Photonic Low-Cost Sensors for in-Line Fluid Monitoring

Design Methodology

Jon Mabe Álvarez

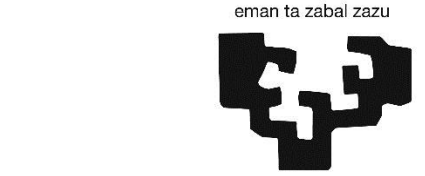

PhD Thesis
Bilbao, 2017

Supervisors:
Joseba Zubia Zaballa
Ana Aranzabe Garcia

Kai eta Alazne, zuentzat
Ama, Aita eskerrik asko

Preface

The paradigm of process monitoring has evolved in the last years, driven by a clear need for improving efficiency, quality and safety of processes and products. Sectors as manufacturing, energy, food and beverages, etc. are fostering the adoption of innovative methods for controlling their processes and products, in a non-destructive, in-place, reliable, fast, accurate and cost-efficient manner. Furthermore, the parameters requested by the industry for the quality assessment are evolving from basic magnitudes as pressures, temperatures, humidity, etc. to complete chemical and physical fingerprints of these products and processes. In this situation, techniques based on the UV/VIS/NIR light-matter interaction appear to be optimum candidates to face the request of the industry. Moreover, at this moment, when we are witnessing a technological revolution in the field of optoelectronic components, which are required for setting up these light-based analyzers.

However, being able to integrate these optoelectronic components with the rest of subsystems (electronics, optics, mechanics, hydraulics, data processing, etc.) is not straightforward. The development of these multi-domain and heterogeneous sensor products, meeting not just technological but also market objectives, poses a considerable technical and organizational challenge for any company.

In this context, a methodological hybrid and agile integration of photonic components within the rest of subsystems, towards a sensor product development, is presented as the main outcome of the thesis. The methodology has been validated in several industrial scenarios, being three of them included in this thesis, which covers from hydraulic fluid quality control to real-time monitoring of alcoholic beverage fermentation process.

Index

1.
Introduction

This introductory chapter aims at setting the motivation of the thesis and to establish its scope. Since this thesis' overall goal is contributing to the development of fully functional cost effective photonic sensors for the in–line analysis of fluids, the first section of the introduction is devoted to clarify this concept. The section starts analyzing the opportunity opened for sensor manufacturers thanks to the requirements of pervasive monitoring of industrial processes within the Industry 4.0 paradigm. The different blocks involved in the photonic sensors are reviewed here, as well as the main strategies followed by the most significant players in the field of sensors companies in this regard. Subsequently, the new generation of cost effective and compact photonic devices (light sources, light detectors, optic components, electronics, etc.) are presented here, analyzing the opportunity generated by their presence but also considering the challenges and risks related to their integration into reliable sensor products. Finally, we position this thesis in the photonic equipment landscape, establishing its scope and its objectives and highlighting the main results.

1.1 Industry 4.0 and Smart Sensors

Surely, some of the most hyped concepts in industry today are the industrial internet, Industry 4.0, Cyber–Physical systems (CPS) or the Industrial Internet of Things (IIoT) and it is difficult to avoid reading about these terms in the industry press and in the marketing of industry technology vendors [1][2][3]. Like it or not, this industrial revolution has already started, driven by the need for more efficient and cost–effective manufacturing [4][5][6].

Foreseeing the convergence of industrial and manufacturing systems with the features of advanced computing, data analytics, cost–effective sensing and new levels of connectivity enabled by the internet, Industry 4.0 is envisaged as the next great breakthrough step in industrial evolution. The promise of unprecedented advancements in automation, efficiency and flexibility, together with an expected dramatic saving in manufacturing costs and achieving better qualities in good production and supply, has sufficed to foster a tremendous amount of effort on providing a full portfolio of solutions within the Industry 4.0 paradigm.

The giants of the process automation and manufacturing equipment, such as Siemens, Bosch, General Electric, ABB, Schneider Electric, Honeywell, etc. are ensuring that all the research efforts reach the market in due time. These companies are going through the most insightful change in their corporate histories, attempting to switch from being makers of machines into fully digital businesses [7], where cloud services, big data analytics and pervasive smart sensing are the most important technologies supporting this revolution (see Figure 1.1–1).

In this context, in 2015 General Electric (Fairfield, CT, USA) launched Predix® as an operating system of the Industrial Internet for connecting industrial equipment, analyzing data, and delivering real–time insights [8], and where smart and connected sensors play a crucial role in the very bottom of the Predix system architecture: data and information gathering. Additionally, again in 2015, Siemens (Munich, Germany) presented MindSphere®, their Industry 4.0 platform, offering to its customers the online monitoring and analysis of globally distributed machine tools, industrial robots, or industrial equipment such as compressors and pumps.

On the other hand, manufacturers as Bosch (Stuttgart, Germany) are not only focusing on the higher tiers of the digitalization of industry [9], but also, they are shifting to generate novel sensor technologies that meet the expectations of the IIoT in terms of integrability, connectivity, intelligence, flexibility and indeed cost [10][11]. Some of the latest examples of this paradigm shift in the Bosch sensor portfolio are found in the APAS®, a bunch of intelligent

systems for man–machine collaboration, including fully sensorized and connected robots and workplaces.

Following the same trend, ABB (Zurich, Switzerland) is showing a strategy to instrumentalize with smart and low-cost sensors legacy industrial machines. This approach enables the equipment operators to upgrade their existing industrial processes with a condition monitoring strategy with a really low investment. For instance, one of the latest solutions launched by ABB in the 2016, the ABB Ability™ Smart Sensor, is designed to be directly attached to a motor frame and picks up data on vibration, temperature and other parameters and, using on–board algorithm, is able to deliver information about the motor's health that is used to reduce motor downtime by up to 70 percent, extend lifetime by as much as 30 percent and lower energy use by up to 10 percent [12].

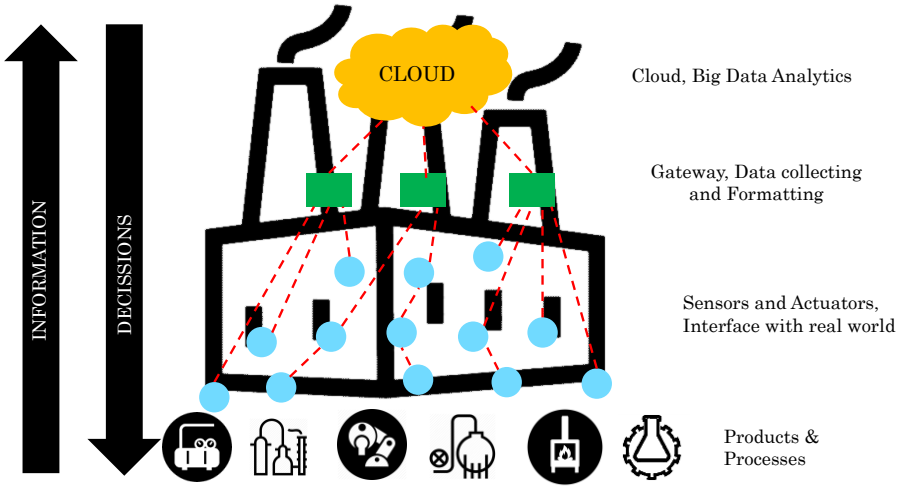

Figure 1.1–1: Schematic overview of the role of sensors within the IIoT or Industry 4.0 paradigm

Along with its analytics platform for the IIoT, the Uniformance® Suite, Honeywell is upgrading and expanding its smart sensor portfolio. As one of the historical references in process automation, Honeywell has identified that fluid management industries such as power, chemicals, and oil and gas, often require complex software architecture to ensure their operations are safe, efficient and reliable, and is proposing a IIoT technology to help solving some of these challenges [13]. The SmartLine® product family for pressure, level and fluid temperature sensing are one of Honeywell's latest example in this field, combining the smart sensor systems with software solutions and open interfaces for data access, which enable users to manage their plant assets better and optimize their productivity [14].

Even if the use of process and diagnostic data from the field level is nothing new [15], it is evident that the context of the Industry 4.0 has fostered the key stakeholders on the industrial automation to consider a huge ramp–up in terms of plant monitoring, being the smart sensors the true enabler for Industry 4.0, as they represent the data source for any service, cloud and big data applications. However, it is absolutely essential for sensor technology to be intelligent, rugged and reliable when it comes to dealing with important workplace challenges, such as critical infrastructure maintenance, or the safe interaction between people and machines [16].

Therefore, this context of eagerness for pervasive motorization within industrial environments represents an opportunity for sensor manufacturers, with several different applications waiting for in–place and real-time measurement solutions. The specific case of the industrial fluid monitoring is not an exception, delivering several examples as the real-time analysis of lubricant status at off–shore wind turbines where the accessibility is very limited [17], or the monitoring of hydraulic fluids of robotic arms in automotive plants, with several thousands of units deployed working at high loads [18], monitoring of hydraulic fluids in critical actuators as airplanes [19], etc. These use cases are clear examples demanding a tradeoff solution between an immediate availability of in situ information and a reduction in the accuracy of the results, which is the ideal scenario for solutions like the one presented in this thesis.

However, meeting not just requirements in terms of sensor performance, compactness, unitary cost, reliability, etc. but also market and economic objectives poses a considerable technical and organizational challenge for any company. Management of uncertain and evolving specifications, continuous risk assessment, synchronizing of multidisciplinary working teams (e.g. chemistry, micromechanics, optics, electronics, signal processing), pressure to cut development times in order to launch new products into market, and the complexity inherent to the technological bases of the sensor's measurement principles need to be managed efficiently throughout the design, development, validation and certification phases of the sensor product.

In this context, the work presented in this thesis describes a methodology for developing smart sensors for industrial fluidics based on photonic working principles. The work describes the different steps, approaches and considerations for bringing sensor concept ideas through different development stages, into a fully operative, reliable, compact and cost–effective sensor system, focusing on the technical and practical challenges of the use of unattended photonic sensors in the field of fluid monitoring.

1.2 In–line Real Time Fluids Monitoring

As mentioned, in the context of Industry 4.0 or IIoT, the focus is primarily on data and the exchange of data across all system boundaries. In most cases, large amount of this data is generated with the help of sensors that measure different parameters of interest throughout the production process. When these sensors are being placed directly into a process stream and offer continuous information about a certain parameter (pH, temperature, pressure, density, flow, etc.) we call them in–line and real-time sensors (see Figure 1.2–1) [20].

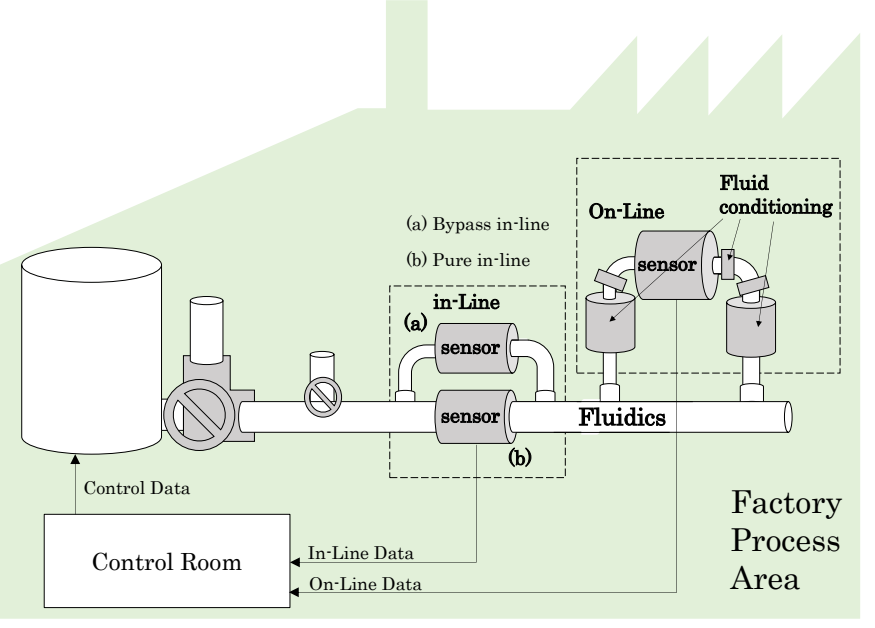

Figure 1.2–1: Schematic overview of in–line and on–line sensors within a process flow.

Among several other magnitudes and elements to monitor in the broad universe of industrial applications, the industrial fluidics (see Table 1.2.1) arise as a very challenging opportunity for smart sensor developers, not only due to the traditional requirements of high sensibility, repeatability and reliability in the measurement, but also because of the extreme working conditions (temperature, pressure, humidity, vibrations, etc.), and the necessity of sample extraction in place (e.g. by pass, in line) at the right flow and in the right volume, dealing with different viscosities, corrosive ambient and samples, non–homogeneous materials, etc. [21].

On the other hand, we may differentiate two kinds of fluids within the industrial applications: fluids that are an important part of a process, part of a machine or equipment, and fluids that represent a product their selves. Monitoring the parameters of the fluids from the first group is crucial for assuring the functionality of the process,

avoiding failures and downtimes, improving efficiency, etc. On the other hand, the products coming out from a manufacturing plant in a fluid format need to be sensed in order to maximize the quality and safety of the production batches, reduce the wastage and to comply with audit and regulatory affairs. Even if both scenarios are well aligned with the Industry 4.0 paradigm, in the first one the fluidics sensing is a fundamental part of predictive maintenance or condition monitoring approach [22], while in the second case, the sensors are part of a Statistical Process Control strategy [23][24].

Table 1.2.1: Examples of fluids present in industrial applications

Fluids / Applications	Function of the sensor
Engine and Gear Box Lubricants Hydraulic Fluids (e.g. phosphate esters)	Viscosity measurement, Water or Air content, Particle content, chemical degradation and oxidations
Coolants (e.g. Glycol)	Viscosity and absorbance
Electrolytes for Redox batteries (e.g. Vanadium)	Viscosity and color
Insulating Oil in Electrical Transformers	Oil oxidation, external contaminations (water leakages, insulating cellulose decomposition)
Gas, Diesels and Biofuels	Water in Oil, Measurement of Aromatic. Monitoring the biofuel chemical & physical characteristics (alcohol fermentation, octane number)
Heat Transfer Fluids	Viscosity and NIR absorption
Cooling Waters	Contaminant detection Plague (e.g. legionella) detection
Food & Beverages: fruit and vegetable sauces and concentrates	Product Quality, Wastage reduction Correlation to consistency and homogeneity for end product quality. Chemical analysis (Fructose, glucose, lactose, fatty acids…)
Food & Beverages: Dairy Products	Product Quality, wastage reduction, viscosity, density, fat, protein and water proportions
Cosmetics	Correlation to texture for end product quality. Surfactant, active ingredient concentration. Moisture.
Pharmaceutics	Product Safety, Product Quality Production SPC records
Pulp & Paper	Inhomogeneity control and fiber concentration. Lignin analysis. Raw water quality, turbidity of white water

Indeed, the monitoring of fluids is nothing new (see Table 1.2.2), and it was an important part of the industrial automation and instrumentalization boost that took place the 1960 decade, with several companies marketing several sensor solutions covering different magnitudes day by day, as pressure, temperature, level, flow, viscosity, moisture, pH, etc. [25][26]. Innovative sensors and actuators came from some key companies, which in a fragmented business, most of them get stuck at growth plateaus and get bought out. For instance, founded in 1956, Rosemount (Shakopee, MN, USA) started with specialty temperature sensors (RTDs) and then grew with the development of its capacitive differential pressure transducers, rapidly overtaking the traditional leaders as Foxboro (Foxboro, MA, USA) and Honeywell, and then the company was eventually acquired by Emerson (Saint Louis, MO, USA) in 1976. These convulse years also witnessed the creation or the consolidation of other reference companies in the field of fluid monitoring as Brooks Instruments (Hatfield, PA, USA) specialized in flow metering, Beckman Coulter (Pasadena, CA, USA) in pH and other chemicals, Yokowaga (Tokyo, Japan) offering flow meters, Balluf (Neuhausen, Germany) with pressure and photoelectric sensors [27][28][29]. In the forthcoming years many other big players started to find their niches in the fluid control and automation field with examples as Parker (founded in 1917, Cleveland, OH, USA), Pall (founded in 1946, New York, NY, USA), Hydac (1963, Sulzbach, Germany) or Burkett (founded in 1946, Ingelfingen, Germany).

Table 1.2.2: Some of the most common physical or chemical parameters of Interest in Fluid Monitoring for industries like Energy, Biotechnology, Chemical, Brewing, Pulp & Paper, Petrochemical, Food and Beverages, etc. [30]

Parameter	Units	Measurement Principles
Viscosity	Poise	Falling–cylinder viscometer, rotating disc viscometer, capillary sensors
Flow [31]	L/min, m^3/s	Ultrasonic flow meters, Electromagnetic flow meters, Pressure flow meters, Rotating flow rate devices, Vortex flow meters

Temperature [32]	Fahrenheit (°F), Celsius(°C), Kelvin(K)	Expansion of materials, Electrical resistance change, Thermistors, Thermocouples, Pyrometers, Semiconductors, Index of Reflection
pH	pH units	Electrolytic principles
Pressure [33]	pounds per square inch (psi), Pascal (Pa), Bar	Manometer, Diaphragms, Capsules, and Bellows, Bourdon Tubes, Piezoelectric pressure gauge, Ionization gauges
Turbidity [34]	Nephelometric turbidity units (NTU)	Optical sensor (scattering), Nephelometry (diffuse radiation), Turbidimetry (attenuation of a radiant flux)
Opacity	mm^2/mass	Optical sensor (absorption)
Moisture [35]	%, ppm	Psychrometers, Resistive hygrometer, capacitive hygrometer, Piezoelectric or sorption hygrometers, Microwave absorption, Infrared absorption
Air presence	%, ppm	Optical sensor (absorption), Imaging sensor
Particle Content	Number of particles	Optical sensor (scattering), Imaging sensor, Ultrasound, Inductive
Color	CIE–Lab, RGB	Optical sensor(absorption)
Density	g/m^3	Vibration sensors, Ultrasound sensors
UV–VIS–NIR Absorption	Arbitrary units	Optical sensor (absorption)
Conductivity [36]	S/m (Siemens/meter)	Amperometric, Potentiometric or inductive probes
Level [37]	n.a.	Ultrasonic, Resistive, Optic, capacitive

The golden age of analog sensors lasted for almost three decades, until the early digitalization of sensors that took place in the mid–nineties. The evolution continued with the connectivity expansion, with a bloom of wirelessly connected industrial sensors around 2005 [38]. These connected sensors paved the way, one decade later, for the already mentioned Industrial Internet of Things, where sensors are supposed to upload to the Industry 4.0 cloud reliable, standardized, significant, real time and in–place information about fluidics used in industrial environments. Therefore, meeting the expectations of the Industry 4.0 will only be possible if, asides the sensor's measurement principle, a full set of on–board algorithms, communications, standard interfaces, auto calibrations, etc. are included within the sensor system itself (see Chapter 3 for smart sensor concept description).

Asides to the addition of layers of intelligence, connectivity, etc. the fluidics sensors have been incorporating different physical and chemical parameters to their sensibility portfolio. The fluidics sensors are gradually becoming into complete integrated mini laboratories, able to measure specific chemicals, contaminants, presence of particles, oxidations, sample homogeneities, etc. which their in–line and real time motorization is very relevant and even critical for several industrial processes (see table 1.2.1). Nevertheless, traditionally, these sensors have been bulky, expensive, difficult to integrate and maintain, and most of them are far from becoming integral part of the IIoT paradigm which is jeopardizing and contributing negatively to their massive deployment in the Industry 4.0 scenario.

However, in this context, photonic sensors arise as a promising technological alternative to close the gap between the Industry 4.0 requirements and the performance of the current sensors. Optical methods can non–invasively assess the microstructure, function, and composition of fluids, as well as deliver a reliable operation while working in the field. Additionally, the revolution in digital electronics has significantly reduced both the price and size of components (sensors, light sources, computing units) critical to most optical systems. Integrating such optical components with compact microfluidics, micromechanics and low–cost electronics and communication systems allows for building robust photonic smart sensor systems that are inexpensive, scalable and ready for their deployment in the Industry 4.0 arena.

1.3 Cost Effective Smart Photonic Sensors

Photonics-enabled sensors deliver a comprehensive measurement of a sample relying on the light-matter interaction processes, which will be reviewed in depth in the Chapter 2. Basically, when a light beam hits a material, the properties of the original light ray get modified depending on the physical and chemical composition of the sample material. Therefore, if these changes in the light are recorded, and compared with the original light, or with the light outputted by other sample materials, relevant information about the composition of the sample can be obtained.

Then, we could define a photonic sensor as a system which integrates all the components for performing a measurement based on the light–matter interaction. If we narrow down to the specific case of photonic sensors for fluidics, the liquid sample conditioning and management should also be included within the sensor to provide a true autonomous operation.

Traditionally, the main subsystems included in a photonic sensor are the ones depicted in Figure 1.3–1.

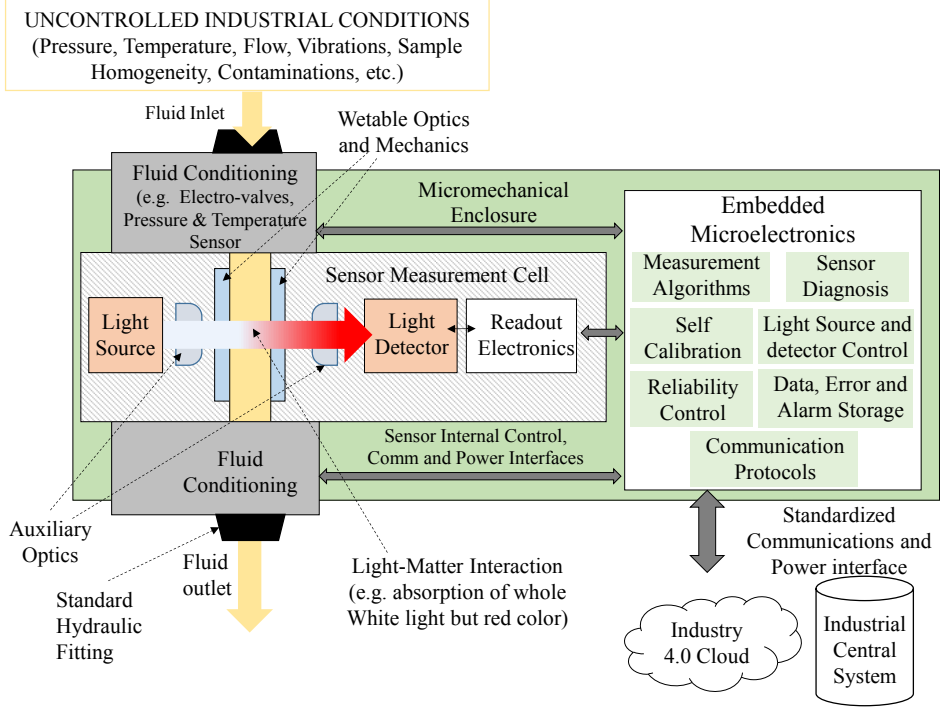

Figure 1.3–1 Block diagram of a Photonic Sensor, working in transmission mode, installed within the industrial process through standard hydraulic fittings and connected to the Industry 4.0 cloud via standardized interfaces.

These main blocks include the **photonic subsystem**, comprising the light emitter and the light detectors, and all the complementary electronics for their driving, readout, signal conditioning and compensation. The system could also require the use of some auxiliary optics as filters, lenses, pinholes, etc. for the conditioning of the light beams.

Another important subsystem in fluidic sensors is known as the **wettable part**. This specific part of the sensor is the one in contact with the fluid and the one responsible for handling and bearing with all the environmental conditions of the sample. The wettable parts should stand high working pressures and temperatures of the fluid, should avoid any leakage under the working flow and viscosities range, should be compatible with the chemical properties of the sample fluids (e.g. corrosive liquids) and for the specific case of photonic inspection techniques, the wettable parts need to be compatible with the properties (e.g. absorption spectrum, index of reflection) of the light incident to and coming out of the sample fluid. Normally, the wettable parts include an optical window transparent to the working spectrum of the light, some sealing and some micro mechanical parts for assuring the water tightness of the whole structure.

Besides, the part of the sensor where the fluid sample is confined or flows through for its analysis is defined as the **measurement cell or chamber**. This is a very important module in the system, with important requirements in terms of fluid dynamics management and fabrication and assembly tolerances. For instance, the microfluidics design should avoid the generation of flow turbulences within the measurement cell contributing to sample homogeneity (as described in Chapter 3). Besides, the mechanical tolerances in the chamber geometry impact, for example, on the light path dimensions (the distance that the light needs to cover from emitter to detector). Not meeting the nominal tolerances, dramatically affects the measured light power due to the exponential dependence of the light absorbed within a medium with the light path distance (as described in Chapter 2).

The different **micromechanical parts** are assembled into the whole sensor body mechanics, which is in charge of: solving the standardized hydraulic fittings and their matching with the measurement cell, assuring the optical alignment of different component, enabling the assembly of all the electronic and connectronic parts, solving or supporting the external enclosure which should be compatible with all the environmental conditions (normally standardized as IP rating of the product).

The smartness concept is brought by the presence of a customized **embedded electronic subsystem**. The embedded CPU will

run different software pieces in charge, among others, of performing the light emitter and detector control, executing the measurement algorithms for outputting the analysis result, applying internal performance assessments and calibrations. This electronic part also, deals with all the power issues, converting the external voltage input (e.g. 24V, 12V) to the internal levels (e.g. 5V, 3.3V) or managing a battery element. In addition, the embedded electronics store all relevant information as measurement results, alarms, errors and key performance indicators that are extremely important for the life management of the sensor. The electronics is also in charge of implementing the standard communication protocols (wired or wireless) for assuring a secure, reliable and seamless information exchange between the sensor and the intermediate layers of the Industry 4.0 architecture.

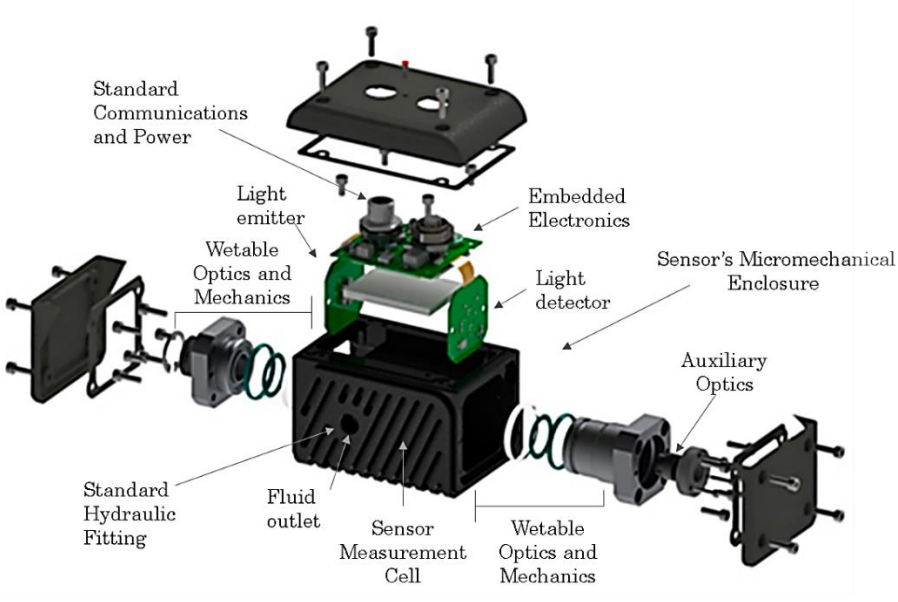

Figure 1.3–2 Teardown of OilWear PICO® sensor product. Different mechanical parts, optoelectronics, electronics, seals, windows, optics and connections are displayed.

In some occasions, some external **fluid conditioning circuitry** is also included within the sensor. Among different alternatives, a combination of some of the following items could be found as part of the sensor systems: electro–valves, flow controllers, pressure limiters, particle filters, pressure sensors, temperature sensors, pumps, etc. However, normally, all the sensor designs try to avoid the need of these bulky hydraulic components that jeopardize the potential low cost and compact size of the photonic sensors. Nevertheless, the system evolution for dealing with non–conditioned fluids is not straightforward, and several modifications especially in the lighting

and detection systems are required as described in one of the use cases of the Chapter 5 (the stroboscopic vision sensor).

Once the Smart Photonic Sensor concept has been described, we will introduce the cost effectiveness term, which requires several considerations. One typical mistake is to reduce the sensor's cost to the aggregation of costs of the individual components, with some contributions from assembly and calibration processes. But this approach is far from being real. The sensor's unitary cost should also consider all the previous research, engineering and tooling costs, normally defined as Non–Recurring Engineering (NRE) costs [39]. Additionally, budget for guaranty period and post–sales support should also be allocated.

Besides, if we widen the perspective, we should not only consider the unitary cost of the sensor, but the Total Cost of Operation [40], that considers the expenses of the sensor installation, maintenance, removal and disposal as part of the investment required by the end user for using the sensor technology (reviewed in depth in Chapter 3). Imagine the real cost behind a situation where a very cheap sensor requires a human operator to calibrate it each week. However, the total cost of operation should also consider the benefit and profit obtained by the end–user due to the installation of the sensor, as, for instance, reducing the downtime of his machinery.

Figure 1.3–3 Colorimetric Sensor for real–time analysis of lubricant oil ageing in gear–boxes.

After having exposed the different considerations behind the real cost of a sensor, we should mention that, currently, we are witnessing a revolution in the photonic and optoelectronic technologies, that are enabling not only to enhance the features of emitters and receivers, but also to reduce their costs dramatically [41] [42], opening the door to the development low cost photonic devices.

Therefore, it is clear that, for achieving the required cost effectiveness, the remaining contributor factors in the sensor costs should be shrunk down (see Figure 1.4–6). While installation and maintenance costs are being controlled thanks to IIoT approaches [43], minimizing the RTD and NRE costs of a photonics–based sensor is not evident, and several risks hinder the achievement of a cost-effective product, as it is described in the next section.

1.4 New photonic devices and their integration into products

Since its emergence at the end of the 60s [44], the idea of fully integrated photonic devices has been captivating scientist and engineers' imagination for more than five decades already. The promise of unmatched features in emission powers, detection sensibilities, longer wavelengths, tunable directivities, etc. together with dramatic reduction of component cost and compactness has sufficed to foster a tremendous amount of effort on providing an integrated platform allowing a monolithic or hybrid integration of photonics, micro–electronics, optics and micro–mechanisms [45].

However, and aside some big exceptions as LEDs and CMOS imagers, despite large R&D investments, photonic integrated circuits with integration levels exceeding a few components did not succeed in entering the commercial marketplace for more than four decades. Skeptics started claiming that integrated optics was only a promising technology and would ever remain so [46].

Therefore, without a true integration, the main trend in photonics device development was to assemble discrete components that are based on a large variety of materials and technologies (lenses, gratings, detectors, electronics, connectors, etc.) into a customized platform. However, the final outcome of this approach was normally crystallized into bulky and expensive photonic systems. Even when huge efforts were put in miniaturization and cost effectiveness of the solution, the results obtained were far from being as compact, lightweight and low cost as expected, as exemplified in Figure 1.4–1).

Nevertheless, as mentioned earlier, there was also a bright side in the integrated photonics landscape centralized in the continuous breakthroughs coming from the LED light emitters or from the CMOS image detectors. Mainly pushed by consumer market, both technologies have unbelievably evolved in parallel in the last decade [47][48][49]. Currently, the availability of a huge portfolio in CMOS detectors (resolution, optical format, sensibility) and LED emitters (spectral range, emission power, form factor), enables the use of high

performance detectors and emitters at minimum costs, even below 1€ per unit. This sort of emitter and detector technology is behind several cost effective industrial machine vision solutions

The current trend is to achieve longer wavelengths, efficiency and stability in LED systems [50], including wide band LEDs [51]. Regarding the imagers, looks like the competition of the solutions in the visible range is to increase the resolution, enhance the dynamic range and sensibility of the detectors [52]. However, several efforts are being put on increasing the wavelength range to NIR and SWIR ranges to enable cost effective Hyperspectral cameras [53].

Nevertheless, even if the LEDs and CMOS imagers have experimented and exponential ramp up in the last decade, from the photonic point of view they are relatively simple structures, since they are basically built upon color filters, diffuser lenses and light sources or receiver. Additionally, it could be fair concluding that the integration achievements witnessed in both cases are much more related with the microelectronics domain rather than with the pure photonic science.

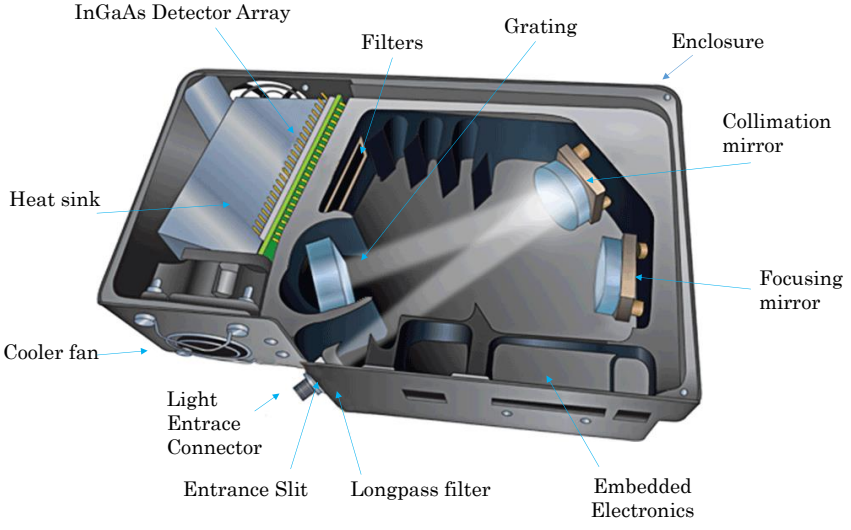

Figure 1.4–1. 182 x 110 x 47 mm, 1.18 kg, 256-pixel Detector Array, NIRQuest ® Device from Ocean Optics ®. Launched in 2015 with an approximate cost of 15K€.

On the other hand, the progresses made in the field of micro–opto – electromechanical systems (MOEMS) could be considered as the true representatives of complex photonic integration [54][55]. Introduced in mid–eighties [56], heterogeneous integration of MOEMS and integrated circuits (ICs) allows the combination of high–quality optical and photonic MOEMS materials such as monocrystalline silicon (Si) with standard CMOS–based electronic circuits in order to realize complex optical systems. Asides the integration of materials

with optical properties, MOEMS, as the MEMS devices do, also take advantages of the mechanical properties of silicon, allowing the integration of moving parts within the device, which are extremely useful for fabrication complex photonic devices as spectrometers [57], projectors (see MOEMS based electro–opto projector by Bosch in Figure 1.4–2), LASERs [58][59], light modulators [60], etc. by companies and research laboratories around the world.

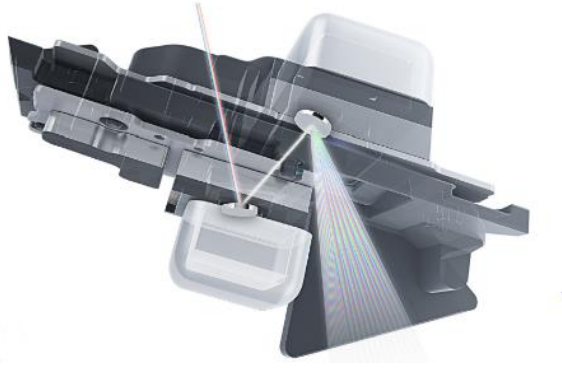

Figure 1.4–2 Bosch SensorTech's new MOEMS technology–enabled micro projector BML050. Featuring compact size, power efficiency, robustness and reliability

An even if the optical MEMS have had a difficult development road during the last thirty years [61], the significant successes reported lately may have finally opened the door to mass commercialization of MOEMS devices. Focusing for instance to the NIR micro spectrometer segment, during the last years a large amount of these research and development efforts have crystalized in breakthrough products and prototypes. In this specific case, in five years, we have witnessed a technological evolution that has enabled the migration from discrete/component based systems, into chip–scale solutions. The new generation of MOEM–based NIR spectrometers offers solutions hundred times more compact at prices hundred times lower.

The latest and most representative examples are coming from large firms as Hamamatsu, from innovative SMEs as Spectral Engines, Si–Ware or PixelTEQ (now acquired by Ocean Optics), or from joint ventures as Viavi (formerly JDSU) and Espross. All of them will be launching new product lines or updating their product portfolio in the area of integrated NIR spectrometers. All these solutions are very compact, cost effective and feature rich (see Figure 1.4–3 and Figure 1.4–4), compared to the latest non–integrated spectrometers (see Figure 1.4–5) which offer faster scanning speeds and better Signal to Noise ratios but at much higher (x10, x100) cost and larger sizes (x10–x100).

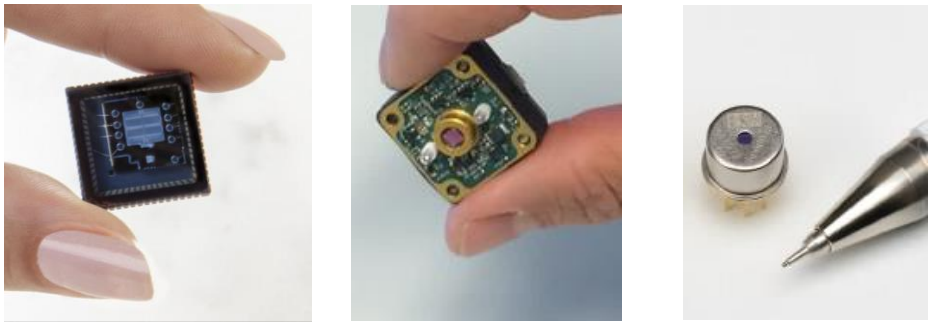

(a) (b) (c)

Figure 1.4–3. Chip scale, single photo–detector NIR micro–spectrometers, (a) NeoSpectra MICRO from Si–Ware, (b) NM series from Spectral Engines, and (c), C13272 series from Hamamatsu.

(a) (b)

Figure 1.4–4. Filter array and 2D photo–detector array based VIS–NIR micro–spectrometers. (a) PixelTEQ's PixelSensor™. (b) Espross's SPM64–NIR.

This new generation of photonic devices, as the extremely compact and cost effective NIR micro spectrometers (see Table 1.4.1), are enabling an enormous number of potential applications and products for improvement and automation of industrial processes, efficiency enhancement, product safety control, etc. answering the demands of process industries for increasing the efficiency of manufacturing processes and the quality of their products. Basically, these industries are requesting to bring photonic measurement solutions for field use, and MEMS-based photonic sensors are considered as true enabler to deliver accurate in-line real–time measurements to applications which are until now only accomplished in laboratories [62].

(a)

(b)

(c)

Figure 1.4–5. Non–integrated spectrometers. (a) MicroNIR PRO from Viavi (formerly JDSU). (b) QRed from RGB Photonics, launched in 2017, (c) FlameNIR micro spectrometer from Ocean Optics, launched in 2016.

Table 1.4.1: Summary of the latest integrated NIR micro spectrometer products.

Device	Working principles	Working Range (nm)	Size (mm)	Cost[1] (€)
NeoSpectra Micro (2017)	Monolithic Michelson interferometer and single uncooled InGaAS Photodiode	1350 – 2500	~18 x 18 x 4	100
NM series (2016 – 2017)	Micromechanical Fabry–Perot Interferometer and single InGaAS Photodiode	1350 – 1650 1550 – 1950 1750 – 2150 1950 – 2450	25 x 25 x 17.5	100
C13272–series (2016–2017)	Single InGaAs Photodetector and Fabry–Perot interferometer	1550 – 1850 1350 – 1650 1750 – 2150	Ø9 x 6	100

[1] Notice that these costs should be considered as an order of magnitude approximation. These costs are estimations based on information from manufacturers but do not represent any official quotation at it may be bonded to volume purchases or other trading conditions.

PixelSensor (2017)	8 channel Thin Film Filter and Si Photodiode array	400 – 1000	9 x 9 x3	10
SPM64–NIR (2017)	64 channel Thin Film Filter and PD array	775 – 1075	17 x 6 x 3	5
MicroNIR PRO (2015)	Linear Variable Filter and uncooled InGaAs Photodiode 128 pixel array	950 – 1650	~ Ø 50 x 50	15K
FlameNIR (2016)	Diffractive grating optics and uncooled InGaAs Photodiode 128 pixel array	950 – 1650	89 x 63 x 32	10K
Qred (2017)	Czerny–Turner approach spectrometer based on fixed surface mirrors, reflective grating and cooled InGaAs 512 pixel array	Default: 950 – 1700 Custom: 800 – 2500	67 × 58 × 20	20K

However, the availability of compact, cost effective cost and feature rich optoelectronic components should not hide the high difficulties, complexity and risks entailed in the design of a photonics-based low-cost sensor system. The uncertainties, the multi-domain nature of the system and time-to-market pressures among others hinder the integration of the novel photonic components into successful products meeting the customer requirements in terms of performance, size, cost and regulations.

Therefore, with the aim of contributing to the field of cost effective sensor solutions (see Figure 1.4–6), the objective of this thesis is to provide a design methodology focused on the integration of these breakthrough photonic devices (see Figure 1.5–1), and several different technological blocks (physics and chemistry, electronics, mechanics, fluidics, optics, data processing, communications, etc.) to assist in the development of fully autonomous, reliable, standardized and cost effective Smart Photonic Sensors for monitoring industrial fluidics.

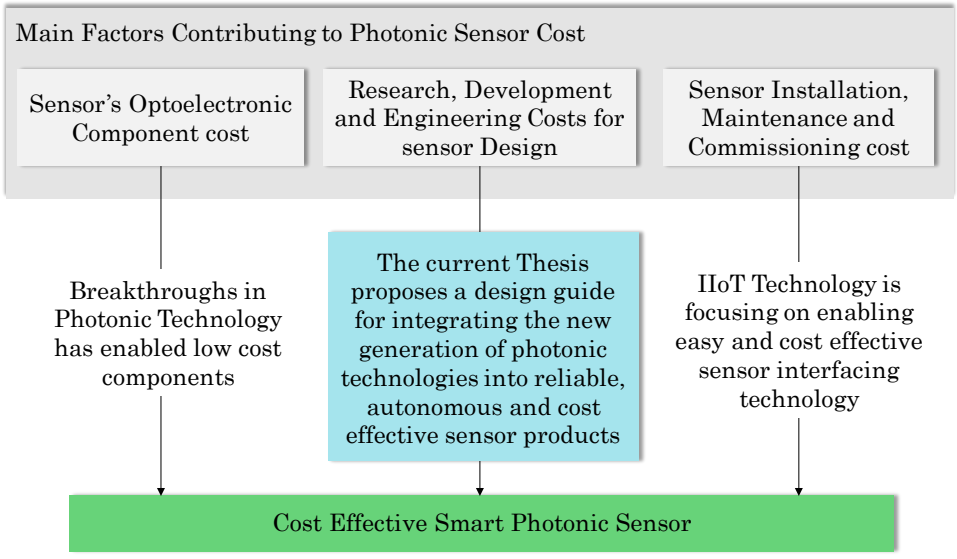

Figure 1.4–6. Diagram displaying the three major factors impacting in the final cost of a sensor system and, how the different technological trends (photonic integration and IIoT approaches) are contributing to lower the cost in two of them evidencing the need of putting some efforts to improve the sensor design and development efficiency, which is, actually, the motivation and objective of this thesis.

1.5 This thesis in the Photonic Sensor landscape

Within the vast landscape of photonics devices, the investigation presented in this thesis focuses on the main challenge of enabling the integration of latest photonic components into autonomous, reliable and cost-effective sensors applied to the in–line monitoring of industrial fluids.

The advent of innovative technology concepts in the field of optoelectronics, with better features, compact integration and dramatically lower costs has opened the door to a high number of potential applications. However, the expectations put on those new potential products enabled by the new photonic components are also increasing, and lower detection limits, lower costs, autonomy, communications and higher compactness are being requested by the end users.

The integration of these photonic components with other fluidic, mechanic, electronic, and data processing subsystems is not evident. In addition, the side effects generated by assembly tolerances, temperature drifts, vibrations, etc. are often underestimated while specifying a sensor. Besides, the impact of verification and validation of a laboratory analysis technique, which has been embedded into a

tiny device, with no sample preparation, and with limited access to it, is often also huge, and not considered in the sufficient manner while planning a fluidic sensor device development.

In addition to the complexity inherent to the photonic measurement principles and their integration into products, stricter regulatory requirements, and the ever-increasing importance of reimbursement decisions for successful sensor commercialization should also be taken into consideration.

The sum of all these factors clearly jeopardizes the crystallization of the original photonic components' low cost, superior performance and reliability into the final smart sensor product.

This integration challenge is exactly where the investigation of this thesis has put the focus. We understand that the development of a smart sensor based on the latest generation of photonic components requires careful planning and strategy–setting, coordinated decisions, and consistent and rigorous development processes.

In this situation, the main contribution of this thesis is to develop a methodology for the effective and agile integration of optoelectronics components within the rest of subsystems, towards a photonic sensor development, focusing on the specific case on in-line fluidics. This methodology aims at guiding the design and engineering teams across the different stages, from proof-of-concept validation to product certification, in the context of complex and uncertain system development with tight project times and costs.

To achieve this general objective, a full review of the light and matter interaction process has been done, with the aim of complementing the engineering view on the sensor integration with a deep and scientific understanding of the physical and chemical processes that define the measurement principle. This step has been considered critical, since several integration risk and performance limitations are found in the most basic fundament of the sensor concept. Additionally, latest alternatives in light emitters, receivers and optic components have been studied, assessing their performance and risks for a cost–effective and reliable deployment in industrial environments. The outcomes of this research could be found in Chapter 2.

Additionally, in Chapter 3, sensor fundamentals and the different approximations for analyzing and extracting relevant information from photonic signals has been studied, which should be embedded into the sensor system to make them smart, fulfilling a basic request from the Industry 4.0. Special attention has been paid at the in–line operation mode and to the fluid management in the proposed sensor systems. The research done in this Chapter 3 is considered also very important because clear heterogeneous

integration (physics, and chemistry, optoelectronics, fluidics, mechanics, electronics, data processing, etc.) problems are identified and addressed.

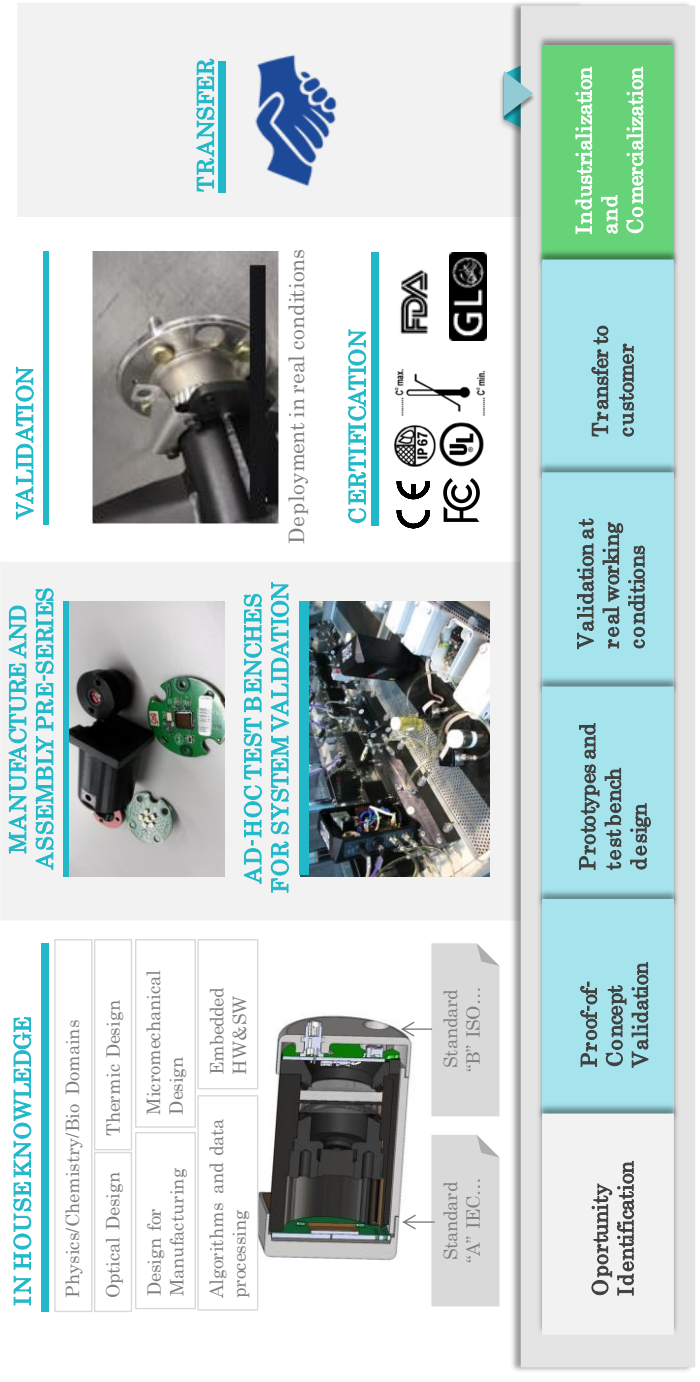

Figure 1.5–1 Stages covered in the methodology proposed in the thesis for assisting the development of Photonic Sensors for in–line monitoring of industrial fluids.

As mentioned, all these insights have been merged in a comprehensive development model that captures all aspects of smart photonic sensor development and commercialization from early–concept selection to post–market surveillance, which is described in Chapter 4. This model was constructed based on scientific review and the analysis of best–practices found in different real developments, as the ones included in the Chapter 5 of this thesis for model validation.

The concluding chapter of the thesis, Chapter 6, includes the main conclusions extracted from this research, and outlines some future investigation lines.

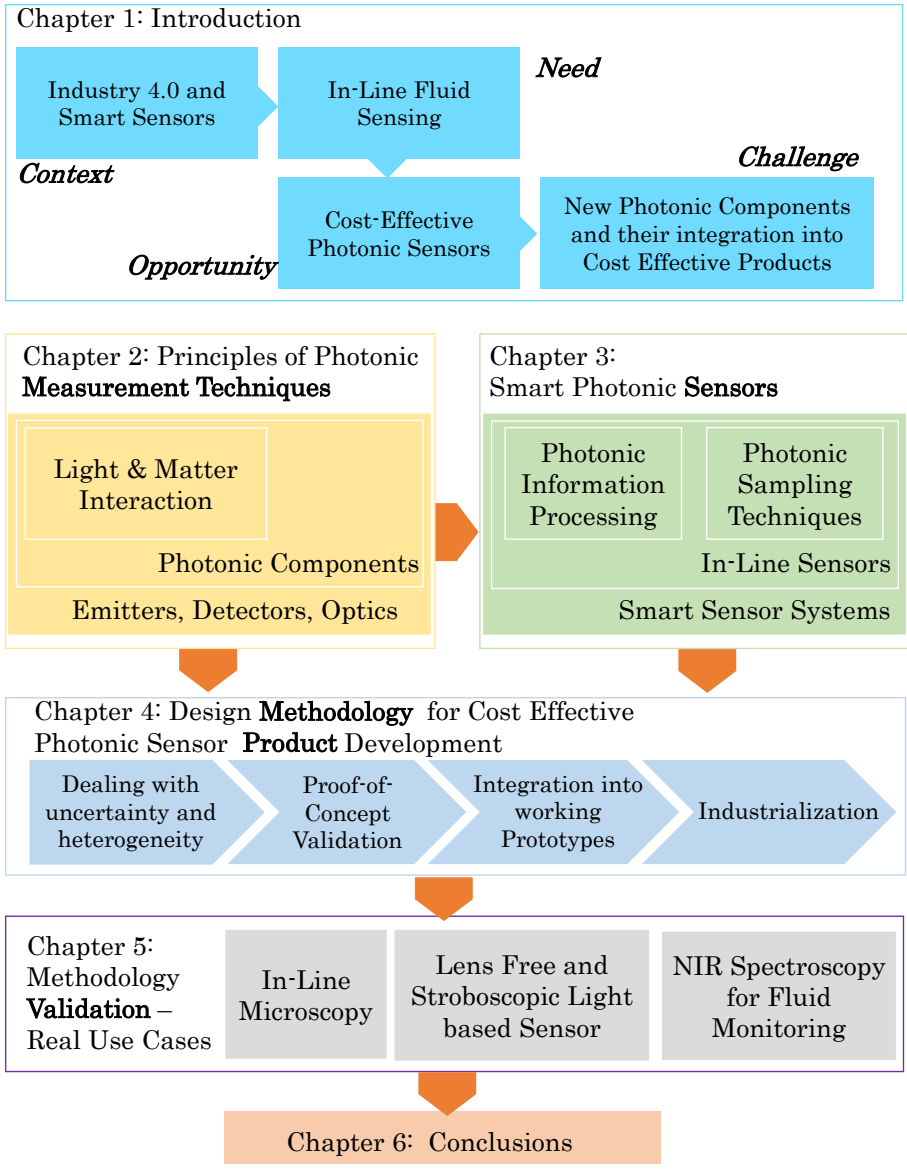

Figure 1.5–2 Thesis Outline.

The most notable scientific, technological and industrial advances of this thesis are listed in Table 1.5.1, together with the chapters and publications in which they are addressed.

Table 1.5.1: Summary of Science, Technology and Industrial advances of this thesis.

Science, Technology and Industrial advances of this thesis	Chapter	Publication
Methodology proposal	[4]	[261]
Integration of Holographic, Lens–Free and Stroboscopic Photonic Sensor	[5]	[260],[261],[262],[263]
Integration of in-line microscopy Sensor	[5]	[259]
Integration of Transmittance NIR Sensor	[5]	[264],[265]

2.

Principles of Photonic Measurement Techniques

The thorough understanding of the photonics–based sensors, including their potential features, intrinsic complexity and the entailed uncertainties requires mastering the basic scientific fundaments involved in the process of using the light for accomplishing measurements about chemical and physical parameters. This is the reason why this chapter reviews and outlines the fundaments of the light and matter interaction processes, describing the most important effects and phenomena happening when the light radiation enters a sample and how they could be used for measuring certain parameters of the matter. Fundamental processes as reflection, absorption, diffraction, scattering, fluorescence, etc. are reviewed as they constitute the core of any photonic sensing technique, and the main considerations for bringing these principles to sensor products is introduced. Additionally, the different light sources (emitters), light receivers (detectors and spectrometers) and light modulator and conditioning elements (optic components) are presented and described in the context of low cost sensor systems.

2.1 Photonic Inspection: The Interaction between Light and Matter

The interaction between the light and matter (e.g. solids, liquids, gases) is one of the most exciting chemo–physical effects that can be witnessed, and has been subject of deep studies by several scientists since the dawn of the science. When the light meets the matter a cascade of reactions and effects happens. The incoming light suffers different modifications, mostly depending on the structure of the matter and the wavelength and power of the light. The possibility of analyzing chemical and physical properties of the matter through the study of these modifications that happened to the emitted light is straightforward and is the base for the development of a photonic inspection technique.

This chapter will review the most important interaction between the light and matter, paying special attention to those with highest potential for being translated into a low-cost inspection technique.

2.1.1 Fundamental Description of the Light

The light radiation is a relatively narrow part within the electromagnetic spectrum, covering the Ultraviolet, Visible and Infrared regions (see Figure 2.1-1). This light is generated by different means, being the most famous one the Thermic Radiation, which, according to Planck's Law, defines that any body in a thermal equilibrium with its environment, will emit electromagnetic radiation in a frequency band defined only by its temperature, radiating the same intensity in all directions.

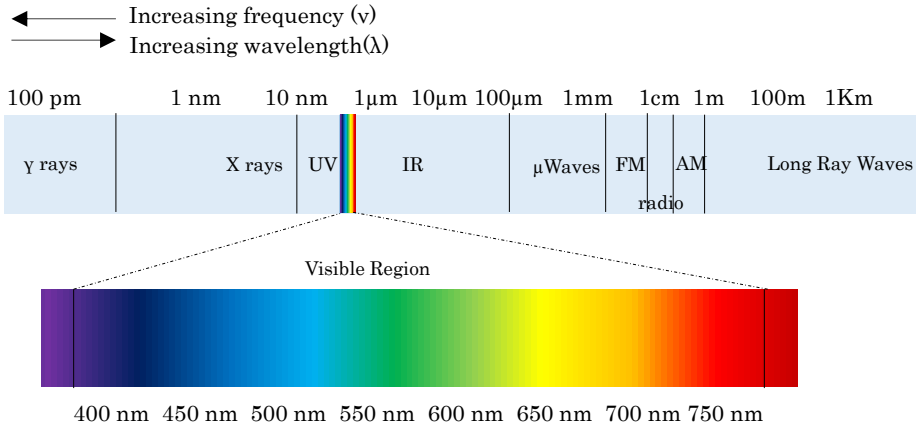

Figure 2.1-1 Electromagnetic spectrum with detailed view of visible light

This propagation of the light will be dependent on the medium that light rays are crossing, affecting their direction and its speed. This effect is described as the Index of Refraction, n_{medium}, of a certain medium, which defines the velocity of the light across it (see Eq. 2.1–1), and will be later used for defining the direction of the light rays with the Schnell's Law.

$$n_{medium} = \frac{c}{v} \quad \text{(dimension less)} \qquad \text{Eq. 2.1–1}$$

Being c (299,792,458 m/s) the speed of light in a vacuum and v (m/s) the speed of light in the medium.

However, the detailed description of the light propagation across different mediums has historically been under scientific discussion. After several attempts to define the behavior of the light, the most accurate description came from Newton[2] and his contemporaries Hooke[3] and Huygens[4], representing their works the controversy in understanding the light as a wave or as a particle.

While Newton described the light with a corpuscular approach, considering that the light was composed of several finite elements, Hooke and Huygens mathematically refined the wave viewpoint for understanding the light as a propagating wave. The wave theory was later developed by Fresnel[5] and Young[6], with his famous double slit–interference, and the wave description became predominant theory until the atomic theory was refined in the early 1900. At that time, the already mentioned Planck[7] and Einstein[8] found several evidences while working on their black body radiation and photoelectric effect, which seemed impossible to describe with the wave approximation of the light, and the scientific community shifted towards the light-as-particle description.

Nowadays, the controversy continues, but there is broad acceptance of a mixed approximation for defining the light as a train or particles, photons, that somehow describe features of waves. This property is referred to as the wave–particle duality

Unlike regular waves, that will lose their energy gradually while propagating in a medium, the light waves will lose some of its particles or photons. At this point, it is important to understand the energy of a photon E, (see Eq. 2.1–2) and the fact that, as described by

[2] Isaac Newton, British physicist, 1643- 1727.
[3] Robert Hooke, British scientist, 1635-1703.
[4] Christiaan Huygens, Dutch scientist, 1629-1695.
[5] Augustin-Jean Fresnel, French engineer and physicist, 1788-1827
[6] Tomas Young, British physicist, 1773-1829.
[7] Max Planck, German physicist, 1858-1947.
[8] Albert Einstein, German physicist, 1879-1955.

quantum theory, its energy cannot decrease: the photon will exist or it will be fully absorbed in a medium.

$$E_{photon} = h \cdot f = h \cdot \frac{c}{\lambda} \quad (J = kg \cdot m^2/s^2) \qquad \text{Eq. 2.1–2}$$

Being h the Planck Constant (6.626×10^{-34} m^2 kg / s), f (1/s) the frequency of the light, c (m/s) the speed of light in a vacuum and λ (m) the wavelength of light in the medium. This equation clearly displays that light of higher frequencies (UV) will have more energy than light of lower frequencies (IR).

So, if the energy of the photon must be conserved, this means that the photon will keep its frequency f, and so will do the light. This is an important consideration to understand the effect on the wavelength λ of the light when passing through a medium. The wavelength of the light, **λ,** defines the distance travelled by a photon in a given period of time across a certain medium, which is described by Eq. 2.1–3 for the vacuum, and generically by Eq. 2.1–4 for any given medium (combining Eq. 2.1–3 and Eq. 2.1–1). Therefore, the wavelength and the speed of the light depends on the medium (see eq. Eq. 2.1–1 and Eq. 2.1–5), but not its frequency, which remains constant for each propagating photon.

$$f = \frac{c}{\lambda_0} \quad (Hz = 1/s) \qquad \text{Eq. 2.1–3}$$

$$f = \frac{v}{\lambda} = \frac{c \cdot n}{\lambda_0} \quad (Hz = 1/s) \qquad \text{Eq. 2.1–4}$$

$$\lambda = \frac{\lambda_0}{n_{medium}} \quad (m) \qquad \text{Eq. 2.1–5}$$

Therefore, the main characteristics describing the light radiation are **intensity of the radiation** (number of photons), **frequency** (vibration of the photon), propagation direction (from the emitter to the observer) and **polarization**, which describes the spatial evolution of the electromagnetic wave across the propagation plane.

With regard to the intensity of the light, its interest is twofold, because sometimes, the interaction of the light with the matter requires achieving a certain level of excitation, which is achieved increasing the light intensity, as it is the case for instance in the fluorescence effect. Additionally, the ability of understanding the slight changes that may occur in the original light due to the properties of the target matter will require the acquisition of the resulting light intensity for post processing it.

There are two main measurement formats for quantifying the intensity of the light: the radiometric and the photometric domains

[63], and the different light sources or detectors may reference to one or both of them for specifying their properties. The photometric units were defined for emulating the response of the human eye, which was defined by the Commission of Illumination (CIE) in 1924, and therefore only covers the frequency range to which the humans are sensible.

Depending on the application, the specifications might be given using any of the following radiometric quantities: power, also called radiant flux and measured in watts (W), irradiance (measured in W/m^2), radiant intensity (measured in watts per steradian (W/sr), and radiance (measured in W/m^2 sr). The equivalent photometric quantities, which are listed in the Table 2.1–1, are based on the international system unit for luminous intensity, the candela (cd).

Table 2.1–1: Radiometric and Photometric quantities.

Quantity	Description	Diagram	Radiometric Unit	Photometric Unit
Flux	Total light emitted in all directions		Watts	Lumens
Intensity	$\frac{\text{Flux}}{\text{Solid Angle}}$	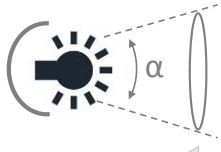	Watts/ steradian	Lumen/ steradian = candela
Irradiance	$\frac{\text{Flux}}{\text{Area}}$	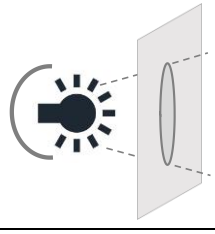	Watts/ $meter^2$	Lumen/ meter = LUX

Focusing on the light frequency, among the different sub–bands of the UV, visible and IR spectrums, this thesis will mainly focus on the long–wave UV (215 – 400 nm), on the whole visible range (400 – 800 nm), on the Near Infrared or NIR (800 – 1100 nm), on the Short-Wave Infrared or SWIR (1100–2500 nm), and the short leg of the Medium Infrared (MIR) that ranges up to the 5000 nm. It should be noted that matter may be responsive to certain frequencies of the light while remains inert to others, which is, actually, the base for the different principle of operation of the analysis of the matter through the light.

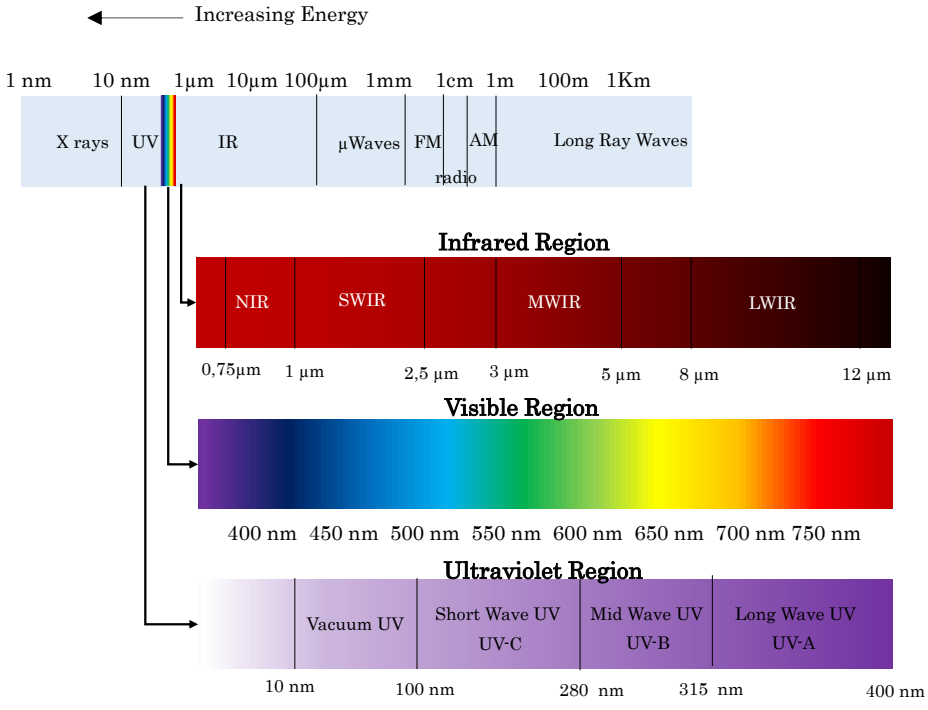

Regions not to scale

Figure 2.1-2: Detailed view of the frequency and wavelengths of the light of interest for the current work, UV, VIS and IR ranges

The polarization is also an important factor to take into account, since several optical settings require to work with polarized light, which may not be an evident effect and it has been depicted in Figure 2.1-3 (the Magnetic Field $\vec{B}$ has been omitted from the diagram). Light is considered as polarized if the Electric Field oscilates in one single direction (linearly polarized), or in spherical or elliptical plane (spherical or elliptical polarizations). Light is considered not polarized, when at any given moment, the $\vec{E}$ field gets to the observer in any direction.

Once the most important characteristics of the light have been summarized, the next section will describe the atomic and molecular processes that may occur when the matter is excited under a light of a given frequency band and intensity.

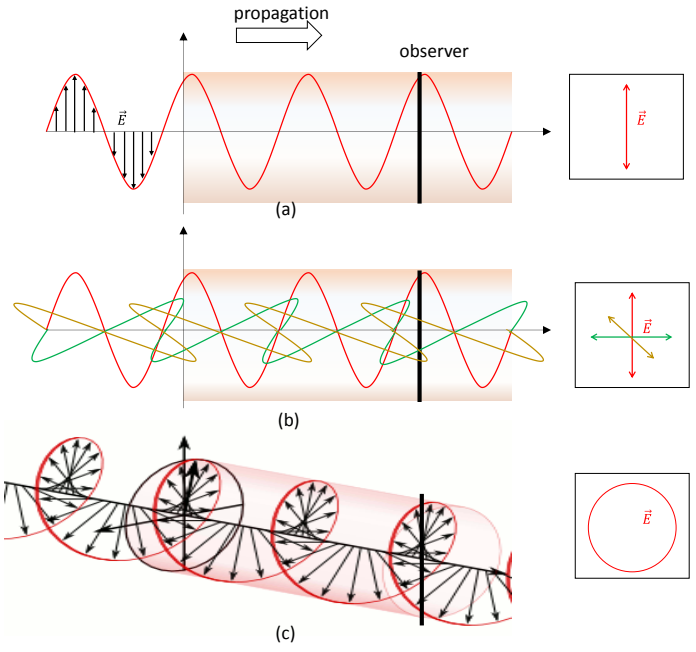

Figure 2.1-3 Polarized (a), not polarized (b), and spherically polarized (c) light. The frames in the left display the intensity pattern at the observer, after a certain observation period longer than the period of the wave. C diagram source Wikipedia.

2.1.2 Fundamental Physical Processes

When VIS, UV, or IR light impacts onto a surface or passes through a medium, unavoidable interaction occurs between the light and the electrons of the atoms and molecules of the material. Basically, this interaction entails two fundamental processes: first, the energy transferred by the photon on the electron and, second, as a charged particle, the excited electron radiates electromagnetic waves (light).

Steeping into a more detailed description, as the one provided by the quantum theory, the electron of an atom, a molecule, or an atomic lattice can absorb a photon and use its energy to jump into an energetically higher state. Equally, an electron can fall into a state of lower energy, with the energy difference being sent out as a photon (see Figure 2.1-4) [64].

It is important to stress that each part of the spectrum poses quantum energies (energy carried by a photon at a certain frequency) appropriate for exciting specific types of physical processes within the matter. As described by the quantum theory, the energy levels for all physical processes at atomic and molecular levels are quantized, and if the incident photon energy does not match with any available energy

level within the matter, then the material is considered transparent to that radiation. If the photon is absorbed but it is not able the translate electrons from the atom, then it is classified as non–ionizing radiation, and will normally just be converted in heat energy.

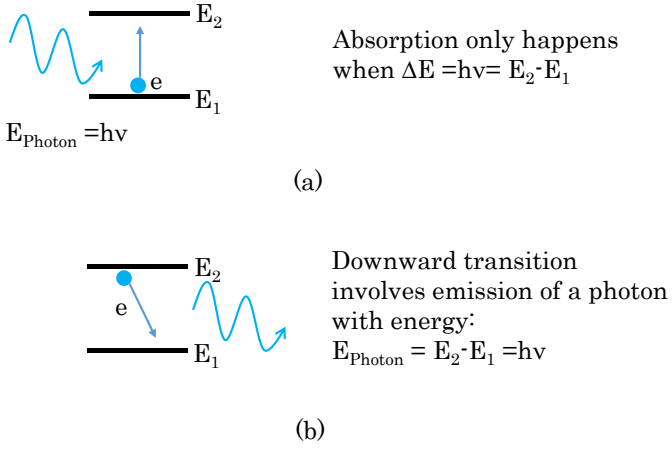

Figure 2.1-4 Photon absorption and photon emission process. (a) Absorption of a photon. Its energy is transferred to the atom and raises its electron shell onto a higher energetic state. This process is only possible when the photon's energy "fits" a gap in the atom's energy spectrum. (b) Spontaneous emission of a photon by an excited atom or molecule. Typically, this process occurs spontaneously, often only a few nanoseconds after the absorption of energy. The energy difference between the two atomic states determines the frequency (and, thus, the wavelength) of the departing photon. The direction of the emitted photon is random

For example, normally, the UV light and some part of the visible light, due to the energy of the photons (>2 eV) is able to generate Electron Level Changes. However, the quantum energy of infrared photons (is in the range 0.001 to 1.7 eV) matches the quantum states of molecular vibrations, which generates elastic absorption of the photon by the molecular bonds of the matter, resulting in a heating of the matter, but without affecting the electronic state.

Some of these physical processes happening between the photon and the atomic and molecular elements could be already introduced, even if they will be described in deep in the next sections.

For instance, the descriptions of the light scattering, absorption, fluorescence and Raman[9] scattering fit quite simply into this picture of elementary processes. Scattering means that a photon is absorbed and immediately emitted again. The absorbed and emitted energies remain the same and, as a result, it does not change the frequency of the light, but the phase and direction associated with the

[9] Chandrashekhara Venkata Raman, Indian physicist, 1888-1970.

photon that is emitted is random. The physical process underneath is called spontaneous emission that happens when, due to the absorption of the photon, an electron migrates from a lower to a higher energy level. However, the electron will not stay in the excited state perpetually, and may decay to a lower energy level, which is not occupied, after a specific time constant characterizing that transition. This transition releases a new photon without any external influence. Besides, the absorption of the light by the matter happens when, due to the absorption of a photon, an atom or a molecule migrates to a state of higher energy. The energy of the photon is converted into vibrations of the material that generates the already mentioned heating of the matter.

Particularities of these process could be found in the Fluorescence and Raman Scattering Principles. Fluorescence happens when the incident light is fully absorbed, transferring the material to an excited state. Then, after a certain resonance time, a part of the absorbed photon energy is released as the ejection of a new photon, which will show higher wavelength (less frequency) due to the energy loss between the absorption of the excitation photon and the emission of the new one, which again is converted into heat. On the other hand, even if due to Raman Effect a light with a different wavelength is emitted by the matter after being excited with a radiation, the processes underneath are completely different. The Raman radiation is due to a specific scattering process and it is independent from the excitation wavelength with a Raman emission peak keeping a constant separation from the excitation frequency, whereas in the fluorescence, the emission peak is anchored to a specific frequency due to the resonant nature of the process.

The abovementioned physic processes occurring when a radiation hits a material have been widely described during centuries by great scientist as Newton, Rayleigh, Fresnel, Planck, Einstein, etc. and even today, several studies continue trying to understand the elementals of the light. The latest example is found in the Higg's[10] boson theory, formulated in 1960 and demonstrated in 2013, this theory describes the light photon as a boson (type of fundamental particle) without any mass, demonstrating that, regardless all the scientific findings, the light nature still remains as a great unknown for the human being.

2.1.3 Light and Matter Interaction

Scientific domain of the optics summarizes in a set of fundamental principles the different effects generated by the

[10] Peter Higgs, British physicist, 1929-

processes mentioned above (see Figure 2.1-5 and Figure 2.1-6 for an outline of most common effects). These definitions describe in a very simple manner the effects of the light–matter interaction in the properties of the original light rays. Moreover, these basic optical principles are the base for developing most of the detection and sensing methods described later. The forthcoming sections will review the different fundamental processes involved in the light and matter interaction and how these effects can be used for developing photonic sensors.

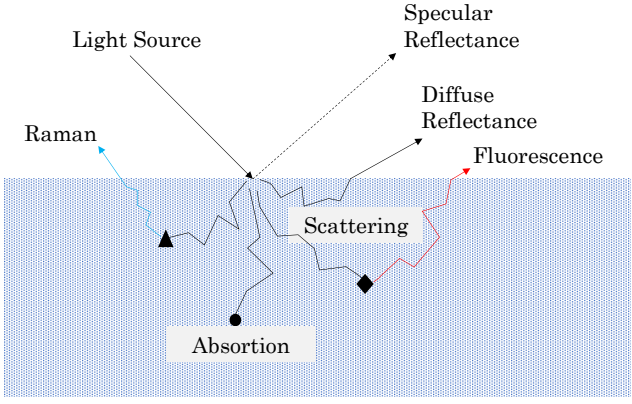

Figure 2.1-5: Summary of the different processes happened after the interaction between an incident light ray and a sample material.

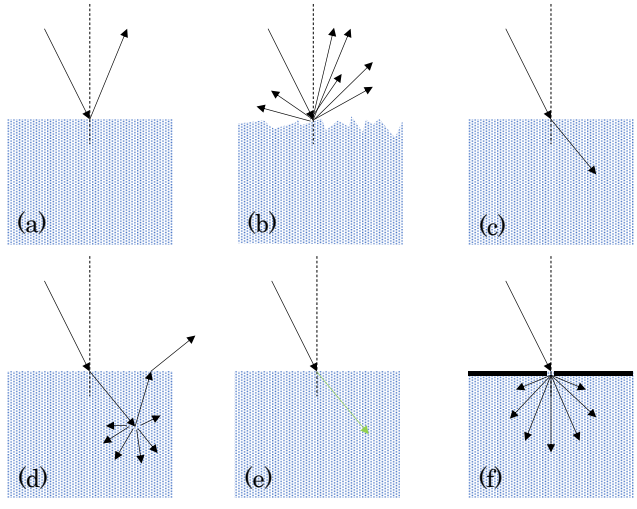

Figure 2.1-6: Some interactions of white light with surfaces and media. (a) specular reflection, (b) diffuse surface reflection, (c) refraction, (d) scattering and diffuse reflection, (e) absorption without scattering, and (f) diffraction.

2.1.4 Transparency

Transparency is a property of a material that allows the light passing through it almost without interaction. Because, even assuming the perfect transparent material, with no absorption or scattering happening, the light suffers an important interaction while crossing the molecular structure of the media, effectively reducing the velocity of the photon. This slowing down is quantified as the refractive index n_{medium} that was mentioned at the beginning of the chapter, and describes the relation of the light speed in vacuum or in a certain medium. Typical examples of refractive indexes are, $n_{vacuum} = 1$, $n_{air} = 1.000293$, $n_{water} = 1.33$, $n_{glass} = 1.458$ or $n_{oil} = 1.4$.

The availability of transparent elements is crucial for the development of photonics-based in–line inspection systems. These transparent mediums allow for instance the fluid sample confinement without impacting in the chemo–physical properties to measure. Traditional cuvettes for absorbance measurements are clear example of the use of transparent means. However, it is important to highlight that a medium is always transparent only to a certain part of the electromagnetic spectrum, and is determined by the dependency of the refractive index with the frequency of the incoming ray (see section 2.1.4.2 Dispersion) and by the absorbance of the material to the different energies of the incident photons (see section 2.1.8 Absorbance).

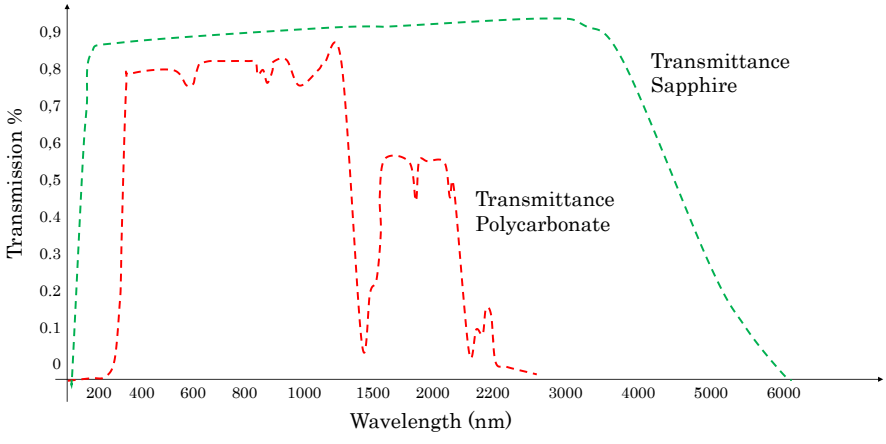

Figure 2.1-7: Approximate Transmittance spectrums of the Sapphire glass and Polycarbonate plate.

Therefore, the selection of the right non–interfering material should be taken once the light bands of interest are defined (see Figure 2.1-7). For instance, plastics such as PS (Polystyrene), PMMA (Polymethyl methacrylate) or Polycarbonate (PC) offer a decent transparency in the visible range, but are not transparent in the UV

or NIR bands. Consequently, if we need to deliver a solution for working in the UV or NIR bands, alternative materials should be used, being the Quartz (SiO2), Sapphire (Al_2O_3) or the Fuzzed Silica good candidates. Materials and low-cost configuration alternatives will be later discussed in section 3.3.3 Wettable interfaces.

2.1.5 Refraction, Reflection and Dispersion

The refraction and reflection of light is the basis for developing several optic elements that are key components for the design of fluid sensors. Additionally, the refraction and reflection laws describe how the emitted light beam travels inside the target matter, and gets to the detector.

When a light ray meets an interface between two materials with different refractive indexes, both reflection and refraction will occur. The proportion of reflected or refracted light will depend on the ratio of the refractive indices of the two media, the incidence angle of the light and its frequency spectrum. This behavior is described by the Snell[11] or Descartes[12] law, which is a further elaboration of the Fermat's[13] principle that describes that the light will always follow the path of least time, which is, evidently, the path with the shortest distance. This assumption is taken to describe the path followed by a ray when it is reflected by a surface, as seen in Figure 2.1-8:

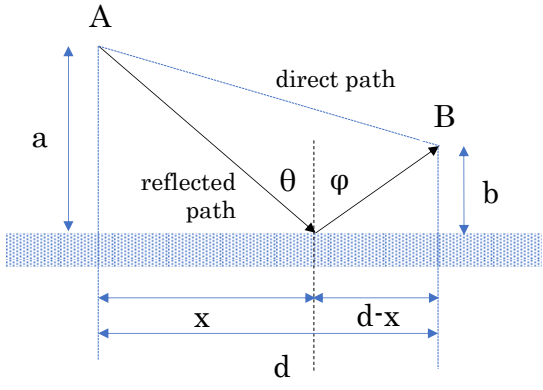

Figure 2.1-8: The reflection of a light ray.

The reflected path length, L, to get from the source point A to the destination point B is:

$$L = \sqrt{a^2 + x^2} + \sqrt{b^2 + (d - x)^2} \qquad \text{Eq. 2.1–6}$$

[11] Willebrord Snellius, Snell, Dutch astronomer and mathematician, 1580–1626.

[12] René Descartes, French mathematician and philosopher, 1596- 1650.

[13] Pierre de Fermat, French mathematician, 1607- 1665.

Since the light ray remains within the same medium across all the path, its speed will be constant. Therefore, the path with the shortest propagation time is directly the minimum distance path, which can be mathematically calculated equaling to zero the derivative of L with respect to x.

$$\frac{dL}{dx} = \frac{1}{2}\frac{2x}{\sqrt{a^2 + x^2}} + \frac{1}{2}\frac{2(d-x)(-1)}{\sqrt{b^2 + (d-x)^2}} = 0 \qquad \text{Eq. 2.1–7}$$

then

$$\frac{x}{\sqrt{a^2 + x^2}} = \frac{(d-x)}{\sqrt{b^2 + (d-x)^2}} \qquad \text{Eq. 2.1–8}$$

switching to trigonometric domain, Eq. 2.1–8 could be described as in the Eq. 2.1–9, which defines the **Law of Reflection**

$$\sin(\theta) = \sin(\varphi) \qquad \text{Eq. 2.1–9}$$

Now, let's take the problem one step further to describe the path length of the light ray amidst two mediums. In this case, the derivative of the time needed by the ray to get from source point A to the destination B ($t = L/v$), and considering the speed of light in the two mediums as function of the index of refraction ($v = c/n$).

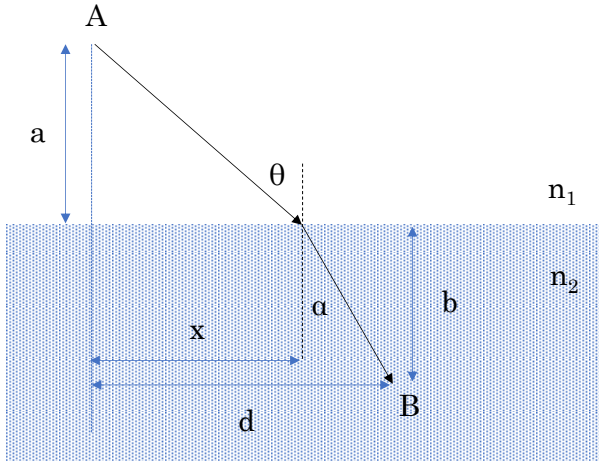

Figure 2.1-9: The refraction of a light ray across two mediums.

$$t = \frac{\sqrt{a^2 + x^2}}{v} + \frac{\sqrt{b^2 + (d-x)^2}}{v'} \qquad \text{Eq. 2.1–10}$$

$$\frac{dt}{dx} = \frac{1}{v}\frac{x}{\sqrt{a^2 + x^2}} - \frac{1}{v'}\frac{(d-x)}{\sqrt{b^2 + (d-x)^2}} = 0 \qquad \text{Eq. 2.1–11}$$

$$0 = \frac{1}{v}\sin(\theta_1) - \frac{1}{v'}\sin(\theta_2) \qquad \text{Eq. 2.1–12}$$

$$\frac{n_1}{n_2} = \frac{\sin(\theta_2)}{\sin(\theta_1)} \qquad \text{Eq. 2.1–13}$$

Which describes the Snell's Law for refraction of light across two mediums.

However, asides the mathematical definition for the refraction, this effect could be also described from the consequence of the differing speeds of light in two media. As already mentioned, the energy, hence, the frequency of the photon vibration must remain the same at the both sides of the interface. Therefore, inside the material with slower light velocity, the wavelength is shortened proportionately because the wave front is compressed at the interface. The Figure 2.1-10 demonstrates that the continuity of the light beam from a fast medium (smaller index of refraction) to a slow one is only possible with the bending of the rays.

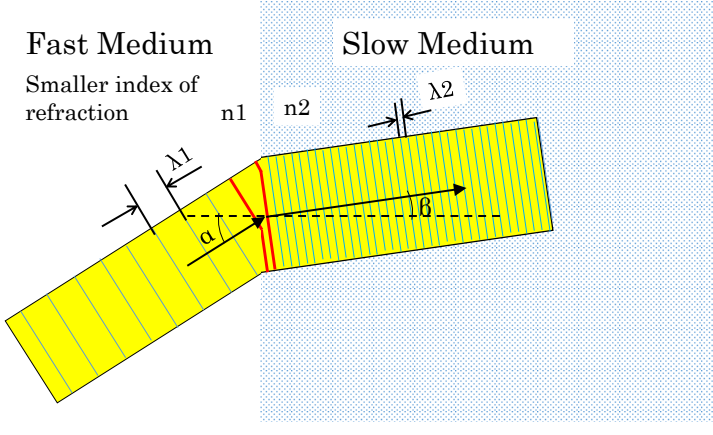

Figure 2.1-10: Graphical demonstration of wavelength shortening when a light radiation propagates from a medium with higher index of refraction to a material with the smaller one. Bottom part of incident rays reaches the slow medium first and is slowed down first, which rotates the ray towards the normal line between the two mediums

The ratio of the wavelength at both sides of interface is described with the refraction indexes of the materials (n_1 and n_2). From previous equations Eq. 2.1–3 to Eq. 2.1–5 the ratio is defined as:

$$\frac{\lambda_1}{\lambda_2} = \frac{n_2}{n_1} \qquad \text{Eq. 2.1–14}$$

The importance of the reflection and refraction laws is foremost since they describe the propagation of the light across not only the sample under test, but also through the different means and materials that constitute the sensor (protective windows, micromechanical structures, etc.)

2.1.5.1 Reflectance and transmittance

In addition to the changes occurring in the light wavelength when the propagating radiation meets a different medium, it is interesting to understand which portion of the light (number of photons) will be reflected and which will be refracted at the interface. This ratio was described by Fresnel, who defined the fraction of the incident power that is reflected from the interface as the Reflectance, R, and the fraction that is refracted as the transmittance, T. As described by Fresnel, these parameters are highly dependent on the electromagnetic properties of the two interfacing materials and, also, on the polarization of the incident light (parallel or perpendicular to the plane of incidence). For instance, the Reflectance for the perpendicularly polarized incident light, also defined as s–polarized light, is defined in Eq. 2.1–15, where μ_1, μ_2 and ε_1, ε_2 are the magnetic and electric permeability and of the two materials at the frequency of the light wave, and θ_i and θ_t are the angles of the incident and refracted rays respectively.

$$R = \left| \frac{\sqrt{\frac{\mu_2}{\epsilon_2}} \cdot \cos\theta_i - \sqrt{\frac{\mu_1}{\epsilon_1}} \cdot \cos\theta_t}{\sqrt{\frac{\mu_2}{\epsilon_2}} \cdot \cos\theta_i + \sqrt{\frac{\mu_1}{\epsilon_1}} \cdot \cos\theta_t} \right|^2 \qquad \text{Eq. 2.1–15}$$

Additionally, due to the conservation of energy, the transmittance is defined as:

$$T = 1 - R \qquad \text{Eq. 2.1–16}$$

The Reflectance and Transmittance are terms referenced all over the thesis. Not only because they are basic physical properties of the matter in concerning its interaction with the light (and reviewed in section 2.1.8), but because the transmission or reflection also refers to different setups for inspection a certain material and configuring photonic sensors as described in section 3.2.1.

2.1.5.2 Dispersion

Due to the different energy carried by photons at different frequencies, the material does no respond equally to all the incident light. This generates that refractive index of a transparent medium is slightly dependent on the wavelength (see for instance Figure 2.1-11), and the direct effect of this property is that not all the rays of a light beam will be refracted in the same direction. The most common example of the consequences of the dispersion happens when the white light incident to a prism is separated into a color spectrum.

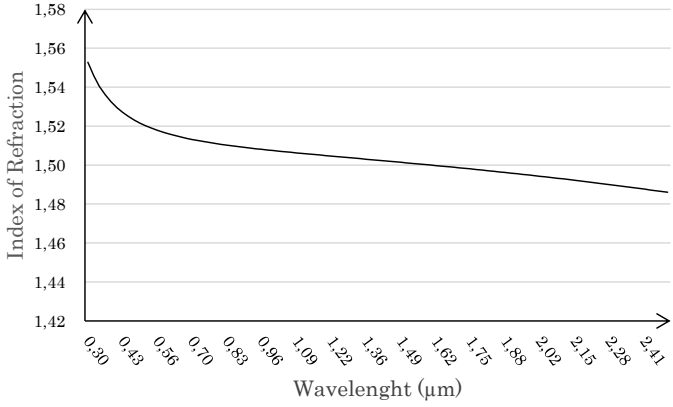

Figure 2.1-11: Dependency of the index of refraction with the light wavelength for the N–BK7 Glass (data source: Scott AG.)

The effect of the dispersion in optical system is also referred as the chromatic aberration, which becomes evident in lens based settings (see Figure 2.1-12) and should be taken into consideration when deciding the plane for placing the light detector.

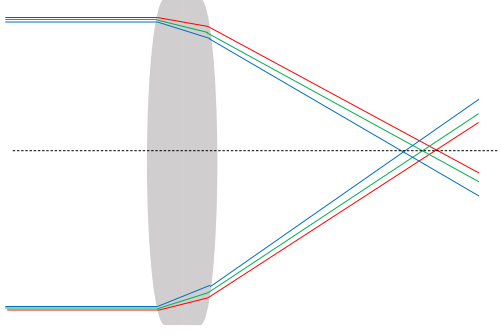

Figure 2.1-12: Chromatic aberration. Rays of different wavelength do not converge in the same point.

Actually, due to the significant impact of the material dispersion in optical setups, transparent materials as glasses reference this effect with the Abbe[14] number, or V–number, which quantifies the variation of refractive index versus wavelength, as:

[14] Ernst Abbe (1840–1905), German physicist.

$$V_D = \frac{n_D - 1}{n_F - n_C} \qquad \text{Eq. 2.1–17}$$

Being, n_D, n_F and n_C the index of refraction of the material at the wavelengths of the Fraunhofer[15] D–, F– and C– lines, which correspond to 589.3 nm, 486.1 nm and 656.3 nm respectively. Therefore, the higher the Abbe number, the less chromatic dispersion is expected for the material. For instance, the N–BK7 glass offers a V_{D-BK7}= 64.17, while for the PC plastics it drops down to V_{D-PC} = 27.86, showing that the plastic option would negatively contribute to the optical setting with a higher chromatic aberration.

Therefore, the variation of the index of refraction with the frequency of the light is an optical property that may help us creating components (prisms, gratings, mono-chromators, filters, etc.) or degrade the performance (chromatic dispersion, non-linearities, etc.) but definitively it is a factor to consider while designing an optical setup. Note that, according to the equations Eq. 2.1–9 and Eq. 2.1–13, the refraction of the light rays is affected by n, and thus, by the dispersion, while the reflection does not.

2.1.5.3 Specular Reflection, Diffuse Reflection and Internal Diffuse Reflection

So far, different physical and chemical processes have been used for describing the behavior of the light amidst different mediums. However, the roughness of the surface where the different materials interface is very important parameter that highly modifies the ideal theories presented for ray tracing. Thus, the rays reflected at a smooth or polished surface generate a sharp image of the mirrored object, which is known as specular reflection. On the other hand, rough, uneven or convoluted surfaces will reflect the incoming rays in arbitrary directions and generate a diffuse reflection.

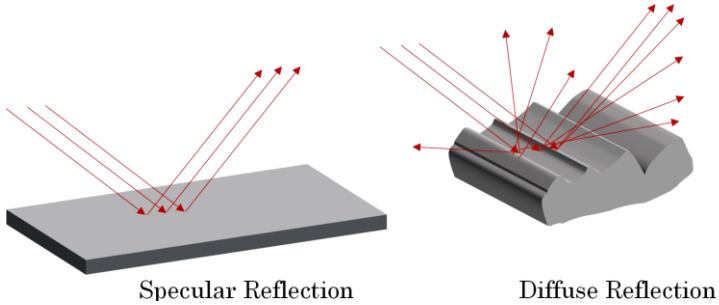

Figure 2.1-13: Difference between the two types of reflection happening in the material surface when irradiated with a light beam (a) specular reflection and (b) surface diffuse reflection.

[15] Joseph von Fraunhofer, German physicist, 1787–1826.

Sometimes, the diffuse reflection is confused with the diffused light coming back from the sample due to the internal reflections happening at the material, which is the fundament where the diffuse reflection spectroscopy is based [65]. The reason is that for a spectroscopic analysis, an effective interaction between the light and the sample should take place, and this is only possible if the light is able to penetrate, at least slightly, in the material. Therefore, true diffuse reflection is the result of light penetration into one or more particles and its diffusion in the material. This component of the radiation also exits the material at any direction, however, since it has gone through the particles, it holds information about the absorption properties of the sample. Understanding the diffuse reflectance process is fundamental for setting up spectroscopic sensors for solids or very opaque fluids, where the transmitted radiation is not sufficient for performing any processing.

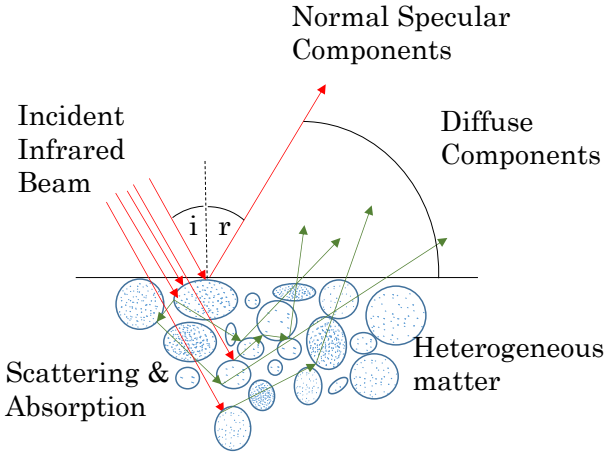

Figure 2.1-14: Mechanisms generating the reflectance spectrum of a sample.

2.1.5.4 Critical Angle and Total Internal Reflection

When a ray of light arrives to an interface with a material of a lesser refraction index, the refracted ray bends away from the normal, being the exit angle greater than the angle of incidence. The reflection happening in this case is called internal reflection. From the Snell's law, it can be observed that the exit angle will eventually get to 90º for a certain angle of incidence θ_C, which is known as the Critical Angle, and generates that no light is refracted and all the energy is internally reflected (see Figure 2.1-15). Beyond this critical angle, the incident radiation will be confined in the medium with higher index of refraction due to the so–called total internal reflection effect.

$$\theta_c = \arcsin\left(\frac{n_2}{n_1}\right) \qquad \text{Eq. 2.1–18}$$

Additionally, there is an interesting effect happening when the light radiation undergoes a total internal reflection process, which is

the generation of an evanescent wave in the vicinity of the incident point of the light ray. The physical explanation for the existence of the evanescent wave is that the electric and magnetic cannot be discontinuous at a boundary, as would be the case if there was no evanescent wave field.

These are very important effect since no energy is loss, and techniques based in the total internal reflection are the base for several optic components and processes as the light propagation within the fiber optics, for the polarizing prisms or for configuring different measurement setups as the Attenuated Total Reflectance sensors.

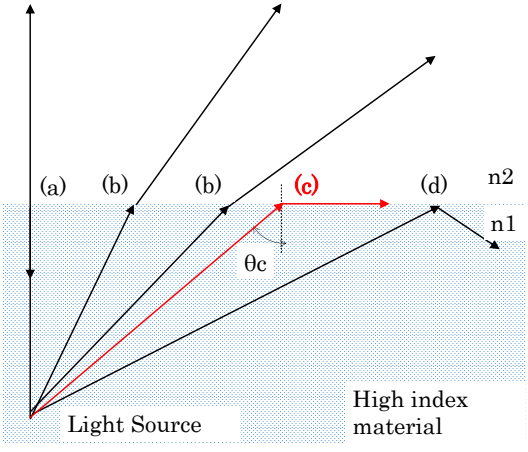

Figure 2.1-15: Diagram showing the different potential reflection effects depending on the angle of incidence. (a) Rays normal to the surface are not bent but a part of the radiation goes back parallel to the normal. (b) non-normal incident rays are reflected and transmitted, (c) displays the situation happening when a radiation hits a medium with lower index of refraction and if the angle meets the critical angle's definition θc. (d) shows that light rays incident at any angle greater that the θc will be totally reflected.

2.1.6 Light Diffraction

Diffraction is described as the apparent bending of the light when it hits an obstacle that is similar in size to its wavelength, or the spreading of the light when it passes through a sufficiently small opening. The proportion between the wavelength of the radiation and the size of the opening determines how much the rays will bend.

Optical effects resulting from diffraction are produced through the interference of light waves, as it is defined by Huygens–Fresnel principle, and exemplified with the single and double slit Young's experiments. This interference basically describes that all the new waveforms generated across the small objects or slits, interact with each other, resulting on higher (constructive interference) or darker

(destructive interference) intensity areas along the wave front propagation.

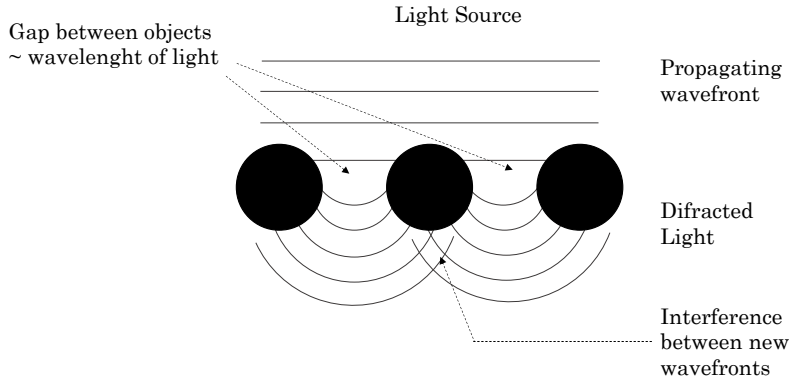

Figure 2.1-16: Example of diffraction

Both, Fresnel and Fraunhofer, described the diffraction effects from different approaches. Both scientist achieved to mathematical approximations for describing the light intensity fringes generated by diffracted light under different setups, such as the single or multiple slits, the light diffraction at an opaque edge, or the diffraction happening at circular apertures.

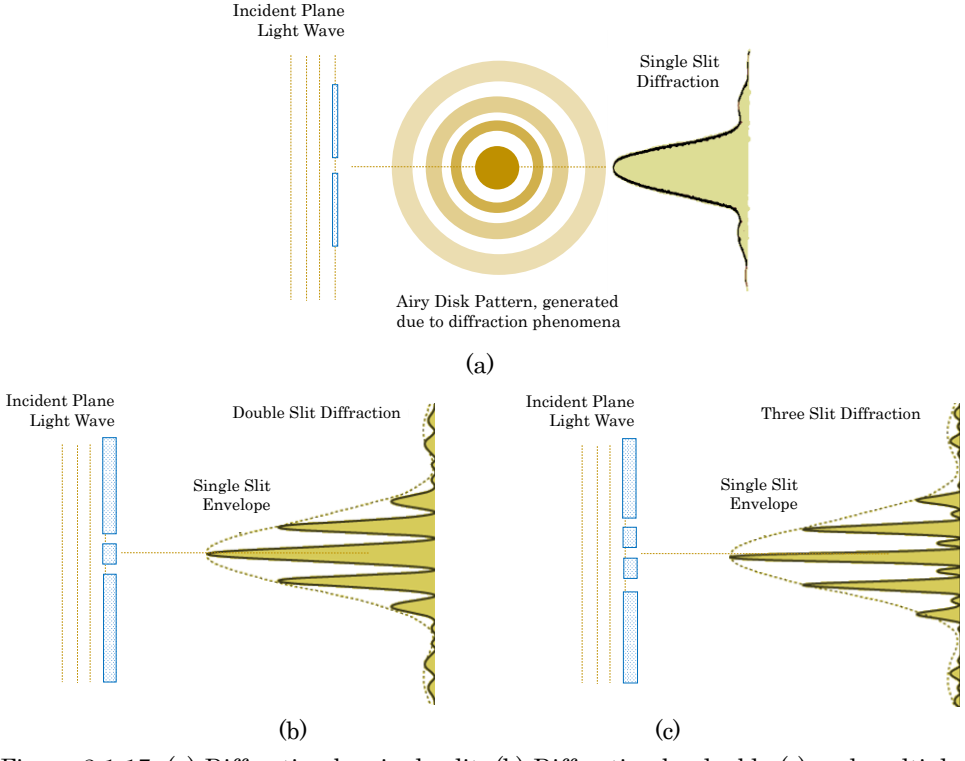

Figure 2.1-17: (a) Diffraction by single slit, (b) Diffraction by double (c) and multiple slits.

Actually, the diffraction generated by a circular aperture takes special importance due to its impact on the limit of resolution of imaging systems. The light from a point source passing through a tiny circular aperture, instead of generating a bright dot image, it produces a diffuse circular disk surrounded by blurred concentric rings, known as Airy's[16] disk. This effect limits the effectivity of an optical system to discriminate between two near objects even if both of them were perfectly focused. This limitation is quantified in terms of the Rayleigh criterion, which defines that an imaging system is limited by diffraction when the first diffraction minimum of the image of one object coincides with the maximum of the adjacent object (see Figure 2.1-18). This is an important consideration when defining the resolution limit of an in-line microscopic sensor.

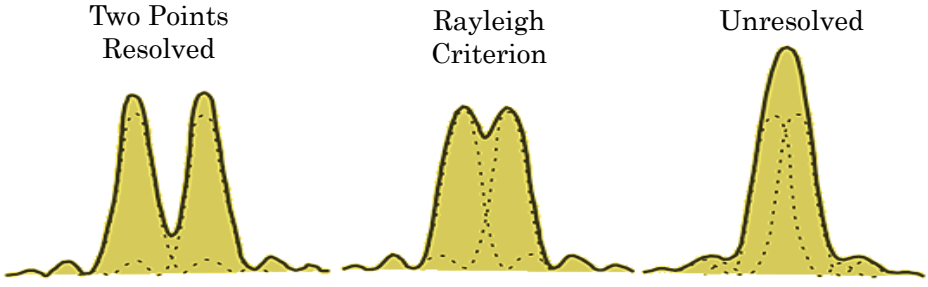

Figure 2.1-18: Description of Rayleigh criterion for resolving two adjacent points.

2.1.7 Light Scattering in Media

Scattering is the physical process describing the change in the trajectory of the light rays due to the non–uniformities in the propagation medium. Those non–uniformities basically represent scattering centers of variant refractive index that interact with the incident photon and modify its propagating direction randomly.

Particles, bubbles, droplets, molecules, dust, etc. are examples of the non–uniformities, and depending on the relation between their size and the radiation wavelength, one of the different predominant scattering processes will take place. This relation is described by the size parameter α, which is defined in Eq. 2.1–19, where D_P is the circumference of the particle and λ the wavelength of the incident radiation.

$$\alpha = \frac{\pi D_p}{\lambda} \qquad \text{Eq. 2.1–19}$$

Objects with $\alpha \gg 1$ act directly as geometric shapes, scattering the light according to their projected area. Around $\alpha \simeq 1$ Mie scattering happens, generating interference effects through phase variations over the object's surface. Rayleigh scattering will take place

[16] George Biddell Airy, British astronomer and mathematician, 1801-1892.

when the scattering particle is very small ($\alpha \ll 1$, with a particle size < 1 /10 wavelength) and the whole surface re–radiates with the same phase.

As mentioned in section 2.1.2, Rayleigh[17] scattering comes from an elastic process due the electric polarizability of particles. The energy of the incoming photon excites the state of the molecule to a higher level, but it almost immediately goes back to the original state, releasing the excess of energy in a form of a new photon, with exactly the same energy as the original one.

The phase and direction of the generated photon is, however, completely random, and normally it is different to the incoming trajectory, but the whole surface of the molecule reradiates with the same phase. However, as the molecules are distributed unevenly within the medium that the light is crossing, the scattered light reaches at a particular point with a random collection of phases and its resulting intensity is described as in Eq. 2.1–20.

$$I = I_0 \frac{8\pi^4 N\alpha^2}{\lambda^4 R^2} (1 - \cos^2\theta) \qquad \text{Eq. 2.1–20}$$

Where I_0 is the light intensity before the interaction with the objects, N represents the number of scatterers (e.g. molecules), α is the polarizability of the objects, and R is the distance from the scattered to the point where intensity I is being measured. The strong dependence of Rayleigh scattering with the wavelength of the incoming radiation (inversely proportional to λ^4) enhances the intensity of shorter wavelengths.

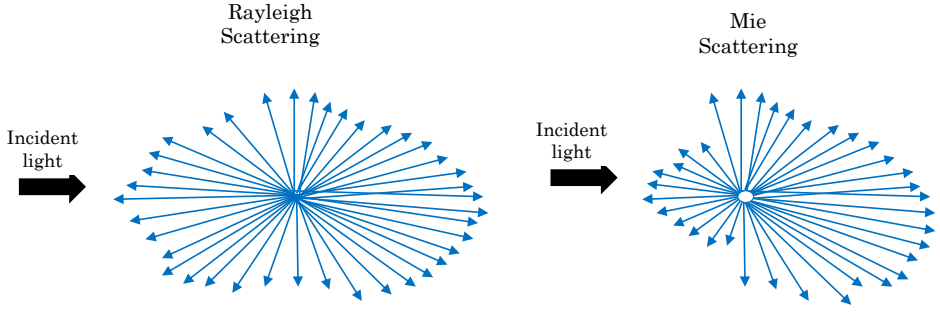

Figure 2.1-19: Graphical representation of Rayleigh and Mie scattering effect.

For larger particle diameters, scattering by spheres larger than the Rayleigh range is therefore usually known as Mie Scattering. In the Mie regime, the shape of the scattering center becomes much more significant in scattering shape, generating an antenna lobe like pattern, with a lobe directivity and intensity dependent on the particle size. However, notice that Mie scattering is not affected by the wavelength. If the general formulae for the Rayleigh scattering is

[17] John William Strutt, Third Rayleigh Baron, British physicist, 1842-1919.

taken (Eq. 2.1–21), the effect of λ is compensated with the particle diameter d, which for Mie case should be much larger than the wavelength (d>> λ).

$$I = I_0 \left(\frac{2\pi}{\lambda}\right)^4 \frac{(1-\cos^2\theta)}{2R^2} \left(\frac{n^2-1}{n^2+2}\right)^2 \left(\frac{d}{2}\right)^6 \qquad \text{Eq. 2.1–21}$$

The scattering is a process of special relevance in sensor design, because in fluids and solids, absorption and scatter happen together, both contributing to the reduction of light transmission through the material. Additionally, the scattering favors the photon propagation and absorption across the sample, redirecting unevenly the incident light radiation to potentially absorbent molecules.

2.1.8 Absorption

Absorption is the physical process describing the energy transference between a photon with a certain amount of energy that matches the quantum energy gap between the initial and final states of a material that the photon is passing through.

Therefore, the absorption spectrum of a certain material will show the fraction of incident radiation that is absorbed by the material over a range of frequencies. These frequencies, known as absorption lines, mainly depend on the molecular and atomic structure of the sample. However, the interaction between the molecules in the sample, the crystal structure and some other environmental conditions such as temperature, pressure or electromagnetic field also impact on the absorption lines happening in a material [66][67]. Notice that, atomic absorption lines have widths typically below 0.05 nm, and Molecular absorption transitions in the visible and ultraviolet span ~10 – 50 nm [68]

Normally, the absorption lines are divided by the nature of the quantum mechanical change that the photon induces in the atoms or molecules. Additionally, these different mechanical processes are bound to different wavelengths of the electromagnetic spectrum, due to the different energy carried by the photons.

Thus, Rotational lines are those absorption lines at which the molecules suffer a change in their rotational state after being excited by a radiation of the microwave spectral region. X–ray absorption, due to the higher energy of this short of radiation, induce deeper changes in the matter exciting electrons of the inner shells of the atoms. Electronic lines occur when a change in the electronic state of the atom or molecule is generated by a photon, which normally correspond to visible or ultraviolet region. In addition, vibrational lines relate to changes in the vibrational state of the molecule and are normally found in the infrared region. The changes generated in the matter by

the incident radiation due to the absorption process, are also classified as ionizing or non–ionizing, being the limit of ionization around the highest energy ultraviolet frequencies. The ionization alters the molecular or atomic structure of the material as it is able to extract electrons from their orbital generating ions, as it happens with the X–ray absorption. On the other hand, in the non–ionizing absorption, the atoms and molecules remain intact as there is a strong tendency for them to return to the ground state energy after a short period of time, releasing the absorbed energy in form of heat (due to random molecular motion or vibration) or emitting a new photon in the same frequency as the original one.

Quantifying the vibrational and electronic lines of chemical samples allows the determination of an unknown solution concentration, the monitoring of reaction progress as a function of time, and many other quantitative uses. For the specific case of the current thesis domain, the absorption happening at UV–Visible and Infrared regions are the most interesting ones for developing cost effective sensors thanks to the huge availability of emitters and detectors working in these frequency ranges.

Therefore, narrowing down to the UV–VIS range, the absorption of a UV–VIS photon by a compound generates an electron transition from lower energy orbital to higher energy orbital, this means that the energy is electronically transferred from the photon to the molecular structure.

The energy of absorbed photon is equal to the energy difference between the highest energy electronic occupied orbital (E_{OO}) and the closest unoccupied orbital (E_{UO}), or equivalently, the energy difference between the ground state and the excited state. Mathematically, this relationship is expressed by Eq. 2.1–22.

$$E_{light} = h \cdot \nu_{light} = \frac{h \cdot c}{\lambda_{light}} = \Delta E = E_{U0} - E_{00} \qquad \text{Eq. 2.1–22}$$

The wavelength of light required to promote an electron from the ground to the excited state is specific to each chemical, and this property is used for identifying the matter with UV–VIS spectroscopy.

The vibrational lines happen when the frequency of the photon matches the vibrational frequencies of the atoms of the chemical compound, and it is normally generated by IR radiation. In that case, the energy of the photon is transferred elastically to the material and it start to vibrate, compressing and stretching the chemical bond lengths and angles. Unlike in UV–VIS range, in this case, the electrons are not able to promote to a higher-level due to the lack of energy of the IR radiation, and the molecule remains in some intermediate excitation states known as vibrational states.

The bonds that keep atoms molecules together are not rigid, and they vibrate at certain frequencies that correspond to their vibrational states. Therefore, the vibrating bond process induced by IR photon is analogous to the physical model of a vibrating spring system, which is described by the Hooke's law. Considering the bond and the attached atoms as a spring with two masses connected, the Eq. 2.1–23 and Eq. 2.1–24 describes how the vibration frequency v of the system varies depending on the properties of the system.

$$v = \frac{1}{2x}\sqrt{\frac{k}{\mu}} \qquad \text{Eq. 2.1–23}$$

$$\mu = \frac{m_1 \cdot m_2}{m_1 + m_2} \qquad \text{Eq. 2.1–24}$$

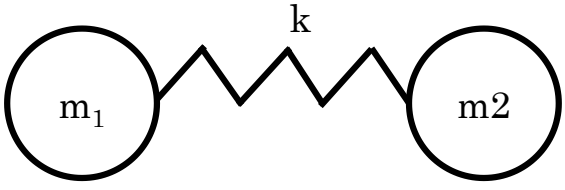

Figure 2.1-20: Diagram of elastically bonded masses

Where m_1 and m_2 represent the masses, k is the force constant of the spring and x is the distance between masses, v is the frequency and μ is the reduced mass [69]. The equivalence to the atomic system comes considering the bond as the k value, the x is the distance between the atomic nuclei, and evidently, the atomic masses represent the masses at the two ends of the spring. In this situation, the stronger bonds (larger k values) will increase the frequency at which the atomic system vibrates. Besides, for heavier atoms attached (larger m value), frequency decreases.

These frequencies represent the frequencies at which the atomic system will resonate with the incident photons absorving their energy and converting it to vibration forces; and again, bond strength is directly related to frequency. and more radiation energy (a higher frequency) will be required to excite a vibration on a stronger bond. Consequently, the combination of masses and bonds of mollecules will show unique vibrational frequencies, that are used by the IR spectroscopy to identify the type of bond between atoms and accordingly, the functional groups.

Additionally, the excitation of complex mollecules where several different possible bond vibrations may happen, implies the presence of several vibrational lines as well. This means that the identification of a specific molecule could be accomplished through the

study of the IR absorption spectrum, where the combination of the different vibration lines represents the unique fingerprint of the molecule, and is the base for several in-line sensors.

2.1.9 Light emission, Fluorescence

Fluorescence is a result of a three–stage process that occurs in some molecules called fluorescent dyes or fluorophores. The first stage is known as the Excitation, where a photon from a source is absorbed by the die, creating an excited electronic state S_1'. Next, a rapid decay to a lower quantum state follows, known as emitting energy level S_1 follows. This energy downgrade is the result of the interaction between the excited electron with the crystal lattice or some collisional process. The third stage is called Emission and occurs when a photon is emitted while the dye returns to the ground state S_0. Note that, due to the energy loss happened when the excited electron is transferred to the intermediate lower quantum state S1, the energy of the emitted photon must be lower than the energy from incident one, which implies equivalently an emission of longer wavelength (see Eq. 2.1–21).

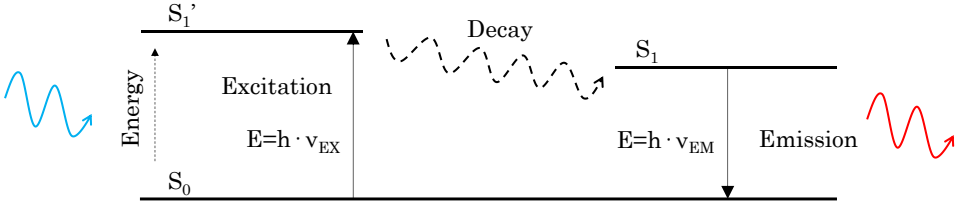

Figure 2.1-21: Basic diagram describing the fluorescence emission, at which, the emitted photon delivers lower energy than the excitation one.

The difference in energy between the emitted and the absorbed photons is shown as a shift between the excitation and the emission spectra of the dye and is called Stokes Shift. Notice that, a large Stokes Shift will allow a good spectral separation of excitation and emission spectra, and thus, a simpler fluorescent optical setup in sensors. Actually, one of the problems of molecules fluorescing in the range of NIR is that typically they have an overlap between excitation and emission and small stokes shift, hindering their use in simple settings, even if currently new NIR fluorophore dyes are being developed with larger stokes shifts [70].

The atomic sub processes involved in the fluorescent emission are summarized in the Jablonski[18] diagram (Figure 2.1-22). The different states described in the diagram include the non–radiative

[18] Aleksander Jabłoński, Polish physicist, 1898-1980.

processes by which the energy of the excited electron moves down to intermediated quantum states. These non–radiative processes include the internal conversion and the vibrational relaxation, which is followed by the fluorescent emission, or the intersystem crossing that can give rise to the phosphorescence.

The thin horizontal lines around the S_0, S_1 and S_1' depicted above represent vibrational/rotational sublevels at which the electrons of the molecules may stick after the excitation. This basically implies that the atomic absorption and emission spectra are broadened by molecular vibronic states to excitation and emission bands. The practical effect of this process is that the molecules may be excited by radiation of different wavelength, but the emission only occurs around a specific frequency band; being just the emission power dependent on the excitation wavelength.

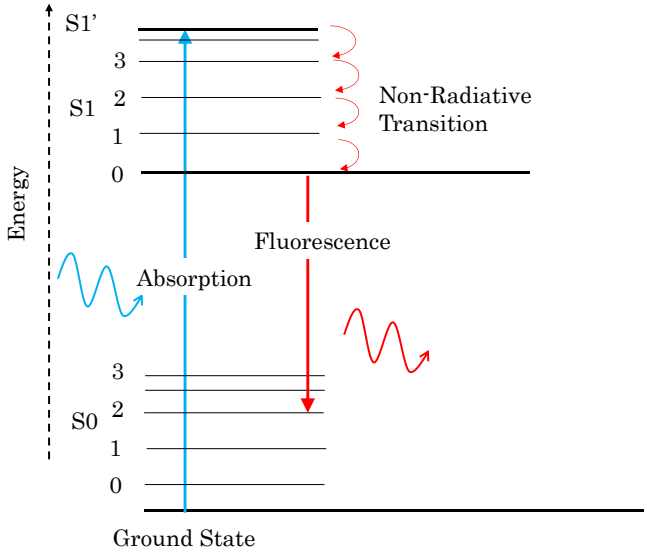

Figure 2.1-22: Jablonski diagram (partial representation), showing the vibrational sublevels between the S_0, S_1 and S_1'.

Additionally, note that not all the incident photos are able to excite the sample to its fluorescent levels. The probability that a photon will be absorbed varies with wavelength (energy). The number of photons fluoresced relative to the number absorbed is the quantum efficiency (see Eq. 2.1–25), indeed, the higher the absorption and quantum efficiency, the brighter the fluorescence.

$$\emptyset_F = \frac{K_{rad}}{K_{rad}+K_{non-rad}} = \frac{\tau_F}{\tau_{rad}} \qquad \text{Eq. 2.1–25}$$

Where k_{rad} is the radiative decay rate, $k_{non-rad}$ is sum of all non–radiative decay rates, τ_F is the observed excited state lifetime (fluorescence lifetime) and τ_{rad} is the radiative lifetime.

However, notice that even if quantum yield may fall between 0.1 to 0.9 [71], meaning that up to 90% of emitted photons shall generate a fluorescent signal, the effective readings in real setups in far from that ration. For instance, an experimental setup results using Cy5.5 fluorescent dye (Amersham, GE Healthcare), with a $\emptyset_F$=0.28, after setting the emitter (VCSEL laser), receivers (CMOS photo–detector) and filters (excitation and emission) the net result in terms of injected intensity over the received one displayed a disappointing 10^{-6} ratio, far from the 0.28 claimed by the quantum yield [72].

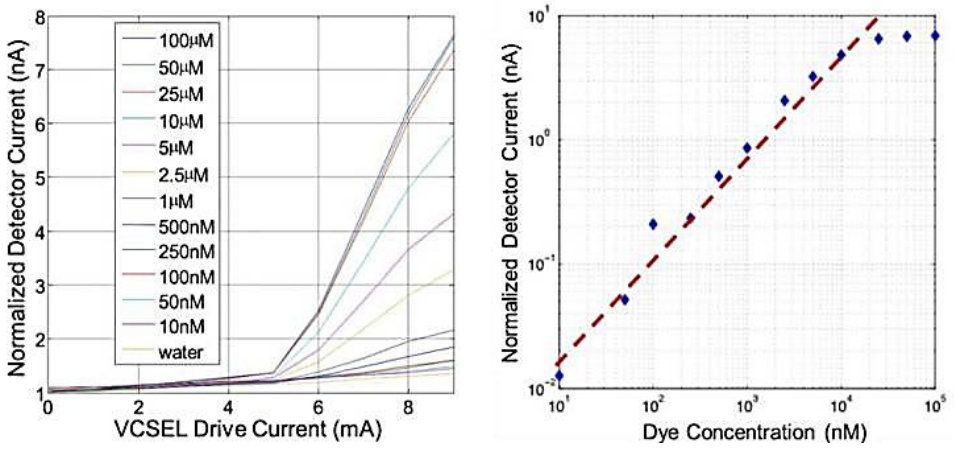

Figure 2.1-23: Measurements of Excitation drive currents and the photo-current received at the detector for different concentrations of Cy5.5 fluorescent dye. Considering the efficiencies and losses of the whole fluorescent setup, the efficiency in terms of required/generated power (and thus photons) is in the range of 10^{-6}, far from the ranges of the Quantum yield efficiency, which cannot be considered in an isolated manner [72].

2.1.10 Raman Scattering

First discovered in 1928, Raman or inelastic Scattering is the process describing the interaction between the light and the matter where scattered photons have either a higher or lower energy than the incident one, depending upon the vibrational state of the molecule under study. As mentioned earlier in section 2.1.6, when photons are scattered from a material, most of them are elastically scattered by Rayleigh or Mie effects, and the energy of the emitted photons remains the same as the incident ones. However, a small part of these photons, around 1 out of 10^7[73], excite the molecules in such a way that some of the incident energy is either lost, or coupled with internal

vibrational states generating that the scattered photons display different frequencies than the original ones.

Therefore, asides the Rayleigh scattering, two inelastic radiations happen, the Stokes and Anti–Stokes radiations, showing lower and higher energy respectively. This energy loss or gain is directly related to the vibrational energy levels of the ground state of the molecule, and therefore, the analysis of Stokes or anti–Stokes frequency shifts are directly translated into a measurement of the vibration energies of the molecule.

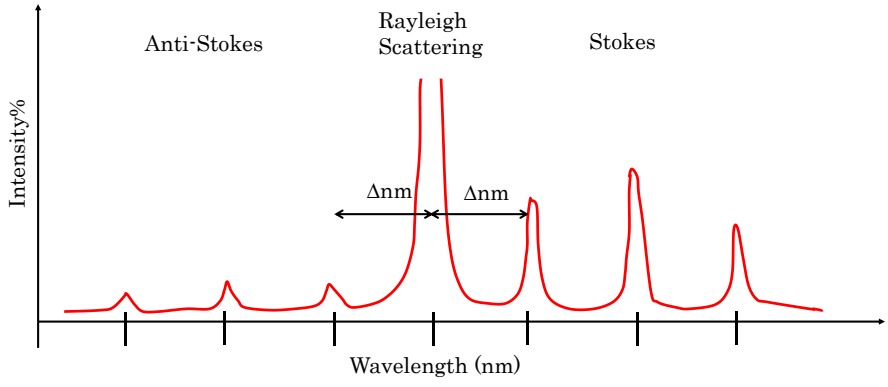

Figure 2.1-24: Schematic Raman spectrum. The energy of the scattered radiation is less than the incident radiation for the Stokes line and the energy of the scattered radiation is more than the incident radiation for the anti–Stokes line. The wavelength shift occurring from the excitation frequency to stokes and anti-stokes ONES is always the same regardless of the excitation, and it is always dependent on the material.

As it can be observed in Figure 2.1-24, the Stokes and anti–Stokes frequencies are equidistant from the Rayleigh frequency (the incident frequency), due to the loss or gain of one vibrational quantum of energy. And this is one of the main differences between the Raman scattering and the Fluorescence, because while the fluorescent peak remains static for a wide excitation spectrum, the Raman Stokes or anti–Stokes frequencies maintains a constant separation from the excitation frequency, which depends on the material and not on the excitation wavelength.

However, as described in Eq. 2.1–20, notice that the scattered signal intensity is proportional to the inverse of the wavelength to the fourth power, Intensity $\propto 1/\lambda^4$, which can lead to low signals at longer excitation wavelengths [74]. So, whenever possible, the excitation wavelength should be kept the minimum the possible.

Nowadays, Raman spectroscopy is generally considered as a complementary technique to IR spectroscopy, being suitable for analyzing organic and inorganic compounds. Additionally, Raman techniques are ideal candidates for measuring aqueous samples,

because, unlike the IR spectroscopy where the water absorption hide other absorption bands of molecules of interest, Raman scattering is more immune to the presence of water, because the intensity of Raman scattering from water is usually weak and direct absorption interferes only when near–infrared lasers (e.g., 1064 nm) are used. This is the reason why, even if high excitation power and strict optical tolerances are required, Raman-based in-line sensors are an interesting topic of research [179].

2.1.11 Attenuation

The attenuation represents the decay occurring to the incident radiation power while it crosses a certain material. Normally, the attenuation is the consequence of the combination of different process as the scattering or the absorbance, but it basically describes the relation between the light power that goes into a sample material and the power that comes out from the opposite end.

The simplest expression for describing the attenuation through a material is defined by the Bouguer[19]–Lambert[20]– Beer[21] law of absorption. This empiric formula defines the relationship between light absorption at a certain wavelength, A(λ), and the properties of the medium as:

$$\log_{10} = \frac{I_0(\lambda)}{I(\lambda)} = \varepsilon(\lambda) \cdot c \cdot l = A(\lambda) \qquad \text{Eq. 2.1–26}$$

Where, I_0 is the incident light intensity at wavelength λ, I is the transmitted intensity at same wavelength, ε is the molar absorption coefficient ($liter \cdot mol^{-1} \cdot cm^{-1}$) also called the molar extinction coefficient, c is the concentration ($mol \cdot liter^{-1}$) or Molar (M) and l is the light path along absorbing material (cm).

Therefore, the absorbance of a certain compound is directly proportional to the concentration, because a higher molecule number implies higher interaction with the light. Additionally, the absorbance is also dependent on the path length travelled by the light across the compound solution, just because the interaction with the molecules will occur along a longer distance. And finally, the absorbance is determined by a proportional constant ε(λ), the extinction coefficient, which basically quantifies the absorption properties of the compound for a certain light frequency.

[19] Pierre Bouguer, French astronomer and physicist, 1698-1758.

[20] Johann Heinrich Lambert, Swiss physicist, 1728-1777.

[21] August Beer, German physicist, chemist, and mathematician, 1825-1863.

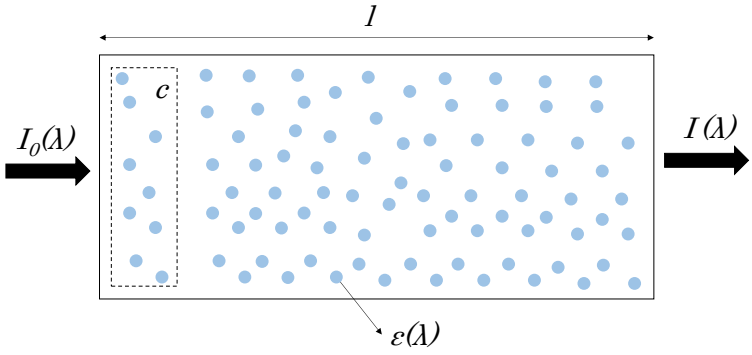

Figure 2.1-25: Schematic representation of the Attenuation process.

However, it should be considered that, normally, the materials are not composed of a single compound, but for a heterogeneity of molecules and components. Therefore, the light across a sample is attenuated by a sum of absorbents in different concentration. This accumulation is known as the absorption coefficient μ_a (cm^{-1}) and is defined by the following equation:

$$\mu_a = \ln(10) \cdot \sum_i C_i \cdot \varepsilon_i \qquad \text{Eq. 2.1–27}$$

Additionally, the approximation described by the Lambert–Beer law only remains valid for diluted solutions (e.g. A < 3). As c increases, the ε(λ) varies with the concentration due to the scattering process, aggregation of molecules, changes in the medium, etc. As concentrations change, turbidity may increase, macromolecules and other larger aggregates appear, etc. which normally contribute to larger light scattering. Since the optical density resulting from scatter is proportional to $1/\lambda^4$ (see Eq. 2.1–20), this effect is easily recognizable as a background absorption that increases rapidly with decreasing wavelength. Additionally, these molecular changes, typically also modify the structure of solvents and refractive index, may change consequently. Since the transmission of a radiation across two different media depends on the index of refraction and not only on the absorbance of the second media, these molecular changes will vastly impact on the Lambert–Beer assumptions [75][76]. The situation gets even more complicated when the Kramers–Krönig relationships are considered, which state that the refractive and absorptive properties of the medium are not independent [77].

Therefore, approximations for understanding and defining the light attenuation through a complex sample matrix are required as

the ones based in a combined consideration of both, absorption and scattering [78], described as in Eq. 2.1–28.

$$I(\lambda) = I_0(\lambda) \cdot \exp(-\mu_t \cdot x) = I_0(\lambda) \cdot \exp[-(\mu_a + \mu_s) \cdot x] \qquad \text{Eq. 2.1–28}$$

Where $\mu_t(cm^{-1})$ represents the extinction coefficient, being μ_a and μ_s coefficients the contributions from the absorption and scattering processes. In thin materials, scatter to larger angles is small and a simple estimate of light attenuation might be used. However, in thicker samples, scatter to larger angles is important, and the anisotropy coefficient, g, needs to be considered in the scattering contribution. In most organic materials, g is approximately in the 0.9 to 0.95 range, indicating mostly forward scatter of the light in the material. The anisotropy coefficient defines the effective scattering coefficient, μ_s', which also determines the Transport Mean Free Path (MFP') (cm), that describes the different trajectories within the material that a photon may travel due to the scattering [79][80]

$$\mu_s' = \mu_s(1 - g) \qquad \text{Eq. 2.1–29}$$

$$MFP' = \frac{1}{\mu_a + \mu_s'} \qquad \text{Eq. 2.1–30}$$

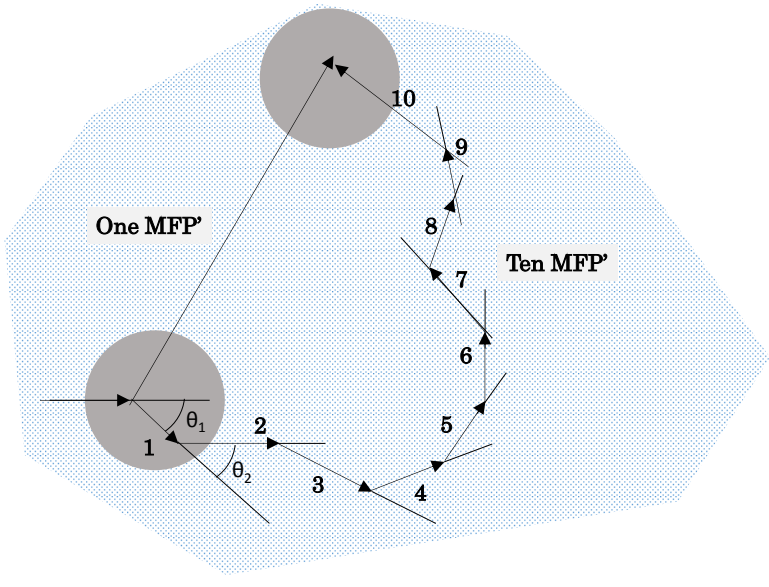

Figure 2.1-26: Effect of multi scattering points

Actually, since the propagation and attenuation of the light through heterogeneous sample matrix is subject to several, complex and interrelated processes, different numerical and analytical solving approaches have been developed. Some of them as the Radiative

Transfer Equation (RTE) are based on differential equations which are difficult to solve for non–homogenous samples. Additionally, mainly driven by the studies of the light propagation across human tissues, different statistical and probabilistic methods, as the Monte Carlo based ones, are being used to model and simulate the photon propagation across multi–layered tissues. In the Monte–Carlo simulation model, the rules of light propagation are described as probability distributions that define the step size of photon transport between points of photon–tissue interaction and the angles of reflection in the trajectory of the photon when a scattering process happens (see Figure 2.1-27).

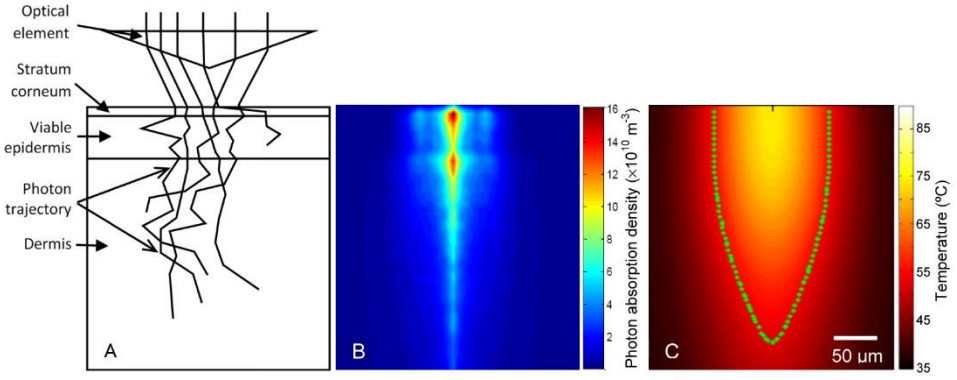

Figure 2.1-27: Schematic diagram of a cross–section of the three–dimensional model used in the Monte Carlo simulations comprising a three–layer skin model and an optical element. B: A typical numerical photon absorption map. C: A typical skin thermal map in pseudo-color [81].

Another interesting approach for understanding the light attenuation across a medium is the one proposed by Kubelka[22]-Munk. These equations are used as an analogy of the Lambert-Beer, but instead describing the attenuation (and thus concentration) in transmissive setups, Kubelka-Munk works for case of diffuse reflectance. The equations consider an opaque sample as a sequence of layers of infinitesimal thickness to generate a simple model of transmission and reflection for a layer, but once with the simplified model a layer with infinite thickness is modeled, where Transmission tends to zero [82]. Following with these approximations, Kubelka-Munk delivered the following equation:

$$f(R_\infty) = \frac{K}{s} \qquad \text{Eq. 2.1–31}$$

being k, the absorption coefficient, as in the Lambert-Beer law, and s the diffusion factor, which is difficult to determine. From Eq.

[22] Paul Kubelka, Czechoslovakian chemical engineer, 1900–1956

2.1–26, we can take k by Ln(10) × ε(ν) × c, where: ε is extinction coefficient (function of the wavenumber ν) and c is the sample concentration, what gives accordingly:

$$f(R_\infty) = \frac{\mathrm{Ln}(10)\varepsilon(\nu)c}{s} \qquad \text{Eq. 2.1–32}$$

Eq. 2.1–32 produces a similar expression to the Lambert-Beer attenuation expression, enabling to obtain a spectrum similar to the transmission spectrum, for the cases when the s parameter remains constant. In these cases, $f(R_\infty)$, at a given frequency, varies with the concentration c.

2.1.12 Optical rotation

The optical rotation is the process by which linearly polarized light radiation rotates its plane as it crosses a certain material. This optical activity occurs only at certain types of materials, as chiral ones, which are compounds with no mirror symmetry on their symmetric structure.

This effect is very useful because it allows measuring the concentration of certain materials by observing the phase shift suffered by a light radiation while crossing it. The interest about this method comes because the molecular groups of glucoses deliver a strong optical activity.

2.2 Optics and Optoelectronic Elements

This section will summarize the most important building blocks for developing a photonics sensor system, including the light sources or emitters, light detectors or receivers, and light conditioning and coupling optics components. Additionally, main trends and latest innovations in the field of microspectrometers are also reviewed.

2.2.1 Emitters

Light Sources or light emitters are the family of devices that transform energy into light photons of a certain wavelength and polarization. The emitters are a fundamental part of any photonics–based sensor as it provides the required excitation for accomplishing the measurement.

Asides the features of the emitted light (irradiance, wavelength and polarization), other important features must be considered when selecting a light emitter. For instance, the efficiency will determine the ability of the source to convert energy into radiated photons, the dynamics of the emitter will describe the possibilities of modulating the generated light and the optical properties, in terms of the geometry of the emission beam, will describe the volumetric concentration of the emitted photons.

Other important factors as the stability of the emitted light, its dependency with ambient temperature, lifetime, compactness and indeed cost may also determine the selection of the light source.

However, the most determining parameter is normally the emitted light spectrum limits, because not all the technologies are able to deliver light power at any wavelength. Table 2.2–1 gives a summary of the available wavelength ranges depending on the emitter technology or material.

Table 2.2–1: Examples of Emitter technologies and emissivity ranges [83][84]

Source Emissivity Ranges (μm)	Start	End
Quartz tungsten halogen	0.22	2.7
Glass tungsten halogen	0.25	2.25
DC deuterium lamp	0.185	3.75
Pulsed xenon arc lamp	0.18	2.5
DC arc lamp	0.20	2.5
Silicon Carbide	1	100
Carbon arc	0.5	100
Mercury lamp	0.3	100

Helium–neon laser (He:Ne)	0.6327	0.6328
Neodymium yttrium aluminum garnet (Nd:YAG) laser	1.0639	1.0640
Laser Diodes	0.7	1
Indium Phosphide (InP) LED	0.92	
Indium Arsenide (InAs) LED	3.6	
Gallium Phosphide (GaP)	0.55	
Gallium Arsenide (GaAs)	0.87	
Aluminum Arsenide (AlAs)	0.59	
Gallium Indium Phosphide (GaInP)	0.64	0.68
Aluminum Gallium Arsenide (AlGaAs)	0.8	0.9
Indium Gallium Arsenide (InGaAs)	1.0	1.3
Indium Gallium Arsenide Phosphide (InGaAsP)	0.9	1.7
Zinc Selenide (ZnSe)	0.45	0.5
Indium Gallium Nitride (InGaN)	0.385	0.45

The next sections introduce the main parameters describing the performance of a certain light source and then list, brief and compare the predominant emitter technologies

2.2.1.1 Main Features of Light Emitters

As mentioned, different parameters should be considered when describing a light source, which range from the characteristics of the generated light, to additional performance data as the efficiency, the driving circuitry, stability etc.

The most basic and traditional feature for describing a light source is the color temperature of the emitted light. This parameter describes somehow the wavelength–amplitude response of the source, assuming its equivalence with an ideal black body emission spectrum, and the value is given in Kelvins. Basically, the color temperature describes the human perception of the light that is generated as the result of a thermal radiator, which matches the reality for incandescent lamps, but is only an approximation when the light source is a LED or a fluorescent lamp [85]. As reference, notice that a tungsten lamp emits a 2500 K light, a warm white LED generates a 3000 K radiation and a fluorescent lamp emits a 5000 K light,

However, the color temperature should be understood as a very basic way for defining the light wavelength within the visible spectrum and the applications of this classification are mostly focused on illumination or photography, but are not useful for the design of photonic instrumentation or sensors.

When more accurate information is needed for understanding the characteristics of the light generated by a source, wavelength–

amplitude charts should be used. This type of graphic displays the emission power across a range of frequencies or wavelengths (in the vacuum) offered by a light source under certain conditions, as, for instance, the ambient temperature of the test and the polarization settings of the source. These charts are essential when the performance of the light iteration with the matter must be studied under a given wavelength band, because the graphs tells the amount of incident energy at a certain wavelength at which the molecules may react.

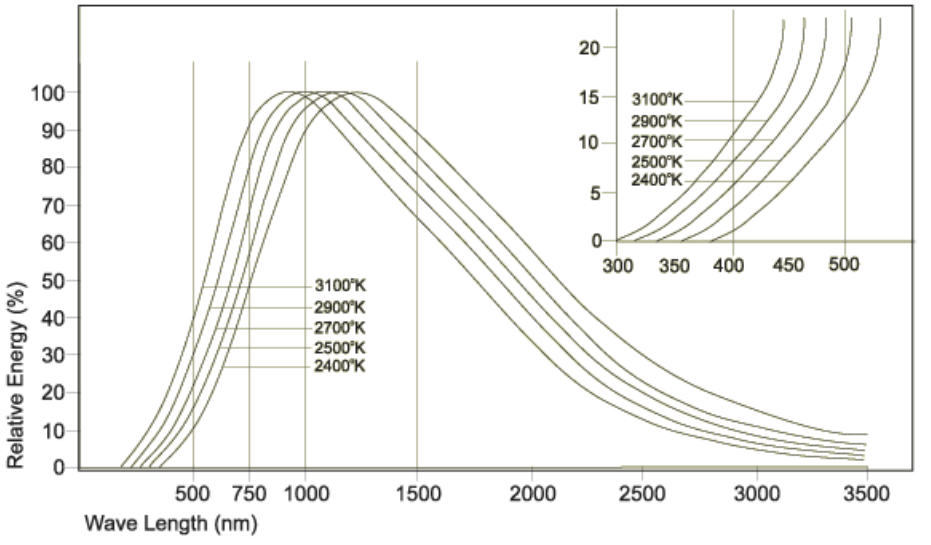

Figure 2.2-1: Spectral radiation output for tungsten filament lamps, including information regarding not only the relative emission energy across the frequency spectrum but also indicating the equivalent color temperature of each (courtesy of International Light Tech., Peabody, MA, USA)

The wavelength–amplitude chart also tells important information about the bandwidth of the light source, especially when narrow emitters are required. In this case, the emission peak (λ_{PEAK}) and the spectral half wave width or alternatively, the full width at half maximum (FWHM) spectrum are normally specified. The emission peak defines the wavelength at which the emitter shows the maximum emission power, and the FWHM quantifies the frequency range where power drops by less than half (see Figure 2.2-2).

Additional feature of the light sources is the directivity of the emission beam, which describes the radiation intensity along the different angles measured from the normal to the emitter surface. Sometimes the emitters include some sort of optics to modify or enhance the natural directivity of the emitter material.

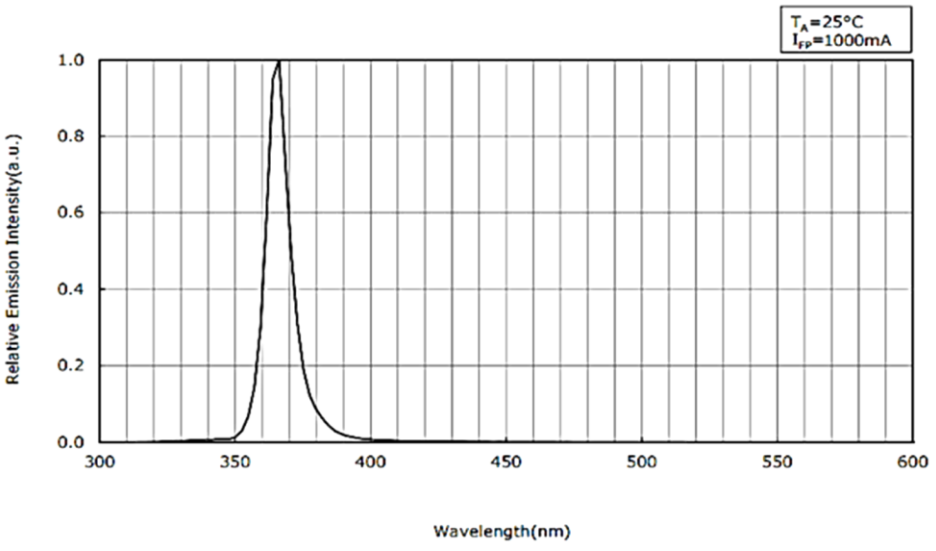

Figure 2.2-2: Spectrum of the U365 UV LED from Nichia manufacturer, showing an emission peak in 365 nm and FWHM of 9.0 nm. Notice that in this case, the emission intensity is displayed as a relative value in arbitrary units (courtesy of Nichia Corp., Tokushima, Japan)

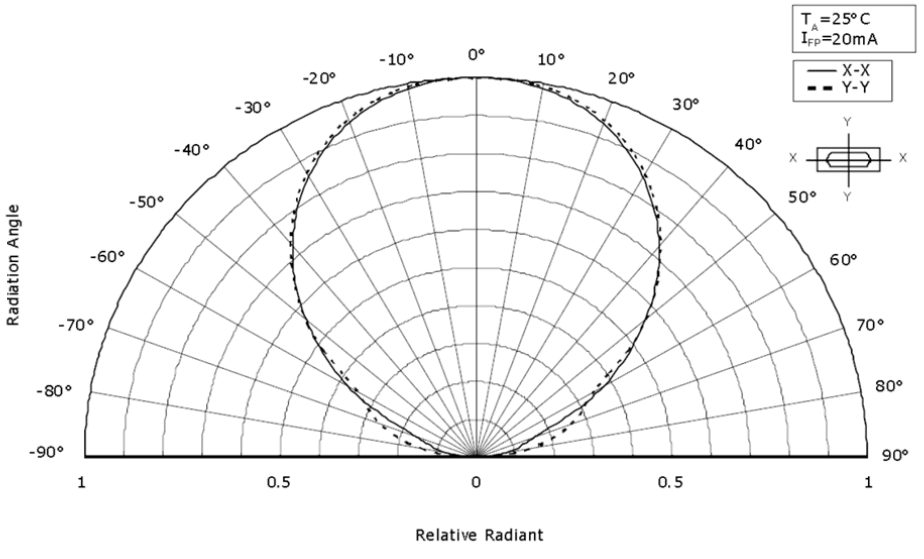

Figure 2.2-3: Directivity of PICOLED SML–P24 RGB LEDs from ROHM Semiconductor (Kyoto, Japan)

Temperature coefficient defines the dependence of the emitter features with the temperature. This is normally a very critical parameter since almost all the emitting technologies present an important dependence with the temperature and not only the radiated flux but also the wavelength gets modified with increasing temperatures [86][87].

Coherence, spatial and temporal, is another factor that may have to be considered in certain applications where the light phase and polarization is relevant, as it happens with interferometry applications. A radiation is called coherent when there is a fixed phase relationship between the electric field values at different locations or at different times. Partial coherence describes that there is some (although not perfect) correlation between those phase values.

Spatial coherence happens when the radiation shows a high fixed phase relationship between the electric fields at different locations across the beam profile. Temporal coherence means a strong correlation between the electric fields at one location but different times. For instance, Lasers have the potential for generating radiation beams with very strong spatial coherence, and this is perhaps the most fundamental difference between laser light and radiation from other light sources.

In addition, ageing of the emitters is another important feature, since it may determine the whole sensor system's lifetime. Not all the technologies offer the same performance stability over time, and it also vastly depend on the operating conditions. Thus, a tungsten lamp designed to operated 10,000 hours keeping at least the 50% of its nominal power may show a totally different performance if the operating temperature differs from the nominal values.

2.2.1.2 Emitter Technologies

This section outlines the most common technological alternatives for radiation sources, covering from simple filament sources to the new generation of light sources based on MEMS devices.

2.2.1.3 Incandescent Bulb

The most basic light emitter technology is the incandescent bulb, where a material like the tungsten is heated up by circulating a current, and the heated body generates a light radiation due to the Thermic Radiation Effect; and until recent years, these incandescent lamps have been the most common light sources. They require a simple control to operate, just a regulated power supply, but when lifetime of the bulb is important, several considerations must be taken to efficiently control the lamp driving current, as ramped pre–heating, controlled startups, etc. [88]. These kind of lamps (tungsten, halogen, quartz tungsten halogen, gas–filled) offer a reasonable short-term stability, but the lifetime is not high (around 10,000 – 50,000 hours), and the intensity decays slowly right from the initial uses.

The spectral ranges of these kind of light sources start around 400nm and may reach the NIR region, but with relatively low efficiencies as 20% (see Figure 2.2-1). Additionally, these light sources are relatively slow, so no light modulation possibilities are possible in setups using incandescent lamps.

2.2.1.4 Electric and Gas Arc Lamps

Historically, the second most common light sources are the arc lamps, even if these were invented fifty years before the filament lamps. In this kind of technology, the light is generated by a high voltage arc between two electrodes, and the most typical ones were the carbon arc sources, which were widespread solution for street lighting until they were substituted by the filament emitters.

The evolution of electric arc lamps continued during the nineteen Century with gas discharge lamps that generate light stimulating an electrical discharge through an ionized gas, which is normally a noble gas (argon, neon, krypton, and xenon) or a combination of these gases. The most know example of these kind of lamps were the famous neon lights and the fluorescent lamps used for lighting.

Sometimes, these lamps even include additional vaporized compounds as mercury, sodium or metal halides, which allow reaching higher irradiances or wider wavelength emissivity. These sources use a filament and anode, but in this case, the filament is not the light source, but the arc that is generated between the filament and the anode. The arc excites the molecules of the gases included in the light bulb which emit light when they return to their initial state. This technology normally requires a warm–up time to stabilize, since the filament needs to be at high temperature to generate the arc, therefore, in these kinds of solutions the light modulation is not an option either.

These kind of lamps, specially deuterium and mercury based versions are the most common UV light sources, and were the unique candidates until the UV LEDs (Light Emitting Diode) where launched around year 2000, and are currently steadily replacing the gas lamps [89].

2.2.1.5 Light Emitting Diodes (LEDs)

Actually, the solid-state lighting is the biggest revolution in lighting system since the development of filament lamp, and the UV wavelength case is just another example after what we have already witnessed in VIS, NIR and MIR ranges in the last decade. Based on the electroluminescence principle, which was discovered around the late years of 1900 decade, the revolution of the LED emitters started

around 1950, but it wasn't until early sixties when the first visible red LED light by Nick Holonyak[23] at General Electric laboratories

The electroluminescence effect defines that in a semiconductor P–N junction, in some materials as gallium arsenide phosphide (GaAsP) or gallium phosphide (GaP), the electron and hole recombination when electric current is applied will dissipate energy in form of heat and photons, and not only in heat as it happens with Silicon (Si) or Germanium (Ge) semiconductor. The wavelength emitted by these diodes is, by definition, a narrow band because the emitted photon's frequencies depend on the band gap energy of the materials forming the p–n junction. Several different materials and combinations have been developed with band gap energies corresponding to near–infrared, visible, or near–ultraviolet light (see Table 2.2–1).

Actually, there are only a few examples of wide spectrum LEDs, as the white LEDs that are not strictly pure LEDs because they generate the white visible spectrum thanks to a phosphor coating over a blue LED, which light excites the phosphor and generates a yellowish light due to fluorescence. Being the combination of that yellow with remaining blue an apparent white light.

LED lights are available in a wide range of packages and beams and currently are able to deliver relatively high efficiency and radiation powers, in the VIS and NIR regions with technological developments driven by commercial lighting and telecommunication industries.

Additionally, using a GaInAsSb/AlGaAsSb–based hetero–structure lattice matched to a GaSb substrate allows creating LEDs for the 1.6–2.4 μm spectral range and by using an InAsSb/InAsSbP–based lattice matched to an InAs substrate LEDs for the 2.8–5.0 μm spectral range can be manufactured. Other approximations use quantum dot doped silicon semiconductor to generate LEDs in the NIR range [90].

In addition, due to their semiconductor nature, LEDs are fast, and offer very high switching frequencies that enable modulating the intensities not only in amplitude but also in time, allowing, among others the direct generation of stroboscopic lighting systems.

2.2.1.6 LASERs

Asides the LEDs, the twentieth century delivered another big breakthrough in photonic emitting technologies, the LASERs. Based on the spontaneous emission described by Albert Einstein, the LASER (Light amplification by stimulated emission of radiation) technology

[23] Nick Noyack, American Electrical Engineer (1928)

started its evolution around 1920 and the fits LASER device was developed in 1960 by Theodore Maiman[24]. The working principle of the LASERs is to amplify a small excitation (either optical or electrical) or pumping with a resonator cavity filled with an active medium where the optical amplification occurs.

The active medium as well as the cavity is designed so that a high gain is obtained for a specific wavelength, delivering spatial and temporally coherent light beam at high radiation powers.

There are several types of LASERs, with gases as Helium–Neon (HeNe) used as active cavities for 633 nm, solid state ones with crystal active mediums as YAG (Yttrium Aluminum Garnet) emitting in 1064nm, etc. However, the most typical LASER sources are the LASER Diodes, which combine a semiconductor emitter as the active medium, with a Fabry–Perot cavity for generating the stimulated generation. As it happens with the LEDs, the emission wavelength of a laser diode is essentially determined by the band gap of the laser–active semiconductor material. Thanks to the variety of semiconductor materials is possible to cover wide spectral regions. Principally, the accurate wavelength availability comes from the ternary and quaternary semiconductor compounds, where the band gap energy can be adjusted in a wide range merely by changing the composition details. For instance, a higher aluminum content (increased x) in $Al_xGa_{1-x}As$ causes an increase in the band gap energy and therefore a shorter emission wavelength.

There are also developments working and marketing white LASER solutions, named Super–continuum LASER, delivering high power solutions (e.g. > 500 mW) in the 450 nm to 2500 nm spectrum [91].

2.2.1.7 VCSELs

Additionally, in the last two decades, another LASER technology is rising as a low cost, low power, fast switching and high flux emitter alternative. Started around 1993 at Honeywell labs, the VCSEL (vertical–cavity surface–emitting lasers) technology presented a paradigm shift due to its surface emitting feature. A VCSELs is a semiconductor laser diode that generates a highly efficient light beam vertically from its top surface. The internal cavities containing the amplifying layers are surrounded by electrically conductive layer stacks that form the laser mirrors. The most common VCSELs emission wavelengths where in the range of 750 to 980 nm targeting communication applications thanks to the good modulation capabilities offered and potential low cost.

[24] Theodore Harold Maiman, American Physicist (1927-2007)

Because VCSELs emit light perpendicular to the surface of the laser, the manufacturing process is fully compatible with traditional semiconductor processing equipment. Additionally, the surface emission also contributes to easy testability, because the VCSELs are verified and burned–in while still in wafer, increasing the manufacturing yield and lowering the cost [92].

Another important practical benefit provided by VCSEL technology [93] are the integrability of VCSEL structures with other semiconductor and detector devices allowing the development of complete systems (see Figure 2.2-4). Besides, the LED packaging technologies are directly applicable to VCSEL allowing a reduced investment cost and enables direct replacement of LED systems by VCSELs. Additionally, when individual device's radiation flux is not enough, the VCSELs can be aggregated in one or two-dimensional arrays (within the same wafer) to scale up the power output. The relatively low power requirements and operation reliability are also important assets offered by this LASER devices.

The benefits of VCSELs are making them good candidates for different sensing applications as fluorescence measurement [94], distance and velocity measurements based on interferometry [95] on a very compact and low-cost settings. Additionally, as mentioned, the small size and the compatibility of VCSEL manufacturing process with semiconductor wafer regular processing, allows to integrate within the same substrate a whole emitter–detector system as the ones described in [94]. In these monolithically integrated devices, the major challenge is to limit the crosstalk between sources and detectors while maintaining the performance of the individual components (laser, detector, filters)

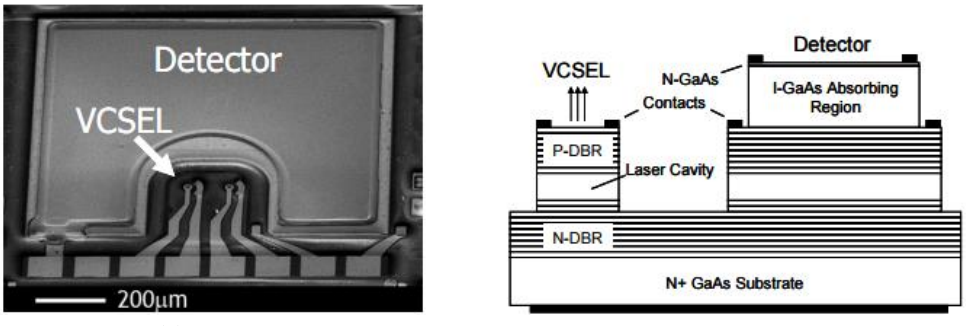

Figure 2.2-4: (a) SEM photography of a hybrid sensor including the VCSEL light source and the InGaAs detector, and (b) cross–section of the integrated device [94].

As mentioned, the most typical emission wavelengths of VCSELs fall in the range of 750–980 nm, based on GaAs/AlGaAs semiconductor system. However, longer wavelengths of e.g. 1.3, 1.55 or even beyond 2 µm can be obtained with dilute nitrides (GaInNAs quantum wells on GaAs) and from devices based on indium phosphide (InAlGaAsP on

InP) [96]. Having emitter in these ranges enables the use of VCSELs for gas monitoring because several molecules present the absorbance lines at these wavelengths. For instance, carbon monoxide and dioxide show several absorption lines around a wavelength of 1.58µm and close to 2µm – Methane in comparison shows absorption between 1.6 and 1.8µm.

2.2.1.8 MEMS based IR sources

As it has been presented, the tungsten filament micro–bulbs are a standard, low cost and well know technology for applications requiring working in the IR range. However, due to their intrinsic properties, they present a number of limitations in terms of limited modulation frequency (max 5 Hz), high power consumption (>100mW), or optical drift (>2%/1000h). Additionally, due to the cover glass (e.g. Quartz), the IR efficiency falls down to 60% at 4200 nm and is almost 0% above 5000 nm. Additionally, their form factor (3mm diameter, ~6mm long) jeopardizes the compactness of the final system and hinders the optical alignment due to their broad emission beam.

Indeed, the latest LED alternatives covering the near, short wave and mid IR ranges (1000 – 5000 nm), address some of the aforementioned issues. These solid-state emitters allow fast responses (>20 KHz), offer narrow emission bands (500 – 700 nm) and relatively high optical power (>0.3 mW radiant flux) at 4300 nm (e.g. L13201–0430M from Hamamatsu, Hamamatsu City, Japan). However, these devices show a relatively high-power consumption (~160mW if I_F=80mA and V_F=2 V) and their optical efficiency depends tightly with the ambient temperature showing a coefficient of 1.2%/ºC [97], converting the LEDs in a non–stable alternative for wide temperature span applications as industrial use cases (e.g. –20ºC to 80ºC).

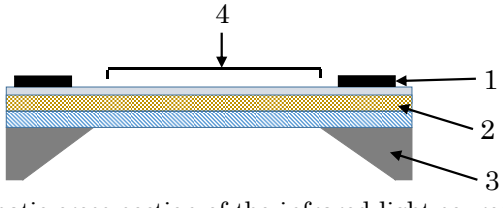

Figure 2.2-5: Schematic cross section of the infrared light source chip and the source mounted in a TO–5 housing. (1) Bonding pads: (2) a–NAC multilayer membrane; (3) silicon support; (4) active emitter area.

In this situation, MEMS IR sources appear as good candidates for solving some of the disadvantages of micro–bulbs and LEDs. The MEMS based emitters normally include a heater (e.g. tungsten) embedded within a dielectric membrane made of nano amorphous carbon (NAC). The substrate is made of Silicon with a back etched membrane. The last layer of the IR emitter chip is typically a

protective layer consisting of silicon nitride, which protects the active element against environmental influences [98].

When current is applied, the heater temperature can reach 400 – 700°C and emits radiation. A thin dielectric membrane is used to thermally isolate the heater from the substrate and hence reduce power consumption. The MEMS IR source can be made compact (3mm x 3mm x 1.5mm) where the IR emitter can be treated as a point source, thereby simplifying the design of the optics, such as reflectors and filter positioning [99]. However, even if these devices offer fast electrical modulation and high modulation depth the emissivity is not that high [100][101].

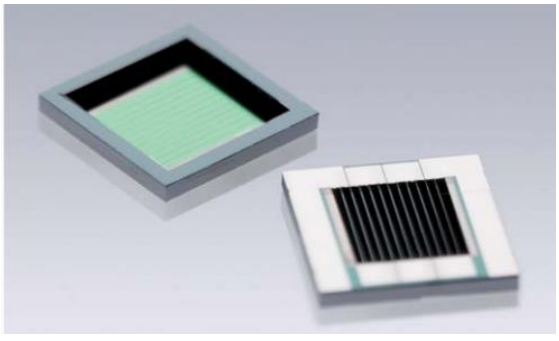

Figure 2.2-6: Front and backside of the IR Source MEMS chip. (overall size: 3.2 x 3.2 mm^2, membrane size: 2.1 x 1.8 mm2), (Axetris, Munich, Germany).

These kinds of sources offer a wide spectral output covering 1 – 20 µm, what is probably the widest bandwidth available in emitter technologies. Additionally, these MEMS–based IR sources can be modulated at frequencies over 100 Hz and achieve 25,000 working hours.

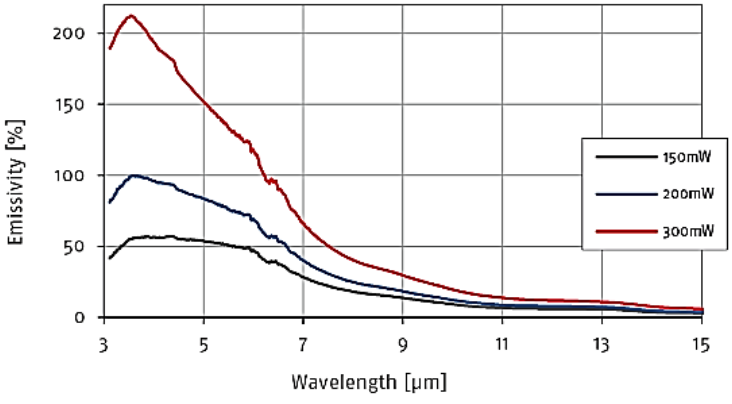

Figure 2.2-7: Emissivity spectrum of the JSIR 350-5 (micro-Hybrid Electronic GmbH, Hermsdorf, Germany) at different power levels

2.2.1.9 Emitter Technology Comparing Chart

Table 2.2–2 outlines the major advantages and disadvantages of the reviewed light sources.

Table 2.2–2: Summary of Emitter Technologies with advantages and disadvantages of each solution.

Light Source	Advantages	Disadvantages
Incandescent	– Low cost – Rugged – Broad spectral coverage – Easy electrical drive – Relatively compact	– Inefficient – Non–uniform spectrum – Continuous decay – Short lifetime – Limited modulation
Gas Arc	–Best solution for UV emission	–High Voltage required –Warm–up required –Bulky equipment
LED	–Very Low cost –Efficient in VIS –Ultra compact –Includes optical guiding –Fast modulation available –High Flux	–Requires active control for stable operation –Not efficient in UV, NIR and MIR ranges –High Temperature Coefficients
LASER	–Narrow Spectrums in UV, VIS and NIR, from 240 nm to 1500 nm (Quantum cascade laser up to 20 μm) –Available in Wide spectrum 450 – 2500 nm (super continuum versions) –Long spatial and temporal coherence –Modulation available	–Very expensive –May require complex electronics (not the diode lasers) –Bulky equipment

VCSEL	–Potentially low cost –Narrow Spectrum –VIS and NIR available –Very compact –Integrable with other semiconductor devices –Easy optical coupling –Modulable in GHz range	–Low reliability –Low power output (0.5–5 mW)
MEMS IR	–Wide MIR source –Modulation available –Compact	–Relatively expensive –Not available for NIR (>3 μm)

2.2.2 Detectors

Light detectors are the family of devices that transform photons of a certain wavelength and polarization into some sort of electrical energy. As emitters, the receivers are essential part of any photonics–based sensor as they deliver quantitative information about the properties of a light radiation incident to its sensitive or active surface.

Detectors are sensitive to certain types of light, specially defined by the wavelength and by the minimum detectable intensity. Not all the radiations may generate the same signal level and moreover, some light levels and frequencies may even be *invisible* for the detectors (see Table 2.2–3 for more details about the detection ranges). However, matching the detector sensitivity with the working wavelengths is not the only feature to consider while selecting the photo–detector.

The quantum efficiency, the spectral response, the aperture number, the bandwidth, element number and disposition, etc. are important design parameters that will determine the suitability of a certain photo–detector technology. In addition, other critical factors as dependency with the temperature, noise, lifetime, compactness and cost should also be considered for deciding the photo–detector technology.

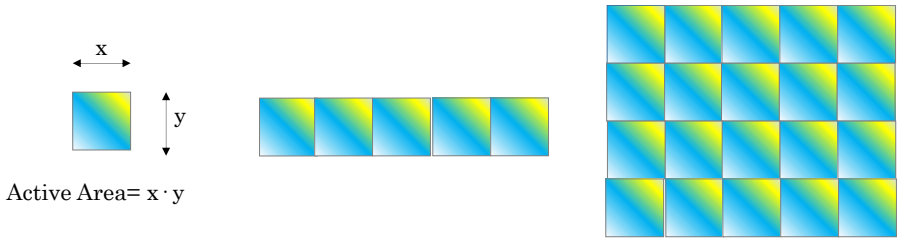

Figure 2.2-8: From left to right, Point, Linear and Matrix Photodetector structures. The matrix or image detectors are well known as they are the base for current popular digital photo-camera's sensors.

The UV/VIS/IR spectral ranges are currently covered by different material and technologies, either in point, linear or image arrangement of detectors (see Figure 2.2-8). Asides the typical structures, photo–detector technology reveals examples as the pyroelectric detectors, thermopiles, microbolometers, narrow–bandgap photovoltaic detectors [102], Schottky barrier detectors [103], extrinsic photoconductors [104], multi–quantum–well semiconductor hetero-structures for quantum cascade detectors (QCD) [105], etc. However, there are four main technologies which cover the majority of the applications: the photomultiplier tubes (PMTs), silicon photo-multipliers (SiPMs), avalanche photodiodes (APDs), and silicon photodiodes.

Table 2.2–3: Examples of Detector technologies and sensitivity ranges.

Source Emissivity Ranges (μm)	**Start**	**End**
Silicon (Si)	0.3	1.2
Lead Sulfide (PbS)	1.1	3
Indium Arsenide (InAs)	1.7	5.7
Indium Gallium Arsenide (InGaAs)	0.65	2.7
Germanium (Ge)	2	40
Lead Selenide (PbSe)	1.7	5.5
Deuterated Triglycine Sulfate	10	120
Indium Antimonide (InSb)	1.8	6.8
Triglycine Sulfate (TGS)	10	120
Pyroelectric Lithium Tantalate ($LiTaO_3$)	1.5	30

As with the light emitters, the following sections summarizes the main parameters describing the features of light detectors, introduces the main technological families and additionally, gives a deep review of the current trends and innovations in the field of microspectrometers, which represent a specific case of light detector,

allowing the discrimination of the light power across different wavelengths.

2.2.2.1 Main Features of Light Detectors

This section outlines some of the most important but basic features that describe a photo-detector technology. Notice that some of the features described in this section, as responsivity, response times, etc. are further elaborated along the Chapter 3, while describing generic sensor systems part of generic sensor system.

As mentioned, the spectral response (see Figure 2.2-9), or the efficiency of the detector to convert a received photon into electronic signal, is the very first parameter to review. Indeed, it is wavelength dependent and it is normally given in terms of quantum efficiency, QE, (see Eq. 2.2–5), which defines the number of electrons generated over the number of incident photons. Sometimes the quantum efficiency and the relative responsivity terms are used indistinctly, and even if they both refer to the detector efficiency to convert light into electrical energy, they are not strictly interchangeable (see section 3.2.1.1).

Alike the QE, the responsivity defines the generated amperes or volts per watt of incident radiant power (see Eq. 2.2–6).

$$\text{Responsivity} = \frac{\text{Electric Energy}}{\text{Incident Radiant Power}} \ (\text{A/W}) \qquad \text{Eq. 2.2–1}$$

$$\text{Quantum Efficiency} = \frac{\text{Electrons Generated}}{\text{Incident Photons}} \ \% \qquad \text{Eq. 2.2–2}$$

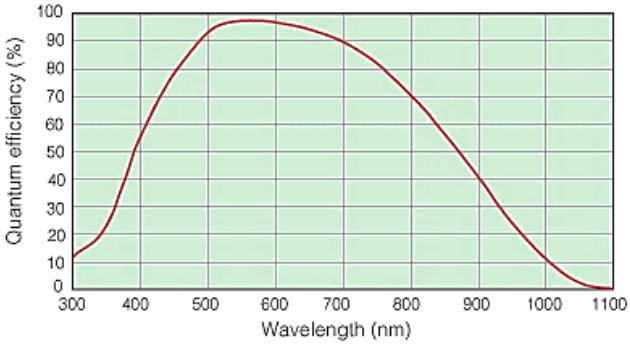

Figure 2.2-9: Spectral response of C10600-10B photodetector from Hamamatsu (Hamamatsu, Japan), where the quantum efficiency is displayed against the wavelength.

Therefore, the spectral response describes the efficiency of the detector material for detecting light over a certain wavelength span (see Figure 2.2-10).

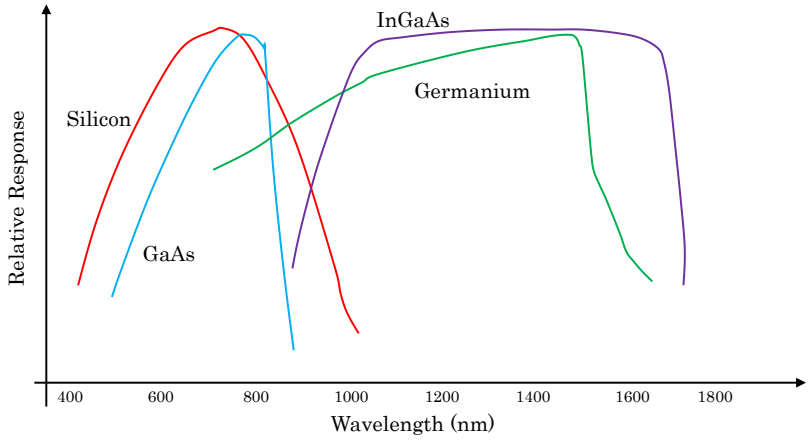

Figure 2.2-10: Typical spectral responses of different semiconductor materials.

Besides, the Numerical Aperture (NA) of a photo–detector help us understanding the percentage of a radiation beam that effectively gets to the detector surface. The NA is a specification indicating the acceptance angle of a system, measured from the detector's surface normal as described in Figure 2.2-11 and Eq. 2.2–3, where n is the index of refraction. The NA should be carefully chosen because exceeding the NA tends to increase the stray light[25] and not meeting the optimum NA reduces the overall system efficiency. Typically, the photo–detector material are flat surfaces with limited natural acceptance angle and, therefore, extra optics are normally used for enhancing the light collection and focusing into the receiver's sensitive area. In lenses, the numerical aperture is normally specified as the f-number or f/# as in Eq. 2.2–4.

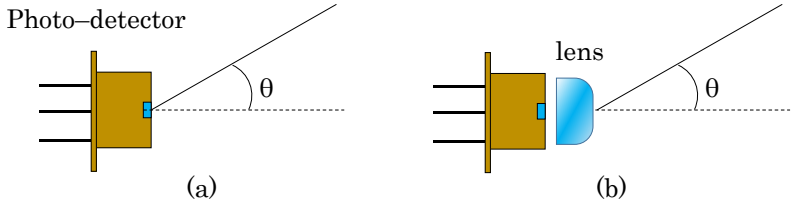

Figure 2.2-11: (a) Open air configuration for photo-detector. (b) photo-detector and a coupled Lens for enhancing the light collection.

[25] Stray Light is the light entering into a system that is not intended to be there.

$$NA = n \cdot \sin(\theta), \qquad \text{Eq. 2.2–3}$$

$$f/\# = \frac{1}{2NA} \qquad \text{Eq. 2.2–4}$$

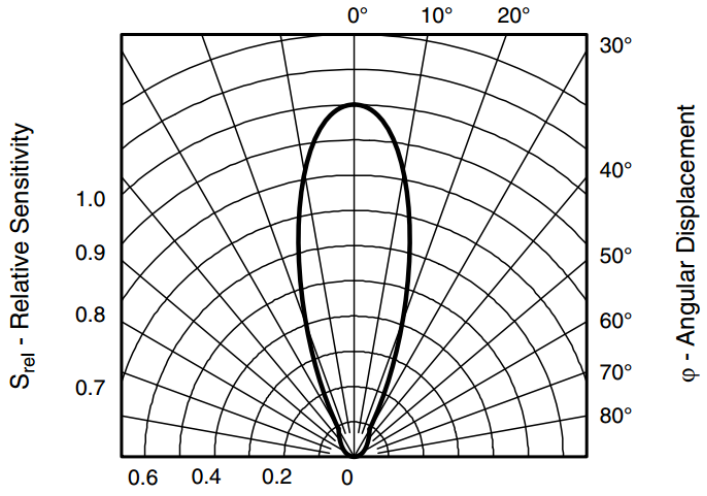

Figure 2.2-12: Typical graph representing the relative radiant sensitivity versus the angular displacement of a Silicon PIN Photodiode (VEMD2500X01) from Vishay (Malvern, PA, USA)

Another important remark that should be considered while dealing with photo-detectors is the Dark current (see section 3.1.1.13 for further details), which is one of the major contributors to the noise of the photo-detectors that hinders the detection of low light intensities. The point is that the electrical energy delivered by photo-receivers is not always originated from the detection of a photon, but from the consequence of some internal and unwanted effects that also generate micro–currents.

The dark current is described as the random generation of electrons in the absence of incoming photons. It is material dependent (e.g. silicon has much lower dark current than germanium) and sensors with larger active areas tend to have higher levels of dark current. Additionally, notice that the dark current approximately doubles its intensity for every 10 ºC rise in temperature. The dark current, especially in certain materials is the reason why photo–detectors may require operating under temperature controlled conditions, and often active cooling system (e.g. Peltier cell) is attached to the photo–detector case. The variation of the detectors responsivity due to changes in temperature are also material dependent, and in the semiconductor based technologies, this dependence has its origin in the increase of decrease of the band gap due to temperature. However, the relative variations in responsivity

can be reduced to less than 1% in certain technologies as in the Silicon Photodiodes (see Figure 2.2-13)

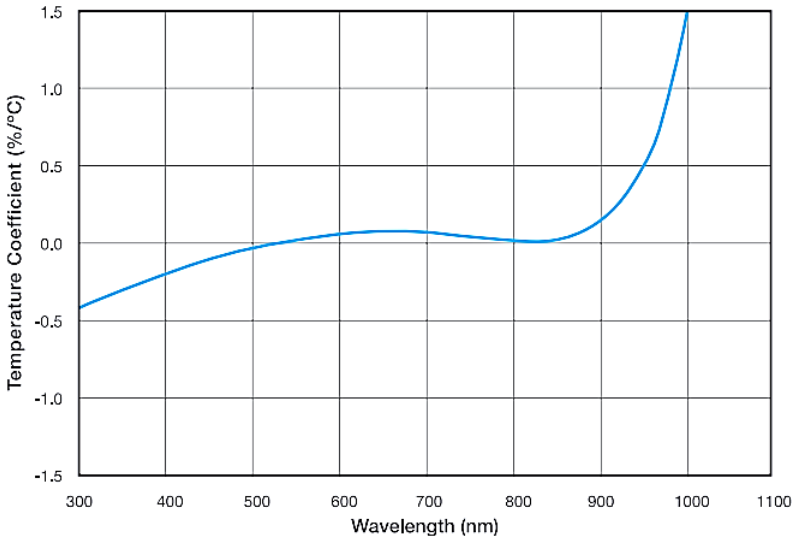

Figure 2.2-13: Typical temperature coefficient of responsivity for silicon photodiode [106].

Another relevant contributor to the noise level in the signal delivered from the photo–detectors is the readout noise, which represent the noise associated with reading the detectors current or accumulated charge. This perturbation is not strictly generated at the detector but at the readout electronics required for amplifying the photocurrent.

In addition, the integration time is another important parameter defining the operation of a photo–detector as it describes the amount of time a detector is allowed to collect photons. During the active periods, the photocurrent is either used for charging capacitors or it is continuously read out. On the other hand, during the inactive periods, the detector's charge is effectively coupled to ground.

In applications requiring responding to very fast switching light pulses, the time response (see section 3.1.1.10) of photo-receivers could be limiting the suitability of a certain solution. The time response defines the minimum light pulse duration that the detector is able to follow and convert into a readable photocurrent.

2.2.2.2 Detector Technologies

The following five sections describe the main photo–detectors technologies, emphasizing their typical physical, optoelectronic, and operational characteristics.

2.2.2.3 Photomultiplier tubes (PMTs)

PMT are vacuum tubes with integrated photo–detectors and photomultipliers that are extremely sensitive to UV, VIS and NIR radiations. They were first introduced around 1935 after several years of investigations for integrating the two internal processes that are the base of the PMT operation mode: the photoelectric effect (emission of electrons from an illuminated metal surface) and the secondary emission which defines that metal surfaces impacted by electron beams emitted a larger number of electrons than the incident ones.

The internal structure (see Figure 2.2-14) of a PMT is based on a vacuum tube comprising a photocathode, a sequence of dynodes and the anode where the signal is collected and delivered to the amplifying electronics. The photocathode is where the light is converted to the first set of electrons due to the photoelectric effect. These electrons are then sequentially multiplied in a series of dynodes where the secondary electron emission happens. Thanks to this cascaded multiplication of electron number, PMTs are able to achieve gains around $x10^6$.

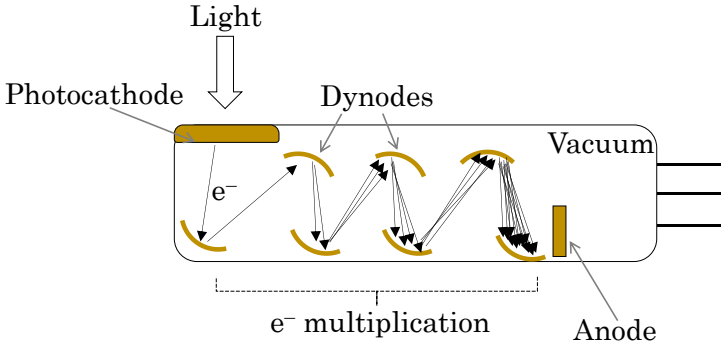

Figure 2.2-14: Internal structure of a PMT detector.

Due to the high gain, low noise, fast speed and large spectral response (especially in the UV range) the PMTs are still a good candidate for applications requiring high sensitivities, but their requirements in driving voltage (e.g. >1000 volts) and readout electronics hinder they use in low cost and integrated applications.

2.2.2.4 Photodiodes

Photodiodes are semiconductor devices with a p-n junction. In this case, the light to current conversion happens at the depletion layer due to the absorption of photons and the generation of an electrons-hole pair, which are then recombined at the N-layer generating the photocurrent, in a process known as the intrinsic photoelectric effect. The sensibility of the photodiode to radiations of

different wavelengths is determined by the band gap energy (eV) of the semiconductor material, defined by its absorption coefficient. Currently, since the first photodiode was developed in late forties at Bells Laboratories, several different materials (Si, Ge, InGaAs, etc.) have been applied to develop photodiode alternatives with the aim of covering different spectral ranges.

Nowadays the photodiodes are a mainstream alternative due to their simplicity, low cost and variety. See sections 3.1.2 for further details about photodiodes.

2.2.2.5 Avalanche photodiodes (APDs)

APDs are is a type of PD that has an internal gain due to avalanche multiplication, which is an intrinsic process in semiconductors by which *n* carriers in the transition region are accelerated by an electric field (see Figure 2.1-15) to energies sufficient to create free electron-hole pairs impact-ionize a lattice atom. The generated charge carriers, may also ionize more atoms while moving through the avalanche region, which leads to a higher gain of charge carriers.

Thanks to this process gains around 10^2 to 10^3 may be achieved by APD but a high reverse bias voltage (from 10 to 150V) to polarize the diode near the breakdown voltage is required.

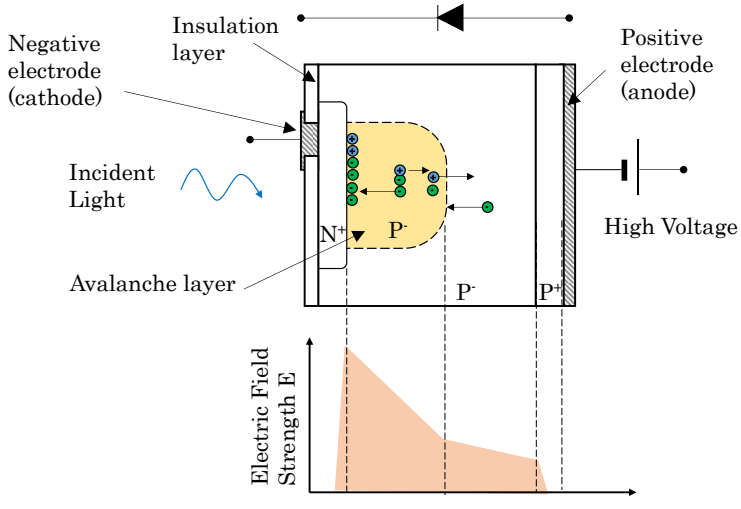

Figure 2.2-15: Internal structure of an APD photodiode detector.

2.2.2.6 PIN Photodiodes

PIN are also a photodiode type comprising not only the typical p-n junction but also an intrinsic region sandwiched between the p-n, which is this case are heavily doped regions (p+ and n+). In this case, the depletion layer is almost completely defined by the intrinsic region.

The PIN photodiodes may deliver some advantages compared to the regular PDs, especially in terms of fast switching times, thanks to the possibility of increasing the width of the depletion layer and thus the capacitance of the PD.

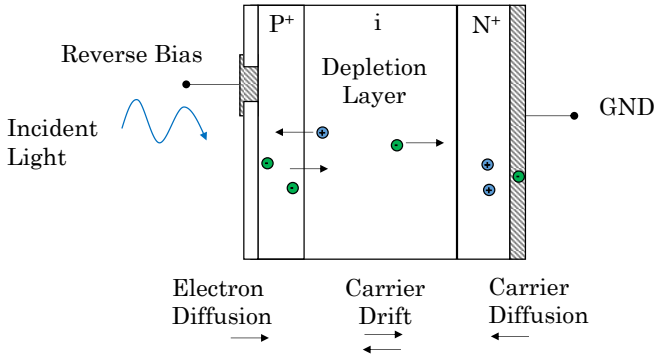

Figure 2.2-16: Internal structure of PIN photodiode detector.

2.2.2.7 Silicon photomultiplier (SiPM)

SiPMs are the only devices than somehow could compete with the PMTs in terms of sensitivity. They are formed by an array of APD working in parallel. The low-light detection capabilities of the SiPM along with the benefits of solid-state technology are reason behind the rapid penetration of this kind of devices [107].

2.2.2.8 Detector Technology Comparing Chart

Table 2.2–4 outlines the main features of the reviewed light sources.

Table 2.2–4: Examples of Detector technologies and main features.

Photodetector	**Wavelength (nm)**	**Responsivity (A/W)**	**Gain**	**Dark Current (nA)**	**Rise Time (ns)**
Silicon PN	550-850	0.41-0.7	1	1-5	5-10
Silicon PIN	850-950	0.6-0.8	1	10	0.070
InGaAs PIN	1310-1550	0.85	1	0.5-1.0	0.005-5
InGaAS APD	1310-1550	0.80	100	30	0.100
Germanium PN	1000-1500	0.7	1	1000	1-2
PMT	115-1700	$1\text{-}5 \cdot 10^6$	10^6	2 (30mins)	5
SiPM	320-900	0.4	10^6		1

2.2.3 Common Passive Optical Elements

This section will give a brief overview of some of the most typical passive optic components. These elements are the responsible for modifying filtering, reflecting, dispersing the light to enhance certain properties the optical system with the aim of making the most of the light generated at the emitters and providing the optimum light radiation to the detector. Therefore, sensor system developers in the UV/VIS/IR spectral domain profit from the availability of a large number of refractive/reflective/diffractive optical devices such as lenses, mirrors, beam–splitters and gratings for setting up the photonic systems. For a deeper review about optical components, the reader could be referred to the vast bibliography available about the topic, as for instance, [108] or [109].

Asides the specific function or feature offered by a certain optic component, the compatible spectral range of the optical material should also be considered, since not all the materials behave the same under different light wavelengths. Table 2.2–5 provides a summary of spectral ranges of most common optical materials, indeed, the ranges are approximations because the absorption does not remain constant along the whole specified range. The material selection is a fundamental part when designing a photonic system which works either in UV, VIS or IR range.

Table 2.2–5: Examples of Optical Materials and their associated spectral ranges

Optical Materials Spectral Ranges (μm)	Start	End
Methacrylate polymer	0.25	1.1
UV Grade Fuzzed Silica (SiO_2)	0.2	2.5
Quartz	0.19	2.7
BK7 Glass	0.315	2.35
Pyrex® Glass	0.31	2.5
Sapphire (Aluminum Oxide Al_2O_3)	0.15	5.1
Germanium	1.1	30
Silver Bromide	0.5	35

2.2.3.1 Lenses

Lenses are optical elements that, based on a geometric disposition of a material with a certain refractive index, are able to converge or diverge the incident light into a certain point or plane. The lenses are normally described by their focal length, which defines how strongly the optical system converges or diverges the light.

Lenses could be used as single elements or as a group of devices that sequentially modifies the light ray propagation geometry until it reaches the output of the lens system.

However, as the index of refraction depends on the wavelength, not all the light rays will bend equally if the incident light is not monochrome, generating a distorted light convergence or divergence, called chromatic aberration. To avoid this effect, specific lens system devices are found named Achromatic lenses which have been specifically designed to minimize the chromatic aberration effects.

Another typical artifact generated at convex lenses in the spherical aberration, which due to the convexity radius, the rays hitting the surface near the edges of the lens are reflected alike the ones hitting right in the center. This generates that even monochrome light beams get distorted due to the lens surface geometry. Another specific design of lens systems contributes to mitigate this effect: the aspheric lenses, which is a solution that instead of a single radius curvature combines a double radius surface to gradually bend back the rays to the ideal focal point.

There are certain applications where the light does not necessarily need to be condensed, but rather parallelized radiation is required. In these cases, collimation lenses should be used. These lenses allow users to control the field of view, collection efficiency and spatial resolution of the photonic setup, and to configure illumination and collection angles for fluid sampling.

Lenses could be manufactured in different materials as plastics or glasses, but indeed, the geometry accuracy and light transmission properties are superior in the glass versions, even though they are one order of magnitude more expensive.

2.2.3.2 Filters

Filters are optical devices that selectively transmit the wavelengths of an incident light radiation. They are normally defined by their frequency response, which specifies the how the filter modifies the magnitude and phase over the whole wavelength spectrum of the incident radiation.

There are two main categories for developing the optical filters, the absorptive ones and the dichroic filters or interference–based ones. Absorptive filters basically are made of a material that absorbs certain wavelengths. This kind of filters is a cheap option, but their frequency response is not usually very sharp, and when accurate spectrum cleaning is required they are not usually suitable options. On the other hand, dichroic filters are able to deliver very accurate frequency response thanks to the interferometric working principle. These filters are formed with a stack of layers in their surface that work as a cavity

(actually, as a Fabri–Perot interferometer), where the light is reflected back and forth generating destructive or constructive interferences by which some wavelengths get blocked. However, even if the optical characteristics of interference type filters are very accurate, they show a strong dependency with the angle of incidence of the light rays, with frequency responses normally shifting to shorter wavelengths as the incidence angle displaces from the normal [109]. Therefore, in this kind of filters there is a position dependent color sensitivity.

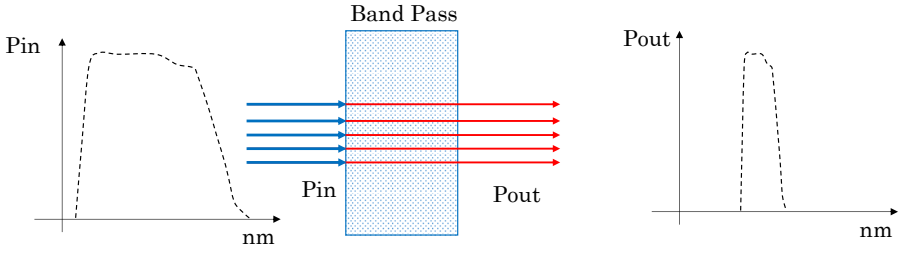

Figure 2.2-17: Filtering Effect on input radiation frequency spectrum.

Filters could be low–pass, high–pass, band–pass or notch filters. Low pass filters block all the wavelengths beyond the cut–off frequency, high–pass ones only transmit the radiation above the cut–off filter and blocks the low frequencies. Band pass filters just transmit the wavelengths between low and high cut–off frequencies, and notch filters just eliminate the portion of the spectrum within the high and low cut–off frequencies.

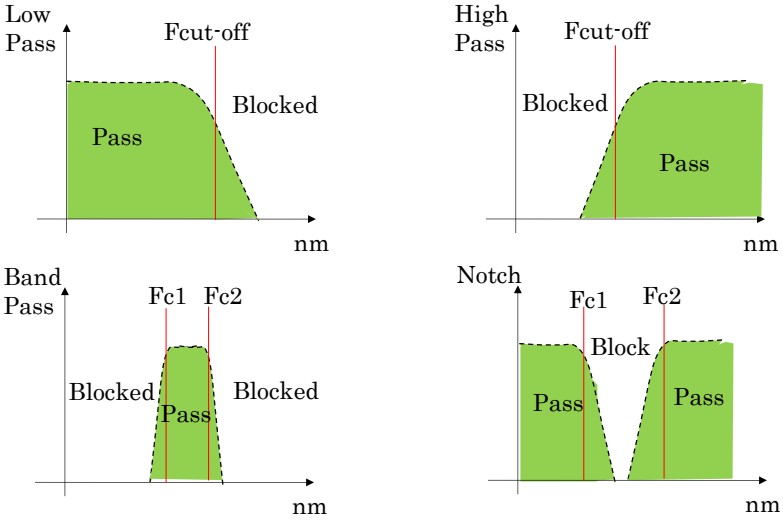

Figure 2.2-18: Different filters configurations.

2.2.3.3 Windows

Windows are the simplest optical elements because they just need to let the light be transmitted across their volume, assuring

minimal losses. However, the relevance of the optical windows in fluidics sensors is not trivial, because they represent the interface between the optoelectronic component and the target fluid, and are responsible of isolating the photonic elements from the potentially harsh fluid conditions in pressure, temperature, corrosion, etc. Chapter 3 gives a deep review of this specific topic.

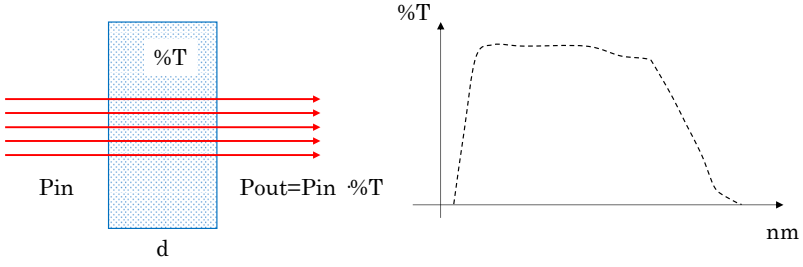

Figure 2.2-19: Optical Window, where the transmitted light power depends on the transmittance of the material, the thickness of the window and the wavelength of the radiation.

2.2.3.4 Mirrors

Mirrors are optical components, somehow similar to the lenses because they are able to concentrate the light into a certain point or plane, with the difference that the mirror do not suffer from chromatic aberration because alike the refracted light, the reflected one is not dependent on its wavelength, and just on the incident angle.

Therefore, the geometry of the mirror can be tuned to reflect the light as desired, and planar, curved and parabolic mirrors can be found, each of one delivering a different light reflection performance.

Alike lenses and windows, mirrors need to offer a highly reflective surface to enhance the light throughput. For this purpose, different coatings, normally metallic, are used to maximize the specular reflectance. Materials as aluminum, silver or gold are common elements for these coatings.

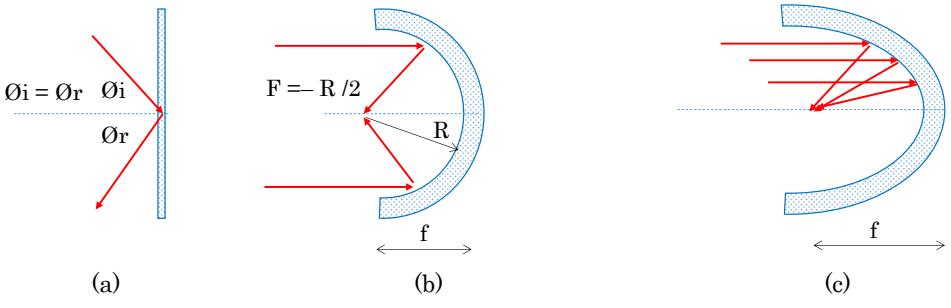

Figure 2.2-20: (a) planar mirror, (b) spherical mirror and (c) parabolic mirror.

2.2.3.5 Diffractive Gratings

In optics, when a certain structure is arranged periodically it normally becomes a diffractive grating. Diffraction grating, due to the periodicity of its structure splits and diffracts light into several beams travelling in different directions depending on the wavelength. Therefore, when a wide spectrum light radiation hits a diffractive grating, it is decomposed in a spatial sequence of singular wavelength radiations. Periodicity and shape of the diffractive grating structure defines the efficiency and light throughput as well as the amount of strayed light.

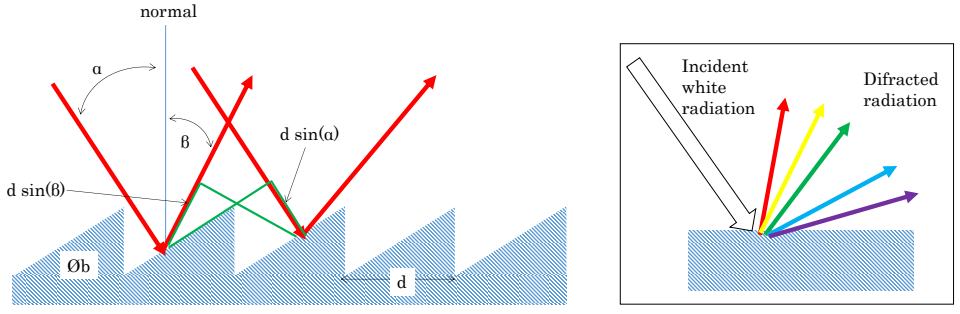

Figure 2.2-21: Basis diagram of a blazed diffractive grating structure.

In Littrow configuration based diffraction gratings, the following Eq. 2.2–5 to Eq. 2.2–7 describe the functionality.

$$d(\sin\alpha + \sin\beta) = m\lambda \quad \text{where } m = 0, \pm1, \pm2, \ldots \qquad \text{Eq. 2.2–5}$$

$$\sin\alpha = \sin\beta = \sin\emptyset_b \qquad \text{Eq. 2.2–6}$$

$$2d\sin\emptyset_b = m\lambda \qquad \text{Eq. 2.2–7}$$

2.2.3.6 Pinholes

Pinholes are plane plates with a small slit or aperture on their surface, with diameters between a few micrometers and a hundred micrometers. Pinholes are commonly used either as spatial filter where the small pinhole acts as a low–pass filter for spatial frequencies in the image plane of the beam, or as light diffractors, generating an airy disk pattern at the pinhole output.

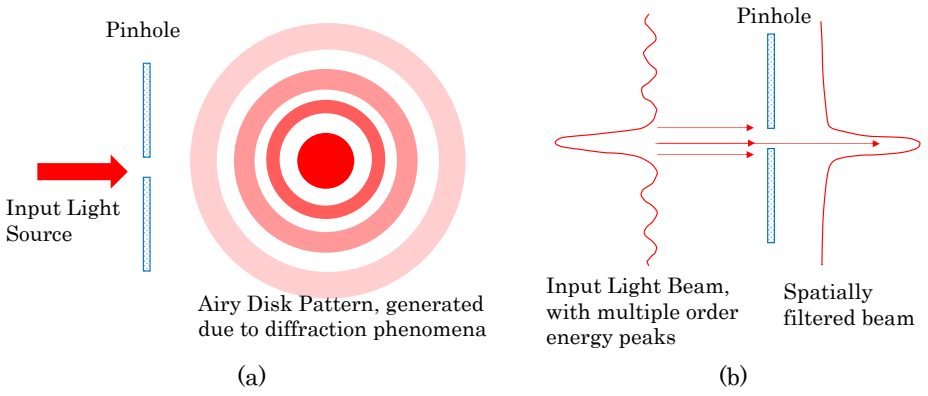

Figure 2.2-22: (a) pinhole as diffractor device and (b) pinhole acting as spatial filter.

2.2.3.7 Bean splitters

These optical devices are used to split or combine optical beams. The beam separation could be performed based on the radiation wavelength or on its polarization, and the separation–combination ratio is also normally adjustable. The beam splitters are available in different configuration as cubic, plate, pellicle or dichroic.

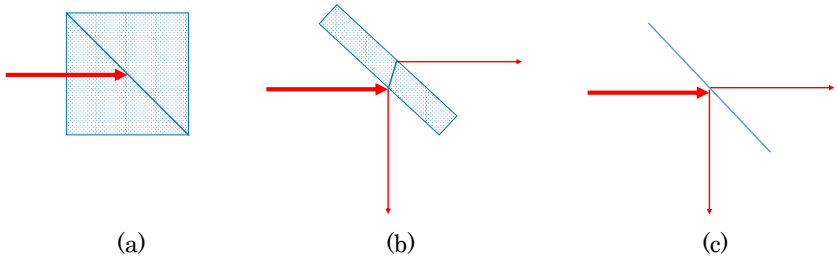

Figure 2.2-23: (a) planar mirror, (b) spherical mirror and (c) parabolic mirror.

2.2.4 Micro-spectrometers

Spectrometers, or their miniature versions, so–called micro-spectrometers, are optical systems designed for collecting a wide spectrum light beam and delivering the corresponding intensity values across a predefined wavelength range, with a certain spectral resolution. Their basic structure comprises a light collection, light splitting system and a single or multiple detector element [110].

When the collected wavelength is unique, then the spectrometer is defined as a non–dispersive system or as a monochromator (see Figure 2.2-24). And, even if they do not offer a

deep spectral information, these configurations are widely used when the relevant information is located in a certain and know wavelength range, as it happens with the gas molecule sensors, where the absorbance of the molecule of interest is known.

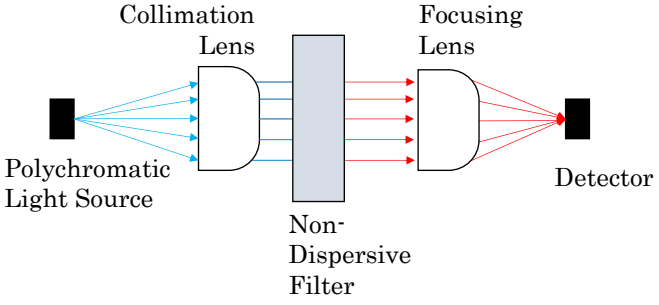

Figure 2.2-24: Basic structure of a non–dispersive spectrometer.

The monochromator configurations are sometimes adjustable, and if this wavelength tuning can be accomplished in an automated way, then a complete spectrometer can be developed, where radiation power information is given for certain wavelength slots. This kind of devices are known as single detector spectrometers, and represent a sensible and economic option when fast acquisition times are not required. The single–element spectrometers will be slower by definition, because a time–based filter multiplexation is required for measuring the light irradiance over the whole wavelength span.

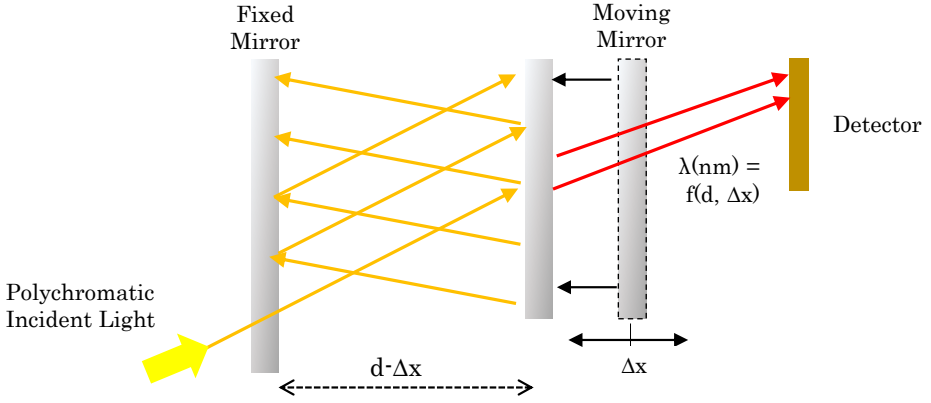

Figure 2.2-25: Schematic structure of Fabri-Perot Etalon interferometer with a moving cavity wall that tunes the wavelength of the outputted radiation

The single element spectrometers are normally based on interferometric configurations using Fabry–Perot or Michelson[26] approaches, where the destructive interference wavelengths depend on the internal geometry (distances between elements) of the resonant

[26] Albert Abraham Michelson (1852-1931), American physicist.

cavities [111][112] (see Figure 2.2-25 Figure 2.2-26). There are also some other approaches using moving mirrors based gratings following the Czerny–Turner[27] approach [113][114]. All of these setups require to generate micro–movements in one or various internal optical structures to modulate the wavelength at which the detector is instantly receiving the power.

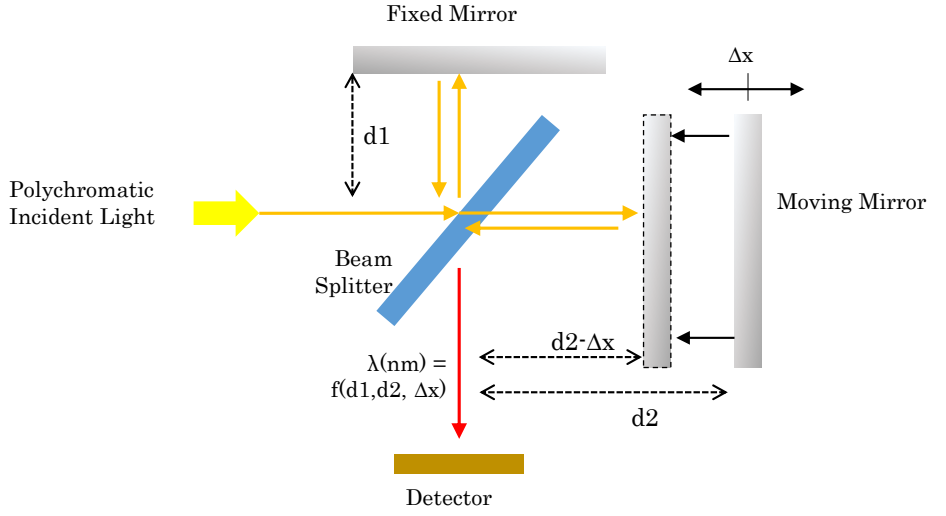

Figure 2.2-26: Schematic structure of Michelson interferometer with a moving mirror that may be used to tune the constructive frequency of the setup.

Alternatively, the multiple element spectrometers are designed to simultaneously receive and read the light irradiance over a defined wavelength range. In this kind of setups, a linear array is arranged for collecting on each of its individual elements, the portion of the wavelength spectra split or filtered by the optical system. Therefore, in this kind of systems, the geometrical disposition of the elements normally defines the wavelength range detected.

There are another setups for filtering the light delivered to the linear array spectrometer, as the Linear Variable Filters (see Figure 2.2-27), which are thin–film coatings, deposited in the top of the detector. The singularity of these thin–film filter is that the coating height defines the cut–off frequency of a band–pass filter. Therefore, if the coating height is gradually modified along the linear detector array, each individual photo–receiver will detect the light intensity of the wavelength corresponding to the height of the coating located above [115].

[27] Arthur Francis Turner (1906-1996) American physicist and Marianus Czerny German physicist (1896-1985).

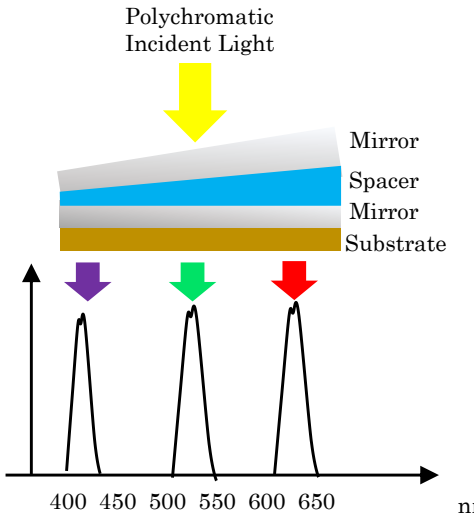

Figure 2.2-27: Example structure of a linear variable filter based on the effect of incremental high on interferometric cavity [115].

One of the latest structure presented for delivering spectrometer system is to merge a 2D spatial filter matrix, with N different band–pass areas, with a 2D photo–receiver array, with N pixels. Then, above each pixel a certain wavelength filter is located, and therefore, the pixel only receives the light intensity of the corresponding wavelength [116][117].

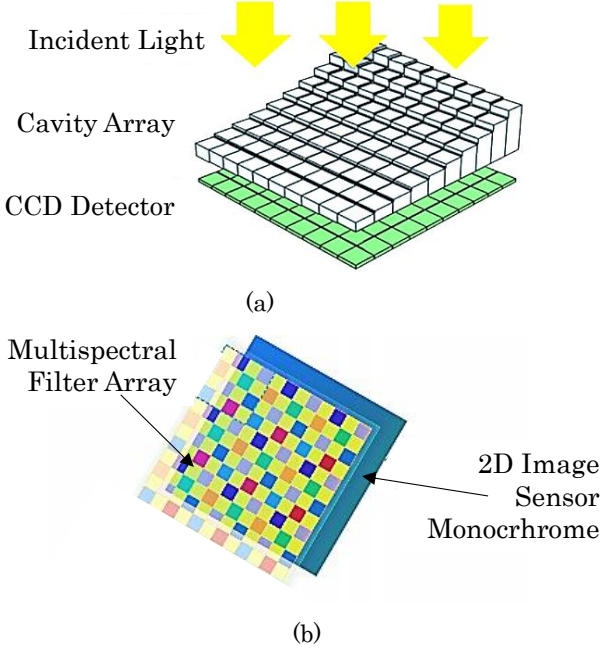

Figure 2.2-28: (a) Fabri Perot multi–cavity 2D array [116] and (b) Thin Film 2D filter structure [117].

Table 2.2–6: Summary of Spectrometer technologies with advantages and disadvantages of each solution.

Type	Technology	Advantages	Disadvantages
Single Element / Single Wavelength	Non–Dispersive (Filters) Mono–chromator	–Simple systems and very compact setting –Low cost – Immediate readout	–Limited spectral information
Single Element Detector	Fabry–Perot Michelson Czerny–Turner	–Low cost –Detailed spectral information –Compact size	–Slow readout
Linear Detector Array	Diffractive Grating Linear Variable Filter	–Immediate readout –Detailed spectral information	–larger than others –high cost, especially in NIR version
2D Detector Array	Multispectral Filter Arrays Etalon Arrays	–Immediate readout –Compact size	–limited spectral information (N channels) – high cost, especially in NIR version

For a detailed description of the different spectrometer setups as the Diffractive grating based, Michelson interferometer, Etalon Fabry–Perot cavities, Czerny–Turner approaches and others, for instance, please refer to [118] [119].

3.

Smart Photonic Sensors

In this chapter, a fundamental overview regarding sensors is given, presenting the concept of transducer, analyzing the main static and dynamic characteristics of sensors and introducing noise, cross–talk, cross–sensibility and other important concepts that should be considered for understanding the response of any sensor system. The section follows presenting the Smart Sensor term, which is a concept of sensor system that embeds the transducer, the algorithms and the communication means within an integrated solution. The chapter continues introducing the most important photonic sampling techniques, susceptible of being integrated in a cost-effective and compact system. Additionally, the section outlines the main techniques or approaches for analyzing the information contained in the light beam outputted by a photonic sensor, allowing the extraction of relevant data about the material under observation. Finally, the in–line sensing approach is described and compared to other monitoring approaches as the at–line, off–line or on–line setups, describing the main challenges of the wettable parts and in-situ calibration of these in-line sensors.

3.1 Fundamental Description of Sensors

Sensors are devices which transform a certain physical phenomenon into an electrical signal, representing a part of the interface between the physical world and the electric devices domain. This capability of perceiving the surrounding is described by the root Latin word *sentire*, which is the origin of the English word *sensor*, formulated around 1350–1400. A sensor is supposed to react to an input stimuli generating processable outputs, which are functionally related to the input's quality or quantity parameters, normally referred as measurands.

Sometimes, the word Transducer is used instead of sensor, but they entail substantial differences. The word Transducer was first coined in 1525–1535 and its source is the term *transduce*, which defines *to transfer*. A transducer is a device that converts one type of energy to another, and even if this generic definition covers the specific case of sensing elements, it also describes the actuators, which convert an electrical signal into a physical phenomenon.

The lack of specificity while describing the function of a sensor is because this is a multidisciplinary field by nature. The sensors may respond to several different domains (chemical, radiant, mechanical, magnetic, thermal) generating processable electrical outputs processes. Each sensor presents its working principles, fundamented in the concatenation of different physical or chemical processes that convert the information describing a material or phenomenon into an electrical signal in form of Volts, Amperes or Watts. These processes are well described in the literature as for instance photoconductivity (radiant energy into electrical energy), piezoelectricity (mechanical energy into electrical energy), Seebeck effects (heat energy into electrical energy), Hall effect (magnetic energy into electrical energy), etc. [120].

Even if this chapter outlines the main characteristics for sensor devices, we should consider that the focus is put on photonic sensors, and more specifically on smart photonic sensors for in–line fluidics monitoring. As depicted in Figure 3.1–1, photonic sensors are based on the analysis of an incoming light beam, which embeds into its properties (amplitude, spectrum, phase, etc.) information concerning the measurands. This incoming light radiation is normally conditioned using optic elements before its detection on an optoelectronic detector, which basically converts certain incident photons (e.g. depending on the photons wavelength) into an electrical signal. The resulting electric signal needs to be cleaned, analyzed and interpreted to extract the significant information about the measurand or analyte. Besides, some other photonic sensors also include the light source, required to generate the excitation radiation that interacts with the phenomenon

being monitorized changing the original properties of the radiation. Additionally, sometimes, this light emitter needs to be controlled (e.g. modulation, synchronization, etc.) to enhance the quality of the measurements delivered by the sensor.

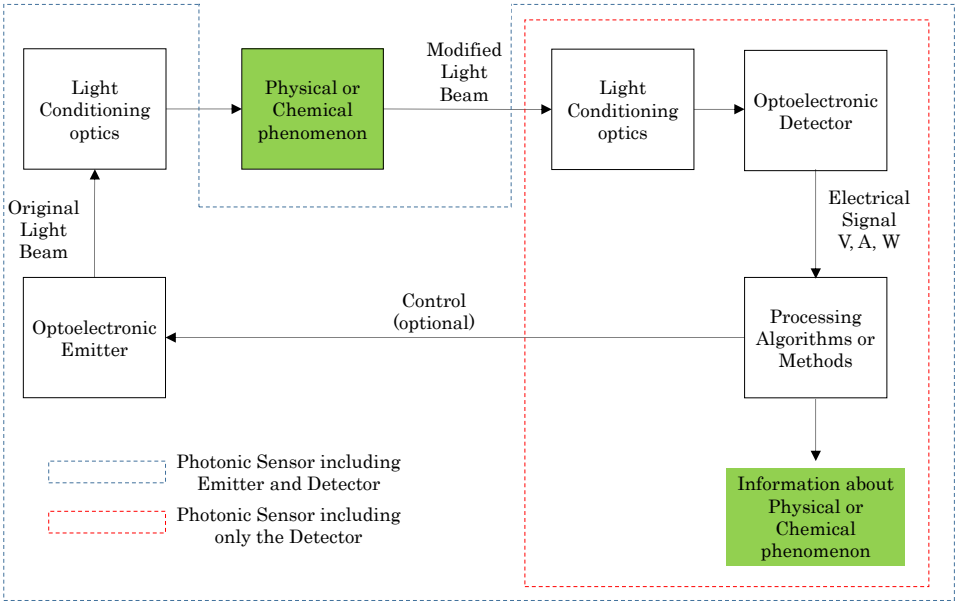

Figure 3.1–1: Basic Block of a Photonic Sensor.

The following sections within the chapter overview fundamental information about sensor characteristics, present some practical considerations concerning the use of sensors, including the different concepts impacting in the final sensor cost, and introduces the formal description of the Smart Sensor Concept. The remaining sections in the chapter include more specific information about photonic sensors (section 3.2.2) and about in–line fluidics sensors (section 3.3)

3.1.1 Sensor Performance Characteristics Definitions

Before describing the different performance parameters that describe a sensor operation, we must introduce the basic concepts that define what is expected for an optimum sensor.

Sensors should be sensitive to their target analytes, and insensitive to any other input quantities or environmental condition. Sensors are expected to deliver reliable, accurate and stable measurements [121], without affecting the analyte itself, avoiding the observer effect which describes the unintended alteration in system

behavior caused by measuring that system [122]. The limit of detection, generally, is required to be as low as possible to enable the sensor measuring small quantities of the measurand. Additionally, sensor size, power consumption and communication interfaces need always to be considered while engineering a sensor, towards a compact, autonomous and easy to integrate sensor system. The sensor life is also an important parameter to consider because a stable behavior is expected for the entire life span of the sensor, which could go from one single use (disposable sensors) to several years, as it is normally the case for the in–line sensors.

Finally, all the above mentioned features should also comply with cost efficiency requirements in terms of sensor development and sensor unitary cost.

After having given a general introduction about the desired features for a sensor device, the following sections offer a brief description of the different key performance indicators used when defining a sensor system. Since there is no a standardized method for describing these parameters, contributions from reference sources as Fraden [123], Kourosh [124] or Meijer [125] has been used for generating the following descriptions

3.1.1.1 Transfer Function

The transfer function describes the functional relationship between the physical parameter under measurement and the electrical output signal generated by the sensor. This functional relationship is normally described in a graphic manner, depicting the correlation between the measurand properties (e.g. concentration of a certain molecule, concentration of particles, etc.) and the signal generated by the sensor (see Figure 3.1–2).

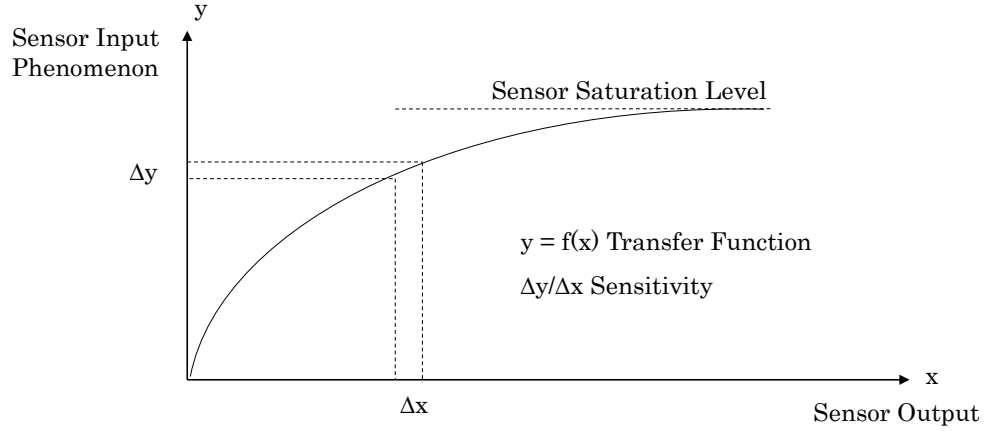

Figure 3.1–2: Graphical description of Sensor's Transfer Function and Sensitivity in a non–linear sensor response.

Sometimes, this Transfer Function is not stable amidst a sensor production batch and may require a calibration (see section 3.1.1.9) of that function for each element or for each fabrication order. This is a typical consequence when using solid state light emitters as a part of the photonic sensor, because the light properties delivered by those components are always batch dependent [126].

3.1.1.2 Sensitivity

Sensitivity, also defined sometimes as Responsivity, defines the ratio of the incremental change happening at the sensor output (Δy) when an incremental change is applied at the input of the sensor (Δy), thus, the sensitivity represents the derivative of the transfer function with respect to the input physical signal.

Sometimes, it could happen that the sensor sensitivity does not remain constant across the whole dynamic range of the sensor (see section 3.1.1.4), describing a non–linear sensor response (see section 3.1.1.8), that, for instance, may hinder the sensor calibration. Another typical issue is when the sensor response eventually reaches a saturation level, a state in which it can no longer respond to any changes (see Figure 3.1–2). Therefore, an ideal sensor should deliver a large and rather constant sensitivity in its operating range.

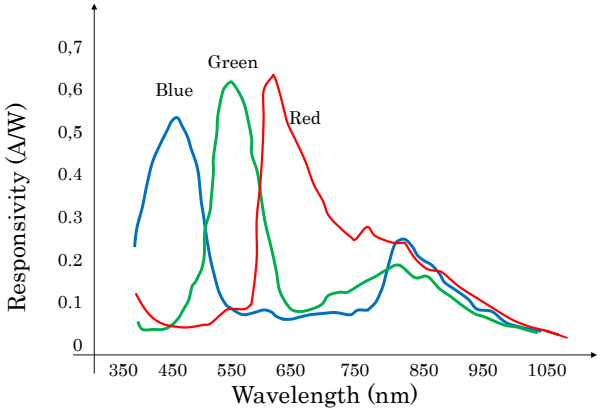

Figure 3.1–3: Relative Sensitivity (quantum efficiency) against wavelength graph for the MT9P006 image sensor (Red, Green and Blue channels) from On Semiconductor, which also delivers a sensitivity (responsivity) of 1.74 V/Lux/s at 540 nm.

The sensitivity is a critical parameter in photo–detectors describing the relation between the irradiance hitting the detector surface and the electrical signal generated. Additionally, in photo–detectors, this relationship is also normalized with a time constant, representing the electrical signal generated by unit of time under a given irradiance (e.g. V / Lux / s as seen in Figure 3.1–3). This parameter is also represented against the wavelength of the incident

radiation, because normally, the photosensitive materials do not respond equally to all the wavelengths (as described previously in section 2). Therefore, this kind of information is critical for understanding the behavior of a photo–detector.

Notice that these sensitivities are normally given for a certain temperature (e.g. T= 25ºC) because the response of the detectors normally varies with the temperature, due to the electronic changes happening at the detectors semiconductor.

3.1.1.3 Limit of detection

The limit of detection (LD) represents the minimum level, quantity, signal or effect of the measurand that is observed by the sensor, when all the interfering factors have been taken into account. As it will be described while assessing the noise (see section 3.1.1.13), when interferences are important, the LD is normally high and the sensor system is not able to detect slight changes in the measurand.

This parameter is especially relevant when dealing with chemical measurements, therefore, if the photonic sensor application deals with analytical measurements, the LD calculation should follow the recommendations delivered by standardization committees [127][128], which defines the LD not only as the minimum concentration of a given analyte to be detectable by the sensor, but the minimum concentration that can be measured in a reliable manner, with known probabilities α and ß of making false positives and false negatives. For analytical measurements, the LD is normally given as parts per million (ppm), percentage (%), or concentration (mg/L) of the analyte of interest detectable by the sensor.

In photonic setups, smallest detectable input signal is defined as standard deviation of input referred noise under dark conditions [129].

3.1.1.4 Span or Dynamic Range

This parameter defines the maximum and minimum ranges of the measurand which may be converted to electrical signals by the sensors, with acceptable accuracy. Therefore, the sensor span defines the working range from the limit of detection level up to the saturation level. All sensor systems are designed to operate within a specific range, and different engineering decisions are taken to optimize the performance over this specified range. Fabricating a sensor with a high dynamic range is not straightforward, and normally requires sacrificing limit of detection, resolution, sensitivity and the linearity.

Continuing the example for the analytical measurements, the dynamic range could be expressed as the range, for instance, 0.1% to

50% of concentration of a certain compound in a dissolution. Below 0.1% the sensor is not able to detect the compound and above 50%, the sensor is saturated.

Achieving a high Dynamic Range in the optoelectronic detectors is a general requirement for the photonic industry, mainly driven by the imaging and machine vision industry, where the CMOS cameras are required to deliver good imaging performance under low light, high light and high contrast (bright and dark areas within the same scene) conditions. This situation has led the development of a new generation of CMOS detectors (arrays of pixel elements), named High Dynamic Range (HDR) image sensors, that are able to operate efficiently under high contrast lighting environments [130].

3.1.1.5 Resolution

The resolution of a sensor system is described as the minimum observable signal fluctuation, being this fluctuation described by its amplitude and by the timescale when it happens. So, the sensors deliver a temporal and a spatial resolution as part of their features.

The temporal resolution is normally in relation with sensor's response time or bandwidth (see section 3.1.1.10) and basically describes the time slots when the sensor measures the physical phenomenon. Some changes may happen too fast to be observed by the sensor. The spatial or amplitude resolution defines the minimal change of the measurand that can produce a detectable increment in the output signal.

Even if the sensor nature is important for defining the resolution, currently, these terms are more often associated with the digitalization process applied to the sensor's output, defined by the sampling frequency (time resolution) and quantification (spatial resolution) processes that convert the electrical signal (V, A, W) into a digital signal expressed in bits (see section 3.1.2).

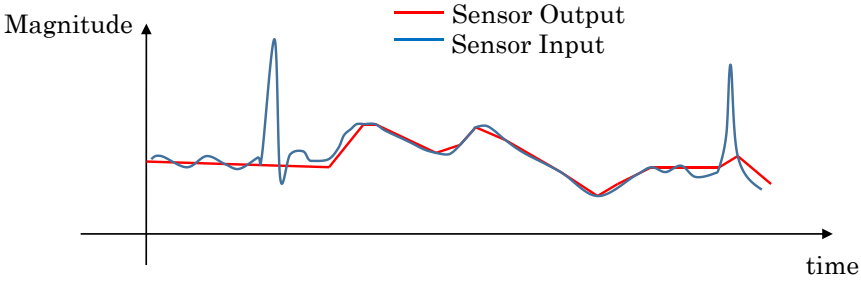

Figure 3.1–4: The lack of temporal resolution hinders the detection of input spikes. The lack of spatial resolution does not allow to follow the slight changes happening at the input.

3.1.1.6 Accuracy

The accuracy is generally defined as the largest expected error between the real value of the measurand and the value outputted by the sensor, and therefore, describes the rightness of the measured value. The accuracy assessment can only be accomplished if the sensor system is benchmarked against a standard model or compared against the values outputted by a sensor with better accuracy. Sometimes the accuracy is defined as a fraction of the full scale output (FSO).

Obtaining an accurate measurement is normally one of the major goals when designing a sensor, but this is hindered by several factors as noise, interferences, cross–sensibilities, etc. Additionally, delivering a high accuracy along the whole dynamic range is also a challenging requirement, and normally sensors offers worse performance at the edges of the dynamic range.

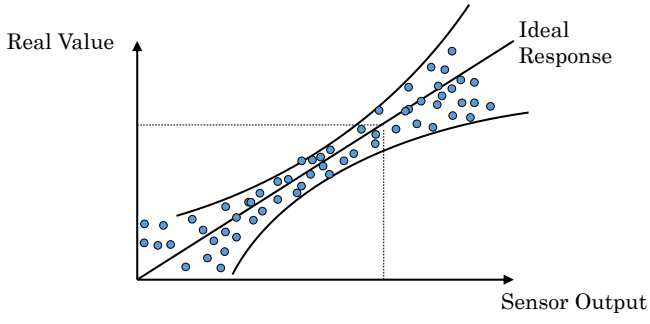

Figure 3.1–5: Sensor Accuracy across the whole dynamic range. Occasionally, sensors deliver better accuracies at the center of the measurement span.

3.1.1.7 Precision, Repeatability, Uniformity and Stability

This list of terms describes the performance of the sensor over a period of time, and generally describe its operation from a statistical point of view, defining the variance observed in the measurement value while the parameters of the measurand and the environmental conditions remain the same.

The Precision or Repeatability terms describes the ability of the sensor to deliver the same output while measuring continuously the same measurand under the same conditions, regardless the correctness of the outputted value. Therefore, Precision defines how consistent a particular sensor is against itself, and it typically limited by random noises, which is often outside of our control.

Besides, Uniformity is described as the systematic error that defines consistency of a measured value, either in a spatial distribution or compared to another sensor taking the same measurement. Uniformity describes the performance dispersion present in a sensor production batch.

Stability is the parameter that describes the ability of the sensor system to maintain its characteristics unaltered over a period of time, therefore, it defines the stability of the outputted value when measuring the same analyte over time. Changes in stability, also known as drift, are considered as systematic errors, which can be attributed to interfering parameters such as mechanical instability and temperature instability, contamination, the sensor's materials degradation, components aging, decrease in sensitivity of components, and/or a change in the signal to noise ratio, etc.

Understanding the degradation mechanisms that dominate critical components in photonic sensors is required for assuring their stable performance over time. For instance, typical conditions that deteriorate the responsivity of photo–detectors are their continuous exposure to UV radiation that damages both, the semiconductor and the optical components of the detector [131][132].

3.1.1.8 Linearity

The linearity of a sensor defines the approximation of the transfer function to a linear response over the specified dynamic range, and its degree of resemblance to a straight line describes how linear a system is. Typically, the linear response of a sensor is defined using the Coefficient of determination, denoted R^2 or r^2, of the simple linear regression made to the sensor outputs over the dynamic range, which considers not only the linearity but also the accuracy of the sensor.

In the optoelectronic domain, a photodiode is defined to be linear when its photoelectric conversion efficiency (responsivity) is independent of the incident optical power. Each photodiode behaves as a linear detector for a certain range of optical power and becomes nonlinear for higher intensity optical power, the nonlinearity threshold being a characteristic of the particular photodiode. As the power of the input optical signal reaches a certain level, the response of the photo–detector starts to saturate, thereby deviating from the linearity [133].

The nonlinearity of a photodiode is a function of several factors like generated photocurrent, incident optical power, the ambient temperature, etc. [134] However, the series resistance of the photodiode appears to be the most important factor in determining the linearity. One also needs to mention the incident beam diameter because it has been observed it has an influence on the linearity, but in a different manner for various types of photodiodes, however the influence is not wavelength dependent [135].

3.1.1.9 Calibration

When the response of the sensor is not constant over the production batch, a calibration process is required for assuring the uniformity of the sensors' output within the whole batch. The calibration process basically requires trimming the sensor output against a benchmark or against a known output to assure that each sensor delivers correct outputs. Calibrations in temperature is a typical factory process for optoelectronic sensors, at it may require one, two or even more calibration points depending on the linearity of the sensor. Some systems require being recalibrate after a certain period of time to adjust the sensor output to the response drifts.

However, calibration is a critical issue when dealing with sensors deployed in the field, because the accessibility is not always easy or even possible, as it happens with the off–shore wind turbines [136]. Therefore, unattended sensors will always foster the application of self–calibration or self–referencing approaches to mitigate the need of in–situ sensor calibrations.

In the specific case of photonics–enabled sensors, there are several ways of introducing self–compensating solutions within the sensor structure. For instance, NDIR sensors (see chapter 2), are normally equipped with a dual detector, one tuned for the target analyte detection and the other used just as reference. This approach enables to remove all the signal fluctuations coming from unstable light emission and detection sensitivities (generated by component ageing, temperature effects, etc.) by simply subtracting the reference detector intensity to the target detector intensity (see Figure 3.1–6).

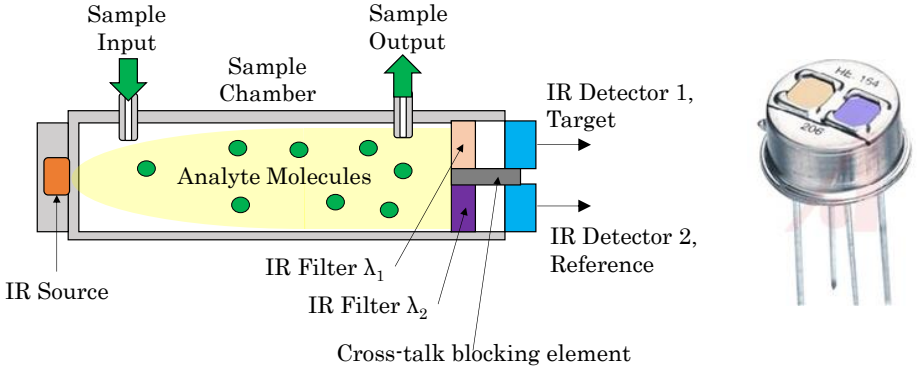

Figure 3.1–6: (a) NDIR fluid or gas sensor, where a dual detector schema is used, with two equal receivers and two IR filters, the first with the band–pass frequency matching the absorbance lines of the target analyte and the second IR band–pass completely aside from these lines. Therefore, the second detector gets information about the source and not about the measurand, and thus, this information is used to compensate any fluctuation on the emitter and on the detectors. (b) Displays a PYS 3228 IR detector with built–in filters for NDIR sensors, from Excelitas Technologies (Waltham, MA, USA)

Another approximation for self–calibrating photonic sensors is to include a secondary photo–detector for continuously assessing the emitters light intensity (and sometimes wavelength) and modulating it to keep a constant level of excitation. This is required for instance when working with reflectance or fluorescence configurations, where a minimum level of light excitation needs to be guaranteed to generate the reflected or fluorescent emission. This approach is observed in sensors for lubricant grease monitoring by reflectance [137] (see Figure 3.1–7), in sensors for lubricant oils monitoring (see Figure 3.1–9), or in UV Absorption sensors for use in the biotech and chemical industries [138] (see Figure 3.1–8)

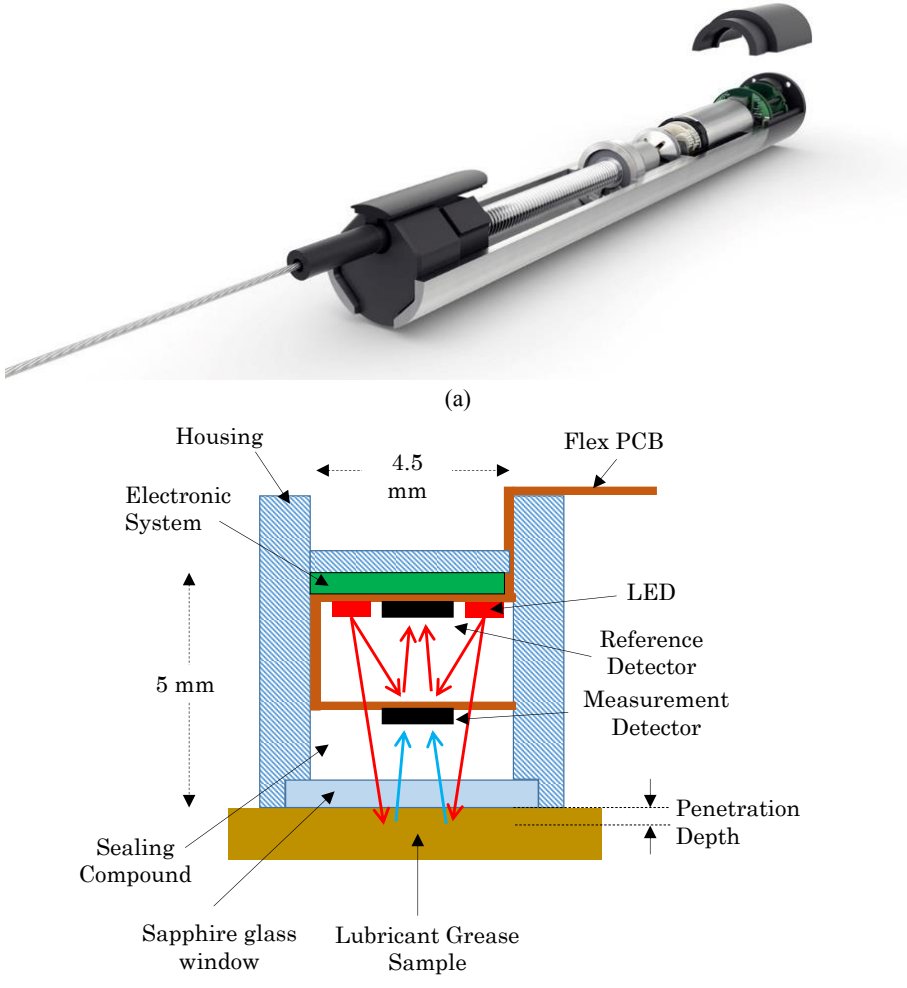

Figure 3.1–7: (a) NIR Reflectance Grease sensor, GreaseCheck from FAG–Schaeffler (Schweinfurt, Germany). (b) Presents the block diagram of the grease sensor, where the reference photodiode is included in the emitter's sensor plane, while the measurement detector is faced in perpendicular to the grease sample.

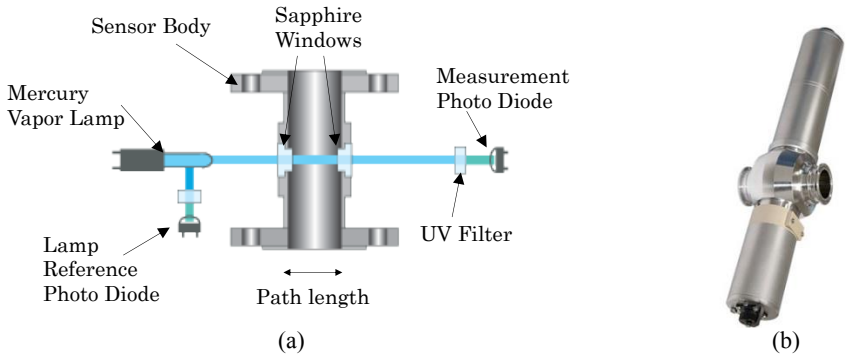

Figure 3.1–8: (a) Block diagram of fluid UV absorbance sensor, with a reference photodiode attached perpendicular to the light beam normal and received part of the emitted intensity through a beam splitter. In this case, while interpreting the signal measurement photodiode the original emitted intensity is always known and can be used for correcting the bias. (b) AF45 / AF46 sensor system including the (a) approach from Optek Danulat (Essen, Germany).

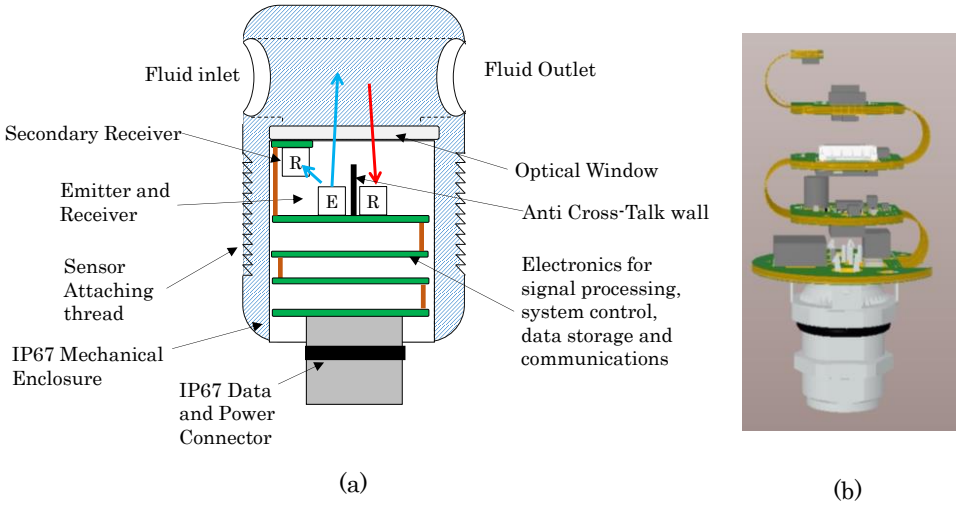

Figure 3.1–9: (a) and (b) Show block diagram of the OilProbe ® [139] sensor from Atten2 Monitoring Technologies (Eibar, Spain). In this case, a reference receiver is located slightly above the emitter, blocking a part of the emission lobule. The measurement detector is located besides the emitter, isolated from the cross–talk effects by a blocking wall.

3.1.1.10 Bandwidth

The bandwidth, sensor speed or the frequency response terms describe the finite response times that sensors deliver to an instantaneous change in the physical signal at the input. Additionally, normally, sensors also present decay times, which basically defines the time needed by the sensor output to reach the original state once the physical signal at the input has changed again. The response and decay times also represent the upper and lower cut–off frequencies of the sensor, defining the sensor bandwidth parameter, which

characterizes the ability of the sensor to respond to changes happening in the time lapses (t = 1 / f) within the cut–off frequency ranges.

In optoelectronics, these response times are normally defined by the Rising and Falling times (t_{RISE} and t_{FALL}), and normally represent the time needed by the optical component output to move from the 10% to the 90%, or the other way around, of the dynamic range. Relation between rise time and detectors bandwidth is given in Eq. 3.1–1 as demonstrated in [140]. Mainly driven by the requirements imposed by optical communications, the response and switching times found in optical semiconductors are currently in the range of nanoseconds and picoseconds.

$$B(\mathrm{Hz}) = \frac{0.35}{t_{RISE}(\mathrm{s})} \qquad \text{Eq. 3.1–1}$$

Because the quantity of noise in the output increases with bandwidth (see section 3.1.1.13 for noise description), a well–designed system has just enough bandwidth for the purpose of the observation [141].

3.1.1.11 Selectivity and Cross–Sensitivity

Selectivity defines the capability of the sensor to measure a target analyte in the presence of other interferences, which is an especially critical when dealing with heterogeneous samples and variable conditions as it happens in the in–line measurement of fluids. The cross–sensitivity means that the presence of other parameters or conditions apart from the target measurand are able to generate changes at the sensor output.

When dealing with optoelectronics, the performance (responsivity, quantum efficiency, etc.) of both emitters and detectors is vastly affected by the temperature. Normally this dependence is well documented as part of the system specification, with graphs and coefficients defining the variation of the emitter or detector efficiency with changing temperature conditions [142].

On the other hand, spectroscopy–based sensors, especially those ones working in the NIR bands, suffer from low selectivity due to the overlapping of absorption lines of different compounds. This is a typical situation when samples with high concentration of water need to be monitored. The huge absorption happening due to the water molecules could hide the absorption of other compound that vibrate near the H_2O molecules [143].

3.1.1.12 Hysteresis

Hysteresis is the effect defining a difference between outputs delivered by a sensor measuring the same, depending on the trajectory followed by the sensor. Indeed, this effect impacts on system accuracy and hinders the calibration process because not only instantaneous information about the environmental conditions are required, but also their historic trajectory. This situation is quite common is systems affected by temperature, as it happens with photonic emitters, which at low temperatures are able to self-heat their junction, but when moving from high temperatures to low temperatures, they are not able to refrigerate.

3.1.1.13 Noise, Signal to Noise Ratio

In photo–detectors, the lower limit of signal detection is defined by the noise characteristics of the receiver device and its amplifiers. There are three main sources of noise in any optoelectronic detector system: photon–related shot noise, detector dark noise, thermal noise and amplifier noise. The first three are related to the detector while the fourth one is originated at the signal conditioning electronics (see section 3.1.2.2 Managing the Photocurrent).

Shot noise is inherent in any signal generated by the detector and is caused by the quantum nature of light. Photons arrive at random intervals, and therefore, the number of electrons produced is also random. Additionally, not all the electrons effectively generate photocurrent, and some just get absorbed or recombined. Being the output current defined by the number of electrons in a certain time interval, it is evident that due to the aforementioned factors, the current generation is dominated by random or statistical process. This probability of generating n electrons is defined by a Poisson distribution [144], and its impact of signal deviation is defined by the Eq. 3.1–2.

$$I_{SHOT\ NOISE} = \sqrt{2eI_{Ph}\Delta B}\ (\text{rms noise}) \qquad \text{Eq. 3.1–2}$$

being e the electron charge, I_{PH} the average photocurrent (A) and ΔB the electrical bandwidth of detector amplifier combination (Hz). Notice that the shot noise is independent of the frequency.

Dark noise describes the statistical variation in the number of electrons thermally generated within the detector regardless of the incident photons, and is the electron equivalent of photon shot noise. Then, the dark noise can be considered as another sort of shot noise, but in this case its description is:

$$I_{DARK} = \sqrt{2eI_D\Delta B}\ (\text{rms noise}) \qquad \text{Eq. 3.1–3}$$

being, I_D the average dark current.

There is another source of noise in photo–detectors called the *1/f* noise, which origins are not fully clear but have been correlated with contacts, surfaces and other potential barriers. The noise power is inversely proportional to the modulation frequency *f*, which gives the noise its name. This noise is usually smaller than the shot noise but in low frequencies, when it becomes an important contributor to the detectors noise level. The formulae describing this noise is defined in Eq. 3.1–4

$$I_f = I_{PH}\sqrt{\frac{\Delta B}{f}}\ (\text{rms noise}) \qquad \text{Eq. 3.1–4}$$

being, I_{PH} (A) the average photodiode current, ΔB (Hz) the electrical bandwidth of detector, and *f* the modulation frequency (Hz).

However, normally, the major contributor to the detectors noise is the thermal or Johnson noise of the device shunt resistance, series resistance and load resistance. Johnson noise is originated due to thermal fluctuations in conductive materials which triggers a random electron movement within the conductor. These constant movement of electrons eventually generate micro currents that over a large period of observation represents a net zero power, but in small time interval generates a fluctuation in the photocurrent which constitute the Johnson noise as described in Eq. 3.1–5.

$$I_j = \sqrt{\frac{4kT\Delta B}{R_{sh}}}\ (\text{rms noise}) \qquad \text{Eq. 3.1–5}$$

being, *k* the Boltzmann's constant (1.3807 x 10^{-23} $\boldsymbol{J}$ K^{-1}), T the absolute temperature of the photodiode (in K) and R the equivalent resistance (ohms), and again ΔB the bandwidth (Hz).

Figure 3.1–10 displays the contributions of the aforementioned noise sources across the photo–detectors frequency bandwidth.

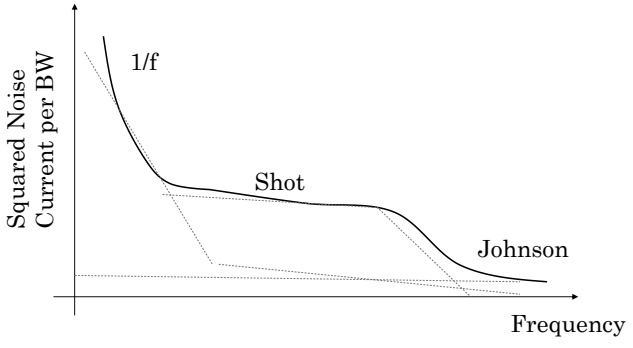

Figure 3.1–10: Distribution of different noise contributors along the photodiode working frequencies.

After having reviewed the photo–detector internal noise sources, one can assume that the output signal from a photo–detector is a chronological sequence of current pulses, each originating from a single photo–generated charge carrier, with a stability affected by statistical and physical factors. The Signal to Noise Ratio (S/N) will represent the proportion of valid or meaningful electrons generated at the photo–detectors over the noisy or undesired ones and the engineering efforts should be focused on increasing this S/N figure of merit.

Eq. 3.1–8 to Eq. 3.1–13 describe how the number of generated electrons depends linearly on the product of I and A, thus, P. Maximizing S/N entails maximizing the signal S and/or of minimizing the noise N. For a given I, increasing S may be feasible by achieving higher P with light–collection optics or by choosing a photo–detector with a larger active area.

With this regard, there is another common parameter for determining the photo–detectors minimum detectable power, described as the noise equivalent power (NEP, in units of W/√Hz), and defined in Eq. 3.1–6, which is the incident optical power yielding S/N = 1 at the output of the detector or the power that generates a photocurrent equal to the rms noise current for 1 Hz bandwidth [145]. Notice that NEP is function of the wavelength of the incident radiation.

$$\mathrm{NEP}(\lambda) = \frac{\text{rms noise}}{\sigma(\lambda)} \qquad \text{Eq. 3.1–6}$$

So far, the photo–detector internal noise sources have been outlined, but there are still important noise sources in the forthcoming stages, exemplified by the amplifier noise. The amplifiers used for conditioning the photocurrent to the needs of the electronic circuitry will amplify both, the signal and the noise, therefore is not straightforward improving the S/N by just adding amplifier stages at the detectors output and different filtering and circuit design approaches (e.g. reduce the bandwidth as much as possible) to keep or slightly enhance the S/N of the photo–detector.

3.1.1.14 Cross–Talk

The cross–talk is the effect by which in a system including an emitter and a receiver, the receiver is directly affected by the radiation generated at the emitter. This measurable leakage of optical energy happening from one optical element to the other, also known as optical coupling, is typical in compact systems, where emitters and receiver sit together, and may arise within the optical receiver from a variety of sources including directly from the optical emitter within or indirectly from the optical emitter via losses.

In addition to the optical cross talk, sometimes, monolithical emitter and detector systems also suffer from electrical cross talk, that may be originated for example at the electrical transmission lines of the optical transmitter and optical receiver.

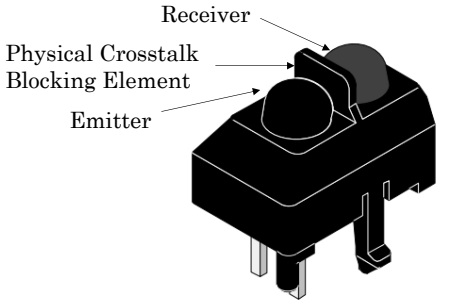

Figure 3.1–11: Example of optical crosstalk mitigation via a physical wall integrated in the TCRT5000 device from Vishay Semiconductor (Malvern, PA, USA), which is a optoelectronic sensors contain infrared–emitting diodes as a radiation source and phototransistors as detectors.

Indeed, this is an unwanted effect because increases the baseline signal at detector, impacting (in addition to the dark current) in the lowest photoelectric current that can be processed as a useful signal in the sensor's detector and defines the sensitivity of the sensor. Therefore, the effect should be mitigated and different approaches have been developed with this regard as physical light blocking elements between emitters and detectors [146] or the use of secondary detectors for compensating the crosstalk signal [147].

3.1.2 Introduction to Photonic Sensor Electronics

So far, we have described the main parameters which objectively define the performance of a given sensor, mainly focusing on the basic processes that enables the sensor converting one type of energy into electrical energy. However, this section will offer a wider view, defining the whole process entailed in the measurement of light, including not only the basic physical principles of light into electricity conversion, but also its effective analogic conditioning, digitalization and processing. Similar process chain is expected when some sort of light modulation is required as a part of the photonic sensor: modulation decision, digital to analog conversion, power stages and electricity to light radiation conversion.

3.1.2.1 Light into Electricity Conversion, Photocurrent

Narrowing down to the specific case of photonics, the energy transduction is possible thanks to three different effects: photoconductivity, photovoltaic effect or photoemission. The process

underneath these transductions, is the reaction of a photosensitive P–N junction of a certain semiconductor under the influence of incident light. When photons of the right frequency hit the photosensitive surface (the P region), due to the energy carried by the photon, *hv,* the valence band electrons are excited to the conduction band, leaving holes in their place in the valence band, thus, resulting in the creation of an electron–hole pair. Under the influence of a bias voltage, these carriers move through the material and induce a current in the external circuit, resulting in a new electron flowing in the circuit per each new e–h pair created.

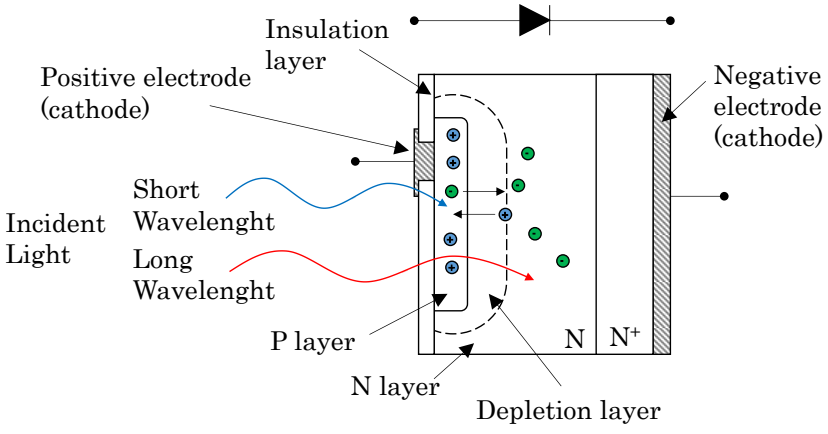

Figure 3.1–12: Schematic cross–section of a photodiode electronic structure.

The capability of the semiconductor lattice to convert the incident photons into electrical energy depends on several factors as the wavelength of the light, absorption coefficient, thickness of P–N layers, doping of the semiconductor, geometry, etc. [148].

This efficiency in energy conversion is normally defined as the Quantum Efficiency, expressed as QE or η, of the detector, representing the number of effectively converted electrons by the number of incident photons. Operating under ideal conditions of reflectance, crystal structure and internal resistance, a high quality silicon photodiode may reach a QE around the 80%.

$$\eta = \mathrm{QE} = \frac{r_e}{r_p} = \frac{\text{Electrons Generated/s}}{\text{Incident Photons/s}} = (1 - R)\xi(1 - e^{-\alpha\omega}) \qquad \text{Eq. 3.1–7}$$

Being R is the reflection coefficient at the air–semiconductor surface, ξ the fraction of the e–h pairs contributes to the photo–current, α the absorption coefficient in the semiconductor material, and ω is the distance where light energy is absorbed. Additionally, r_P represents the photon flux and r_e the electron rate.

The QE is related to the detectors Responsivity, already described in 3.1.1.2, which defines the ability of the detectors to convert the incident radiant energy (in watts), *P*, to the photocurrent output in amperes I_P.

$$R_\lambda = \frac{I_P(\frac{A}{cm^2})}{P\,(\frac{W}{cm^2})} = \frac{I_P}{P}\,(\frac{A}{W}) \qquad \text{Eq. 3.1–8}$$

The radiation energy is defined as the sum of individual photon energy, being r_p the photon flux and $h\nu$ the photon energy

$$P = E_{Photon} \cdot r_p = h\,\nu \cdot r_p \qquad \text{Eq. 3.1–9}$$

$$r_p = \frac{P}{h\,\nu} = \text{number of photons/s} \qquad \text{Eq. 3.1–10}$$

Then, the electron rate r_e and the photocurrent, I_P, may be expressed as:

$$r_e = \eta r_p = \frac{\eta P}{h\,\nu} \qquad \text{Eq. 3.1–11}$$

$$I_P = e\,\frac{\eta P}{h\,\nu} \qquad \text{Eq. 3.1–12}$$

The responsivity may be then written as:

$$R_\lambda = e\eta\,\frac{1}{h\,\nu} = e\eta\,\frac{\lambda}{h\,c} = \frac{\eta\,\lambda}{1.24}\,(\frac{A}{W}) \qquad \text{Eq. 3.1–13}$$

Where h is the Planck Constant (6.63×10^{-34} joule–second), e is the Electron Charge (1.6×10^{-19} coulombs) and c is the speed of light (2.99×10^{8} meter / second), and λ (meter) is the wavelength of the light at which the Responsivity is being given.

But regardless detector responsivity, if the generated photocurrent is not efficiently managed in the following stages within the photonic sensor, the detected information may be lost. The sections below outline briefly the steps required to acquire, condition, filter, digitalize and process the signals outputted by the detector. The low noise electronics and sensor readout circuits is a very wide technological domain and its details fall out from the scope of the current thesis, therefore only a brief introduction is given here. Further information could be found in the topic literature, as the following references [149][150]

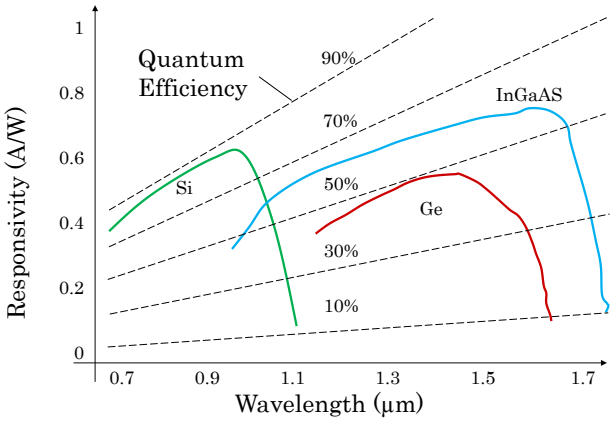

Figure 3.1–13: Responsivities of different semiconductor materials over the visible and near infrared wavelengths.

3.1.2.2 Managing the Photocurrent

The first stage for managing the photocurrent delivered by the photo–receptor is to feed it into a signal conditioning analog circuit, which has the main objective of enhancing the Signal to Noise ratio. This stage normally implies the use of low noise operational amplifiers, filters, compensations, etc. with the objective of delivering a clean and amplified signal to the next stage.

The next step is the signal digitalization, which requires to introduce terms as the sampling frequency, Nyquist[28] frequency, aliasing and quantification resolution. The digitalization entails converting a signal from a continuous time and amplitude (either volts, amperes or watts) domains, to a digital domain with quantified observation times and quantified signal amplitudes. The quantification of the time domain is represented by the sampling frequency of the digitalization system, which defines the specific time instants where the value of the amplitude is latched. Defining the sampling frequency is not straightforward, and the original signal bandwidth should be taken into consideration to avoid odd effects as the aliasing. The aliasing defines the situation originated when a signal with a certain maximum frequency is under–sampled, generating a false representation of the original signal.

The aliasing could be prevented if the sampling frequency meets the Nyquist criterion, which sets the minimum sampling frequency as the double of the signal's maximum frequency (see Eq. 3.1–14).

$$F_{Sampling} >= F_{Nyquist} = 2 \cdot F_{MAX} \qquad \text{Eq. 3.1–14}$$

[28] Harry Nyquist, Swedish engineer (1889-1976)

However, even if the signal frequency spectra may be known, the noise is spread all over a wide bandwidth, so to avoid artifacts generated by the aliasing, it is recommended to include a low pass filter to reduce all the energy belonging to frequencies above the signal's maximum.

Therefore, once the signal has been filtered and sampled, the quantification starts, which is the last step for getting a digital representation of the original photocurrent. The quantification means to assign a digital value within a scale to the analog amplitude. Indeed, the maximum and minimums of the digital scale should match the peak values of the analog signal in order to maximize the use of the whole scale.

These digital values, as it happened with the sampling instant, are discrete steps, being the number of available steps defined by the number of bits and the range of the analog signal to cover. The resolution describes the analog signal span (normally in volts) represented by each increment in the digital value.

$$N_{Steps}(V/bit) = \frac{A_{Max-Signal} - A_{Min-Signal}}{2^{n\ bit}} \qquad \text{Eq. 3.1–15}$$

It may happen that different analog values are converted into the same digital value if enough resolution is not available. Therefore, some engineering is required for defining the minimum length in bits for the digitalization.

3.1.2.3 Processing the Signals

Once the signal has been properly converted into the digital domain, and represented by a train of digital values updated at the sampling frequency, its processing may start. Normally, the signal processing is accomplished in a processor that performs different digital signal treatments and calculations to extract relevant information contained in the digital signal. Sections 3.1.5 Smart Sensors and 3.2.2 Analysis of photonic information provide more information about the calculations that may be applied in the processors.

After the relevant information has been extracted, it may be stored, displayed or communicated away.

3.1.3 Quantitative, Qualitative and Indirect Measurements

The final objective of any sensor is to offer a valuable information about parameters, status, quantities, etc. of a certain measurand. However, the way of getting this information and the nature of the requested data is not always the same.

Basically, the measurements can be a direct translation of a physical or chemical effect into an electric magnitude. In these cases, the working principles are defined as a Direct Measurement method, as it happens with elongation sensors, where the net elongation distance generates a change in the resistivity of the elongation transducer.

Alternatively, the data delivered by the sensor can be the result of several calculations applied to the parameters observed. These situations define the Indirect Measurement methods, which require more steps, are more prone to cross–sensibilities, and normally are only used when the direct measurement is an inconvenient [151]. However, there are several examples based on indirect measurements offering very valuable information about the process being monitored [152].

In the photonic field, examples of direct measurement methods are found in: observation of the color of the measurand, measurement of the absorbed intensity, opacity and reflectivity measurements. For instance, quantifying the light intensity emitted by a fluorescent dye can be considered as a direct measurement [153], because the intensity is directly proportional to the concentration of the fluorophore, as depicted in Figure 3.1–14.

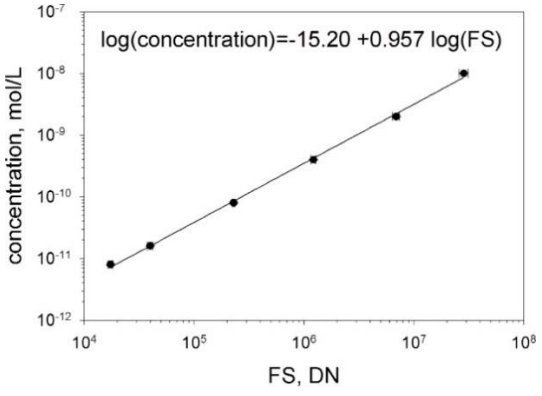

Figure 3.1–14: The plot of the log of the concentration of a fluorophore solution versus the log of the integrated fluorescence signal (FS) associated with the known concentration. The ideally linear response has a slope of 1.0. [153].

Another example of direct measurements performed by photonic sensors is found in the particle counting, where the effective detection and classification of particles suspended in a fluid is accomplished by directly imaging (Figure 3.1–15) them and analyzing by machine vision algorithms (see section 3.2.2.3).

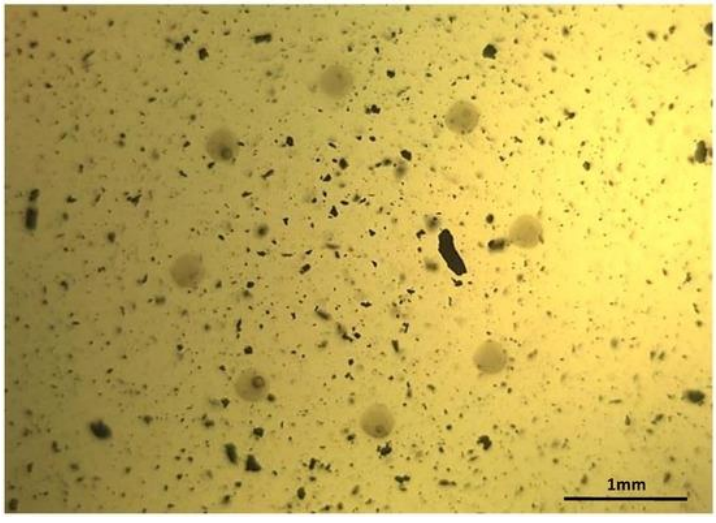

Figure 3.1–15: Image of a real lubricant sample from a gearbox in a wind mill, where large and small particles suspended in the fluid can be observed directly applying a photonic setup.

On the other hand, when a certain parameter of the sample is inferred from these basic direct measurements offered by the transducer, we talk about indirect method. For instance, chemometric methods (see section 3.2.2.2) are a clear example of indirect methods for determining a certain parameter of the sample, because based on the absorbance happening over a range of wavelengths, and the empirical results obtained from a reference sample collection, the value of the parameter of interest is calculated through mathematical calculations. Among a vast number of examples, determining the geographical origin of red wines based on their UV–VIS–NIR absorbance patterns is classical application of chemometrics–enabled indirect measurement [154].

Figure 3.1–16: The changes in the oil color have several causes, so measuring the color does not offer a direct measurement of any of them due to the lack of selectivity of the measurement principle.

Another example of indirect measurement deals with the lubricant degradation, which is somehow associated with a change in the oil color that becomes more reddish and opaque (see Figure 3.1–16). The two most common causes of oil darkening are thermal stress and oxidation, thus, tracking the color changes could be used as a value of the status of the oil. However, the color observation can never deliver a direct measurement of oxidation, nor about the thermal stress, because both processes cause the same consequence, the darkening of the oil [155].

Regardless of the measurement method, direct or indirect, the nature of the sensor results also deserves a clarification. Understanding the differences between qualitative and quantitative analysis is relevant for any sensor application, because the approach, objectives and challenges are totally different depending on the expected result type.

The minimum operation normally requested for a sensor system is to offer a Qualitative analysis of a certain property of the measurand, which means giving a categorical response based on observed parameters or conditions of the sample. The main objectives while delivering a quantitative analysis are either to identify or to qualify the new sample according to previously defined groups.

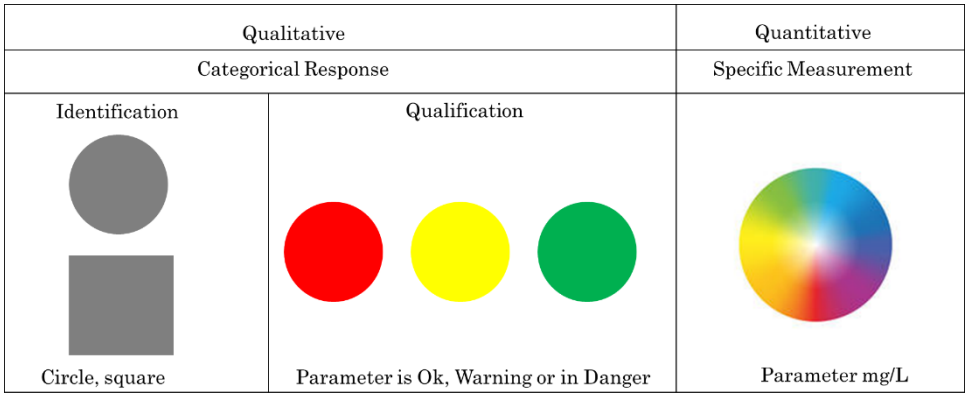

Figure 3.1–17: Differences between qualitative and quantitative measurements.

When a sensor is supposed to identify a sample, it needs to discriminate it as belonging to one of at least two well–defined groups. The qualification goes one step further, and the samples are classified in groups depending on defined thresholds, that categorize the samples based on quality, etc. On the other hand, a sensor delivers a quantitative analysis when is able to output specific information about the process or the measurand being observed, as it happens, for instance, when the sensor outputs the concentration of the unknown sample composition in real time [156][157].

3.1.4 Cost of Sensors

Already introduced in the section 1.3 Cost Effective Smart Photonic Sensors, the true cost of a sensor solution is far for being limited to the device cost, and several other factors increase significantly the Total Cost of Ownership [158]. The cost accounting for any measurement system deployed in the field should always considered the impact of the items outlined in the Table 3.1–1. The photonics–enabled in–line sensors are not an exception, and costs concerning calibration, installation and maintenance are sometimes one order of magnitude bigger than the device cost.

Table 3.1–1: Concepts impacting on the Total Cost of Ownership of industrial sensor systems.

Other costs	Description
Installation	Requirements of any extra mounting system for installing the sensor, installation and setup times and skill and knowledge required for deployment (e.g. technician, engineering work)
Cabling, Connectors, Signal Conditioning, Data Receivers,	Requirements for power or communications cabling, as well as the need of data receivers (PLC, SCADA, PC, Ethernet Switch, etc.)
Reliability	Implications concerning the lifetime of the sensor product and its mean time before failure (MTBF), as well as the reliability statistics. These unexpected failures may impact on the end–users' equipment unscheduled downtimes.
Scheduled Down time, Calibration	Requirements in terms of sensor calibration or maintenance, calibration frequencies, time to accomplish it, can it be done in–situ or the sensor needs to be taken away from the installation point.
Repairs	Implications regarding product reparability and the disposal costs at the end of the lifetime. Requirements for reparations similar to calibration ones, can it be accomplished in situ?
Usability	Requirements for any other external equipment or software to process the signal outputted by the sensor.

Lead time	Implications regarding the lead time of the sensor. Long manufacturing time may require producing a sensor inventory which generates stocking expenses.
Environmental Protection	Requirement of any specific enclosure to be used on certain environments? (e.g. ATEX for explosive atmospheres)
Shipping	Requirements in terms of shipping cost that depend on product volume, weight and on shipping conditions (e.g. is it care handling required?)

3.1.5 Smart Sensors

Even if the term Smart Sensor may have been hyped in the last decade, in its origins, it entailed a whole new vision on how to understand the sensors, their use and their design. First introduced in late eighties [159], the smart or intelligent sensors presented a new paradigm for presenting the signals measured to the operators: the raw signals needed to be processed and combined and delivered in a normalized way either to a display or to a PC system for further processing [160]. This new approach paved the way for the digitalization of the analog transducers, benefiting from the breakthrough in embedded processing capabilities that was about to become a reality.

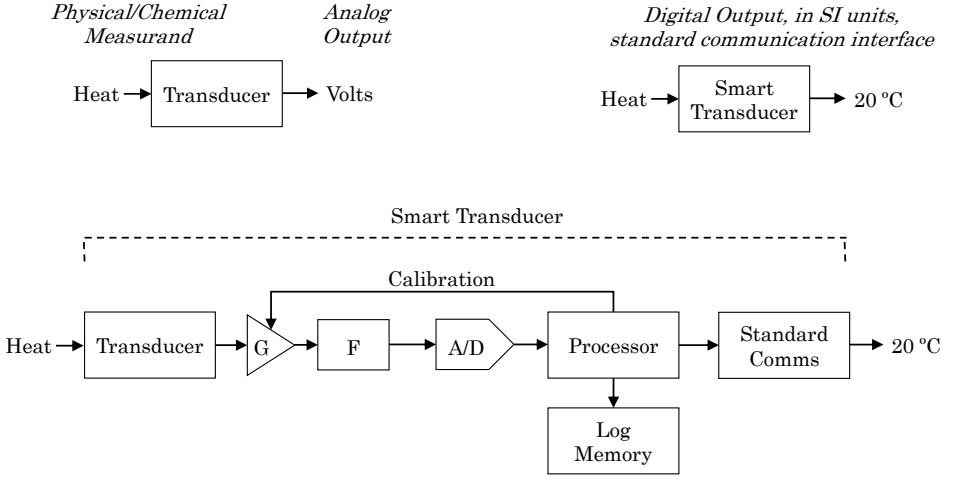

Figure 3.1–18: Difference between a traditional analog transducer and a Smart one, additionally displaying all the modules entailed in an intelligent transduction.

The structure of a Smart Sensor basically includes all the blocks already mentioned in the section 3.1.2 where the different

electronic modules required for a sensor system were introduced. Thus, a Smart Sensor needs to include all the transducer, analog and digital stages to acquire, condition, filter, digitalize, process, calibrate, store and communicate in a standardized way a measurement information, as depicted in Figure 3.1–18.

A smart sensor can be a monolithically integrated system, with all the components sharing the same semiconductor lattice, or alternatively, it could be based on hybrid approaches, where the transducer and the digitalization and processing parts belong to different manufacturing processes or even stand physically in different components as off the shelf modules (see Figure 3.1–19 and Figure 3.1–20) [161]. During the last few years, almost all of the photonic sensor systems where based on the integration of different components (emitters, detectors, optics, processors) into compact settings, however, recently, the heterogeneous integration technologies is moving one step forward and complete systems are being integrated in the same chip [162][163], either sharing the semiconductor die, as it is the case for VIS region solutions with monolithic silicon chips, or merging different technologies as InGaAs and Silicon for the NIR region solutions.

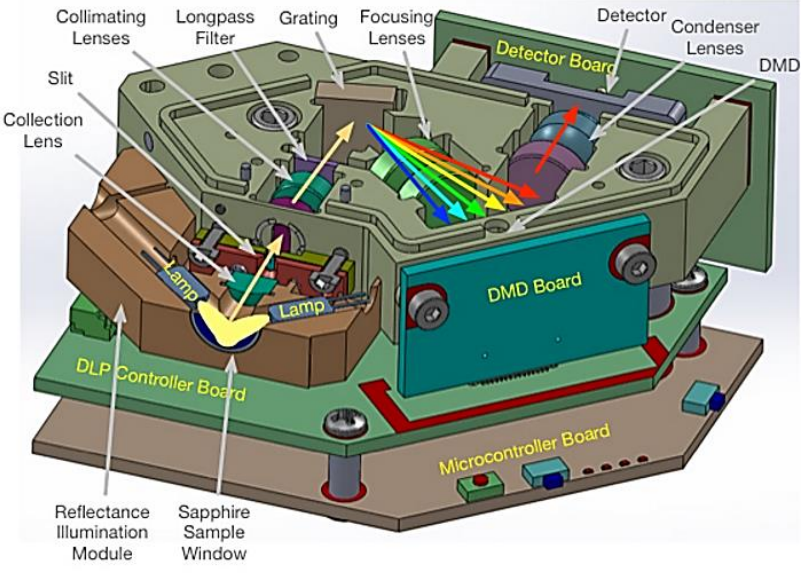

(a)

(b)

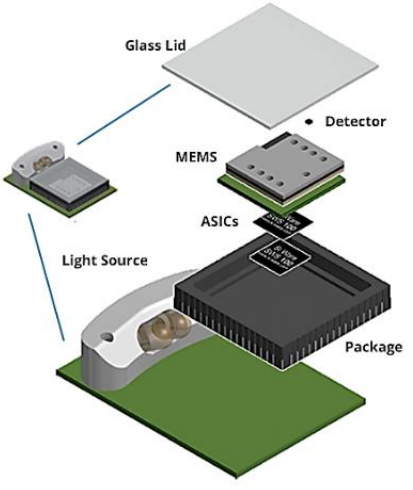

(c)

(d)

Figure 3.1–19: (a) and (b) display the 2014 Texas Instruments NIR spectrometer, which achieved a high compactness integrating different off–the–self components. (c) And (d) show the block diagram and the effective chip size of the NeoSpectra Micro device from Si–Ware launched in 2017.

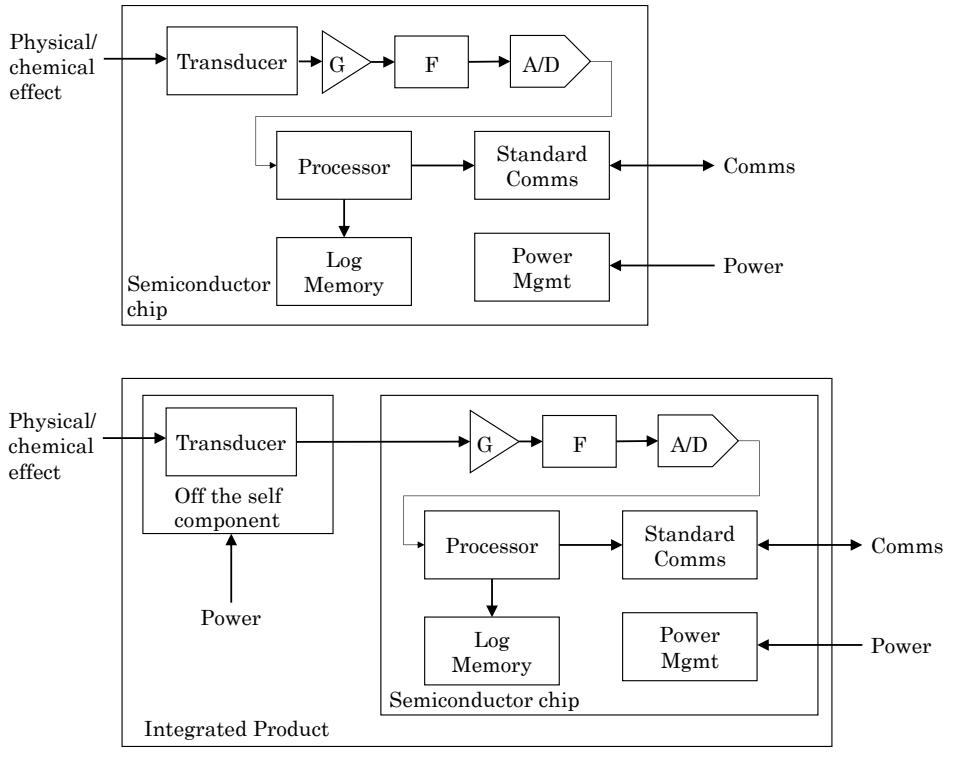

Figure 3.1–20: Smart Sensor Chip integrated in the same semiconductor die or smart sensor product, comprising different components but delivering the same inputs/and outputs as the chip version.

The following sections define the main functions expected for a smart sensor system, according to the IEEE 1451 Smart Transducer Compliant standard [164].

3.1.5.1 Compensation,

An intelligent sensor is expected to accomplish an internal evaluation about the reasonability of the measured values, controlling the dynamics of the changes at the input, checking it with the short and long-term evolutions, etc. Additionally, the intelligent sensor needs to be equipped with internal offset and drift compensation system and offer programmable gains to maximize the ADC ranges, etc.

According to the IEEE 1451 standard, smart sensors should store any factory calibration information in the sensor's internal memories.

3.1.5.2 Computation,

There are different sort of computation elements included within the smart sensor processing means, including the signal conditioning (digital filtering), logic functions as triggers and alarms,

data reductions as feature extractions, decision making and classifications, etc.

3.1.5.3 Communications

Smart sensors include a set of standardized interfaces to communicate the results, alarms, etc. and to receive parametrizations and new calibration data. These standardized solutions include not only the communication logic and protocols, but also the electrical and mechanical characteristics of the connection means as described by the IEC 61076 standard family [165].

In case of wireless communication systems, several protocols and solutions available (e.g. Wireless Hart, WIFI, Thread) for connecting sensors with each other or with gateways or centralized systems.

3.2 Photonic Sensors

So far, the different characteristics of the sensor systems have been introduced, outlining the performance indicators and describing how to upgrade a traditional transducer into a smart sensor system. During this section, we will move on to the specific case of the photonic sensors, describing some of the different sensor settings utilized for implementing a measurement technique (section 3.2.1) and introducing the different computing approaches to process the signals obtained with the presented sensor settings (section 3.2.2).

3.2.1 Photonic Sampling and Sensing Techniques

This section describes different settings for implementing certain photonics–based measurement principles, describing the layout and configuration of the different optoelectronic components and the basic physical processes involved in the working principles.

Sampling Techniques refer to how the sample, light source and light detector are arranged for performing the photonic inspection. Even if general principles are very well known in analytical chemistry, several practical issues rise when moving to in–line operation, and therefore, this section will focus on these practical problems. Sampling techniques need to deal with angles of incidence, angles of observation, mechanical and optical tolerances, wavelengths of interests, absorbance of the mediums between photonic elements and sample, etc. with the aim of maximizing the effects of interest for the effective sample measurement.

Notice that, the different cases described here do not represent the totality of photonics–enabled measurement techniques available in the scientific community, but the ones includes in this section have been considered as good candidates for being implemented in the specific case of in–line monitoring of fluids. Thus, transmission, reflectance, and Raman spectroscopy, fluorescence and in–line microscopy are presented.

Methods such as Laser–induced breakdown spectroscopy (LIBS), Attenuated Total Reflectance (ATR) settings, Plasmonics setups or the Tunable diode laser absorption spectroscopy (TDLS) have been also considered as techniques susceptible to contribute in the field of the in–line sensor, but due to the complexity in the settings or due to the high cost in components have not been covered in the current review.

3.2.1.1 Transmission/Absorption Sampling Setup

This is one of the most common sampling technique for analyzing non–opaque fluids and gases. The basic setup displays the excitation light source, the sample, the holder optics and the detector aligned in different parallel planes. It is a traditional sampling technique for in–line inspection of fluids and gases at industrial processes, either bypassing the main flow or directly attached to it. The excitation light beam travels across the sample, and its properties get modified due to the absorption generated at the molecular groups, and due to the attenuation occurring while penetrating in the sample volume. Consequently, the light received at the detector is characterized by the properties of the sample and the medium, at its post processing could give significant information about the chemical and physical composition of the sample.

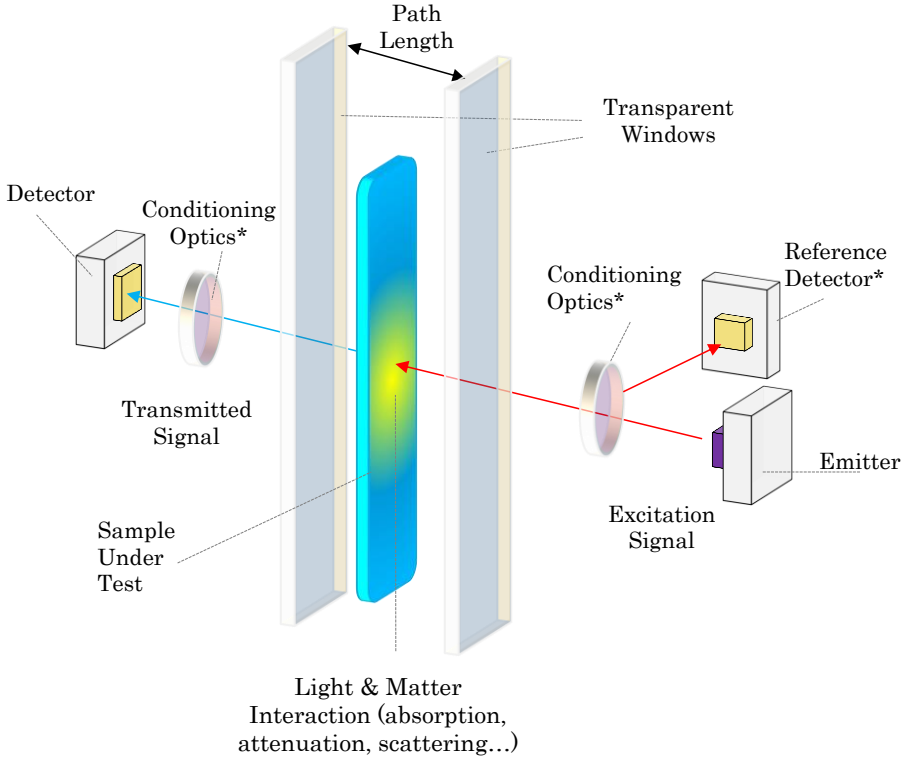

Figure 3.2–1: Schematic overview of the main components for a transmission/ absorption measurement setting. Some components, marked with *, are optional.

The basic setup for a transmission/absorption measurement setting requires to integrate different components following the mechanical and positioning arrangement depicted in Figure 3.2–1. The emitter should be chosen considering the required light power and spectrum, being its stability and reliability under changing thermic and vibration conditions an important feature to consider. The

receiver is also a fundamental part, and depending on the application, a single photo–receptor, a 2D imager or a complete spectrometer may be integrated. Occasionally, some light conditioning, filtering or focusing may be required to maximize the throughput of the system; however, simple setups with emitter and receiver working with open air interfaces are also feasible. Then, two windows fabricated in transparent material should be used to confine the sample under test. Depending on the hydraulic requirements (pressure and temperature of the fluid) and the working wavelengths, different materials (e.g. PMMA or PS plastics, borosilicate glass, quartz, sapphire) and thicknesses will be required. The width of the window will be defined by the diameter of the emission and reception radiation beams.

The separation between the windows is defined by the desired sample path length. Fluid viscosities, working pressures, etc. should be taken into consideration if very narrow (250 μm – 1 mm) are required.

Asides the free space losses[29], the physical processes governing the modifications happening into the light while crossing the sample include reflection, absorption and scattering. This generates a wavelength dependent attenuation in the light power that gets to the detectors. As described in section 2.1, in low concentrations, where analyte molecules are individually solvated and do not noticeably perturb the solvent, absorbance is well described by the Lambert–Beer law. However, as the absorbance increases (e.g. $A > 3$) [166][167], the changes in concentrations may tend to form molecular clusters, modify the solvent structure, etc. that may also change the refractive index of the sample, impacting both, in the reflected light power and in the absorbance itself, as described by the Kramers–Krönig relationships (see section 2.1.4, 2.1.7 and 2.1.10).

The main challenges in transmission/absorption settings is to assure a stable or at least known emission power and spectrum. Otherwise, changes in the source may be wrongly recognized as changes in the sample under test. Therefore, sometimes, a secondary receiver is used to verify and compensate changes in the emitted light. In these cases, a beam splitter may be used, but in other simpler configurations, the detector is mechanically placed towards the emission beam, receiving a part of the radiation lobule.

In this kind of configurations, the tolerances of the optical, optoelectronic and mechanic components are important for assuring that the optical power budget remains as designed. Depending on the optical components, the required positioning accuracies may. Additionally, notice that for quantification applications, the accuracy

[29] The free space power losses (FSPL) are described by the Friss Formula as $FSPL = (4\pi \times D/\lambda)^2$, being the losses negligible if distances are small.

in the path length becomes critical, since the absorbance happening at the sample is logarithmically bonded to this distance.

This kind of settings are very useful for measuring changes in opacity, turbidities, fluid color, and chemical analysis through UV, VIS or IR spectroscopy, provided that the absorbance of the sample allows significant light power being transmitted across the sample. If this is not the case, as it happens with very opaque fluids as lubricants for gas engines.

3.2.1.2 Reflectance Sampling Setup

When the fluids to be monitored present a high opacity in the wavelengths of interest, and even with very narrow path lengths very little power is transmitted across the sample, diffuse reflectance settings may be used as inspection method [168].

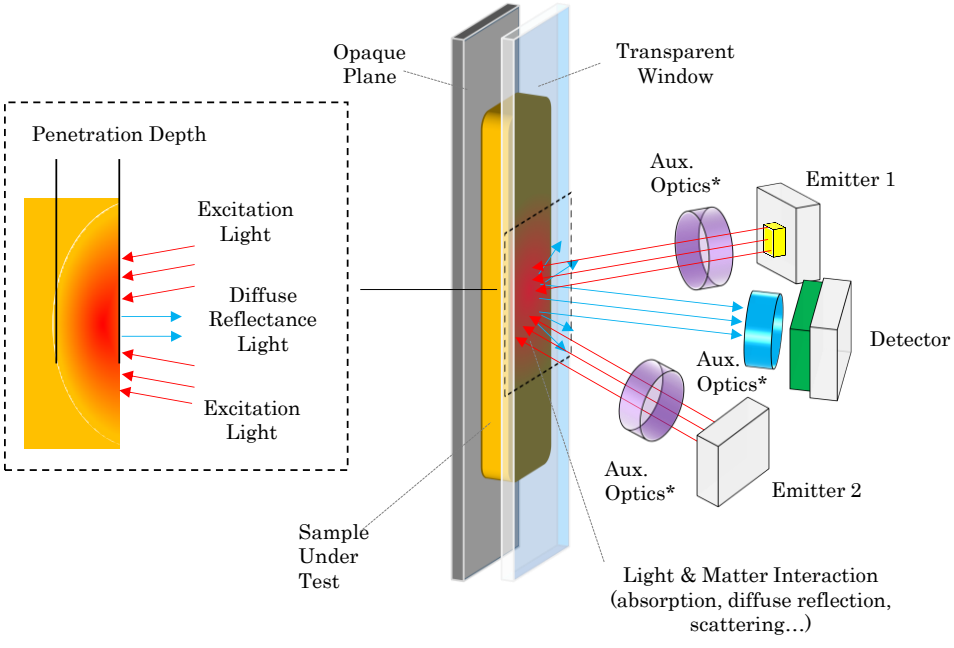

Figure 3.2–2: Schematic overview of the main components for a diffuse reflectance measurement setting. Some components, marked with *, are optional.

The fundaments of this sampling methods rely on the analysis of diffuse reflectance, which, as described in chapter 2, is the consequence of the penetration and multiple diffusions and reflections of the incident photons within the sample. A proportion of this excitation radiation may exit the sample at any angle, but due to its diffusion across the sample particles, it also contains information about the absorption of the material, because mainly the non–absorbed wavelengths are prone to exit the sample. Therefore, this

diffuse reflectance contains similar information to those acquired through a transmission setup.

However, in addition to the diffuse reflectance which carries information about the absorption properties of the sample, reflected radiation is also contributed by the specular reflection happening at the sample surface due to the changes in the refraction index between the two media. Actually, this specular reflection is the main contributor to the distortion of the diffuse reflectance spectra, generating changes in band shapes, their relative intensity, and, occasionally, it is liable for complete band inversions, due to Restrahlen effect [169].

Other factors such as the refractive index of the sample, particle dimensions, packing density, homogeneity, concentration and absorption coefficients of the sample are also susceptible of influencing in the quality of the reflectance spectra [170].

From the analytical point of view, the complexity inherited from the factors described above, combined with the intrinsic statistical distribution of the reflected radiation angles (as described in section 2.1.10), hinder the extraction of any reliable linear relation between reflectance band intensities and concentration of the target compound [171]. In this situation, Lambert–Beer law is not applicable, and even if approaches like Kubelka–Munk's (see section 2.2) could be used to estimate concentrations in reflectance setups, diffuse reflection measurements are mostly limited to semi–quantitative analyses

Diffuse reflectance working principle depends on the focused projection of the detector beam into the sample where the excitation light is being reflected, scattered and transmitted through the sample material. The back reflected, diffusely scattered light, a part of which is absorbed at the sample molecules, is then collected by the detector optics. Only the part of the beam that is scattered within the sample (suffering the absorption by the molecules) and returned to the surface is considered to be diffuse reflection and it is the one used for further processing.

Therefore, from the optical point of view, it is very important to control the intersection points between the area of the illumination spot and the Field of View, Focal point and Deep of Field of the detector. The probabilities of having effective absorbed and reflected radiation are much higher in the nearby of the illumination spot, so the detector must be focused on this volume for maximizing the collection of diffuse reflectance spectrum as depicted in Figure 3.2–3. This spatial coincidence normally requires setting the emitter and detector in a certain angular arrangement, which increases the mechanical integration difficulty. Additionally, the use of optical

components for maximizing the light collection at the detector, such as collimator lenses is also quite common in reflectance setups [172].

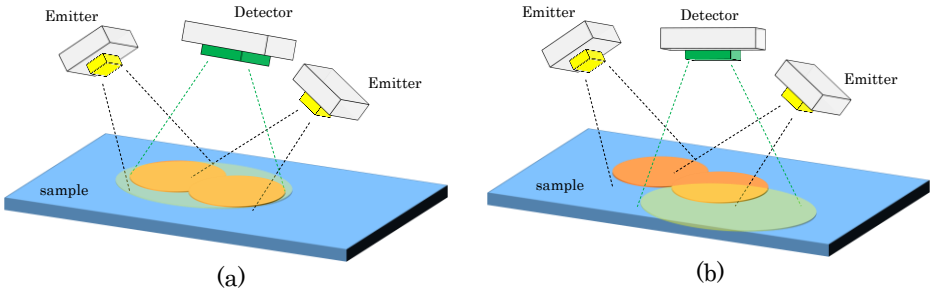

Figure 3.2–3: (a) illumination spot and detector's field of view coincidence. (b) Illumination spot and detector's field of view mismatch.

Additionally, the lack of awareness about the penetration depth may result in completely inaccurate results because the absorbance may be happening at layers outside the sample volume, for instance in the opaque plates used at the back of the samples (see Figure 3.2–2) [173] [174] [175].

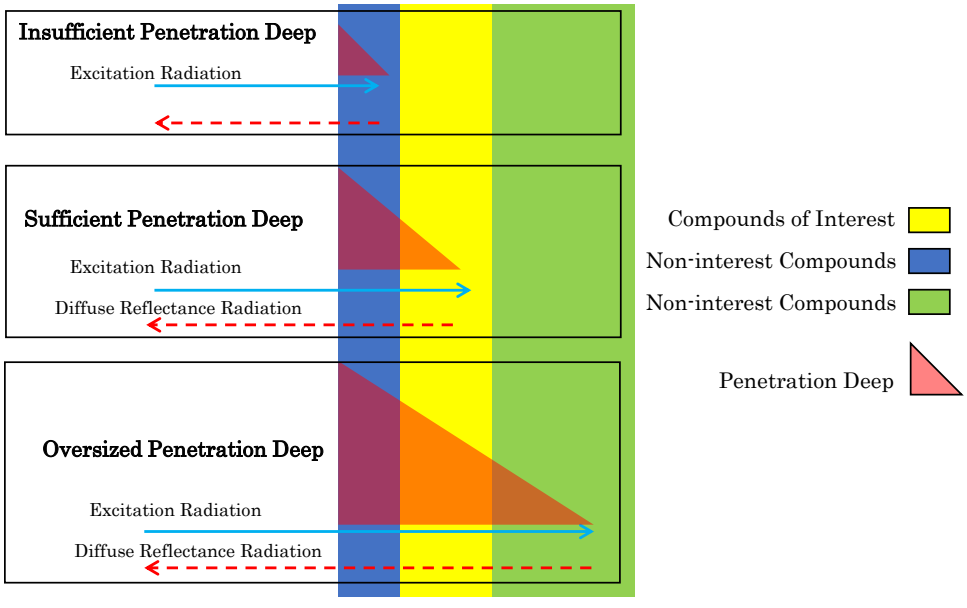

Figure 3.2–4: The penetration deep should match the volume of the compounds of interest localization in a non–homogeneous sample, otherwise, the diffuse reflectance spectrum will contain the absorbance properties of the non–interest compounds. Therefore, the excitation power should be carefully tuned to the sample requirements.

3.2.1.3 Fluorescence Setup

The inspection of the matter through fluorescent setups require understanding that, alike the previously described techniques, fluorescent analysis is not measuring changes occurring in the excitation light, but changes occurring in the sample itself while being illuminated. Under this approach, the excitation subsystem needs to assure a light source fulfilling stability, power and spectral requirements, which is able to illuminate the sample volume under inspection. Additionally, the detection subsystem needs to be able to collect the signal emitted by the sample, getting rid of any other stray light generated within the inspection system.

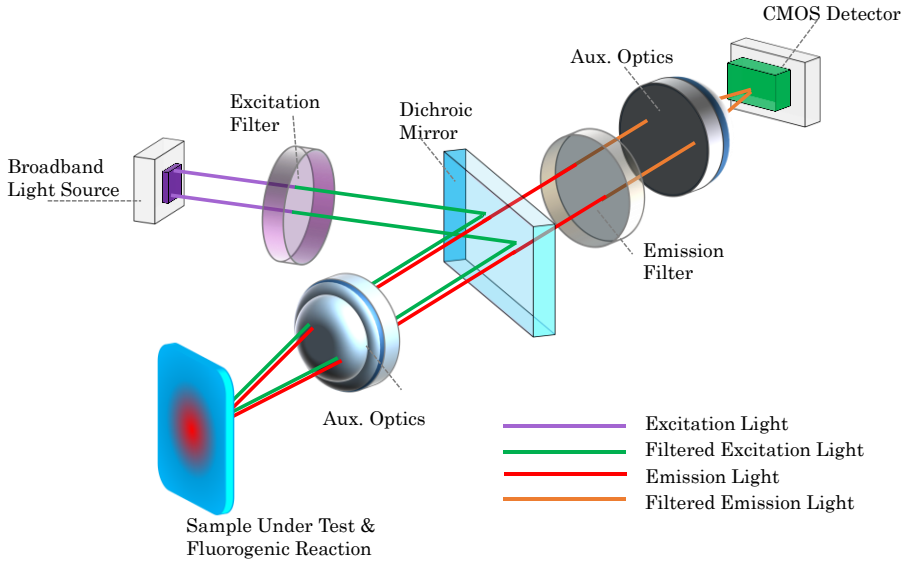

Figure 3.2–5: Fluorescence Setup based on Epifluorescence setting.

Traditional setups for fluorescent analysis, as the epifluorescence microscope, rely on dichroic mirrors, which are elements used to selectively reflect light of a range of wavelengths while transmitting others (see Figure 3.2–5). This setup requires a high-power lamp source, traditionally a mercury or xenon arc lamp but nowadays being replaced by solid state LED solutions. An excitation filter transmits the band of the excitation radiation, blocking undesired bands to avoid noise sources. The excitation radiation is reflected by the dichroic mirror towards the optics that condense the light on the sample. The excitation light triggers the fluorescence process, and radiation emitted by the fluorophore molecules is collected by the same lens and is transmitted by the dichroic mirror towards the detection optics.

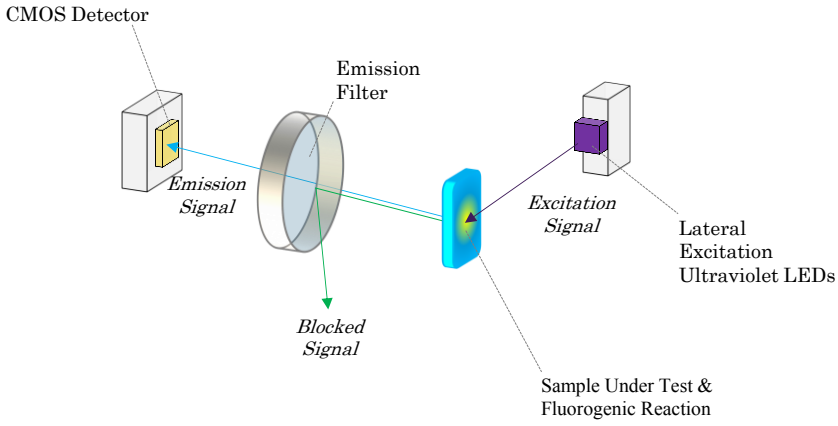

Figure 3.2–6: Orthogonal Excitation–Detection setup for Fluorescence Sampling.

Even if the dichroic mirror based setups are really simple and usually fit in in–line measurement cells, the cost of excitation and emission filters (100€ each) along with the cost of dichroic mirror (100€) and the assembly tolerances for the mirror placement (+–5º) could jeopardize the low costs objective. Alternatively, reduced bill of material configurations can be reached making the most of novel narrow band and narrow beam emitters and orthogonal excitation and detection setup.

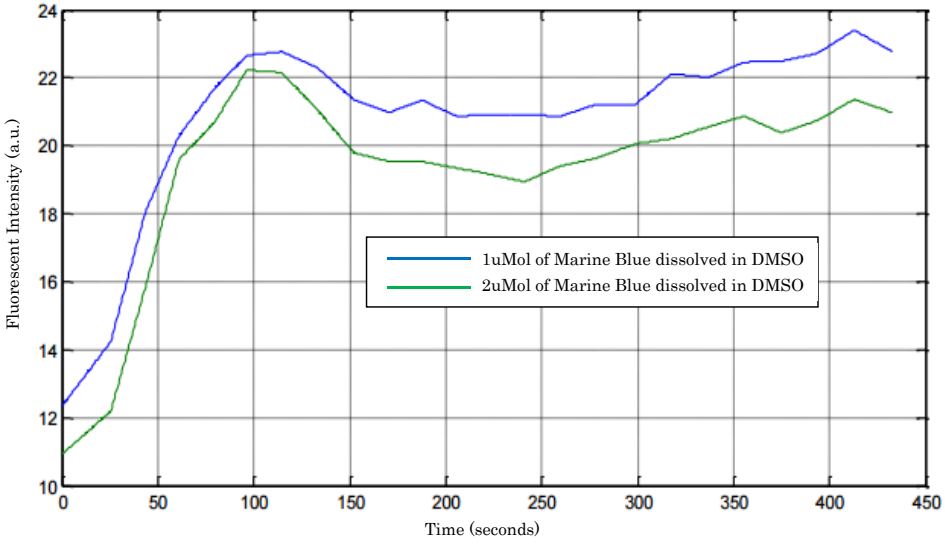

Figure 3.2–7: Example of an emission signal level readout for 450 seconds, for two different concentrations of fluorophore.

It should be taken into account that normally, fluorogenic reactions are not immediate and follow a non–constant time response (e.g. enzymatic fluorogenic responses are normally logarithmic). Therefore, the fluorogenic sampling techniques need to measure not

only the intensity of the emission signal of a given sample, but also its variation across the reaction time (see Figure 3.2–7). This may require stablishing a light modulation approach (e.g. on–off cycles) to avoid overheating in the excitation emitters, due to the long monitoring cycles.

Additionally, notice the importance of sample volumes when measuring fluorescent reactions, especially when very low sample quantities have to be handled, because linearity and detection limits are affected by the sample volume [176]. In general, the greater the sample volume under inspection, the lower the upper end of the linear range, and the lower the limits of detection. There is a clear dependency between the fluorescent intensity and the sample volume excited by the light. Basically, hitting larger volume, at a given concentration, means hitting more molecules, which will generate larger emission signal. Figure 3.2–8 shows this mentioned effect.

Regarding the materials used in fluorescence setups, these not only need to meet the optical requirements of transparency, filtering, etc. but also the auto–fluorescence of the materials needs to be validated. This is especially critical when plastic materials are used within the sensor, because they tend to display much more auto–fluorescence signals than glasses or metallic parts. However, if the auto–fluorescence spectrum falls out of the emission spectrum band, the filters at the detectors may eliminate the unwanted signals.

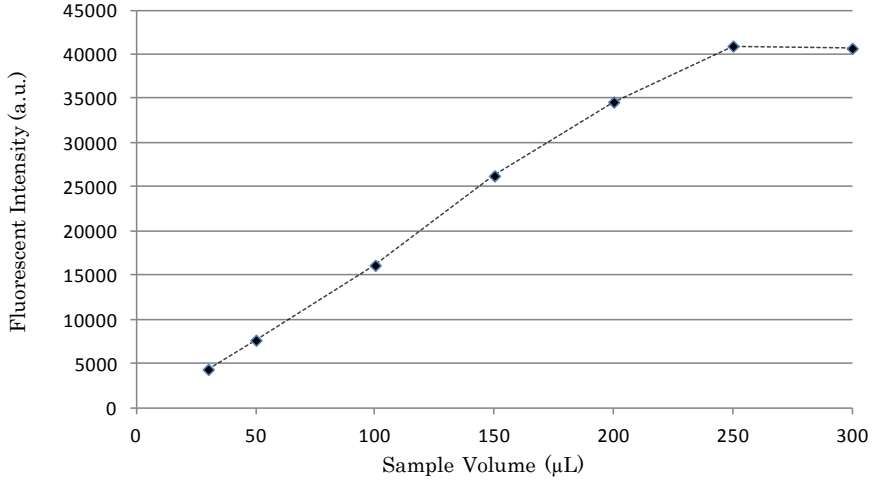

Figure 3.2–8: Results of the fluorescent signal emitted by 1uMol concentration of Marine Blue dissolved in DMSO[30]. Maintaining the photonic configuration (Fluostar Optima, BMG Labtech, Gain: 1400, Excitation Filter 365nm, Emission Filter 470nm) and changing the inspected sample volume the differences in the emission signal are evident.

[30] Marine Blue succinimidyl Ester (M-10165, Molecular probes ThermoFisher). DMSO: Dimetilsulfóxido, (SU0159, Scharlau)

In Fluorescence processes, alike in the Raman ones (see next section), the excitation wavelength must be thoroughly chosen, because even if the absorption spectrum of fluorophores is relatively wide, compared to the emission one, there is always an excitation frequency at which the fluorescence process becomes much more efficient. However, this optimum excitation wavelength is normally relatively near to the emission band, and choosing it requires higher expenses in signal filtering (see Figure 3.2–9).

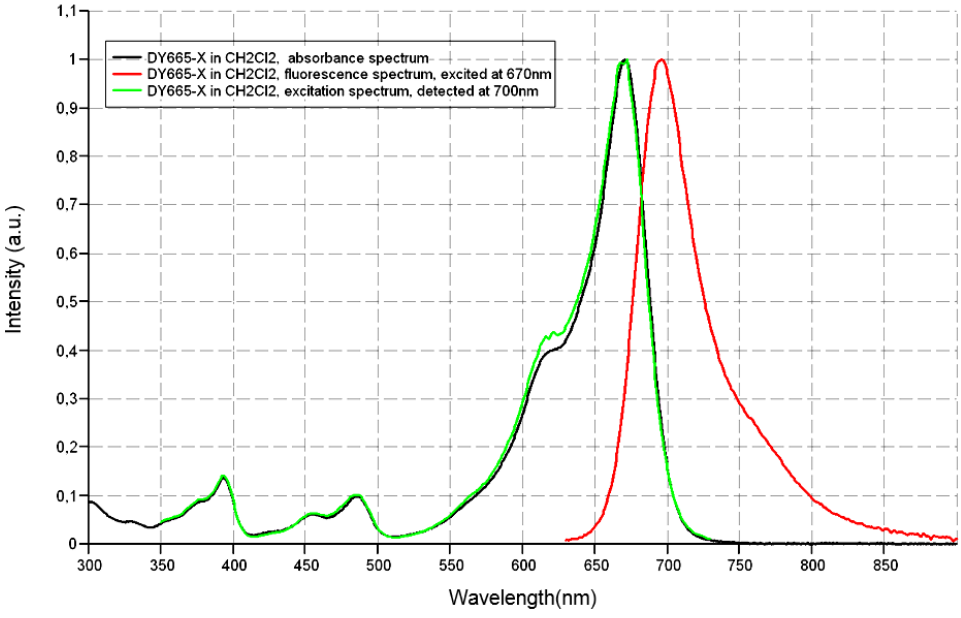

Figure 3.2–9: Emission and excitation spectrums of the DY665–X NIR fluorophore dye in CH_2CI_2 [177].

3.2.1.4 RAMAN Setup

Low signal levels expected in Raman scattering based photonic sensors, with approximately only one in every one million incident photons being scattered via the Raman Effect, requires a complex system setting that represent a true challenge to implement in low cost and in–field deployment. However, thanks to Raman's immunity to water absorption bands, it is an interesting method to analyze fluids with a high proportion of water molecules in them.

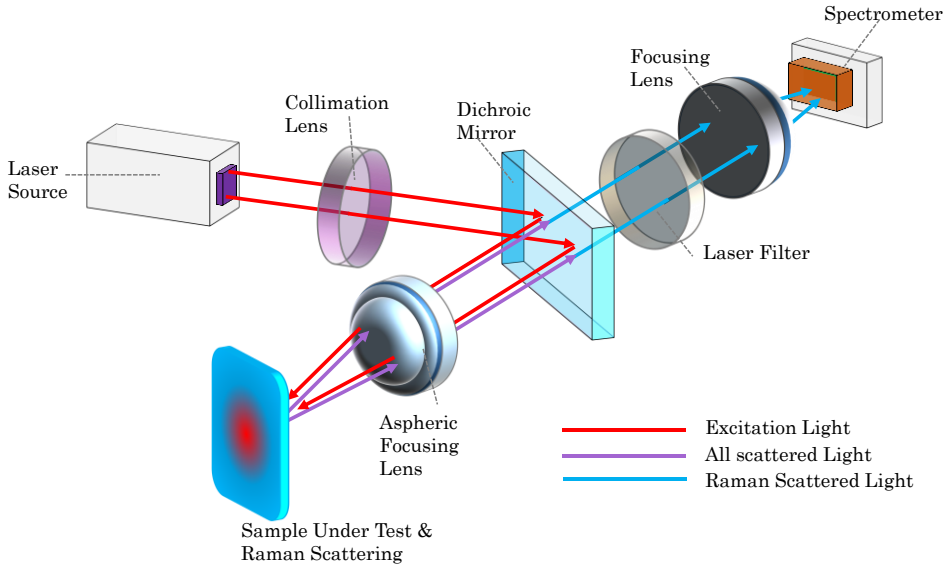

Figure 3.2–10: Block diagram of a typical Raman–based sampling setting.

Raman effect based sensor system analyzes the spectrum results that return from the sample after being excited with a monochromatic light, typically from a laser. A sample's Raman signature displays a series of signal peaks that are shifted in wavelength from the excitation source, offering the molecular fingerprint of the analyte. Figure 3.2–10 represents a standard Raman sampling setup, where the target sample is illuminated through a dichroic mirror and the scattered light is captured by optical elements, which filter all other scattered or reflected light except the inelastic Raman scattered signal that is focused back to a spectrometer detector [178].

Perhaps, the most important decision when selecting components for a Raman system is the excitation wavelength. Notice that Raman shift is a measure of the amount of energy between vibrational energy levels for bonds within the analyte, which is solely a property of the molecules itself and independent of excitation wavelength. However, the returned Raman signal intensity does depend on the excitation wavelength, being proportional to the inverse of the wavelength to the fourth power

$$\text{Intensity}_{\text{RAMAN}} \propto \frac{1}{\lambda_{EXCITATION}^{\ 4}} \qquad \text{Eq. 3.2–1}$$

In addition to this relation with the expected Raman intensity, the excitation wavelength must be chosen taken into consideration the fluorescence properties of the material under analysis, because the signal baseline generated by compounds fluorescence is one of the most important noise sources in Raman Spectroscopy. For instance, many organic compounds fluoresce in visible range (around 300nm to

800nm), so if these organic molecules are to be monitored with Raman UV or IR excitation would be preferred.

Regardless of the wavelength choice, due to the high intensity requirements for the excitation, LASERs are required as sources in Raman settings. Diode lasers in the range of 100mW, available in standard TO–56 packages which include beam filtering optics and heat sinks are a possible alternative for compact and relatively low-cost system [179]. Due to the self–heating of this kind of lasers, active coolers as Peltier effect thermo–electric cooler systems are recommended for avoiding the wavelength drift that occurs in these laser lights due to heating.

While designing a Raman–based detector, another important challenge is removing Rayleigh scattered light from the desired Raman signal. Normally Dichroic filters, or mirrors, are used for such purpose thanks to their ability to reflect or transmitting the light depending on light's wavelength. The dichroic filter is used to reflect the excitation light towards the sample and to filter the light scattered back to the detector due Rayleigh only letting the Raman spectrum propagating to the detection optics.

The dichroic mirrors need to be specified on angles of incidence and in transmission and reflection efficiency above and below the cutoff frequencies. Actually, this angle of incidence is one of the most crucial parameters in terms of opto–mechanical tolerances (see chapter 4.6.1) and deviating from the optimum angle will vastly decrease the system performance, because cutoff frequencies may shift and even block the Raman Signals. Additionally, with the aim of enhancing the signal to noise ratio, normally an extra filter is placed after the dichroic mirror to clean up the radiation from stray light and potential excitation light that propagates through the dichroic mirror to the detector.

Indeed, assuring an optimum alignment in focal position of the excitation and collection optics remains as one of the most important factor for obtaining a maximum Raman signal, making the most of the emission light power. The mechanical complexity for meeting these tolerances, along with the cost of the light source and filters are the main contributors keeping the cost of Raman–based systems one order of magnitude above Transmission, Reflectance or Fluorescence based sensors.

3.2.1.5 Microscopy

The microscopy techniques are used when physical features of the samples need to be monitored, which in the case of in–line fluidic inspection could be reduced to detection of suspended solids or aggregations, and the detection of sample heterogeneity (e.g. presence of air or water bubbles, etc.). The working principles are based on the

optical magnifications enabled by the lenses and the most important features are the Field–Of–View (FOV), Deep–of–Field (DOF), resolution or the minimum resolvable object size, and the whole system compactness. For in–line solutions, it is desired to minimize the system size, while offering a large FOV (e.g. tens of mm^2), and DOF (1 to 2 mm) and high resolution (around 1um), which requires using multi–element lens solutions configured for working in macro mode.

The in–line microscopes require a light source, which could be arranged either in reflexive or transmissive position, require the sample isolating optics, which should be transparent to the working wavelengths, require the 2D detector (e.g. CMOS or CCD camera) and of course require the lens system that enables the detector to focus on the sample. The lens choice and the definition of the working distances is one of the most critical points in the development of this kind of systems, and vastly impacts on the systems manufacturability at low cost, due to the requirements in tolerances (see Figure 3.2–13). Mitigation solutions as self–calibration patterns are used to relax the fabrication and assembly tolerances in the optical and mechanical components of the microscope systems [180].

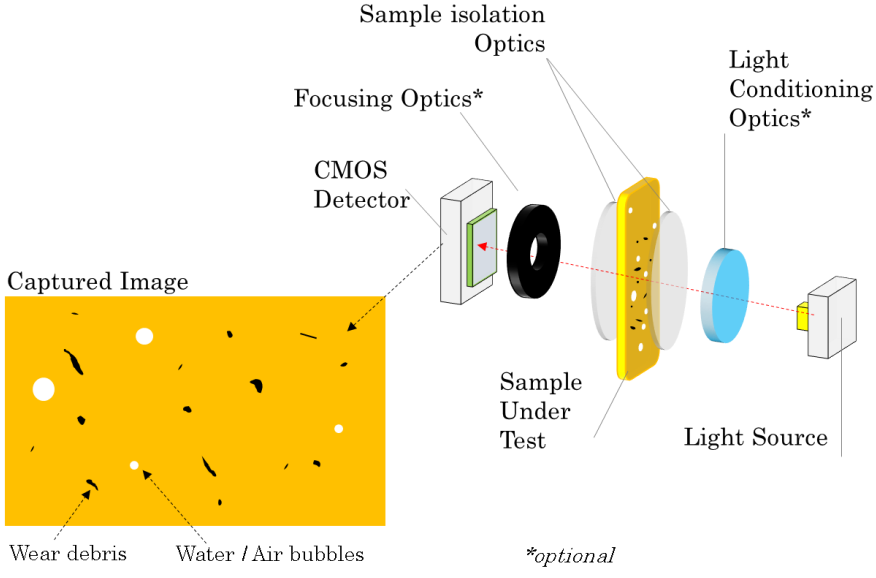

Figure 3.2–11: Block diagram of an in–Line, lens–based microscope with transmission light setting. In this example, wear particles and air bubbles are detected in the image.

There are several cases where the visual inspection of the fluid delivers very useful information about its status. This inspection could be human based or performed with automatic machine vision algorithms.

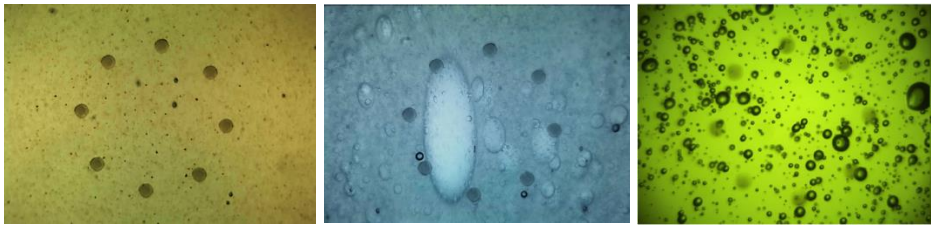

(a) (b) (c)

Figure 3.2–12: Examples of lubricant samples captured with an in–line microscope, showing contamination by shoot, by water and by air bubbles.

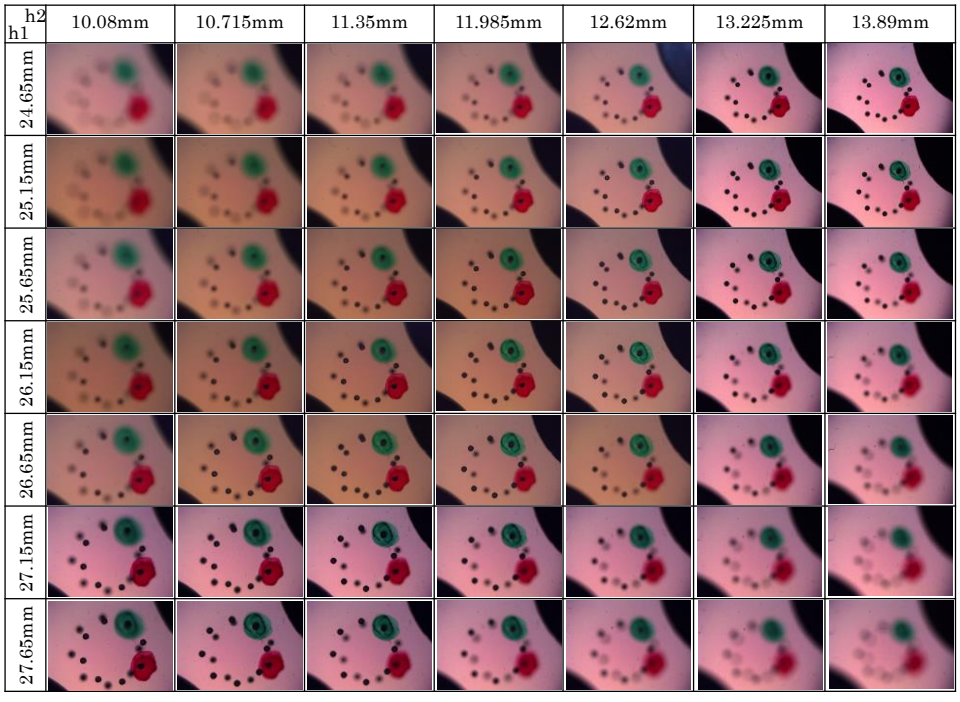

(a)

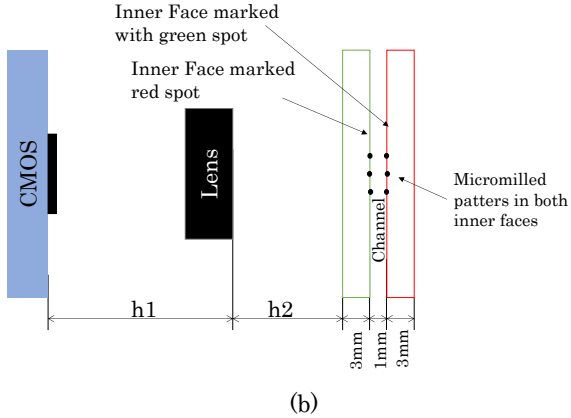

(b)

Figure 3.2–13: Experiment displaying the impact of tolerances of distances between the optoelectronic elements in a microscope setting.

3.2.2 Analysis of photonic information

The previous section has introduced different settings for setting up a photonic inspection of a given fluidic sample. Those setups delivered the method for arranging different optoelectronic, mechanic and optic components for accomplishing a matter inspection though an emitted light radiation, which interacts with the material under inspection, and where the resulting light is received by a photo–detector system. This section will discuss about several potential methods for interpreting and processing the changes happened in the light radiation after interacting with the matter. In the end, the objective of any sensor is to give an objective measurement of a parameter of interest contained in the sample under analysis; therefore, the changes in the light need to be understood, measured, calibrated and translated to a real value of the magnitude of interest.

The methods for analyzing photonic information outlined in this section will cover very basic processing approaches, based on the amplitude, phase or frequency change measurement, in addition spectrometry and chemometrics advanced mathematical analysis are described and finally the imaging and machine vision techniques will be reviewed.

3.2.2.1 Basic analysis: Amplitude, frequency, phase analysis

Considering the fundamental description of a light wave (see Eq. 3.2–2 for the electric field of the light wave), there are three main parameters that define its instantaneous state: Amplitude (E_0), phase or polarization (kz) and frequency or wavelength (w). Therefore, the basic way of analyzing any change happening at the emitted radiation when it interferes with the sample is to track differences in any of these three main parameters.

$$E = E_0 \cdot \cos(kz - wt) \qquad \text{Eq. 3.2–2}$$

Indeed, the physical and chemical effects that might generate a change in the parameters of light are numerous. For instance, the presence of certain compounds in the fluid will generate and attenuation in the light intensity, another molecules might generate a frequency shift between the emitted and the received light (Fluorescence or Raman effects). Additionally, the presence of certain molecular structures (e.g. helical secondary structures or chiral molecules) may generate the rotation of the light's polarization as it happens with glucose solutions.

Indeed, tracking the changes in any of the light parameters require specific emitters and detector. The emitters need to assure the required amplitude, wavelength and frequency properties for the original radiation and the detector should be able to detect the changes happening at the parameter of importance.

The simplest analysis is based on light amplitude measurement, which only requires a matched photo–emitter and photo–receptor, and the calculations are based on the analysis of the received light power.

When the measurement principle requires to analyze not only the amplitude but its distribution in different wavelengths or across a whole spectrum, even if the emitter may remain relatively simple, the detection subsystem requires being able to discriminate the light power received at different frequencies. This is normally accomplished by filtering the light before getting into the detector or using spectrometer systems.

When the phase changes need to be analyzed, emitter needs to assure a certain light polarization and the receiver needs to detect only the light corresponding to predefined polarization. This is accomplished either with tunable polarizers before the detector as in Polarimeter devices, which blocks all but the phase of interest, or by interferometers that are able to quantify the phase [181].

3.2.2.2 Spectrometry and Chemometrics

When the information contained in an absorbance spectrum is the consequence of a series of overlapping bands, the direct measurement of the absorption lines and amplitudes does not give any reliable information about the sample due to the interferences. This is the case with the NIR absorbance spectrums, that due to the spectral coincidence of several compounds' absorption lines (see Figure 3.2–14), the selectivity of the spectroscopic analysis is very low, and advanced processing techniques are required for performing identification, qualitative or quantitative measurements.

These techniques are known as Chemometrics and were defined around 1972 as a chemical discipline based on mathematics, statistics and formal logic to deliver maximum relevant chemical information by analyzing chemical data [182]. These techniques are designed to extract relevant information from complex absorbance, reflectance, fluorescence, etc. spectrums which possess broad overlapping bands and when the chemical, physical and structural properties of the sample also influence the measured spectra. This situation means that the absorption data from the sample depends on more than one variable simultaneously, and thus, the absorbance could be considered multivariate, which represents a challenge for any processing approach.

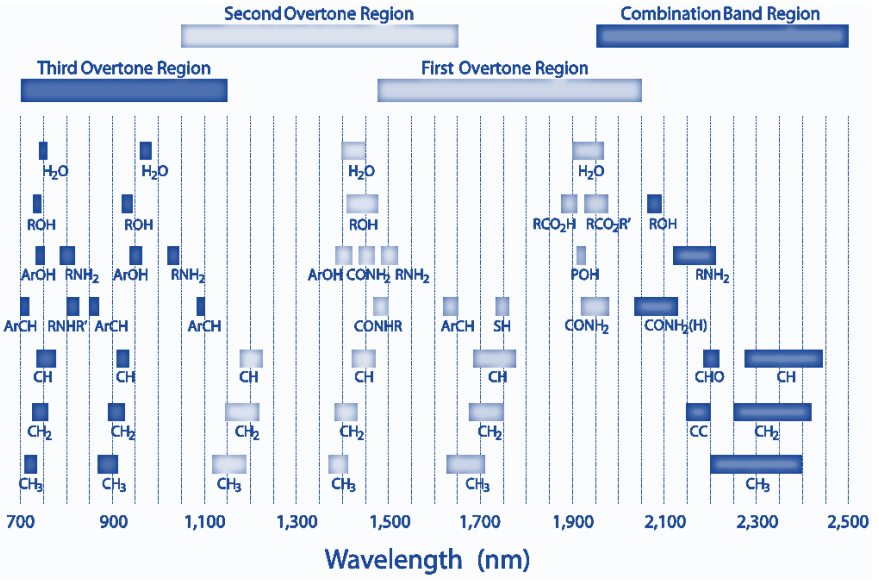

Figure 3.2–14: Major absorption lines and relative peak positions within the NIR region.

Chemometrics combine mathematical and statistical procedures that allow analyzing multivariate spectrums, filtering information that correlates to a certain property of the sample from other distorting data present in the absorbance signal.

Chemometrics rely importantly in the availability of sufficient number of representative samples along with accurate results from reference analytical methods (see Figure 3.2–16). This baseline information is used for calibrating and validating the chemometric measurement methods, being these, qualitative or quantitative.

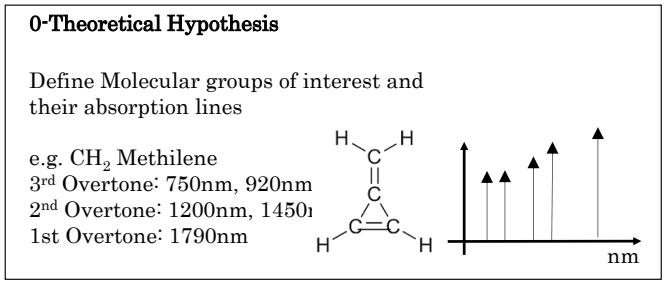

Figure 3.2–15: The first stage in any chemometric model development is to accomplish a theoretical approximation to the problem to solve.

Before starting any mathematical analysis, a theoretical overview to the problem is recommended, identifying the molecular groups of interest that will be analyzed through chemometrics and recognizing their absorption lines along the working wavelength range (see Figure 3.2–15).

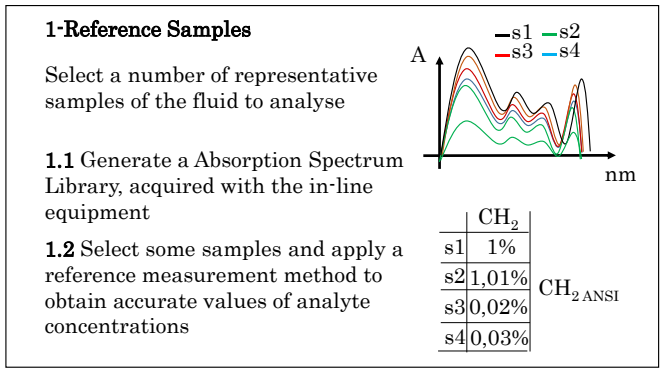

Figure 3.2–16: The second stage in any chemometric model development includes the spectrum library generation and the accomplishment of reference laboratory measurements.

After the hypothesis definition, the first stage in a chemometric method is the data pretreatment, which tries to mitigate the effects of amplitude differences from sample–to–sample. These systematic variations are originated mainly due to scattering effects at sample's non–homogeneities. The pretreatment is applied to the spectrum collection with the aim of normalizing the information for its further processing (see Figure 3.2–17). The literature covers several different pretreatment methods as Multiplicative Scatter Correction (MSC), Standard Normal Variate (SNV), Orthogonal Signal Correction (OSC), mean centering, first and second order derivatives, etc. [183].

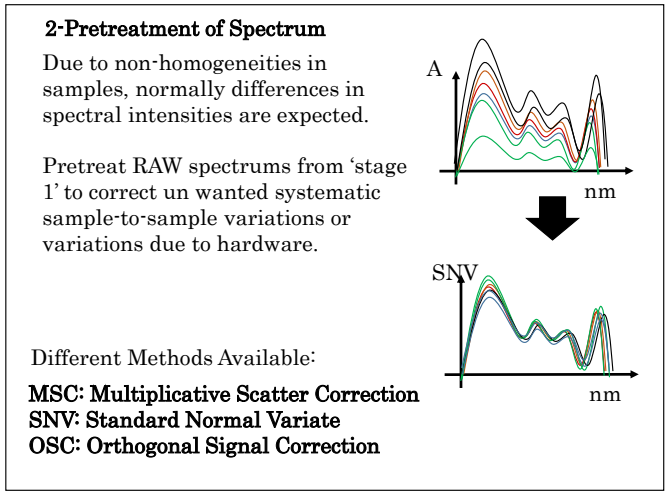

Figure 3.2–17: The pretreatment stage homogenizes the spectrum library for feeding these preprocessed data into the next stages.

The pretreatment stage is followed by different processing methods with the aim of reducing the large volume of information contained in the sample collection, filtering it to identify uncorrelated latent variables, known as Principal Components (PC). In qualitative

analysis, the Principal Component Analysis (PCA) is the most common method, while for quantitative methods, the Partial Least Square (PLS) regression is normally accomplished.

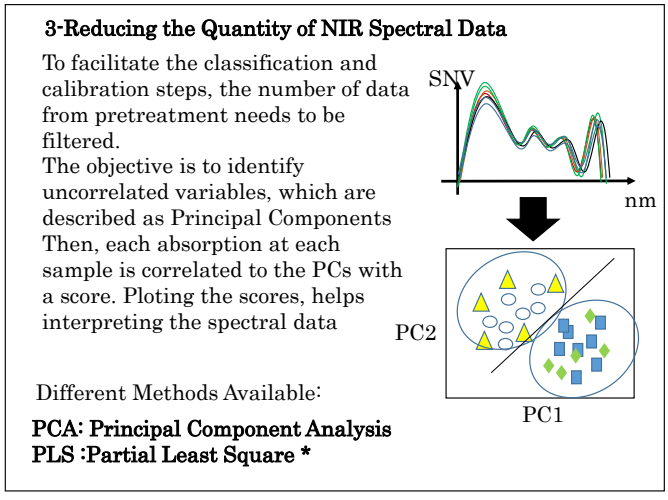

Figure 3.2–18: The large amount of data available for a chemometric model development is not practically processable, so significant information filtering is applied before model development.

While looking for the PCs, one should always take into account the theoretical analysis of the problem to solve. The PCs selected should be located in wavelength bands that have been previously identified as significant from a molecular point of view. Otherwise, the chemometrics may classify the samples according to an unwanted compound.

Once a sensible number of PCs have been identified, avoiding over–fitting or under–fitting the calibration, the spectrums can be graphically displayed according to their absorbance correspondence to the PCs, which is really helpful to understand the complexity of the calibration required.

The last stages are the multivariate calibration model development and its validation against the reference values (see Figure 3.2–19). The calibration is accomplished using appropriate models that describe relationships between the PCs and the absorbance values of different spectrums to provide prediction results about sample identification, qualification or quantification. Basically, the calibration looks for regression models that match the reference values with the analytical information pieces extracted in the previous stages. Indeed, this is a critical process and achieving reliable results that guarantee reliable predictions beyond the calibration library is not straightforward [184]. Normally, this reliability is related to the number of PCs used for the model regression, being 2 to 10 wavelengths a reasonable number for developing the model. Typical

regression models that may be used include Multiple Linear Regression (MLR), Partial Least Squares (PLS) regression, Principal Component Regression (PCR) and Artificial Neural Network (ANN) based regressions recommended when the relation between the spectral absorbance and the sample property to measure is non–linear [185].

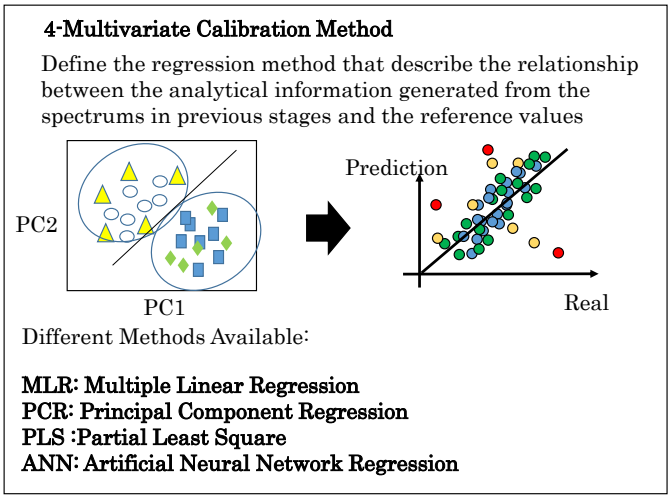

Figure 3.2–19: Calibration method development allows identifying, qualifying or quantifying new spectral information based on the insights gained in the thorough analysis of the spectrum library and reference values.

The model is assessed and verified with a validation set of samples (which have not taken part in the calibration of the model) to understand its predictive ability. The performance of the model is characterized by statistical parameters such as the root mean square error of calibration and prediction (RMSEC and RMSEP), which represent the deviation of the predicted values from the reference values.

It goes beyond the scope of this summary to cover every mathematical detail of the different pretreatment and calibration models and further insights into chemometrics can be obtained consulting examples in the vast literature about the topic, as [186].

3.2.2.3 Imaging and Machine Vision

Even if Imaging and Machine Vision techniques are a clear paradigm of a photonic system, they are often left apart from the pure analytical techniques as the afore mentioned ones. However, machine vision techniques are often really helpful at in–line applications where not only light radiation intensities and wavelengths are important but also when their spatial distribution amidst a volume or geometry, or when the morphology of the sample may contain significant

information. Machine vision or imaging techniques are able to automatize the extraction of these features.

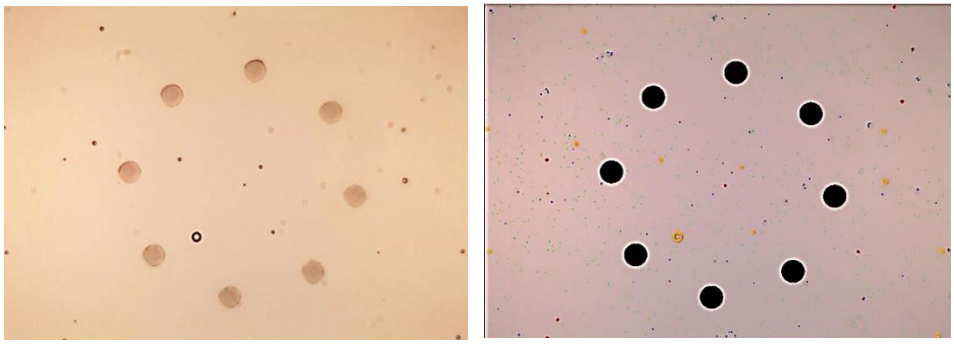

Figure 3.2–20: Results of machine vision algorithms for particle and bubble detection, as well as the self–calibration precision pattern that allows calibrating the size of the particles and bubbles at each image taken. Source: OilWear® sensor, Atten2 Technologies.

Sometimes machine vision or imaging techniques are used in combination with Fluorescence or Raman setups to analyze the presence of singular components that react to the excitation lights. Even if these approaches are not very common with industrial fluidics, these mixed techniques are being widespread in biological applications, such as cytometry or cell identification [187].

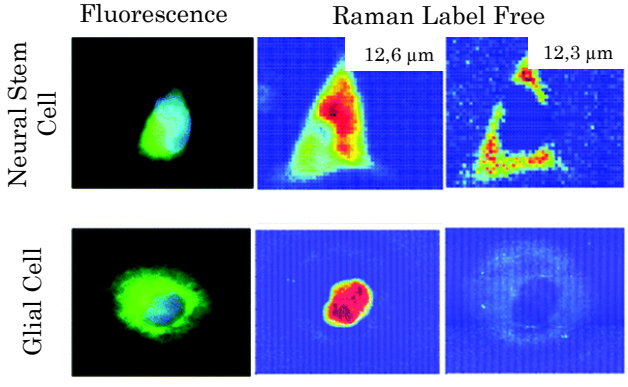

Figure 3.2–21: Fluorescent and Raman imaging used for demonstrating the differences between glial and neural stem cells. The Raman band at 788 cm−1 is associated with the nucleic acids of DNA and RNA, whilst the band at 813 cm−1 is associated with RNA only. Source [188].

The most accurate description for the Imaging or Machine Vision technologies is a combination of a set of algorithms of operations that a system is able to perform over an image or a sequence of images to extract significant information, based on geometrical forms, movements and other effects. For more information about machine vision techniques refer to literature references as [189].

The images used for imaging or machine vision processing are normally captured in the visible color region, at infrared region and

lately more and more examples can be seen in the near infrared hyperspectral domain [190][191].

The potentials of these technologies are evident and complementary to the previously mentioned signal analyzing techniques. This is the case, for instance, when machine vision helps identifying uncontrolled sample conditions that may jeopardize a chemometrics analysis (e.g. high concentration of air bubbles would not allow a correct fluid absorbance reading) or helping to localize regions of interest before accomplishing the full in–deep spectral analysis.

3.3 In Line Sensors

Integrating the aforementioned photonic setups and analysis methods is not an easy task, especially when requirements in terms of compactness and low cost becomes part of the equation. However, things get even more complex when these configurations need to deal with in–line operation, where the fluid sample is directly taken for the process under test and fed into the sensor element.

The advantages of acquiring in–situ and real-time information about the fluids directly from the process flow are evident: the fluid conditions remain unaltered; the reaction time is very fast and the sensors can be installed in locations relevant for process monitoring. The in–line monitoring helps guaranteeing and improving product quality and repeatability, enables increasing the efficiency and safety of the process, and also allows understanding the fundamentals of the process thanks to the acquired insights about process statistics.

Even if the cost of the in–line sensor is going down constantly, normally this is one of the factors hindering their deployment. However, this cost is rapidly paid off due to improved process efficiency, lower raw materials consumption and waste generation, and, most important, the ability to manufacture high quality products.

Nevertheless, dealing with an in–line operation imposes several challenging working conditions that need to be matched with the photonic and optoelectronic requirements. Different factors need to be addressed when designing and in–line sensor system:

i. Definition of the information and parameters necessary to monitor and control (chemical compounds, physical parameters, etc.).

ii. Accuracies, response times, reliabilities expected.

iii. Average values, normal fluctuations, dynamic ranges, extreme values of the parameters to monitorize

iv. Sampling frequencies with respect to the process timescale and expected dynamics of the changes.

v. Implications for installation, operation and calibration of the sensors, always assuring an easy deployment and automated operation

vi. Number and measurement locations

vii. Data output formats and compatibility with already deployed control systems

viii. Safety and certification considerations.

ix. Total cost of operation.

Next section will review the differences between the process monitoring approaches, from the off–line analysis to the proposed in–line systems, also covering the associated calibration issues entailed in the in–line operation solutions. Additionally, the requirements for the wettable parts of the sensors will be outlined, including the possible wear or fouling on these parts in contact with the fluid.

3.3.1 In–line, On–line, At–line and Off–line Sensors

Process Analysis at industrial deployments as production, processing, energy or manufacturing plants could be defined as the set of methods for providing sufficiently accurate and immediate information on variables that describe the state of the industrial activity. These process analyses can be accomplished in four options: Off–line or laboratory analysis, At–line measurements or On–Line and In–line systems (see Figure 3.3–1) [192]. However, there is no clear–cut line between the different classes, and these boundaries are even moving, with an increasing number of off–line techniques having been converted into on–line methods by automated, robot–assisted sample extraction from the processes or from bypasses that directly feed samples into in–line instruments [193].

For instance, the laboratory analysis of oil samples looking for wear evidences was first introduced in 1948 [194], and this traditional off–line fluid analysis is still an important asset for several maintenance programs, especially when high accuracy and low detection limits are needed. However, due to the potential benefits of real time operation, in situ sampling, reduced prices and size, and the decent accuracy and reliability (which increased day by day), the number of in–line sensor solutions is increasing unstoppably in the last decades [195][196].

Off–line analysis relies in high–end equipment operated by trained personal located in environmentally controlled laboratories. They offer the greatest versatility of analysis methods and achieve the

highest accuracies, reliabilities, etc. However, they require samples being physically extracted and sent to laboratory for their analysis, which, obviously implies long turnaround times and the delivery may change some sample properties that could be significant for the measurement.

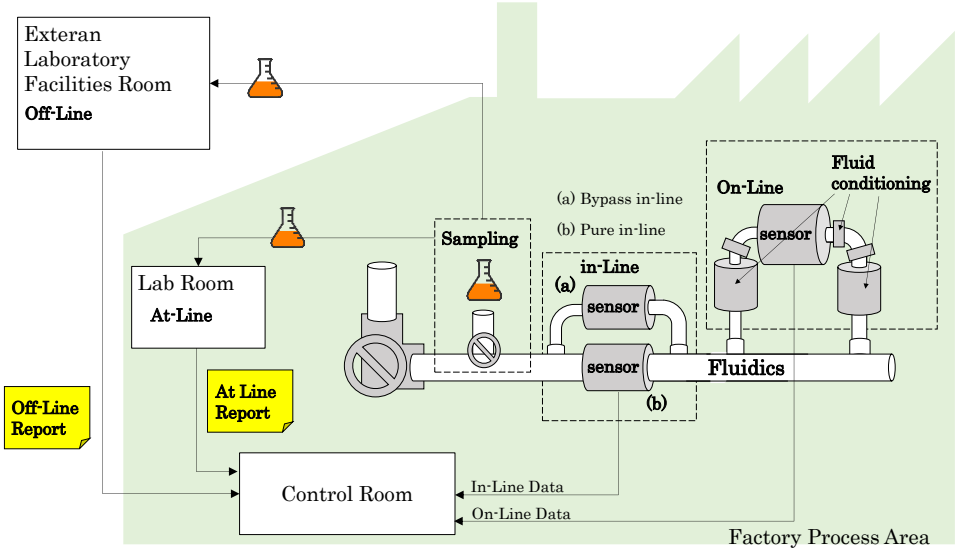

Figure 3.3–1: Diagram depicting the differences between the fluidic process analysis approaches.

At–Line systems are mini–laboratory solutions intended to be installed within the process area and used by a skilled operator. They still require extracted samples to perform measurements, but they are normally ready to deliver a high sample throughput (5–10 per hour) with high accuracies. Even if they can still be considered as laboratory equipment, they are designed to work under relatively dirt environments with no special environment conditioning.

In addition to the laboratory analysis performed either in–house (at–line) or in external facilities (off–line), there is another family of process measurement approach represented by the on–line and in–line sensor systems, terms which are sometimes used indistinctly.

On–line sensors are fully automated systems, located very close to the process under monitoring. Normally, an on–line system includes not only the sensor or transducer but also sample conditioning hydraulics as pumping, filters, electro–valves, heating, cooling, pressure reductions, and could also, sometimes, asides the hydraulic conditioning, include some sort of chemical preparation controlling external devices as dosing pump. Thanks to these pretreatments, on–line systems are able to include delicate transducers and offer very good sensor performances in terms of accuracy, reliabilities, etc. Additionally, on–line sensors deliver the measurement results directly

to the central point through a standardized communication protocol. However, the required external equipment makes on–line solutions normally expensive and bulky.

On the other hand, in–line system represents the most integrated version of process monitoring equipment since they need to be placed directly into the process stream. As it has already been detailed in chapter 1, these in–line devices have traditionally been used for measuring relatively simple parameters as pressure, PH, density, flows, etc. but with approaches as the one presented in this thesis, in–line sensors are evolving to offer readings of much more complex parameters.

One of the biggest difference between the on–line and in–line devices is that on–line sensors remove a lot of uncertainty sources thanks to the fluid conditioning applied before the measurement is done. For instance, on–line devices add bubble removing systems, may include particle filters, flow controllers that avoid turbulences and assure sample homogeneity, etc. [197][198][199], contributing to a much more stable sample conditions that lead to higher accuracies and repeatabilities in on–line sensor systems.

However, integrating more complicated transduction in harsh conditions as the ones imposed by the industrial fluidics requires a careful hydraulics, fluidics, optics, mechanics and electronics integration for offering reliable measurements. The next sections describe two important design considerations when dealing with photonics sensors in industrial fluidics applications: the calibration and the wettable parts.

Table 3.3–1: Comparison chart of process analysis approaches.

	Off–Line	**At–Line**	**On–Line**	**In–Line**
Installation Site	Laboratory	Plant	Process	Process
Sampling	manually	manually	Automatically	integrated
Sampling Points	Potentially many	Potentially many	few	few
Analysis Frequency	low	Low–mid	high	Real time
Sample Transport	To remote laboratory	To local analytical equipment	integrated	No transport
Analysis Procedure	Automated /manual	Automated/ quick check	Automated	Automated
Turnaround time	Hours / days	hours	minutes	Real time
Parameters Measured	many	1–10	1–2	1–2

Measurement Range	Flexible	Fixed	Fixed	Fixed
Accuracy	Very High	High	Medium	Medium
Sample Preparation	manually	manually	automatically	No preparation
Operation	Lab assistant	Plant Operator	Automatically	Automatically
Maintenance	Lab assistant	Plant Operator	Plant Operator	Plant Operator
Data communication	LIMS[31]	LIMS	Process Signal / LIMS*	Process Signal / LIMS*
Environmental compatibility	Room temp.	Room Temp.	Industrial range	Harsh environments
Environmental protection	IP23	IP54	IP67 / Hazardous area certified	IP67/ Hazardous area certified

*Smart sensors are supposed to be deliver LIMS

3.3.2 Calibrating in–Line sensors, White and Dark Level measurements

The different measurement techniques presented in the previous chapters are normally the integrated versions of well–stablished laboratory methods. Indeed, transmission, fluorescence, microscopy, etc. have been routine processes in laboratories since hundreds of years ago. However, the migrations of these methods to low cost compact settings does not only present integration problems, and meeting some of the method–fundamentals is almost no possible in systems as the ones presented in this thesis. We are talking about spectroscopy calibration (white and dark signals), detector calibration (as in colorimetry), or dimensional calibrations performed in microscopy.

Laboratory equipment normally include a calibration procedure, either for calibrating the instrument, or to be accomplished prior to the measurement acquisition as baseline signal. These reference values are used for normalizing measurements and for compensating the measured signal removing the effects of variations in emitters, detectors or optical settings.

For instance, in reflectance spectrometry, the standard procedure, require measuring the White and Dark signals. White signal represents the maximum value detectable, and thus requires using a mock sample that reflects ideally the 100% of the emitted light. Several reference samples are available for this purpose, but

[31] Laboratory Information Management System

basically are composed of a highly reflective material (see Figure 3.3–2). Dark signal represents the intensity value delivered by the detector whit the emitter lights switched off. The dark signal represents the noise level at the detector, which increases with integration times, gain, etc. In transmittance, even if some standard materials could be used, the White signal is acquired just measuring an empty cuvette. These reference spectrums are then mathematically applied to the sample's measured spectrum and its normalized and compensated reflectance is obtained, which is fed into subsequent processing stages (e.g. chemometrics).

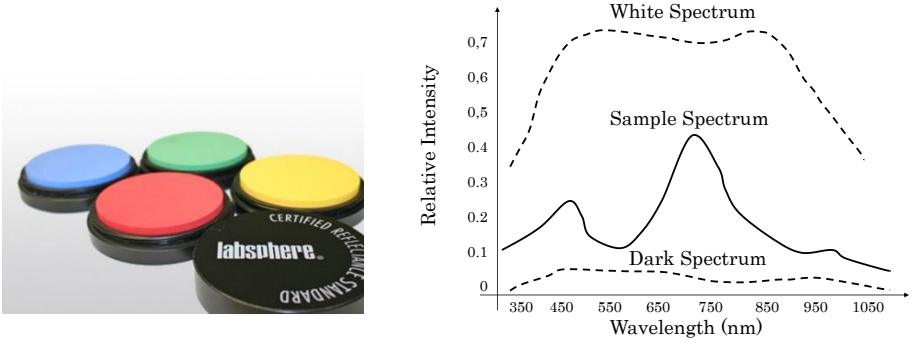

(a) (b)

Figure 3.3–2: (a) Reference samples for diffuse reflectance (Lapsphere, North Sutton, NH, USA). (b) Example representation of white, dark and real sample spectrums.

$$\text{Transmittance} = \frac{I_{SAMPLE} - I_{DARK}}{I_{WHITE} - I_{DARK}} \qquad \text{Eq. 3.3–1}$$

Something similar happens with microscopes, where either the equipment is calibrated on regular basis or reference patterns are used to determine the size of the measured targets. Colorimetric measurements are accomplished following the same approach, calibrated equipment or reference color.

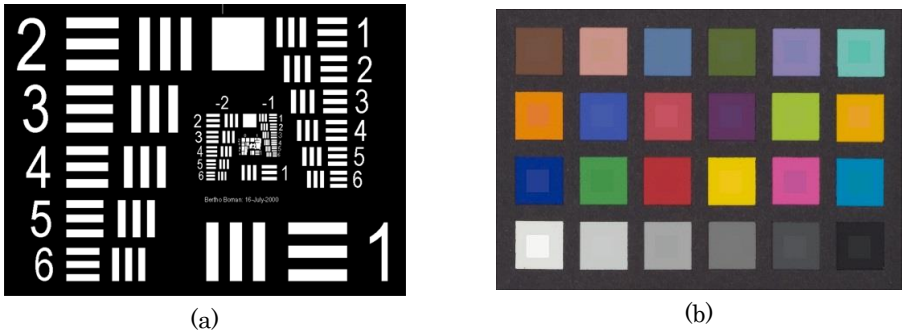

(a) (b)

Figure 3.3–3: (a) Microscope calibration and resolution resolving pattern (1951 USAF resolution test chart). (b) Color calibration patter (Leica, Wetzlar, Germany).

But, indeed, the migration of the aforementioned techniques is not straightforward, and in some occasions, is even practically impossible. Notice that the in–line sensors are permanently in contact with the sample fluid, with little or null possibilities of completely removing it for taking a reference reading.

In this situation, there are only two possible solutions left for the integrated in–line sensors: either they work without calibration, which could perfectly fit several applications where no absolute readings are required, or some sort of calibration system is included within the system.

Notice that we are not talking about detector or emitter compensation systems (already outlined in section 3.1.1.9 Calibration), but presenting the implications of enabling the in–line sensors to offer a calibrated measurement against a standard. And this requires somehow measuring the reference pattern along with the sample analysis [200].

For instance, the measurement of the white reference patterns is a traditional challenge that has been faced with several clever and even artistic engineering solutions, which at certain moments, between measurements, are able to introduce a physical component, named white tiles, for accomplishing a white signal reading. Even if sometimes, these engineering solutions use two parallel systems, one measuring the reference and the other the sample [201], the solutions normally require some sort of moving parts within the sensor system, either for displacing the physical white tile to the measurement point, blocking the sample, or, moving some optical component (e.g. mirror) that alternatively focuses the sample or the white tile [202] [203] [204] [205].

Regarding the calibration of in–line microscopy solutions, a good approximation is to include reference and accurate patterns within the FOV of the system [180]. This reduces the active area available for inspecting the sample, but removes all the dependencies with mechanical, optical and assembly tolerances.

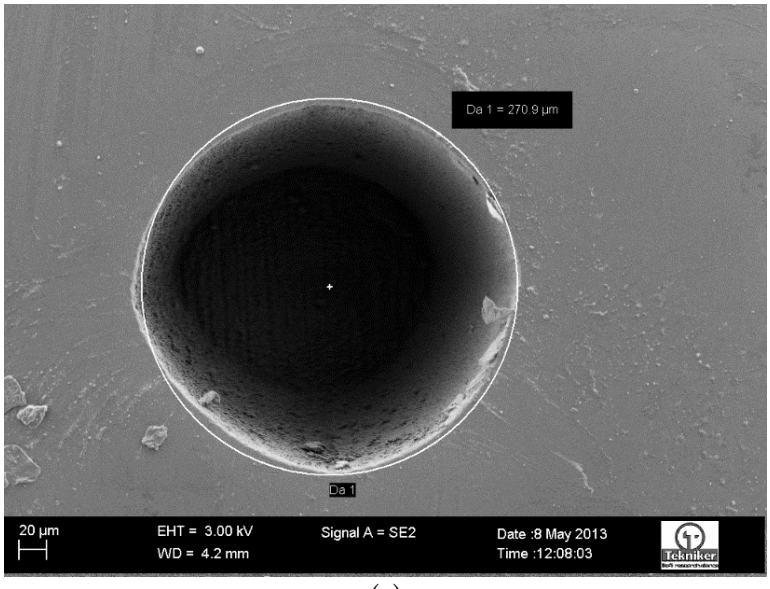

(a)

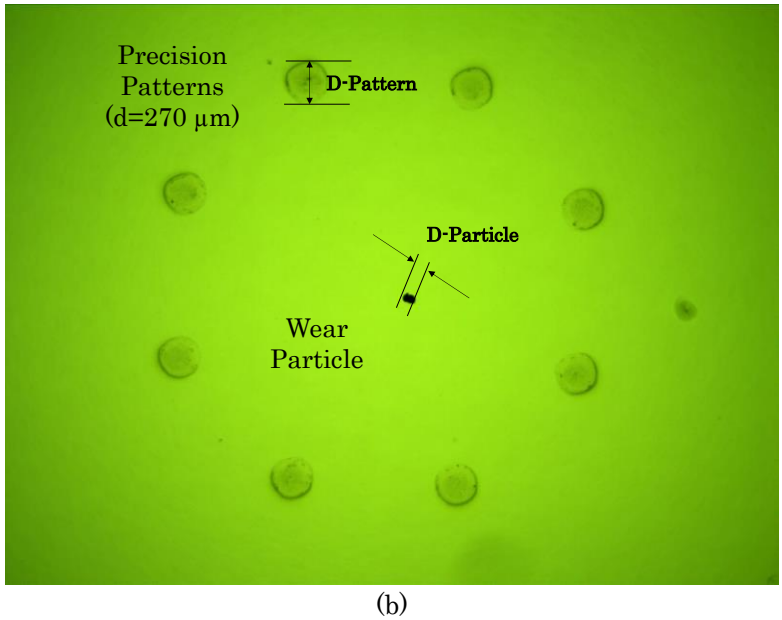

(b)

Figure 3.3–4: (a) Calibrated Pattern inspected in SEM microscope. (b) Rings of patterns included in the FOV of the in–line microscope. All the wear particle dimensions are calculated referenced to the precision pattern dimensions.

3.3.3 Wettable Parts

The wettable parts are one of the most critical parts within an in–line sensor for fluidics. Wettable parts are defined as all the components that will be in contact with the fluid, which individual properties and integration need to assure a reliable operation under the given working conditions (pressure, temperature, corrosion, wear…).

Regarding the compatibility of the sensor with the fluid, it needs to be assured in both directions, especially when dealing with bio samples that may be contaminated by the sensor itself. This is the case for the Food&Beverages and medical applications, where all the optics, seals and metals need to be accepted for the biological uses.

From the practical point of view, the design of the wettable parts normally relies in several laboratory analyses for compatibility studies, and simulations (see chapter 4) for assessing the reliability of the different parts under the working conditions.

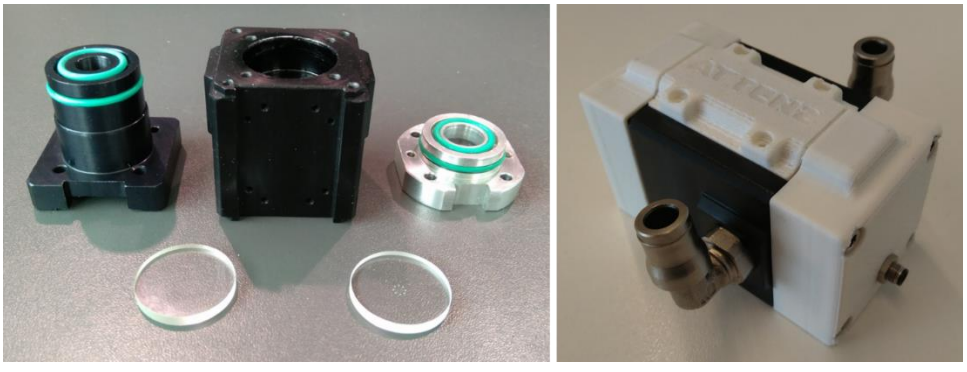

(a) (b)

Figure 3.3–5: Example of wettable parts included within a sensor prototype for wear particle detection. (a) Shows optics, mechanics, and sealings and (b) shows the hydraulic fittings.

Normally, these parts will include the following items:

3.3.3.1 Hydraulic fittings

These elements allow connecting the sensor with the hydraulic infrastructure to monitorize. Normally these parts are standard hydraulic components (BSP, GAS, etc. connectors) and are fully compatible with a large range of fluids and do not represent a major problem in sensor integration.

3.3.3.2 Sealings

The seals are required to assure a proper sealing between the different optic and metallic parts. These flexible elements are accommodated to absorb the effects of the mechanical imperfections and to seal the junctions avoiding leakages due to capillarity effects. The sealing material, normally elastomers, should be selected depending on the fluid to be monitorized, because not all the materials are suitable to all applications. For instance, when dealing with mineral or synthetic lubricant fluids fluorocarbon may be used for sealings, while Phosphate Ester based hydraulic fluids require the use of EPDM (Ethylene–Propylene) or Teflon.

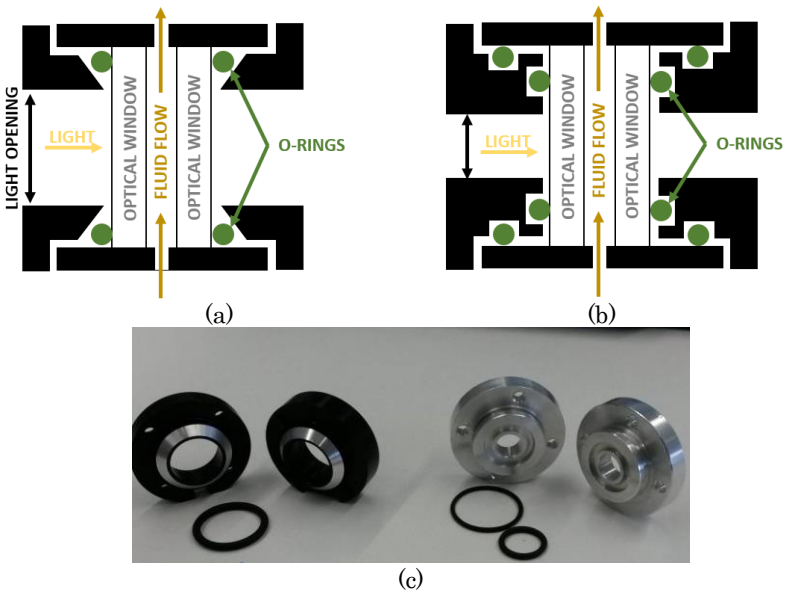

Figure 3.3–6: (a), (b) Different mechanical approaches for installing a single seal or double seal solution for photonic sensors. (c) Mechanical parts and seals according to the (a) and (b) designs.

3.3.3.3 Mechanical parts and sensor internal embodiment

Normally the channels by which the fluid moves within the sensor are made in metallic elements. Corrosion and chemical compatibility needs to be checked because not all the metals and metal surface treatments (e.g anodizing) are compatible with the different fluids.

3.3.3.4 Optics

This is perhaps the most challenging part in the structural design of the sensor. The optics in contact with the fluid may do not have any optical function but to let the light come in and out from the sample. However, as it needs to stand the fluidics pressure, temperature, etc. it has to be carefully selected not only for its transparency properties but also for its mechanical roughness. For instance, the following Eq. 3.3–2 describes the minimum thickness of glass disk before it breaks under a given pressure.

$$T(\text{inch}) = \sqrt{\frac{P\max(\text{psi}) \times A(\text{sq.inch}) \times F}{3.12 \times M}} \qquad \text{Eq. 3.3–2}$$

Whereas, T represents the minimum thickness in inches, A defines the unsupported area in sq/inches (see Figure 3.3–7 depicting different apertures), P is the maximum pressure in psi, F is a safety factor that normally is set to 7 and M defines the Modulus of Rupture of the glass (in psi). As reference a BK7 glass delivers a M~2,400 psi

and Gorilla® Glass from Corning (Corning, NY, USA) a M~100,000 psi, which allows a compatibility with higher working pressures.

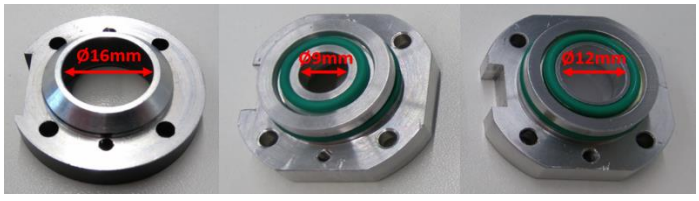

Figure 3.3–7: Different optical apertures. Increasing the diameter allow higher radiation flux availability, while reducing the compatible maximum pressure.

Besides, the ageing, fouling and scratches on the surfaces of the optical parts in contact with the fluid is also one of the major drawbacks of this kind of photonic sensors and hinders long life time of the sensors. The wear of the surface will produce a wrong measurement due to either increase or decrease the intensity of scattered light onto the sensor surface, changes in absorptivity, modified index of reflection, etc. Even if several coatings and surface nano–structuration, [206] [207] [208] [209], have been tried for protecting the optics against wear and fouling, they do not offer a definitive solution and only delay the effects of the surface degradation.

4.

Design Methodology for Cost Effective Photonic Sensor Product Development

Photonic component developers usually do not provide any specific support for bringing their systems into products, leaving an important technological gap to be faced by system integrators. Moreover, the intrinsic complexity of the fundamental processes involved in photonic measurement techniques, requires the availably of a multi-domain engineering team, including physicist, chemist, mechanics, optics, electronics and data processing experts. The integration of this bunch of heterogeneous domains is not evident, which, added to the uncertainties and risks typically entailed in complex and innovative products hinders the technological, economic and time-to-market success of the development. The situation aggravates if strict certification framework regulates the application, as it happens in the industrial, energy or manufacturing domains.

In this context, this chapter reviews different New Product Development processes targeting complex and innovative products. Since none of the state of the art models satisfy the abovementioned situation, a development methodology is presented and specified for guiding the design and development of cost effective photonic sensor products Development. The presented methodology merges contributions identified from different development models with customized approaches tailored to the use case of fluidics sensors. The definition of the methodology is continuously complemented with specific examples taken from real developments that illustrate different details at each stage of the design process.

4.1 Background and Main Objectives of the Design Methodology

The main challenges faced by a photonics–enabled smart sensor integrator derive from manifold reasons. First, the nature of the working principles (as described in Chapter 2) require a deep understanding of the physical and chemical processes behind the measurement principle, and normally, advanced knowledge in chemistry, fluid dynamics, thermodynamics, etc. is essential for specifying the problem–to–solve and formulating the solution hypothesis. Then, the interaction with the photonics starts, when the suitability of the properties of the light–matter interaction processes is assessed for enabling a solution to the identified problem. Therefore, it becomes evident that the insights and expertise of a photonic expert is required to evaluate the benefits and risks of applying a certain photonic principle to sort out a fluidics sensing problem.

At this stage, the engineering review starts, where the issues coming from the effective integration of the aforementioned techniques into a system need to be solved. Optical alignment of the photonic components, mechanical tolerances, fluid sample acquisition and conditioning, assuring the sensor performance under operational conditions (pressure, temperature, vibrations, etc.), enabling the easy calibration, installation and maintenance of the sensor, embedding all the data processing and communications, etc. are some of the task to be solved by the multidisciplinary engineering team (mechanics, hydraulics, electronics, control and automation and software engineers).

Besides the complexity inherited from the mentioned scientific, technological and operational challenges, photonics–enabled smart sensor integrators need to deal with severer regulatory requirements and the constantly increasing importance of reducing time–to–market and investment payback for successful device commercialization.

Fluid sensing problems looks solvable at laboratories, and the availability of continuously improving low cost, compact and feature–rich photonic emitters and detectors seems to enable the easy migration of multiple monitoring techniques from the lab to the market, requiring little effort and time. The real situation is completely opposite to this appreciation, because, asides the traditional difficulties found in bringing innovative products to the market, known as crossing the 'valley of the death' [210][211][212], in this case additional technological, integration, regulatory and market originated risks and strict requirements [213][214][215] [216][217][218] seriously jeopardize the successful evolution from photonic measurement principles into autonomous sensor systems.

The objective of the proposed methodology is to bridge the gap between the theoretical measurement principle formulation and the photonic smart sensor manufacturing, providing a device development model, which has been empirically formulated based on insights acquired during the sequence of different photonics–enabled product development.

One of the major concerns faced while shaping the model has been, indeed, the management of the aforementioned heterogeneity of technologies, but also how to deal with the uncertainty in terms of lack of specifications and lack of awareness about the risks involved in the project.

The reason behind this lack of information and knowledge about the product is because normally, the sort of sensors addressed by this methodology are novel devices. This novelty is generated either because the sensors target a new application scenario, which is quite common situation for the in–line sensors since they are supposed to replace or assist an off–line laboratory method but the conditions for the in–line operations are unclear. Alternatively, the novelty may be justified because, even if other sensor technologies might cover an application, the integration of photonic measurement principles for that specific case has not been tackled previously.

The proposed methodology is based on different approaches of New Product Development processes, specifically on those models focused on technological products and on incremental product developments, as the traditional Phase–Gate or Stage–Gate models [219], and the newer generation as the Triple A System (Adaptive, Agile, Accelerated) [220], because they accommodate better the uncertainty that normally surrounds the development of new sensor products.

The work presented here, describes the generic methodology but also highlights some specific steps which are considered critical for a successful development of a photonic–enabled smart sensor for in–line fluid monitoring. Notice that, even if the final goal of the methodology is to achieve a product, its business model formulation [221][222] is out of the scope of the topics covered here, so value propositions, distribution channels, revenue streams, etc. are not considered while formulating the product structure.

4.2 Product Innovation and Development Process Models

Bringing a new sensor product successfully from the laboratory to the real field is highly complex and depends heavily on the implementation of rigorous processes or methodologies. These

methodologies should allow or assist developers to optimally synchronize development, prototyping, verification, production, etc. successfully meeting manifold requirements of third parties, including end users, regulators and investors [223]. However, this traditional situation has evolved collaterally to the raise of Industry 4.0.

In the Industrial Internet of Things world, the boundaries between traditional industry and internet companies are becoming increasingly blurred, and connectivity is opening up new business opportunities for sensor manufacturers, which require very fast reaction times once the opportunity has been identified [224].

As described in section 4.2.1, dealing with this complex and innovative product development in successively shorter product life cycles is not straightforward, and different development strategies has been proposed in the last years. However, while various models may exist in the sensor industry, no comprehensive development process has been published so far.

The sections from 4.2.2 to 4.2.7 review different existing model representations, looking for the best approaches that might be applied to the formulation of a new development model that captures all aspects of photonic sensor system integration and commercialization from early–concept development to after–sales support.

4.2.1 Smart Photonic Sensors: Complex and Technological Product development

Known as novel, disruptive, vanguard, breakthrough, or exploratory projects, etc. what they all have in common is that, in this sort of project scenario neither the objectives, nor the capabilities, means and resources to achieve them, are clearly specified at the beginning of the development. This uncertain situation poses clear differences when compared to a routine project execution (see Table 4.2-1), and therefore, the management approaches for both project types could not share the same vision, tools and criteria [225] [226].

Table 4.2-1: Differences between routine and complex project execution [244].

	Routine Projects	Novel and Complex Projects
Objectives and Requirements	Fully specified with little probability of change	General view of the project known, but without detailed objectives and with emerging and evolving requirements
Tasks	Can be specified and could be derived from previous experience	Only the big picture of the project is envisaged

Means and Capabilities	Identified beforehand, with known sources or suppliers	Not necessarily existent, not necessarily specifiable
Uncertainty	Variation (plan deviations) and risks (stochastic estimable changes in known project variables)	Unexpected uncertainty: new variables, new effects, new actions, which could not be foreseen at the beginning
Risks	Normally known, and therefore, mitigation plans could be allocated early	Mostly unknown
Examples of Domains of Relevance	▪ Well Known markets and customer expectations ▪ Well Known performance drivers of the developed system ▪ Well Known environmental parameters	▪ New markets and unknown customer feedback and reaction ▪ New performance drivers of the developed system ▪ Unknown or new technology ▪ Complexity with unexpected interactions among parts ▪ New markets and application domains with unforeseeable regulatory constraints ▪ New stakeholders with unforeseeable requirements

Additionally, as mentioned earlier, in todays globalized and digitalized modern economy, it is often impossible to envisage how a digital product will evolve. The needs from the end users evolve, the economic and market conditions change rapidly and new competitive pressures arise suddenly from any part of the world. Therefore, apart from the uncertainty intrinsic to technologically complex projects, the volatility of the globalized economy does not contribute to having the full set of requirements defined at the outset of the projects [227].

If we narrow down to the photonics–enabled smart sensors, we found a set of challenges that the methodology is supposed to help developers dealing with.

Table 4.2-2: Description of the challenges present in the Smart Photonic Fluid Sensor product development.

Challenge	Description
Critical Requirements	▪ High sensibility ▪ Reliable and Autonomous operation ▪ harsh environments (corrosive ambient, high temperature range)

	▪ Almost zero maintenance ▪ Plug & Play installation and calibration free operation
Heterogeneous technology integration	▪ Physics and Chemistry, Optics, optoelectronics, micromechanics, hydraulics and microfluidics, hardware and software, algorithms, communications, industrial processes.
Multidisciplinary working teams	▪ Chemistry, Optics, Photonics, Mechanics, Design, Electronics, Software and data analytics.
Managing key providers	▪ Novel Photonic components
Uncertainty	▪ Novel applications ▪ Unspecified working conditions (environmental, sample conditions, contaminations…) ▪ Little accessibility to devices once deployed in the field (little feedback)
Little time to market	▪ From problem identification by the end–user, 0.5 years concept proto, ~1 years working prototype, ~1.5 years volume production
Regulatory, investment and market constraints	▪ Several Certifications may apply (e.g. CE, UL, FDA, IP, vibrations and Shock, ATEX…) ▪ Unit cost constraints, impacting on product margin ▪ Fierce competition

In addition to the challenges described in Table 4.2-1 and Table 4.2-2, the proposed methodology also needs to address the traditional objectives considered a must for any new product development technology [228]:

- Foster optimum Quality of Execution
- Sharp the focus for better project prioritization
- Focus the development of the competitive advantage of the product
- Keep a strong market and end–user orientation
- Sharp, early, and stable product definition
- Fast parallel and flexible processing by different disciplines
- Rely on a true cross–functional team approach

The next sections will review different development models, looking for the best contributions to the specific product we have in hands. Then from section 4.3 on, we will summarize these diverse contributions and visions in the Design Methodology for Cost Effective Photonic Sensor Product Development.

4.2.2 Design for Six Sigma

Design for Six Sigma (DFSS), which was introduced as an evolution from the traditional Six Sigma approach in the early 2000s [229], is a product development process that uses metrics, data, statistics, and project management tools with the final goal of having a robust and failure–free product in the market, and has been applied in the sensor product development industry [230]. The DFSS focuses all the development in the deep understanding of the customer needs, which are translated to requirements that drive design and development, which is then optimized and finally validated. In this situation, some interesting contributions from the DFSS philosophy [231] to the photonic sensor development have been identified:

i. Only if you focus on measuring the defects of a process, you will be able to figure out how to solve them,

ii. Use objective metrics or key performance indicators (KPI) to measure processes

iii. Track changes occurring at these KPIs for early problem identification

iv. Keep the customer in the loop for detecting problems and deviations occurring at customer's site

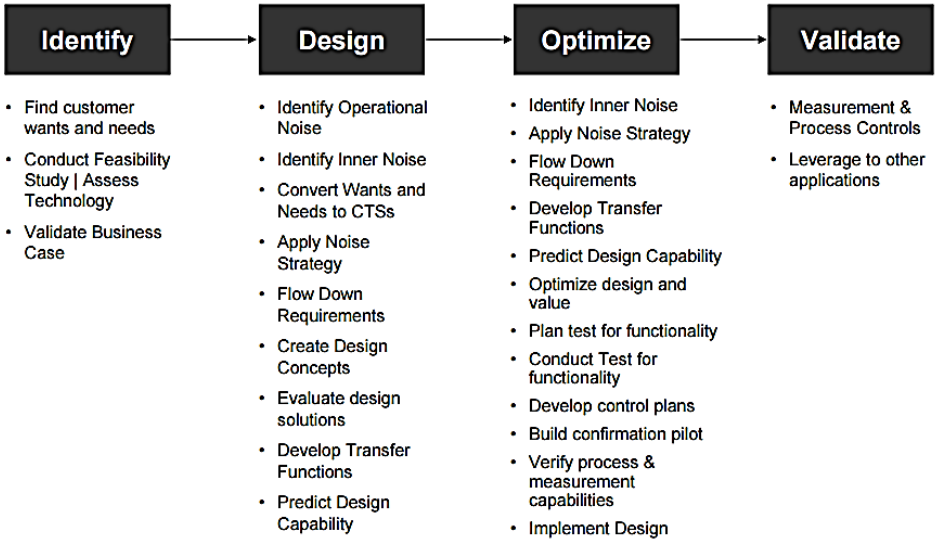

Figure 4.2-1: DFSS phases and internal actions [231].

4.2.3 Lean Product Development

Even if the Lean thinking was originated after the World War II in japan at the Toyota factories, it was reformulated during the nineties decade [232] for maximizing the value (meeting or exceeding customer requirements) while minimizing or removing the waste (cost reduction), by simplifying and continuously assessing and improving all processes and relationships in an environment of trust, respect and full employee involvement.

After being widely adopted, the Lean principles were shaped into the Lean Product Development (LPD) approach fifteen years later [233], with the aim of helping the design teams to be fast, flexible and highly effective to be able to answer the demands of today's globally competitive environment. Basically, the successful application of Lean models in product development involves improving the growth of knowledge about the product, customer and manufacturing [234], achieving a practical approach for accelerating the time–to–market focusing on efficient planning, resource management, design control, and interdisciplinary communication.

The LPD also highlights the importance of the deep knowledge and insight gathering about the product while it is being developed, and concludes that engineering decisions in product development must be based on proven knowledge and experience [235]. This asseveration should be directly translated to the Photonic sensor design flow, because due to their intrinsic complexity, design decisions that do not rely on proven scientific evidences may be prone to generate failures in later stages.

Besides interiorizing the importance of always relying on the knowledge for driving the design, the Photonic Sensor development could also benefit from LPD's proposals about team management and organizational procedures [233].

v. Develop a chief engineer system to integrate development from start to finish.

vi. Organize to balance functional expertise and cross–functional integration.

vii. Develop towering competence in all engineers.

viii. Fully integrate suppliers into the product development system.

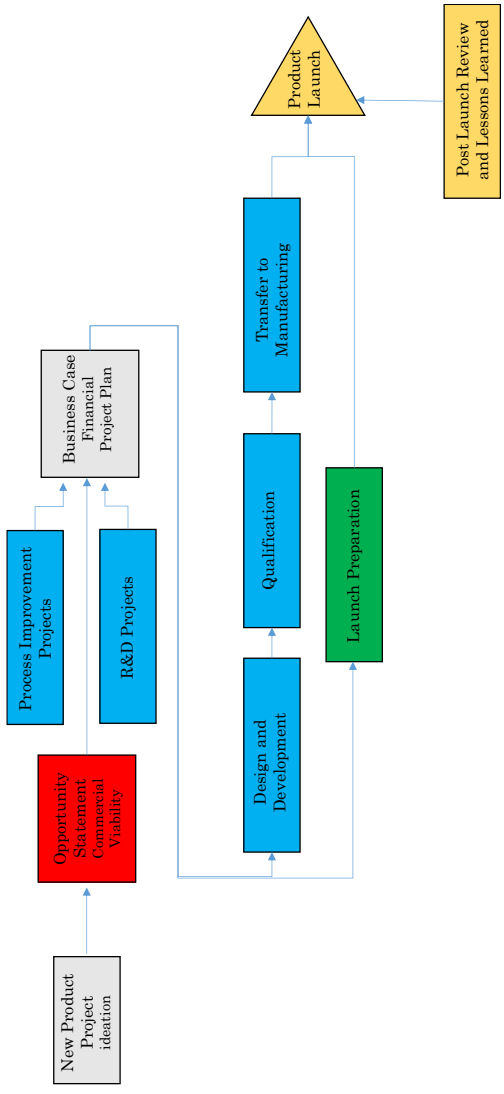

Figure 4.2-2: Lean Product Development process flow [233].

4.2.4 Lean Startup

The Lean for Startups is a particularization of the Lean process and provides a scientific approach to get the right product to the customer faster. Introduced around 2008 [236], the Lean Startup model suggests some interesting ideas based on eliminating the uncertainty, prototyping fast and validating with the customer the product concept as early as possible, rather than trying to perfecting it. Actually, the Lean Startup recommend including the potential customers in the loop from the very beginning of the product development, in order to incorporate their request in the design while it is being built. This approach should allow to reach the market with already stablished customers with the minimum investment possible.

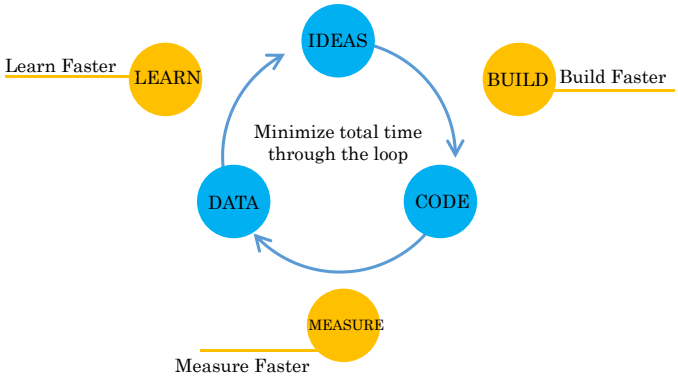

Figure 4.2-3 The Lean Startup process diagram [236].

The Lean Startup process is based on the Build–Measure–Learn feedback loop. *Build* is referred to focus the efforts on putting together the minimum pieces to have a working prototype, known as the Minimum Viable Product (see next section). The MVP is the version of the product that enables a full turn of the Build–Measure–Learn cycle with a minimum amount of effort in the minimum development time.

Measure defines the need to observe the performance of your prototypes, not only from your perspective, but also from the customers' point of view. This measurement requires a comprehensive and scientific assessment of the product and relies on the analysis of a predefined KPIs. The *Learn* word suggests the need to measure the effective progress achieved in the product development, which is the only way to progressively mitigate the uncertainty. This last part is also defined as *Validated Learning*, and suggests validating the learning by running scientific experiments that allow developers to test each element of our vision.

Even if Lean Startup method claims that is suitable for any kind of business, it addresses best the pure software and web products rather than a complex system like the Photonic Sensors. However, there are still some interesting points that could be applicable to our methodology proposal as:

ix. Shape the product specifications hand by hand with the customer.

x. Analyze thoroughly the progress of the development by scientific experiments and by the feedback of the customer.

4.2.5 Minimum Viable Product, Hardware products

As mentioned, the Lean Startup model does not consider with the appropriate importance the differences between the software and

the hardware developments, which dramatically impact on the Minimum Viable Product concept for non–software products. Regulatory compliances (e.g. CE or UL marks) are required to install or use almost any kind of hardware products. The tooling costs for being able to manufacture or even prototype the hardware MVP have a huge impact on the companies' finances. And, last but not least, even the most basic minimum viable hardware product will be bound to certain durability and reliability requirements that are not evident to meet for use cases as the industrial ones [237].

However, the MVP concept is not new to hardware designers, and it was a basic process applied by product design firms already twenty years ago or even earlier, as demonstrated by the popular Ideo's shopping cart example [238]. And even if the MVP concept has now gained attention due to its massive adoption by software and web engineers, hardware integrators need to understand the main differences between the two worlds and need to deal with them.

Getting hardware products to market is harder and costlier due to the need of building tools, managing manufacturing, acquisition of components and raw materials, shipping and distribution, stocking, etc. In this situation, it is evident that hardware products present a more probable risk of failure, because, asides the higher expenses, the expectations witch such products are normally also higher. Software is perceived and assumed to be ephemeral, and consumers are far more tolerant of imperfections, but this is not applicable to physical products, where the end users want their expectations to be met [239].

Moreover, the product type we have in hands, the Photonic Sensor, is not even a mere hardware product. The problem's complexity management, the smartness and the connectivity are to be solved by software means. Having a look at smart sensor products that combine an advanced hardware with several software applications, we realize that the development effort may fall around 60–70% in software and algorithm development [240].

Considering both, the budgetary requirements for launching the hardware series, and the importance of delivering advanced functionalities through customized software, the following statements could be assimilated for the Photonic Sensors development from the Minimum Viable Hardware Product philosophy.

xi. Plan scalable hardware and schedule different software releases for the same hardware.

xii. Plan modular hardware so that you can replace blocks with less effort.

xiii. Focus of minimum viable, but reliable, hardware products, shipping first versions with basic software functionalities.

4.2.6 Phase–Gate or Stage–Gate®

It is evident that efforts, time and budget for the development of photonic sensors, including not only hardware and software, but also optoelectronics, micromechanics, chemistry, etc. increases as the complexity of the system does. Therefore, providing means to control the progress of the development becomes crucial for the success of the product, or just for stopping the projects early to minimize the losses.

The sensor systems covered in this thesis could be considered as the result of research intensive activities, and normally address critical use cases, with important technical and regulatory specifications. In this challenging scenario, the probabilities of not meeting certain requirements are high. Consequently, the methodology suggested for assisting the integration of photonic sensors should cover the continuous technical, economical, regulatory and market assessment of the development, monitoring the progress and identifying risks.

This challenging scenario is well suited for the Phase–Gate, or Stage–Gate® methodologies, which suggest an operational roadmap for conceiving, developing and launching new products improving effectiveness and efficiency. Devised during the mid–1980s and implemented around 1995 [228], the core idea of these methods is a staging and gating process, where *Stages* represent the development of the project, executed by multidisciplinary teams, and the *Gates* symbolize intermediate assessment points. At each Gate the continuation of the project is decided based on the information generated within the previous Stages, including not only the technological progress but also the business case, risk analysis, and availability of necessary resources.

The structure of each stage is quite the similar, formed by the specific Activities to be carried out by the project leader and the team, a *Comprehensive Analysis* of the results and the preparation of the Deliverables which integrate the conclusions of the analysis and which are submitted to the Gate. There are 6 basic stages:

Table 4.2-3: Description of the Stages included in the traditional Stage–Gate development process.

Stage	Activities
0. Discovery	The phase covering the activities planned to discover opportunities and to generate new product ideas.

1. Scoping	During this step, the main goal is to launch an inexpensive assessment of the technical strengths, weaknesses, market prospects and status of the competence regarding the new product idea.
2. Build Business Case	This phase deals with the comprehensive analysis of the technical, marketing and business feasibility of the product and it is a difficult, complex and resource intensive task. There are four main components to be defined within this phase: product and project definition; project justification; project plan and feasibility review.
3. Development	Plans defined at early stages are translated into concrete deliverables. The actual design and development of the new product happens at this phase, as well as the scheduling of manufacturing and operations, and the test plans for the next stage are defined. The ultimate deliverable of this stage is the prototype, which will go through extensive testing and validation in the next stage of the process.
4. Testing and Validation	The objective of this stage is to validate the entire project, covering the product itself, the production and manufacturing process, customer acceptance, and the economics of the project. The tests include near testing, field testing and market testing
5. Launch	The product launch is the conclusion of the product having passed all previous gate. This phase covers the full commercialization of the product – the beginning of full production, selection of distributors and commercial launch.

As mentioned, prior to each Stage, we found a decision point, Gates, where the continuity of the project is decided based on the information generated so far. At each Gate, the next steps of the project are decided and resources are allocated based on three quality parameters: quality of execution, business rationale and quality of the action plan.

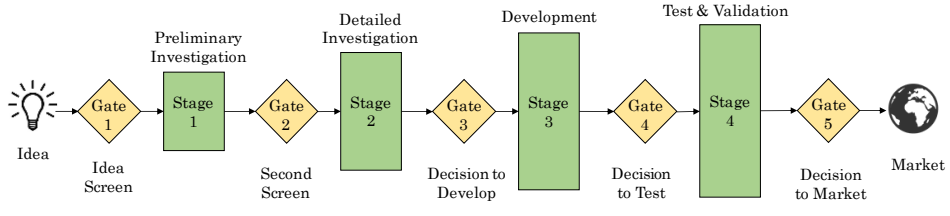

Figure 4.2-4: The generic Stage–Gate Process.

As it happens with the Stages, the Gates are structured in three components: *Deliverables*, which are the inputs to the Gate and collect all the information generated within the previous stages. The *Criteria* by which the project is validated, including normally technical, financial and qualitative parameters. And finally, the *Outputs* of each gate, which include a decision (go, kill, hold, recycle) and a path forward (approved project plan, date and deliverables for the next gate agreed upon).

The benefits from this paced process are evident and, since its launch, Stage–Gate has been present in more than 80% of the companies in the United States [241]. This method has also been reported as an ideal candidate for assisting the development of medical devices [242], covering from their embryonic research phases, clinical trials, clearance from regulatory bodies until the commercial launch. This is an interesting scenario, because medical devices is a really challenging development field, dealing with research intensive products, heterogeneous and multi–domain technologies, strict regulations and testing, and requiring huge investment that need to be carefully justified and allocated.

Additionally, as it can be seen in Figure 4.2-5, Stage–Gate has been merged with other traditional new product development processes as the DFSS.

There are also some references of application of Stage Gate modifications in the field of MEMS devices [243], which is also a challenging application field, intrinsically heterogeneous, highly dependable on functional prototypes for concept validations and with important investment requirements even at early stages.

As described in the next section, the traditional Stage Gate process is evolving to better accommodate iterative projects. However, some interesting contributions can be extracted even from its original principles, as:

xiv. Control the process development through a structured process, with clear check–points, helping to introduce discipline into an ordinarily chaotic process

xv. Create multi–domain working groups to cover both, the development and the assessment of the project

xvi. Focus on three different testing scenarios: near, field and market testing.

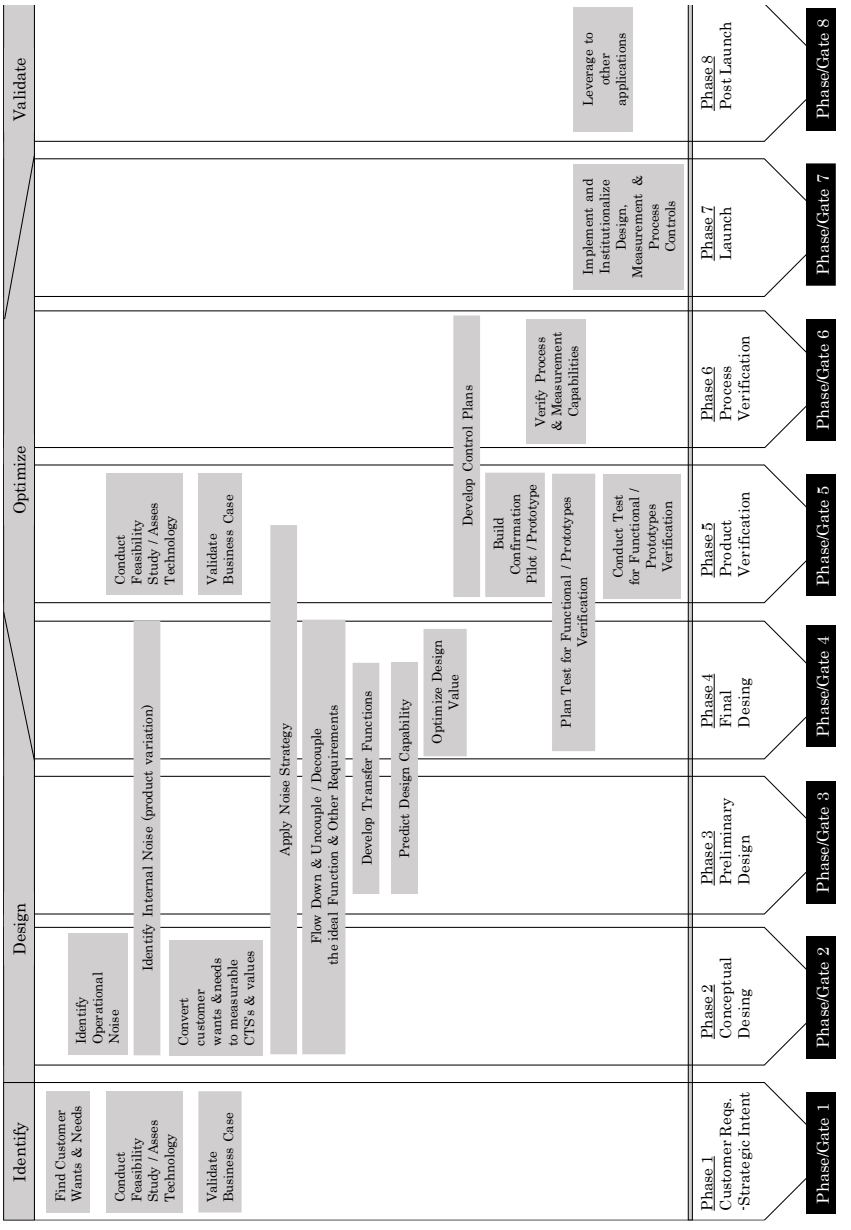

Figure 4.2-5: Design for Six Sigma phases mapped into a phase–gate development process [231].

4.2.7 New Development models: Hybrid Approaches

The traditional vision of the Stage–Gate process is clearly lineal or sequential, and may lack from the flexibility needed to accommodate to fast changing scenarios [244]. This weakness has led to the generation of different hybrid models lately, as the Agile Stage–Gate [245] [246] [247], Open Innovation and Stage–Gate [248], or the Triple A System (Adaptive, Agile, Accelerated) [220].

These evolutions are always looking for a better management of product development under evolving requirements, uncertain environments and unforeseeable risk management, which are the common denominator in ambitious novel projects [249] as the ones represented by the Smart Photonics Sensors, and described in Table 4.2-1. Basically, all the new features added to sequential processes like the Stage–Gate try to incorporate the iteration or looping approaches within the general project phases, as depicted in Figure 4.2-6, assuming that the information at the beginning of each phase is not solid.

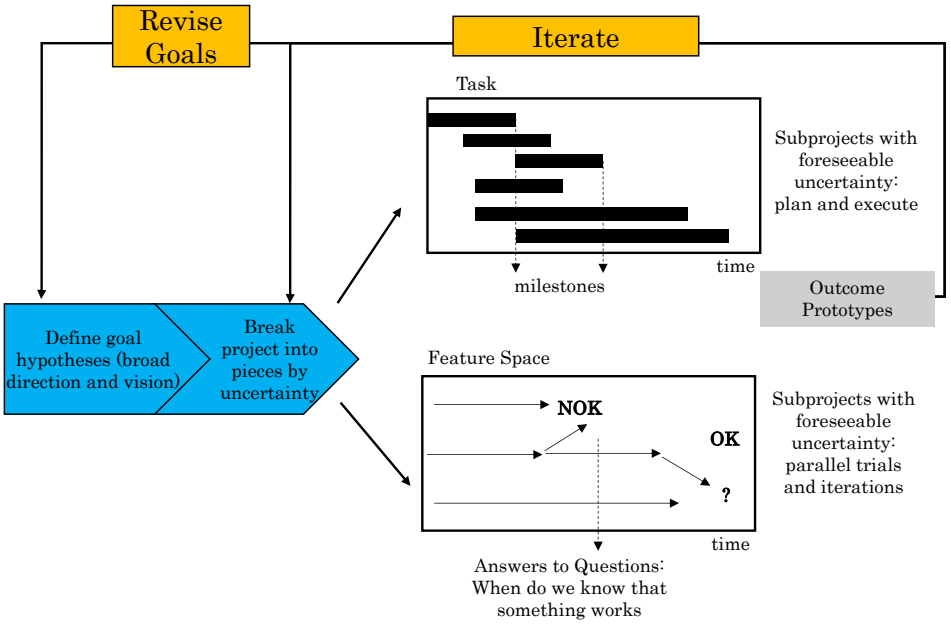

Figure 4.2-6: Template of flexible process to complement the Stage approach [244].

Agile development methods were elaborated by the software industry and described for the first time in the 2001 book, *Manifesto for Agile Software Development*. Basically, this approach splits the development into small incremental pieces, so–called 'sprints', requiring minimum planning, with clear goals, short delivery times (2–3 weeks) and focused on creating working version of the product, which will be used to demonstrate a certain functionality to stakeholders (management, customers, end users, investors, etc.). Therefore, this methodology suggests micro–planning management approach, with incremental and iterative design, where requirements and solutions evolve through cooperation between cross–functional and self–organizing teams.

While this approach has proved to be very suitable for software environments, as mentioned in section 4.2.5, physical products represent a much more complex challenge, and it may not be feasible

to manufacture a working version of the product in a few weeks. However, when applied to physical or hardware products, the goal of an Agile–based approach, the objective is similar: deliver something that is tangible and can be evaluated and tested with stakeholders.

xvii. Parallelize as much as possible the different proof–of–concepts required to validate technologies, mitigate risk, verify integrations, etc. considering each of work lines as an isolated sprint.

Understanding the differences between Agile and Stage–Gate models, displayed in Table 4.2-4 helps to assimilate the diverse approaches that have been proposed for their merge.

The first approach is to consider Agile as a useful micro–planning or project management method that can be used within Stage–Gate to accelerate some of its stages. The next evolution of the integration of Agile within Stage–Gate is the Spiral concept. This evolution was suggested to bridge the gap between the Agile principles and the requirements from physical product developers facing a dynamic and fluid market with changing product specifications. The spiral development devises a series of *build–test–feedback–revise* iterations with each iteration delivering an increasingly more complete version of the product.

When applying the Spiral approach to the development of physical products, unlike it happens with the software ones, each iteration does not deliver a working product, but a product version that the end user can respond to or give his feedback. These product versions can be virtual prototypes, crude models, working models, rapid prototypes, or early prototypes, i.e. usually something physical that the customer can respond to

Table 4.2-4: Key differences between Stage–Gate and Agile models, from [246]

Characteristic	Stage–Gate	Agile
Type of model	Macro–planning	Micro–planning, project management
Scope	Idea–to–Launch, end–to–end	Development & Testing stages only
Organizational breadth	Cross–functional: Development, Marketing, Sales, Operations	Technical (software code writers, engineers, IT people)
End point	A launched new product in the market	Developed and tested working software product

Decision model	Investment model: Go/Kill Involves a senior management group	Principally tactical: the actions needed for the next sprint

The next evolution of Stage–Gate under the influence of Agile is the Triple A System, which apart from the Agility, it empowers the Adaptive and Accelerated development. The Triple A system basically suggests to incorporate the *Agility* by the previously mentioned spiral's *build–test–feedback–revise* loop or iteration within each phase of the generic Stage–Gate approach. Additionally, the development needs to be *Adaptive*, to accommodate to new scenarios, because, especially for more innovative products, end users are not able to specify what they want or need until they see it.

However, continual adaptation without any forward progress accomplishes little to the project development [227]. Therefore, not only adaptability, but also means for fast progressing are required, and, we need to offer versions of the product very fast to enable the validations of the product concept by the end users early, cheaply and often. Consequently, an Accelerated development flow is expected.

The Triple A System also suggests to increase the development emphasis on the clarifying the key unknowns, risks and uncertainties of the project. The objective should be to identify them as early as possible and determine whether new technology or development might be required. Keeping the focus on specifying the uncertainty, many problems later in the project can be prevented and much time and money saved.

But the Triple A proposal it is clear on this specific point, for achieving a truly accelerated design, the resources should be properly accommodated and supported by a dedicated cross–functional team for maximum speed to market. According to the Tripe A System, to achieve this commitment, the integration of the Stage–Gate approach with the company's portfolio management and resource management is required. This technical and management integration should guarantee that the number of projects under development and the resources available are equilibrated so that project team members are not stretched too thin and a true Acceleration, Adaptation and Agility is achieved.

Even if several suggestions claimed by the Agile and Stage–Gate merged view are also present in the Lean Startup proposal, some interesting approaches have been also identified in these methods, as:

xviii. Integrate technical, economic and human resource management to enable a true accelerated project development.

xix. Prototype fast (generate something tangible) to enable the end user giving feedback about the project concept, contributing to its specification.

xx. Focus on the unknown, uncertain and risky parts of the project, to clarify them as early as possible with the aim of minimizing project development time and cost.

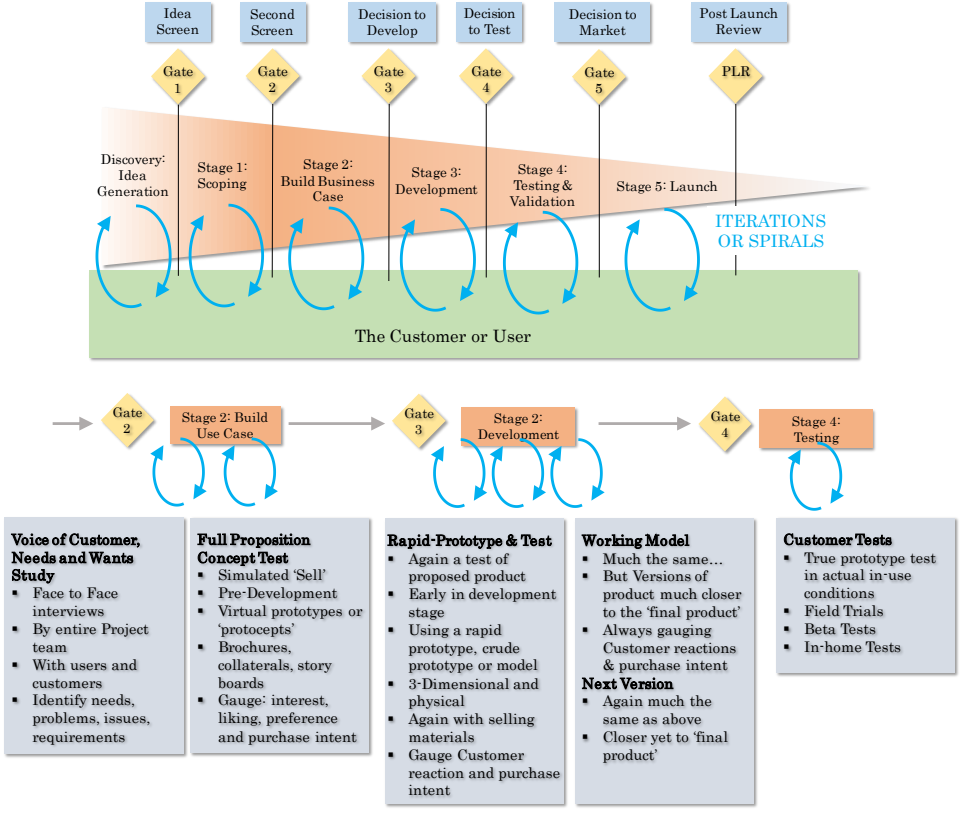

Figure 4.2-7: The Spiral development within the Stage–Gate process, from [220].

Continuing with the Stage–Gate evolutions, the Open Innovation Stage–Gate is found. Open Innovation is a concept pioneered around 2003 [250] with the aim of moving forward from the classic Closed Innovation scenario, where the companies rely solely on internal resources for envisaging new ideas, for developing them and for selling the final outcomes. The Open Innovation claims that projects may be generated inside or outside the boundaries of the companies, while their development and commercialization could, eventually, accommodate or be transferred to third parties. This new model is really suitable for helping companies to expand to new markets, to assimilate new technologies or to make profit from developments out of the companies' core businesses.

When merged with the Stage–Gate process, different activities are fitted into the Stages, and some new Criterions are considered at Gates. The philosophy change gets more evident at the first pre–Development stages (scoping and business model), including actions that involve potential partners or outsourced suppliers who may provide technical, marketing or manufacturing competences to develop and commercialize the product. Additionally, the Criteria at the Gates should deal with a completely new perspective like the lack of knowledge within the development team, or the unalignment with business of the company.

The new set of actions suggested by the Open Innovation Stage–Gate approach suits perfectly to the case of Photonics–enable Sensors. The multi–domain nature of these systems evidently could be benefited from the inclusion of external experts to support the development. This is clearly the case for the photonic component providers, whose insights are always an important asset for the sensor product design. Therefore, the Open Innovation version of the Stage–Gate could contribute to the specific case of this thesis with the following suggestions:

xxi. Identify the missing internal capabilities and seek potential partners or outsourced suppliers early in the projects.

xxii. Develop an IP strategy for the project to help handling the IP and legal issues with external firms.

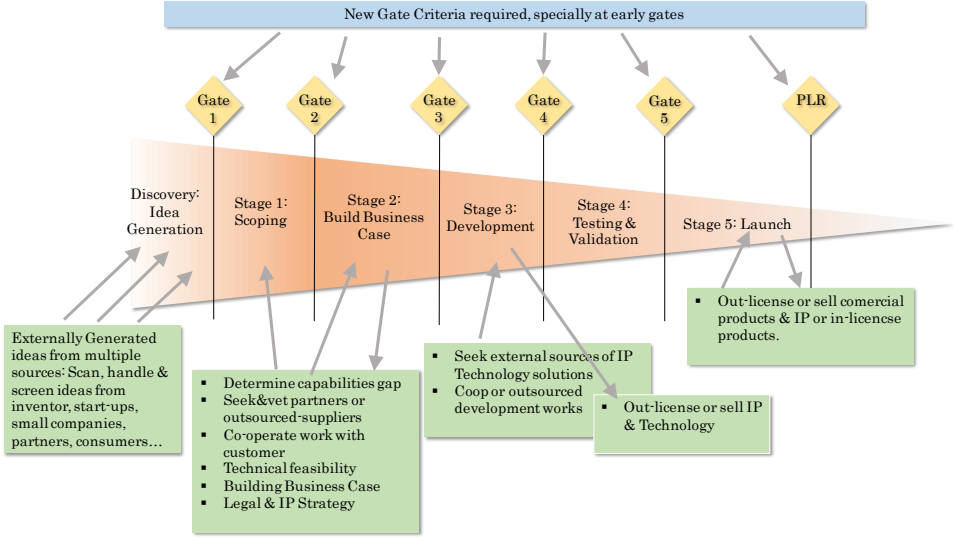

Figure 4.2-8: Open Innovation Stage–Gate, External interfaces (in–bound and out–bound) at multiple points in the process, from [250].

4.2.8 Summary of Key Contributions from Baseline Models

The review of the state of the art of the different models for the development of new products done in the sections so far, has served as starting point for our custom methodology elaboration. Different contributions have been identified while assessing the structure and approach of the baseline processes, which have been summarized in Table 4.2-5. These contributions have been fed into the different stages of the proposed methodology for photonics–enabled sensor engineering.

Table 4.2-5: Summary of identified contributions from the different new product development processes.

	Contribution	Baseline model
i.	Only if you focus on measuring the defects of a process, you will be able to figure out how to solve them,	DFSS
ii.	Use objective metrics or key performance indicators (KPI) to measure processes	
iii.	Track changes occurring at these KPIs for early problem identification	
iv.	Keep the customer in the loop for detecting problems and deviations occurring at customer's site	
v.	Develop a chief engineer system to integrate development from start to finish.	Lean Product Development
vi.	Organize to balance functional expertise and cross–functional integration.	
vii.	Develop towering competence in all engineers.	
viii.	Fully integrate suppliers into the product development system.	
ix.	Shape the product specifications hand by hand with the customer.	Lean Startup
x.	Analyze thoroughly the progress of the development by scientific experiments and by the feedback of the customer.	
xi.	Plan scalable hardware and schedule different software releases for the same hardware.	MVP Hardware
xii.	Plan modular hardware so that you can replace	

	blocks with less effort.	
xiii.	Focus of minimum viable, but reliable, hardware products, shipping first versions with basic software functionalities.	
xiv.	Control the process development through a structured process, with clear check–points, helping to introduce discipline into an ordinarily chaotic process	
xv.	Create multi–domain working groups to cover both, the development and the assessment of the project	Stage-Gate
xvi.	Focus on three different testing scenarios: near, field and market testing.	
xvii.	Parallelize as much as possible the different proof–of–concepts required to validate technologies, mitigate risk, verify integrations, etc. considering each of work lines as an isolated sprint.	Agile Stage Gate
xviii.	Integrate technical, economic and human resource management to enable a true accelerated project development.	
xix.	Prototype fast (generate something tangible) to enable the end user giving feedback about the project concept, contributing to its specification.	Tripe A Stage Gate
xx.	Focus on the unknown, uncertain and risky parts of the project, to clarify them as early as possible with the aim of minimizing project development time and cost.	
xxi.	Identify the missing internal capabilities and seek potential partners or outsourced suppliers early in the projects.	Open Innovation Stage Gate
xxii.	Develop an IP strategy for the project to help handling the IP and legal issues with external firms.	

4.3 Methodology proposal

This chapter introduces a comprehensive methodology for Photonics–enabled in–line fluid sensor engineering. The following sections give an overview of the method, and then dives deep down into the details of the individual methodology blocks. For each of the

Stages and Gates, a detailed description of their objectives, restrictions, inputs and outputs and criteria is given. The description of the different Stages is complemented with specific examples as well. Additionally a design flow chart that leads through the development of the project is provided.

4.3.1 Audience for the Methodology

This methodology is intended to answer the concerns and curiosities of Research and Development Teams, Design houses or Engineering teams that typically have to face the development and integration of products for end customers, being those either within the same company or outside. Therefore, even if innovative ideas may come up from the aforementioned teams, these are not normally the main promoters of the innovations neither they are the ones with the better insights on the final application.

However, these teams need to be imaginative, flexible and fast to adapt to the new development scenario and maximize the expertise and knowledge gained in previous experiences to generate a development team that answers and anticipates to the customers' needs.

The intention of the methodology is to help these design teams understanding the intrinsic complexity of the photonics-enabled sensors, providing a structured approach developed for uncertainty reduction, guiding on multi-domain and heterogeneous integration and to maximize the incremental outcomes towards the product development.

Indeed, customers promoting and requesting this kind of products would also benefit from this methodology because this approach should help them understanding the technological complexity of the product, allowing them to specify it better and plan de development in a more accurate way.

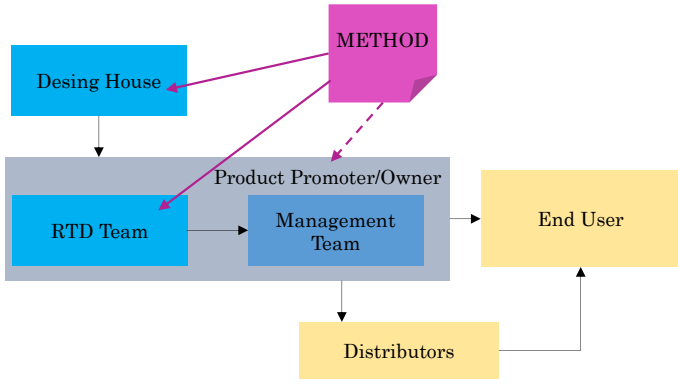

Figure 4.3-1: Schematic showing potential stake holders in a product structure and the main audience at which the methodology is aiming.

4.3.2 Overview

The assessment of the baseline methods reviewed in previous sections revealed that a combination of principles, suggestions and visions taken from the different models (see Table 4.2-5) represents a promising approach for New Product Development in the context of Photonics–enabled Smart Sensors for fluidics.

Additionally, we found that the backbone of the traditional **Stage–Gate process, enhanced with Agile and Open Innovation** concepts, could serve as an ideal framework for controlling the development process, from the management of the early stages to the materialization of the final product.

Sections 4.1 and 4.2.1 have already introduced the main objectives and challenges set out by the photonic sensor integration, and most of them deal with the **management of heterogeneous technologies** by a **multi-domain team** and with the **lack of awareness about specifications and risks** of the project. Therefore, these two conditions have been considered as the main drivers for the model elaboration, and all the focus and efforts of the different stages, iterations and gates are devoted to solve the heterogeneous integration in an efficient and reliable manner and to clarify the uncertainty (specifications and risks) as early as possible.

Another important asset in the suggested development model is the continuous **presence of the end–user or customer in the development loop**. Their insights and feedback is a key factor for the success of the idea generation, proof-of-concept validation, prototype testing, product shaping and product launch. This is because, the customers and end–users are the ones who really look after strengthening the competitive advantage and added value of the sensor under development.

The methodological approach proposed here is tailored for **projects that must integrate photonic component provided by third parties or outsourced into autonomous sensor products**. Therefore, the management of this supply chain, and the characterization and wise selection of these components is also addressed by the methodology.

The development **process has been divided into five different stages** with its corresponding gates where efforts and resource requirement increase with each subsequent stage. The stages are (i) Opportunity identification, (ii) Proof of concept validation, (iii) Prototypes and Test Bench design, (iv) Validation in real field, (v) Industrialization and commercialization (see Figure 4.3-2), and will be described in deep in the next sections. Notice that, from now on, the methodology will be called Photonic Sensor Development (PSD) process.

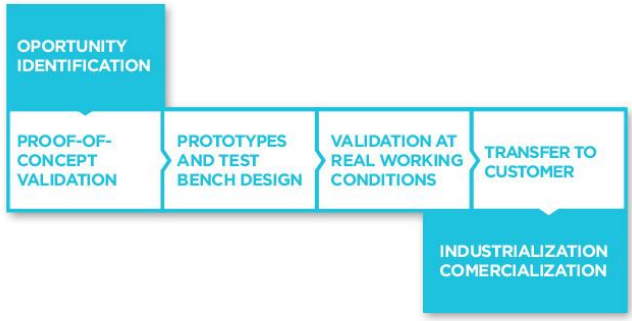

Figure 4.3-2: Basic structure of the Photonic Sensor Development (PSD) process.

4.4 Opportunity Identification

The first step towards a new product is to envisage an idea, vision, or concept that looks promising for a certain application or to identify a clear need to be covered. The first situation is known as technology push and the second is clearly a market pull scenario. Both innovation strategies are valid for generating the seed of a new product, because the first one looks for promoting or expanding a promising technology and the second one set outs a market need that may become an opportunity for technological developments. Even if both approaches may drive a new product conceptualization, the strategy to follow on each case should not be the same [251].

Some examples of market-pull product requests may be found in: (i) the enforcement of new regulations that require to measure or control a new parameter of the fluid (e.g. detection of allergens proteins in beverage production). (ii) The application of preventive maintenance programs, which requires to check the status of a certain fluid in real time to detect failures early and prevent them (e.g. monitoring wear debris on hydraulic fluids). (iii) The execution of cost cutting strategies that look for replacing certain fluid only when it is strictly needed to reduce the cost in consumables (fluid liters) and in human resources devoted to change the fluids (e.g. replacement of lubricant oils in automotive robots).

On the other hand, new developments driven by technological innovation are quite common in the photonics field. We should notice that photonic analysis techniques are very transversal to any application, and several use cases may benefit from the outcomes achieved in similar, but different, use cases. Imagine the possibilities of the spectroscopy analysis of a fluid; the capabilities of analyzing the presence of certain molecules by the measurement of the absorption bands happening in a fluid could be applied to recognize the

degradation of a lubricant (e.g. presence of oxidation molecules) or to quantify the fat proportion (e.g. presence of fatty acid molecules) on dairy products.

In this scenario, the purpose of the Opportunity Capturing Stage does not strictly deal with the process of new idea generation but with the evaluation of its feasibility. The Opportunity Identification is done almost exclusively by the customer company, however, for some preliminary investigations done within the stage, potential development partners might be included for consulting. Therefore, the focus of the proposed methodology with this regard is to perform a wise assessment of the opportunities identified.

The Opportunity Screening Gate is the place where the newly identified product ideas are assessed from technological and market views.

4.4.1 Opportunity Capturing Stage

Normally, we enter this stage with a rough formulation about the problem to solve made by the customer or end-user, with parameters of interest somehow defined and the process where to install the in-line monitoring system more or less identified. This situation represents an opportunity for the photonic sensor developer, who rapidly should identify the potential measurement principles that could address the problem or challenge outlined by the customer.

As mentioned earlier, the opportunities may come from different origins, but the first step is to identify if their nature is either technology push or a market pull. The reason behind this need for classification is because the origin of the idea will determine how the relationship with the end users and the specifications of requirements develop in later stages.

Additionally, the nature of the idea will modulate the efforts to be put on this early stage. Opportunities originated by market requests may require smaller efforts on the business model definition and the market assessment of the idea, but will entail a deeper technological review. On the other hand, technological ideas looking to be accommodated to an end user's need will have to focus on the economical feasibilities and implications of the new use case scenarios.

Once the basic idea has been defined, the objective of the Opportunity assessment stage is to briefly define technical, economical, intellectual property and business advantages that will help evaluating in more detail the suitability of the idea.

Usually, this Stage should not occupy more than one month, and the objective is to deliver the conclusions as soon as possible because a preliminary overview is requested rather than a deep

analysis. So far, the assessment work group should be composed of the headcount listed in the Table 4.4-1.

Table 4.4-1: Roles and equipment required and their expected activities for the Opportunity Identification Stage.

Headcount	
Role	**Activities expected**
Project Leader/ Senior Engineer	Deal with integration approach, IP and patent search, general feasibility, general plans, may require assistance from Legal and Financial depts.
Optoelectronic Engineer	Assessment of the proposed photonic method
Mechanical Engineer	Assessment of the proposed size, installation and environmental conditions
Chemical Engineer / Physicist	Assessment of the requested measurement performance, measurands
IP and Patent Advisor	Assessment of any potential IP or patent issue
Market and Financial Advisor	Assist the project leader on the economic plan
Equipment	
Item	**Use expected**
Bench-top Laboratory analyzers	Fast feasibility assessment

The specific deliverable outputs generated during this stage are described below, but it should be noticed that these documents will contain only basic and preliminary information that needs to be further elaborated in later stages. Notice that this is the only stage in the whole process where no physical deliverable is expected, since all these outputs deal with a generic feasibility assessment of the idea, each of them focusing on different aspects to be considered so far.

Table 4.4-2: Deliverables generated during the Opportunity Identification Stage and the involved team members.

id	Name	Participants
1.1	Technical Feasibility Report	Project Leader & Technical members
1.2	Capability Assessment Report	Project Leader
1.3	IP, Regulation and Legal Assessment Report	Project Leader & Technical members IP and Legal Advisor
1.4	Business and Economic Assessment Report	Project Leader Market and Financial Advisor

The first deliverable is the Technical Feasibility Report, which is coordinated by the Project Leader, but gathers the insights of the whole technical team. This document gives an overview about the measurement principle, the different implementation technologies and their interfaces, an estimation regarding the development plan, costs and times, an estimation about the expected unitary and volume prices of the product and the potential risks foreseen.

For the technical assessment of the measurement principle a bibliographic review and the internal technical expertise and resources are used. At this stage, the use of certain bench–top laboratory equipment (e.g. spectrometers, colorimeters, microscopes, rheometers) might be required. These laboratory analyzers could be useful for performing a rapid evaluation of the chemo–physical properties over some representative fluid samples provided by the end-user or for cross verifying some bibliographic findings.

At this stage already, the heterogeneous building blocks of the envisaged solutions should be, at least, identified. This enables not only a better estimation of resources and planning of the project, but also finding missing capabilities within the partners involved, which is critical for the next deliverables.

Another additional output of this stage is the Capability Assessment Report, which contains information concerning the foreseen capabilities and equipment required for project execution. Besides, the critical photonic components are listed and the associated key suppliers identified. Moreover, if any missing capability is found, a list of potential partners or outsourcers is provided. If required, this list is used in the following Gate by the stakeholders to decide which potential partners to approach for a joined engineering undertaking. An outline and example of this deliverable is given in Table 4.4-3.

.

Table 4.4-3: Example of information to be provided in the Deliverable 1.2 Capability Assessment Report

Equipment	
Item	**Activities expected**
Hydraulic Test Bench up to 15 bars	
UV/VIS/NIR Optic Test Bench	Preliminary feasibility test
Climatic Chamber	
Vibration and Shock generator	
Missing Equipment	
Item	**Potential Provider**
Hydraulic Test Bench up to 100 bars	Laboratory A
Fast prototyping of Plastic and Metallic pieces	Workshop A

Capabilities	
Role	**Activities expected**
Hardware Engineer	HW prototypes
Software Engineer	SW prototypes
Mechanical Engineer	Fluidics and Mechanics Simulations
Mechanical Designer	Micromechanical System design. Enclosure design
Optical Engineer	Optical design and simulations
UL and CE Advisor	Assessment of the envisaged regulatory requirements and their impact on design
Missing Capabilities	
Item	**Potential Provider**
Chemometrics Expert	University A, Company B
FDA Certification Expert	Company C
Core Photonic Component	
Item	**Potential Provider**
NIR micro–spectrometer 1600-2200nm	Company D, Company E

The next deliverable at this stage is the IP, Regulation and Legal Assessment Report, responsibility of the Project Leader and the IP and legal advisor and its content is outlined in Table 4.4-4. This document includes the declaration of the background knowledge for all the parties, and the list of the envisaged foreground technology generated during the project [252].

The background knowledge represents the pieces of technology that might be used during the project execution, but were developed previously and belong to the party's IP portfolio. The general conditions (e.g. license to use, deployment conditions, and royalties) for using these technological blocks should also be addressed here. On the contrary, the foreground knowledge is the innovation generated as the result of the project execution, and its ownership should be agreed among the partners, as well as its protection strategy (new patent submission, trade secret, etc.).

Of course, the information included in this very first version of the document is only an intention declaration, and should not be consider as legally binding. The specific term of each item will be later discussed and agreed among the partners, but having at least identified all the hot topics lubricates the forthcoming negotiations.

This deliverable should also include the conclusions of a preliminary patent review report, which has been accomplished with a twofold aim: early identifying any blocking or competing patent and

understanding the potential patentability of the foreground technology.

Last but not least, this report should gather the conclusions drawn by all the parties concerning the applicable regulations and potential compliance requirements, including the framework set up for monitoring the progress in terms of regulations along the next stages. Besides, this document needs to raise the awareness of the regulatory and compliance implications, especially concerning delivery time and cost of the development.

Table 4.4-4: Summary of the items and the expected information to collect in the 1.3 IP, Regulation and Legal Assessment Report deliverable.

Item
Background declaration
Foreground estimation
Patent review
Regulations and compliance requirements

The activities within this stage conclude with the Business and Economic Assessment Report. Notice that, as mentioned earlier in this chapter, the proposed methodology is not focusing on how to develop a comprehensive business and market review of the product; this is supposed to be the responsibility of the customer, and the information contained in this last deliverable must be generated with their close collaboration. The customer is supposed to have accomplished at least a preliminary scoping of the market existence, market size, potential sales, expected maximum investment, market opportunity window, competitors, and product placement. Based on this assessment, the information outlined below, and summarized in Table 4.4-5, should be included in this document.

The expected production volume and the approximated unit cost are significant information that may drive several technical decisions and may even jeopardize the whole feasibility of the project, either because the unit cost is not achievable, or because the project, or the non–recurring engineering (NRE) cost is not paid back by the margin profit of each unit at the expected commercialization volume.

Additionally, the market opportunity window will be used as baseline for the project planning and timeline, basically analyzing the feasibility and uncertainty of having the product ready by the time requested by the customer. The document is concluded with a very rough estimate of potential project cost, including personnel cost, consumable cost and equipment cost or amortization.

Table 4.4-5: Information contained in deliverable 1.4 Business and Economic Assessment Report.

Information	Responsibility of
Market existence, market size, potential sales, expected maximum investment, market opportunity window, competitors, and product placement	Customer
Production Volume and Target Unit Cost	Customer
Project Planning and Timeline	Project Leader
Project Cost (Personnel, Consumables, Equipment)	Project Leader & Economic Advisor

4.4.2 Opportunity Screen Gate

The main activity to accomplish at this first Gate is authorize or not the initialization of the project. This resolution is based on a thorough assessment performed by a decision group formed by customer representatives and the project leader. The particular decisions to be taken deal with the evaluation and acceptance of the individual deliverables generated during the Opportunity Capturing Stage (see Table 4.4-6). In addition to the continuation acceptance, a plan for the next stage is also provided, including the required resource allocation based on the estimations provided in the deliverable 1.4.

Table 4.4-6: Detailed inputs, decisions and outputs at 4.5.2 Opportunity Screen Gate.

Input	Decisions	Outputs
Technical Feasibility Report	Project risks and uncertainties acceptable	Approved initialization Proof-of-concept stage plan
Capability Assessment Report	Partner and provider list acceptable	Potential partners list
IP, Regulation and Legal Assessment Report	IP and regulatory perspective acceptable	Authorization to proceed
Business and Economic Assessment Report	Unit cost, project cost and project timeline acceptable	

4.5 Proof–of–Concept Validation

The objective of this second stage is to consolidate the estimations made on the previous one, confirming the measurement principle hypothesis, clarifying the integration needs, better understanding the project and technological risks and providing a more accurate vision on project's economics and schedule. Additionally, during this stage a first version of system requirements are expected.

During this stage, certain scientific or technological work is expected, but the level of detail and the intensity of these developments depend on the budget availability agreed at the Opportunity Screen Gate. The outcomes of this research will be decisive for the conclusions to be taken at the Prototype Development Decision Gate.

4.5.1 Proof–of–Concept Stage

The main objective during this Proof-of-Concept Stage is to confirm the feasibility of the envisaged sensor, and this is started primarily from the technical assessment of the devised measurement principles. In the previous stage, the customer's problem-to-solve has been somehow defined and the potential technical approaches have been identified based on internal expertise, literature review and some eventual laboratory measurements. At this point, these solution proposals will be further elaborated and verified against a first set of requirements already identified by the customer (see Table 4.5-3 for examples of requirement definition at this stage), with the aim of concluding if they are suitable for the use case, identifying their constraints and risk, and finally proposing a potential system architecture.

Normally, this stage should not cover more than one or two months, and the technical staff are the main active members. The roles, activities and required equipment and outsourcing for this stage is outlined in Table 4.5-1.

Table 4.5-1: Roles, equipment and outsourcing required and their expected activities for the Proof-of-Concept Stage.

Role	Headcount Activities expected
Project Leader/ Senior Engineer	Risk identification, identify the heterogeneous interfaces, provide the integrated view and assure the integrability of the proposed methods into an in-line sensor.

Optoelectronic Engineer	Define suitable optical and optoelectronic components. Define working settings.
Mechanical Engineer	Assess the feasibility mechanic, hydraulic, fluidic and environmental requirements. Validate the manufacturability of optoelectronic settings
Chemical Engineer / Physicist	Validate the chemo–physical measurement principles

Equipment	
Item	**Use expected**
Bench-top Laboratory analyzers (spectrometers, colorimeters, microscopes)	Validate the chemo–physical measurement principle
Sample optoelectronic equipment (emitter and detector evaluation systems)	Validate the integrability of the chemo–physical measurement principle into a sensor system
Climatic Chamber, Vibration test bed, etc.	Emulate different working conditions to validate the chemo–physical measurement principle under the required operation environment

Outsourcing	
Item	**Use expected**
Plastic/Metallic Fast Prototyping	Fabricate mechanical parts for the integration validation

The specific deliverables belonging to this stage (see Table 4.5-2) are generated during different sub–stage activities, which cover a theoretical approach to the problem, a laboratory validation of the theoretical hypothesis and a first assessment of the integrability of the method.

Table 4.5-2: Deliverables generated during the Proof-of-Concept Stage and the involved team members.

id	Name	Participants
2.1	Theoretical Description Report	Technical members
2.2	Laboratory Result Report	Technical members

2.3	Photonic Integration Report	Project Leader & Technical members
2.4	System Specification and Project Plan	Project Leader

4.5.1.1 Theoretical Approach

The vast majority of the applications of the fluid monitoring sensors are based on the measurement of a certain chemo-physical parameter. In the first stage, some photonic working mode have already been identified as potential candidates for extracting this relevant information from a fluid sample. In this sub-stage, the theoretical approach to the problem should be accomplished, which merges the theoretical principles with the very preliminary set of requirements already brought by the customer (see Table 4.5-3 for examples of this kind of requirements).

Table 4.5-3: examples of raw requirements brought by customer at this stage

Examples of Raw Requirements
Parameter to measure
Sensibility
Throughput
Size
Working conditions
Cost
Number of units required
Idea of potential regulations that may apply

This work is based on the application of the Photonic principles explained in the Chapter 2, to the specific use case under development. Thus, concepts like light transmission, reflection angles, absorption bands, focal points, etc. are particularized for the analysis of the parameters of interest of the target fluid. References to bibliographic sources as well as internal calculations are expected in this phase.

This theoretical study is fully dependent on the target application, and the experience of the chemo-physical and optoelectronics technicians is fundamental here for defining the right formulation of the problem. In the Table 4.5-4, we display some examples of possible outputs generated at this stage.

Table 4.5-4: Examples of parameters defined during the Proof-of-concept stage when analyzing a generic photonic system.

Example Parameters defined at Proof-of-Concept	Sub-stage
Absorption lines of compounds	Theoretical Approach
Working Spectral Range	
Sample Volume to analyze	
Expected Absorbance of typical sample	
Order of magnitude of the light source	
Order of magnitude of the detector sensibility	
Numerical Apertures of source and detector	
Optical Focal Lengths	
Optical Path Length	Lab. Validation
Optical Spot Size	
Field of View	
Deep of Field	
Integration time of detector	Integrated Validation
Intensity of emitters	

For instance, applications interested in either the identification of the material (qualitative analysis) or how much of a particular compound is present (quantitative analysis), require first to identify the functional groups of the target compound, map their absorption on the spectral region, and identify any other compound present in the sample that overlaps the absorption lines of interest (see Figure 4.5-1). This allows specifying the spectral working range for emitters and detectors.

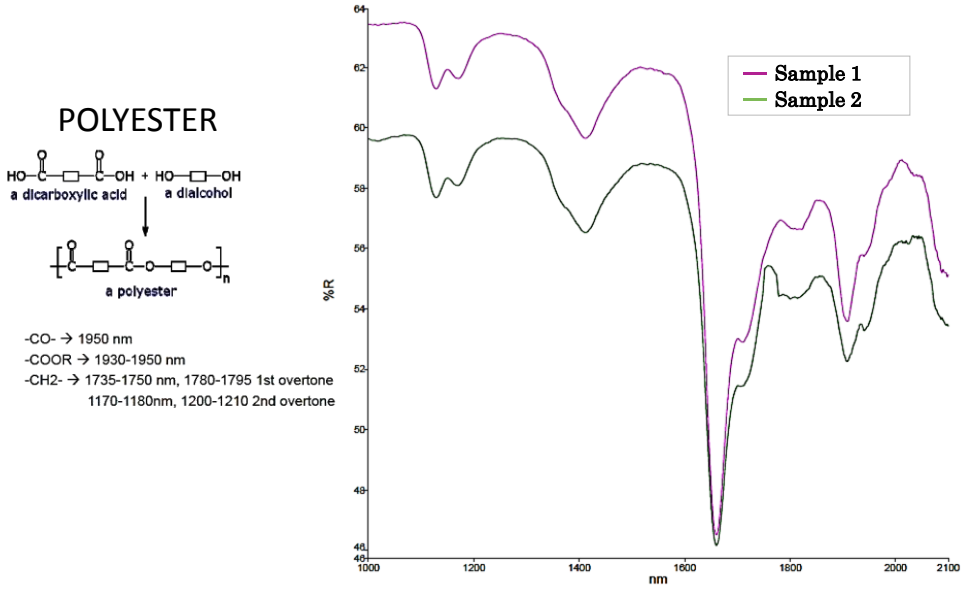

Figure 4.5-1: Functional groups of the Polyester compound, their absorption lines, and the correspondence of these lines with the reflectance spectra in the NIR region of two analyzed samples.

Then we should define the molar absorptivity of the compounds and apply theoretical models (e.g. Beer-Lambert, Kubelka–Munk or Kramers–Krönig) for estimating the light behavior and thus, the required emission light power and detector's sensibility. At this stage, the impact of other side effects should also be at least identified, such as the effect of the temperature changes in the absorption lines, or the variation of moisture concentration in the sample.

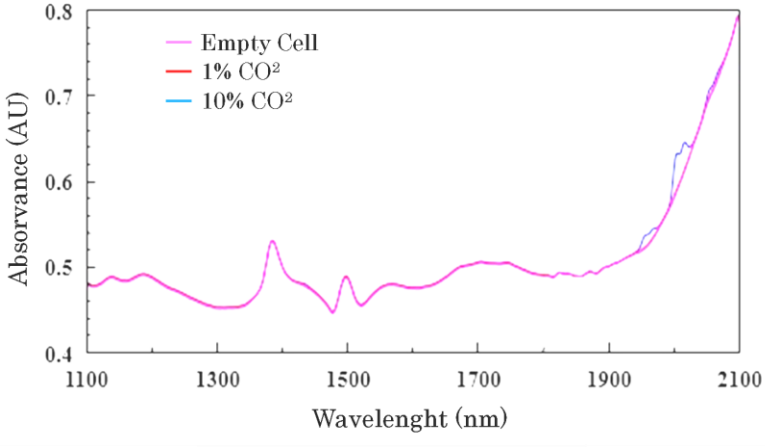

Figure 4.5-2: NIR spectra of empty cell, cell with 1% CO^2, and cell with 10% CO^2 sample. The differences between the empty cell and the 1% sample are insufficient to perform any measurement, and thus, this is the detection limit [253].

Some typical conclusions at this stage that could hinder the project execution could be that the analyte concentration is too little for a reliable measurement (see Figure 4.5-2), or that the overlapping noisy-compounds present stronger absorptions that hide the effect of the compound of interest, as depicted in the Figure 4.5-3.

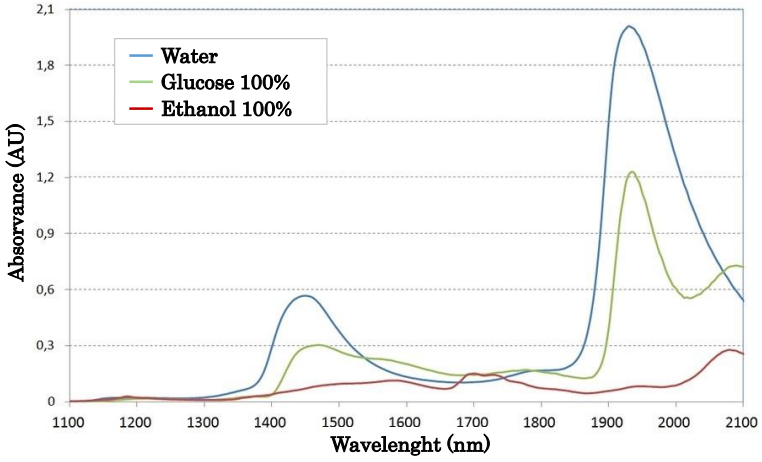

Figure 4.5-3: Absorption spectrum in the NIR range of Ethanol, Glucose and Water samples, showing the overlap of the absorption peaks. This situation complicates the quantitative analysis of mixed samples (e.g. fermentation of alcoholic beverages [254], or at bioreactor processes [255]) based on NIR spectroscopy.

Another example is the motorization of micro-particles. In this specific application, the problem to solve is the definition of the optical and focusing properties and the definition of the light intensity requirement at the detector to perform a valid detection through machine vision algorithms (see section 5.2).

Of course, this theoretical approach needs to be consolidated whit real experimentation, which is accomplished in the following sections.

Table 4.5-5: Summary of the items and the expected information to collect in the 2.1 Theoretical Description Report.

Item
Theoretical description of the measurement principle
Assessment of working conditions in the measurement principle
Identification of main Photonic Component
Formulae to calculate (orders of magnitude) emitters, detectors, …

4.5.1.2 Laboratory Verification

Basically, at this stage, the theoretical hypothesis and definitions are taken one step further and are validated against real measurements performed at bench-top laboratory equipment.

This is one of the first points where the cooperation of the end-user or customer is strictly required, since the availability of real and representative samples is mandatory. Depending on the photonic principle that is going to be used as measurement method, a different minimum number of samples will be required. For instance, a chemometrics-based method will require at least 50 or 70 representative samples.

These samples will be used as reference, so the validated values of the parameters of interest need to be provided as well, if not, we should also accomplish these measurements. Once the samples with their reference values have been identified, we proceed to apply the selected photonic measurement setup to extract the information.

Notice that applying a photonic inspection does not necessarily give a measurement result. Remember that the photonic techniques are mainly indirect methods for extracting relevant information from a sample, but always some sort of algorithm, method or processing mean is required to convert the photonic information into a valid sensor measurement.

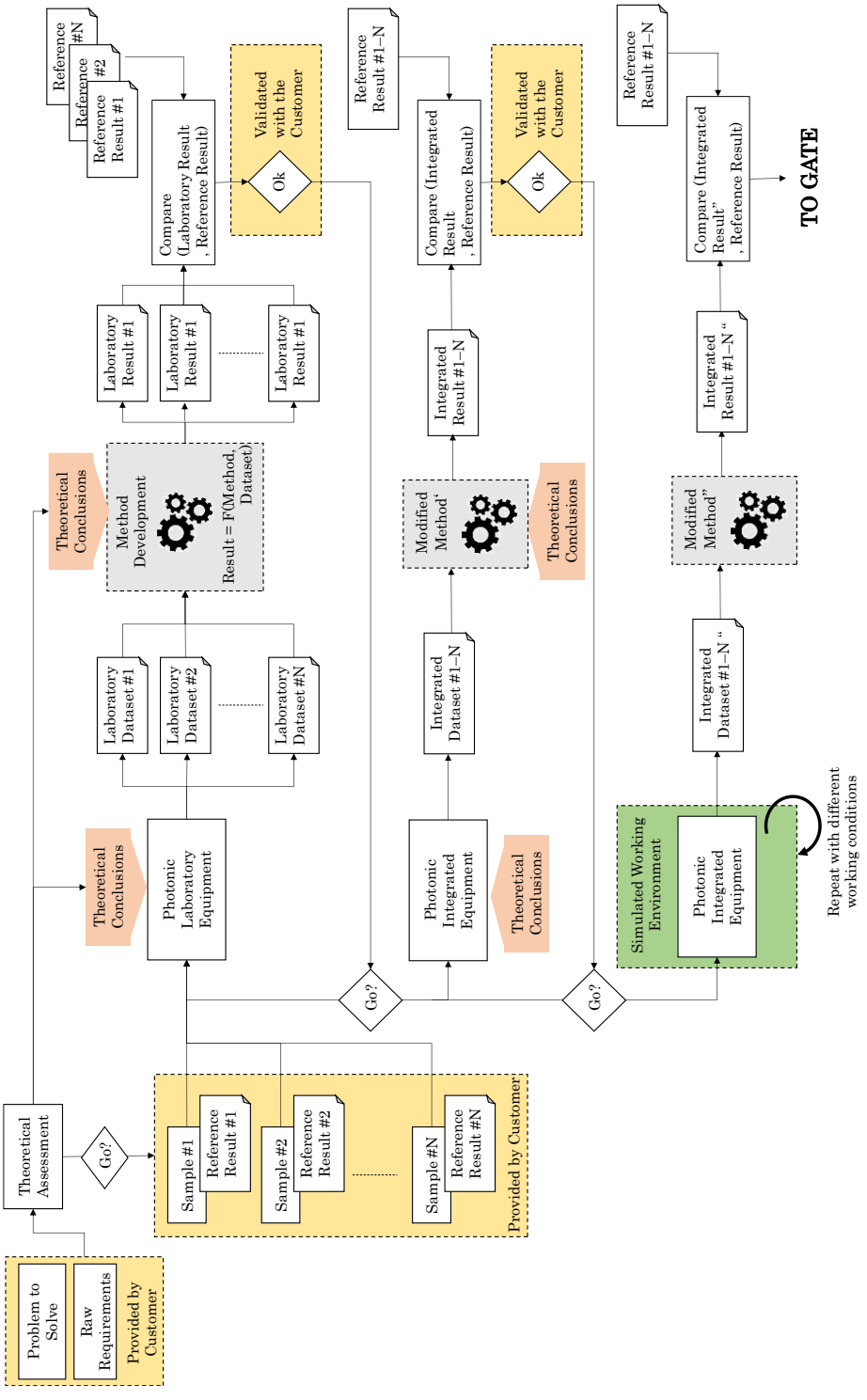

Figure 4.5-4: Workflow amidst the different sub-stages within the Proof-of-Concept phase.

Depending on the complexity of this method, including it within the Proof-of-Concept stage may be overambitious, because sometimes the method itself is the core of the photonic integration project. In these cases, the extent of the method development and the expected soundness of the laboratory results should be agreed with the customer. Same happens with the decisions about the feasibility of the idea, they may depend entirely on the capabilities of the method to be developed. In these cases, the experienced verdict given by the technicians after analyzing the laboratory data needs to be validated by the customer, assuming that with the current level of dedication no further guarantee is possible.

Concerning some specific information extracted during these laboratory studies, sample volume and inspection area are normally defined based on the settings of the laboratory equipment and the data obtained (see Table 4.5-4). For instance, for a transmission spectrometric system, the sample volume is defined by the path length (the section of the cuvette) and by the spot size, or the intersected area between the emitted light beam and the detectors viewing area. On the other hand, for an optical setup, the inspected volume equals the field of view by the deep of field. The specification of this kind of parameters and their tolerances is critical for the later hydraulic and mechanic system specification.

Notice that, apart from the abovementioned parameters and the photonic results, no relevant information may be taken from the photonic settings of the laboratory equipment, because normally, these include detectors, emitters and optical components which installation on the field is not feasible. This is the reason why we move forward to the next sub-stage.

4.5.1.3 Integrability assessment

The very first thing to take into account while planning to develop an integrated photonic sensor is that, likely, the performance and characteristics available in the integrated components will be worse than the ones available at laboratory equipment. And even if, as described in Chapter 1, the integrated photonic components are enhancing their features day by day, the reality is that the laboratory equipment is doing the same, so we will always have to consider this performance gap.

This is the reason why this third stage is required while validating the proof-of-concept, because the results achieved with the bench-top equipment may not be migrated into an embedded sensor system at the required cost, size, sensibility, etc.

Besides, it is almost impossible to replicate any industrial working condition with bench-top analyzers, basically because these have been designed to work under stabilized environments, rather

than dealing with broad temperature spans, humidity and vibrating conditions as expected for the in-line sensors. On the other hand, if required for the proof-of-concept, we could emulate different working conditions (e.g. using a climatic chamber, vibration bench, etc.) and have the integrated photonic components operating under these conditions for verifying the performance of the system.

Actually, the photonic components tested at this stage (emitters, detectors and optics) will become the first option to be integrated in the hypothetic forthcoming prototypes, and therefore, should be selected with the aim of meeting not only the technical specifications identified in the previous theoretical and laboratory studies, but also the requirements in terms of cost, size, and operation conditions specified by the customer.

However, even if the providers of the integrated photonic components offer a full range of evaluation systems to test their devices, at this stage we may require manufacturing mechanical mock parts for enabling the use of the devices more similar to their intended use once integrated in the sensor. These mechanical parts could be considered as the very first version of the sensor prototype (see Figure 4.5-5). Therefore, the implication of the mechanical and hydraulic engineers may be required for designing and accomplishing the fabrication and assembly of these parts with the optoelectronic components.

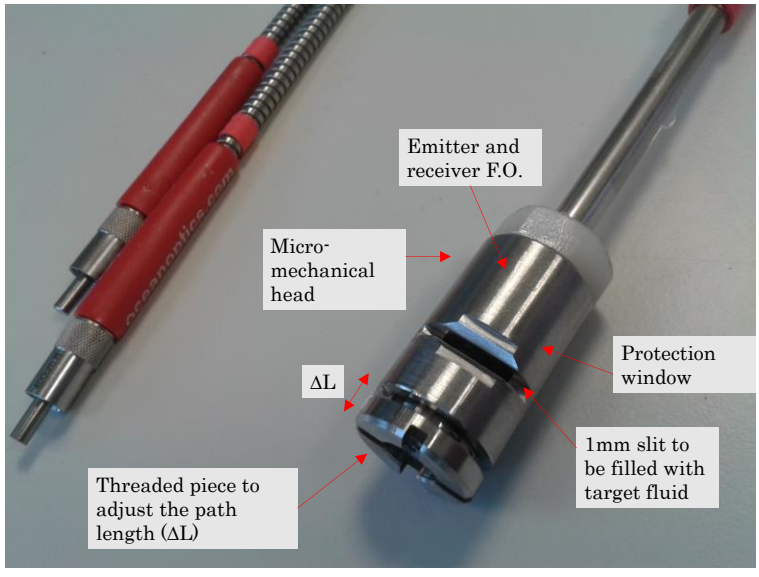

Figure 4.5-5: Example of customized mechanics system to enable the proof-of-concept of the integrated components. In this case, a micro mechanical head was developed to submerge a dual F.O. system into a running fluid to analyze it with visible spectrometry. Since the path length was not defined yet, the design includes a threaded piece that allows enlarging the path length. This specific prototype belongs to the proof-of-concept of the OilProbe® sensor.

In addition, in some occasions, dedicated electronic system is required for enabling certain working modes of the photonic components, and not all the features are available in the evaluation versions. In these situations, we may also require developing a custom hardware-software solution for the tests. In Figure 4.5-6, we display an example of this situation, with a CMOS detector required to drive and synchronize a stroboscopic lighting system; but with no evaluation board supporting this feature, a customized hardware was built. So, already at the proof-of-concept stage we realize about the multi-domain skill set required to accomplish the verification of the first integrated version of the measurement principle.

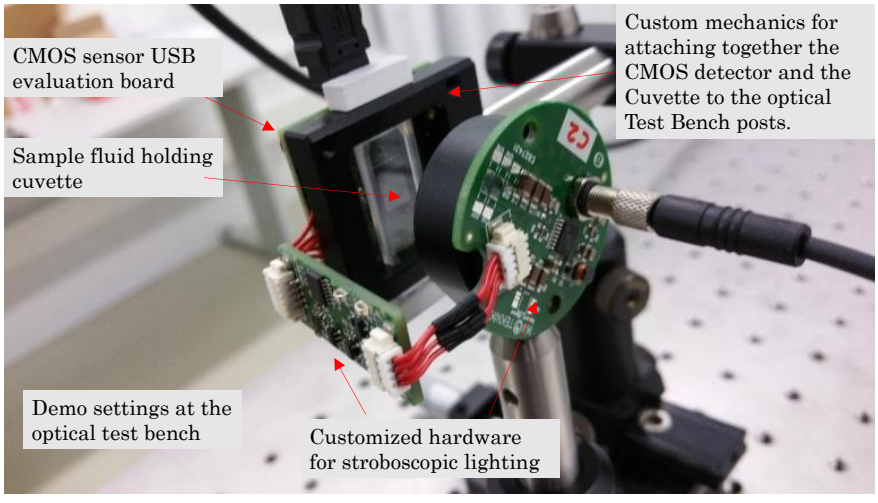

Figure 4.5-6: Example of customized hardware system to enable the proof-of-concept of the integrated components. In this case, the settings belong to the proof-of-concept of a micro-particle detector.

Even if we may require certain customized parts, our objective at this stage is using as much standard components as possible to keep the development cost down. The availably of an optical test bench is very useful at this point, because several optical and mechanic components are accessible at relatively low cost. Sometimes, as depicted in Figure 4.5-6, even if we develop our custom parts, we still fabricate them compatible with standard optical test benches to allow using them along with the rest of compatible optical components.

4.5.1.4 System Specification and Project Plan

This is the wrapping up sub-stage, where the developments and conclusions of the previous tasks are summed up to deliver a system architecture, with all the heterogeneous blocks clearly identified (see Figure 4.5-7), and including a first version of system

specification answering to the customers' requirements. If the project moves on to the next stage, these preliminary specifications will be the base for the prototype development.

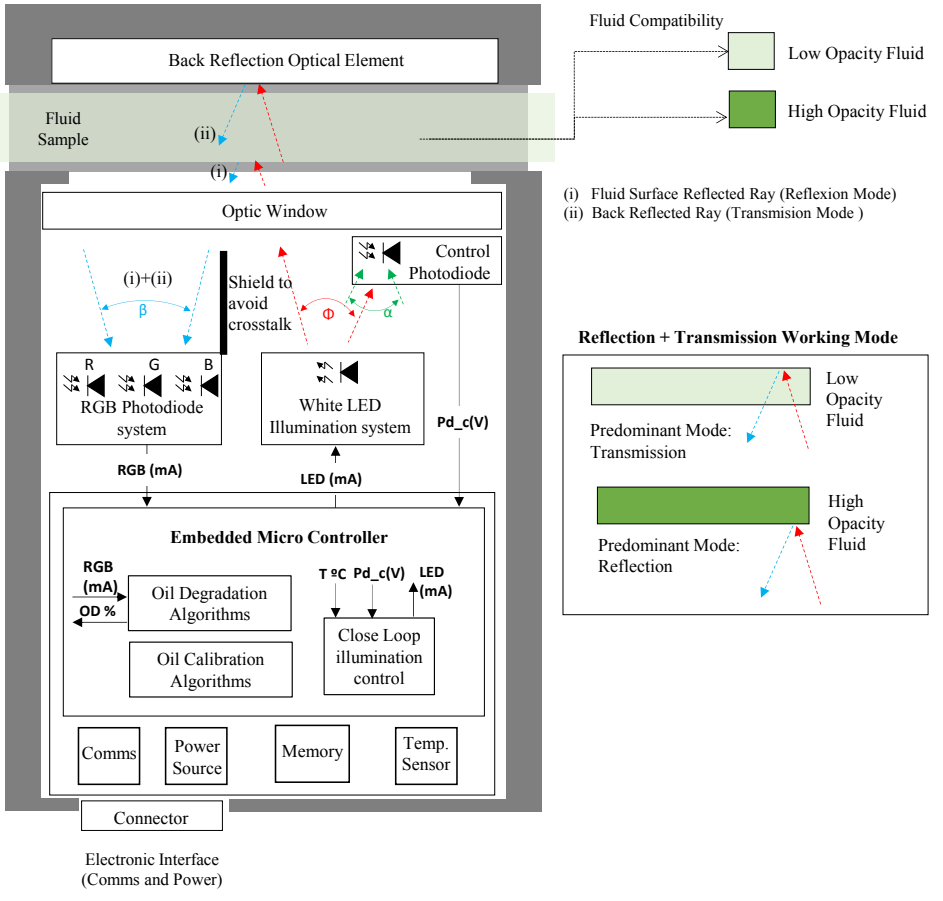

Figure 4.5-7: Typical block diagram of sensor system generated at this stage, where Different building blocks are depicted and working mode is outlined. In this case, the diagram belongs to the OilProbe® lubricant sensor.

Additionally, this is the place where the risks, uncertainties, and the potential heterogeneous integration problems are risen up. Besides, an updated and much more accurate view of the whole project cost and schedule is provided.

Table 4.5-6: Information contained in deliverable 2.4 System Specification and Project Plan.

Item
System Architecture
Heterogeneous blocks and interfaces
selection of photonic components and their settings

Identification of hydraulic components and their specifications
Identification of electronic component and their settings
Specification of working ranges
Revised expected unitary cost
Revised Project cost
Revised Project Plan
Revised Risk and Uncertainty assessment

4.5.2 Prototype Development Decision Gate

The main activity to accomplish at this second Gate is authorize or not the launch of the prototyping stage. Up to now only initial checks, feasibility tests and perhaps some minor prototypes have been performed. However, in the coming phase a real prototype of the product will be developed. Therefore, this Gate needs to be executed very thoroughly with higher management as well as customer involvement to reach sign-off on the product definition, and the development plan. Additionally, agreement on the commitment of the required resources (capital, personnel, etc.) needs to be achieved.

Notice that, even if this final Gate represents the final checkpoint, the stage's workflow (see Figure 4.5-4) already includes some internal decision points at which, in front of negative intermediate results or major risks, the customer may stop the development.

All the deliverables will be taken into consideration, but the continuation of the project normally depends on the following four questions. If all of them have a positive answer, very likely the project will proceed to the next stage.

1. Are we able to measure the parameters of interest with the envisaged photonic principles?
2. Are we able to integrate them into a sensor and maintain the performance over the industrial working condition span?
3. Does the unitary cost of the sensor and does the project cost meet the target?
4. Are the risks and uncertainties accepted by all the parties?

Table 4.5-7: Detailed inputs, decisions and outputs at 4.5.2 Prototype Development Decision Gate.

Input	Decisions	Outputs
Theoretical Description Report	Photonic Measurement principle proven	Prototypes stage plan and resources

Laboratory Result Report	Integrabiltity and reliability in operation conditions feasible	Potential partners list
Photonic Integration Report	Unit cost, project cost and project timeline meet target	Authorization to proceed
System Specification and Project Plan	Project risks and uncertainties acceptable	

4.6 Design of Prototypes and Test–Bench Verifications

The objective of this third stage is to iterate in the fabrication of the different versions of the sensor prototypes, until the whole set of client's requirements (the already known and the ones to be defined) are met and the system is ready for its validation in real environments in the next stage. The different technological developments will help us progressing in the system integration, will enable the optimization of the measurement principle, will allow reducing the uncertainties and mitigating risks, and will serve as the first pilot versions for the customer, enabling him to narrow down in the specification and to define unforeseen requirements or working modes.

Why we talk about Test-Benches along with Sensor Prototypes? This is because this stage is not only responsible for the prototype development, but also for its deep verification, and this task is usually underestimated when talking about photonic sensors. These prototypes need to be verified with many different fluid samples, at several operating environments, under different fluid conditions, etc. and this implies a huge effort and time spent in testing. Things get worse when not only a single device needs to be tested but a batch of them in order to provide the repeatability of the prototypes and the variance coefficient of the measurement. Consequently, any little support concerning the test would maximize our productivity, and this is the specific reason why we conceive the prototypes with their paired test-bench.

Test-benches are automatized and parameterizable hydraulic equipment, which may already exist at customer's or design house's premises, may be subcontracted or may be designed and developed within the project. These Test-benches usually enable to install more than one sensor simultaneously (in parallel and in series), allow modifying the hydraulic setup (e.g. pressure, flow, temperature of the sample) and normally permits an easy fluid sample interchangeability. Merging all these features, we are able to

dramatically speed up the prototype testing time and maximize our insights about the sensor performance.

This is a technological intensive stage, with all the technical members devoted to the definition and fabrication of the different working prototypes. In this case, the headcount and budget availability needs to be assured for enabling an accelerated work rhythm that allows iterating fast. In this occasion, only if the conclusions and results achieved at test benches and controlled environments are successful it will make sense to move forward to the next stage (Validation in real field), but this will be judged at the Real Field Deployment Decision Gate.

4.6.1 Prototype Development and Test Bench Setup Stage

This is the phase where the system briefly specified in the previous stage is crystalized in a physical system, with all the heterogeneous building blocks efficiently integrated to deliver an autonomous sensor system for in-line fluidics monitoring. Additionally, all the required efforts are put for having the system massively verified at laboratory scale, assuring its suitability for a real field validation. This verification implies the setup and use of dedicated Test-Benches that will allow achieving high productivity in testing activities.

Of course, all the project partner should assume an evolving design of the prototypes, which iteratively answer to the new specifications that arise as we, and the customer, learn about the problem and about the application, as new risks to mitigate are recognized, or as new use cases are identified.

The duration of this stage depends on the difficulty of the sensor system, but in the current fast Time-to-Market scenario, customers normally require having sound results in 6 - 9 months. Therefore, the resources should be dimensioned considering this tight schedule. The roles, hardware and software equipment and the outsourcing needs normally present in this stage are outlined in Table 4.6-1.

Table 4.6-1: Roles, equipment and outsourcing required and their expected activities for the Prototypes and Test-Bench Stage.

Headcount	
Role	**Activities expected**
Project Leader/ Senior Engineer	Risk identification, identify the heterogeneous interfaces, provide the integrated view and assure the integrability of the proposed methods into an in-line sensor.

Optoelectronic Engineer	Simulate the photonic subsystem
Mechanical Engineers	Simulate the hydraulics and mechanics Simulate the microfluidics Design and develop the different versions sensor body and enclosure Design/Modify the sensor Test-Bench
Hardware Engineers	Design and develop the sensor electronics
Software Engineers	Design and Develop the sensor control firmware Codify the measurement algorithms
Automation Engineers	Program the test bench and automate the tests
Verification Engineers	Define and implement the verification plans
Chemical Engineer / Physicist	Design the chemo–physical measurement method

Equipment/Software	
Item	**Use expected**
Hydraulic Test Benches	Emulate the different hydraulic operating conditions, enable fluid sample interchangeability, enable multi sensor measurements
CFD Simulation Software	Simulate the mechanical stresses, and the fluidics behavior across the micromechanical structures
Optics Simulation Software	Simulate the ray traces, absorptions, light intensities
Climatic Chamber, Vibration test bed, etc.	Emulate different working conditions to validate the prototypes under the required operation environment

Outsourcing	
Item	**Use expected**
Plastic/Metallic Fast Prototyping	Fabricate mechanical parts for the prototypes
Hardware Electronics manufacturing	Fabricate and assembly the prototype electronics
Photonic Components	Integrate as core part of the sensor system

Again, this stage is divided in different sub-stages that are supposed to generate specific deliverables for its later assessment at the stage's Gate. However, on this occasion, we found an iterative loop in the sensor prototyping and verification, because, until the customer's expectations are fulfilled (or the project is stopped), we should remain in this loop.

Table 4.6-2: Deliverables generated during the Proof-of-Concept Stage and the involved team members.

id	Name	Participants
3.1	Heterogeneous Integration Report	Project Leader & Technical members
3.2	Simulation Report	Technical members
3.3	Verification Plan	Project Leader & Technical members
3.4.i	Prototypes	Technical members
3.5.i	Verification Report	Project Leader & Technical members
3.6.i	Technical and Economic Progress Report	Project Leader
3.7	Final Version Prototype	Technical members
3.8	Validation and Industrialization Plan	Project Leader

i: 1…N, being N the number of iterations

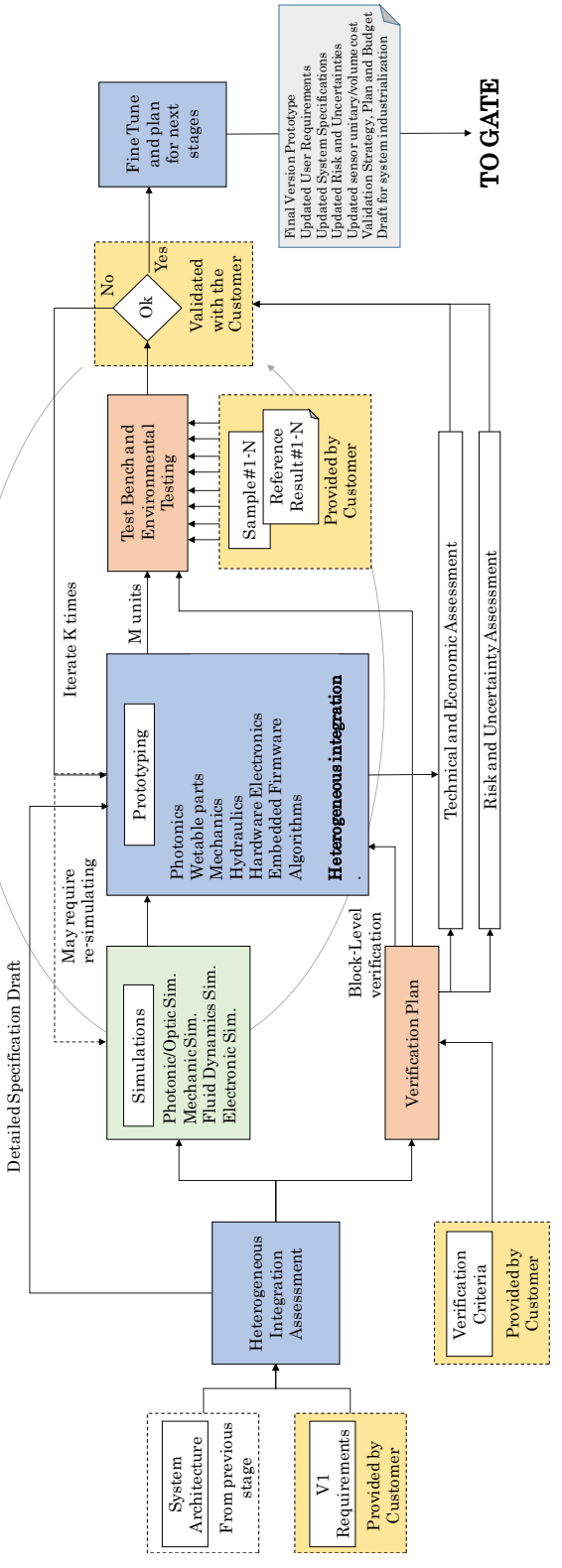

Figure 4.6-1: Workflow amidst the different sub-stages within the Prototyping phase.

4.6.1.1 Heterogeneous Integration Assessment

The heterogeneous integration does not only imply putting all the different building blocks together and having them running. It also implies performing a thorough study about the dependences between the blocks, identification of potential error propagation, definition of tolerances and recognition of weaknesses and risks. In this sub-stage, the system will be treated as a whole, and specifications for all the sub-systems will be generated.

The analysis of the dependences between the blocks is a crucial part before starting the integration. This is a task to accomplish among the whole technical work-team since it is a truly multi-domain activity. This study should reveal how the system works thanks to the internal connections between the blocks. Indeed, these connections and interfaces will pose a heterogeneous nature, and the blocks could be tied together through a physical, chemical, mechanical, electronic, photonic, etc. interface.

The analysis of the risks and uncertainties present in the system follows a similar multi-domain approach. However, due to this heterogeneity, it is not possible to define a single manner to proceed in this definition of dependences, but following the next steps may help:

1. To define a responsible person for each building block.
2. Make them define how their block works, and which are the limitations and risks within it
3. Make them define which are the inputs and outputs and their most important parameters (key performance indicators)
4. Make them define what can fail in their block
5. Make them define what concerns them about the boundary blocks and about the quality of their inputs
6. Merge all answers and define the sensor as a plant with several blocks connected (inputs and outputs), each of them with internal information (KPI) and different risks and weaknesses identified at each block level and at block interface level.

The outcome of this sound analysis reveals the dependences and the risks present in the sensor at this stage.

Additionally, and fully related with the analysis of the interfaces between the building blocks, we found the study of tolerances. Tolerance assessment and budgeting is the process of defining the required design specifications for each block within the context of the whole system to guarantee both the optimal performance and the manufacturability of the final sensor product. In a system that includes photonic elements, from source to detector,

with all the precision optics in between, the analysis of the tolerance of the optical design is critically important [256]; optical and mechanical engineers need to understand how tightly the size, surface figure, thickness, tilt, centering, and other parameters of the optics must be controlled. In addition, it is equally important to simultaneously analyze mechanical and assembly tolerances, to avoid overlooking at the optics and not to the entire system [257]. This task is extremely important because inadequate tolerance analysis during design frequently results in system shortfalls. Under-specifying tolerances may generate performance deficits or issues during final assembly, either of which will require expensive and time-consuming redesign. Similarly, over-specifying optical and mechanical tolerances normally implies incrementing unnecessarily cost, complexity, and lead time to a project.

Table 4.6-3: Information contained in deliverable 3.1 Heterogeneous Integration Report.

Item
Detailed System Architecture
Detailed identification of building blocks: Function, Input, Output and KPI
Detailed identification of interfaces between the building blocks
Detailed system and block specification
Detailed optical and mechanical tolerance definition
Risk and uncertainties at block and at system level

4.6.1.2 Simulation Support

Once all the building blocks have been clearly identified and the first version of the specifications has been defined, we now should take advantage of the benefits brought by the simulation tools to speed up the system design and to minimize uncertainties in a fast and flexible manner. The simulation tools enable to understand how different critical parts of the system will behave, and help us driving some design decision based on the simulation outputs.

The simulations rely on dedicated software tools, that must be configured properly and that normally require some engineering work to define the settings, to prepare the required input dataset and to interpret the output results. However, all the effort pays off, because all the conclusions are very valuable to specify the first version of the prototypes.

Normally, the simulation will be used in four different domains, each one with its own objectives, based on different software

tools, requiring different input information and generating different results.

i. **Optics and Optoelectronics:** The objective of these simulations is to clarify how the light behaves across the different elements of the system. It includes simulation models for emitters, receivers, optical components and mechanical parts, including their finishing materials, which is important for simulating the ray reflections and identifying potential stray rays. Normally, the photonic component manufacturers provide these simulation models for easing the integration work. However, if this data is not available, reference or standard models could be used instead, but the accuracy of the results will be less accurate. Besides the models of the individual components, a 3D model depicting their relative positions (e.g. a CAD model) is essential for the simulation, therefore, a collaborative work between the optic and mechanic engineers is required here.

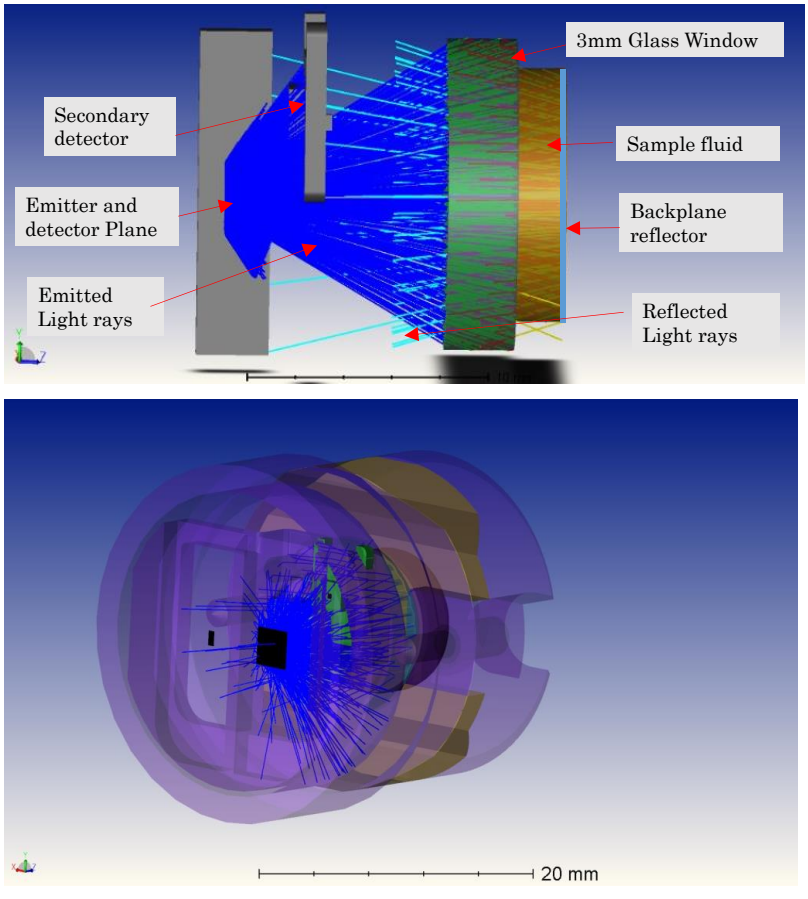

Figure 4.6-2: Simulation results of the optoelectronic, optic and mechanic components. This specific case belongs to the OilProbe® system already introduced in Figure 4.5-7

The results provided by these simulators illustrate the different trajectories followed by the light rays from the source to the detector (see Figure 4.6-2)., and help us defining for instance, positioning tolerances of the different components. Additionally, the intensities of these light beams are also provided (see Figure 4.6-3 and Figure 4.6-4), based on the light flux generated at the emitter and the different constructive or destructive interactions, reflections, absorptions, etc. This output is extremely useful for the light budget calculation and for validating the theoretical results from the previous stages.

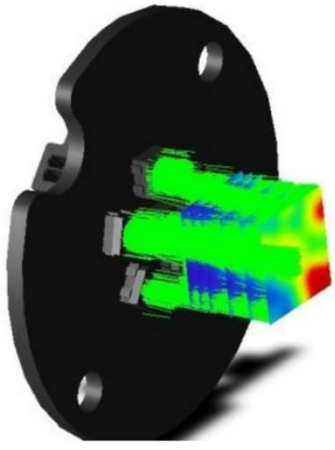

Figure 4.6-3: Simulation of the light irradiance generated by a custom multi-LED light source. This specific design belongs to the OilWear® product.

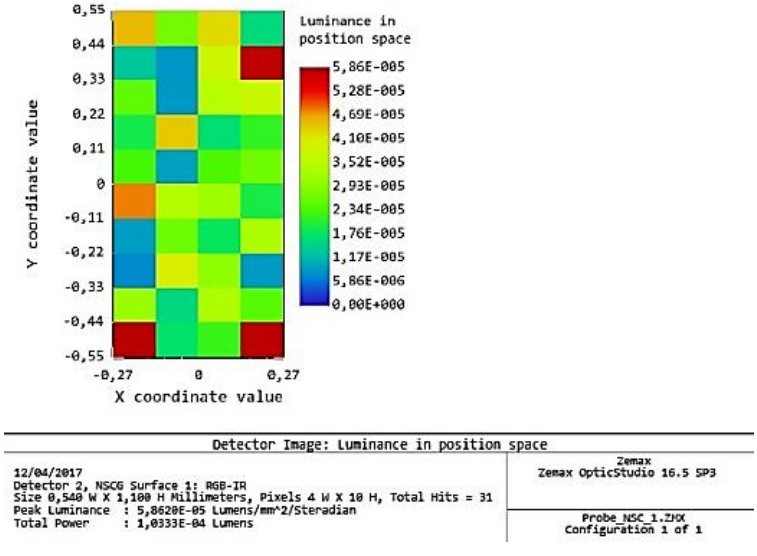

Figure 4.6-4: Example of results generated by simulation tool. This specific case represents the luminance getting to a 2D detector of the OilHealth® product.

Additionally, these tools are able to estimate the scattering, absorption and diffuse reflection that may occur at the sample fluids (see Figure 4.6-5). Setting up this feature in the simulation tools is not straightforward and normally requires very specific knowledge about the sample in order to generate a valid simulation model. These features are based on statistical and numerical approximations of Mie and Rayleigh scattering phenomena for calculating the estimated trajectory of the photons entering the sample. Using input parameterization about the particle distribution and absorption, the simulation tool usually performs a Monte-Carlo based statistical representation of the different light rays across the sample. This information is very useful for understanding where the light-matter interaction effectively happens, and eases the design and interpretation of quantitative measurement methods in spectrometry and fluorescence.

Some reference tools for optical design simulations include OpticsStudio from Zemax (Kirkland, WA, USA), TracePro from Lambda Research Corporation (Littleton, MA, USA) or ASAP by Breult Research (Tucson, Arizona, USA).

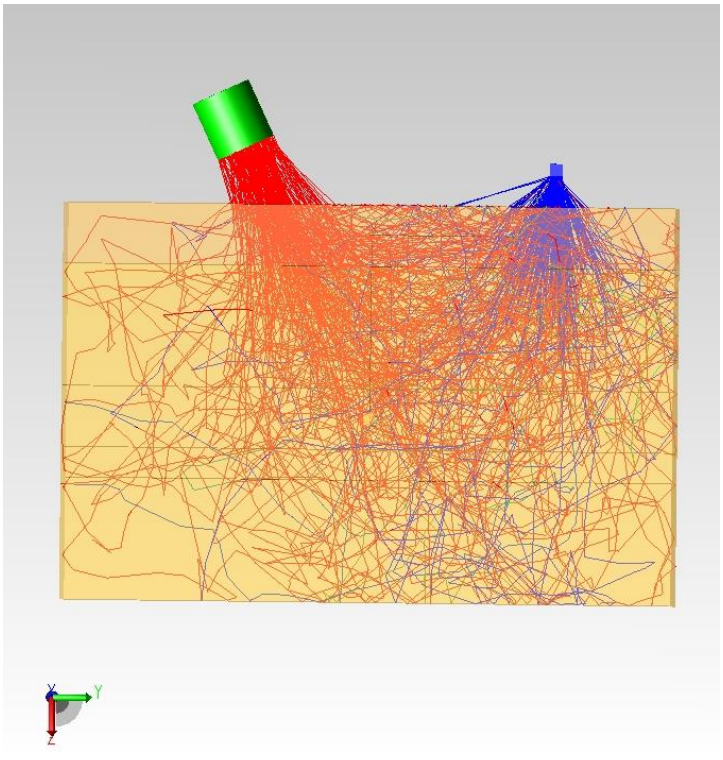

Figure 4.6-5: Ray trace simulation within a tissue, the emitter is on the left and the receiver on the right. Image courtesy of Lambda Research Corporation.

ii. **Structural Analysis of Wettable parts:** The objective of this simulation is to calculate how the glass; plastic or metallic parts behave under the extreme working conditions required for the sensor. The hydraulic conditions are often very challenging because the photonic sensors require a transparent interface between the optoelectronics and the fluid sample, which may be a high pressure, temperatures, etc. This wettable part is normally the weakest point of the system and solving it is not straightforward due to the high maximum pressures of the fluid and the necessity of keeping the compactness and the low cost of the components. Therefore, engineering and validating efforts are expected there for assuring the reliable design. The input parameters are normally mechanical properties of the materials (young modulus, shear limits, etc.), the 3D model or CAD file of the wettable part (see Figure 4.6-6-a), fluidic properties of the liquid (e.g. viscosity) and the hydraulic parameters to simulate with (e.g. temperature, pressure). Then a Finite Element Model of each part under test is developed (see Figure 4.6-6-b) and the finite element analysis is then executed by the tool.

The results generated by the simulation are normally the efforts and tensions suffered by the different mechanic parts at different points (see Figure 4.6-6-c), and thus, the engineer could verify if these values remain far from critical levels. Additionally, thanks to these simulators, we can directly calculate misalignments and tolerances in the parts may dramatically impact on the tension and effort values.

Some examples of tools performing this kind of simulations are: Mechanical from Ansys (Canonsburg, PA, USA), SolidWorks Simulation from Dassault Systemes (Vélizy-Villacoublay, France), or FEA tools from MSC Software (Newport Beach, CA, USA).

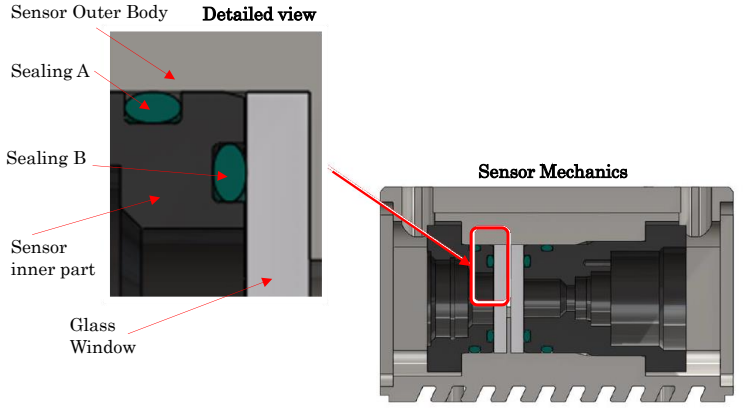

(a)

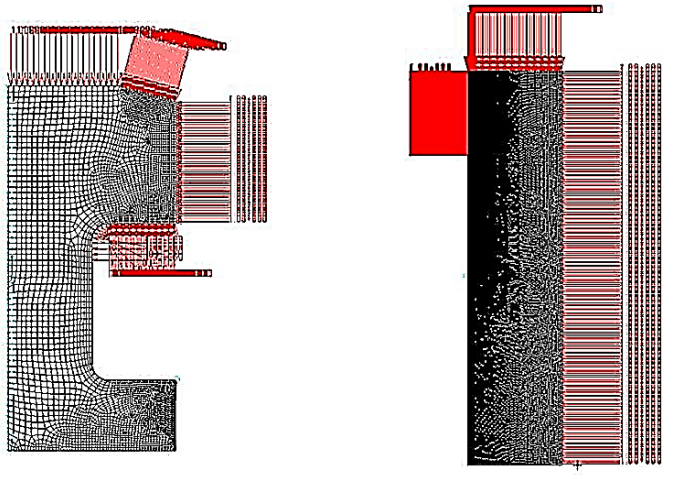

(b)

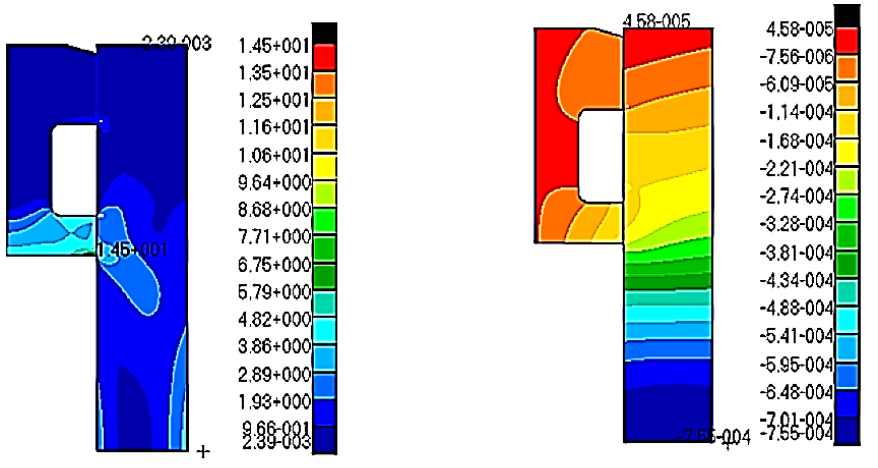

(c)

Figure 4.6-6: Example of Finite Element Model for simulation the different forces supported by the glass and metallic parts under 10bar fluidic pressure. This specific design belongs to the OilWear Piko® product.

iii. **Fluid Dynamics:** The aim of these simulations is to understand how the fluid behaves within the measurement cell, identifying potential turbulence vortexes, flow homogeneities, sample renovation, etc. The simulations are based on Computational Fluid Dynamics (CFD) calculations, which basically apply the Fluid Dynamics formulae to the specific problem configure into the simulation tool.

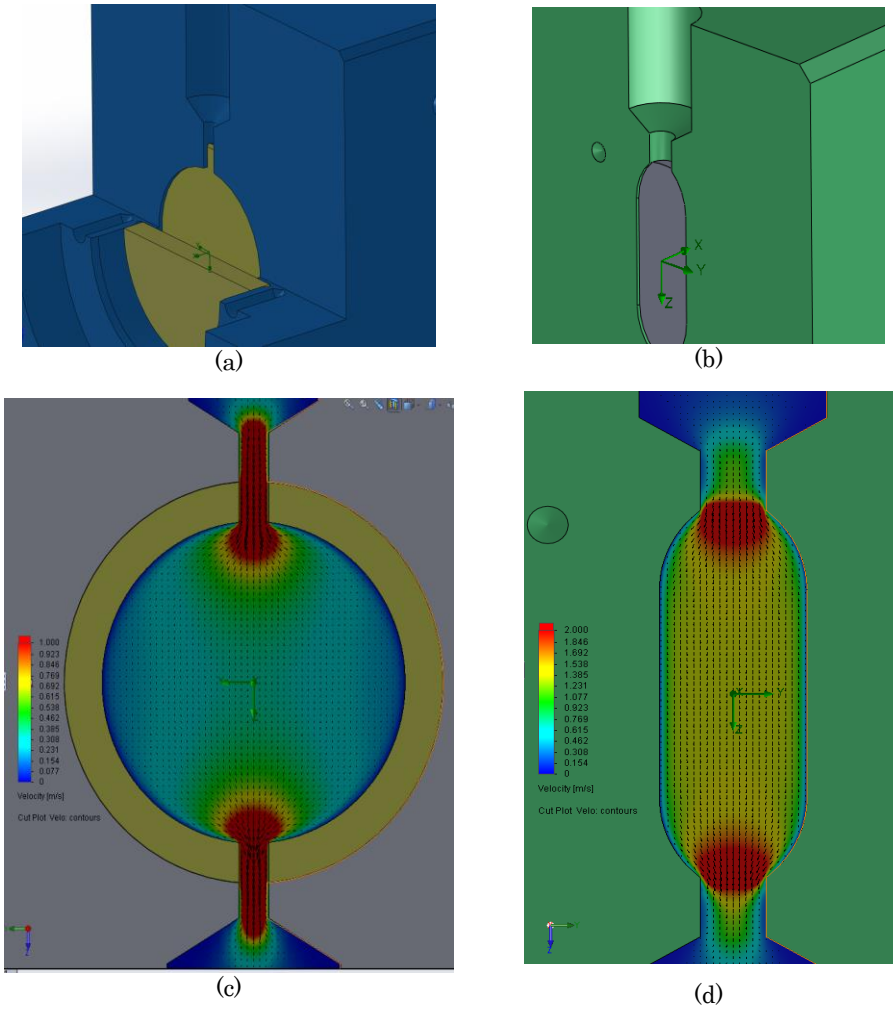

Figure 4.6-7: (a) and (b) represent Mechanical CAD model of different generations of OilWear® bypass sensors, where the geometry of the cavity was modified to homogenize the fluid flow. (c) and (d) Output results displaying how the fluid flows across the cavities and how the (d) version present a smaller flow speed gradient.

The input information is normally the 3D model of the mechanical cavities crossed by the fluid (see Figure 4.6-7-a and -b), hydraulic conditions (input and output pressures, temperature) and properties of the fluid (viscosity, density

and temperature). Then, the structure to be simulated is converted into a mesh (see Figure 4.6-8) and the tool calculates the 3D distribution of the flow speed across the mechanical structure (see Figure 4.6-7-c and -d). The typical system configurations for the fluidic sensors are in bypass, with a fluid inlet and a fluid outlet and the immersion systems, with the whole structure at the same pressure point (see Figure 4.6-9).

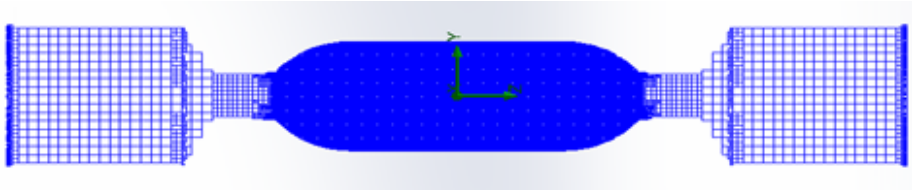

Figure 4.6-8: Mesh structure of the fluidic sensor cavity to setup the simulation.

These kinds of simulations are extremely useful for validating the geometry of the measurement cavity and assist the mechanical engineer in the selection of the best approach for solving the microfluidic structure.

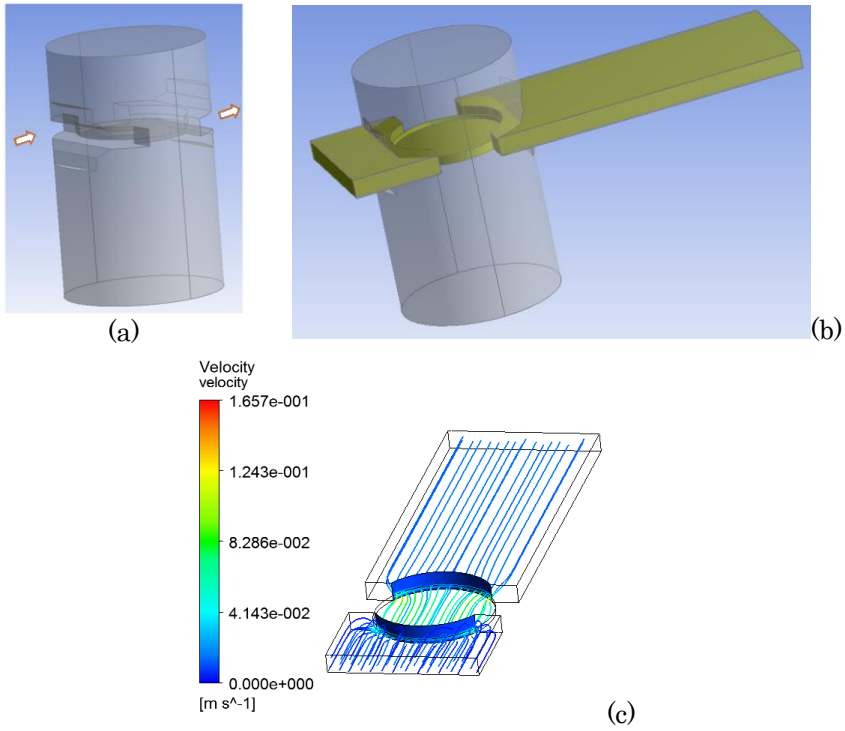

Figure 4.6-9: (a) Mechanical CAD model of the OilProbe® immersion sensor. (b) Geometry of the fluid section under simulation, considering not only the liquid contained in the measurement cavity, but also on its surroundings, simulating the immersion. (c) Output results displaying how the fluid flows across the cavity once the sensor is immersed.

Some example of simulation tools for CFD are Fluent from Ansys, scFLOW from MSC Software or Flow Simulations from SolidWorks.

iv. **Hardware Electronics:** The objective of these simulations is to assist in the design of the analog electronic subsystems, which are sometimes required either for driving and modulating the light sources, for reading out and conditioning of the signals coming from detectors or for synchronizing both. It is true that the integration of digitalized interfaces into current photonic components avoids the need of designing custom electronic solutions for controlling them, but not all the system includes these digital communication channels and in these occasions, some sort of analog electronic design should be delivered by the design team.

The analog circuit behavior simulators enable the designer to tailor the development avoiding any investment in hardware until the confidence in the design is much higher. Typical applications of these simulations include power sources and control system for light emitters (Figure 4.6-10-a), and signal conditioners for reading the information collected by the detector. Simulated results normally display the performance of Voltage, Intensity or Power signals in the time or frequency domains (see Figure 4.6-10-b).

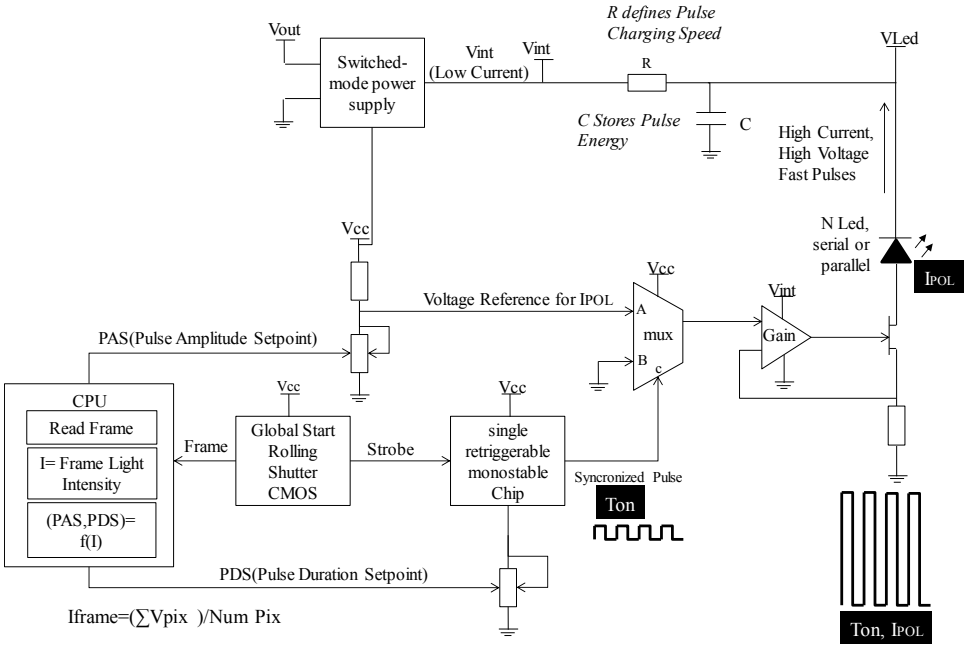

(a)

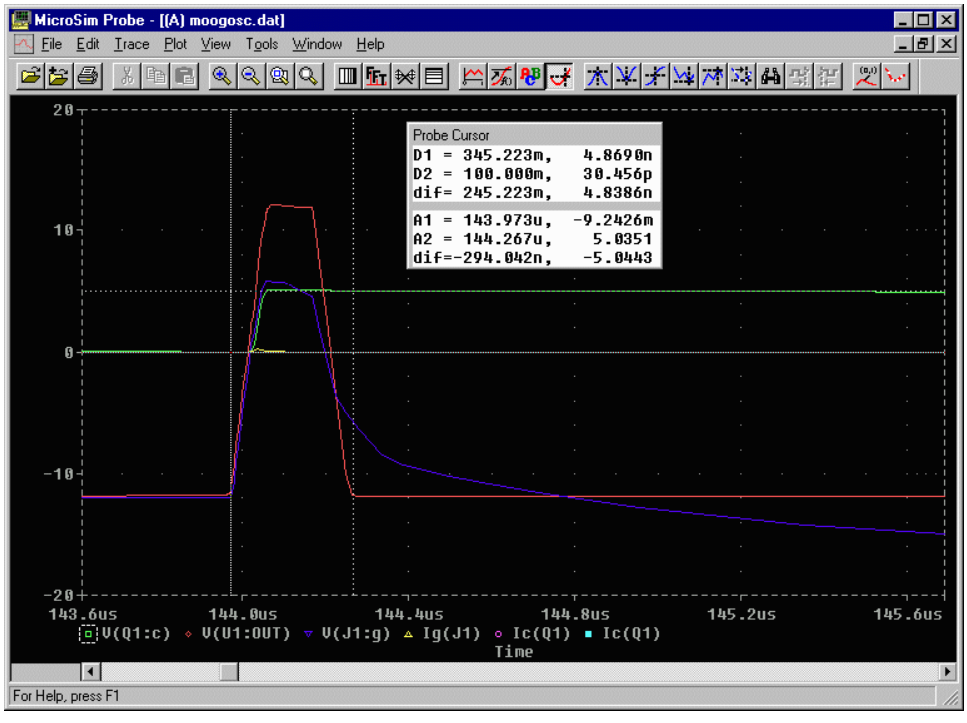

(b)

Figure 4.6-10: (a)Example of Analog Circuit for synchronizing and driving a stroboscopic illumination system for a Lens Free wear particle sensor system. (b) Simulation result of the stroboscopic light pulse generation circuit, where the x-axis shows the duration of the pulse in microseconds and the y-axis the amplitude in Amperes.

Typical simulation tools include Altium Simulator from Altium Designer (Sydney, Australia), LTSpice from Linear Technologies (Milpitas, CA, USA) or Orcad Pspice from Cadence (San José, CA, USA).

The results and conclusions from these simulations (included in the deliverable 3.2 Simulation Report) are directly fed into the design of the different building blocks of the prototypes. However, notice that simulated results need to be confirmed by real physical verifications. Additionally, the input data of these simulation environments may be updated as new information and new scenarios are being defined while progressing in the project development.

4.6.1.3 Verification Approach

This sub-stage is devoted to defining the verification plan to accomplish at the prototyping stage. The verification presents a manifold objective and should cover, among others the items outlined in Table 4.6-4.

Table 4.6-4: Examples of topics to be covered by the verification plan at the Prototyping Stage.

Topic to Verify
Performance of the measurement principle (e.g. algorithm result, stability and variance coefficient of the measurement) under different status conditions of the fluid.
Stability of the measurement under different hydraulic and operating conditions.
Stability of emitters and detectors under different operating conditions (e.g. Temperature, humidity).
Reliability of the sensor under hydraulic operating conditions (e.g. Pressure, flow, fluid temperature).
Reliability of the sensor under environmental conditions (e.g. temperature, humidity, vibrations, EMC).
Impact of fabrication/assembly tolerances.
Durability of wettable parts under the continuous contact with target fluid under different status of the fluid (e.g. degraded, contaminated) under different hydraulic and operating conditions.
Installation and operation easiness.

The analysis carried out at this sub-stage should be able to generate verification plans for the individual building blocks as well as for the entire, integrated, system. During this phase, the requirements for the test-benches and specific equipment (e.g. climatic chambers, vibration benches, anechoic chambers) are identified and the test to be performed there are also specified.

During the verification of the sensor, the availability of relevant samples is critical for performing a thorough assessment of the sensors operation, therefore, the verification team should agree with the customer the provision of these sample library. Additionally, the acceptance criteria for all the test is agreed with the customer and the required staff and resources are allocated for accomplishing the verification task, which include among others, the activities listed in the Table 4.6-5.

Table 4.6-5: Activities included in the Verification Approach sub-stage

Activity
Definition of Individual and Integrated Verification plans
Specification of tests
Agree with the customer the availability of representative samples
Agree the acceptance criteria with the customer
Specification of resources to accomplish the tests
Configure and operate the testing equipment
Configure, program and operate the test-benches
Execute the tests
Document the test and provide feedback about the successes

4.6.1.4 Prototype development

This is the sub-stage where the physical implementation of the different building blocks is accomplished. Based on the specifications and simulation results from previous tasks, here the efforts on technical developments ramp-up for having the different modules developed, individually verified and integrated into a working prototype. These prototypes are fed-into the test-benches and testing equipment's for their exhaustive verifications.

Due to the nature of the development already described in section 4.1, different iterations are expected for the prototype refinement until the customer's expectations are meet. Thanks to the agility applied to the development iterations (*build–test–feedback–revise*) these are delivered fast to the customer. These evolving prototypes serve as unique demonstrators for specifying the required sensing capabilities, identifying weaknesses, clarifying uncertainties,

and devising methods for mitigating the risks. The iterative development approach helps shaping the product much better and changes included at this relatively early phase impacts much less in project cost and times (see Figure 4.6-11) because late-stage design iterations (occurring at every product) are avoided [258].

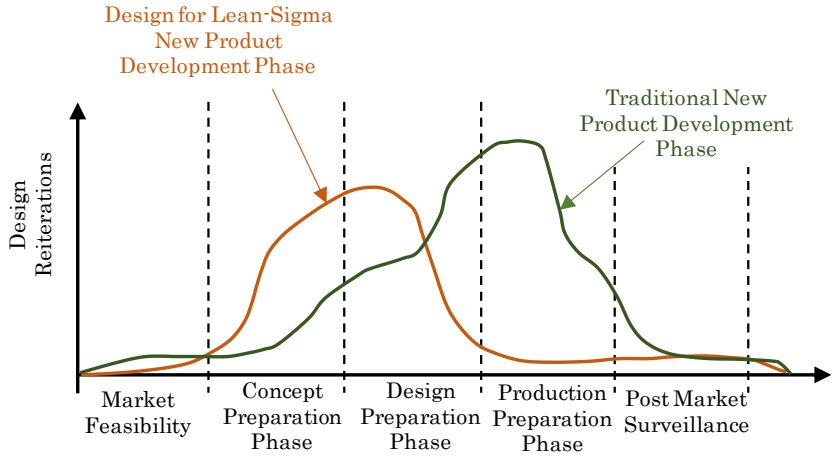

Figure 4.6-11: Example of how the design iterations move backwards on time using novel development technologies as LeanSigma [258].

These prototypes should encompass all the design variations, intermediate designs, etc. that may contribute in increasing the knowledge about the product and about the problem-to-solve. For instance, we may manufacture N different prototype versions where N different light sources are tested because neither the simulation results nor the theoretical studies clarified the most appropriate candidate, so this is solved by prototyping. Notice that prototype development comprises the following steps to be accomplished at each iteration:

- Development of individual building blocks,
- Fabrication and partial verification of individual blocks
- Integration and assembly
- Testing and customer feedback (see next section)

This is the sub-stage where the photonic components are integrated with the rest of blocks to form the photonic sensor. Therefore, a close collaboration with the component provider should be fostered, received their insights about reference designs, integration tips, verification details, etc.

Notice that this stage may represent an intense resource consumer. The technical efforts are high (e.g. 2-3 Full Time Person Efforts during 4-5 months) and the expenses to cover the fabrication of different prototypes are also considerable. Especially during these

early developments, the components, manufacturing and assembly costs are relatively high compared to the final prices and labor costs achieved in the later stages. Thus, the economic impact of each iteration needs to be validated by all the partners.

Additionally, expect an increasing budget allocation to cover the fabrication of an increased number of units at each iteration, even if sometimes components utilized in previous iterations are reused in the later ones. As the design is getting closer to the final specifications, a larger number of units is required for performing the different tests, as depicted in Table 4.6-6.

Table 4.6-6: Number of Units per prototype iteration for the OilWear-Piko® Product.

Iteration	Units	Prototype Example
1	2-3	Figure 4.6-12.a
2	5-10	Figure 4.6-12.b
3	10-20	-
4	10-20	Figure 4.6-12.c
5	40-50	Figure 4.6-12.d

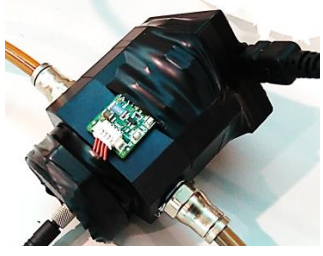

(a)

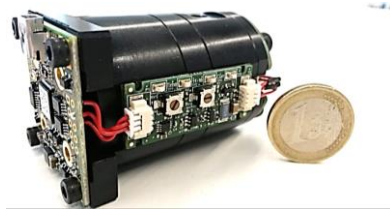

(b)

(c)

(d)

Figure 4.6-12: Examples of different prototypes accomplished during the OW-Piko® sensor design. (a) Concept prototype, (b) improved version, (c) first complete integration and (d) final prototype.

4.6.1.5 Test–Bench Verification

This stage is crucial for accomplishing a thorough verification of the sensor system performance under controlled conditions. These

conditions may be gradually modified towards being much closer to the real working conditions.

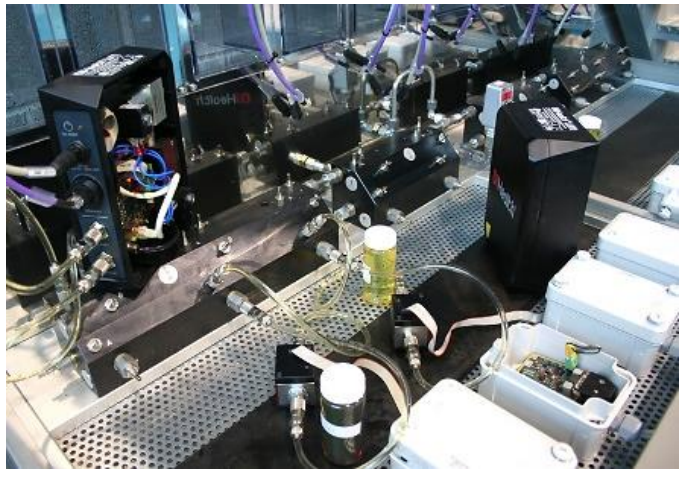

Figure 4.6-13: Example of test bench with different OilHealth® sensors installed simultaneously.

The availability of these kind of test-benches should serve a twofold purpose. First, they need to ease the testing of several units in a row to maximize the generation of results and to assess the sensor's performance, reliability and repeatability and stability of the measurements (see Figure 4.6-13). The second main outcome of the test-benches is to allow a fast test setup modification, either changing the sample under measure or by changing the sample or environmental conditions.

The test-benches are typically used for testing the whole integrated system, but sometimes they are a very useful tool for verifying system's sub–modules as for instance the Wettable parts (see Figure 4.6-14)

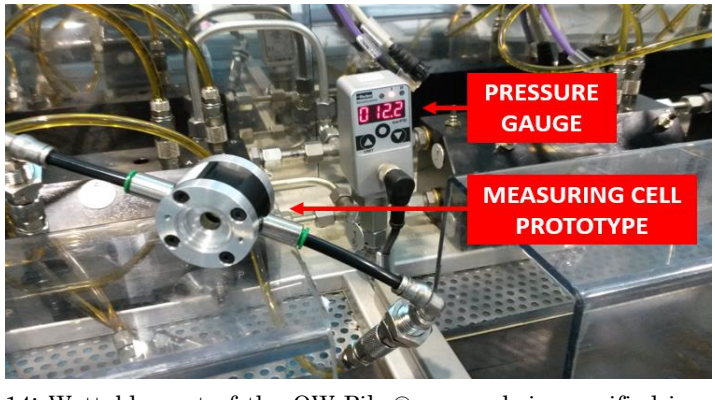

Figure 4.6-14: Wettable part of the OW-Piko® sensor being verified in a test-bench setup.

Notice that it is not required to combine all the test equipment within the same setup. Even if having the complete set of conditions and test parameters available in the same setting would be the ideal situation, this is not always feasible and different test-benches are normally designed or arranged for covering the different testing scenario. Thus, in fluidics sensor verification, it is quite typical to require the following types of test-equipment:

- Sample test bench, where different sensors can be installed in a row and the fluid samples are easily exchanged. These kinds of test-benches may include the option to modify some hydraulic conditions as flow or pressure.
- Hydraulic test bench, with controllable hydraulic conditions as pressure, flow, temperature and viscosity of the fluid.
- Climatic Chamber, with controllable temperature and relative humidity environment.
- Vibrations and shock test bench, with different vibration modes.
- EMC test equipment, to verify the electromagnetic compatibility of the device.

Some other test equipment as Saline mist and condensation chamber or UV irradiation chambers may be required if the sensor enclosure needs to be tested against harsh climatic conditions.

4.6.1.6 Technical and Economic Assessment

This parallel task basically tracks the technical and economic progress of the project at each prototype iteration, because new resource allocation may be required at the end of each iteration loop. The Project Leader is in charge of generating a periodic technical and economic report including the budgetary request for the next planed iteration. This information should be reviewed and accepted by the customer to proceed to the next iteration.

4.6.1.7 Fine–tuning and deployment plan for real scenarios

This is the last sub-stage within the Prototyping phase and includes the minor changes to apply to the prototypes preparing them for their deployment in the real use cases. During this task, the deployment of the prototypes in the real scenarios should be planned, identifying the responsibilities of each party (e.g. designer, customer, and end-user) and quoting the cost of the different activities, consumables, prototypes, etc. Additionally, this stage includes the final set of system specifications and risk identification for answering

the latest definition of the user requirement prepared by the customer. The different topics covered in the deliverables 3.7 Final Version Prototype and 3.8 Validation and Industrialization Plan, which belong to this phase are outlined in the Table 4.6-7.

Table 4.6-7: Topics covered in deliverables 3.7 Final Version Prototype and 3.8 Validation and Industrialization Plan

Item
Final Version Prototype, including all the photonic, mechanic, hydraulic, electronic and software elements integrated in a working prototype
Updated User Requirements
Updated System Specifications
Updated Risk and Uncertainty Assessment
Updated sensor unitary/volume cost estimation
Validation Strategy, Plan and Budget
Draft for system industrialization

4.6.2 Real Field Deployment Decision Gate

The conclusions from the test-bench verifications along with the economical assessment will determine the suitability of moving forward to the real scenarios for the sensor validation. Notice that once the sensor is installed in the field its accessibility will be very limited, and with little room for system modifications and improvements. Additionally, the impact of a sensor failure once at customer's premises may be critical for the system acceptance, and therefore, only sensors with a proven reliability at test-bench scale should move forward to the next stage.

4.7 Validation in real field

4.7.1 Validation and fine-tuning Stage

This stage represents the final validation of the sensor concept. At this point, all the insights gained about the sensor performance concerning measurement quality and system reliability are confronted with real working conditions, real sensor users and real samples.

Notice, that even the best test-bed could only give an approximate and not solid feedback about the sensor behavior. Additionally, normally, it is not even physically possible to simulate or emulate the different working conditions all together, so the coverage of the test performed at test station is, by definition, limited.

Therefore, expect unexpected conditions, unforeseen working modes and odd performances while executing the first set of tests at real deployment.

However, if the development so far has been accomplished in a sensible manner, the probabilities are high for overcoming from these initial disappointments.

The activities start with the sensor installation on end user's site. This might be carried out by the customer technicians, so, by now, the sensor installation may require to be easy enough for not requiring an expert supervisor. However, during the first field tests, it is recommended to accommodate resources for on-site assistance, since the first deployments are always complex and last-minute setting and tuning may be required. The suggestions for including tools enabling sensor remote monitoring, parameterization, performance assessment and even software update becomes a true requirement for sensor developers, and will ease all the validation activities.

Indeed, testing at customer's site, where all the definitive working conditions impact on the sensor together, may evidence some hidden weaknesses in sensor design and even some new and unforeseeable requirement may be included at this moment. Therefore, once sufficient feedback has been acquired, a fine-tuning stage starts, where the conclusions from the real validations are turned into specifications which may be integrated into the prototype system or perhaps leave the implementation for the latter industrialization stage.

4.7.2 Industrialization Decision Gate

This is one of the most important gate so far since it is the responsible for launching the final industrialization of the prototypes, which in terms of economy requirements may represent an amount of several times the already invested budget. Indeed, at this point, all the technical uncertainties and risk must be under control, and only minor concerns may remain in terms of the specific final product cost (e.g. ±5-10%). However, and specially in new products with no previous references in the market, doubts and uncertainties may remain until the final product hits the market, because even if feedback has been gathered from end users so far, their purchasing intentions may change once the final economic conditions are set.

Therefore, the people involved in this gate (technical and economic managers as well as the rest of stakeholders) gate should be responsible of taking the decision and for allocating the required resources based on estimations provided by the project manager.

4.8 Industrialization

This is the final stage, where the product finally crystalizes into an industrial reality. The objective of this stage is to accomplish all the modifications in the previous prototypes to assure the industrialization of the sensor, considering the outsourcing management, manufacturing, assembly and all the processes entailed in the volume production of the sensor system.

Additionally, this is the stage where the knowledge transference should be performed from the design house to the final customer. Actually, in some occasions, the relation may finish at this point because the customer may be able to manage the production by itself, provided that the knowledge transference has been managed in a proper way.

This stage also involves the regulatory and certification processes, and the definition of the product life-cycle management strategy, which in both cases, from this point on, becomes the responsibility of the product owner

Notice that the industrialization is a resource intensive stage, with high expenses not only due to development of the industrial version, but also because of subcontracting for certificate emissions and for the manufacturing of the first pre–series, which require investment in tooling and materials.

4.8.1 Industrialization of prototypes

The industrialization of the sensor system may be straightforward activity depending on the status of the final prototypes. Indeed, more mature prototypes could be reused in a larger extent and will be closer to industrial version. However, some short of redesigning is typically required, either in the electronic hardware, in mechanics or in software.

In addition to the sensor system itself, some extra technical side developments shall start at this stage, including design and fabrication of tools, molds and any other specific development for assisting the manufacturing and assembly of the mechanical parts. If custom optics are required, the associated tooling cost should also be covered during this stage.

Additionally, specific electronic hardware is normally required for series manufacturing of the sensors electronics, which include specific test and programming equipment. Aligned with this activity, additional software and firmware pieces are required by the Electronic Manufacturing Supplier for accomplishing the system factory verifications.

Production, assembly and calibration lines must be prepared and setup in time for the first production batches, which will serve for evaluating the final manufacturing costs because until now, the costs in terms of assembly and calibrations were based on estimations.

During this stage, the strategy for purchase and supplier management should be defined, as well as the production strategy (minimum stocking, delivery times, pre-orders, etc.)

Table 4.8-1: Items covered during the industrialization stage.

Item
Final Version of Hardware, Software, Mechanics and optics
Molds and Tools for series manufacturing of mechanics, optics and sensor embodiments
Test beds for series manufacturing of electronic hardware
Specific firmware and software for verification of electronic hardware
Specific firmware and software for sensor calibration
Production, Assembly and calibration plant
Purchases and supplier management plan
Production strategy: stock, delivery time, order management
Definitive unitary cost of the product

4.8.2 Certification and Regulatory affairs

Even if regulatory requirements have been considered from the early stages of the project, it is not until now when the project-product auditing starts by an authorized body. Indeed, different products may entail different certification and regulatory requirements, but even aside the critical markets as Medical, Automotive, Aeronautics or Military, industrial product certification may represent a difficult challenge to accomplish with.

With the aim of giving a brief overview of potential certifications that may apply to the sort of products covered by this thesis, three main categories may be found.

- Compatibility certifications as the EMC (Europe) or FCC (USA) directives, which defines the electronic compatibility tests and levels to be applied to the product.

- Operation Environment certifications, that normally defines the different tests and conditions at which the product performance must remain unaltered. These tests normally cover the International Protection Marking (IPXX), the temperature and humidity tests, vibrations and shocks, transportation, etc.
- Safety certifications as the UL for the USA market, which looks after electrical, fire, or risk of other nature that may impact of safety of the system users or installers. Additionally, if the sensor system is supposed to be installed and operative in explosive environments, ATEX certification is required, which takes its name from the French directive *Appareils destinés à être utilisés en Atmosphères Explosives*.
- Market Specific Regulations as the Food and Drug Administration (FDA) in the USA that regulates and provides clearance for the use of sensor system at food & beverage industries; or the Det Norske Veritas - Germanischer Lloyd (DNV-GL), formerly two different firms, which provides independent accredited certification services for the renewable energy industry.

Depending on the application, the documentation to be provided include, but are not limited to, user and installation manuals, risk assessments; historic design files describing the development methodology, design inputs and outputs, etc.; record of evidences, etc.

On the other hands, other certifications as the EMC, IP, Vibrations, Temperature, etc. require running real test at the certified body premises to verify that the system under test behaves as expected under the whole environmental condition span. For this purpose, normally specific test-assistance tools are required by the certification technicians.

Figure 4.8-1: The product is not able to reach the market without the corresponding certifications and regulatory clearance.

Be sure to allocate an important budget (several tens of thousands of euros) for accomplishing just the subcontracting of the certification agencies, without considering any possible modification of the product that might be required if any test is not successfully passed. Even if the product owner is the final, and legal, responsible for the regulatory issues, the design house is normally required for assisting the test and for compiling all the design documentation.

4.8.3 Life Cycle Management strategy

The kind of product presented in this thesis are complex product, which may require a continuous assessment of the performance especially when the first units are rolled out in the market. Even if the design house is typically required for giving support to the product owner, they are supposed to stablish a post-sales and life-cycle management strategy to support the product.

All, but specially this kind of advanced products, will require reviews, updates, amendments, etc. and the product owner must stablish an internal structure or a collaboration framework to assist the product launch, operation and maintenance of the sensor (installation, calibrations, etc.), substitution, evolution and disposal. Section 3.1.4 gives an outline of some of the most important points to consider in the life cycle management of sensor systems.

5.

Methodology Validation: Photonic Sensor Examples

While sections 1 to 3 have been focused on explaining the fundaments behind the photonic-sensors for cost effective in-line fluid monitoring, and section 4 describes the proposed methodology for accomplishing the development of such a product, this fifth chapter is all about the practice. Based on the real-world experience of the author in the photonic sensor development, three application scenario that have been benefited from the methodology are presented. First use case describes an in-line microscopy solution for detecting wear particles suspended on industrial fluids. The second use case is an evolution of the first, where holography, lens-free microscopy and stroboscopic photonic technologies are merged for delivering a real time flowing particle detector. The last use case deals with the application of NIR spectroscopy and chemometrics for analyzing alcoholic beverages with an in-line sensor.

5.1 In-Line Microscopy: Wear Debris Sensor

This use case deals with the development of a sensor product for the detection of micro particles suspended in hydraulic fluids. The detection of such wear particles is becoming an important asset for the predictive maintenance strategies since the presence of these microscopic particles is often the symptom of latent or incoming faults in the machines where the fluids are being used.

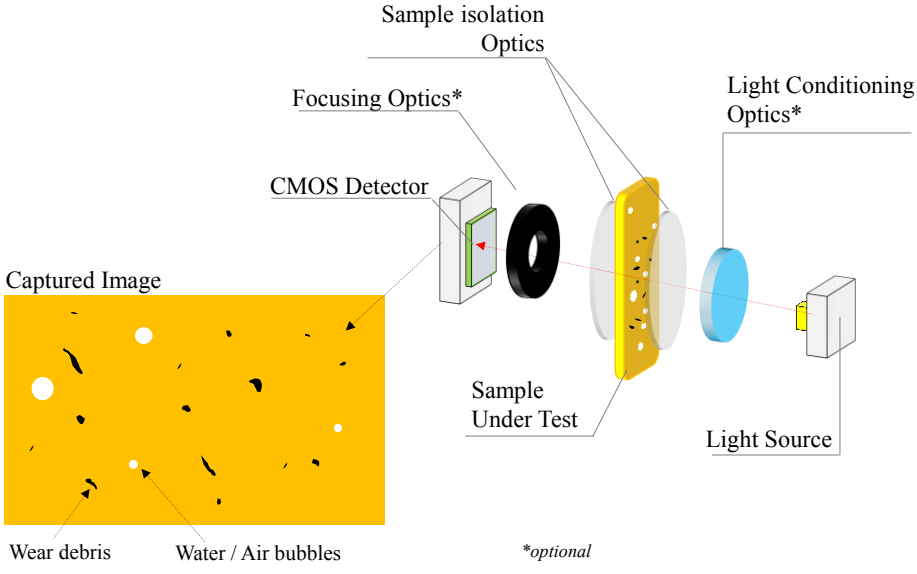

Figure 5.1-1: Working principle of the in-line microscopy. Block diagram depicting a direct imaging wear debris sensor analyzing a flowing lubricant

The working principle is based on a transmissive setup, with white light emitters, a diffuser, two transparent windows, and the light collection subsystem comprising a 2D CMOS imager and a macro lens optics. The optoelectronic system is illuminating a fluid volume, confined between the windows, and capturing a high-resolution image that enables the later detection and classification of solid particles above 4 µm. The key features of the system come not only from its ability to detect, count and classify by size and shape the particles, but also because it is a plug&play sensor, delivering standardized outputs (ISO normalized data over Modbus RTU or Modbus TCP) in a compact setting, and at very effective cost.

Indeed, the development of such a system, with no reference in the market was far from being a straightforward integration. The uncertainties where more than the specifications and the multi domain nature of the technology jeopardized any direct development. Therefore, a set of evolving prototypes were manufactured, each of them with incremental features answering to the newly discovered requirements. These prototypes were tested not only by the customer

(vendor of the technology) but also by end users who gave invaluable feedback that allowed having the right product at the right time.

Figure 5.1-2: OilWear S100 version (Atten2, Advanced Monitoring Technologies), the sensor module and the particularized embodiment for wind turbine applications.

Requirements in terms of reliability but without compromising the target cost effectiveness also hindered the time to market, due to the long verification periods. However, thanks to the use of specific test benches, the impact of these intensive testing sessions was kept under control.

The outcomes of this research and developments efforts where put together in an already accepted patent [259] and are now core part of a successful line of products of the Atten2 Advanced Monitoring Technologies in the field of in-line wear particle counting and classification (see Figure 5.1-2). Currently the devices are being used in wind turbines all over the world; it is also being installed on high load hydraulic and equipment in USA and Korea for serving automotive industry; the sensor is also being used for monitoring the status of gas turbines, compressors, presses, etc.

5.2 Lens Free and Stroboscopic Lighting: Next Generation of Wear Debris Sensor

This second use case, even if aligned with the wear detection applications, presents three completely different photonic technologies to accomplish several major changes to in-line microscopy approach followed by the Wear Debris Sensor of the section 5.1. While the operation of the previous development was based on light transmission and a macro focus system, the new developments integrated holography, lens-free imaging and stroboscopic lighting to remove the macro lens and allows working in continuous flow enabling the detection of particles below the 4 µm.

Achieving the aforementioned enhancements allows the OilWear product moving one step forward in terms of lowering the cost (avoid the macro lens) and size of the system, enabling a true hydraulic plug&play thanks to the compatibility with continuous flows, and reducing the minimum resolvable particle. However, the integration of holography and diffraction processes to setup a lens-free microscope presented several difficulties, because, even if it is well known technique, with several developments (specially from 2010 on), these have been always focusing to biological samples and low pressure; a scenario which has little in common with the highly absorptive and pressurized industrial fluidics.

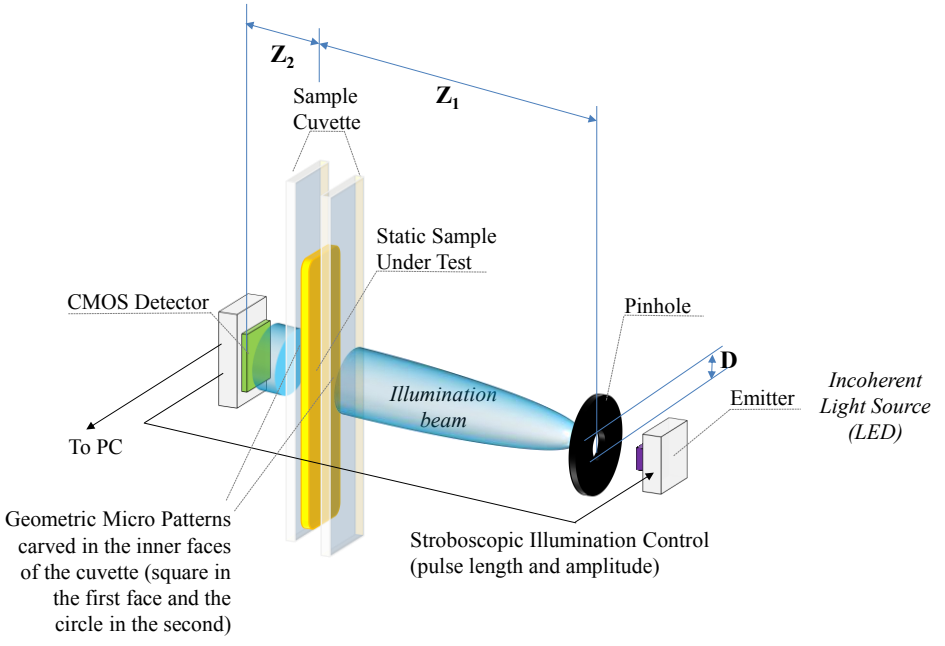

Figure 5.2-1: Schematic diagram of the Lens-Free sensor setup.

The situation was even worse because non-stationary samples had to be monitored to allow an effective particle detection on running fluids. Therefore, in addition to the spatial filtering of the light radiation required for generating the holographic pattern for the lens free operation, imaging moving objects requires to illuminate the sample during very short time slots (stroboscopic imaging). Thus, the available net light power was a real challenge in the prototype hypothesis.

Again, in order to assess the feasibility of the envisaged product idea, several simulations and prototyping sessions were accomplished iteratively, being some of them already used as examples during the methodology description in Chapter 4. A detailed description of the operation and working principles is described in [260] and [261].

During the prototype phases, two parallel development were followed, the first one dealt with the pure lens free operation setup, focusing on static hydraulic fluids (see [260] and Figure 5.2-1), while the second focused on the flowing particles part of the problem. When both investigations delivered relatively successful and potentially patentable results, (already submitted and pending approval [262][263]), the integrated approach was launched, as described in [261] (see Figure 5.2-2).

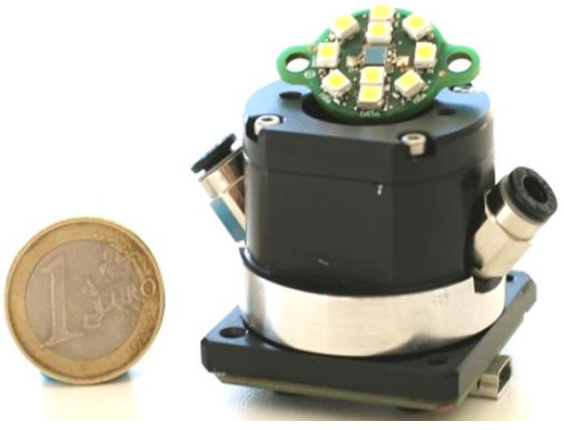

Figure 5.2-2: Prototype of Lens-Free sensor integrating the stroboscopic lighting system.

However, even if the scientific results demonstrated the feasibility of the Lens-Free sensor for flowing objects, the risks and uncertainties for having a reliable product jeopardized the whole product development. Therefore, at that GATE, the decision was to leave a part of the developments for the future, but to integrate the pieces of technology offering the highest confidence to the whole decision team.

Thus, lens-free operation was replaced by the lens based one but the system was enhanced with the stroboscopic lighting system and the integrated electronics, delivering a totally new product.

The figures summarizing this development are 2 patents issued and waiting for approval, and one new product (see Figure 5.2-3) which halves the price of the original version, in a much smaller form factor, offering a total new functionality enabling the monitoring of continuous flows. Additionally, even if the lens-free line was eventually stalled, it is now part of the new development lines with the aim of achieving sub-micron resolutions. It took around 16 months from the concept to the pre-series manufacturing, employing approximately 2.5-3 FTP effort.

Figure 5.2-3: Oilwear PIKO version (Atten2, Advanced Monitoring Technologies), renovated version of OilWear device including the outcomes from the developments of section 5.1 and section 5.2.

5.3 NIR Spectroscopy for Fluid Monitoring: Cider and Wine Use Cases

The last use case is focused on the integration of VIS-NIR spectroscopy in transmissive setup for the monitoring of the fermentation process of cider and wines. The objective of this kind of sensors is to monitorize the process of the alcoholic fermentation, which basically comprises the gradual conversion of glucoses and fructose molecules to Ethanol. Both molecular groups present absorption lines in the NIR (SWIR) range: CH3 and CH2 groups of Ethanol present at 1670-1780nm with the first overtone of the CH-stretch; 2200-2300 nm with the absorption of glucoses; at 380-780nm the phenolic compounds (anthocyanin); and at 1450 and 1950 nm the first overtone of the OH stretch is present, due to the water and ethanol molecules-

The solution integrates not only the sensor hardware but also the chemometric algorithms for delivering an estimation about the fermentation state rather than only providing RAW spectral information.

Due to technological availability of low cost spectrometers, the development started with a VIS-NIR spectrometer in the range of 400–1100 nm, but during the project development, larger wavelengths

become available at integrated spectrometer versions. The work accomplished for cider monitoring is referenced in [264].

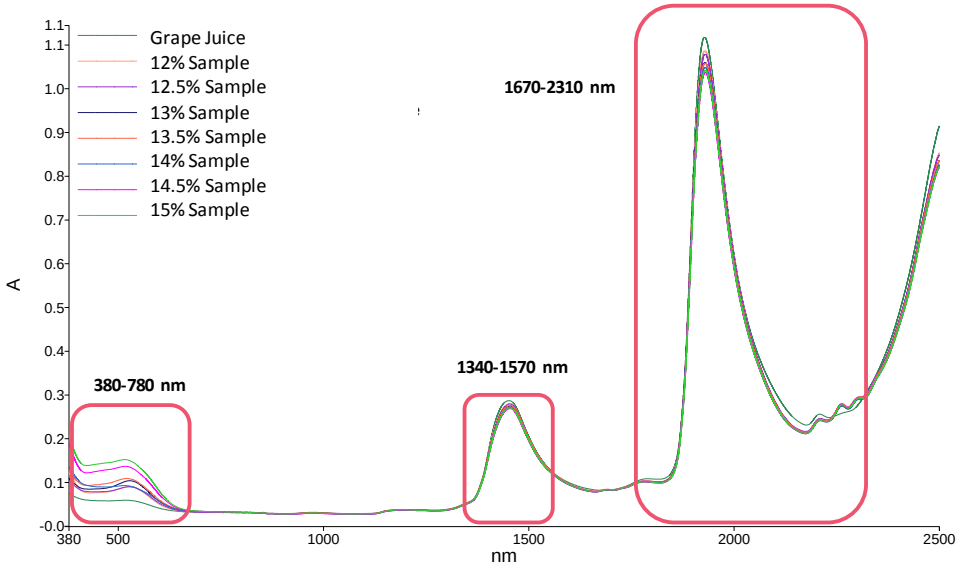

Figure 5.3-1: Absorbance spectra from different samples with incremental alcoholic concentration. As the alcohol concentration rises, the absorbance around 1670-1780nm increases.

Based on the feasibility study accomplished with the cider, the development of a compact and low version of the sensor was launched (see Figure 5.3-2), integrating a tungsten light source, sapphire windows, a collimating lens and a 1700 – 2200 nm spectrometer. The prototype was designed for operating on immersion mode, submerged in the wine/cider barrel using the cork hole (see Figure 5.3-3).

Figure 5.3-2: Detail of the NIR prototype, with the 1 mm slit designed to be filled by capillary forces of the fluid.

Figure 5.3-3: Wine-NIR prototype immersed in a barrel through the cork hole.

The work accomplished so far has led to a patent submission [265], but the cost of the prototypes is still too high, hindering the decision for the industrialization of the system. Newest spectrometers being launched during the 2017 are, however, opening new opportunities to move on the development of a second generation of devices based on the IPs and insights gathered with the early versions of the system. Actually, the knowledge in the field of the in-line chemometric analysis has also driven other families of products in the field of food sorting by reflectance measurements as the ones presented in the patent application [266].

6.
Conclusions

This chapter includes a discussion about the most significant results presented in this thesis together with the concluding remarks and the identified future research lines. The opportunity–challenge paradox, entailed in the outlook of photonics-based fluidics sensors, is highlighted as the main driver of the work accomplished during this thesis. In this context, a methodological hybrid and agile integration of photonic components within the rest of subsystems towards a sensor product development is presented as the main outcome of the thesis. The methodology has been validated in several industrial scenarios, being three of them included in this book, which covers from hydraulic fluid quality control and real-time monitoring of alcoholic beverage fermentation process.

Additionally, the future research lines are outlined, including some specific developments already requested by the industry, setting out new paradigms of the opportunity-challenge binomial in the landscape of photonics-enabled in-line fluidic sensors.

6.1 Low Cost Photonic Sensors, the opportunity-challenge paradox

It is evident that the paradigm of process monitoring has evolved in the last years, driven by a clear necessity for improving the production efficiency, quality and safety of products and processes. In this context, so-called Industry 4.0, sectors as manufacturing, energy, pharma, food and beverages, etc. are fostering the adoption of innovative methods for controlling their processes and products, in a non-destructive, in-place, reliable, fast, accurate and cost-efficient manner. Furthermore, the parameters of interest requested by the industry for the quality assessment are evolving from basic magnitudes as pressures, temperatures, humidity, etc. to complete chemical and physical fingerprints of these products and processes.

In this situation, the measurement techniques based on the UV/VIS/IR light-matter interaction appear to be optimum candidates to face the request of the industry. Moreover, at this moment, when we are witnessing a technological revolution in the field of optoelectronic components, which are required for setting up these light-based analyzers. A complete range of cost effective, compact and feature rich emitters, detectors, modules is being launched to the market paving the way for developing photonic sensor products.

Thus, the opportunity is, clear: the industry requests sensor systems, photonics arises as optimum candidate for answering their needs, and the fundamental pieces for delivering a complete solution are becoming a reality. However, being able to integrate these optoelectronic components with the rest of subsystems (electronics, optics, mechanics, hydraulics, data processing, etc.) is not straightforward.

The development of these multi-domain and heterogeneous sensor products, meeting not just technological but also market objectives, poses a considerable technical and organizational challenge for any company. The synchronizing of multidisciplinary working teams, the pressure to cut development times to launch new products into the market, and the complexity inherent in the technological bases of this kind of product, need to be managed efficiently throughout the design, development, validation and certification phases of the photonics-enabled sensors.

The review of the different development models concludes that even if these different processes propose interesting contributions, no one provides a comprehensive coverage for the kind of product we are presenting.

Therefore, a custom methodological solution is presented as the main outcome of the thesis, with the aim of answering the concerns

and curiosities of Research and Development Teams, Design houses or Engineering teams facing the design of Cost Effective Photonic Sensor Products for in-line fluid analysis.

6.2 Methodological Hybrid and Agile Integration for sensor product development

With the aim of fulfilling the requirements of the abovementioned situation, a custom methodology has been proposed to guide and help Engineering teams in the different steps from the proof-of-concept to the product launch in the area of photonic sensor systems. The thorough revision of the traditional and innovative methods for managing the development of complex technological projects involving a high hardware load, concluded that these methodologies were lacking important features for an effective management of the uncertainties, lack of specifications and risks in a multi domain environment.

The reason behind this lack of information and knowledge about the product is because, normally, the sort of sensors addressed by this methodology are novel devices. This novelty is generated either because the sensors target a new application scenario, which is quite common situation for the in–line sensors as they replace an off–line laboratory method but the conditions for the in–line operations are unclear. Alternatively, the novelty may be justified because, even if other sensor technologies might cover an application, the integration of photonic measurement principles for that specific case has not been tackled previously.

Therefore, assuming the Stage-Gate model as starting point, and taking contributions from Agile, Open Innovation, Lean and Six Sigma, a customized product development approach has been proposed. The methodology splits the development in five stages (Opportunity identification, Proof-of-Concept validation, Design of Prototypes and Test Benches, Validation in Real Field and Industrialization) but identifies specific activities, responsibilities and deliverables on each of them. Indeed, the focus is put on the integration of photonic components into complete smart sensor systems for delivering in-line and real-time measurement solutions in the field of industrial fluidics. The proposed methodology has been validated in several real industrial sensor domains and three of them have been included as use cases.

The main conclusions about the application of the methodology for the development of cost effective photonic sensors for in-line fluidics monitoring, is that it helps cutting the development times,

allows tailoring the product to the exact customer evolving demands without hindering the development cost, maximizes the exploitation of the generated IP cores, and assures the compliance with the identified regulations.

6.3 Future research lines

Three main reasons motivate the continuity in the structuration of a development process in the field of photonics sensors: (i) enabling the integration of new but complex core measurement techniques and increasing the autonomy of the deployed sensors; (ii) minimizing their maintenance and calibration needs and maximizing the lifetime; (iii) and providing the means for delivering hardware independent solutions.

Processes like Raman Spectroscopy presents important advantages in the field of fluid monitoring, especially due to its immunity against the interferences of water molecules. However, the required excitation powers, low detection limits and strict optical tolerances hinder the development of low cost and in-line solutions and push the limits of the proposed methodological approach.

On the other hand, the durability of optic sensors, in a continuous exposure to harsh fluid conditions is also a factor limiting the total and long-term autonomy of in-line photonic sensors. Solutions like protective coatings, the use of micro-actuated white tiles for self-calibration, etc. need to be incorporated to the photonic sensors and the methodology requires evolving to consider these new requirements.

Additionally, newer components, with better features, lower costs and higher compactness will continuously be hitting the market specially in the forthcoming years. Sensor product developers need tools for integrating new photonic components without being required to modify to legacy development (e.g. chemometrics or machine vision algorithms). Thus, the development methodology will also have to deal with this required hardware agnosticism to allow rapid migration to newer platforms.

7.

References

[1] Lee, J., Bagheri, B., Kao and H. A. (2015). A Cyber-Physical Systems architecture for Industry 4.0-based manufacturing systems. Manufacturing Letters, 3, pp. 18-23.

[2] Evans P.C. and Annunziata M., (2012). Industrial Internet: Pushing the Boundaries of Mind and Machines. White paper, General Electric.

[3] Drath R. and Horch, A. (2014). Industry 4.0 Hit or Hype? IEEE Industrial Electronics Magazine, 8(2), pp 56-58.

[4] Franklin, C. (2015). General Electric Announces Predix Cloud, The World's First Cloud Service Built for Industrial Data and Analytics. Press Release, General Electric, New York, NY, USA.

[5] Gantz, J. and Reinsel, D. (2012). The Digital Universe in 2020: Big Data, Bigger Digital Shadows, and Biggest Growth in the Far East. Report, International Data Corporation (IDC), retrieved from: https://www.emc.com/collateral/analyst-reports/idc-the-digital-universe-in-2020.pdf (accessed on 14/05/2017)

[6] Evans, D. (2011). The Internet of Things. How the Next Evolution of the Internet Is Changing Everything. White Paper, Cisco, retrieved from: http://www.cisco.com/web/innov/IoT_IBSG_0411FINAL.pdf (accessed on 16/04/2017)

[7] Simonds, D. (2016). Siemens and General Electric gear up for the internet of things. Press Article, The Economist, New York, USA, December 3, 2016. Retrieved from: http://www.economist.com/news/business/21711079-american-industrial-giant-sprinting-towards-its-goal-german-firm-taking-more (accessed on 16/05/2017)

[8] General Electric (2016). PREDIX, The industrial Internet Platform. White paper, General Electric Company.

[9] Möller, M. (2016). Industry 4.0 in action at Bosch Rexroth Homburg facility. White paper, Rexroth, Bosch Group.

[10] Hoenicke, C. (2016). Intelligent sensor systems for Industry 4.0. Press Release, Bosch Group, May 27, 2016.

[11] Thomä, M. (2016). Machine monitoring with smart sensors. Press Release, Bosch Group, July 26, 2016.

[12] Bertheau, T. (2016). ABB's new condition monitoring solution is a quantum leap for millions of motors. Press Release, January 21, 2016.

[13] Honeywell (2013). Analytical Sensors and Measurement Solutions. Brochure, Honeywell, retrieved from: https://www.honeywellprocess.com/library/marketing/brochures/HPS-SmartSensors-Analytical-Instruments-Brochure.pdf (accessed on 17/05/2017)

[14] Honeywell (2017). SmartLine Temperature Transmitters, Modular, Accurate and Reliable for the Lowest Cost of Ownership. Brochure, Honeywell, retrieved from: https://www.honeywellprocess.com/library/marketing/brochures/smartline-temperature-transmitter-brochure.pdf (accessed on 17/05/2017)

[15] Grönzin, H. (2017). Fit for Industry 4.0 with smart sensor business 4.0. White Paper, Leuze Electronics, retrieved from: http://www.leuze.it/media/assets/whitepaper/WP_I40_Smart_Sensor_Business_40_en.pdf (accessed on 20/04/2017).

[16] Lorenz, M., Rüssman, M., Strack, R. and Bolle, M. (2015). Man and Machine in Industry 4.0. White Paper, Boston Consulting, retrieved from:http://www.bcg.com.cn/en/files/publications/reports_pdf/BCG_Man_and_Machine_in_Industry_4_0_Sep_2015_ENG.pdf (accessed on 17/05/2017).

[17] Coronado, D. and Kupferschmidt, C. (2014). Assessment and Validation of Oil Sensor Systems for On-line Oil Condition Monitoring of Wind Turbine Gearboxes. Procedia Technology, 15, pp. 747-754.

[18] Amin, M., Majid, A. and Fudzin, F. (2017). Study on Robots Failures in Automotive Painting Line. ARPN Journal of Engineering and Applied Sciences, 12(1), pp. 62-67.

[19] Sumit, P., Legner, W., Krenkow, A. et al. (2010) Chemical Contamination Sensor for Phosphate Ester Hydraulic Fluids. International Journal of Aerospace Engineering, 2010, 156281.

[20] Kress-Rogers, E., Brimelow, C. (2001), Instrumentation and Sensors for the food Industry, CRC Press, Woodhead Publishing Limited, Cambridge, England, pp. 404-405.

[21] GEM Sensors (2017). Tackling Tough Fluid Sensing Challenges. White paper, GEM Sensors, retrieved from: http://www.gemssensors.com/
(accessed on 26/03/2017)

[22] (ed.) Bøving, K. G. (2014). NDE handbook: Non-destructive examination methods for condition monitoring. Butterworths, Silkerborg, Denmark, pp. 286-295.

[23] Qin, S. J. (2014). Process data analytics in the era of big data. AIChE Journal, 60(9), pp. 3092-3100.

[24] LIM, S. A. H., Jiju, A. and, Saja, A. (2014). Statistical Process Control (SPC) in the food industry–A systematic review and future research agenda. Trends in food science & technology, 37(2), pp 137-151.

[25] Bennet, S. (1993). A History of Control Engineering, 1930-1955. IEE Control Engineering series, 47, London, UK, pp. 28-34.

[26] Bennett, S. (1994). Automatic on-line fluid monitoring. Industrial Lubrication and Tribology, 46(4), pp.8-9.

[27] Yokogawa (2012). Flowmeter History. White Paper, LF 01E00A00-03EN, 2nd Edition, Yokogawa, retrieved from: https://web-material3.yokogawa.com/LF01E00A00-03EN.us.pdf
(accessed on 2017/04/28)

[28] Wemyss, C. (2017). Next Generation Flowmeters for Fluid Measurement and Control Solutions. White Paper, Litre Meter Ltd. Retrieved from: http://litremeter.info/tag/flowmeter-history/
(accessed on 2017/04/28)

[29] Pinto, J. (2010). Brief history of Industrial Instrumentation. InTech Magazine, ISA publications, January-February 2010.

[30] Dunn, W. C. (2006), Introduction to Instrumentation, Sensors, and Process Control. ARTECH HOUSE, INC, Boston,

[31] Yoder, J. (2003). Flow Meters and Their Application; an Overview. Sensors Magazine, 20 (10).

[32] Desmarais, R., and Breuer, J. (2001). How to Select the Right Temperature Sensor. Sensors Magazine, 18(1), January 2001.

[33] Wilson, J. S. (2003). Pressure Measurement Principles and Practice. Sensors Magazine, 20(1).

[34] ISO 7027-1 (2016). Water quality, Determination of turbidity, Part 1: Quantitative methods. International Organization for Standardization.

[35] Roveti, D. K. (2001). Choosing a Humidity Sensor. A Review of Three Technologies. Sensors Magazine, 18(7).

[36] Radiometer Analytical SAS, (2004). Conductivity Theory and Practice. White paper, Radiometer Analytical SAS, retrieved from: http://www.analytical-chemistry.uoc.gr/ (accessed on 2017/04/17).

[37] Hambrice, K., and Hooper, H. (2004). A Dozen Ways to Measure Fluid Level and How They Work. Sensors Magazine, 21(12).

[38] Gungor, V. C. and Hancke, G. P. (2009). Industrial Wireless Sensor Networks: Challenges, Design Principles, and Technical Approaches. IEEE Transactions On Industrial Electronics, 56(10), pp. 4258–4265.

[39] (ed.) Alioto, M. (2017). Enabling the Internet of Things: From Integrated Circuits to Integrated Systems, Springer International Publishing, Basel, Switzerland, pp. 35-36.

[40] (ed.) Wilson, J. (2005). Sensor Technology Handbook, Volume 1, Newnes, Elsevier, Burlington, MA, USA, pp. 591-597.

[41] Willner, A. E. et al. (2012). Optics and Photonics: Key Enabling Technologies. Proc. IEEE, Special Centennial Issue, 100, pp. 1604-1643.

[42] (ed.) Zheludev, N. I. (2009). The next photonic revolution. J. Opt. A: Pure Appl. Opt., 11, pp. 1-2.

[43] Forbes, H. (2016). The IIoT Edge: Why is Industrial Sensing Difficult and Expensive?.retrieved from: https://industrial-iot.com/2016/05/iiot-edge-industrial-sensing-difficult-expensive/ (accessed on 2017/03/28)

[44] Miller, S. E. (1969). Integrated optics: an introduction. Bell Syst. Tech. J., 48, pp. 2059– 2069.

[45] Smit, M., Tol, J. and Hill, M. (2012), Moore's law in photonics. Laser & Photon. Rev., 6, pp. 1–13.

[46] M. Smit et al. (2012). A generic foundry model for InP-based photonic ICs. OFC/NFOEC, Los Angeles, CA, pp. 1-3.

[47] Nomoto, T., Oike, Y. and Wakabayashi, H. (2016). Accelerating the Sensing world through imaging evolution. VLSI Circuits (VLSI-Circuits) 2016 IEEE Symposium on, pp. 1-4

[48] Sanderson, S. W. and Simons, K. L. (2012). Light Emitting Diodes and the Lighting Revolution: The Emergence of a Solid-State Lighting Industry. Rensselaer Polytechnic Institute, NY, USA.

[49] Wang, Y., Alonso, J. M. and Ruan, X. (2017). A Review of LED Drivers and Related Technologies. IEEE Transactions on Industrial Electronics, 99, pp. 1-1.

[50] Kim, J. K., Krames, M. R., Tu, L. W. and Strassburg, M. (2017). Proc. SPIE 10124 Light-Emitting Diodes: Materials, Devices, and Applications for Solid State Lighting XXI, 10124.

[51] Reichl, M. (2016). Osram presents the world's first broadband infrared LED. Osram, Regensburg, November 4, 2016, retrieved from: https://www.osram.com/os/press/press-releases/
(accessed on 2017/04/14)

[52] Cambou, P. and Jaffard, J. L. (2016). Status of the CMOS Image Sensor Industry 2016: New Market and Technology Dynamics. Yole Technologies, Market Report, Lyon, France.

[53] (ed.) Bannon, D. P. (2016). Hyperspectral Imaging Sensors: Innovative Applications and Sensor Standards 2016. Proc. SPIE, 9860.

[54] Warren, M. E. (2014). Micro-opto-electro-mechanical Systems (MOEMS). Access Science, McGraw-Hill Education, 2014.

[55] Fischer, A. C., Forsberg, F., Lapisa, M., Bleiker, S. J., Stemme, G., Roxhed, N. and Niklaus,F. (2015). Integrating MEMS and ICs. Nat. Microsyst. Nanoeng., 1, pp. 15005.

[56] Ford, J. (2005). Optical Mems: A Brief History and Future Trends. Mems Journal, 10 (8), pp.45-46.

[57] Antila, J., Tuohiniemi, M., Rissanen, A., Kantojärvi, U., Lahti, M., Viherkanto, K., Kaarre, M. and Malinen, J. (2014). MEMS- and MOEMS-Based Near-Infrared Spectrometers. Encyclopedia of Analytical Chemistry, John Wiley & Sons, Lt, pp. 1–36.

[58] Havermeyer, F., Ho, L. and Moser, C. (2012). Discrete Tunable Laser for 3D Imaging. International Conference on Optical MEMS and Nanophotonics, Banff, AB, 2012, pp. 11-12.

[59] Jayaraman, V., Jiang, J., Potsaid, B., Cole, G. and Fujimoto, J.C.A. (2012). Design and Performance of Broadly Tunable, Narrow Line-width, High Repetition Rate 1310nm VCSELs for Swept Source Optical Coherence Tomography. Proc. SPIE, 8276, 1–10.

[60] Sinning, S., Wullinger, I., Schmidt, J.-U., Friedrichs, M., Dauderstädt, U., Wolschke, S., Hughes, T., Pahner, D. and Wagner, M. (2012). One dimensional light modulator. Proc. SPIE 8252, MOEMS and Miniaturized Systems XI, 82520H.

[61] Johnson, R. C. (2010). Optical MEMS finally arriving. MEMS Journal, retrieved from:
http://www.memsjournal.com/2010/08/optical-mems-finally-arriving.html
(accessed on 2017/03/01)

[62] Kantojärvi et al. (2015). MEMS spectral sensors bring laboratory measurements to field use. Laser and Photonics, 10(1) pp. 66- 69.

[63] Parr, A. C. (2001). The Candela and Photometric and Radiometric Measurements. Journal of Research of the National Institute of Standards and Technology, 106(1), pp. 151–186.

[64] J. Flammer et al. (2013). Basic Sciences in Ophthalmology. Springer-Verlag Berlin, Germany, pp. 20-35.

[65] (ed.) Calmers, J.M. and Dent, G. (1976). Industrial Analysis with Vibrational Spectroscopy. The Royal Society of Chemistry, Cambridge, UK.

[66] Qingbo, F. (2012). Short-Wave Near- Infrared Spectrometer for Alcohol Determination and Temperature Correction Journal of Analytical Methods in Chemistry, 2012, Article ID 728128.

[67] Wulfert, F. and Smilde K. (1998). Influence of Temperature on Vibrational Spectra and Consequences for the Predictive Ability of Multivariate Models. Anal. Chem., 70, pp. 1761-1767.

[68] Scheeline, A. (2016). What must be specified to achieve a valid spectroscopic measurement? Hamamatsu Articles, retrieved from:
http://www.hamamatsu.com/us/en/community/optical_sensors/article/scheeline_spectroscopic_measurement/index.html
(accessed on 2017/17/04)

[69] (ed.) Polfer, N. C. and Dugourd, P. (2013). Laser Photodissociation and Spectroscopy of Mass-separated Biomolecular Ions. Lecture Notes in Chemistry 83, Springer International Publishing, Basel, Switzerland.

[70] Gong, Y. J. et al. (2016). A unique approach toward near-infrared fluorescent probes for bioimaging with remarkably enhanced contrast. Chem. Sci., 7, pp. 2275-2285.

[71] Abramowitz, M. and Davidson, M. W. (2015). Fluorescence: Overview of Excitation and Emission Fundamentals. The Florida State University, retrieved from: https://micro.magnet.fsu.edu/primer/lightandcolor/fluoroexcitation.ml (accessed on 2017/05/16).

[72] O'Sullivan, T. D., Heitz, R. T., Parashurama, N., Barkin, D. B., Wooley, B. A., Gambhir, S. S. and Levi, O. (2013). Real-time, continuous, fluorescence sensing in a freely-moving subject with an implanted hybrid VCSEL/CMOS biosensor. Biomedical Optics Express, 4(8), pp. 1332–1341.

[73] Banwell, C. N., (1972). Fundamentals of Molecular Spectroscopy. McGraw-Hill, Berkshire, UK, pp. 121-156.

[74] Struve, Walter S., (1989). Fundamentals of Molecular Spectroscopy, John Wiley & Sons, New York, NY, USA, pp. 307-330.

[75] Davis, B. J., Carney, P. S., and R. Bhargava, (2010). Theory of Mid-infrared Absorption Micro-spectroscopy: II. Heterogeneous Samples. Analytical Chemistry, 82(9), pp. 3487–3499.

[76] Davis, B. J., Carney, P. S., and R. Bhargava, (2010). Theory of Mid-infrared Absorption Micro-spectroscopy: I. Homogeneous Samples," Analytical Chemistry, 82(9), pp. 3474–3486

.

[77] Yamamoto, K. and Ishida, H. (1997). Kramers-Kronig analysis applied to reflection-absorption spectroscopy. Vibrational Spectroscopy, 15(1), pp. 27-36.

[78] Jacques, S.L. (2013). Optical properties of biological tissues: a review. Phys. Med. Bio., 58 (11), pp. R37-R61.

[79] Saccomandi, P. et al., (2014). Estimation of anisotropy coefficient and total attenuation of swine liver at 850 nm based on a goniometric technique: Influence of sample thickness. Proc. IEEE Eng. Med. Biol. Soc., pp. 5332-5335.

[80] Pu, Y., Chen, J. and Wang, W. (2014). Investigation of scattering coefficients and anisotropy factors of human cancerous and normal

prostate tissues using Mie theory. Proc. SPIE 8941, Optical Interactions with Tissue and Cells XXV; and Terahertz for Biomedical Applications, 894115.

[81] Mignon, C., Rodriguez, A., Palero, J., Varghese, B. and M. Jurna, (2016). Fractional laser photothermolysis using Bessel beams. Biomed. Opt. Express, 7, pp. 4974-4981.

[82] Armaroli1, T., Bécue, T. and Gautier, S. (2004). Diffuse Reflection Infrared Spectroscopy (DRIFTS): Application to the in situ Analysis of Catalysts. Oil & Gas Science and Technology – Rev. IFP, 59(2), pp. 215-237.

[83] Workman, J. (2016). The Concise Handbook of Analytical Spectroscopy: Theory, Applications, and Reference Materials. Volume 3. World Scientific Publishing, London, UK, pp. 52.

[84] Hamamatsu, Solid State Division (2017). Technical Information LEDs. Hamamatsu, retrieved from: http://www.hamamatsu.com/resources/pdf/ssd/led_kled9001e.pdf (accessed on 2017/02/01).

[85] Grum, F., Saunders, S. B. and Macadam, D. L. (1978). Concept of correlated color temperature. Color Res. Appl., 3, pp. 17–21.

.

[86] Osram (2001). Led Fundamentals, Thermal Characteristics of LEDs. Osram Opto Semiconductors, retrieved from: https://ledlight.osram-os.com/wp-content/uploads/2013/01/OSRAM-OS_LED-FUNDAMENTALS_Thermal-Characteristics-of-LEDs_v2_08-16-11_SCRIPT.pdf (accessed on 2017/02/13)

[87] Olafsen, L. J., Ice, L. D. and Ball, B. (2012). Nonlinear Temperature Dependence of Resonant Pump Wavelengths in Optical Pumping Injection Cavity Lasers. IEEE Journal of Selected Topics in Quantum Electronics, 17(5), pp. 1453-1459.

[88] Excelsys. Driving Halogen Lamps. Application Note 1604, Excelsys, retrieved from: http://www.excelsys.com/wp-content/uploads/2016/07/AN1604_Driving_Halogen_Lamps.pdf (accessed on 2017/03/14).

[89] Muramoto, Y., Kimura, M. and Nouda, S. (2014). Development and future of ultraviolet light-emitting diodes: UV-LED will replace the UV lamp. Semicond. Sci. Technol., 29, 084004.

[90] Liangfeng, S. et al. (2012). Bright infrared quantum-dot light-emitting diodes through inter-dot spacing control. Nature Nanotechnology, 7, pp. 369–373.

[91] Thorlabs (2009). Supercontinuum Generation in Photonics Crystal Fibers. Thorlabs Application Note, retrieved from: https://www.thorlabs.com/images/TabImages/SupercontinuumGeneralApplicationNoteThorlabs.pdf
(accessed on 2017/02/25).

[92] Michalzik, R. and Ebeling, K. J. (2003). Operating Principles of VCSELs. Chapter 3, in Vertical-Cavity Surface-Emitting Laser Devices, Springer Series in Photonics, 6, pp. 53-98.

[93] Overton, G. (2013). VCSEL Illumination: High-power VCSELs rule IR illumination. Laser Focus World, 49(08).

[94] O'Sullivan, T. D., Munro, E., Harris, J. S. and Levi, O. (2010). Fabrication of an integrated 670nm VCSEL-based sensor for miniaturized fluorescence sensing. Proc. SPIE, Vertical-Cavity Surface-Emitting Lasers XIV, 76150D.

[95] Van der Lee, A., Carpaij, M., Monch, H., Schemmann, M. and Pruijmboom, A. (2008). A miniaturized VCSEL based sensor platform for velocity measurement. Proc. IEEE Instrumentation and Measurement Tech. pp. 141-143.

[96] Maute, M. and Amann, M. C. (2004). Long-wavelength VCSELs. Proc. Indium Phosphide and Related Materials (IRPM), pp. 695-699.

[97] Koerperick, E. J. (2009). High power mid-wave and long-wave infrared light emitting diodes: device growth and applications. Thesis, University of Iowa.

[98] Weise, S., Steinbach, B. and Biermann, S. (2016). MEMS-based IR-sources. Proc. SPIE, 9752, 97521E 7.

[99] Chowdhury, M. F., Hopper, R., Ali, S. Z., Gardner, J. W. and Udrea, F. (2016). MEMS Infrared Emitter and Detector for Capnography Applications. Procedia Engineering, 168, pp. 1204 - 1207.

[100] Ali, S. Z. et al (2015). A Low-Power, Low-Cost Infra-Red Emitter in CMOS Technology. IEEE Sen Jour, 15(12), pp. 6775 – 6782.

[101] Calaza, C., Salleras, M., Sabaté, N., Santander, J., Cané, C. and Fonseca, L. (2012). A MEMS-based thermal infrared emitter for an integrated NDIR spectrometer. Microsystem Technologies, 18(7-8), pp. 1147-1154.

[102] Hossein, L. et al. (2013). Narrow-bandgap photovoltaic devices operating at room temperature and above with high open-circuit voltage. Applied Physics Letters, 102(21), 10.1063.

[103] Kosonocky, W. F. (1987). Infrared Image Sensors With Schottky-Barrier Detectors. Proc. SPIE, 869, pp.90 - 106.

[104] Watanabe, K. et al (2008). GaAs extrinsic photoconductors for the terahertz astronomy. Proc. SPIE 6840, Terahertz Photonics, 68401F.

[105] Giorgetta , F., Baumann , E., Graf, M. and Hofstetter , D. (2009). Quantum Cascade Detectors. IEEE Journal of Quantum Electronics, 45(8), pp. 1039 - 1052.

[106] Osi Optoelectronics. (2007). Photodiode Characteristics and Applications. Osi Optoelectronics, retrieved from: http://www.osioptoelectronics.com/application-notes/an-photodiode-parameters-characteristics.pdf (accessed on 2017/04/18)

[107] Pagano, R., Libertino, S., Corso, D., Valvo, G. and Sanfilippo, D. et al. (2014). Potentialities of silicon photomultiplier. Proc. SPIE 8990, Silicon Photonics IX, 899018.

[108] Haus, J. (2010). Optical Sensors: Basics and Applications, John Wiley & Sons, Weinheim, Germany.

[109] (ed.) Kubitscheck, U. (2017). Fluorescence Microscopy: From Principles to Biological Applications. John Wiley & Sons, NY, USA.

[110] Manzardo, O. (2002). Micro-Sized Fourier Spectrometers. Master Thesis, Universit´e de Neuchˆatel Institut de Microtechnique.

[111] Sabry, Y. M, Hassan, K., Anwar, M., Alharon, M. H., Medhat, M. et al. (2017). Ultra-compact MEMS FTIR spectrometer. Proc. SPIE 10210, Next-Generation Spectroscopic Technologies X, 102100H.

[112] Rissanen, A., Akujärvi, A., Antila, J., Blomberg, M. and Saari, H. (2012). MOEMS miniature spectrometers using tuneable Fabry-Perot interferometers. J. Micro/Nanolith. MEMS MOEMS. 11(2), 023003.

[113] Grüger, H., Knobbe, J., Pügner, T. and Schenk, H. (2013). Design and characterization of a hybrid-integrated MEMS scanning grating spectrometer. Proc. SPIE 8616, MOEMS and Miniaturized Systems XII, 86160L.

[114] Pügner, T., Knobbe, J., and Grüger, H. (2016). Near-Infrared Grating Spectrometer for Mobile Phone Applications. Applied Spectroscopy, 70(5), 734–745.

[115] Friedrich, D. M., Hulse, C. A., Gunten, M.V., Williamson, E. P., Pederson, C. G. and O'Brien, N. A. (2014). Miniature near-infrared

spectrometer for point-of-use chemical analysis. Proc. SPIE, 8992, Photonic Instrumentation Engineering, 899203.

[116] Huang, E. et al. (2017). Etalon Array Reconstructive Spectrometry. Scientific Reports, 7, 40693.

[117] Lapray, P. J., Wang, X., Thomas, J. B. and Gouton, P. (2014) Multispectral Filter Arrays: Recent Advances and Practical Implementation. Sensors 2014, 14, 21626-21659.

[118] Loewen, E. G. and Popov, E. (1997). Diffraction Gratings and Applications. CRC Press, NY, USA.

[119] Martin, A. E. (1980). Infrared interferometric spectrometers. Vibrational Spectra and Structure, 8, Elsevier, Amsterdam, The Netherlands.

[120] Middelhoek, S. and Audet, S. A. (1989). Silicon Sensors, Academic Press, London, UK.

[121] Hashemian, H. M and Knovel (Firm) (2005). Sensor performance and reliability. ISA - The Instrumentation, Systems, and Automation Society, Triangle Park, NC. pp. 23-40.

[122] Sassoli de Bianchi, M. (2013). The Observer Effect. Foundations of Science 18, pp. 213-243.

[123] Fraden, J. (2010). Handbook of Modern Sensors. Springer-Verlag New York. pp. 13-52.

[124] Kourosh, K. (2013). Sensors, An Introductory Course. Springer-Verlag New York. pp. 12-19.

[125] Meijer, G. (2008). Smart Sensor Systems. John Wiley & Sons, Sussex. pp. 23-50.

[126] Cree, (2016). Binning & Labeling, Cree® XLamp® XM Family LEDs. White Paper, Cree Inc., retrieved from: http://www.cree.com/led-components/media/documents/XLampXMBL.pdf (accessed on 2017/04/17).

[127] International Organization for Standardization (1997). ISO 11843-1. Capability of detection. Part 1: Terms and definitions. ISO, Genève.

[128] International Union of Pure and Applied Chemistry IUPAC (1995). Nomenclature in Evaluation of Analytical Methods including Detection and Quantification Capabilities, Pure & Appl. Chem., 67, pp. 1699-1723.

[129] El Gamal, A. (2001). High Dynamic Range Image Sensors. 392b Lectures and Class notes, Department of Electrical Engineering, Stanford University.

[130] Kavusi, S. and El Gamal, A. (2004). Quantitative study of high-dynamic-range image sensor architectures. Proc. SPIE 5301, Sensors and Camera Systems for Scientific, Industrial, and Digital Photography Applications V, 264.

[131] Arp, U., Shaw, P.S., Gupta, R. and Lykke, K. R. (2005). Damage to solid-state photodiodes by vacuum ultraviolet radiation, Journal of Electron Spectroscopy and Related Phenomena, 144–147, pp. 1039-1042

[132] Bostian, K. (2006). Long Term Stability and Reliability of Permanently Installed On-Line UV Sensors. Proc. Radtech Technical Conference.

[133] Liu, J.M. (2005). Photonic Devices. Cambridge University Press. Cambridge. pp. 941-942

[134] Rahimi, N., Patadia, A., Babic, D. and Grubisic, D. (2016). Characterization of the Linearity of InGaAs Photodetectors Using Series Resistance. GMA/ITG-Fachtagung Sensoren und Messsysteme 2016, pp. 519 - 523.

[135] L. P. Boivin, (1993). Automated absolute and relative spectral linearity measurements on photovoltaic detectors. Metrologia, 30(4), pp. 355-415.

[136] Martini, M., Guanche, R., Losada, I. J., and Vidal, C. (2017) Accessibility assessment for operation and maintenance of offshore wind farms in the North Sea. Wind Energy, 20, pp. 637–656.

[137] Whitby, D. (2012). Online condition monitoring of greases. Tribology and lubrication technology, STLE Publication, 68(5), pp. 72.

[138] Meyer, R. G., (2008). Inline photometer device and calibration method. Optek-Danulat Gmbh, US Patent, US2008100845 (A1).

[139] Lopez, P., Mabe, J., Iturbe, I. (2017). Sistema y Método de Monitorización del Estado de un Fluido (Spanish). IK4-Tekniker, Pending Patent, P201730848. See annexed documents.

[140] Rao, P. R. (2008). Signal and Systems. Tata McGraw Hill, New Delhi, pp. 415-420

[141] Hergert, E. (2015). WITS$- A Rough Guide to Selecting a Photodetector. Industrial Photonics, 2(3), pp.19 - 22.

[142] (ed.) Lasance, C. and Poppe, A. (2014). Thermal Management for LED Applications. Springer, New York, pp. 21 - 23.

[143] Du, Y. P., Liang, Y. Z., Kasemsuran, S., Maruo, K. and Ozaki, Y. (2004). Removal of Interference Signals Due to Water from in vivo Near-Infrared (NIR) Spectra of Blood Glucose by Region Orthogonal Signal Correction (ROSC). Analytical Sciences, 20(9), pp. 1339-1345.

[144] Newman, R. (1995). Visible light from a silicon p-n junction. Physics Review, 100(2), pp. 700 - 703.

[145] Mackowiak, V., Peupelmann, J. and Ma, Y. NEP – Noise Equivalent Power. Thorlabs White Paper, retrieved from: https://www.thorlabs.com/images/TabImages/Noise_Equivalent_Power_White_Paper.pdf
(accessed on 2017/04/29).

[146] Vishay Semiconductors (2002). Application of Optical Reflex Sensors. Application Note, 80107.

[147] Watson, C. and Vitic, M. (2011). Crosstalk mitigation in optical transceivers. Onechip Photonics Inc. , US Patent, US20110217045 A1.

[148] Osada, B. (2014). Handbook of Photodiodes. Hamamatsu, retrieved from: https://www.hamamatsu.com/resources/pdf/ssd/e02_handbook_si_photodiode.pdf
(accessed on 2017/03/17).

[149] (ed.) Dobkin, B. and Hamburger, J. (2015). Analog Circuit Design Volume Three: Design Note Collection. Elsevier, Oxford, UK.

[150] (ed.) Turchetta, R. (2016). Analog Electronics for Radiation Detection. CRC Press, Boca Ratón, FL, USA.

[151] Ping, W. and Qingjun, L., (2011). Biomedical Sensors and Measurement. Springer-Verlag, Hangzhou, China, pp. 25 - 27.

[152] Greanya, V. (2016). Bioinspired Photonics: Optical Structures and Systems Inspired by Nature. CRC press, London, UK, pp. 292 - 294.

[153] Gaigalas, A. K., Wang, L., Schwartz, A., Marti, G. E., and Vogt, R. F. (2005). Quantitating Fluorescence Intensity from Fluorophore: Assignment of MESF Values. Journal of Research of the National Institute of Standards and Technology, 110(2), pp. 101 - 114.

[154] Martelo-Vidal, M. J., Domínguez-Agis, F. and Vázquez, M. (2013), Ultraviolet/visible/near-infrared spectral analysis and chemometric tools for the discrimination of wines between subzones inside a

controlled designation of origin: a case study of Rías Baixas. Australian Journal of Grape and Wine Research, 19, pp. 62 - 67.

[155] Weeks, J. (2016). Why Hydraulic Oil Changes Color. Machine Lubrication, retrieved from http://machinerylubrication.com/Read/30495/hydraulic-oil-color
(accessed on 2017/04/17)

[156] Nørgaard, L., Haunstrup, I., Petersen, M., Weimann, J. and Sørensen, K. M., (2014). Chemometric terminology for qualitative and quantitative analysis. White Paper, P/N 1026715, Issue 1, Foss.

[157] Micklander, E. (2014). Quantitative, Qualitative and Exploratory Analysis of Food using Spectrometry and Quimiometry. The Royal Veterinary and Agricultural University Denmark.

[158] Denton, R. (2016). Sensor reliability impact on predictive maintenance program costs. Wilcoxon Research White paper, retrieved from:
https://wilcoxon.com/wp-content/uploads/2016/07/Sensor-reliability-impact-on-PdM-cost.pdf
(accessed on 2017/04/20).

[159] Ohba, R. (1992). Intelligent Sensor Technology. John Wiley & Sons, Ltd, Chichester, UK, pp. 5 -19.

[160] Brignell, J. E. and White, N. M. (1996). Intelligent Sensor Systems. Taylor & Francis, Oxford, UK, pp. 143 - 148.

[161] Kazior, T. E. (2014). Beyond CMOS: heterogeneous integration of III–V devices, RF MEMS and other dissimilar materials/devices with Si CMOS to create intelligent microsystems. Philosophical Transactions. Series A, Mathematical, Physical, and Engineering Sciences, 372.

[162] Geum, D.-M., Park, M.-S., Lim, J. Y., Yang, H.-D., Song, J. D., Kim, C. Z. and Choi, W. J. (2016). Ultra-high-throughput Production of III-V/Si Wafer for Electronic and Photonic Applications. Scientific Reports, 6, 20610.

[163] Roelkens, G. et al. (2015). III–V-on-silicon photonic integrated circuits for communication and sensing applications, 2015 IEEE Photonics Conference (IPC), pp. 593 - 594.

[164] IEEE Standard for a Smart Transducer Interface for Sensors and Actuators". IEEE Standards Association, IEEE STD.2007.4346346.

[165] International Electrotechnical Commission (2012). IEC 61076-2-101, Connectors for electronic equipment.

[166] Scheeline, A. (2016). What must be specified to achieve a valid spectroscopic measurement? Hamamatsu Articles, retrieved from: http://www.hamamatsu.com/us/en/community/optical_sensors/article/scheeline_spectroscopic_measurement/index.html (accessed on 2017/04/21).

[167] Scheeline, A. (2015). Is "good enough" good enough for portable visible and near-visible spectrometry? Proc. SPIE 9482, Next-Generation Spectroscopic Technologies VIII, 94820H.

[168] Workman, J. (2016). The Concise Handbook of Analytical Spectroscopy: Theory, Applications, and Reference Materials. World Scientific, London, UK, 3, pp. 21 - 23.

[169] (ed.) Coleman, P. C. (1994). Practical Sampling Techniques for Infrared Analysis. CRC Press, Boca Raton, FL, USA, pp. 151.

[170] (ed.) Lindon, J. C., Tranter, G. E. and Koppenaal, D. W. (2017). Encyclopedia of Spectroscopy and Spectrometry. Elsevier, Oxford, UK, pp. 752 - 755.

[171] Armaroli, T., Bécue, T. and Gautier, S. (2004). Diffuse Reflection Infrared Spectroscopy (DRIFTS): Application to the in situ Analysis of Catalysts. Oil & Gas Science and Technology - Rev. IFP, 59(2), pp. 215-237.

[172] Ocean Optics, (2015). Sampling Accessories for Reflection. Applications blog, retrieved from: https://oceanoptics.com/sampling-accessories-for-reflection/ (accessed on 2017/04/21).

[173] Padalkar, M. V. and Pleshko, N. (2015). Wavelength-Dependent Penetration Depth of Near Infrared Radiation into Cartilage. The Analyst, 140(7), pp. 2093 - 2100.

[174] Jianwei, Q. and Renfu, L. (2008). Measurement of the optical properties of fruits and vegetables using spatially resolved hyperspectral diffuse reflectance imaging technique. Postharvest Biology and Technology, 49(3), pp. 355 - 365.

[175] Huang, M., Kim, M.S., Chao, K., Qin, J., Mo, C., Esquerre, C., Delwiche, S. and Zhu, Q. (2016). Penetration Depth Measurement of Near-Infrared Hyperspectral Imaging Light for Milk Powder. Sensors. 16(4), pp. 441-449.

[176] Turner Designs (2014). Introduction to Fluorescence Measurements. Technical Note, retrieved from: https://www.turnerdesigns.com/t2/doc/appnotes/998-0050.pdf (accessed on 2017/04/26).

[177] Fischer, G., Ehlers, M., Andreas P., Zumbusch, A. and Daltrozzo, E. (2007). Near-Infrared Dyes and Fluorophores Based on Diketopyrrolopyrroles. Angewandte Chemie International Edition, 46, pp. 3750 - 3753.

[178] Gnyba, M., Smulko, J., Kwiatkowski, A. and Wierzba, P. (2011). Portable Raman spectrometer – design rules and applications. Bulleting of the Polish Academy of Sciences, 59(3).

[179] Bryan, A., Bonvallet, J., Rodriguez, J. and Olmstead, T. (2017). Miniature Raman spectroscopy utilizing stabilized diode lasers and 2D CMOS detector arrays. Proc. SPIE 10110, Photonic Instrumentation Engineering IV, 1011019.

[180] Gorritxategi, E. and Mabe, J. (2013). System and method for monitoring a fluid. Atten2 Monitoring Technologies, Patent EP2980557 A1.

[181] Salik, E. (2009). Optical phase measurement emphasized. Education and Training in Optics and Photonics, OSA Technical Digest Series (CD) (Optical Society of America), paper EMB3.

[182] Massart, D. L. (2003). Chemometrics: A Textbook. Elsevier Health Sciences, London, UK.

[183] Devos O., Downey G. and Duponchel L. (2014). Simultaneous data pre-processing and SVM classification model selection based on a parallel genetic algorithm applied to spectroscopic data of olive oils. Food Chem., 148, pp. 124 - 130.

[184] Sileoni V., van den Berg F., Marconi O., Perretti G. and Fantozzi P. (2011). Internal and external validation strategies for the evaluation of long-term effects in NIR calibration models. J. Agric. Food Chem. 59, pp. 1541–1547.

[185] Zhao, N., Wu, Z., Zhang, Q., Shi, X., Ma, Q., and Qiao, Y. (2015). Optimization of Parameter Selection for Partial Least Squares Model Development. Scientific Reports, 5, 11647.

[186] Brereton, R.G. (2003). Chemometrics: Data Analysis for the laboratory and Chemical Plant. Willey, Chichester, UK.

[187] (ed.) Johnson, R.W. (2016). Handbook of Fluid Dynamics. CRC Press, Boca Raton, FL, USA, pp. 502 - 506.

[188] Ghita, A., Pascut, F. C., Mather, M., Sottile, V. and Notingher, I. (2012). Cytoplasmic RNA in Undifferentiated Neural Stem Cells: A Potential Label-Free Raman Spectral Marker for Assessing the

Undifferentiated Status. Analytical Chemistry, 84 (7), pp. 3155 - 3162.

[189] Jain, R., Kasturi, R. and Schunk, B.G. (1995) Machine Vision. McGraw Hill, London, UK.

[190] Tack, N., Lambrechts, A., Soussan, P. and Haspeslagh, L. (2012). A compact, high-speed, and low-cost hyperspectral imager. Proc. SPIE 8266, Silicon Photonics VII, 82660Q.

[191] Lambrechts, A., Gonzalez, P., Geelen, B., Soussan, P., Tack, K. and Jayapala, M. (2014). A CMOS-compatible, integrated approach to hyper- and multispectral imaging. IEEE International Electron Devices Meeting, San Francisco, CA, USA, pp. 10.5.1-10.5.4.

[192] Hergeth, W.D. (2014). Process Analytical Chemistry. Wiley-VCH Verlag GmbH & Co. KGaA, Weinheim, Germany.

[193] Kress-Rogers, E. and Brimelow, C. J. B. (2000). Instrumentation and Sensors for the Food Industry. CRC Press, Boca Raton, FL, USA, pp. 404 - 410.

[194] Johnson, M. (2007). Past, Present and Future of Oil Analysis: An Expert Panel Discussion on the Future of Oil 705 Analysis. Tribology and Lubrication Transactions.

[195] Poley, J. (2011). Metallic wear Debris Sensors: promising Developments in Failure Prevention for Wind Turbine Gear sets and Similar Components. Wind turbine Condition Monitoring Workshop.

[196] Zhu, J., Yoon, J.M., He D. and Bechhoefer, E. (2014). Online particle-contaminated lubrication oil condition monitoring and remaining useful life prediction for wind turbines. Wind Energy, 18(6), pp. 1131-1149.

[197] O'Toole, M. and Diamond, D. (2008). Absorbance Based Light Emitting Diode Optical Sensors and Sensing Devices. Sensors (Basel, Switzerland), 8(4), pp. 2453 - 2479.

[198] (ed.) Gaonkar, A. G. (1995) Characterization of Food: Emerging Methods. Elsevier, New York, NY, USA, pp. 192 - 195.

[199] Siesler, H.W. and Eschenauer, U. (1998). NIR absorbance measuring instrument with ATR probe. Perstorp Analytical, Inc., US Patent, US5739537 A.

[200] Bereta, G. (1999). Spectrophotometer Calibration and Certification. HP Laboratories Palo Alto, HPL-1999-2.

[201] Gordon, D.A., Alguard, M. J. (1998). Dual spectrometer color sensor. Honeywell, Patent, US5793486 A.

[202] Color Sentinel Systems. In Line & Hand Held Self-Calibrating Modeling Spectrophotometers. White Paper, retrieved from: http://www.colorsentinelsystems.com/ (accessed on 2017/04/11).

[203] Ehbets, P., Frick, B., Wegmuller, M., Hunkemeier, J. and Niederer, G. (2014). Hand-Held Measurement Device for Capturing the Visual Impression of a Measurement Object. X-Rite Switzerland GmbH, Patent, US20140152990 A1.

[204] Frick, B. (2015). Color Measuring Apparatus. X-Rite Switzerland GmbH, Patent, US20160011052 A1.

[205] Frick, B., Feri, L. and Knechtle, S. (2012). Hand-held light measuring device. X-Rite Switzerland GmbH, Patent, US8279440 B2.

[206] Navarro-Villoslada, F., Orellana, G., Moreno-Bondi, M.C. Vick, T., Driver, M., Hildebrand, G. and Liefeith, K. (2001). Fiber-optic luminescent sensors with composite oxygen-sensitive layers and anti-biofouling coating. Anal. Chem., 73, pp. 5150 - 5156.

[207] Chae, K. H., Jang, Y. M., Kim, Y.H., Sohn, O. J. and Rhee, J. I. (2007). Anti-fouling epoxy coatings for optical biosensor application based on phosphorylcholine. Sensors and Actuators B: Chemical, 124(1), pp. 153 - 160.

[208] Omar, A. F. B. and MatJafri, M. Z. B. (2009). Turbidimeter Design and Analysis: A Review on Optical Fiber Sensors for the Measurement of Water Turbidity. Sensors (Basel, Switzerland), 9(10), 8311 - 8335.

[209] Mignani, A.G., Bizzarri, P. and Driver, M. (2002). Anti-biofouling coatings for optical fiber sensors. Proc. SPIE 4578, Sensor Technology and Applications, 0277-786X.

[210] Gulbrandsen, K. E. (2009). Bridging the valley of death: The rhetoric of technology transfer, PhD Thesis, Univ Iowa.

[211] Hargadon, A. (2011). Into the Valley of Death, University of California Davis Graduate School of Management.

[212] Cooper, R. G. and Scott J. E. (2012). Best Practices in the Idea-to-Launch Process and Its Governance. Research-Technology Management. 55 (2), pp. 43 - 54.

[213] Kuroda, R. and Sugawa, S. (2015). UV/VIS/NIR imaging technologies: challenges and opportunities. Proc. SPIE 9481, Image Sensing Technologies: Materials, Devices, Systems, and Applications II, 948108.

[214] Manuela Reitzig, M., Katzmann, J., Schuster, C. and Härtling, T. (2015). Optical nanosensor technology – from basic research to industrial applications. Proc. SENSOR 2015, AMA Science, pp. 25 – 29.

[215] European Commission. (2012). Towards 2020 - Photonics Driving Economic Growth in Europe. Photonics PPP Multi Annual Roadmap, pp.6-8, retrieved from: https://ec.europa.eu/research/industrial_ technologies/pdf/photonics-ppp-roadmap_en.pdf (accessed on 2017/04/ 21).

[216] El Hagrasy, A. S., Chang S.Y. and Kiang, S. (2006). Evaluation of Risk and Benefit in the Implementation of Near-Infrared Spectroscopy for Monitoring of Lubricant Mixing. Pharmaceutical Development and Technology, 11(3), pp. 303-315.

[217] Huang, H., Yu, H., Xu, H. and Ying, Y. (2008). Near infrared spectroscopy for on/in-line monitoring of quality in foods and beverages: A review. Food Engineering, 87(3), pp. 303-313.

[218] Tokhtuev, E., Owen, C. J., Skirda, A. and Christensen, W. M. (2015). Self-cleaning optical sensor. Ecolab Usa Inc., US Patent, US9001319 B2.

[219] Cooper, R. G. (2007). Managing Technology Development Projects, IEEE Engineering Management Review, 35 (1), pp. 67 - 76.

[220] Cooper, R. G. (2014). What's next? After Stage-Gate. Research Technology Management, 157(1), pp 20 - 31.

[221] Osterwalder, A. and Pigneur, Y. (2010). Business Model Generation: A Handbook for Visionaries, Game Changers, and Challengers. John Wiley and Sons, New York, NY, USA.

[222] Osterwalder, A. Pigneur, Y., Bernarda, G. and Smith, A. (2014). Value Proposition Design: How to Create Products and Services Customers Want. John Wiley and Sons, New York, NY, USA.

[223] Photonics 21, (2011). Our Vision for a Key Enabling Technology of Europe. White Paper, Photonics 21, pp. 8-12

[224] Resenhoeft, T. (2015). The fast track to success with agile product development, Bosch Press Release, June 16, 2015.

[225] McGrath, R. and McMillan, I. (2009). Discovery-Driven Growth. A Breakthrough Process to Reduce Risk and Seize Opportunity. Harvard Business School Press: Cambridge, MA, pp. 1 - 26.

[226] Loch, C., DeMeyer, A. and Pich, M. (2006). Managing the Unknown. A New Approach to Managing High Uncertainty and Risks in Projects. John Wiley & Sons, Hoboken, NJ, USA, pp. 1 - 5

[227] Pressman, R. (2009). Software Engineering: A Practitioner's Approach. McGraw-Hill, International Editions, 5th Ed...

[228] Cooper, R.G. (1998). Product Leadership – Creating and Launching Superior New Products. Perseus Books, New York, USA.

[229] Hasenkamp, T. and Olme, A. (2008). Introducing design for Six Sigma at SKF. International Journal of Six Sigma and Competitive Advantage, 4 (2), pp. 172 - 189.

[230] Korb, W. and Helmut, K. (2013). Innovation and robust sensor product development with Design for Six Sigma. Proc. SENSOR 2013, AMA Science, pp. 743 – 745.

[231] Eskandari, R. (2006). Role of Design for Six Sigma in Total Product Development. Six Sigma Academy International LCC, MIT LGO seminars May 2006.

[232] Womack, J. P., Jones, D. T. and Roos, D. (1990). The Machine that Changed the World: The Story of Lean Production. Harper Perennial, New York, NY, USA.

[233] Morgan, J. P. and Liker, J. K. (2006). The Toyota Product Development System: Integrating People, Process, and Technology. Productivity Press, New York, NY, USA.

[234] McMahon, T. (2010). Lean Product Development. CONNSTEP's 2010 Manufacturing and Business.

[235] Sorli, M., Maksimovic, M., Al-Ashaab, A., Sulowski, R., Shehab, E. and Sopelana, A. (2012). Development of KBE system to support LeanPPD application. 18th International ICE Conference on Engineering, Technology and Innovation, pp. 1 - 8.

[236] Ries, E. (2011). The Lean Startup: How Today's Entrepreneurs Use Continuous Innovation to Create Radically Successful Businesses. Crown Business, Crown Publishing Group, New York. NY, USA.

[237] Chen, E. (2015). Bringing a Hardware Product to Market: Navigating the Wild Ride from Concept to Mass Production. Concept Spring.com, pp. 9-31.

[238] Ideo (1999). Reimagining the shopping cart, Ideo, Palo Alto, CA, retrieved from:
https://www.ideo.com/post/reimagining-the-shopping-cart
(accessed on 2017/04/15).

[239] Ostrower, D. (2014). MVP for Hardware. Insight, page 8, retrieved from: http://www.altitudeinc.com (accessed on 2017/04/15).

[240] Hof, R. (2014). How Fitbit Survived as A Hardware Startup. Forbes, retrieved from: https://www.forbes.com/sites/roberthof/2014/02/04/how-fitbit-survived-as-a-hardware-startup/
(accessed on 2017/04/15).

[241] Sheehan, M. (2009). Ready, fire… aim: balancing speed and accuracy in new product development. PDMA Ontario, retrieved from: http://www.ontariopdma.ca/events/pastevents.htm
(accessed on 17/04/ 2017).

[242] Pietzsch, J.B., Shluzas, L.A., Paté-Cornell, M., Yock, P.G. and Linehan, J.H. (2009). Stage-Gate Process for the Development of Medical Devices. ASME. J. Med. Devices., 3(2), pp. 021004 - 021004-15.

[243] Ortloff, D. et al. (2014). MEMS Product Engineering: Handling the Diversity of an Emerging Technology. Best Practices for Cooperative Development. Springer-Verlag Wien, New York, USA, pp. 85 - 129.

[244] Lenfle, S. and Loch, C. (2010). Lost Roots: How Project Management Came to Emphasize Control Over Flexibility and Novelty. California Management Review, 53(1), pp. 32 - 55.

[245] Karlström, D. and Runeson, P. (2006). Integrating agile software development into stage-gate managed product development. Empirical Software Engineering, 11(2), pp. 203 - 225.

[246] Cooper, R. G. (2016). Agile–Stage-Gate Hybrids. Journal of Research-Technology Management, 59(1), pp. 21 - 29.

[247] Sommer, A. F., Hedegaard, C., Dukovska-Popovska, I., and Steger-Jensen, K. (2015). Improved product development performance through Agile/Stage-Gate hybrids: The next-generation Stage-Gate process? Research-Technology Management, 58(1), pp. 34 - 44.

[248] Grönlund, J., Rönnberg, D. and Frishammar, J. (2010). Open Innovation and the Stage-Gate Process: A Revised Model for New Product Development. California Management Review, 52(3), pp. 106-131.

[249] Unnger D. W., and Eppinger, S. D. (2009). Comparing product development processes and managing risk. Int. J. Product Development, 8(4), pp. 382 - 402.

[250] Chesbrough, H. W. (2003). Open Innovation: The new imperative for creating and profiting from technology. Boston: Harvard Business School Press, Boston, MA, USA.

[251] Mierzwa, T. J. (2016). Strategies for Managing Innovation. Lectures, University of Maryland's Master of Technology Entrepreneurship Program, Innovation Theory.

[252] European Commission, (2011). Guide to Intellectual Property Rules for FP7 projects. European Commission, Version 3, pp. 5 - 13.

[253] Metrohm AG. (2016). Using Online Near-Infrared Spectroscopy for Real-Time Analysis of Industrial Gases. Application Work, AW NIR-US-073-092015, Metrohm AG, retrieved from: https://www.metrohm.com/ (accessed on 2017/04/17)

[254] Di Egidio, V., Sinelli, N., Giovanelli, G. et al. (2010). NIR and MIR spectroscopy as rapid methods to monitor red wine fermentation. Eur Food Res Technol , 230(6), 947 - 955.

[255] Miller, R., Princz, S., Hessling, M. and Nurtdinow, I. (2012). Goal: online glucose sensor for bioreactors. Online Article. Ulm University of Applied Sciences, retrieved from: https://www.biooekonomie-bw.de/en/articles/news/goal-online-glucose-sensor-for-bioreactors/ (accessed on 2017/04/17).

[256] Filhaber, J. (2013). How Wedge and Decenter Affect Aspheric Optics. Photonics Spectra, Laurin Publishing, pp. 44 - 47.

[257] Hill, D. and McEuen, K. (2015). 4 Big Mistakes in Developing Photonics-Enabled Medical Devices. White Paper, Zygo Corporation.

[258] Mazurek, W. and Badve, A. (2017). Applying Design for LeanSigma® in the Medical Device Industry. White Paper, ConMed Corp. retrieved from: http://www.tbmcg.com.br/practitioner_assets/ Practitioner_Briefing_DLS.pdf (accessed on 2017/04/17)

[259] Mabe, J. and Gorritxategi, E. (2013). System and method for monitoring a fluid. Atten2 Advanced Monitoring Technologies, Patent, EP2980557A1, US20160069856, WO2014154915A1.

[260] Mabe, J., Zubia, J. and Gorritxategi, E. (2017). Lens-free imaging-based low-cost microsensor for in-line wear debris detection in lube

oils. Proc. SPIE 10110, Photonic Instrumentation Engineering IV, 101101D.

[261] Mabe, J., Zubia, J., Gorritxategi, E. (2017). Photonic Low Cost Micro-Sensor for in-Line Wear Particle Detection in Flowing Lube Oils. Sensors 2017, 17, 586.

[262] Mabe, J. (2016). Fluid Monitoring System, IK4-Tekniker, Pending Patent, EP16382179. See Annexed Documents.

[263] Mabe, J. (2017). Monitoring System and Method for Detecting Flowing Microscopic Objects. IK4-Tekniker, Pending Patent, EP17382007. See Annexed Documents.

[264] Villar, A., Vadillo, J., Santos, J.I., Gorritxategi, E., Mabe, J., Arnaiz, A. and Fernández, L. A. (2017) Cider fermentation process monitoring by Vis-NIR sensor system and chemometrics. Food Chemistry, 221(15), pp. 100-106.

[265] Gorritxategi, E., Mabe, J., Delgado, A. (2015). Fluid Monitoring System Based on Near-Infrared Spectroscopy. Atten2 Advanced Monitoring Technologies, Pending Patent, EP15382609.
See Annexed Documents.

[266] Villar, A., Mabe, J. et al. (2017). Equipo de Inspección para la Clasificación o Discriminación Automatizada de Almendras en Función de la Concentración de Amigdalina y Procedimiento de Inspección. (Spanish) Arboreto SL, Pending Patent, P201730562.

Photonic Low-Cost Sensors for in-Line Fluid Monitoring

Design Methodology

ANEXES

Jon Mabe Álvarez

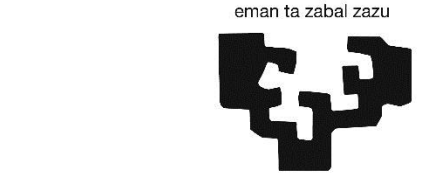

PhD Thesis
Bilbao, 2017

Supervisors:
Joseba Zubia Zaballa
Ana Aranzabe Garcia

Kai eta Alazne, zuentzat
Ama, Aita eskerrik asko

Preface

This volume compiles the different papers and patents that have been generated under the umbrella of the Photonic Low Cost sensor design methodology elaboration.

Index

sensors

MDPI

Article

Photonic Low Cost Micro-Sensor for in-Line Wear Particle Detection in Flowing Lube Oils

Jon Mabe [1,*], Joseba Zubia [2] and Eneko Gorritxategi [3]

1 IK4-Tekniker, Eibar 20600, Spain
2 Department of Communications Engineering, ETSI de Bilbao, University of the Basque Country (UPV/EHU), Alameda de Urquijo s/n, Bilbao 48013, Spain; joseba.zubia@ehu.es
3 Advanced Monitoring Technologies, Eibar 20600, Spain; egorritxategi@atten2.com
* Correspondence: jon.mabe@tekniker.es; Tel.: +34-688-819-784

Academic Editor: Vittorio M. N. Passaro
Received: 10 February 2017; Accepted: 10 March 2017; Published: 14 March 2017

Abstract: The presence of microscopic particles in suspension in industrial fluids is often an early warning of latent or imminent failures in the equipment or processes where they are being used. This manuscript describes work undertaken to integrate different photonic principles with a micro- mechanical fluidic structure and an embedded processor to develop a fully autonomous wear debris sensor for in-line monitoring of industrial fluids. Lens-less microscopy, stroboscopic illumination, a CMOS imager and embedded machine vision technologies have been merged to develop a sensor solution that is able to detect and quantify the number and size of micrometric particles suspended in a continuous flow of a fluid. A laboratory test-bench has been arranged for setting up the configuration of the optical components targeting a static oil sample and then a sensor prototype has been developed for migrating the measurement principles to real conditions in terms of operating pressure and flow rate of the oil. Imaging performance is quantified using micro calibrated samples, as well as by measuring real used lubricated oils. Sampling a large fluid volume with a decent 2D spatial resolution, this photonic micro sensor offers a powerful tool at very low cost and compacted size for in-line wear debris monitoring.

Keywords: optoelectronic and photonic sensors; object recognition, optical sensors; optical microscopy; optical diffraction; lubricating oils, hydraulic fluids; maintenance

1. Introduction

The presence of solid particles in suspension in industrial fluids, such as lubricants or hydraulic fluids, is frequently an early warning of latent or imminent faults in the machines or processes where they are being used [1,2], as it can be seen in Figure 1, where the contaminated lubricant of a gearbox about to fail is displayed. Therefore, the early detection of the presence of these wear particles is a key objective in a proper predictive maintenance program, complementing other machine condition monitoring approaches (CMS) such as vibration analysis [3]. The laboratory analysis of oil samples looking for evidence of wear was first introduced in 1948 [4], and this traditional off-line fluid analysis is still an important asset for several maintenance programs, especially when high accuracy and low detection limits are needed. However, the number of in-line sensor solutions is increasing steadily in the last decades [5–8]. The reason behind this growing number of in-line fluid monitoring technologies is found in a clear market request for: (i) real time results for critical infrastructure monitoring (gas turbines, aircraft engines) where the latency of the off-line laboratory tests is not acceptable [9,10]; (ii) solutions for applications with challenging and expensive off-line sample acquisition (e.g., off-shore wind turbines) [11,12]; and (iii) solutions for closing the control loops, as for example in torque regulation in run-in phases of gears or drive trains manufacturing [13]. These use cases are clear

examples demanding a tradeoff solution between an immediate availability of information and a reduction in the accuracy of the results, which is the ideal scenario for solutions like the one presented in this paper.

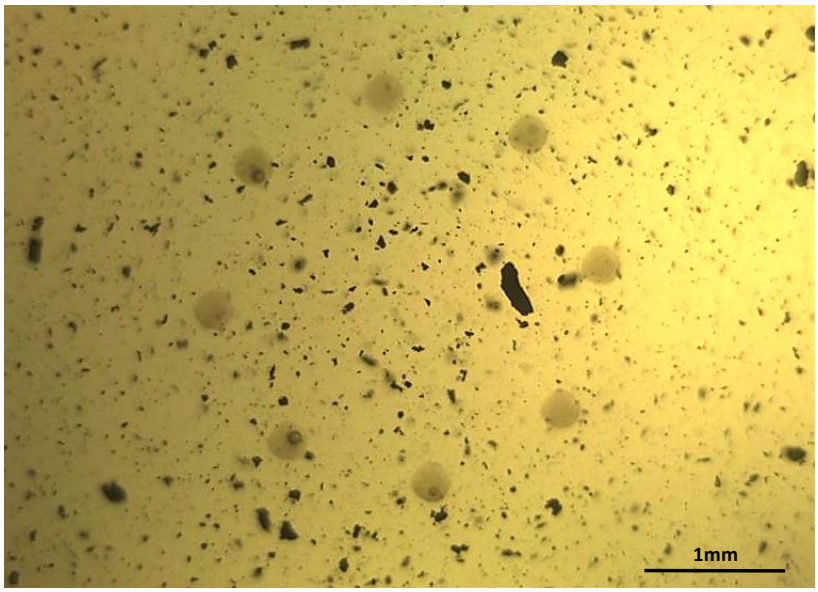

Figure 1. Image of a real lubricant sample from a gearbox in a wind mill, where large and small particles can be observed suspended in the fluid. The presence of this wear was evidencing a failure.

1.1. Wear Debris Sensors

Considering the features normally required of a wear debris monitoring sensor (asides the chemical and physical fluid compatibility), the following items can be highlighted [14,15]:

1. Output of normalized and calibrated data as specified by relevant standards of fluid cleanliness levels like ISO 4406, NAS 1638 or SAE AS4059, that basically summarize the particle count per mL classified in different size ranges (e.g., >4 μm, >6 μm, >14 μm)
2. Achieve a minimum detection limit of approximately 2 μm in particle size, which is directly proportional to the ability of the sensor to detect changes in contamination levels earlier.
3. Offer sensibility to metallic and non-metallic particles, allowing the sensor to detect either endogenous debris (e.g., iron or steel particles from mechanical parts, debris from seals) or exogenous contamination such as silicon dust, water or air.
4. Maximize sampling volume, while minimizing the measurement latency, which is proportional to mL analyzed per unit of time and determines the significance of the measurement.
5. Classify particles in groups (e.g., cutting, sliding or fatigue) for root cause analysis of the faults, which is normally determined by the particle shape and size.
6. Operate reliably and offer accurate measurements in conditions of turbidity, opacity and water and air bubble presence in fluid samples.
7. Offer a competitive total cost of operation (price, installation and maintenance of the sensor) compared to the off-line laboratory tests.

Regarding the measurement principles, there are two predominant technologies for in-line wear debris sensors: magnetic or inductive detectors and photonic detectors [16,17]. While the magnetic or inductive solutions offer a very good performance for high flow rates, allowing them to monitor large fluid volumes in real time, they suffer some drawbacks in terms of resolution and minimum detectable particle size, and they are affected by electrical noise and vibrations [18]. Additionally, they are not able to detect non-metallic particles, and shape recognition is not an option either [19].

On the other hand, photonic-based particle counters can be found, with different measurement principles available such as light scattering, light obscuration, or direct imaging [20,21]. However, among the different alternatives, the direct imaging systems (described in the Figure 2) are efficient solutions when the target for the minimum particle size is above 1 or 2 µm, preferably 4 µm, as it is the case for the ISO 4406 standardized applications, which are the most common ones for in-situ systems. The direct imaging systems offer a good ferrous and non-ferrous particle detection sensibility, allow shape recognition, and normally these solutions are relatively reliable in the presence of air and water bubbles [22]. However, these systems are normally constrained to very low flow applications and normally require a dedicated pumping system for bypassing the sample to the sensor in a regulated flow rate.

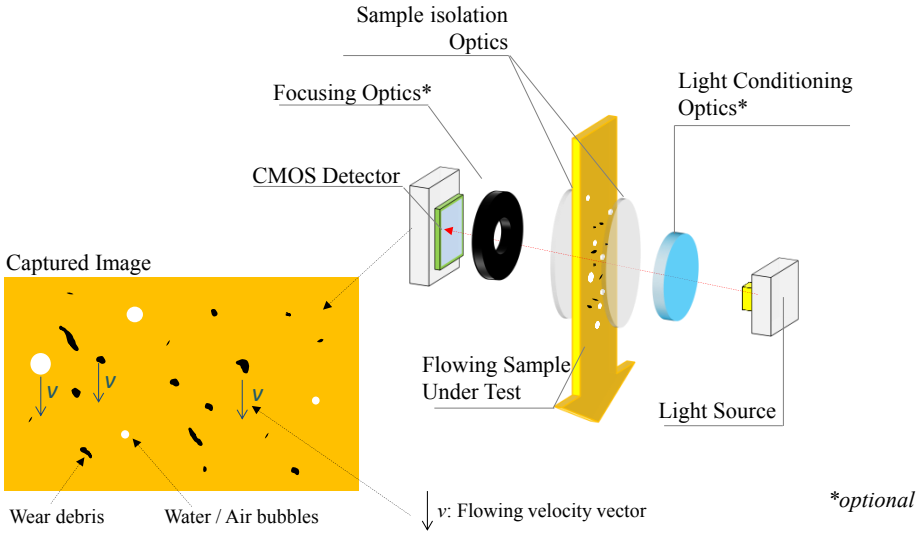

Figure 2. Block diagram depicting a direct imaging wear debris sensor analyzing a flowing lubricant.

In addition, due to the physical limits of the focusing optics needed for Direct Imaging, these solutions are not able to measure large samples of fluids. The limitations of traditional microscopes straightly affect in the direct imaging solutions, because, if high resolution is required (e.g., 4 µm) the field of view (FOV) and depth of field (DOF) are constrained, which aggravates the problem of probing large sample volumes in real time. The situation gets even worse if relatively simple lens solutions are required (instead of bulky tele-centric optics for instance) due to restrictions in the cost and dimensions of the final system. As a reference for the reader, a sensor system mounting a lens with an effective focal length of 9.6, and a CMOS of 10 M Pix is able to measure approximately 0.025 mL (FOV 36 mm^2/DOF 250 µm) of fluid per each sampling, achieving a resolution of around 3 µm [23]. These major limitations in resolution, FOV and DOF of traditional lens-based direct imaging sensors pave the way for applying lens-less microscopy techniques to wear debris monitoring. Lens-less microscopy is an emerging cost-effective technique that enables capturing high resolution images of 1 µm or below, over large FOV and long DOF with simple, compact and lightweight settings [24,25].

1.2. Lens-Less Imaging

Formulated in the late 1940s by the Hungarian engineer Dennis Gabor, the principle of lens-less imaging describes a new way for getting a perfect image. He proposed to capture an image of the interference pattern between the light that illuminates an object and the light diffracted by that object. Thanks to the amplitude and phase information, the collected light pattern contains all the information to reconstruct an image of the object [26]. Therefore, a lens-less imaging system only requires a light source, an aperture (pinhole) for generating the diffraction pattern, and an image sensor for capturing this light pattern.

Based on these theoretical principles, the lens-less imaging or microscopy was later developed in the 1960s [27], and it has been evolving since then. Recently, mainly driven by technological developments in CMOS cameras, light sources and data processing resources, there has been an increasing number of applications and published works in the field of lens-less microscopy, but these have been mainly oriented to biological applications, focusing on the inspection of microorganisms and cells in biological samples [28].

There are different configurations for constructing a lens-less imaging system, basically depending on the properties of the light source, their detection/imaging geometries and reconstruction or image-processing algorithms (e.g., FFT based original object reconstructions or direct use of the interference patterns). Each configuration is able to generate images of focused objects situated between the light source and the image sensor, but the details of these captured images will differ. With several particularizations, we found two main categories, Digital In-line Holography (DIH) using coherent light and Incoherent Lens-Less On-Chip imaging [29] (see Figure 3).

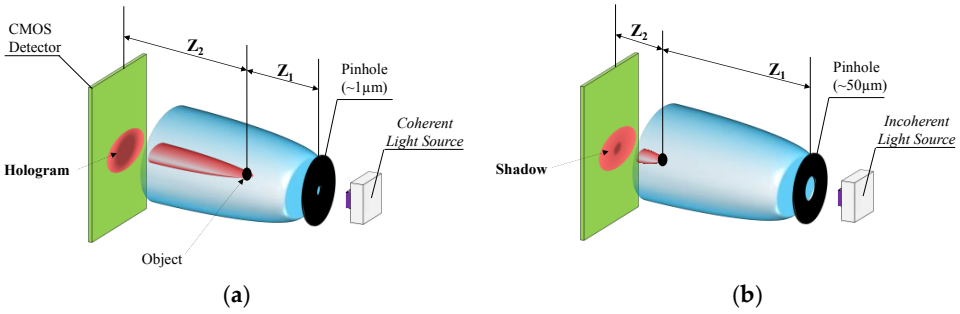

Figure 3. Coherent (**a**) and Incoherent (**b**) lens-less approaches.

The coherent lens-less option requires integrating a coherent light source, such as a LASER, with a pin hole with an aperture diameter of approximately 1 µm. This configuration assures the temporal and spatial coherence of the light hitting the sample object, enabling a later reconstruction of the captured holographic images into the original objects with a resolution below the micrometer. This configuration requires to set a distance in the range of some millimeters ($\sim 1000 \cdot \lambda$) between the object and the aperture (Z_1), whereas the distance between the CMOS sensor and the object (Z_2) is about some centimeters, therefore $Z_2 \sim 10 \times Z_1$.

The incoherent lighting approach represents the simplest alternative within the lens-less arena because it avoids the need for advanced optical components like lasers, replacing them with standard light sources. In this configuration, the detector receives a self-interfering diffraction pattern generated when the light beam hits the target object. This pattern could be understood as the shadow generated by the object blocking the incoming light to the detector and could be directly used for the object's size recognition, avoiding the use of computationally intensive holographic reconstruction algorithms [30,31]. In this case, the target objects should be located right above the detector, minimizing Z_2 distance to 1 or 2 mm, and the distance from the objects to the pinhole should meet $Z_1 >> Z_2$ relation. Additionally, in the incoherent mode, the aperture diameter is normally above 50 µm.

One of the best advantages of the incoherent mode is its suitability for dense samples (samples with a lot of particles) because the cross-interference in the diffraction patterns of the different adjacent particles is near zero, whereas it is an important factor for the coherent version [32].

It becomes evident that the potential benefits of the lens-less imaging in terms of resolution, FOV, DOF and simplicity of the solution described in the literature, would positively contribute in the field on the in-line/on-line wear particle counting and classification. Even in the simplest expression of the lens-less microscopy, the incoherent mode, the solution looks promising due to a relatively large sample volume monitoring (FOV ~20 mm^2, DOF ~1 mm), resolutions of approximately 2 µm, simplicity and robustness of the hardware setup, small size of 50 mm × 50 mm × 10 mm allowing the

integration of the solution on larger structures [33,34], and last but not least, the possibility of avoiding the holographic reconstruction algorithms (which take several seconds in a PC station with a graphical processing unit) and working directly with the 'spatial signatures' or shadows generated by the light absorbed by particles in the sample volume.

An application of a lens-less approach for solving the detection of wear particles is presented in [35], however, it only dealt with static fluids and requires some external hydraulic conditioning systems, such as electro-valves or flow controllers, to stall the fluid while the images of the sample are taken. The need of these bulky hydraulic components jeopardize the low cost and compact size potential of the lens-less approach. However the system evolution for dealing with non-static fluid conditions is not straightforward, and several modifications especially in the lighting and image capture system, are required as described in the next section.

1.3. Precision Imaging of Moving Objects

The current sensor proposal addresses the problem of the low sampling volume from a twofold approach. It is evident that the enhancements brought by the lens-less technology in terms of higher FOV, DOF and resolutions are contributing to acquire a sharp image of a larger sample volume. However, as mentioned above, the direct application of the lens-less solution still requires to regulate or stop the flow of the sample crossing the acquisition area.

The problem is related with the distortion or blur occurring at images capturing objects moving at relatively high velocities (see Figure 4). This distortion is caused because the target objects displaces its position within the acquisition area faster than the pixel acquisition time, being this acquisition divided in the pixel exposure time and on the pixel read-out time. This is widespread problem in the machine vision and imaging fields, and applications such as traffic management, metrology and robotics inspection all need to image fast-moving objects without smear or distortion. Techniques such as Global Shutter Imagers or Global Reset Rolling Shutter CMOS systems have risen as candidates to meet the requirement of capturing smear-free images of fast moving objects [35,36]. Additionally, there are some software based approaches to restore motion blurred particle images [37] applied to the in-line wear debris monitoring, however, they have only been validated at low flow rates of 1 mL/min and large particles.

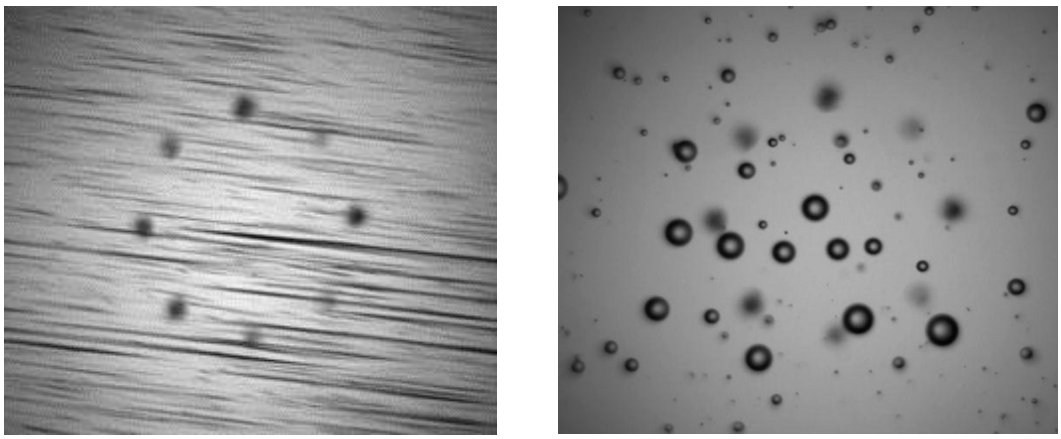

(**a**) (**b**)

Figure 4. Example of distorted image due to the Rolling Shutter effect recording moving objects suspended in a fluid (**a**). Same objects recorded using synchronized stroboscopic illumination (**b**) generating a non-distorted image. (**a**) image has been recorded using an exposure time of 23 ms and a flash gain of $\times 1$ with a duration equal or longer than the exposure time. The (**b**) image instead uses a flash pulse of 4 µs to allow the smear-free images but requires applying a flash gain of $\times 40$ to achieve a similar image luminance level. In the (**b**) case, the effective exposure time is limited by the flash pulse duration, regardless of the configured pixel exposure.

The solution implemented in the current sensor proposal uses a stroboscopic light control (high amplitude pulsed light) system emulating a Global Shutter CMOS mode using a Rolling Shutter CMOS (with global pixel reset feature enabled). The CMOS frame capture trigger is synchronized with the LED light switching on, allowing the acquisition of semi-static images of moving objects avoiding the Jello effect or the diagonal bending of images, characteristic of rolling shutter captures of fast moving objects. Indeed, a Global Shutter CMOS could have been chosen for enabling non-distorted images, but the cost and size of Global Shutter sensors against the Rolling Shutter ones is much higher, especially in high resolution versions [38].

The stroboscopic-based illumination and capture system enables working with higher flow rates as the flash pulse duration is reduced, provided that enough light power reaches the detector for the later processing of the images. However, reducing the pulse length drastically impacts the effective amount of light available, which is especially important when illuminating opaque fluid samples. From Figure 5, it can be concluded that, if the design goal is to maintain the same light level at the CMOS detector ($V_{PIX}' \sim V_{PIX}$), then the emitted light power should meet $I_{LED}' >> I_{LED}$ as described in Equations (1) to (4) (these calculations are further discussed in later sections). As the maximum light power amplitude (I_0') is limited by the technology, the optimal pulse duration (T_{ON}) for each sensor configuration is a trade-off between the maximum flow rate and the compatibility with darker fluid samples:

$$I_1 \propto I_{LED}\,, I_1' \propto I_{LED}' \tag{1}$$

$$V_{pix} = R\left(\frac{V}{Lux{\cdot}s}\right) \times I_1(Lux) \times T_{EXP}(s) \tag{2}$$

$$V_{pix}' = R\left(\frac{V}{Lux{\cdot}s}\right) \times I_1'(Lux) \times T_{ON}(s) \tag{3}$$

$$T_{EXP} \gg T_{ON} \rightarrow I_1' \gg I_1 \rightarrow V_{pix}' \sim V_{pix} \tag{4}$$

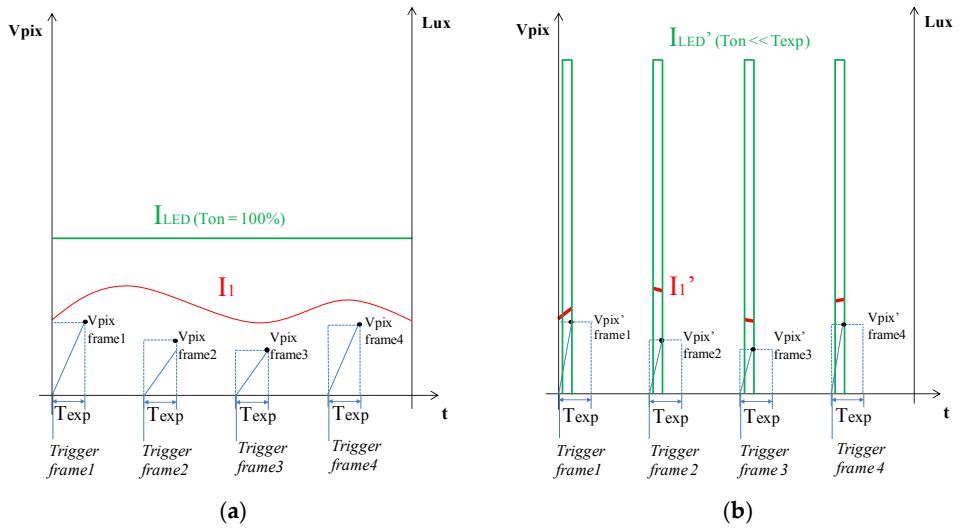

Figure 5. Graphical example of the irradiance received by the CMOS sensor ($V_{PIX} = R\left(\frac{V}{Lux{\cdot}s}\right){\cdot}I_1(Lux){\cdot}T(s)$) on each frame on a continuously illuminated case (**a**) and on the stroboscopic case (**b**). I_{LED} and I_{LED}' represents the light power generated at the emitter, whereas I_1 and I_1' are the light remaining after crossing the whole system (optics, sample, etc.) and getting to the CMOS surface. Indeed, I_1 and I_1' are proportional to the light emitted by the sources, I_{LED} and I_{LED}'. T_{EXP} represents the exposure time configured at the CMOS, being the amount of time that each pixel is integrating the light received with the given sensor responsivity $R\left(\frac{V}{Lux{\cdot}s}\right)$. Additionally, T_{ON} describes the light pulse duration, being 100% of time for the (**a**) case and $T_{ON} << T_{EXP}$ for the (**b**) configuration. Note that the pulse start is synchronized with the frame triggering.

Additionally, this light shortage is aggravated due to inclusion of the pinhole requested by the lens-less configuration, which acts as a spatial filter blocking an important amount of the light emitted by the source.

Therefore, bringing all the potential advantages of the lens-less optics and stroboscopic illumination system to an integrated sensor is not straightforward, due to some application-specific requirements that need to be met as the mentioned maximum sample flow rate or the maximum pressure to be born by the sample cell. The target operating conditions for the lubricant sensors may require standing working or burst pressures above 10 bars, requiring a protective mean between the running sample and the CMOS detector that will directly impact on the possibility of reducing the lens-less Z_2 distance.

The following sections describe the work performed for the application of the aforementioned photonic principles into an optical microsensor for the detection of wear particles in running industrial fluids with clear maximum pressure and flow rate specifications.

2. Materials and Methods

This section describes the different test benches and prototypes developed with the objective of validating the proposed sensor approach that enables the largest FOV, DOF, highest resolution and maximum compatible flow rate to fulfill the industrial requirements for particle counters. The development starts with a theoretical approach for describing the lens-less setup, and a proof-of-concept validation phase in an optical test bench. Some theoretical approximations follow, defining the light power budget in relation with the maximum compatible fluid flowing velocity, and calculating the different structural constraints due to maximum fluid pressure. Some intermediate results are displayed along the section, which verify the different modules later included in the sensor.

2.1. Optical Test Bench

As a first step in the proof-of-concept realization, a custom optical test bench has been arranged. The main objectives of this setup are: (i) definition of the Z_1 and Z_2 distances, (ii) definition of the pinhole diameter D; (iii) characterization of system performance in terms of resolution, FOV and DOF; and (iv) characterization of the stroboscopic light for enabling the maximum compatible sample flowing rate.

The photonic test bench (see Figure 6) comprises a customized light source based on an array of XLamp white LEDs from Cree (Durham, NC, USA) providing a light flux of 535 lumens/3W at 120° viewing angle per each LED and being able to generate a tunable amplitude and length light pulses synchronized with the image captures. The CMOS sensor is a 5 Mpix rolling shutter device in $\frac{1}{2}$" format, 2.2 × 2.2 μm pixel size, with a responsivity of 1.76 V/Lux-s and 5.7 × 4.28 mm active area (MT9P006 from On Semiconductors, Phoenix, AZ, USA). For the aperture definition, a set of precision pinholes 50, 200 and 500 μm) from Thorlabs (Newton, NJ, USA) has been selected. Additionally, a thin quartz cuvette (ref. 106-0.50-40, Hellma Analytics, Müllheim, Germany) has been used as fluid sample container. The cuvette is placed adjacent to the CMOS surface, making Z_2 distance equal to the cuvette wall thickness (~1.25 mm).

Therefore, the sample volume is determined by the cuvette light path, which is 0.5 mm. Asides, the light source and pinhole have been attached to a micrometer translation stage (Thorlabs MT1/M) allowing precision Z_1 tuning. Additionally, note that the inner walls of the cuvette walls have been micro milled with precision marks (65 μm side square and 75 μm diameter circle) that allow us to characterize the DOF, FOV and resolution of the setup. The detailed view of these micro patterns is displayed in Figure 7.

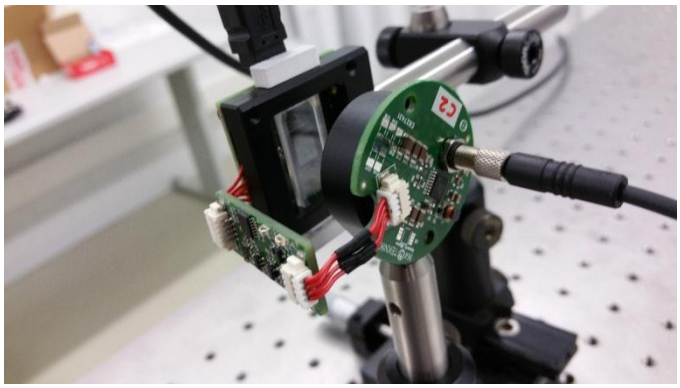

(**a**)

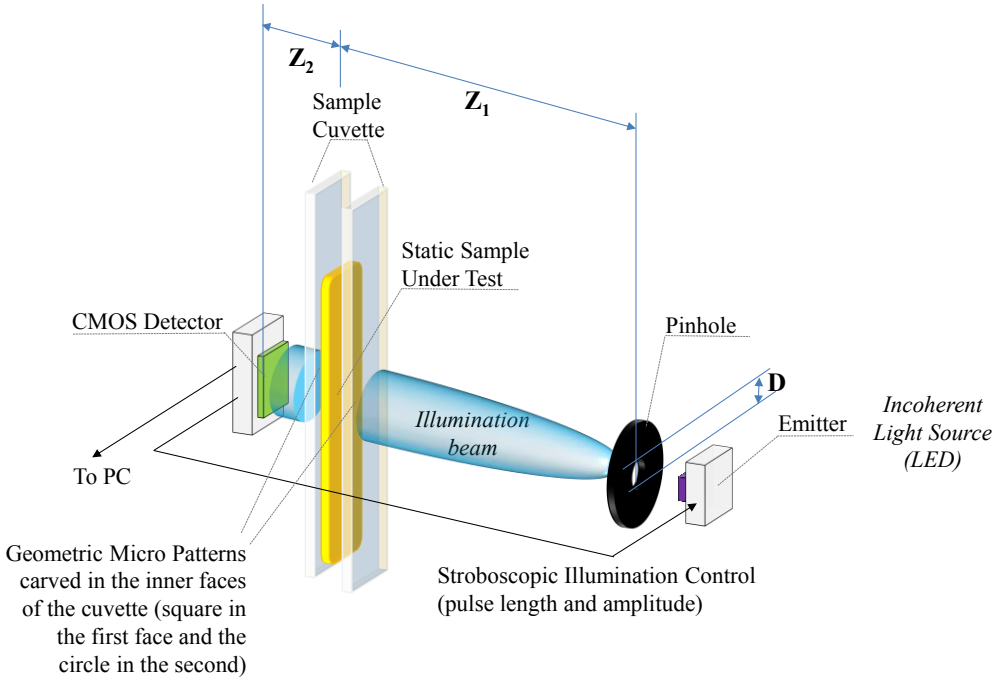

(**b**)

Figure 6. (**a**) Photo and (**b**) block diagram of the optical test bench.

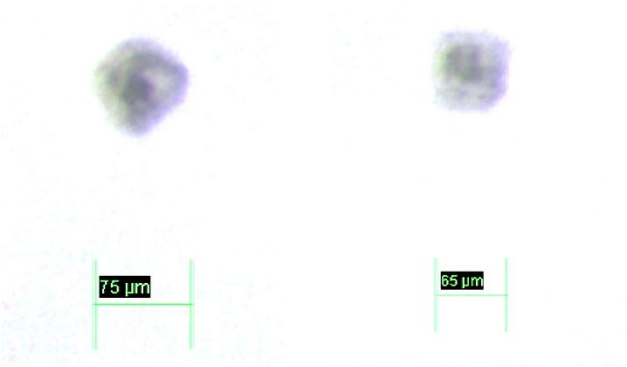

Figure 7. Detailed view of the patterns micro milled in the inner faces of the quartz cuvette.

2.2. Theoretical Approach

The optical requirements for the wear debris sensor have been used as the starting point for the theoretical calculations. The minimum resolution required for the detection of particles of 4 µm has been considered around 1–2 µm. The largest particle size expected should not exceed 200–400 µm. The DOF and FOV definition derives from the general request of offering the highest sampling volume possible. According to the references, in an incoherent lens-less setup, one could expect a FOV equal to the active area of the CMOS sensor, which for the current example is 5.70 mm (H) × 4.28 mm (V).

Regarding the DOF, two important considerations are needed. First, the effective DOF depends on the particle size, and different DOF are expected for 4 µm, 6 µm and >14 µm particle sizes. For instance, in the lens-based system referenced in [22], the DOF for small particles is approximately 250 µm, for medium particles it raises to 400 µm, and for large particles the system reaches almost 1 mm. Secondly, the DOF will not only be limited by the lens-less performance, but also by the light absorption happening at the sample, which according to the Lambert-Beer law, decreases logarithmically proportional to the light path length. This may generate that even at sharply focused planes a non-valid particle image may be acquired by the detector due to the lack of light intensity.

The already mentioned issue of the amount of light received at the CMOS needs to be further elaborated because it is a critical parameter allowing the acquisition of valid images for particle detection, especially when they are moving at relatively high velocities. As can be seen in Figure 8, this light intensity will depend on several factors as the light power emitted by the source (Lux/mA), the switch on time of the light pulse (T_{ON}), the aperture diameter of the pin-hole ($D_{pinhole}$), the free-space loses happening at Z_1 and Z_2 distances, the responsivity at the CMOS (V/lux-s), and of course, the light absorption occurring at the fluid sample which depends on its absorptivity (ε) and on the path length (L).

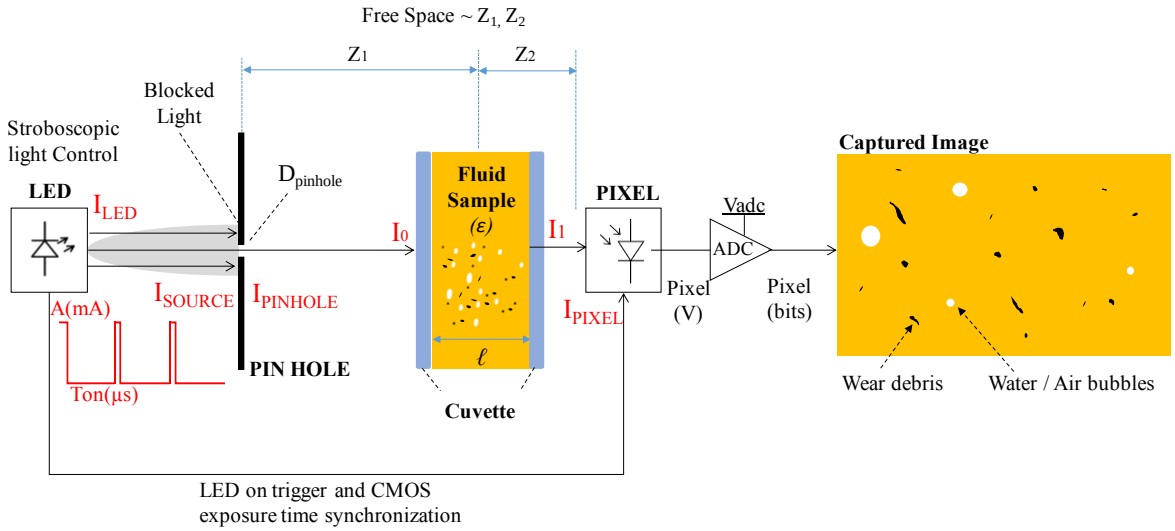

Figure 8. Block diagram depicting the main factors impacting in the light intensity detected at the CMOS sensor.

Some of these variables are defined by the state-of-the-art technology (e.g. light source efficiency, detector responsivity), whereas some others are constrained by the application requirements as the T_{ON} time, which for the target fluid flows should be sent in the range of 40 ns to 40 µs, or the path length, which for the compatible fluid range opacity, it has been set to 0.5–1 mm. These considerations will be later elaborated in Section 3.3 where the lighting system of the sensor is described.

However, parameters such as the pin-hole diameter D and Z_1–Z_2 distances are totally dependent on the lens-less setup selected. The following calculations are based on the work described in [39], and define the lens-less setup for meeting the requirements described above.

As mentioned earlier, for non-coherent light based lens-less setups, Z_2 distance must be minimized. However, for the current sensor setup, there is a minimum limit for the Z_2 defined by the sample holder structure (either a cuvette in the optical test bench or a window in the sensor prototype) is defined by the cuvette wall thickness. This holding structure needs to stand pressures of 10–15 bars, which depending on the constructive material and the area, requires to be at least 0.5 mm thick. With this assumption, and considering a sample path length of 0.5 mm:

$$\begin{array}{c} Z_{2-\min} = \text{sample holder wall} = 1.25 \text{ mm} \\ Z_{2-\max} = \text{sample holder wall} + \text{path} = 1.75 \text{ mm} \end{array} \quad (5)$$

Considering that this setup requires a fringe magnification factor, $F = (Z_1 + Z_2)/Z_1 \sim 1$, then $Z_1 >> Z_2$, typical Z_1 values in the literature are 2–5 cm. This relation also defines the FOV of the system, defined as FOV = Area of the sensor/F, which for F~1 remains almost equal to the full active area of the CMOS detector.

Regarding the diameter of the pin-hole, the incoherent lens-less setup requires a relatively large aperture (e.g., > 100λ–200λ). Considering the central emission peak of the white LEDs used at λ_0 = 580 nm, we obtain: $D_{pinhole} > 58$ μm.

The diameter of holographic coherent diffraction (D_{coh}) for each object in the focus plane is proportional to $\lambda_0 \, Z_1/D_{pinhole}$. Note that for this specific case, we are targeting a direct use of the images collected, rather than needing a holographic reconstruction of the captured light intensity. Therefore, the setup will look for decreasing Z_1 as much as possible.

The effective width at the detector plane of each point scattered on the sample plane is defined as $d_{scat} = D_{pinhole} \, Z_2/Z_1$. This is relatively important for understanding the DOF and resolution performance of the proposed setup: the objects (particles) located at higher Z_2 distances will show a higher scattering. It is clear that towards minimizing enhancing the sharpness of the images captures in the largest DOF, we should reduce $D_{pinhole}$ and Z_2 as much as possible.

Therefore, the choice of both the $D_{pinhole}$ and Z_1 is driven by a tradeoff solution for minimizing the d_{scat} and D_{coh}, whereas Z_2 must be keep the minimum possible. Additionally, for defining $D_{pinhole}$, the impact on the light intensity filtered also needs to be taken into consideration.

Table 1 summarizes the dependencies between the lens-less parameters with the targeted optical performance indicators.

Table 1. Critical Parameters of the lens-less system.

Parameter	Design Target	Impacts on	Dependencies
D_{coh}	Minimize	Resolution, DOF	$\propto 1/D_{pinhole}$, $\propto Z_1$
I_{light}	Maximize	Contrast, Flow Rate	$\propto D_{pinhole}$, $\propto 1/Z_1$, $\propto 1/Z_2$
d_{scat}	Minimize	Resolution, DOF	$\propto D_{pinhole}$, $\propto 1/Z_1$, $\propto Z_2$

Following sections present the results obtained with different settings for $D_{pinhole}$, Z_1, Z_2 and light power for imaging real lubricants (Optigear X320 Synthetic, Castrol, Berkshire, UK). Therefore, the sample volume is determined by the cuvette light path, which is 0.5 mm. Asides, the light source and pinhole have been attached to a micrometer translation stage (Thorlabs MT1/M) allowing precision Z_1 tuning. Therefore, the sample volume is determined by the cuvette light path, which is 0.5 mm. Asides, the light source and pinhole have been attached to a micrometer translation stage (Thorlabs MT1/M) allowing precision Z_1 tuning.) artificially contaminated with metallic particles (LS277298 Stainless Steel >45 μm AISI 316 ,GoodFellow, Huntingdon, UK).

2.3. Test Bench Results

Figures 9 and 10 show different detailed views of the cuvette sample acquired with a benchtop microscope. The presence of the wear particles and their size can be observed against the already mentioned micropatterned structures.

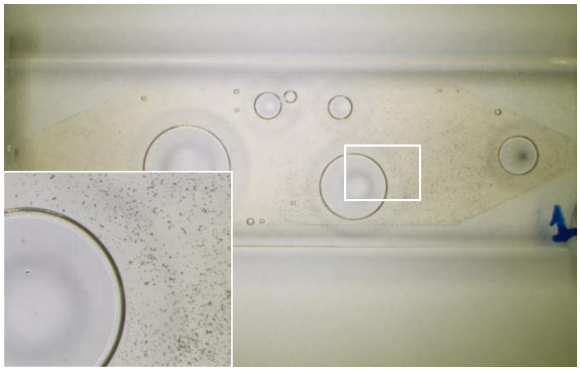

Figure 9. General (0.8×) and detailed view (2×) of the 0.5 mm quartz cuvette containing the contaminated lubricant sample and air bubbles.

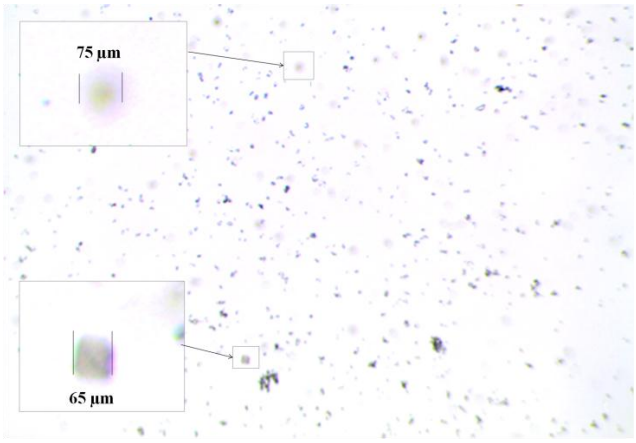

(**a**)

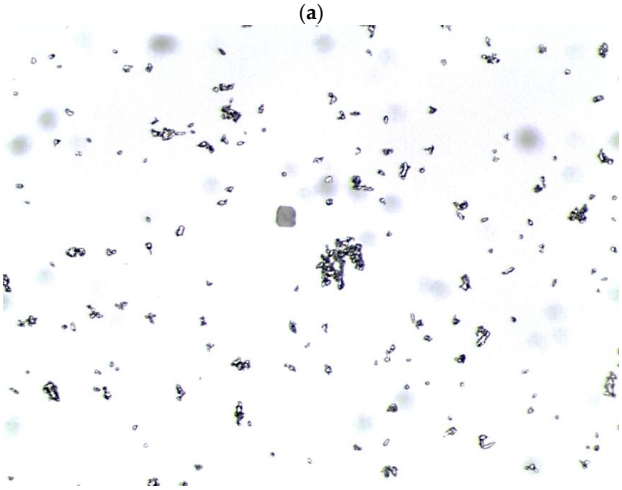

(**b**)

Figure 10. (**a**) General view (5×) and (**b**) detailed view (11.5×) of wear debris within the quartz cuvette. A detail of the micro patterns is also displayed in (**a**), where the limitation of the DOF becomes evident. In (**b**) the squared pattern could be found in the center of the image.

The cuvette has been analyzed first using the microscope optics in different magnification setups. Indeed, the level of detail achieved with the microscope observation is very high, however, the FOV and DOF is limited to the properties of regular optics. For instance, in Figure 10a the limitation in DOF is evident: when using a 5× magnification, the FOV achieved is 5485 µm by 4100 µm, but the performance in terms of DOF is very poor, as the system is almost unable to focus the two micromilled patterns that are 500 µm deep far from each other.

When comparing with the images acquired with the lens-less test bench (for instance Figure 12a), both micropatterns are in the focus range, while the FOV is 4500 × 3400 μm^2 remaining almost the same as for the microscope in 5× mode. However, the quality and resolution of the images acquired with the lens-less setup are affected by the diffraction patterns generated at each particle, which are inversely proportional to the pinhole diameter as described by Fraunhofer diffraction pattern for a circular aperture [40]. Figure 11 displays the diffraction patterns generated with the different pinholes.

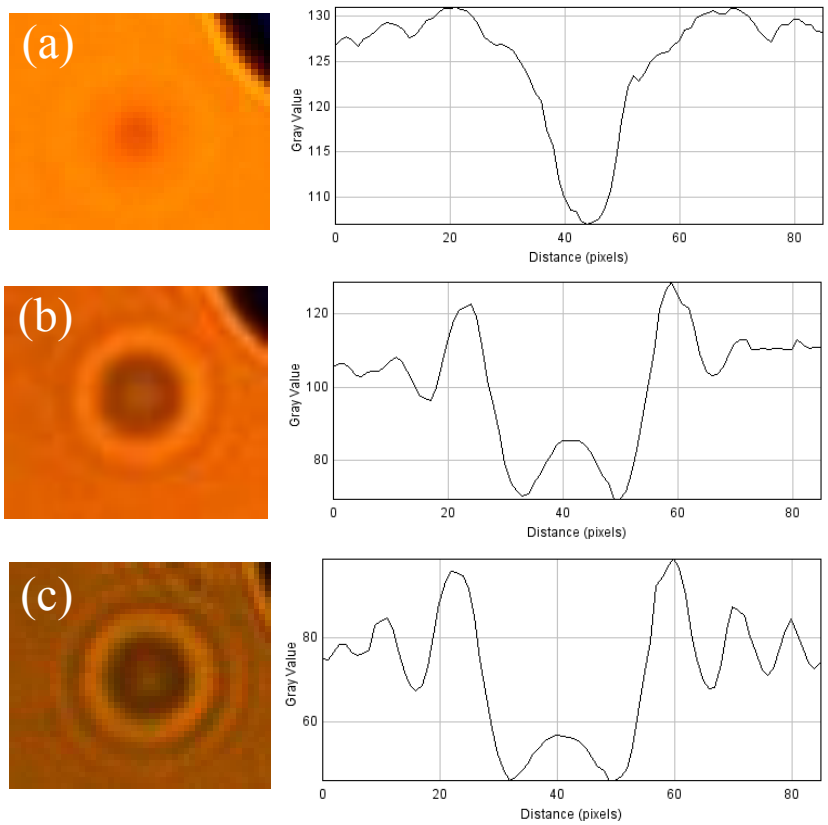

Figure 11. Examples of the different diffraction patterns and their linear intensity profile for different pinholes (**a**) $D_{pinhole}$ = 500 µm; (**b**) $D_{pinhole}$ = 200 µm; and (**c**) $D_{pinhole}$ = 50 µm all of them with Z_1 = 11 mm and Z_2 = 1 mm.

Note that the objective of the proposed sensor system is to work with direct imaging, avoiding the need of reconstructing holograms. For this specific case, the diffraction patterns are considered as a noise source, and therefore, the design specification should work towards mitigating their presence. The following images show the result of inspecting the same fluid sample under different pinhole configurations. Additionally, even if in this case the samples were static, a stroboscopic illumination system has been used, with pulses durations ranging from T_{ON} 500 ns to 5 µs and amplitude intensities from 2 to 6 A. The settings that displayed the best performance were based on the biggest pinhole diameter, Z_1 around 10–11 mm and the smallest Z_2 possible, in this case approximately 1 mm and limited by the cuvette wall.

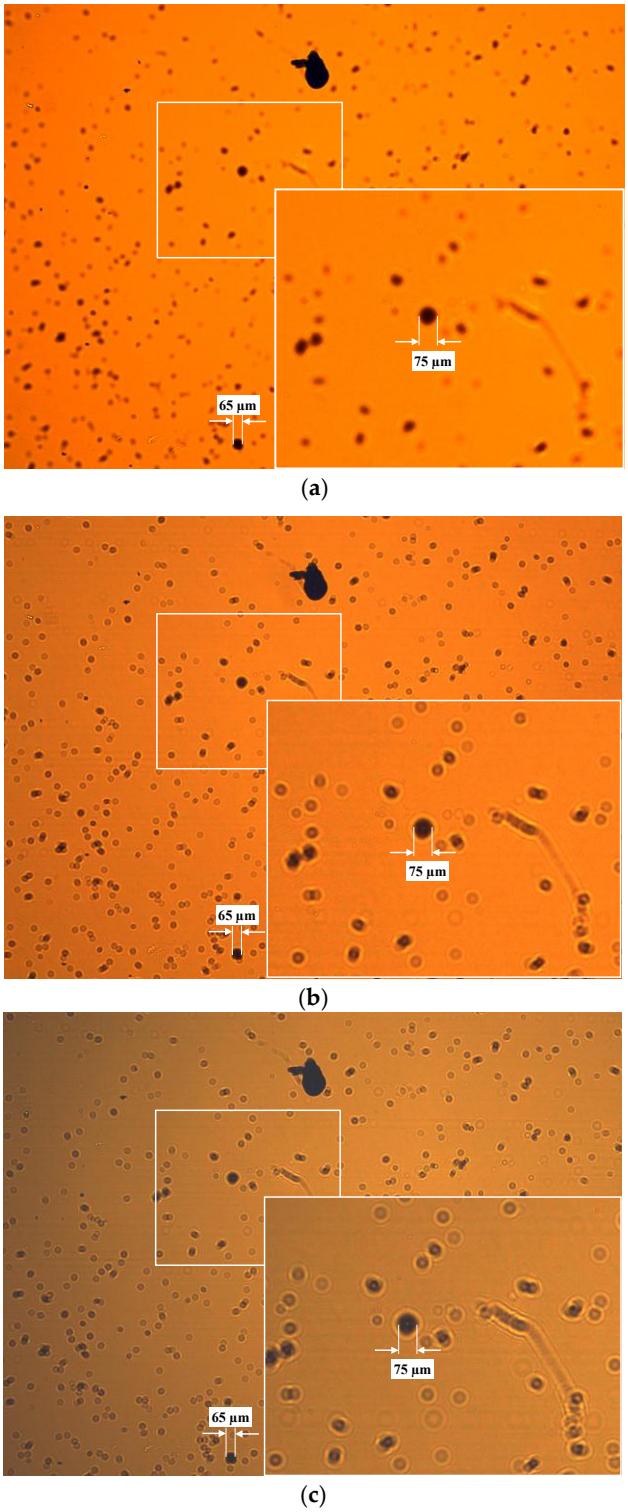

Figure 12. Examples of results with the lens-less test bench. Full FOV and Detailed view of a contaminated fluid sample with (**a**) $D_{pinhole}$ = 500 µm; (**b**) $D_{pinhole}$ = 200 µm; and (**c**) $D_{pinhole}$ = 50 µm all of them with Z_1 = 11 mm and Z_2 = 1 mm. Light Power and T_{ON} pulses have been configured for achieving similar image intensity on all configurations.

3. Sensor Design

The results accomplished during the experiments at the optical test bench were considered promising enough for launching the design of the proof-of-concept sensor prototype.

3.1. Sensor Description

The sensor solution integrates different building blocks, including micromechanics, microfluidics, photonics and electronic subsystems (see Figure 13). The micro mechanical solution includes the hydraulic connections, microfluidic sample cell, deals with positioning of optical and electronic components and additionally solves the external enclosure. The photonic subsystem integrates the CMOS camera, stroboscopic lighting, pinhole, light diffuser and two transparent glass disks to confine the fluid within the sampling cell. Besides, the sensor includes a custom embedded electronics for video acquisition, lighting control and execution of the machine vision algorithms for object recognition. The following sections describe the most challenging subsystem of the sensor: the mechanics, optics and the lighting system.

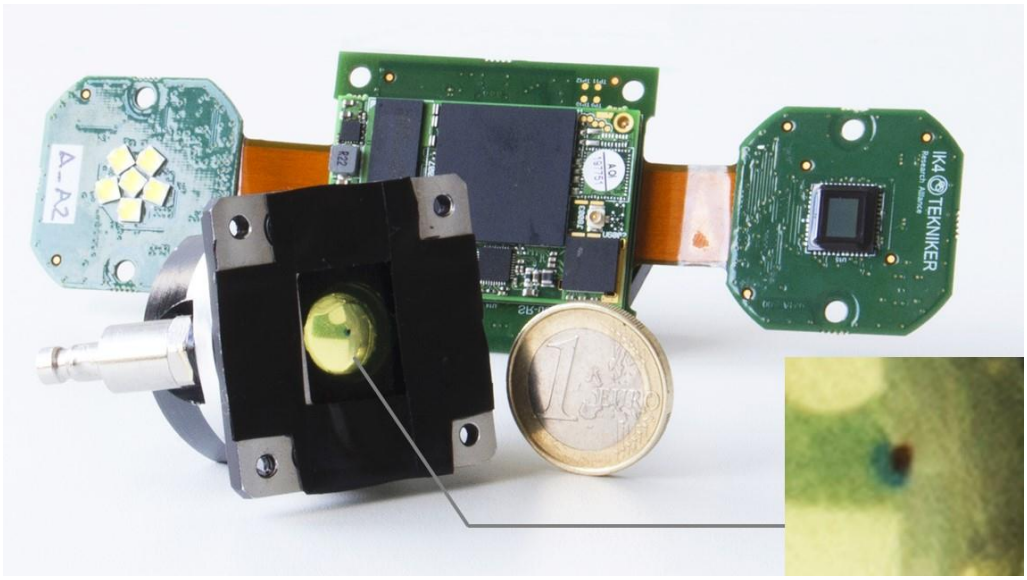

Figure 13. Sensor Prototype. The micromechanical sensor body is in the front, where the measurement cell is detailed. The electronic subsystem with the processor, the CMOS and the LED lighting is in the background.

3.2. Mechanics and Optical Design

The conclusions regarding FOV, Z_1, Z_2 and $D_{pinhole}$ dimensions were fed into the specifications for mechanical design of the sensor body. Matching these micro-scale requirements with relatively challenging pressures (e.g., 10–15 bar), flows (e.g., 1–3 liter/min), viscosities (e.g., 320–480 cSt), etc. requires a careful system design. For instance, the requirement for using standardized hydraulic fast plug connectors (BSP Gas 1/8) in combination with the design target of reducing Z_2 as much as possible (~0.5 mm) has required to introduce crosswise sample inlet and outlets, due to space restrictions, as it can be observed in Figure 14.

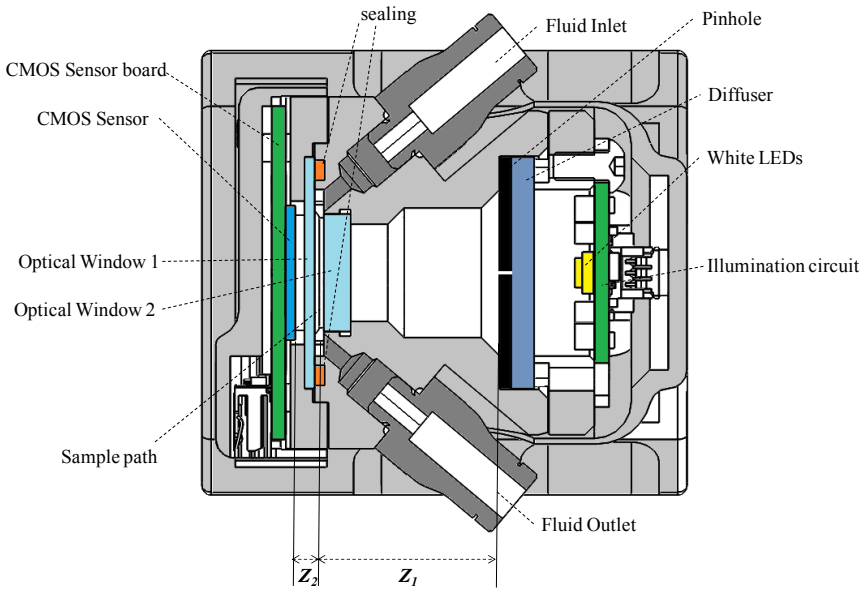

Figure 14. Block Diagram depicting the sensor system.

Integrating the electronics, mechanics and optics, the sensor dimensions are approximately 35 × 45 × 45 mm, which could be considered as a very compact solution. The sensor body is fabricated in anodized aluminum and the sealing materials are fluorocarbons (for mineral or synthetic lubricant fluids) or EPDM (for measuring phosphate ester-based hydraulic fluids). Regarding the optical window closest to the CMOS sensor, which defines the Z_2 distance, it should be keep the thinnest possible while standing the fluid pressure specification. The following formula describes the minimum thickness of glass disk before it breaks under a given pressure:

$$\mathrm{T(inch)} = \sqrt{\frac{\mathrm{Pmax(psi)} \times \mathrm{A(sq.inch)} \times \mathrm{F}}{3.12 \times \mathrm{M}}} \quad (6)$$

Whereas, T represents the minimum thickness in inches, A defines the unsupported area in sq/inches, P is the maximum pressure in psi, M defines the modulus of rupture (in psi) and F is a safety factor that normally is set to 7. Therefore, depending on the type of glass, different thickness could be used for tolerating a specified maximum pressures of 10 bars. In the current proof of concept, two different glass materials and thicknesses have been used. The first option is a 0.2 mm ultra-thin BK7 (M ~2400 psi) window from Edmund Optics (Barrington, NJ, USA), that have been selected with the aim of demonstrating the best optical performance as it allows a high reduction in the Z_2 distance. Unfortunately, according to Equation (6), this BK7 option only bears 0.01 bars, meaning that its use is restricted to low pressure applications. The second candidate is a 1.1mm thick Gorilla® Glass (M ~100,000 psi) disk, which allows working up to 11 bars but sets Z_2 a little bit further, but still in the range of operation for incoherent lens-less applications. The second optical window (the one closest to the pinhole) has been resolved with a thicker BK7 glass disk (3 mm). The sample path is 0.5 mm, equivalent to tests performed with the cuvettes.

Additionally, in order to protect the CMOS sensor from the bending occurring at the glass window, a small security air gap of 0.2 mm has been defined. Therefore, the system is able to offer a minimum Z_2 of 0.4 mm mounting the ultrathin glass disk and a maximum of Z_2 1.3 mm when using the Gorilla® glass. Implementing the Z_1 distance is much straightforward, and the sensor integrates a mechanical solution for holding the pinhole plate at 10 mm from the center of the sample path.

3.3. Light System Design

Pinhole selection and the light emitter design has been driven by the light power requirements for properly illuminating flowing lubricants. As it has been explained in earlier sections, due to the instant velocity of the particulate flowing within the lubricant, a stroboscopic lighting system is required for avoiding the generation of distorted images. In this context, the duration of these pulses is defined by the expected velocity of the objects (particles) suspended in the fluid under supervision when they go through the focusing area of the CMOS. Indeed, the duration of the illumination pulse is inversely proportional to the maximum velocity of the moving objects.

According to the Computational Fluid Dynamics (CFD) simulation displayed in Figure 15, considering a range of working pressures of 2, 5 and 10 bars, the expected laminar flow speeds of the lubricant across the microfluidic structure of the sensor are 3, 11 and 22 m/s, respectively. Therefore, the particulate suspended in the fluid will also move at similar velocities (not considering turbulence effects, etc.).

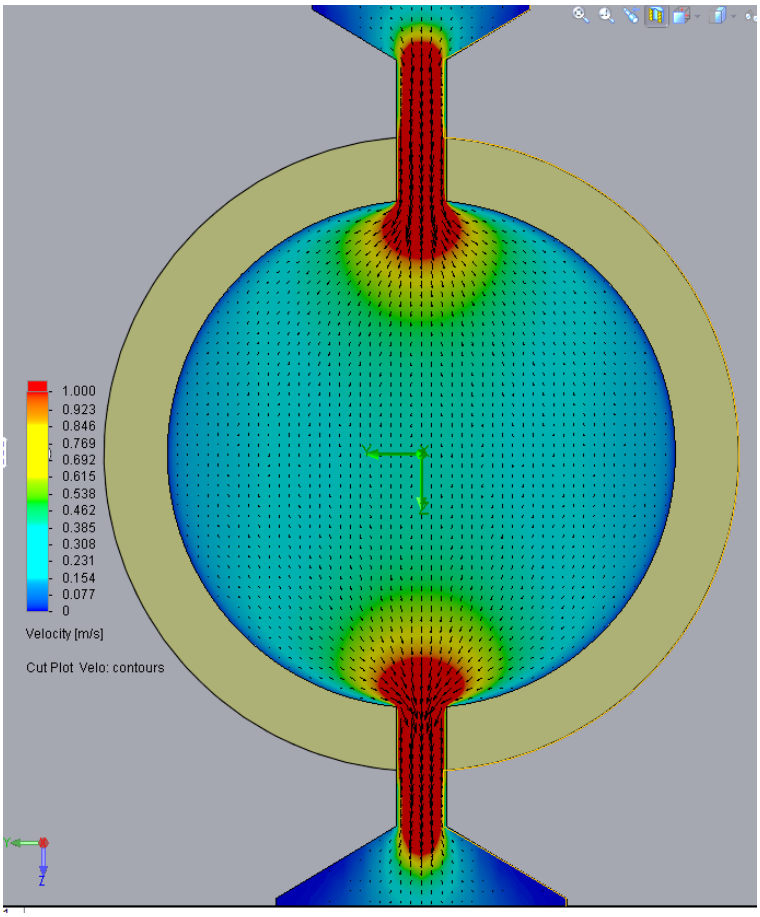

Figure 15. CFD simulation of sensor fluidic structure displaying the flowing velocity of the lubricant normalized to 1 m/s.

However, even if all particles are moving at the same velocity, the effect of the image capture distortion does not affect large and small particles alike. Large particles, even with a small distortion, will be detectable by the machine vision algorithms and there is no significant impact, being the real particle size very close to the size of the object detected. However, as the particle size gets smaller, the effects of the distortion are more pronounced, impacting both on the size and on its apparent shape, even making the smallest particles non-perceptible for the detection algorithms, as it can be observed in the example displayed in Figure 16.

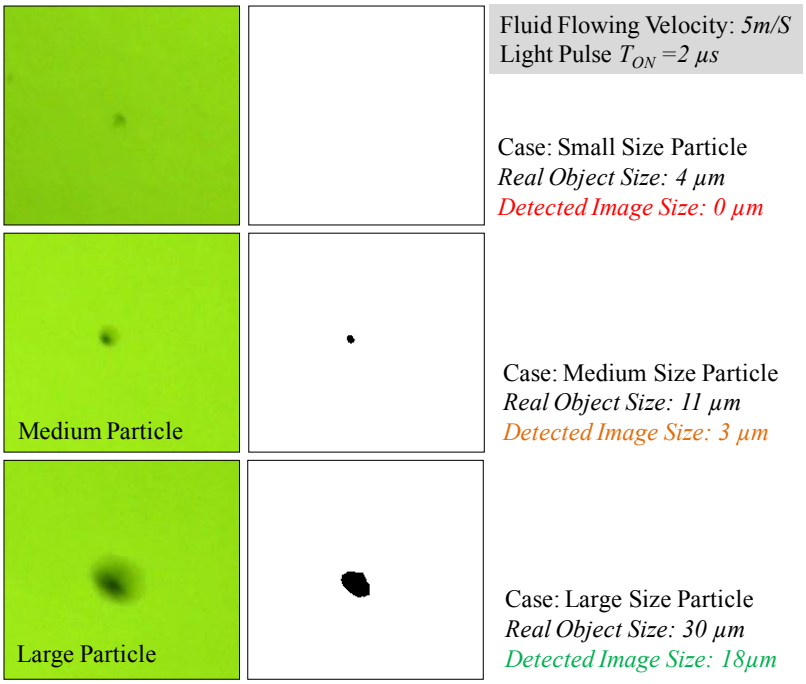

Figure 16. Impact of the object distortion (images on the right column) on its recognition through machine vision depending on its original size (images on the left column) for a given flowing and illumination conditions.

In this situation, a criterion has been defined to determine which percentage of distortion generates a fatal impact for the particle detection. Considering for example that distortion will cause a bad detection if 50% of the area of the object is affected, the Table 2 shows the maximum duration of the stroboscopic light pulse for different object sizes (largest dimension) and velocity of the fluid, calculated as:

$$\text{Max. Acceptable Distortion } (\mu\text{m}) = \text{Particle Size } (\mu\text{m}) \times 0.5 \quad (7)$$

$$\text{Max. Acceptable Time Lapse}(\mu\text{s}) = \frac{\text{Max. Acceptable Distortion } (\mu\text{m})}{\text{Flow Velocity } \left(\frac{\text{m}}{\text{s}}\right)} \quad (8)$$

Table 2. Maximum Time Lapse for Illuminating a Moving Particles.

Particle Size	**Small ~4 μM**	**Medium ~10 μM**	**Large ~20 μm**
Maximum Acceptable Distortion (50% Blur)	**2 μm**	**5 μm**	**10 μm**
Flow Velocity	**Maximum Acceptable Time Lapse**		
	Small	**Medium**	**Large**
1.5 (m/S)	1.3 μs	3.3 μs	6.6 μs
3 (m/S)	600 ns	1.6 μs	3.3 μs
11 (m/S)	180 ns	450 ns	900 ns
22 (m/S)	90 ns	230 ns	450ns

The time lapse limits the interval of time that a particle of a certain size could be moving without generating a distortion that would impact on its later recognition. Therefore, this interval defines the maximum allowed pulse duration, T_{ON}, for the stroboscopic lighting system.

With such a little time (e.g., 500 ns < T_{ON} < 4 μs) for illuminating the fluid sample, it is straightforward to conclude that a high-power light source will be required for generating a decent signal level at the detector; moreover considering the current responsivity or sensitivity of

industrial CMOS with 2.2 μm^2 pixel sizes is approximately 1 to 2 V/Lux-s (e.g., MT9P006 sensor features 1.76 V/Lux-s and the AR0330 1.9 V/Lux-s at λ = 550 nm). If generating a mid-scale intensity value at each pixel of the CMOS is set as the design objective, the light intensity budget calculation across the system could be approximately described with the following equations and considerations:

$$V_{PIXEL\ mid-scale} = 0.5 \times V_{ADC-PIXEL} = 0.5\ \times 2.4\ V = 1.4\ V \tag{9}$$

$$V_{PIXEL\ mid-scale} = R\left(\frac{V}{Lux{\cdot}s}\right) \times I_{PIXEL\ mid-scale}(Lux) \times T_{ON}(s) \tag{10}$$

$$1.4\ V = 1.76\left(\frac{V}{Lux{\cdot}\ sec}\right) \times I_{PIXEL\ mid-scale}(Lux)4{\cdot}10^{-6}(s) \tag{11}$$

$$I_{PIXEL\ mid-scale} = 0.2{\cdot}10^{6}(Lux) \tag{12}$$

Therefore, sufficient light energy needs to be provided by the system to allow that light flux getting to each pixel. The diagram depicted in the Figure 8, describes the different main considerations for the light power budget required for the current application as the light absorption happening at the sample, free space losses and the light filtering occurring at the pinhole.

Considering that the absorptions across the free space (FSPL) and at the cuvette walls are both negligible, then, the most important factors for the light intensity losses are the absorption happening at the fluid sample and the light filtering at the pinhole. Friss Formula, which describes free space power losses as FSPL = $(4\pi \times D/\lambda)^2$, allows us to demonstrate the assumption of FSPL~0, being D~Z_1~0.01 m or D~Z_2~0.001 m. In addition, the high transmission of the quartz (above %90) across the visible light spectrum [41], demonstrates the low impact of the glass disks in the light intensity budget. Therefore, we assume that $I_{pinhole}$~I_0 and I_1~I_{PIXEL}.

The absorption of the light crossing through the sample fluid is defined by the Lambert-Beer law, which describes an exponential relation between the light entering the sample (I_0) and the light getting across it (I_1) as $I_1 = I_0 \times 10^{-\varepsilon \ell c} = I_0 \times 10^{-A}$, whereas ε is the attenuation coefficient; c is the amount concentration of the absorbent; and ℓ is the path length of the beam of light through the fluid sample; and their product represents the absorptivity (A) happening at the sample. A value of A = 0.5 is taken as an average absorptivity of used lubricant oil at λ_0 = 580 nm for 0.5 mm path length [42,43], accordingly, the incoming light power will be lowered in a factor of: $10^{-A} = 10^{-0.5} = 0.316$. Therefore:

$$I_{PIXEL}\ = 0.316 \times I_{pinhole}(Lux) \tag{13}$$

and from Equation (12):

$$I_{pinhole\ mid-scale}\ = \frac{I_{PIXEL\ mid-scale}(Lux)}{0.316}\ =\ 0.633{\cdot}10^{6}(Lux) \tag{14}$$

At this point, the I_{LED} to $I_{pinhole}$ relation needs to be defined to calculate the minimum light power that needs to be generated by the illumination solution to deliver an image on the camera sensor with decent brightness. As the aperture could be considered as an spatial filter that blocks a significant portion of the emitted light flux, it is straightforward to correlate the light power transmitted through the pinhole with the area of the aperture ($I_{pinhole} \propto D_{pinhole}$).

Based on the output from ZEMAX simulation (see Figure 17), a set of six LEDs have been validated for illuminating the pinhole from a distance of ~5 mm within a polished aluminum case. The white LEDs chosen offer a light flux of 178 lumens/W (9 W maximum) at 120° viewing angle. This means, that at a 5 mm distance, the illumination system, per each LED, is able to generate approximately 2,266,000 Lux/W spread following a Gaussian distribution in an area of 235 mm^2 right before the pinhole. However, only a minimal proportion of this light flux will get across the aperture, and could be described as:

$$I_{source} = 2,260,000\left(\frac{LUX}{W}\right)\cdot\frac{1}{235\ mm^2}\cdot W_{LED}(W) \quad (15)$$

$$I_{pinhole} = I_{source} \times A_{pinhole} = 2,260,000\left(\frac{LUX}{W}\right)\cdot\frac{1}{235\ mm^2}\cdot W_{LED}(W).\pi.\frac{D_{pinhole}(mm^2)}{2} \quad (16)$$

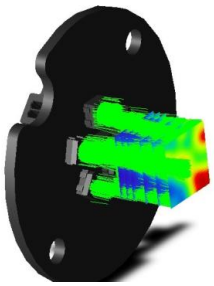

Figure 17. Output example of the ZEMAX simulation of the light source.

Combining Equation (16) with Equation (13), I_{PIXEL} is defined in dependence with the polarization of the LED and with the diameter of the pinhole:

$$I_{PIXEL} = 0.316 \times I_{pinhole} = 47,000\left(\frac{LUX}{W\ .mm^2}\right)\cdot D_{pinhole}(mm^2)\cdot W_{LED}(W) \quad (17)$$

Then, for each of candidate pinholes, different LED number and polarization currents are needed for achieving the targeted mid-scale intensity level of $I_{PIXEL} = 0.2 \times 10^6$ Lux. If the saturation current is reached, and considering a fixed number of LEDs (a circular array of 6 LEDs have been arranged for the current setting), we would be forced to increase the stroboscopic pulse time above the cited 4 µs.

As mentioned, due to the pinhole filtering, only a small proportion of this light beam power will be transmitted to the sample. Table 3 summarizes the expected light power at the pixel plane considering all the assumptions and design parameters described so far. The data displayed concludes that the only feasible pinhole diameter is the 500 µm for the target fluid absorptivity and fluid flowing velocity, because it is the only setting that enables achieving the requested design objective of I_{PIXEL} of 0.2×10^6.

Table 3. Calculations of the light budget within the sensor for different pinhole diameters and different LED polarization power. Assuming that the six LEDs are on, the different light flux intensities at the pixel are presented.

$D_{pinhole}$	$A_{pinhole}$	Pixel Polarization (W)				
		1 (W)	3(W)	5(W)	7(W)	9(W)
		I_{PIXEL} (Lux)				
0.5 mm	0.19 (mm^2)	53,580	160,740	267,900	375,060	482,220
0.2 mm	0.03 (mm^2)	8460	25,380	42,300	59,220	76,140
0.05 mm	0.001 (mm^2)	282	846	1410	1974	2538

A custom circuit has been designed for controlling the pulse length and intensity of the LEDs using an algorithm that is executed on the CPU. The activation time (T_{ON}) and polarization current (I_0) of the LEDs for achieving the frame intensity set point is computed for every new frame. As depicted in the Figure 18, a capacitors array is used for storing the energy required for driving the LEDs. This setup allows meeting the requirement of a very fast (T_{RISE} < 10% T_{ON}) pulse switching times even for very short pulses, which is a critical design challenge, as described in [44,45].

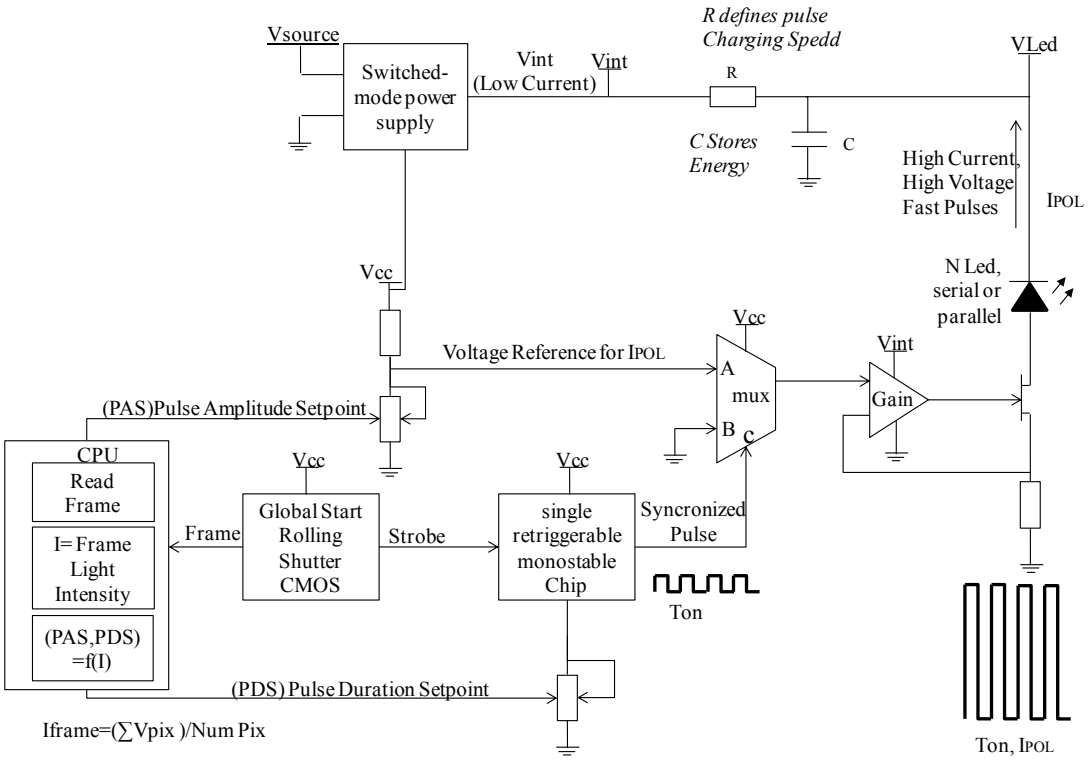

Figure 18. Block diagram of the stroboscopic light source of the sensor. Including the pulse length and amplitude control and the synchronization (strobe) control from the CMOS for triggering the pulse start.

4. Results and Discussion

This section describes the optical performance achieved with the sensor prototype sampling real used lubricant samples. Additionally, the performance of the machine vision algorithms is evaluated in terms of particle counting capabilities and algorithm execution time on different embedded CPU architectures.

4.1. Optical Results

The objective of the first test was determining the particle detection limit in the sensor, the FOV and the DOF. For this purpose, the glass disks were marked with ink in their faces in contact with the fluid, being these marks previously measured in the microscope as reference. Then, sensor was assembled with these disk and particles were fed into the measurement cell. Sample images of this experiment are found in Figures 19 and 20.

The detection limit was calculated using the scattering diameter for each sensor configuration, which, as described in Section 2.2, is theoretically defined as $d_{scat} = D_{pinhole}\, Z_2/Z_1$. The resolution has been defined calculating the µm/pix ratio using the real dimensions of the blue marks against the number of pixels. For the DOF, the glass in the face opposite to the first glass disk is also marked (see the images of the next experiment in Figures 21–24). Therefore, introducing the values of the dimensions used in the sensor we get the following:

$$d_{scat\ GORILLA} = D_{pinhole}\frac{Z_2}{Z_1} = 500\ \mu m\frac{1.1 + 0.2\ mm}{10\ mm} = 65\ \mu m \quad (18)$$

$$d_{scat\ BK7} = D_{pinhole}\frac{Z_2}{Z_1} = 500\ \mu m\frac{0.2 + 0.2\ mm}{10\ mm} = 20\ \mu m \quad (19)$$

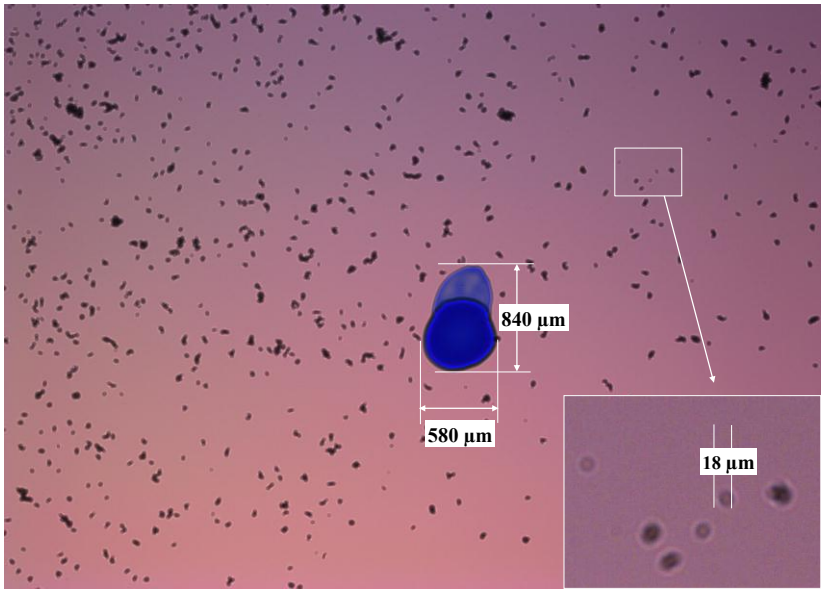

Figure 19. Sample image acquired with the sensor mounting the BK7 glass disk of 0.2 mm.

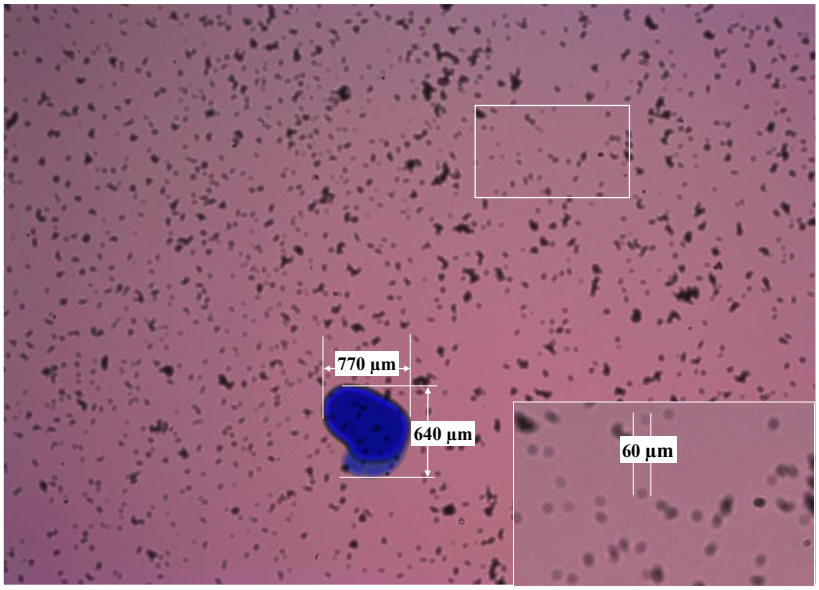

Figure 20. Sample image acquired with the sensor mounting the Gorilla glass disk of 1.1 mm.

These theoretical values match what it is observed in the sample images. The µm/pix ratio obtained in the case of the BK7 glass disk is ~2.5 µm/pix and for the Gorilla glass is 2.43 µm/pix. The blue mark dimensions in the Gorilla® glass were 770 × 640 µm and represent 307 × 282 pix in the image. On the other hand, marks in the BK7 alternative measure 580 × 840 µm and cover 238 × 357 pixel in the captured image. The FOV is calculated directly extrapolating the um/pix value to the CMOS resolution, Therefore, the FOV is covering approximately 6480 × 4860 μm^2 due to the ~2.5 µm/pix in the 2592 × 1944 pixel matrix.

After the initial performance measurements, the sensor was plugged into the lubricant test bench. There, different fluid samples and different hydraulic settings were applied, obtaining the images displayed in the Figures 21–24. As in the previous example, Gorilla® glass and BK7 glass sensor configurations have been used and three different lubricant samples from real machines have been feed into them. These samples due to their original formulation and because of the different

conditions in use (time of use, working temperatures, type of machine, mechanical stress, etc.) present different absorptivity ranges, which impacts in the frame intensity, and in the case of very opaque fluids, the sample is hardly illuminated in a homogenous way. The sample types are Renolyn (Fuchs, Staffordshire, UK), Meropa (Texaco, San Ramon, CA, USA) and Optigear Castrol and they present different contaminations (bubbles, fibers, particles, varnishes), which will be later identified through machine vision processing. Note that in this case, the sensor glass disks have been marked to help identifying the full DOF; the red ink mark is located in the first glass disk and the blue one in the second glass disk.

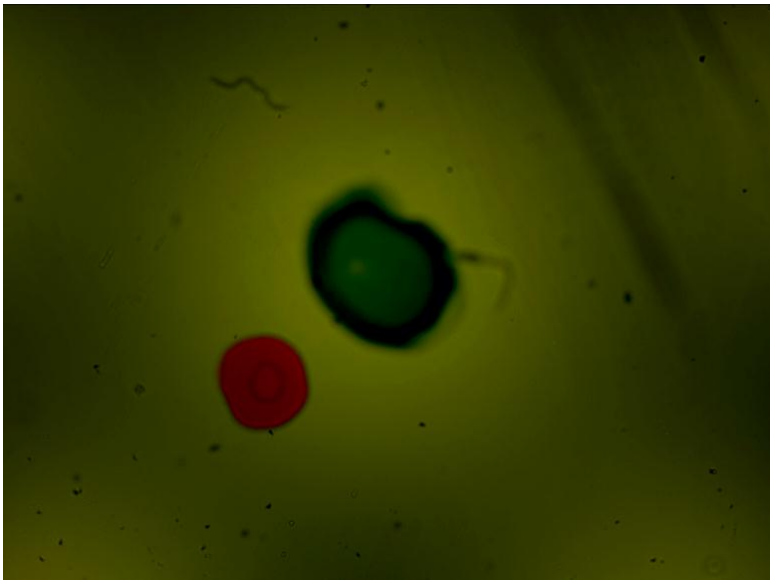

Figure 21. In this case the sensor mounts the Gorilla® glass. Sample is Castrol Optigear (opaque sample) and the flow speed is approximately 1.0 L/min. Different particles and fibers are present in the image.

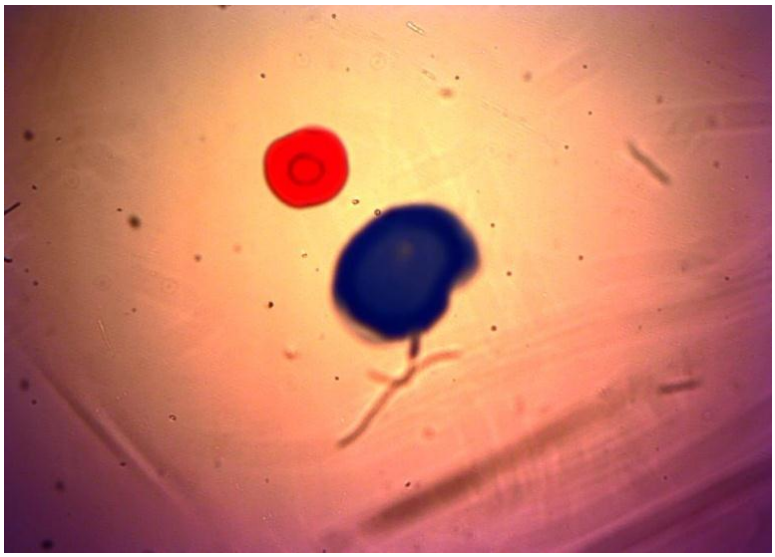

Figure 22. Sensor mounting the Gorilla® glass disk. Sample is Texaco Meropa (medium absorptivity) and the flow speed is approximately 1.5 L/min. Asides, fibers and particles, non-homogeneity of the sample is evident, which may indicate the presence of other contaminants as varnishes.

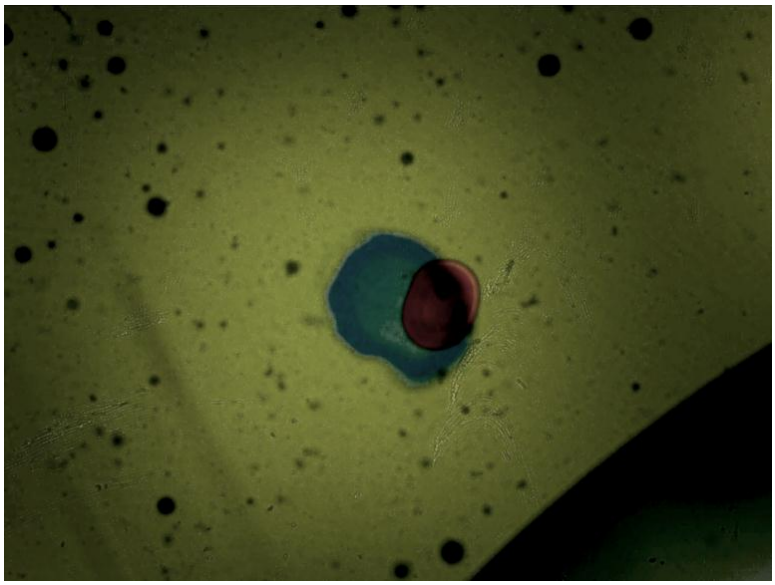

Figure 23. In this case the sensor is mounting the BK7 Glass disk of 0.2 mm. Sample is Castrol Optigear and the flow speed is approximately 1.0 L/min. Different particles and fibers are present in the image as well as a part of a big bubble in the bottom right corner.

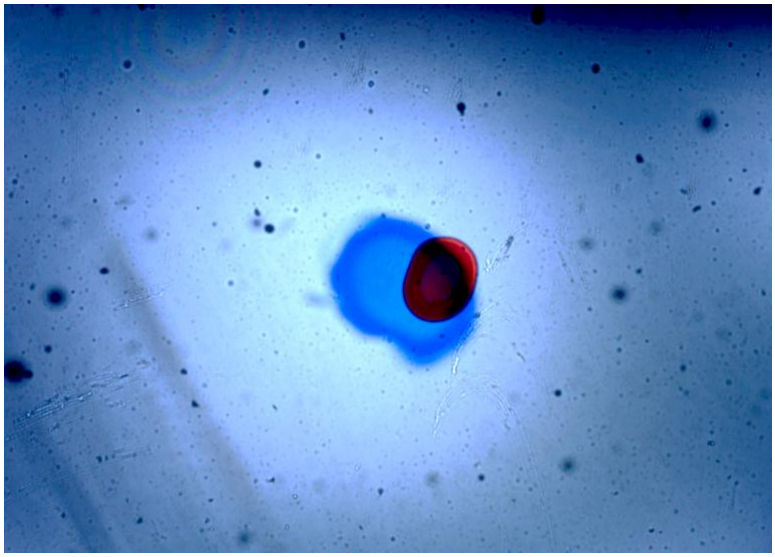

Figure 24. Sensor mounting the BK7 glass. Sample is Fuch Renolyn (clear fluid) and the flowing speed is approximately 1.5 L/min. Different particles and fibers are present in the image.

Table 4 summarizes a comparison between the proposed sensor, in the BK7 and Gorilla Glass configurations, with some of the most widely used commercial wear particle in-line detection systems. Notice that the sensibility to the minimum particle size of the lens-less sensor remains above the target 4 µm because no hologram reconstruction has been applied so far. According to the literature review, the use of these advanced algorithms would allow to increase the sensibility up to 1 µm as described in Section 1.2.

Table 4. Particle detection and classification execution time using the different CPUs architectures.

Sensor	Working Principle	Particle Type	Flow	Max. Pressure	Min. Particle	Shape Recognition
Parker FG-K19567-KW	Inductive	Only Metallic	<1.9 m/s	<20 bar	>40 µm	No
Gastops MetalScan MS4000	Inductive	Only Metallic	16.2 L/min	<35 bar	>65 µm	No
Atten2 OilWear S100	Direct Imaging	Metallic and non-metallic	Static Sample	<20 bar	>4 µm	Yes
CCJensen OCM 15	Light Extinction	Metallic and non-metallic	Static Sample	Built-in Pressure Reduction-Pumping	>4 µm	No
Lens-Less Sensor (BK7 glass)	Direct Imaging	Metallic and non-metallic	<3 m/s	<0.01 bar	>18 µm	Potential
Lens-Less Sensor (Gorilla glass)	Direct Imaging	Metallic and non-metallic	<3 m/s	<10 bar	>60 µm	Potential

4.2. Particle detection through Machine Vision Image Processing

After evaluating the optical performance of the sensor, in order to validate the measurement principle, particle counting algorithms should be validated in real samples monitoring. Therefore, a set of machine vision functions are executed to preprocess the image, segmentate the regions of interest, and identify and classify the objects presents on each new frame. Basically, the machine vision operations include a dynamic background compensation for eliminating the static particles or mitigating the effects of the soiling occurring at the glass disks. Then, a set of image conditioning stages are applied, such as a high pass filter and a binarization based on a variance threshold. This binary image is processed and the regions of interest are segmentated and the different features are extracted. Finally, based on these features, the bubbles and particles are separated and they are classified by their size according to the ISO standards. Halcon Embedded Machine Vision library from MVTEC Company (Munich, Germany) has been used for programming the different machine vision functions.

The execution time is a critical feature for the sensor, as it is also correlated with the ability of measuring more fluid volume per unit of time. Machine vision algorithms for high resolution images (e.g., 5 Mpix) are computationally intensive operation and, indeed, its execution speed depends on the computational power available at the embedded processor. Even if the CPU power is continuously increasing unstoppably, the results reached several ms per frame, which may be a limitation in latency critical applications. However, the current standardized structure of the embedded CPUs allows migrating the same piece of code to different processors, so the processing speed performance can be easily tested in current and future microprocessors. Therefore, depending on the real time requirements of each use case, the response time of the system could be accommodated choosing the right embedded platform.

For instance, the i.MX6 processor (Cortex A9 structured) offers the possibility of acquiring a CPU 1, 2 or 4 cores. The execution times of the algorithms have been measured in different i.MX6 CPUs and in the new family of ARM Cortex A53 devices, the Qualcomm Snapdragon 410, and are summarized in Table 5. Note that the object number within the image also impacts in the execution time, just because the decision algorithms need to be applied to a larger number of elements.

Figure 25 shows the results of applying the aforementioned algorithms to the original frame depicted in Figure 21. The particles are detected and the result is overlaid in the image. Result data outputted by the algorithms is summarized in Table 6. The absolute object measurement values are based on a prefixed parameter determining the µm/pixel proportion, which, for the example below is set to 2.5 µm/pix.

Table 5. Particle detection and classification execution time using the different CPUs architectures.

CPU	ARM Family	Core Number	Core Bus	Core Freq.	Objects in the Image			
					0	30	68	92
					Execution Time (ms)			
i.MX6 Solo	Cortex A9	1	32 bit	1 GHz	608	865	1133	1315
i.MX6 Dual	Cortex A9	2	32 bit	1 GHz	456	648.75	849.75	986.25
i.MX6 Quad	Cortex A9	4	32 bit	1 GHz	413.44	588,2	770.44	894.2
SD 410	Cortex A53	4	64 bit	1 GHz	322.24	458.45	600.49	696.95

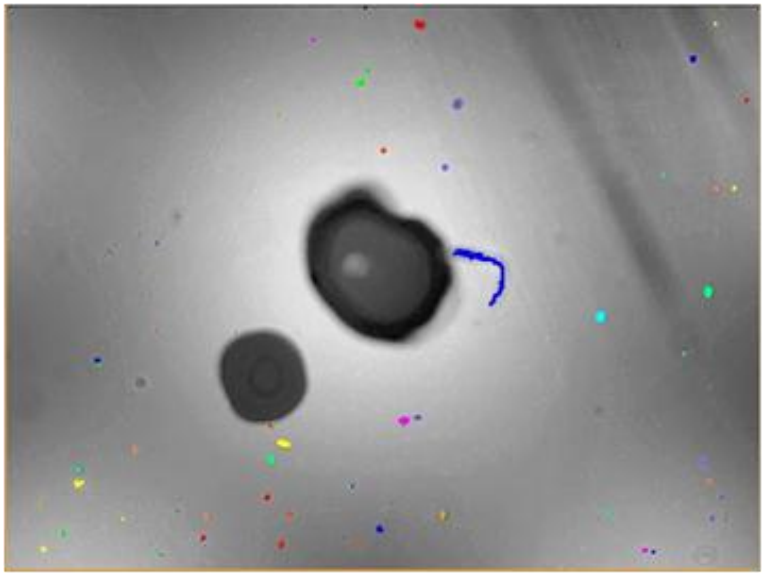

Figure 25. Result of processing the image of the Figure 21 with the particle detection algorithms. The processed image overlays the detected particles.

Table 6. Particle classification results according to ISO 4406 size groups for the sample image of Figure 21.

Particle Size Group	Elements Detected
>70 µm and <400 µm	1
>38 µm and <70 µm	13
>21 µm and <38 µm	29
>14 µm and <21 µm	7
>6 µm and <14 µm	22
>4 µm and <6 µm	5

5. Conclusions

In this manuscript, we have presented a detailed study on the performance of a photonic micro-sensor aimed at in-line analysis of wear debris focused on the use case of industrial fluidics monitoring. The integration of lens-less microscopy and stroboscopic illumination has been accomplished to answer the challenging operation conditions in terms of sample opacity, sample flowing velocity and working fluid pressure. Specifically, we have validated the proof-of-concept analyzing the presence of wear particles in flowing lube oils based on the direct use of images acquired with a stroboscopic and incoherent lighting lens-less setup. The system settings have been optimized in a custom test-bench, achieving as preliminary results an optical performance of FOV = 5.5 mm by 4.1 mm, DOF = 500 µm (for ~70 µm objects) and 2.5 µm/pix resolution, requiring stroboscopic light pulses of about 4 µs

and 6 A for dealing with fluid flow rate around 1–3 L/min. These optical settings have been transferred into the sensor design specifications, which, along with specific electronic design (including CMOS detector, stroboscopic light control, embedded CPU and communications) and the customized mechanical and micro fluidic solution, have been integrated into a compact 35 × 45 × 45 mm wear debris sensor with a really cost effective bill of materials. Additionally, examples of real lubricant samples have been described, including their particle counting and classification, as well as the execution times for the machine vision algorithms, running on reference embedded platforms such as the Cortex-A9 or the Cortex-A53. Migration from the direct use of the shadow images to the holographic reconstruction techniques for enhancing the sensor resolution towards the sub-pixel sampling has been identified as the most promising future work, as this is the way for achieving much lower detection limits for particles below 1 µm. The main advantages achieved with this proposed sensor include the cost effectiveness, compatibility with metallic and non-metallic particles, sampling volume and resolution and the potential particles shape recognition. Additionally, the compact size of the sensor allows its integration in larger hydraulic components as filters, valves, pressure sensors, etc. enabling the development of true added-value solutions in the field of industrial fluidics. Asides the industrial market, other applications, as the pharmaceutical membrane filtration systems, could benefit from the compact size and high sensibility of the proposed solution for continuously monitoring the performance of the purification and separation processes. Sampling a large fluid volume in continuous fluid flow with a decent 2D spatial resolution, this photonic micro sensor could provide a powerful tool for in-line wear debris monitoring at low resource settings.

Acknowledgments: This work has been funded in part by the Fondo Europeo de Desarrollo Regional (FEDER); by the Ministerio de Economía y Competitividad under project TEC2015-638263-C03-1-R; by the Gobierno Vasco/Eusko Jaurlaritza under projects IT933-16 and ELKARTEK (KK-2016/0030 and KK-2016/0059).

Author Contributions: J.M. conceived the sensor system, the test bench and stroboscopic illumination, J.Z. validated the theoretical approach, E.G. contribute to the use case definition and validation. J.M. wrote the paper.

Conflicts of Interest: The authors declare no conflict of interest.

References

1. Kumar, M.; Mukherjee, P.S.; Misra, N.M. Advancement and current status of wear debris analysis for machine condition monitoring: A review. *Ind. Lubr. Tribol.* **2013**, *65*, 3–11. [CrossRef]
2. Rabinowicz, E. *Friction and Wear of Materials*, 2nd ed.; John Wiley & Sons: Hoboken, NJ, USA, 1995; pp. 6–7.
3. Peng, Z.; Kessissoglou, N.J.; Cox, M. A study of the effect of contaminant particles in lubricants using wear debris and vibration condition monitoring techniques. *Wear* **2005**, *258*, 1651–1662. [CrossRef]
4. Johnson, M. Past, Present and Future of Oil Analysis: An Expert Panel Discussion on the Future of Oil Analysis. *Tribol. Lubr. Trans.* **2007**, *64*, 32–39.
5. Johnson, M. Machine Lubrication Best Practices Volume 28: Oil Analysis Program Development: On Site Analysis and Sensory Inspections. *Tribol. Lubr. Trans.* **2010**, *28*, 18–23.
6. Poley, J. Metallic Wear Debris Sensors: Promising Developments in Failure Prevention for Wind Turbine Gearsets and Similar Components. *Proc. SPIE* **2011**, *7979*, 79790I.
7. Zhu, J.; Yoon, J.M.; He, D.; Bechhoefer, E. Online particle-contaminated lubrication oil condition monitoring and remaining useful life prediction for wind turbines. *Wind Energy* **2014**, *18*, 1131–1149. [CrossRef]
8. Gorritxategi, E.; García-Arribas, A.; Aranzabe, A. Innovative On-Line Oil Sensor Technologies for the Condition Monitoring of Wind Turbines. *Key Eng. Mater.* **2015**, *644*, 53–56. [CrossRef]
9. Dempsey, P.J. *Gear Damage Detection Using Oil Debris Analysis*; NASA TM 210936; NASA Glenn Research Center: Cleveland, OH, USA, 2001.
10. Miller, J.L.; Kitaljevich, D. In-line oil debris monitor for aircraft engine condition assessment. In Proceedings of the 2000 IEEE Aerospace Conference Proceedings, Big Sky, MT, USA, 22–25 March 2000; pp. 49–56.
11. Coronado, D.; Kupferschmidt, C. Assessment and Validation of Oil Sensor Systems for On-line Oil Condition Monitoring of Wind Turbine Gearboxes. *Procedia Technol.* **2014**, *15*, 747–754. [CrossRef]
12. Tavner, P.J. *Offshore Wind Turbines-Reliability, Availability and Maintenance*; Institution of Engineering and Technology Press: London, UK, 2012; pp. 119–121.

13. Link, H.; Lacava, W.; Van Dam, J.; Mcniff, B. *Gearbox Reliability Collaborative Project Report: Findings from Phase 1 and Phase 2 Testing*; National Renewable Energy Laboratory (NREL): Golden, CO, USA, 2011.
14. Coronado, D.; Bustamante, A.; Kupferschmidt, C. Oil-sensors test bench—An approach to validate oil condition monitoring systems for wind turbine applications. In Proceedings of the OilDoc Conference and Exhibition, Rosenheim, Germany, 27–29 January 2015; pp. 27–29.
15. Pall Corporation. Industrial Manufacturing Pocket Book. Pall Corporation: USA. Available online: https://www.pall.com/pdfs/Industrial-Manufacturing/POCKET_BOOK_EN_Standard.pdf (accessed on 20 January 2017).
16. Han, L.; Hong, W.; Wang, S. The key points of inductive wear debris sensor. In Proceedings of the International Conference on Fluid Power and Mechatronics, Beijing, China, 17–20 August 2011; pp. 809–815.
17. Crabtree, C.J. *Survey of Commercially Available Condition Monitoring Systems for Wind Turbines*; Durham University Press: Durham, NC, USA, 2010.
18. Peng, L.C.; Liang, M. Enhancement of the wear particle monitoring capability of oil debris sensors using a maximal overlap discrete wavelet transform with optimal decomposition depth. *Sensors* **2014**, *14*, 6207–6228.
19. Hamilton, A.; Quail, F. Detailed state of the art review for the different online/inline oil analysis techniques in context of wind turbine gearboxes. *ASME J. Tribol.* **2011**, *133*, 044001–044019. [CrossRef]
20. Reintjes, J.F.; Howard, P.L. Fluid Sampler Utilizing Optical Near-Field Imaging. US Patent US5572320 A, 5 November 1996.
21. Kong, H. Method and Apparatus for Monitoring Oil Deterioration in Real Time. US Patent Application 20080024761 A, 3 November 2008.
22. Kolp, J.P.; Sebok, T.J.; Russell, D.E. Tribological Debris Analysis System. US Patent US 7385694 B, 28 March 2008.
23. Mabe, J.; Gorritxategi, E. System and Method for Monitoring a Fluid. US Patent US9341612 B, 17 May 2013.
24. Kim, S.B.; Bae, H.; Koo, K.; Dokmeci, M.R.; Ozcan, A.; Khademhosseini, A. Lens-Free Imaging for Biological Applications. *J. Lab. Autom.* **2012**, *17*, 43–49. [CrossRef] [PubMed]
25. Stahl, R.; Vanmeerbeeck, G.; Lafruit, G.; Huys, R.; Reumers, V.; Lambrechts, A.; Liao, C.-K.; Hsiao, C.-C.; Yashiro, M.; Takemoto, M.; et al. Lens-free digital in-line holographic imaging for wide field-of-view, high-resolution and real-time monitoring of complex microscopic objects. *Proc. SPIE* **2014**, *8947*, 342–348.
26. Gabor, D. A new microscopic principle. *Nature* **1948**, *161*, 777–778. [CrossRef] [PubMed]
27. Han, Y.; Gu, Y.; Zhang, A.C.; Lo, Y.-H. Review: imaging technologies for flow cytometry. *Lab. Chip R. Soc. Chem.* **2016**, *16*, 4639–4647.
28. Lee, H.; Xu, H.; Koh, D.; Nyayapathi, N.; Oh, K.W. Various on-chip sensors with microfluidics for biological applications. *Sensors* **2014**, *14*, 17008–17036. [CrossRef] [PubMed]
29. Göröcs, Z.; Ozcan, A. On-Chip Biomedical Imaging. *IEEE Rev. Biomed. Eng.* **2013**, *6*, 29–46. [CrossRef] [PubMed]
30. Seo, S.; Isikman, S.O.; Sencan, I.; Mudanyali, O.; Su, T.-W.; Bishara, W.; Ozcan, A. High-throughput lens-free blood analysis on a chip. *Anal. Chem.* **2010**, *82*, 4621–4627. [CrossRef] [PubMed]
31. Isikman, S.O.; Bishara, W.; Mavandadi, S.; Yu, F.W.; Feng, S.; Lau, R.; Ozcan, A. Lens-free optical tomographic microscope with a large imaging volume on a chip. *Proc. Natl. Acad. Sci. USA* **2011**, *108*, 7296–7301. [CrossRef] [PubMed]
32. Stahl, R.; Vercruysse, D.; Claes, T.; Vanmeerbeeck, G.; Mukund, V.; Jansen, R.; Song, J.; Hoffman, L.; Rottenberg, X.; Lambrechts, A.; et al. Microscope-on-chip: Combining lens-free microscopy with integrated photonics. *Proc. SPIE* **2015**, *9328*. [CrossRef]
33. Mudanyali, O.; Tseng, D.; Oh, C.; Isikman, S.O.; Sencan, I.; Bishara, W.; Ozcan, A. Compact, light-weight and cost-effective microscope based on Lensless incoherent holography for telemedicine applications. *Lab Chip* **2010**, *10*, 1417–1428. [CrossRef] [PubMed]
34. Bishara, W.; Su, T.-W.; Coskun, A.F.; Ozcan, A. Lens free on-chip microscopy over a wide field-of-view using pixel super-resolution. *Opt. Express* **2010**, *18*, 11181–11191. [CrossRef] [PubMed]
35. Mabe, J.; Zubia, J.; Gorritxategi, E. Lens-free imaging-based low-cost microsensor for in-line wear debris detection in lube oils. *Proc. SPIE* **2017**, *10110*. [CrossRef]
36. Behnam, R.; Fox, E. The Evolution of CMOS Imaging Technology. White Paper. 2011. Available online: https://www.teledynedalsa.com/public/mv/appnotes/EvolutionofCMOS_Technology_wp.pdf (accessed on 20 January 2017).

37. Peng, Y.; Wu, T.; Wang, S.; Kwok, N.; Peng, Z. Motion-Blurred Particle Image Restoration for On-Line Wear Monitoring. *Sensors* **2015**, *15*, 8173–8191. [CrossRef] [PubMed]
38. Linkemann, J.; Weber, B. Global Shutter, Rolling Shutter—Functionality and Characteristics of Two Exposure Methods (Shutter Variants). White Paper. 2014. Available online: http://s.baslerweb.com/dist/live/news/data/2/7/8/9/5/BAS1401_White_Paper_Rolling-Shutter_en.pdf (accessed on 20 January 2017).
39. Gamal, A.E.; Eltoukhy, H. CMOS image sensors. *IEEE Circuits Devices Mag.* **2005**, *21*, 6–20. [CrossRef]
40. Seward, G.H. *Basic Physical Optics, Fundamentals of Photonic*; SPIE Digital Library: Bellingham, WA, USA, 2008; pp. 35–51.
41. Schilowitz, A.M.; Szobota, J.S.; Vann, W.D. Method for On-Line Monitoring of Lubricating Oil Using Light in the Visible and Near IR Spectra. US Patent US 7172903 B, 6 February 2003.
42. Hellma Analytics. Certificate of High-Precision Cells. Hellma GmbH & Co, Müllheim. Available online: http//www.hellma-analytics.com (accessed on 20 January 2017).
43. Villar, A. Chemometric Methods Applied to the Optimization of Calibration of Vis-Nir Sensor Systems for Real Time Fluids Monitoring. Ph.D. Thesis, University of the Basque Country, Spain, 2014; pp. 50–55.
44. Fu, G. Light-Emitting Diodes Flash Light for Inspecting Printing Image and Its Driving Circuit. China Patent CN 2899386, 9 May 2007.
45. Chung, X.-C. Controlling System and Method of Moving Object Detection Light Source to Realize a Variety of Illuminations. Taiwan Patent TW 201547325, 5 June 2014.

Food Chemistry 221 (2017) 100–106

Contents lists available at ScienceDirect

Food Chemistry

journal homepage: www.elsevier.com/locate/foodchem

Cider fermentation process monitoring by Vis-NIR sensor system and chemometrics

Alberto Villar [a,*], Julen Vadillo [a], Jose I. Santos [b], Eneko Gorritxategi [c], Jon Mabe [d], Aitor Arnaiz [e], Luis A. Fernández [f]

[a] Surface Chemistry Unit, IK4-Tekniker, Iñaki Goenaga 5, 20600 Eibar, Spain
[b] SGIKER-UPV, University of the Basque Country, Tolosa Hiribidea 7, 20018 Donosti, Spain
[c] Atten2 Advanced Monitoring Technologies, Iñaki Goenaga 5, 20600 Eibar, Spain
[d] Electronics and Comms. Unit, IK4-Tekniker, Iñaki Goenaga 5, 20600 Eibar, Spain
[e] Intelligent Information Systems Unit, IK4-Tekniker, Iñaki Goenaga 5, 20600 Eibar, Spain
[f] Department of Analytical Chemistry, University of the Basque Country, 48080 Bilbao, Spain

ARTICLE INFO

Article history:
Received 25 April 2016
Received in revised form 11 October 2016
Accepted 11 October 2016
Available online 14 October 2016

Keywords:
Visible-Near Infrared
Cider
Fermentation
Chemometrics
Sensor system

ABSTRACT

Optimization of a multivariate calibration process has been undertaken for a Visible-Near Infrared (400–1100 nm) sensor system, applied in the monitoring of the fermentation process of the cider produced in the Basque Country (Spain). The main parameters that were monitored included alcoholic proof, L-lactic acid content, glucose + fructose and acetic acid content. The multivariate calibration was carried out using a combination of different variable selection techniques and the most suitable pre-processing strategies were selected based on the spectra characteristics obtained by the sensor system. The variable selection techniques studied in this work include Martens Uncertainty test, interval Partial Least Square Regression (iPLS) and Genetic Algorithm (GA). This procedure arises from the need to improve the calibration models prediction ability for cider monitoring.

1. Introduction

Asturias and the Basque Country are the main cider production areas in Spain. The cider production in the Basque Country (northern Spain) has doubled in the last 25 years with a total production of 10 millions liters per year, becoming an important economic activity in the Basque country. The production process of cider in the Basque Country can be divided in the following stages: reception, cleaning, crushing, pressing, decanting, alcoholic and malolactic fermentation, racking, maturation and bottling. (Del Campo, Santos, Berregi, & Munduate, 2005).

Apple collection begins in the early October. The apples are picked up directly from the soil in baskets or bags. Afterwards, apples are transported to the cider farmhouse where are stored in silos (reception). After that, apples are washed by a float system, followed by manual separation of the defective ones. Then, apples go through some pressurized water rotary drums to remove mud, leaves and other impurities (cleaning). Afterwards, apples are crushed obtaining the pulp, which is soaked for several hours (crushing). In the next stage (pressing), the apple juice is extracted in successive pressings. Yields between 50% and 70% are obtained depending on the varieties of apples used. Depending on the variety of apple, ripening vintage and pressing process, the composition of the juice is as follows: water (75–90%), sugars (9–18%), acids (0.1–1%), pectic substances (0.05–2%) and phenolic substances (0.02–0.6%). In addition, the apple juice contains small amounts of proteins, vitamins, minerals, enzymes and nitrogenous substances. The liquid that comes from the press is subject to clarification process by the sedimentation of the heavier particles (decanting).

Once the procedure described above is completed the most important stages of elaboration process take place: the alcoholic and malolactic fermentation processes. The quality of the cider mainly depends on apple juice compounds transformations, essentially acids and sugars, undergo during the fermentation process. The fermentation takes place in wooden, polyester or stainless steel casks at a controlled temperature of 10–16 °C. The entire process can take from 1 to 4 months. During alcoholic fermentation process, fructose and glucose are processed by the *Saccharomyces cerevisiae fermenting yeast* obtaining ethanol and carbonic acid as main products. The malolactic fermentation is performed by lactic

* Corresponding author.
E-mail address: alberto.villar@tekniker.es (A. Villar).

http://dx.doi.org/10.1016/j.foodchem.2016.10.045
0308-8146/

acid bacteria and involves the conversion of malic acid into lactic acid and carbon dioxide. During this fermentation process, the cider suffers important sensory changes. Bacterial transformation of malic acid into lactic acid produces a drink deacidification improving the cider's organoleptic characteristics. The malolactic fermentation also produces an aromatic modification caused by the formation of esters. After the fermentation processes, lees and microorganisms are removed from cider in order to ensure an adequate physical-chemical and microbiological stability of the cider (racking). Afterwards, the maturation of the cider takes place, a slow evolution process of the broth, which can last several months. This process is produced by the contact of the broth with its fine lees, increasing the aromatic strength of the final product. Finally, when the density of cider is less than 1.000 g/L, it is bottled without making any kind of filtration so that the product does not lose its carbonic gas. (Del Campo et al., 2003, 2005).

Unlike other food products, such as wine or milk, Vis-NIR spectroscopy has not been widely used for quality control in the cider industry. There are not too many articles about the application of Vis-NIR spectroscopy for cider quality monitoring. The examples found in the literature include the application of hyperspectral imaging reflectance and the measurement of CIELab colour parameters (Alonso-Salces et al., 2005; Chen & Liu, 2007; Dambergs, Kambouris, Francis, & Guishen, 2002; Mehl, Chen, Kin, & Chan, 2004; Queji, Wosiacki, Cordeiro, Peralta-Zamora, & Nagata, 2010). In the same way, there are few examples in the literature related with sensor systems for cider quality or fermentation process monitoring. James, Parry, and Jones (1987) developed an on-line sensor system based on headspace analysis, with electrochemical fuel cell sensor as detector, for the on-line determination of ethanol content during the alcoholic fermentation process. Bureau et al. (2002) developed an infrared glass fiber for in-situ sensing chemical and biochemical reactions. This sensor measures in the range of 1800–900 cm^{-1}, and it was applied to follow the fermentation process in cider fabrication and to detect and monitor a bacterial biofilm formation. Meyes, Blyth, Kyrolainen-Reay, Millington, and Lowe (1999) developed a holographic alcohol sensor based on a reflection hologram distributed through the volume of a cross-linked polyhydroxyethyl methacrylate film. The sensor was tested with different spirit beverages, including cider. Finally, Bleibaum et al. (2002) applied an electronic nose and tongue sensor to monitor the sensory quality parameters of cider. The research was focused on comparing the results obtained by a trained sensory panel with the results obtained by the ASTREE Liquid Taste Analyzer (electronic tongue) and the Prometheus (electronic nose sensor array and mass spectrometry) (Castillo et al., 2004).

The main goal of this work is to explain the multivariate calibration and validation process of Vis-NIR sensor system developed for the elaboration process monitoring of cider. Alcohol proof and glucose + fructose content are some of the main control parameters of cider. Meanwhile, L-lactic acid content can be used to monitor the malolactic fermentation process. On the other hand, acetic acid can be applied for volatile acidity monitoring and to prevent the generation of vinegar by pitting. Acetic acid may be generated due to the degradation of sugars present in the medium and by malolactic bacteria inducing a process called acetic acidification (acetic pitting). This work involves correlating the spectra obtained by the Vis-NIR sensor system with the cider quality parameters and explores the possibility of using variable selection techniques for the improvement of the calibration models performance. By means of this sensor system, the main manufacturing process of cider is intended to monitor: alcoholic/malolactic fermentation and maturation processes. The implementation of this sensor system would allow greater control of these processes and the possibility to take corrective actions in real time.

2. Materials

2.1. Vis-NIR sensor design

Previous Vis-NIR sensors prototypes were successfully employed by the authors for milk and marine diesel engine lubricating oil monitoring (Villar, Fernández, Gorritxategi, Ciria, & Fernández, 2014; Villar et al., 2012). This new prototype provides a more robust sensor system able to carry out more reliable spectroscopic measurements with better resolution in Vis-NIR range by means of the improvement of its optical and mechanical design.

2.1.1. Optical design

The main objective of the optical design is to provide an optical system, which works in the range of 400–1100 nm and that separates the light signal into different wavelengths after passing through the fluid sample. The components used for the development of the optical system of the Vis-NIR sensor are: (a) halogen white light source, (b) a 150 μm pinhole, which is a mechanical shutter of the light with a circular opening in the center, to make the light source extended on an approximation point source; (c) a spherical concave mirror to collimate the light towards the diffraction grating; (d) a diffraction grating to split the light into different wavelengths; and (e) a second spherical concave mirror that focalizes the light at the detector. The spectral range defines the type of light source, the coating for the mirrors and the characteristics of the diffraction grating. Concerning the light source, the most suitable for this design will be a tungsten halogen lamp of high intensity. The coatings of the windows are made of silver, as they have a good response in the spectral range. The grating reflection is gold plated and optimized for wavelengths close to 800 nm. The detector, which collects the light, is a 128 photodiode array that works in the range of 400–1100 nm.

The optical design was carried with the Zemax® Optical and illumination design software (Radiant Zemax LLC, Redmond, WA, U.S.A).

2.1.2. Mechanical design

The mechanical design of the sensor was performed taking into account the following features: (a) high accuracy in the position of the optical components; (b) prevention of the entrance of external light on the optical system; and (c) lightweight. The mechanical components developed and assembled are the optical components housing, the fluidic cell, the light source fixing and the detector fixing.

The fluidic cell comprises a chamber independent from the rest of the housing, designed to hold the sample, light source, the optical window and the light filter. The optical path is just 1 mm. By means of this cell different kind of samples with different types of light source and different sensor devices can be analyzed.

The mechanical components are made of aluminium with the objective that once assembled the whole set is as light as possible and easy to manufacture. In addition, each piece is given a treatment of anodized matte black so that if a beam of light deviates from the desired trajectory is not reflected and impacts on the photodiode detector. Seals are placed between the housing and the lid in order to prevent the entering of light and the particles from the outside. Fig. 1 shows a Vis-NIR sensor used for cider's fermentation process monitoring.

2.2. Cider samples

A total of 96 cider samples were supplied by different cider houses of the Basque Country. The samples were obtained from different barrels containing cider in different degrees of fermenta-

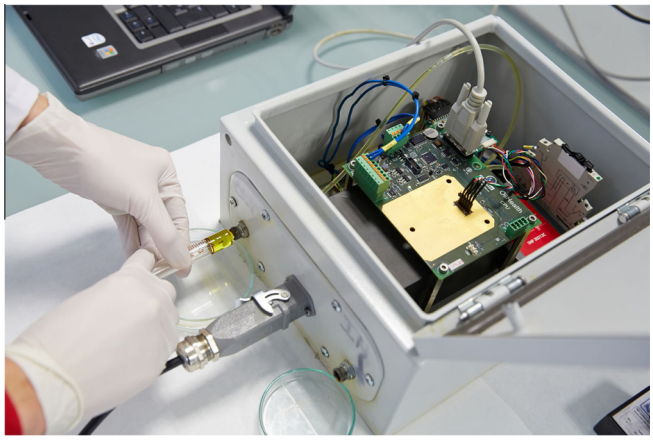

Fig. 1. Vis-NIR sensor system used for cider's fermentation process monitoring.

tion and maturation. The cider samples were divided into two groups, 78 samples were used in the calibration and another 18 samples were used as prediction samples in the validation of the model. All the cider samples were stored in a freezer at −20 °C in order to preserve them and stop the different fermentation processes that could take place.

3. Experimental methods

3.1. Laboratory measurements

The cider samples were analyzed in the Agrifood Laboratories of The Provincial Council of Gipuzkoa, FRAISORO. The parameters analyzed were alcoholic proof, acetic acid, glucose + fructose and L-lactic acid, according to the internal procedures PNTE/LF/502, 505, 507, and enzymatic autoanalyzer respectively. The PNTE/LF/502 method consists in the determination of alcoholic proof by electronic densimetry. The method PNTE/LF/505 involves the acetic acid measurement by UV–Vis spectrometry based on an enzymatic method and the method PNTE/LF/507 provides the detection of glucose + fructose by UV–Vis spectrometry based on an enzymatic method too.

3.2. Sensor measurements

The first step before performing the measurements was the defrosting of the cider samples that were in the freezer. Once defrosted, the cider samples were measured in the sensor system previous adjustment of the integration time. Three measurements per sample were done and from each measurement three replicates were carried out in order to obtain an average measurement of each cider sample. Cider samples were introduced in the fluidic cell using a 5 ml syringe. After inserting the samples two minutes of standby were allowed in order to stabilize the samples in the fluidic cell. The fluidic cell was cleaned with water between measurements. To minimize the effect of temperature variation all the samples were measured in a temperature range of 19–21 °C.

3.3. Multivariate data analysis

The final purpose of the multivariate data analysis was to correlate the spectra obtained by the Vis-NIR sensor system in the range between 400 and 1100 nm with the quality parameters of the cider samples analyzed in the laboratory, in order to obtain the best calibration model for each parameter. With the aim of obtaining spectroscopic data for an optimal analysis, different pre-processing methods were applied. Once the pre-processing strategy was defined, the most significant predictor variables were chosen by means of Martens Uncertainty test, interval Partial Least Squares (iPLS) and Genetic Algorithm (GA) variables selection techniques. Finally, the validation of the models was carried out by K-fold cross validation and with a prediction test set. A similar procedure has been successfully applied by author in previous researches (Villar et al., 2014).

The data analysis was carried out with The Unscrambler ver. 9.8 software (CAMO Software AS, Oslo, Norway) and with the PLS Toolbox (Eigenvector Research, Inc., Wenatchee, U.S.A) for Matlab ver. 7.4 (The Mathworks, Inc., Natick, U.S.A).

3.3.1. Spectra pre-processing

Considering the characteristics of the spectra obtained with the sensor system such as spectral resolution and the constant background signals presence (noise, offset or scatter effects), different pre-processing methods were applied so as to choose the best pre-processing strategy. The first step in the pre-processing was the average of the all the measurements obtained with the sensor (9 measurements), the next step was to transform all the transmittance spectra into absorbance in order to reduce the dynamic range of the measurements. Afterwards, different pre-processing methods such as Savitzky-Golay smoothing, derivatives, Multivariate Scatter Correction (MSC) or Standard Normal Variate (SNV) were applied. Finally, all the spectra were centered.

3.3.2. Development of the calibration model

The mathematical models were developed by Partial Least Squares Regression (PLSR). PLSR is often presented as the major regression technique for multivariate data calibration (Brereton, 2003, Chapter 5). PLSR has been previously applied by other authors to obtain calibration models for cider quality monitoring by MIR and NIR Spectroscopy (Dambergs et al., 2002; Picinelli Lobo, Súarez Valles, Fernández Tascón, Rodríguez Madera, & Fernández García, 2006; Queji et al., 2010).

3.3.3. Variable selection

Variable selection applied to spectroscopic data is a critical step in data analysis as it allows the quality improvement of the data during the calibration procedure. There are some variables that contain useless or irrelevant information like noise and background which can worsen the predictive ability of the model. Variable selection removes non-informative variables so as to obtain better and simpler prediction models by the identification of the most relevant predictor variables (Villar et al., 2014; Wu, He, Nie, Cao, & Bao, 2010; Xiaobo, Jiewen, Povey, Holmes, & Hanpin, 2010). The variable selection methods employed in this work are the Martens Uncertainty Test, iPLS and GA. The GA and iPLS variable selection analysis was carried out the PLS Toolbox for Matlab and the Martens uncertainty test was made with The Unscrambler ver. 9.8.

The Martens Uncertainty test is a method for variable selection proposed by Westad & Martens, 2000. The principle of Jack-knifing is applied for estimating standard errors of the regression coefficients estimates in the PLSR. The regression coefficients are divided by their estimated standard errors to give *t*-test values for testing the significance of the variables used in the model. This method can be applied both for PCR and PLSR. This is a fast and reliable method with low risk of overfitting (Villar et al., 2014).

iPLS is a method developed by Norgaard et al. (2000). This method gives an overall idea of the relevant information in different spectral intervals, focusing on more relevant spectral regions and removing interferences from the other ones. The principle of this method is to split the spectra into smaller non-overlapping

equidistant sections. At that point, each section undergoes a separate PLS modelling to determine the most useful variable range, choosing the region with lowest prediction error during the validation. iPLS can work in backward (BiPLS) mode, where the intervals are successively eliminated from the analysis, or in forward mode (FiPLS), where the intervals are successively added to the analysis (Villar et al., 2014; Xiaobo et al., 2010).

Genetic Algorithms (GAs) are a set of heuristic optimization techniques that employ a probabilistic, non-local search process inspired by Darwin's theory of natural selection. The idea of GA is to copy the biological evolution (Wu et al., 2010; Xiaobo et al., 2010). GA manipulates binary strings called chromosomes that contain genes that encode the predictor variables. There are two genetic operators used to obtain a new generation: crossover and mutation. Crossover involves the mixing of two chromosomes. The split point is chosen randomly along the length of either chromosome. In mutation each bit in a single chromosome is changed from a 1 to a 0 or viceversa. The steps included in a usual GA analysis combined with PLSR are the following (Balabin & Smirnov, 2011; Laxalde et al., 2011; Mehmood, Liland, Snipen, & Saebo, 2012; Villar et al., 2014); a) Creation of an initial population, encoding the spectrum as a binary string, where bits 1 and 0 represent selected and unselected variables; b) Assessment of the fitness of each individual in the population developing a PLSR model for each chromosome and evaluating the model taking the Root Mean Square Error of Cross Validation (RMSECV) as fitness value; c) Creation of a new generation by the recombination of the original chromosomes by single-point or double point crossover, where chromosomes with a better fitness value will have more chance to reproduce; and d) Mutation which consist of an inversion of a gene in a chromosome, ensuring that all variables have been chosen at least once during the analysis. Steps b and d are repeated until achieve the termination condition based on a convergence criterion. The algorithm completes the analysis when a given percentage of the chromosomes are identical.

3.3.4. Validation

The validation of the calibration models was first made by K-fold cross validation (8 splits, 9 iterations) and then by means of a prediction test set. The calibration models performance was assessed by means of the statistical parameters achieved from the prediction test set such as the coefficient of determination (r^2), Root Mean Square Error of Prediction (RMSEP), Standard Error of Performance (SEP), bias, and Ratio of Prediction of Deviation (RPD). The optimum number of Latent Variables (LVs) of the model was selected considering the variation of RMSEP with the number of LVs. The RPD is a statistics used to estimate the prediction accuracy of the calibration model. It is calculated as the ratio of the standard deviation (SD) of the data set to the RMSECV or RMSEP. Considering the bibliography, five different levels of prediction accuracy can be suggested on the RPD value (Joffre, Goge, Jolivet, Ross, & Ranjard, 2012; Rudnitskaya, Rocha, Legin, Pereira, & Marques, 2010; Saeys, Mouazen, & Ramon, 2005; Sun, Kamruzzaman, El Masry, & Allen, 2012; Villar et al., 2014):

- RPD below 1.5 indicates that the method is not admissible for prediction.
- RPD between 1.5 and 2 indicates that it is possible to differentiate between high and low concentration levels.
- RPD between 2.0 and 2.5 indicates that approximate quantitative prediction can be carried out.
- RPD between 2.5 and 3 indicates that the method performs a good prediction.
- RPD above 3 indicates the prediction can be classified as exceptional.

4. Results and discussion

4.1. Choosing the best pre-processing strategy

The type of pre-processing applied to the spectra is explained in detail in this section. The pre-processing applied was determined considering the features of the spectra obtained with the sensor system. The pre-processing strategy chosen for alcoholic proof, L-lactic, acetic acid and glucose + fructose quantification was the following: (i) Transmittance-Absorbance conversion; (ii) 1st Derivative Savitzky-Golay (size = 5, polynomial order = 2); and (iii) MSC. The segment size for Savitzky-Golay derivative was selected taking into account the experience gained in the similar spectra's pre-processing and the photodiode detector's spectral resolution which is 5.4 nm. Table 1 summarizes the results obtained applying different pre-processing strategies.

4.2. Optimization of calibration model performance

iPLS analyses were carried out in reverse mode with an interval size of 1. GA analyses were performed with the settings shown in Table 2. GA parameters were changed until the best performance was obtained.

Table 3 shows the performance of the calibration models without variable selection and with the three variable selection methods

Table 1
Results of the different pre-processing strategies used for the quantitative determination of alcoholic proof, glucose + fructose, L-lactic and acetic acid content.

Parameter	Pre-processing Strategy	r^2	RMSECV	LVs
Alcoholic proof (%vol)	1	0.389	0.207	9
	2	0.405	0.179	8
	3	0.519	0.170	6
	4	**0.568**	**0.162**	**6**
	5	0.543	0.166	6
Gluc + fruct (g/L)	1	0.403	1,575	8
	2	0.484	1.446	7
	3	0.581	1.288	7
	4	**0.667**	**1.146**	**8**
	5	0.654	0.167	7
Acetic acid (g/L)	1	0.456	0.334	8
	2	0.493	0.321	9
	3	0.591	0.301	9
	4	**0.607**	**0.272**	**9**
	5	0.602	0.279	9
L-Lactic acid (g/L)	1	0.420	0.268	11
	2	0.476	0.254	11
	3	0.605	0.227	12
	4	**0.671**	**0.212**	**12**
	5	0.628	0.219	13

The bold terms indicate the most suitable pre-processing strategy.

Table 2
Best performance settings of GA analyses.

GA Parameters	Best performance settings
Population size	128
Window width	1
% Initial terms	40
Penalty slope	0
Max generations	100
% at convergence	75
Mutation rate	0.01
Crossover	Double
Regression choice	PLS
Cross-validation	Contiguous (8 splits, 9 iterations)
Replicate runs	3

Table 3
Performance of the calibration models developed for the Vis-NIR sensor system without variable selection and applying the three variable selection methods tested in this work.

Parameter	Variable Selection Method	No. Of Variables	r^2	RMSECV	Bias	RPD	LVs
Alcoholic proof (% vol)	None	124	0.568	0.162	−0.002	1.530	6
	Martens test	24	0.625	0.161	−0.003	1.549	5
	iPLS	74	0.657	0.153	−0.003	1.621	6
	GA	**28**	**0.748**	**0.123**	**−0.003**	**2.017**	**4**
Gluc + fruct (g/L)	None	124	0.667	1.146	0.009	1.755	8
	Martens test	23	0.801	0.887	−0.010	2.267	8
	iPLS	34	0.904	0.616	0.019	3.265	8
	GA	**24**	**0.945**	**0.442**	**0.005**	**4.551**	**8**
Acetic acid (g/L)	None	124	0.606	0.272	−0.008	1.602	9
	Martens test	18	0.646	0.256	0.004	1.703	7
	iPLS	52	0.798	0.197	−0,013	2.213	8
	GA	**33**	**0.837**	**0.184**	**0.003**	**2.369**	**8**
L-Lactic acid (g/L)	None	124	0.671	0.212	−0.006	1.761	12
	Martens test	20	0.666	0.216	0.000	1.723	8
	iPLS	54	0.728	0.193	−0.015	1.934	8
	GA	**38**	**0.839**	**0.149**	**0.001**	**2.507**	**9**

The bold terms indicate the most suitable variable selection strategy.

Table 4
Performance of the calibration models with a prediction test set in the validation.

PLSR parameters	Alcoholic Proof (% vol)	Gluc + Fruct (g/L)	Acetic acid (g/L)	L-Lactic acid (g/L)
Number of samples	18	10	18	18
Measurement range	5.40–6.28	0.22–7.48	0.59–1.90	1.76–3.33
Number of LVs	4	8	8	9
r^2p	0.737	0.847	0.770	0.834
RMSEP	0.132	1.043	0.203	0.187
SEP	0.133	1.051	0.210	0.189
Uncertainty (95%)	±0.266	±2.102	±0.420	±0.378
RPD (SD/RMSEP)	1.770	2.374	1.440	2.323
Bias	−0.034	0.370	−0.038	−0.074

applied in this work. In all cases the best performance was obtained by the GA analysis. In the case of the alcoholic proof, the number of variables is reduced from 124 to 28, the value of RMSECV decreases from 0.162 to 0.123, the RPD value increases from 1.530 to 2.017, and the number of LVs decreases from 6 to 4. For Glucose + Fructose, the number of variables is reduced from 124 to 24, the value of RMSECV decreases from 1.146 to 0.442, the value of RPD increases from 1.755 to 4.551 and the number of LVs remains the same. In the case of acetic acid, the number of variables is reduced from 124 to 33, the value of RMSECV decreases 0.272 to 0.184, the value of RPD increases from 1.602 to 2.369 and the number of LVs decreases from 9 to 8. Finally, for lactic acid, the number of variables is reduced from 124 to 29, the value of RMSECV decreases from 0.212 to 0.149, the value of RPD increases from 1.761 to 2.507 and the number of LVs decreases from 12 to 9. In all cases the performance improvement obtained by variable selection has been considerable, being Martens Uncertainty test the method which shows the worst improvement in the calibration models performance including the statistical parameters and LVs decrease.

Fig. 2 shows the results obtained by GA analyses, showing the fitness versus the number of variables. The variables that made the RMSECV worse for each model are located the top of the figure and the variables which tend to improve the RMSECV on each model are located towards the bottom of the figure. The variables not shown in the figure are not useful in the developments of models.

4.3. Validation

The calibration models validation was made using a prediction test set. Table 4 shows the performance of each calibration model during the validation process. The results obtained in the validation with the prediction test set are worse than those obtained by cross-validation. In every case the value of RMSEP increased leading to a decrease in the value of RPD. Taking into consideration the RPD classification, by means of the alcoholic proof sensor system method it could be possible to distinguish between high and low concentration levels, the glucose + fructose and lactic acid sensor system methods could be suitable for approximate quantitative determination. Nevertheless, the acetic acid sensor system method cannot be considered suitable for prediction.

5. Conclusions

The main conclusion obtained in this work is the adequate combination of spectroscopic pre-processing techniques with variable selection methods are great chemometric tools to improve the prediction ability of the multivariate calibration models developed for the Vis-NIR sensor systems. They help to decrease the RMSECV/RMSEP and SECV/SEP values, to increase the RPD and to reduce the number of LVs of the models. These techniques and methods can improve the prediction ability of the new analytical methods developed by means of the Vis-NIR sensor systems. The spectroscopic pre-processing methods are able to correct the scatter effects or to remove the spectroscopic noise. However, the way to operate them is not straightforward. The choice of the suitable pre-processing strategy is usually based on the user expertise and sometimes it must be optimized using a trial and error approach. Moreover, a suitable pre-processing strategy can improve the performance of the calibration models, but in order to achieve the optimum performance it is necessary to combine pre-processing and variable selection methods.

The second important conclusion achieved in this work is the Vis-NIR sensor system developed by IK4-Tekniker can be a really

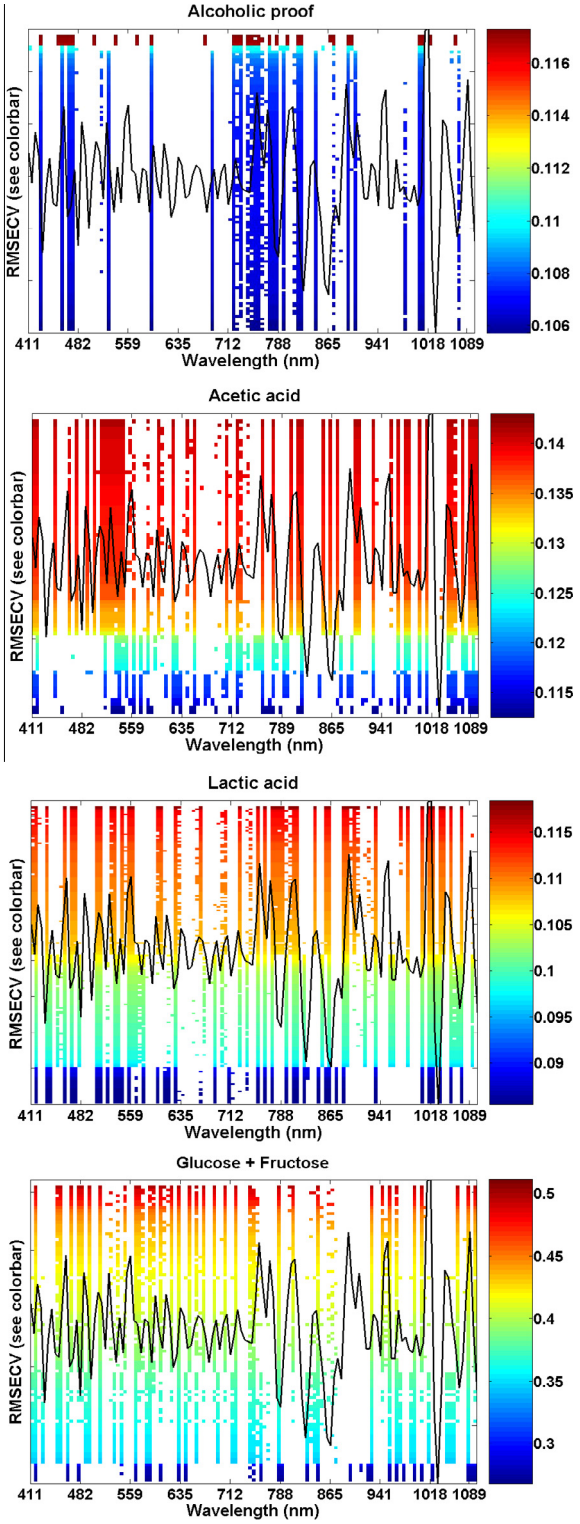

Fig. 2. The fitness versus the variable number in GA analyses. The variables that get worse the RMSECV of each model are located towards the top of the figure and the variables which tend to improve it are located towards the bottom of the figure. The variables not shown in the figure are not useful in the developments of models. The mean of the spectra is overlain in black.

helpful tool for real time quality and safety monitoring of foodstuff. The main advantages of the Vis-NIR sensor system compared to current technology for cider quality monitoring are the following: (a) real-time monitoring of alcoholic and malolactic fermentation and maturation process of the cider; (b) low level of knowledge required from the operators; (c) easy to install in each barrel; and (d) finally – were a final product developed-the sensor's cost would be easily paid for, being more economical than the cost of the samples analysis in the laboratory. Nevertheless, the accuracy of the sensor system method is worse than the accuracy obtained from the laboratory method. Furthermore, some adjustment in the calibration model from one year to another would be required.

References

Alonso-Salces, R. M., Guyot, S., Herrero, C., Berrueta, L. A., Drilleau, J.-F., Gallo, B., et al. (2005). Chemometric classification of Basque and French ciders based on their total polyphenol contents and CIELab parameters. *Food Chemistry, 91*, 91–98.

Balabin, R. M., & Smirnov, S. V. (2011). Variable selection in near-infrared spectroscopy: Benchmarking of feature selection methods on biodiesel data. *Analytica Chimica Acta, 692*, 63–72.

Bleibaum, R. N., Stone, H., Tan, T., Labreche, S., Saint-Martin, E., & Isz, S. (2002). Comparison of sensory and consumer results with electronic nose and tongue sensors for apple juice. *Food Quality and Preference, 13*, 409–422.

Brereton, R. (2003). *Chemometrics: Data analysis for the laboratory and chemical plant* (2nd ed.). Chichester: John Wiley and Sons Ltd (Chapter 5).

Bureau, B., Le Coq, D., Michel, K., Keirsse, J., Boussard-Pledel, C., Fonteneau, G., et al. (2002). Infrared glass fibers for in-situ sensing, chemical and biochemical reactions. *Comptes Rendus Chimie, 5*, 907–913.

Castillo, J., Gáspar, S., Leth, S., Niculescu, M., Mortari, A., Bontidean, I., et al. (2004). Biosensors for life quality: Design, development and applications. *Sensors and Actuators B, 102*, 179–184.

Chen, Y.-R., & Liu, Y. (2007). Development of simple algorithms for the detection of fecal contaminants on apples from visible-near infrared hyperspectral reflectance imaging. *Journal of Food Engineering, 81*, 412–418.

Dambergs, R. G., Kambouris, A., Francis, L., & Guishen, M. (2002). Rapid analysis of methanol on grape-derived distillation products using near-infrared transmission spectroscopy. *Journal of Agricultural Food Chemistry, 50*, 3079–3084.

Del Campo, G., Santos, J. I., Berregi, I., & Munduate, A. (2005). Differentiation of Basque cider apple juices from different cultivars by means of chemometric techniques. *Food Control, 16*, 551–557.

Del Campo, G., Santos, J. I., Berregi, I., Velasco, S., Ibarburu, I., Dueñas, M. T., et al. (2003). Cider produced by two types of press and fermented in stainless steel and wooden vats. *Journal of the Institute of Brewing, 109*, 342–348.

James, W., Parry, K. W., & Jones, T. P. (1987). On-line determination of ethanol during fermentation processes using a fuel cell sensor. *Analyst, 112*, 615–618.

Joffre, R., Goge, F., Jolivet, C., Ross, I., & Ranjard, L. (2012). Optimization criteria in sample selection step of local regression for quantitative analysis of large soils NIRS database. *Chemometrics and Intelligent Laboratory Systems, 110*, 168–176.

Laxalde, J., Rukesbuch, C., Devos, O., Caillol, N., Wahl, F., & Duponchel, L. (2011). Characterization of heavy fuels oils using near-infrared spectroscopy: Optimization of pre-processing methods and variable selection. *Analytica Chimica Acta, 705*, 227–234.

Mehl, P. M., Chen, Y.-R., Kin, M. S., & Chan, D. E. (2004). Development of hyperspectral imaging technique for the detection of apple surface defects and contaminations. *Journal of Food Engineering, 61*, 67–81.

Mehmood, T., Liland, K. H., Snipen, L., & Saebo, S. (2012). A review of variable selection methods in Partial Least Squares Regression. *Chemometrics and Intelligent Laboratory Systems, 118*, 62–69.

Meyes, A. G., Blyth, J., Kyrolainen-Reay, M., Millington, R. B., & Lowe, C. R. (1999). A holographic alcohol sensor. *Analytical Chemistry, 71*, 3390–3396.

Norgaard, A. S. L., Saudland, A., Wagner, J., Nielsen, J. P., Munck, L., & Engelsen, S. B. (2000). Interval partial least squares-regression (iPLS): A comparative chemometric study with an example from near-infrared spectroscopy. *Applied Spectroscopy, 54*, 413–419.

Picinelli Lobo, A., Súarez Valles, B., Fernández Tascón, N., Rodríguez Madera, R., & Fernández García, O. (2006). Calibration models for routine analysis of cider by min-infrared spectroscopy. *LWT-Food Science and Technology, 39*, 1026–1032.

Queji, M. D., Wosiacki, G., Cordeiro, G. A., Peralta-Zamora, P. G., & Nagata, N. (2010). Determination of simple sugars, malic acid and total phenolic compounds in apple pomace by infrared spectroscopy by PLSR. *International Journal of Science, 45*, 602–609.

Rudnitskaya, A., Rocha, S. M., Legin, A., Pereira, V., & Marques, J. C. (2010). Evaluation of the feasibility of the electronic tongue as a rapid analytical tool for wine age prediction and quantification of the organic acids and phenolic compounds. *Analytica Chimica Acta, 662*, 82–89.

Saeys, W., Mouazen, A. M., & Ramon, H. (2005). Potential for onsite and online analysis of pig manure using visible and near-infrared reflectance spectroscopy. *Biosystems Engineering, 91*, 393–402.

Sun, D.-W., Kamruzzaman, M., El Masry, G., & Allen, P. (2012). Prediction of some quality attributes of lamb meat using near-infrared hyperspectral imaging and multivariate analysis. *Analytica Chimica Acta, 714*, 57–67.

Villar, A., Fernández, S., Gorritxategi, E., Ciria, J. I., & Fernández, L. A. (2014). Optimization of the multivariate calibration of a Vis-NIR sensor for the on-line monitoring of marine diesel engine lubricating oil by variable selection methods. *Chemometrics and Intelligent Laboratory Systems, 130*, 68–75.

Villar, A., Gorritxategi, E., Aranzabe, A., Fernández, S., Otaduy, D., & Fernández, L. A. (2012). Low-cost visible-near infrared sensor for on-line monitoring of fat and fatty acids content during the manufacturing process of the milk. *Food Chemistry, 135*, 2756–2760.

Westad, F., & Martens, H. (2000). Variable selection in near-infrared spectroscopy based on significance testing in partial least squares regression. *Journal of Near Infrared Spectroscopy, 8*, 117–124.

Wu, D., He, Y., Nie, P., Cao, F., & Bao, Y. (2010). Hybrid variable selection in visible and near-infrared spectral analysis for non-invasive quality determination of grape juice. *Analytica Chimica Acta, 659*, 229–237.

Xiaobo, Z., Jiewen, Z., Povey, M. J. W., Holmes, M., & Hanpin, M. (2010). Variable selection methods in near-infrared spectroscopy. *Analytica Chimica Acta, 667*, 14–32.

Lens-Free Imaging based low cost micro sensor for in-line wear debris detection in lube oils

Jon Mabe*[1a], Joseba Zubia[b], Eneko Gorritxategi[c]
[a]IK4-Tekniker Research Center, Iñaki Goenaga 5, Eibar, Spain; [b] Dept. of Communications, University of the Basque Country, Bilbao, Spain; [c]Atten2 Advanced Monitoring Technologies, Iñaki Goenaga 5, Eibar, Spain.

ABSTRACT

The current paper describes the application of lens-free imaging principles for the detection and classification of wear debris in lubricant oils. The potential benefits brought by the lens-free microscopy techniques in terms of resolution, deep of field and active areas have been tailored to develop a micro sensor for the in-line monitoring of wear debris in oils used in lubricated or hydraulic machines as gearboxes, actuators, engines, etc. The current work presents a laboratory test-bench used for evaluating the optical performance of the lens-free approach applied to the wear particle detection in oil samples. Additionally, the current prototype sensor is presented, which integrates a LED light source, CMOS imager, embedded CPU, the measurement cell and the appropriate optical components for setting up the lens-free system. The imaging performance is quantified using micro structured samples, as well as by imaging real used lubricant oils. Probing a large volume with a decent 2D spatial resolution, this lens-free micro sensor can provide a powerful tool at very low cost for in-line wear debris monitoring.

Keywords: Optoelectronic and photonic sensors, Object recognition, Optical sensors, Optical microscopy, Optical diffraction, Lubricating oils, Hydraulic fluids, Maintenance.

1. INTRODUCTION

Low cost smart sensors are becoming more and more popular in the industrial sector, especially due to their potential contributions for increasing productivity and safety in the industry. These sensors are normally installed in-situ at production environments and allow real time monitoring of parameters of interest for the control of processes, test and inspection of products or for assisting predictive maintenance approaches. The promising outlook of these sensors gets consolidated when critical equipment or machines with very restricted spatial or temporal accessibility need to be monitorized. Examples of this paradigm could be found in the inspection of lubricant or hydraulic fluids in new off-shore wind turbines as part of their predictive maintenance program [1][2] or in run-in phases of drive trains manufacturing, where the load is regulated based on the increasing presence of cutting wear particles in the lubricant [3], or when the safety of an aircraft or helicopter relies on the accurate measuring of a certain parameter of the lubricant [4][5].

Among several other magnitudes and elements to monitor in the broad universe of industrial applications, fluidics arise as a very challenging opportunity for smart sensor developers, not only due to the traditional requirements of high sensibility, repeatability and reliability in the measurement but also because of the extreme working conditions (temperature, pressure, and humidity), and the necessity of sample extraction in place (e.g. by pass, in line) at the right flow and in the right volume, dealing with different viscosities, not homogeneous samples, etc. Traditionally, several different technological principles have been used for designing sensors for fluidics inspection, such as capacitive, magneto-resistive, inductive or photonic sensors, focusing on a single parameter, which is directly or indirectly correlated with a certain magnitude of interest in the fluid. This manuscript described the work accomplished for bringing a very fundamental photonic principle as the lens-free imaging, to a very challenging industrial use case for the in-line wear debris detection in lube oils.

[1] *jon.mabe@tekniker.es; phone 1 +34 943 20 67 44; tekniker.es

1.1 Wear Debris on Industrial Fluids

Solid particulate in suspension in industrial fluids, such as lubricants or hydraulic fluids, is frequently an early warning of latent or incoming failures in the machines or processes where they are being used [6]. Reference [7] observed that 70% of component and part replacements in industrial equipment is due to surface degradation, whereas in hydraulic and lubricating systems, 20% of these replacements result from corrosion with 50% resulting from mechanical wear. Therefore, obtaining reliable, accurate and fast fluid cleanliness information in order to detect anomalous contamination is a key operation for ensuring the efficiency of industrial processes and minimizing downtime [8][9]. First introduced in late 40s [10], the laboratory analysis of oil samples, the traditional off-line fluid analysis, is still an important asset for several maintenance programs, especially when high accuracy and low detection limits are needed and the response time is not critical. However, thanks to the potential benefits brought by real time operation, in situ sampling, reduced price and size, and a decent accuracy and reliability (which improve day by day), the number of in-line sensor solutions is increasing steadily in the last decades [11][12][13][14]. Additionally, as reported in [15] in relatively clean fluids, the level recorded by the off-line analysis imprecisely reports the oil status compared to in-line analysis, motivating erroneous maintenance actuations.

1.2 Wear Debris Sensors

With regard to the measurement principles, asides the inductive, capacitive, ultrasound or pressure difference technologies [16][17][18][19], the photonic detectors represent a predominant alternative for the inline wear debris sensors [20][21]. Photonic particle counters are based in different measurement principles, as the light obscuration or light scattering, but the direct imaging alternative (see figure 1) offers a simple and efficient solution when the minimum particle size is above 1 or 2 µm, preferably 4 µm, as it is the case for the ISO 4406, a standard which normalizes the fluid cleanliness based on the particle count per mL classified in different size ranges (e.g. > 4 µm, > 6 µm, > 14 µm). In addition, the direct imaging solutions offer a good non-ferrous particle detection sensibility, allow shape recognition, and typically they are relatively accurate even under the presence of water and air bubbles [22], which are also basic requests from the industry.

Nevertheless, direct imaging solutions suffer from low volume sampling capability, which derive from the restrictions of traditional linear optics, whereas, if resolution should be minimized (e.g. 4 µm) the Deep of field (DOF) and Field of View (FOV) will be constrained. For instance, in [23], a direct imaging wear debris sensor is described, which, using a lens with an Effective Focal Length of 9.6, and a CMOS of 10 MPix, is able to sample approximately 0.025 mL (FOV 36 mm2 / DOF 250 µm) of fluid with a resolution of 3 µm with every new image acquisition.

Therefore, in this situation of intrinsic trade-off between FOV, DOF and resolution of traditional lens-based systems, the lens-free imaging techniques arises as a potential breakthrough solution for enhancing the optical performance of wear particulate sensors.

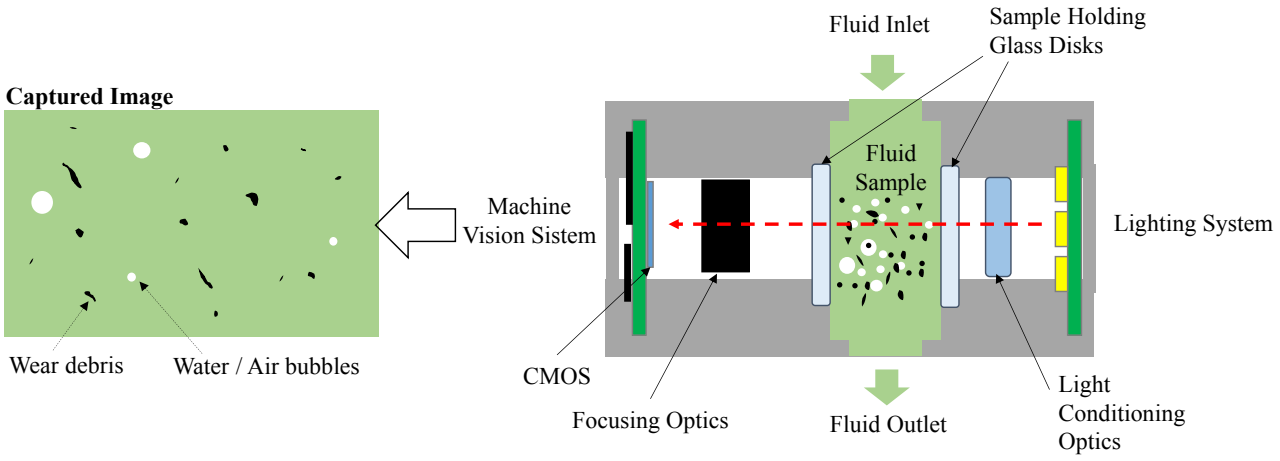

Figure 1. Block diagram depicting a direct imaging wear debris sensor.

1.3 Lens-Free Imaging

Lens-free microscopy is an cost-effective technique that allows capturing high resolution images, over large FOV and DOF with simple and compacted settings [24] [25], which only requires a light source, a pinhole for generating a diffraction pattern, and an image sensor for capturing this light pattern. This technique is based on the hologram theory formulated by Denis Gabor in the late 40s, which describes that the interference between the light illuminating an object and the light diffracted by that object generates an amplitude and phase information that can be used to reconstruct a perfect image of the object [26].

The application of lens-free principles has increased in the last decade, mainly focused on biological use cases, dealing with the inspection of cells and microorganisms in bio samples [27][28]. The literature reviews several different configurations of the lens-free setups, describing different sample illumination approaches (e.g. coherent, incoherent or semi coherent), image processing algorithms (e.g. FFT based original object reconstructions or direct use of the interference patterns), and several system geometries, defining distances and locations of light sources, detectors, pinholes and samples [29] [30] [31]. In this specific research work, the development has been focused on the Incoherent lens-free approach.

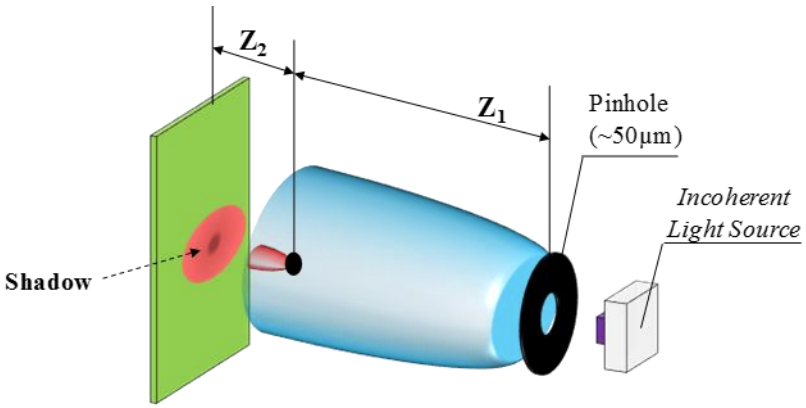

Figure 2. Incoherent lens-free setup [30].

Incoherent lighting approach represents the simplest alternative within the lens-free arena because it gets rid of advanced optical components as lasers, replacing them by standard light sources. In this configuration, the detector receives a self-interfering diffraction pattern generated when the light beam hits the target object. This pattern could be understood as the shadow generated by the object blocking the incoming light to the detector and could be directly used for the object's size recognition, avoiding the use of computationally intensive holographic reconstruction algorithms [32][33]. In this case, the target objects should be located right above the detector, minimizing Z_2 distance to 1 or 2 mms, and the distance from the objects to the pinhole should meet $Z_1 >> Z_2$ relation. Additionally, in the incoherent mode, the aperture diameter is normally above 50 µm.

Optical performances reported in the literature for incoherent lens-free systems describe: large sample volume monitoring (FOV ~ 20 mm2, DOF~1 mm), resolutions of approximately 2 µm, simplicity and robustness of the hardware setup and small size of the solution (50 mm × 50 mm × 10 mm) [34][31]. According to this information, even the simplest expression of the lens -ree microscopy, the incoherent mode, could positively contribute in the field on the in-line/on-line wear particle counting and classification.

The forthcoming sections present the work performed for the application of the incoherent lens-free principles into an optical micro sensor for the detection of wear particles in industrial fluids.

2. OPTICAL TEST BENCH FOR SENSOR SYSTEM DESIGN

A custom test-bench has been developed for accomplishing the proof-of-concept of the lens-free based wear debris sensor. The objective with this setup is to find the optimal configuration of Z_1 and Z_2 distances and pinhole that enables the largest FOV, DOF and highest resolution to fulfil the industrial requirements for particle counters.

The expected minimum resolution could be set around 1 or 2 µm, enabling an accurate detection of small particles of 4 µm. The DOF and FOV definition derives from the general request of offering the highest sampling volume possible. According to the typical incoherent lens-free specifications, the FOV is normally as big as the active area of the CMOS sensor. Regarding the DOF, it will be limited by the optical performance of the lens-free setup and by the light absorbed at the sample fluid. It could happen that, with very opaque fluids, the light is not able to penetrate the full optical DOF and therefore limits it. Additionally, it should be noted that the system will offer different effective DOFs depending on the size of the target object, and, consequently, different DOF are expected for 4 µm, 6 µm and >14 µm particles. For instance, in the lens-based system referenced in [23], the DOF for small particles is approximately 250 µm, for medium particles it raises to 400 µm, and for large particles the system reaches almost 1 mm.

2.1 Optical Test Bench Description: Materials and Method

The optical test bench includes a set of precision pinholes from Thorlabs (50, 200 and 500 µm), a custom light source based on an array of XLamp white LEDs from Cree offering a light flux of 535 Lumens/3W at 120º viewing angle per each led. The CMOS sensor is a half inch 5Mpix, 2.2 × 2.2 µm pixel size, with a sensibility of 1.76 V/Lux-sec and 5.7 × 4.28 mm active area rolling shutter device (MT9P006 from On Semiconductors). As fluid sample container a thin a quartz cuvette from Hellma Analytics (ref. 106-0.50-40) has been used. The cuvette is placed in close contact with the CMOS surface, making Z_2 distance equal to the cuvette wall thickness (~1.25 mm). Therefore, the sample volume is determined by the cuvette light path, which is 0.5 mm. Asides, the light source and pinhole have been attached to a micrometer translation stage (Thorlabs MT1/M) for allowing an accurate Z_1 tuning. In addition, the inner walls of the cuvette have been micro milled with precision marks (65 µm side square and 75 µm diameter circle) for allowing the characterization of the DOF.

2.2 Theoretical Approach

The starting point for defining the optimal lens-free setup in the test bench is based on a theoretical approximation to the problem. The following calculations are based on the work described in [31], and define the lens-free setup for meeting the requirements described above.

The incoherent lens-free setups requires a Fringe Magnification Factor, $F = (Z_1 + Z_2) / Z_1 \sim 1$, then $Z_1 >> Z_2$, being typical Z_1 values reported in the literature in the range of 10 – 50 mm. Besides, incoherent lens-free systems also involves minimizing the Z_2 distance. As mentioned earlier, in our specific case, there is a minimum limit for the Z_2 defined by the thickness of the cuvette (~1.25 mm) containing the specimen sample. Additionally, the sample path length must be considered, which for the cuvettes chosen is limited to 0.5 mm. Therefore, we get that in the current Test Bench, $Z_{2\text{-}min}$ = *Sample Holder Wall Thickness = 1.25 mm* and $Z_{2\text{-}max}$ = *Sample Holder Wall Thickness + sample path-length = 1.25 mm + 0.5 mm = 1.75 mm.*

Another important parameter to define is the diameter of the pinhole, which for the incoherent lens-free mode requires a rather large aperture of approximately 100 ʎ - 200 ʎ. The white LEDs used in the test bench have their central emission peak at $ʎ_0$ *=580 nm*, and therefore we obtain: $D_{pinhole} > 58\ µm$. Additionally, for defining $D_{pinhole}$, the impact on the light intensity filtered also needs to be taken into consideration, as the aperture acts as a spatial filter for the light beam reducing its intensity.

The FOV of the system is defined as $FOV = Area\ of\ the\ sensor / F^2$. For $F \sim 1$, the FOV remains almost equal to the full active area of the CMOS detector, which for the current case is 5.7 × 4.28 mm.

The resolution and DOF of the proposed setup is limited by two main factors: the diameter of holographic Coherent Diffraction (D_{coh}) for each object in the focus plane and the effective dimensions (d_{scat}) at the detector plane of each point scattered on the sample plane. The design objective is to minimize both. As we are not looking for any reconstruction of the diffraction patterns, larger D_{coh} will increase the noise for particle detection. Additionally, increasing the d_{scat} will directly impact on the minimum resolution achievable.

According to the references cited, D_{coh} is proportional to $ʎ_0 Z_1 / D_{pinhole}$ and $d_{scat} = D_{pinhole}\ Z_2/Z_1$.detector. Therefore, the optimal $D_{pinhole}$ and Z_1 selection is based on the trade-off for minimizing the d_{scat} and D_{coh}, whereas Z_2 must be keep the minimum possible.

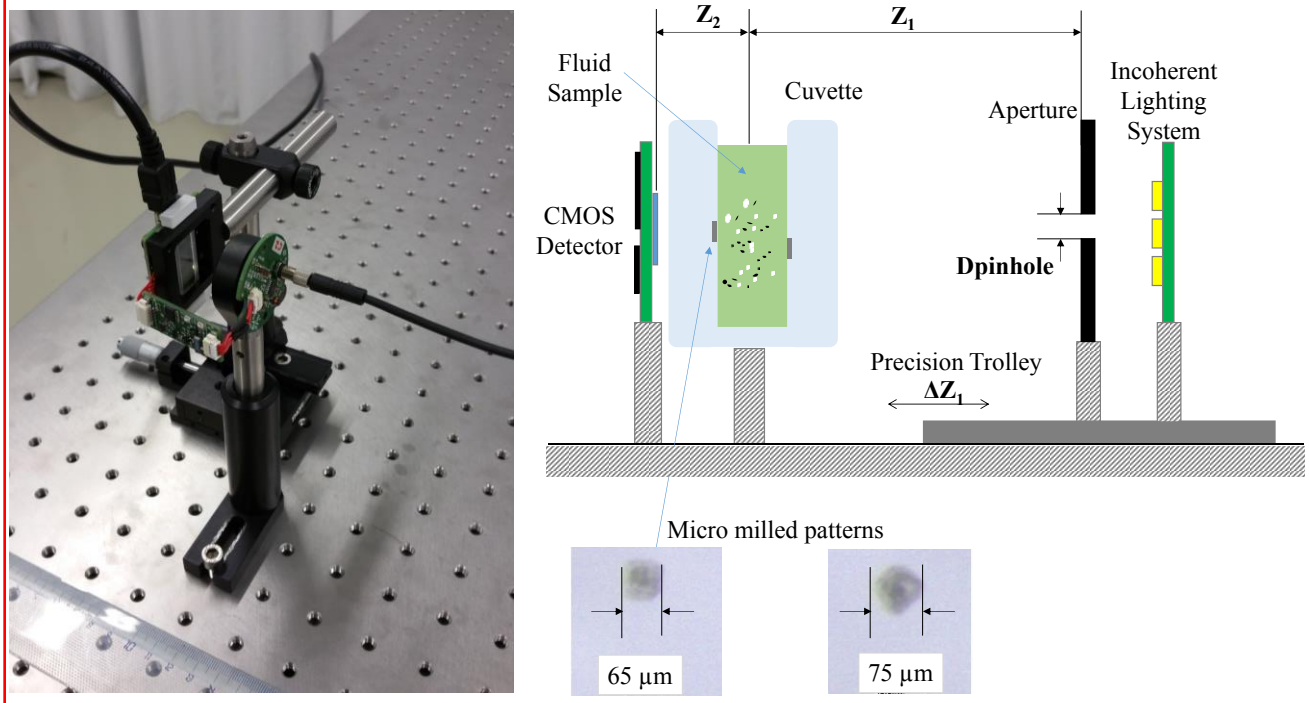

Figure 3. Photo and Schematic of the Optical Test Bench.

Regarding the intensity of light required for properly illuminating the fluid sample, parameters of different nature have an impact on the contrast and brightness of the image acquired at the detector. These factors are summarized in the figure. 4, being: constructional parameters of the LED (quantum efficiency *η-lux/A*) and CMOS pixels (sensibility *S- V/lux-sec*); and design parameters, such as the LED polarization current (A), the exposure time of the pixel (sec); the light absorption occurring at the fluid sample which depends on its absorptivity (ε) and on the path length (ℓ); and of course, parameters regarding lens-free setup as the pinhole diameter or the free space distances Z_1 and Z_2, which mainly contribute negatively to the light received at the detector due to the light blocking happening at the aperture and due to the free space losses across Z_1 and Z_2.

The LED polarization current, the exposure time and the lens-free setup are the only parameters under designer's choice to adjust the power of the received light in order to analyze a sample of fluid with enough contrast towards a correct discrimination of objects (particles, bubbles) suspended in the fluid. On the other hand, we must consider that minimizing the exposure time would allow monitoring at faster frame rate, and consequently maximizing the effective sample volume analyzed per second; therefore, a starting value of T_{exp}=*200 ms* has been used in the calculations.

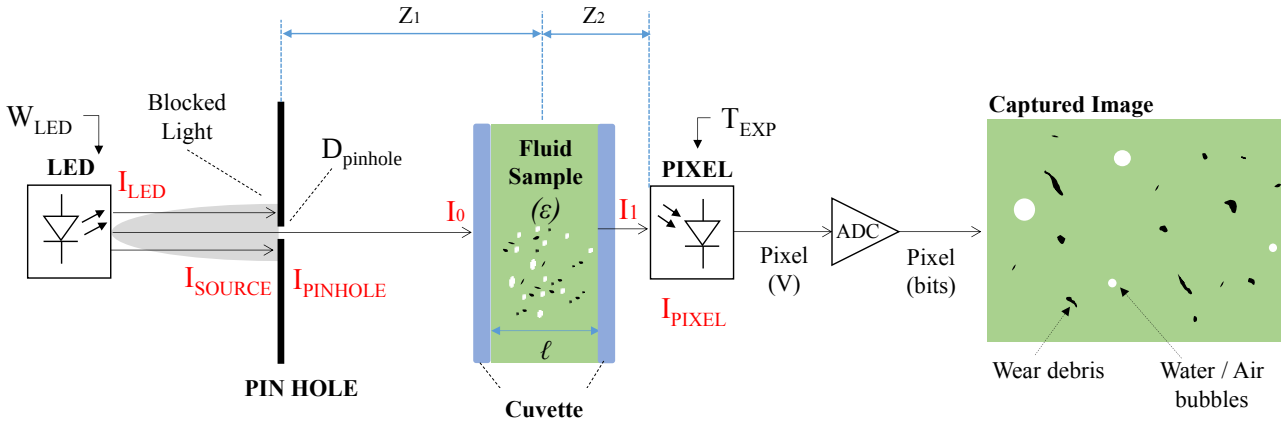

Figure 4. Block Diagram depicting the main factors impacting in the light intensity detected at the CMOS sensor.

If acquiring a mid-scale intensity value at each pixel of the CMOS is defined as the design target, the light intensity budget calculation across the system could be approximately described with the following equations and considerations:

$$V_{PIXEL\ mid-scale} = 0.5 \times V_{ADC-PIXEL} = 0.5 \times 2.4\,V = 1.4\,V \quad (1)$$

$$V_{PIXEL\ mid-scale} = S\left(\frac{V}{Lux \cdot sec}\right) \times I_{PIXEL\ mid-scale}(Lux) \times \mathrm{T_{exp}}(sec) \quad (2)$$

$$1.4V = 1.76\left(\frac{V}{Lux \cdot sec}\right) \times I_{PIXEL\ mid-scale}(Lux) \times 200 \cdot 10^{-3}(sec) \quad (3)$$

$$I_{PIXEL\ mid-scale} = 3.9(Lux) \quad (4)$$

If we consider that the absorption happening across the free space (FSPL) and at the cuvette walls are both negligible, then, the main contributors to the light intensity loss within the system are clearly the absorption at the fluid sample and the light blocking at the pinhole. The assumption made above is demonstrated first based on the Friss Formula, which describes free space power losses as $FSPL = (4\pi \times D / \lambda)^2$, being $D \sim Z_1 \sim 0.01m$ or $D \sim Z_2 \sim 0.001m$, then FSPL~0. Additionally, the losses at the cuvette are omitted due to the high transmission of the quartz (above %90) in the visible light spectrum [35]. Therefore, we assume that $I_{PINHOLE} \sim I_0$ and $I_1 \sim I_{PIXEL}$.

The light loss across the sample fluid is described by the Lambert-Beer law, which defines an exponential relation between the light entering the sample (I_0) and getting through it (I_1) as $I_1 = I_0 \times 10^{-\varepsilon \ell c} = I_0 \times 10^{-A}$, whereas ε is the attenuation coefficient in the fluid sample; c is the amount concentration of the absorbent in the fluid sample; and ℓ is the path length of the beam of light through the material sample; and their product represents the absorptivity (A) happening at the sample. A value of $A=0.25$ could be considered as an average absorptivity of an used lubricant oil at $\lambda_0 = 580nm$ for 0.5 mm path length [36][37], consequently, the incoming light power will be reduced in a factor of: $10^{-A} = 10^{-0.25} = 0{,}56$. Therefore, we can conclude that:

$$I_{PIXEL} = 0.56 \times I_{PINHOLE}(Lux) \quad (5)$$

and from eq. (4)

$$I_{PINHOLE\ mid-scale} = \frac{I_{PIXEL\ mid-scale}(Lux)}{0.56} = 6.9(Lux) \quad (6)$$

At this point, we are only missing the I_{LED} to $I_{PINHOLE}$ transfer function to define the minimum light power that needs to be emitted by the LED lighting system to generate an image on the CMOS with decent brightness. The aperture acts as a spatial filter blocking a significant amount of the emitted light power. Indeed, the light power transmitted through the pinhole is proportional to the pinhole aperture area $I_{PINHOLE} \propto D_{PINHOLE}$.

The white LEDs chosen for the test bench are able to generate a light flux of $I_{LED}=178\ Lumens/W$ (9W maximum) at 120º viewing angle and they have been placed 5 mm away from the pinhole. This means, that the illumination system, per each LED, is able to deliver a light beam of approximately *22600 Lux/W* spread following a Gaussian distribution in an area of 235 mm^2 (almost the whole area of the pinhole mounting disk) right before the pinhole. But it is clear that only a small proportion of that light beam will be transmitted across the pinhole, that could be described as $I_{SOURCE}=22600\ Lux/W/235\ mm^2=96\ Lux/W/mm^2$ and therefore:

$$I_{PINHOLE} = I_{SOURCE} \times A_{PINHOLE} = 96\left(\frac{LUX}{W \cdot mm^2}\right) \times \pi \cdot \frac{D_{PINHOLE}(mm^2)}{2} = 150 \cdot D_{PINHOLE}(mm^2)\left(\frac{LUX}{W}\right) \quad (7)$$

Combining this with eq. (5), we could now define I_{PIXEL} in dependence with the aperture diameter and with the LED polarization.

$$I_{PIXEL} = 0.56 \times I_{PINHOLE} = 84 \cdot D_{PINHOLE}(mm^2)\left(\frac{LUX}{W}\right) \quad (8)$$

Therefore, for the different candidate pinholes, different LED number and polarization currents are expected for achieving

the target mid-scale value for I_{PIXEL} of *3.9 Lux*. If we reach the saturation current and we cannot add any more LEDs devices within the source (a circular array of 6 LEDs have been arranged), we would need to increase the exposure time above the cited *200 ms*.

2.3 Results of the Test Bench

The next section discusses the results achieved with different setups for $D_{pinhole}$, Z_1, Z_2 and light power for capturing images of a real used lubricant (Castrol Optigear X320 Synthetic) artificially contaminated with metallic particles (GoodFellow LS277298 Stainless Steel >45 µm AISI 316).

First of all, for using as reference benchmark, the cuvette was analyzed with a laboratory microscope. Even if the resolution and level of detail is very high, the limitations of the regular microscopes gets evident from the very beginning (see figure 5), when, setting the target FOV (approximately the CMOS area and achieved with 5X gain) the two micro milled patterns (the square and the circle) cannot be sharply focused at the same time, evidencing a poor DOF even for relatively large objects (~70 µm).

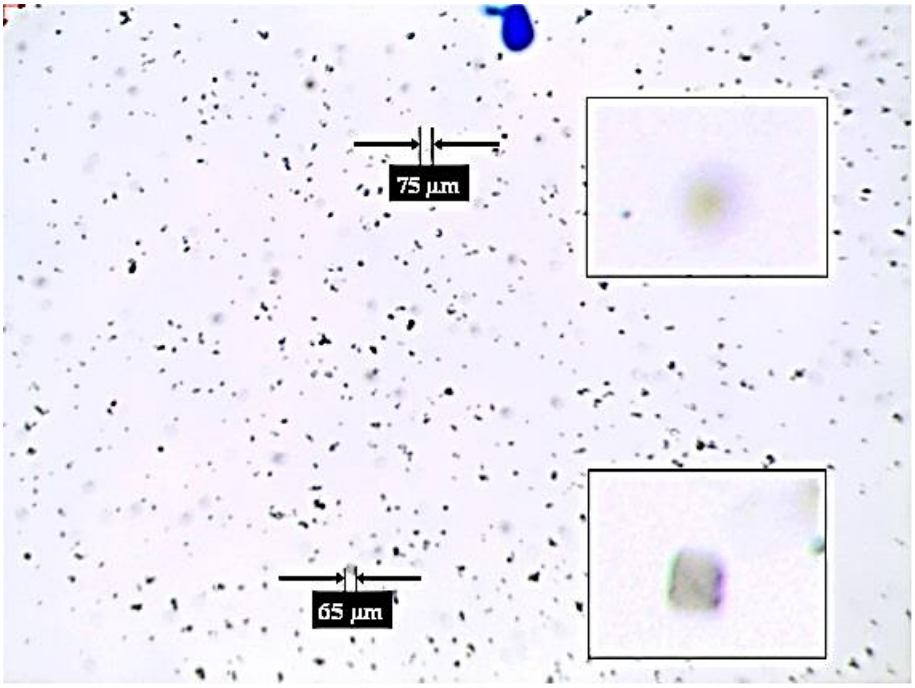

Figure 5. Image from the sample cuvette acquired with a laboratory microscope (5X). The FOV is 5,485 µm by 4,100 µm and the DOF limitation is evident in the image quality of the two patterns.

The first experiments with the lens-free setup in the test-bench already reported an improved DOF while keeping a FOV performance similar to the 5X microscope. For instance, in figure 6, the enhancement in the image quality of the patterns is manifest.

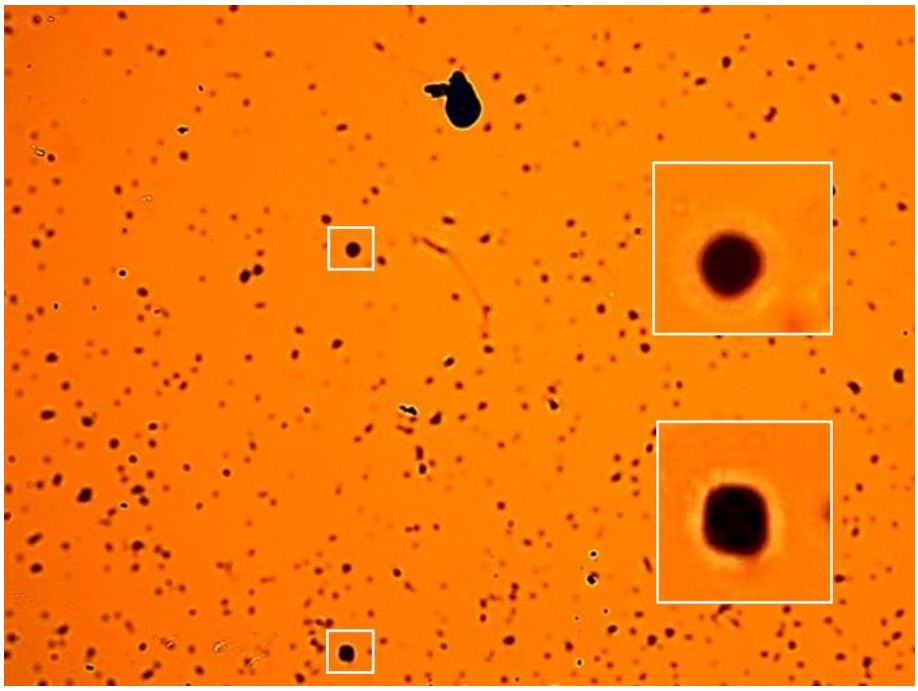

Figure 6. Image from the sample cuvette acquired with the lens-free test bench. The FOV in this case is 5,485 µm by 4,100 µm and the DOF enhacement is evident in the image quality of the two patterns. The lens-free setup used was $D_{PINHOLE}$ = 500 µm, Z_1=11 mm and Z_2 = 1.5 mm. Light Power 0.9 W and Exposure Times 200 ms. With this setup, the resolution achieved is 1.625 µm/pix (the 65 µm squared pattern is 40 by 40 pixel large).

The following images show the result of inspecting the same fluid sample under different pinhole, Z_1 and light power configurations. The starting light power for each pinhole has been the following, even if it has been regulated at each Z_1 distance to normalize the image brightness. With 500 µm pinhole the light source was polarized with 900 mW, the 200 µm one required1.2W and finally using the 50 µm pinhole 3W were applied (the LED saturation current). Photographic high pass filtering has been applied to the images for easing the detailed review of the readers. The images are centered in the circled micro pattern. The quality and resolution of the images is affected by the diffraction patterns generated by each particle, which increase in size and intensity while the aperture diameter reduces. Additionally, note that the FOV of the image shrinks as the pinhole gets closer to the sample (smaller Z_1).

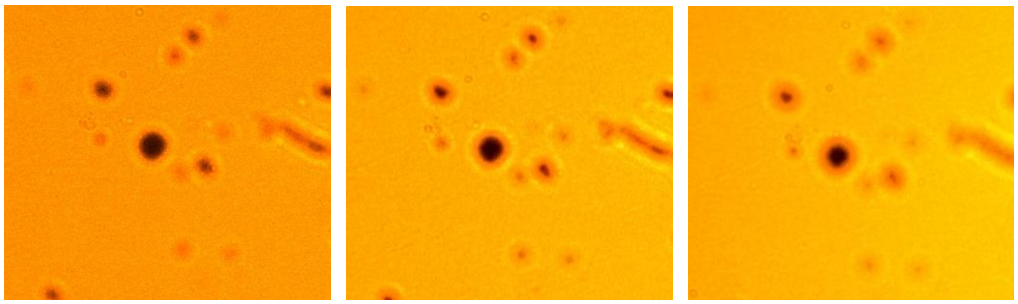

Figure 7. Sequence of images with $D_{PINHOLE}$=500 µm, Z_2 = 1 mm. Light Power ~0.9 W and Exposure Times 200 ms. From left to right Z_1 = 11mm, Z_1 = 7 mm and Z_1 = 4 mm.

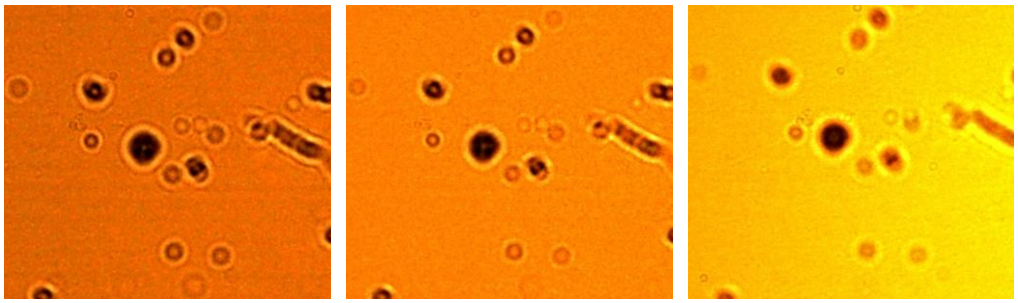

Figure 8. Sequence of images with $D_{PINHOLE}$=200 µm, Z_2 = 1.5 mm. Light Power ~1.2 W and Exposure Times 200 ms. From left to right Z_1 = 11 mm, Z_1 = 7 mm and Z_1 = 4 mm.

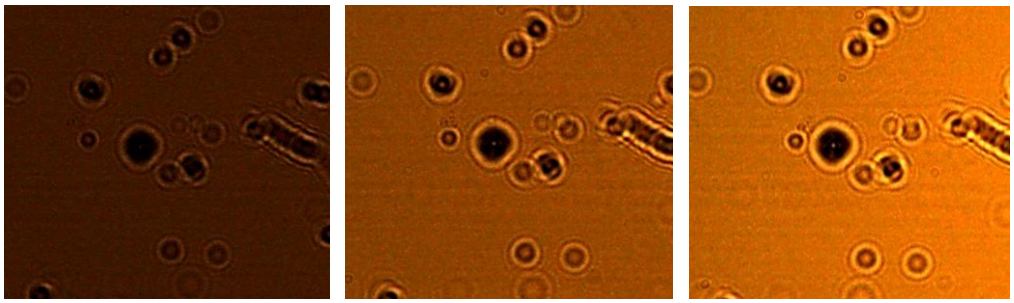

Figure 9. Sequence of images with $D_{PINHOLE}$=50 µm, Z_2 = 1.5 mm. Light Power ~3 W and Exposure Times 200 ms. From left to right Z_1 = 11 mm, Z_1 = 7 mm and Z_1 = 4 mm.

As mentioned earlier, instead of targeting a holographic reconstruction, the direct use of the acquired images has been selected as the first step in the sensor development. Therefore, the diffraction patterns are only contributing as noise factors, and therefore the design objective is to mitigate then. In this situation, the most promising results have been obtained with the largest pinhole diameter and the smallest Z_1 possible, in this case approximately 1mm and limited by the cuvette wall. Besides, the system offers the best performance when Z_2 is set to 10-11mm.

3. SENSOR DESING

The positive conclusions drawn from the experiments at the test bench were directly fed into the sensor prototype design specifications. However, bringing all the potential advantages achieved at laboratory experiments is not straightforward and some constructive and application specific constraints need to be solved. Some of these requirements directly impact on the applicability of the lens-free setup parameters, as it is the case for minimizing the Z_2 distance while the maximum pressure of the fluid is borne within the sample cell.

3.1 Sensor Description

The sensor solution is the outcome of the integration of different building blocks. The sensor includes a micro mechanical subsystem, with different parts as the hydraulic connections, microfluidic sample cell, which also deals with positioning of optical and electronic components and serves as external enclosure additionally. The optical subsystem includes the pinhole, light source and two transparent glass disks to confine the lubricant within the sampling cell. The glass disk in direct contact with the CMOS defines the Z_2 distance and its optimal thickness is a trade-off between enhanced optical performance and the maximum working pressure of the fluid.

Additionally, the sensor is equipped with the same CMOS camera and lighting solution as described in the Test Bench setup. Besides, the sensor includes all the auxiliary embedded electronics for processing the video and executing the machine vision algorithms for object recognition (the CPU is an i.MX6 from NXP manufacturer) and communicating (through Modbus TCP/IP) the results of the particle counting.

Reducing Z2 as much as possible (~ 0.5 mm) while maintaining the sensor reliability to high pressures and allowing the use of common hydraulic fast plug connectors (BSP Gas 1/8) has required to introduce crosswise sample inlet and outlets.

Integrating the electronics, mechanics and optics, the sensor dimensions are approximately 30x30x45 mm. The sensor body is fabricated in anodized aluminum and the sealing materials are fluorocarbons (for mineral or synthetic lubricant fluids) or EPDM (for measuring Phosphate Ester based hydraulic fluids).

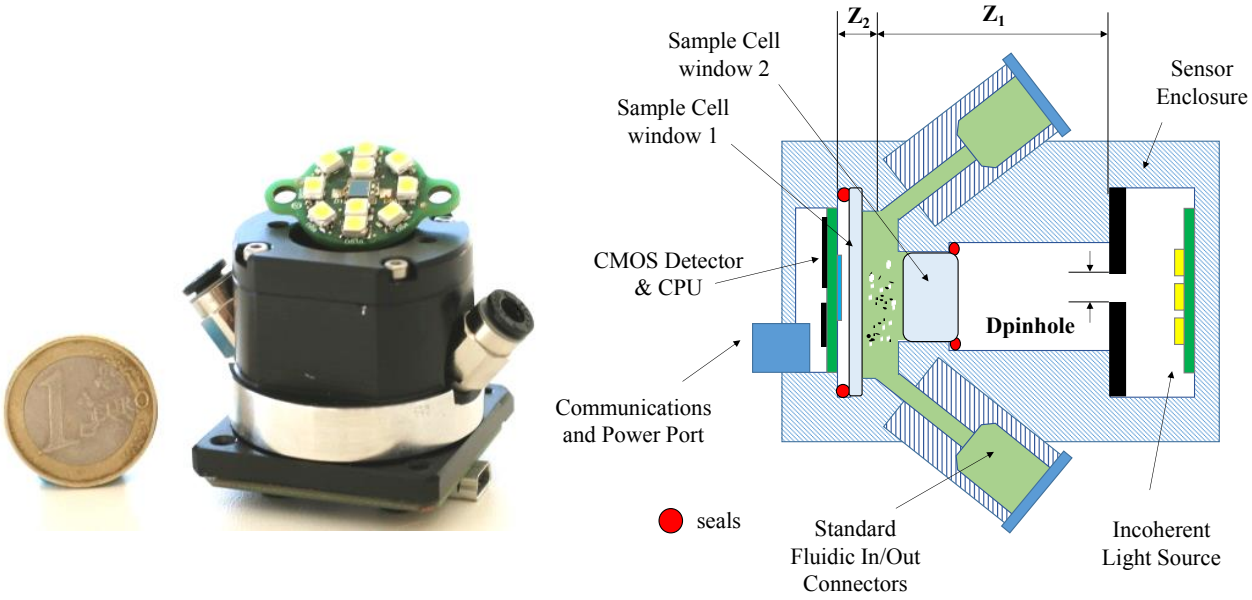

Figure 8. Sensor Prototype block diagram a photo. The light source is located in the top and the CMOS sensor at the bottom. The hydraulic inlet and outlet are located crosswise to the sensor body.

3.2 Sample Images

The sensor was connected to the lubricant test bench, which allows selecting different samples and different hydraulic configurations. The following images are examples captured with the sensor once installed in the test bench. Three different real lubricant samples have been feed into the system. These samples cover different absorptivity ranges: from very clear fluids (Fuch Renolyn), regular (Texaco Meropa) to very opaque lubricant (Castrol Optigear). The impact of the fluid opacity is evident in the frame intensity, and in the case of very dark samples, the sample is hardly illuminated in a homogenous way. On each image, different contamination sources are present (bubbles, fibers, particles) which will be later processed with the machine vision algorithms. In these configurations, the red ink mark is located in the first sample cell glass window disk and the blue one in the second glass window.

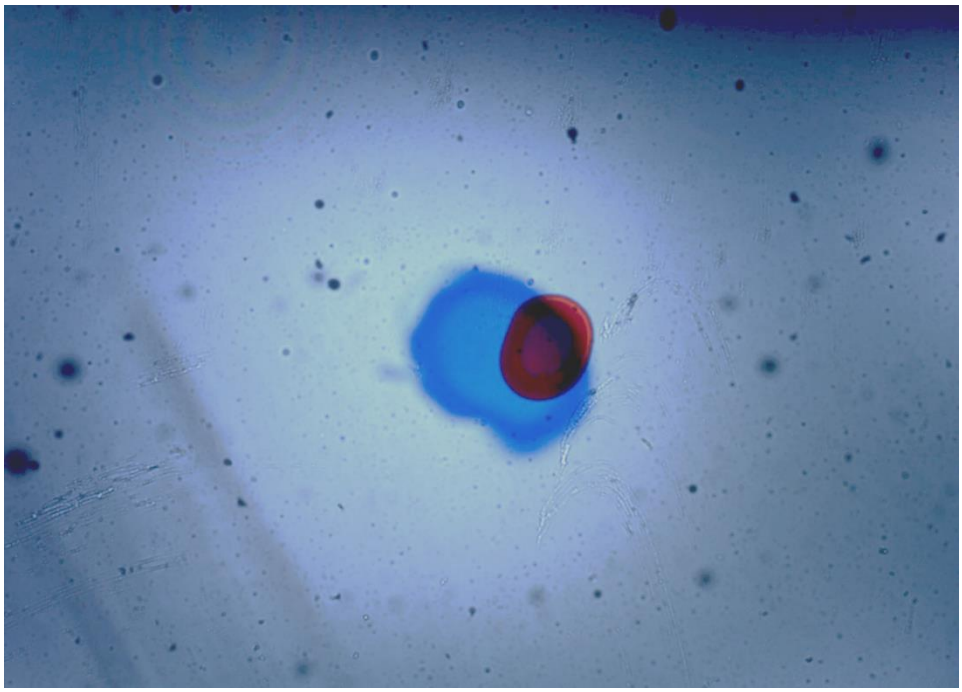

Figure 9. Fuch Renolyn sample. Different particles and fibers are present in the image.

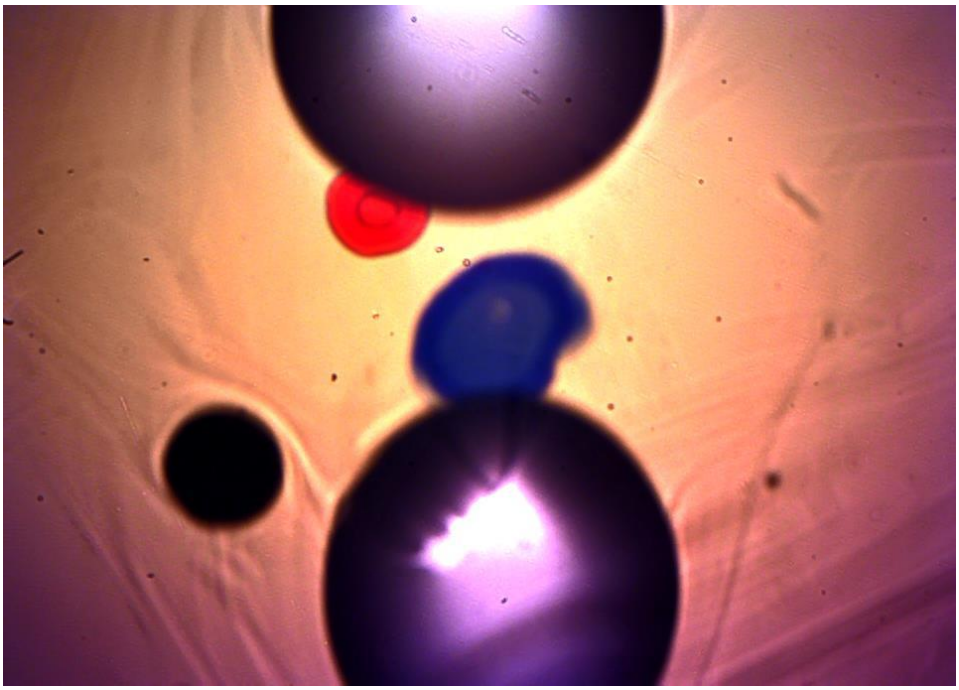

Figure 10. Texaco Meropa sample. In this case, big air bubbles could be observed. Asides, fibers and particles, non-homogeneity of the sample is evident, which may indicate the presence of other contaminants as varnishes.

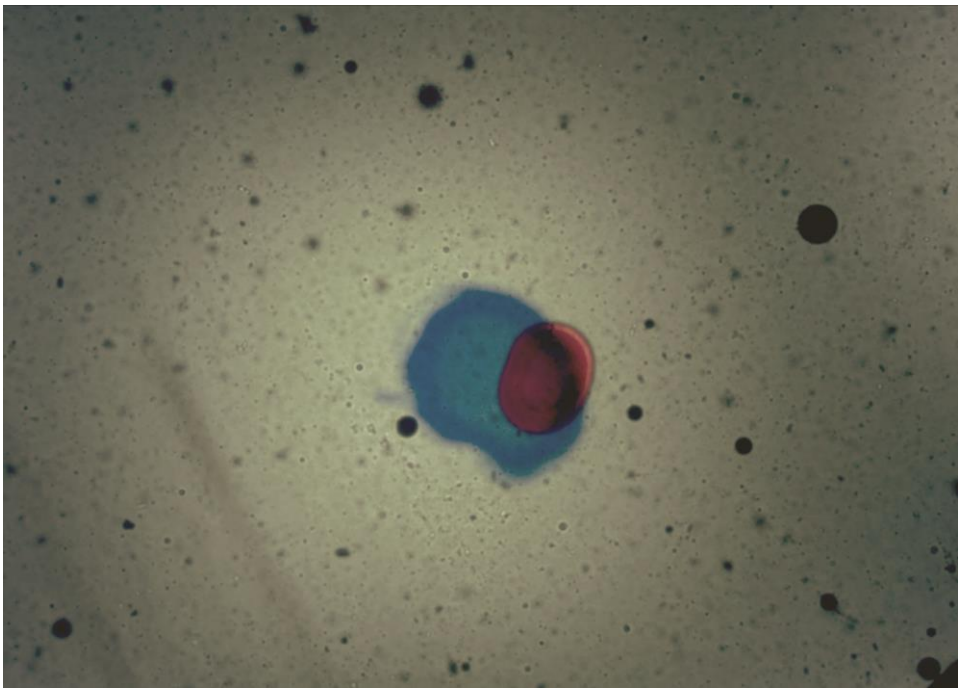

Figure 11. Castrol Optigear sample. Different particles and bubbles are present in the image.

3.3 Particle detection through Machine Vision Image Processing

So far, all the descriptions have been focused on the optical performance of the lens-free sensor. However, in order to validate the suitability of the proposed imaging solution, particle counting in real fluids must be accomplished successfully. A set of machine vision algorithms are applied to the images for the particle detection in the fluid sample. The summary of the operations include a dynamic background compensation (for elimination the static particles, effects of soiling in the optical windows, etc.), image preprocessing using a high pass filter and binarization based on a variance threshold. Then, the different regions of interest are analyzed and classified either as bubbles or particles, and finally the detected objects are classified by their size. These operations have been programmed using the Halcon Embedded Machine Vision library from MVTEC Company.

The execution time of these algorithms depends on the number of cores within the CPU used and in the number of objects present on the captured image. The i.MX6 processor (Cortex A9 structured) family allows executing the very same SW piece using 1, 2 or 4 cores. Therefore, depending on the applications real time or latency criticity, the sensor response time could be accommodated choosing the right CPU. This potential execution time reduction has been measured in different i.MX6 CPUs and in the new family of ARM Cortex A53 devices, the Qualcomm Snapdragon 410, being these results referenced in table 1. The execution times achieved processing different sample images are the described in table 2 (take into consideration that the resolution of the input images is 5 Mpix).

Table 1. Execution times of the algorithms being processed in different CPU architectures.

CPU	ARM Family	Core Number	Core Structure	Core Frequency	Execution time (%)
i.MX6 Solo from NXP (Qualcomm)	Cortex A9	1	32 bit	1 GHz	100%
i.MX6 Dual from NXP (Qualcomm)	Cortex A9	2	32 bit	1 GHz	75%
i.MX6 Quad from NXP (Qualcomm)	Cortex A9	4	32 bit	1 GHz	68%
Snapdragon 410 from Qualcomm	Cortex A53	4	64 bit	1 GHz	53%

Table 2. Particle detection and classification execution time using the i.MX6 Solo CPU, and the acceleration with the alternative CPUs.

CPU	Objects in the image			
	0	30	68	92
	Execution time (ms)			
i.MX6 Solo	608	865	1133	1315
i.MX6 Dual	456	648,75	849,75	986,25
i.MX6 Quad	413,44	588,2	770,44	894,2
SD 410	322,24	458,45	600,49	696,95

3.4 Sample Results

Applying the algorithms described above to the images acquired with the sensor, the particles present in one image are detected and classified by size. In the sample image below, the result data outputted by the embedded algorithms are summarized in table 3.

Table 3. Particle classification results according to ISO 4406 size groups for the sample image of figure 12.

Size Group	Particle Number
> 70 µm and < 400µm	1
> 38 µm and < 70 µm	13
> 21 µm and < 38 µm	29
> 14 µm and < 21 µm	7
> 6 µm and < 14 µm	22
> 4 µm and < 6 µm	5

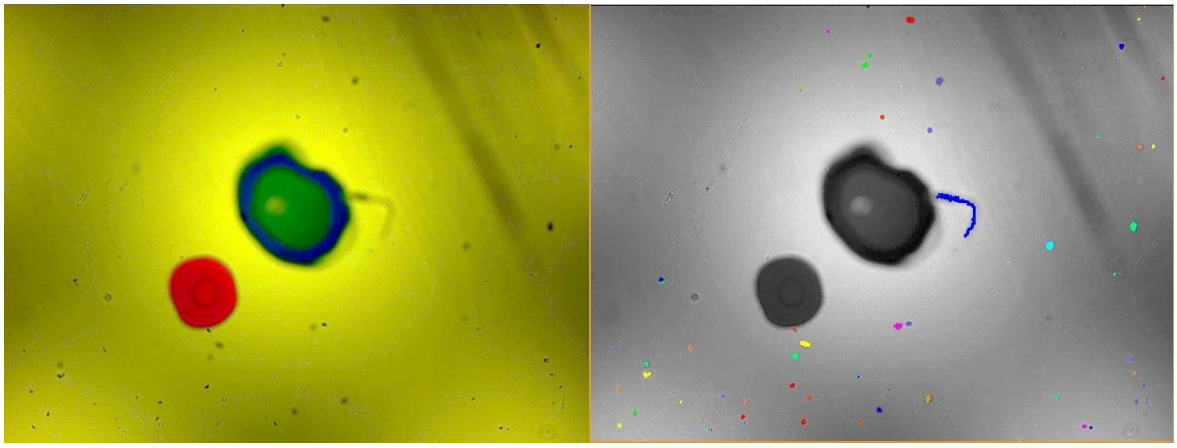

Figure 12. Original (left) and processed (right) images. The processed one overlays the detected particles.

The absolute size measurement values outputted by the algorithm are based on a prefixed parameter defining the µm/pixel value, which, for the example below have been set to 2.5 µm/pix. The way for practically avoiding this by-default parameterization is to include a precision marks within the FOV and use them to calibrate automatically every single sensor manufactured, this technique is out of the scope of this manuscript (as is reported in the patent [23]) but an example of this approach could be found in figure 10, where 8 precision patterns have been marked in the first glass disk to calibrate every measurement.

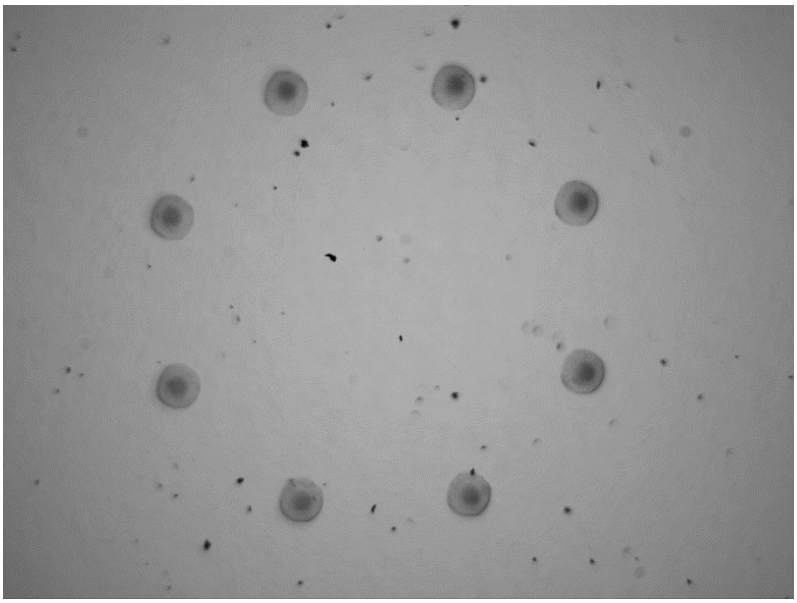

Figure 13. Precision marks with a diameter of 300µm added to the sample cell window for enabling a continuous auto-calibration.

4. CONCLUSIONS AND FUTURE WORK

In this manuscript, we have presented a detailed research on the performance of incoherent lens-free microscopy towards in-line analysis of wear debris focused on the use case of industrial fluidics monitoring. Specifically, we have validated the proof-of-concept analyzing the presence of wear particles in lube oils based on the direct use of images acquired with an incoherent lens-free setup. The values of the lens-free parameters have been optimized in a custom test-bench, achieving as preliminary results an optical performance of FOV=5.5 mm by 4.1 mm, DOF=500 µm (for ~70 µm objects) and 1.6 µm/pix resolution. These conclusions have been fed into the sensor design specification set, which, along with specific electronic design (including the lighting, CPU and communications) and the customized micromechanical solution, have been integrated into a tiny 30x30x45 mm wear debris sensor with a really cost effective bill of materials. Furthermore, examples of real lubricant measurements have been presented, including their particle counting and classification, as well as the execution times for accomplishing the machine vision algorithms, running on reference CPUs as the Cortex-A9 or the Cortex-A53. Future work has also been identified, as the inclusion of dimensional micrometric auto-calibration patterns within the FOV or the evolution from the direct use of the lens-free images to the utilization of holographic reconstruction for enhancing the sensor resolution towards the sub-pixel sampling. Probing a large sample volume with a decent 2D spatial resolution, this lens-free micro sensor could provide a powerful tool at very low cost for in-line wear debris monitoring.

REFERENCES

[1] Coronado, D. and Kupferschmidt, C., "Assessment and Validation of Oil Sensor Systems for On-line Oil Condition Monitoring of Wind Turbine Gearboxes," Procedia Technology 15, 747-754 (2014)
[2] Tavner, P. J., [Offshore Wind Turbines- Reliability, Availability and Maintenance], Institution of Engineering and Technology Press, London, 119-121 (2012).
[3] Link, H., Lacava, W., Van Dam, J.and B. Mcniff, "Gearbox Reliability Collaborative Project Report : Findings from Phase 1 and Phase 2 Testing," National Renewable Energy Laboratory (NREL), (2011).
[4] Dempsey, P. J., "Gear Damage Detection Using Oil Debris Analysis," NASA TM 210936, (2001).
[5] Miller, J. L. and Kitaljevich, D., "In-line oil debris monitor for aircraft engine condition assessment," Proc. IEEE Aerospace Conference 6, 49-56 (2000).

[6] Kumar, M., Mukherjee, P. S., Misra, N. M., "Advancement and current status of wear debris analysis for machine condition monitoring: a review," Industrial Lubrication and Tribology 65(1), 3 – 11 (2013).
[7] Rabinowicz, E, [Friction and Wear of Materials, 2nd Edition], John Wiley & Sons, 6-7 (1995).
[8] Peng, Z., Kessissoglou, N.J. and Cox, M., "A study of the effect of contaminant particles in lubricants using wear debris and vibration condition monitoring techniques," Wear 258(11), 1651-1662 (2005).
[9] Pall Corporation, "Industrial Manufacturing Pocket Book," Pall Corporation, USA,. https://www.pall.com/pdfs/Industrial-Manufacturing/POCKET_BOOK_EN_Standard.pdf (2016)
[10] Johnson, M., "The Past, Present and Future of Oil Analysis: An Expert Panel Discussion on the Future of Oil Analysis," Tribology and Lubrication Transactions, (2007).
[11] Johnson, M., "Machine Lubrication Best Practices Volume 28: Oil Analysis Program Development: On Site Analysis and Sensory Inspections," Tribology and Lubrication Transactions, (2010).
[12] Poley, J., "Metallic wear Debris Sensors: promising Developments in Failure Prevention for Wind Turbine Gearsets and Similar Components," Wind turbine Condition Monitoring Workshop, (2011).
[13] Zhu, J., Yoon, J., He. D., and Bechhoefer, E., "Online particle-contaminated lubrication oil condition monitoring and remaining useful life prediction for wind turbines," Wind Energy 17, (2014).
[14] Gorritxategi, E., Arnaiz, A., Aranzabe, E., and Villar, A., "On-line sensors for condition monitoring of lubricating oil". Proc. Int. Congress on Condition Monitoring and Diagnostic Engineering Management 22, 465–471 (2009).
[15] Day, M. J., Rinkinen, J. "Contaminant Monitoring of Hydraulic Systems - The Need for Reliable Data," Proc. Int. Congress on Condition Monitoring and Diagnostic Engineering Management 10, 171-182 (1997)
[16] Coronado, D., Bustamante, A., Kupferschmidt, C., "Oil-sensors test bench - an approach to validate oil condition monitoring systems for wind turbine applications," OilDoc Conference and Exhibition, 27-29 (2015).
[17] Appleby, M. P., [Wear Debris Detection and Oil Analysis Using Ultrasonic and Capacitance Measurements], Ph.D. dissertation, Analytic Chemistry Dept., University of Akron, USA, 68-81(2010).
[18] Han, L., Hong, W., and Wang, S., "The key points of inductive wear debris sensor," Proc. Int. Conference on Fluid Power and Mechatronics, 809-815 (2011).
[19] Crabtree, C.J., "Survey of Commercially Available Condition Monitoring Systems for Wind Turbines," Durham University, (2010).
[20] Reintjes, J. F., and Howard, P. L., "Fluid sampler utilizing optical near-field imaging," US Patent US5572320 A, (1996).
[21] Kong, H., "Method and apparatus for monitoring oil deterioration in real time," US Patent Application 20080024761 A, (2008).
[22] Kolp, J. P., Sebok, T. J., and Russell, D. E., "Tribological debris analysis system," US Patent 7385694 B, (2008).
[23] Mabe, J., and Gorritxategi, E., "System and method for monitoring a fluid," US Patent 9341612 B, (2013).
[24] Kim, S. B. et al. "Lens-Free Imaging for Biological Applications," Journal of laboratory automation 17(1), 43–49 (2012).
[25] Stahl, R. et.al, "Lens-free digital in-line holographic imaging for wide field-of-view, high-resolution and real-time monitoring of complex microscopic objects," Proc. SPIE 8947, (2014).
[26] Gabor, D. "A new microscopic principle," Nature 161, 777-778 (1948).
[27] Yuanyuan, H., Gu, Y., Zhanga, A. C., and Yu-Hwa, L., "Review: imaging technologies for flow cytometry," Lab Chip The Royal Society of Chemistry 16(24), 4639-4647 (2016).
[28] Lee, H. Xu, H., Koh, D., Nyayapathi, N., Oh, K.W., "Various On-Chip Sensors with Microfluidics for Biological Applications". Sensors 14(9), 17008-17036 (2014).
[29] Göröcs, Z., and Ozcan, A., "On-Chip Biomedical Imaging," IEEE reviews in biomedical engineering 6, 29–46 (2013).
[30] Kim, S. B., Bae, H., Koo, K., Dokmeci, M. R., Ozcan, A., and Khademhosseini, A. "Lens-Free Imaging for Biological Applications," Journal of Laboratory Automation, 17(1), 43–49 (2012)
[31] Mudanyali, O., Tseng, D., Oh, C., Isikman, S. O., Sencan, I., Bishara, W., Ozcan, A., "Compact, Light-weight and Cost-effective Microscope based on Lensless Incoherent Holography for Telemedicine Applications," Lab on a Chip 10(11), 1417–1428 (2010).
[32] Seo, S., Isikman, S. O., Sencan, I., Mudanyali, O., Su, T.-W., Bishara, W., Ozcan, A. "High-Throughput Lens-Free Blood Analysis on a Chip," Analytical chemistry 82(11), 4621–4627 (2010).
[33] Isikman, S. O., Bishara, W., Mavandadi, S., Yu, F. W., Feng, S., Lau, R., and Ozcan, A., "Lens-free optical tomographic microscope with a large imaging volume on a chip," Proc. of the National Academy of Sciences of the United States of America 108(18), 7296-7301 (2011)

[34] Bishara, W., Su, T.-W., Coskun, A. F., and Ozcan, A. "Lens free on-chip microscopy over a wide field-of-view using pixel super-resolution," Optics Express, 18(11), 11181–11191 (2010).

[35] Hellma Analytics, "Certificate of High-Precision Cells," Hellma GmbH & Co, Müllheim. www.hellma-analytics.com (2010)

[36] Villar, A., [Chemometric Methods Applied to the Optimization of Calibration of Vis-Nir Sensor Systems for Real Time Fluids Monitoring], Ph.D. dissertation, Analytic Chemistry Dept., University of the Basque Country, Spain, 50-55 (2014).

[37] Schilowitz, A.M., Szobota, J. S. and Vann, W. D., "Method for on-line monitoring of lubricating oil using light in the visible and near IR spectra," US 7172903 B, (2003).

(19) Europäisches Patentamt
European Patent Office
Office européen des brevets

(11) EP 2 980 557 A1

(12) EUROPEAN PATENT APPLICATION
published in accordance with Art. 153(4) EPC

(43) Date of publication:
03.02.2016 Bulletin 2016/05

(21) Application number: **13734813.2**

(22) Date of filing: **27.03.2013**

(51) Int Cl.:
G01N 15/02 *(2006.01)* ***G01N 33/28*** *(2006.01)*

(86) International application number:
PCT/ES2013/070207

(87) International publication number:
WO 2014/154915 (02.10.2014 Gazette 2014/40)

(84) Designated Contracting States:
AL AT BE BG CH CY CZ DE DK EE ES FI FR GB GR HR HU IE IS IT LI LT LU LV MC MK MT NL NO PL PT RO RS SE SI SK SM TR
Designated Extension States:
BA ME

(71) Applicant: **Atten2 Advanced Monitoring Technologies S.L.U.**
20600 Eibar Guipuzcoa (ES)

(72) Inventors:
- **Gorritxategi, Eneko**
  E-20600 Eibar (Guipúzcoa) (ES)
- **Mabe, Jon**
  E-20600 Eibar (Guipúzcoa) (ES)

(74) Representative: **Balder IP Law, S.L.**
Paseo de la Castellana 93
5a planta
28046 Madrid (ES)

(54) SYSTEM AND METHOD FOR MONITORING A FLUID

(57) System (18, 28) for inspecting oil, which comprises a cell (280) through which oil (281) flows through a pipe. Inside said cell (280) the system comprises a lighting system (284) based on at least one LED diode and configured to supply a beam of white light to the flow of oil (281); a diffuser (286) situated between the lighting system (284) and the flow of oil (281), configured to provide homogeneous lighting to the lit area; an image capture system (282, 382) situated on the opposite side of the pipe through which the oil (281) flows in respect of the lighting system (284) and configured to capture a sequence of images of the oil which flows inside said pipe; a lens (283) situated between the image capture system (282) and the flow of oil (281), configured to focus the captured images; a calibration device (287) situated between the lens (283) and the flow of oil (281); a processor (2851) configured to process said sequence of images and to determine the presence of particles and bubbles and a degradation value of the oil.

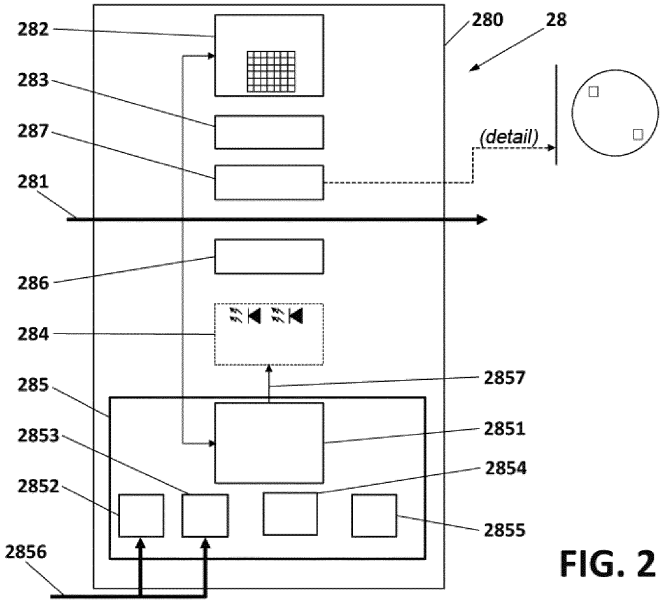

FIG. 2

EP 2 980 557 A1

Description

TECHNICAL FIELD

[0001] The present invention relates to the field of fluid monitoring for determining the general condition of fluids from the point of view of their degradation and also particle content. More specifically, it relates to the field of oil monitoring, in particular lubricating oils, in order to obtain through said monitoring their state of degradation, and also to obtain information on the machinery lubricated by said oils on the basis of their particle content.

BACKGROUND OF THE INVENTION

[0002] Industrial machinery, whether engines or power generating turbines, compressors, multipliers, etc. undergo unforeseen shutdowns and failures, often associated to aspects related to lubrication. The reduction in the service life of this industrial machinery often gives rise to unnecessary maintenance costs. Current 'off-line' measurement methodologies (oil sample analysis in the laboratory) do not provide a sufficiently early detection of the degradation process due to the low frequency with which these measurements are usually taken. Furthermore, in many contexts (transport, industrial, power...) this control methodology entails a significant logistical and financial burden. To deal with this drawback, the idea is to develop a new generation of sensors capable of analysing the machine's condition in real time.

[0003] Critical machinery could benefit from an increase in reliability, reduction in maintenance costs and early problem identification through the use of smart sensors.

[0004] Lubricating oil is one of the key components in some of these machines and provides a lot of information regarding the machine's condition. Oil heating, for example, can be a sign that the machine is not operating in optimum conditions, and the presence of particles in the oil may indicate a future failure or considerable wear in the lubricated components. It could even point to the existence of cracks or faults in joints that could allow the entry of external contaminants.

[0005] Some of the parameters that it could be interesting to monitor in lubricating oil are as follows: particle determination (for example, quantification, classification of size or determination of shape), bubble content in the system or oil degradation based on colour. Below is a brief description of these parameters.

[0006] Particle determination in lubricated systems is a key aspect in many sectors and applications, since the particles provide information on the condition of the machine that is being monitored. In other words, the detection of particles in the oil is indicative in many cases of a situation that will generate a future failure or a breakdown in the machine, or the presence of a fault in filters or joints.

[0007] At present, most of these lubricated systems install filtering solutions that remove the particles from the lubrication system. However, filtering systems do not act on the root cause of the problem, and instead are limited to reducing the consequences of particle generation, whose presence in the lubrication system could accentuate the generation of more serious problems. At the same time, filtering systems present a series of limitations: they can become clogged or saturated, not being capable of removing any more particles.

[0008] Traditionally, laboratory techniques have been used in order to determine the quantity and type of wear particles present in lubricating oil, and also to classify them according to size. Subsequently, different technologies for on-line particle detection have started to emerge, such as:

[0009] Detectors through light blockage: These systems are based on the reduction in intensity that the detectors receive when a particle passes through the measuring cell to which a beam of light is supplied. No image is collected, instead this reduction in light is observed, principally on some wavelength. It is not possible to determine the shape of the particles but it is possible to determine their size. The main problem with these systems is the presence of water or air bubbles, which are counted as particles.

[0010] Detectors through pore blockage: They also use optical detection, but without image gathering. However, before this, the oil is made to pass through a mesh (10 micras approx.) for classification avoiding the presence of water and air bubbles at the time that the measurement is taken.

[0011] Magnetic/electric detectors: Sensors that use a magnetic principle to detect ferromagnetic particles on the fluid, by making the fluid pass through a magnetic field that is altered by the presence of the ferromagnetic particles.

[0012] Detectors through image analysis: These analyse an image, quantifying particle content according to size, shape and type, using a neural network algorithm. One would cite, for example, analysis equipment that uses an image capture system, together with a laser lighting system and powerful image processing software installed on a computer. It is also capable of identifying contaminants, free water, and fibres. The equipment quantifies wear particles having a size between 4-100 micras, and the shape of particles larger than 20 micras. Particle analysis in this range is useful for detecting mechanical faults in a wide variety of lubricated systems. Depending on the shape, the particle is classified as: a) cutting; b) fatigue; c) sliding; d) non- metallic.

[0013] Below is a mention of patents that disclose image-analysis detectors:

[0014] For example, patent US5572320 describes an image analysis detector that includes a lighting system based on a pulsed laser. Detection is carried out by means of a planar array of light sensitive photodiodes or phototransistors. However, the system of US5572320 is not capable of discriminating between particle shapes. Also, the measuring cell of US5572320 consists of a moving part that positions the oil in a specific place, and this complicates development and can be an important source of errors.

[0015] Meanwhile, patent US7385694B2 describes a detector through image analysis that includes a lighting system based on a pulsed laser and a camera for gathering images of the oil subjected to such lighting. However, the device of this patent does not allow a homogenous lighting to be provided over an inspection area that is greater than the beam of light itself. Also, the device requires a pump in order to pump the fluid to the measuring zone.

[0016] Another of the parameters that it could be interesting to monitor in lubricating oil is the bubble content in the system, since this can be indicative of foam generation in the oil and air retention in the system, which is undesirable. Both must be controlled and reduced to a maximum in order to achieve optimum functioning of the oil inside the system. This is critical in systems such as the multipliers of wind turbines. The maximum acceptable foam levels for used oil, according to method ASTM-D892, must not exceed:

Temperature	*Formation (5'blowing)*	*Stability (10 blowing)*
24ºC	100	10
93.5ºC	200	20
24ºC	100	10

[0017] The content in retained oil must not exceed 25% in respect of new oil according to ASTM-D3427.

[0018] Finally, oil degradation based on colour is another parameter that may be interesting to monitor in lubricating oil:

[0019] Oil degradation is a key indicator of oil quality and how it fulfils its lubricating mission. It does not provide information on the machine directly, but indirectly from the speed of degradation it would be possible to extract information regarding the machine's operation. The degradation process of oil follows several very well-known steps: first it suffers a loss in additive content, then acidic compounds are generated, and finally, when it is in an advanced state of degradation, polymerisation processes begin in these acidic compounds that have been generated. The percentage of acidic constituents (in the form of additives in the case of new lubricating oils and in the form of oxidation compounds in the case of lubricating oils in service) is determined through analytical techniques.

DESCRIPTION OF THE INVENTION

[0020] The present invention attempts to resolve the drawbacks mentioned above by means of a system for inspecting oil, which comprises a cell through which oil flows along a pipe. The system comprises inside said cell: a lighting system based on at least one LED diode and configured to supply a beam of white light to the flow of oil; a diffuser situated between the lighting system and the flow of oil, configured to provide homogeneous lighting in the lit area; an image capture system situated on the opposite side of the pipe through which the oil flows in respect of the lighting system and configured to capture a sequence of images of the oil that flows inside said pipe; a lens situated between the image capture system and the oil flow, configured to focus the captured images; a calibration device situated between the lens and the oil flow; a processor configured to process said sequence of images and to determine the presence of particles and a value for the oil degradation.

[0021] Preferably, the lighting system comprises a polarisation control system of at least one LED diode configured to avoid emission fluctuations due to changes in temperature.

[0022] Preferably, the diffuser is situated closing and sealing a hole made in the pipe through which the fluid flows.

[0023] In a possible embodiment, the diffuser is a frosted glass.

[0024] Preferably, the image capture system is a camera.

[0025] In a possible embodiment, the calibration device situated between the lens and the oil flow comprises a plurality of markings designed to calibrate the system. Preferably, the calibration device is situated closing and sealing a hole made in the pipe through which the oil flows.

[0026] In another aspect of the present invention, a method is provided for auto-calibration of the system for inspecting oil mentioned above, which comprises the stages of:

- carrying out on the calibration device at least one marking of known dimensions;
- capturing an image of an oil using the image acquisition system;
- adjusting the capture parameters to increase the contrast of the captured image until finding the system's optimum

polarisation;
- capturing a new image;
- binarising said image with dynamic threshold;
- in said image, identifying the geometry of said at least one marking;
- carrying out the horizontal and vertical measurement of the number of pixels and applying a correction in respect of their real sizes;
- saving said correction as the calibration measurement for the absolute dimensional measurements obtained by the system during its subsequent use.

[0027] In another aspect of the present invention, a method is provided for the detection and discrimination of particles and bubbles in an oil by means of the system for inspecting an oil described above, which comprises the stages of:

- capturing an image of the oil using the image acquisition system;
- adjusting the capture parameters to increase the contrast of the captured image until finding the system's optimum polarisation;
- capturing a new image;
- binarising said image with dynamic threshold;
- conditioning the binary image;
- detecting the objects that are considered bubbles or particles by means of applying techniques for searching for connected components or for detection and dimensional identification of pixel groupings;
- in order to distinguish between bubble and particle:

    - applying an inversion of the binary image in those regions where potential particles or bubbles have been detected;
    - applying dilation-based conditioning to those inverted regions of interest;
    - applying to those zones techniques for detecting connected components in order to detect holes in the original groupings of pixels, identifying as bubbles those zones that present pixel groupings with holes, and identifying as particles those pixel groupings detected without an inner hole;

- based on the pixel groupings, counting and calculating the size of the bubbles and particles, wherein the calculation of said size comprises applying to those pixels the dimensional correction obtained in the auto-calibration method described above.

[0028] In another aspect of the present invention, a method is provided for obtaining an oil degradation parameter using the system for inspecting an oil described above, which comprises the stages of:

- applying to the lighting system described above, a temperature compensation algorithm;
- capturing an image of the oil with the three colour channels - red, green, blue - using the system's image acquisition system;
- extracting from said image the regions with pixel groupings and generating an image with those zones marked with a negative value;
- carrying out a measurement of the transmittance in the red band I_R, transmittance in the blue band I_B and transmittance in the green band I_G, adding up the value of each one of the pixels divided by the number of pixels used for the inspection;
- applying an algorithm to obtain a degradation parameter n the basis of said three colour channels.

[0029] Preferably, said obtaining of a degradation parameter based on said three colour channels is obtained from the formula $CI=1*I_R+0.5*I_G+0.5*I_B$, wherein CI is the value of the oil's colour index.

BRIEF DESCRIPTION OF THE DRAWINGS

[0030] As a complement to the description and with a view to contributing towards an improved understanding of the characteristics of the invention, according to an example of a practical example thereof, a set of drawings is attached as an integral part of this description, which by way of illustration and not limitation, represent the following:

Figure 1 represents a general outline of the monitoring system of the invention.
Figure 2 shows an outline of the measurement module according to a possible embodiment of the invention.
Figure 3 illustrates schematically a method for auto-calibration of the measurement system, according to a possible

embodiment of the invention.

DESCRIPTION OF AN EMBODIMENT OF THE INVENTION

[0031] Figure 1 represents a general outline of the monitoring or inspection system of the invention. The system is composed of a series of sub-systems connected to each other and contained within a receptacle or container 10. The sub-systems are as follows:

[0032] A hydraulic conditioning sub-system, made up of components for flow control 12, oil flow control by means of electrovalves 11 19, pressure control 13, safety filter 14 and the inlet 15i and outlet 15o piping. The reading and operation of the active hydraulic elements is carried out from the electronic sub-system 16. It is noteworthy that the hydraulic conditioning sub-system does not include any pump, unlike the system described in US7385694B2. In a preferred embodiment, the system of the invention is designed to be installed in a by-pass of the lubricating system of certain machinery. The installation takes advantage of the pressure differences for the fluid to circulate to the measurement module 18 where the oil inspection will take place.

[0033] An electronic sub-system formed by an embedded electronic platform 16 for managing all active sub-systems and managing data channels. This embedded electronic platform 16 performs the global management of information and control of the hydraulic and measurement sub-systems. This sub-system is considered to include the internal and external connection technologies and the power system 17.

[0034] A sensor sub-system or measurement sub-system 18, which represents the sub-system where the measurement is carried out and which is described below. The measurement module 18 delivers totally valid measurement values without the need for processing.

[0035] The container and fastening system 10 which incorporates the external hydraulic and electrical connections and the fastening system (not shown in figure 1) to the installation's place of destination. The system 10 is specifically designed for its direct integration into the lubricating systems of machinery but without affecting the operating conditions thereof. This is achieved by means of the hydraulic sub-systems of the sensor which make it possible to carry out controlled sampling with low content in lubricating oil. The container and the fastening system 10 houses and integrates the different elements in an appropriate manner and allows external communication for the intake and output of the fluid, through the respective inlet 15i and outlet 15o (as the measurement is carried out in the measurement sub-system 18) and provides the communication interfaces and power supply 17 in order to be able to carry the sensor's results to the machine in question or wherever required.

[0036] The hydraulic sub-systems in turn allow the fluid to be measured to be conditioned, thereby reducing the effects of external conditions or factors on the end result. The system has also been developed to avoid the influence of environmental factors such as changes in temperature. In this sense, the sensor system has temperature measurers that actuate the intensity of the light emitting diode and thereby prevent differences in emission related to changes in temperature.

[0037] As can be seen from figure 1, the fluid enters the container 10 through the inlet 15i. The flow of fluid follows the direction of the dotted arrow line. The fluid circulates through the inside of the container 10 through appropriate channelling means, such as pipes. Through the inlet and outlet fittings and the sub-systems it is possible to carry out a representative sampling of the fluid (for example, oil) and to condition it to obtain representative measurements of its real condition.

[0038] Flow control 12 makes it possible for the system to obtain a fixed flow which makes it possible to know the amount of fluid that is being measured and thereby to obtain the particle concentration therein. In other words, the flow control 12 makes it possible to give values of, for example 100 particles per millilitre. Otherwise, it would only be possible to say that 100 particles were detected, in absolute terms.

[0039] Optionally there may be a safety filter or filter with pressure control 14 which serves to prevent large-sized particles from entering the measurement module 18, which could damage or soil the module's windows and even ensure that the system does not become clogged with large particles.

[0040] The pressure switch 13 is a pressure system that ensures that there is pressure in the system and therefore guarantees that there is a flow of the fluid (for example, of oil). Therefore, it is a pressure switch designed to identify low pressures. The issue is that the machines in which the sensor is installed (module 18) are not functioning continuously, and when they are stopped there is no oil pressure, meaning that there is no entry of oil in the sensor, which results in the measurement eventually taken not being representative, because oil is not being measured. With the pressure switch 13 there is detection of pressure when there is and when there isn't pressure, in order to validate a taken measurement and thereby ensure that it is oil and not air that is being measured.

[0041] Both the inlet electrovalve 11 and the outlet electrovalve 19 perform the function of allowing the oil in or not. When the electrovalve is "ON", the system is open for the oil to pass; and when the electrovalve is "OFF", the system is closed and the oil does not enter. This is carried out so that the oil is not continuously flowing through the system, for two important reasons: (1) to carry out controlled sampling and interfere as little as possible with the machine's lubricating

systems; (2) to ensure that the hydraulic sub-systems are not affected by dirt that could be generated by the continuous flow of oil.

[0042] The ON/OFF arrows indicate in respect of the components next to which they appear in figure 1, that these components are controlled electronically. Specifically, on electrovalves 11 19 the ON/OFF arrows indicate the opening and closing off of entry to the oil; and in the pressure switch 13 and filter 14 the ON/OFF arrows provide an indication of the pressure level in the system. The pressure switch 13 is "ON" when a specific pressure value is exceeded and then it is assumed that oil has entered; in filter 14, the pressure control that it incorporates ensures that the oil does not exceed a maximum pressure value.

[0043] Figure 2 represents an outline of the measurement sub-system or sensor sub-system of the invention (sub-system 18 in figure 1). This module or measurement sub-system 28 has been conceived as an autonomous sub-system with totally independent functioning, which delivers auto interpretable measurements, calibrated and corrected for the entire defined operating range. As described below, the measurement sub-system 28 operates on a micromechanical cell 280 through which the fluid 281 under supervision circulates. In a preferred embodiment, this fluid is oil, more preferably lubricating oil. The fluid 281 is driven inside channelling means, such as for example a pipe.

[0044] The measurement sub-system or module 28 comprises an optical part and an electronic part (or video acquisition and processing sub-system). As can be seen, this video acquisition and processing sub-system is an independent electronic from the embedded electronic platform 16 of the complete system. The first is found inside the measure module 18 28, whereas the second is a module 16 extraneous to the measurement module. This video acquisition and processing sub-system carries out the activities related to measurements, among other things. The video acquisition and processing sub-system is made up of an embedded image capture system 282 and by electronics 285 which comprise an embedded processor 2851. The measurement sub-system 28 is based on an embedded artificial vision measurement system, wherein by means of an image capture system 282 a video sequence is captured which is processed in an embedded processor 2851. The objective of the processing is to determine the presence of particles and/or bubbles and the degradation value of the fluid (for example, oil) (OD). The arrow between the image capture system 282 and the embedded processor 2851 outlines the video data and control lines.

[0045] In a possible embodiment, an acquisition and processing system of 4 frames per second (4FPS) is used. For example, and Omnivision detector can be used with a 14 megapixel camera.

[0046] The optical part comprises a lighting system 284 to subject the flow of fluid 281 to a beam of light and an image capture system 282 to capture a video sequence that will afterwards be processed in an embedded processor 2851 of the electronics part 285. In a preferred embodiment, the embedded processor 2851 is a DSP device (*Digital Signal Processor*).

[0047] The lighting system 284 is designed to supply a beam of white light to the fluid. Preferably, the lighting system is based on one or more LED diodes which continuously light the flow 281 which circulates through the micromechanical cell 280. In other words, preferably, the lighting system is a LED emitter 284. Preferably, the emission system 284 has a control system (closed loop control) of the polarisation of the LED emitter based on changes in temperature which prevent fluctuations in emission due to said changes in temperature. As a person skilled in the art knows, when the temperature rises there is a reduction in the emission of the LEDs due to a decrease in the efficiency of the photons. By means of this control, if the temperature rises the power is increased so that the apparent emitted light remains constant. In a possible embodiment, the lighting system 284 comprises also a photodiode near the lighting zone to calculate the error of that closed loop. The embedded processor 2851 controls the lighting system 284, through LED control signals and compensation data 2857.

[0048] Between the lighting system 284 (preferably LED emitter) and the flow of fluid 281 (which circulates inside a pipe), a diffuser 286 is placed having the principal mission of diffusing the amount of light emitted by the lighting system 284 in order to obtain a homogenous lighting over the entire area (amount of fluid, preferably oil) that is being inspected. In a preferred embodiment, the diffuser 286 is a window. The diffuser 286 is called a "window" because it is the element that provides visual access to the fluid under inspection. Thanks to this diffuser 286 it is possible to light the area under inspection in a homogeneous manner.

[0049] The diffuser (diffuser window) 286 is placed closing a hole made in the pipe through which the fluid 281 flows. In other words, the fluid (oil) passes through the pipe or conduit, but transversally to the direction of the fluid a hole is made through which the fluid will be inspected and measured. The hole is preferably circular and the diffuser window 286 is also preferably. This diffuser 286 prevents the fluid (oil) leaking through the holes made. This window 286 acts as a seal so that the fluid does not leak through the transversal hole. The diffuser 286 is moreover made of a transparent material that allows light through it. Therefore, the lighting system 284 can light the fluid appropriately, and by means of the detection system 282 it is possible to visualise this zone and to capture the image of the fluid. In a preferred embodiment, the window 286 is a glass, for example a frosted glass.

[0050] The light that is not absorbed by the fluid is gathered by means of a detector (for example, a photodiode or photodiode array). In an inspection system by means of artificial vision, by using back lighting, the optical receiver element (the 2D photodiode array) collects the light that passes through the flow of fluid (for example, oil).

[0051] Opposite the lighting system 284 (LED emitter), on the other side of the pipe through which the flow 281 circulates, an image capture system 282 is situated to capture the video sequence (which is no more than a train of images) of the zone of interest in the passage of the fluid (preferably oil). This image capture is carried out with a defined spatial resolution and maintaining the general criteria of reduced size and low cost. In other words, the "defined spatial resolution" refers to the fact that the capture system 282 is capable of determining a defined minimum size of particle, which is in the region of 4 micras over an inspection area of about 100 mm^2. This resolution is achieved by optimising several conditions, such as the area to be inspected, the size of the camera, its number of pixels, and the characteristics of the lens 283 (which is mentioned below). The module 28 and in general the complete system 10 must have a small size and be as compact as possible.

[0052] In a preferred embodiment, the image capture system 282 is a camera, more preferably a camera based on CMOS sensor or CMOS detector (the CMOS sensor is the camera component that receives the image). Therefore, a CMOS camera has a 2D array of photoreceptors manufactured with CMOS technology. For this reason, occasionally in this text the expression "CMOS sensor" or "CMOS detector" is used to refer to the camera 282. The images captured by this camera are processed in the embedded processor 2851 of the electronics part 285. In a preferred embodiment, the embedded processor 2851 is a DSP device (*Digital Signal Processor*). This embedded processor 2851 is the one that analyses for each image whether there are bubbles and particles and counts them following the procedure described further below. In other words, the processor is responsible for extracting the image from the CMOS and processing it. To do this, it has an intermediate memory 2854 for subsequent processing. In a possible embodiment, this intermediate memory is a DDR2 external memory.

[0053] Between the image capture system (CMOS detector) 282 and the flow of fluid 281 under inspection there is a lens 283, preferably a macro lens, responsible for transporting the image from the object to the camera 282, in other words, it is responsible for the camera 282 appropriately focusing what is required to be detected. The lens allows objects to be focused in the light-reactive element and objects to be captured. The lens carries the light in focus to the light receiving area.

[0054] Between the lens (macro lens) 283 and the pipe that collects the flow of fluid 281 under inspection another optical device or optical window 287 is placed which is also placed sealing a hole made in the pipe through which the fluid 281 flows. This hole is opposite the hole described above (and covered by the diffuser 286). This second optical window 287 also acts as a seal so that the fluid does not leak through the transversal hole. It is also made of a transparent material that allows light to pass through it. The hole is preferably circular and the optical window 287 is also preferably. Preferably, the window 287 is a calibration window which comprises markings or patterns that allow it to be auto-calibrated (as explained below). The markings are of a specific size and in this way it is possible to automatically calibrate the equipment avoiding errors or dispersions due to assembly or manufacture. Figure 2 illustrates an enlarged close-up of the optical device or optical window 287 which includes two markings by way of an example.

[0055] The minimum size of particle that it must be possible to discriminate is of approximately 4 μm. The area to be captured in each image by the image capture system (CMOS detector) 282 must be such that it is capable of capturing particles of 4 μm and more. In a preferred embodiment, the area to be captured is of several square millimetres. In one example, said area to be captured is of 100 mm^2. At the same time, the distance between the object (plane of passage of the fluid under inspection) and the CMOS detector 282 is desirably as minimum as possible and does not exceed approximately 100 mm, so that the system can be as compact and small as possible. The maximum depth of field (range in which the lens 283 is capable of providing a focused image) is marked by the width of the passage of the oil through the micromechanical cell 280.

[0056] As has been explained, the measurement sub-system or module 28 comprises diffuser means 286 of the inspected area. Thanks to the LED diodes and to these diffuser means, it is possible to obtain a homogeneous lighting of all of the inspected area. Conventional oil supervision systems do not homogenise the area under supervision, meaning that particle detection is not optimal. The inventors have observed that, especially when white light is used, this homogenisation is important in order to obtain reliable results.

[0057] The video acquisition and processing sub-system (embedded image capturer 282 and electronics 285 with embedded processor 2851) is the one responsible for acquiring and processing the video sequence supplied by the camera 282 of the optical sub-system. The power and precision of the measurement or sensor sub-system 28 is the direct result of the processing algorithms run by this video acquisition and processing sub-system.

[0058] In figure 2, the electronic part 285 comprises, in addition to the embedded processor 2851, auxiliary systems (communication interface 2852, power source 2853, memory 2854, temperature sensor 2855...). Reference 2856 indicates the electronic interface of communication and the power source). Also, there is a software part, formed by the group of algorithms in charge of the detection and classification of particles, bubble detection and determination of degradation.

[0059] In a particular embodiment, the video acquisition and processing sub-system is responsible for applying algorithms for the dimensional calibration of the measurement module 28. Basically, the auto-calibration is based on identifying using the image capture system (CMOS detector) 282 markings, of a known size, made on the calibration window 287

so that any identified image can then be scaled. One example of these markings is shown in the close-up of the calibration window 287 of figure 2. Although this is explained in detail further below, figure 3 illustrates schematically the auto-calibration of the proposed measurement system. The calculation of the size of the detected particles is the product of the entire configuration of the optical sub-system. It is known that the manufacturing and assembly tolerances introduce a dispersion in the system's focus, and consequently in the apparent size of the objects captured on the camera. In order to correct this deviation, compensation is applied through dimensional auto-calibration of the module. This auto-calibration is the result of applying some algorithms of dimensional identification (which are explained further below) to known shapes marked in the calibration window 287 and then applying said proportionality to all of the dimensions calculated by the system.

[0060] The inventors have observed that this auto-calibration makes it possible to diminish the effects of the mechanical and assembly tolerance on the size of the images of particles captured on the camera. The auto-calibration allows, in contrast to conventional oil supervision systems, automatic compensation of these differences in the sizes of the objects captured due to the manufacturing and assembly dispersion. It also means that it is not necessary to dimensionally calibrate each unit of equipment. Also, it makes the system more robust against potential degradations occurring in the machine. In other words, the auto-calibration system and algorithm impose the required precision of the system (4 μm) on the auto-calibration markings and not on the entire micromechanical system, although in practice the result is equivalent to imposing said precision requirements on the whole system.

[0061] What follows is a description of the different algorithms and procedures of the invention, for the detection and classification of particles, fluid (oil) degradation, and others:

Detection, discrimination and classification of particles and bubbles algorithm (DDC-PB)

[0062] The particle detection and discrimination algorithm must one the one hand discriminate between bubble and particle, and count and classify particles by size. Optionally, it comprises also algorithms for control of lighting/exposure to improve detection sensitivity. The particle detection and discrimination algorithm comprises the following steps:

a. Capturing an image with the image acquisition system 282 382. Preferably, this image is taken at the system's medium resolution and in gray scale.
b. Adjusting the capture parameters, preferably by means of applying control of the exposure time of the image acquisition system 282 382 and current control of the LED 2857 in order to increase the contrast of the captured image until finding the system's optimum polarisation.
c. After adjusting the capture parameters, capturing a new image, preferably with maximum resolution in gray scale.
d. Binarising the image with dynamic threshold (based preferably on analysis of the mean and standard deviation of luminance in different zones of the image).
e. Conditioning the binary image, preferably by means of the 2D enlargement technique, which makes it possible to group dispersed pixels together and to generate denser pixel concentrations.
f. Applying techniques for searching for connected components or dimensional detection and identification of pixel groupings. This technique is used to detect objects that are considered to be bubbles or particles. From this point onwards, methods of discrimination between bubble and particle are applied.
g. Applying an inversion of the binary image in those regions where objects have been detected (potential particles or bubbles).
h. Applying a conditioning based on enlargement to those inverted regions of interest.
i. Applying in those zones the same techniques of connected component detection. In this case, holes in the original pixel groupings are being detected.
j. Those zones that present pixel groupings with holes are identified as bubbles due to the fact that the proposed lighting system makes the bubbles be captured as circular objects having a very shiny zone within their circumference due to the light diffraction occurring in the air contained by the bubble.
k. Consequently, those pixel groupings detected as not having a hole inside are considered to be particles.
l. Next, the bubbles and particles are counted and classified. Size classification is carried out preferably in number of pixels of the highest value between the height and the width of the pixel grouping.
m. To conclude, with regard to calculating the real size of the particles and delivering a normalised value based on standard classifications, applying to those sizes in pixels the dimensional correction provided by the dimensional auto-calibration algorithm (see the following point).

Dimensional auto-calibration (ACD)

[0063] The calculation of the size of the particles is the product of the entire configuration of the optical sub-system. It is known that the manufacturing and assembly tolerances introduce a dispersion in the system's focus, and consequently

in the apparent size of the objects captured on the image capture system. In order to correct this deviation, in a particular embodiment, compensation is applied through dimensional auto-calibration of the measurement module 28. Basically, the auto-calibration is based on identifying by means of the image capture system 282 markings, of a known size, made on the optical device 287 so that it is then possible to scale (apply that proportionality to) any identified image.

[0064] The auto-calibration algorithm presents the following stages:

a. Capturing an image using the image acquisition system 282 382. Preferably, this image is taken at medium resolution and in gray scale.
b. Adjusting the capture parameters, preferably by means of applying control of the exposure time of the image acquisition system 282 382 and current control of the LED 2857 in order to increase the contrast of the captured image until finding the system's optimum polarisation.
c. After adjusting the capture parameters, capturing a new image preferably with maximum resolution in gray scale.
d. Binarising the image with dynamic threshold (based preferably on the analysis of the mean and standard deviation of luminance in different zones of the image).
e. Identifying the geometry of each pattern shape, by means of applying classification techniques to the areas found (the markings of known size made on window 287) taking into account the size and characteristics of the shape, such as length, circularity, compactness, roundness, rectangularity, or others.
f. After identifying the geometries of the pattern shapes, carrying out the horizontal and vertical measurement of the number of pixels and applying a correction in respect of their real sizes in micrometres.
g. Using this correction as a calibration measurement of all absolute dimensional measurements supplied by the system during its subsequent use.

[0065] Figure 3 shows an example of execution of stage f above: The image acquisition system 382 captures one of the markings or patterns of the optical device 387. Given that this marking has been made intentionally on the optical device 387, it is known that its real dimensions are, for example, 100μmx200μm. At the same time, the capture made by the image acquisition system 382 provides a size of the captured object of, for example 12 pixels x 24 pixels. After applying the processing and the corresponding algorithm, it is established that the correction factor to be applied is 0.12 pixel per μm.

Oil degradation parameter calculation algorithm (OD)

[0066] In order to calculate the fluid (preferably oil) degradation parameter there is a discrimination made to segment the image and use only those areas that are "clean" of particles and bubbles. In those segments, colorimetry algorithms are applied. Due to the fact that this is an analysis of colour intensity, in this case, a known lighting/exposure configuration must be used, corrected only to offset the effect of the temperature.

[0067] The algorithm for calculating the degradation parameter presents the following stages:

a. Applying a compensation algorithm for the temperature of the lighting system.
b. Capturing an image preferably at medium resolution with the three colour channels (RGB).
c. Applying an algorithm of detection and discrimination of particles and bubbles (DDC-PB) and extracting the regions with pixel groupings to generate an image having those zones marked with a negative value (nonexistent).
d. Carrying out a mean of the intensity of each one of the channels or bands I_R I_B I_G (red band transmittance, blue band transmittance, and green band transmittance, respectively), adding up the value of each one of the pixels divided by the number of pixels used for the inspection.
e. Applying an algorithm to obtain a degradation parameter based on the three colour channels RGB. In a preferred embodiment, applying the following formula: $CI=1*I_R+0.5*I_G+0.5*I_B$, wherein CI is the value of the fluid's colour index.

[0068] Not all processing must be performed in the same cycle, meaning that response time requirements are relaxed.

[0069] Throughout this document, the word "comprises" and variants thereof (such as "comprising", etc.) must not be interpreted as having an exclusive meaning, in other words, they do not exclude the possibility of what is being described incorporating other elements, steps, etc.

[0070] At the same time, the invention is not limited to the specific embodiments described herein and also extends, for example, to variants that may be embodied by an average person skilled in the art (for example, with regard to the choice of materials, dimensions, components, configuration, etc.), within the scope of what is inferred from the claims.

Claims

1. A system (18, 28) for inspecting oil, which comprises a cell (280) through which oil (281) flows through a pipe, the system (18, 28) being **characterised in that** it comprises inside said cell (280):

   a lighting system (284) based on at least one LED diode and configured to supply a beam of white light to the flow of oil (281);
   a diffuser (286) situated between the lighting system (284) and the flow of oil (281), configured to provide homogeneous lighting to the lit area;
   an image capture system (282, 382) situated on the opposite side of the pipe through which the oil (281) flows in respect of the lighting system (284) and configured to capture a sequence of images of the oil that flows inside said pipe;
   a lens (283) situated between the image capture system (282) and the flow of oil (281), configured to focus the captured images;
   a calibration device (287) situated between the lens (283) and the flow of oil (281);
   a processor (2851) configured to process said sequence of images and to determine the presence of particles and bubbles and a degradation value of the oil.

2. The system (18, 28) of claim 1, wherein said lighting system (284) comprises a system for controlling the polarisation of at least one LED diode configured to prevent emission fluctuations due to changes in temperature.

3. The system (18, 28) of any of the preceding claims, wherein said diffuser (286) is situated closing off and sealing a hole made in the pipe through which the fluid (281) flows.

4. The system (18, 28) of claim 3, wherein said diffuser (286) is a frosted glass.

5. The system (18, 28) of any of the preceding claims, wherein said image capture system (282, 382) is a camera.

6. The system (18, 28) of any of the preceding claims, wherein said calibration device (287) situated between the lens (283) and the flow of oil (281) comprises a plurality of markings designed to calibrate the system.

7. The system (18, 28) of claim 6, wherein said calibration device (287) is situated closing off and sealing a hole made in the pipe through which the oil (281) flows.

8. A method for auto-calibration of the system (18, 28) for inspecting oil according to any of the preceding claims, which comprises the stages of:

   - making on the calibration device (287) at least one marking of known dimensions;
   - capturing an image of an oil using the image acquisition system (282, 382);
   - adjusting the capture parameters to increase the contrast of the captured image until finding the system's optimum polarisation;
   - capturing a new image;
   - binarising said image with dynamic threshold;
   - in said image, identifying the geometry of said at least one marking;
   - taking the horizontal and vertical measurement in the number of pixels and applying a corrector in respect of their real sizes;
   - saving that correction as a calibration measurement for the absolute dimensional measurements obtained by the system (18, 28) during its subsequent use.

9. A method for detecting and discriminating particles and bubbles in oil by means of the system (18, 28) for inspecting oil according to any of claims 1 to 7, which comprises the stage of:

   - capturing an image of an oil using the image acquisition system (282, 382);
   - adjusting the capture parameters to increase the contrast of the captured image until finding the system's optimum polarisation;
   - capturing a new image;
   - binarising said image with dynamic threshold;
   - conditioning the binary image;

- detecting the objects that are considered bubbles or particles by applying techniques for the search of connected components or for dimensional detection and identification of pixel groupings;
- in order to discriminate between bubble and particle:

  - applying an inversion of the binary image in those regions where potential particles or bubbles have been detected;
  - applying a conditioning based on enlargement of those inverted regions of interest;
  - applying in those zones techniques for the detection of connected components in order to detect holes in the original pixel groupings, identifying as bubbles those zones that present pixel groupings with holes, and identifying as particles those pixel groupings not having a hole inside them;

- based on the pixel groupings, counting and calculating the size of the bubbles and particles, wherein the calculation of said size comprises applying to those pixels the dimensional correction obtained using the auto-calibration method of claim 8.

10. A method for obtaining an oil degradation parameter using the system (18, 28) for inspecting oil of any of claims 1 to 7, which comprises the stage of:

- applying to the lighting system (284) of the system (18, 28) of any of claims 1 to 7, a temperature compensation algorithm;
- capturing an image of the oil with the three colour channels - red, green, blue - using the image acquisition system (282, 382) of the system (18, 28);
- extracting from said image the regions with pixel groupings and generating an image with those zones marked with a negative value;
- taking a mean of transmittance in the red band I_R, transmittance in the blue band I_B and transmittance in the green band I_G, adding up the value of each one of the pixels divided by the number of pixels used for the inspection;
- applying an algorithm to obtain a degradation parameter based on said three colour channels.

11. The method of claim 10, wherein obtaining a degradation parameter based on said three colour channels is obtained on the basis of the formula $CI=1*I_R +0.5*I_G +0.5*I_B$, wherein CI is the value of the oil's colour index.

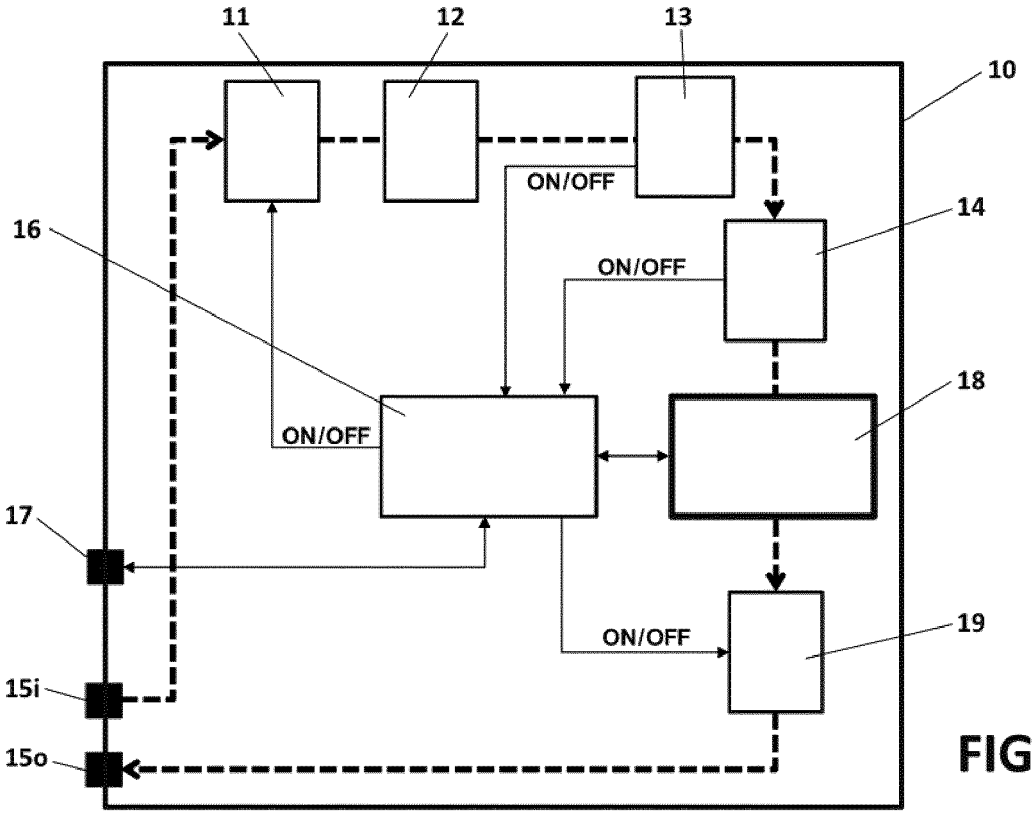

FIG. 1

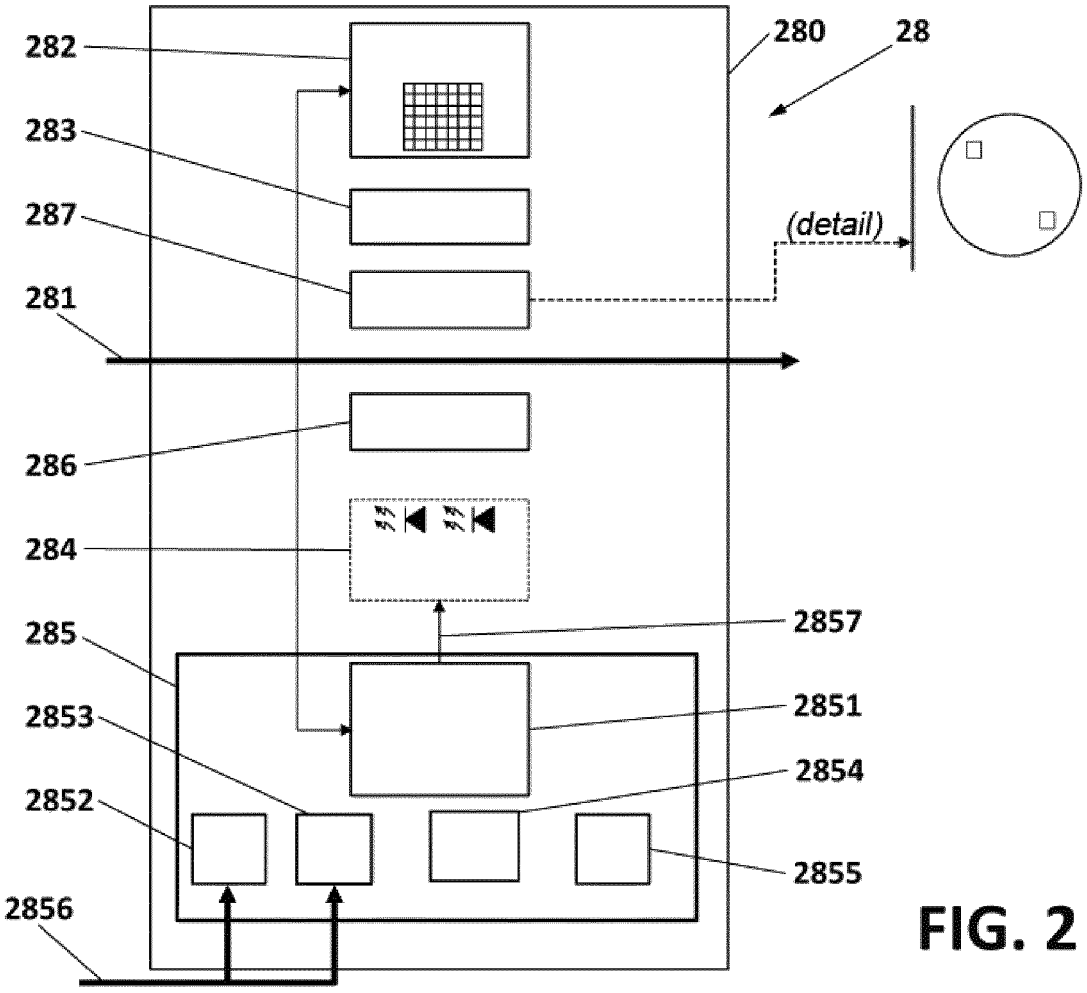
282
283
287
281
286
284
285
2853
2852
2856
280
28
(detail)
2857
2851
2854
2855

FIG. 2

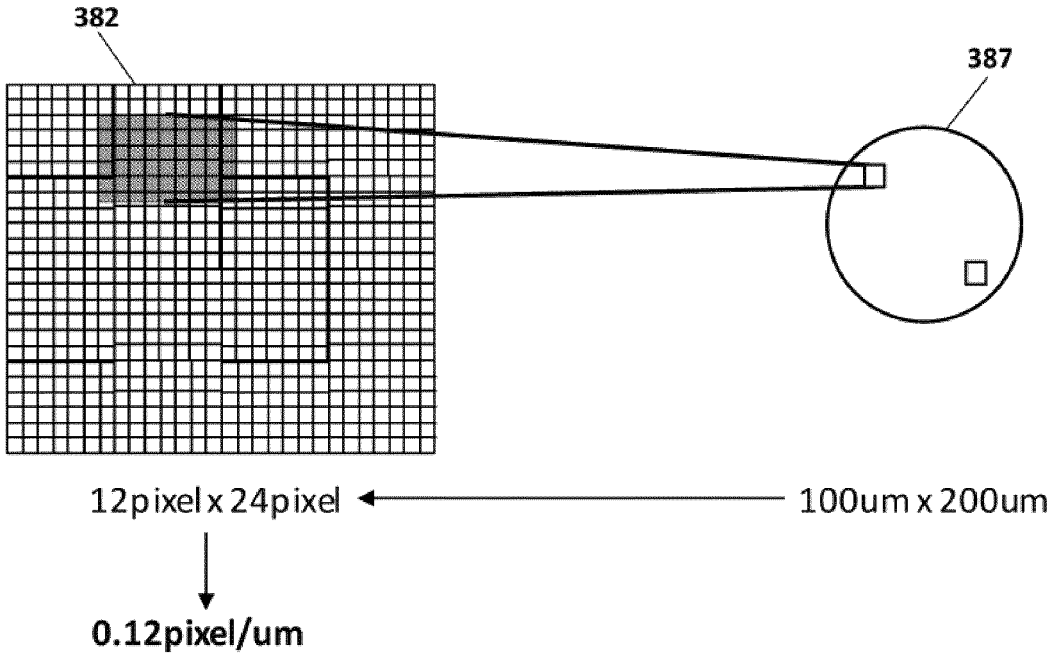

FIG. 3

INTERNATIONAL SEARCH REPORT

International application No
PCT/ES2013/070207

A. CLASSIFICATION OF SUBJECT MATTER
INV. G01N15/02 G01N33/28
ADD.

According to International Patent Classification (IPC) or to both national classification and IPC

B. FIELDS SEARCHED

Minimum documentation searched (classification system followed by classification symbols)
G01N

Documentation searched other than minimum documentation to the extent that such documents are included in the fields searched

Electronic data base consulted during the international search (name of data base and, where practicable, search terms used)
EPO-Internal, COMPENDEX, INSPEC, WPI Data

C. DOCUMENTS CONSIDERED TO BE RELEVANT

Category*	Citation of document, with indication, where appropriate, of the relevant passages	Relevant to claim No.
X	WO 97/40360 A1 (MONTORES PTY LTD [AU]; MONTECH MEDICAL DEVELOPMENTS P [AU]; DENTIRE PT) 30 October 1997 (1997-10-30) figure 9 page 3, line 5 - line 18 page 13, line 24 - line 32 page 15, line 24 - page 17, line 24	1-7
A	WO 01/55768 A1 (CELLVISION TECHNOLOGIES B V I [NL]; KOCK ALFONS PETRUS ANTONIUS GE [NL]) 2 August 2001 (2001-08-02) figure 4 page 1, line 6 - line 38	1-11
A	US 2008/024761 A1 (KONG HOSUNG [KR] ET AL) 31 January 2008 (2008-01-31) figure 3 paragraphs [0050], [0051], [0058]	1-11

-/--

[X] Further documents are listed in the continuation of Box C. [X] See patent family annex.

* Special categories of cited documents :

"A" document defining the general state of the art which is not considered to be of particular relevance

"E" earlier application or patent but published on or after the international filing date

"L" document which may throw doubts on priority claim(s) or which is cited to establish the publication date of another citation or other special reason (as specified)

"O" document referring to an oral disclosure, use, exhibition or other means

"P" document published prior to the international filing date but later than the priority date claimed

"T" later document published after the international filing date or priority date and not in conflict with the application but cited to understand the principle or theory underlying the invention

"X" document of particular relevance; the claimed invention cannot be considered novel or cannot be considered to involve an inventive step when the document is taken alone

"Y" document of particular relevance; the claimed invention cannot be considered to involve an inventive step when the document is combined with one or more other such documents, such combination being obvious to a person skilled in the art

"&" document member of the same patent family

Date of the actual completion of the international search	Date of mailing of the international search report
27 January 2014	05/02/2014

Name and mailing address of the ISA/	Authorized officer
European Patent Office, P.B. 5818 Patentlaan 2 NL - 2280 HV Rijswijk Tel. (+31-70) 340-2040, Fax: (+31-70) 340-3016	Rasmusson, Marcus

Form PCT/ISA/210 (second sheet) (April 2005)

INTERNATIONAL SEARCH REPORT

International application No
PCT/ES2013/070207

C(Continuation). DOCUMENTS CONSIDERED TO BE RELEVANT

Category*	Citation of document, with indication, where appropriate, of the relevant passages	Relevant to claim No.
A	CN 102 818 756 A (USTC UNIV SCIENCE TECH CN) 12 December 2012 (2012-12-12) figure 4	1-11

Form PCT/ISA/210 (continuation of second sheet) (April 2005)

INTERNATIONAL SEARCH REPORT

Information on patent family members

International application No
PCT/ES2013/070207

Patent document cited in search report	Publication date	Patent family member(s)	Publication date
WO 9740360 A1	30-10-1997	AU 706758 B2	24-06-1999
		AU 2281797 A	12-11-1997
		CA 2251861 A1	30-10-1997
		EP 0900370 A1	10-03-1999
		JP 2001503848 A	21-03-2001
		KR 20000010549 A	15-02-2000
		NZ 332306 A	28-01-1999
		US 5790246 A	04-08-1998
		WO 9740360 A1	30-10-1997
WO 0155768 A1	02-08-2001	AT 382880 T	15-01-2008
		AU 3424301 A	07-08-2001
		DE 60132173 T2	24-12-2008
		EP 1256027 A1	13-11-2002
		ES 2296728 T3	01-05-2008
		NL 1014217 C2	31-07-2001
		US 2003107731 A1	12-06-2003
		WO 0155768 A1	02-08-2001
US 2008024761 A1	31-01-2008	KR 100795373 B1	17-01-2008
		US 2008024761 A1	31-01-2008
CN 102818756 A	12-12-2012	NONE	

Form PCT/ISA/210 (patent family annex) (April 2005)

REFERENCES CITED IN THE DESCRIPTION

This list of references cited by the applicant is for the reader's convenience only. It does not form part of the European patent document. Even though great care has been taken in compiling the references, errors or omissions cannot be excluded and the EPO disclaims all liability in this regard.

Patent documents cited in the description

- US 5572320 A **[0014]**
- US 7385694 B2 **[0015] [0032]**

MINISTERIO
DE INDUSTRIA, ENERGÍA
Y TURISMO

Oficina Española
de Patentes y Marcas

Acknowledgement of receipt

We hereby acknowledge receipt of your request for grant of a European patent as follows:

Submission number	300178393	
Application number	EP15382609.4	
File No. to be used for priority declarations	EP15382609	
Date of receipt	04 December 2015	
Your reference	P152422EP	
Applicant	Atten2 Advanced Monitoring Technologies S.L.U.	
Country	ES	
Title		
Documents submitted	package-data.xml	ep-request.xml
	application-body.xml	ep-request.pdf (5 p.)
	DRAWNONEPO.pdf\DIBUJOS.pdf (4 p.)	SPECNONEPO.pdf\descripcion.pdf (20 p.)
	OLF-ARCHIVE.zip\P152422EP-spec-draft-(NIR)-20151106-v4.zip	f1002-1.pdf (2 p.)
Submitted by	CN=Manuel Barrero 34075	
Method of submission	Online	
Date and time receipt generated	04 December 2015, 15:14:27 (CET)	
Official Digest of Submission	55:68:66:E3:C3:89:DD:C6:DD:C3:C1:53:F3:C1:24:57:EE:72:87:9D	

/Madrid, Oficina Receptora/

Europäisches Patentamt
European Patent Office
Office européen des brevets

Request for grant of a European patent

For official use only		
1 Application number:	MKEY	
2 Date of receipt (Rule 35(2) EPC):	DREC	
3 Date of receipt at EPO (Rule 35(4) EPC):	RENA	
4 Date of filing:		

5 Grant of European patent, and examination of the application under Article 94, are hereby requested. ☒

Request for examination in an admissible non-EPO language: Se solicita el examen de la solicitud según el artículo 94.

5.1 The applicant waives his right to be asked whether he wishes to proceed further with the application (Rule 70(2)) ☐

Procedural language: en

Description and/or claims filed in: es

6 Applicant's or representative's reference: P152422EP

Applicant 1

7-1 Name: Atten2 Advanced Monitoring Technologies S.L.U.

8-1 Address:
Iñaki Goenaga 5
20600 Eibar, Gipuzkoa
Spain

10-1 State of residence or of principal place of business: Spain

14.1 The/Each applicant hereby declares that he is an entity or a natural person under Rule 6(4) EPC. ☒

Representative 1

15-1 Name: BALDER IP Law, S.L.

Association No.: 639

16-1 Address of place of business:
Castellana 93
5ª planta
28046 Madrid
Spain

17-1	Telephone:	0034911336879
17-1	Fax:	0034911331384
17-1	E-mail:	info@balderip.com

Inventor(s)

23 Inventor details filed separately ☒

24 Title of invention

25 Declaration of priority (Rule 52)

A declaration of priority is hereby made for the following applications

25.2 This application is a complete translation of the previous application ☐

25.3 It is not intended to file a (further) declaration of priority ☐

26 Reference to a previously filed application

27 Divisional application ☐

28 Article 61(1)(b) application ☐

29 Claims

Number of claims: 11

29.1 ☒ as attached

29.2 ☐ as in the previously filed application (see Section 26.2)

29.3 ☐ The claims will be filed later

30 Figures

It is proposed that the abstract be published together with figure No. 2

31 Designation of contracting states

All the contracting states party to the EPC at the time of filing of the European patent application are deemed to be designated (see Article 79(1)).

32 Different applicants for different contracting states

33 Extension/Validation

This application is deemed to be a request to extend the effects of the European patent application and the European patent granted in respect of it to all non-contracting states to the EPC with which extension or validation agreements are in force on the date on which the application is filed. However, the request is deemed withdrawn if the extension fee or the validation fee, whichever is applicable, is not paid within the prescribed time limit.

33.1 It is intended to pay the extension fee(s) for the following state(s):

33.2 It is intended to pay the validation fee(s) for the following state(s):

34 Biological material

38 Nucleotide and amino acid sequences

The European patent application contains a sequence listing as part of the description ☐

The sequence listing is attached in computer-readable format in accordance with WIPO Standard ST.25 ☐

The sequence listing is attached in PDF format ☐

Further indications

39 Additional copies of the documents cited in the European search report are requested

Number of additional sets of copies:

40 Refund of the search fee under to Article 9 of the Rules relating to Fees is requested ☐

Application or publication number of earlier search report:

42 Payment

Mode of payment: Debit from deposit account

The European Patent Office is hereby authorised, to debit from the deposit account with the EPO any fees and costs indicated on the fees section below.

Currency: EUR

Deposit account number: 28120253

Account holder: BALDER IP Law,S.L.

43 Refunds

Any refunds should be made to EPO deposit account: 28120253

Account holder: BALDER IP Law,S.L.

Fees	Factor applied	Fee schedule	Amount to be paid
001 Filing fee - EP direct - online	0.7	120.00	84.00
002 Fee for a European search - Applications filed on/after 01.07.2005	1	1 285.00	1 285.00
015 Claims fee - For the 16th to the 50th claim	0	235.00	0.00
015e Claims fee - For the 51st and each subsequent claim	0	580.00	0.00
501 Additional filing fee for the 36th and each subsequent page	0	15.00	0.00
Total:		EUR	1 369.00

44-A Forms		Details:	System file name:
A-1	Request		as ep-request.pdf
A-2	1. Designation of inventor	1. Inventor	as f1002-1.pdf

44-B Technical documents		Original file name:	System file name:
B-1	Specification in admissible non-EPO language	descripcion.pdf 11 claims 5 figure(s)	SPECNONEPO.pdf
B-2	Drawings / Translation of text in drawings	DIBUJOS.pdf 5 figure(s)	DRAWNONEPO.pdf
B-3	Pre-conversion archive	P152422EP-spec-draft-(NIR)-20151106-v4.zip	OLF-ARCHIVE.zip

44-C Other documents	Original file name:	System file name:

45

General authorisation:

46 Signature(s)

Place: **MADRID**

Date: **04 December 2015**

Signed by: **/M.STIEBE/**

Association: **BALDER IP Law, S.L.**

Representative name: **Lars Magnus STIEBE**

Capacity: **(Representative)**

Form 1002 - 1: Public inventor(s)

Designation of inventor 123

User reference: P152422EP
Application No:

Public

	Inventor	
	Name:	GORRITXATEGI ARRONDO, Mr. Eneko
	Address:	Iñaki Goenaga 5 20600 Gipuzkoa Spain
	The applicant has acquired the right to the European patent:	As employer
	Inventor	
	Name:	MABE ÁLVAREZ, Mr. Jon
	Address:	Iñaki Goenaga 5 20600 Gipuzkoa Spain
	The applicant has acquired the right to the European patent:	Under agreement:
	Inventor	
	Name:	DELGADO CASTRILLO, Mr. Andoni
	Address:	Iñaki Goenaga 5 20600 Gipuzkoa Spain
	The applicant has acquired the right to the European patent:	Under agreement:
	Inventor	
	Name:	VILLAR VERGUIZAS, Mr. Alberto
	Address:	Iñaki Goenaga 5 20600 Gipuzkoa Spain
	The applicant has acquired the right to the European patent:	Under agreement:
	Inventor	
	Name:	URRETA PRIETO, Mr. Harkaitz
	Address:	Arriaga Kalea 2 20870 Gipuzkoa Spain
	The applicant has acquired the right to the European patent:	Under agreement:

Signature(s)

Place: **MADRID**

Date:	**04 December 2015**
Signed by:	**/M.STIEBE/**
Association:	**BALDER IP Law, S.L.**
Representative name:	**Lars Magnus STIEBE**
Capacity:	**(Representative)**

SISTEMA DE MONITORIZACIÓN DE FLUIDOS BASADO EN ESPECTROSCOPIA EN EL INFRARROJO CERCANO

CAMPO TÉCNICO

La presente invención pertenece al campo de la monitorización y control de fluidos durante su proceso de producción. Más concretamente, pertenece al campo de la monitorización de la fermentación de alimentos, tales como vinos, tanto blancos como tintos, cervezas, zumos, tomates o lácteos, para obtener a partir de dicha monitorización un control sobre ciertos parámetros críticos durante el proceso de fermentación y/o envejecimiento. La invención se refiere asimismo a la integración de un sistema de monitorización en depósito para la medición continua del fluido, a altura constante y asegurando el llenado completo de la cavidad de medida del sistema de monitorización.

ANTECEDENTES DE LA INVENCIÓN

El empleo de técnicas espectroscópicas para la determinación de ciertos parámetros críticos de calidad en un fluido, por ejemplo vino, ha resultado exitoso, pero solo cuando el analito en cuestión es elemental (potasio, calcio o hierro). Por ejemplo, la patente estadounidense US8794049B1 describe un sistema para la monitorización online de ciertos parámetros de interés en el control del proceso de fermentación del vino. En este caso, se monitoriza la presión creada por el flujo de dióxido de carbono que emana como consecuencia de la actividad de fermentación. A su vez, la solicitud de patente US2002/0023849A1 describe un método para detectar la presencia de etanol en muestras de un fluido utilizando una barrera no porosa de PVC sin plastificar interpuesta entre la muestra y un detector de etanol.

En los últimos años, la espectroscopia de infrarrojo cercano (NIRs, del inglés Near InfraRed, en español Infrarrojo Cercano) se ha convertido en una alternativa a los métodos físicos, químicos y cromatográficos tradicionales. Por ejemplo, dentro del sector vitivinícola, la tecnología de infrarrojo cercano NIRs permite la medida de parámetros de calidad del vino necesarios para el control de los procesos de fermentación. Resulta de mucha utilidad poder realizar un control automático para medir la calidad del producto y determinar si una intervención correctiva es necesaria durante la fermentación para mantener la calidad. Además el NIRs tiene la ventaja añadida de ser capaz de cuantificar múltiples parámetros al mismo tiempo empleando

un único espectro. Las aplicaciones y parámetros de medida para otros sectores también son muy variadas, desde el control de calidad de la leche hasta el porcentaje de maduración de frutas y verduras. La región espectral del infrarrojo cercano (NIR) se extiende desde el extremo de las longitudes más altas del visible (alrededor de 780 ηm) hasta los 3000 ηm (13 000 cm-1 hasta 3300 cm-1).

Las ventajas que ofrece la tecnología NIRs se basan principalmente en la rapidez en el procesado y la facilidad de uso y manejo, debido principalmente a la escasa necesidad de pre-procesado del analito a analizar. A pesar de que supone una cierta inversión en sistemas para la monitorización on-line integrados en los procesos de producción, la espectroscopia NIR ha tomado ventaja sobre el resto de métodos analíticos debido sobre todo a su capacidad de realidad medidas no-destructivas rápidas tanto de compuestos sólidos como líquidos. Sin embargo, comparada con la espectroscopia FTIR, la NIR se caracteriza por su baja especificidad, ya que en muchos casos las bandas obtenidas se encuentran solapadas y tienen baja sensibilidad debido a que grandes variaciones de las propiedades dan lugar a pequeñas variaciones en el espectro Visible-NIR. Por lo tanto es necesaria la utilización de técnicas de calibración multivariante para poder correlacionar la información útil de los espectros obtenidos con las medidas de referencia obtenidas en el laboratorio. La calibración multivariante es una disciplina dentro de la Quimiometría (disciplina que utiliza métodos matemáticos y estadísticos para diseñar y seleccionar procedimientos de medida y experimentos óptimos, para proporcionar la máxima información química mediante el análisis de datos químicos) imprescindible en espectroscopia NIR debido a la complejidad de la señal obtenida por esta técnica. El objetivo de la calibración multivariante es buscar la relación entre una serie de medidas indirectas fáciles de obtener y una serie de medidas directas de laboratorio que son caras o requieren una mano de obra intensiva. Es decir, crear un buen modelo de calibración de tal manera que los parámetros medidos en laboratorio mediante técnicas costosas se pueden determinar cuantitativamente de manera rápida y económica a partir de medidas realizadas con métodos más baratos. El desarrollo de un modelo de calibración multivariante es un proceso complejo donde el objetivo principal es relacionar las N variables experimentales (datos espectroscópicos) frente a una o varias propiedades conocidas de las muestras. La estrategia típica a seguir en el desarrollo de un modelo de calibración multivariante consiste en los siguientes pasos: Selección del Conjunto de Muestras; Determinación del Parámetro de Referencia; Obtención de la Señal

Analítica; Tratamiento de los Datos; Generación del Modelo de Calibración; y Validación.

Por otra parte, habitualmente el gran número de variables espectrales que se encuentra en la mayoría de los conjuntos de datos espectrales hace difícil la predicción de una variable dependiente. Además, la existencia de un gran número de muestras y variables hace que el proceso de calibración pueda llegar a ser muy costoso en el tiempo. Es por ello que hoy en día es necesario utilizar la selección de variables predictoras, con el objetivo no solo de ahorrar tiempo en la calibración, sino también para eliminar aquellas variables predictoras (longitudes de onda) que no contienen información relevante o que puedan dañar el resultado final de la calibración multivariante. La exclusión de las variables no relevantes mejora las características del modelo en términos de exactitud y robustez. Por otra parte, la selección de variables es una herramienta muy útil en la mejora de la robustez de los modelos de calibración multivariantes. Mediante la selección de variables es posible eliminar aquellas variables que no aportan información útil o relevante obteniendo de esta manera un mejor modelo de calibración en términos exactitud y robustez.

La solicitud de patente estadounidense US2010/0297291A1 describe un método de análisis del espectro visible/infrarrojo cercano para monitorizar ciertos parámetros del proceso de fermentación del vino. Para ello se utilizan dispositivos de medida de laboratorio, no integrados en el propio proceso de producción. En concreto, el método se desarrolla sobre una muestra de uva.

Por su parte, la solicitud de patente china CN103234923, propone un método on-line de monitorización del contenido de azúcar en un vino en fermentación mediante técnicas espectroscópicas.

DESCRIPCIÓN DE LA INVENCIÓN

La presente invención ofrece un dispositivo de medida y sistema de monitorización basado en espectroscopia de infrarrojo cercado (NIRs) que permite implementar de forma sencilla y rápida la monitorización on-line de parámetros críticos en fluidos. El sistema es especialmente útil dentro del sector agroalimentario, aunque puede aplicarse a otros sectores. Con el presente sistema, es posible determinar diversos parámetros, tales como grado de alcohol, acidez y azúcares, en las cubas de

fermentación del vino o de otros productos, tales como cervezas, zumos, tomates y lácteos, entre otros, sin necesidad de extraer una muestra de la cuba de fermentación. Por el contrario, el dispositivo de sensado/medida se deja introducido en la cuba y el dispositivo toma medidas de forma periódica (o a petición). Mediante este nuevo sistema sensor integrado en depósito se realizan mediciones a altura constante asegurando el llenado completo de la cavidad.

En un primer aspecto de la invención, se proporciona un sistema de monitorización de al menos un parámetro de un fluido contenido en un depósito, que comprende un dispositivo de medida basado en espectroscopia de infrarrojo cercano diseñado para sumergirse en el citado fluido a monitorizar y para tomar medidas de dicho fluido, donde dicho dispositivo de medida comprende una zona de medida. El sistema de monitorización comprende un sistema de flotación conectado a dicho dispositivo de medida, estando dicho sistema de flotación dispuesto, durante el uso del sistema de monitorización, en flotación sobre el fluido a monitorizar, de forma que la zona de medida del dispositivo de medida queda sumergida en el fluido a una profundidad constante con respecto al nivel de fluido en el depósito, de forma que todas las medidas tomadas por el dispositivo de medida se toman a la misma profundidad con respecto al nivel de fluido.

En una posible realización, el dispositivo de medida está conectado al sistema de flotación mediante una barra de una determinada longitud.

En una posible realización, el sistema de flotación comprende medios de conexión configurados para conectar el sistema de flotación con el exterior del depósito.

En una posible realización, el dispositivo de medida está configurado para tomar medidas del fluido de forma periódica o de forma aleatoria.

En una posible realización, el dispositivo de medida comprende una fuente de iluminación que trabaja en el espectro de luz visible e infrarrojo cercano y un sistema de detección basado en espectroscopia de infrarrojo cercano, donde dicha fuente de iluminación está configurada para iluminar el fluido a monitorizar y dicho sistema de detección está configurado para tomar al menos una medida del espectro de luz que ha atravesado dicho fluido a monitorizar. El dispositivo de medida comprende

preferentemente medios para registrar la temperatura del fluido a monitorizar, medios para registrar la temperatura del sistema de detección y medios para registrar la temperatura de la fuente de iluminación. También preferentemente, el dispositivo de medida comprende medios de procesado configurados para procesar las medidas tomadas por sistema de detección y por los tres medios para registrar la temperatura del fluido, del sistema de detección y de la fuente de iluminación.

En una realización preferida, el sistema de monitorización comprende además un sistema de posicionamiento configurado para girar el dispositivo de medida en el interior del fluido, de forma que la zona de medida quede dispuesta en el interior del fluido con su abertura hacia arriba.

Preferentemente, el sistema de posicionamiento comprende un mecanismo de apertura y cierre formado por una primera pieza y una segunda pieza articuladas entre sí mediante un eje común, y un cable, donde la primera pieza está fijada al dispositivo de medida y la segunda pieza está fijada a la barra, estando dicho sistema de posicionamiento configurado para, una vez introducido en el depósito lleno de fluido el conjunto formado por la barra y el dispositivo de medida, unidos por dicho mecanismo de apertura y cierre dispuesto formando un ángulo de unos 90º, tirar desde el exterior del depósito del cable hasta que el mecanismo de apertura y cierre se pliegue formando un ángulo de unos 0º entre dichas primera y segunda piezas, quedando la cavidad dispuesta en posición vertical, facilitando la liberación de burbujas de aire.

En una realización particular, el sistema de posicionamiento comprende además un sistema de amarre del cable configurado para fijar la posición del mismo tras el giro del dispositivo de medida y mantener la ranura en posición vertical durante el tiempo de muestreo.

En una posible realización, el fluido cuyo al menos un parámetro se desea monitorizar es un vino y el al menos un parámetro a monitorizar es uno de los siguientes: el grado de alcohol, el grado de acidez o el grado de azúcares presentes en el vino.

Las ventajas de la invención resultarán aparentes a la vista de la descripción que se presenta a continuación.

BREVE DESCRIPCIÓN DE LOS DIBUJOS

Para complementar la descripción y con objeto de ayudar a una mejor comprensión de las características de la invención, de acuerdo con un ejemplo de realización práctica de la misma, se acompaña como parte integrante de la descripción, un juego de figuras en el que con carácter ilustrativo y no limitativo, se ha representado lo siguiente:

La figura 1 muestra un diagrama de bloques de un dispositivo de medida NIRs de acuerdo con una posible implementación de la invención. El diagrama de bloques ilustra el funcionamiento del dispositivo de medida.

La figura 2 muestra un esquema de un sistema de monitorización integrado en un depósito, de acuerdo con una primera realización de la invención. El sistema de monitorización comprende un dispositivo de medida como el esquematizado en la figura 1.

La figura 3 muestra un esquema de otro sistema de monitorización integrado en un depósito, de acuerdo con una segunda realización de la invención. El sistema de monitorización comprende un dispositivo de medida como el esquematizado en la figura 1.

Las figuras 4A y 4B muestran un sistema de monitorización de acuerdo con una posible realización de la invención, que incluye un sistema mecánico que permite girar el dispositivo de medida y dejar la cavidad en perpendicular para obtener un llenado adecuado que evita la presencia de burbujas de aire en la zona de medida.

Las figuras 5A y 5B muestran un sistema de monitorización que incluye un sistema mecánico de acuerdo con otra realización de la invención.

DESCRIPCIÓN DE UN MODO DE REALIZACIÓN DE LA INVENCIÓN

En este texto, la palabra “comprende” y sus variantes (como “comprendiendo”, etc.) no deben interpretarse de forma excluyente, es decir, no excluyen la posibilidad de que lo descrito incluya otros elementos, pasos etc.

En el contexto de la presente invención, el término "aproximadamente" y los términos de su familia (tales como "aproximado", etc.) deberían entenderse como valores indicativos muy próximos a los que acompañan al término anteriormente mencionado. Es decir, se debería aceptar una desviación dentro de los límites aceptables a partir de un valor exacto, ya que la persona experta en la técnica comprenderá que dicha

desviación a partir de los valores indicados resulta inevitable debido a las imprecisiones de la medición, etc. Lo mismo resulta aplicable a los términos "alrededor" y "sustancialmente".

El sistema de monitorización de la invención comprende un dispositivo de medida 10 diseñado para integrarse en un depósito. El dispositivo de medida 10 es un dispositivo de espectroscopia de infrarrojo cercano (NIRs) y está diseñado para introducirse en la cuba de fermentación del fluido que se esté produciendo (por ejemplo, vino) y dejarse introducido en la cuba a lo largo del proceso de fermentación. De esta forma, el dispositivo de medida 10 puede tomar medidas de diversos parámetros que afectan al proceso de fermentación sin necesidad de extraer una muestra de fluido de la cuba. Interpretando correctamente los valores que toman los parámetros medidos, se puede actuar sobre el fluido en cuestión o tomar decisiones basadas por ejemplo en su grado de madurez. El dispositivo 10 puede tomar medidas periódicas o no periódicas (por ejemplo, a petición). Las medidas se toman a altura constante, asegurando además el llenado completo de la cavidad (zona de medida) en la que se toman las medidas. El fluido recogido en la cuba es preferentemente un líquido. Ejemplos no limitativos de líquidos cuyo proceso de fermentación o envejecimiento puede monitorizarse con el dispositivo de medida 10 son vinos, cervezas, zumos, tomate o lácteos, tales como leche, yogures, etc. Los parámetros de estos productos que pueden monitorizarse son por ejemplo, de forma no limitativa, el grado de alcohol, de acidez o de azúcares.

La figura 1 muestra un diagrama de bloques o esquema funcional del dispositivo de medida 10. La medida o medidas se toma(n) disponiendo el analito/fluido a medir entre un sistema de iluminación (fuente de iluminación NIR) 11 y un sistema de detección (espectrómetro NIR) 15, tal y como se describe a continuación. Ambos sistemas (de iluminación y de detección) quedan sellados mediante sendas ventanas de protección 12 14 transparentes en el rango de trabajo. Es decir, las ventanas de protección no absorben luz en el rango de trabajo (NIR). Además se monitorizan la temperatura del fluido a medir, la temperatura del sistema de iluminación y la temperatura del sistema espectrométrico (sistema de detección) que recoge la señal. Integrados en el propio sistema se encuentran los algoritmos quimiométricos que realizan el cálculo de las variables de interés a partir del espectro detectado, para el control del estado del analito/fluido que se analiza.

El dispositivo de medida 10, del que se muestra un diagrama de bloques en la figura 1, tiene una serie de elementos optoelectrónicos integrados en una carcasa, vaina o encapsulado. La figura 1 muestra un esquema de un corte de este encapsulado, lo que permite ver esquemáticamente su interior. La carcasa, vaina o encapsulado tiene una forma que permite el paso del fluido entre dos paredes externas del dispositivo. Es decir, el fluido pasa por una zona 13 exterior al dispositivo 10. Esta zona 13 es una especie de túnel o conducto entre la superficie exterior de una parte 101 del dispositivo y la superficie exterior de otra parte 102 del dispositivo. Es decir, como se aprecia en las figuras 2 y 3, la vaina tiene un determinado grosor en la parte o porción inferior 101 y en la parte o porción superior 102, y experimenta un estrechamiento 103 en una parte o porción intermedia entra las partes inferior 101 y superior 102 (estrechamiento 103 que se aprecia en las figuras 2 y 3), de forma que la vaina queda dividida en una parte superior 102 y una parte inferior 101, unidas por una parte estrecha 103 de la vaina, quedando un hueco 13 por el que fluye el fluido cuando el dispositivo 10 se ha insertado o sumergido en el fluido bajo supervisión. En la parte inferior 101 con respecto a la zona estrecha 103, es decir, en la parte destinada a quedar más sumergida en el fluido, es decir, en la parte opuesta al extremo por el que el dispositivo 10 se sujeta o conecta desde el exterior de la cuba o depósito 30, el dispositivo 10 tiene una fuente de luz (sistema de iluminación) 11. La pared de la parte inferior 101 en contacto con la muestra de fluido (que pasa por el canal o túnel 13) está sellada herméticamente por una ventana de protección transparente 12 (transparente a la longitud de onda de trabajo). La fuente de luz 11 es una fuente de luz en el espectro de luz visible e infrarrojo (VIS + IR). Preferentemente es una fuente de luz de banda ancha, por ejemplo, pero de forma no limitativa, una lámpara halógena, que ofrece espectro estable desde el ultravioleta hasta el infrarrojo lejano o profundo. La fuente de luz 11 está a una determinada temperatura T_3 registrada por un sensor de temperatura dispuesto junto a la misma. La fuente de luz 11 está orientada hacia la zona 13 por la que fluye el fluido. La ventana de protección transparente 12 se sitúa entre la fuente de luz 11 y la zona 13 por la que fluye el fluido. En una posible realización, no limitativa, esta ventana de protección transparente 12 se realiza de cuarzo. A través de esta ventana transparente 12 la luz emitida por la fuente de luz 11 viaja hasta el fluido que se encuentra en el hueco 13.

Al otro lado del fluido bajo supervisión, es decir, en la parte superior 101 de la carcasa o vaina, el dispositivo 10 tiene otra ventana de protección transparente 14 similar a la

ventana 12 de la parte inferior 102. Como indican las flechas punteadas en la figura 1, la luz que, procedente de la fuente 11, atraviesa la primera ventana transparente 12 y el fluido que circula por la zona 13 que queda entre la parte inferior 101 y superior 102 de la carcasa, continúa viajando y atraviesa también la ventana transparente 14 hasta llegar un sistema de detección 15. El sistema de detección es un espectómetro NIR 15. El espectómetro NIR 15 es un dispositivo con el que se obtiene una señal de transmitancia en el rango NIR. El espectómetro 15 está a una temperatura T_2, registrada por un sensor de temperatura dispuesto junto al mismo. A su vez, un tercer sensor de temperatura registra la temperatura T_1 del fluido muestra. Este sensor se sitúa en las proximidades del fluido muestra, preferentemente en la parte superior 102 de la vaina. En el esquema de la figura 1, el sensor de temperatura que registra la temperatura T_1 del fluido muestra se sitúa en la parte superior 102 de la vaina. En una posible realización, los sensores de temperatura que miden las temperaturas T_1, T_2 y T_3 son termopares.

Es preciso controlar las temperaturas del fluido y de los sistemas de iluminación y detección porque las medidas tomadas por el espectómetro NIR 15 fluctúan con la temperatura y ésta puede experimentar cambios muy pronunciados. De hecho, la influencia de la temperatura afecta en la señal obtenida de dos maneras diferentes. En primer lugar, si cambia la temperatura T_3 del emisor 11 y/o la temperatura T_2 del detector 15, la medida tomada de la muestra (considerando que la muestra no varía) variará con respecto a la medida que se tomaría si dichas temperaturas T_2 T_3 no se viesen alteradas. Si varía la temperatura T_3 del emisor de luz 11, la cantidad de luz que emite el emisor 11 puede variar hasta en un 50%. Algo parecido ocurre si varía la temperatura T_2 del receptor o espectrómetro NIR 15. Para minimizar el impacto de estas variaciones de temperatura, el dispositivo 10 tiene integrado un sistema, no ilustrado, para realizar las medidas a una temperatura nominal. El segundo aspecto clave en relación con la temperatura es que cambios de temperatura T_1 de la propia muestra pueden alterar la señal, ya que cambia la formulación del propio analito que se está analizando. Es decir, debe tenerse en cuenta la temperatura a la que se han tomado las medidas para interpretar correctamente los parámetros bajo análisis. Esto es especialmente relevante en el caso concreto de las cubas de fermentación de vino, en las que la temperatura puede pasar de unos 2/3ºC a unos 40/42ºC.

La parte superior 102 de la vaina, es decir, la parte que alberga el espectómetro NIR 15 comprende también medios de procesado 16 para procesar las medidas tomadas por el espectómetro NIR 15 y por los tres sensores de temperatura (para controlar emisor, receptor y analito). Nos referimos a esta parte 102 como “parte superior” porque es la parte que, durante la inmersión del dispositivo 10 en el fluido recogido en un depósito, queda más cercana al cable o cordón 31 41 que une el dispositivo 10 con el exterior del depósito (ver por ejemplo figuras 2 y 3). No obstante, en las realizaciones de las figuras 4 y 5 se apreciará que, en uso del sistema de monitorización, no siempre la parte llamada “parte superior” queda necesariamente más cerca del extremo superior del depósito. Esto mismo es aplicable, pero a la inversa, al término “parte inferior”. En una posible realización, los medios de procesado 16 son un microcontrolador embebido, pero puede usarse cualquier procesador, microprocesador o dispositivo hardware que albergue el software necesario para realizar las tareas de control y procesado de la información registrada. Los medios de procesado 16 albergan los algoritmos quimiométricos 165, implementados mediante software, que realizan el cálculo de las variables de interés a partir de la información espectral NIR registrada por el espectómetro 15 y de las temperaturas del fluido a medir T_1, la temperatura del sistema de iluminación T_3 y la temperatura del sistema espectrométrico T_2 que recoge la señal. Estos algoritmos quedan fuera del alcance de la invenciónEn el caso particular en el que el fluido es un vino fermentando en una cuba, las variables de interés que se calculan a partir del espectro detectado y de las temperaturas registradas son: el grado alcohólico y el contenido de azúcares para monitorizar el proceso de fermentación del vino.

La parte superior 102 de la vaina puede incorporar algunos elementos adicionales, como un sensor de temperatura 171 para controlar la temperatura del sistema electrónico, una fuente de alimentación o batería 172, medios de almacenamiento de información 173, como por ejemplo una memoria y electrónica de comunicaciones 174 para el intercambio de información con otros dispositivos o entre componentes del propio dispositivo, por ejemplo para controlar el encendido de la fuente de iluminación 11 y el tiempo que ésta permanece encendida.

Por último, el dispositivo 10 incluye, preferentemente en la parte superior 102, y más preferentemente en el extremo de la misma opuesto al extremo en el que se encuentra la primera lámina transparente 12, un conector o interfaz de conexión 18. Esta interfaz

18 se utiliza para el intercambio de información de control, comunicaciones y alimentación. La parte del dispositivo 10 donde se encuentra esta interfaz 18 está preferentemente protegida por un anillo protector 19, preferentemente de plástico o de cualquier otro material que haga un sellado para evitar que el aire entre en contacto con la muestra que se está analizando.

A continuación se describen dos realizaciones de sistemas de medida integrados en un depósito, basados en un dispositivo de medida 10 como el descrito en este texto. El modo de llenado de las cubas, depósitos o recipientes de almacenamiento del fluido hace que el nivel de llenado sea diferente de una cuba a otra frecuentemente. Además, el nivel de fluido en la cuba puede variar durante el proceso de fermentación, envejecimiento o proceso de tratamiento de que se trate. Los inventores han observado que es interesante realizar mediciones a la misma altura (profundidad), tomando como referencia por ejemplo el nivel máximo de llenado, ya que las condiciones pueden cambiar en función de la altura a la que se realiza la medida. En el caso concreto del vino, durante su proceso de fermentación y envejecimiento, uno de los aspectos claves es la turbidez del mismo. Esta turbidez indica la cantidad de partículas sólidas suspendidas en el fluido, y esta turbidez puede variar significativamente a diferentes alturas, ya que la generación de CO_2 durante la fermentación hace que estas partículas sólidas vayan hacía arriba. Es decir, se ha observado que la profundidad con respecto al nivel de fluido en el depósito a la que se toman las medidas condiciona el resultado de las mismas. Para solucionar este problema, se ha desarrollado un sistema para mantener en todo momento el dispositivo de medida 10 a una misma distancia relativa respecto al nivel de llenado de la cuba o depósito de almacenamiento. El sistema de regulación en altura permite anclar el dispositivo de medida 10 a una distancia fija respecto al nivel de llenado, solucionando así el problema detectado.

La figura 2 muestra un esquema de un sistema de monitorización 300 integrado en un depósito 30, de acuerdo con una primera realización de la invención. La regulación de la altura se consigue mediante un sistema de flotación 32. El sistema de flotación 32 es preferentemente un elemento, preferentemente un cilindro, de un material flotante en el fluido o líquido bajo supervisión. Un ejemplo no limitativo de tal material es el corcho. El sistema de flotación 32 se sitúa en flotación sobre el nivel del fluido dentro de la cuba, tanque o depósito 30. El dispositivo de medida 10 se une o conecta al

sistema de flotación 32 mediante una barra 31 de longitud determinada (seleccionada en función de las dimensiones del depósito 30, del producto a monitorizar, etc.), de forma que el dispositivo de medida 10 queda sumergido en el fluido a una profundidad determinada por la longitud de la barra 31. El sistema de flotación 32 puede controlarse desde el exterior del depósito 30 mediante medios de conexión 33, que pueden tomar la forma por ejemplo de un cordón o cable 33 conectado al sistema de flotación 32 en un extremo. Alternativamente, este primer extremo del cordón o cable 33 no termina en el sistema de flotación 32, sino que una vez enganchado al sistema de flotación 32, se introduce en el interior de la barra 31, a lo largo de la misma, o discurre paralelo a la barra 31. El otro extremo del cordón o cable 33 queda dispuesto en el exterior de la cuba o depósito, para manipulación desde el exterior del sistema de medida 300. Preferentemente el cable 33 es además un cable de comunicaciones para hacer llegar el resultado de las medidas y procesado posterior hacia el exterior de la cuba. Alternativamente, el cable 33 es un cable mecánico convencional y junto al mismo, en paralelo o en su interior, se encuentra un cable de comunicaciones para el transporte de los datos mencionados hacia el exterior. La cuba o depósito 30 está preferentemente cerrada/sellada para que su contenido no entre en contacto con el aire exterior, mediante una tapa 301, por ejemplo de plástico. El cordón o cable 33 que conecta el sistema de flotación 32 con el exterior de la cuba atraviesa la tapa que cierra el depósito por un agujero o ranura diseñado a tal efecto.

La figura 2 muestra la zona de medida M (13 en la figura 1) y la distancia D entre la zona de medida M y el nivel máximo de llenado del depósito 30. En la figura 2 se muestra también, con línea gruesa, el nivel de llenado N y en torno a este nivel de llenado N, los posibles cambios de nivel, con sendas líneas punteadas. Estos posibles cambios de nivel indican los cambios de nivel que pueden ocurrir en el proceso de fermentación y envejecimiento del fluido, por ejemplo vino. De esta forma, gracias al sistema de flotación 32 se consigue un sistema de monitorización autorregulable en altura. Así, se garantiza que todas las medidas sobre el fluido se toman a la profundidad de interés (D). La barra 31 contiene el cable 33 (o cable mecánico más cable de comunicaciones). El cable de comunicaciones se utiliza para extraer los datos del sensor 10. Dicho cable de comunicaciones se conecta al interfaz de comunicaciones y alimentación 18. El sistema de monitorización 300 de esta realización es especialmente ventajoso para la monitorización de fluidos en cuyos procesos se pueda producir una variación significativa del nivel del fluido en la cuba

(por ejemplo porque fruto del proceso de fermentación, varíe significativamente la cantidad de producto en proceso de producción). En estos casos, el sistema de flotación 32 mantiene el dispositivo de medida 10 al mismo nivel con respecto a la altura o nivel de fluido N, independientemente de si ocurre un cambio en el nivel total del fluido en el depósito. Alternativamente al envío de la información al exterior mediante el cable de comunicaciones, este envío puede realizarse de manera inalámbrica, en función del sistema de adquisición presente en el al planta.

La figura 3 muestra un esquema de otro sistema de monitorización 400 integrado en un depósito 30, de acuerdo con una segunda realización de la invención. El sistema de monitorización 400 comprende un dispositivo de medida 10 como los ilustrados en las figuras 1 y 2. El sistema de medida 400 comprende un sistema de regulación en altura 42 configurado para que el dispositivo de medida 10 sumergido en el fluido mantenga siempre la misma distancia (profundidad) con respecto al nivel máximo de fluido N. El sistema de regulación en altura 42 comprende un anclaje que, destornillándolo, permite regularlo/moverlo en altura y una vez atornillado queda fijo a una altura concreta. La figura 3 muestra la zona de medida M (13 en la figura 1) del dispositivo de medida 10 y la distancia D entre la zona de medida M y el nivel N de llenado del depósito 30. El sistema de regulación en altura 42 se sitúa a una cierta altura sobre el nivel máximo de fluido N. En una realización preferente, en la que la cuba, tanque o depósito 30 dispone de una tapa 401 para su cerrado, el sistema de regulación en altura 42 se acopla o inserta en la tapa 401. El dispositivo de medida 10 se une o conecta al sistema de regulación en altura 42 mediante un cable o cuerda 41 que puede desplegarse o recogerse en el sistema de regulación en altura 42, en función de las variaciones del nivel de llenado N del fluido en la cuba. Así, como en la realización anterior, el dispositivo de medida 10 queda sumergido en el fluido a una profundidad determinada por la longitud del cable o cuerda 41, que en este caso se controla por el sistema de regulación en altura 42. El sistema de regulación en altura 42 se controla desde el exterior del depósito 30. De esta forma, gracias al sistema de regulación en altura 42, se garantiza que todas las medidas sobre el fluido se toman a la profundidad de interés. Las medidas tomadas se envían al exterior como en la realización de la figura 2, es decir, o bien de forma cableada o bien de forma inalámbrica.

Los inventores han observado que un aspecto importante para llevar a cabo la medida correcta es que la ranura o cavidad de medida (13 en la figura 1, M en las figuras 2 y

3) esté completamente llena del líquido a medir. Por otra parte, el dispositivo de medida 10 debe introducirse en la cuba o depósito 30 tal y como se ilustra en las figuras 1 a 3, ya que la tapa 301 401 de la cuba tiene normalmente un diámetro muy pequeño, que solo permite la inserción del dispositivo 10 de forma tal que la cavidad de medida 13, M queda en posición horizontal. Situando la ranura o cavidad 13, M en horizontal (como se muestra en las figuras 2 y 3) puede provocar que no se llene la cavidad completamente, ya que en ocasiones esta disposición horizontal provoca que no todo el aire (burbujas indeseadas en las medidas) salga de la ranura. El sistema de la invención supera el inconveniente anterior como se explica a continuación.

Las figuras 4A y 4B muestran una realización particular del sistema de monitorización 300 de la figura 2, en el que se incorpora un sistema de posicionamiento 34 para favorecer el llenado de la zona de medida M, M'. Las figuras 5A y 5B muestran una realización particular del sistema de monitorización 400 de la figura 3, en el que se incorpora un sistema de posicionamiento 44. El sistema mecánico (sistema de posicionamiento) 34 44 permite girar el dispositivo de medida 10 para orientar la ranura M, M' en disposición vertical, favoreciendo así la salida del aire y favoreciendo el llenado de la ranura o cavidad M' con el líquido o analito medir. Nótese que la cavidad o ranura se ha referenciado como M cuando se sitúa en horizontal (figuras 4A y 5A) y como M' cuando se ha girado y está dispuesta en vertical (figuras 4B y 5B), pero en realidad la cavidad delimitada por las paredes 101 102 103 del dispositivo 10 no varía con el giro del mismo. Es decir, el sistema de posicionamiento 34 44 permite girar el dispositivo de medida 10 unos 90º y dejar la cavidad o zona de medida M' en perpendicular a su posición original (es decir, con la abertura hacia arriba), para obtener un llenado adecuado que evita la presencia de burbujas de aire en la zona de medida. Esta posición favorece la evacuación de burbujas de aire, que pueden abandonar la cavidad de forma natural, ascendiendo en vertical hacia la zona abierta de la misma.

A continuación se describe una posible implementación de un sistema de posicionamiento 34 44. La vaina o carcasa del dispositivo de medida 10 comprende un mecanismo de apertura y cierre 341 formado por dos piezas articuladas por un eje común. Una de las piezas se fija a la vaina o carcasa del dispositivo 10 y la otra pieza se fija a la barra 31, en la parte de la misma que queda junto a la vaina o carcasa. En una posible realización, el mecanismo de apertura y cierra 341 es una bisagra. El

mecanismo 341 está diseñado para que su apertura máxima sea de 90º, tal y como se ilustra en la figura 4A. Además, la vaina o carcasa lleva incorporado en su exterior un cable 342, por ejemplo en la misma pared en la que se encuentra la primera pieza del mecanismo de apertura y cierre 341 o, como se muestra en la figura 4A, en una pared perpendicular a la pared en la que se encuentra la primera pieza del mecanismo de apertura y cierre 341. El funcionamiento del sistema de posicionamiento 34 es el siguiente: Una vez introducido en el depósito 30 lleno de fluido el conjunto formado por la barra 31 y el dispositivo de medida 10, unidos por el mecanismo de apertura y cierre 341 dispuesto formando un ángulo de unos 90º, hasta que el dispositivo de medida 10 quede totalmente sumergido en el interior del fluido, se tira desde el exterior del depósito del cable 342, cuyo extremo libre debe quedar asomando por la tapa 301 del depósito, hasta que el mecanismo de apertura y cierre 341 se pliegue o cierre, formando un ángulo de 0º entre las dos piezas que la forman. Esta posición final tras la manipulación del sistema de posicionamiento se muestra en la figura 4B. Como la segunda pieza del mecanismo 341 está unida a la vaina o carcasa, al tirar hacia arriba del cable 342 el mecanismo 341, al cerrarse acercándose a la primera pieza (unida a la barra 31), hace girar a la vaina o carcasa hasta que, en su posición de cerrado completo, la cavidad M' queda dispuesta en posición vertical, facilitando la liberación de burbujas de aire. Opcionalmente, el sistema de posicionamiento 34 comprende además un sistema de amarre del cable 342, para fijar la posición del mismo tras el giro del dispositivo de medida 10 y mantener la ranura M' en posición vertical durante el tiempo de muestreo. Este sistema de amarre, no ilustrado en las figuras, se sitúa en el exterior del depósito 30. En las figuras 5A y 5B se ilustra un sistema de posicionamiento 44, en esta ocasión en un sistema de monitorización como el de la figura 3. En las figuras se muestra un mecanismo de apertura y cierre 441 y un cable 442 como los de las figuras 4A y 4B,

En ambas realizaciones, al girar dispositivo 10 para situar su cavidad o ranura M' en posición vertical, la distancia a la que se toman las medidas varía ligeramente: mientras que con el dispositivo 10 situado en la posición de inserción (figuras 4A y 5A) esta distancia era D, con el dispositivo 10 girado y con la cavidad M' en vertical la distancia del punto medio de la cavidad M' hasta la línea de llenado N es D'. Nótese que lo importante es que todas las medidas se realicen a profundidad constante, ya sea D o D'.

Por otra parte, la invención no está limitada a las realizaciones concretas que se han descrito sino abarca también, por ejemplo, las variantes que pueden ser realizadas por el experto medio en la materia (por ejemplo, en cuanto a la elección de materiales, dimensiones, componentes, configuración, etc.), dentro de lo que se desprende de las reivindicaciones.

REIVINDICACIONES

1. Un sistema de monitorización (300) de al menos un parámetro de un fluido contenido en un depósito (30), que comprende:
-un dispositivo de medida (10) basado en espectroscopia de infrarrojo cercano diseñado para sumergirse en el citado fluido a monitorizar y para tomar medidas de dicho fluido, donde dicho dispositivo de medida (10) comprende una zona de medida (13, M, M').

estando el sistema de monitorización (300) caracterizado por que comprende un sistema de flotación (32) conectado a dicho dispositivo de medida (10), estando dicho sistema de flotación (32) dispuesto, durante el uso del sistema de monitorización (300), en flotación sobre el fluido a monitorizar, de forma que la zona de medida (13, M, M') del dispositivo de medida (10) queda sumergida en el fluido a una profundidad constante (D, D') con respecto al nivel de fluido (N) en el depósito (30), de forma que todas las medidas tomadas por el dispositivo de medida (10) se toman a la misma profundidad con respecto al nivel de fluido (N).

2. El sistema (300) de la reivindicación 1, donde dicho dispositivo de medida (10) está conectado a dicho sistema de flotación (32) mediante una barra (31) de una determinada longitud.

3. El sistema (300) de cualquiera de las reivindicaciones anteriores, donde el sistema de flotación (32) comprende medios de conexión (33) configurados para conectar dicho sistema de flotación (32) con el exterior del depósito (30).

4. El sistema (300) de cualquiera de las reivindicaciones anteriores, donde dicho dispositivo de medida (10) está configurado para tomar medidas del fluido de forma periódica o de forma aleatoria.

5. El sistema (300) de cualquiera de las reivindicaciones anteriores, donde dicho dispositivo de medida (10) comprende una fuente de iluminación (11) que trabaja en el espectro de luz visible e infrarrojo cercano y un sistema de detección (15) basado en

espectroscopia de infrarrojo cercano, donde dicha fuente de iluminación (11) está configurada para iluminar el fluido a monitorizar y dicho sistema de detección (15) está configurado para tomar al menos una medida del espectro de luz que ha atravesado dicho fluido a monitorizar.

6. El sistema (300) de la reivindicación 5, donde dicho dispositivo de medida (10) comprende medios para registrar la temperatura (T_1) del fluido a monitorizar, medios para registrar la temperatura (T_2) del sistema de detección (15) y medios para registrar la temperatura (T_3) de la fuente de iluminación (11).

7. El sistema (300) de la reivindicación 6, donde dicho dispositivo de medida (10) comprende medios de procesado (16) configurados para procesar las medidas tomadas por sistema de detección (15) y por dichos tres medios para registrar la temperatura del fluido (T_1), del sistema de detección (T_2) y de la fuente de iluminación (T_3).

8. El sistema (300) de cualquiera de las reivindicaciones anteriores, que comprende además un sistema de posicionamiento (34) configurado para girar el dispositivo de medida (10) en el interior del fluido, de forma que la zona de medida (M') quede dispuesta en el interior del fluido con su abertura hacia arriba.

9. El sistema (300) de las reivindicaciones 2 y 8, donde dicho sistema de posicionamiento (34) comprende un mecanismo de apertura y cierre (341) formado por una primera pieza y una segunda pieza articuladas entre sí mediante un eje común, y un cable (342), donde dicha primera pieza está fijada al dispositivo de medida (10) y dicha segunda pieza está fijada a la barra (31), estando dicho sistema de posicionamiento (34) configurado para, una vez introducido en el depósito (30) lleno de fluido el conjunto formado por la barra (31) y el dispositivo de medida (10), unidos por dicho mecanismo de apertura y cierre (341) dispuesto formando un ángulo de unos 90º, tirar desde el exterior del depósito (30) del cable (342) hasta que el mecanismo de apertura y cierre (341) se pliegue formando un ángulo de unos 0º entre dichas primera y segunda piezas, quedando la cavidad (M') dispuesta en posición vertical, facilitando la liberación de burbujas de aire.

10. El sistema (300) de la reivindicación 9, donde dicho sistema de posicionamiento (34) comprende además un sistema de amarre del cable (342) configurado para fijar la posición del mismo tras el giro del dispositivo de medida (10) y mantener la ranura (M') en posición vertical durante el tiempo de muestreo.

11. El sistema (300) de cualquiera de las reivindicaciones anteriores, donde dicho fluido cuyo al menos un parámetro se desea monitorizar es un vino y dicho al menos un parámetro a monitorizar es uno de los siguientes: el grado de alcohol, el grado de acidez o el grado de azúcares presentes en el vino.

RESUMEN

Un sistema de monitorización (300) de al menos un parámetro de un fluido contenido en un depósito (30), que comprende: un dispositivo de medida (10) basado en espectroscopia de infrarrojo cercano diseñado para sumergirse en el citado fluido a monitorizar y para tomar medidas de dicho fluido, donde dicho dispositivo de medida (10) comprende una zona de medida (13, M, M'). El sistema de monitorización (300) comprende un sistema de flotación (32) unido a dicho dispositivo de medida (10), estando dicho sistema de flotación (32) dispuesto, durante el uso del sistema de monitorización (300), en flotación sobre el fluido a monitorizar, de forma que la zona de medida (13, M, M') del dispositivo de medida (10) queda sumergida en el fluido a una profundidad constante (D, D') con respecto al nivel de fluido (N) en el depósito (30), de forma que todas las medidas tomadas por el dispositivo de medida (10) se toman a la misma profundidad con respecto al nivel de fluido (N).

[Fig. 2]

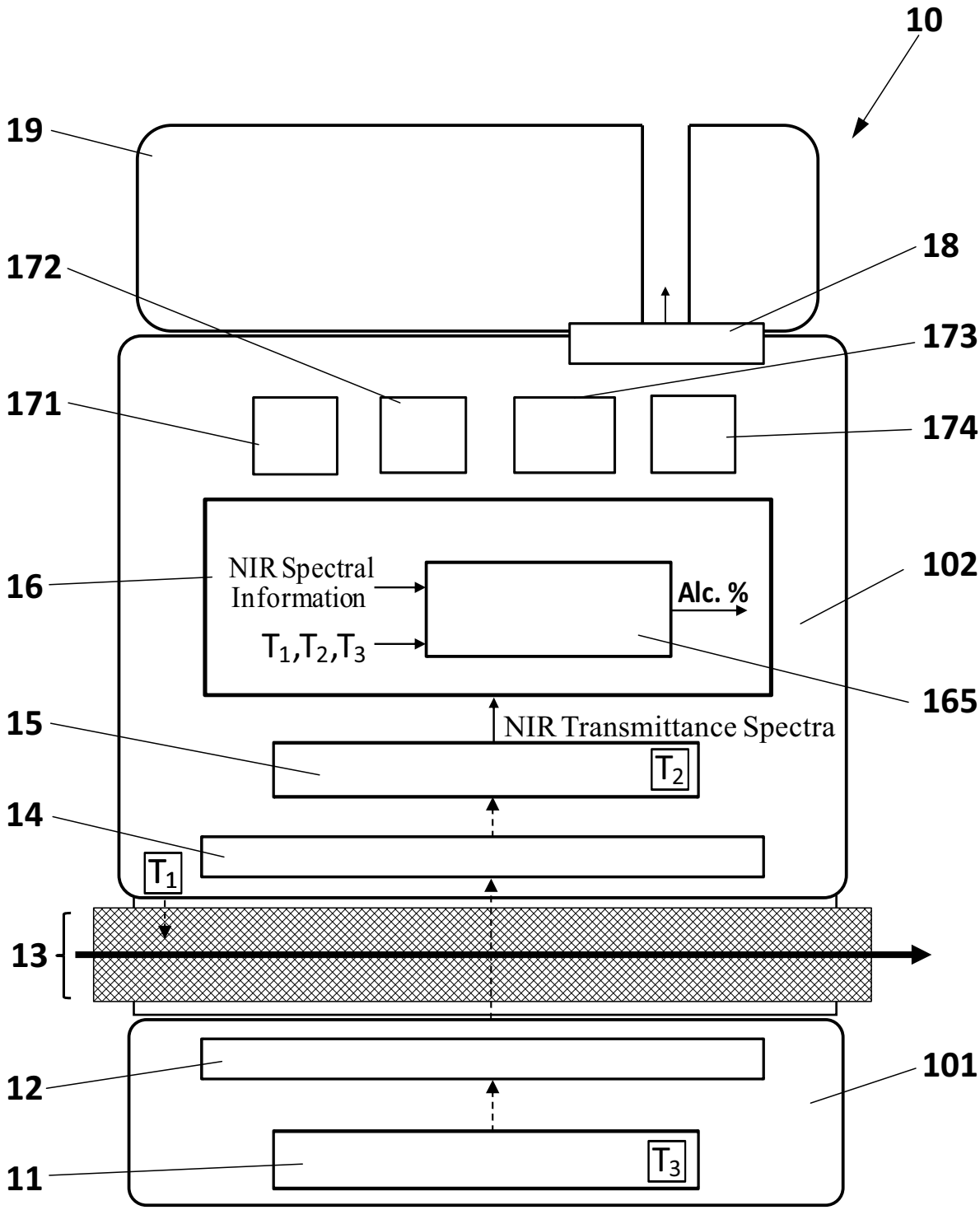
10
19
172
18
173
171
174
16
NIR Spectral Information
T_1,T_2,T_3
Alc. %
102
165
15
NIR Transmittance Spectra
T_2
14
T_1
13
12
101
11
T_3

FIG. 1

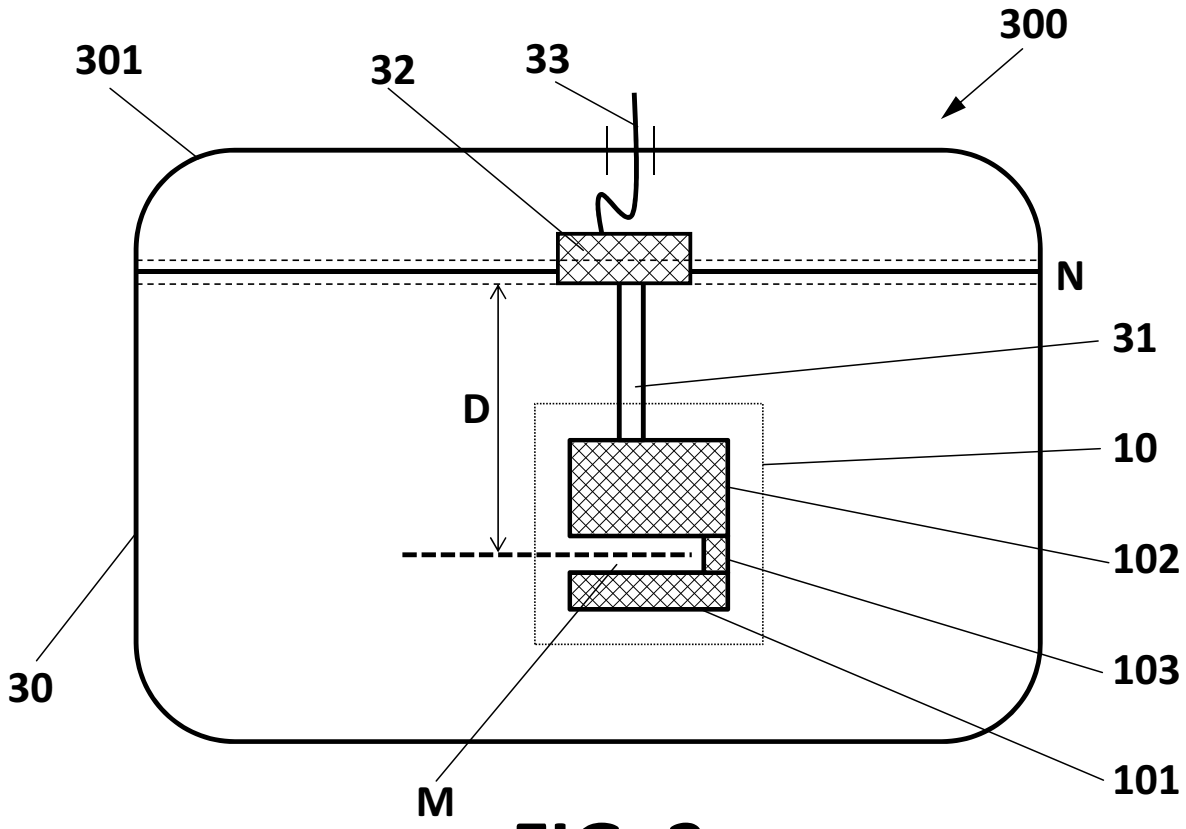
300
301
32
33
N
31
D
10
102
103
101
30
M

FIG. 2

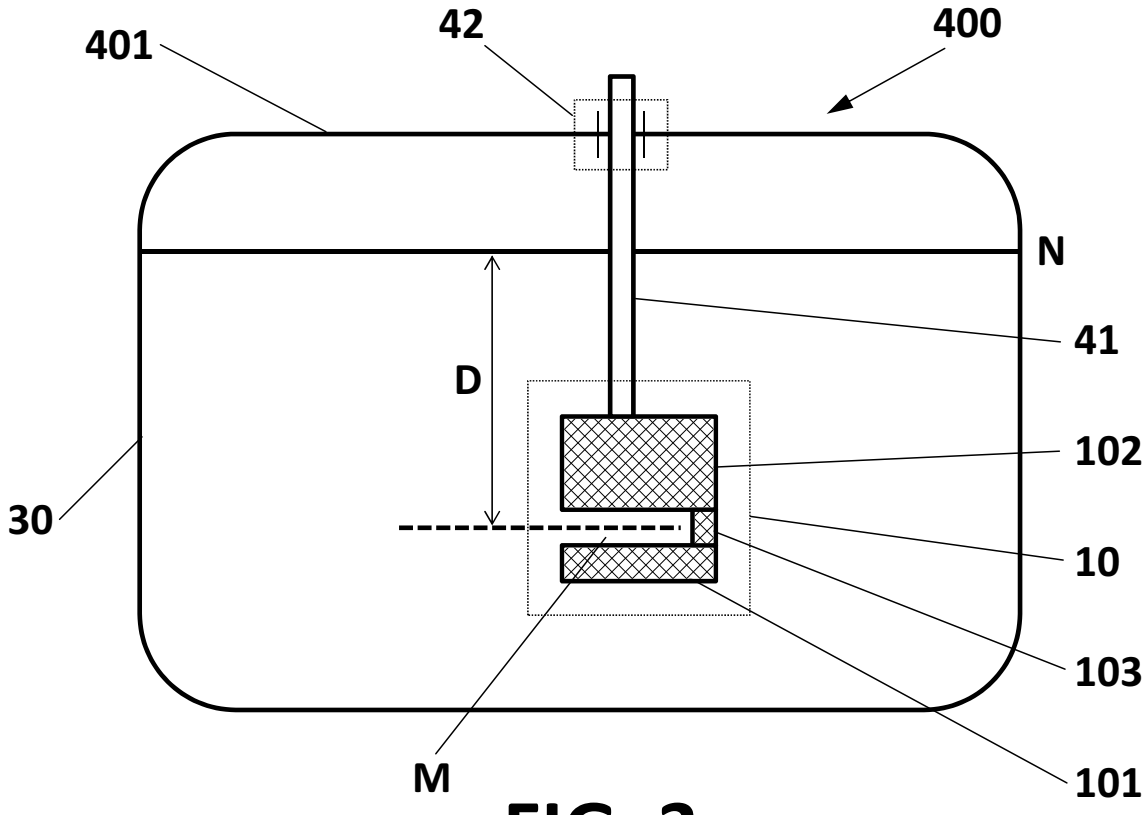
401
42
400
N
41
D
102
10
103
101
30
M

FIG. 3

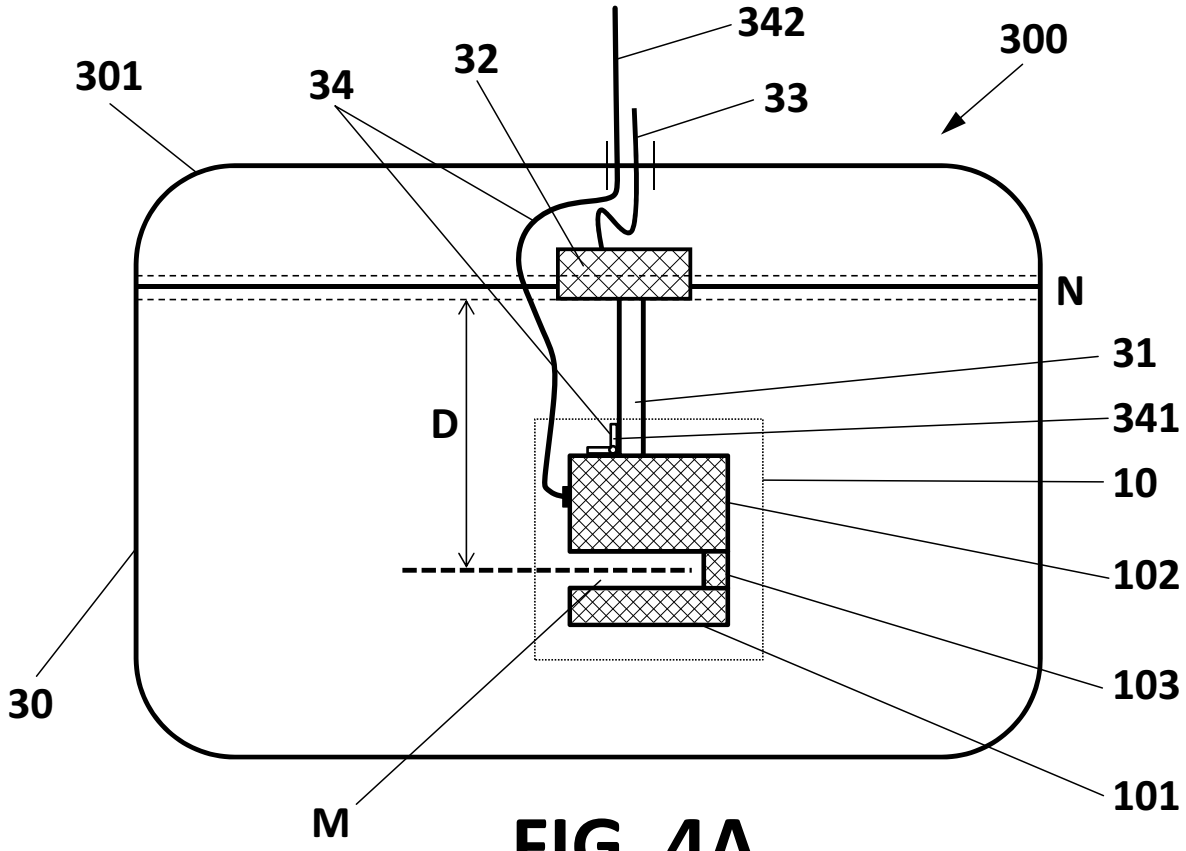
342
300
301
34
32
33
N
31
D
341
10
102
30
103
M
101

FIG. 4A

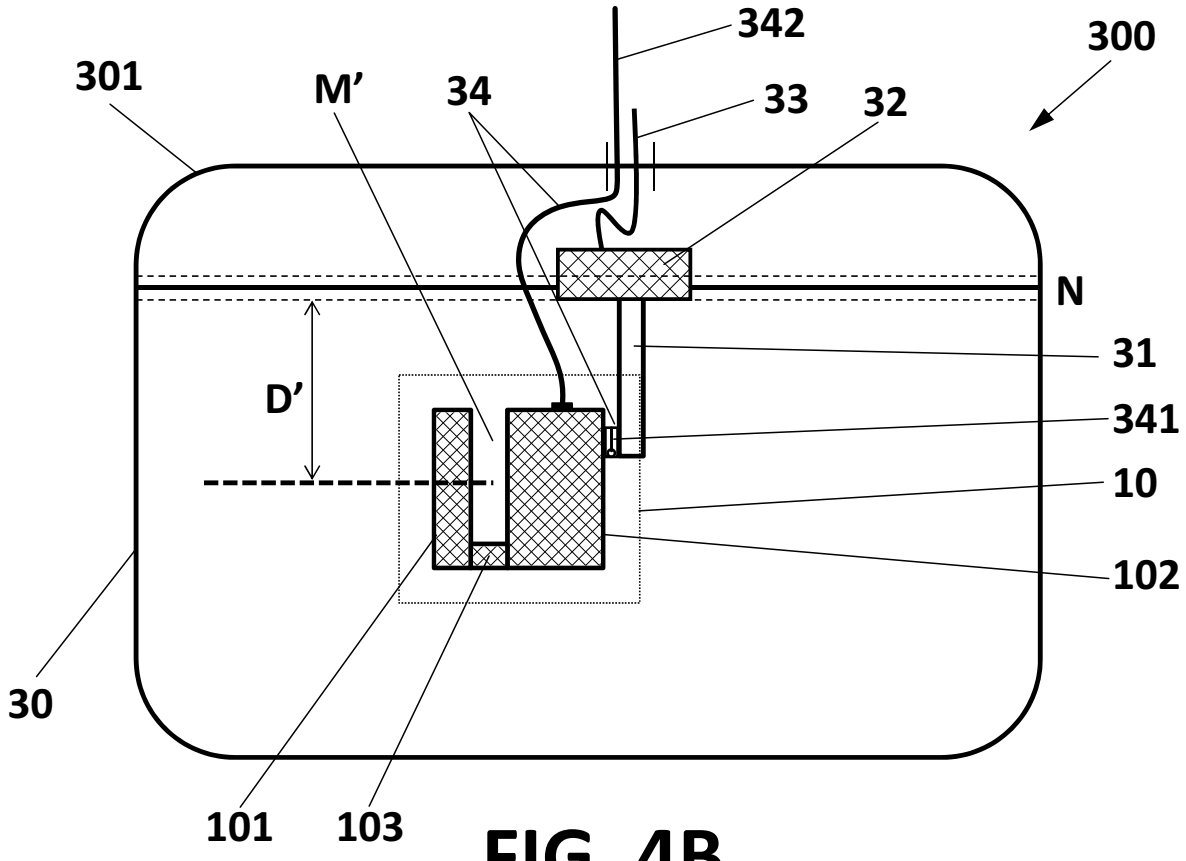
342
300
301
M'
34
33
32
N
31
D'
341
10
102
30
101
103

FIG. 4B

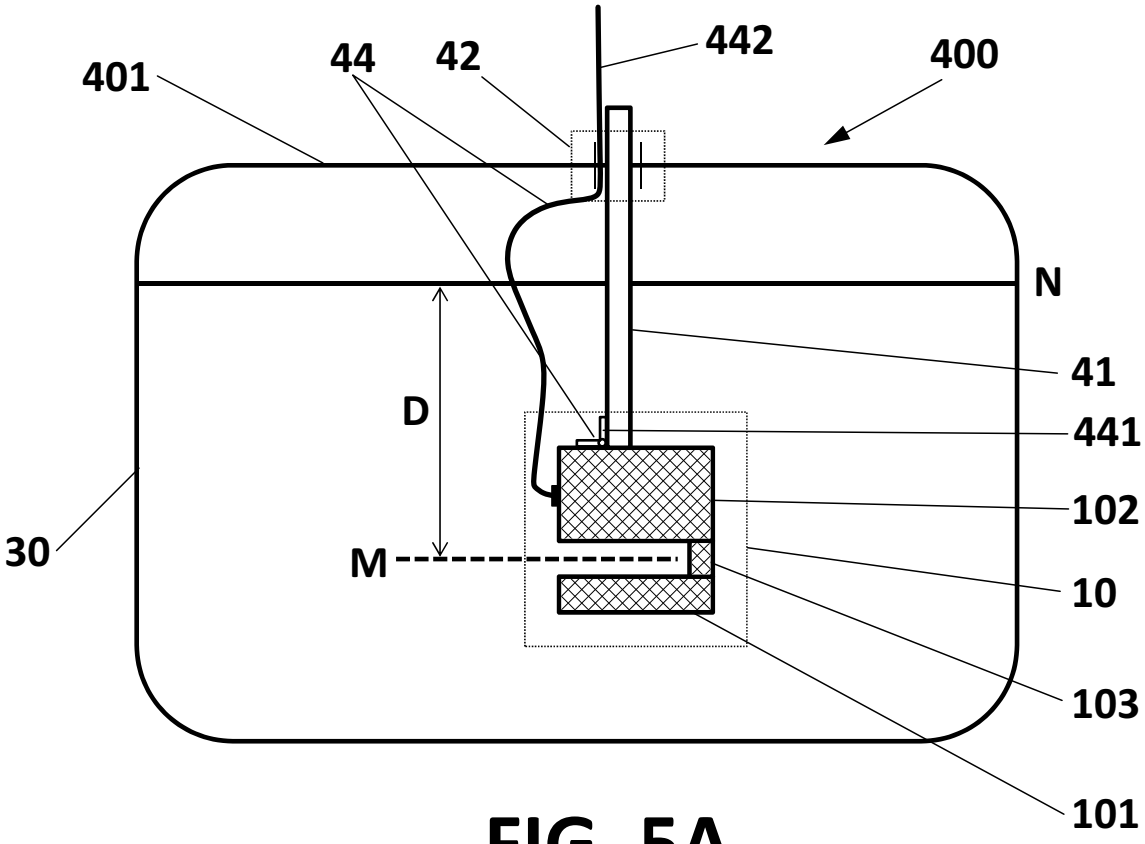
401
44
42
442
400
N
41
D
441
102
30
M
10
103
101

FIG. 5A

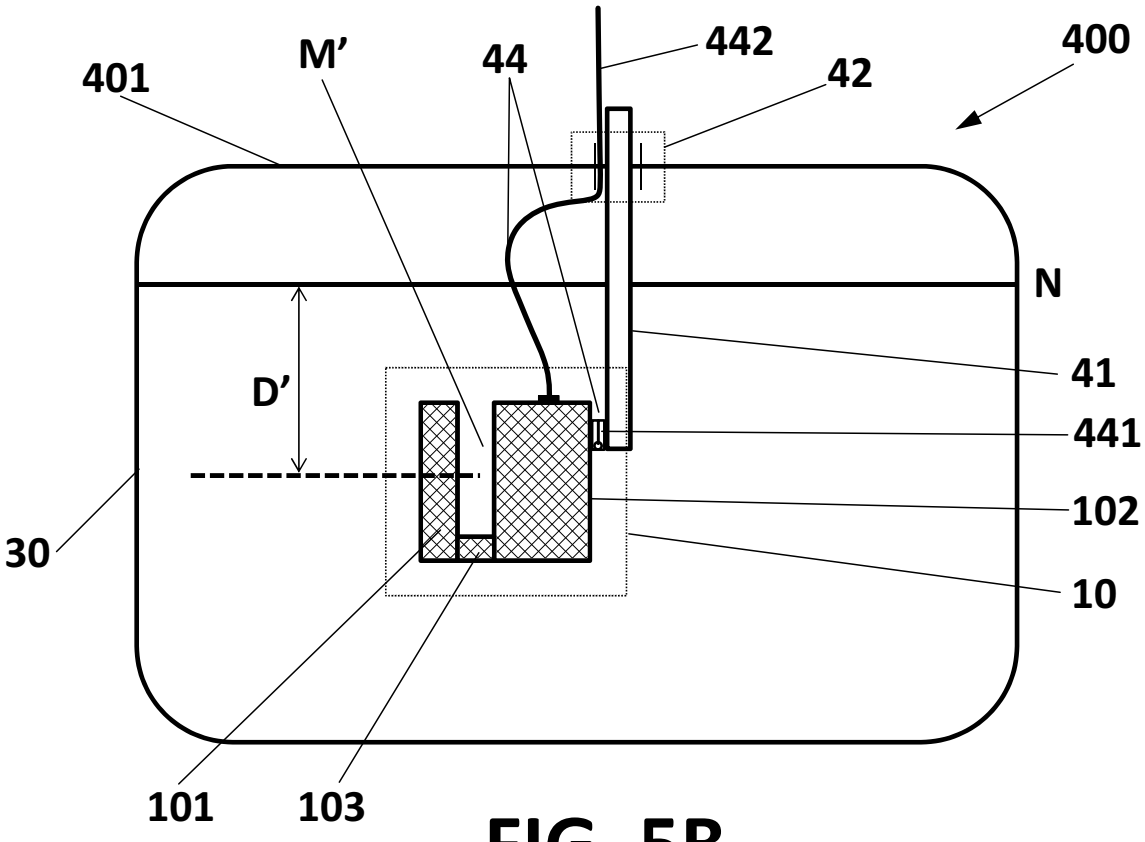
401
M'
44
442
42
400
N
41
D'
441
102
30
10
101
103

FIG. 5B

MINISTERIO
DE INDUSTRIA, ENERGÍA
Y TURISMO

Oficina Española
de Patentes y Marcas

Acknowledgement of receipt

We hereby acknowledge receipt of your request for grant of a European patent as follows:

Submission number	300191449	
Application number	EP16382179.6	
File No. to be used for priority declarations	EP16382179	
Date of receipt	26 April 2016	
Your reference	P152931EP	
Applicant	FUNDACIÓN TEKNIKER	
Country	ES	
Title	FLUID MONITORING SYSTEM	
Documents submitted	package-data.xml	ep-request.xml
	application-body.xml	ep-request.pdf (5 p.)
	SPECEPO-1.pdf\P152931EP-spec-draft-(oilwearPICO)-20160425-vFINAL.pdf (19 p.)	SPECEPO-2.pdf\P152931EP-drawings-(oilwearPICO)-20160425-vFINAL.pdf (10 p.)
	f1002-1.pdf (1 p.)	
Submitted by	CN=Manuel Barrero 34075	
Method of submission	Online	
Date and time receipt generated	26 April 2016, 10:04:17 (CEST)	
Official Digest of Submission	57:63:56:95:D7:EA:5E:6D:DE:51:5D:65:5D:2E:7B:E3:83:57:93:38	

/Madrid, Oficina Receptora/

Europäisches Patentamt
European Patent Office
Office européen des brevets

Request for grant of a European patent

For official use only		
1 Application number:	MKEY	
2 Date of receipt (Rule 35(2) EPC):	DREC	
3 Date of receipt at EPO (Rule 35(4) EPC):	RENA	
4 Date of filing:		

5 Grant of European patent, and examination of the application under Article 94, are hereby requested. ☒

5.1 The applicant waives his right to be asked whether he wishes to proceed further with the application (Rule 70(2)) ☐

Procedural language: en

Description and/or claims filed in: en

6 Applicant's or representative's reference: P152931EP

Applicant 1

7-1 Name: FUNDACIÓN TEKNIKER

8-1 Address:
Polo tecnológico de Eibar, c/ Iñaki Goenaga 5
20600 Eibar
Spain

10-1 State of residence or of principal place of business: Spain

14.1 The/Each applicant hereby declares that he is an entity or a natural person under Rule 6(4) EPC. ☐

Representative 1

15-1 Name: BALDER IP Law, S.L.

Association No.: 639

16-1 Address of place of business:
Castellana 93
5ª planta
28046 Madrid
Spain

17-1 Telephone: 0034911336879

17-1 Fax: 0034911331384

17-1 E-mail: info@balderip.com

Inventor(s)

23 Inventor details filed separately ☒

24 Title of invention

Title of invention: FLUID MONITORING SYSTEM

25 Declaration of priority (Rule 52)

A declaration of priority is hereby made for the following applications

25.2 This application is a complete translation of the previous application ☐

25.3 It is not intended to file a (further) declaration of priority ☐

26 Reference to a previously filed application

27 Divisional application ☐

28 Article 61(1)(b) application ☐

29 Claims

Number of claims: 15

29.1 ☒ as attached

29.2 ☐ as in the previously filed application (see Section 26.2)

29.3 ☐ The claims will be filed later

30 Figures

It is proposed that the abstract be published together with figure No. 1

31 Designation of contracting states

All the contracting states party to the EPC at the time of filing of the European patent application are deemed to be designated (see Article 79(1)).

32 Different applicants for different contracting states

33 Extension/Validation

This application is deemed to be a request to extend the effects of the European patent application and the European patent granted in respect of it to all non-contracting states to the EPC with which extension or validation agreements are in force on the date on which the application is filed. However, the request is deemed withdrawn if the extension fee or the validation fee, whichever is applicable, is not paid within the prescribed time limit.

33.1 It is intended to pay the extension fee(s) for the following state(s):

33.2 It is intended to pay the validation fee(s) for the following state(s):

34 Biological material

38 Nucleotide and amino acid sequences

The European patent application contains a sequence listing as part of the description ☐

The sequence listing is attached in computer-readable format in accordance with WIPO Standard ST.25 ☐

The sequence listing is attached in PDF format ☐

Further indications

39 Additional copies of the documents cited in the European search report are requested

Number of additional sets of copies:

40 Refund of the search fee under to Article 9 of the Rules relating to Fees is requested ☐

Application or publication number of earlier search report:

42 Payment

Mode of payment: Debit from deposit account

The European Patent Office is hereby authorised, to debit from the deposit account with the EPO any fees and costs indicated on the fees section below.

Currency: EUR

Deposit account number: 28120253

Account holder: BALDER IP Law, S.L.

43 Refunds

Any refunds should be made to EPO deposit account: 28120253

Account holder: BALDER IP Law, S.L.

Fees	Factor applied	Fee schedule	Amount to be paid
001 Filing fee - EP direct - online	1	120.00	120.00
002 Fee for a European search - Applications filed on/after 01.07.2005	1	1 300.00	1 300.00
015 Claims fee - For the 16th to the 50th claim	0	235.00	0.00
015e Claims fee - For the 51st and each subsequent claim	0	585.00	0.00
501 Additional filing fee for the 36th and each subsequent page	0	15.00	0.00
Total:		EUR	1 420.00

44-A Forms		Details:	System file name:
A-1	Request		as ep-request.pdf
A-2	1. Designation of inventor	1. Inventor	as f1002-1.pdf

44-B Technical documents		Original file name:	System file name:
B-1	Specification	P152931EP-spec-draft-(oilwearPICO)-20160425-vFINAL.pdf Description; 15 claims; abstract	SPECEPO-1.pdf
B-2	Specification	P152931EP-drawings-(oilwearPICO)-20160425-vFINAL.pdf 10 figure(s)	SPECEPO-2.pdf

44-C Other documents	Original file name:	System file name:

45 General authorisation:

46 Signature(s)

Place: **MADRID**

Date: **26 April 2016**

Signed by: **/M.STIEBE/**

Association: **BALDER IP Law, S.L.**

Representative name: **Lars Magnus STIEBE**

Capacity: **(Representative)**

Form 1002 - 1: Public inventor(s)

Designation of inventor 123

User reference: P152931EP
Application No:

Public

	Inventor	
	Name:	MABE, Mr. Jon
	Address:	Polo tecnológico de Eibar, c/ Iñaki Goenaga 5 20600 Eibar Spain
	The applicant has acquired the right to the European patent:	As employer

Signature(s)

Place:	**MADRID**
Date:	**26 April 2016**
Signed by:	**/M.STIEBE/**
Association:	**BALDER IP Law, S.L.**
Representative name:	**Lars Magnus STIEBE**
Capacity:	**(Representative)**

FLUID MONITORING SYSTEM

TECHNICAL FIELD

The present invention relates to the field of fluid monitoring for determining the general condition of fluids from the point of view of their degradation and particle content. More specifically, it relates to the field of oil monitoring, in particular lubricating oils, in order to obtain their state of degradation and to obtain information on the machinery lubricated by those oils on the basis of their particle content.

BACKGROUND OF THE INVENTION

Lubricating oil is one of the key components in many industrial machines and provides a lot of information regarding the machine's condition. Oil heating, for example, can be a sign that the machine is not operating in optimum conditions, and the presence of particles in the oil may indicate a future failure or considerable wear in the lubricated components. It could even point to the existence of cracks or faults in joints that could allow the entry of external contaminants. Some of the parameters that are interesting to monitor in lubricating oil are as follows: particle determination (for example, quantification, classification of size or determination of shape), bubble content in the system or oil degradation based on colour.

In order to prevent shutdowns and failures in industrial machinery due to lubrication-related reasons, different techniques are currently used. Some of these techniques are 'off-line' measurement methodologies (oil sample analysis in the laboratory). However, they do often not provide a sufficiently early detection of the degradation process due to the low frequency with which these measurements are usually taken. Furthermore, in many contexts (transport, industrial, power…) this control methodology entails a significant logistical and financial burden.

To deal with this drawback, alternative technologies based on sensors have been developed for analysing the machine's condition in real time. Among these detectors, those based on image analysis are remarkable. As a matter of example, patent US5572320 describes an image analysis detector that includes a lighting system based on a pulsed laser. Detection is carried out by means of a planar array of light sensitive photodiodes or phototransistors. However, this system is not capable of discriminating between particle shapes. Also, its measuring cell consists of a moving part that positions the oil in a specific place, and this complicates development and can be an important source of errors.

In turn, patent US7385694B2 describes a detector through image analysis that includes a lighting system based on a pulsed laser and a camera for gathering images of the oil subjected to such lighting. However, the device of this patent does not allow a homogenous lighting to be provided over an inspection area that is greater than the beam of light itself. Also, the device requires a pump in order to pump the fluid to the measuring zone.

International patent application WO97/40360 discloses an apparatus based on an optical sensor for determining contamination on machine wear by measuring wear particles in a fluid used in the machine.

Also, international patent application WO2014/154915A1 discloses a system for inspecting oil based on a lighting system, an image capture system and a lens disposed between the image capture system and the oil flow.

The above mentioned disclosures are based on complex systems requiring many components; they are bulky and difficult to deploy in target applications in industrial environments. Taking into account that they need to be submerged in oil and installed in the field, the risk of failure is high, which implies maintenance work and cost and potential failure in the machine under supervision. Additionally, the moving parts require a semi-static sample in order to obtain a proper image, which is not compatible with a running sample.

On the other hand, a lens-free imaging technology has been reported for biological applications, for example by Sang Bok Kim et al. (Lens-Free Imaging for Biological Applications, Journal of Laboratory Automation, 17(1) 43-49, ©2012 Society for Laboratory). Lens-free imaging is based on a light source that illuminates an object through a pin-hole or aperture and an image sensor located at the other side of the object. The object is correctly focused thanks to diffraction effects generated at the pin-hole when hit by the coherent, incoherent or partially coherent light. A focusing lens is therefore not required. This technology has been proved to have remarkable biomedical applications in microscopy, for example in portable diagnostic systems.

As a matter of example, international patent application WO2012/094523A2 discloses a system for three dimensional imaging of an organelle contained within a sample that includes an image sensor, a sample holder adjacent the image sensor and an illumination source comprising coherent light or partially coherent light. The source illuminates the sample through at least one aperture, fiber-optic cable or optical waveguide, based on the lens-free imaging concept. The system illuminates the sample through a plurality of different angles. In order to achieve this illumination in different angles, the light source is rotated. A portable tomographic imager is also described. It is based on the same lens-free imaging principle. Instead of rotating a

single light source, a plurality of light sources is used.

Also, United States patent application US2015204773A1 discloses a system for three dimensional imaging of motile objects, such as sperm, based on an image sensor and a sample holder adjacent to the image sensor. In this system, two illumination sources are used, each one illuminating at a different wavelength.

Both the system disclosed in WO2012/094523A2 and the one disclosed in US2015204773A1 imply 'off-line' measurement methodologies (sample analysis in the laboratory). The sample is confined within a sample holder or chamber and the imaging technique is applied. These approaches are not suitable for online measurements, where especial mechanical parts are needed for allowing a continuous flow through the detection cell. Additionally, these solutions rely on algorithms with a huge computational need for reconstructing the images, which may jeopardize their application in systems where a high throughput and real time response is needed, for example when measuring running fluids.

However, as already explained, industrial machines require an analysis on their condition in real time. Therefore, there is a need for developing new systems for oil inspection in real time and with as much sample volume as possible, overcoming the cited drawbacks.

DESCRIPTION OF THE INVENTION

The present invention attempts to resolve the drawbacks mentioned above by means of a system for inspecting oil with reduced size and number of components with respect to conventional ones. The reduction in size improves its portability and its capacity to be implemented in many more types of industrial machines, including inside other larger components, like filters or pumps. Its reduction in number of components reduces the risk of failure, increases its lifetime and eases the assembly. Additionally, it is remarkable that the current invention is able to improve the inspection area and the optical performance (contrast and spatial aberrations) while keeping the same detector size. This contribution is the key for increasing the sample volume inspected by the sensor.

In a first aspect of the present invention, it is provided a sensor system for inspecting oil, which comprises a micromechanical cell defining a cavity, the micromechanical cell being configured for allowing the entrance of oil within said cavity and the outcome of oil from said cavity through respective inlet and outlet. The sensor system comprises inside said micromechanical cell: a first transparent protective means configured to isolate the inner part of said first member from said cavity to be occupied with oil; a

second transparent protective means configured to isolate the inner part of said second member from said cavity to be occupied with oil; a light source disposed in said first member and configured to emit incoherent light towards said oil disposed within said cavity; an opaque plate disposed between said light source and said first transparent protective means, said plate having a pin-hole configured to permit the passage of illumination towards said cavity to be occupied with oil, said pin-hole being located at a first distance from a focussing plane defined by said cavity; an image sensor disposed in said second member situated on the opposite side of the cavity with respect to said first member and configured to capture a sequence of images of the oil disposed within said cavity, said image sensor being located at a second distance from said focussing plane defined by said cavity.

In a particular embodiment, the system further comprises a diffuser disposed between said light source and said plate defining the pin-hole, said diffuser being configured to provide homogeneous lighting to said cavity.

In a particular embodiment, the system further comprises processing means configured to process said sequence of images and to determine the presence of particles and bubbles and a degradation value of the oil.

In a particular embodiment, the light source comprises on one or more LED diodes.

In a particular embodiment, the image sensor comprises a CMOS sensor or a CCD camera.

In a particular embodiment, the pin-hole has a diameter varying in the range of 30 μm to about 300 μm. Said diameter preferably varies in the range of 50 μm to about 150 μm.

In a particular embodiment, the first distance at which said pin-hole is located from said focussing plane is in the range of 10 mm to about 30 mm. Said distance preferably varies in the range of 15 mm to about 25 mm.

In a particular embodiment, the distance at which said image sensor is located from said focussing plane is in between 1 and 3 mm. The distance preferably varies between 1 and 2 mm.

In a particular embodiment, the oil is static within said cavity. Alternatively, the oil is in motion within said cavity.

In a particular embodiment, the micromechanical cell comprises a first member and a second member defining said cavity therebetween.

In a particular embodiment, the inlet and outlet are inclined with respect to said cavity, thus minimizing the separation between the oil located within said cavity and said

image sensor.

Additional advantages and features of the invention will become apparent from the detail description that follows and will be particularly pointed out in the appended claims.

BRIEF DESCRIPTION OF THE DRAWINGS

To complete the description and in order to provide for a better understanding of the invention, a set of drawings is provided. Said drawings form an integral part of the description and illustrate an embodiment of the invention, which should not be interpreted as restricting the scope of the invention, but just as an example of how the invention can be carried out. The drawings comprise the following figures:

Figure 1 shows an outline of a sensor system according to a possible embodiment of the invention.

Figure 2A shows a sensor system according to another embodiment of the invention. This configuration has inclined inlet/outlet points.

Figure 2B shows an outline of the sensor system of figure 2A.

Figure 3 shows in detail the image sensor, the focussing plane, the pin-hole and the distances between image sensor and focussing plane and between focussing plane and pin-hole.

Figure 4 represents a general outline of a monitoring system, including the sensor system of the invention.

Figure 5 shows an image captured in a first experiment of the inventive sensor system.

Figure 6 shows the setup of a second experiment of the inventive sensor system.

Figures 7A-7C show the results of a second experiment taken with diameter of pinhole = 500μm.

Figures 8A-8C show the results of the second experiment taken with diameter of pinhole = 200μm.

Figures 9A-9C show the results of the second experiment taken with diameter of pinhole = 50μm.

Figures 10A-10C represent images captured in a third experiment of the inventive sensor.

DESCRIPTION OF AN EMBODIMENT OF THE INVENTION

Figure 1 represents a scheme of a sensor system 1 for inspecting a fluid, of the invention. The fluid may include undesired particles and/or undesired bubbles. The fluid is inspected in order to determine the amount, nature and size of these particles and/or bubbles. This sensor system 1 has been conceived as an autonomous system with totally independent functioning, which delivers auto interpretable measurements, calibrated and corrected for the entire defined operating range.

The sensor system is based on lens-free imaging. The sensor system 1 comprises an optical part 1-O and an electronic part 1-E (or video acquisition and processing sub-system). The electronic part 1-E, schematically represented in figure 1 on the left, is a conventional one. In a preferred embodiment, it is similar to the one described in WO2014/154915A1. Figure 1 illustrates a fluid 5 to be imaged that is disposed in a cavity, space or area 12 between a light source 14 and an image sensor 17.

As described below, the sensor system 1 operates on a micromechanical cell 10 through which the fluid 5 under supervision circulates. In a preferred embodiment, this fluid is oil, more preferably lubricating oil. The fluid 5 is either static or in motion (circulating fluid) and accesses the area under supervision (supervision cavity, area or space 12) through two inlet/outlet points 11a 11b. In other words, the fluid 5 under supervision is supervised when it fills a supervision area 12 disposed within micromechanical cell 10. Inlet/outlet points 11a 11b are not necessarily parallel to the cavity 12 in which fluid 5 is supervised. They can alternatively be inclined with respect to this area 12. In fact, a configuration having inclined inlet/outlet points 11a 11b, as shown in figure 2A and 2B, contributes to reduce the separation between the sample and the image sensor (not yet described).

Two members 101 102 form the micromechanical cell 10 which defines therebetween a cavity, space or area 12 in fluid contact with input portion 11a and output portion 11b. Space 12 is separated from the remainder of the interior of micromechanical cell 10 (defined by members 101 102) by transparent protective means 13a 13b. In this context, “transparent” means “transparent in the wavelength operated by light source 14”, not yet described, that Is to say, the transparent protective means 13a 13b allow light to pass through them. The protective means 13a 13b, also referred to as protective windows, are made of any suitable transparent material. Non-limiting examples of suitable transparent materials are plastics, such as PMMA or polystyrene (PS), or glass, such as borosilicate, quartz or sapphire. These transparent windows 13a 13b seal the cavity or space 12 occupied by the fluid 5 under supervision. These windows 13a 13b act as a seal so that the fluid does not leak towards the optical equipment housed within the micromechanical cell 10. In other words, the fluid passes

through (or statically fills) space or area 12 and the fluid is “transversally” inspected and measured. Getting rid of the focusing lens mitigates the problems related with the assembly tolereance dependent optical magnifications. Therefore, the proposed system can work without an optical autocalibration. However, if even more accurate size measurements are needed, the seals or windows 13a and/or 13b may be marked with precision patterns to calibrate every single measurement, as described by the inventors in WO2014/154915A1.

The optical part 1-O of the sensor system 1 comprises a light source 14 configured to emit light, in such a way that the fluid 5 (or flow of fluid) which fills cavity or space 12 is subjected to a beam of light. In the scheme of figure 1, the light source 14 is embedded or integrated within a board, such as a PCB (printed circuit board) 15. The light source 14 has light modulation capabilities in terms of light power and light pulse duration. In a preferred embodiment, light source 14 is a source of incoherent light. In other words, the light source 14 preferably supplies a beam of white light to the fluid 5. In a particular embodiment, light source 14 comprises on one or more LED diodes (Light Emitting Diodes) which continuously light the flow 5 which circulates through or fills cavity or space 12 between members 101 102. A diffuser or frosted window 19 may be disposed in front of light source 14. The diffuser 19 is discussed in detail later. In other words, in this embodiment the light source is a LED emitter. Preferably, the light emitting system has a control system (closed loop control) of the polarisation of the LED emitter based on changes in temperature which prevent fluctuations in emission due to said changes in temperature. As a person skilled in the art knows, when the temperature rises there is a reduction in the emission of the LEDs due to a decrease in the efficiency of the photons. By means of this control, if the temperature rises the power is increased so that the apparent emitted light remains constant. In a possible embodiment, the light source 14 also comprises a photodiode 21 near the lighting zone to calculate the error of that closed loop. An embedded processor, not specifically shown, but for example integrated within PCB 15, preferably controls the light source 14 through LED control signals and compensation data. In an alternative embodiment, light source 14 is a conventional light bulb or a Xenon lamp with a filter. In fact, any source of incoherent light could be used (for example a broadband extended source). The light source 14 preferably has a spectral bandwidth that is between 400 and about 700 nm, although the spectral bandwidth may be even smaller or larger.

Opposite the light source 14, on the other side of the cavity, space or area 12 through which the flow 5 circulates (or simply, the cavity, space or area 12 filled with fluid 5), an image sensor or image capture system 17 is placed. The light emitted by the light source 14 that is not absorbed by the fluid 5 is gathered by means of a detector (for example, a photodiode or photodiode array). In an inspection system implementing

artificial vision, as is the case of the sensor system 1, back lighting is used, which means that the optical receiver element (i.e. photodiode array) collects the light that passes through the flow of fluid 5. In the scheme of figure 1, the image sensor 17 is embedded or integrated within a board, such as a PCB (printed circuit board) 18. The image sensor 17 is configured to capture a video sequence (i.e. a train of images) of the zone of interest 12 in the passage of the fluid (preferably oil). This image capture is carried out with a defined spatial resolution and maintaining a general criterion of reduced size and low cost. In other words, the “defined spatial resolution” refers to the fact that the image sensor 17 is capable of determining a defined minimum size of particle, which is in the region of 4 microns over an inspection cavity or area 12 of about 100 mm^2. This resolution is achieved by optimising several conditions, such as the area to be inspected, the size of the image sensor 17 and its number of pixels. It is remarked that the system 1 must have a small size and be as compact as possible.

In a preferred embodiment, the image sensor or image capture system 17 is a camera, more preferably a camera based on complementary metal-oxide semiconductor (CMOS) sensor or CMOS detector (the CMOS sensor is the camera component that receives the image). Therefore, a CMOS camera has a 2D array of photoreceptors manufactured with CMOS technology. For this reason, occasionally in this text the expression “CMOS sensor” or “CMOS detector” is used to refer to the image sensor 17. Alternatively, the image sensor 17 may include, for example, a charged coupled device (CCD) camera. The image sensor 17 may be monochromatic or colour. The image sensor 17 has a small pixel size and therefore produces higher resolutions. In a particular embodiment, the pixel size of the image sensor 17 is less than 10.0 μm in size and preferably smaller than 6.0 μm (for example, 2.0 μm or smaller). In a possible embodiment, an acquisition and processing system of 15 frames per second (15 FPS) is used. For example, and Omnivision detector can be used with a 14 megapixel camera. With this image sensor 17 a spatial resolution better than pixel size is obtained. It is remarkable that the proposed invention is able to use an inspection area larger than a lens-based system at the same object-detector-light component placing distances.

The minimum size of particle that it must be possible to discriminate is of approximately 4 μm. The area to be captured in each image by the image sensor 17 must be such that it is capable of capturing particles of 4 μm and more. In a preferred embodiment, the area to be captured is of several square millimetres. In one example, said area to be captured is of 100 mm^2. The distance z2 between the object (focussing plane or plane of passage of the fluid under inspection) and the image sensor 17 is desirably as minimum as possible and does not exceed approximately 5 mm, so that the system 1 is remarkably compact and small. Distance z2 is selected to be above 1 mm, in order

to leave room to place transparent protective means 13b, which is necessary in order to prevent fluid from leaking into the inner cavity of member 102. In particular, distance z2 is preferably between 1 and 3 mm and more preferably between 1 and 2 mm approximately. The outline represented in figure 3 shows in detail the image sensor 17, the focussing plane F located at the fluid 5 under supervision and distance z2.

The images (for example video sequence) captured by this camera are processed in an embedded processor of the electronics part 1-E (for example integrated within PCB 18). In a preferred embodiment, the not shown embedded processor is a DSP device (*Digital Signal Processor*). This embedded processor is the one that analyses for each image whether there are bubbles and particles and counts them. In other words, the processor is responsible for extracting the image from the CMOS and processing it. To do this, it has an intermediate memory for subsequent processing. In a possible embodiment, this intermediate memory is a DDR2 external memory. In figure 1, the electronic part 1-E comprises, in addition to the embedded processor and memory means, auxiliary systems such as communication interface, power source, memory, temperature sensor, among others. Also, there is a software part, formed by the group of algorithms in charge of the detection and classification of particles, bubble detection and determination of degradation. Details on the video acquisition, processing of images and counting of bubbles and particles are out of the present invention. This acquisition and processing is preferably similar to the one described in detail in WO2014/154915A1. In a particular embodiment, in which more accuracy is required, the acquisition and processing unit is responsible for applying algorithms for the dimensional calibration of the measurement. Basically, the auto-calibration is based on identifying using the image sensor 17 markings, of a known size, made on windows 13a and/or 13b, which also work as calibration windows, so that any identified image can then be scaled. Machine vision algorithms are used, which directly use the image captured by the image sensor, rather than requiring a reconstruction of the image or a pre-processing of the image using holographic techniques. This auto-calibration makes it possible to diminish the effects of the mechanical and assembly tolerance on the size of the images of particles captured on the camera. The auto-calibration allows, in contrast to conventional oil supervision systems, automatic compensation of these differences in the sizes of the objects captured due to the manufacturing and assembly dispersion. It also means that it is not necessary to dimensionally calibrate each unit of equipment. Also, it makes the system more robust against potential degradations occurring in the machine. In other words, the auto-calibration algorithms impose the required precision of the system on the auto-calibration markings and not on the entire micromechanical system, although in practice the result is equivalent to imposing said precision requirements on the whole system.

Between the light source 14 and the protective means 13a (the protective means closest to the light source or, in other words, the protective means that separates member 101 from the supervision cavity, area or space 12), there is a sheet, plate or spatial filter 16. The sheet or plate 16 is opaque. In the context of the present invention, "opaque" means "opaque in the wavelength operated by light source 14". The sheet, plate or spatial filter 16 can be made of any material, such as plastic or metal. The sheet or plate 16 has an aperture or pin-hole 165 contained therein that is configured to permit the passage of illumination (e.g., spatial aperture or pin-hole). The pin-hole 165 can have any section. In a particular embodiment, it has been implemented with circular section. The pin-hole 165 has a diameter that is typically in the range of 30 μm to about 300 μm. More preferably, it varies in the range of 50 μm to about 150 μm. The smaller the hole is, the more is improved the beam quality, but the more is reduced the power. If, on the contrary, a too large hole is selected, the beam quality may not be improved as much as desired.

Thanks to the use of the aperture or pin-hole 165, there is no need to use a lens for transporting the image from the object (the fluid 5) to the image sensor 17, as was required in conventional sensing systems. In other words, thanks to the pin-hole 165, the image sensor (camera) 17 is capable of appropriately focusing the object. The diameter of the pin-hole 165 also affects in the depth of field, but with the proposed diameters, the current invention is able to offer a larger depth of field than a lens-based solution. It is remarked that avoiding the use of a lens, which in this application was normally a macro-lens, saves a great deal of space in the sensor system 1 while keeps even a larger sampling volume and image quality. A reduction in size, an increase in compactness and an improvement in sampling volume and image quality across all that volume is therefore achieved.

As seen in figure 1, the aperture or pin-hole 165 is located at a distance z1 from the focusing plane or plane of passage of the fluid under inspection (plane of the area or space 12 occupied by the fluid 5 under supervision). Distance z1 between the object (focusing plane or plane of passage of the fluid under inspection) and the pin-hole 165 is desirably as minimum as possible, because it enables a reduction in the size of the cell 10. The outline represented in figure 3 shows in detail the pin-hole 165, the focussing plane F located at the fluid 5 under supervision and distance z1. In a particular embodiment, distance z1 is in the range of 10 mm to about 30 mm. More preferably, it varies in the range of 15 mm to about 25 mm.

The values of z1, z2 and diameter of pin-hole D_{ph} may vary depending on the application for which the sensor system is used. In general, the larger the diameter of the pin-hole D_{ph}, the less light power will be needed, but the larger z1 is required and

the smaller z2 is achieved. On the contrary, reducing the diameter of the pin-hole D_{ph}, will require increasing the light power applied, but a smaller z1 and a larger z2 could be reached, allowing a thicker protection glass between the sample and the detector and enabling a much more compact complete system. As an approximation, the following relation may be used:

*Minimum object Diameter in detector=pin-hole Diameter * z2/z1*

The selection of these values also depends on the fluid under supervision. For example, if the fluid is static, a pin-hole with smaller diameter can be chosen, because although less amount of light goes through the pin-hole, the shutter of the image sensor (camera) 17 can remain open for a longer time without risking the quality of the image taken (because the fluid does not substantially move). On the contrary, if the fluid is in motion, the higher its velocity, the larger the diameter of the pin-hole must be, in order to let more light go through the pin-hole, thus minimizing the time required for the image sensor shutter to be open to capture the image. Additionally, the amount of light permitted to go through the diameter of the pin-hole can be compensated with an increase in power in the light source.

In a preferred embodiment, between the light source 14 and the fluid 5 under supervision, a diffuser 19 is placed. In particular, the diffuser 19 is located between the light source 14 and the sheet, plate or spatial filter 16 defining the pin-hole 165. Still more preferably, the diffuser 19 is placed adjacent to sheet, plate or spatial filter 16. The principal mission of diffuser 19 is diffusing the amount of light emitted by the light source 14 in order to obtain a homogenous lighting over the entire cavity or area 12 (amount of fluid 5) that is being inspected. In other words, diffuser 19 increases the incoherence of the light emitted by the light source 14. The diffuser 19 is made of a transparent material that allows light through it. Therefore, the light source 14 can light the fluid 5 appropriately, and by means of the detection system (image system 17) it is possible to visualise the illuminated zone and to capture the image of the fluid. In a preferred embodiment, the diffuser 19 is made of glass, for example a frosted glass. Thanks to this diffuser 19 it is possible to light the area under inspection still in a more homogeneous manner. It has been observed that this is important in order to obtain reliable results (optimal particle detection). As shown in the embodiment represented in figure 1, it is desirable to leave a certain distance d1 between the board (for example PCB) 15 and the closest surface of diffuser 19 in order not to heat diffuser 19 above a certain temperature. Taking into account the typical values of power of the light source 14, it has been experimentally observed that distance d1 may be in the range of about 1 mm to about 5 mm. More preferably, it may be in the range of about 1 mm to about 3 mm (for example 2 mm). The space within the micromechanical cell 10 which is not

occupied by any component is occupied with open air. This space is referred to as 20 in figure 1.

In sum, the proposed sensor system 1 is very compact and of reduced size. A prototype has been developed having a total length of 45 mm approximately. This length includes the length L-O of the optical part 1-O and the length L-E of the electrical part 1-E, wherein L-O = 31 mm approximately and L-E = 14 mm approx. The width of the sensor system 1 is 20 mm approx. Its height is 23 mm approx.

Figure 4 represents a general outline of a monitoring or inspection system in which the sensor system 1 of figures 1 and 2A-2B can be included. Apart from the sensor system 1 already described, the complete system is composed of a series of sub-systems connected to each other and contained within a receptacle or container 50. This monitoring or inspection system is similar to the one described in WO2014/154915A1. The sub-systems are as follows:

A hydraulic conditioning sub-system, made up of components for flow control 52, oil flow control by means of electrovalve 51, pressure control 53, safety filter 54 and the inlet 55i and outlet 55o piping. The reading and operation of the active hydraulic elements is carried out from an electronic sub-system 56. It is noteworthy that the hydraulic conditioning sub-system does not include any pump. In a preferred embodiment, the system of the invention is designed to be installed in a by-pass of the lubricating system of certain machinery. The installation takes advantage of the pressure differences for the fluid to circulate to the measurement module 1 (sensor system) where the oil inspection will take place.

The electronic sub-system 56 is formed by an embedded electronic platform for managing all active sub-systems and managing data channels. This embedded electronic platform performs the global management of information and control of the hydraulic and measurement sub-systems. This sub-system is considered to include the internal and external connection technologies and the power system 57.

The container and fastening system 50 incorporates the external hydraulic and electrical connections and the fastening system (not shown in figure 4) to the installation's place of destination. The system 50 is specifically designed for its direct integration into the lubricating systems of machinery but without affecting the operating conditions thereof. This is achieved by means of the hydraulic sub-systems of the sensor which make it possible to carry out controlled sampling with low content in lubricating oil. The container and the fastening system 50 houses and integrates the different elements in an appropriate manner and allows external communication for the intake and output of the fluid, through the respective inlet 55i and outlet 55o (as the measurement is carried out in the measurement sub-system 1) and provides the

communication interfaces and power supply 57 in order to be able to carry the sensor's results to the machine in question or wherever required.

The hydraulic sub-systems in turn allow the fluid to be measured to be conditioned, thereby reducing the effects of external conditions or factors on the end result. The system has also been developed to avoid the influence of environmental factors such as changes in temperature. In this sense, the sensor system has temperature measurers that actuate the intensity of the light emitting diode and thereby prevent differences in emission related to changes in temperature.

As can be seen from figure 4, the fluid enters the container 50 through the inlet 55i. The flow of fluid follows the direction of the dotted arrow line. The fluid circulates through the inside of the container 50 through appropriate channelling means, such as pipes. Through the inlet and outlet fittings and the sub-systems it is possible to carry out a representative sampling of the fluid (for example, oil) and to condition it to obtain representative measurements of its real condition.

Flow control 52 makes it possible for the system to obtain a fixed flow which makes it possible to know the amount of fluid that is being measured and thereby to obtain the particle concentration therein. In other words, the flow control 52 makes it possible to give values of, for example 100 particles per millilitre. Otherwise, it would only be possible to say that 100 particles were detected, in absolute terms.

The pressure switch 53 is a pressure system that ensures that there is pressure in the system and therefore guarantees that there is a flow of the fluid (for example, of oil). Therefore, it is a pressure switch designed to identify low pressures. The issue is that the machines in which the sensor system 1 is installed are not functioning continuously, and when they are stopped there is no oil pressure, meaning that there is no entry of oil in the sensor system, which results in the measurement eventually taken not being representative, because oil is not being measured. With the pressure switch 53 there is detection of pressure when there is and when there isn't pressure, in order to validate a taken measurement and thereby ensure that it is oil and not air that is being measured.

The inlet electrovalve 51 performs the function of allowing the oil in or not. When the electrovalve is "ON", the system is open for the oil to pass; and when the electrovalve is "OFF", the system is closed and the oil does not enter. This is carried out so that the oil is not continuously flowing through the system, for two important reasons: (1) to carry out controlled sampling and interfere as little as possible with the machine's lubricating systems; (2) to ensure that the hydraulic sub-systems are not affected by dirt that could be generated by the continuous flow of oil.

The ON/OFF arrows indicate in respect of the components next to which they appear in

figure 4, that these components are controlled electronically. Specifically, on electrovalve 51 the ON/OFF arrow indicates the opening and closing off of entry to the oil; and in the pressure switch 53 the ON/OFF arrow provide an indication of the pressure level in the system. The pressure switch 53 is “ON” when a specific pressure value is exceeded and then it is assumed that oil has entered.

Next some experiments are explained. They have been monitored by establishing a USB connection between board 18 and a computer.

Experiment 1

The goal of this experiment is to illustrate the general performance of the system shown in figures 2A-2B in terms of its ability to generate a useful image of the fluid sample for its later processing. The fluid sample used is lube oil contaminated with wear debris and air and water bubbles.

Figure 5 represents an image captured in this experiment using a prototype according to figures 2A-2B. The light source was a white LED having beam aperture of 60º. The plate defining the pin-hole was placed at a distance 1mm from the LED. The diameter of the pin-hole was 150 µm. A diffuser of 3mm thickness was placed adjacent to the plate. In the prototype, lube oil was isolated from the sensor system by two protective windows of 1mm thickness made of quartz. Lube oil was fed into that cavity with an auxiliary hydraulic pump at a flow rate of 0.5L/minute. Distance z1 from the cavity to the pinhole was selected to be 19 mm. The image sensor was a CMOS sensor of 5 Megapixel. Distance z2 from the CMOS sensor to the cavity was selected to be 2.1 mm.

As can be observed in figure 5, the system is able to capture a valid image of the running fluid where the wear particulates and bubbles are recognizable.

Experiment 2

The goal of this experiment is to illustrate the effect of the diameter of the pinhole 165 and of the z1/z2 distances in the system magnifications and depth of field. The setup of the experiment is described in the figure 6. The experiment setup shows a 10Mpix CMOS imager 17, a sample object 25 located at distance z2 from the CMOS imager 17, a plate having a pinhole 165 placed at distance z1 from the object 25, a diffuser (3mm thick / PMMA material) 19 placed immediately after the pinhole 165 and a partially incoherent light source (White LED) 14 at 1mm from diffuser 19. The sample

object 25 is a 1mm thick quartz transparent window in which 8 circles (with diameter=200μm) have been micromachined on its inner (4 circles) and outer surfaces (4 circles). In the outline of figure 6 only two circles 250 are shown.

In the experiment, different pinhole diameters are combined with different z1/z2 distances to illustrate the impact on the focusing plane and on the depth of field which becomes evident at the sharpness of the circles and their apparent diameter in the captured image. In particular, different configurations of pinholes (500μm, 200μm and 50μm) have been used, in order to observe the behavior of each of them. For each pinhole configuration, different values of distances z1 and z2 have been tried. First, the sample object 25 has been located close to the CMOS imager 17 (z2=0) and the optimal value of z1 has been determined, in terms of achieving best focus. Once z1 is determined, the light source 14 and the pinhole 165 are placed. Next, the position of the sample object 25 is modified, thus obtaining new values for z1 and z2. In each position a capture of the image is taken. Based on the formula:

*Minimum object Diameter in detector=pin-hole Diameter * z2/z1*

We have observed that:

-Given a sample object and having a certain distance z2, the bigger the diameter of the pinhole, the bigger is the distance z1 at which the sample object becomes focused.

-Given each pinhole and given a sample object, if distance z2 is increased, the distance z1 at which the sample object becomes focused is also increased. This increase is linearly proportional.

Figures 7A-7C show the results obtained with diameter of pinhole = 500μm. Figure 7A shows the image taken when z2=0mm and z1+z2=z1=35mm (optimal focus). Figure 7B shows the image taken when z2=2,45mm and z1=35-2,45=32,55mm. Figure 7C shows the image taken when z2=4,9mm and z1= 35-4,9mm=30,1mm.

Figures 8A-8C show the results obtained with diameter of pinhole = 200μm. Figure 8A shows the image taken when z2=0mm and z1+z2=z1=28mm (optimal focus). Figure 7B shows the image taken when z2=2,45mm and z1=28-2,45=25,55mm. Figure 7C shows the image taken when z2=4,9mm and z1= 28-4,9mm=23,1mm.

Figures 9A-9C show the results obtained with diameter of pinhole = 50μm. Figure 9A shows the image taken when z2=0mm and z1+z2=z1=15mm (optimal focus). Figure 9B shows the image taken when z2=2,45mm and z1=15-2,45=12,55mm. Figure 9C shows the image taken when z2=4,9mm and z1= 15-4,9mm=10,1mm.

Experiment 3: The effect of the pinhole diameter in the focus plane and depth of field

Figures 10A-10C represent images captured in this experiment. For this experiment, even if the same prototype system as in Experiment 1 has been used, in this case, the lube fluid sample is replaced by a transparent solid sample with a micromachined pattern on it. The solid sample is 1mm thick and the pattern is 100μm deep. The pattern is faced up, therefore placed at a distance of 900μm from the protective window inner plane. With this prototype set up, the experiment evaluates the image captured using different pin-hole diameters (1.5mm in figure 10A, 0.5mm in figure 10B and 150 μm in figure 10C). It can be observed that the smaller the diameter of the pin-hole, the best image focusing is achieved due to the focusing plane displacement and increase in depth of field.

Throughout this document, the word “comprises” and variants thereof (such as “comprising”, etc.) must not be interpreted as having an exclusive meaning, in other words, they do not exclude the possibility of what is being described incorporating other elements, steps, etc.

Finally, the invention is not limited to the specific embodiments described herein and also extends, for example, to variants that may be embodied by an average person skilled in the art (for example, with regard to the choice of materials, dimensions, components, configuration, etc.), within the scope of what is inferred from the claims.

CLAIMS

1. A sensor system (1) for inspecting oil, which comprises a micromechanical cell (10) defining a cavity (12), the micromechanical cell (10) being configured for allowing the entrance of oil (5) within said cavity (12) and the outcome of oil (5) from said cavity (12) through respective inlet (11a) and outlet (11b),

the sensor system (1) being characterised in that it comprises inside said micromechanical cell (10):

-a first transparent protective means (13a) configured to isolate the inner part of said first member (101) from said cavity (12) to be occupied with oil (5);

-a second transparent protective means (13b) configured to isolate the inner part of said second member (102) from said cavity (12) to be occupied with oil (5);

-a light source (14) disposed in said first member (101) and configured to emit incoherent light towards said oil (5) disposed within said cavity (12);

-an opaque plate (16) disposed between said light source (14) and said first transparent protective means (13a), said plate (16) having a pin-hole (165) configured to permit the passage of illumination towards said cavity (12) to be occupied with oil (5), said pin-hole (165) being located at a first distance (z1) from a focussing plane (F) defined by said cavity (12);

-an image sensor (17) disposed in said second member (102) situated on the opposite side of the cavity (12) with respect to said first member (102) and configured to capture a sequence of images of the oil disposed within said cavity (12), said image sensor (17) being located at a second distance (z2) from said focussing plane (F) defined by said cavity (12).

2. The system (1) of claim 1, further comprising a diffuser (19) disposed between said light source (14) and said plate (16) defining the pin-hole (165), said diffuser (19) being configured to provide homogeneous lighting to said cavity (12).

3. The system (1) of any of the preceding claims, further comprising processing means configured to process said sequence of images and to determine the presence of particles and bubbles and a degradation value of the oil.

4. The system (1) of any of the preceding claims, wherein said light source (14) comprises on one or more LED diodes.

5. The system (1) of any of the preceding claims, wherein said image sensor (17) comprises a CMOS sensor or a CCD camera.

6. The system (1) of any of the preceding claims, wherein said pin-hole (165) has a diameter varying in the range of 30 μm to about 300 μm.

7. The system (1) of claim 6, wherein said diameter varies in the range of 50 μm to about 150 μm.

8. The system (1) of any of the preceding claims, wherein said first distance (z1) at which said pin-hole (165) is located from said focussing plane (F) is in the range of 10 mm to about 30 mm.

9. The system (1) of claim 8, wherein said distance (z1) varies in the range of 15 mm to about 25 mm.

10. The system (1) of any of the preceding claims, wherein said first distance (z2) at which said image sensor (17) is located from said focussing plane (F) is in between 1 and 3 mm.

11. The system (1) of claim 10, wherein said distance (z2) varies between 1 and 2 mm.

12. The system of any of the preceding claims, wherein said oil (5) is static within said cavity (12).

13. The system of any of claims 1-11, wherein said oil (5) is in motion within said cavity (12).

14. The system of any of the preceding claims, wherein said micromechanical cell (10) comprises a first member (101) and a second member (102) defining said cavity (12) therebetween.

15. The system of any of the preceding claims, wherein said inlet (11a) and outlet (11b) are inclined with respect to said cavity (12), thus minimizing the separation between the oil (5) located within said cavity (12) and said image sensor (17).

FLUID MONITORING SYSTEM

ABSTRACT

A sensor system (1) for inspecting oil, which comprises a micromechanical cell (10) defining a cavity (12), the micromechanical cell (10) being configured for allowing the entrance of oil (5) within said cavity (12) and the outcome of oil (5) from said cavity (12) through respective inlet (11a) and outlet (11b). The sensor system (1) comprises inside said micromechanical cell (10): a first transparent protective means (13a) configured to isolate the inner part of said first member (101) from said oil (5); a second transparent protective means (13b) configured to isolate the inner part of said second member (102) from said oil (5); a light source (14) disposed in said first member (101) and configured to emit incoherent light towards said oil (5) disposed within said cavity (12); an opaque plate (16) disposed between said light source (14) and said first transparent protective means (13a), said plate (16) having a pin-hole (165) configured to permit the passage of illumination towards said oil (5), said pin-hole (165) being located at a first distance (z1) from a focussing plane (F) defined by said oil (5) in cavity (12); and an image sensor (17) disposed in said second member (102) situated on the opposite side of the space (12) with respect to said first member (102) and configured to capture a sequence of images of the oil disposed within said cavity (12), said image sensor (17) being located at a second distance (z2) from said focussing plane (F) defined by said oil (5) in cavity (12).

[FIG. 1]

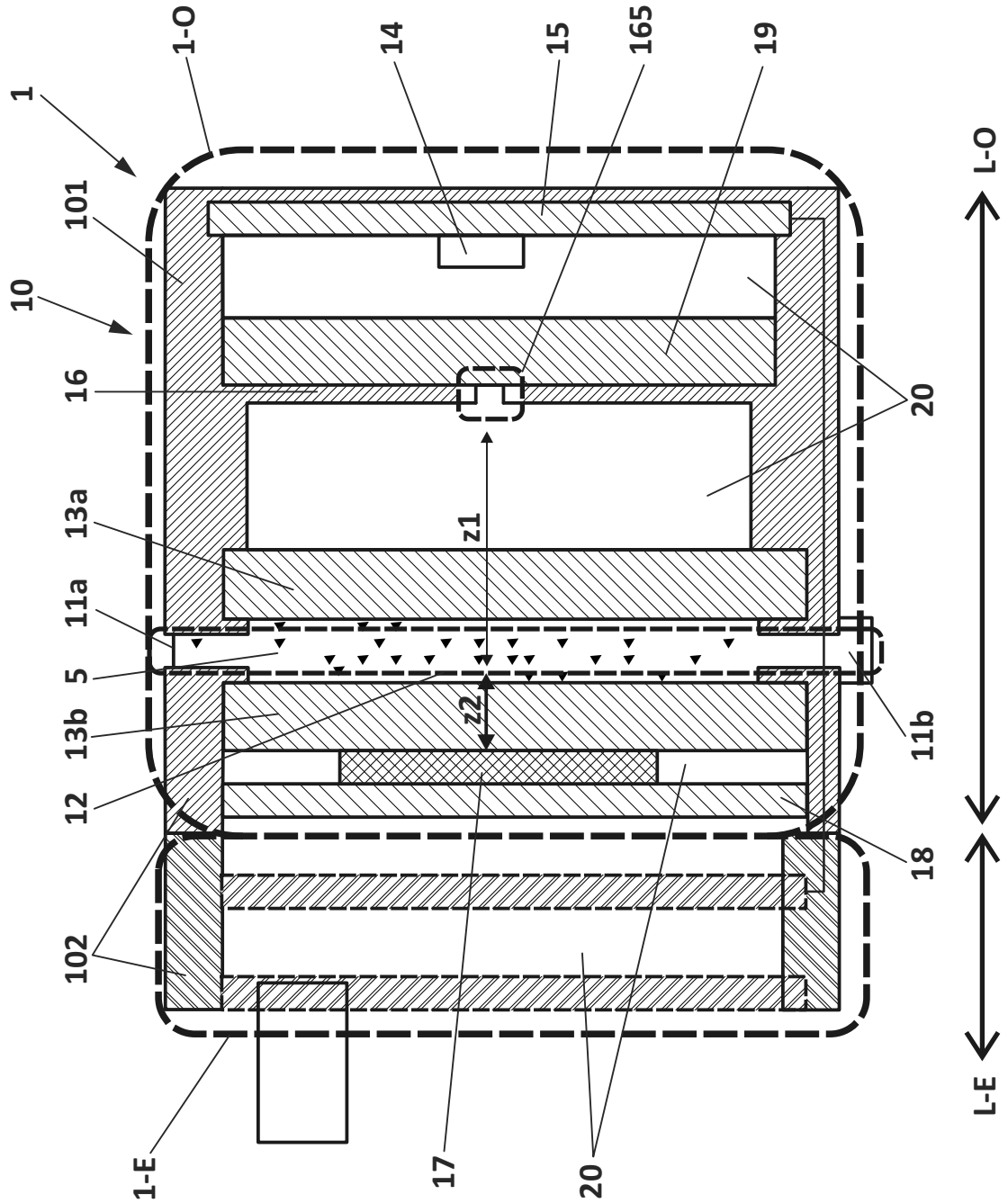
1
1-O
14
15
165
19
101
10
16
20
13a
z1
11a
5
z2
13b
11b
12
18
102
1-E
17
20
L-O
L-E

FIG. 1

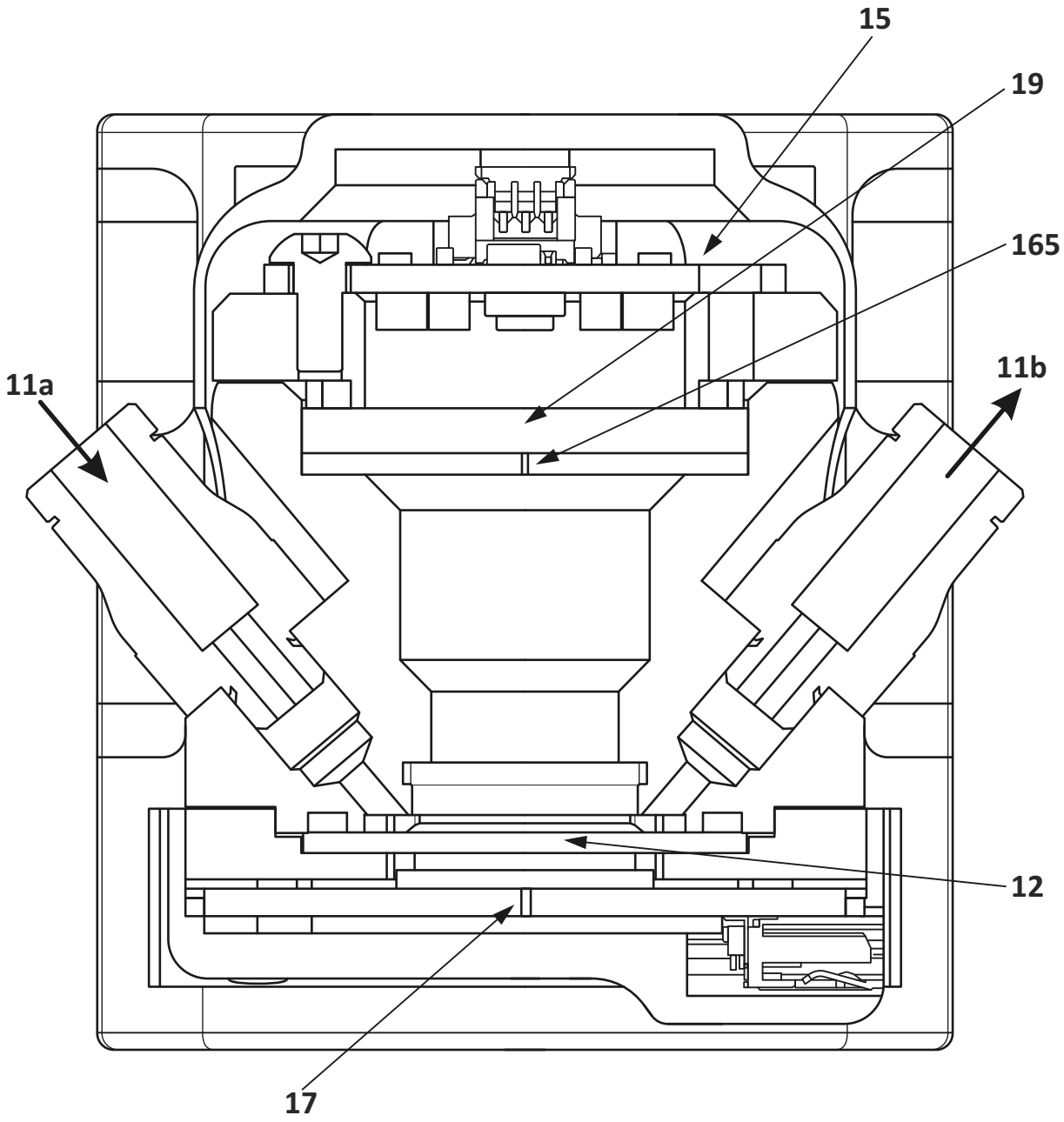

FIG. 2A

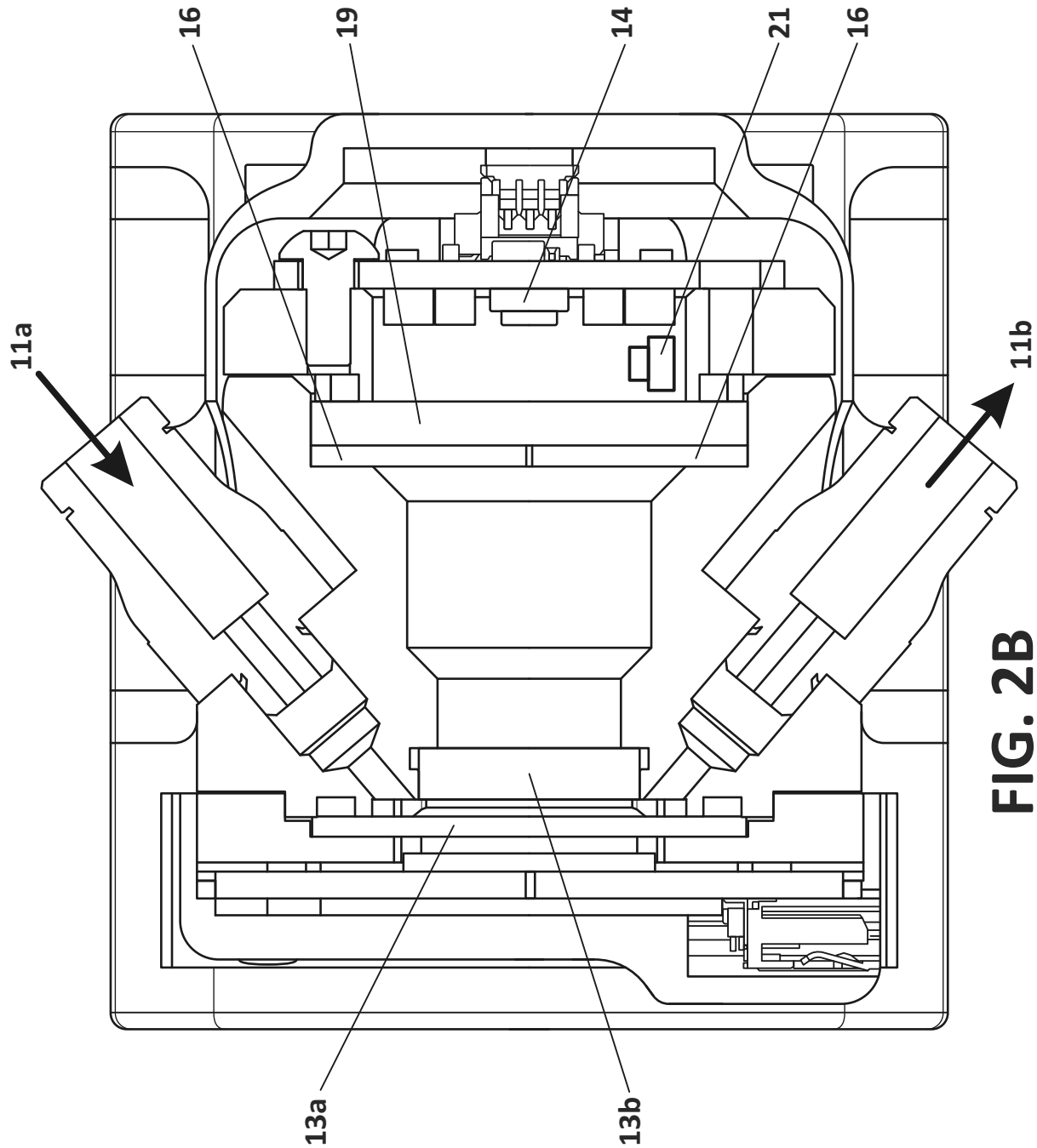

FIG. 2B

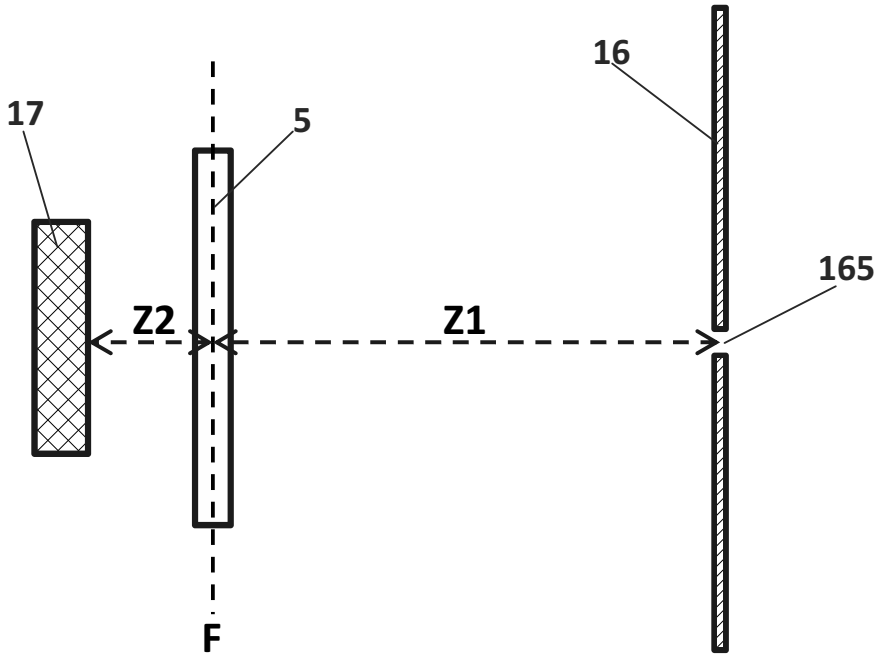

FIG. 3

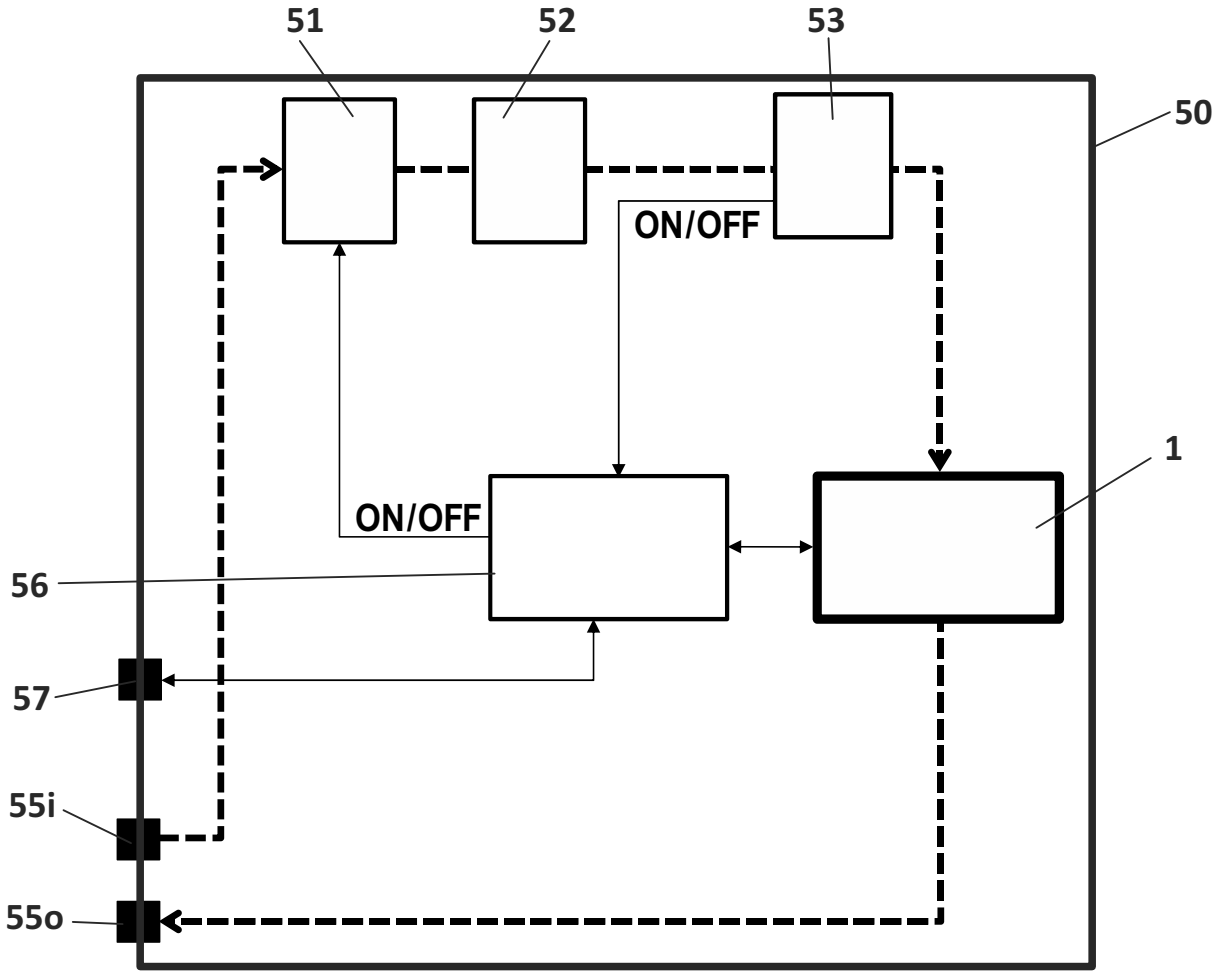

FIG. 4

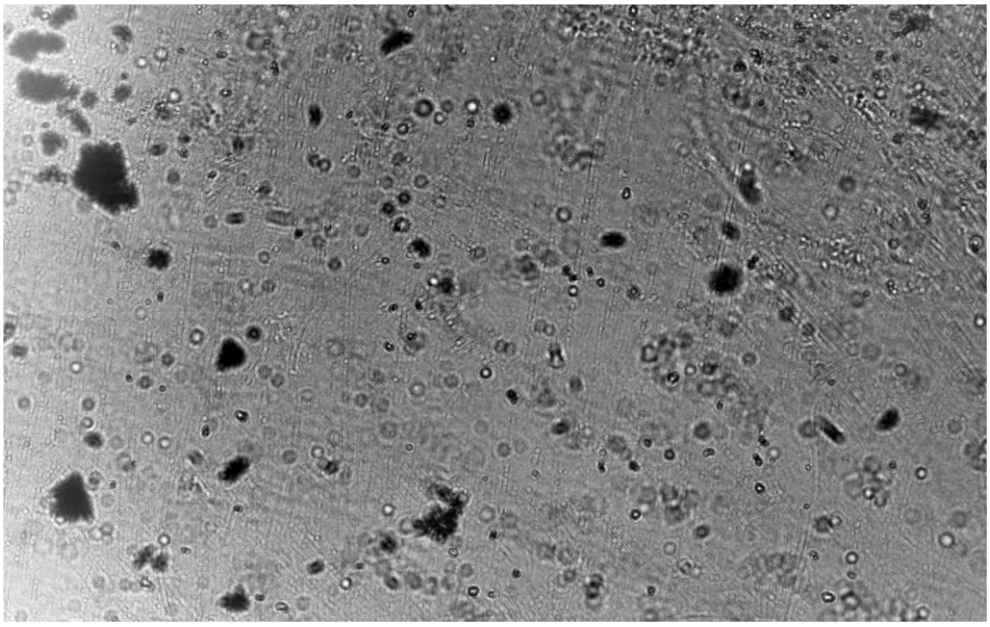

FIG. 5

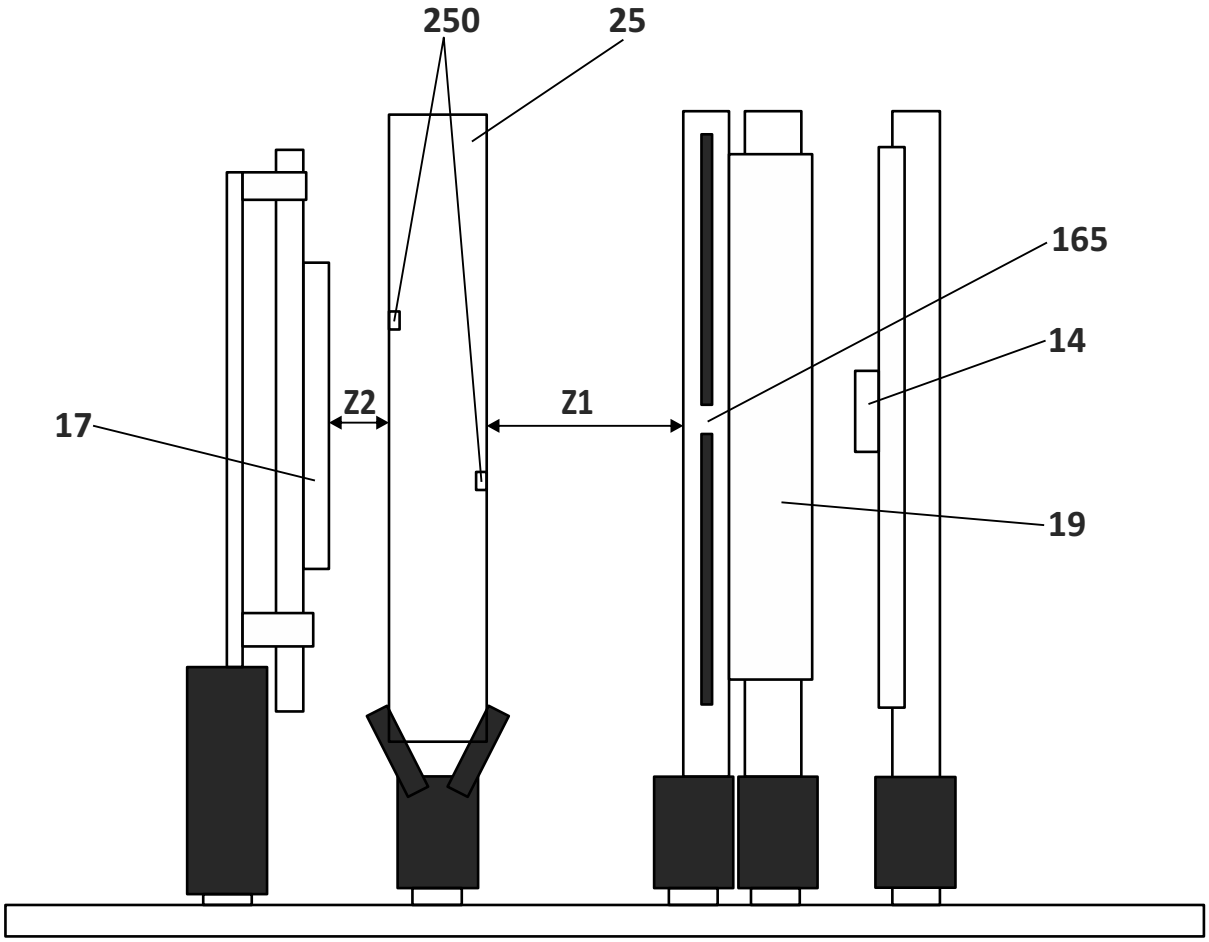

FIG. 6

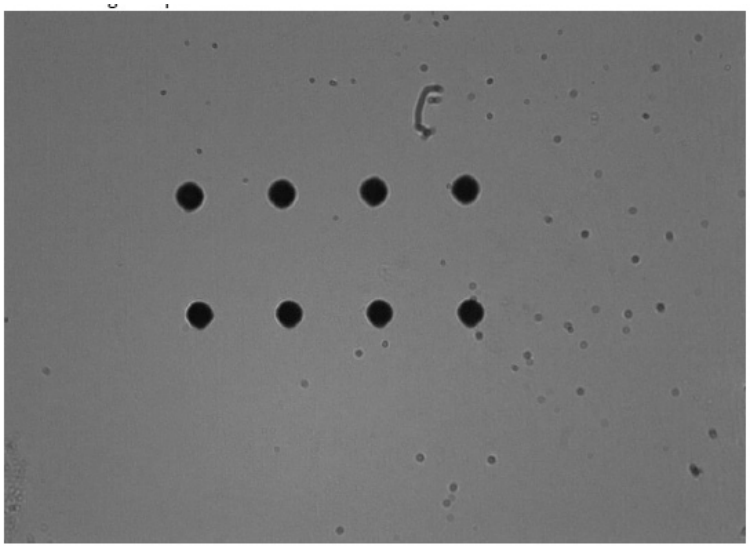

FIG. 7A

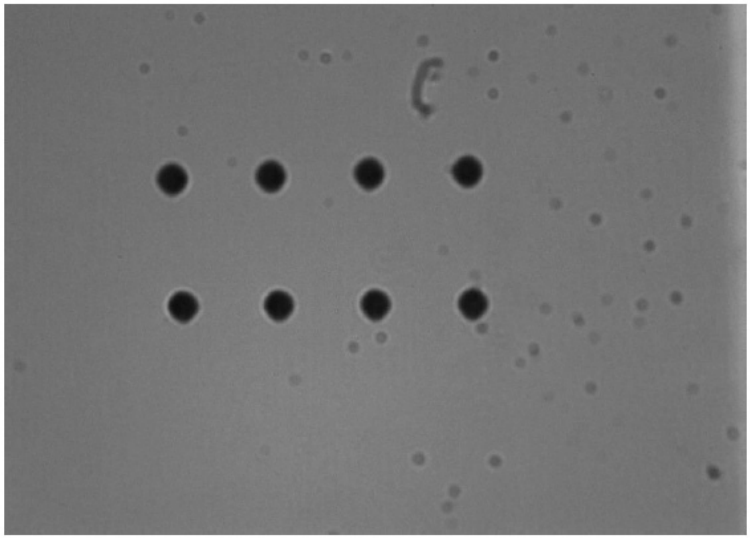

FIG. 7B

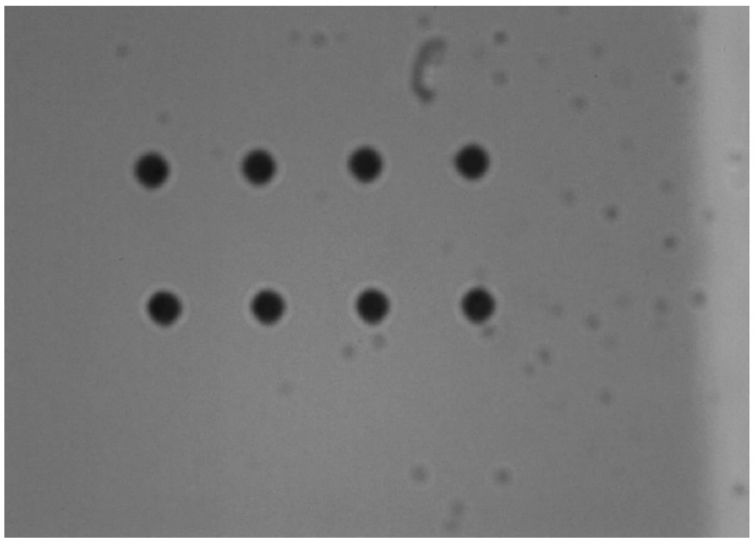

FIG. 7C

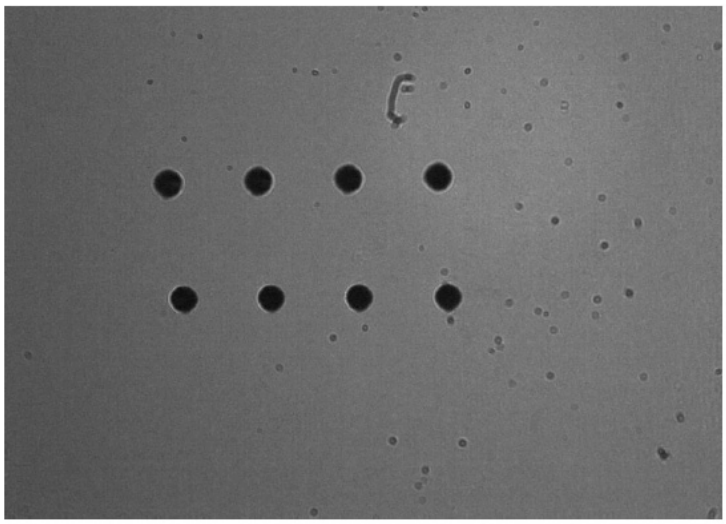

FIG. 8A

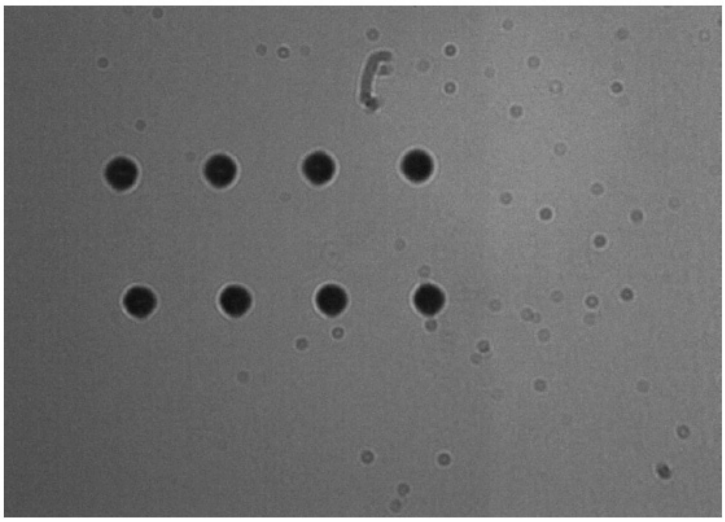

FIG. 8B

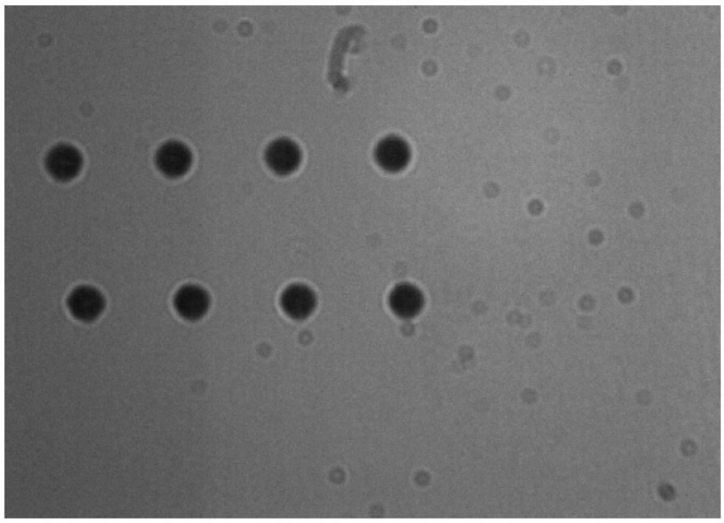

FIG. 8C

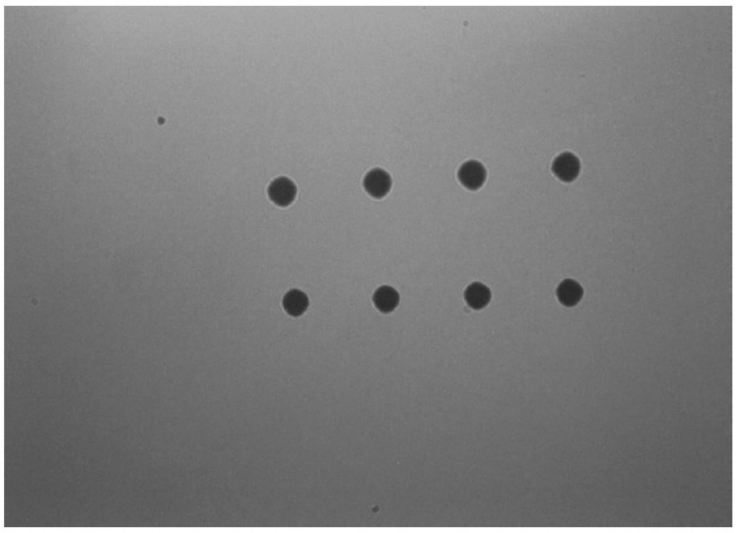

FIG. 9A

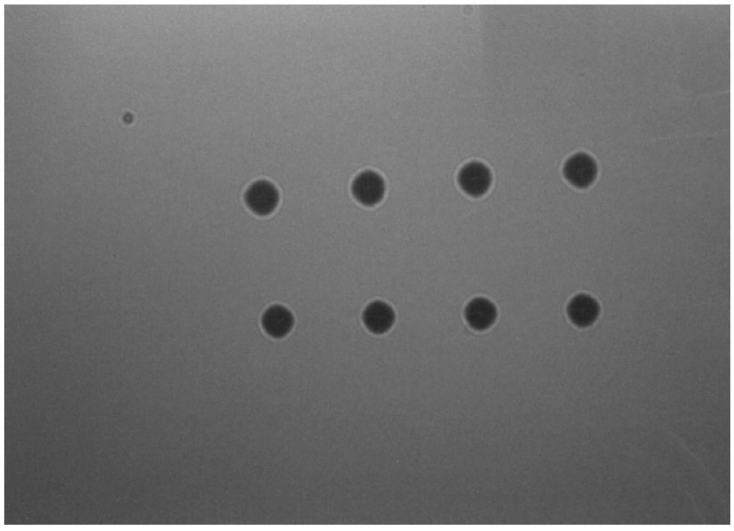

FIG. 9B

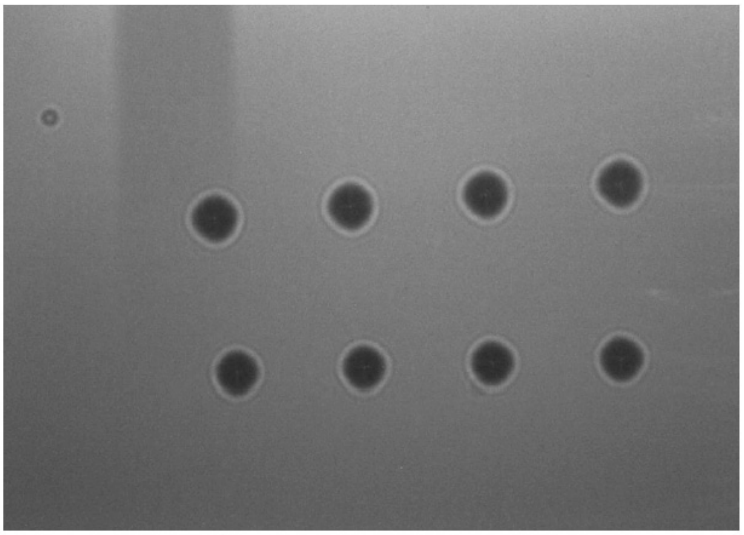

FIG. 9C

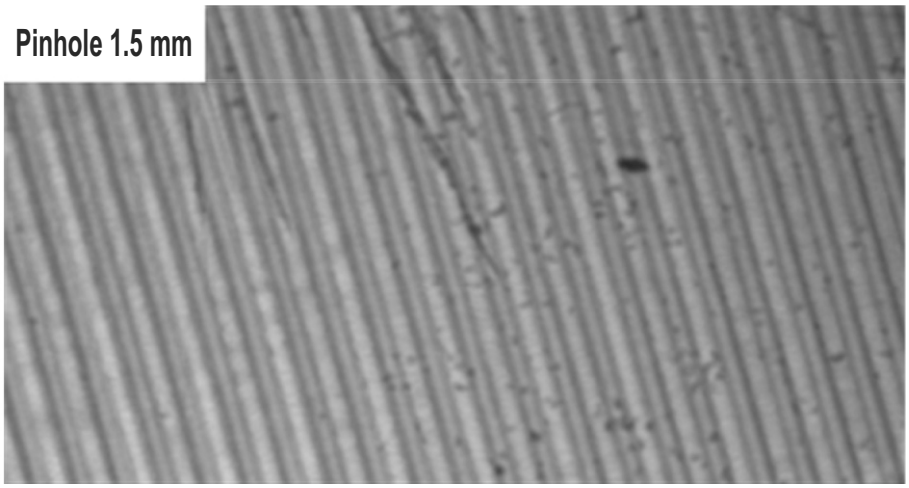

FIG. 10A

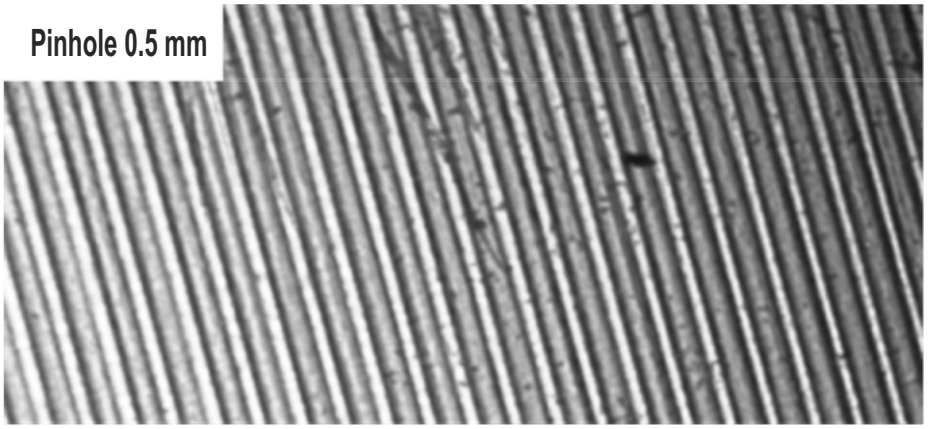

FIG. 10B

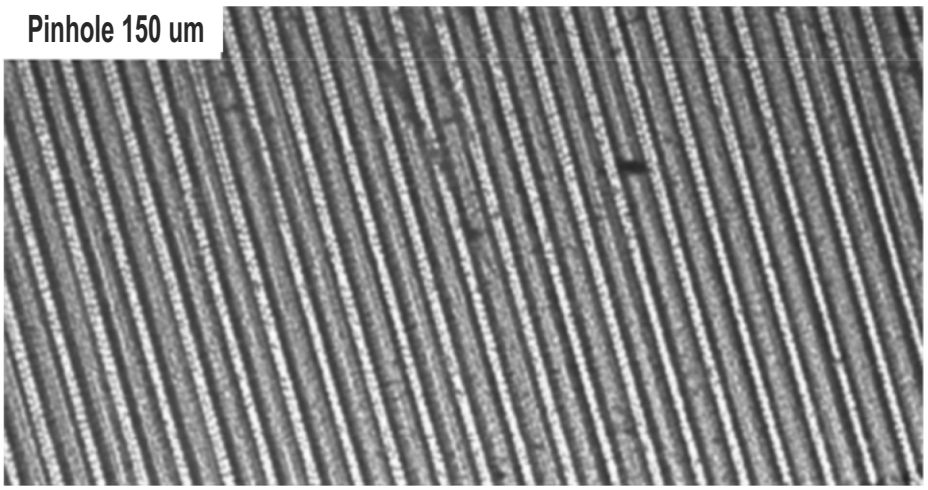

FIG. 10C

MINISTERIO
DE INDUSTRIA, ENERGÍA
Y TURISMO

Oficina Española
de Patentes y Marcas

Acknowledgement of receipt

We hereby acknowledge receipt of your request for grant of a European patent as follows:

Submission number	300219445	
Application number	EP17382007.7	
File No. to be used for priority declarations	EP17382007	
Date of receipt	11 January 2017	
Your reference	P162291EP	
Applicant	FUNDACIÓN TEKNIKER	
Country	ES	
Title	MONITORING SYSTEM AND METHOD FOR DETECTING FLOWING MICROSCOPIC OBJECTS	
Documents submitted	package-data.xml	ep-request.xml
	application-body.xml	ep-request.pdf (5 p.)
	SPECEPO-2.pdf\P162291EP-figs.pdf (11 p.)	OLF-ARCHIVE.zip\P162291EP.zip
	SPECEPO-1.pdf\P162291EP-(spec-fraft)-(oilwear mejorado)-20170111-vFINAL.pdf (28 p.)	f1002-1.pdf (1 p.)
Submitted by	CN=Manuel Barrero 34075	
Method of submission	Online	
Date and time receipt generated	11 January 2017, 18:49:18 (CET)	
Official Digest of Submission	25:AD:7C:D0:6E:7A:E1:06:F7:A3:67:3C:20:AE:C7:27:50:F2:A6:17	

Europäisches Patentamt
European Patent Office
Office européen des brevets

Request for grant of a European patent

For official use only		
1 Application number:	MKEY	
2 Date of receipt (Rule 35(2) EPC):	DREC	
3 Date of receipt at EPO (Rule 35(4) EPC):	RENA	
4 Date of filing:		

5 Grant of European patent, and examination of the application under Article 94, are hereby requested. ☒

5.1 The applicant waives his right to be asked whether he wishes to proceed further with the application (Rule 70(2)) ☐

Procedural language: en

Description and/or claims filed in: en

6 Applicant's or representative's reference: P162291EP

Filing Office: ES

Applicant 1

7-1 Name: FUNDACIÓN TEKNIKER

8-1 Address:
Polo tecnológico de Eibar, c/ Iñaki Goenaga 5
20600 Eibar
Spain

10-1 State of residence or of principal place of business: Spain

14.1 The/Each applicant hereby declares that he is an entity or a natural person under Rule 6(4) EPC. ☐

Representative 1

15-1 Name: BALDER IP Law, S.L.

Association No.: 639

16-1 Address of place of business:
Castellana 93
5ª planta
28046 Madrid
Spain

17-1 Telephone: 0034911336879

17-1 Fax: 0034911331384

17-1 E-mail: info@balderip.com

Inventor(s)

23 Inventor details filed separately ☒

24 Title of invention

Title of invention: MONITORING SYSTEM AND METHOD FOR DETECTING FLOWING MICROSCOPIC OBJECTS

25 Declaration of priority (Rule 52)

A declaration of priority is hereby made for the following applications

25.2 This application is a complete translation of the previous application ☐

25.3 It is not intended to file a (further) declaration of priority ☐

26 Reference to a previously filed application

27 Divisional application ☐

28 Article 61(1)(b) application ☐

29 Claims

Number of claims: 15

29.1 ☒ as attached

29.2 ☐ as in the previously filed application (see Section 26.2)

29.3 ☐ The claims will be filed later

30 Figures

It is proposed that the abstract be published together with figure No. 8

31 Designation of contracting states

All the contracting states party to the EPC at the time of filing of the European patent application are deemed to be designated (see Article 79(1)).

32 Different applicants for different contracting states

33 Extension/Validation

This application is deemed to be a request to extend the effects of the European patent application and the European patent granted in respect of it to all non-contracting states to the EPC with which extension or validation agreements are in force on the date on which the application is filed. However, the request is deemed withdrawn if the extension fee or the validation fee, whichever is applicable, is not paid within the prescribed time limit.

33.1 It is intended to pay the extension fee(s) for the following state(s): BA ME

33.2 It is intended to pay the validation fee(s) for the following state(s): MA MD

34 Biological material

38 Nucleotide and amino acid sequences

The European patent application contains a sequence listing as part of the description ☐

The sequence listing is attached in computer-readable format in accordance with WIPO Standard ST.25 ☐

The sequence listing is attached in PDF format ☐

Further indications

39 Additional copies of the documents cited in the European search report are requested

Number of additional sets of copies:

40 Refund of the search fee under to Article 9 of the Rules relating to Fees is requested ☐

Application or publication number of earlier search report:

42 Payment

Mode of payment: Debit from deposit account

The European Patent Office is hereby authorised, to debit from the deposit account with the EPO any fees and costs indicated on the fees section below.

Currency: EUR

Deposit account number: 28120253

Account holder: BALDER IP Law, S.L.

43 Refunds

Any refunds should be made to EPO deposit account: 28120253

Account holder: BALDER IP Law, S.L.

Fees	Factor applied	Fee schedule	Amount to be paid
001 Filing fee - EP direct - online	1	120.00	120.00
002 Fee for a European search - Applications filed on/after 01.07.2005	1	1 300.00	1 300.00
015 Claims fee - For the 16th to the 50th claim	0	235.00	0.00
015e Claims fee - For the 51st and each subsequent claim	0	585.00	0.00
501 Additional filing fee for the 36th and each subsequent page	4	15.00	60.00
Total:		EUR	1 480.00

44-A Forms		Details:	System file name:
A-1	Request		as ep-request.pdf
A-2	1. Designation of inventor	1. Inventor	as f1002-1.pdf

44-B Technical documents		Original file name:	System file name:
B-1	Specification	P162291EP-figs.pdf 11 figure(s)	SPECEPO-2.pdf
B-2	Specification	P162291EP-(spec-fraft)-(oilwear mejorado)-20170111-vFINAL.pdf Description; 15 claims; abstract	SPECEPO-1.pdf
B-3	Pre-conversion archive	P162291EP.zip	OLF-ARCHIVE.zip

44-C Other documents	Original file name:	System file name:

45 General authorisation:

46 Signature(s)

Place: **MADRID**

Date: **11 January 2017**

Signed by: **/M.STIEBE/**

Association: **BALDER IP Law, S.L.**

Representative name: **Lars Magnus STIEBE**

Capacity: **(Representative)**

Form 1002 - 1: Public inventor(s)

Designation of inventor

User reference: P162291EP
Application No:

Public

	Inventor	
	Name:	MABE ÁLVAREZ, Mr. Jon
	Address:	Polo tecnológico de Eibar, c/ Iñaki Goenaga 5 20600 Eibar Spain
	The applicant has acquired the right to the European patent:	As employer

Signature(s)

Place:	**MADRID**
Date:	**11 January 2017**
Signed by:	**/M.STIEBE/**
Association:	**BALDER IP Law, S.L.**
Representative name:	**Lars Magnus STIEBE**
Capacity:	**(Representative)**

MONITORING SYSTEM AND METHOD FOR DETECTING FLOWING MICROSCOPIC OBJECTS

TECHNICAL FIELD

The present invention relates to the field of fluid monitoring for determining the general condition of fluids, such as their degradation and particle content. This monitoring is for example applicable to lubricating oils, since their state of degradation and particle content provides information on the machinery lubricated by said oil.

BACKGROUND OF THE INVENTION

Industrial machines often undergo unforeseen shutdowns and failures, often associated to aspects related to lubrication. Lubricating oil is one of the key components in some of these machines and provides a lot of information regarding the machines condition. It may be interesting to monitor some parameters in lubricating oil, such as particle determination (for example, quantification, classification of size or determination of shape), bubble content in the system or oil degradation based on colour. Oil degradation is a key indicator of oil quality and how it fulfils its lubricating mission. It does not provide information on the machine directly, but indirectly, from the speed of degradation, it is possible to extract information regarding the machine's operation.

European patent application EP2980557A1 discloses a system for inspecting oil, which comprises a cell through which oil flows along a pipe. The system is based on a lighting system having a LED diode, configured to supply a light beam to the flow of oil, and an image capture system situated on the opposite side of the pipe in respect of the lighting system. The image capture system is configured to capture a sequence of images of the oil that flows inside the pipe. The lighting system and the image capture system are disposed within the cell. A processor processes the sequence of images and determines the presence of particles and a value for the oil degradation.

The system disclosed in EP2980557A1 performs as expected when the oil, and therefore the particles comprised therein, travel along the pipe at low speed. However, it has been observed that when the instant velocity of the particles is relatively high, when they pass by the area of image capture, the system is unable to capture an image of the passing particles or it manages to capture an image in which the particles have an incorrect morphology. This has for example been observed for particles travelling with instant velocity varying between 3 and 20 m/s (the smaller the particle, the lower the threshold of instant velocity above which the particle is not captured in the

image or it is captured with incorrect morphology).

Capturing undistorted images of objects moving at relatively high speed at the image capture area is a traditional problem. If the sampling rate of each pixel is not fast enough, the captured images will tend to be blurry and with shapes that do not correspond to reality. The sampling rate of each pixel depends mainly on two factors: the exposure time (the time for which each pixel collects the instant light that comes to it) and the reading time of each pixel (the maximum rate at which information from each pixel in the camera is transferred to a buffer). The capture of images on very dark oils can be compensated with an increase of the exposure time or with an increase of the intensity on the lighting source. While the exposure time is dependent on each application and is a function of the maximum illumination power available and of the opacity of the fluid to be analyzed, the reading time of each pixel depends on the technology of the video sensor.

Indeed, the problem of moving objects can be avoided by mechanical means using devices for flow regulation (in order to reduce the flow speed) or solenoid valves for stopping the oil sample under analysis. However, stopping or reducing the fluid flow rate directly impacts of the significance of the measurement, because samples are not being taken in real conditions. Flow regulators, such as needle valves for instance, tend to filter particles by themselves and can be easily stoppled by the accumulation of wear debris in highly contaminated fluids (like the ones targeted in the present invention) and the valves only allow the measurement of static samples with no flow at all, which impacts in the sampling speed and in the representativeness of the sample. Ideally, reducing the number of hydraulic elements enhances the measurement significance of an in-line or by-pass sensor.

Besides, certain techniques have been developed for overcoming the problem of capturing images of moving objects at the image capture area. One of the traditional techniques is called Rolling Shutter (RS). In RS, the pixels are activated sequentially one after the other. The temporal difference of the activation of a pixel with the forthcomings causes the captured images to appear moved and not focused if the objects move faster than the reading speed of each pixel. Another technique is called Global Shutter: This technology allows all pixels to be activated simultaneously, so regardless of the speed of the object to be captured, it appears static in the captured image. A third technique is called Rolling Shutter with Global Start (RSGS): This technology is a particular case of the Rolling Shutter, and allows all the pixels to be activated at the same instant, although the duration of the activation depends on the reading instant of each one, which is still sequential, which causes that some pixels are active longer than others.

However, in order to apply these techniques to the detection of microscopic particles comprised in a moving fluid, some parameters must be considered: (a) the resolution of the detector (height x width in pixels), (b) the pixel size and (c) the sensor area, because these three parameters determine (1) the minimum detectable size of a particle (which is dependent on the ratio between resolution and pixel size) and (2) the volume of analyzed fluid in each image (which is dependent on the sensor's active area). For this reason, Global Shutter techniques are discouraged for the detection of small particles in a moving fluid because in the state of the art solutions, due to their higher complexity in the pixel structure, they tend to offer lower resolutions and larger pixel sizes. Besides, even if Rolling Shutter solution is able to offer decent resolutions, pixel sizes for this specific application are not an option due to their limitations for capturing sharp images of moving objects. On the contrary, RSGS allows maintaining the advantages of the RS sensors while offering a performance in the capture of moving objects similar to the GS, under certain conditions, such as the isolation of CMOS detector of the non-controlled light sources (e.g. ambient lighting).

Nevertheless, when applying traditional RSGS setups to the detection of particles in a moving fluid, it has been observed that the system does not perform as expected for two reasons: (1) the image capture system does not receive enough light power (flash gain), which is normally required for the images and particles suspended on the fluid to have enough contrast in order to enable their discrimination; and (2) the time for which the lighting system is on (flash duration) is too elevated and therefore the images are not captured in a clear way.

Chinese patent application CN2899386 discloses a LED-array source for inspecting a printing image, in which the LED source provides a pulsed signal synchronized with the image printing speed. In order to synchronize the pulse signal with the printing speed, a circuit is designed for adjusting the frequency of the pulse signal. However, this disclosure does not give any clue regarding as how to provide very high power pulses from a conventional low current DC power source. Additionally, in systems for inspecting a moving fluid, the light pulses cannot be synchronized with the particle velocity because the inspection system does not know this velocity.

Therefore, there is a need for a system for inspecting a moving fluid which overcomes the former drawbacks.

DESCRIPTION OF THE INVENTION

The present invention attempts to solve the drawbacks mentioned above by means of a monitoring system and method for detecting microscopic objects disposed in a flowing fluid. The microscopic objects flow at high flow rates. In the context of the

present invention, the term “high” in “high flow rates” refers to flow rates varying between 1 and 40 m/s, that is to say, flow rates of up to 40 m/s. The monitoring system uses a pulsed lighting system, that is to say, a lighting system that produces regular flashes of light, synchronized with the video capturing speed. In the context of the present invention, the term “microscopic” refers to objects having a largest dimension (i.e. diameter) smaller than 20 µm. The monitoring system of the invention has been proved to detect and correctly identify objects in motion (objects suspended in a flowing fluid) having a largest dimension smaller than 10 µm and even smaller than 3 µm when they move at instant velocity of 20 m/s. The pulsed lighting system ensures that the light it provides is on (flash duration) in a controlled way, in particular for a shorter time than the exposure time selected in the sensor (i.e. CMOS) of the image capture system, since in that way, once the light source is turned off, even if there are still active pixels (until the exposure time is finished) the active pixels will have no effect, since there are no more photons to be received (the CMOS is isolated from any external light source). Besides, the lighting system is synchronized with the image capture system to trigger the flash pulses at the beginning of every new video frame. What is more, the system is designed for the image capture system to receive enough flash gain so as to correctly discriminate particles within the moving fluid. In this context, the exposure time is the time for which each pixel collects the instant light that comes to it and it is limited in practice by the duration of the flash pulse.

As mentioned earlier, because the monitoring system is isolated from outside light (the only light source is that of the monitoring system) and the lighting system allows a total shutdown, applying the RSGS technique is possible.

Therefore, the system and method for inspecting a fluid manages to perform correctly without needing to actuate on the speed of the fluid flow. In other words, the system of the invention is capable of capturing images of the passing particles in continuous flow and of determining the real size and shape of the microscopic objects shown in the captured images (and not a distorted version of the objects).

In a first aspect of the invention, a system is provided for detecting microscopic objects located in a flowing fluid. The system comprises: a lighting system comprising at least one LED diode and configured to supply light to the flowing fluid; an image capture system situated on the opposite side of the flowing fluid in respect of the lighting system, the image capture system being configured to capture a sequence of images of the flowing fluid, the image capture system comprising a camera in turn comprising a plurality of pixels; processing means configured to process the sequence of images and to determine the presence of microscopic objects within the flowing fluid and the shape of the microscopic objects. The lighting system is configured to supply high

power light pulses having amplitude Io' and very short time duration T_{ON}. In the context of the present invention, the term "high" in "high power light pulses" refers to power pulses varying between 20 mA and 20 A, preferably between 2 A and 15 A. In the context of the present invention, the expression "very short" in "very short time duration" refers to time duration varying between 50 ns and 50 µs, preferably between 50 ns and 20 µs, more preferably between 50 ns and 10 µs, and still more preferably varying between 50 ns and 5 µs. The time instant at which these pulses are triggered is synchronized with the time instants at which pixels in the image capture system start to capture an image frame. The processing means is configured to control the amplitude Io' and time duration T_{ON} of the light pulses supplied by the lighting system by means for calculating, from the light intensity I_{frame} of each captured image frame, a pulse amplitude setpoint (PAS) and a pulse duration setpoint (PDS) for adjusting respective potentiometers configured to respectively fix the amplitude Io' and pulse duration T_{ON}. The means for calculating the pulse amplitude setpoint (PAS) and the pulse duration setpoint (PDS) is configured to execute an algorithm that prioritizes amplitude rises over pulse duration rises. The lighting system also comprises an energy loading system configured to make the amplitude requirement and response time of the lighting system independent from a power supply unit of the system.

Preferably, the image capture system operates in RSGS mode.

In embodiments of the invention, the image capture system is configured to provide the processing means with an image frame captured every T_{frame} seconds, T_{frame} being less than or equal to T_{EXP}, wherein T_{EXP} is the exposure time of the pixels comprised in the image capture system.

In embodiments of the invention, the lighting system comprises a pulse generator for generating from the pulse duration setpoint (PDS) and from a strobe signal provided by the image capture system, a pulsed signal having period T_{frame} and having pulses of duration T_{ON}, $T_{ON} << T_{EXP} \leq T_{frame}$, the duration T_{ON} being obtained from the pulse duration setpoint (PDS) and said strobe signal being used for synchronizing the pulses of duration T_{ON} with the time instant at which the pixels in the image capture system start to capture an image frame. In a particular embodiment, the pulse generator is implemented with a single retriggerable monostable forming, together with the potentiometer adjustable by the pulse duration setpoint (PDS), an RC network configured to fix the pulse duration T_{ON}.

In embodiments of the invention, the lighting system further comprises a multiplexor configured to provide a reference voltage V_{MUX} of duration T_{ON}, and a substantially null voltage of duration $T_{frame} - T_{ON}$, wherein the reference voltage V_{MUX} is calculated from the pulse amplitude setpoint (PAS) obtained at processing means, the reference

voltage V_{MUX} being used for obtaining a polarization current of the at least one LED.

In embodiments of the invention, the energy loading system comprises a switched-mode power supply configured to provide a voltage V_{int} and a low current I_{int} from a DC power supply source V_{out}; and an RC network comprising at least one capacitor and a resistor, wherein the at least one capacitor works as a pulse energy storage means and the resistor regulates the charging speed of the pulse energy storage means. The RC network is configured for the at least one capacitor to become fully charged in a time duration T_{frame} - T_{ON} , wherein T_{frame} is the time period between two consecutive image frames captured by the image capture system, the switched-mode power supply thus providing a voltage V_{LED} in turn enabling to provide the at least one LED with current Io'.

In embodiments of the invention, the system further comprises a diffuser situated between the lighting system and the flow of fluid, configured to provide homogeneous lighting to the area to be illuminated.

In embodiments of the invention, the diffuser is situated closing off and sealing a hole made in the pipe through which the fluid flows.

In embodiments of the invention, the system further comprises a lens situated between the image capture system and the flow of fluid, configured to focus the captured images.

In embodiments of the invention, the system further comprises a calibration device situated between the lens and the flow of fluid.

In embodiments of the invention, the processing means is configured to determine the presence and shape of objects having a largest dimension smaller than 20 µm.

In embodiments of the invention, the light pulses supplied by the lighting system have amplitude Io' varying between 20 mA and 20 A and time duration T_{ON} varying between 50 ns and 50 µs.

In another aspect of the invention, a method for detecting microscopic objects located in a flowing fluid is disclosed. It comprises: supplying light emitted by at least one LED to a flowing fluid having microscopic objects suspended thereon; capturing a sequence of images of the flowing fluid by means of an image capture system comprising a plurality of pixels; processing the sequence of images and determining the presence of microscopic objects within the flowing fluid and the shape thereof; at the image capture system, capturing an image frame every T_{frame} seconds, T_{frame} being higher than or equal to T_{EXP}, wherein T_{EXP} is the exposure time of the pixels comprised in the image capture system; providing a strobe signal the said image capture system; for each image frame, calculating (controlling) a pulse amplitude setpoint (PAS) and a pulse

duration setpoint (PDS) from the intensity of each frame I_{frame} by executing an algorithm that prioritizes rises in the pulse amplitude (PAS) rather than rises in the pulse duration (PDS); at a pulse generator (655), receiving the pulse duration setpoint (PDS) and generating from the pulse duration setpoint (PDS) and from the strobe signal a pulsed signal having period T_{frame} and having pulses of duration T_{ON}, $T_{ON} << T_{frame}$, the duration T_{ON} being obtained from the pulse duration setpoint (PDS) and the strobe signal being used for synchronizing the pulses of duration T_{ON} with the time instant at which the pixels in the image capture system start to capture an image; calculating a reference voltage V_{MUX} of duration T_{ON} from the pulse amplitude setpoint (PAS), the reference voltage V_{MUX} being used for obtaining a polarization current of the at least one LED; providing a voltage V_{LED} enabling to provide a current Io' to the at least one LED at pulses of duration T_{ON}, the voltage V_{LED} being provided by an RC network comprising at least one capacitor and a resistor, wherein the at least one capacitor works as a pulse energy storage means and the resistor regulates the charging speed of the pulse energy storage means, the RC network being configured for the at least one capacitor to become fully charged.

In embodiments of the invention, the stage of, for each frame, calculating a pulse amplitude setpoint (PAS) and a pulse duration setpoint (PDS) from the intensity of each frame (I_{frame}), is done as follows: from current PAS, PDS and luminance generated with the PAS and PDS, checking whether the current luminance is within a design range $LUMA_{MIN}$ < current LUMA < $LUMA_{MAX}$; if $LUMA_{MIN}$ < current LUMA < $LUMA_{MAX}$, then no control is required; otherwise, it is checked whether the time duration of the deviation with respect to the established range ($LUMA_{MIN}$, $LUMA_{MAX}$) is larger than a design hysteresis time and if the current luminance is out of the design range for a time duration shorter than the defined hysteresis time, then no control is required; otherwise, it is checked whether or not the current pulse amplitude setpoint PAS corresponds to a maximum value of intensity and, if not, then the following calculation is performed: new_PAS = (I_{frame} – $I_{frame\_setpoint}$) x Gain_PAS, the new_PAS value being used to update said potentiometer; if the current pulse amplitude setpoint PAS corresponds to a maximum value of intensity, the pulse duration is adjusted as follows: new_PDS = (I_{frame} – $I_{frame\_setpoint}$) x Gain_PDS, the value of new_PDS being used to update said potentiometer.

In another aspect of the invention, a computer program comprising computer program code means adapted to perform the steps of the previous method is provided when the program is run on a computer, a digital signal processor, a field-programmable gate array, an application-specific integrated circuit, a micro-processor, a micro-controller, or any other form of programmable hardware.

In sum, the proposed system and method permits to work with conventional DC voltage sources of very low current, in spite of the fact that the light pulses illuminating the fluid under inspection are of very high current. With the proposed system and method, for example a conventional 24 VDC and 1 mA power source is enough to feed pulses of 6A and duration of 4 µs at frequencies of for example 1 KHz. This enables to operate with any conventionally available power supply, normally not able to directly feed power for high current (e.g. 6A) short pulses (4µs) due to their switching on and off ramp times.

A collateral advantage of the system of the invention is the elimination of the need to control the light source in order to dampen the efficiency changes of the light source as a function of temperature, because the light source does not self-heat as it works in small duty cycles (<1%).

Additional advantages and features of the invention will become apparent from the detail description that follows and will be particularly pointed out in the appended claims.

BRIEF DESCRIPTION OF THE DRAWINGS

As a complement to the description and with a view to contributing towards an improved understanding of the characteristics of the invention, according to an example of a practical example thereof, a set of drawings is attached as an integral part of this description, which by way of illustration and not limitation, represent the following:

Figure 1 represents a general outline of the monitoring or inspection system according to an embodiment of the invention.

Figure 2 represents the problem observed when applying RS in a system for inspecting a moving fluid.

Figure 3 represents the power received in a system for inspecting a moving fluid when applying conventional RS.

Figure 4 shows the focusing area of a typical CMOS sensor, in which particles move at velocities varying between 3 and 22 m/s.

Figure 5 shows a comparison of the performance of RS in moving fluids with respect to the size of the particles comprised in the moving fluid.

Figure 6 represents the power received in a system for inspecting a moving fluid according to an embodiment of the invention, in which the duration of the flash light

applied by the lighting system is much shorter than the exposure time of the pixels of the image capture system.

Figure 7 shows in block diagram the image capturing system, processing means and lighting system of the monitoring system according to an embodiment of the invention.

Figure 8 shows a more detailed scheme of the lighting system of the monitoring system according to an embodiment of the invention.

Figure 9 shows a flow chart of an algorithm for calculating a pulse amplitude setpoint and a pulse duration setpoint from the frame light intensity according to an embodiment of the invention.

Figure 10 shows an example of exposure time T_{EXP}, T_{frame} and T_{ON} according to an embodiment of the invention.

Figure 11 shows a comparison of performance of a system according to the invention (right) versus a conventional system based on Rolling Shutter (left).

DESCRIPTION OF AN EMBODIMENT OF THE INVENTION

Figure 1 represents a general outline of a monitoring or inspection system 1 according to an embodiment of the invention. At the monitoring system 1 measurements of a moving fluid are taken. This system 1 has been conceived as an autonomous system with totally independent functioning, which delivers auto interpretable measurements, calibrated and corrected for the entire defined operating range. In other words, the measurement system 1 delivers measurement values that have no need of further processing. The system is specifically designed for its direct integration into the lubricating systems of machinery without affecting the operating conditions thereof. This is achieved by means of hydraulic piping (not shown) which make it possible to carry out controlled sampling in lubricating fluid (for example, oil) either by by-pass or by in-line installation. Communication interfaces and power supply units are also used in order to carry the system's results to the machine in question or wherever required. It is remarked that any conventional low current power source (such as, but not limiting, a conventional power source of 24 V (DC) and current of 1 mA) suffices for powering the proposed system, in spite of the lighting system requiring to be fed with pulses having for example 6 A (current) and extremely short duration (for example around 4 µs) in frequencies of around 1 kHz. This is enabled by means of the proposed driving circuit for the lighting system, which is described in detail later in this text.

The system 1 must have a small size and be as compact as possible to be fitted within larger hydraulic subsystems, such as filters or valves. The measurement system 1

operates on a micromechanical cell 20 through which the fluid 21 under supervision circulates. In a preferred embodiment, this fluid is oil, more preferably lubricating or hydraulic oil. The fluid 21 is driven inside channelling means, such as for example a regular pipe and circulates thanks to a small pressure difference between the input and the output of the system (0.05 Bar or larger is enough).

The measurement system 1 comprises an optical part and an electronic part (or video acquisition and processing sub-system). The video acquisition and processing sub-system carries out the activities related to measurements, among other things. It is made up of an embedded image capture system 201 and by electronics 206 comprising processing means 2061. The measurement system 1 is based on an embedded artificial vision measurement system, wherein by means of an image capture system 201 a video sequence is captured which is processed in processing means 2061, such as an embedded processor. In some embodiments of the invention, the processing means 2061 is a DSP device (*Digital Signal Processor*) or a CPU (Central Processing Unit). The goal of the processing is to determine the presence of particles and/or bubbles and the degradation value of the fluid (for example, oil)-and to determine the shape of the particles. For this purpose, processing means 2061 comprises software means, formed by a group of algorithms for the detection and classification of particles, bubble detection and determination of degradation. The arrow connecting the image capture system 201 and the processing means 2061 outlines the video data and control lines.

The image capture system 201 is configured to work in RSGS mode. In a possible embodiment, an acquisition and processing system of 4 frames per second (4FPS) is used. For example, a 5 Mpix On Semiconductor device can be used.

The optical part comprises a lighting system 205 to subject the flow of fluid 21 to a beam of light, in such a way that the image capture system 201 captures a video sequence that will afterwards be processed in the processing means 2061. The lighting system 205 is designed to supply a pulsed beam of white light to the fluid. The lighting system 205 is a stroboscopic lighting system where light pulses are synchronized with the video capture. Preferably, the lighting system 205 is based on one or more LED diodes which light the flow 21 which circulates through the micromechanical cell 20 at regular flashes of light. In other words, the lighting system preferably comprises at least one LED emitter 205. More preferably, a plurality of LED diodes is used. In embodiments of the invention, between 3 and 6 LED diodes are used. When more than one LED is used, the plurality of LEDs may be disposed in serial configuration or in parallel configuration. The lighting system 205 is described in detail later in this text.

Between the lighting system 205 and the flow of fluid 21 (which circulates inside a

pipe), a diffuser 204 may be placed for diffusing the amount of light emitted by the lighting system 205 in order to obtain a homogenous lighting over the entire area (amount of fluid) that is being inspected. In embodiments of the invention, the diffuser 204 is a window, understood as an element providing visual access to the fluid under inspection. The diffuser or diffuser window enables to light the area under inspection in a homogeneous manner. The diffuser or diffuser window 204 may be implemented as closing a hole made in the pipe through which the fluid 21 flows. The diffuser 204 is moreover made of a transparent material, such as a glass, for example a frosted glass, which allows light passing through it after diffusing it.

Opposite the lighting system 205, on the other side of the pipe through which the flow 21 circulates, the image capture system 201 is situated to capture the video sequence (a train of images) of the zone of interest in the passage of the fluid. This image capture is carried out with a defined spatial resolution and maintaining the general criteria of reduced size and low cost. In other words, the “defined spatial resolution” refers to the fact that the capture system 201 is capable of determining a defined minimum size of particle (even particles having a largest dimension of 1 µm (for example diameter of 1 µm) can be measured) taking into account the instant velocity of the fluid in which the particles are suspended. This is exemplified later with respect to figure 5.

The image capture system 201 is a camera implementing the Rolling Sutter with Global Start (RSGS) functionality. More preferably, it is a RSGS camera based on CMOS sensor or CMOS detector (the CMOS sensor is the camera component that receives the image). Therefore, a CMOS camera has a 2D array of photoreceptors manufactured with CMOS technology. For this reason, occasionally in this text the expression “CMOS sensor” or “CMOS detector” is used to refer to the image capture system 201. Alternatively, the image capture system 201 is a charge-coupled device camera (CCD camera) implementing the (RSGS) functionality. The images captured by this camera are processed in the processing means 2061, which analyses for each image whether there are bubbles and particles (and, in embodiments of the invention, counts them) and determines the size and shape of the detected objects (bubbles and particles). In other words, the processor extracts the image from the CMOS and processes it. To do this, it has an intermediate memory (not shown) for subsequent processing. In a possible embodiment, this intermediate memory is a DDR2 external memory.

Between the image capture system 201 and the flow of fluid 21 under inspection there may be a lens 202, preferably a macro lens, for transporting the image from the object to the camera 201. The lens allows objects to be focused in the light-reactive element

and objects to be captured. The lens carries the light in focus to the light receiving area.

Between the lens 202 and the pipe that collects the flow of fluid 21 under inspection there may be an optical window 203 sealing a hole made in the pipe. This hole is opposite the hole described above (and covered by the diffuser 204). This second optical window 203 is also made of a transparent material that allows light to pass through it. The window 203 is a calibration window which comprises markings or patterns that allow it to be auto-calibrated, as explained in EP2980557A1.

The minimum size of objects that the system is capable of discriminating is of approximately 1 µm. The area to be captured in each image by the image capture system 201 must be such that it is capable of capturing objects of 1 µm (and of course, bigger ones) across a total capture area of several tens of mm^2. In a preferred embodiment, the area to be captured is of several mm^2. In one example, said area to be captured is of 100 mm^2. At the same time, the distance between the object (plane of passage of the fluid under inspection) and the image capture system 201 is desirably as minimum as possible and does not exceed approximately 40 mm, so that the system can be as compact and small as possible. The maximum depth of field (range in which the lens 202 is capable of providing a focused image) is marked by the width of the passage of the fluid through the micromechanical cell 20.

Figure 2 represents the problem observed when applying RSGS in a system as shown in figure 1. This problem relates to the received optical power at the image capture system 201. In order for the system 1 to perform correctly, there must be enough light travelling through the fluid under supervision, in such a way that an image having enough contrast is generated and captured. A person skilled in the art knows that the image processing is only possible with images of enough quality in terms of focusing contrast. Figure 2 shows the amount of light Pixel(V) captured by each pixel 282 and converted into a digital voltage level Pixel(bits) by an analog-to-digital converter ADC 290 included adherent to the pixels within the CMOS sensor device. Pixel(bits) refers to the digital representation (in bits) of an analogue magnitude, such as the current or voltage (Pixel V) generated by each pixel when it receives light. Pixel(bits) = Pixel(V) / Vref(V/bit). Vref refers to the voltage reference of the CMOS in order to perform such digitalization of the received light. LED 205 emits light pulses (stroboscopic pulses) of duration T_{on} (ms), having certain light intensity I_O wherein $I_0(lux) = I_{pol}(A)\ \rho(lux/A)$, $I_{pol}(A)$ being the polarization current and ρ(lux/A) being the LED efficiency. The light I_1 received by pixel 282 (this light I_1 is essential for achieving good contrast) depends on the intensity of the emitted light I_O, on the absorbance $10^{-\alpha \ell c}$ that takes place in the sample 21 under analysis (the absorbance is dependent on the chemical properties c,

α of the fluid and on the width ℓ of the pipe; for example, opaque fluids have much larger absorbance than transparent fluids), on the responsivity R of the photodiodes forming each pixel (responsivity refers to the efficiency of the photodiodes in converting light energy into volts) and on the selected exposure time T_{exp} (time for which a pixel is accumulating incident light) which, in RSGS systems is determined (limited) by the pulse duration T_{ON}, as will be explained later. As can be observed, parameters of different nature have an impact on the performance of the system: constructional parameters of the LED and pixels (*ρ, R*); physical and chemical parameters (absorbance, dependent on the fluid under supervision); and design parameters, such as the LED polarization current I_{pol}, the exposure time T_{exp} of the pixel (or its photodiodes) and the pulse duration T_{ON}. These last parameters are the only ones under designer's choice to adjust the power of the received light in order to analyze a sample of fluid with enough contrast towards a correct discrimination of objects (particles, bubbles) suspended in the fluid. The range of LED polarization current I_{pol} permits to inspect a certain range of fluids, defined by their absorbance which, together with the pulse duration T_{ON} (which limits the exposure time T_{exp}) determines the maximum velocity of the particles.

Figure 3 represents a conventional system in which the lighting system continuously provides a flash light (flash always on or T_{on}=100%). Under these circumstances, the following equation describes the signal received by each pixel in each frame (a frame comprises a plurality of pixels forming a MxN matrix, being M~1900pix and N~2600pix), considering that the variations of I_1 within the time interval T_{exp} are negligible (in figure 3, I_1 is represented as non-constant in order to express that the fluid under supervision may vary its absorbance as it is a flowing, non-static, sample):

$$Vpix(V) = I_1(lux) \times T_{exp}\,(sec) \times R(\frac{V}{lux \times sec})$$

The duration of the lighting pulse of the stroboscopic lighting system 205 is defined by the expected velocity of the objects (particles) suspended in the fluid under supervision when they go through the focusing area. In other words, since the goal is to detect moving particles, the maximum pulse duration is given by the maximum particle velocity under observation. The lower the travelling velocity of the particles under examination is, the higher the duration of the lighting pulse may be. In contrast, the higher the travelling velocity of the particles under examination is, the lower the duration of the lighting pulse will have to be in order to avoid distortion. In a particular embodiment in which the supervision system 1 is applied to industrial machines, and more precisely to the lubricating oil they use, it has been observed that a typical working pressure may vary for example between 2 bar and 10 bar. In this case, the

velocity of the objects (particles) suspended in the fluid (in this case, oil) varies between 3 m/s and 22 m/s, respectively. This means that it is expected that the samples under analysis travel following a laminar flow of velocities varying between 3 and 22 m/s. This means that the particles suspended in the fluid will also move at similar velocities (not considering turbulence effects, etc.). Figure 4 shows the focusing area of a typical CMOS sensor, in which particles move at velocities varying between 3 and 22 m/s.

However, even if all particles are moving at the same velocity, the effect of the image capture distortion in Rolling Shutter does not affect large and small particles alike. Large particles, even with a small distortion, will be detectable by the vision algorithms (that are out of the scope of the present invention; see for example EP2980557A1) and there is no significant impact (actual particle size ~ object size detected). However, as the particle size is reduced, the effects of the distortion are more pronounced, impacting both on the size and in its apparent shape (for example, a circular particle will be seen as an ellipse due to the effect of distortion). What is more, in small particles, the distortion causes them to be non-perceptible.

Figure 5 shows a comparison of the performance of RSGS in moving fluids with respect to the size of the particles comprised in the moving fluid. First column refers to a big particle 51 (for example having a largest dimension larger than 14 µm), second column refers to a medium-size particle 52 (for example having a largest dimension between 6 and 14 µm) and third column refers to a small particle 53 (for example having a largest dimension varying between 1 and 6 µm). Second row shows how each particle 51 52 53 is captured with distortion 51’ 52’ 53’. Third row shows how the applied vision algorithms recognize each particle: the big particle is correctly recognized 51’’ (with minimum –negligible- impact), the medium-size particle is detected, but its size and shape is erroneously identified 52’’. Finally, the small particle is not detected at all 53’’.

Therefore, a criterion can be applied to determine from which percentage of distortion we have a fatal impact for detection. Defining for example that distortion will cause a bad detection if 50% of the area of the object is affected, the following table shows the maximum duration of the lighting pulse of the stroboscopic lighting system 205 for different object sizes (largest dimension) and speeds:

Object size	4µm (small object)	10µm (medium object)	20µm (big object)
50% distortion	*2µm*	*5µm*	*10µm*

Flowing velocity (m/s)	Maximum acceptable duration of lighting pulse		
	4µm (small object)	10µm (medium object)	20µm (big object)
1,5	*1,3 µs*	*3,3 µs*	*6,6 µs*
3	*600 ns*	*1,6 µs*	*3,33 µs*
11	*180 ns*	*450 ns*	*900 ns*
22	*90 ns*	*230 ns*	*450 ns*

This means that, depending on the target object size and on its expected velocity, the duration of the lighting pulse should vary between 80 ns and 10 µs approx.

Figure 6 represents a system in which the duration of the lighting pulse (flash on) T_{ON} from the lighting system has been selected to be << T_{exp}. Then, the effective exposition time = T_{ON}. Under these circumstances, the following equation describes the signal received by each pixel in each frame (a frame comprises a plurality of pixels), considering that the variations of I_1' within the time interval T_{exp} are negligible:

$$Vpix'(V) = I_1'(lux) \times \left(T_{exp}\,(\mathrm{sec}) \cap \mathrm{T}_{Flas\,h\,on}\,(\mathrm{sec})\right) \times \mathrm{R}\left(\frac{\mathrm{V}}{\mathrm{lux} \times \mathrm{sec}}\right) = \mathrm{I}_0'(\mathrm{lux}) \times 10^{-\mathrm{A}} \times T_{Flas\,h\,on}\,(\mathrm{sec}) \times \mathrm{R}\left(\frac{\mathrm{V}}{\mathrm{lux} \times \mathrm{sec}}\right)$$

Therefore, since the design goal is to maintain the signal generated by each pixel (V_{PIX} == V_{PIX}'), that is to say, in spite of having pulses of short duration, the total light power must be similar to the one that would be obtained with a pulse always on (because high light power is required for acquiring images with good contrast), given certain values of absorbance (A) and pixel responsivity (R), the light intensity I_0' emitted by the lighting system must be modulated. However, because T_{ON} << T_{exp}, in order to achieve that V_{PIX} == V_{PIX}', the applied light power must be very high: I_0' >> I_0.

Therefore, coming back to figure 1, in order to be able to inspect opaque fluids (worst case, since opaque fluids require more light power than transparent ones) having suspended objects having a largest dimension as small as 1 µm, flowing at high flow rates, the lighting system 205 must be capable of delivering very high power pulses for very short time duration. Besides, these pulses must be synchronized with the start instants of capture at image capture system 201. In the context of the present invention, the term “high” in “high flow rates” refers to flow rates varying between 1 and 40 m/s, that is to say, flow rates of up to 40 m/s. In the context of the present invention, the term “high” in “high power pulses” refers to power pulses varying between 20 mA

and 20 A, preferably between 2 and 15 A. In the context of the present invention, the expression “very short” in “very short time duration” refers to time duration varying between 50 ns and 50 µs, preferably between 50 ns and 20 µs, more preferably between 50 ns and 10 µs, and still more preferably varying between 50 ns and 5 µs.

This is achieved by a monitoring system 1 having an image capturing system 601 (201 in figure 1), processing means 6061 (2061 in figure 1) and lighting system 305 (205 in figure 1) as schematized in figures 7 and 8. The lighting system 305 is configured for operating synchronized with an image capturing system configured in RSGS mode.

Figure 7 shows in block diagram the image capturing system 601 (201 in figure 1), processing means 6061 (2061 in figure 1) and lighting system 305 for operating synchronized with the image capturing system 601 configured in RSGS mode, of the monitoring system 1. The lighting system 305 comprises at least one LED diode 605 and light driving means 360 for operating the at least one LED diode 605. Figure 8 shows in detail the blocks of figure 7. In particular, the light driving means 360 for operating the at least one LED diode 605 is shown in more detail. The lighting system 305 is capable of detecting objects (such as particles and bubbles) of microscopic size, suspended in moving fluids potentially very opaque. With the lighting system 305 of the invention, particles having a dimension (i.e. diameter) larger than 1 µm are detected.

The lighting system 305 has one or more LED diodes 605 (also referred to as LED or LEDs) that may be disposed in serial or in parallel or in a mixed serial/parallel configuration. The current Io’ travelling through the at least one LED 605 must be a high current and high voltage delivered at fast pulses. In a particular embodiment, each LED needs current I_O’ = 6 A and voltage = 5 V. In an exemplary implementation, in which 6 LEDs are disposed in serial configuration, the required current and voltage is: I_O’ = 6 A, V = 30 V. In another exemplary implementation, in which 6 LEDs are disposed in parallel configuration, the required current and voltage is: I_O’ = 36 A, V = 5 V. The value of the amplitude of this current I_O’ and the duration of the current pulses delivered by the at least one LED 605 is controlled by processing means 6061 from the frames provided by the image capture system 601.

Each of these frames comprises the information captured by at least some of the pixels comprised in the image capture system 601 (preferably CMOS camera). The information captured by each pixel is a voltage (Vpix), then converted into digital value (bits), as explained with reference to figure 2. The Vpix resolution is given by the number of bits of the CMOS sensor (normally 8, 10 or 12 bits), in such a way that the information kept by a pixel can be discriminated into 2^n steps within the range 0-Vref, n being the number of bits used by each pixel (in other words, the pixel resolution). In a particular embodiment, each frame comprises the voltage captured by all of the pixels

comprised in the image capture system 601. Each pixel carries a digital value representing the received light intensity.

Referring now to figure 8, processing means 6061 has means 611 for reading each frame, means 612 for calculating, from each read frame, a frame light intensity I_{frame} and means 613 for calculating a pulse amplitude setpoint (PAS) and pulse duration setpoint (PDS) from said frame light intensity I_{frame}. These setpoints PAS, PDS are instructions to be sent to respective digital potentiometers 651 652 in order to respectively establish the current and pulse duration. An algorithm calculates setpoints PAS, PDS from the frame light intensity (intensity of each frame) I_{frame}. In embodiments of the invention, the algorithm is a proportional-integral (PI) controller that prioritizes current increases over pulse duration in order to make it compatible with higher flows. In other embodiments, the setpoints PAS, PDS are calculated from the intensity of each frame I_{frame} and from the contrast of each frame. Figure 9 shows a flow chart of the algorithm for calculating setpoints PAS, PDS according to an embodiment of the invention. The algorithm is described next.

The frame light intensity I_{frame} is preferably calculated as follows:

$$I_{frame}=(\sum Vpix\ )/NumPix$$

wherein Vpix is the voltage captured by each pixel in the image capture system 601 and NumPix is the amount of pixels in the image capture system 601.

As mentioned, block 613 comprises an algorithm for calculating a pulse amplitude setpoint (PAS) and pulse duration setpoint (PDS) from every new frame light intensity I_{frame}. The goal of this block 613 is to determine the new values of PAS and PDS in order to obtain a value of frame light intensity I_{frame} (referred to as LUMA in figure 9) within lower and upper limits I_{frame_MIN}, I_{frame_MAX} (respectively referred to as $LUMA_{MIN}$, $LUMA_{MAX}$ as in figure 9) defined by design. The starting points are current PAS 901 and PDS 902, together with the frame light intensity I_{frame} (or LUMA) generated with the initial configuration of PAS, PDS. The goal of this control algorithm is to reach a value of I_{frame}, such that $I_{frame\_MIN} < I_{frame} < I_{frame\_MAX}$ ($LUMA_{MIN} < LUMA < LUMA_{MAX}$) while prioritizing raising the pulse amplitude (PAS) rather than raising the pulse duration (PDS), because it has been observed that this prioritizing scheme optimizes the compatibility with higher particle velocities. It is remarked that PAS and PDS values respectively control the values of potentiometers 651 652 respectively controlling the current I_O' (Amperes) and the pulse duration T_{ON} (µs). In a particular embodiment, potentiometers 651 652 are digital potentiometers. For example, they may be 8-bits potentiometers. This means that PAS and PDS are values varying between 0 and 255. In turn, the frame intensity is also represented as a certain level. In a particular

embodiment, in which the camera is a CMOS camera of, for example, 8 bits, a level varying between 0 and 255 represents a mean luminance of all the pixels of the image captured by the CMOS. Therefore, the threshold intensity values $LUMA_{MIN}$, $LUMA_{MAX}$ correspond to certain luminance levels (varying for example between 0 and 255). A non-limiting typical design value of LUMA for a certain frame is 150. So, turning back to figure 9, the starting points of PAS 901 and PDS 902 provide a starting point of luminance (or LUMA) 903.

Then, considering threshold design parameters $LUMA_{MIN}$ 904 and $LUMA_{MAX}$905, the algorithm checks (block 906) whether the current luminance 903 is within the established threshold: current LUMA > $LUMA_{MIN}$ and current LUMA < $LUMA_{MAX}$. Non-limiting exemplary values of minimum luma $LUMA_{MIN}$ 904 and maximum luma $LUMA_{MAX}$ 905 are $LUMA_{MIN}$ = 130 and $LUMA_{MAX}$ =170 (for levels varying between 0 and 255). If $LUMA_{MIN}$ < current LUMA < $LUMA_{MAX}$, then (block 907) no control is required (end of the algorithm). If, on the contrary, the former condition is not fulfilled, in block (909) it is checked the time duration of the deviation with respect to the established range ($LUMA_{MIN}$, $LUMA_{MAX}$). In other words, it is checked whether or not the deviation is stable in time, that is to say, how many consecutive frames have luminance out of ($LUMA_{MIN}$, $LUMA_{MAX}$). This hysteresis time 908 is also a design parameter. A non-limiting example of hysteresis time may be 5 seconds. So, if the current LUMA is out of the design range for a time duration shorter than the defined hysteresis time 908, no control is applied (block 910) and the algorithm is ended. If, on the contrary, the current LUMA is out of the design range for a time duration larger than the defined hysteresis time 908, a control must be applied.

Then, it is first checked (block 911) whether or not the current pulse amplitude setpoint PAS corresponds to a maximum value of intensity (saturation current). In a non-limiting example, the saturation current may be 6 A. In other words, it is checked (block 911) whether current PAS = PAS_{MAX}. If PAS < PAS_{MAX} (that is to say, current I < $I_{saturation}$), then (block 912) the following calculation is performed: new_PAS = (I_{frame} – $I_{frame\_setpoint}$) x Gain_PAS, wherein I_{frame} is the actual current (LUMA) and $I_{frame\_setpoint}$ (also referred to as $LUMA_{setpoint}$) is the frame intensity (LUMA) to be reached. For example, if $I_{frame\_setpoint}$ = 160 and I_{frame} = 120, the control algorithm will try to obtain I_{frame} = 160 for the following frames by applying a gain. In a particular example, $LUMA_{setpoint}$ = ($LUMA_{MAX}$ + $LUMA_{MIN}$)/2. In block 912, the applied gain is referred to as G_{PAS}. The value of new_PAS (block 914) is used to update potentiometer 651. In other words, the resistance value of potentiometer 651 is adjusted to the value that enables the pulse amplitude to be as required.

If, on the contrary, PAS = PAS_{MAX} (that is to say, current I = $I_{saturation}$), then the pulse

amplitude cannot be raised anymore. Therefore, the only parameter to be adjusted in order to control I_{frame} (that is, LUMA) is the pulse duration. In order to do so, in block 913 the following calculation is performed: new_PDS = (I_{frame} – $I_{frame\_setpoint}$) x Gain_PDS. In block 913, the applied gain is referred to as G_{PDS}. The value of new_PDS (block 915) is used to update potentiometer 652. In other words, the resistance value of potentiometer 652 is adjusted to the value that enables the pulse duration to be as required.

As explained in relation to the algorithm illustrated in figure 9, the PDS is used for controlling the pulse duration T_{ON} of a pulse signal, that is to say, the time for which the lighting system 305, or more precisely, the at least one LED 605, is on (emitting power). The pulse signal (and pulse duration T_{ON}) is created at a pulse generator 655. In a particular embodiment, the pulse generator 655 is implemented with a single retriggerable monostable, such as a single retriggerable monostable chip, provided for example by Texas Instruments. The pulse generator 655 provides a pulse signal having period T_{frame} and having pulses of duration T_{ON}, $T_{ON} << T_{frame}$. In order to define the pulse duration T_{ON}, the pulse generator 655 uses the PDS (that basically configures an RC net of the retriggerable monostable, which is a common way of configuring chips of this kind). The pulse generator 655 also uses a flash signal (also referred to as strobe signal) provided by the image capture system 601. The strobe signal triggers the start of the flash duration, and it is a parameter of the image capture system, in particular, of the CMOS camera, which provides a strobe signal having certain frequency correlated with the Frames per Second (T_{frame}) configuration. Therefore, the strobe signal is used as a trigger signal. This strobe signal provided by the image capture system 601 is used by the pulse generator 655 for synchronizing the generated signal (having period T_{frame} and having pulses of duration T_{ON}) with the strobe signal of the image capture system 601. The PDS signal is fed into the digital potentiometer 652. Potentiometer 652 controls, by means of its variable resistance R (adjusted from PDS) in a RC network (capacitor not explicitly shown in figure 8), the duration of the short pulses (duration T_{ON}) generated by pulse generator 655. In other words, potentiometer 652 fixes a value of the RC network that defines the operation of the pulse. Therefore, the pulse generator 655 calculates the pulse duration T_{ON} (the very short time duration of the high power pulses emitted by the at least one LED 605) from the PDS. The strobe signal is used for triggering each pulse of duration T_{ON}. In other words, the strobe signal permits to work in synchronization between lighting system and image capture system. This way, the light pulses emitted by the at least one LED 605 are synchronized with the strobe signal of the image capture system 601 (the light pulses emitted by the at least one LED 605 are triggered at the time instant at which each pixel starts to capture a frame). As a matter of example, let’s consider an image

capture system 601 whose pixels have exposure time T_{EXP}=150 ms and video is captured at 4 FPS (frames per second, that is to say, T_{frame} = 250 ms). This is exemplified in figure 10. If for example T_{ON} = 1 µs, with every new frame (that is to say, every 250 ms, since T_{frame} is the time period between two consecutive captured image frames) a new LED pulse is triggered. This triggering of each pulse of duration T_{ON} = 1 µs is synchronized with the starting of each exposure time T_{EXP}=150 ms.

The pulse duration T_{ON} is directed to multiplexor 656 which provides at its output a reference voltage of duration the pulse duration T_{ON}, and a substantially null voltage when there is no pulse duration T_{ON}. The duration of the null voltage depends of the frames per second (FPS) at which the camera works. For example, if it works at 20 FPS, then the duration of the null voltage is 50 ms. The minimum duration of the null voltage is approximately 1 ms. In other words, multiplexor 656 provides a reference voltage V_{MUX} for the time the at least one LED 605 must be on and provides a null voltage for the time the at least one LED 605 must be off. This reference voltage V_{MUX} is then converted into the polarization current of the at least one LED 605. How this reference voltage V_{MUX} is calculated is explained next.

Turning back to processing means 6061, processing means 6061 delivers a PAS to a potentiometer 651. As explained in relation to the algorithm illustrated in figure 9, PAS value defines the value taken by variable potentiometer 651, in such a way that V_{MUX} = (resistance of potentiometer 651)/(resistance of potentiometer 651 + resistance of resistor 653) x Vcc. So, the PAS is used for calculating a reference voltage V_{MUX}, in turn used for calculating current Io' travelling through the at least one LED 605. This is done at multiplexor 656, wherein either V_{MUX} or a null voltage is provided to amplifying means 657, which provides flash gain. As explained above, V_{MUX} is provided for the time duration T_{ON} of the pulse generated by pulse generator 655, while a null voltage is provided for the time duration at which the pulse generated by pulse generator 655 has null amplitude. This time duration can be referred to as T_{OFF}. Processing means 6061 configures the frames per second (FPS) at which the camera (CMOS) works. These FPS in turn fixes $T_{OFF} = T_{frame} - T_{ON}$. At the output of amplifying means 657 a driving voltage is applied to the mosfet transistor circuit 658, 654, which drives finally the high current Io' for the one or more LEDs 605. This high current Io' can be switched on and off very fast, allowing the generation of clean pulses. In a preferred embodiment, the on & off switching times of high current Io' are less than 10% of the time duration T_{ON}.

So far, a circuit has been described, capable of generating a current Io' delivered at pulses of duration T_{ON} (for example 4 µs or less) and having high amplitude (for example 10 A) and $T_{OFF} = T_{frame} - T_{ON}$, of for example 20 ms (depending on the FPS at which the camera works). However, in order for the lighting system 205, 305 to

correctly operate in RSGS mode, it is required that the very high power pulses maintain their amplitude exactly for the time duration T_{ON} (pulses as square as possible), as represented in figure 6. In other words, Io' must switch from several Amperes to 0 Amperes immediately (preferably in less than 10% of the time duration T_{ON}) and the other way around. In order to fulfil such strict requirement, the lighting system 305 comprises a loading system 670 that makes the lighting system 305 independent from the power supply unit and that permits the lighting system 305 to work with a very low current power source (for example, 100 mA or even less). Loading system 670 stores energy in such a way that current Io' is available very quickly for driving the one or more LEDs 605. Therefore, system 670 is an energy storage means capable of transferring current very quickly. Because $T_{OFF} >> T_{ON}$, T_{OFF} is used for loading a capacitor, thus having the energy required for providing current Io' ready to be used. As one skilled in the art is aware of, the energy stored by a capacitor is given by $E=1/2*C*V^2$ wherein $V= V_{Led}$.

System 670 comprises a switched-mode power supply 659 which, from an external common DC power supply source V_{out} provided by the industrial system in which the monitoring or inspection system 1 (figure 1) is integrated, generates a low current I_{int} and voltage V_{int} (voltage V_{int} at the output of switched-mode power supply 659). A typical voltage V_{out} provided by the industrial system is, for example, 24 V. Alternative typical values of V_{out} are 5 V and 12 V. In other words, voltage V_{int} is an intermediate voltage generated in order to enable the "low" loading of capacitor 662. In an exemplary embodiment, V_{int} varies between 30 and 40 V. V_{int} may vary depending on the configuration of the LED diodes 605 (serial or parallel configuration). This means that, although the lighting system 305 needs current Io' (for example, 10 A), a switched-mode power supply 659 may only provide a low current I_{int}. This low current I_{int} is limited by the resistor 661 and sets the charging speed of the capacitor 662. In other words, resistor 661 regulates current I_{int} because V_{int} is normally fixed (design value). In embodiments of the invention, low current I_{int} varies between 1 mA and 50 mA. The higher is current I_{int}, the quicker the capacitor 662 will be loaded. There may be one or more capacitors 662. In other words, capacitor 662 works as a pulse energy storage means, while resistor 661 regulates the charging speed of the pulse energy storage means 662 ($I_{int} = V_{int}$ / resistance value of 661). The RC circuit (661, 662) is configured in such a way that capacitor 662 becomes fully charged in a time T smaller than T_{EXP} (T_{EXP} depends on the image capture system). So, when capacitor 662 is fully charged, it stores enough energy to commute Io' current keeping V_{LED} stable. In other words, V_{Led} works as the source that provides the current Io' imposed by processing means 6061 (through PAS). V_{Led} is V_{int} but with capacity of providing a high current through the energy stored in the capacitors 662. Finally, Vcc is the voltage for feeding

the remaining electronic circuits (a typical value of Vcc is 3.3 V).

Figure 11 shows a comparison of performance of a system according to the invention (right) versus a conventional system based on Rolling Shutter (left). In both cases the frame rate = 42 fps (T_{frame} = 1/42 = 23 ms) and the exposure time T_{EXP} = T_{frame} = 23 ms. Using a conventional system (left), having flash always on (T_{ON} = 23 ms (100%), the objects (bubbles) captured by the image capture system and processed at processing means are distorted. In other words, with an exposure time (that is to say, a flash time on) of 23ms, moving objects appear distorted. In this case, the brightness (or contrast) of the image is determined by the 23 ms of exposure time (T_{EXP}). In the conventional system (left), Io' = 200 mA. On the contrary, using a system according to the invention (right), having flash duration (T_{ON}) = 4 µs (that is to say, in the order of 0.01% of T_{frame}), the objects (bubbles) captured by the image capture system and processed at processing means are not distorted. In this case (right), Io' = 10 A. In this case, the effective exposure time is defined by the duration of the 4 µs Flash (T_{ON}), in spite of the exposure time (T_{EXP}) of the CMOS being 23 ms, allowing moving objects to be much clearer. What is more, the brightness of the image is also determined by the flash pulse because the flash duration (T_{ON}) and its power (Io') determine the amount of light received by the CMOS and therefore the brightness of the image. It is observed in this case that it has been necessary to amplify 50 times the illumination power (x50) (from 200 mA to 10 A) in order to obtain a contrast similar to the one on the left. However, in terms of LED life, it is much better to operate with short pulses of higher current than with 100% on with lower current, due to overheating occurring with the LED always on.

In sum, detection of moving objects having a largest dimension as small as 1 µm at flow rates of up to 40 m/s in opaque fluids and determination of their size and shape has been achieved by the system of the invention, provided that the image capture system receives enough power ($\propto T_{ON}$ and Io') for the fluid images and the objects suspended thereon to have enough contrast for its correct discrimination, and that the flash duration (duration of light pulses) is very short in order to obtain clear capture of the objects suspended in the fluid. This is achieved by a lighting system delivering very high power pulses (varying between 20 mA and 20 A) for very short time instants (varying between 50 ns and 50 µs). The microscopic objects shown in the images captured by the image capture system 601 substantially have the shape of the original microscopic objects located in the flowing fluid. This permits the later detection of their real size and identification of actual shape of the original microscopic objects suspended in the flowing fluid by means of techniques which are out of the scope of the present invention.

Throughout this document, the word "comprises" and variants thereof (such as

“comprising”, etc.) must not be interpreted as having an exclusive meaning, in other words, they do not exclude the possibility of what is being described incorporating other elements, steps, etc.

At the same time, the invention is not limited to the specific embodiments described herein and also extends, for example, to variants that may be embodied by an average person skilled in the art (for example, with regard to the choice of materials, dimensions, components, configuration, etc.), within the scope of what is inferred from the claims.

CLAIMS

1. A system (1) for detecting microscopic objects located in a flowing fluid, the system (1) comprising:

a lighting system (205, 305) comprising at least one LED diode (605) and configured to supply light to the flowing fluid;

an image capture system (201, 601) situated on the opposite side of the flowing fluid in respect of the lighting system (205, 305), said image capture system (201, 601) being configured to capture a sequence of images of the flowing fluid, said image capture system (201, 601) comprising a camera in turn comprising a plurality of pixels;

processing means (2061, 6061) configured to process said sequence of images and to determine the presence of microscopic objects within said flowing fluid and the shape of the microscopic objects,

the system (1) being characterized in that said lighting system (205, 305) is configured to supply high power light pulses having amplitude Io' and very short time duration T_{ON}, the time instant at which said pulses are triggered being synchronized with the time instants at which pixels in the image capture system (601) start to capture an image frame, wherein said processing means (2061, 6061) is configured to control said amplitude Io' and time duration T_{ON} of the light pulses supplied by the lighting system (205, 305) by means (613) for calculating, from the light intensity ($I_{frame,}$ LUMA) of each captured image frame, a pulse amplitude setpoint (PAS) and a pulse duration setpoint (PDS) for adjusting respective potentiometers (651, 652) configured to respectively fix the amplitude Io' and pulse duration T_{ON}, said means (613) for calculating the pulse amplitude setpoint (PAS) and the pulse duration setpoint (PDS) being configured to execute an algorithm that prioritizes amplitude rises over pulse duration rises, said lighting system (305) further comprising an energy loading system (670) configured to make the amplitude requirement and response time of the lighting system (305) independent from a power supply unit (Vout) of the system (1).

2. The system (1) of claim 1, wherein said image capture system (601) is configured to provide said processing means (6061) with an image frame (Frame) captured every T_{frame} seconds, T_{frame} being less than or equal to T_{EXP}, wherein T_{EXP} is the exposure time of the pixels comprised in said image capture system (601).

3. The system (1) of either claim 1 or 2, wherein said lighting system (305) comprises a pulse generator (655) for generating from said pulse duration setpoint (PDS) and from a strobe signal provided by said image capture system (601), a pulsed signal having period T_{frame} and having pulses of duration T_{ON}, $T_{ON} << T_{EXP} \leq T_{frame}$, said

duration T_{ON} being obtained from said pulse duration setpoint (PDS) and said strobe signal being used for synchronizing the pulses of duration T_{ON} with the time instant at which the pixels in the image capture system (601) start to capture an image frame.

4. The system (1) of claim 3, wherein the pulse generator (655) is implemented with a single retriggerable monostable forming, together with the potentiometer (652) adjustable by the pulse duration setpoint (PDS), an RC network configured to fix said pulse duration T_{ON}.

5. The system (1) of any preceding claims, wherein said lighting system (305) further comprises a multiplexor (656) configured to provide a reference voltage (V_{MUX}) of duration T_{ON}, and a substantially null voltage of duration T_{frame} - T_{ON} , wherein said reference voltage V_{MUX} is calculated from said pulse amplitude setpoint (PAS) obtained at said processing means (6061), said reference voltage (V_{MUX}) being used for obtaining a polarization current of said at least one LED (605).

6. The system (1) of any preceding claims, wherein said energy loading system (670) comprises a switched-mode power supply (659) configured to provide a voltage (V_{int}) and a low current (I_{int}) from an external DC power supply source (V_{out}); and an RC network comprising at least one capacitor (662) and a resistor (661), wherein said at least one capacitor (662) works as a pulse energy storage means and said resistor (661) regulates the charging speed of the pulse energy storage means, said RC network being configured for the at least one capacitor (662) to become fully charged in a time duration T_{frame} - T_{ON} , wherein T_{frame} is the time period between two consecutive image frames captured by the image capture system (601), the switched-mode power supply (659) thus providing a voltage (V_{LED}) in turn enabling to provide said at least one LED (605) with said current Io'.

7. The system (1) of any preceding claims, further comprising a diffuser (204) situated between the lighting system (205, 305) and the flow of fluid (21), configured to provide homogeneous lighting to the area to be illuminated.

8. The system (1) of claim 7, wherein said diffuser (204) is situated closing off and sealing a hole made in the pipe through which the fluid (21) flows.

9. The system (1) of any preceding claims, further comprising a lens (202) situated between the image capture system (201, 601) and the flow of fluid (21), configured to focus the captured images.

10. The system (1) of claim 9, further comprising a calibration device (203) situated between the lens (202) and the flow of fluid (21).

11. The system (1) of any preceding claim, wherein said processing means (2061, 6061) is configured to determine the presence and shape of objects having a largest

dimension smaller than 20 µm.

12. The system (1) of any preceding claim, wherein the light pulses supplied by the lighting system (305) have amplitude Io' varying between 20 mA and 20 A and time duration T_{ON} varying between 50 ns and 50 µs.

13. A method for detecting microscopic objects located in a flowing fluid, comprising:

supplying (205, 305) light emitted by at least one LED (605) to a flowing fluid having microscopic objects suspended thereon;

capturing a sequence of images of the flowing fluid by means of an image capture system (601) comprising a plurality of pixels;

processing said sequence of images and determining the presence of microscopic objects within said flowing fluid and the shape thereof,

the method being characterized by:

at said image capture system (601), capturing an image frame every T_{frame} seconds, T_{frame} being higher than or equal to T_{EXP}, wherein T_{EXP} is the exposure time of said pixels comprised in said image capture system (601);

providing a strobe signal from said image capture system (601);

for each frame, calculating a pulse amplitude setpoint (PAS) and a pulse duration setpoint (PDS) from the intensity of each frame (I_{frame}, LUMA) by executing an algorithm that prioritizes rises in the pulse amplitude (PAS) rather than rises in the pulse duration (PDS);

at a pulse generator (655), receiving said pulse duration setpoint (PDS) and generating from said pulse duration setpoint (PDS) and from said strobe signal a pulsed signal having period T_{frame} and having pulses of duration T_{ON}, $T_{ON} << T_{frame}$, said duration T_{ON} being obtained from said pulse duration setpoint (PDS) and said strobe signal being used for synchronizing the pulses of duration T_{ON} with the time instant at which the pixels in the image capture system (601) start to capture an image;

calculating a reference voltage (V_{MUX}) of duration T_{ON} from said pulse amplitude setpoint (PAS), said reference voltage (V_{MUX}) being used for obtaining a polarization current of said at least one LED (605);

providing (670) a voltage (V_{LED}) enabling to provide a current Io' to said at least one LED (605) at pulses of duration T_{ON}, said voltage (V_{LED}) being provided by a an RC network (661, 662) comprising at least one capacitor (662) and a resistor (661), wherein said at least one capacitor (662) works as a pulse energy storage means and

said resistor (661) regulates the charging speed of the a pulse energy storage means, said RC network being configured for the at least one capacitor (662) to become fully charged in a time duration T_{frame} - T_{ON} , wherein T_{frame} is the time period between two consecutive image frames captured by the image capture system (601).

14. The method of claim 13, wherein said stage of, for each frame, calculating a pulse amplitude setpoint (PAS) and a pulse duration setpoint (PDS) from the intensity of each frame (I_{frame}, LUMA), is done as follows:

from current PAS (901), PDS (902) and luminance (903) generated with said PAS (901) and PDS (902), checking (906) whether the current luminance (903) is within a design range $LUMA_{MIN}$ < current LUMA < $LUMA_{MAX}$;

if $LUMA_{MIN}$ < current LUMA < $LUMA_{MAX}$, then (907) no control is required;

otherwise, it is checked (909) whether the time duration of the deviation with respect to the established range ($LUMA_{MIN}$, $LUMA_{MAX}$) is larger than a design hysteresis time (908) and

if the current luminance is out of the design range for a time duration shorter than the defined hysteresis time (908), then (910) no control is required;

otherwise, it is checked (911) whether or not the current pulse amplitude setpoint PAS corresponds to a maximum value of intensity (911) and,

if not, then (912) the following calculation is performed: new_PAS = (I_{frame} – $I_{frame\_setpoint}$) x Gain_PAS, the new_PAS value being used (914) to update said potentiometer (651);

if the current pulse amplitude setpoint PAS corresponds to a maximum value of intensity (911) the pulse duration is adjusted as follows (913): new_PDS = (I_{frame} – $I_{frame\_setpoint}$) x Gain_PDS, the value of new_PDS (915) being used to update said potentiometer (652).

15.- A computer program comprising computer program code means adapted to perform the steps of the method according to claims 13 or 14 when said program is run on a computer, a digital signal processor, a field-programmable gate array, an application-specific integrated circuit, a micro-processor, a micro-controller, or any other form of programmable hardware.

MONITORING SYSTEM AND METHOD FOR DETECTING FLOWING MICROSCOPIC OBJECTS

ABSTRACT

A system (1) for detecting microscopic objects located in a flowing fluid. It comprises a lighting system (205, 305) comprising at least one LED diode (605) for supplying light to the flowing fluid; an image capture system (201, 601) configured to capture a sequence of images of the fluid. The image capture system comprises a camera comprising a plurality of pixels. The sequence of images is processed and the presence and shape of microscopic objects is determined. The lighting system (205, 305) is configured to supply high power light pulses having amplitude Io' and very short time duration T_{ON}, the time instant at which said pulses are triggered being synchronized with the time instants at which pixels in the image capture system (601) start to capture an image frame. The amplitude Io' and time duration T_{ON} of the light pulses are controlled by calculating, from the light intensity (I_{frame}) of each captured image frame, a pulse amplitude setpoint (PAS) and a pulse duration setpoint (PDS) for adjusting respective potentiometers (651, 652) configured to respectively fix the amplitude Io' and pulse duration T_{ON} by executing an algorithm that prioritizes amplitude rises over pulse duration rises. The lighting system (305) comprises an energy loading system (670) configured to make the amplitude requirement and response time of the lighting system (305) independent from the power supply unit. Method for detecting microscopic objects suspended in a flowing fluid.

(FIG. 8)

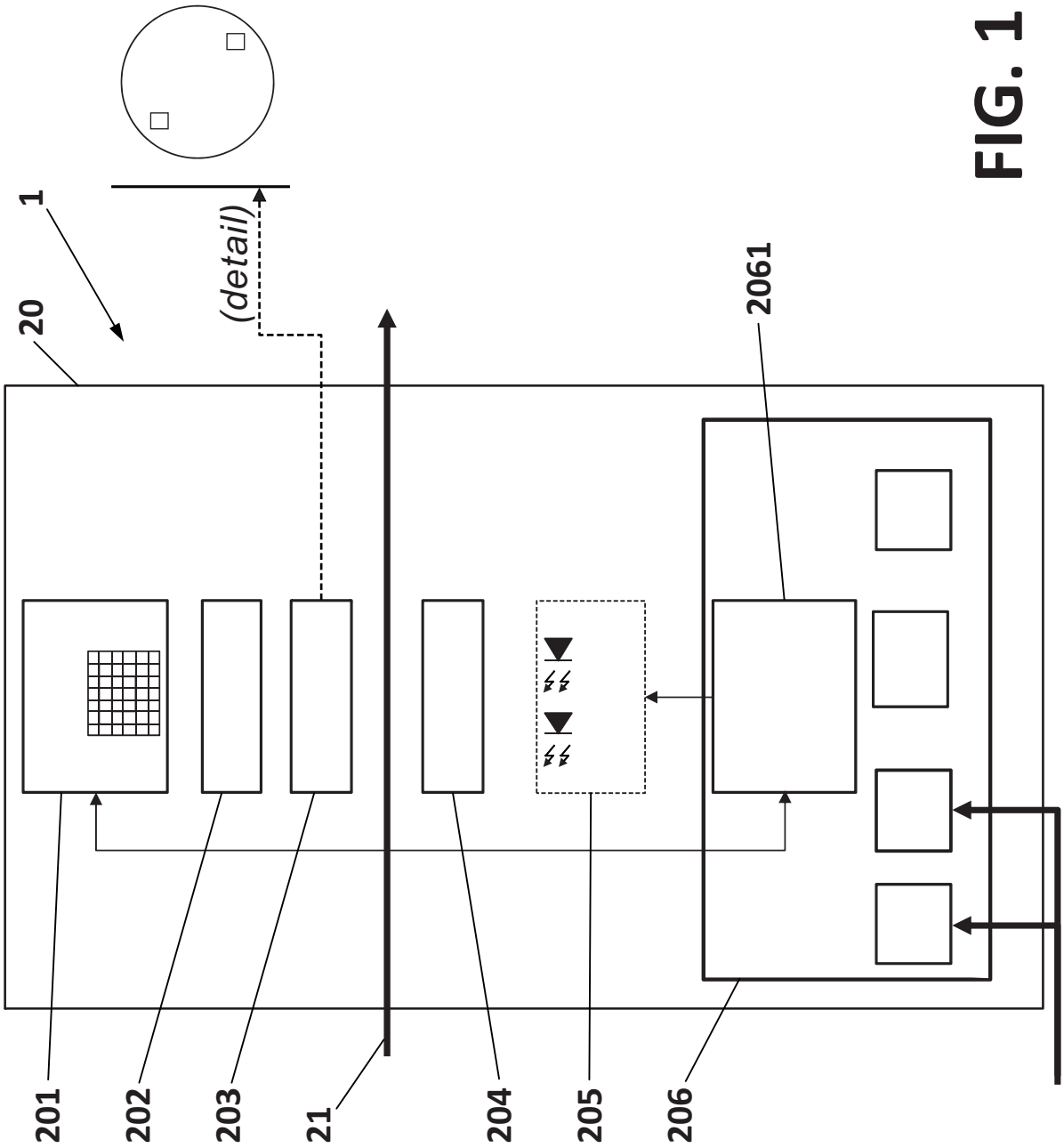

FIG. 1

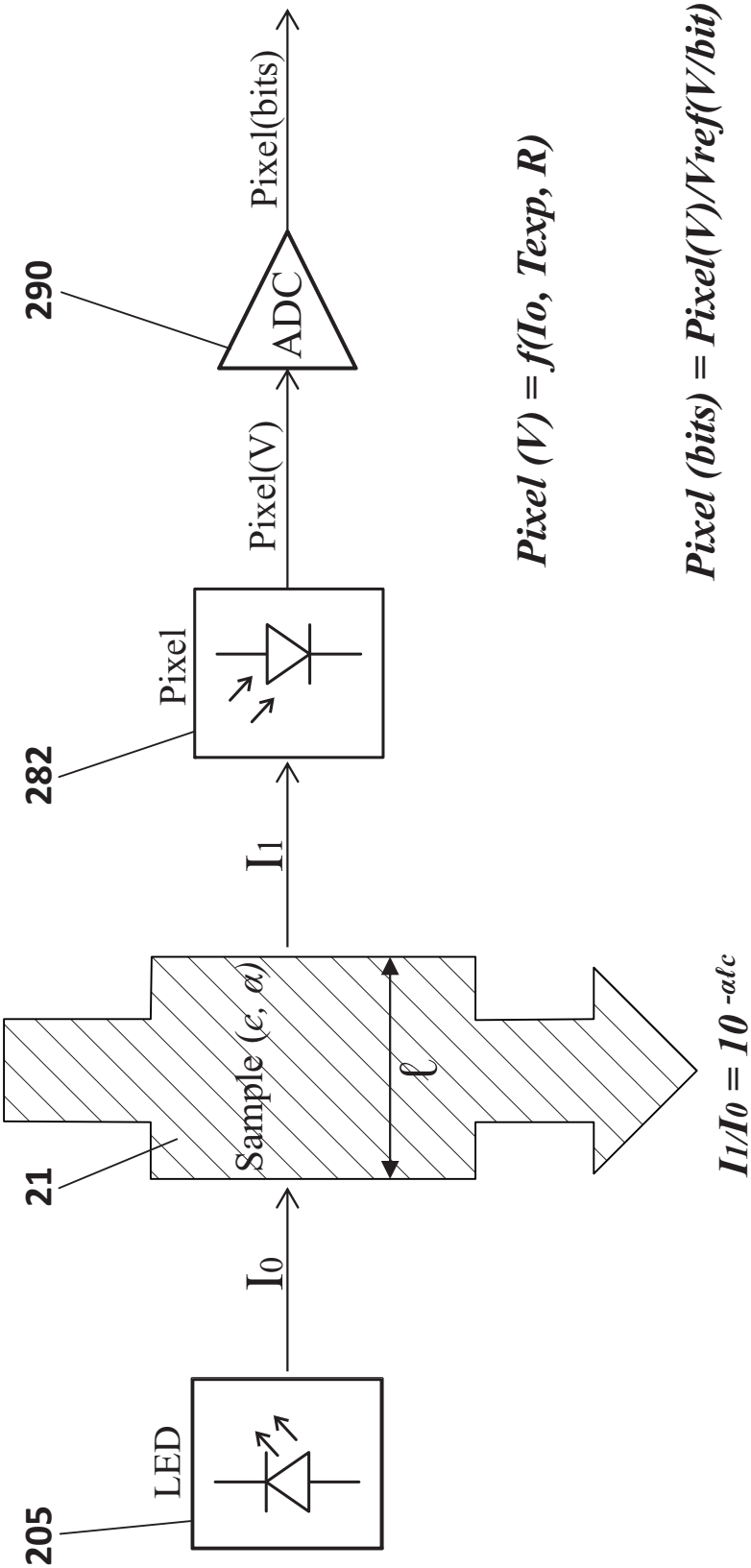
205
LED
I_0
21
Sample (ϵ, α)
ℓ
I_1
282
Pixel
Pixel(V)
290
ADC
Pixel(bits)
Pixel (V) = f(Io, Texp, R)
Pixel (bits) = Pixel(V)/Vref(V/bit)
$I_1/I_0 = 10^{-\alpha \ell c}$

FIG. 2

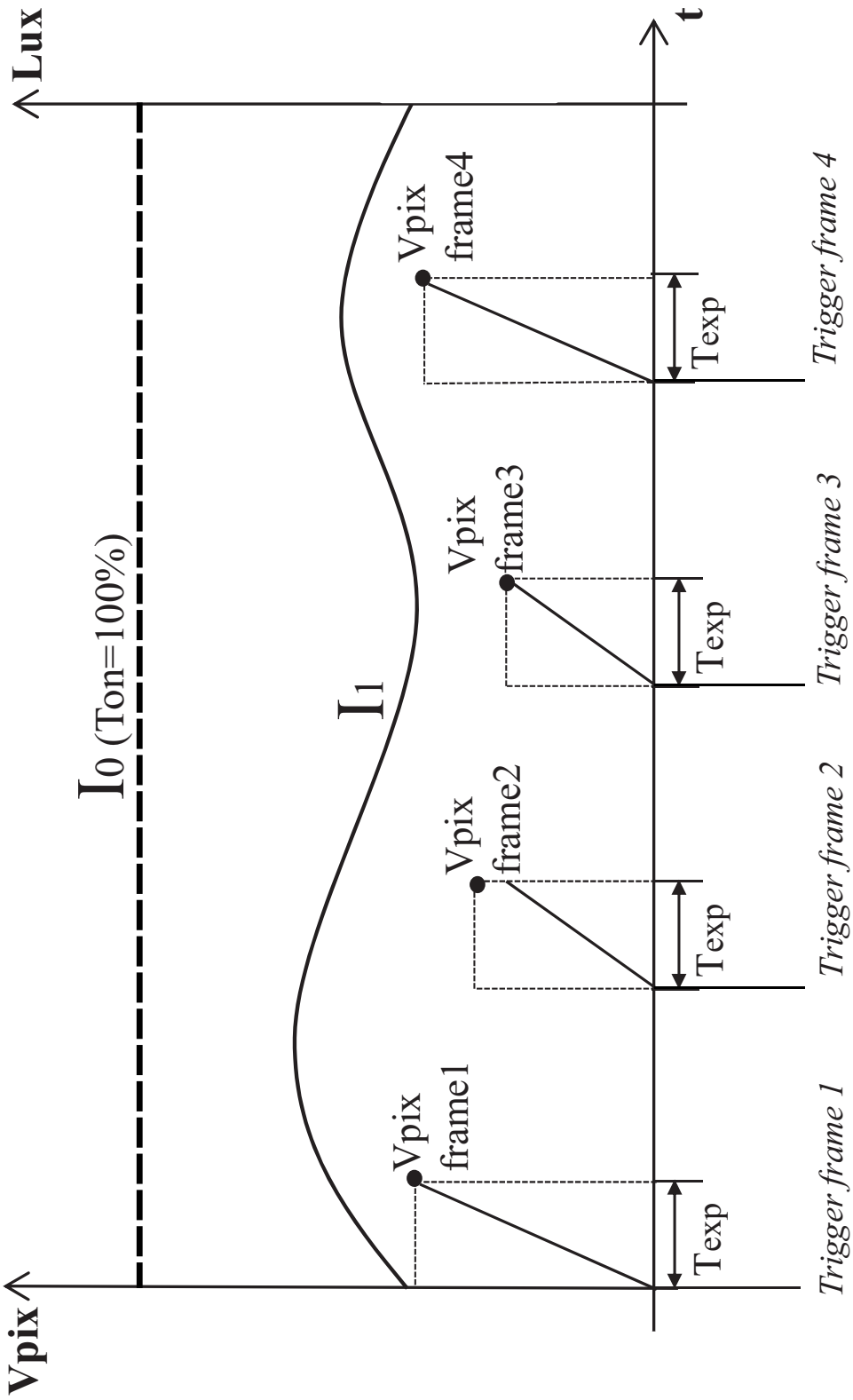
Lux
t
Vpix
I0 (Ton=100%)
I1
Vpix frame1
Vpix frame2
Vpix frame3
Vpix frame4
Texp
Texp
Texp
Texp
Trigger frame 1
Trigger frame 2
Trigger frame 3
Trigger frame 4

FIG. 3

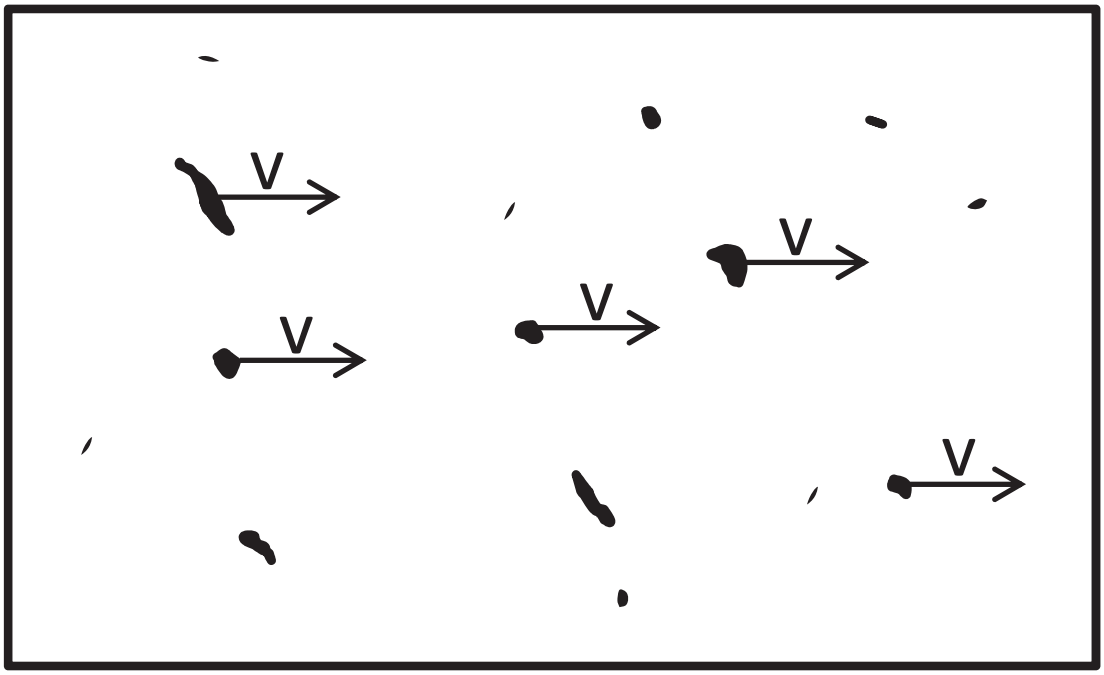

FIG. 4

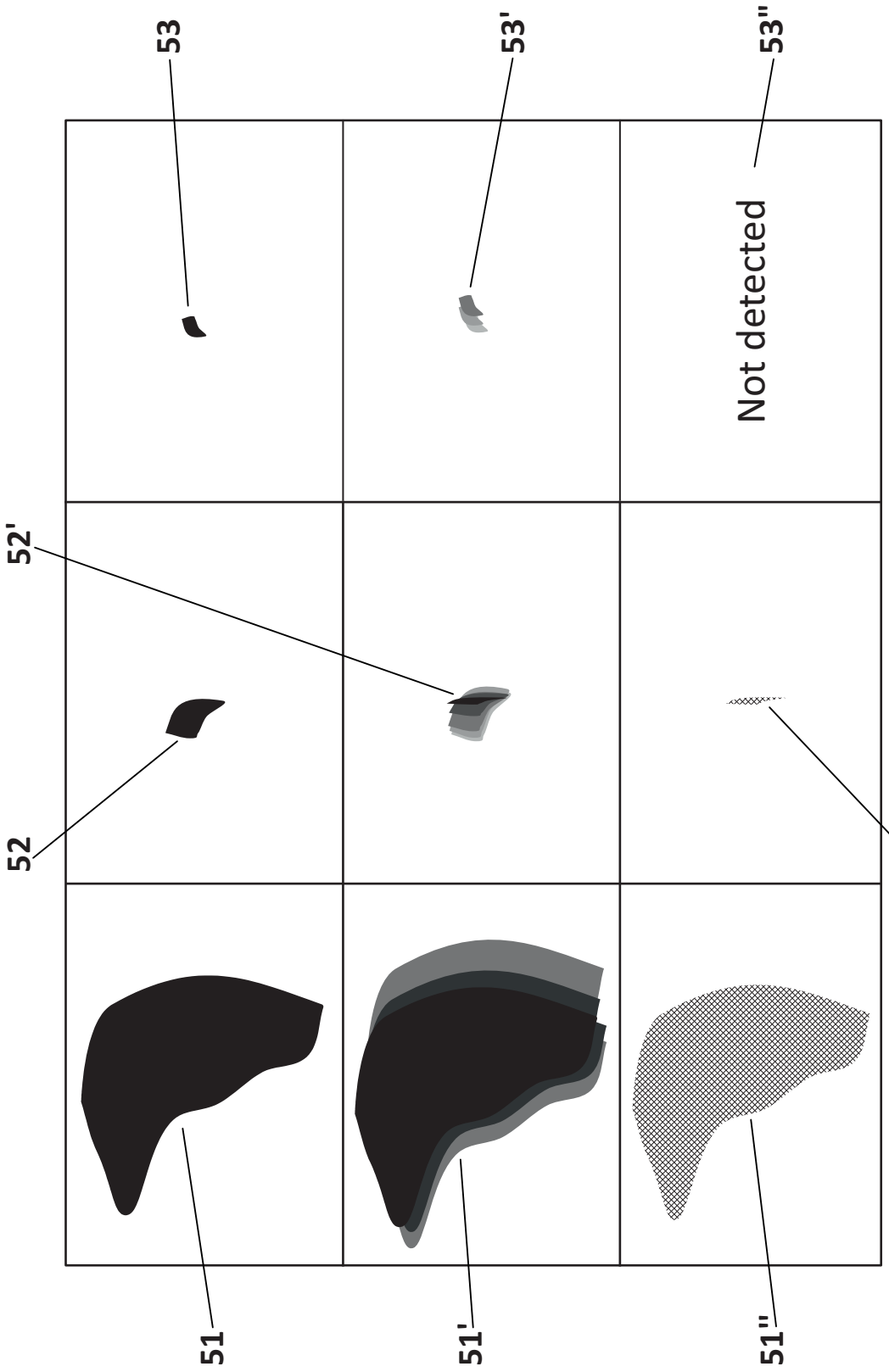

FIG. 5

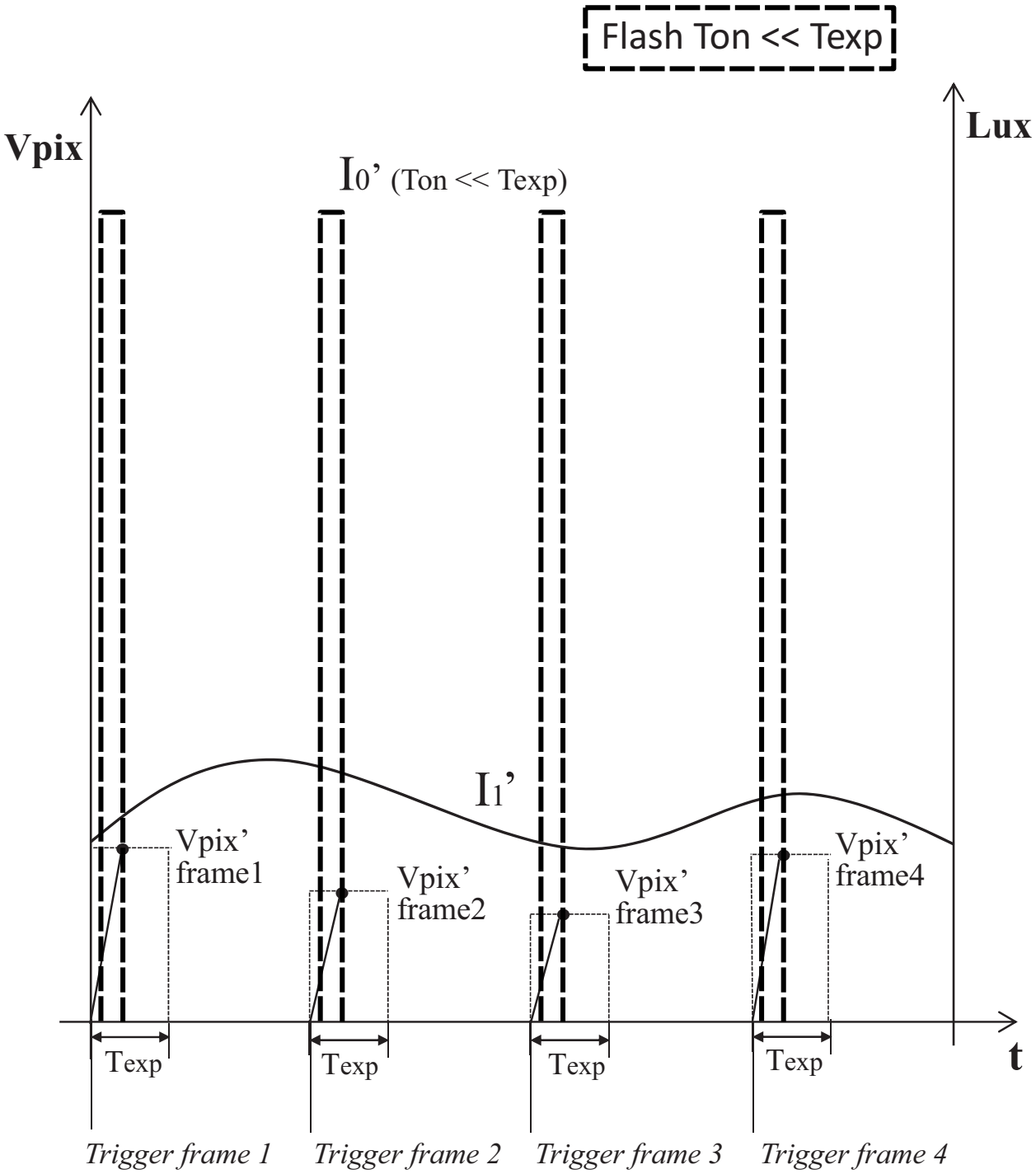
Flash Ton << Texp
Vpix
Lux
I0' (Ton << Texp)
I1'
Vpix' frame1
Vpix' frame2
Vpix' frame3
Vpix' frame4
Texp
Texp
Texp
Texp
t
Trigger frame 1
Trigger frame 2
Trigger frame 3
Trigger frame 4

FIG. 6

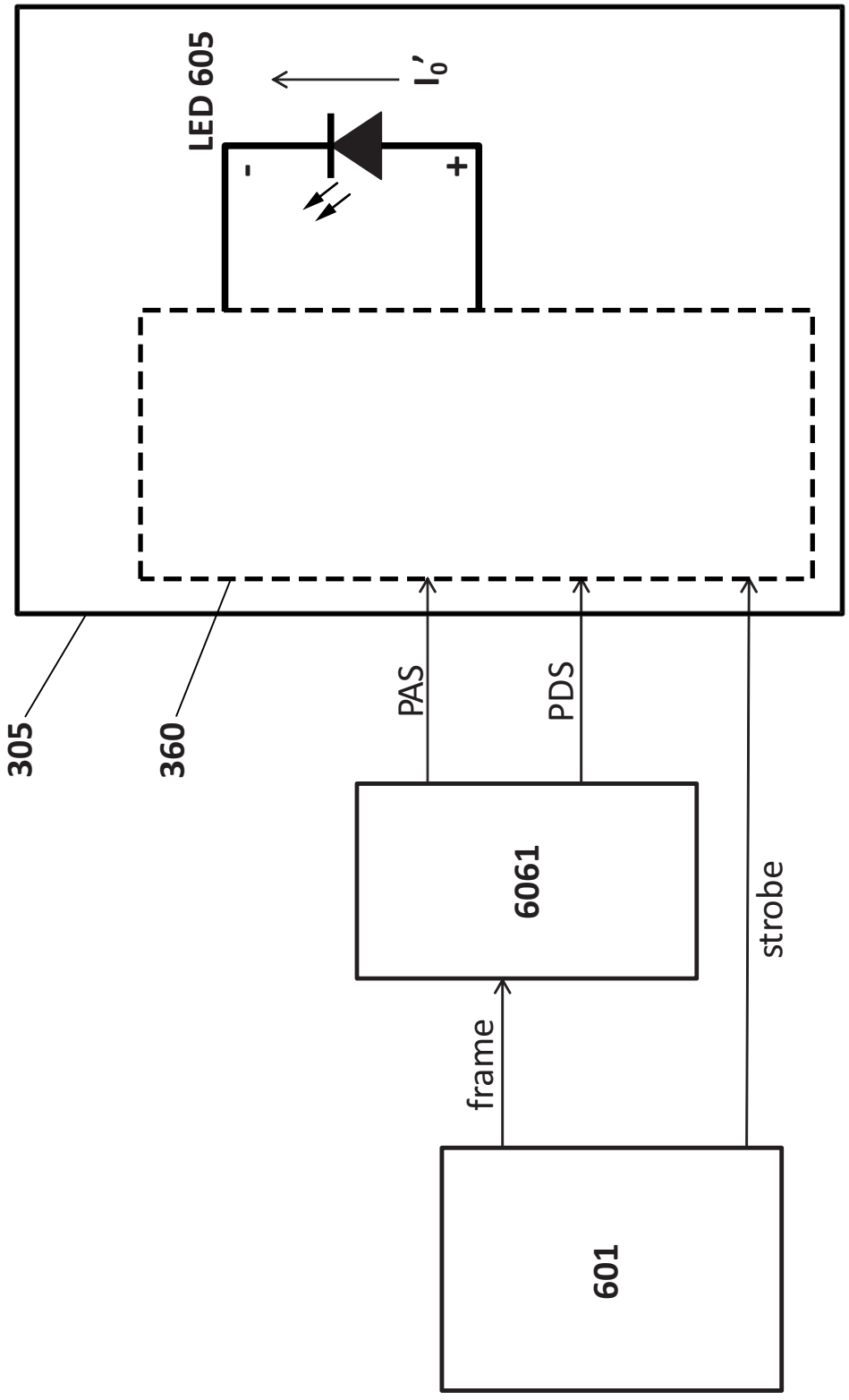

FIG. 7

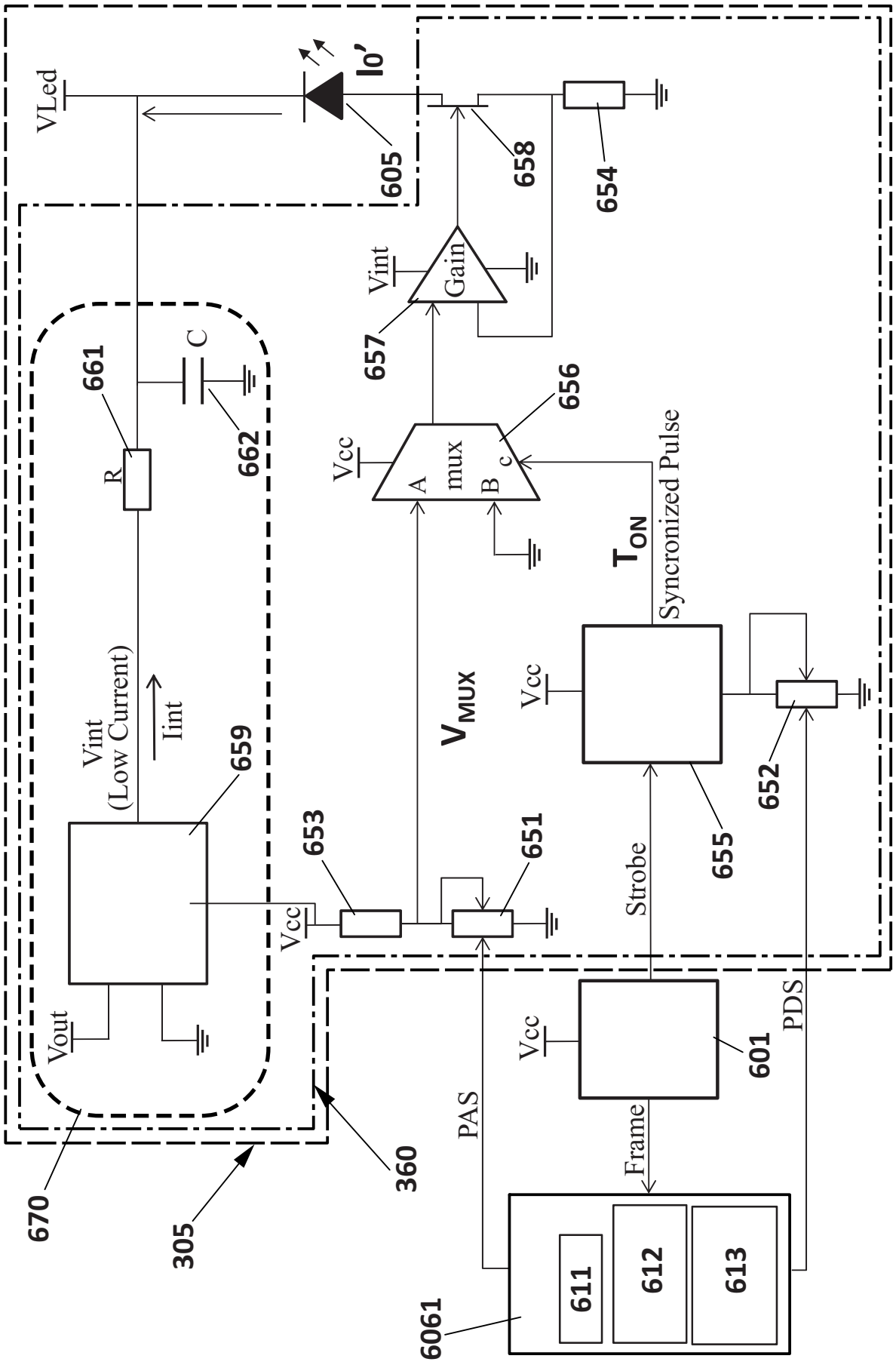
VLed
Io'
605
658
654
Vint
Gain
657
661
C
662
R
656
Vcc
A
mux
B
c
Syncronized Pulse
T_{ON}
Vint
(Low Current)
Iint
659
V_{MUX}
Vcc
652
653
651
Strobe
655
Vcc
601
PDS
Vout
PAS
Frame
360
670
305
6061
611
612
613

FIG. 8

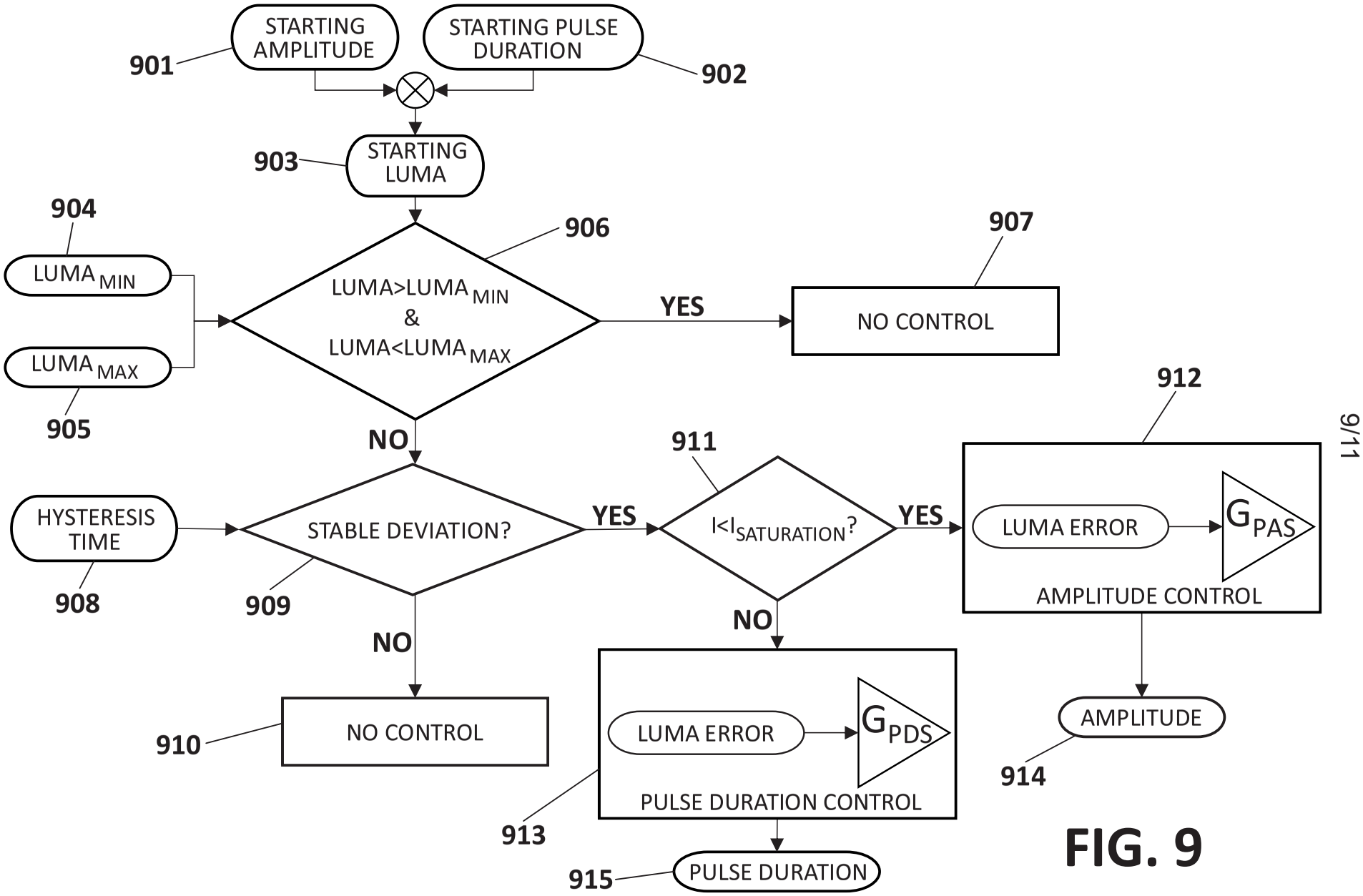
STARTING AMPLITUDE
STARTING PULSE DURATION
901
902
STARTING LUMA
903
904
LUMA MIN
LUMA MAX
905
906
LUMA>LUMA MIN & LUMA<LUMA MAX
YES
907
NO CONTROL
NO
HYSTERESIS TIME
908
STABLE DEVIATION?
909
YES
911
I<I SATURATION?
YES
912
LUMA ERROR
G PAS
AMPLITUDE CONTROL
NO
NO
910
NO CONTROL
LUMA ERROR
G PDS
PULSE DURATION CONTROL
913
AMPLITUDE
914
PULSE DURATION
915

FIG. 9

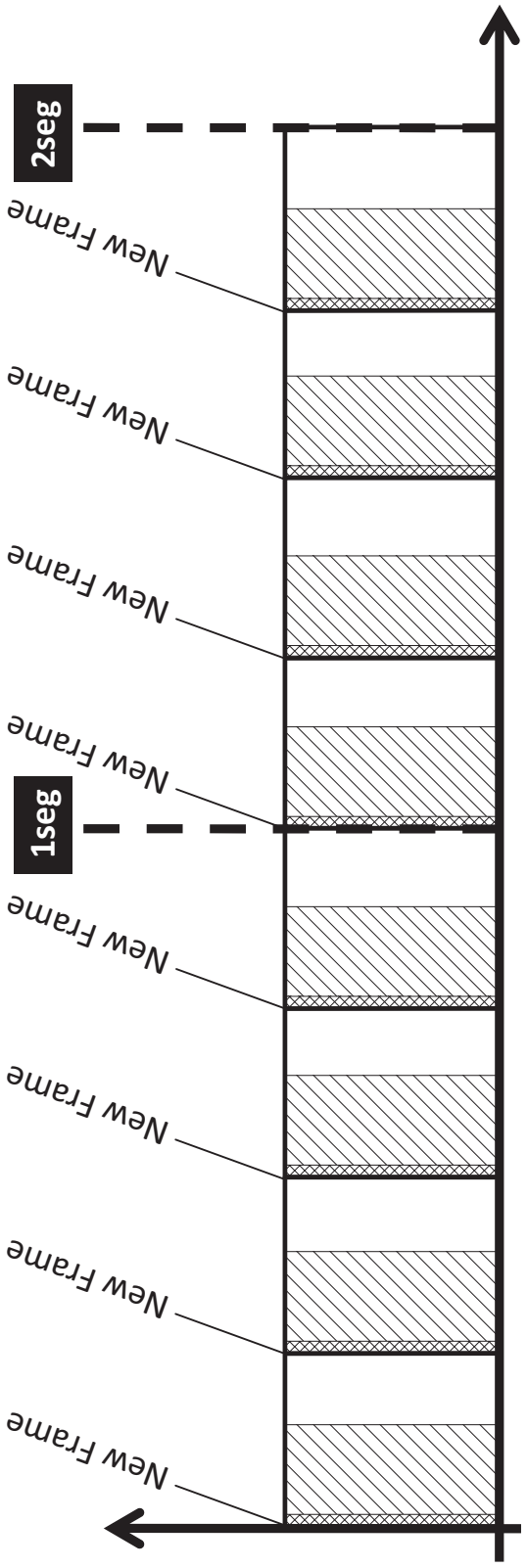
2seg
1seg
New Frame
New Frame
New Frame
New Frame
New Frame
New Frame
New Frame
New Frame
Video at 4 FPS
Tframe = 250 ms
Texp = 150 ms
Ton = 1 µs

FIG. 10

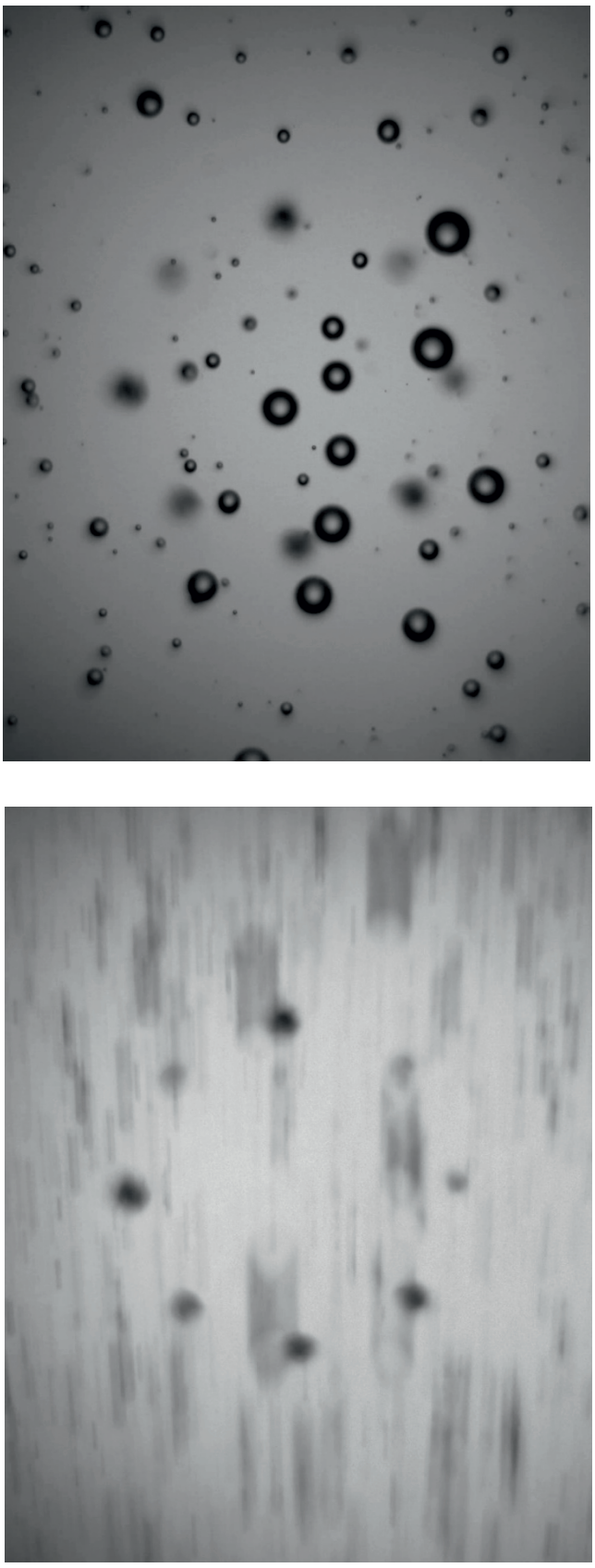

FIG. 11

MINISTERIO
DE INDUSTRIA, ENERGÍA
Y TURISMO

Oficina Española
de Patentes y Marcas

Justificante de presentación electrónica de solicitud de patente

Este documento es un justificante de que se ha recibido una solicitud española de patente por vía electrónica utilizando la conexión segura de la O.E.P.M. De acuerdo con lo dispuesto en el art. 16.1 del Reglamento de ejecución de la Ley 24/2015 de Patentes, se han asignado a su solicitud un número de expediente y una fecha de recepción de forma automática. La fecha de presentación de la solicitud a la que se refiere el art. 24 de la Ley le será comunicada posteriormente.

Número de solicitud:	P201730848	
Fecha de recepción:	27 June 2017, 17:14 (CEST)	
Oficina receptora:	OEPM Madrid	
Su referencia:	P170847ES	
Solicitante:	FUNDACIÓN TEKNIKER	
Número de solicitantes:	1	
País:	ES	
Título:	SISTEMA Y MÉTODO DE MONITORIZACIÓN DEL ESTADO DE UN FLUIDO	
Documentos enviados:	Descripcion.pdf (23 p.) Reivindicaciones.pdf (3 p.) Dibujos.pdf (8 p.) Resumen.pdf (1 p.) OLF-ARCHIVE.zip FEERCPT-1.pdf (3 p.)	package-data.xml es-request.xml application-body.xml es-fee-sheet.xml feesheet.pdf request.pdf
Enviados por:	CN=VALLEJO LOPEZ JUAN PEDRO - 33501382L,givenName=JUAN PEDRO,SN=VALLEJO LOPEZ,serialNumber=33501382L,C=ES	
Fecha y hora de recepción:	27 June 2017, 17:14 (CEST)	
Codificación del envío:	9A:CC:20:63:D8:8A:2E:C7:7A:58:74:4C:63:6E:DF:46:9D:03:71:D8	

AVISO IMPORTANTE

Las tasas pagaderas al solicitar y durante la tramitación de una patente o un modelo de utilidad son las que se recogen en el Apartado "Tasas y precios públicos" de la página web de la OEPM (http://www.oepm.es/es/propiedad_industrial/tasas/). Consecuentemente, si recibe una comunicación informándole de la necesidad de hacer un pago por la inscripción de su patente o su modelo de utilidad en un "registro central" o en un "registro de internet" posiblemente se trate de un fraude.

La anotación en este tipo de autodenominados "registros" no despliega ningún tipo de eficacia jurídica ni tiene carácter oficial.

En estos casos le aconsejamos que se ponga en contacto con la Oficina Española de Patentes y Marcas en el correo electrónico informacion@oepm.es.

ADVERTENCIA: POR DISPOSICIÓN LEGAL LOS DATOS CONTENIDOS EN ESTA SOLICITUD PODRÁN SER PUBLICADOS EN EL BOLETÍN OFICIAL DE LA PROPIEDAD INDUSTRIAL E INSCRITOS EN EL REGISTRO DE PATENTES DE LA OEPM, SIENDO AMBAS BASES DE DATOS DE CARÁCTER PÚBLICO Y ACCESIBLES VÍA REDES MUNDIALES DE INFORMÁTICA.

Para cualquier aclaración puede contactar con la O.E.P.M.

/Madrid, Oficina Receptora/

MINISTERIO
DE INDUSTRIA, ENERGÍA
Y TURISMO

Oficina Española
de Patentes y Marcas

(1) MODALIDAD: **PATENTE DE INVENCIÓN** **MODELO DE UTILIDAD**	 [✓] [ ]
(2) TIPO DE SOLICITUD: PRIMERA PRESENTACIÓN SOLICITUD DIVISIONAL CAMBIO DE MODALIDAD TRANSFORMACIÓN SOLICITUD PATENTE EUROPEA PCT: ENTRADA FASE NACIONAL	 [✓] [ ] [ ] [ ] [ ]
(3) EXP. PRINCIPAL O DE ORIGEN: MODALIDAD: N.º SOLICITUD: FECHA SOLICITUD:	
4) LUGAR DE PRESENTACIÓN:	OEPM, Presentación Electrónica
(5-1) SOLICITANTE 1: DENOMINACIÓN SOCIAL: UNIVERSIDAD PÚBLICA NACIONALIDAD: CÓDIGO PAÍS: NIF/NIE/PASAPORTE: CNAE: PYME: DOMICILIO: LOCALIDAD: PROVINCIA: CÓDIGO POSTAL: PAÍS RESIDENCIA: CÓDIGO PAÍS: TELÉFONO: FAX: CORREO ELECTRÓNICO: EMPRENDEDOR: PERSONA DE CONTACTO: MODO DE OBTENCIÓN DEL DERECHO: INVENCIÓN LABORAL: CONTRATO: SUCESIÓN: PORCENTAJE DE TITULARIDAD:	 FUNDACIÓN TEKNIKER [ ] España ES G20545729 Polo tecnológico de Eibar, c/ Iñaki Goenaga 5 Eibar 20 Guipúzcoa 20600 España ES [ ] [✓] [ ] [ ] 100,00 %
(6-1) INVENTOR 1: APELLIDOS: NOMBRE: NACIONALIDAD: CÓDIGO PAÍS: NIF/NIE/PASAPORTE: DOMICILIO: LOCALIDAD: PROVINCIA: CÓDIGO POSTAL: PAÍS RESIDENCIA: CÓDIGO PAÍS:	 MABE ÁLVAREZ Jon España ES 30678164-M Polo tecnológico de Eibar, c/ Iñaki Goenaga 5 Eibar 20 Guipúzcoa 20600 España ES

TELÉFONO:	
FAX:	
CORREO ELECTRÓNICO:	
EL INVENTOR RENUNCIA A SER MENCIONADO:	[ ]
(6-2) INVENTOR 2:	
APELLIDOS:	LÓPEZ ALONSO
NOMBRE:	Patricia
NACIONALIDAD:	España
CÓDIGO PAÍS:	ES
NIF/NIE/PASAPORTE:	78879606-W
DOMICILIO:	Polo tecnológico de Eibar, c/ Iñaki Goenaga 5
LOCALIDAD:	Eibar
PROVINCIA:	20 Guipúzcoa
CÓDIGO POSTAL:	20600
PAÍS RESIDENCIA:	España
CÓDIGO PAÍS:	ES
TELÉFONO:	
FAX:	
CORREO ELECTRÓNICO:	
EL INVENTOR RENUNCIA A SER MENCIONADO:	[ ]
(6-3) INVENTOR 3:	
APELLIDOS:	DELGADO CASTRILLO
NOMBRE:	Andoni
NACIONALIDAD:	España
CÓDIGO PAÍS:	ES
NIF/NIE/PASAPORTE:	78886562-N
DOMICILIO:	Polo tecnológico de Eibar, c/ Iñaki Goenaga 5
LOCALIDAD:	Eibar
PROVINCIA:	20 Guipúzcoa
CÓDIGO POSTAL:	20600
PAÍS RESIDENCIA:	España
CÓDIGO PAÍS:	ES
TELÉFONO:	
FAX:	
CORREO ELECTRÓNICO:	
EL INVENTOR RENUNCIA A SER MENCIONADO:	[ ]
(6-4) INVENTOR 4:	
APELLIDOS:	ITURBE BERISTAIN
NOMBRE:	Ion
NACIONALIDAD:	España
CÓDIGO PAÍS:	ES
NIF/NIE/PASAPORTE:	15386217-E
DOMICILIO:	Polo tecnológico de Eibar, c/ Iñaki Goenaga 5
LOCALIDAD:	Eibar
PROVINCIA:	20 Guipúzcoa
CÓDIGO POSTAL:	20600
PAÍS RESIDENCIA:	España
CÓDIGO PAÍS:	ES
TELÉFONO:	
FAX:	
CORREO ELECTRÓNICO:	
EL INVENTOR RENUNCIA A SER MENCIONADO:	[ ]
(7) TÍTULO DE LA INVENCIÓN:	SISTEMA Y MÉTODO DE MONITORIZACIÓN DEL ESTADO DE UN FLUIDO
(8) NÚMERO DE INFORME TECNOLÓGICO DE PATENTES (ITP):	P

(9) SOLICITA LA INCLUSIÓN EN EL PROCEDIMIENTO ACELERADO DE CONCESIÓN	
SI	[ ]
NO	[✓]
(10) EFECTUADO DEPÓSITO DE MATERÍA BIOLÓGICA:	
SI	[ ]
NO	[✓]
(11) DEPÓSITO:	
REFERENCIA DE IDENTIFICACIÓN:	
INSTITUCIÓN DE DEPÓSITO:	
NÚMERO DE DEPÓSITO:	
ORÍGEN BIOLÓGICO:	
(12) RECURSO GENÉTICO:	
NÚMERO DE REGISTRO:	
NÚMERO DE CERTIFICADO DE ACCESO AL RECURSO:	
UTILIZACIÓN DEL RECURSO GENÉTICO:	
CONOCIMIENTO TRADICIONAL ASOCIADO A UN RECURSO GENÉTICO:	
(13) DECLARACIONES RELATIVAS A LA LISTA DE SECUENCIAS:	
LA LISTA DE SECUENCIAS NO VA MÁS ALLÁ DEL CONTENIDO DE LA SOLICITUD	[ ]
LA LISTA DE SECUENCIAS EN FORMATO PDF Y ASCII SON IDENTICOS	[ ]
(14) EXPOSICIONES OFICIALES:	
NOMBRE:	
LUGAR:	
FECHA:	
(15) DECLARACIONES DE PRIORIDAD:	
PAÍS DE ORIGEN:	
CÓDIGO PAÍS:	
NÚMERO:	
FECHA:	
(16) REMISIÓN A UNA SOLICITUD ANTERIOR:	
PAÍS DE ORIGEN:	
CÓDIGO PAÍS:	
NÚMERO:	
FECHA:	
(17) AGENTE DE PROPIEDAD INDUSTRIAL:	
APELLIDOS:	VALLEJO LÓPEZ
NOMBRE:	Juan Pedro
CÓDIGO DE AGENTE:	0994/6
NÚMERO DE PODER:	
(18) DIRECCIÓN A EFECTOS DE COMUNICACIONES: SÓLO EN CASO DE DIRECCIÓN DIFERENTE DE LA INDICADA PARA EL PRIMER SOLICITANTE	
DOMICILIO:	
LOCALIDAD:	
PROVINCIA:	
CÓDIGO POSTAL:	
PAÍS RESIDENCIA:	
CÓDIGO PAÍS:	
TELÉFONO:	
FAX:	
CORREO ELECTRÓNICO:	
MEDIO PREFERENTE DE COMUNICACIÓN	
(19) RELACIÓN DE DOCUMENTOS QUE SE ACOMPAÑAN:	
DESCRIPCIÓN:	[✓] N.º de páginas: 23
REIVINDICACIONES:	[✓] N.º de reivindicaciones: 16
DIBUJOS:	[✓] N.º de dibujos: 8
RESUMEN:	[✓] N.º de páginas: 1
FIGURA(S) A PUBLICAR CON EL RESUMEN:	[✓] N.º de figura(s): 2A
ARCHIVO DE PRECONVERSION:	[✓]
DOCUMENTO DE REPRESENTACIÓN:	[ ] N.º de páginas:

JUSTIFICANTE DE PAGO (1): LISTA DE SECUENCIAS PDF: ARCHIVO PARA LA BUSQUEDA DE LS: OTROS (Aparecerán detallados):	[✓] N.º de páginas: 3 [ ] N.º de páginas: [ ]
(20) EL SOLICITANTE SE ACOGE A LA REDUCCIÓN DE TASAS PARA EMPRENDEDORES PREVISTA EN EL ART. 186 DE LA LEY 24/2015 DE PATENTES Y, A TAL EFECTO, APORTA LA SIGUIENTE DOCUMENTACIÓN ADJUNTA:	[ ]
(21) NOTAS:	
(22) FIRMA: FIRMA DEL SOLICITANTE O REPRESENTANTE: LUGAR DE FIRMA: FECHA DE FIRMA:	 VALLEJO LOPEZ JUAN PEDRO - 33501382L MADRID 27 Junio 2017

MINISTERIO
DE INDUSTRIA, ENERGÍA
Y TURISMO

Oficina Española
de Patentes y Marcas

OFICINA ESPAÑOLA DE PATENTES Y MARCAS

Hoja informativa sobre pago de tasas de una solicitud de patente o modelo de utilidad

1. REFERENCIA DE SOLICITUD	**P170847ES**	
2. TASAS	**Importe (en euros)**	
Concepto	**Código de barras asignado**	**Importe**
IE01 - Solicitud de demanda de depósito o de rehabilitación.	88160368957	85,32
IE02 - Solicitud de cambio de modalidad en la protección		0,00
IE04 - Petición IET	88160369051	581,95
IE06 - Prioridad extranjera (0)		0,00
IE22 - Solicitud de examen sustantivo		0,00
Importe total		667,27
Importe abonado		667,27

Se ha aplicado el 15% de descuento sobre la tasa de solicitud de acuerdo con la D. Adic. 8.2 Ley de Marcas.

MINISTERIO DE INDUSTRIA, ENERGÍA Y TURISMO

Oficina Española de Patentes y Marcas

TASA en materia de Propiedad Industrial
CODIGO 511

Modelo 791

Identificación

Ejercicio: 2017
Nro Justificante: 7915113343286

Sujeto Pasivo

NIF:

Apellidos y Nombre o Razón Social:

Agente o Representante legal

NIF: 33501382L

Apellidos y Nombre o Razón Social: JUAN PEDRO VALLEJO LÓPEZ

Código de Agente o Representante 0994

Autoliquidación

Titular del expediente si es distinto del pagador:

Modalidad Expediente: L Número

Clave: LOTE Año: 2017 Concepto: Lote

Unidades: 2 Importe: 667,27

Este código de barras corresponde al pago global del lote. No utilice este código para justificar el pago de cada una de las tasas individuales, sino el que consta en cada una de las páginas siguientes.

Referencia OEPM: 88160369164

90999210020018816036916 4

Declarante

Fecha: 27/06/17 14:29

Firma: JUAN PEDRO VALLEJO LÓPEZ

Ingreso

Importe en 667,27 Adeudo en ☒

Entidad: 2100

NRC Asignado: 7915113343286Q1B052E64

Modelo 791

(1) Solo cuando el pago se realice con cargo a la cuenta corriente del representante o agente.
(2) En el caso de que tenga asignado un número por la OEPM.
(3) En el caso de patentes europeas, se pondrá una P si es el número de publicación o una S si es el número de solicitud.

MINISTERIO DE INDUSTRIA, ENERGÍA Y TURISMO

Oficina Española de Patentes y Marcas

TASA en materia de Propiedad Industrial
CODIGO 511

Modelo 791

Identificación

Ejercicio: 2017
Nro Justificante: 7915113343286

Sujeto Pasivo

NIF:

Apellidos y Nombre o Razón Social:

Agente o Representante legal

NIF: 33501382L

Apellidos y Nombre o Razón Social: JUAN PEDRO VALLEJO LÓPEZ

Código de Agente o Representante 0994

Autoliquidación

Titular del expediente si es distinto del pagador: FUNDACIÓN TEKNIKER

Modalidad Expediente: P Número Tipo

Clave: IE04 Año: 2017 Concepto: SOLICITUD I.E.T. INTERNET

Unidades: 1 Importe: 581,95

Referencia OEPM: 88160368957

90999210020018816036895 7

Declarante

Fecha: 27/06/17 14:29

Firma: JUAN PEDRO VALLEJO LÓPEZ

Ingreso

Importe en 581,95 Adeudo en ☒

NRC Asignado: 7915113343286000000001

Modelo 791

(1) Solo cuando el pago se realice con cargo a la cuenta corriente del representante o agente.
(2) En el caso de que tenga asignado un número por la OEPM.
(3) En el caso de patentes europeas, se pondrá una P si es el número de publicación o una S si es el número de solicitud.

MINISTERIO DE INDUSTRIA, ENERGÍA Y TURISMO

Oficina Española de Patentes y Marcas

TASA en materia de Propiedad Industrial
CODIGO 511

Modelo 791

Identificación

Ejercicio: 2017
Nro Justificante: 7915113343286

Sujeto Pasivo

NIF:

Apellidos y Nombre o Razón Social:

Agente o Representante legal

NIF: 33501382L

Apellidos y Nombre o Razón Social: JUAN PEDRO VALLEJO LÓPEZ

Código de Agente o Representante 0994

Autoliquidación

Titular del expediente si es distinto del pagador: FUNDACIÓN TEKNIKER

Modalidad Expediente: P Número Tipo

Clave: IE01 Año: 2017 Concepto: SOL. DE INVENCION O REAHABILITACIÓN POR INTERNET

Unidades: 1 Importe: 85,32

Referencia OEPM: 88160369051

90999210020018816036905 1

Declarante

Fecha: 27/06/17 14:29

Firma: JUAN PEDRO VALLEJO LÓPEZ

Ingreso

Importe en 85,32 Adeudo en ☒

NRC Asignado: 7915113343286000000002

Modelo 791

(1) Solo cuando el pago se realice con cargo a la cuenta corriente del representante o agente.
(2) En el caso de que tenga asignado un número por la OEPM.
(3) En el caso de patentes europeas, se pondrá una P si es el número de publicación o una S si es el número de solicitud.

DESCRIPCIÓN

SISTEMA Y MÉTODO DE MONITORIZACIÓN DEL ESTADO DE UN FLUIDO

CAMPO DE LA INVENCIÓN

La presente invención pertenece al campo de los métodos y sistemas de monitorización de fluidos, tales como aceites, y en particular aceites lubricantes, para determinar su estado general (degradación, contenido de partículas, etc.). Más concretamente, la invención pertenece al campo de la medición del estado de fluidos, tales como aceites, por colorimetría o espectroscopia óptica.

ANTECEDENTES DE LA INVENCIÓN

La maquinaria industrial utiliza a menudo fluidos lubricantes para el correcto funcionamiento de los componentes de la máquina en cuestión. Ejemplos de estos fluidos incluyen lubricantes y aceites que pueden estar basados en hidrocarburos, productos sintéticos y/o basados en petróleo, así como fluidos hidráulicos. Estos fluidos deben mantenerse dentro de un intervalo preferido de composición y limpieza para un rendimiento eficiente de la máquina. Por ejemplo, la adición no deseada de agua o residuos puede hacer que la máquina pierda eficiencia o sufra daños. Es decir, la maquinaria industrial sufre a menudo fallos o interrupciones imprevistas ocasionados por problemas asociados a la lubricación. Estos fallos o interrupciones pueden reducir la vida de servicio de la maquinaria, así como costos innecesarios de mantenimiento. Es por tanto necesario supervisar el fluido (normalmente, aceite) utilizado para la lubricación y determinar el estado de dicho fluido.

Una forma convencional de supervisión del estado del aceite lubricante es mediante medición “off-line”, es decir, mediante análisis de muestras de aceite en laboratorio. Sin embargo, las técnicas “off-line” no proporcionan una detección suficientemente temprana del proceso de degradación debido a que no se realizan con suficiente frecuencia debido a su vez al esfuerzo humano y material que la toma y análisis de estas muestras requiere. Por ejemplo, es frecuente que al tomar la muestra el lubricante se mezcle con sedimento, complicando el control del aceite. También puede ocurrir que el muestreo requiera que la máquina se detenga o incluso se vacíe de lubricante, causando una pérdida de producción de la máquina.

Para superar los inconvenientes inherentes a las técnicas de análisis “off-line”, se han desarrollado técnicas “on-line” para analizar el estado del fluido en cuestión durante su propio funcionamiento, en movimiento, sin necesidad de extraer muestras del mismo para su análisis posterior y sin pérdida temporal de producción. Por ejemplo, la patente española ES2455465B1 describe un sistema para la inspección de la degradación de un fluido lubricante “on-line” en una celda de medida mediante un sensor óptico. Para la inspección “on-line”, el sistema necesita elementos externos de control de flujo para detener el fluido, desairear la celda de medida y asegurar que la muestra de fluido no presenta burbujas. Además, este sistema requiere una diferencia de presión entre la entrada y la salida del sensor, lo que limita su uso a configuraciones e instalaciones en bypass.

En otro ejemplo, la solicitud de patente internacional WO2012032197A1 describe un sistema para conocer la degradación de un aceite a partir de un análisis de sus características de absorción espectral. Este sistema también requiere ser instalado en bypass en un sistema de lubricación, inmerso en el fluido bajo inspección.

Sin embargo, existen escenarios en los que no es posible realizar una monitorización en modo bypass. Tal es el caso, por ejemplo, de entornos con poco espacio de medida, tales como sistemas de retro-fitting, no diseñados para ser instrumentados con sensores. O entornos en los que, como mucho, existe un único punto de toma de muestra. Ejemplos de este tipo son algunos sistemas mecatrónicos lubricados, tales como robots y grúas. Muchos de estos sistemas requieren la monitorización de miles de puntos de interés en una planta. Por ejemplo, en una planta de producción de automóviles, cada uno de los muchos robots tiene dos o tres sistemas hidráulicos a monitorizar. O, en una planta de montaje de automoción, cada articulación de cada robot (de los que puede haber miles) incorpora un sistema de engranajes que a su vez incorpora su propio microsistema de lubricación (de un litro de aceite aproximadamente). Para monitorizar un sistema de tal magnitud, es deseable poder utilizar sistemas de bajo coste que proporcionen recogida automática de datos de interés. En suma, en ocasiones es deseable poder realizar el análisis de un fluido en una toma simple, es decir, que no requieran una diferencia de presión.

Por otra parte, un sistema convencional de monitorización del grado de degradación de un fluido (por ejemplo, un aceite lubricante) se basa en iluminar el fluido con una fuente de luz y observar la luz que se transmite a traves de él. Según el estado del fluido (típicamente más oscuro cuanto más degradado el fluido), la luz transmitida varía.

Utilizando diversas técnicas e implementaciones (luz visible o no visible, análisis espectral o de intensidad, etc.) se puede conseguir información más o menos detallada del estado del fluido. Sin embargo, al trabajar en transmisión, cuando el fluido es o se vuelve muy oscuro, la luz trasmitida es tan escasa que no es posible realizar la medida adecuadamente. Este es el caso de los fluidos lubricantes, que experimentan debido a su uso como lubricantes un cambio sustancial en su color. Por ello, se ha observado que, si bien los dispositivos on-line de monitorización de aceites basados en el principio de transmitancia (es decir, que trabajan en modo transmisión), son efectivos cuando el aceite bajo supervisión es muy translúcido (es decir, normalmente al principio de su uso, cuando el aceite está relativamente limpio), estos dispositivos de monitorización pierden efectividad a medida que el aceite se vuelve opaco por su uso continuado. Un ejemplo de estos sistemas que trabajan en transmitancia es el de la citada patente ES2455465B1. Sería posible realizar las mismas medidas analizando la luz reflejada de manera difusa en lugar de analizar la luz transmitida por el fluido. Sin embargo, en este caso, en lugar de tener el problema con fluidos oscuros, el problema surge con fluidos claros o traslúcidos, que no reflejan, de manera difusa, sufciente luz como para tener una medida adecuada.

La solicitud de patente internacional WO2016/080824A1 propone un sistema para monitorizar la dinámica del color de un fluido, formado por una sonda sumergible en el fluido bajo análisis. La sonda está acoplada a una videocámara para capturar imágenes de la muestra de fluido. El sistema utiliza dos fuentes de luz: una fuente de luz en el plano de la videocámara (sistema de iluminación frontal) para trabajar en modo de reflexión difusa para la supervisión de muestras opacas; y una fuente de luz enfrentada a la videocámara (sistema de iluminación a contraluz) para trabajar en modo de transmisión para la supervisión de muestras transparentes o traslúcidas. Este sistema es complejo, por requerir dos emisores de luz, además de frágil, por incorporar una de las fuentes de luz en la parte del dispositivo más expuesta a la presión del fluido bajo análisis. Además, el sistema está diseñado para introducirse en el recipiente que alberga el fluido de forma perpendicular al mismo, y por tanto perpendicular a la evacuación de aire por desaireación, por lo que se dificulta dicha evacuación y por tanto se dificulta el movimiento de fluido en la zona de inspección, impidiéndose así la renovación de las muestras bajo análisis.

DESCRIPCIÓN DE LA INVENCIÓN

La presente invención proporciona un sistema para la monitorización de un fluido en una toma simple, es decir, sin requerir una diferencia de presión entre dos puntos de acceso al fluido bajo análisis, que resuelve los inconvenientes de propuestas anteriores. El sistema de la invención facilita el análisis de un fluido en tanque de forma muy compacta y de bajo coste. Con respecto a los sistemas que realizan medidas en transmitancia (propuesta por ejemplo de la patente ES2455465B1), el sistema de la presente divulgación supone una evolución a un sistema de reflexión/transmisión, facilitando la medida tanto en fluidos opacos como en fluidos traslúcidos o transparentes, pero minimizando la implementación de elementos ópticos activos, concretamente de emisores de luz, tanto en número como en disposición. Esto permite monitorizar con mayor resolución –y a la vez con sencillez de diseño- tanto fluidos que desde su estado limpio inicial son opacos (es decir, cuya absorbancia en dicha longitud de onda es mayor de 1,0, como mayor de 2,0 o mayor de 3,0), como fluidos que en su vida útil pasan de ser traslúcidos (es decir, cuya absorbancia en una cierta longitud de onda es menor de 1,0, tal como menor de 0,5, o menor de 0,2 o menor de 0,1) a opaco (es decir, cuya absorbancia en dicha longitud de onda es mayor de 1,0, como mayor de 2,0 o mayor de 3,0). Se ofrece así una solución compacta, simple y autónoma para la monitorización de fluidos sin necesidad de extraer muestras del mismo de su entorno de operación.

El sistema propuesto presenta además una configurabilidad que permite adaptarse a distintas tipologías y/o estado de degradación del fluido bajo supervisión, seleccionando una u otra implementación para su tapa trasera (plano trasero).

En el contexto de la presente divulgación, se entiende por fluidos opacos aquellos que presentan una absorbancia en una determinada banda espectral mayor de 1,0. A partir de una absorbancia en la banda espectral de trabajo mayor de 3,0 un fluido se considera muy opaco. Asimismo, se entiende por fluidos traslúcidos aquellos que presentan una absorbancia en una determinada banda espectral menor de 1,0, y muy traslúcidos si su absorbancia es menor de 0,1. En general, la luz no penetra en los fluidos opacos, sino que se absorbe en una profundidad cercana a la superficie y la parte que no es absorbida puede salir otra vez de la muestra en forma de reflexión difusa debido al scattering (dispersión) producido por las reflexiones internas en el fluido en las moléculas que lo forman o partículas que pueda haber. La figura 8 ilustra estos fenómenos. Este efecto tiene más posibilidades de existir en fluidos opacos que en traslúcidos, pero depende fuertemente de la absorbancia y de la composición molecular y de las partículas presentes en el mismo. Independientemente del scattering, en términos generales, a mayor absorbancia, menor es la cantidad de luz que atraviesa el fluido propagándose a

través del mismo. En el caso de los fluidos traslúcidos, en general, la luz atraviesa (se transmite) a través del mismo.

En un primer aspecto de la invención, se proporciona un sistema de monitorización para la inspección de un fluido contenido en un depósito mediante la inserción de dicho sistema de monitorización en una toma de dicho depósito, que comprende: una zona de medida configurada para que circule por ella una muestra de dicho fluido. El sistema de monitorización comprende además: unos medios de emisión/recepción de luz que consisten en un sistema de iluminación y un sistema detector de luz situados en un mismo lado del sistema de monitorización con respecto a dicha zona de medida; una ventana óptica dispuesta entre dichos medios de emisión/recepción de luz y dicha zona de medida; y un elemento óptico trasero situado al otro lado del sistema de monitorización con respecto a dicha zona de medida. El sistema de iluminación está configurado para emitir radiación óptica hacia dicha zona de medida. El sistema detector de luz está configurado para detectar una radiación óptica que comprende la luz reflejada por dicho fluido que circula por dicha zona de medida y/o la luz transmitida a través de dicho fluido y reflejada en dicho elemento óptico trasero. El sistema de monitorización comprende además un subsistema electrónico que comprende medios de procesado configurados para controlar la activación/desactivación del sistema de iluminación y para procesar las señales obtenidas procedentes del sistema detector de luz.

En realizaciones de la invención, el elemento óptico trasero se implementa mediante un elemento absorbente desde el punto de vista óptico, estando dicho elemento óptico trasero configurado para impedir la reflexión de la luz transmitida a través de dicho fluido.

En realizaciones de la invención, el elemento óptico trasero se implementa mediante un elemento reflexivo desde el punto de vista óptico, estando dicho elemento óptico trasero configurado para favorecer la reflexión de la luz transmitida a través de dicho fluido. Este elemento reflexivo desde el punto de vista óptico puede ser un elemento reflexivo plano. Alternativamente, el elemento reflexivo desde el punto de vista óptico puede ser un elemento reflexivo cóncavo, con el objeto de concentrar los rayos reflejados.

En realizaciones de la invención, el elemento óptico trasero es intercambiable, de forma que en función de la absorbancia del fluido bajo inspección, se elige un elemento óptico trasero absorbente o reflexivo.

En realizaciones de la invención, el sistema de monitorización comprende además al menos un fotodiodo de control configurado para medir la intensidad emitida por el sistema de iluminación.

En realizaciones de la invención, el sistema de monitorización está comprendido en una carcasa, en la que dichos medios de emisión/recepción de luz están situados en una porción de dicha carcasa y dicho elemento óptico trasero está situado en otra porción de dicha carcasa, donde dichas porciones de carcasa definen dicha zona de medida, delimitando dicho elemento óptico trasero y dicha ventana óptica la zona de medida.

En realizaciones de la invención, la altura de dicha zona de medida es regulable para garantizar la renovación de la muestra de fluido dentro de dicha zona de medida.

En realizaciones de la invención, la ventana óptica tiene una inclinación con respecto al plano definido por elemento óptico trasero para evitar la acumulación de aire en la zona de medida.

En realizaciones de la invención, el sistema de monitorización comprende un difusor dispuesto entre dicho sistema de iluminación de dichos medios de emisión/recepción de luz y dicho al menos un fotodiodo de control.

En otro aspecto de la invención, se proporciona un método de monitorización de un fluido contenido en un depósito, que comprende: insertar un sistema de monitorización en una toma simple de dicho depósito, donde dicho sistema de monitorización comprende: una zona de medida configurada para que circule por ella una muestra de dicho fluido; unos medios de emisión/recepción de luz que consisten en un sistema de iluminación y un sistema detector de luz situados en un mismo lado del sistema de monitorización con respecto a dicha zona de medida; una ventana óptica dispuesta entre dichos medios de emisión/recepción de luz y dicha zona de medida; y un elemento óptico trasero situado al otro lado del sistema de monitorización con respecto a dicha zona de medida; hacer incidir una radiación óptica desde dicho sistema de iluminación hacia dicha zona de medida; detectar por dicho sistema detector de luz una radiación óptica que comprende la luz reflejada por dicho fluido que circula por dicha zona de medida y/o la luz transmitida a través de dicho fluido y reflejada en dicho elemento óptico trasero; en un subsistema electrónico comprendido en dicho sistema de monitorización, controlar la activación/desactivación del sistema de iluminación y procesar las señales obtenidas procedentes del sistema detector de luz.

En realizaciones de la invención, cuando dicho fluido tiene una absorbancia mayor de 1,0 en su estado inicial, dicho elemento óptico trasero es un elemento óptico trasero absorbente.

En realizaciones de la invención, cuando dicho fluido tiene una absorbancia menor de 1,0 en su estado inicial, dicho elemento óptico trasero es un elemento óptico trasero reflexivo.

En realizaciones de la invención, el método comprende además regular la altura de dicha zona de medida para garantizar la renovación de la muestra de fluido dentro de dicha zona de medida.

En realizaciones de la invención, el método comprende además inclinar dicha ventana óptica con respecto al plano definido por elemento óptico trasero para evitar la acumulación de aire en la zona de medida.

Ventajas y características adicionales de la invención serán evidentes a partir de la descripción en detalle que sigue y se señalarán en particular en las reivindicaciones adjuntas.

BREVE DESCRIPCIÓN DE LAS FIGURAS

Para complementar la descripción y con objeto de ayudar a una mejor comprensión de las características de la invención, de acuerdo con un ejemplo de realización práctica de la misma, se acompaña como parte integrante de la descripción, un juego de figuras en el que con carácter ilustrativo y no limitativo, se ha representado lo siguiente:

La figura 1A ilustra esquemáticamente un sistema de monitorización de un fluido mediante su inserción en una toma simple de un depósito que contiene dicho fluido, de acuerdo con una posible realización de la invención. Las figuras 1B y 1C muestran sendas vistas (frontal y de perfil, respectivamente) del sistema de monitorización de acuerdo con una posible realización de la invención, en la que puede observarse el canal por el que fluye la muestra bajo inspección. Una parte del fluido contenido en el tanque en el que se acople el sistema de monitorización circula por este canal, en cuyo momento se toman las muestras. La figura 1D muestra una vista en perfil de un sistema de monitorización de acuerdo con otra realización de la invención, en la que puede observarse el canal que se forma en el exterior del mismo, como un estrechamiento de la carcasa que recubre al sistema.

La figura 2A muestra un esquema del sistema de monitorización del estado de un fluido por espectrometría, de acuerdo con una posible realización de la invención. La figura 2B

muestra una posible carcasa en la que se inserta la estructura o soporte en la que se colocan los elementos ópticos y electrónicos del sistema. La figura 2C muestra la electrónica albergada en el interior de la carcasa mostrada en la figura 2B, en cuyo interior pueden observarse los elementos ópticos y electrónicos esquematizados en la figura 2A. La figura 2D muestra en detalle la disposición del sistema detector de luz y de la al menos una fuente de iluminación, ambos del mismo lado o porción del sistema con respecto del canal.

Las figuras 3A-3C esquematizan el recorrido de la radiación óptica emitida por una fuente de iluminación al viajar hacia un fluido (transmitiéndose a través del mismo y/o reflejándose en el volumen cercano a la superficie del mismo y/o en el elemento trasero, en función de ciertos parámetros del fluido y de las características del elemento trasero) y la luz detectada por un sistema detector de luz dispuesto en el mismo plano que la fuente de iluminación.

Las figuras 4A y 4B representan el funcionamiento del sistema de monitorización en modo de operación transmisión/reflexión.

La figura 5 ilustra el problema de la introducción del sistema de monitorización en un depósito de forma totalmente vertical, dificultándose la evacuación de aire en el canal de medida.

La figura 6 muestra un sistema de monitorización con altura del canal de medida variable, de acuerdo con una posible realización de la invención.

La figura 7 muestra un sistema de monitorización cuya ventana óptica está inclinada con respecto al plano definido por la placa trasera, de acuerdo con una posible realización de la invención.

La figura 8 ilustra los fenómenos de transmisión, absorción, scattering y reflexión difusa que pueden tener lugar en un medio en función de las características del mismo en términos de absorbancia, transmitancia y reflectancia. Nótese que se ha obviado el efecto de la reflexión especular.

DESCRIPCIÓN DE UN MODO DE REALIZACIÓN DE LA INVENCIÓN

La figura 1A ilustra un esquema de un posible escenario de aplicación de un sistema de monitorización (o sistema de medida) 3 de un fluido mediante la inserción o acople del sistema de monitorización 3 en una toma estándar (toma simple) 5 de un tanque, tubería,

o en general, depósito 1 en el que se encuentra dicho fluido 2, de acuerdo con una posible realización de la invención. Al sistema de monitorización o medida se le denomina en ocasiones “sensor” a lo largo de la presente divulgación. La monitorización o medida se realiza por espectrometría. El sistema de monitorización 3 de la invención está diseñado para integrarse en un depósito 1, acoplándose al mismo a través de una toma simple, tal como una toma hidráulica estándar, sin necesidad de realizar un bypass mediante conductos o tuberías, que desvíen el fluido para su monitorización. El sistema de monitorización 3 está diseñado para dejarse introducido en el depósito 1, de forma que el sistema 3 pueda tomar medidas del fluido sin necesidad de extraer una muestra de fluido del depósito 1. Aplicando una serie de algoritmos para la interpretación de las medidas tomadas relativas a diversos parámetros, tales como al color del fluido 2, se obtiene información sobre el fluido, por ejemplo sobre su grado de degradación, y por tanto se puede actuar sobre el fluido en cuestión o tomar decisiones basadas por ejemplo en su grado de deterioro. El sistema de monitorización 3 puede tomar medidas periódicas o no periódicas (por ejemplo, a petición). El fluido 2 recogido en el depósito 1 es preferentemente un aceite lubricante industrial.

El sistema de monitorización 3 esquematizado en la figura 1A tiene una serie de elementos optoelectrónicos (no ilustrados en el esquema de la figura 1A) integrados en una carcasa, vaina o encapsulado, que constituye la parte externa del sistema o sensor. Las figuras 1B y 1C representan vistas de frente y perfil, respectivamente, de una posible implementación del sistema de monitorización 3. En ella, la carcasa, vaina o encapsulado tiene una forma que permite el paso del fluido 2 entre cuatro superficies externas 31 32 33 34 de la carcasa. Es decir, el fluido 2 pasa por una zona exterior 20 a la carcasa. Esta zona exterior es una especie de túnel, canal, conducto o zona de medida entre la superficie exterior de una primera porción 35 de la carcasa y la superficie exterior de una segunda porción 36 de la carcasa enfrentada a la primera porción 35 de la carcasa, definiendo ambas porciones el conducto o zona de medida 20 para el fluido. La segunda porción 36 tiene forma de U, definiendo esta forma el canal o zona de medida 20 por el que fluye el fluido cuando el sistema de monitorización 3 se ha acoplado al depósito 1 de fluido 2 bajo supervisión.

La figura 1D representa una vista de perfil de otra posible implementación del sistema de monitorización 3. Como en el caso anterior, la carcasa, vaina o encapsulado del sistema o sensor tiene una forma que permite el paso del fluido 2 entre tres superficies externas 31’ 32’ 33’ de la carcasa. Estas tres superficies 31’ 32’ 33’ definen el canal o zona de medida entre la superficie exterior de una primera porción 35 de la carcasa y la superficie

exterior de una segunda porción 36 de la carcasa enfrentada a la primera porción 35 de la carcasa, definiendo ambas porciones el conducto o zona de medida 20 para el fluido. Es decir, como se aprecia en la figura 1B, la carcasa tiene un determinado grosor, espesor o fondo “z1” en la primera y en la segunda porciones, y experimenta un estrechamiento en su espesor “z2” en una porción intermedia 37 entra las primera y segunda porciones 35 36, de forma que la carcasa queda dividida en dos porciones unidas por una parte estrecha 37 de la carcasa, quedando un hueco o canal 20 por el que fluye el fluido cuando el sistema de monitorización 3 se ha acoplado al depósito 1 de fluido 2 bajo supervisión. Aunque en las figuras 1B-1D la superficie que delimita la zona de medida 20 se ha ilustrado como paredes o superficies planas (31-34, 31’-33’), otras implementaciones de la carcasa podrán realizarse con superficies curvadas, por ejemplo una superficie curvada sustancialmente, en la que por tanto no pueda establecerse una clara diferenciación entre dichas superficies 31-34 o 31’-33’.

En función de la configuración del depósito 1 que recoge el fluido 2 bajo análisis, la toma o acople 5 en el depósito 1, a través de la cual se inserta o acopla el sensor o sistema de monitorización 3 en el depósito 1, puede estar en un lateral del depósito 1, como es el caso de la configuración mostrada en la figura 1A, o puede estar en la parte superior (por ejemplo, tapa) del depósito 1. En el primer caso, el sistema de monitorización 3 se inserta en el depósito 1 de forma oblicua al mismo. En el segundo caso, el sistema de monitorización 3 se inserta en el depósito 1 de forma perpendicular al mismo.

En la figura 2A se ilustra en mayor detalle el sistema de monitorización 13 de acuerdo con una posible implementación de la invención. En relación con esta figura se describen elementos optoelectrónicos del sistema, que se integran o soportan en una estructura que a su vez se inserta en la carcasa, vaina o encapsulado descritos anteriormente. La figura 2B muestra una posible carcasa en la que se inserta la estructura o soporte (mostrada en la figura 2C) en la que se colocan los elementos ópticos y electrónicos del sistema. El sistema de monitorización tiene una parte óptica (subsistema óptico) 140 y una parte electrónica (subsistema electrónico) 150. El subsistema óptico 140 ocupa la segunda porción 136 de la carcasa del sistema y una parte de la primera porción 135 de la carcasa, entendiéndose por primera y segunda porciones las referenciadas como 35, 36 en las figuras 1B-1D anteriores. En concreto, de la primera porción 135 de la carcasa, el subsistema óptico 140 ocupa la parte más próxima al canal externo 120 al sistema de monitorización 13, por el que fluye el fluido bajo supervisión. La figura 2A muestra dicho canal 120. La flecha a lo largo del canal 120 representa el flujo de fluido en el canal 120. El subsistema electrónico 150 ocupa la parte de la primera porción 135 de la carcasa más

alejada al canal 120 definido por la superficie externa de la carcasa (31-34 en la figura 1B, 31'-33' en la figura 1D).

El subsistema óptico 140 está formado, entre otros elementos, por unos medios de emisión/recepción de luz 41. Los medios de emisión/recepción de luz 41 se componen de un sistema de iluminación 411 y un sistema detector de luz 412. El sistema de iluminación 411 está formado por al menos una fuente de iluminación. El sistema detector de luz 412 está formado por uno o más detectores de luz. Los medios de emisión/recepción de luz 41 se encuentran en la primera porción 135 de la carcasa, que es la porción de la carcasa más robusta habida cuenta, por ejemplo, de sus dimensiones, frente a la segunda porción 136 de la carcasa, más expuesta al volumen total del fluido que ocupa el depósito 1 (véase las figuras 1A-1D). A modo de ejemplo, la primera porción 135 de la carcasa puede tener un diámetro que varía entre 25 y 30 mm (milímetros, 10^{-3} metros) y una altura que varía entre 40 y 45 mm, mientras que la segunda porción 136 de la carcasa puede tener un diámetro que varía entre 20 y 25 mm y una altura que varía entre 7 y 12 mm. Es decir, el sistema de iluminación 411 y el sistema detector de luz 412 están situados en un mismo lado con respecto a la zona de medida 20, 120. Ejemplos no limitativos de fuentes de iluminación 411 son uno o más diodos emisores de luz (LED), una o más lámparas de tungsteno (lámpara que comprende tungsteno en sus filamentos), una o más lámparas de luz halógena, una o más lámparas de vapor de mercurio, entre otras. La fuente o fuentes de iluminación 411 puede(n) ser de banda ancha (como es el caso, por ejemplo, de la lámpara halógena), que ofrece espectro estable desde el ultravioleta hasta el infrarrojo lejano o profundo. En una posible implementación, la al menos una fuente de iluminación 411 es uno o más LEDs que emiten luz blanca para iluminar el fluido que fluye por el canal 120. Ejemplos no limitativos de sistemas detectores de luz 412 son detectores de luz ultravioleta (UV), detectores de luz visible (VIS), detectores de luz en el infrarrojo cercano (NIR) y combinaciones de los mismos. En una posible implementación, se utiliza al menos un sensor de color, por ejemplo un sensor de color RGB (configurado para captar la luz visible en la banda del rojo (R, *red*), verde (G, *green*) y azul (B, *blue*)). Con objeto de evitar o minimizar diafonía (más comúnmente conocida como *crosstalk*, por su término en inglés), es decir, que parte de la intensidad emitida por la al menos una fuente de iluminación llegue de vuelta al receptor sin efecto de la muestra, los medios de emisión/recepción de luz 41 pueden incorporar unos medios de apantallamiento 413, implementados por ejemplo como una pared separadora realizada por ejemplo de un material absorbente o de un material reflectante a las longitudes de onda de trabajo, entre la al menos una fuente de iluminación 411 y el

al menos un sistema detector de luz 412.

El sistema detector de luz 412 está preferentemente dispuesto en el mismo plano que la al menos una fuente de iluminación 411 (ambos del mismo lado o porción del sistema con respecto del canal 20, 120), como ilustra la figura 2D. Como se explica más adelante, el sistema detector de luz 412 está configurado para detectar la luz reflejada en una profundidad cercana a la superficie del fluido (reflexión difusa) y para detectar la luz transmitida a través del fluido y reflejada en un elemento óptico trasero que se describe más adelante.

El subsistema óptico 140 puede incluir también uno o más fotodiodos de control 43, configurados para emparejarse a la al menos una fuente de iluminación 411 de los medios de emisión/recepción de luz 41. La función del uno o más fotodiodos de control 43 es medir la intensidad emitida por la al menos una fuente de iluminación 411, para poder controlar dicha intensidad emitida. Al aumentar la temperatura del sistema, la intensidad luminosa emitida por la fuente de iluminación disminuye y, por lo tanto, disminuye la cantidad de luz que incide en la muestra. Esta disminución en la cantidad de luz que incide en la muestra puede llegar a causar que la medida no sea correcta. Para evitar este efecto, preferentemente se implementa un control en lazo cerrado de la potencia de emisión de la fuente de iluminación. Este control en lazo cerrado puede implementarse como sigue: en base a la cantidad de luz recibida en el fotodiodo de control 43, se calcula el valor de intensidad al que hay que encender la fuente de iluminación para conseguir que la intensidad de luz emitida sea la adecuada para realizar la medida. El valor de intensidad adecuado se obtiene mediante un proceso de calibración que se realiza preferentemente en fabricación. En la figura 2A, el ángulo ϕ representa el ángulo de emisión de la fuente de iluminación 411, el ángulo α representa el ángulo de recepción del fotodiodo de control 43 y el ángulo β representa el ángulo de recepción del sistema detector de luz 412. Además, Pd-c(V) se refiere al valor de la medida realizada por el fotodiodo de control 43, RGB(mA) representa el valor de la medida del sistema detector de luz 412 y LED(mA) representa el valor de la corriente a la que se tiene que encender el al menos un emisor de la fuente de iluminación 411. La al menos una fuente de iluminación 411, el al menos un sistema detector de luz 412 y el al menos un fotodiodo de control 43 se controlan desde el subsistema electrónico 150. Por ejemplo, desde el subsistema electrónico 150 se proporciona la corriente necesaria para la alimentación de la al menos una fuente de iluminación 411, en el subsistema electrónico 150 se recibe y procesa la señal detectada por el al menos un sistema detector de luz 412 y se recibe y procesa la señal proporcionada por el fotodiodo de

control 43.

Preferentemente, entre la al menos una fuente de iluminación 411 y el al menos un fotodiodo de control 43 se dispone un difusor 48 cuya misión principal es la difusión de la cantidad de luz emitida por la al menos una fuente de iluminación 411 para conseguir una iluminación homogénea en toda la zona bajo inspección (zona 120 ocupada por el fluido, tal como aceite, bajo análisis). El difusor 48 es de un material sustancialmente transparente a las longitudes de onda de trabajo pero que tiene la función de dispersar la luz. Así, la al menos una fuente de iluminación 411 puede iluminar adecuadamente el fluido que circula por la zona de medida 120. En una posible realización, el difusor 48 es un cristal, por ejemplo un cristal esmerilado.

El subsistema óptico 140 incluye también una ventana óptica 44. En la figura 2B, la referencia 44 se refiere al hueco ocupado por esta ventana óptica 44, que en la figura 2B no se ha ilustrado. Es decir, la superficie de la segunda porción 35, 135 de la carcasa del sensor o sistema de monitorización, que es una de las superficies del sistema que definen el canal 20, 120, y por tanto una de las superficies en contacto con la muestra de fluido que pasa por el canal 20, 120, está sellada herméticamente por una ventana de protección transparente 44 (transparente a la longitud de onda de trabajo). La superficie sellada corresponde con la pared 33 en la figura 1B y con la pared 33' en la figura 1D de la segunda porción 35 de la carcasa del sensor o sistema de monitorización. La fuente de iluminación 411 está orientada hacia el canal 20, 120 por el que fluye el fluido. La ventana de protección transparente 44 se sitúa entre los medios de emisión/recepción de luz 41 y la zona 20, 120 por la que fluye el fluido. En una posible realización, no limitativa, esta ventana de protección transparente 44 se realiza, por ejemplo, de vidrio borosilicato (Vidrio óptico BK7) o de un material plástico, tal como PMMA. A través de esta ventana óptica 44 la luz emitida por la fuente de iluminación 411 viaja hasta el fluido que se encuentra en el hueco, ranura o canal 120. La ventana óptica 44 permite que sustancialmente toda la luz que llega a la misma se transmita por su interior hacia el canal 20, 120.

Al otro lado del canal 120, es decir, en la segunda porción 136 de la carcasa del sistema, se encuentra otro elemento del subsistema óptico 140. Se trata de un elemento óptico trasero o placa trasera 45. Este elemento óptico trasero 45 forma al menos parte de la superficie de la primera porción 36, 136 de la carcasa que define el canal de medida 20, 120. Por ejemplo, en el esquema de la figura 1B, el elemento óptico trasero está integrado en la pared 31, o en el esquema de la figura 1D, el elemento óptico trasero está

integrado en la pared 31'. En función de diversos factores, tales como el tipo de fluido (tal como aceite) empleado o del grado de degradación previsible del fluido bajo análisis, el elemento óptico trasero 45 se diseña de forma que proporcione un cierto (mayor o menor) grado de reflexión. En posibles implementaciones de la invención, el elemento óptico trasero 45 se implementa como una superficie negra, o como un espejo plano o como un espejo cóncavo o parabólico configurado para concentrar los rayos reflejados en el sistema detector de luz 412. Es decir, la región de fluido en la que se realiza la medida está definida por el canal 20, 120, la ventana óptica 44 y el elemento óptico trasero 45.

A su vez, el subsistema electrónico 150 tiene unos medios de procesado 51 para las tareas de activación/desactivación de la iluminación (control de la(s) fuentes de iluminación) y para el procesado y cálculo de las señales obtenidas, procedentes del sistema detector de luz, para obtención de indicadores de degradación de aceite en función de las medidas tomadas. En una posible realización, no limitativa, los medios de procesado 51 se implementan mediante un microcontrolador embebido, programado para realizar dichas tareas de activación/desactivación de iluminación y de cálculo y procesado de señales. Los medios de procesado 51 albergan los siguientes algoritmos (cuyo contenido concreto queda fuera del alcance de la presente invención):

-uno o más algoritmos de control de la iluminación 511, que se encargan de que la intensidad de la luz emitida por la al menos una fuente de iluminación 411 se ajuste a una consigna de iluminación; los parámetros de entrada de este algoritmo son la medida del fotodiodo de control 43 (Pd_c(V)) y una consigna de iluminación, mientras que el parámetro de salida es la corriente que debe aplicarse al sistema de iluminación (Led(mA));

-uno o más algoritmos de cálculo de degradación de aceite 512, diseñados para calcular un indicador de degradación a partir de la lectura RGB realizada en el sistema detector de luz 412; y

-uno o más algoritmos de calibración 513, diseñados para un ajuste de intensidades de trabajo y toma de referencia.

El subsistema electrónico 150 tiene además otros elementos, como drivers de comunicación 52 que permiten al sistema 13 comunicarse con equipos externos para recibir comandos (instrucciones para realizar medidas, realizar calibración, etc.) y para transmitir medidas o resultados del procesado realizado en los medios de procesado 51; fuente de alimentación 53, diseñada para alimentar todos los dispositivos electrónicos del sistema 13; medios de memoria 54, configurados para almacenar resultados de medidas

y parámetros de los algoritmos; y sensor de temperatura 55, para conocer y monitorizar la temperatura del sistema 13.

El sistema de monitorización 13 comprende también medios de conexión, que pueden ser cableados, como por ejemplo el conector 60 mostrado en la figura 2A o el cableado 4 mostrado en la figura 1A, o inalámbricos, para la comunicación con equipos externos o para recibir alimentación externa en caso de que sea necesaria.

En función de las circunstancias, tales como el tipo de sistema industrial bajo monitorización, o del tipo (y por tanto, de la absorbancia y reflectancia) de fluido –preferentemente aceite lubricante- que se esté monitorizando, o de la previsible velocidad de degradación que de dicho fluido se pueda esperar, se podrá elegir entre distintas implementaciones del elemento óptico trasero 45. Como se ilustra en la figura 2A, el fluido que fluye en el canal 20, 120 puede ser un fluido considerado opaco (es decir, un fluido de absorbancia mayor de 1,0) o un fluido considerado traslúcido (es decir, un fluido de absorbancia menor de 1,0). En el caso de aceites lubricantes para maquinaria industrial, como por ejemplo motores de gas, existen aceites opacos (absorbancia mayor de 1,0, tales como mayor de 2,0 o mayor de 3,0 a la longitud de onda de trabajo) incluso cuando están limpios, es decir, antes de empezar a usarse y por tanto degradarse; y también existen aceites que inicialmente (por ejemplo cuando están limpios) son traslúcidos (absorbancia menor de 1,0, tales como menor de 0,5 o menor de 0,2 o menor de 0,1 a la longitud de onda de trabajo) y que, a lo largo de su vida útil, su absorbancia va aumentando con el paso del tiempo y del uso como lubricante de la maquinaria de que se trate, hasta llegar a tener una alta opacidad al final de su vida útil (por ejemplo, presentando una absorbancia en torno a 1,0 o superior, como 2,0 o 3,0 en la longitud de onda de medida). En cualquier caso, a medida que se usan como lubricantes, su absorbancia va aumentando debido a procesos de oxidación, entre otros.

El sistema de monitorización de la presente divulgación se implementa preferentemente de forma que el elemento óptico trasero 45 sea intercambiable, para adaptarse al tipo de fluido que se desee monitorizar. Así, con el diseño de los medios de emisión/recepción de luz 41 y del elemento óptico trasero 45, es posible cubrir distintos casos de uso, seleccionando el elemento óptico trasero 45 entre distintas posibles opciones. Las figuras 3A-3C esquematizan el recorrido de la radiación óptica emitida por la al menos una fuente de iluminación 411 al viajar hacia un fluido que ocupa el canal 20, 120 y la luz detectada por el al menos un sistema detector de luz 412 dispuesto en el mismo lado que la al menos una fuente de iluminación 411 (ambos del mismo lado del canal 20, 120) y,

preferentemente, en un mismo plano para facilitar el diseño óptico. En estas figuras, se explica el papel desempeñado por el elemento óptico trasero 45 con respecto a la radiación óptica procedente de la al menos una fuente de iluminación 411 que consigue llegar a dicho elemento óptico trasero 45 (flecha continua). Las flechas punteadas representan la reflexión difusa en el fluido, presente en mayor o menor medida en función del tipo de fluido.

El modo de operación predominante está determinado por el tipo de elemento óptico trasero 45 elegido y las características del fluido monitorizado. Así, en la figura 3A, en la que se ha usado un material absorbente desde el punto de vista óptico (es decir, un material que a la longitud de onda (o longitudes de onda) de trabajo sustancialmente no refleja nada de luz) para implementar el elemento óptico trasero 451, se observa cómo este material absorbente no refleja nada, de forma que sustancialmente toda la contribución de señal recibida en el sistema detector de luz 412 corresponde (línea punteada) a la señal de reflexión difusa en la muestra. Ejemplos no limitativos de materiales absorbentes son nylon negro y aluminio anodizado, entre otros. Se recomienda la configuración de la figura 3A cuando se desea asegurar que solo se mide reflexión difusa generada en la muestra. En este caso, el modo de operación predominante es modo reflexión, pues la medida principal de radiación óptica realizada por el al menos un sistema detector de luz 412 es la relativa a la reflexión difusa (flecha discontinua).

Por su parte, en la figura 3B, en la que el elemento óptico trasero 452 se ha implementado mediante un material reflexivo no curvado desde el punto de vista óptico (es decir, un material que a la longitud de onda (o longitudes de onda) de trabajo refleja sustancialmente toda la luz que incide sobre dicho material reflexivo), se observa cómo el elemento óptico trasero 452 refleja todo (flecha continua que parte del elemento óptico trasero 452), por lo que el sistema detector de luz 412 recibe intensidad de reflexión difusa (línea punteada) y señal de transmisión que se corresponde con la porción de luz transmitida a través del fluido y reflejada en la placa trasera 452 que se transmite de vuelta a través del fluido (línea continua que llega al sistema detector de luz 412). Ejemplos no limitativos de materiales reflexivos son aluminio pulido, nylon blanco, y en general, cualquier material que actúe como un espejo. En este caso, el elemento óptico trasero 452 actúa como emisor virtual, ya que el comportamiento es como si hubiese un emisor virtual al otro lado del fluido que ocupa el canal 20, 120. La flecha continua procedente del elemento trasero 452 se refiere a la radiación reflejada por dicho elemento trasero 452. En este caso, el modo de operación predominante es modo transmisión,

pues la medida principal de radiación óptica realizada por el al menos un sistema detector de luz 412 es la relativa a la radiación óptica procedente del elemento óptico trasero 452 que actúa como un emisor virtual (flecha continua).

Por último, en la figura 3C, en la que el elemento óptico trasero 45 se ha implementado mediante un material reflexivo curvado, reflexivo focalizado o reflector curvado 453, éste concentra los rayos procedentes de la al menos una fuente de iluminación 411 que llegan hasta la placa trasera 453, en el área activa del sistema detector de luz 412, para maximizar la señal recibida. Es decir, el elemento óptico trasero 45 se ha implementado mediante un material que a la longitud de onda (o longitudes de onda) de trabajo refleja sustancialmente toda la luz que incide sobre dicho material reflexivo y además se diseña para que concentre la luz en el sistema detector de luz 412. Ejemplos no limitativos de implementaciones como ésta son las implementaciones mediante espejos curvos (parabólicos o cóncavos). Como en el caso de la figura 3B, en la figura 3C el sistema detector de luz 412 recibe intensidad de reflexión difusa (línea punteada) y señal de transmisión que se corresponde con la porción de luz transmitida a través del fluido y reflejada en la placa trasera 453 que se transmite de vuelta a través del fluido (línea continua que llega al sistema detector de luz 412), ésta última optimizada (llega focalizada del emisor virtual). Es decir, como en el caso de la figura 3B, el modo de operación predominante es modo transmisión, pues la medida principal de radiación óptica realizada por el al menos un sistema detector de luz 412 es la relativa a la radiación óptica procedente del elemento óptico trasero 453 que actúa como un emisor virtual (flecha continua).

Estas configuraciones (figuras 3B y 3C) se recomiendan para medir el nivel de transmitancia de la muestra. Sin embargo, si el fluido a monitorizar tiene una absorbancia elevada (fluidos opacos o muy opacos), no llegará apenas señal a la placa trasera y el comportamiento del sistema será similar al descrito en el caso de la figura 3A, es decir, se trabaja en modo reflexión a pesar de tener una placa trasera reflectante 452, 453.

Es decir, gracias a la ubicación de los medios ópticos de emisión/recepción 41 del mismo lado del fluido, y del elemento óptico trasero 45 situado al otro lado del fluido con respecto a los medios ópticos de emisión/recepción 41, se consigue un modo de operación en reflexión o en transmisión que va a permitir monitorizar un amplio rango de fluidos en términos de absorbancia (transmitancia) y reflectancia.

Las figuras 4A y 4B representan el funcionamiento del sistema de monitorización. Concretamente, la figura 4A representa el comportamiento óptico de los rayos

transmitidos por la al menos una fuente de iluminación 411 al entrar en contacto con el fluido que llena el canal 20, 120 cuando el fluido que llena el canal 20, 120 es un fluido de alta opacidad 72, es decir, cuando el fluido presenta una absorbancia mayor de 1,0, tal como mayor de 2,0 o mayor de 3,0 (parte inferior de la figura 4A); y cuando el fluido que llena el canal 20, 120 es un fluido de baja opacidad 71, es decir, cuando el fluido presenta una absorbancia menor de 1,0, tal como menor de 0,5 o menor de 0,2 o menor de 0,1 (parte superior de la figura 4A).

Cuando se emite una radiación óptica que incide en un fluido de alta opacidad 72, prácticamente nada de la luz consigue atravesar el fluido 72 debido a la opacidad de éste, ya que la luz se absorbe en una profundidad cercana a la superficie y la parte que no es absorbida puede salir otra vez de la muestra en forma de reflexión difusa debido al scattering (dispersión) producido por las reflexiones internas en el fluido (véase figura 8). En este caso, el modo de operación predominante es el modo en reflexión. En estas circunstancias, el comportamiento de los rayos de luz en el fluido es sustancialmente el mismo independientemente del tipo de placa trasera utilizada 45, ya que prácticamente ningún rayo llega hasta la placa trasera.

Por el contrario, cuando se emite una radiación óptica que incide en un fluido de baja opacidad 71, una alta proporción de la luz emitida por la fuente atraviesa el fluido. En este caso, el modo de operación predominante es el modo en transmisión, porque la radiación luminosa es capaz de atravesar el fluido y la componente debida al scattering es en proporción mucho menor (debe tenerse en cuenta además que el efecto del scattering depende de las características propias del fluido). En caso de que la placa trasera del sistema sea reflectante 452, 453, toda la luz que llegue a esta superficie se reflejará y volverá de vuelta a través del fluido. Si, por el contrario, la placa trasera es absorbente 451, toda la luz que incide en esta superficie será absorbida y nada volverá de vuelta a través del fluido.

La elección de la placa trasera 451, 452, 453 depende de las características del fluido a monitorizar y de su evolución durante su uso. La utilización de una placa trasera absorbente 451 permite obtener información sobre el nivel de reflexión difusa debida al scattering en la muestra, lo que puede dar información sobre la aparición de partículas en la misma, puede indicar por ejemplo la aparición de barnices. Mientras que una placa trasera reflectante 452, 453 permite realizar por ejemplo una monitorización del nivel de absorbancia de la muestra, cambios en el color, etc. Todos estos efectos son indicativos del estado de degradación del aceite.

Como se ha indicado, el fluido lubricante en su estado inicial y su evolucióndurante su uso condicionan la elección del placa trasera 45, de forma que un fluido lubricante considerado opaco en estado inicial (limpio) podrá determinar la elección de una placa trasera absorbente 451, mientras que un fluido lubricante considerado traslúcido en estado inicial, podrá determinar la elección de una placa trasera reflexiva 452, 453. La figura 4B muestra en detalle los principales componentes del subsistema óptico 140 y los modos predominantes (modo reflexión y modo transmisión) en función de la opacidad del fluido que ocupa el canal 20, 120 y de la placa trasera o elemento óptico de reflexión 45 elegido. La referencia (i) se refiere a rayos de luz reflejados en las inmediaciones de la superficie del fluido (reflexión difusa) que son detectados en el sistema detector de luz 412, mientras que la referencia (ii) se refiere a rayos de luz que atraviesan el fluido y que son reflejados por el elemento óptico trasero 45 (cuando éste actúa como emisor virtual), de forma que viajan de vuelta por el fluido. Así, cuando se elige una placa trasera absorbente 451, el sistema detector de luz 412 sustancialmente solo recibe los rayos (i), es decir, los rayos de luz reflejados por reflexión difusa, independientemente de que el fluido tenga mayor o menor opacidad, ya que los rayos emitidos por la fuente de iluminación 411 que hayan logrado atravesar el fluido, si los hubiera, son absorbidos por elemento óptico trasero absorbente 451. El sistema trabaja en este caso de forma predominante en modo reflexión, porque la mayor parte de la radiación detectada por el detector 412 es la componente (i) reflejada en el fluido. Por el contrario, cuando se elige una placa trasera reflexiva 452, 453, el sistema detector de luz 412 recibe los rayos (i) (reflexión difusa) más los rayos reflejados (ii) por el elemento óptico trasero reflexivo 452, 453 que hayan logrado atravesar de vuelta el fluido. En este caso, si el fluido es opaco, es decir, de absorbancia mayor de 1,0, tal como mayor de 2,0 o mayor de 3,0, la componente (i) podrá ser mayor que la (ii), porque el fluido opaco 72 permite el paso de poca radiación reflejada. El sistema trabaja en este caso de forma predominante en modo reflexión (difusa). Por el contrario, si el fluido es traslúcido (absorbancia menor de 1,0, tal como menor de 0,5 o menor de 0,2 o menor de 0,1), la componente (i) podrá ser menor que la (ii), porque el fluido de baja opacidad 71 permite el paso de mayor cantidad de radiación reflejada por la placa trasera 453, 453. El sistema trabaja en este caso de forma predominante en modo transmisión. En general, de las dos componentes de luz (i), (ii) que son detectadas por el sistema detector de luz 412, la menor de ellas puede llegar a ser nula.

Por otra parte, el hecho de trabajar con un sistema de monitorización diseñado para acoplarse de forma compacta y sencilla en una toma simple de un depósito y trabajar por

tanto en modo sumergido, obliga a superar ciertos inconvenientes: Por una parte, debe garantizarse que haya una renovación efectiva del fluido dentro del canal 20, 120. Nótese que el flujo del fluido a lo largo del canal de medida 20, 120 depende de las pequeñas diferencias de presión que existen en el depósito 1 debido a turbulencias internas, de la viscosidad del fluido y de la temperatura del fluido. Por ejemplo, se ha obtenido mediante simulación que con un incremento de presión de 17,07 Pascales entre la entrada y salida del sistema de monitorización, para un canal 20, 120 de 2 mm de espesor (distancia entre la ventana 44 y placa trasera 45) se consigue un caudal volumétrico de 0,053 ml/s.

Por tanto, la renovación de fluido en el canal de medida 20, 120 está garantizada en las condiciones de presión descritas. Por otra parte, debe garantizarse que a la hora de introducir el sistema de monitorización 3, 13 en el depósito 1, el sistema de monitorización 3, 13, evacue el aire que pueda contener en su cavidad de medida (canal de medida) 20, 120. La probabilidad de no evacuar el aire contenido en el canal de medida 20, 120 es mayor cuanto más verticalmente se introduce el sistema de monitorización 3, 13 en el depósito 1, y cuanto más viscoso sea el fluido bajo monitorización. El caso mayor riesgo de acumulación de aire en el canal de medida 20, 120 es aquel en el que se introduce el sistema de monitorización de forma totalmente vertical en un depósito que contiene un fluido muy viscoso (por ejemplo, 320 cSt), donde cSt son centiStokes, es decir, unidades de viscosidad, siendo 1cSt = 10^{-6} m^2/s^3.

La figura 5 ilustra el problema de la introducción del sistema de monitorización 3 en un depósito 1 de forma totalmente vertical, en cuyo caso las burbujas de aire acumuladas en el canal de medida tienen dificultades para evacuar el canal y, por tanto, éste no se llena con el fluido que se desea monitorizar 2.

Para garantizar la renovación de la muestra de fluido dentro del canal de medida 20, 120, garantizándose así que el sistema de monitorización tome medidas sobre muestras diferentes de fluido a lo largo del tiempo, en realizaciones de la invención se diseña un canal de medida 20, 120 de altura regulable para cada tipo de fluido. La figura 6 muestra un sistema de monitorización con altura H del canal de medida 20, 120 variable. En realizaciones de la invención, la altura H del canal 20, 120 puede variar entre 0,5 mm y 5 mm, por ejemplo entre 0,75 mm y 4 mm, o entre 1 mm y 3,5 mm, o entre 1,5 mm y 3 mm, o entre 1,75 mm y 2,75 mm.

Para evitar la acumulación de aire en el canal de medida 20,120, es decir, para favorecer la evacuación de aire de dicho canal 20, 120, en realizaciones de la invención se diseña la unión entre la ventana óptica 44 y el cuerpo o carcasa del sistema de monitorización

sin aristas. En otras realizaciones de la invención, se diseña dicha ventana óptica 44, que es preferentemente plana, con una cierta inclinación con respecto al plano definido por el elemento óptico trasero 45. Esta inclinación favorece la evacuación de aire del canal 20, 120. La figura 7 muestra un sistema de monitorización cuya ventana óptica 44 está inclinada con respecto al plano definido por el elemento óptico trasero 45. En realizaciones de la invención, la inclinación ρ puede variar entre 5 y 15º, por ejemplo entre 6 y 14º, o entre 7 y 13º, o entre 8 y 12º, o entre 9 y 11º. En realizaciones de la invención, se diseña la unión entre la ventana óptica 44 y el cuerpo o carcasa del sistema de monitorización sin aristas, y además se diseña la ventana óptica 44 inclinada un ángulo ρ con respecto al plano definido por el elemento óptico trasero 45.

Se ha construido un prototipo del sistema de monitorización descrito. El prototipo está compuesto por un emisor LED de luz blanca, un detector de color RGB y una anchura de canal (distancia entre ventana óptica y placa trasera) de 2 mm. La siguiente tabla muestra los valores obtenidos al realizar medidas con diferentes fluidos (fluido 1 a fluido 6) y diferentes configuraciones del sistema (placa trasera absorbente o reflectante) frente a datos obtenidos en el laboratorio. En todas las medidas realizadas con el prototipo y con la misma configuración de placa trasera el emisor envía la misma cantidad de luz. Este valor se determina durante el proceso de calibración del sensor (sistema de monitorización) en condiciones de vacío, es decir, sin fluido en el canal. En estas condiciones, el valor medido en el detector es del 80% respecto a su fondo de escala. Este valor se ha escogido por cuestiones de resolución del sensor, tales como para evitar situaciones de saturación del detector. Las dos últimas columnas se refieren a la medida tomada por el detector de color RGB en presencia de fluido en el canal. El fluido 1 es Beslux degradado. El fluido 2 es Beslux degradado intermedio. El fluido 3 es Beslux Referencia. El fluido 4 es Cepsa degradado. El fluido 5 es Cepsa degradado intermedio. El fluido 6 es Cepsa referencia.

	Absorbancia medida en laboratorio	Reflectancia medida en laboratorio	Medida Detector (Placa trasera Reflectante)	Medida Detector (Placa trasera Absorbente)
Fluido 1	3	4	32%	66%
Fluido 2	2	3,25	39%	62%
Fluido 3	1	4,5	44%	66%
Fluido 4	0,5	5,25	55%	67%
Fluido 5	0,2	6	63%	68%
Fluido 6	0,04	6,75	79%	69%

Como puede observarse, cuando se usa una placa trasera absorbente 451 (primera

columna por la derecha), y por tanto sustancialmente toda la radiación que pueda haber atravesado el fluido es absorbida por la placa trasera 451, para cualquiera de las muestras (fluido 1 a fluido 6) el detector mide un valor en torno al 60-70% de su fondo de escala. En este caso el sistema trabaja en modo reflexión. Por el contrario, cuando se usa una placa trasera reflexiva 452, 453 (segunda columna por la derecha), la medida obtenida por el detector de color RGB, varía mucho en función de la absorbancia del fluido, desde valores de fondo de escala próximos al 80% en fluidos muy translúcidos (fluido 6) hasta valores próximos al 30% en fluidos muy opacos (fluido 1). En este caso el sistema trabaja en modo predominante transmisión.

Como puede observarse, con respecto a sistemas de monitorización en toma simple del estado de la técnica, como por ejemplo el descrito en la solicitud de patente internacional WO2016/080824A1, la presente divulgación simplifica y abarata el diseño, fabricación y mantenimiento del sistema de monitorización, debido a que se necesita una única fuente de iluminación, que además se ubica en la zona más robusta del sistema de monitorización. En suma, el sistema de monitorización de la presente divulgación se implementa como un sensor 'enchufable' (acoplable a una toma simple de un depósito) que puede entregar una salida de degradación de aceite (o de su capacidad de lubricación), así como otros parámetros indicativos del aceite, como su nivel de aditivos antioxidantes, su grado de acidez, su nivel de oxidación y/o su nivel de presencia de barnices tanto si el fluido es opaco o traslúcido. El sistema puede ser roscable, o de cualquier otra forma de acoplamiento sencilla, que no precise de canal de bypass en el depósito para la selección de la muestra de fluido. El sistema permite la medida en reflexión y/o transmisión de fluidos tanto opacos como transparentes, pasando por los diversos grados de traslucidez. Se pueden emplear diversos elementos ópticos traseros, ya sean de material absorbente o reflectante, y en este caso tanto planos como curvados para focalizar los rayos. El sistema se ha optimizado para que, al introducirse en el depósito, se elimine el aire que pueda haber en el canal de medida, evitándose la presencia de aire en la zona de medida. Además, se ha optimizado para que se regeneren las muestras sobre las que se toman las medidas.

En este texto, la palabra "comprende" y sus variantes (como "comprendiendo", etc.) no deben interpretarse de forma excluyente, es decir, no excluyen la posibilidad de que lo descrito incluya otros elementos, pasos etc.

Por otra parte, la invención no está limitada a las realizaciones concretas que se han descrito sino abarca también, por ejemplo, las variantes que pueden ser realizadas por el

experto medio en la materia (por ejemplo, en cuanto a la elección de materiales, dimensiones, componentes, configuración, etc.), dentro de lo que se desprende de las reivindicaciones.

REIVINDICACIONES

1.- Un sistema de monitorización (3, 13) para la inspección de un fluido (2, 71, 72) contenido en un depósito (1) mediante la inserción de dicho sistema de monitorización (3, 13) en una toma (5) de dicho depósito (1), que comprende:

una zona de medida (20, 120) configurada para que circule por ella una muestra de dicho fluido (2, 71, 72);

estando el sistema de monitorización (3, 13) caracterizado por que comprende:

unos medios de emisión/recepción de luz (41) que consisten en un sistema de iluminación (411) y un sistema detector de luz (412) situados en un mismo lado del sistema de monitorización (3, 13) con respecto a dicha zona de medida (20, 120);

una ventana óptica (44) dispuesta entre dichos medios de emisión/recepción de luz (41) y dicha zona de medida (20, 120);

y un elemento óptico trasero (45, 451, 452, 453) situado al otro lado del sistema de monitorización (3, 13) con respecto a dicha zona de medida (20, 120),

estando dicho sistema de iluminación (411) configurado para emitir radiación óptica hacia dicha zona de medida (20, 120),

estando dicho sistema detector de luz (412) configurado para detectar una radiación óptica que comprende la luz (i) reflejada por dicho fluido (2, 71, 72) que circula por dicha zona de medida (20, 120) y/o la luz (ii) transmitida a través de dicho fluido (2, 71, 72) y reflejada en dicho elemento óptico trasero (45, 451, 452, 453),

comprendiendo además dicho sistema de monitorización (3, 13) un subsistema electrónico (150) que comprende medios de procesado (51) configurados para controlar la activación/desactivación del sistema de iluminación (411) y para procesar las señales obtenidas procedentes del sistema detector de luz (412).

2.- El sistema de monitorización (3, 13) de la reivindicación 1, en el que dicho elemento óptico trasero (45, 451) se implementa mediante un elemento absorbente desde el punto de vista óptico, estando dicho elemento óptico trasero (45, 451) configurado para impedir la reflexión de la luz transmitida a través de dicho fluido (20, 120).

3.- El sistema de monitorización (3, 13) de la reivindicación 1, en el que dicho elemento óptico trasero (45, 452, 453) se implementa mediante un elemento reflexivo desde el punto de vista óptico, estando dicho elemento óptico trasero (45, 452, 453) configurado para favorecer la reflexión de la luz transmitida a través de dicho fluido (20, 120).

4.- El sistema de monitorización (3, 13) de la reivindicación 3, en el que dicho elemento reflexivo desde el punto de vista óptico (452, 453) es un elemento reflexivo plano (452).

5.- El sistema de monitorización (3, 13) de la reivindicación 3, en el que dicho elemento reflexivo desde el punto de vista óptico (452, 453) es un elemento reflexivo cóncavo (453).

6.- El sistema de monitorización (3, 13) de la reivindicación 1, en el que dicho elemento óptico trasero (45, 451, 452, 453) es intercambiable, de forma que en función de la absorbancia del fluido bajo inspección (2, 71, 72), se elige un elemento óptico trasero absorbente (451) o reflexivo (452, 453).

7.- El sistema de monitorización (3, 13) de cualquiera de las reivindicaciones anteriores, que comprende además al menos un fotodiodo de control (43) configurado para medir la intensidad emitida por el sistema de iluminación (411).

8.- El sistema de monitorización (3, 13) de cualquiera de las reivindicaciones anteriores, estando dicho sistema de monitorización (3, 13) comprendido en una carcasa, en la que dichos medios de emisión/recepción de luz (41) están situados en una porción (136) de dicha carcasa y dicho elemento óptico trasero (45, 451, 452, 453) está situado en otra porción (135) de dicha carcasa, donde dichas porciones (135, 136) de carcasa definen dicha zona de medida (20, 120), delimitando dicho elemento óptico trasero (45, 451, 452, 453) y dicha ventana óptica (44) la zona de medida (20, 120).

9.- El sistema de monitorización (3, 13) de cualquiera de las reivindicaciones anteriores, donde la altura (H) de dicha zona de medida (20, 120) es regulable para garantizar la renovación de la muestra de fluido (2, 71, 72) dentro de dicha zona de medida (20, 120).

10.- El sistema de monitorización (3, 13) de cualquiera de las reivindicaciones anteriores, donde dicha ventana óptica (44) tiene una inclinación con respecto al plano definido por elemento óptico trasero (45, 451, 452, 453) para evitar la acumulación de aire en la zona de medida (20,120).

11.- El sistema de monitorización (3, 13) de cualquiera de las reivindicaciones anteriores, que comprende un difusor (48) dispuesto entre dicho sistema de iluminación (411) de dichos medios de emisión/recepción de luz (41) y dicho al menos un fotodiodo de control (43).

12.- Un método de monitorización de un fluido (2, 71, 72) contenido en un depósito (1), que comprende:

insertar un sistema de monitorización (3, 13) en una toma simple (5) de dicho depósito (1), donde dicho sistema de monitorización (3, 13) comprende: una zona de

medida (20, 120) configurada para que circule por ella una muestra de dicho fluido (2, 71, 72); unos medios de emisión/recepción de luz (41) que consisten en un sistema de iluminación (411) y un sistema detector de luz (412) situados en un mismo lado del sistema de monitorización (3, 13) con respecto a dicha zona de medida (20, 120); una ventana óptica (44) dispuesta entre dichos medios de emisión/recepción de luz (41) y dicha zona de medida (20, 120); y un elemento óptico trasero (45, 451, 452, 453) situado al otro lado del sistema de monitorización (3, 13) con respecto a dicha zona de medida (20, 120);

hacer incidir una radiación óptica desde dicho sistema de iluminación (411) hacia dicha zona de medida (20, 120);

detectar por dicho sistema detector de luz (412) una radiación óptica que comprende la luz (i) reflejada por dicho fluido (2, 71, 72) que circula por dicha zona de medida (20, 120) y/o la luz (ii) transmitida a través de dicho fluido (2, 71, 72) y reflejada en dicho elemento óptico trasero (45, 451, 452, 453);

en un subsistema electrónico (150) comprendido en dicho sistema de monitorización (3, 13), controlar la activación/desactivación del sistema de iluminación (411) y procesar las señales obtenidas procedentes del sistema detector de luz (412).

13.- El método de la reivindicación 12, en el que cuando dicho fluido (2, 71, 72) tiene una absorbancia mayor de 1,0 en su estado inicial, dicho elemento óptico trasero (45, 451, 452, 453) es un elemento óptico trasero absorbente (451).

14.- El método de la reivindicación 12, en el que cuando dicho fluido (2, 71, 72) tiene una absorbancia menor de 1,0 en su estado inicial, dicho elemento óptico trasero (45, 451, 452, 453) es un elemento óptico trasero reflexivo (452, 453).

15.- El método de cualquiera de las reivindicaciones 12 a 14, que comprende además regular la altura (H) de dicha zona de medida (20, 120) para garantizar la renovación de la muestra de fluido (2, 71, 72) dentro de dicha zona de medida (20, 120).

16.- El método de cualquiera de las reivindicaciones 12 a 115 que comprende además inclinar dicha ventana óptica (44) con respecto al plano definido por elemento óptico trasero (45, 451, 452, 453) para evitar la acumulación de aire en la zona de medida (20,120).

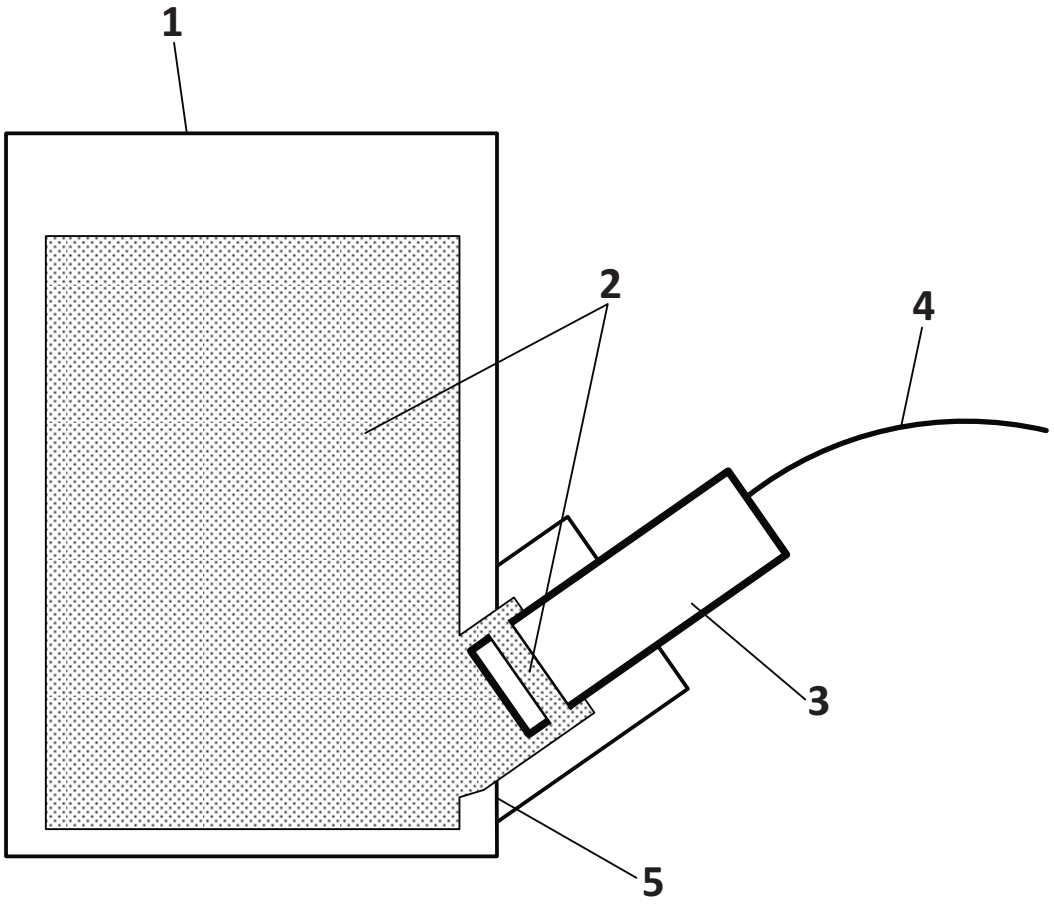

FIG. 1A

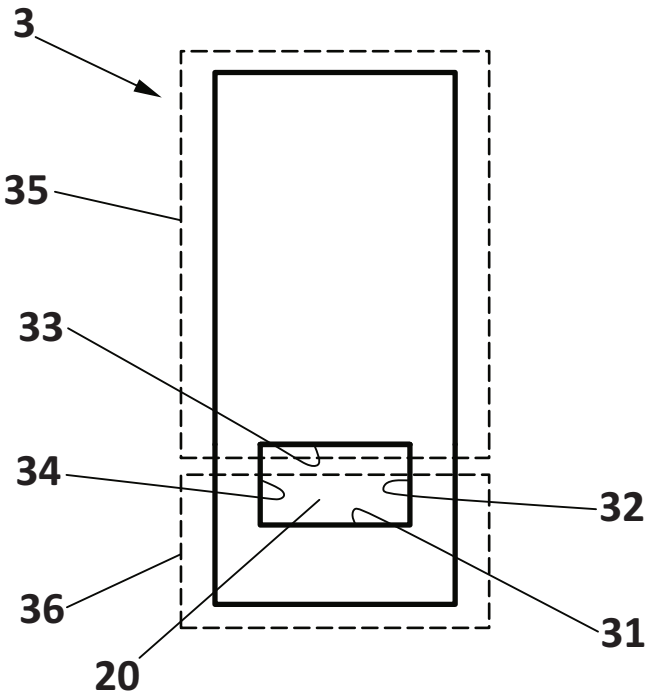

FIG. 1B

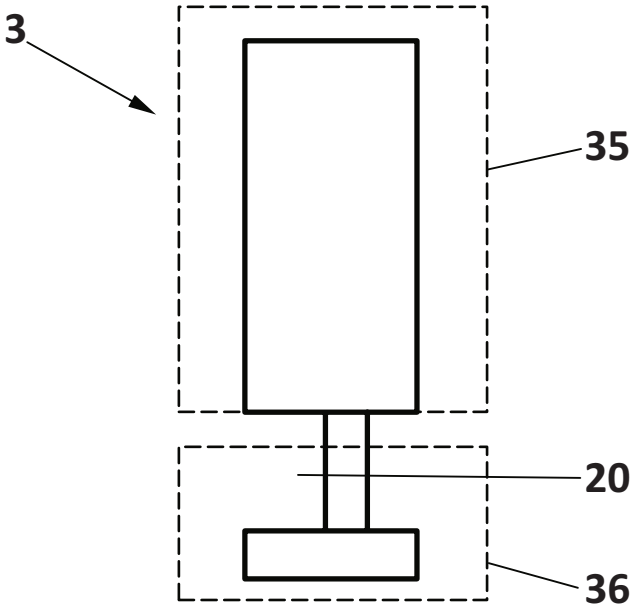

FIG. 1C

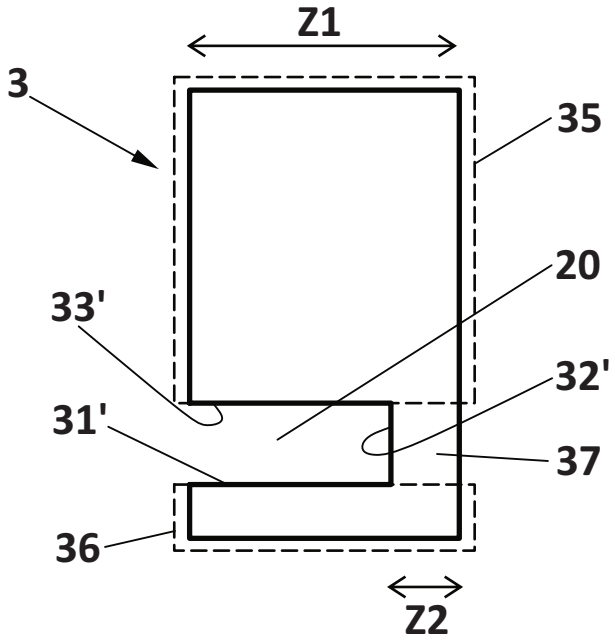

FIG. 1D

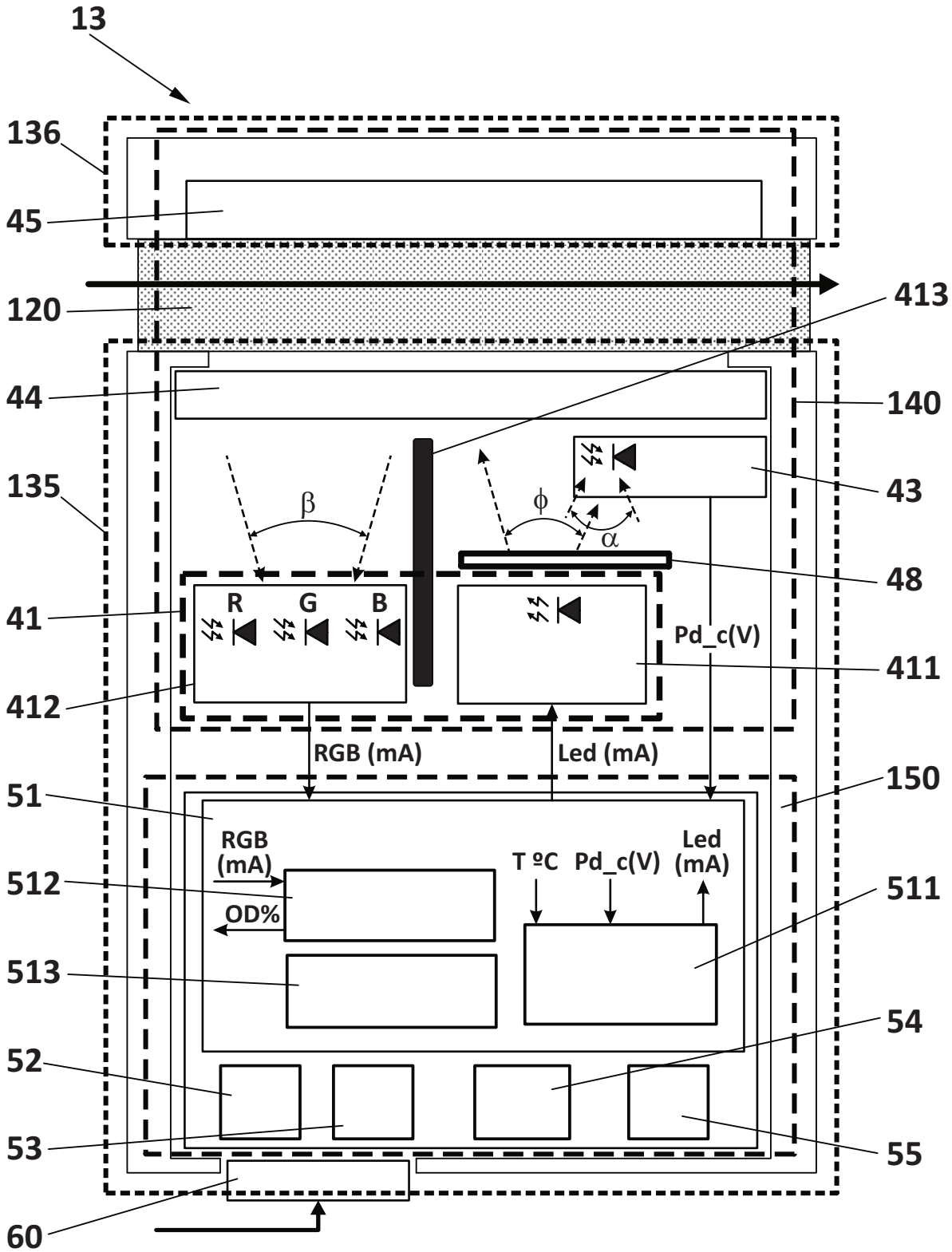
13
136
45
120
413
44
140
135
β
ϕ
α
43
48
41
R
G
B
Pd_c(V)
411
412
RGB (mA)
Led (mA)
150
51
RGB (mA)
T ºC
Pd_c(V)
Led (mA)
512
OD%
511
513
54
52
53
55
60

FIG. 2A

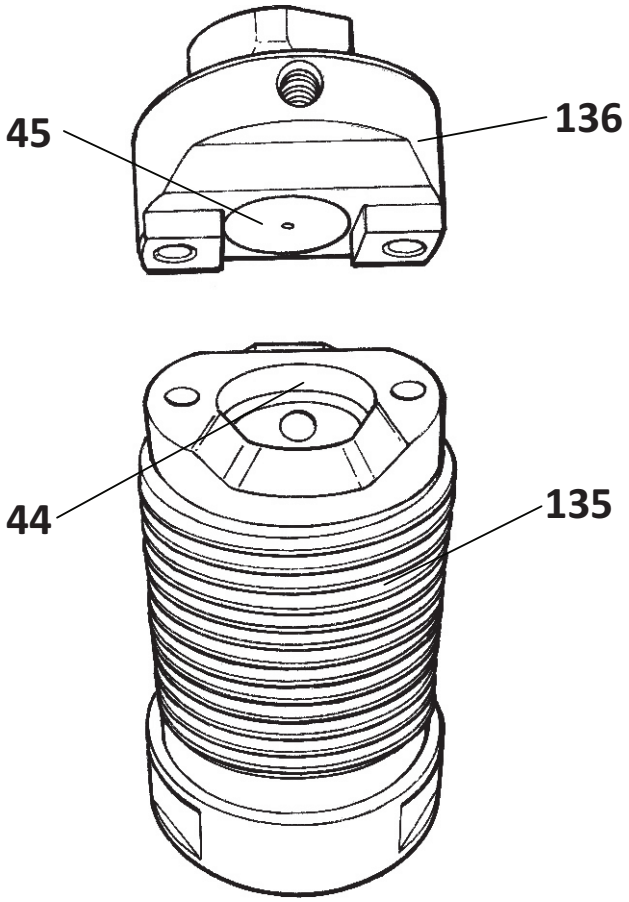

FIG. 2B

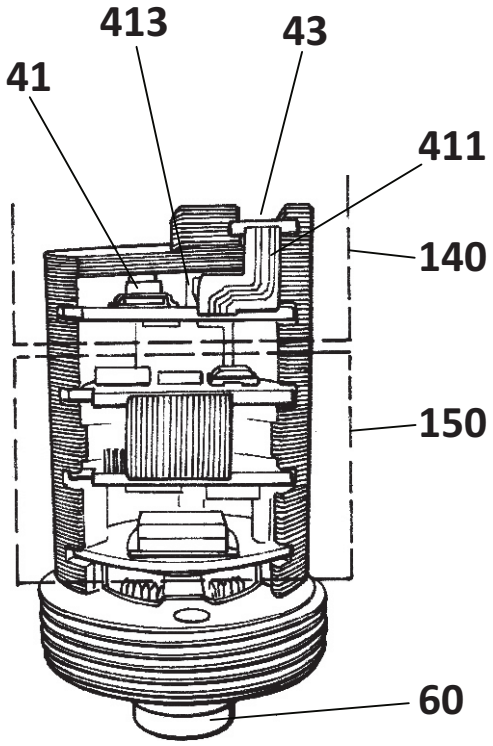

FIG. 2C

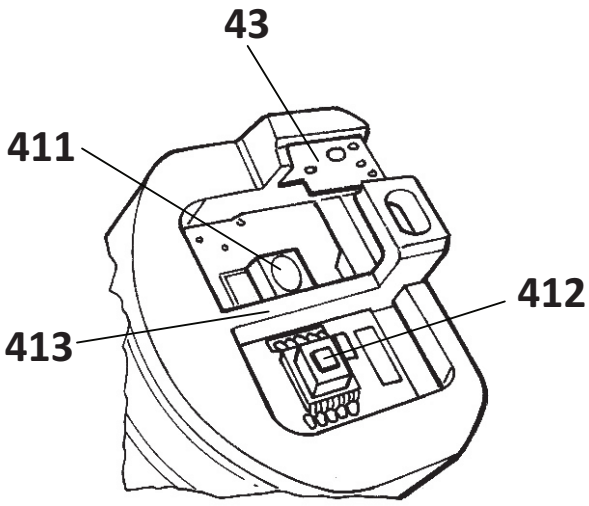

FIG. 2D

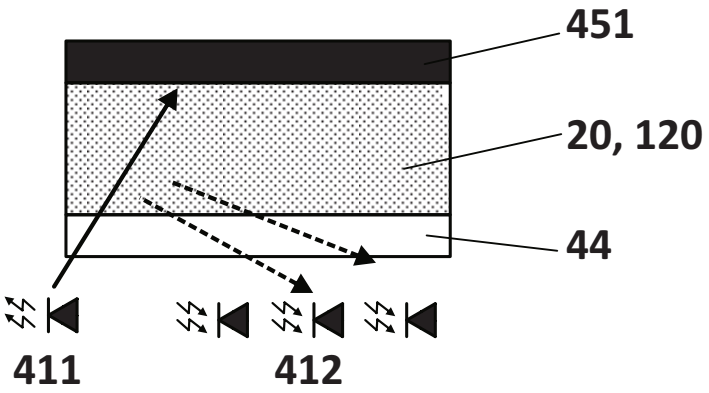

FIG. 3A

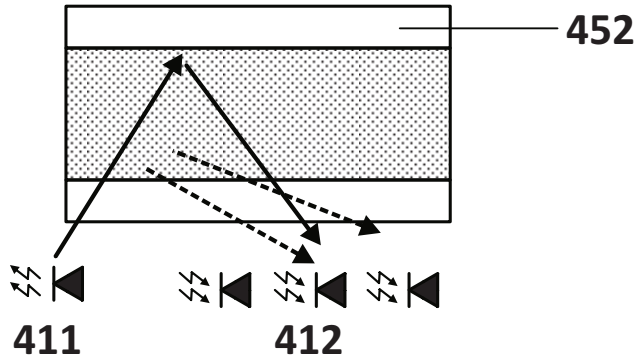

FIG. 3B

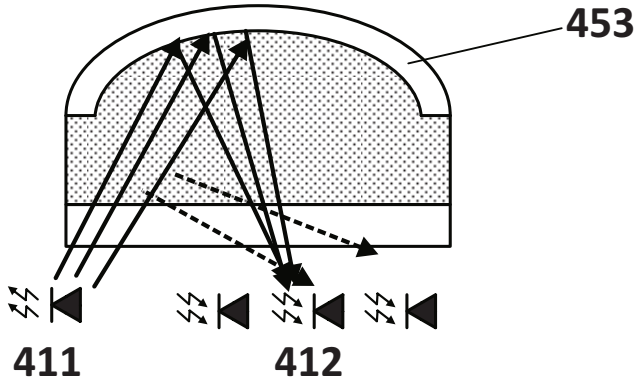

FIG. 3C

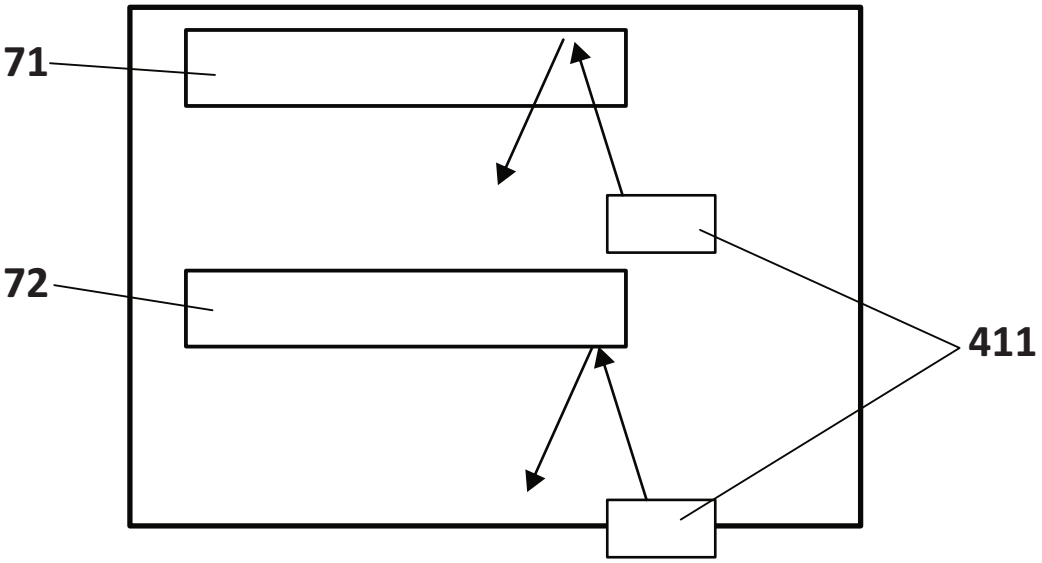
71
72
411

FIG. 4A

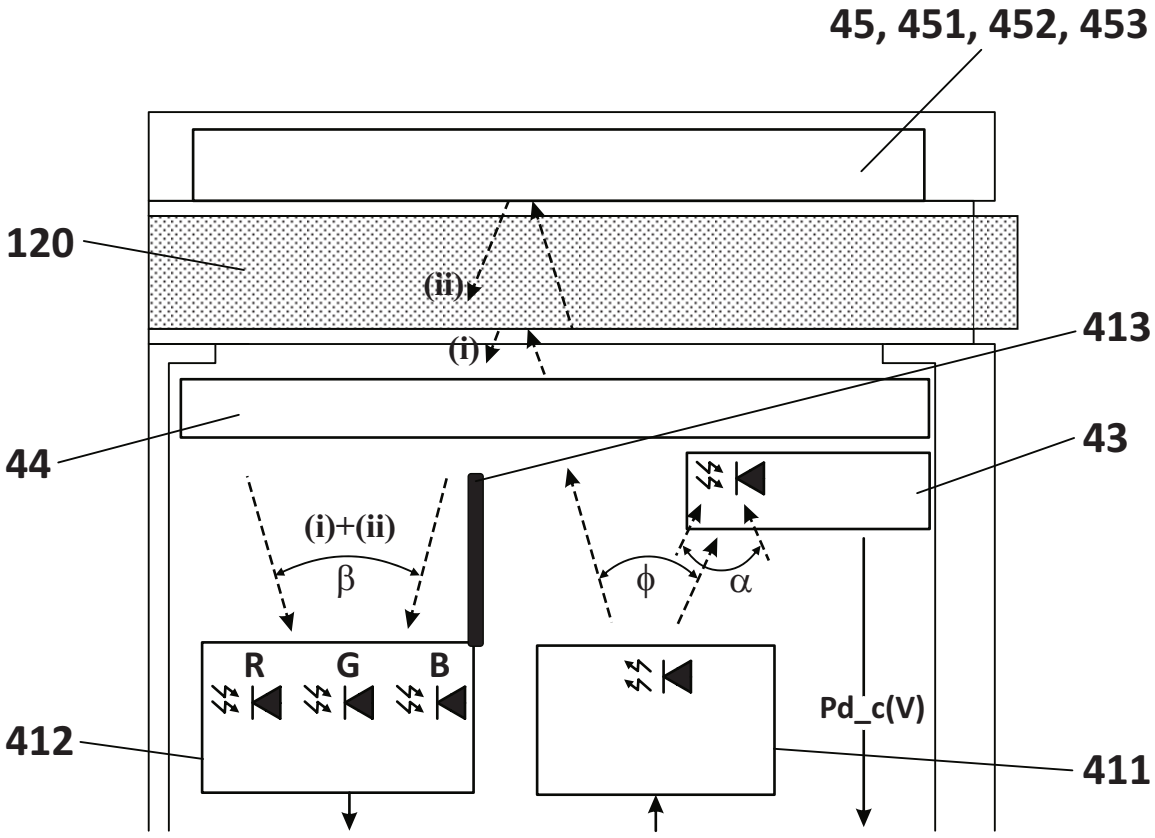
45, 451, 452, 453
120
(ii)
(i)
413
44
43
(i)+(ii)
β
ϕ
α
R
G
B
412
Pd_c(V)
411

FIG. 4B

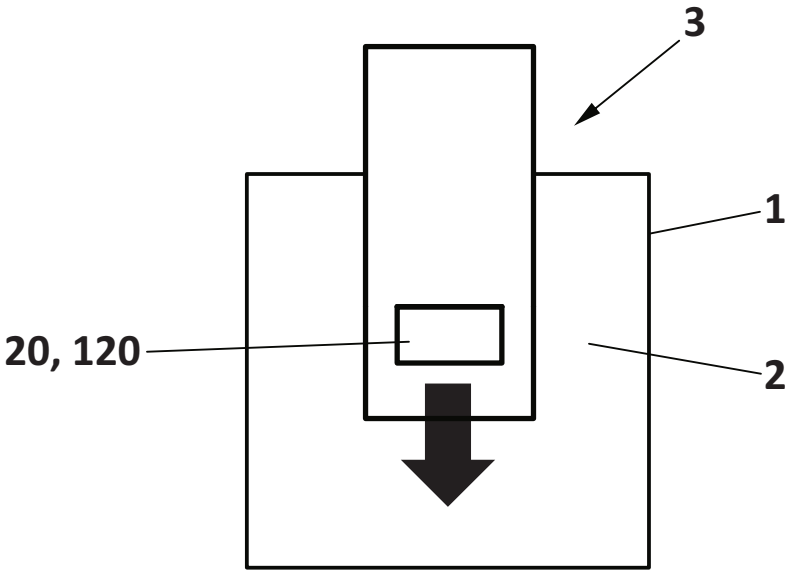

FIG. 5

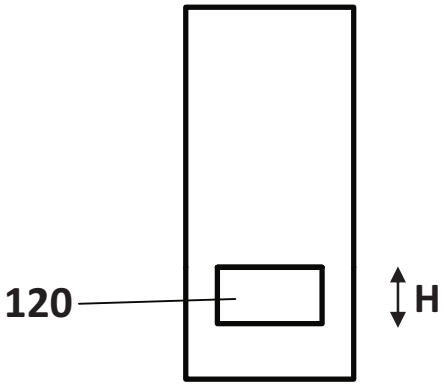

FIG. 6

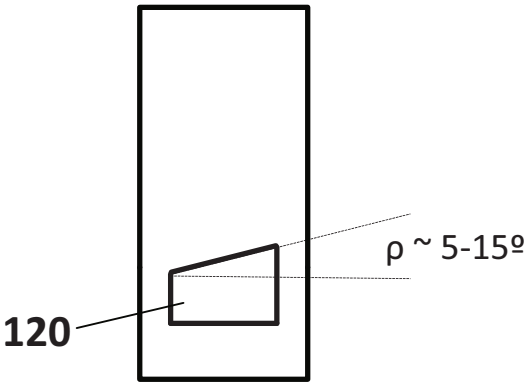

FIG. 7

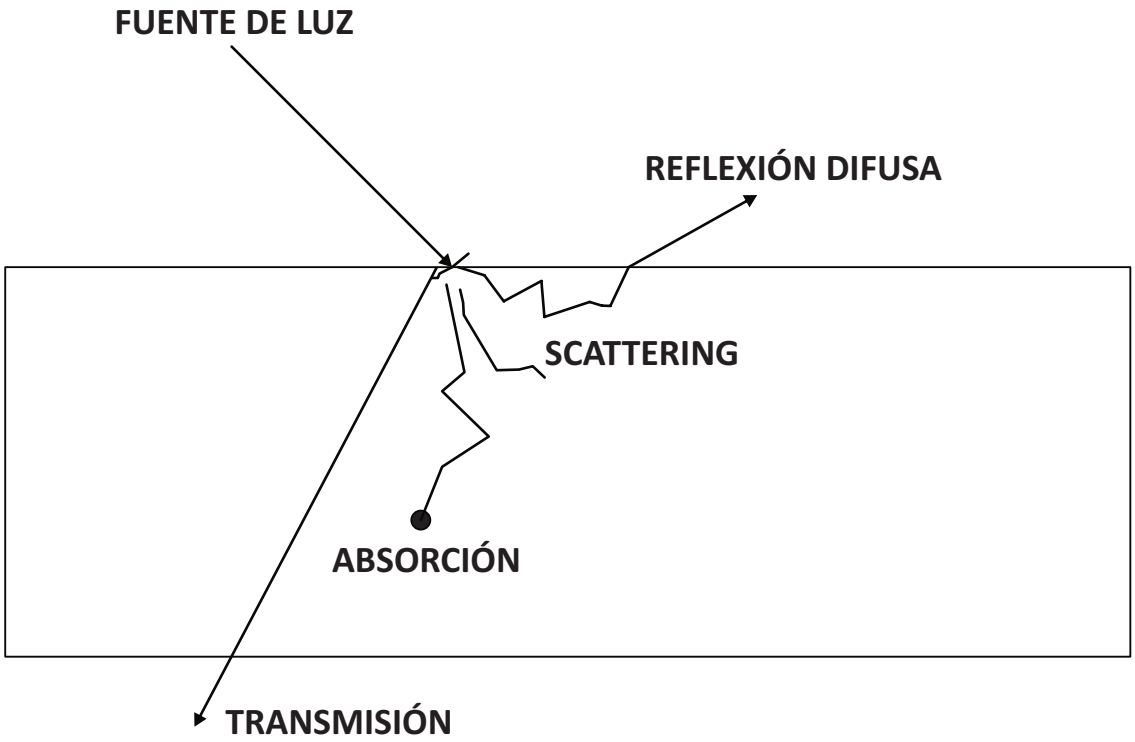
FUENTE DE LUZ
REFLEXIÓN DIFUSA
SCATTERING
ABSORCIÓN
TRANSMISIÓN

FIG. 8

RESUMEN

SISTEMA Y MÉTODO DE MONITORIZACIÓN DEL ESTADO DE UN FLUIDO

Un sistema de monitorización (3, 13) para la inspección de un fluido (2, 71, 72) contenido en un depósito (1) mediante su inserción en una toma (5) del depósito (1), que comprende: una zona de medida (20, 120) configurada para que circule por ella una muestra de dicho fluido (2, 71, 72); unos medios de emisión/recepción de luz (41) que consisten en un sistema de iluminación (411) y un sistema detector de luz (412) situados en un mismo lado del sistema de monitorización (3, 13) con respecto a dicha zona de medida (20, 120); una ventana óptica (44) dispuesta entre dichos medios de emisión/recepción de luz (41) y dicha zona de medida (20, 120); y un elemento óptico trasero (45, 451, 452, 453) situado al otro lado del sistema de monitorización (3, 13) con respecto a dicha zona de medida (20, 120),. El sistema de iluminación (411) está configurado para emitir radiación óptica hacia dicha zona de medida (20, 120), y el sistema detector de luz (412) está configurado para detectar una radiación óptica que comprende la luz (i) reflejada por dicho fluido (2, 71, 72) y/o la luz (ii) transmitida a través de dicho fluido (2, 71, 72) y reflejada en dicho elemento óptico trasero (45, 451, 452, 453). El sistema de monitorización (3, 13) comprende además un subsistema electrónico (150) que comprende medios de procesado (51) configurados para controlar la activación/desactivación del sistema de iluminación (411) y para procesar las señales obtenidas procedentes del sistema detector de luz (412). Método de monitorización.

[FIG. 2A]

Photonic Low-Cost Sensors for in-Line Fluid Monitoring

Design Methodology

Jon Mabe Álvarez

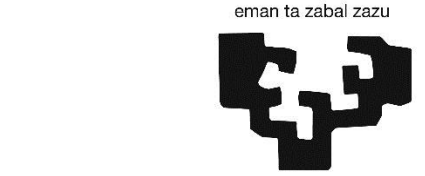

PhD Thesis
Bilbao, 2017

Supervisors:
Joseba Zubia Zaballa
Ana Aranzabe Garcia

Kai eta Alazne, zuentzat
Ama, Aita eskerrik asko

Preface

The paradigm of process monitoring has evolved in the last years, driven by a clear need for improving efficiency, quality and safety of processes and products. Sectors as manufacturing, energy, food and beverages, etc. are fostering the adoption of innovative methods for controlling their processes and products, in a non-destructive, in-place, reliable, fast, accurate and cost-efficient manner. Furthermore, the parameters requested by the industry for the quality assessment are evolving from basic magnitudes as pressures, temperatures, humidity, etc. to complete chemical and physical fingerprints of these products and processes. In this situation, techniques based on the UV/VIS/NIR light-matter interaction appear to be optimum candidates to face the request of the industry. Moreover, at this moment, when we are witnessing a technological revolution in the field of optoelectronic components, which are required for setting up these light-based analyzers.

However, being able to integrate these optoelectronic components with the rest of subsystems (electronics, optics, mechanics, hydraulics, data processing, etc.) is not straightforward. The development of these multi-domain and heterogeneous sensor products, meeting not just technological but also market objectives, poses a considerable technical and organizational challenge for any company.

In this context, a methodological hybrid and agile integration of photonic components within the rest of subsystems, towards a sensor product development, is presented as the main outcome of the thesis. The methodology has been validated in several industrial scenarios, being three of them included in this thesis, which covers from hydraulic fluid quality control to real-time monitoring of alcoholic beverage fermentation process.

Index

1.
Introduction

This introductory chapter aims at setting the motivation of the thesis and to establish its scope. Since this thesis' overall goal is contributing to the development of fully functional cost effective photonic sensors for the in–line analysis of fluids, the first section of the introduction is devoted to clarify this concept. The section starts analyzing the opportunity opened for sensor manufacturers thanks to the requirements of pervasive monitoring of industrial processes within the Industry 4.0 paradigm. The different blocks involved in the photonic sensors are reviewed here, as well as the main strategies followed by the most significant players in the field of sensors companies in this regard. Subsequently, the new generation of cost effective and compact photonic devices (light sources, light detectors, optic components, electronics, etc.) are presented here, analyzing the opportunity generated by their presence but also considering the challenges and risks related to their integration into reliable sensor products. Finally, we position this thesis in the photonic equipment landscape, establishing its scope and its objectives and highlighting the main results.

1.1 Industry 4.0 and Smart Sensors

Surely, some of the most hyped concepts in industry today are the industrial internet, Industry 4.0, Cyber–Physical systems (CPS) or the Industrial Internet of Things (IIoT) and it is difficult to avoid reading about these terms in the industry press and in the marketing of industry technology vendors [1][2][3]. Like it or not, this industrial revolution has already started, driven by the need for more efficient and cost–effective manufacturing [4][5][6].

Foreseeing the convergence of industrial and manufacturing systems with the features of advanced computing, data analytics, cost–effective sensing and new levels of connectivity enabled by the internet, Industry 4.0 is envisaged as the next great breakthrough step in industrial evolution. The promise of unprecedented advancements in automation, efficiency and flexibility, together with an expected dramatic saving in manufacturing costs and achieving better qualities in good production and supply, has sufficed to foster a tremendous amount of effort on providing a full portfolio of solutions within the Industry 4.0 paradigm.

The giants of the process automation and manufacturing equipment, such as Siemens, Bosch, General Electric, ABB, Schneider Electric, Honeywell, etc. are ensuring that all the research efforts reach the market in due time. These companies are going through the most insightful change in their corporate histories, attempting to switch from being makers of machines into fully digital businesses [7], where cloud services, big data analytics and pervasive smart sensing are the most important technologies supporting this revolution (see Figure 1.1–1).

In this context, in 2015 General Electric (Fairfield, CT, USA) launched Predix® as an operating system of the Industrial Internet for connecting industrial equipment, analyzing data, and delivering real–time insights [8], and where smart and connected sensors play a crucial role in the very bottom of the Predix system architecture: data and information gathering. Additionally, again in 2015, Siemens (Munich, Germany) presented MindSphere®, their Industry 4.0 platform, offering to its customers the online monitoring and analysis of globally distributed machine tools, industrial robots, or industrial equipment such as compressors and pumps.

On the other hand, manufacturers as Bosch (Stuttgart, Germany) are not only focusing on the higher tiers of the digitalization of industry [9], but also, they are shifting to generate novel sensor technologies that meet the expectations of the IIoT in terms of integrability, connectivity, intelligence, flexibility and indeed cost [10][11]. Some of the latest examples of this paradigm shift in the Bosch sensor portfolio are found in the APAS®, a bunch of intelligent

systems for man–machine collaboration, including fully sensorized and connected robots and workplaces.

Following the same trend, ABB (Zurich, Switzerland) is showing a strategy to instrumentalize with smart and low-cost sensors legacy industrial machines. This approach enables the equipment operators to upgrade their existing industrial processes with a condition monitoring strategy with a really low investment. For instance, one of the latest solutions launched by ABB in the 2016, the ABB Ability™ Smart Sensor, is designed to be directly attached to a motor frame and picks up data on vibration, temperature and other parameters and, using on–board algorithm, is able to deliver information about the motor's health that is used to reduce motor downtime by up to 70 percent, extend lifetime by as much as 30 percent and lower energy use by up to 10 percent [12].

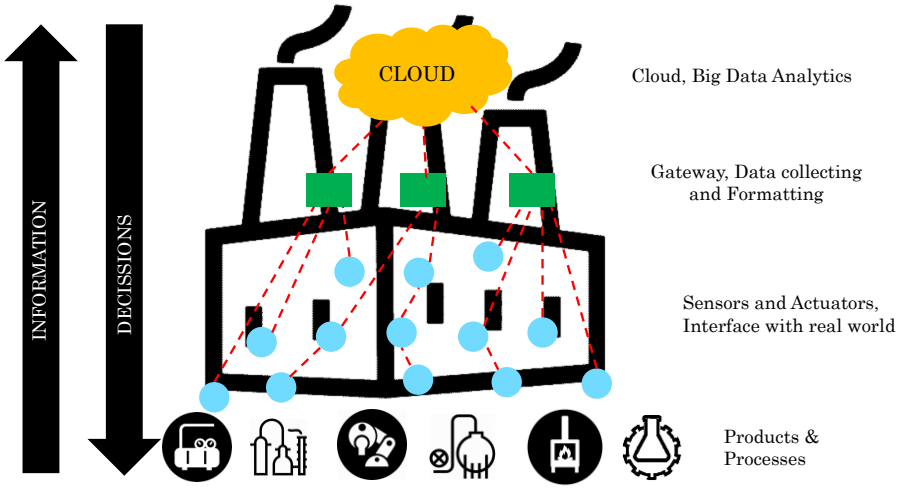

Figure 1.1–1: Schematic overview of the role of sensors within the IIoT or Industry 4.0 paradigm

Along with its analytics platform for the IIoT, the Uniformance® Suite, Honeywell is upgrading and expanding its smart sensor portfolio. As one of the historical references in process automation, Honeywell has identified that fluid management industries such as power, chemicals, and oil and gas, often require complex software architecture to ensure their operations are safe, efficient and reliable, and is proposing a IIoT technology to help solving some of these challenges [13]. The SmartLine® product family for pressure, level and fluid temperature sensing are one of Honeywell's latest example in this field, combining the smart sensor systems with software solutions and open interfaces for data access, which enable users to manage their plant assets better and optimize their productivity [14].

Even if the use of process and diagnostic data from the field level is nothing new [15], it is evident that the context of the Industry 4.0 has fostered the key stakeholders on the industrial automation to consider a huge ramp–up in terms of plant monitoring, being the smart sensors the true enabler for Industry 4.0, as they represent the data source for any service, cloud and big data applications. However, it is absolutely essential for sensor technology to be intelligent, rugged and reliable when it comes to dealing with important workplace challenges, such as critical infrastructure maintenance, or the safe interaction between people and machines [16].

Therefore, this context of eagerness for pervasive motorization within industrial environments represents an opportunity for sensor manufacturers, with several different applications waiting for in–place and real-time measurement solutions. The specific case of the industrial fluid monitoring is not an exception, delivering several examples as the real-time analysis of lubricant status at off–shore wind turbines where the accessibility is very limited [17], or the monitoring of hydraulic fluids of robotic arms in automotive plants, with several thousands of units deployed working at high loads [18], monitoring of hydraulic fluids in critical actuators as airplanes [19], etc. These use cases are clear examples demanding a tradeoff solution between an immediate availability of in situ information and a reduction in the accuracy of the results, which is the ideal scenario for solutions like the one presented in this thesis.

However, meeting not just requirements in terms of sensor performance, compactness, unitary cost, reliability, etc. but also market and economic objectives poses a considerable technical and organizational challenge for any company. Management of uncertain and evolving specifications, continuous risk assessment, synchronizing of multidisciplinary working teams (e.g. chemistry, micromechanics, optics, electronics, signal processing), pressure to cut development times in order to launch new products into market, and the complexity inherent to the technological bases of the sensor's measurement principles need to be managed efficiently throughout the design, development, validation and certification phases of the sensor product.

In this context, the work presented in this thesis describes a methodology for developing smart sensors for industrial fluidics based on photonic working principles. The work describes the different steps, approaches and considerations for bringing sensor concept ideas through different development stages, into a fully operative, reliable, compact and cost–effective sensor system, focusing on the technical and practical challenges of the use of unattended photonic sensors in the field of fluid monitoring.

1.2 In–line Real Time Fluids Monitoring

As mentioned, in the context of Industry 4.0 or IIoT, the focus is primarily on data and the exchange of data across all system boundaries. In most cases, large amount of this data is generated with the help of sensors that measure different parameters of interest throughout the production process. When these sensors are being placed directly into a process stream and offer continuous information about a certain parameter (pH, temperature, pressure, density, flow, etc.) we call them in–line and real-time sensors (see Figure 1.2–1) [20].

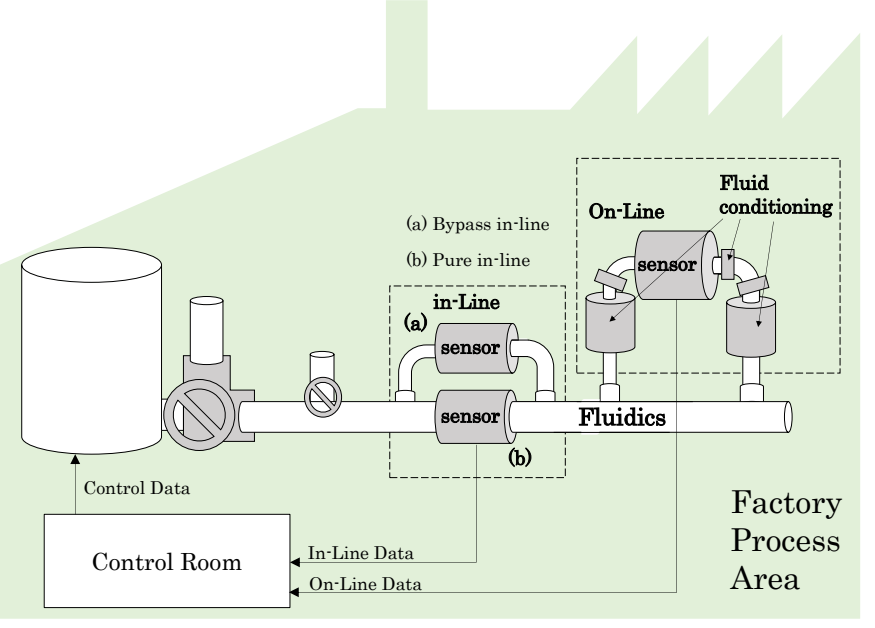

Figure 1.2–1: Schematic overview of in–line and on–line sensors within a process flow.

Among several other magnitudes and elements to monitor in the broad universe of industrial applications, the industrial fluidics (see Table 1.2.1) arise as a very challenging opportunity for smart sensor developers, not only due to the traditional requirements of high sensibility, repeatability and reliability in the measurement, but also because of the extreme working conditions (temperature, pressure, humidity, vibrations, etc.), and the necessity of sample extraction in place (e.g. by pass, in line) at the right flow and in the right volume, dealing with different viscosities, corrosive ambient and samples, non–homogeneous materials, etc. [21].

On the other hand, we may differentiate two kinds of fluids within the industrial applications: fluids that are an important part of a process, part of a machine or equipment, and fluids that represent a product their selves. Monitoring the parameters of the fluids from the first group is crucial for assuring the functionality of the process,

avoiding failures and downtimes, improving efficiency, etc. On the other hand, the products coming out from a manufacturing plant in a fluid format need to be sensed in order to maximize the quality and safety of the production batches, reduce the wastage and to comply with audit and regulatory affairs. Even if both scenarios are well aligned with the Industry 4.0 paradigm, in the first one the fluidics sensing is a fundamental part of predictive maintenance or condition monitoring approach [22], while in the second case, the sensors are part of a Statistical Process Control strategy [23][24].

Table 1.2.1: Examples of fluids present in industrial applications

Fluids / Applications	Function of the sensor
Engine and Gear Box Lubricants Hydraulic Fluids (e.g. phosphate esters)	Viscosity measurement, Water or Air content, Particle content, chemical degradation and oxidations
Coolants (e.g. Glycol)	Viscosity and absorbance
Electrolytes for Redox batteries (e.g. Vanadium)	Viscosity and color
Insulating Oil in Electrical Transformers	Oil oxidation, external contaminations (water leakages, insulating cellulose decomposition)
Gas, Diesels and Biofuels	Water in Oil, Measurement of Aromatic. Monitoring the biofuel chemical & physical characteristics (alcohol fermentation, octane number)
Heat Transfer Fluids	Viscosity and NIR absorption
Cooling Waters	Contaminant detection Plague (e.g. legionella) detection
Food & Beverages: fruit and vegetable sauces and concentrates	Product Quality, Wastage reduction Correlation to consistency and homogeneity for end product quality. Chemical analysis (Fructose, glucose, lactose, fatty acids…)
Food & Beverages: Dairy Products	Product Quality, wastage reduction, viscosity, density, fat, protein and water proportions
Cosmetics	Correlation to texture for end product quality. Surfactant, active ingredient concentration. Moisture.
Pharmaceutics	Product Safety, Product Quality Production SPC records
Pulp & Paper	Inhomogeneity control and fiber concentration. Lignin analysis. Raw water quality, turbidity of white water

Indeed, the monitoring of fluids is nothing new (see Table 1.2.2), and it was an important part of the industrial automation and instrumentalization boost that took place the 1960 decade, with several companies marketing several sensor solutions covering different magnitudes day by day, as pressure, temperature, level, flow, viscosity, moisture, pH, etc. [25][26]. Innovative sensors and actuators came from some key companies, which in a fragmented business, most of them get stuck at growth plateaus and get bought out. For instance, founded in 1956, Rosemount (Shakopee, MN, USA) started with specialty temperature sensors (RTDs) and then grew with the development of its capacitive differential pressure transducers, rapidly overtaking the traditional leaders as Foxboro (Foxboro, MA, USA) and Honeywell, and then the company was eventually acquired by Emerson (Saint Louis, MO, USA) in 1976. These convulse years also witnessed the creation or the consolidation of other reference companies in the field of fluid monitoring as Brooks Instruments (Hatfield, PA, USA) specialized in flow metering, Beckman Coulter (Pasadena, CA, USA) in pH and other chemicals, Yokowaga (Tokyo, Japan) offering flow meters, Balluf (Neuhausen, Germany) with pressure and photoelectric sensors [27][28][29]. In the forthcoming years many other big players started to find their niches in the fluid control and automation field with examples as Parker (founded in 1917, Cleveland, OH, USA), Pall (founded in 1946, New York, NY, USA), Hydac (1963, Sulzbach, Germany) or Burkett (founded in 1946, Ingelfingen, Germany).

Table 1.2.2: Some of the most common physical or chemical parameters of Interest in Fluid Monitoring for industries like Energy, Biotechnology, Chemical, Brewing, Pulp & Paper, Petrochemical, Food and Beverages, etc. [30]

Parameter	Units	Measurement Principles
Viscosity	Poise	Falling–cylinder viscometer, rotating disc viscometer, capillary sensors
Flow [31]	L/min, m^3/s	Ultrasonic flow meters, Electromagnetic flow meters, Pressure flow meters, Rotating flow rate devices, Vortex flow meters

Temperature [32]	Fahrenheit (°F), Celsius(°C), Kelvin(K)	Expansion of materials, Electrical resistance change, Thermistors, Thermocouples, Pyrometers, Semiconductors, Index of Reflection
pH	pH units	Electrolytic principles
Pressure [33]	pounds per square inch (psi), Pascal (Pa), Bar	Manometer, Diaphragms, Capsules, and Bellows, Bourdon Tubes, Piezoelectric pressure gauge, Ionization gauges
Turbidity [34]	Nephelometric turbidity units (NTU)	Optical sensor (scattering), Nephelometry (diffuse radiation), Turbidimetry (attenuation of a radiant flux)
Opacity	mm^2/mass	Optical sensor (absorption)
Moisture [35]	%, ppm	Psychrometers, Resistive hygrometer, capacitive hygrometer, Piezoelectric or sorption hygrometers, Microwave absorption, Infrared absorption
Air presence	%, ppm	Optical sensor (absorption), Imaging sensor
Particle Content	Number of particles	Optical sensor (scattering), Imaging sensor, Ultrasound, Inductive
Color	CIE–Lab, RGB	Optical sensor(absorption)
Density	g/m^3	Vibration sensors, Ultrasound sensors
UV–VIS–NIR Absorption	Arbitrary units	Optical sensor (absorption)
Conductivity [36]	S/m (Siemens/meter)	Amperometric, Potentiometric or inductive probes
Level [37]	n.a.	Ultrasonic, Resistive, Optic, capacitive

The golden age of analog sensors lasted for almost three decades, until the early digitalization of sensors that took place in the mid–nineties. The evolution continued with the connectivity expansion, with a bloom of wirelessly connected industrial sensors around 2005 [38]. These connected sensors paved the way, one decade later, for the already mentioned Industrial Internet of Things, where sensors are supposed to upload to the Industry 4.0 cloud reliable, standardized, significant, real time and in–place information about fluidics used in industrial environments. Therefore, meeting the expectations of the Industry 4.0 will only be possible if, asides the sensor's measurement principle, a full set of on–board algorithms, communications, standard interfaces, auto calibrations, etc. are included within the sensor system itself (see Chapter 3 for smart sensor concept description).

Asides to the addition of layers of intelligence, connectivity, etc. the fluidics sensors have been incorporating different physical and chemical parameters to their sensibility portfolio. The fluidics sensors are gradually becoming into complete integrated mini laboratories, able to measure specific chemicals, contaminants, presence of particles, oxidations, sample homogeneities, etc. which their in–line and real time motorization is very relevant and even critical for several industrial processes (see table 1.2.1). Nevertheless, traditionally, these sensors have been bulky, expensive, difficult to integrate and maintain, and most of them are far from becoming integral part of the IIoT paradigm which is jeopardizing and contributing negatively to their massive deployment in the Industry 4.0 scenario.

However, in this context, photonic sensors arise as a promising technological alternative to close the gap between the Industry 4.0 requirements and the performance of the current sensors. Optical methods can non–invasively assess the microstructure, function, and composition of fluids, as well as deliver a reliable operation while working in the field. Additionally, the revolution in digital electronics has significantly reduced both the price and size of components (sensors, light sources, computing units) critical to most optical systems. Integrating such optical components with compact microfluidics, micromechanics and low–cost electronics and communication systems allows for building robust photonic smart sensor systems that are inexpensive, scalable and ready for their deployment in the Industry 4.0 arena.

1.3 Cost Effective Smart Photonic Sensors

Photonics-enabled sensors deliver a comprehensive measurement of a sample relying on the light-matter interaction processes, which will be reviewed in depth in the Chapter 2. Basically, when a light beam hits a material, the properties of the original light ray get modified depending on the physical and chemical composition of the sample material. Therefore, if these changes in the light are recorded, and compared with the original light, or with the light outputted by other sample materials, relevant information about the composition of the sample can be obtained.

Then, we could define a photonic sensor as a system which integrates all the components for performing a measurement based on the light–matter interaction. If we narrow down to the specific case of photonic sensors for fluidics, the liquid sample conditioning and management should also be included within the sensor to provide a true autonomous operation.

Traditionally, the main subsystems included in a photonic sensor are the ones depicted in Figure 1.3–1.

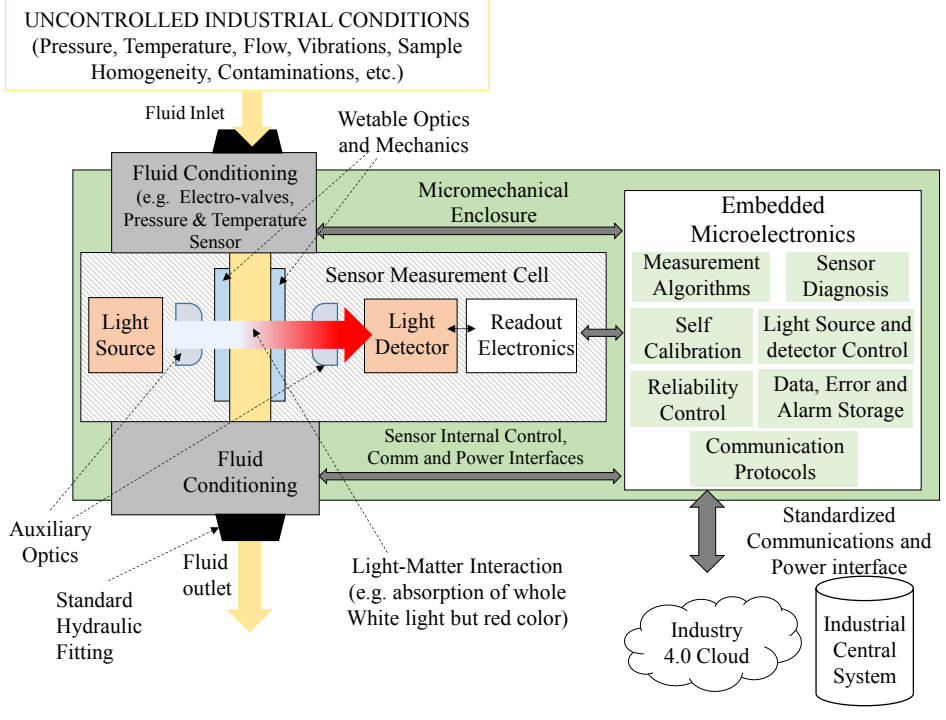

Figure 1.3–1 Block diagram of a Photonic Sensor, working in transmission mode, installed within the industrial process through standard hydraulic fittings and connected to the Industry 4.0 cloud via standardized interfaces.

These main blocks include the **photonic subsystem**, comprising the light emitter and the light detectors, and all the complementary electronics for their driving, readout, signal conditioning and compensation. The system could also require the use of some auxiliary optics as filters, lenses, pinholes, etc. for the conditioning of the light beams.

Another important subsystem in fluidic sensors is known as the **wettable part**. This specific part of the sensor is the one in contact with the fluid and the one responsible for handling and bearing with all the environmental conditions of the sample. The wettable parts should stand high working pressures and temperatures of the fluid, should avoid any leakage under the working flow and viscosities range, should be compatible with the chemical properties of the sample fluids (e.g. corrosive liquids) and for the specific case of photonic inspection techniques, the wettable parts need to be compatible with the properties (e.g. absorption spectrum, index of reflection) of the light incident to and coming out of the sample fluid. Normally, the wettable parts include an optical window transparent to the working spectrum of the light, some sealing and some micro mechanical parts for assuring the water tightness of the whole structure.

Besides, the part of the sensor where the fluid sample is confined or flows through for its analysis is defined as the **measurement cell or chamber**. This is a very important module in the system, with important requirements in terms of fluid dynamics management and fabrication and assembly tolerances. For instance, the microfluidics design should avoid the generation of flow turbulences within the measurement cell contributing to sample homogeneity (as described in Chapter 3). Besides, the mechanical tolerances in the chamber geometry impact, for example, on the light path dimensions (the distance that the light needs to cover from emitter to detector). Not meeting the nominal tolerances, dramatically affects the measured light power due to the exponential dependence of the light absorbed within a medium with the light path distance (as described in Chapter 2).

The different **micromechanical parts** are assembled into the whole sensor body mechanics, which is in charge of: solving the standardized hydraulic fittings and their matching with the measurement cell, assuring the optical alignment of different component, enabling the assembly of all the electronic and connectronic parts, solving or supporting the external enclosure which should be compatible with all the environmental conditions (normally standardized as IP rating of the product).

The smartness concept is brought by the presence of a customized **embedded electronic subsystem**. The embedded CPU will

run different software pieces in charge, among others, of performing the light emitter and detector control, executing the measurement algorithms for outputting the analysis result, applying internal performance assessments and calibrations. This electronic part also, deals with all the power issues, converting the external voltage input (e.g. 24V, 12V) to the internal levels (e.g. 5V, 3.3V) or managing a battery element. In addition, the embedded electronics store all relevant information as measurement results, alarms, errors and key performance indicators that are extremely important for the life management of the sensor. The electronics is also in charge of implementing the standard communication protocols (wired or wireless) for assuring a secure, reliable and seamless information exchange between the sensor and the intermediate layers of the Industry 4.0 architecture.

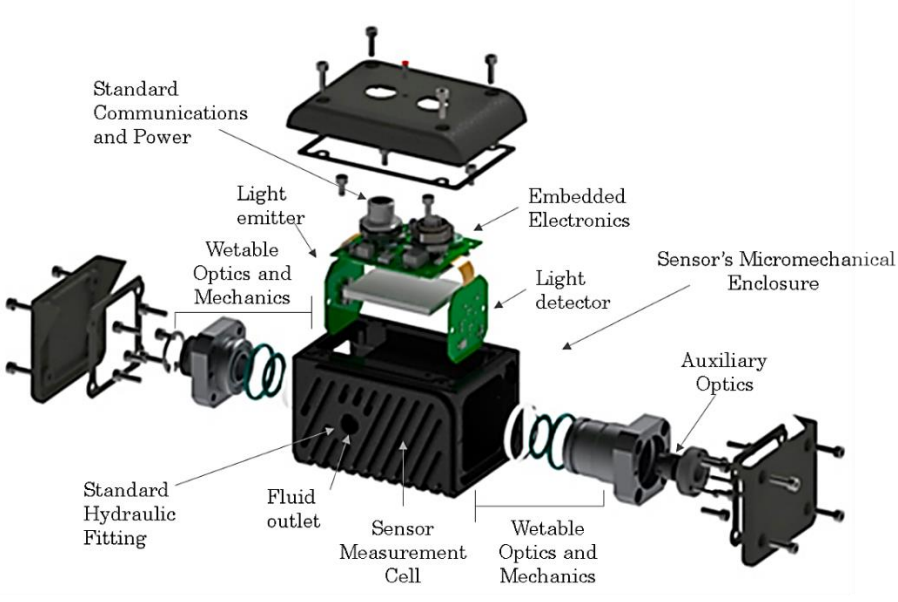

Figure 1.3–2 Teardown of OilWear PICO® sensor product. Different mechanical parts, optoelectronics, electronics, seals, windows, optics and connections are displayed.

In some occasions, some external **fluid conditioning circuitry** is also included within the sensor. Among different alternatives, a combination of some of the following items could be found as part of the sensor systems: electro–valves, flow controllers, pressure limiters, particle filters, pressure sensors, temperature sensors, pumps, etc. However, normally, all the sensor designs try to avoid the need of these bulky hydraulic components that jeopardize the potential low cost and compact size of the photonic sensors. Nevertheless, the system evolution for dealing with non–conditioned fluids is not straightforward, and several modifications especially in the lighting

and detection systems are required as described in one of the use cases of the Chapter 5 (the stroboscopic vision sensor).

Once the Smart Photonic Sensor concept has been described, we will introduce the cost effectiveness term, which requires several considerations. One typical mistake is to reduce the sensor's cost to the aggregation of costs of the individual components, with some contributions from assembly and calibration processes. But this approach is far from being real. The sensor's unitary cost should also consider all the previous research, engineering and tooling costs, normally defined as Non–Recurring Engineering (NRE) costs [39]. Additionally, budget for guaranty period and post–sales support should also be allocated.

Besides, if we widen the perspective, we should not only consider the unitary cost of the sensor, but the Total Cost of Operation [40], that considers the expenses of the sensor installation, maintenance, removal and disposal as part of the investment required by the end user for using the sensor technology (reviewed in depth in Chapter 3). Imagine the real cost behind a situation where a very cheap sensor requires a human operator to calibrate it each week. However, the total cost of operation should also consider the benefit and profit obtained by the end–user due to the installation of the sensor, as, for instance, reducing the downtime of his machinery.

Figure 1.3–3 Colorimetric Sensor for real–time analysis of lubricant oil ageing in gear–boxes.

After having exposed the different considerations behind the real cost of a sensor, we should mention that, currently, we are witnessing a revolution in the photonic and optoelectronic technologies, that are enabling not only to enhance the features of emitters and receivers, but also to reduce their costs dramatically [41] [42], opening the door to the development low cost photonic devices.

Therefore, it is clear that, for achieving the required cost effectiveness, the remaining contributor factors in the sensor costs should be shrunk down (see Figure 1.4–6). While installation and maintenance costs are being controlled thanks to IIoT approaches [43], minimizing the RTD and NRE costs of a photonics–based sensor is not evident, and several risks hinder the achievement of a cost-effective product, as it is described in the next section.

1.4 New photonic devices and their integration into products

Since its emergence at the end of the 60s [44], the idea of fully integrated photonic devices has been captivating scientist and engineers' imagination for more than five decades already. The promise of unmatched features in emission powers, detection sensibilities, longer wavelengths, tunable directivities, etc. together with dramatic reduction of component cost and compactness has sufficed to foster a tremendous amount of effort on providing an integrated platform allowing a monolithic or hybrid integration of photonics, micro–electronics, optics and micro–mechanisms [45].

However, and aside some big exceptions as LEDs and CMOS imagers, despite large R&D investments, photonic integrated circuits with integration levels exceeding a few components did not succeed in entering the commercial marketplace for more than four decades. Skeptics started claiming that integrated optics was only a promising technology and would ever remain so [46].

Therefore, without a true integration, the main trend in photonics device development was to assemble discrete components that are based on a large variety of materials and technologies (lenses, gratings, detectors, electronics, connectors, etc.) into a customized platform. However, the final outcome of this approach was normally crystallized into bulky and expensive photonic systems. Even when huge efforts were put in miniaturization and cost effectiveness of the solution, the results obtained were far from being as compact, lightweight and low cost as expected, as exemplified in Figure 1.4–1).

Nevertheless, as mentioned earlier, there was also a bright side in the integrated photonics landscape centralized in the continuous breakthroughs coming from the LED light emitters or from the CMOS image detectors. Mainly pushed by consumer market, both technologies have unbelievably evolved in parallel in the last decade [47][48][49]. Currently, the availability of a huge portfolio in CMOS detectors (resolution, optical format, sensibility) and LED emitters (spectral range, emission power, form factor), enables the use of high

performance detectors and emitters at minimum costs, even below 1€ per unit. This sort of emitter and detector technology is behind several cost effective industrial machine vision solutions

The current trend is to achieve longer wavelengths, efficiency and stability in LED systems [50], including wide band LEDs [51]. Regarding the imagers, looks like the competition of the solutions in the visible range is to increase the resolution, enhance the dynamic range and sensibility of the detectors [52]. However, several efforts are being put on increasing the wavelength range to NIR and SWIR ranges to enable cost effective Hyperspectral cameras [53].

Nevertheless, even if the LEDs and CMOS imagers have experimented and exponential ramp up in the last decade, from the photonic point of view they are relatively simple structures, since they are basically built upon color filters, diffuser lenses and light sources or receiver. Additionally, it could be fair concluding that the integration achievements witnessed in both cases are much more related with the microelectronics domain rather than with the pure photonic science.

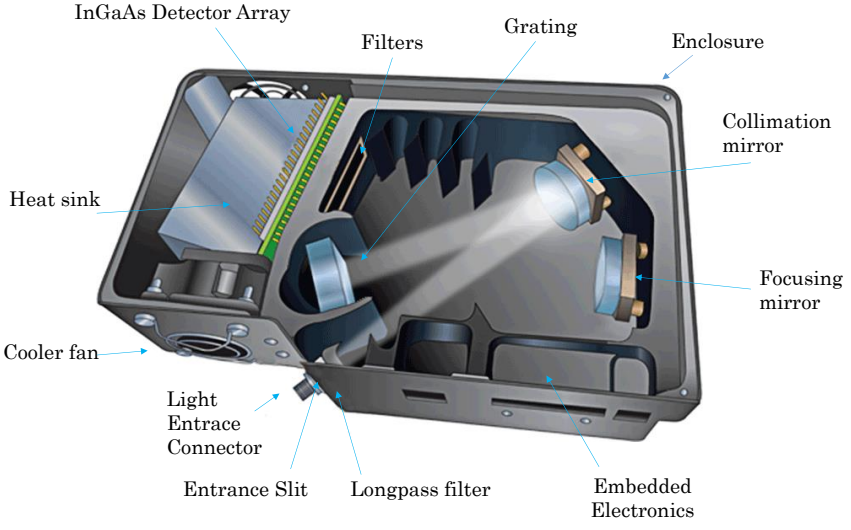

Figure 1.4–1. 182 x 110 x 47 mm, 1.18 kg, 256-pixel Detector Array, NIRQuest ® Device from Ocean Optics ®. Launched in 2015 with an approximate cost of 15K€.

On the other hand, the progresses made in the field of micro–opto – electromechanical systems (MOEMS) could be considered as the true representatives of complex photonic integration [54][55]. Introduced in mid–eighties [56], heterogeneous integration of MOEMS and integrated circuits (ICs) allows the combination of high–quality optical and photonic MOEMS materials such as monocrystalline silicon (Si) with standard CMOS–based electronic circuits in order to realize complex optical systems. Asides the integration of materials

with optical properties, MOEMS, as the MEMS devices do, also take advantages of the mechanical properties of silicon, allowing the integration of moving parts within the device, which are extremely useful for fabrication complex photonic devices as spectrometers [57], projectors (see MOEMS based electro–opto projector by Bosch in Figure 1.4–2), LASERs [58][59], light modulators [60], etc. by companies and research laboratories around the world.

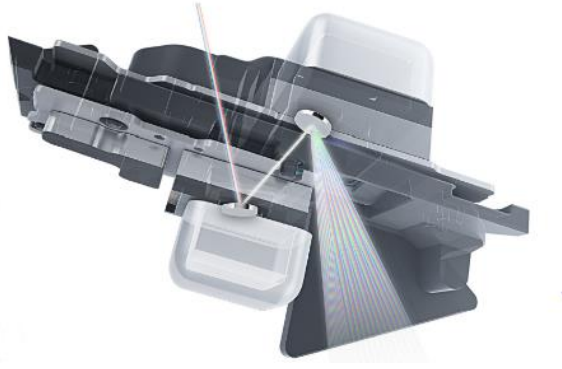

Figure 1.4–2 Bosch SensorTech's new MOEMS technology–enabled micro projector BML050. Featuring compact size, power efficiency, robustness and reliability

An even if the optical MEMS have had a difficult development road during the last thirty years [61], the significant successes reported lately may have finally opened the door to mass commercialization of MOEMS devices. Focusing for instance to the NIR micro spectrometer segment, during the last years a large amount of these research and development efforts have crystalized in breakthrough products and prototypes. In this specific case, in five years, we have witnessed a technological evolution that has enabled the migration from discrete/component based systems, into chip–scale solutions. The new generation of MOEM–based NIR spectrometers offers solutions hundred times more compact at prices hundred times lower.

The latest and most representative examples are coming from large firms as Hamamatsu, from innovative SMEs as Spectral Engines, Si–Ware or PixelTEQ (now acquired by Ocean Optics), or from joint ventures as Viavi (formerly JDSU) and Espross. All of them will be launching new product lines or updating their product portfolio in the area of integrated NIR spectrometers. All these solutions are very compact, cost effective and feature rich (see Figure 1.4–3 and Figure 1.4–4), compared to the latest non–integrated spectrometers (see Figure 1.4–5) which offer faster scanning speeds and better Signal to Noise ratios but at much higher (x10, x100) cost and larger sizes (x10–x100).

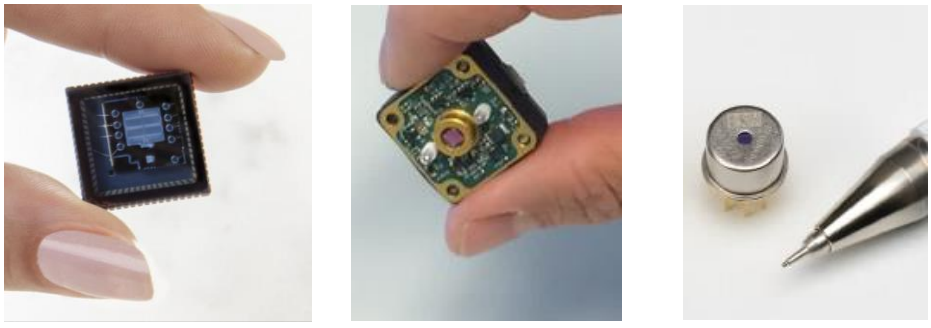

(a) (b) (c)

Figure 1.4–3. Chip scale, single photo–detector NIR micro–spectrometers, (a) NeoSpectra MICRO from Si–Ware, (b) NM series from Spectral Engines, and (c), C13272 series from Hamamatsu.

(a) (b)

Figure 1.4–4. Filter array and 2D photo–detector array based VIS–NIR micro–spectrometers. (a) PixelTEQ's PixelSensor™. (b) Espross's SPM64–NIR.

This new generation of photonic devices, as the extremely compact and cost effective NIR micro spectrometers (see Table 1.4.1), are enabling an enormous number of potential applications and products for improvement and automation of industrial processes, efficiency enhancement, product safety control, etc. answering the demands of process industries for increasing the efficiency of manufacturing processes and the quality of their products. Basically, these industries are requesting to bring photonic measurement solutions for field use, and MEMS-based photonic sensors are considered as true enabler to deliver accurate in-line real–time measurements to applications which are until now only accomplished in laboratories [62].

(a)

(b)

(c)

Figure 1.4–5. Non–integrated spectrometers. (a) MicroNIR PRO from Viavi (formerly JDSU). (b) QRed from RGB Photonics, launched in 2017, (c) FlameNIR micro spectrometer from Ocean Optics, launched in 2016.

Table 1.4.1: Summary of the latest integrated NIR micro spectrometer products.

Device	Working principles	Working Range (nm)	Size (mm)	Cost[1] (€)
NeoSpectra Micro (2017)	Monolithic Michelson interferometer and single uncooled InGaAS Photodiode	1350 – 2500	~18 x 18 x 4	100
NM series (2016 – 2017)	Micromechanical Fabry–Perot Interferometer and single InGaAS Photodiode	1350 – 1650 1550 – 1950 1750 – 2150 1950 – 2450	25 x 25 x 17.5	100
C13272–series (2016–2017)	Single InGaAs Photodetector and Fabry–Perot interferometer	1550 – 1850 1350 – 1650 1750 – 2150	Ø9 x 6	100

[1] Notice that these costs should be considered as an order of magnitude approximation. These costs are estimations based on information from manufacturers but do not represent any official quotation at it may be bonded to volume purchases or other trading conditions.

PixelSensor (2017)	8 channel Thin Film Filter and Si Photodiode array	400 – 1000	9 x 9 x3	10
SPM64–NIR (2017)	64 channel Thin Film Filter and PD array	775 – 1075	17 x 6 x 3	5
MicroNIR PRO (2015)	Linear Variable Filter and uncooled InGaAs Photodiode 128 pixel array	950 – 1650	~ Ø 50 x 50	15K
FlameNIR (2016)	Diffractive grating optics and uncooled InGaAs Photodiode 128 pixel array	950 – 1650	89 x 63 x 32	10K
Qred (2017)	Czerny–Turner approach spectrometer based on fixed surface mirrors, reflective grating and cooled InGaAs 512 pixel array	Default: 950 – 1700 Custom: 800 – 2500	67 × 58 × 20	20K

However, the availability of compact, cost effective cost and feature rich optoelectronic components should not hide the high difficulties, complexity and risks entailed in the design of a photonics-based low-cost sensor system. The uncertainties, the multi-domain nature of the system and time-to-market pressures among others hinder the integration of the novel photonic components into successful products meeting the customer requirements in terms of performance, size, cost and regulations.

Therefore, with the aim of contributing to the field of cost effective sensor solutions (see Figure 1.4–6), the objective of this thesis is to provide a design methodology focused on the integration of these breakthrough photonic devices (see Figure 1.5–1), and several different technological blocks (physics and chemistry, electronics, mechanics, fluidics, optics, data processing, communications, etc.) to assist in the development of fully autonomous, reliable, standardized and cost effective Smart Photonic Sensors for monitoring industrial fluidics.

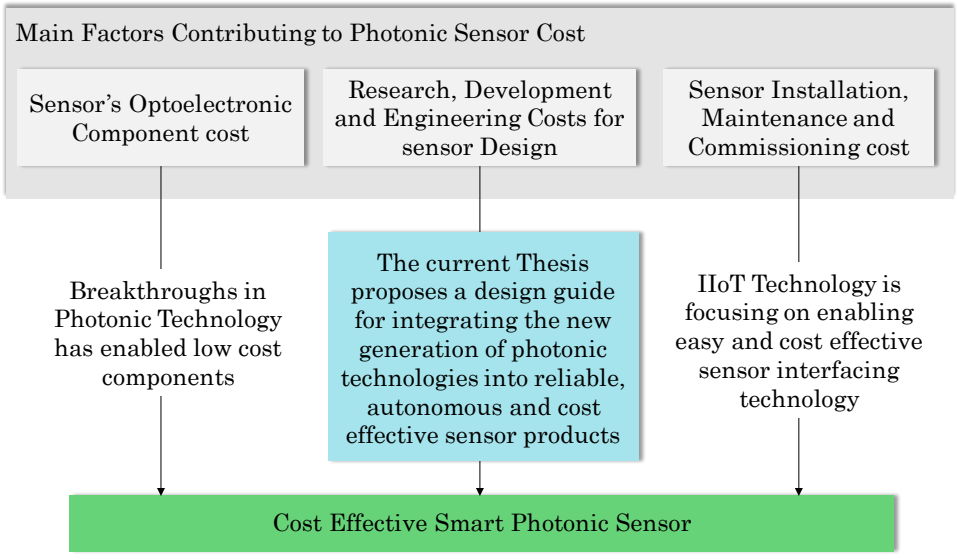

Figure 1.4–6. Diagram displaying the three major factors impacting in the final cost of a sensor system and, how the different technological trends (photonic integration and IIoT approaches) are contributing to lower the cost in two of them evidencing the need of putting some efforts to improve the sensor design and development efficiency, which is, actually, the motivation and objective of this thesis.

1.5 This thesis in the Photonic Sensor landscape

Within the vast landscape of photonics devices, the investigation presented in this thesis focuses on the main challenge of enabling the integration of latest photonic components into autonomous, reliable and cost-effective sensors applied to the in–line monitoring of industrial fluids.

The advent of innovative technology concepts in the field of optoelectronics, with better features, compact integration and dramatically lower costs has opened the door to a high number of potential applications. However, the expectations put on those new potential products enabled by the new photonic components are also increasing, and lower detection limits, lower costs, autonomy, communications and higher compactness are being requested by the end users.

The integration of these photonic components with other fluidic, mechanic, electronic, and data processing subsystems is not evident. In addition, the side effects generated by assembly tolerances, temperature drifts, vibrations, etc. are often underestimated while specifying a sensor. Besides, the impact of verification and validation of a laboratory analysis technique, which has been embedded into a

tiny device, with no sample preparation, and with limited access to it, is often also huge, and not considered in the sufficient manner while planning a fluidic sensor device development.

In addition to the complexity inherent to the photonic measurement principles and their integration into products, stricter regulatory requirements, and the ever-increasing importance of reimbursement decisions for successful sensor commercialization should also be taken into consideration.

The sum of all these factors clearly jeopardizes the crystallization of the original photonic components' low cost, superior performance and reliability into the final smart sensor product.

This integration challenge is exactly where the investigation of this thesis has put the focus. We understand that the development of a smart sensor based on the latest generation of photonic components requires careful planning and strategy–setting, coordinated decisions, and consistent and rigorous development processes.

In this situation, the main contribution of this thesis is to develop a methodology for the effective and agile integration of optoelectronics components within the rest of subsystems, towards a photonic sensor development, focusing on the specific case on in-line fluidics. This methodology aims at guiding the design and engineering teams across the different stages, from proof-of-concept validation to product certification, in the context of complex and uncertain system development with tight project times and costs.

To achieve this general objective, a full review of the light and matter interaction process has been done, with the aim of complementing the engineering view on the sensor integration with a deep and scientific understanding of the physical and chemical processes that define the measurement principle. This step has been considered critical, since several integration risk and performance limitations are found in the most basic fundament of the sensor concept. Additionally, latest alternatives in light emitters, receivers and optic components have been studied, assessing their performance and risks for a cost–effective and reliable deployment in industrial environments. The outcomes of this research could be found in Chapter 2.

Additionally, in Chapter 3, sensor fundamentals and the different approximations for analyzing and extracting relevant information from photonic signals has been studied, which should be embedded into the sensor system to make them smart, fulfilling a basic request from the Industry 4.0. Special attention has been paid at the in–line operation mode and to the fluid management in the proposed sensor systems. The research done in this Chapter 3 is considered also very important because clear heterogeneous

integration (physics, and chemistry, optoelectronics, fluidics, mechanics, electronics, data processing, etc.) problems are identified and addressed.

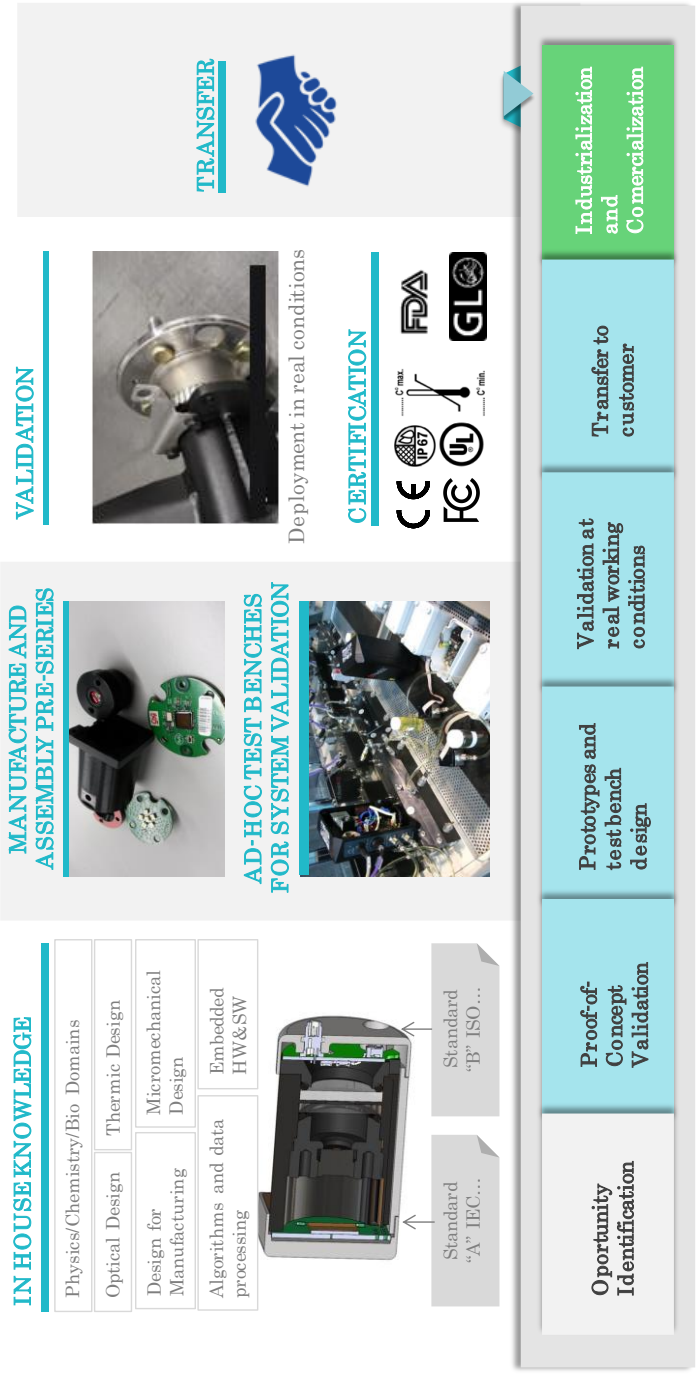

Figure 1.5–1 Stages covered in the methodology proposed in the thesis for assisting the development of Photonic Sensors for in–line monitoring of industrial fluids.

As mentioned, all these insights have been merged in a comprehensive development model that captures all aspects of smart photonic sensor development and commercialization from early–concept selection to post–market surveillance, which is described in Chapter 4. This model was constructed based on scientific review and the analysis of best–practices found in different real developments, as the ones included in the Chapter 5 of this thesis for model validation.

The concluding chapter of the thesis, Chapter 6, includes the main conclusions extracted from this research, and outlines some future investigation lines.

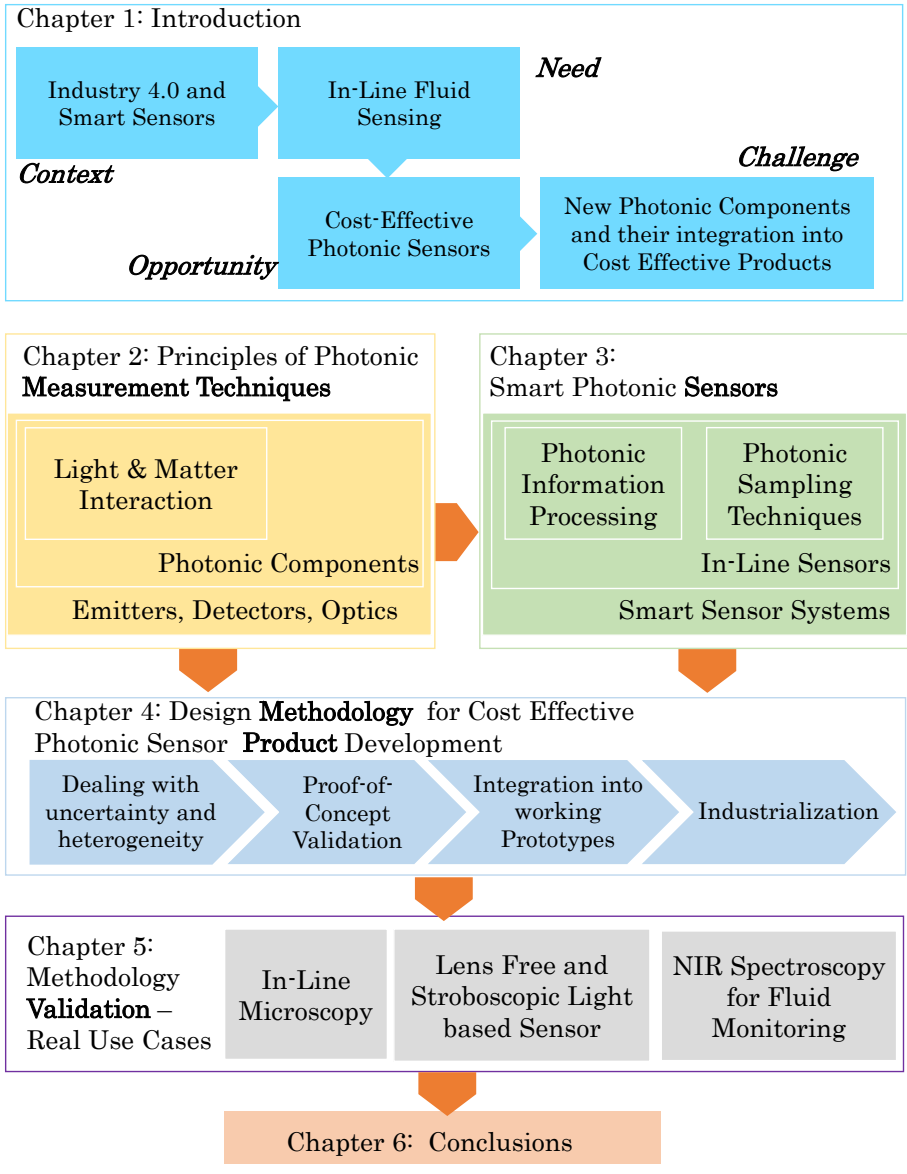

Figure 1.5–2 Thesis Outline.

The most notable scientific, technological and industrial advances of this thesis are listed in Table 1.5.1, together with the chapters and publications in which they are addressed.

Table 1.5.1: Summary of Science, Technology and Industrial advances of this thesis.

Science, Technology and Industrial advances of this thesis	Chapter	Publication
Methodology proposal	[4]	[261]
Integration of Holographic, Lens–Free and Stroboscopic Photonic Sensor	[5]	[260],[261],[262],[263]
Integration of in-line microscopy Sensor	[5]	[259]
Integration of Transmittance NIR Sensor	[5]	[264],[265]

2.

Principles of Photonic Measurement Techniques

The thorough understanding of the photonics–based sensors, including their potential features, intrinsic complexity and the entailed uncertainties requires mastering the basic scientific fundaments involved in the process of using the light for accomplishing measurements about chemical and physical parameters. This is the reason why this chapter reviews and outlines the fundaments of the light and matter interaction processes, describing the most important effects and phenomena happening when the light radiation enters a sample and how they could be used for measuring certain parameters of the matter. Fundamental processes as reflection, absorption, diffraction, scattering, fluorescence, etc. are reviewed as they constitute the core of any photonic sensing technique, and the main considerations for bringing these principles to sensor products is introduced. Additionally, the different light sources (emitters), light receivers (detectors and spectrometers) and light modulator and conditioning elements (optic components) are presented and described in the context of low cost sensor systems.

2.1 Photonic Inspection: The Interaction between Light and Matter

The interaction between the light and matter (e.g. solids, liquids, gases) is one of the most exciting chemo–physical effects that can be witnessed, and has been subject of deep studies by several scientists since the dawn of the science. When the light meets the matter a cascade of reactions and effects happens. The incoming light suffers different modifications, mostly depending on the structure of the matter and the wavelength and power of the light. The possibility of analyzing chemical and physical properties of the matter through the study of these modifications that happened to the emitted light is straightforward and is the base for the development of a photonic inspection technique.

This chapter will review the most important interaction between the light and matter, paying special attention to those with highest potential for being translated into a low-cost inspection technique.

2.1.1 Fundamental Description of the Light

The light radiation is a relatively narrow part within the electromagnetic spectrum, covering the Ultraviolet, Visible and Infrared regions (see Figure 2.1-1). This light is generated by different means, being the most famous one the Thermic Radiation, which, according to Planck's Law, defines that any body in a thermal equilibrium with its environment, will emit electromagnetic radiation in a frequency band defined only by its temperature, radiating the same intensity in all directions.

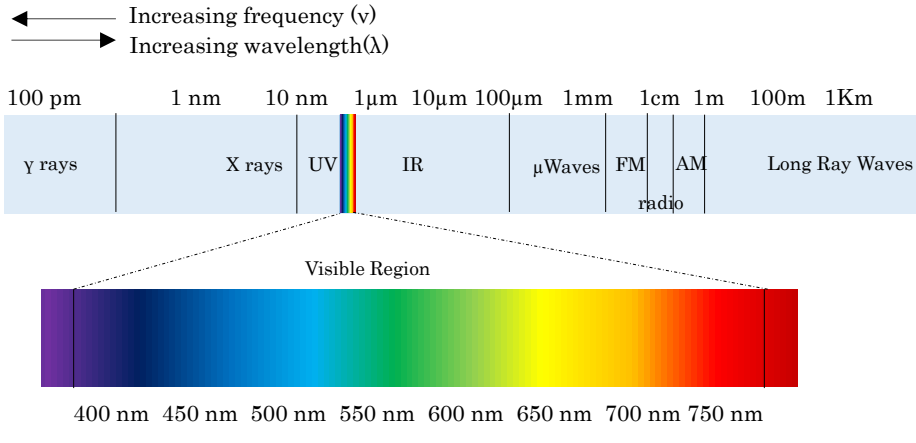

Figure 2.1-1 Electromagnetic spectrum with detailed view of visible light

This propagation of the light will be dependent on the medium that light rays are crossing, affecting their direction and its speed. This effect is described as the Index of Refraction, n_{medium}, of a certain medium, which defines the velocity of the light across it (see Eq. 2.1–1), and will be later used for defining the direction of the light rays with the Schnell's Law.

$$n_{medium} = \frac{c}{v} \quad \text{(dimension less)} \qquad \text{Eq. 2.1–1}$$

Being c (299,792,458 m/s) the speed of light in a vacuum and v (m/s) the speed of light in the medium.

However, the detailed description of the light propagation across different mediums has historically been under scientific discussion. After several attempts to define the behavior of the light, the most accurate description came from Newton[2] and his contemporaries Hooke[3] and Huygens[4], representing their works the controversy in understanding the light as a wave or as a particle.

While Newton described the light with a corpuscular approach, considering that the light was composed of several finite elements, Hooke and Huygens mathematically refined the wave viewpoint for understanding the light as a propagating wave. The wave theory was later developed by Fresnel[5] and Young[6], with his famous double slit–interference, and the wave description became predominant theory until the atomic theory was refined in the early 1900. At that time, the already mentioned Planck[7] and Einstein[8] found several evidences while working on their black body radiation and photoelectric effect, which seemed impossible to describe with the wave approximation of the light, and the scientific community shifted towards the light-as-particle description.

Nowadays, the controversy continues, but there is broad acceptance of a mixed approximation for defining the light as a train or particles, photons, that somehow describe features of waves. This property is referred to as the wave–particle duality

Unlike regular waves, that will lose their energy gradually while propagating in a medium, the light waves will lose some of its particles or photons. At this point, it is important to understand the energy of a photon E, (see Eq. 2.1–2) and the fact that, as described by

[2] Isaac Newton, British physicist, 1643- 1727.
[3] Robert Hooke, British scientist, 1635-1703.
[4] Christiaan Huygens, Dutch scientist, 1629-1695.
[5] Augustin-Jean Fresnel, French engineer and physicist, 1788-1827
[6] Tomas Young, British physicist, 1773-1829.
[7] Max Planck, German physicist, 1858-1947.
[8] Albert Einstein, German physicist, 1879-1955.

quantum theory, its energy cannot decrease: the photon will exist or it will be fully absorbed in a medium.

$$E_{photon} = h \cdot f = h \cdot \frac{c}{\lambda} \quad (J = kg \cdot m^2/s^2) \qquad \text{Eq. 2.1–2}$$

Being h the Planck Constant (6.626×10^{-34} m^2 kg / s), f (1/s) the frequency of the light, c (m/s) the speed of light in a vacuum and λ (m) the wavelength of light in the medium. This equation clearly displays that light of higher frequencies (UV) will have more energy than light of lower frequencies (IR).

So, if the energy of the photon must be conserved, this means that the photon will keep its frequency f, and so will do the light. This is an important consideration to understand the effect on the wavelength λ of the light when passing through a medium. The wavelength of the light, **λ,** defines the distance travelled by a photon in a given period of time across a certain medium, which is described by Eq. 2.1–3 for the vacuum, and generically by Eq. 2.1–4 for any given medium (combining Eq. 2.1–3 and Eq. 2.1–1). Therefore, the wavelength and the speed of the light depends on the medium (see eq. Eq. 2.1–1 and Eq. 2.1–5), but not its frequency, which remains constant for each propagating photon.

$$f = \frac{c}{\lambda_0} \quad (Hz = 1/s) \qquad \text{Eq. 2.1–3}$$

$$f = \frac{v}{\lambda} = \frac{c \cdot n}{\lambda_0} \quad (Hz = 1/s) \qquad \text{Eq. 2.1–4}$$

$$\lambda = \frac{\lambda_0}{n_{medium}} \quad (m) \qquad \text{Eq. 2.1–5}$$

Therefore, the main characteristics describing the light radiation are **intensity of the radiation** (number of photons), **frequency** (vibration of the photon), propagation direction (from the emitter to the observer) and **polarization**, which describes the spatial evolution of the electromagnetic wave across the propagation plane.

With regard to the intensity of the light, its interest is twofold, because sometimes, the interaction of the light with the matter requires achieving a certain level of excitation, which is achieved increasing the light intensity, as it is the case for instance in the fluorescence effect. Additionally, the ability of understanding the slight changes that may occur in the original light due to the properties of the target matter will require the acquisition of the resulting light intensity for post processing it.

There are two main measurement formats for quantifying the intensity of the light: the radiometric and the photometric domains

[63], and the different light sources or detectors may reference to one or both of them for specifying their properties. The photometric units were defined for emulating the response of the human eye, which was defined by the Commission of Illumination (CIE) in 1924, and therefore only covers the frequency range to which the humans are sensible.

Depending on the application, the specifications might be given using any of the following radiometric quantities: power, also called radiant flux and measured in watts (W), irradiance (measured in W/m^2), radiant intensity (measured in watts per steradian (W/sr), and radiance (measured in W/m^2 sr). The equivalent photometric quantities, which are listed in the Table 2.1–1, are based on the international system unit for luminous intensity, the candela (cd).

Table 2.1–1: Radiometric and Photometric quantities.

Quantity	Description	Diagram	Radiometric Unit	Photometric Unit
Flux	Total light emitted in all directions		Watts	Lumens
Intensity	$\frac{\text{Flux}}{\text{Solid Angle}}$	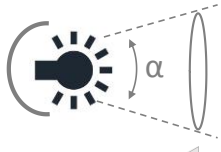	Watts/ steradian	Lumen/ steradian = candela
Irradiance	$\frac{\text{Flux}}{\text{Area}}$	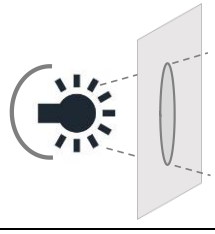	Watts/ $meter^2$	Lumen/ meter = LUX

Focusing on the light frequency, among the different sub–bands of the UV, visible and IR spectrums, this thesis will mainly focus on the long–wave UV (215 – 400 nm), on the whole visible range (400 – 800 nm), on the Near Infrared or NIR (800 – 1100 nm), on the Short-Wave Infrared or SWIR (1100–2500 nm), and the short leg of the Medium Infrared (MIR) that ranges up to the 5000 nm. It should be noted that matter may be responsive to certain frequencies of the light while remains inert to others, which is, actually, the base for the different principle of operation of the analysis of the matter through the light.

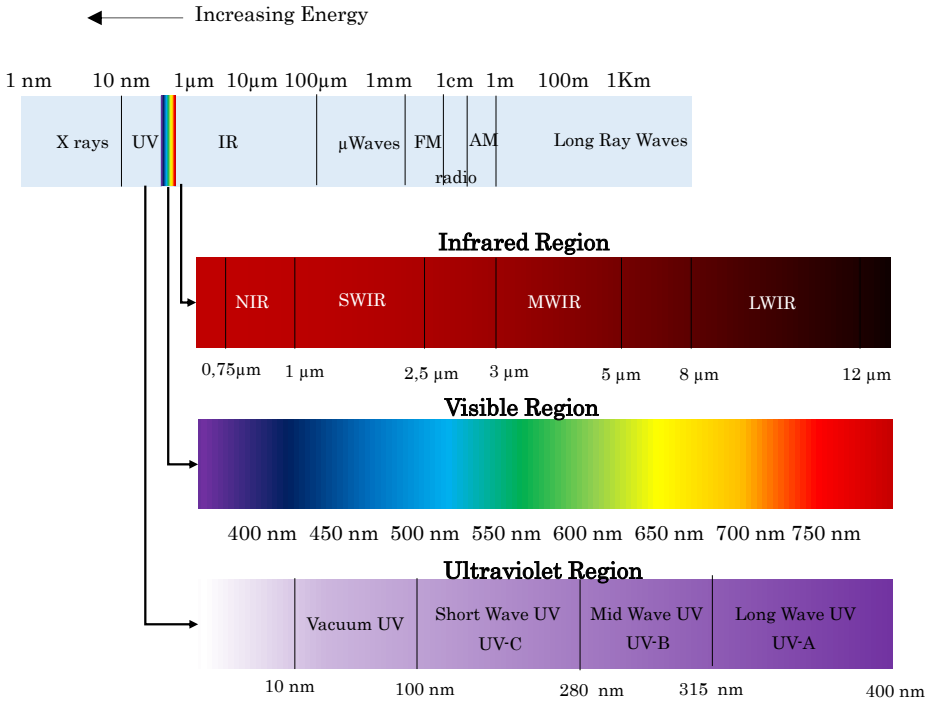

Regions not to scale

Figure 2.1-2: Detailed view of the frequency and wavelengths of the light of interest for the current work, UV, VIS and IR ranges

The polarization is also an important factor to take into account, since several optical settings require to work with polarized light, which may not be an evident effect and it has been depicted in Figure 2.1-3 (the Magnetic Field $\vec{B}$ has been omitted from the diagram). Light is considered as polarized if the Electric Field oscilates in one single direction (linearly polarized), or in spherical or elliptical plane (spherical or elliptical polarizations). Light is considered not polarized, when at any given moment, the $\vec{E}$ field gets to the observer in any direction.

Once the most important characteristics of the light have been summarized, the next section will describe the atomic and molecular processes that may occur when the matter is excited under a light of a given frequency band and intensity.

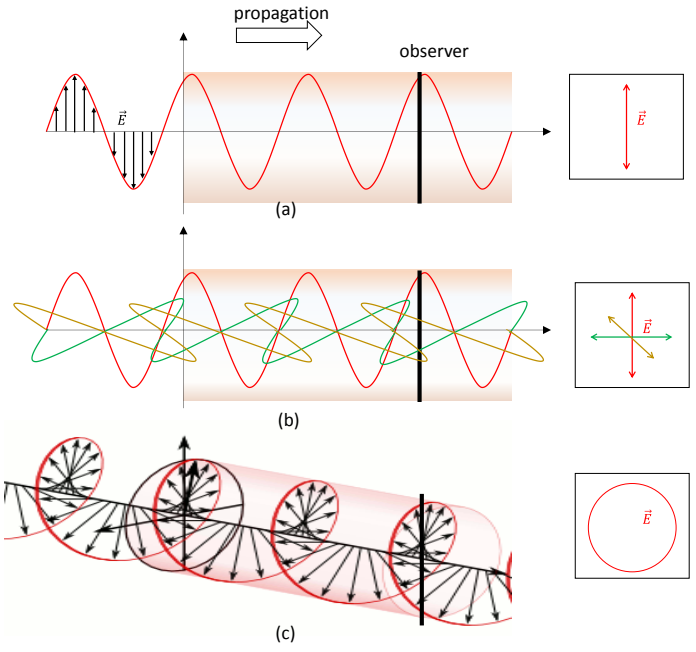

Figure 2.1-3 Polarized (a), not polarized (b), and spherically polarized (c) light. The frames in the left display the intensity pattern at the observer, after a certain observation period longer than the period of the wave. C diagram source Wikipedia.

2.1.2 Fundamental Physical Processes

When VIS, UV, or IR light impacts onto a surface or passes through a medium, unavoidable interaction occurs between the light and the electrons of the atoms and molecules of the material. Basically, this interaction entails two fundamental processes: first, the energy transferred by the photon on the electron and, second, as a charged particle, the excited electron radiates electromagnetic waves (light).

Steeping into a more detailed description, as the one provided by the quantum theory, the electron of an atom, a molecule, or an atomic lattice can absorb a photon and use its energy to jump into an energetically higher state. Equally, an electron can fall into a state of lower energy, with the energy difference being sent out as a photon (see Figure 2.1-4) [64].

It is important to stress that each part of the spectrum poses quantum energies (energy carried by a photon at a certain frequency) appropriate for exciting specific types of physical processes within the matter. As described by the quantum theory, the energy levels for all physical processes at atomic and molecular levels are quantized, and if the incident photon energy does not match with any available energy

level within the matter, then the material is considered transparent to that radiation. If the photon is absorbed but it is not able the translate electrons from the atom, then it is classified as non–ionizing radiation, and will normally just be converted in heat energy.

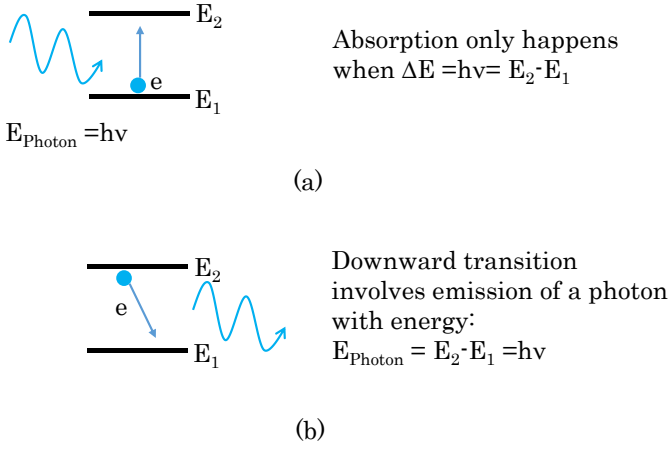

Figure 2.1-4 Photon absorption and photon emission process. (a) Absorption of a photon. Its energy is transferred to the atom and raises its electron shell onto a higher energetic state. This process is only possible when the photon's energy "fits" a gap in the atom's energy spectrum. (b) Spontaneous emission of a photon by an excited atom or molecule. Typically, this process occurs spontaneously, often only a few nanoseconds after the absorption of energy. The energy difference between the two atomic states determines the frequency (and, thus, the wavelength) of the departing photon. The direction of the emitted photon is random

For example, normally, the UV light and some part of the visible light, due to the energy of the photons (>2 eV) is able to generate Electron Level Changes. However, the quantum energy of infrared photons (is in the range 0.001 to 1.7 eV) matches the quantum states of molecular vibrations, which generates elastic absorption of the photon by the molecular bonds of the matter, resulting in a heating of the matter, but without affecting the electronic state.

Some of these physical processes happening between the photon and the atomic and molecular elements could be already introduced, even if they will be described in deep in the next sections.

For instance, the descriptions of the light scattering, absorption, fluorescence and Raman[9] scattering fit quite simply into this picture of elementary processes. Scattering means that a photon is absorbed and immediately emitted again. The absorbed and emitted energies remain the same and, as a result, it does not change the frequency of the light, but the phase and direction associated with the

[9] Chandrashekhara Venkata Raman, Indian physicist, 1888-1970.

photon that is emitted is random. The physical process underneath is called spontaneous emission that happens when, due to the absorption of the photon, an electron migrates from a lower to a higher energy level. However, the electron will not stay in the excited state perpetually, and may decay to a lower energy level, which is not occupied, after a specific time constant characterizing that transition. This transition releases a new photon without any external influence. Besides, the absorption of the light by the matter happens when, due to the absorption of a photon, an atom or a molecule migrates to a state of higher energy. The energy of the photon is converted into vibrations of the material that generates the already mentioned heating of the matter.

Particularities of these process could be found in the Fluorescence and Raman Scattering Principles. Fluorescence happens when the incident light is fully absorbed, transferring the material to an excited state. Then, after a certain resonance time, a part of the absorbed photon energy is released as the ejection of a new photon, which will show higher wavelength (less frequency) due to the energy loss between the absorption of the excitation photon and the emission of the new one, which again is converted into heat. On the other hand, even if due to Raman Effect a light with a different wavelength is emitted by the matter after being excited with a radiation, the processes underneath are completely different. The Raman radiation is due to a specific scattering process and it is independent from the excitation wavelength with a Raman emission peak keeping a constant separation from the excitation frequency, whereas in the fluorescence, the emission peak is anchored to a specific frequency due to the resonant nature of the process.

The abovementioned physic processes occurring when a radiation hits a material have been widely described during centuries by great scientist as Newton, Rayleigh, Fresnel, Planck, Einstein, etc. and even today, several studies continue trying to understand the elementals of the light. The latest example is found in the Higg's[10] boson theory, formulated in 1960 and demonstrated in 2013, this theory describes the light photon as a boson (type of fundamental particle) without any mass, demonstrating that, regardless all the scientific findings, the light nature still remains as a great unknown for the human being.

2.1.3 Light and Matter Interaction

Scientific domain of the optics summarizes in a set of fundamental principles the different effects generated by the

[10] Peter Higgs, British physicist, 1929-

processes mentioned above (see Figure 2.1-5 and Figure 2.1-6 for an outline of most common effects). These definitions describe in a very simple manner the effects of the light–matter interaction in the properties of the original light rays. Moreover, these basic optical principles are the base for developing most of the detection and sensing methods described later. The forthcoming sections will review the different fundamental processes involved in the light and matter interaction and how these effects can be used for developing photonic sensors.

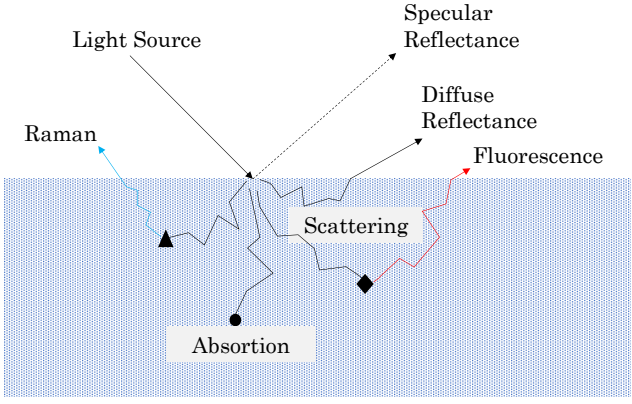

Figure 2.1-5: Summary of the different processes happened after the interaction between an incident light ray and a sample material.

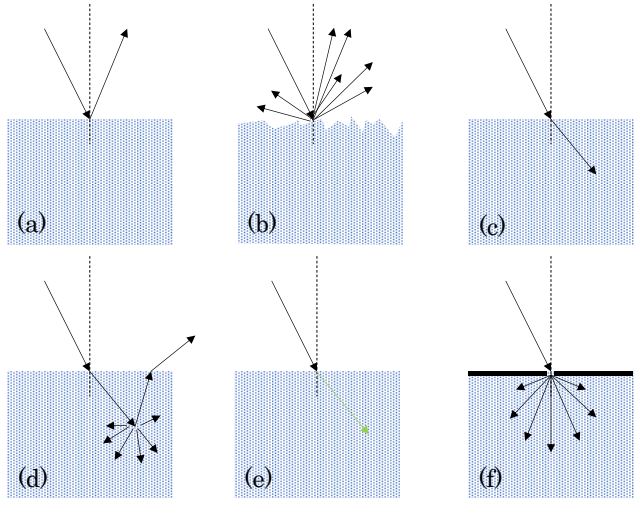

Figure 2.1-6: Some interactions of white light with surfaces and media. (a) specular reflection, (b) diffuse surface reflection, (c) refraction, (d) scattering and diffuse reflection, (e) absorption without scattering, and (f) diffraction.

2.1.4 Transparency

Transparency is a property of a material that allows the light passing through it almost without interaction. Because, even assuming the perfect transparent material, with no absorption or scattering happening, the light suffers an important interaction while crossing the molecular structure of the media, effectively reducing the velocity of the photon. This slowing down is quantified as the refractive index n_{medium} that was mentioned at the beginning of the chapter, and describes the relation of the light speed in vacuum or in a certain medium. Typical examples of refractive indexes are, $n_{vacuum} = 1$, $n_{air} = 1.000293$, $n_{water} = 1.33$, $n_{glass} = 1.458$ or $n_{oil} = 1.4$.

The availability of transparent elements is crucial for the development of photonics-based in–line inspection systems. These transparent mediums allow for instance the fluid sample confinement without impacting in the chemo–physical properties to measure. Traditional cuvettes for absorbance measurements are clear example of the use of transparent means. However, it is important to highlight that a medium is always transparent only to a certain part of the electromagnetic spectrum, and is determined by the dependency of the refractive index with the frequency of the incoming ray (see section 2.1.4.2 Dispersion) and by the absorbance of the material to the different energies of the incident photons (see section 2.1.8 Absorbance).

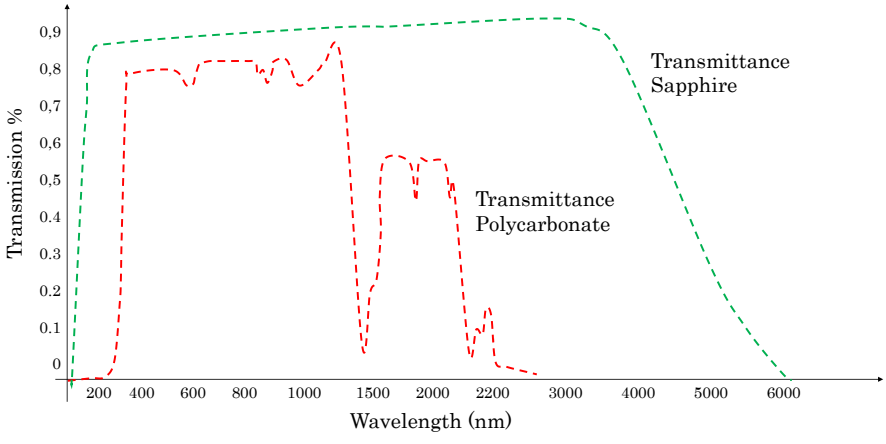

Figure 2.1-7: Approximate Transmittance spectrums of the Sapphire glass and Polycarbonate plate.

Therefore, the selection of the right non–interfering material should be taken once the light bands of interest are defined (see Figure 2.1-7). For instance, plastics such as PS (Polystyrene), PMMA (Polymethyl methacrylate) or Polycarbonate (PC) offer a decent transparency in the visible range, but are not transparent in the UV

or NIR bands. Consequently, if we need to deliver a solution for working in the UV or NIR bands, alternative materials should be used, being the Quartz (SiO2), Sapphire (Al_2O_3) or the Fuzzed Silica good candidates. Materials and low-cost configuration alternatives will be later discussed in section 3.3.3 Wettable interfaces.

2.1.5 Refraction, Reflection and Dispersion

The refraction and reflection of light is the basis for developing several optic elements that are key components for the design of fluid sensors. Additionally, the refraction and reflection laws describe how the emitted light beam travels inside the target matter, and gets to the detector.

When a light ray meets an interface between two materials with different refractive indexes, both reflection and refraction will occur. The proportion of reflected or refracted light will depend on the ratio of the refractive indices of the two media, the incidence angle of the light and its frequency spectrum. This behavior is described by the Snell[11] or Descartes[12] law, which is a further elaboration of the Fermat's[13] principle that describes that the light will always follow the path of least time, which is, evidently, the path with the shortest distance. This assumption is taken to describe the path followed by a ray when it is reflected by a surface, as seen in Figure 2.1-8:

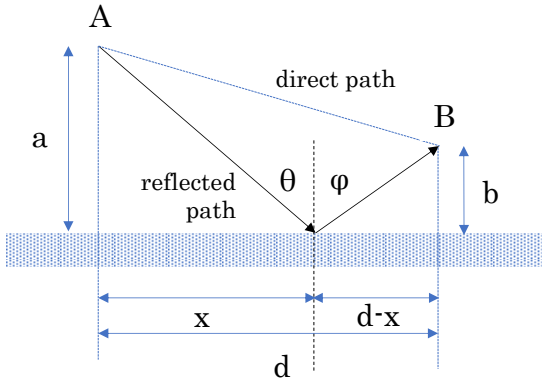

Figure 2.1-8: The reflection of a light ray.

The reflected path length, L, to get from the source point A to the destination point B is:

$$L = \sqrt{a^2 + x^2} + \sqrt{b^2 + (d - x)^2} \qquad \text{Eq. 2.1–6}$$

[11] Willebrord Snellius, Snell, Dutch astronomer and mathematician, 1580–1626.

[12] René Descartes, French mathematician and philosopher, 1596- 1650.

[13] Pierre de Fermat, French mathematician, 1607- 1665.

Since the light ray remains within the same medium across all the path, its speed will be constant. Therefore, the path with the shortest propagation time is directly the minimum distance path, which can be mathematically calculated equaling to zero the derivative of L with respect to x.

$$\frac{dL}{dx} = \frac{1}{2}\frac{2x}{\sqrt{a^2 + x^2}} + \frac{1}{2}\frac{2(d-x)(-1)}{\sqrt{b^2 + (d-x)^2}} = 0 \qquad \text{Eq. 2.1–7}$$

then

$$\frac{x}{\sqrt{a^2 + x^2}} = \frac{(d-x)}{\sqrt{b^2 + (d-x)^2}} \qquad \text{Eq. 2.1–8}$$

switching to trigonometric domain, Eq. 2.1–8 could be described as in the Eq. 2.1–9, which defines the **Law of Reflection**

$$\sin(\theta) = \sin(\varphi) \qquad \text{Eq. 2.1–9}$$

Now, let's take the problem one step further to describe the path length of the light ray amidst two mediums. In this case, the derivative of the time needed by the ray to get from source point A to the destination B ($t = L/v$), and considering the speed of light in the two mediums as function of the index of refraction ($v = c/n$).

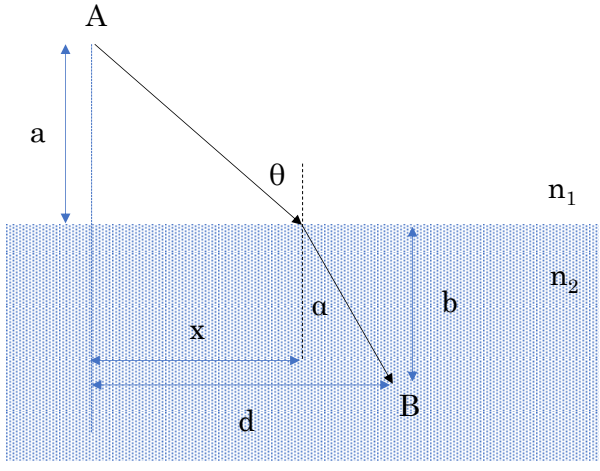

Figure 2.1-9: The refraction of a light ray across two mediums.

$$t = \frac{\sqrt{a^2 + x^2}}{v} + \frac{\sqrt{b^2 + (d-x)^2}}{v'} \qquad \text{Eq. 2.1–10}$$

$$\frac{dt}{dx} = \frac{1}{v}\frac{x}{\sqrt{a^2 + x^2}} - \frac{1}{v'}\frac{(d-x)}{\sqrt{b^2 + (d-x)^2}} = 0 \qquad \text{Eq. 2.1–11}$$

$$0 = \frac{1}{v}\sin(\theta_1) - \frac{1}{v'}\sin(\theta_2) \qquad \text{Eq. 2.1–12}$$

$$\frac{n_1}{n_2} = \frac{\sin(\theta_2)}{\sin(\theta_1)} \qquad \text{Eq. 2.1–13}$$

Which describes the Snell's Law for refraction of light across two mediums.

However, asides the mathematical definition for the refraction, this effect could be also described from the consequence of the differing speeds of light in two media. As already mentioned, the energy, hence, the frequency of the photon vibration must remain the same at the both sides of the interface. Therefore, inside the material with slower light velocity, the wavelength is shortened proportionately because the wave front is compressed at the interface. The Figure 2.1-10 demonstrates that the continuity of the light beam from a fast medium (smaller index of refraction) to a slow one is only possible with the bending of the rays.

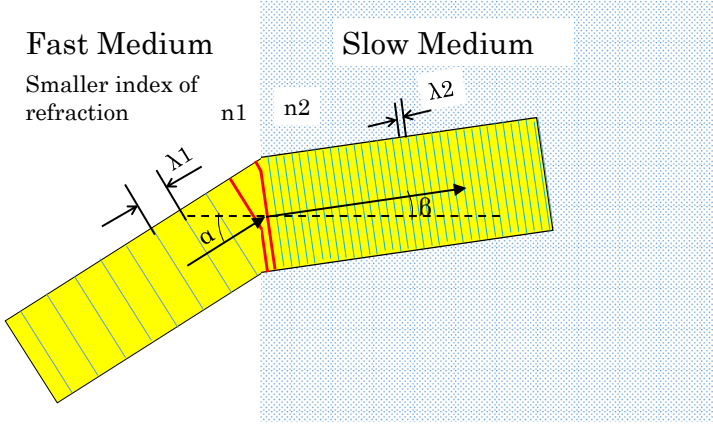

Figure 2.1-10: Graphical demonstration of wavelength shortening when a light radiation propagates from a medium with higher index of refraction to a material with the smaller one. Bottom part of incident rays reaches the slow medium first and is slowed down first, which rotates the ray towards the normal line between the two mediums

The ratio of the wavelength at both sides of interface is described with the refraction indexes of the materials (n_1 and n_2). From previous equations Eq. 2.1–3 to Eq. 2.1–5 the ratio is defined as:

$$\frac{\lambda_1}{\lambda_2} = \frac{n_2}{n_1} \qquad \text{Eq. 2.1–14}$$

The importance of the reflection and refraction laws is foremost since they describe the propagation of the light across not only the sample under test, but also through the different means and materials that constitute the sensor (protective windows, micromechanical structures, etc.)

2.1.5.1 Reflectance and transmittance

In addition to the changes occurring in the light wavelength when the propagating radiation meets a different medium, it is interesting to understand which portion of the light (number of photons) will be reflected and which will be refracted at the interface. This ratio was described by Fresnel, who defined the fraction of the incident power that is reflected from the interface as the Reflectance, R, and the fraction that is refracted as the transmittance, T. As described by Fresnel, these parameters are highly dependent on the electromagnetic properties of the two interfacing materials and, also, on the polarization of the incident light (parallel or perpendicular to the plane of incidence). For instance, the Reflectance for the perpendicularly polarized incident light, also defined as s–polarized light, is defined in Eq. 2.1–15, where μ_1, μ_2 and ε_1, ε_2 are the magnetic and electric permeability and of the two materials at the frequency of the light wave, and θ_i and θ_t are the angles of the incident and refracted rays respectively.

$$R = \left| \frac{\sqrt{\frac{\mu_2}{\epsilon_2}} \cdot \cos\theta_i - \sqrt{\frac{\mu_1}{\epsilon_1}} \cdot \cos\theta_t}{\sqrt{\frac{\mu_2}{\epsilon_2}} \cdot \cos\theta_i + \sqrt{\frac{\mu_1}{\epsilon_1}} \cdot \cos\theta_t} \right|^2 \qquad \text{Eq. 2.1–15}$$

Additionally, due to the conservation of energy, the transmittance is defined as:

$$T = 1 - R \qquad \text{Eq. 2.1–16}$$

The Reflectance and Transmittance are terms referenced all over the thesis. Not only because they are basic physical properties of the matter in concerning its interaction with the light (and reviewed in section 2.1.8), but because the transmission or reflection also refers to different setups for inspection a certain material and configuring photonic sensors as described in section 3.2.1.

2.1.5.2 Dispersion

Due to the different energy carried by photons at different frequencies, the material does no respond equally to all the incident light. This generates that refractive index of a transparent medium is slightly dependent on the wavelength (see for instance Figure 2.1-11), and the direct effect of this property is that not all the rays of a light beam will be refracted in the same direction. The most common example of the consequences of the dispersion happens when the white light incident to a prism is separated into a color spectrum.

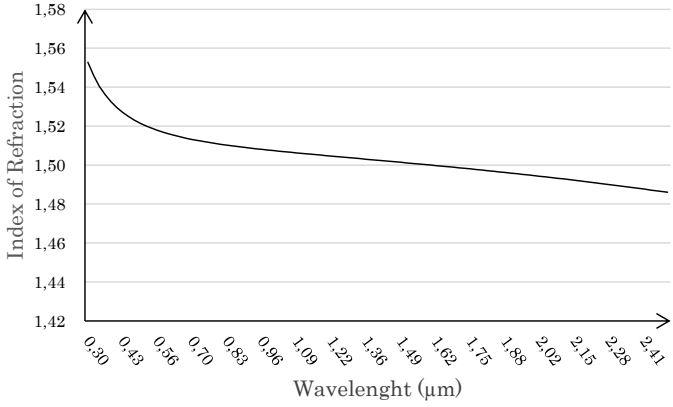

Figure 2.1-11: Dependency of the index of refraction with the light wavelength for the N–BK7 Glass (data source: Scott AG.)

The effect of the dispersion in optical system is also referred as the chromatic aberration, which becomes evident in lens based settings (see Figure 2.1-12) and should be taken into consideration when deciding the plane for placing the light detector.

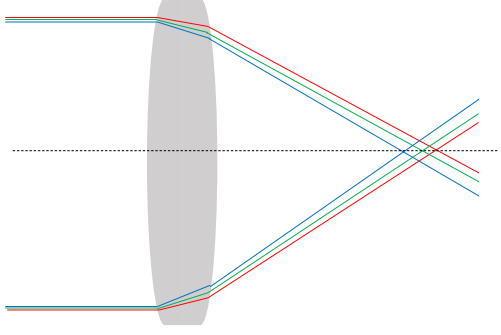

Figure 2.1-12: Chromatic aberration. Rays of different wavelength do not converge in the same point.

Actually, due to the significant impact of the material dispersion in optical setups, transparent materials as glasses reference this effect with the Abbe[14] number, or V–number, which quantifies the variation of refractive index versus wavelength, as:

[14] Ernst Abbe (1840–1905), German physicist.

$$V_D = \frac{n_D - 1}{n_F - n_C} \qquad \text{Eq. 2.1–17}$$

Being, n_D, n_F and n_C the index of refraction of the material at the wavelengths of the Fraunhofer[15] D–, F– and C– lines, which correspond to 589.3 nm, 486.1 nm and 656.3 nm respectively. Therefore, the higher the Abbe number, the less chromatic dispersion is expected for the material. For instance, the N–BK7 glass offers a V_{D-BK7}= 64.17, while for the PC plastics it drops down to V_{D-PC} = 27.86, showing that the plastic option would negatively contribute to the optical setting with a higher chromatic aberration.

Therefore, the variation of the index of refraction with the frequency of the light is an optical property that may help us creating components (prisms, gratings, mono-chromators, filters, etc.) or degrade the performance (chromatic dispersion, non-linearities, etc.) but definitively it is a factor to consider while designing an optical setup. Note that, according to the equations Eq. 2.1–9 and Eq. 2.1–13, the refraction of the light rays is affected by n, and thus, by the dispersion, while the reflection does not.

2.1.5.3 Specular Reflection, Diffuse Reflection and Internal Diffuse Reflection

So far, different physical and chemical processes have been used for describing the behavior of the light amidst different mediums. However, the roughness of the surface where the different materials interface is very important parameter that highly modifies the ideal theories presented for ray tracing. Thus, the rays reflected at a smooth or polished surface generate a sharp image of the mirrored object, which is known as specular reflection. On the other hand, rough, uneven or convoluted surfaces will reflect the incoming rays in arbitrary directions and generate a diffuse reflection.

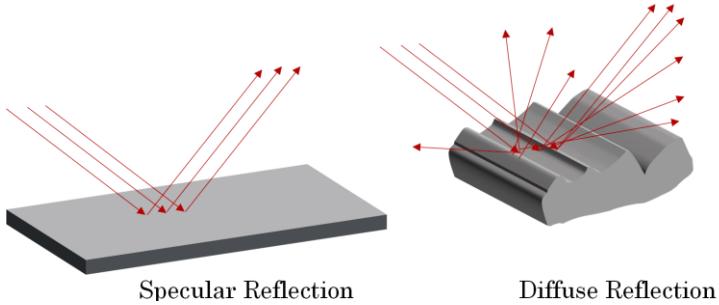

Figure 2.1-13: Difference between the two types of reflection happening in the material surface when irradiated with a light beam (a) specular reflection and (b) surface diffuse reflection.

[15] Joseph von Fraunhofer, German physicist, 1787–1826.

Sometimes, the diffuse reflection is confused with the diffused light coming back from the sample due to the internal reflections happening at the material, which is the fundament where the diffuse reflection spectroscopy is based [65]. The reason is that for a spectroscopic analysis, an effective interaction between the light and the sample should take place, and this is only possible if the light is able to penetrate, at least slightly, in the material. Therefore, true diffuse reflection is the result of light penetration into one or more particles and its diffusion in the material. This component of the radiation also exits the material at any direction, however, since it has gone through the particles, it holds information about the absorption properties of the sample. Understanding the diffuse reflectance process is fundamental for setting up spectroscopic sensors for solids or very opaque fluids, where the transmitted radiation is not sufficient for performing any processing.

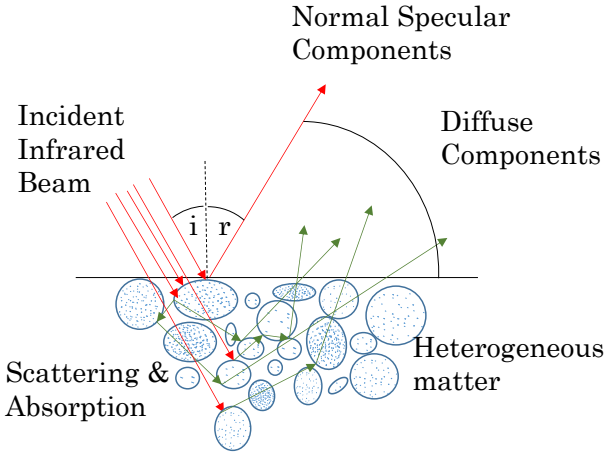

Figure 2.1-14: Mechanisms generating the reflectance spectrum of a sample.

2.1.5.4 Critical Angle and Total Internal Reflection

When a ray of light arrives to an interface with a material of a lesser refraction index, the refracted ray bends away from the normal, being the exit angle greater than the angle of incidence. The reflection happening in this case is called internal reflection. From the Snell's law, it can be observed that the exit angle will eventually get to 90º for a certain angle of incidence θ_C, which is known as the Critical Angle, and generates that no light is refracted and all the energy is internally reflected (see Figure 2.1-15). Beyond this critical angle, the incident radiation will be confined in the medium with higher index of refraction due to the so–called total internal reflection effect.

$$\theta_c = \arcsin\left(\frac{n_2}{n_1}\right) \qquad \text{Eq. 2.1–18}$$

Additionally, there is an interesting effect happening when the light radiation undergoes a total internal reflection process, which is

the generation of an evanescent wave in the vicinity of the incident point of the light ray. The physical explanation for the existence of the evanescent wave is that the electric and magnetic cannot be discontinuous at a boundary, as would be the case if there was no evanescent wave field.

These are very important effect since no energy is loss, and techniques based in the total internal reflection are the base for several optic components and processes as the light propagation within the fiber optics, for the polarizing prisms or for configuring different measurement setups as the Attenuated Total Reflectance sensors.

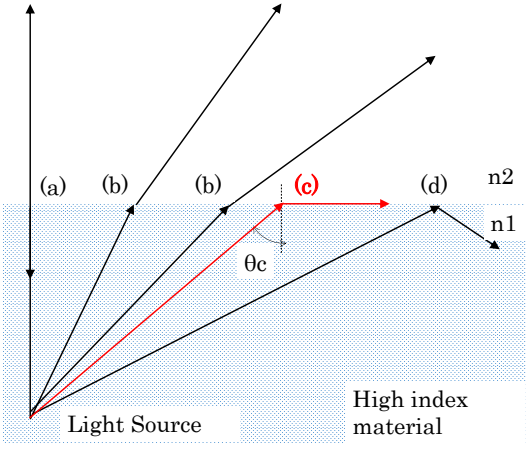

Figure 2.1-15: Diagram showing the different potential reflection effects depending on the angle of incidence. (a) Rays normal to the surface are not bent but a part of the radiation goes back parallel to the normal. (b) non-normal incident rays are reflected and transmitted, (c) displays the situation happening when a radiation hits a medium with lower index of refraction and if the angle meets the critical angle's definition θc. (d) shows that light rays incident at any angle greater that the θc will be totally reflected.

2.1.6 Light Diffraction

Diffraction is described as the apparent bending of the light when it hits an obstacle that is similar in size to its wavelength, or the spreading of the light when it passes through a sufficiently small opening. The proportion between the wavelength of the radiation and the size of the opening determines how much the rays will bend.

Optical effects resulting from diffraction are produced through the interference of light waves, as it is defined by Huygens–Fresnel principle, and exemplified with the single and double slit Young's experiments. This interference basically describes that all the new waveforms generated across the small objects or slits, interact with each other, resulting on higher (constructive interference) or darker

(destructive interference) intensity areas along the wave front propagation.

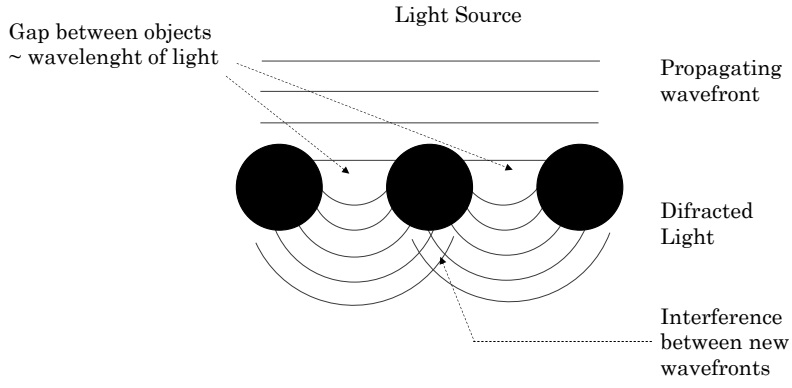

Figure 2.1-16: Example of diffraction

Both, Fresnel and Fraunhofer, described the diffraction effects from different approaches. Both scientist achieved to mathematical approximations for describing the light intensity fringes generated by diffracted light under different setups, such as the single or multiple slits, the light diffraction at an opaque edge, or the diffraction happening at circular apertures.

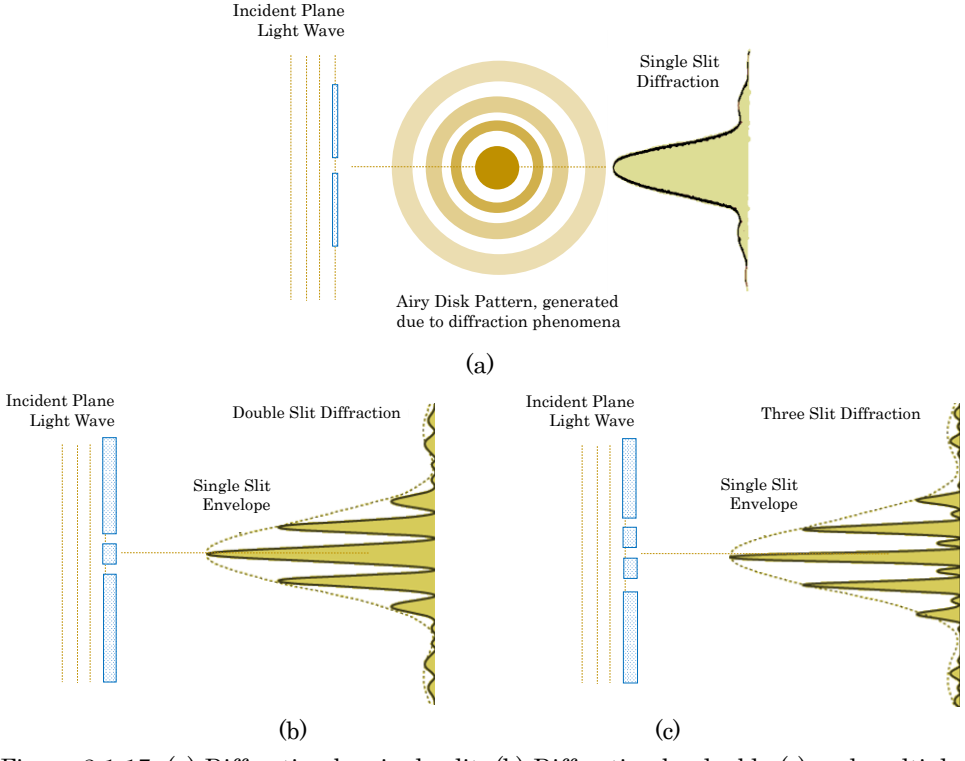

Figure 2.1-17: (a) Diffraction by single slit, (b) Diffraction by double (c) and multiple slits.

Actually, the diffraction generated by a circular aperture takes special importance due to its impact on the limit of resolution of imaging systems. The light from a point source passing through a tiny circular aperture, instead of generating a bright dot image, it produces a diffuse circular disk surrounded by blurred concentric rings, known as Airy's[16] disk. This effect limits the effectivity of an optical system to discriminate between two near objects even if both of them were perfectly focused. This limitation is quantified in terms of the Rayleigh criterion, which defines that an imaging system is limited by diffraction when the first diffraction minimum of the image of one object coincides with the maximum of the adjacent object (see Figure 2.1-18). This is an important consideration when defining the resolution limit of an in-line microscopic sensor.

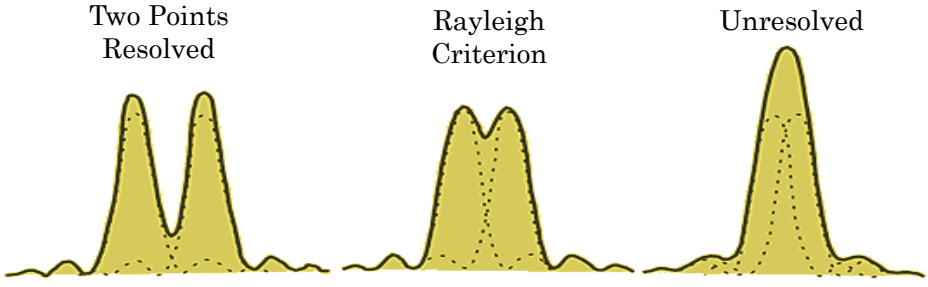

Figure 2.1-18: Description of Rayleigh criterion for resolving two adjacent points.

2.1.7 Light Scattering in Media

Scattering is the physical process describing the change in the trajectory of the light rays due to the non–uniformities in the propagation medium. Those non–uniformities basically represent scattering centers of variant refractive index that interact with the incident photon and modify its propagating direction randomly.

Particles, bubbles, droplets, molecules, dust, etc. are examples of the non–uniformities, and depending on the relation between their size and the radiation wavelength, one of the different predominant scattering processes will take place. This relation is described by the size parameter α, which is defined in Eq. 2.1–19, where D_P is the circumference of the particle and λ the wavelength of the incident radiation.

$$\alpha = \frac{\pi D_p}{\lambda} \qquad \text{Eq. 2.1–19}$$

Objects with $\alpha \gg 1$ act directly as geometric shapes, scattering the light according to their projected area. Around $\alpha \simeq 1$ Mie scattering happens, generating interference effects through phase variations over the object's surface. Rayleigh scattering will take place

[16] George Biddell Airy, British astronomer and mathematician, 1801-1892.

when the scattering particle is very small ($\alpha \ll 1$, with a particle size < 1 /10 wavelength) and the whole surface re–radiates with the same phase.

As mentioned in section 2.1.2, Rayleigh[17] scattering comes from an elastic process due the electric polarizability of particles. The energy of the incoming photon excites the state of the molecule to a higher level, but it almost immediately goes back to the original state, releasing the excess of energy in a form of a new photon, with exactly the same energy as the original one.

The phase and direction of the generated photon is, however, completely random, and normally it is different to the incoming trajectory, but the whole surface of the molecule reradiates with the same phase. However, as the molecules are distributed unevenly within the medium that the light is crossing, the scattered light reaches at a particular point with a random collection of phases and its resulting intensity is described as in Eq. 2.1–20.

$$I = I_0 \frac{8\pi^4 N\alpha^2}{\lambda^4 R^2} (1 - \cos^2\theta) \qquad \text{Eq. 2.1–20}$$

Where I_0 is the light intensity before the interaction with the objects, N represents the number of scatterers (e.g. molecules), α is the polarizability of the objects, and R is the distance from the scattered to the point where intensity I is being measured. The strong dependence of Rayleigh scattering with the wavelength of the incoming radiation (inversely proportional to λ^4) enhances the intensity of shorter wavelengths.

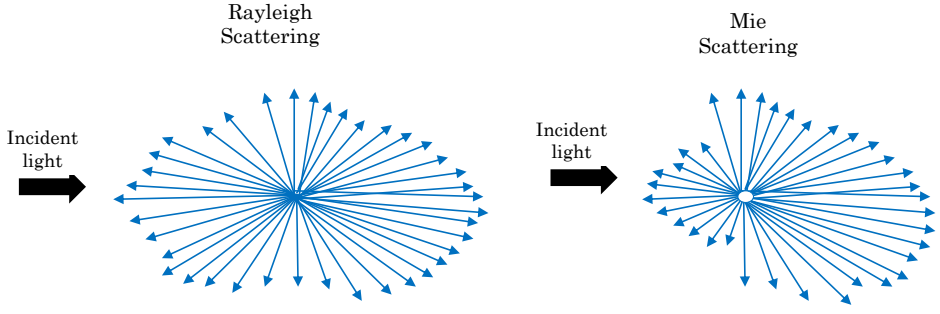

Figure 2.1-19: Graphical representation of Rayleigh and Mie scattering effect.

For larger particle diameters, scattering by spheres larger than the Rayleigh range is therefore usually known as Mie Scattering. In the Mie regime, the shape of the scattering center becomes much more significant in scattering shape, generating an antenna lobe like pattern, with a lobe directivity and intensity dependent on the particle size. However, notice that Mie scattering is not affected by the wavelength. If the general formulae for the Rayleigh scattering is

[17] John William Strutt, Third Rayleigh Baron, British physicist, 1842-1919.

taken (Eq. 2.1–21), the effect of λ is compensated with the particle diameter d, which for Mie case should be much larger than the wavelength (d>> λ).

$$I = I_0 \left(\frac{2\pi}{\lambda}\right)^4 \frac{(1-\cos^2\theta)}{2R^2} \left(\frac{n^2-1}{n^2+2}\right)^2 \left(\frac{d}{2}\right)^6 \qquad \text{Eq. 2.1–21}$$

The scattering is a process of special relevance in sensor design, because in fluids and solids, absorption and scatter happen together, both contributing to the reduction of light transmission through the material. Additionally, the scattering favors the photon propagation and absorption across the sample, redirecting unevenly the incident light radiation to potentially absorbent molecules.

2.1.8 Absorption

Absorption is the physical process describing the energy transference between a photon with a certain amount of energy that matches the quantum energy gap between the initial and final states of a material that the photon is passing through.

Therefore, the absorption spectrum of a certain material will show the fraction of incident radiation that is absorbed by the material over a range of frequencies. These frequencies, known as absorption lines, mainly depend on the molecular and atomic structure of the sample. However, the interaction between the molecules in the sample, the crystal structure and some other environmental conditions such as temperature, pressure or electromagnetic field also impact on the absorption lines happening in a material [66][67]. Notice that, atomic absorption lines have widths typically below 0.05 nm, and Molecular absorption transitions in the visible and ultraviolet span ~10 – 50 nm [68]

Normally, the absorption lines are divided by the nature of the quantum mechanical change that the photon induces in the atoms or molecules. Additionally, these different mechanical processes are bound to different wavelengths of the electromagnetic spectrum, due to the different energy carried by the photons.

Thus, Rotational lines are those absorption lines at which the molecules suffer a change in their rotational state after being excited by a radiation of the microwave spectral region. X–ray absorption, due to the higher energy of this short of radiation, induce deeper changes in the matter exciting electrons of the inner shells of the atoms. Electronic lines occur when a change in the electronic state of the atom or molecule is generated by a photon, which normally correspond to visible or ultraviolet region. In addition, vibrational lines relate to changes in the vibrational state of the molecule and are normally found in the infrared region. The changes generated in the matter by

the incident radiation due to the absorption process, are also classified as ionizing or non–ionizing, being the limit of ionization around the highest energy ultraviolet frequencies. The ionization alters the molecular or atomic structure of the material as it is able to extract electrons from their orbital generating ions, as it happens with the X–ray absorption. On the other hand, in the non–ionizing absorption, the atoms and molecules remain intact as there is a strong tendency for them to return to the ground state energy after a short period of time, releasing the absorbed energy in form of heat (due to random molecular motion or vibration) or emitting a new photon in the same frequency as the original one.

Quantifying the vibrational and electronic lines of chemical samples allows the determination of an unknown solution concentration, the monitoring of reaction progress as a function of time, and many other quantitative uses. For the specific case of the current thesis domain, the absorption happening at UV–Visible and Infrared regions are the most interesting ones for developing cost effective sensors thanks to the huge availability of emitters and detectors working in these frequency ranges.

Therefore, narrowing down to the UV–VIS range, the absorption of a UV–VIS photon by a compound generates an electron transition from lower energy orbital to higher energy orbital, this means that the energy is electronically transferred from the photon to the molecular structure.

The energy of absorbed photon is equal to the energy difference between the highest energy electronic occupied orbital (E_{OO}) and the closest unoccupied orbital (E_{UO}), or equivalently, the energy difference between the ground state and the excited state. Mathematically, this relationship is expressed by Eq. 2.1–22.

$$E_{light} = h \cdot \nu_{light} = \frac{h \cdot c}{\lambda_{light}} = \Delta E = E_{U0} - E_{00} \qquad \text{Eq. 2.1–22}$$

The wavelength of light required to promote an electron from the ground to the excited state is specific to each chemical, and this property is used for identifying the matter with UV–VIS spectroscopy.

The vibrational lines happen when the frequency of the photon matches the vibrational frequencies of the atoms of the chemical compound, and it is normally generated by IR radiation. In that case, the energy of the photon is transferred elastically to the material and it start to vibrate, compressing and stretching the chemical bond lengths and angles. Unlike in UV–VIS range, in this case, the electrons are not able to promote to a higher-level due to the lack of energy of the IR radiation, and the molecule remains in some intermediate excitation states known as vibrational states.

The bonds that keep atoms molecules together are not rigid, and they vibrate at certain frequencies that correspond to their vibrational states. Therefore, the vibrating bond process induced by IR photon is analogous to the physical model of a vibrating spring system, which is described by the Hooke's law. Considering the bond and the attached atoms as a spring with two masses connected, the Eq. 2.1–23 and Eq. 2.1–24 describes how the vibration frequency v of the system varies depending on the properties of the system.

$$v = \frac{1}{2x}\sqrt{\frac{k}{\mu}} \qquad \text{Eq. 2.1–23}$$

$$\mu = \frac{m_1 \cdot m_2}{m_1 + m_2} \qquad \text{Eq. 2.1–24}$$

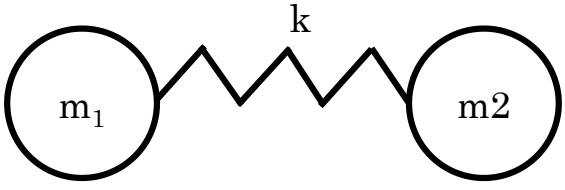

Figure 2.1-20: Diagram of elastically bonded masses

Where m_1 and m_2 represent the masses, k is the force constant of the spring and x is the distance between masses, v is the frequency and μ is the reduced mass [69]. The equivalence to the atomic system comes considering the bond as the k value, the x is the distance between the atomic nuclei, and evidently, the atomic masses represent the masses at the two ends of the spring. In this situation, the stronger bonds (larger k values) will increase the frequency at which the atomic system vibrates. Besides, for heavier atoms attached (larger m value), frequency decreases.

These frequencies represent the frequencies at which the atomic system will resonate with the incident photons absorving their energy and converting it to vibration forces; and again, bond strength is directly related to frequency. and more radiation energy (a higher frequency) will be required to excite a vibration on a stronger bond. Consequently, the combination of masses and bonds of mollecules will show unique vibrational frequencies, that are used by the IR spectroscopy to identify the type of bond between atoms and accordingly, the functional groups.

Additionally, the excitation of complex mollecules where several different possible bond vibrations may happen, implies the presence of several vibrational lines as well. This means that the identification of a specific molecule could be accomplished through the

study of the IR absorption spectrum, where the combination of the different vibration lines represents the unique fingerprint of the molecule, and is the base for several in-line sensors.

2.1.9 Light emission, Fluorescence

Fluorescence is a result of a three–stage process that occurs in some molecules called fluorescent dyes or fluorophores. The first stage is known as the Excitation, where a photon from a source is absorbed by the die, creating an excited electronic state S_1'. Next, a rapid decay to a lower quantum state follows, known as emitting energy level S_1 follows. This energy downgrade is the result of the interaction between the excited electron with the crystal lattice or some collisional process. The third stage is called Emission and occurs when a photon is emitted while the dye returns to the ground state S_0. Note that, due to the energy loss happened when the excited electron is transferred to the intermediate lower quantum state S1, the energy of the emitted photon must be lower than the energy from incident one, which implies equivalently an emission of longer wavelength (see Eq. 2.1–21).

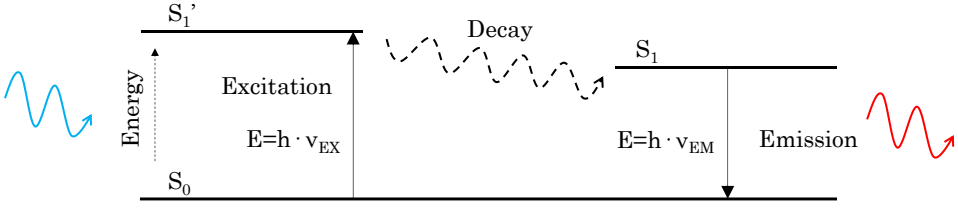

Figure 2.1-21: Basic diagram describing the fluorescence emission, at which, the emitted photon delivers lower energy than the excitation one.

The difference in energy between the emitted and the absorbed photons is shown as a shift between the excitation and the emission spectra of the dye and is called Stokes Shift. Notice that, a large Stokes Shift will allow a good spectral separation of excitation and emission spectra, and thus, a simpler fluorescent optical setup in sensors. Actually, one of the problems of molecules fluorescing in the range of NIR is that typically they have an overlap between excitation and emission and small stokes shift, hindering their use in simple settings, even if currently new NIR fluorophore dyes are being developed with larger stokes shifts [70].

The atomic sub processes involved in the fluorescent emission are summarized in the Jablonski[18] diagram (Figure 2.1-22). The different states described in the diagram include the non–radiative

[18] Aleksander Jabłoński, Polish physicist, 1898-1980.

processes by which the energy of the excited electron moves down to intermediated quantum states. These non–radiative processes include the internal conversion and the vibrational relaxation, which is followed by the fluorescent emission, or the intersystem crossing that can give rise to the phosphorescence.

The thin horizontal lines around the S_0, S_1 and S_1' depicted above represent vibrational/rotational sublevels at which the electrons of the molecules may stick after the excitation. This basically implies that the atomic absorption and emission spectra are broadened by molecular vibronic states to excitation and emission bands. The practical effect of this process is that the molecules may be excited by radiation of different wavelength, but the emission only occurs around a specific frequency band; being just the emission power dependent on the excitation wavelength.

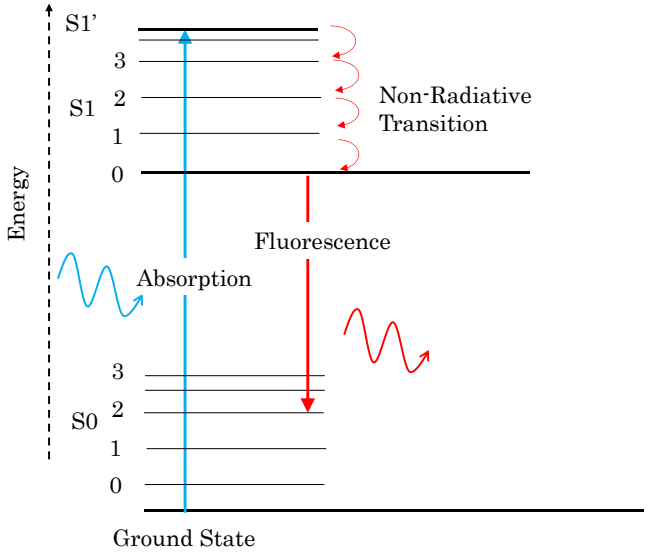

Figure 2.1-22: Jablonski diagram (partial representation), showing the vibrational sublevels between the S_0, S_1 and S_1'.

Additionally, note that not all the incident photos are able to excite the sample to its fluorescent levels. The probability that a photon will be absorbed varies with wavelength (energy). The number of photons fluoresced relative to the number absorbed is the quantum efficiency (see Eq. 2.1–25), indeed, the higher the absorption and quantum efficiency, the brighter the fluorescence.

$$\emptyset_F = \frac{K_{rad}}{K_{rad}+K_{non-rad}} = \frac{\tau_F}{\tau_{rad}} \qquad \text{Eq. 2.1–25}$$

Where k_{rad} is the radiative decay rate, $k_{non-rad}$ is sum of all non–radiative decay rates, τ_F is the observed excited state lifetime (fluorescence lifetime) and τ_{rad} is the radiative lifetime.

However, notice that even if quantum yield may fall between 0.1 to 0.9 [71], meaning that up to 90% of emitted photons shall generate a fluorescent signal, the effective readings in real setups in far from that ration. For instance, an experimental setup results using Cy5.5 fluorescent dye (Amersham, GE Healthcare), with a $\emptyset_F$=0.28, after setting the emitter (VCSEL laser), receivers (CMOS photo–detector) and filters (excitation and emission) the net result in terms of injected intensity over the received one displayed a disappointing 10^{-6} ratio, far from the 0.28 claimed by the quantum yield [72].

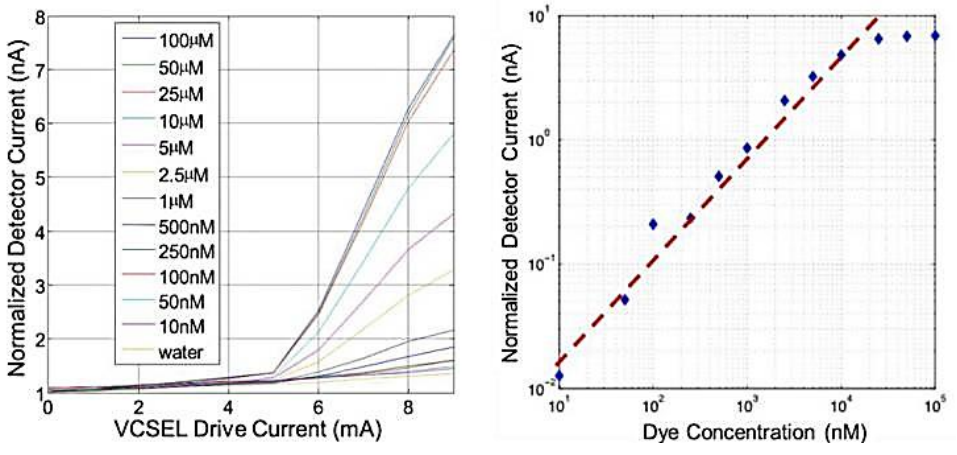

Figure 2.1-23: Measurements of Excitation drive currents and the photo-current received at the detector for different concentrations of Cy5.5 fluorescent dye. Considering the efficiencies and losses of the whole fluorescent setup, the efficiency in terms of required/generated power (and thus photons) is in the range of 10^{-6}, far from the ranges of the Quantum yield efficiency, which cannot be considered in an isolated manner [72].

2.1.10 Raman Scattering

First discovered in 1928, Raman or inelastic Scattering is the process describing the interaction between the light and the matter where scattered photons have either a higher or lower energy than the incident one, depending upon the vibrational state of the molecule under study. As mentioned earlier in section 2.1.6, when photons are scattered from a material, most of them are elastically scattered by Rayleigh or Mie effects, and the energy of the emitted photons remains the same as the incident ones. However, a small part of these photons, around 1 out of 10^7[73], excite the molecules in such a way that some of the incident energy is either lost, or coupled with internal

vibrational states generating that the scattered photons display different frequencies than the original ones.

Therefore, asides the Rayleigh scattering, two inelastic radiations happen, the Stokes and Anti–Stokes radiations, showing lower and higher energy respectively. This energy loss or gain is directly related to the vibrational energy levels of the ground state of the molecule, and therefore, the analysis of Stokes or anti–Stokes frequency shifts are directly translated into a measurement of the vibration energies of the molecule.

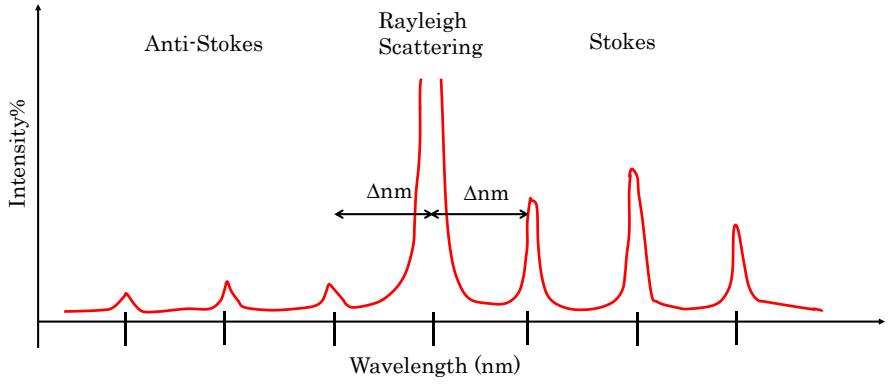

Figure 2.1-24: Schematic Raman spectrum. The energy of the scattered radiation is less than the incident radiation for the Stokes line and the energy of the scattered radiation is more than the incident radiation for the anti–Stokes line. The wavelength shift occurring from the excitation frequency to stokes and anti-stokes ONES is always the same regardless of the excitation, and it is always dependent on the material.

As it can be observed in Figure 2.1-24, the Stokes and anti–Stokes frequencies are equidistant from the Rayleigh frequency (the incident frequency), due to the loss or gain of one vibrational quantum of energy. And this is one of the main differences between the Raman scattering and the Fluorescence, because while the fluorescent peak remains static for a wide excitation spectrum, the Raman Stokes or anti–Stokes frequencies maintains a constant separation from the excitation frequency, which depends on the material and not on the excitation wavelength.

However, as described in Eq. 2.1–20, notice that the scattered signal intensity is proportional to the inverse of the wavelength to the fourth power, Intensity $\propto 1/\lambda^4$, which can lead to low signals at longer excitation wavelengths [74]. So, whenever possible, the excitation wavelength should be kept the minimum the possible.

Nowadays, Raman spectroscopy is generally considered as a complementary technique to IR spectroscopy, being suitable for analyzing organic and inorganic compounds. Additionally, Raman techniques are ideal candidates for measuring aqueous samples,

because, unlike the IR spectroscopy where the water absorption hide other absorption bands of molecules of interest, Raman scattering is more immune to the presence of water, because the intensity of Raman scattering from water is usually weak and direct absorption interferes only when near–infrared lasers (e.g., 1064 nm) are used. This is the reason why, even if high excitation power and strict optical tolerances are required, Raman-based in-line sensors are an interesting topic of research [179].

2.1.11 Attenuation

The attenuation represents the decay occurring to the incident radiation power while it crosses a certain material. Normally, the attenuation is the consequence of the combination of different process as the scattering or the absorbance, but it basically describes the relation between the light power that goes into a sample material and the power that comes out from the opposite end.

The simplest expression for describing the attenuation through a material is defined by the Bouguer[19]–Lambert[20]– Beer[21] law of absorption. This empiric formula defines the relationship between light absorption at a certain wavelength, A(λ), and the properties of the medium as:

$$\log_{10} = \frac{I_0(\lambda)}{I(\lambda)} = \varepsilon(\lambda) \cdot c \cdot l = A(\lambda) \qquad \text{Eq. 2.1–26}$$

Where, I_0 is the incident light intensity at wavelength λ, I is the transmitted intensity at same wavelength, ε is the molar absorption coefficient ($liter \cdot mol^{-1} \cdot cm^{-1}$) also called the molar extinction coefficient, c is the concentration ($mol \cdot liter^{-1}$) or Molar (M) and l is the light path along absorbing material (cm).

Therefore, the absorbance of a certain compound is directly proportional to the concentration, because a higher molecule number implies higher interaction with the light. Additionally, the absorbance is also dependent on the path length travelled by the light across the compound solution, just because the interaction with the molecules will occur along a longer distance. And finally, the absorbance is determined by a proportional constant ε(λ), the extinction coefficient, which basically quantifies the absorption properties of the compound for a certain light frequency.

[19] Pierre Bouguer, French astronomer and physicist, 1698-1758.

[20] Johann Heinrich Lambert, Swiss physicist, 1728-1777.

[21] August Beer, German physicist, chemist, and mathematician, 1825-1863.

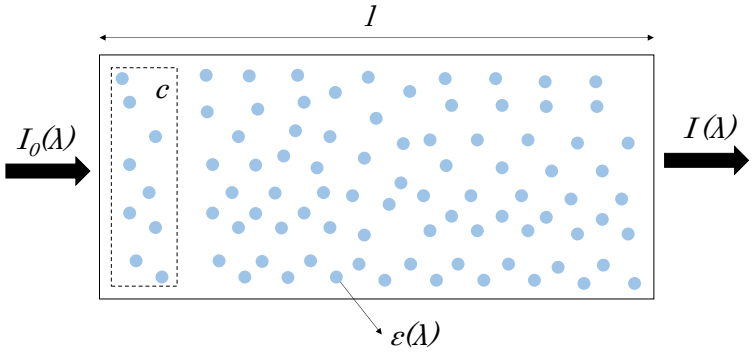

Figure 2.1-25: Schematic representation of the Attenuation process.

However, it should be considered that, normally, the materials are not composed of a single compound, but for a heterogeneity of molecules and components. Therefore, the light across a sample is attenuated by a sum of absorbents in different concentration. This accumulation is known as the absorption coefficient μ_a (cm^{-1}) and is defined by the following equation:

$$\mu_a = \ln(10) \cdot \sum_i C_i \cdot \varepsilon_i \qquad \text{Eq. 2.1–27}$$

Additionally, the approximation described by the Lambert–Beer law only remains valid for diluted solutions (e.g. A < 3). As c increases, the ε(λ) varies with the concentration due to the scattering process, aggregation of molecules, changes in the medium, etc. As concentrations change, turbidity may increase, macromolecules and other larger aggregates appear, etc. which normally contribute to larger light scattering. Since the optical density resulting from scatter is proportional to $1/\lambda^4$ (see Eq. 2.1–20), this effect is easily recognizable as a background absorption that increases rapidly with decreasing wavelength. Additionally, these molecular changes, typically also modify the structure of solvents and refractive index, may change consequently. Since the transmission of a radiation across two different media depends on the index of refraction and not only on the absorbance of the second media, these molecular changes will vastly impact on the Lambert–Beer assumptions [75][76]. The situation gets even more complicated when the Kramers–Krönig relationships are considered, which state that the refractive and absorptive properties of the medium are not independent [77].

Therefore, approximations for understanding and defining the light attenuation through a complex sample matrix are required as

the ones based in a combined consideration of both, absorption and scattering [78], described as in Eq. 2.1–28.

$$I(\lambda) = I_0(\lambda) \cdot \exp(-\mu_t \cdot x) = I_0(\lambda) \cdot \exp[-(\mu_a + \mu_s) \cdot x] \qquad \text{Eq. 2.1–28}$$

Where $\mu_t(cm^{-1})$ represents the extinction coefficient, being μ_a and μ_s coefficients the contributions from the absorption and scattering processes. In thin materials, scatter to larger angles is small and a simple estimate of light attenuation might be used. However, in thicker samples, scatter to larger angles is important, and the anisotropy coefficient, g, needs to be considered in the scattering contribution. In most organic materials, g is approximately in the 0.9 to 0.95 range, indicating mostly forward scatter of the light in the material. The anisotropy coefficient defines the effective scattering coefficient, μ_s', which also determines the Transport Mean Free Path (MFP') (cm), that describes the different trajectories within the material that a photon may travel due to the scattering [79][80]

$$\mu_s' = \mu_s(1 - g) \qquad \text{Eq. 2.1–29}$$

$$MFP' = \frac{1}{\mu_a + \mu_s'} \qquad \text{Eq. 2.1–30}$$

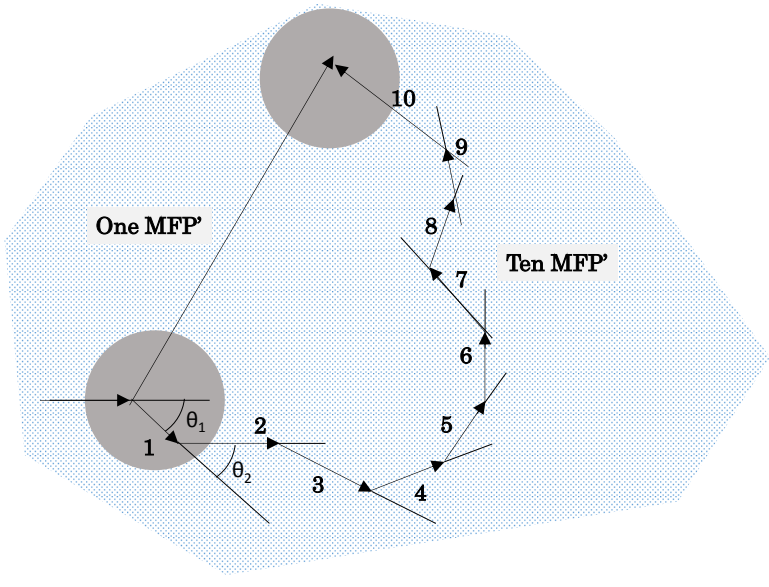

Figure 2.1-26: Effect of multi scattering points

Actually, since the propagation and attenuation of the light through heterogeneous sample matrix is subject to several, complex and interrelated processes, different numerical and analytical solving approaches have been developed. Some of them as the Radiative

Transfer Equation (RTE) are based on differential equations which are difficult to solve for non–homogenous samples. Additionally, mainly driven by the studies of the light propagation across human tissues, different statistical and probabilistic methods, as the Monte Carlo based ones, are being used to model and simulate the photon propagation across multi–layered tissues. In the Monte–Carlo simulation model, the rules of light propagation are described as probability distributions that define the step size of photon transport between points of photon–tissue interaction and the angles of reflection in the trajectory of the photon when a scattering process happens (see Figure 2.1-27).

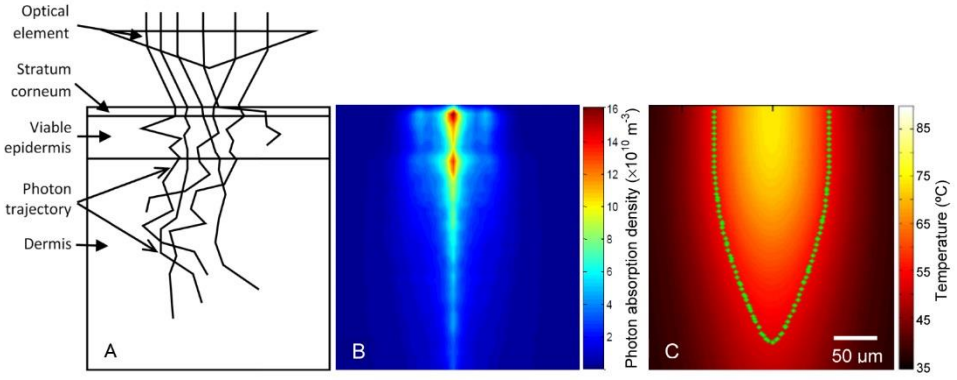

Figure 2.1-27: Schematic diagram of a cross–section of the three–dimensional model used in the Monte Carlo simulations comprising a three–layer skin model and an optical element. B: A typical numerical photon absorption map. C: A typical skin thermal map in pseudo-color [81].

Another interesting approach for understanding the light attenuation across a medium is the one proposed by Kubelka[22]-Munk. These equations are used as an analogy of the Lambert-Beer, but instead describing the attenuation (and thus concentration) in transmissive setups, Kubelka-Munk works for case of diffuse reflectance. The equations consider an opaque sample as a sequence of layers of infinitesimal thickness to generate a simple model of transmission and reflection for a layer, but once with the simplified model a layer with infinite thickness is modeled, where Transmission tends to zero [82]. Following with these approximations, Kubelka-Munk delivered the following equation:

$$f(R_\infty) = \frac{K}{s} \qquad \text{Eq. 2.1–31}$$

being k, the absorption coefficient, as in the Lambert-Beer law, and s the diffusion factor, which is difficult to determine. From Eq.

[22] Paul Kubelka, Czechoslovakian chemical engineer, 1900–1956

2.1–26, we can take k by Ln(10) × ε(ν) × c, where: ε is extinction coefficient (function of the wavenumber ν) and c is the sample concentration, what gives accordingly:

$$f(R_\infty) = \frac{\mathrm{Ln}(10)\varepsilon(\nu)c}{s} \qquad \text{Eq. 2.1–32}$$

Eq. 2.1–32 produces a similar expression to the Lambert-Beer attenuation expression, enabling to obtain a spectrum similar to the transmission spectrum, for the cases when the s parameter remains constant. In these cases, $f(R_\infty)$, at a given frequency, varies with the concentration c.

2.1.12 Optical rotation

The optical rotation is the process by which linearly polarized light radiation rotates its plane as it crosses a certain material. This optical activity occurs only at certain types of materials, as chiral ones, which are compounds with no mirror symmetry on their symmetric structure.

This effect is very useful because it allows measuring the concentration of certain materials by observing the phase shift suffered by a light radiation while crossing it. The interest about this method comes because the molecular groups of glucoses deliver a strong optical activity.

2.2 Optics and Optoelectronic Elements

This section will summarize the most important building blocks for developing a photonics sensor system, including the light sources or emitters, light detectors or receivers, and light conditioning and coupling optics components. Additionally, main trends and latest innovations in the field of microspectrometers are also reviewed.

2.2.1 Emitters

Light Sources or light emitters are the family of devices that transform energy into light photons of a certain wavelength and polarization. The emitters are a fundamental part of any photonics–based sensor as it provides the required excitation for accomplishing the measurement.

Asides the features of the emitted light (irradiance, wavelength and polarization), other important features must be considered when selecting a light emitter. For instance, the efficiency will determine the ability of the source to convert energy into radiated photons, the dynamics of the emitter will describe the possibilities of modulating the generated light and the optical properties, in terms of the geometry of the emission beam, will describe the volumetric concentration of the emitted photons.

Other important factors as the stability of the emitted light, its dependency with ambient temperature, lifetime, compactness and indeed cost may also determine the selection of the light source.

However, the most determining parameter is normally the emitted light spectrum limits, because not all the technologies are able to deliver light power at any wavelength. Table 2.2–1 gives a summary of the available wavelength ranges depending on the emitter technology or material.

Table 2.2–1: Examples of Emitter technologies and emissivity ranges [83][84]

Source Emissivity Ranges (μm)	Start	End
Quartz tungsten halogen	0.22	2.7
Glass tungsten halogen	0.25	2.25
DC deuterium lamp	0.185	3.75
Pulsed xenon arc lamp	0.18	2.5
DC arc lamp	0.20	2.5
Silicon Carbide	1	100
Carbon arc	0.5	100
Mercury lamp	0.3	100

Helium–neon laser (He:Ne)	0.6327	0.6328
Neodymium yttrium aluminum garnet (Nd:YAG) laser	1.0639	1.0640
Laser Diodes	0.7	1
Indium Phosphide (InP) LED	0.92	
Indium Arsenide (InAs) LED	3.6	
Gallium Phosphide (GaP)	0.55	
Gallium Arsenide (GaAs)	0.87	
Aluminum Arsenide (AlAs)	0.59	
Gallium Indium Phosphide (GaInP)	0.64	0.68
Aluminum Gallium Arsenide (AlGaAs)	0.8	0.9
Indium Gallium Arsenide (InGaAs)	1.0	1.3
Indium Gallium Arsenide Phosphide (InGaAsP)	0.9	1.7
Zinc Selenide (ZnSe)	0.45	0.5
Indium Gallium Nitride (InGaN)	0.385	0.45

The next sections introduce the main parameters describing the performance of a certain light source and then list, brief and compare the predominant emitter technologies

2.2.1.1 Main Features of Light Emitters

As mentioned, different parameters should be considered when describing a light source, which range from the characteristics of the generated light, to additional performance data as the efficiency, the driving circuitry, stability etc.

The most basic and traditional feature for describing a light source is the color temperature of the emitted light. This parameter describes somehow the wavelength–amplitude response of the source, assuming its equivalence with an ideal black body emission spectrum, and the value is given in Kelvins. Basically, the color temperature describes the human perception of the light that is generated as the result of a thermal radiator, which matches the reality for incandescent lamps, but is only an approximation when the light source is a LED or a fluorescent lamp [85]. As reference, notice that a tungsten lamp emits a 2500 K light, a warm white LED generates a 3000 K radiation and a fluorescent lamp emits a 5000 K light,

However, the color temperature should be understood as a very basic way for defining the light wavelength within the visible spectrum and the applications of this classification are mostly focused on illumination or photography, but are not useful for the design of photonic instrumentation or sensors.

When more accurate information is needed for understanding the characteristics of the light generated by a source, wavelength–

amplitude charts should be used. This type of graphic displays the emission power across a range of frequencies or wavelengths (in the vacuum) offered by a light source under certain conditions, as, for instance, the ambient temperature of the test and the polarization settings of the source. These charts are essential when the performance of the light iteration with the matter must be studied under a given wavelength band, because the graphs tells the amount of incident energy at a certain wavelength at which the molecules may react.

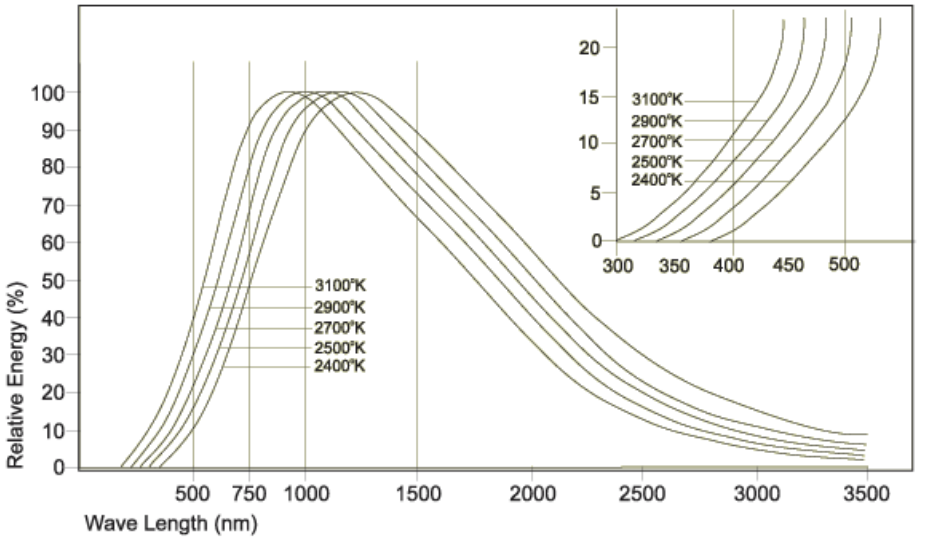

Figure 2.2-1: Spectral radiation output for tungsten filament lamps, including information regarding not only the relative emission energy across the frequency spectrum but also indicating the equivalent color temperature of each (courtesy of International Light Tech., Peabody, MA, USA)

The wavelength–amplitude chart also tells important information about the bandwidth of the light source, especially when narrow emitters are required. In this case, the emission peak (λ_{PEAK}) and the spectral half wave width or alternatively, the full width at half maximum (FWHM) spectrum are normally specified. The emission peak defines the wavelength at which the emitter shows the maximum emission power, and the FWHM quantifies the frequency range where power drops by less than half (see Figure 2.2-2).

Additional feature of the light sources is the directivity of the emission beam, which describes the radiation intensity along the different angles measured from the normal to the emitter surface. Sometimes the emitters include some sort of optics to modify or enhance the natural directivity of the emitter material.

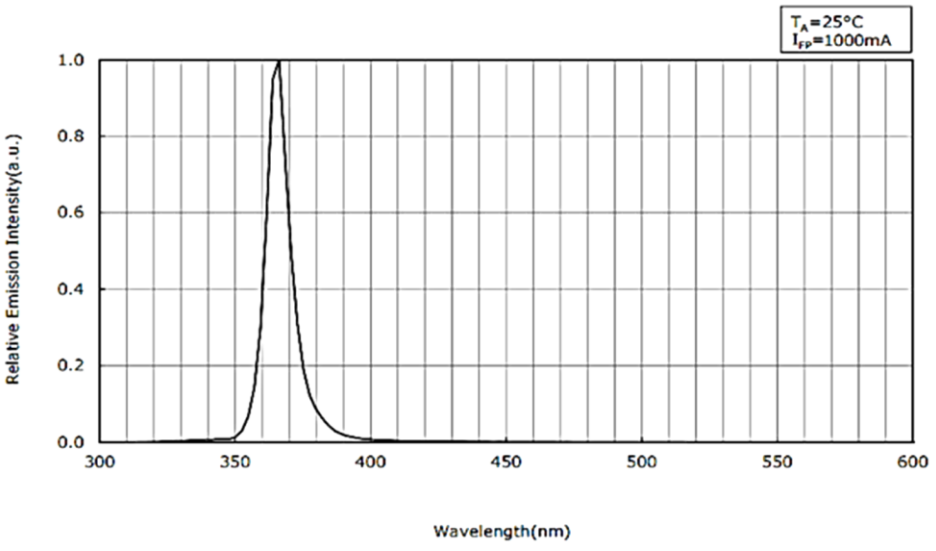

Figure 2.2-2: Spectrum of the U365 UV LED from Nichia manufacturer, showing an emission peak in 365 nm and FWHM of 9.0 nm. Notice that in this case, the emission intensity is displayed as a relative value in arbitrary units (courtesy of Nichia Corp., Tokushima, Japan)

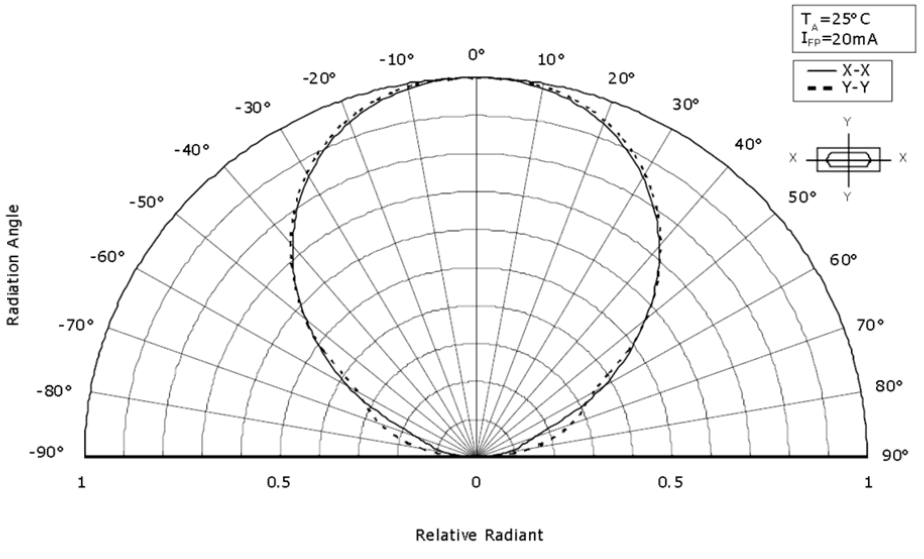

Figure 2.2-3: Directivity of PICOLED SML–P24 RGB LEDs from ROHM Semiconductor (Kyoto, Japan)

Temperature coefficient defines the dependence of the emitter features with the temperature. This is normally a very critical parameter since almost all the emitting technologies present an important dependence with the temperature and not only the radiated flux but also the wavelength gets modified with increasing temperatures [86][87].

Coherence, spatial and temporal, is another factor that may have to be considered in certain applications where the light phase and polarization is relevant, as it happens with interferometry applications. A radiation is called coherent when there is a fixed phase relationship between the electric field values at different locations or at different times. Partial coherence describes that there is some (although not perfect) correlation between those phase values.

Spatial coherence happens when the radiation shows a high fixed phase relationship between the electric fields at different locations across the beam profile. Temporal coherence means a strong correlation between the electric fields at one location but different times. For instance, Lasers have the potential for generating radiation beams with very strong spatial coherence, and this is perhaps the most fundamental difference between laser light and radiation from other light sources.

In addition, ageing of the emitters is another important feature, since it may determine the whole sensor system's lifetime. Not all the technologies offer the same performance stability over time, and it also vastly depend on the operating conditions. Thus, a tungsten lamp designed to operated 10,000 hours keeping at least the 50% of its nominal power may show a totally different performance if the operating temperature differs from the nominal values.

2.2.1.2 Emitter Technologies

This section outlines the most common technological alternatives for radiation sources, covering from simple filament sources to the new generation of light sources based on MEMS devices.

2.2.1.3 Incandescent Bulb

The most basic light emitter technology is the incandescent bulb, where a material like the tungsten is heated up by circulating a current, and the heated body generates a light radiation due to the Thermic Radiation Effect; and until recent years, these incandescent lamps have been the most common light sources. They require a simple control to operate, just a regulated power supply, but when lifetime of the bulb is important, several considerations must be taken to efficiently control the lamp driving current, as ramped pre–heating, controlled startups, etc. [88]. These kind of lamps (tungsten, halogen, quartz tungsten halogen, gas–filled) offer a reasonable short-term stability, but the lifetime is not high (around 10,000 – 50,000 hours), and the intensity decays slowly right from the initial uses.

The spectral ranges of these kind of light sources start around 400nm and may reach the NIR region, but with relatively low efficiencies as 20% (see Figure 2.2-1). Additionally, these light sources are relatively slow, so no light modulation possibilities are possible in setups using incandescent lamps.

2.2.1.4 Electric and Gas Arc Lamps

Historically, the second most common light sources are the arc lamps, even if these were invented fifty years before the filament lamps. In this kind of technology, the light is generated by a high voltage arc between two electrodes, and the most typical ones were the carbon arc sources, which were widespread solution for street lighting until they were substituted by the filament emitters.

The evolution of electric arc lamps continued during the nineteen Century with gas discharge lamps that generate light stimulating an electrical discharge through an ionized gas, which is normally a noble gas (argon, neon, krypton, and xenon) or a combination of these gases. The most know example of these kind of lamps were the famous neon lights and the fluorescent lamps used for lighting.

Sometimes, these lamps even include additional vaporized compounds as mercury, sodium or metal halides, which allow reaching higher irradiances or wider wavelength emissivity. These sources use a filament and anode, but in this case, the filament is not the light source, but the arc that is generated between the filament and the anode. The arc excites the molecules of the gases included in the light bulb which emit light when they return to their initial state. This technology normally requires a warm–up time to stabilize, since the filament needs to be at high temperature to generate the arc, therefore, in these kinds of solutions the light modulation is not an option either.

These kind of lamps, specially deuterium and mercury based versions are the most common UV light sources, and were the unique candidates until the UV LEDs (Light Emitting Diode) where launched around year 2000, and are currently steadily replacing the gas lamps [89].

2.2.1.5 Light Emitting Diodes (LEDs)

Actually, the solid-state lighting is the biggest revolution in lighting system since the development of filament lamp, and the UV wavelength case is just another example after what we have already witnessed in VIS, NIR and MIR ranges in the last decade. Based on the electroluminescence principle, which was discovered around the late years of 1900 decade, the revolution of the LED emitters started

around 1950, but it wasn't until early sixties when the first visible red LED light by Nick Holonyak[23] at General Electric laboratories

The electroluminescence effect defines that in a semiconductor P–N junction, in some materials as gallium arsenide phosphide (GaAsP) or gallium phosphide (GaP), the electron and hole recombination when electric current is applied will dissipate energy in form of heat and photons, and not only in heat as it happens with Silicon (Si) or Germanium (Ge) semiconductor. The wavelength emitted by these diodes is, by definition, a narrow band because the emitted photon's frequencies depend on the band gap energy of the materials forming the p–n junction. Several different materials and combinations have been developed with band gap energies corresponding to near–infrared, visible, or near–ultraviolet light (see Table 2.2–1).

Actually, there are only a few examples of wide spectrum LEDs, as the white LEDs that are not strictly pure LEDs because they generate the white visible spectrum thanks to a phosphor coating over a blue LED, which light excites the phosphor and generates a yellowish light due to fluorescence. Being the combination of that yellow with remaining blue an apparent white light.

LED lights are available in a wide range of packages and beams and currently are able to deliver relatively high efficiency and radiation powers, in the VIS and NIR regions with technological developments driven by commercial lighting and telecommunication industries.

Additionally, using a GaInAsSb/AlGaAsSb–based hetero–structure lattice matched to a GaSb substrate allows creating LEDs for the 1.6–2.4 μm spectral range and by using an InAsSb/InAsSbP–based lattice matched to an InAs substrate LEDs for the 2.8–5.0 μm spectral range can be manufactured. Other approximations use quantum dot doped silicon semiconductor to generate LEDs in the NIR range [90].

In addition, due to their semiconductor nature, LEDs are fast, and offer very high switching frequencies that enable modulating the intensities not only in amplitude but also in time, allowing, among others the direct generation of stroboscopic lighting systems.

2.2.1.6 LASERs

Asides the LEDs, the twentieth century delivered another big breakthrough in photonic emitting technologies, the LASERs. Based on the spontaneous emission described by Albert Einstein, the LASER (Light amplification by stimulated emission of radiation) technology

[23] Nick Noyack, American Electrical Engineer (1928)

started its evolution around 1920 and the fits LASER device was developed in 1960 by Theodore Maiman[24]. The working principle of the LASERs is to amplify a small excitation (either optical or electrical) or pumping with a resonator cavity filled with an active medium where the optical amplification occurs.

The active medium as well as the cavity is designed so that a high gain is obtained for a specific wavelength, delivering spatial and temporally coherent light beam at high radiation powers.

There are several types of LASERs, with gases as Helium–Neon (HeNe) used as active cavities for 633 nm, solid state ones with crystal active mediums as YAG (Yttrium Aluminum Garnet) emitting in 1064nm, etc. However, the most typical LASER sources are the LASER Diodes, which combine a semiconductor emitter as the active medium, with a Fabry–Perot cavity for generating the stimulated generation. As it happens with the LEDs, the emission wavelength of a laser diode is essentially determined by the band gap of the laser–active semiconductor material. Thanks to the variety of semiconductor materials is possible to cover wide spectral regions. Principally, the accurate wavelength availability comes from the ternary and quaternary semiconductor compounds, where the band gap energy can be adjusted in a wide range merely by changing the composition details. For instance, a higher aluminum content (increased x) in $Al_xGa_{1-x}As$ causes an increase in the band gap energy and therefore a shorter emission wavelength.

There are also developments working and marketing white LASER solutions, named Super–continuum LASER, delivering high power solutions (e.g. > 500 mW) in the 450 nm to 2500 nm spectrum [91].

2.2.1.7 VCSELs

Additionally, in the last two decades, another LASER technology is rising as a low cost, low power, fast switching and high flux emitter alternative. Started around 1993 at Honeywell labs, the VCSEL (vertical–cavity surface–emitting lasers) technology presented a paradigm shift due to its surface emitting feature. A VCSELs is a semiconductor laser diode that generates a highly efficient light beam vertically from its top surface. The internal cavities containing the amplifying layers are surrounded by electrically conductive layer stacks that form the laser mirrors. The most common VCSELs emission wavelengths where in the range of 750 to 980 nm targeting communication applications thanks to the good modulation capabilities offered and potential low cost.

[24] Theodore Harold Maiman, American Physicist (1927-2007)

Because VCSELs emit light perpendicular to the surface of the laser, the manufacturing process is fully compatible with traditional semiconductor processing equipment. Additionally, the surface emission also contributes to easy testability, because the VCSELs are verified and burned–in while still in wafer, increasing the manufacturing yield and lowering the cost [92].

Another important practical benefit provided by VCSEL technology [93] are the integrability of VCSEL structures with other semiconductor and detector devices allowing the development of complete systems (see Figure 2.2-4). Besides, the LED packaging technologies are directly applicable to VCSEL allowing a reduced investment cost and enables direct replacement of LED systems by VCSELs. Additionally, when individual device's radiation flux is not enough, the VCSELs can be aggregated in one or two-dimensional arrays (within the same wafer) to scale up the power output. The relatively low power requirements and operation reliability are also important assets offered by this LASER devices.

The benefits of VCSELs are making them good candidates for different sensing applications as fluorescence measurement [94], distance and velocity measurements based on interferometry [95] on a very compact and low-cost settings. Additionally, as mentioned, the small size and the compatibility of VCSEL manufacturing process with semiconductor wafer regular processing, allows to integrate within the same substrate a whole emitter–detector system as the ones described in [94]. In these monolithically integrated devices, the major challenge is to limit the crosstalk between sources and detectors while maintaining the performance of the individual components (laser, detector, filters)

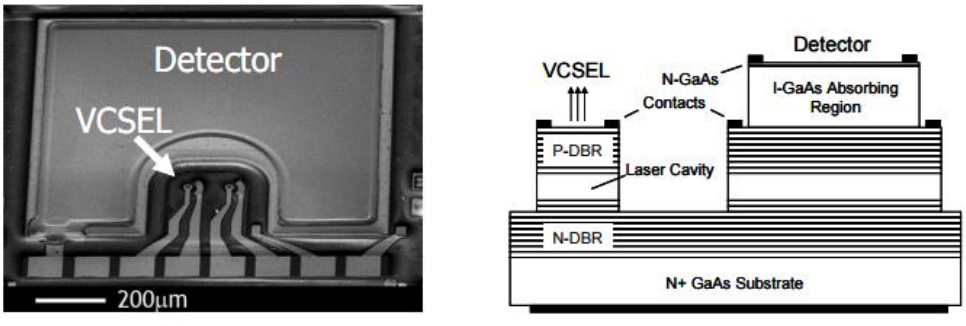

Figure 2.2-4: (a) SEM photography of a hybrid sensor including the VCSEL light source and the InGaAs detector, and (b) cross–section of the integrated device [94].

As mentioned, the most typical emission wavelengths of VCSELs fall in the range of 750–980 nm, based on GaAs/AlGaAs semiconductor system. However, longer wavelengths of e.g. 1.3, 1.55 or even beyond 2 µm can be obtained with dilute nitrides (GaInNAs quantum wells on GaAs) and from devices based on indium phosphide (InAlGaAsP on

InP) [96]. Having emitter in these ranges enables the use of VCSELs for gas monitoring because several molecules present the absorbance lines at these wavelengths. For instance, carbon monoxide and dioxide show several absorption lines around a wavelength of 1.58µm and close to 2µm – Methane in comparison shows absorption between 1.6 and 1.8µm.

2.2.1.8 MEMS based IR sources

As it has been presented, the tungsten filament micro–bulbs are a standard, low cost and well know technology for applications requiring working in the IR range. However, due to their intrinsic properties, they present a number of limitations in terms of limited modulation frequency (max 5 Hz), high power consumption (>100mW), or optical drift (>2%/1000h). Additionally, due to the cover glass (e.g. Quartz), the IR efficiency falls down to 60% at 4200 nm and is almost 0% above 5000 nm. Additionally, their form factor (3mm diameter, ~6mm long) jeopardizes the compactness of the final system and hinders the optical alignment due to their broad emission beam.

Indeed, the latest LED alternatives covering the near, short wave and mid IR ranges (1000 – 5000 nm), address some of the aforementioned issues. These solid-state emitters allow fast responses (>20 KHz), offer narrow emission bands (500 – 700 nm) and relatively high optical power (>0.3 mW radiant flux) at 4300 nm (e.g. L13201–0430M from Hamamatsu, Hamamatsu City, Japan). However, these devices show a relatively high-power consumption (~160mW if I_F=80mA and V_F=2 V) and their optical efficiency depends tightly with the ambient temperature showing a coefficient of 1.2%/ºC [97], converting the LEDs in a non–stable alternative for wide temperature span applications as industrial use cases (e.g. –20ºC to 80ºC).

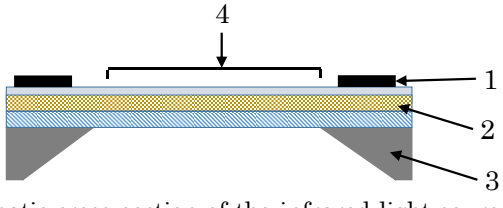

Figure 2.2-5: Schematic cross section of the infrared light source chip and the source mounted in a TO–5 housing. (1) Bonding pads: (2) a–NAC multilayer membrane; (3) silicon support; (4) active emitter area.

In this situation, MEMS IR sources appear as good candidates for solving some of the disadvantages of micro–bulbs and LEDs. The MEMS based emitters normally include a heater (e.g. tungsten) embedded within a dielectric membrane made of nano amorphous carbon (NAC). The substrate is made of Silicon with a back etched membrane. The last layer of the IR emitter chip is typically a

protective layer consisting of silicon nitride, which protects the active element against environmental influences [98].

When current is applied, the heater temperature can reach 400 – 700°C and emits radiation. A thin dielectric membrane is used to thermally isolate the heater from the substrate and hence reduce power consumption. The MEMS IR source can be made compact (3mm x 3mm x 1.5mm) where the IR emitter can be treated as a point source, thereby simplifying the design of the optics, such as reflectors and filter positioning [99]. However, even if these devices offer fast electrical modulation and high modulation depth the emissivity is not that high [100][101].

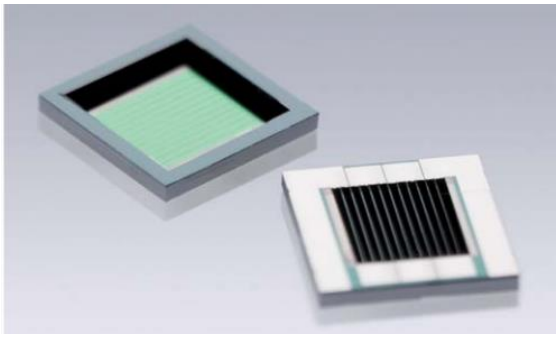

Figure 2.2-6: Front and backside of the IR Source MEMS chip. (overall size: 3.2 x 3.2 mm^2, membrane size: 2.1 x 1.8 mm2), (Axetris, Munich, Germany).

These kinds of sources offer a wide spectral output covering 1 – 20 µm, what is probably the widest bandwidth available in emitter technologies. Additionally, these MEMS–based IR sources can be modulated at frequencies over 100 Hz and achieve 25,000 working hours.

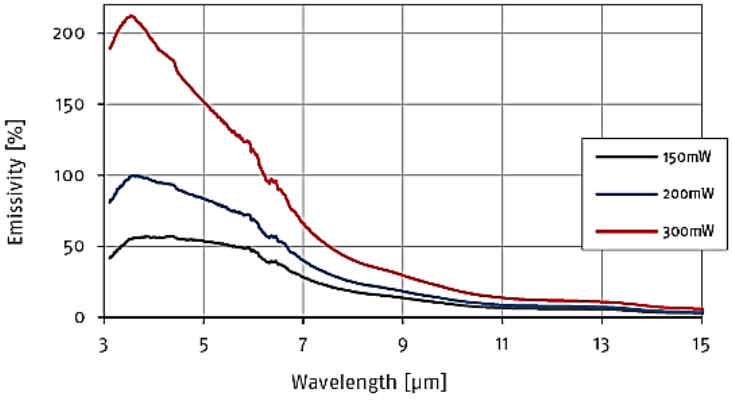

Figure 2.2-7: Emissivity spectrum of the JSIR 350-5 (micro-Hybrid Electronic GmbH, Hermsdorf, Germany) at different power levels

2.2.1.9 Emitter Technology Comparing Chart

Table 2.2–2 outlines the major advantages and disadvantages of the reviewed light sources.

Table 2.2–2: Summary of Emitter Technologies with advantages and disadvantages of each solution.

Light Source	Advantages	Disadvantages
Incandescent	– Low cost – Rugged – Broad spectral coverage – Easy electrical drive – Relatively compact	– Inefficient – Non–uniform spectrum – Continuous decay – Short lifetime – Limited modulation
Gas Arc	–Best solution for UV emission	–High Voltage required –Warm–up required –Bulky equipment
LED	–Very Low cost –Efficient in VIS –Ultra compact –Includes optical guiding –Fast modulation available –High Flux	–Requires active control for stable operation –Not efficient in UV, NIR and MIR ranges –High Temperature Coefficients
LASER	–Narrow Spectrums in UV, VIS and NIR, from 240 nm to 1500 nm (Quantum cascade laser up to 20 μm) –Available in Wide spectrum 450 – 2500 nm (super continuum versions) –Long spatial and temporal coherence –Modulation available	–Very expensive –May require complex electronics (not the diode lasers) –Bulky equipment

VCSEL	–Potentially low cost –Narrow Spectrum –VIS and NIR available –Very compact –Integrable with other semiconductor devices –Easy optical coupling –Modulable in GHz range	–Low reliability –Low power output (0.5–5 mW)
MEMS IR	–Wide MIR source –Modulation available –Compact	–Relatively expensive –Not available for NIR (>3 μm)

2.2.2 Detectors

Light detectors are the family of devices that transform photons of a certain wavelength and polarization into some sort of electrical energy. As emitters, the receivers are essential part of any photonics–based sensor as they deliver quantitative information about the properties of a light radiation incident to its sensitive or active surface.

Detectors are sensitive to certain types of light, specially defined by the wavelength and by the minimum detectable intensity. Not all the radiations may generate the same signal level and moreover, some light levels and frequencies may even be *invisible* for the detectors (see Table 2.2–3 for more details about the detection ranges). However, matching the detector sensitivity with the working wavelengths is not the only feature to consider while selecting the photo–detector.

The quantum efficiency, the spectral response, the aperture number, the bandwidth, element number and disposition, etc. are important design parameters that will determine the suitability of a certain photo–detector technology. In addition, other critical factors as dependency with the temperature, noise, lifetime, compactness and cost should also be considered for deciding the photo–detector technology.

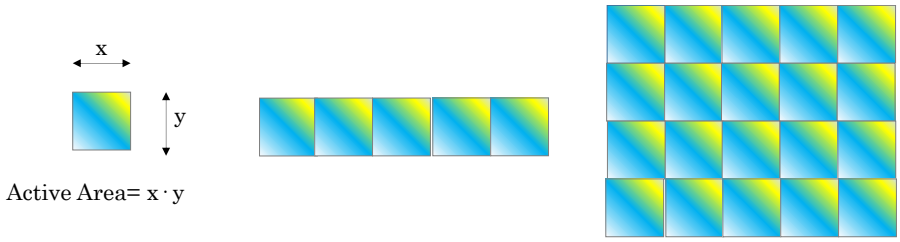

Figure 2.2-8: From left to right, Point, Linear and Matrix Photodetector structures. The matrix or image detectors are well known as they are the base for current popular digital photo-camera's sensors.

The UV/VIS/IR spectral ranges are currently covered by different material and technologies, either in point, linear or image arrangement of detectors (see Figure 2.2-8). Asides the typical structures, photo–detector technology reveals examples as the pyroelectric detectors, thermopiles, microbolometers, narrow–bandgap photovoltaic detectors [102], Schottky barrier detectors [103], extrinsic photoconductors [104], multi–quantum–well semiconductor hetero-structures for quantum cascade detectors (QCD) [105], etc. However, there are four main technologies which cover the majority of the applications: the photomultiplier tubes (PMTs), silicon photo-multipliers (SiPMs), avalanche photodiodes (APDs), and silicon photodiodes.

Table 2.2–3: Examples of Detector technologies and sensitivity ranges.

Source Emissivity Ranges (μm)	**Start**	**End**
Silicon (Si)	0.3	1.2
Lead Sulfide (PbS)	1.1	3
Indium Arsenide (InAs)	1.7	5.7
Indium Gallium Arsenide (InGaAs)	0.65	2.7
Germanium (Ge)	2	40
Lead Selenide (PbSe)	1.7	5.5
Deuterated Triglycine Sulfate	10	120
Indium Antimonide (InSb)	1.8	6.8
Triglycine Sulfate (TGS)	10	120
Pyroelectric Lithium Tantalate ($LiTaO_3$)	1.5	30

As with the light emitters, the following sections summarizes the main parameters describing the features of light detectors, introduces the main technological families and additionally, gives a deep review of the current trends and innovations in the field of microspectrometers, which represent a specific case of light detector,

allowing the discrimination of the light power across different wavelengths.

2.2.2.1 Main Features of Light Detectors

This section outlines some of the most important but basic features that describe a photo-detector technology. Notice that some of the features described in this section, as responsivity, response times, etc. are further elaborated along the Chapter 3, while describing generic sensor systems part of generic sensor system.

As mentioned, the spectral response (see Figure 2.2-9), or the efficiency of the detector to convert a received photon into electronic signal, is the very first parameter to review. Indeed, it is wavelength dependent and it is normally given in terms of quantum efficiency, QE, (see Eq. 2.2–5), which defines the number of electrons generated over the number of incident photons. Sometimes the quantum efficiency and the relative responsivity terms are used indistinctly, and even if they both refer to the detector efficiency to convert light into electrical energy, they are not strictly interchangeable (see section 3.2.1.1).

Alike the QE, the responsivity defines the generated amperes or volts per watt of incident radiant power (see Eq. 2.2–6).

$$\text{Responsivity} = \frac{\text{Electric Energy}}{\text{Incident Radiant Power}} \ (\text{A/W}) \qquad \text{Eq. 2.2–1}$$

$$\text{Quantum Efficiency} = \frac{\text{Electrons Generated}}{\text{Incident Photons}} \ \% \qquad \text{Eq. 2.2–2}$$

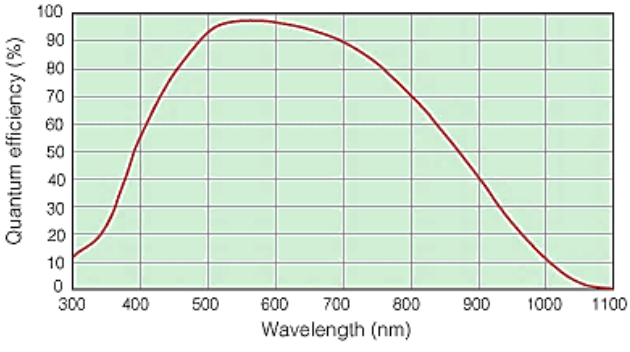

Figure 2.2-9: Spectral response of C10600-10B photodetector from Hamamatsu (Hamamatsu, Japan), where the quantum efficiency is displayed against the wavelength.

Therefore, the spectral response describes the efficiency of the detector material for detecting light over a certain wavelength span (see Figure 2.2-10).

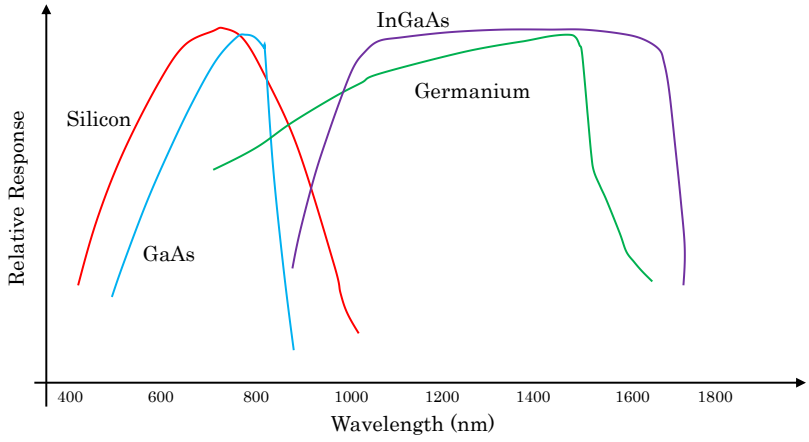

Figure 2.2-10: Typical spectral responses of different semiconductor materials.

Besides, the Numerical Aperture (NA) of a photo–detector help us understanding the percentage of a radiation beam that effectively gets to the detector surface. The NA is a specification indicating the acceptance angle of a system, measured from the detector's surface normal as described in Figure 2.2-11 and Eq. 2.2–3, where n is the index of refraction. The NA should be carefully chosen because exceeding the NA tends to increase the stray light[25] and not meeting the optimum NA reduces the overall system efficiency. Typically, the photo–detector material are flat surfaces with limited natural acceptance angle and, therefore, extra optics are normally used for enhancing the light collection and focusing into the receiver's sensitive area. In lenses, the numerical aperture is normally specified as the f-number or f/# as in Eq. 2.2–4.

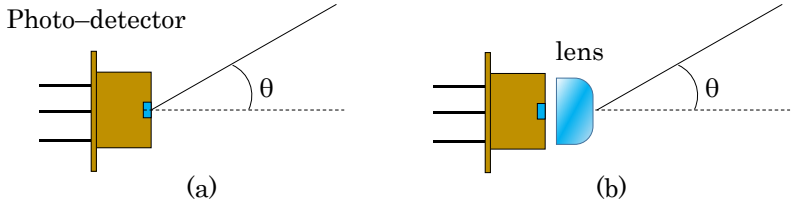

Figure 2.2-11: (a) Open air configuration for photo-detector. (b) photo-detector and a coupled Lens for enhancing the light collection.

[25] Stray Light is the light entering into a system that is not intended to be there.

$$NA = n \cdot \sin(\theta), \qquad \text{Eq. 2.2–3}$$

$$f/\# = \frac{1}{2NA} \qquad \text{Eq. 2.2–4}$$

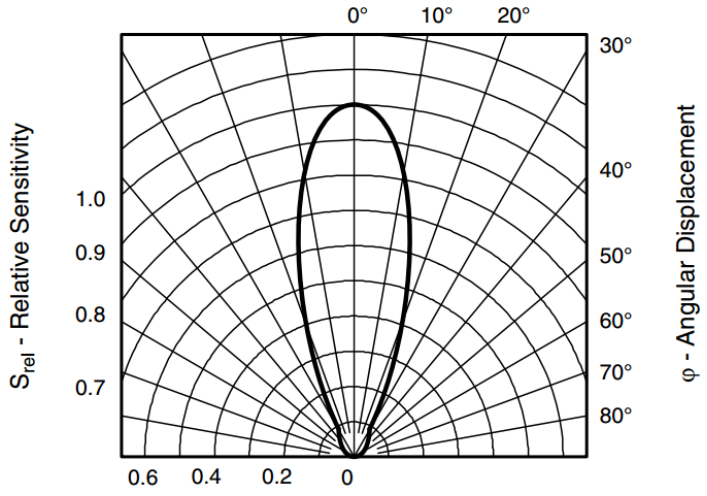

Figure 2.2-12: Typical graph representing the relative radiant sensitivity versus the angular displacement of a Silicon PIN Photodiode (VEMD2500X01) from Vishay (Malvern, PA, USA)

Another important remark that should be considered while dealing with photo-detectors is the Dark current (see section 3.1.1.13 for further details), which is one of the major contributors to the noise of the photo-detectors that hinders the detection of low light intensities. The point is that the electrical energy delivered by photo-receivers is not always originated from the detection of a photon, but from the consequence of some internal and unwanted effects that also generate micro–currents.

The dark current is described as the random generation of electrons in the absence of incoming photons. It is material dependent (e.g. silicon has much lower dark current than germanium) and sensors with larger active areas tend to have higher levels of dark current. Additionally, notice that the dark current approximately doubles its intensity for every 10 ºC rise in temperature. The dark current, especially in certain materials is the reason why photo–detectors may require operating under temperature controlled conditions, and often active cooling system (e.g. Peltier cell) is attached to the photo–detector case. The variation of the detectors responsivity due to changes in temperature are also material dependent, and in the semiconductor based technologies, this dependence has its origin in the increase of decrease of the band gap due to temperature. However, the relative variations in responsivity

can be reduced to less than 1% in certain technologies as in the Silicon Photodiodes (see Figure 2.2-13)

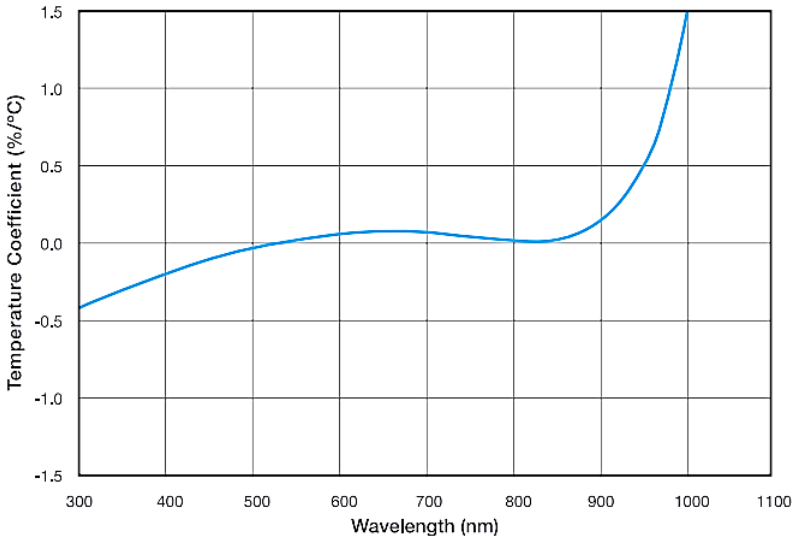

Figure 2.2-13: Typical temperature coefficient of responsivity for silicon photodiode [106].

Another relevant contributor to the noise level in the signal delivered from the photo–detectors is the readout noise, which represent the noise associated with reading the detectors current or accumulated charge. This perturbation is not strictly generated at the detector but at the readout electronics required for amplifying the photocurrent.

In addition, the integration time is another important parameter defining the operation of a photo–detector as it describes the amount of time a detector is allowed to collect photons. During the active periods, the photocurrent is either used for charging capacitors or it is continuously read out. On the other hand, during the inactive periods, the detector's charge is effectively coupled to ground.

In applications requiring responding to very fast switching light pulses, the time response (see section 3.1.1.10) of photo-receivers could be limiting the suitability of a certain solution. The time response defines the minimum light pulse duration that the detector is able to follow and convert into a readable photocurrent.

2.2.2.2 Detector Technologies

The following five sections describe the main photo–detectors technologies, emphasizing their typical physical, optoelectronic, and operational characteristics.

2.2.2.3 Photomultiplier tubes (PMTs)

PMT are vacuum tubes with integrated photo–detectors and photomultipliers that are extremely sensitive to UV, VIS and NIR radiations. They were first introduced around 1935 after several years of investigations for integrating the two internal processes that are the base of the PMT operation mode: the photoelectric effect (emission of electrons from an illuminated metal surface) and the secondary emission which defines that metal surfaces impacted by electron beams emitted a larger number of electrons than the incident ones.

The internal structure (see Figure 2.2-14) of a PMT is based on a vacuum tube comprising a photocathode, a sequence of dynodes and the anode where the signal is collected and delivered to the amplifying electronics. The photocathode is where the light is converted to the first set of electrons due to the photoelectric effect. These electrons are then sequentially multiplied in a series of dynodes where the secondary electron emission happens. Thanks to this cascaded multiplication of electron number, PMTs are able to achieve gains around $x10^6$.

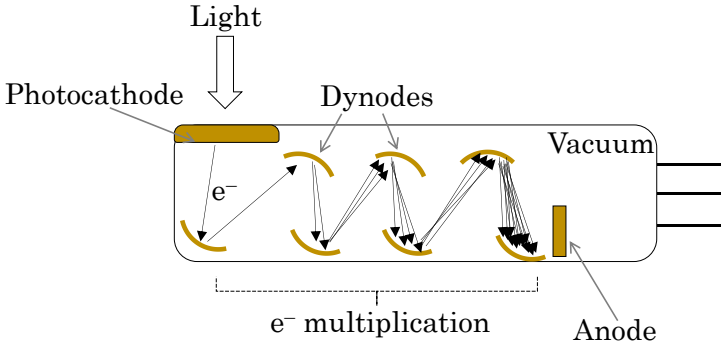

Figure 2.2-14: Internal structure of a PMT detector.

Due to the high gain, low noise, fast speed and large spectral response (especially in the UV range) the PMTs are still a good candidate for applications requiring high sensitivities, but their requirements in driving voltage (e.g. >1000 volts) and readout electronics hinder they use in low cost and integrated applications.

2.2.2.4 Photodiodes

Photodiodes are semiconductor devices with a p-n junction. In this case, the light to current conversion happens at the depletion layer due to the absorption of photons and the generation of an electrons-hole pair, which are then recombined at the N-layer generating the photocurrent, in a process known as the intrinsic photoelectric effect. The sensibility of the photodiode to radiations of

different wavelengths is determined by the band gap energy (eV) of the semiconductor material, defined by its absorption coefficient. Currently, since the first photodiode was developed in late forties at Bells Laboratories, several different materials (Si, Ge, InGaAs, etc.) have been applied to develop photodiode alternatives with the aim of covering different spectral ranges.

Nowadays the photodiodes are a mainstream alternative due to their simplicity, low cost and variety. See sections 3.1.2 for further details about photodiodes.

2.2.2.5 Avalanche photodiodes (APDs)

APDs are is a type of PD that has an internal gain due to avalanche multiplication, which is an intrinsic process in semiconductors by which *n* carriers in the transition region are accelerated by an electric field (see Figure 2.1-15) to energies sufficient to create free electron-hole pairs impact-ionize a lattice atom. The generated charge carriers, may also ionize more atoms while moving through the avalanche region, which leads to a higher gain of charge carriers.

Thanks to this process gains around 10^2 to 10^3 may be achieved by APD but a high reverse bias voltage (from 10 to 150V) to polarize the diode near the breakdown voltage is required.

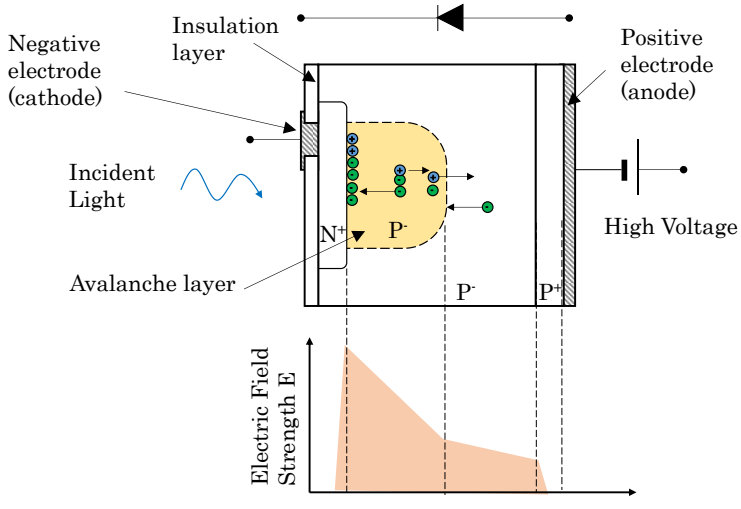

Figure 2.2-15: Internal structure of an APD photodiode detector.

2.2.2.6 PIN Photodiodes

PIN are also a photodiode type comprising not only the typical p-n junction but also an intrinsic region sandwiched between the p-n, which is this case are heavily doped regions (p+ and n+). In this case, the depletion layer is almost completely defined by the intrinsic region.

The PIN photodiodes may deliver some advantages compared to the regular PDs, especially in terms of fast switching times, thanks to the possibility of increasing the width of the depletion layer and thus the capacitance of the PD.

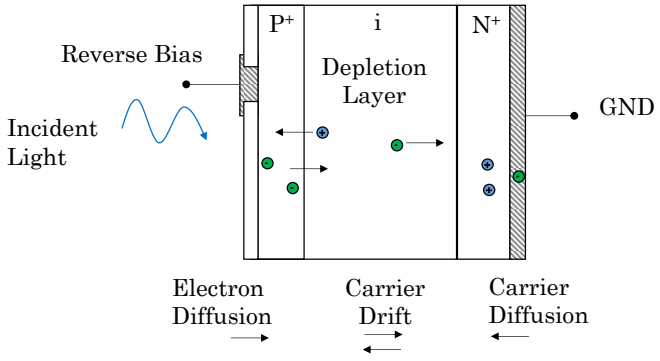

Figure 2.2-16: Internal structure of PIN photodiode detector.

2.2.2.7 Silicon photomultiplier (SiPM)

SiPMs are the only devices than somehow could compete with the PMTs in terms of sensitivity. They are formed by an array of APD working in parallel. The low-light detection capabilities of the SiPM along with the benefits of solid-state technology are reason behind the rapid penetration of this kind of devices [107].

2.2.2.8 Detector Technology Comparing Chart

Table 2.2–4 outlines the main features of the reviewed light sources.

Table 2.2–4: Examples of Detector technologies and main features.

Photodetector	**Wavelength (nm)**	**Responsivity (A/W)**	**Gain**	**Dark Current (nA)**	**Rise Time (ns)**
Silicon PN	550-850	0.41-0.7	1	1-5	5-10
Silicon PIN	850-950	0.6-0.8	1	10	0.070
InGaAs PIN	1310-1550	0.85	1	0.5-1.0	0.005-5
InGaAS APD	1310-1550	0.80	100	30	0.100
Germanium PN	1000-1500	0.7	1	1000	1-2
PMT	115-1700	$1\text{-}5 \cdot 10^6$	10^6	2 (30mins)	5
SiPM	320-900	0.4	10^6		1

2.2.3 Common Passive Optical Elements

This section will give a brief overview of some of the most typical passive optic components. These elements are the responsible for modifying filtering, reflecting, dispersing the light to enhance certain properties the optical system with the aim of making the most of the light generated at the emitters and providing the optimum light radiation to the detector. Therefore, sensor system developers in the UV/VIS/IR spectral domain profit from the availability of a large number of refractive/reflective/diffractive optical devices such as lenses, mirrors, beam–splitters and gratings for setting up the photonic systems. For a deeper review about optical components, the reader could be referred to the vast bibliography available about the topic, as for instance, [108] or [109].

Asides the specific function or feature offered by a certain optic component, the compatible spectral range of the optical material should also be considered, since not all the materials behave the same under different light wavelengths. Table 2.2–5 provides a summary of spectral ranges of most common optical materials, indeed, the ranges are approximations because the absorption does not remain constant along the whole specified range. The material selection is a fundamental part when designing a photonic system which works either in UV, VIS or IR range.

Table 2.2–5: Examples of Optical Materials and their associated spectral ranges

Optical Materials Spectral Ranges (μm)	Start	End
Methacrylate polymer	0.25	1.1
UV Grade Fuzzed Silica (SiO_2)	0.2	2.5
Quartz	0.19	2.7
BK7 Glass	0.315	2.35
Pyrex® Glass	0.31	2.5
Sapphire (Aluminum Oxide Al_2O_3)	0.15	5.1
Germanium	1.1	30
Silver Bromide	0.5	35

2.2.3.1 Lenses

Lenses are optical elements that, based on a geometric disposition of a material with a certain refractive index, are able to converge or diverge the incident light into a certain point or plane. The lenses are normally described by their focal length, which defines how strongly the optical system converges or diverges the light.

Lenses could be used as single elements or as a group of devices that sequentially modifies the light ray propagation geometry until it reaches the output of the lens system.

However, as the index of refraction depends on the wavelength, not all the light rays will bend equally if the incident light is not monochrome, generating a distorted light convergence or divergence, called chromatic aberration. To avoid this effect, specific lens system devices are found named Achromatic lenses which have been specifically designed to minimize the chromatic aberration effects.

Another typical artifact generated at convex lenses in the spherical aberration, which due to the convexity radius, the rays hitting the surface near the edges of the lens are reflected alike the ones hitting right in the center. This generates that even monochrome light beams get distorted due to the lens surface geometry. Another specific design of lens systems contributes to mitigate this effect: the aspheric lenses, which is a solution that instead of a single radius curvature combines a double radius surface to gradually bend back the rays to the ideal focal point.

There are certain applications where the light does not necessarily need to be condensed, but rather parallelized radiation is required. In these cases, collimation lenses should be used. These lenses allow users to control the field of view, collection efficiency and spatial resolution of the photonic setup, and to configure illumination and collection angles for fluid sampling.

Lenses could be manufactured in different materials as plastics or glasses, but indeed, the geometry accuracy and light transmission properties are superior in the glass versions, even though they are one order of magnitude more expensive.

2.2.3.2 Filters

Filters are optical devices that selectively transmit the wavelengths of an incident light radiation. They are normally defined by their frequency response, which specifies the how the filter modifies the magnitude and phase over the whole wavelength spectrum of the incident radiation.

There are two main categories for developing the optical filters, the absorptive ones and the dichroic filters or interference–based ones. Absorptive filters basically are made of a material that absorbs certain wavelengths. This kind of filters is a cheap option, but their frequency response is not usually very sharp, and when accurate spectrum cleaning is required they are not usually suitable options. On the other hand, dichroic filters are able to deliver very accurate frequency response thanks to the interferometric working principle. These filters are formed with a stack of layers in their surface that work as a cavity

(actually, as a Fabri–Perot interferometer), where the light is reflected back and forth generating destructive or constructive interferences by which some wavelengths get blocked. However, even if the optical characteristics of interference type filters are very accurate, they show a strong dependency with the angle of incidence of the light rays, with frequency responses normally shifting to shorter wavelengths as the incidence angle displaces from the normal [109]. Therefore, in this kind of filters there is a position dependent color sensitivity.

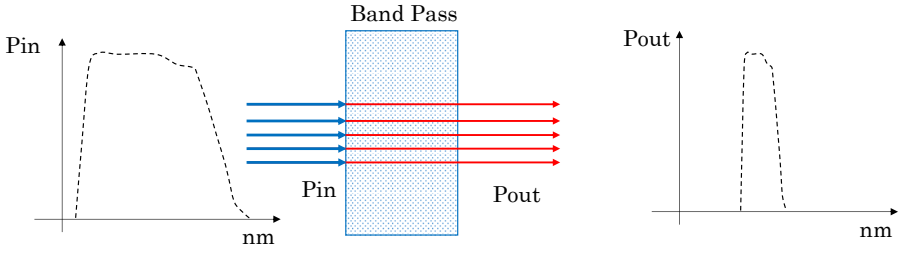

Figure 2.2-17: Filtering Effect on input radiation frequency spectrum.

Filters could be low–pass, high–pass, band–pass or notch filters. Low pass filters block all the wavelengths beyond the cut–off frequency, high–pass ones only transmit the radiation above the cut–off filter and blocks the low frequencies. Band pass filters just transmit the wavelengths between low and high cut–off frequencies, and notch filters just eliminate the portion of the spectrum within the high and low cut–off frequencies.

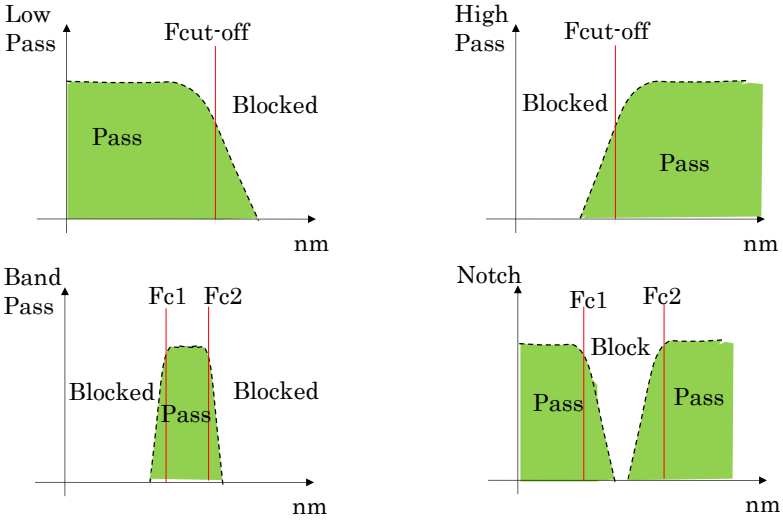

Figure 2.2-18: Different filters configurations.

2.2.3.3 Windows

Windows are the simplest optical elements because they just need to let the light be transmitted across their volume, assuring

minimal losses. However, the relevance of the optical windows in fluidics sensors is not trivial, because they represent the interface between the optoelectronic component and the target fluid, and are responsible of isolating the photonic elements from the potentially harsh fluid conditions in pressure, temperature, corrosion, etc. Chapter 3 gives a deep review of this specific topic.

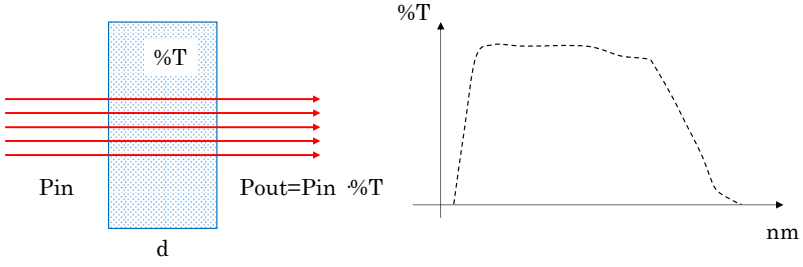

Figure 2.2-19: Optical Window, where the transmitted light power depends on the transmittance of the material, the thickness of the window and the wavelength of the radiation.

2.2.3.4 Mirrors

Mirrors are optical components, somehow similar to the lenses because they are able to concentrate the light into a certain point or plane, with the difference that the mirror do not suffer from chromatic aberration because alike the refracted light, the reflected one is not dependent on its wavelength, and just on the incident angle.

Therefore, the geometry of the mirror can be tuned to reflect the light as desired, and planar, curved and parabolic mirrors can be found, each of one delivering a different light reflection performance.

Alike lenses and windows, mirrors need to offer a highly reflective surface to enhance the light throughput. For this purpose, different coatings, normally metallic, are used to maximize the specular reflectance. Materials as aluminum, silver or gold are common elements for these coatings.

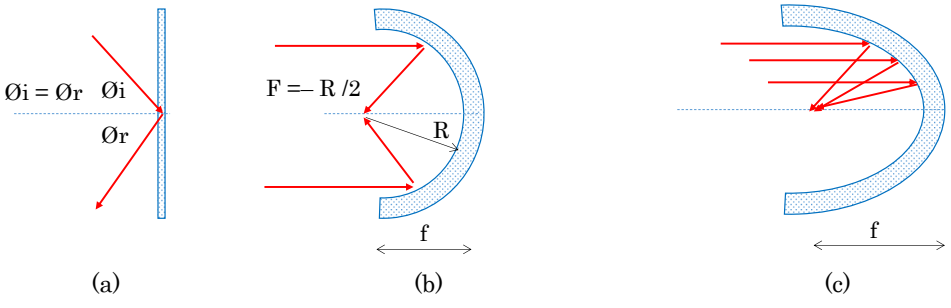

Figure 2.2-20: (a) planar mirror, (b) spherical mirror and (c) parabolic mirror.

2.2.3.5 Diffractive Gratings

In optics, when a certain structure is arranged periodically it normally becomes a diffractive grating. Diffraction grating, due to the periodicity of its structure splits and diffracts light into several beams travelling in different directions depending on the wavelength. Therefore, when a wide spectrum light radiation hits a diffractive grating, it is decomposed in a spatial sequence of singular wavelength radiations. Periodicity and shape of the diffractive grating structure defines the efficiency and light throughput as well as the amount of strayed light.

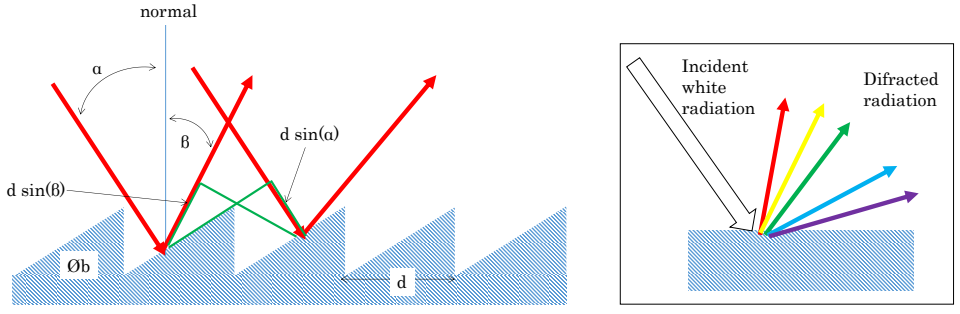

Figure 2.2-21: Basis diagram of a blazed diffractive grating structure.

In Littrow configuration based diffraction gratings, the following Eq. 2.2–5 to Eq. 2.2–7 describe the functionality.

$$d(\sin\alpha + \sin\beta) = m\lambda \quad \text{where } m = 0, \pm1, \pm2, \ldots \qquad \text{Eq. 2.2–5}$$

$$\sin\alpha = \sin\beta = \sin\emptyset_b \qquad \text{Eq. 2.2–6}$$

$$2d\sin\emptyset_b = m\lambda \qquad \text{Eq. 2.2–7}$$

2.2.3.6 Pinholes

Pinholes are plane plates with a small slit or aperture on their surface, with diameters between a few micrometers and a hundred micrometers. Pinholes are commonly used either as spatial filter where the small pinhole acts as a low–pass filter for spatial frequencies in the image plane of the beam, or as light diffractors, generating an airy disk pattern at the pinhole output.

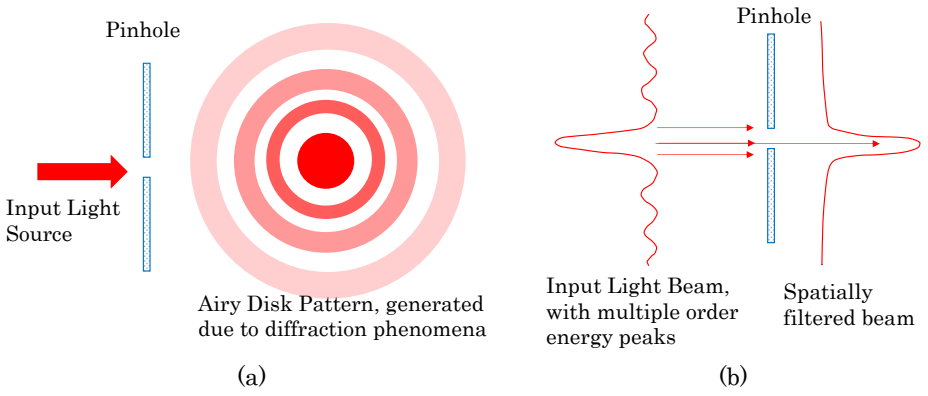

Figure 2.2-22: (a) pinhole as diffractor device and (b) pinhole acting as spatial filter.

2.2.3.7 Bean splitters

These optical devices are used to split or combine optical beams. The beam separation could be performed based on the radiation wavelength or on its polarization, and the separation–combination ratio is also normally adjustable. The beam splitters are available in different configuration as cubic, plate, pellicle or dichroic.

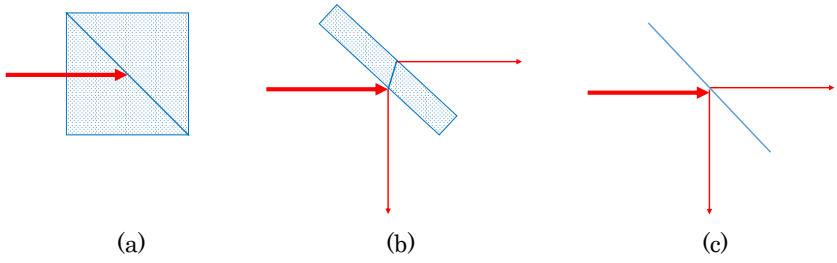

Figure 2.2-23: (a) planar mirror, (b) spherical mirror and (c) parabolic mirror.

2.2.4 Micro-spectrometers

Spectrometers, or their miniature versions, so–called micro-spectrometers, are optical systems designed for collecting a wide spectrum light beam and delivering the corresponding intensity values across a predefined wavelength range, with a certain spectral resolution. Their basic structure comprises a light collection, light splitting system and a single or multiple detector element [110].

When the collected wavelength is unique, then the spectrometer is defined as a non–dispersive system or as a monochromator (see Figure 2.2-24). And, even if they do not offer a

deep spectral information, these configurations are widely used when the relevant information is located in a certain and know wavelength range, as it happens with the gas molecule sensors, where the absorbance of the molecule of interest is known.

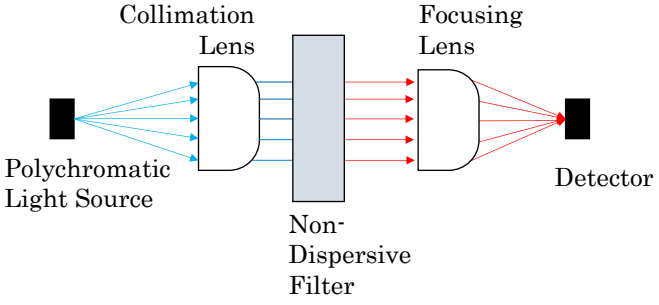

Figure 2.2-24: Basic structure of a non–dispersive spectrometer.

The monochromator configurations are sometimes adjustable, and if this wavelength tuning can be accomplished in an automated way, then a complete spectrometer can be developed, where radiation power information is given for certain wavelength slots. This kind of devices are known as single detector spectrometers, and represent a sensible and economic option when fast acquisition times are not required. The single–element spectrometers will be slower by definition, because a time–based filter multiplexation is required for measuring the light irradiance over the whole wavelength span.

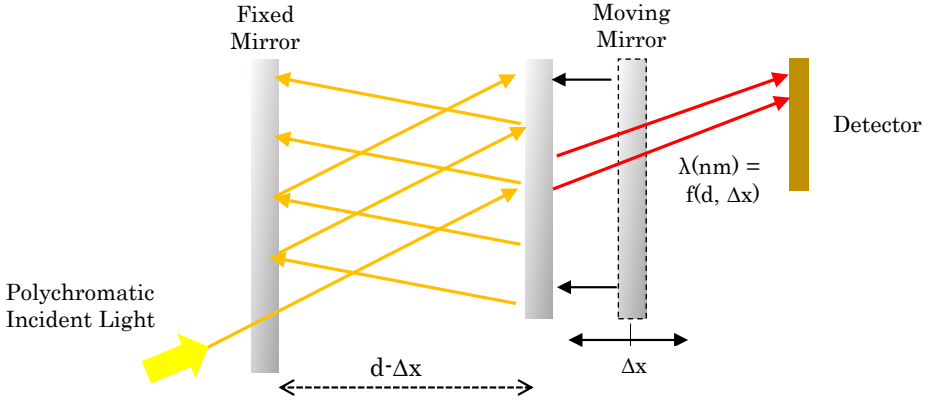

Figure 2.2-25: Schematic structure of Fabri-Perot Etalon interferometer with a moving cavity wall that tunes the wavelength of the outputted radiation

The single element spectrometers are normally based on interferometric configurations using Fabry–Perot or Michelson[26] approaches, where the destructive interference wavelengths depend on the internal geometry (distances between elements) of the resonant

[26] Albert Abraham Michelson (1852-1931), American physicist.

cavities [111][112] (see Figure 2.2-25 Figure 2.2-26). There are also some other approaches using moving mirrors based gratings following the Czerny–Turner[27] approach [113][114]. All of these setups require to generate micro–movements in one or various internal optical structures to modulate the wavelength at which the detector is instantly receiving the power.

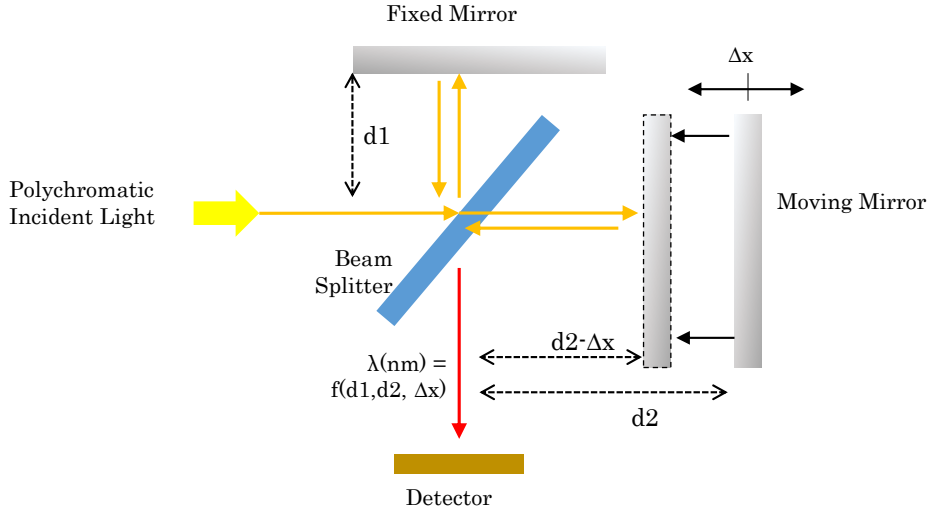

Figure 2.2-26: Schematic structure of Michelson interferometer with a moving mirror that may be used to tune the constructive frequency of the setup.

Alternatively, the multiple element spectrometers are designed to simultaneously receive and read the light irradiance over a defined wavelength range. In this kind of setups, a linear array is arranged for collecting on each of its individual elements, the portion of the wavelength spectra split or filtered by the optical system. Therefore, in this kind of systems, the geometrical disposition of the elements normally defines the wavelength range detected.

There are another setups for filtering the light delivered to the linear array spectrometer, as the Linear Variable Filters (see Figure 2.2-27), which are thin–film coatings, deposited in the top of the detector. The singularity of these thin–film filter is that the coating height defines the cut–off frequency of a band–pass filter. Therefore, if the coating height is gradually modified along the linear detector array, each individual photo–receiver will detect the light intensity of the wavelength corresponding to the height of the coating located above [115].

[27] Arthur Francis Turner (1906-1996) American physicist and Marianus Czerny German physicist (1896-1985).

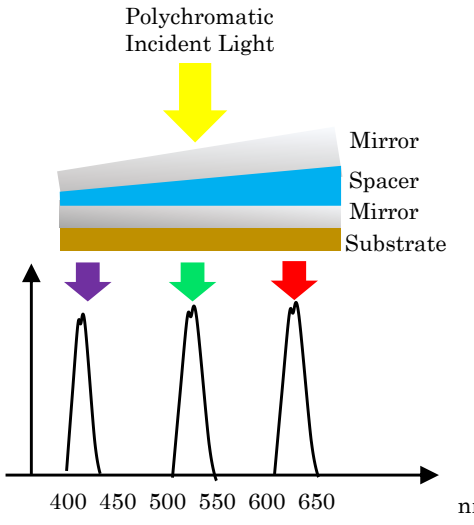

Figure 2.2-27: Example structure of a linear variable filter based on the effect of incremental high on interferometric cavity [115].

One of the latest structure presented for delivering spectrometer system is to merge a 2D spatial filter matrix, with N different band–pass areas, with a 2D photo–receiver array, with N pixels. Then, above each pixel a certain wavelength filter is located, and therefore, the pixel only receives the light intensity of the corresponding wavelength [116][117].

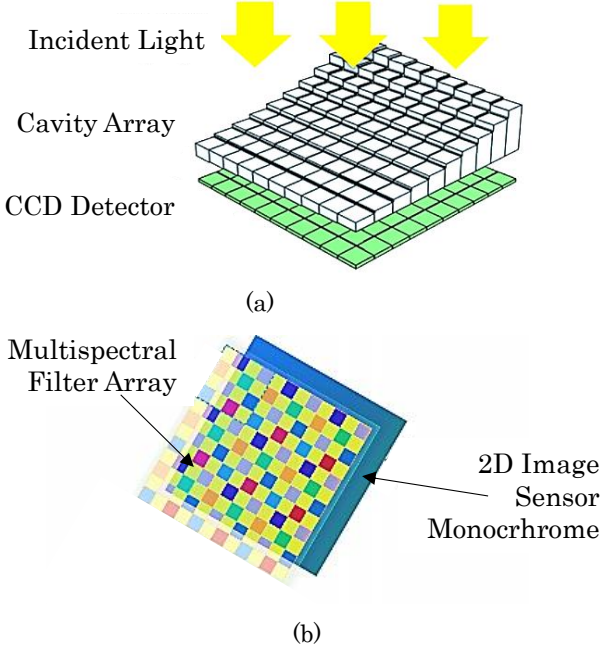

Figure 2.2-28: (a) Fabri Perot multi–cavity 2D array [116] and (b) Thin Film 2D filter structure [117].

Table 2.2–6: Summary of Spectrometer technologies with advantages and disadvantages of each solution.

Type	Technology	Advantages	Disadvantages
Single Element / Single Wavelength	Non–Dispersive (Filters) Mono–chromator	–Simple systems and very compact setting –Low cost – Immediate readout	–Limited spectral information
Single Element Detector	Fabry–Perot Michelson Czerny–Turner	–Low cost –Detailed spectral information –Compact size	–Slow readout
Linear Detector Array	Diffractive Grating Linear Variable Filter	–Immediate readout –Detailed spectral information	–larger than others –high cost, especially in NIR version
2D Detector Array	Multispectral Filter Arrays Etalon Arrays	–Immediate readout –Compact size	–limited spectral information (N channels) – high cost, especially in NIR version

For a detailed description of the different spectrometer setups as the Diffractive grating based, Michelson interferometer, Etalon Fabry–Perot cavities, Czerny–Turner approaches and others, for instance, please refer to [118] [119].

3.

Smart Photonic Sensors

In this chapter, a fundamental overview regarding sensors is given, presenting the concept of transducer, analyzing the main static and dynamic characteristics of sensors and introducing noise, cross–talk, cross–sensibility and other important concepts that should be considered for understanding the response of any sensor system. The section follows presenting the Smart Sensor term, which is a concept of sensor system that embeds the transducer, the algorithms and the communication means within an integrated solution. The chapter continues introducing the most important photonic sampling techniques, susceptible of being integrated in a cost-effective and compact system. Additionally, the section outlines the main techniques or approaches for analyzing the information contained in the light beam outputted by a photonic sensor, allowing the extraction of relevant data about the material under observation. Finally, the in–line sensing approach is described and compared to other monitoring approaches as the at–line, off–line or on–line setups, describing the main challenges of the wettable parts and in-situ calibration of these in-line sensors.

3.1 Fundamental Description of Sensors

Sensors are devices which transform a certain physical phenomenon into an electrical signal, representing a part of the interface between the physical world and the electric devices domain. This capability of perceiving the surrounding is described by the root Latin word *sentire*, which is the origin of the English word *sensor*, formulated around 1350–1400. A sensor is supposed to react to an input stimuli generating processable outputs, which are functionally related to the input's quality or quantity parameters, normally referred as measurands.

Sometimes, the word Transducer is used instead of sensor, but they entail substantial differences. The word Transducer was first coined in 1525–1535 and its source is the term *transduce*, which defines *to transfer*. A transducer is a device that converts one type of energy to another, and even if this generic definition covers the specific case of sensing elements, it also describes the actuators, which convert an electrical signal into a physical phenomenon.

The lack of specificity while describing the function of a sensor is because this is a multidisciplinary field by nature. The sensors may respond to several different domains (chemical, radiant, mechanical, magnetic, thermal) generating processable electrical outputs processes. Each sensor presents its working principles, fundamented in the concatenation of different physical or chemical processes that convert the information describing a material or phenomenon into an electrical signal in form of Volts, Amperes or Watts. These processes are well described in the literature as for instance photoconductivity (radiant energy into electrical energy), piezoelectricity (mechanical energy into electrical energy), Seebeck effects (heat energy into electrical energy), Hall effect (magnetic energy into electrical energy), etc. [120].

Even if this chapter outlines the main characteristics for sensor devices, we should consider that the focus is put on photonic sensors, and more specifically on smart photonic sensors for in–line fluidics monitoring. As depicted in Figure 3.1–1, photonic sensors are based on the analysis of an incoming light beam, which embeds into its properties (amplitude, spectrum, phase, etc.) information concerning the measurands. This incoming light radiation is normally conditioned using optic elements before its detection on an optoelectronic detector, which basically converts certain incident photons (e.g. depending on the photons wavelength) into an electrical signal. The resulting electric signal needs to be cleaned, analyzed and interpreted to extract the significant information about the measurand or analyte. Besides, some other photonic sensors also include the light source, required to generate the excitation radiation that interacts with the phenomenon

being monitorized changing the original properties of the radiation. Additionally, sometimes, this light emitter needs to be controlled (e.g. modulation, synchronization, etc.) to enhance the quality of the measurements delivered by the sensor.

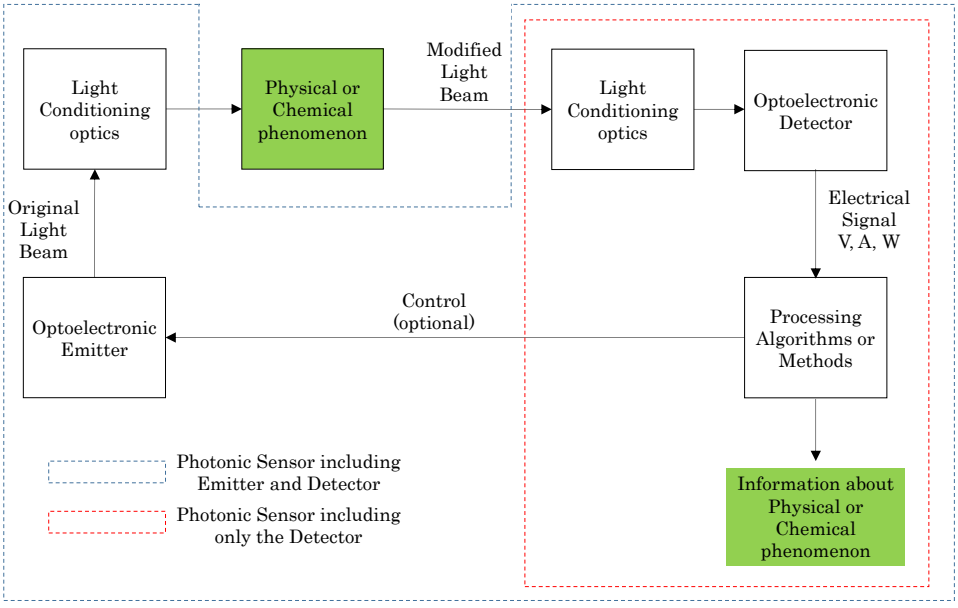

Figure 3.1–1: Basic Block of a Photonic Sensor.

The following sections within the chapter overview fundamental information about sensor characteristics, present some practical considerations concerning the use of sensors, including the different concepts impacting in the final sensor cost, and introduces the formal description of the Smart Sensor Concept. The remaining sections in the chapter include more specific information about photonic sensors (section 3.2.2) and about in–line fluidics sensors (section 3.3)

3.1.1 Sensor Performance Characteristics Definitions

Before describing the different performance parameters that describe a sensor operation, we must introduce the basic concepts that define what is expected for an optimum sensor.

Sensors should be sensitive to their target analytes, and insensitive to any other input quantities or environmental condition. Sensors are expected to deliver reliable, accurate and stable measurements [121], without affecting the analyte itself, avoiding the observer effect which describes the unintended alteration in system

behavior caused by measuring that system [122]. The limit of detection, generally, is required to be as low as possible to enable the sensor measuring small quantities of the measurand. Additionally, sensor size, power consumption and communication interfaces need always to be considered while engineering a sensor, towards a compact, autonomous and easy to integrate sensor system. The sensor life is also an important parameter to consider because a stable behavior is expected for the entire life span of the sensor, which could go from one single use (disposable sensors) to several years, as it is normally the case for the in–line sensors.

Finally, all the above mentioned features should also comply with cost efficiency requirements in terms of sensor development and sensor unitary cost.

After having given a general introduction about the desired features for a sensor device, the following sections offer a brief description of the different key performance indicators used when defining a sensor system. Since there is no a standardized method for describing these parameters, contributions from reference sources as Fraden [123], Kourosh [124] or Meijer [125] has been used for generating the following descriptions

3.1.1.1 Transfer Function

The transfer function describes the functional relationship between the physical parameter under measurement and the electrical output signal generated by the sensor. This functional relationship is normally described in a graphic manner, depicting the correlation between the measurand properties (e.g. concentration of a certain molecule, concentration of particles, etc.) and the signal generated by the sensor (see Figure 3.1–2).

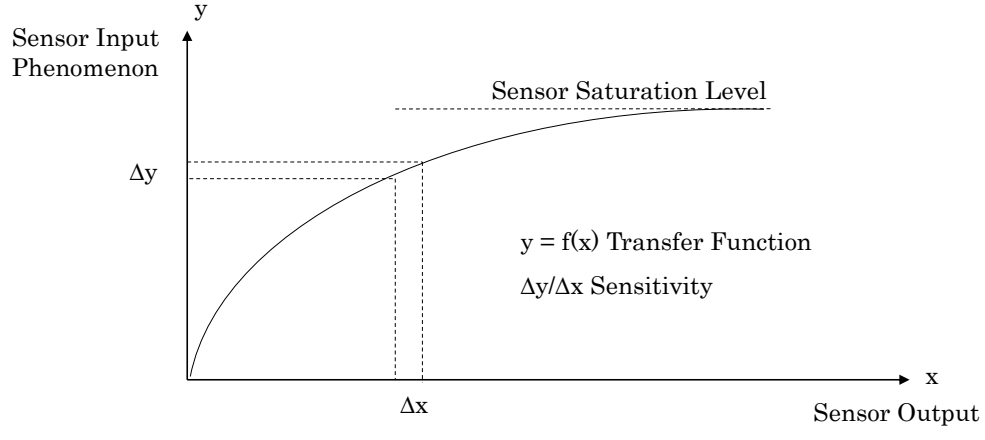

Figure 3.1–2: Graphical description of Sensor's Transfer Function and Sensitivity in a non–linear sensor response.

Sometimes, this Transfer Function is not stable amidst a sensor production batch and may require a calibration (see section 3.1.1.9) of that function for each element or for each fabrication order. This is a typical consequence when using solid state light emitters as a part of the photonic sensor, because the light properties delivered by those components are always batch dependent [126].

3.1.1.2 Sensitivity

Sensitivity, also defined sometimes as Responsivity, defines the ratio of the incremental change happening at the sensor output (Δy) when an incremental change is applied at the input of the sensor (Δy), thus, the sensitivity represents the derivative of the transfer function with respect to the input physical signal.

Sometimes, it could happen that the sensor sensitivity does not remain constant across the whole dynamic range of the sensor (see section 3.1.1.4), describing a non–linear sensor response (see section 3.1.1.8), that, for instance, may hinder the sensor calibration. Another typical issue is when the sensor response eventually reaches a saturation level, a state in which it can no longer respond to any changes (see Figure 3.1–2). Therefore, an ideal sensor should deliver a large and rather constant sensitivity in its operating range.

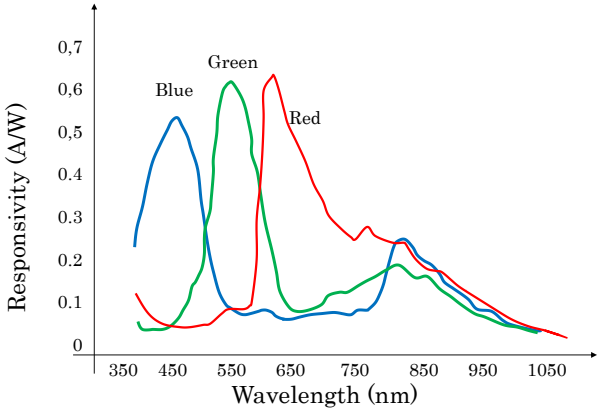

Figure 3.1–3: Relative Sensitivity (quantum efficiency) against wavelength graph for the MT9P006 image sensor (Red, Green and Blue channels) from On Semiconductor, which also delivers a sensitivity (responsivity) of 1.74 V/Lux/s at 540 nm.

The sensitivity is a critical parameter in photo–detectors describing the relation between the irradiance hitting the detector surface and the electrical signal generated. Additionally, in photo–detectors, this relationship is also normalized with a time constant, representing the electrical signal generated by unit of time under a given irradiance (e.g. V / Lux / s as seen in Figure 3.1–3). This parameter is also represented against the wavelength of the incident

radiation, because normally, the photosensitive materials do not respond equally to all the wavelengths (as described previously in section 2). Therefore, this kind of information is critical for understanding the behavior of a photo–detector.

Notice that these sensitivities are normally given for a certain temperature (e.g. T= 25ºC) because the response of the detectors normally varies with the temperature, due to the electronic changes happening at the detectors semiconductor.

3.1.1.3 Limit of detection

The limit of detection (LD) represents the minimum level, quantity, signal or effect of the measurand that is observed by the sensor, when all the interfering factors have been taken into account. As it will be described while assessing the noise (see section 3.1.1.13), when interferences are important, the LD is normally high and the sensor system is not able to detect slight changes in the measurand.

This parameter is especially relevant when dealing with chemical measurements, therefore, if the photonic sensor application deals with analytical measurements, the LD calculation should follow the recommendations delivered by standardization committees [127][128], which defines the LD not only as the minimum concentration of a given analyte to be detectable by the sensor, but the minimum concentration that can be measured in a reliable manner, with known probabilities α and ß of making false positives and false negatives. For analytical measurements, the LD is normally given as parts per million (ppm), percentage (%), or concentration (mg/L) of the analyte of interest detectable by the sensor.

In photonic setups, smallest detectable input signal is defined as standard deviation of input referred noise under dark conditions [129].

3.1.1.4 Span or Dynamic Range

This parameter defines the maximum and minimum ranges of the measurand which may be converted to electrical signals by the sensors, with acceptable accuracy. Therefore, the sensor span defines the working range from the limit of detection level up to the saturation level. All sensor systems are designed to operate within a specific range, and different engineering decisions are taken to optimize the performance over this specified range. Fabricating a sensor with a high dynamic range is not straightforward, and normally requires sacrificing limit of detection, resolution, sensitivity and the linearity.

Continuing the example for the analytical measurements, the dynamic range could be expressed as the range, for instance, 0.1% to

50% of concentration of a certain compound in a dissolution. Below 0.1% the sensor is not able to detect the compound and above 50%, the sensor is saturated.

Achieving a high Dynamic Range in the optoelectronic detectors is a general requirement for the photonic industry, mainly driven by the imaging and machine vision industry, where the CMOS cameras are required to deliver good imaging performance under low light, high light and high contrast (bright and dark areas within the same scene) conditions. This situation has led the development of a new generation of CMOS detectors (arrays of pixel elements), named High Dynamic Range (HDR) image sensors, that are able to operate efficiently under high contrast lighting environments [130].

3.1.1.5 Resolution

The resolution of a sensor system is described as the minimum observable signal fluctuation, being this fluctuation described by its amplitude and by the timescale when it happens. So, the sensors deliver a temporal and a spatial resolution as part of their features.

The temporal resolution is normally in relation with sensor's response time or bandwidth (see section 3.1.1.10) and basically describes the time slots when the sensor measures the physical phenomenon. Some changes may happen too fast to be observed by the sensor. The spatial or amplitude resolution defines the minimal change of the measurand that can produce a detectable increment in the output signal.

Even if the sensor nature is important for defining the resolution, currently, these terms are more often associated with the digitalization process applied to the sensor's output, defined by the sampling frequency (time resolution) and quantification (spatial resolution) processes that convert the electrical signal (V, A, W) into a digital signal expressed in bits (see section 3.1.2).

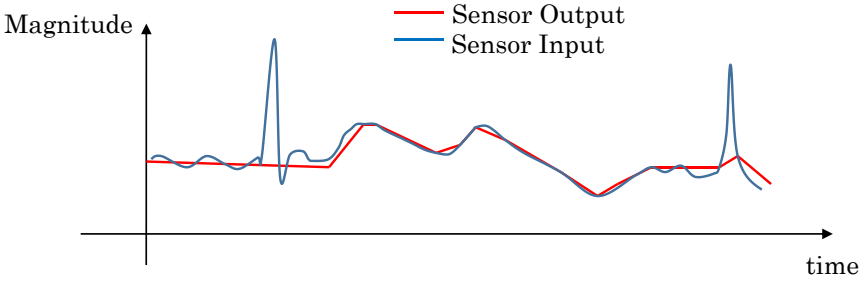

Figure 3.1–4: The lack of temporal resolution hinders the detection of input spikes. The lack of spatial resolution does not allow to follow the slight changes happening at the input.

3.1.1.6 Accuracy

The accuracy is generally defined as the largest expected error between the real value of the measurand and the value outputted by the sensor, and therefore, describes the rightness of the measured value. The accuracy assessment can only be accomplished if the sensor system is benchmarked against a standard model or compared against the values outputted by a sensor with better accuracy. Sometimes the accuracy is defined as a fraction of the full scale output (FSO).

Obtaining an accurate measurement is normally one of the major goals when designing a sensor, but this is hindered by several factors as noise, interferences, cross–sensibilities, etc. Additionally, delivering a high accuracy along the whole dynamic range is also a challenging requirement, and normally sensors offers worse performance at the edges of the dynamic range.

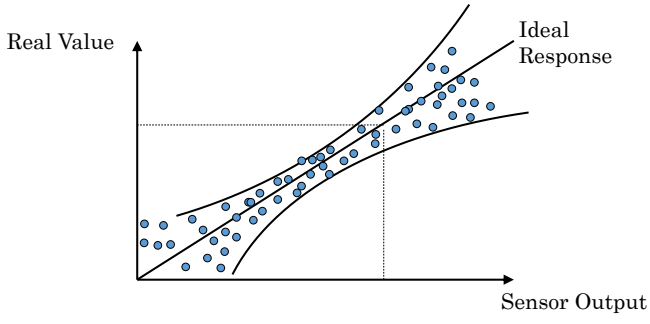

Figure 3.1–5: Sensor Accuracy across the whole dynamic range. Occasionally, sensors deliver better accuracies at the center of the measurement span.

3.1.1.7 Precision, Repeatability, Uniformity and Stability

This list of terms describes the performance of the sensor over a period of time, and generally describe its operation from a statistical point of view, defining the variance observed in the measurement value while the parameters of the measurand and the environmental conditions remain the same.

The Precision or Repeatability terms describes the ability of the sensor to deliver the same output while measuring continuously the same measurand under the same conditions, regardless the correctness of the outputted value. Therefore, Precision defines how consistent a particular sensor is against itself, and it typically limited by random noises, which is often outside of our control.

Besides, Uniformity is described as the systematic error that defines consistency of a measured value, either in a spatial distribution or compared to another sensor taking the same measurement. Uniformity describes the performance dispersion present in a sensor production batch.

Stability is the parameter that describes the ability of the sensor system to maintain its characteristics unaltered over a period of time, therefore, it defines the stability of the outputted value when measuring the same analyte over time. Changes in stability, also known as drift, are considered as systematic errors, which can be attributed to interfering parameters such as mechanical instability and temperature instability, contamination, the sensor's materials degradation, components aging, decrease in sensitivity of components, and/or a change in the signal to noise ratio, etc.

Understanding the degradation mechanisms that dominate critical components in photonic sensors is required for assuring their stable performance over time. For instance, typical conditions that deteriorate the responsivity of photo–detectors are their continuous exposure to UV radiation that damages both, the semiconductor and the optical components of the detector [131][132].

3.1.1.8 Linearity

The linearity of a sensor defines the approximation of the transfer function to a linear response over the specified dynamic range, and its degree of resemblance to a straight line describes how linear a system is. Typically, the linear response of a sensor is defined using the Coefficient of determination, denoted R^2 or r^2, of the simple linear regression made to the sensor outputs over the dynamic range, which considers not only the linearity but also the accuracy of the sensor.

In the optoelectronic domain, a photodiode is defined to be linear when its photoelectric conversion efficiency (responsivity) is independent of the incident optical power. Each photodiode behaves as a linear detector for a certain range of optical power and becomes nonlinear for higher intensity optical power, the nonlinearity threshold being a characteristic of the particular photodiode. As the power of the input optical signal reaches a certain level, the response of the photo–detector starts to saturate, thereby deviating from the linearity [133].

The nonlinearity of a photodiode is a function of several factors like generated photocurrent, incident optical power, the ambient temperature, etc. [134] However, the series resistance of the photodiode appears to be the most important factor in determining the linearity. One also needs to mention the incident beam diameter because it has been observed it has an influence on the linearity, but in a different manner for various types of photodiodes, however the influence is not wavelength dependent [135].

3.1.1.9 Calibration

When the response of the sensor is not constant over the production batch, a calibration process is required for assuring the uniformity of the sensors' output within the whole batch. The calibration process basically requires trimming the sensor output against a benchmark or against a known output to assure that each sensor delivers correct outputs. Calibrations in temperature is a typical factory process for optoelectronic sensors, at it may require one, two or even more calibration points depending on the linearity of the sensor. Some systems require being recalibrate after a certain period of time to adjust the sensor output to the response drifts.

However, calibration is a critical issue when dealing with sensors deployed in the field, because the accessibility is not always easy or even possible, as it happens with the off–shore wind turbines [136]. Therefore, unattended sensors will always foster the application of self–calibration or self–referencing approaches to mitigate the need of in–situ sensor calibrations.

In the specific case of photonics–enabled sensors, there are several ways of introducing self–compensating solutions within the sensor structure. For instance, NDIR sensors (see chapter 2), are normally equipped with a dual detector, one tuned for the target analyte detection and the other used just as reference. This approach enables to remove all the signal fluctuations coming from unstable light emission and detection sensitivities (generated by component ageing, temperature effects, etc.) by simply subtracting the reference detector intensity to the target detector intensity (see Figure 3.1–6).

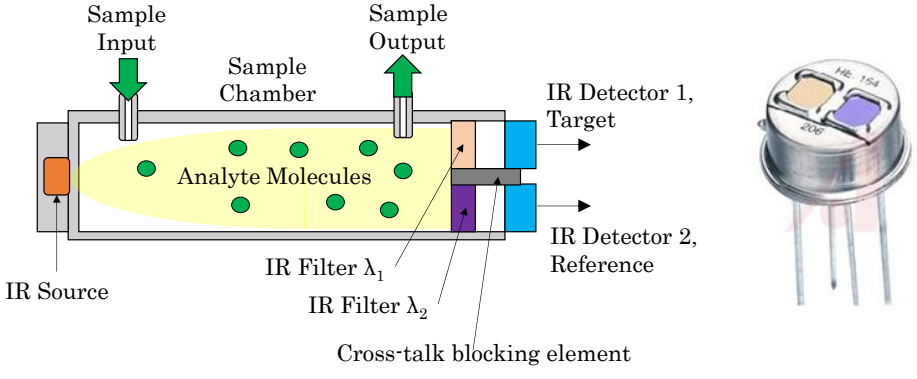

Figure 3.1–6: (a) NDIR fluid or gas sensor, where a dual detector schema is used, with two equal receivers and two IR filters, the first with the band–pass frequency matching the absorbance lines of the target analyte and the second IR band–pass completely aside from these lines. Therefore, the second detector gets information about the source and not about the measurand, and thus, this information is used to compensate any fluctuation on the emitter and on the detectors. (b) Displays a PYS 3228 IR detector with built–in filters for NDIR sensors, from Excelitas Technologies (Waltham, MA, USA)

Another approximation for self–calibrating photonic sensors is to include a secondary photo–detector for continuously assessing the emitters light intensity (and sometimes wavelength) and modulating it to keep a constant level of excitation. This is required for instance when working with reflectance or fluorescence configurations, where a minimum level of light excitation needs to be guaranteed to generate the reflected or fluorescent emission. This approach is observed in sensors for lubricant grease monitoring by reflectance [137] (see Figure 3.1–7), in sensors for lubricant oils monitoring (see Figure 3.1–9), or in UV Absorption sensors for use in the biotech and chemical industries [138] (see Figure 3.1–8)

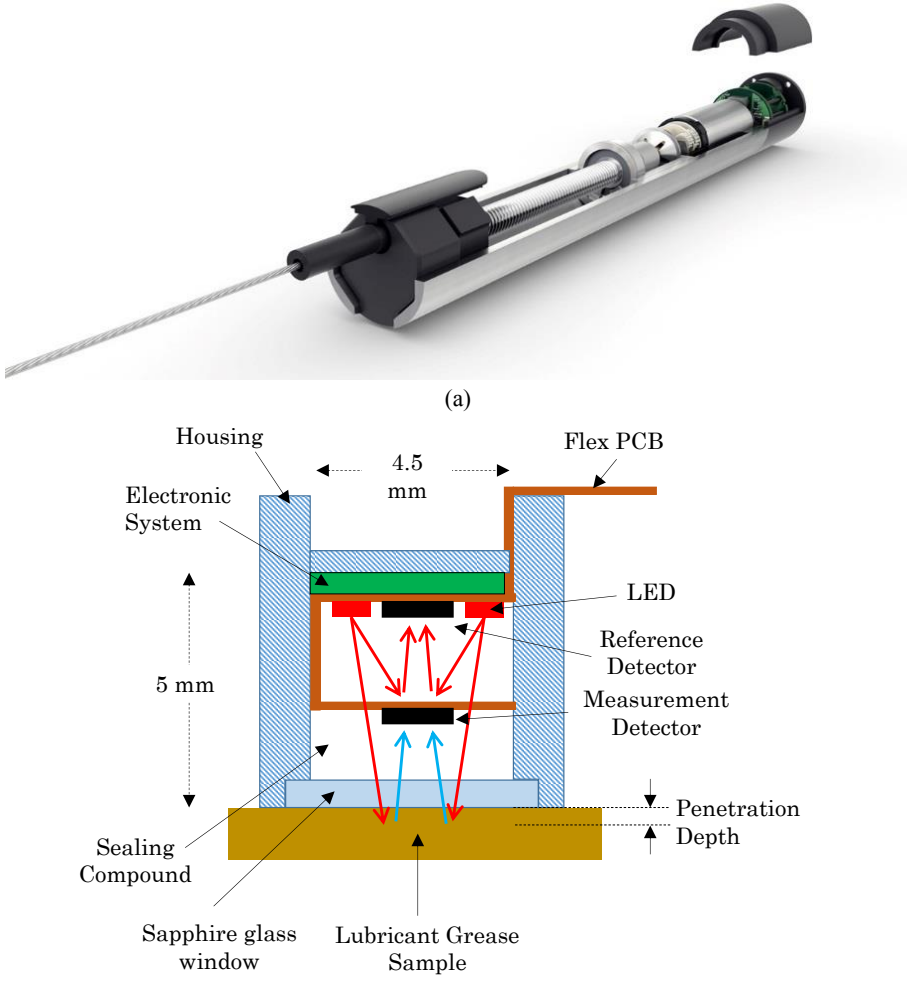

Figure 3.1–7: (a) NIR Reflectance Grease sensor, GreaseCheck from FAG–Schaeffler (Schweinfurt, Germany). (b) Presents the block diagram of the grease sensor, where the reference photodiode is included in the emitter's sensor plane, while the measurement detector is faced in perpendicular to the grease sample.

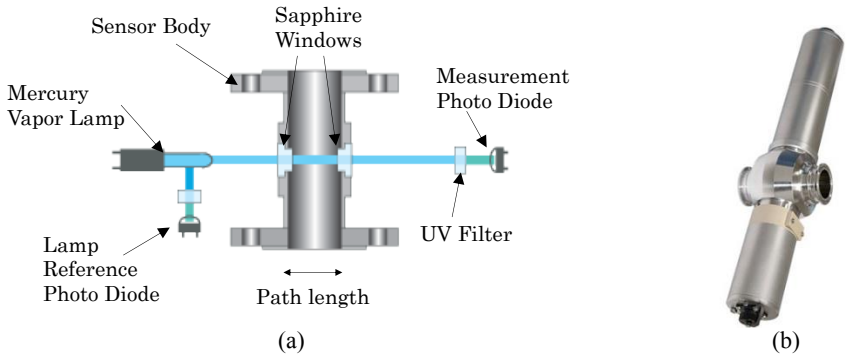

Figure 3.1–8: (a) Block diagram of fluid UV absorbance sensor, with a reference photodiode attached perpendicular to the light beam normal and received part of the emitted intensity through a beam splitter. In this case, while interpreting the signal measurement photodiode the original emitted intensity is always known and can be used for correcting the bias. (b) AF45 / AF46 sensor system including the (a) approach from Optek Danulat (Essen, Germany).

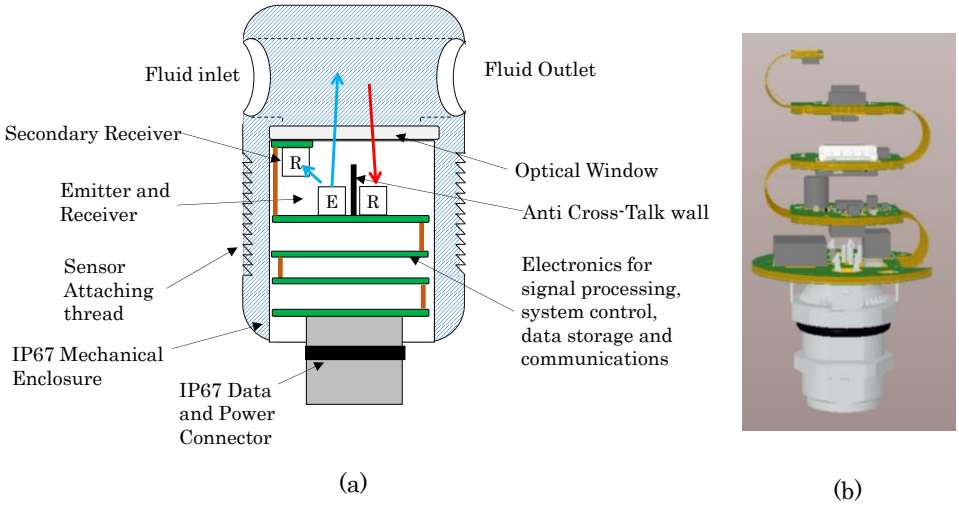

Figure 3.1–9: (a) and (b) Show block diagram of the OilProbe ® [139] sensor from Atten2 Monitoring Technologies (Eibar, Spain). In this case, a reference receiver is located slightly above the emitter, blocking a part of the emission lobule. The measurement detector is located besides the emitter, isolated from the cross–talk effects by a blocking wall.

3.1.1.10 Bandwidth

The bandwidth, sensor speed or the frequency response terms describe the finite response times that sensors deliver to an instantaneous change in the physical signal at the input. Additionally, normally, sensors also present decay times, which basically defines the time needed by the sensor output to reach the original state once the physical signal at the input has changed again. The response and decay times also represent the upper and lower cut–off frequencies of the sensor, defining the sensor bandwidth parameter, which

characterizes the ability of the sensor to respond to changes happening in the time lapses (t = 1 / f) within the cut–off frequency ranges.

In optoelectronics, these response times are normally defined by the Rising and Falling times (t_{RISE} and t_{FALL}), and normally represent the time needed by the optical component output to move from the 10% to the 90%, or the other way around, of the dynamic range. Relation between rise time and detectors bandwidth is given in Eq. 3.1–1 as demonstrated in [140]. Mainly driven by the requirements imposed by optical communications, the response and switching times found in optical semiconductors are currently in the range of nanoseconds and picoseconds.

$$B(\mathrm{Hz}) = \frac{0.35}{t_{RISE}(\mathrm{s})} \qquad \text{Eq. 3.1–1}$$

Because the quantity of noise in the output increases with bandwidth (see section 3.1.1.13 for noise description), a well–designed system has just enough bandwidth for the purpose of the observation [141].

3.1.1.11 Selectivity and Cross–Sensitivity

Selectivity defines the capability of the sensor to measure a target analyte in the presence of other interferences, which is an especially critical when dealing with heterogeneous samples and variable conditions as it happens in the in–line measurement of fluids. The cross–sensitivity means that the presence of other parameters or conditions apart from the target measurand are able to generate changes at the sensor output.

When dealing with optoelectronics, the performance (responsivity, quantum efficiency, etc.) of both emitters and detectors is vastly affected by the temperature. Normally this dependence is well documented as part of the system specification, with graphs and coefficients defining the variation of the emitter or detector efficiency with changing temperature conditions [142].

On the other hand, spectroscopy–based sensors, especially those ones working in the NIR bands, suffer from low selectivity due to the overlapping of absorption lines of different compounds. This is a typical situation when samples with high concentration of water need to be monitored. The huge absorption happening due to the water molecules could hide the absorption of other compound that vibrate near the H_2O molecules [143].

3.1.1.12 Hysteresis

Hysteresis is the effect defining a difference between outputs delivered by a sensor measuring the same, depending on the trajectory followed by the sensor. Indeed, this effect impacts on system accuracy and hinders the calibration process because not only instantaneous information about the environmental conditions are required, but also their historic trajectory. This situation is quite common is systems affected by temperature, as it happens with photonic emitters, which at low temperatures are able to self-heat their junction, but when moving from high temperatures to low temperatures, they are not able to refrigerate.

3.1.1.13 Noise, Signal to Noise Ratio

In photo–detectors, the lower limit of signal detection is defined by the noise characteristics of the receiver device and its amplifiers. There are three main sources of noise in any optoelectronic detector system: photon–related shot noise, detector dark noise, thermal noise and amplifier noise. The first three are related to the detector while the fourth one is originated at the signal conditioning electronics (see section 3.1.2.2 Managing the Photocurrent).

Shot noise is inherent in any signal generated by the detector and is caused by the quantum nature of light. Photons arrive at random intervals, and therefore, the number of electrons produced is also random. Additionally, not all the electrons effectively generate photocurrent, and some just get absorbed or recombined. Being the output current defined by the number of electrons in a certain time interval, it is evident that due to the aforementioned factors, the current generation is dominated by random or statistical process. This probability of generating n electrons is defined by a Poisson distribution [144], and its impact of signal deviation is defined by the Eq. 3.1–2.

$$I_{SHOT\ NOISE} = \sqrt{2eI_{Ph}\Delta B}\ (\text{rms noise}) \qquad \text{Eq. 3.1–2}$$

being e the electron charge, I_{PH} the average photocurrent (A) and ΔB the electrical bandwidth of detector amplifier combination (Hz). Notice that the shot noise is independent of the frequency.

Dark noise describes the statistical variation in the number of electrons thermally generated within the detector regardless of the incident photons, and is the electron equivalent of photon shot noise. Then, the dark noise can be considered as another sort of shot noise, but in this case its description is:

$$I_{DARK} = \sqrt{2eI_D\Delta B}\ (\text{rms noise}) \qquad \text{Eq. 3.1–3}$$

being, I_D the average dark current.

There is another source of noise in photo–detectors called the *1/f* noise, which origins are not fully clear but have been correlated with contacts, surfaces and other potential barriers. The noise power is inversely proportional to the modulation frequency *f*, which gives the noise its name. This noise is usually smaller than the shot noise but in low frequencies, when it becomes an important contributor to the detectors noise level. The formulae describing this noise is defined in Eq. 3.1–4

$$I_f = I_{PH}\sqrt{\frac{\Delta B}{f}}\ (\text{rms noise}) \qquad \text{Eq. 3.1–4}$$

being, I_{PH} (A) the average photodiode current, ΔB (Hz) the electrical bandwidth of detector, and *f* the modulation frequency (Hz).

However, normally, the major contributor to the detectors noise is the thermal or Johnson noise of the device shunt resistance, series resistance and load resistance. Johnson noise is originated due to thermal fluctuations in conductive materials which triggers a random electron movement within the conductor. These constant movement of electrons eventually generate micro currents that over a large period of observation represents a net zero power, but in small time interval generates a fluctuation in the photocurrent which constitute the Johnson noise as described in Eq. 3.1–5.

$$I_j = \sqrt{\frac{4kT\Delta B}{R_{sh}}}\ (\text{rms noise}) \qquad \text{Eq. 3.1–5}$$

being, *k* the Boltzmann's constant (1.3807 x 10^{-23} $\boldsymbol{J}$ K^{-1}), T the absolute temperature of the photodiode (in K) and R the equivalent resistance (ohms), and again ΔB the bandwidth (Hz).

Figure 3.1–10 displays the contributions of the aforementioned noise sources across the photo–detectors frequency bandwidth.

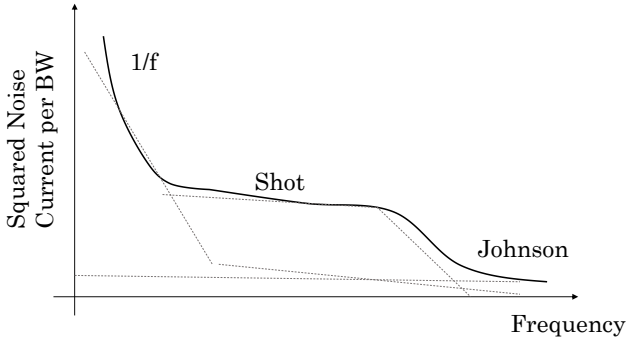

Figure 3.1–10: Distribution of different noise contributors along the photodiode working frequencies.

After having reviewed the photo–detector internal noise sources, one can assume that the output signal from a photo–detector is a chronological sequence of current pulses, each originating from a single photo–generated charge carrier, with a stability affected by statistical and physical factors. The Signal to Noise Ratio (S/N) will represent the proportion of valid or meaningful electrons generated at the photo–detectors over the noisy or undesired ones and the engineering efforts should be focused on increasing this S/N figure of merit.

Eq. 3.1–8 to Eq. 3.1–13 describe how the number of generated electrons depends linearly on the product of I and A, thus, P. Maximizing S/N entails maximizing the signal S and/or of minimizing the noise N. For a given I, increasing S may be feasible by achieving higher P with light–collection optics or by choosing a photo–detector with a larger active area.

With this regard, there is another common parameter for determining the photo–detectors minimum detectable power, described as the noise equivalent power (NEP, in units of W/√Hz), and defined in Eq. 3.1–6, which is the incident optical power yielding S/N = 1 at the output of the detector or the power that generates a photocurrent equal to the rms noise current for 1 Hz bandwidth [145]. Notice that NEP is function of the wavelength of the incident radiation.

$$\mathrm{NEP}(\lambda) = \frac{\text{rms noise}}{\sigma(\lambda)} \qquad \text{Eq. 3.1–6}$$

So far, the photo–detector internal noise sources have been outlined, but there are still important noise sources in the forthcoming stages, exemplified by the amplifier noise. The amplifiers used for conditioning the photocurrent to the needs of the electronic circuitry will amplify both, the signal and the noise, therefore is not straightforward improving the S/N by just adding amplifier stages at the detectors output and different filtering and circuit design approaches (e.g. reduce the bandwidth as much as possible) to keep or slightly enhance the S/N of the photo–detector.

3.1.1.14 Cross–Talk

The cross–talk is the effect by which in a system including an emitter and a receiver, the receiver is directly affected by the radiation generated at the emitter. This measurable leakage of optical energy happening from one optical element to the other, also known as optical coupling, is typical in compact systems, where emitters and receiver sit together, and may arise within the optical receiver from a variety of sources including directly from the optical emitter within or indirectly from the optical emitter via losses.

In addition to the optical cross talk, sometimes, monolithical emitter and detector systems also suffer from electrical cross talk, that may be originated for example at the electrical transmission lines of the optical transmitter and optical receiver.

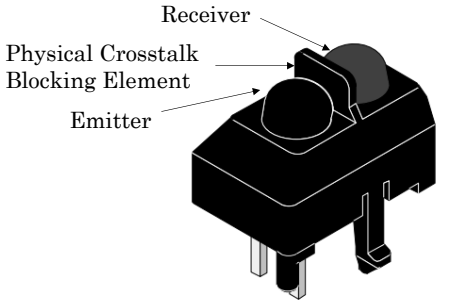

Figure 3.1–11: Example of optical crosstalk mitigation via a physical wall integrated in the TCRT5000 device from Vishay Semiconductor (Malvern, PA, USA), which is a optoelectronic sensors contain infrared–emitting diodes as a radiation source and phototransistors as detectors.

Indeed, this is an unwanted effect because increases the baseline signal at detector, impacting (in addition to the dark current) in the lowest photoelectric current that can be processed as a useful signal in the sensor's detector and defines the sensitivity of the sensor. Therefore, the effect should be mitigated and different approaches have been developed with this regard as physical light blocking elements between emitters and detectors [146] or the use of secondary detectors for compensating the crosstalk signal [147].

3.1.2 Introduction to Photonic Sensor Electronics

So far, we have described the main parameters which objectively define the performance of a given sensor, mainly focusing on the basic processes that enables the sensor converting one type of energy into electrical energy. However, this section will offer a wider view, defining the whole process entailed in the measurement of light, including not only the basic physical principles of light into electricity conversion, but also its effective analogic conditioning, digitalization and processing. Similar process chain is expected when some sort of light modulation is required as a part of the photonic sensor: modulation decision, digital to analog conversion, power stages and electricity to light radiation conversion.

3.1.2.1 Light into Electricity Conversion, Photocurrent

Narrowing down to the specific case of photonics, the energy transduction is possible thanks to three different effects: photoconductivity, photovoltaic effect or photoemission. The process

underneath these transductions, is the reaction of a photosensitive P–N junction of a certain semiconductor under the influence of incident light. When photons of the right frequency hit the photosensitive surface (the P region), due to the energy carried by the photon, *hv,* the valence band electrons are excited to the conduction band, leaving holes in their place in the valence band, thus, resulting in the creation of an electron–hole pair. Under the influence of a bias voltage, these carriers move through the material and induce a current in the external circuit, resulting in a new electron flowing in the circuit per each new e–h pair created.

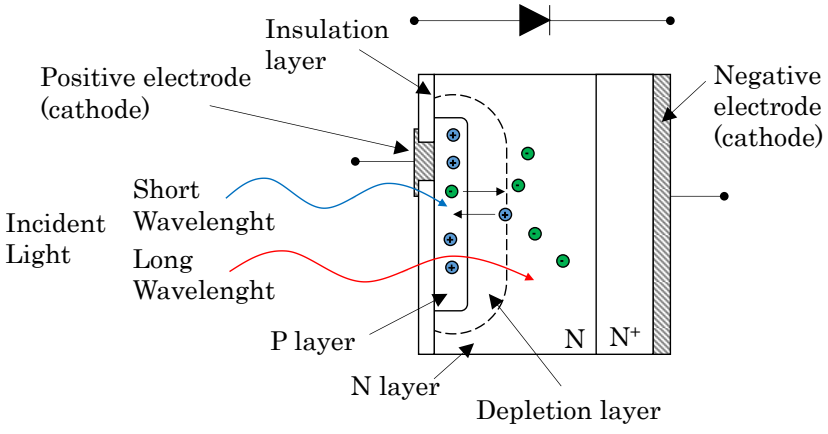

Figure 3.1–12: Schematic cross–section of a photodiode electronic structure.

The capability of the semiconductor lattice to convert the incident photons into electrical energy depends on several factors as the wavelength of the light, absorption coefficient, thickness of P–N layers, doping of the semiconductor, geometry, etc. [148].

This efficiency in energy conversion is normally defined as the Quantum Efficiency, expressed as QE or η, of the detector, representing the number of effectively converted electrons by the number of incident photons. Operating under ideal conditions of reflectance, crystal structure and internal resistance, a high quality silicon photodiode may reach a QE around the 80%.

$$\eta = \mathrm{QE} = \frac{r_e}{r_p} = \frac{\text{Electrons Generated/s}}{\text{Incident Photons/s}} = (1 - R)\xi(1 - e^{-\alpha\omega}) \qquad \text{Eq. 3.1–7}$$

Being R is the reflection coefficient at the air–semiconductor surface, ξ the fraction of the e–h pairs contributes to the photo–current, α the absorption coefficient in the semiconductor material, and ω is the distance where light energy is absorbed. Additionally, r_P represents the photon flux and r_e the electron rate.

The QE is related to the detectors Responsivity, already described in 3.1.1.2, which defines the ability of the detectors to convert the incident radiant energy (in watts), *P*, to the photocurrent output in amperes I_P.

$$R_\lambda = \frac{I_P(\frac{A}{cm^2})}{P\,(\frac{W}{cm^2})} = \frac{I_P}{P}\,(\frac{A}{W}) \qquad \text{Eq. 3.1–8}$$

The radiation energy is defined as the sum of individual photon energy, being r_p the photon flux and $h\nu$ the photon energy

$$P = E_{Photon} \cdot r_p = h\,\nu \cdot r_p \qquad \text{Eq. 3.1–9}$$

$$r_p = \frac{P}{h\,\nu} = \text{number of photons/s} \qquad \text{Eq. 3.1–10}$$

Then, the electron rate r_e and the photocurrent, I_P, may be expressed as:

$$r_e = \eta r_p = \frac{\eta P}{h\,\nu} \qquad \text{Eq. 3.1–11}$$

$$I_P = e\,\frac{\eta P}{h\,\nu} \qquad \text{Eq. 3.1–12}$$

The responsivity may be then written as:

$$R_\lambda = e\eta\,\frac{1}{h\,\nu} = e\eta\,\frac{\lambda}{h\,c} = \frac{\eta\,\lambda}{1.24}\,(\frac{A}{W}) \qquad \text{Eq. 3.1–13}$$

Where h is the Planck Constant (6.63×10^{-34} joule–second), e is the Electron Charge (1.6×10^{-19} coulombs) and c is the speed of light (2.99×10^{8} meter / second), and λ (meter) is the wavelength of the light at which the Responsivity is being given.

But regardless detector responsivity, if the generated photocurrent is not efficiently managed in the following stages within the photonic sensor, the detected information may be lost. The sections below outline briefly the steps required to acquire, condition, filter, digitalize and process the signals outputted by the detector. The low noise electronics and sensor readout circuits is a very wide technological domain and its details fall out from the scope of the current thesis, therefore only a brief introduction is given here. Further information could be found in the topic literature, as the following references [149][150]

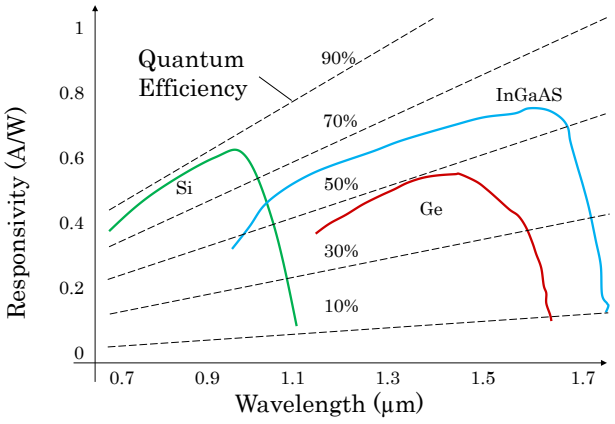

Figure 3.1–13: Responsivities of different semiconductor materials over the visible and near infrared wavelengths.

3.1.2.2 Managing the Photocurrent

The first stage for managing the photocurrent delivered by the photo–receptor is to feed it into a signal conditioning analog circuit, which has the main objective of enhancing the Signal to Noise ratio. This stage normally implies the use of low noise operational amplifiers, filters, compensations, etc. with the objective of delivering a clean and amplified signal to the next stage.

The next step is the signal digitalization, which requires to introduce terms as the sampling frequency, Nyquist[28] frequency, aliasing and quantification resolution. The digitalization entails converting a signal from a continuous time and amplitude (either volts, amperes or watts) domains, to a digital domain with quantified observation times and quantified signal amplitudes. The quantification of the time domain is represented by the sampling frequency of the digitalization system, which defines the specific time instants where the value of the amplitude is latched. Defining the sampling frequency is not straightforward, and the original signal bandwidth should be taken into consideration to avoid odd effects as the aliasing. The aliasing defines the situation originated when a signal with a certain maximum frequency is under–sampled, generating a false representation of the original signal.

The aliasing could be prevented if the sampling frequency meets the Nyquist criterion, which sets the minimum sampling frequency as the double of the signal's maximum frequency (see Eq. 3.1–14).

$$F_{Sampling} >= F_{Nyquist} = 2 \cdot F_{MAX} \qquad \text{Eq. 3.1–14}$$

[28] Harry Nyquist, Swedish engineer (1889-1976)

However, even if the signal frequency spectra may be known, the noise is spread all over a wide bandwidth, so to avoid artifacts generated by the aliasing, it is recommended to include a low pass filter to reduce all the energy belonging to frequencies above the signal's maximum.

Therefore, once the signal has been filtered and sampled, the quantification starts, which is the last step for getting a digital representation of the original photocurrent. The quantification means to assign a digital value within a scale to the analog amplitude. Indeed, the maximum and minimums of the digital scale should match the peak values of the analog signal in order to maximize the use of the whole scale.

These digital values, as it happened with the sampling instant, are discrete steps, being the number of available steps defined by the number of bits and the range of the analog signal to cover. The resolution describes the analog signal span (normally in volts) represented by each increment in the digital value.

$$N_{Steps}(V/bit) = \frac{A_{Max-Signal} - A_{Min-Signal}}{2^{n\ bit}} \qquad \text{Eq. 3.1–15}$$

It may happen that different analog values are converted into the same digital value if enough resolution is not available. Therefore, some engineering is required for defining the minimum length in bits for the digitalization.

3.1.2.3 Processing the Signals

Once the signal has been properly converted into the digital domain, and represented by a train of digital values updated at the sampling frequency, its processing may start. Normally, the signal processing is accomplished in a processor that performs different digital signal treatments and calculations to extract relevant information contained in the digital signal. Sections 3.1.5 Smart Sensors and 3.2.2 Analysis of photonic information provide more information about the calculations that may be applied in the processors.

After the relevant information has been extracted, it may be stored, displayed or communicated away.

3.1.3 Quantitative, Qualitative and Indirect Measurements

The final objective of any sensor is to offer a valuable information about parameters, status, quantities, etc. of a certain measurand. However, the way of getting this information and the nature of the requested data is not always the same.

Basically, the measurements can be a direct translation of a physical or chemical effect into an electric magnitude. In these cases, the working principles are defined as a Direct Measurement method, as it happens with elongation sensors, where the net elongation distance generates a change in the resistivity of the elongation transducer.

Alternatively, the data delivered by the sensor can be the result of several calculations applied to the parameters observed. These situations define the Indirect Measurement methods, which require more steps, are more prone to cross–sensibilities, and normally are only used when the direct measurement is an inconvenient [151]. However, there are several examples based on indirect measurements offering very valuable information about the process being monitored [152].

In the photonic field, examples of direct measurement methods are found in: observation of the color of the measurand, measurement of the absorbed intensity, opacity and reflectivity measurements. For instance, quantifying the light intensity emitted by a fluorescent dye can be considered as a direct measurement [153], because the intensity is directly proportional to the concentration of the fluorophore, as depicted in Figure 3.1–14.

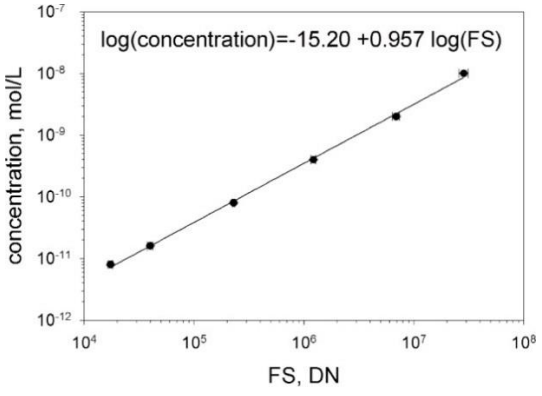

Figure 3.1–14: The plot of the log of the concentration of a fluorophore solution versus the log of the integrated fluorescence signal (FS) associated with the known concentration. The ideally linear response has a slope of 1.0. [153].

Another example of direct measurements performed by photonic sensors is found in the particle counting, where the effective detection and classification of particles suspended in a fluid is accomplished by directly imaging (Figure 3.1–15) them and analyzing by machine vision algorithms (see section 3.2.2.3).

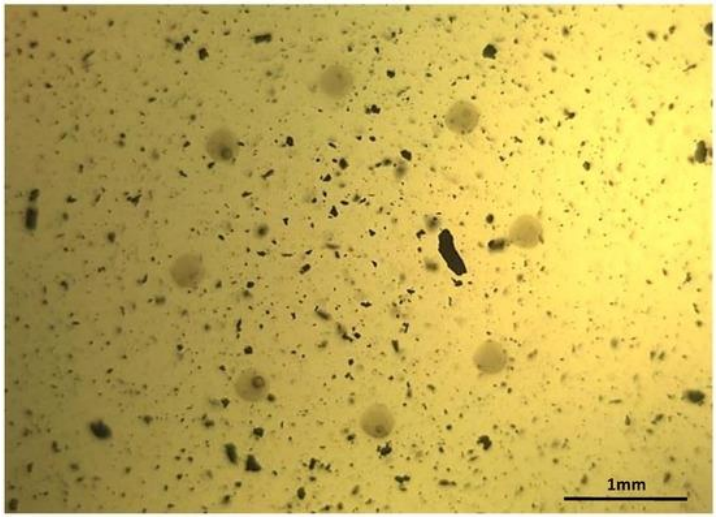

Figure 3.1–15: Image of a real lubricant sample from a gearbox in a wind mill, where large and small particles suspended in the fluid can be observed directly applying a photonic setup.

On the other hand, when a certain parameter of the sample is inferred from these basic direct measurements offered by the transducer, we talk about indirect method. For instance, chemometric methods (see section 3.2.2.2) are a clear example of indirect methods for determining a certain parameter of the sample, because based on the absorbance happening over a range of wavelengths, and the empirical results obtained from a reference sample collection, the value of the parameter of interest is calculated through mathematical calculations. Among a vast number of examples, determining the geographical origin of red wines based on their UV–VIS–NIR absorbance patterns is classical application of chemometrics–enabled indirect measurement [154].

Figure 3.1–16: The changes in the oil color have several causes, so measuring the color does not offer a direct measurement of any of them due to the lack of selectivity of the measurement principle.

Another example of indirect measurement deals with the lubricant degradation, which is somehow associated with a change in the oil color that becomes more reddish and opaque (see Figure 3.1–16). The two most common causes of oil darkening are thermal stress and oxidation, thus, tracking the color changes could be used as a value of the status of the oil. However, the color observation can never deliver a direct measurement of oxidation, nor about the thermal stress, because both processes cause the same consequence, the darkening of the oil [155].

Regardless of the measurement method, direct or indirect, the nature of the sensor results also deserves a clarification. Understanding the differences between qualitative and quantitative analysis is relevant for any sensor application, because the approach, objectives and challenges are totally different depending on the expected result type.

The minimum operation normally requested for a sensor system is to offer a Qualitative analysis of a certain property of the measurand, which means giving a categorical response based on observed parameters or conditions of the sample. The main objectives while delivering a quantitative analysis are either to identify or to qualify the new sample according to previously defined groups.

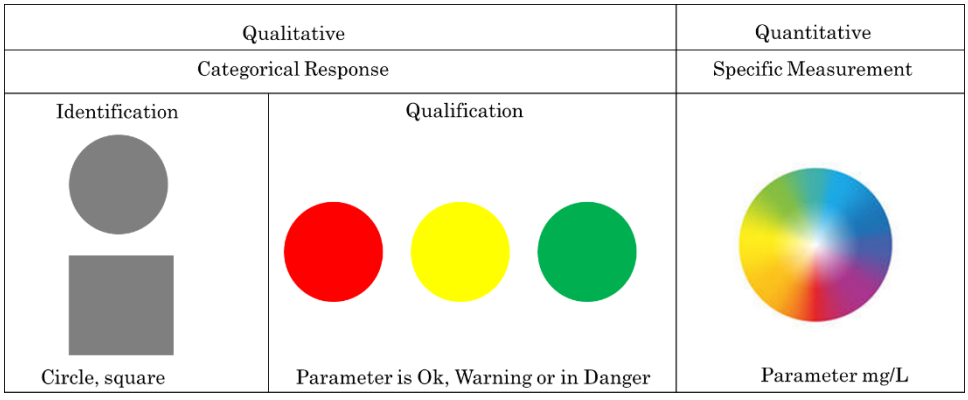

Figure 3.1–17: Differences between qualitative and quantitative measurements.

When a sensor is supposed to identify a sample, it needs to discriminate it as belonging to one of at least two well–defined groups. The qualification goes one step further, and the samples are classified in groups depending on defined thresholds, that categorize the samples based on quality, etc. On the other hand, a sensor delivers a quantitative analysis when is able to output specific information about the process or the measurand being observed, as it happens, for instance, when the sensor outputs the concentration of the unknown sample composition in real time [156][157].

3.1.4 Cost of Sensors

Already introduced in the section 1.3 Cost Effective Smart Photonic Sensors, the true cost of a sensor solution is far for being limited to the device cost, and several other factors increase significantly the Total Cost of Ownership [158]. The cost accounting for any measurement system deployed in the field should always considered the impact of the items outlined in the Table 3.1–1. The photonics–enabled in–line sensors are not an exception, and costs concerning calibration, installation and maintenance are sometimes one order of magnitude bigger than the device cost.

Table 3.1–1: Concepts impacting on the Total Cost of Ownership of industrial sensor systems.

Other costs	Description
Installation	Requirements of any extra mounting system for installing the sensor, installation and setup times and skill and knowledge required for deployment (e.g. technician, engineering work)
Cabling, Connectors, Signal Conditioning, Data Receivers,	Requirements for power or communications cabling, as well as the need of data receivers (PLC, SCADA, PC, Ethernet Switch, etc.)
Reliability	Implications concerning the lifetime of the sensor product and its mean time before failure (MTBF), as well as the reliability statistics. These unexpected failures may impact on the end–users' equipment unscheduled downtimes.
Scheduled Down time, Calibration	Requirements in terms of sensor calibration or maintenance, calibration frequencies, time to accomplish it, can it be done in–situ or the sensor needs to be taken away from the installation point.
Repairs	Implications regarding product reparability and the disposal costs at the end of the lifetime. Requirements for reparations similar to calibration ones, can it be accomplished in situ?
Usability	Requirements for any other external equipment or software to process the signal outputted by the sensor.

Lead time	Implications regarding the lead time of the sensor. Long manufacturing time may require producing a sensor inventory which generates stocking expenses.
Environmental Protection	Requirement of any specific enclosure to be used on certain environments? (e.g. ATEX for explosive atmospheres)
Shipping	Requirements in terms of shipping cost that depend on product volume, weight and on shipping conditions (e.g. is it care handling required?)

3.1.5 Smart Sensors

Even if the term Smart Sensor may have been hyped in the last decade, in its origins, it entailed a whole new vision on how to understand the sensors, their use and their design. First introduced in late eighties [159], the smart or intelligent sensors presented a new paradigm for presenting the signals measured to the operators: the raw signals needed to be processed and combined and delivered in a normalized way either to a display or to a PC system for further processing [160]. This new approach paved the way for the digitalization of the analog transducers, benefiting from the breakthrough in embedded processing capabilities that was about to become a reality.

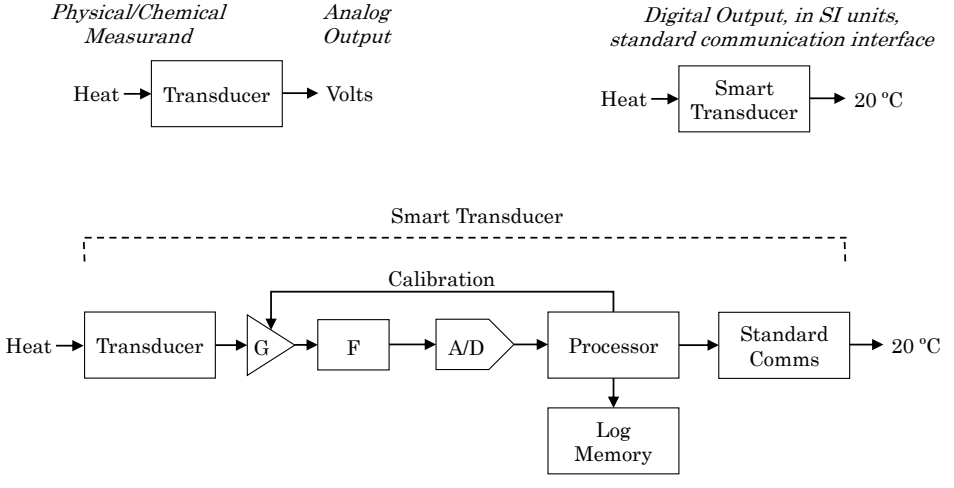

Figure 3.1–18: Difference between a traditional analog transducer and a Smart one, additionally displaying all the modules entailed in an intelligent transduction.

The structure of a Smart Sensor basically includes all the blocks already mentioned in the section 3.1.2 where the different

electronic modules required for a sensor system were introduced. Thus, a Smart Sensor needs to include all the transducer, analog and digital stages to acquire, condition, filter, digitalize, process, calibrate, store and communicate in a standardized way a measurement information, as depicted in Figure 3.1–18.

A smart sensor can be a monolithically integrated system, with all the components sharing the same semiconductor lattice, or alternatively, it could be based on hybrid approaches, where the transducer and the digitalization and processing parts belong to different manufacturing processes or even stand physically in different components as off the shelf modules (see Figure 3.1–19 and Figure 3.1–20) [161]. During the last few years, almost all of the photonic sensor systems where based on the integration of different components (emitters, detectors, optics, processors) into compact settings, however, recently, the heterogeneous integration technologies is moving one step forward and complete systems are being integrated in the same chip [162][163], either sharing the semiconductor die, as it is the case for VIS region solutions with monolithic silicon chips, or merging different technologies as InGaAs and Silicon for the NIR region solutions.

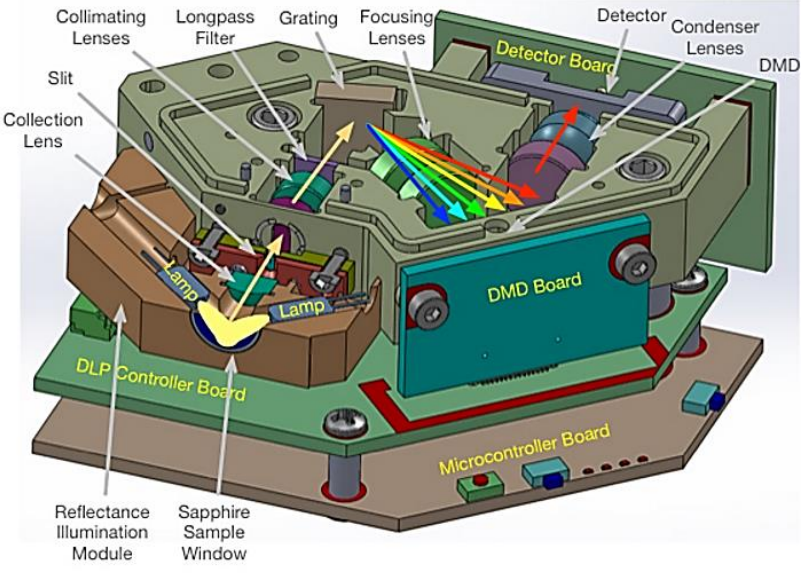

(a)

(b)

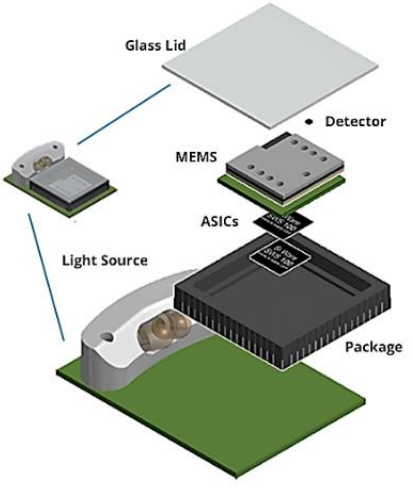

(c)

(d)

Figure 3.1–19: (a) and (b) display the 2014 Texas Instruments NIR spectrometer, which achieved a high compactness integrating different off–the–self components. (c) And (d) show the block diagram and the effective chip size of the NeoSpectra Micro device from Si–Ware launched in 2017.

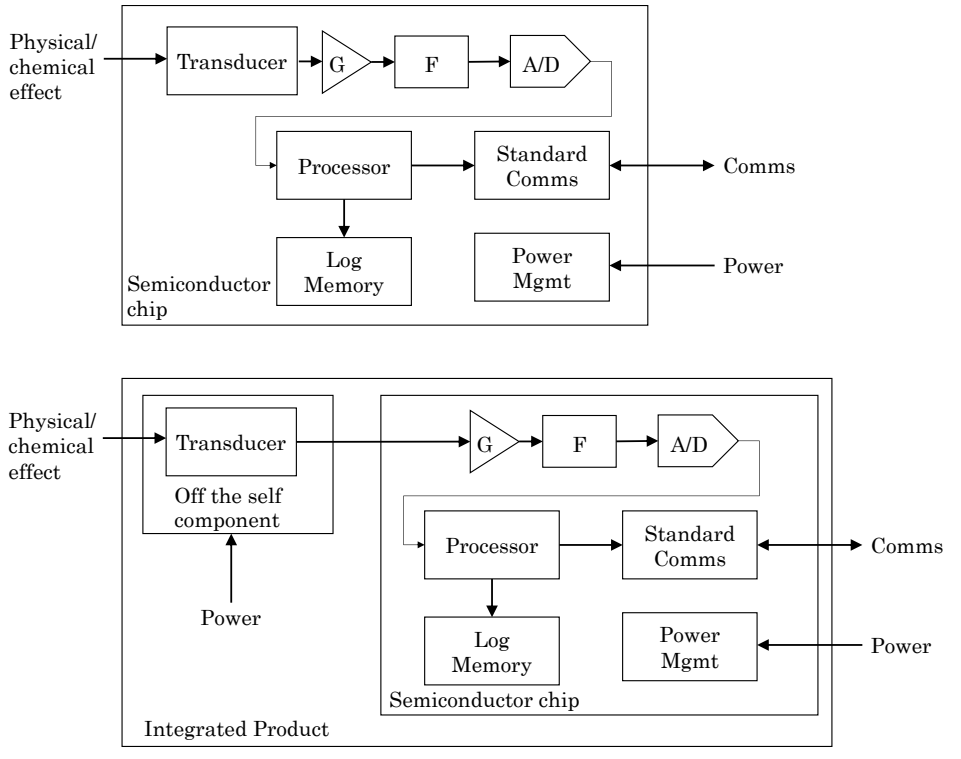

Figure 3.1–20: Smart Sensor Chip integrated in the same semiconductor die or smart sensor product, comprising different components but delivering the same inputs/and outputs as the chip version.

The following sections define the main functions expected for a smart sensor system, according to the IEEE 1451 Smart Transducer Compliant standard [164].

3.1.5.1 Compensation,

An intelligent sensor is expected to accomplish an internal evaluation about the reasonability of the measured values, controlling the dynamics of the changes at the input, checking it with the short and long-term evolutions, etc. Additionally, the intelligent sensor needs to be equipped with internal offset and drift compensation system and offer programmable gains to maximize the ADC ranges, etc.

According to the IEEE 1451 standard, smart sensors should store any factory calibration information in the sensor's internal memories.

3.1.5.2 Computation,

There are different sort of computation elements included within the smart sensor processing means, including the signal conditioning (digital filtering), logic functions as triggers and alarms,

data reductions as feature extractions, decision making and classifications, etc.

3.1.5.3 Communications

Smart sensors include a set of standardized interfaces to communicate the results, alarms, etc. and to receive parametrizations and new calibration data. These standardized solutions include not only the communication logic and protocols, but also the electrical and mechanical characteristics of the connection means as described by the IEC 61076 standard family [165].

In case of wireless communication systems, several protocols and solutions available (e.g. Wireless Hart, WIFI, Thread) for connecting sensors with each other or with gateways or centralized systems.

3.2 Photonic Sensors

So far, the different characteristics of the sensor systems have been introduced, outlining the performance indicators and describing how to upgrade a traditional transducer into a smart sensor system. During this section, we will move on to the specific case of the photonic sensors, describing some of the different sensor settings utilized for implementing a measurement technique (section 3.2.1) and introducing the different computing approaches to process the signals obtained with the presented sensor settings (section 3.2.2).

3.2.1 Photonic Sampling and Sensing Techniques

This section describes different settings for implementing certain photonics–based measurement principles, describing the layout and configuration of the different optoelectronic components and the basic physical processes involved in the working principles.

Sampling Techniques refer to how the sample, light source and light detector are arranged for performing the photonic inspection. Even if general principles are very well known in analytical chemistry, several practical issues rise when moving to in–line operation, and therefore, this section will focus on these practical problems. Sampling techniques need to deal with angles of incidence, angles of observation, mechanical and optical tolerances, wavelengths of interests, absorbance of the mediums between photonic elements and sample, etc. with the aim of maximizing the effects of interest for the effective sample measurement.

Notice that, the different cases described here do not represent the totality of photonics–enabled measurement techniques available in the scientific community, but the ones includes in this section have been considered as good candidates for being implemented in the specific case of in–line monitoring of fluids. Thus, transmission, reflectance, and Raman spectroscopy, fluorescence and in–line microscopy are presented.

Methods such as Laser–induced breakdown spectroscopy (LIBS), Attenuated Total Reflectance (ATR) settings, Plasmonics setups or the Tunable diode laser absorption spectroscopy (TDLS) have been also considered as techniques susceptible to contribute in the field of the in–line sensor, but due to the complexity in the settings or due to the high cost in components have not been covered in the current review.

3.2.1.1 Transmission/Absorption Sampling Setup

This is one of the most common sampling technique for analyzing non–opaque fluids and gases. The basic setup displays the excitation light source, the sample, the holder optics and the detector aligned in different parallel planes. It is a traditional sampling technique for in–line inspection of fluids and gases at industrial processes, either bypassing the main flow or directly attached to it. The excitation light beam travels across the sample, and its properties get modified due to the absorption generated at the molecular groups, and due to the attenuation occurring while penetrating in the sample volume. Consequently, the light received at the detector is characterized by the properties of the sample and the medium, at its post processing could give significant information about the chemical and physical composition of the sample.

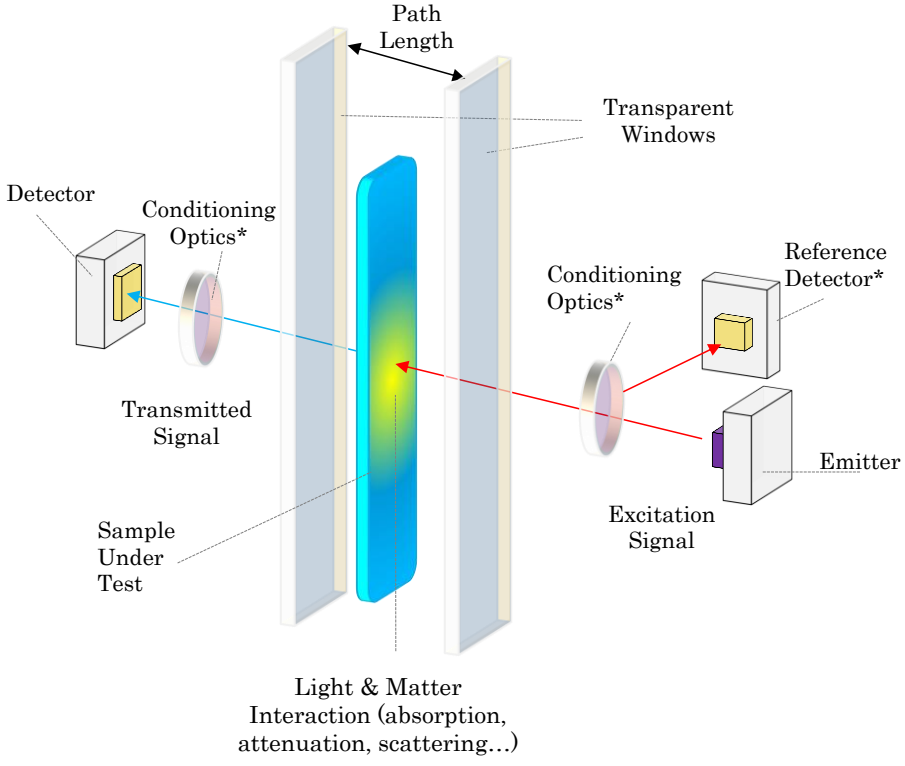

Figure 3.2–1: Schematic overview of the main components for a transmission/ absorption measurement setting. Some components, marked with *, are optional.

The basic setup for a transmission/absorption measurement setting requires to integrate different components following the mechanical and positioning arrangement depicted in Figure 3.2–1. The emitter should be chosen considering the required light power and spectrum, being its stability and reliability under changing thermic and vibration conditions an important feature to consider. The

receiver is also a fundamental part, and depending on the application, a single photo–receptor, a 2D imager or a complete spectrometer may be integrated. Occasionally, some light conditioning, filtering or focusing may be required to maximize the throughput of the system; however, simple setups with emitter and receiver working with open air interfaces are also feasible. Then, two windows fabricated in transparent material should be used to confine the sample under test. Depending on the hydraulic requirements (pressure and temperature of the fluid) and the working wavelengths, different materials (e.g. PMMA or PS plastics, borosilicate glass, quartz, sapphire) and thicknesses will be required. The width of the window will be defined by the diameter of the emission and reception radiation beams.

The separation between the windows is defined by the desired sample path length. Fluid viscosities, working pressures, etc. should be taken into consideration if very narrow (250 μm – 1 mm) are required.

Asides the free space losses[29], the physical processes governing the modifications happening into the light while crossing the sample include reflection, absorption and scattering. This generates a wavelength dependent attenuation in the light power that gets to the detectors. As described in section 2.1, in low concentrations, where analyte molecules are individually solvated and do not noticeably perturb the solvent, absorbance is well described by the Lambert–Beer law. However, as the absorbance increases (e.g. $A > 3$) [166][167], the changes in concentrations may tend to form molecular clusters, modify the solvent structure, etc. that may also change the refractive index of the sample, impacting both, in the reflected light power and in the absorbance itself, as described by the Kramers–Krönig relationships (see section 2.1.4, 2.1.7 and 2.1.10).

The main challenges in transmission/absorption settings is to assure a stable or at least known emission power and spectrum. Otherwise, changes in the source may be wrongly recognized as changes in the sample under test. Therefore, sometimes, a secondary receiver is used to verify and compensate changes in the emitted light. In these cases, a beam splitter may be used, but in other simpler configurations, the detector is mechanically placed towards the emission beam, receiving a part of the radiation lobule.

In this kind of configurations, the tolerances of the optical, optoelectronic and mechanic components are important for assuring that the optical power budget remains as designed. Depending on the optical components, the required positioning accuracies may. Additionally, notice that for quantification applications, the accuracy

[29] The free space power losses (FSPL) are described by the Friss Formula as $FSPL = (4\pi \times D/\lambda)^2$, being the losses negligible if distances are small.

in the path length becomes critical, since the absorbance happening at the sample is logarithmically bonded to this distance.

This kind of settings are very useful for measuring changes in opacity, turbidities, fluid color, and chemical analysis through UV, VIS or IR spectroscopy, provided that the absorbance of the sample allows significant light power being transmitted across the sample. If this is not the case, as it happens with very opaque fluids as lubricants for gas engines.

3.2.1.2 Reflectance Sampling Setup

When the fluids to be monitored present a high opacity in the wavelengths of interest, and even with very narrow path lengths very little power is transmitted across the sample, diffuse reflectance settings may be used as inspection method [168].

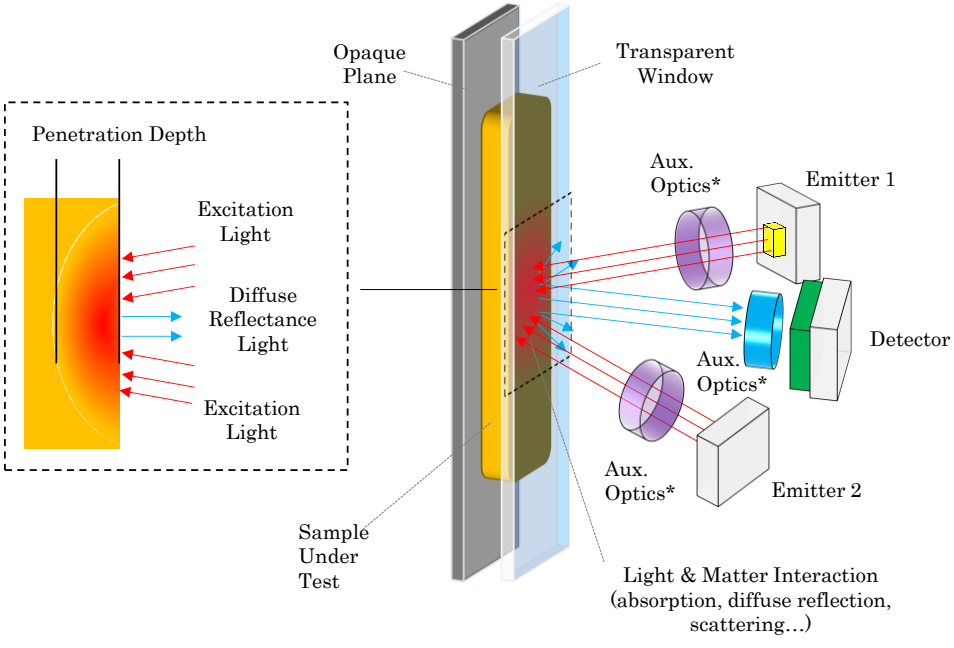

Figure 3.2–2: Schematic overview of the main components for a diffuse reflectance measurement setting. Some components, marked with *, are optional.

The fundaments of this sampling methods rely on the analysis of diffuse reflectance, which, as described in chapter 2, is the consequence of the penetration and multiple diffusions and reflections of the incident photons within the sample. A proportion of this excitation radiation may exit the sample at any angle, but due to its diffusion across the sample particles, it also contains information about the absorption of the material, because mainly the non–absorbed wavelengths are prone to exit the sample. Therefore, this

diffuse reflectance contains similar information to those acquired through a transmission setup.

However, in addition to the diffuse reflectance which carries information about the absorption properties of the sample, reflected radiation is also contributed by the specular reflection happening at the sample surface due to the changes in the refraction index between the two media. Actually, this specular reflection is the main contributor to the distortion of the diffuse reflectance spectra, generating changes in band shapes, their relative intensity, and, occasionally, it is liable for complete band inversions, due to Restrahlen effect [169].

Other factors such as the refractive index of the sample, particle dimensions, packing density, homogeneity, concentration and absorption coefficients of the sample are also susceptible of influencing in the quality of the reflectance spectra [170].

From the analytical point of view, the complexity inherited from the factors described above, combined with the intrinsic statistical distribution of the reflected radiation angles (as described in section 2.1.10), hinder the extraction of any reliable linear relation between reflectance band intensities and concentration of the target compound [171]. In this situation, Lambert–Beer law is not applicable, and even if approaches like Kubelka–Munk's (see section 2.2) could be used to estimate concentrations in reflectance setups, diffuse reflection measurements are mostly limited to semi–quantitative analyses

Diffuse reflectance working principle depends on the focused projection of the detector beam into the sample where the excitation light is being reflected, scattered and transmitted through the sample material. The back reflected, diffusely scattered light, a part of which is absorbed at the sample molecules, is then collected by the detector optics. Only the part of the beam that is scattered within the sample (suffering the absorption by the molecules) and returned to the surface is considered to be diffuse reflection and it is the one used for further processing.

Therefore, from the optical point of view, it is very important to control the intersection points between the area of the illumination spot and the Field of View, Focal point and Deep of Field of the detector. The probabilities of having effective absorbed and reflected radiation are much higher in the nearby of the illumination spot, so the detector must be focused on this volume for maximizing the collection of diffuse reflectance spectrum as depicted in Figure 3.2–3. This spatial coincidence normally requires setting the emitter and detector in a certain angular arrangement, which increases the mechanical integration difficulty. Additionally, the use of optical

components for maximizing the light collection at the detector, such as collimator lenses is also quite common in reflectance setups [172].

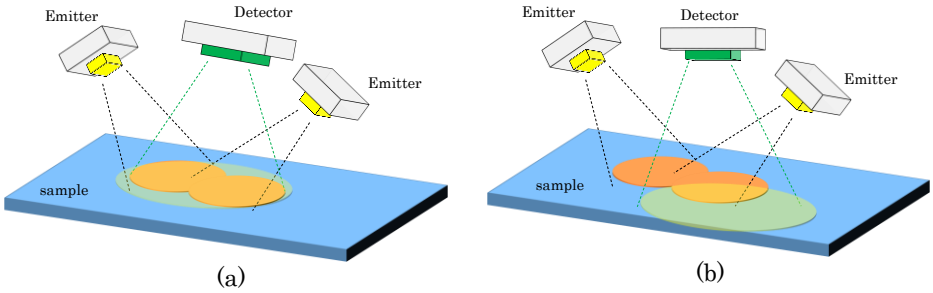

Figure 3.2–3: (a) illumination spot and detector's field of view coincidence. (b) Illumination spot and detector's field of view mismatch.

Additionally, the lack of awareness about the penetration depth may result in completely inaccurate results because the absorbance may be happening at layers outside the sample volume, for instance in the opaque plates used at the back of the samples (see Figure 3.2–2) [173] [174] [175].

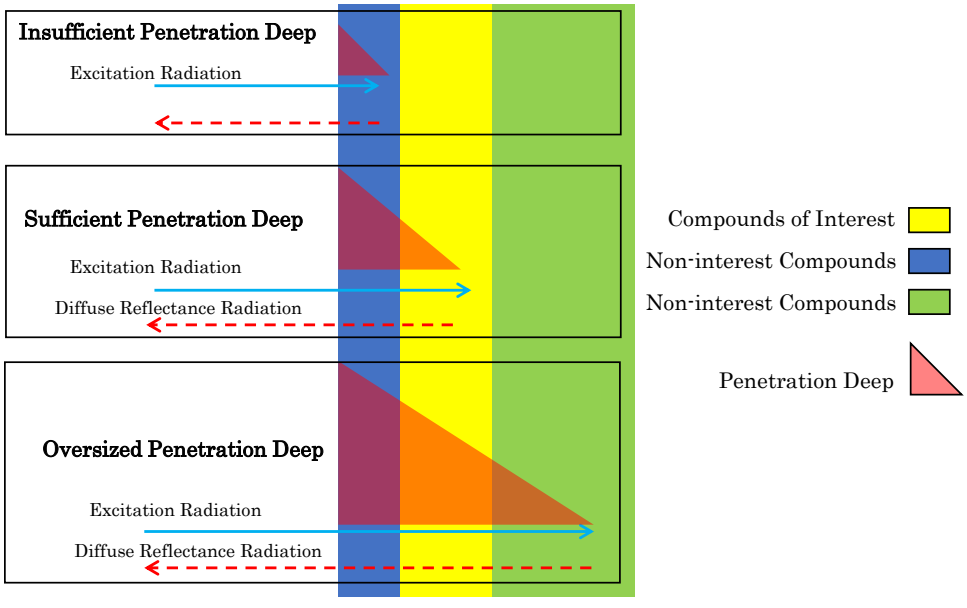

Figure 3.2–4: The penetration deep should match the volume of the compounds of interest localization in a non–homogeneous sample, otherwise, the diffuse reflectance spectrum will contain the absorbance properties of the non–interest compounds. Therefore, the excitation power should be carefully tuned to the sample requirements.

3.2.1.3 Fluorescence Setup

The inspection of the matter through fluorescent setups require understanding that, alike the previously described techniques, fluorescent analysis is not measuring changes occurring in the excitation light, but changes occurring in the sample itself while being illuminated. Under this approach, the excitation subsystem needs to assure a light source fulfilling stability, power and spectral requirements, which is able to illuminate the sample volume under inspection. Additionally, the detection subsystem needs to be able to collect the signal emitted by the sample, getting rid of any other stray light generated within the inspection system.

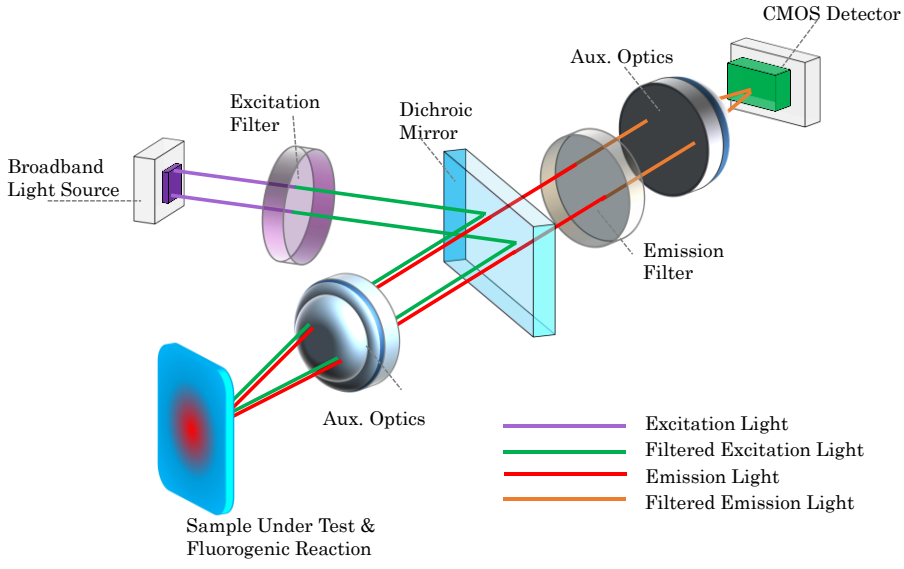

Figure 3.2–5: Fluorescence Setup based on Epifluorescence setting.

Traditional setups for fluorescent analysis, as the epifluorescence microscope, rely on dichroic mirrors, which are elements used to selectively reflect light of a range of wavelengths while transmitting others (see Figure 3.2–5). This setup requires a high-power lamp source, traditionally a mercury or xenon arc lamp but nowadays being replaced by solid state LED solutions. An excitation filter transmits the band of the excitation radiation, blocking undesired bands to avoid noise sources. The excitation radiation is reflected by the dichroic mirror towards the optics that condense the light on the sample. The excitation light triggers the fluorescence process, and radiation emitted by the fluorophore molecules is collected by the same lens and is transmitted by the dichroic mirror towards the detection optics.

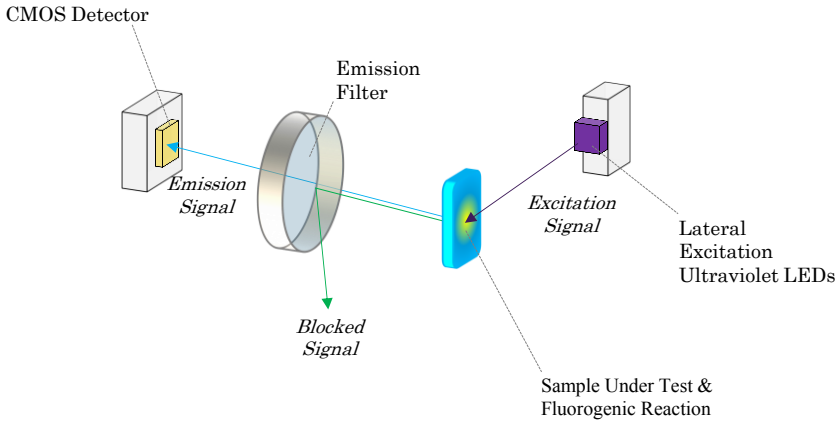

Figure 3.2–6: Orthogonal Excitation–Detection setup for Fluorescence Sampling.

Even if the dichroic mirror based setups are really simple and usually fit in in–line measurement cells, the cost of excitation and emission filters (100€ each) along with the cost of dichroic mirror (100€) and the assembly tolerances for the mirror placement (+–5º) could jeopardize the low costs objective. Alternatively, reduced bill of material configurations can be reached making the most of novel narrow band and narrow beam emitters and orthogonal excitation and detection setup.

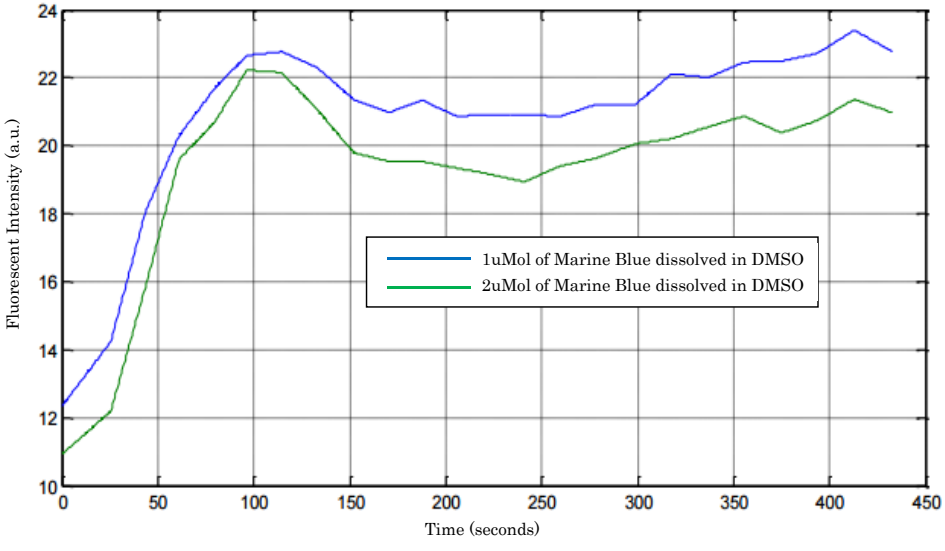

Figure 3.2–7: Example of an emission signal level readout for 450 seconds, for two different concentrations of fluorophore.

It should be taken into account that normally, fluorogenic reactions are not immediate and follow a non–constant time response (e.g. enzymatic fluorogenic responses are normally logarithmic). Therefore, the fluorogenic sampling techniques need to measure not

only the intensity of the emission signal of a given sample, but also its variation across the reaction time (see Figure 3.2–7). This may require stablishing a light modulation approach (e.g. on–off cycles) to avoid overheating in the excitation emitters, due to the long monitoring cycles.

Additionally, notice the importance of sample volumes when measuring fluorescent reactions, especially when very low sample quantities have to be handled, because linearity and detection limits are affected by the sample volume [176]. In general, the greater the sample volume under inspection, the lower the upper end of the linear range, and the lower the limits of detection. There is a clear dependency between the fluorescent intensity and the sample volume excited by the light. Basically, hitting larger volume, at a given concentration, means hitting more molecules, which will generate larger emission signal. Figure 3.2–8 shows this mentioned effect.

Regarding the materials used in fluorescence setups, these not only need to meet the optical requirements of transparency, filtering, etc. but also the auto–fluorescence of the materials needs to be validated. This is especially critical when plastic materials are used within the sensor, because they tend to display much more auto–fluorescence signals than glasses or metallic parts. However, if the auto–fluorescence spectrum falls out of the emission spectrum band, the filters at the detectors may eliminate the unwanted signals.

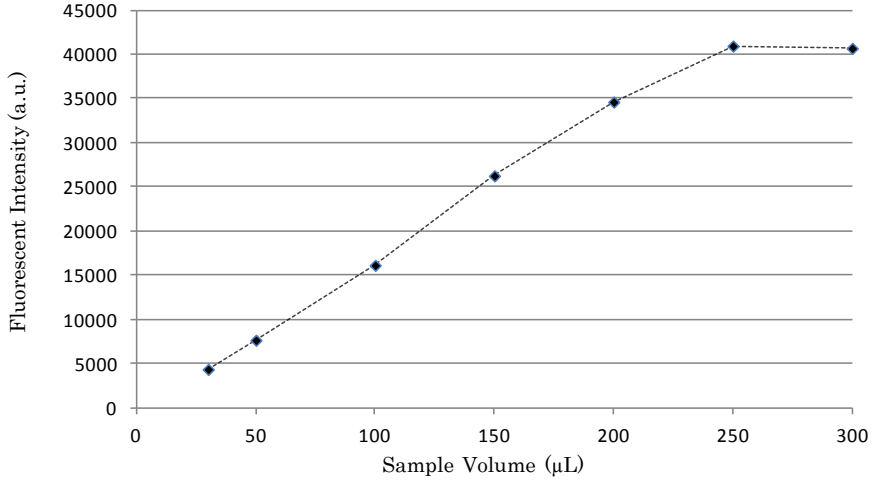

Figure 3.2–8: Results of the fluorescent signal emitted by 1uMol concentration of Marine Blue dissolved in DMSO[30]. Maintaining the photonic configuration (Fluostar Optima, BMG Labtech, Gain: 1400, Excitation Filter 365nm, Emission Filter 470nm) and changing the inspected sample volume the differences in the emission signal are evident.

[30] Marine Blue succinimidyl Ester (M-10165, Molecular probes ThermoFisher). DMSO: Dimetilsulfóxido, (SU0159, Scharlau)

In Fluorescence processes, alike in the Raman ones (see next section), the excitation wavelength must be thoroughly chosen, because even if the absorption spectrum of fluorophores is relatively wide, compared to the emission one, there is always an excitation frequency at which the fluorescence process becomes much more efficient. However, this optimum excitation wavelength is normally relatively near to the emission band, and choosing it requires higher expenses in signal filtering (see Figure 3.2–9).

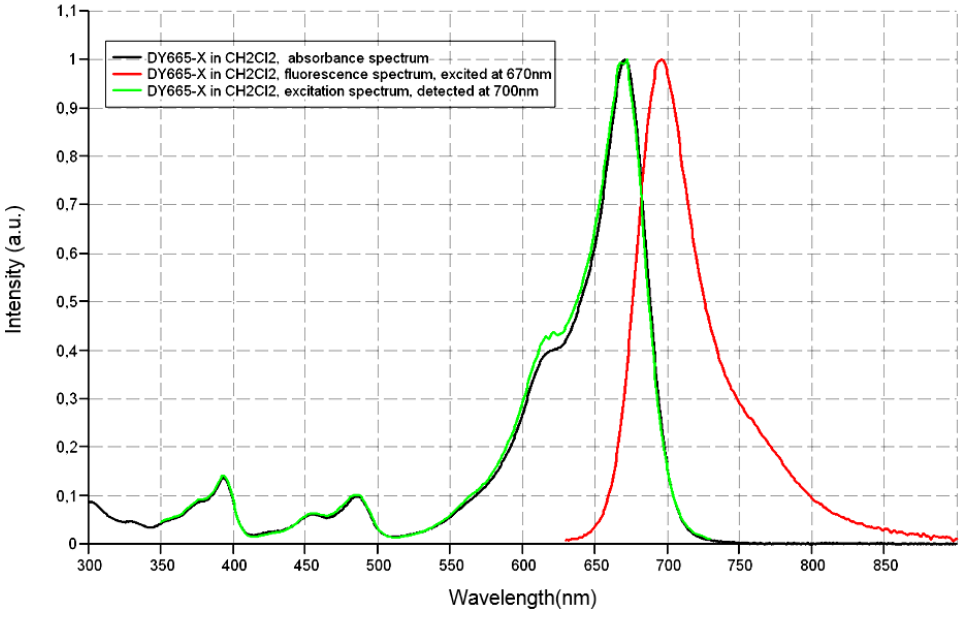

Figure 3.2–9: Emission and excitation spectrums of the DY665–X NIR fluorophore dye in CH_2CI_2 [177].

3.2.1.4 RAMAN Setup

Low signal levels expected in Raman scattering based photonic sensors, with approximately only one in every one million incident photons being scattered via the Raman Effect, requires a complex system setting that represent a true challenge to implement in low cost and in–field deployment. However, thanks to Raman's immunity to water absorption bands, it is an interesting method to analyze fluids with a high proportion of water molecules in them.

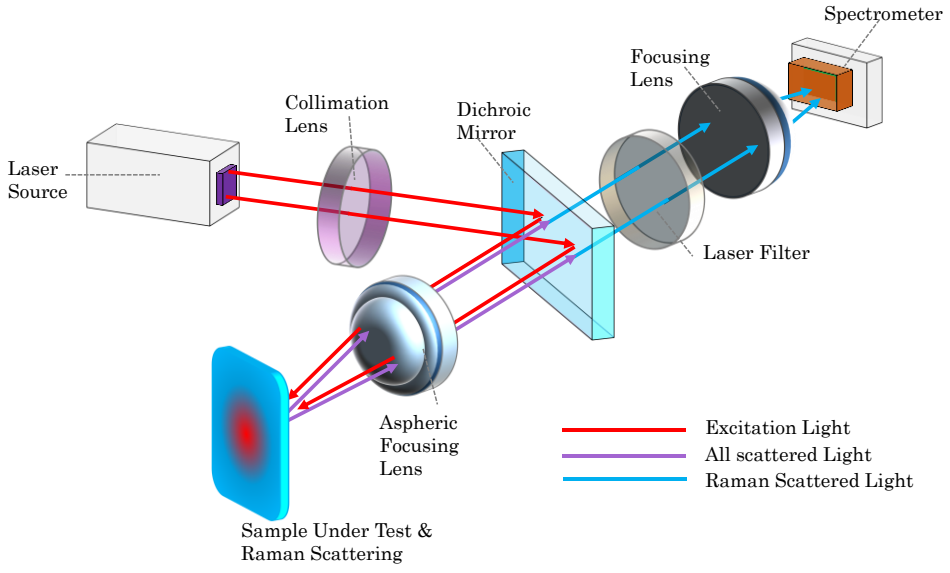

Figure 3.2–10: Block diagram of a typical Raman–based sampling setting.

Raman effect based sensor system analyzes the spectrum results that return from the sample after being excited with a monochromatic light, typically from a laser. A sample's Raman signature displays a series of signal peaks that are shifted in wavelength from the excitation source, offering the molecular fingerprint of the analyte. Figure 3.2–10 represents a standard Raman sampling setup, where the target sample is illuminated through a dichroic mirror and the scattered light is captured by optical elements, which filter all other scattered or reflected light except the inelastic Raman scattered signal that is focused back to a spectrometer detector [178].

Perhaps, the most important decision when selecting components for a Raman system is the excitation wavelength. Notice that Raman shift is a measure of the amount of energy between vibrational energy levels for bonds within the analyte, which is solely a property of the molecules itself and independent of excitation wavelength. However, the returned Raman signal intensity does depend on the excitation wavelength, being proportional to the inverse of the wavelength to the fourth power

$$\text{Intensity}_{\text{RAMAN}} \propto \frac{1}{\lambda_{EXCITATION}^{\ 4}} \qquad \text{Eq. 3.2–1}$$

In addition to this relation with the expected Raman intensity, the excitation wavelength must be chosen taken into consideration the fluorescence properties of the material under analysis, because the signal baseline generated by compounds fluorescence is one of the most important noise sources in Raman Spectroscopy. For instance, many organic compounds fluoresce in visible range (around 300nm to

800nm), so if these organic molecules are to be monitored with Raman UV or IR excitation would be preferred.

Regardless of the wavelength choice, due to the high intensity requirements for the excitation, LASERs are required as sources in Raman settings. Diode lasers in the range of 100mW, available in standard TO–56 packages which include beam filtering optics and heat sinks are a possible alternative for compact and relatively low-cost system [179]. Due to the self–heating of this kind of lasers, active coolers as Peltier effect thermo–electric cooler systems are recommended for avoiding the wavelength drift that occurs in these laser lights due to heating.

While designing a Raman–based detector, another important challenge is removing Rayleigh scattered light from the desired Raman signal. Normally Dichroic filters, or mirrors, are used for such purpose thanks to their ability to reflect or transmitting the light depending on light's wavelength. The dichroic filter is used to reflect the excitation light towards the sample and to filter the light scattered back to the detector due Rayleigh only letting the Raman spectrum propagating to the detection optics.

The dichroic mirrors need to be specified on angles of incidence and in transmission and reflection efficiency above and below the cutoff frequencies. Actually, this angle of incidence is one of the most crucial parameters in terms of opto–mechanical tolerances (see chapter 4.6.1) and deviating from the optimum angle will vastly decrease the system performance, because cutoff frequencies may shift and even block the Raman Signals. Additionally, with the aim of enhancing the signal to noise ratio, normally an extra filter is placed after the dichroic mirror to clean up the radiation from stray light and potential excitation light that propagates through the dichroic mirror to the detector.

Indeed, assuring an optimum alignment in focal position of the excitation and collection optics remains as one of the most important factor for obtaining a maximum Raman signal, making the most of the emission light power. The mechanical complexity for meeting these tolerances, along with the cost of the light source and filters are the main contributors keeping the cost of Raman–based systems one order of magnitude above Transmission, Reflectance or Fluorescence based sensors.

3.2.1.5 Microscopy

The microscopy techniques are used when physical features of the samples need to be monitored, which in the case of in–line fluidic inspection could be reduced to detection of suspended solids or aggregations, and the detection of sample heterogeneity (e.g. presence of air or water bubbles, etc.). The working principles are based on the

optical magnifications enabled by the lenses and the most important features are the Field–Of–View (FOV), Deep–of–Field (DOF), resolution or the minimum resolvable object size, and the whole system compactness. For in–line solutions, it is desired to minimize the system size, while offering a large FOV (e.g. tens of mm^2), and DOF (1 to 2 mm) and high resolution (around 1um), which requires using multi–element lens solutions configured for working in macro mode.

The in–line microscopes require a light source, which could be arranged either in reflexive or transmissive position, require the sample isolating optics, which should be transparent to the working wavelengths, require the 2D detector (e.g. CMOS or CCD camera) and of course require the lens system that enables the detector to focus on the sample. The lens choice and the definition of the working distances is one of the most critical points in the development of this kind of systems, and vastly impacts on the systems manufacturability at low cost, due to the requirements in tolerances (see Figure 3.2–13). Mitigation solutions as self–calibration patterns are used to relax the fabrication and assembly tolerances in the optical and mechanical components of the microscope systems [180].

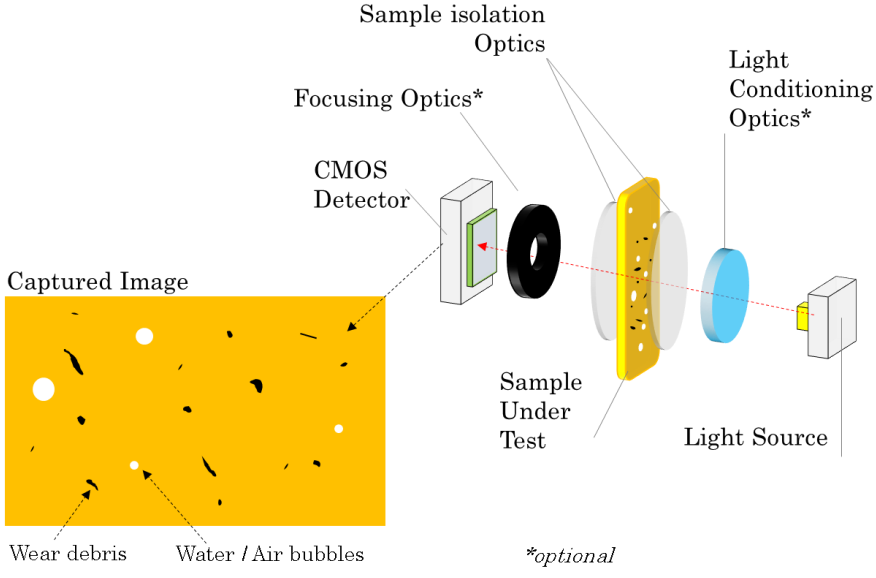

Figure 3.2–11: Block diagram of an in–Line, lens–based microscope with transmission light setting. In this example, wear particles and air bubbles are detected in the image.

There are several cases where the visual inspection of the fluid delivers very useful information about its status. This inspection could be human based or performed with automatic machine vision algorithms.

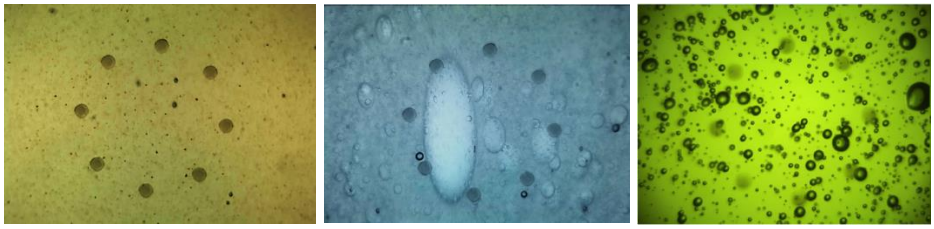

(a) (b) (c)

Figure 3.2–12: Examples of lubricant samples captured with an in–line microscope, showing contamination by shoot, by water and by air bubbles.

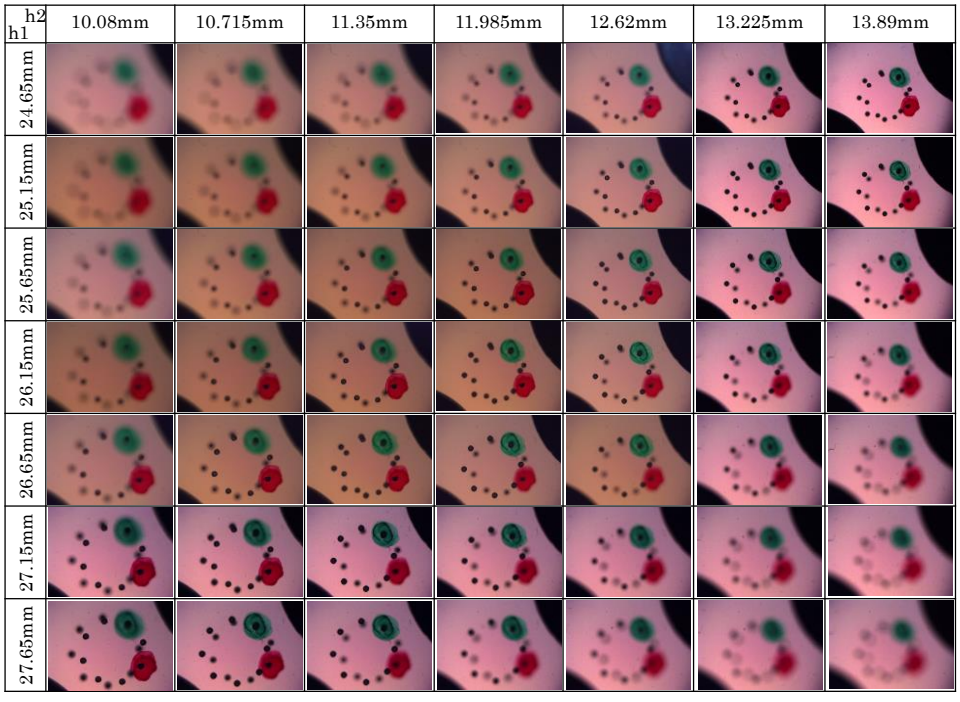

(a)

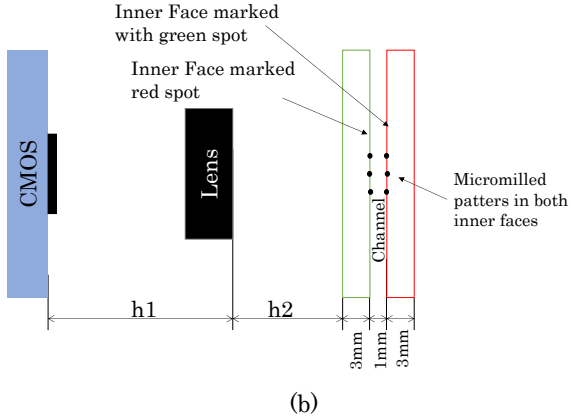

(b)

Figure 3.2–13: Experiment displaying the impact of tolerances of distances between the optoelectronic elements in a microscope setting.

3.2.2 Analysis of photonic information

The previous section has introduced different settings for setting up a photonic inspection of a given fluidic sample. Those setups delivered the method for arranging different optoelectronic, mechanic and optic components for accomplishing a matter inspection though an emitted light radiation, which interacts with the material under inspection, and where the resulting light is received by a photo–detector system. This section will discuss about several potential methods for interpreting and processing the changes happened in the light radiation after interacting with the matter. In the end, the objective of any sensor is to give an objective measurement of a parameter of interest contained in the sample under analysis; therefore, the changes in the light need to be understood, measured, calibrated and translated to a real value of the magnitude of interest.

The methods for analyzing photonic information outlined in this section will cover very basic processing approaches, based on the amplitude, phase or frequency change measurement, in addition spectrometry and chemometrics advanced mathematical analysis are described and finally the imaging and machine vision techniques will be reviewed.

3.2.2.1 Basic analysis: Amplitude, frequency, phase analysis

Considering the fundamental description of a light wave (see Eq. 3.2–2 for the electric field of the light wave), there are three main parameters that define its instantaneous state: Amplitude (E_0), phase or polarization (kz) and frequency or wavelength (w). Therefore, the basic way of analyzing any change happening at the emitted radiation when it interferes with the sample is to track differences in any of these three main parameters.

$$E = E_0 \cdot \cos(kz - wt) \qquad \text{Eq. 3.2–2}$$

Indeed, the physical and chemical effects that might generate a change in the parameters of light are numerous. For instance, the presence of certain compounds in the fluid will generate and attenuation in the light intensity, another molecules might generate a frequency shift between the emitted and the received light (Fluorescence or Raman effects). Additionally, the presence of certain molecular structures (e.g. helical secondary structures or chiral molecules) may generate the rotation of the light's polarization as it happens with glucose solutions.

Indeed, tracking the changes in any of the light parameters require specific emitters and detector. The emitters need to assure the required amplitude, wavelength and frequency properties for the original radiation and the detector should be able to detect the changes happening at the parameter of importance.

The simplest analysis is based on light amplitude measurement, which only requires a matched photo–emitter and photo–receptor, and the calculations are based on the analysis of the received light power.

When the measurement principle requires to analyze not only the amplitude but its distribution in different wavelengths or across a whole spectrum, even if the emitter may remain relatively simple, the detection subsystem requires being able to discriminate the light power received at different frequencies. This is normally accomplished by filtering the light before getting into the detector or using spectrometer systems.

When the phase changes need to be analyzed, emitter needs to assure a certain light polarization and the receiver needs to detect only the light corresponding to predefined polarization. This is accomplished either with tunable polarizers before the detector as in Polarimeter devices, which blocks all but the phase of interest, or by interferometers that are able to quantify the phase [181].

3.2.2.2 Spectrometry and Chemometrics

When the information contained in an absorbance spectrum is the consequence of a series of overlapping bands, the direct measurement of the absorption lines and amplitudes does not give any reliable information about the sample due to the interferences. This is the case with the NIR absorbance spectrums, that due to the spectral coincidence of several compounds' absorption lines (see Figure 3.2–14), the selectivity of the spectroscopic analysis is very low, and advanced processing techniques are required for performing identification, qualitative or quantitative measurements.

These techniques are known as Chemometrics and were defined around 1972 as a chemical discipline based on mathematics, statistics and formal logic to deliver maximum relevant chemical information by analyzing chemical data [182]. These techniques are designed to extract relevant information from complex absorbance, reflectance, fluorescence, etc. spectrums which possess broad overlapping bands and when the chemical, physical and structural properties of the sample also influence the measured spectra. This situation means that the absorption data from the sample depends on more than one variable simultaneously, and thus, the absorbance could be considered multivariate, which represents a challenge for any processing approach.

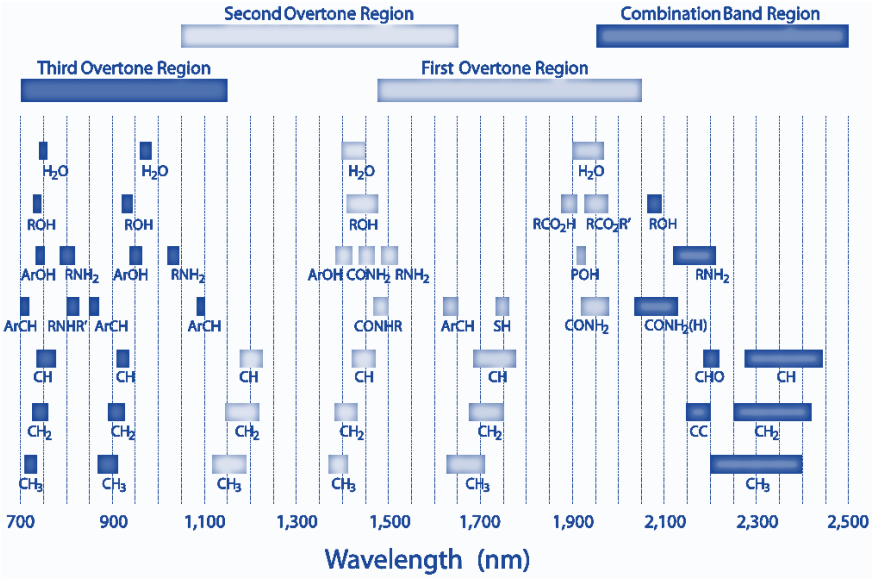

Figure 3.2–14: Major absorption lines and relative peak positions within the NIR region.

Chemometrics combine mathematical and statistical procedures that allow analyzing multivariate spectrums, filtering information that correlates to a certain property of the sample from other distorting data present in the absorbance signal.

Chemometrics rely importantly in the availability of sufficient number of representative samples along with accurate results from reference analytical methods (see Figure 3.2–16). This baseline information is used for calibrating and validating the chemometric measurement methods, being these, qualitative or quantitative.

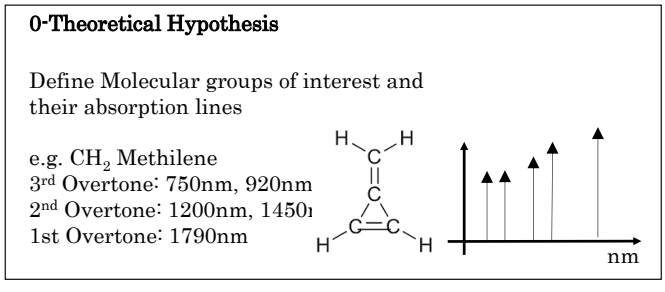

Figure 3.2–15: The first stage in any chemometric model development is to accomplish a theoretical approximation to the problem to solve.

Before starting any mathematical analysis, a theoretical overview to the problem is recommended, identifying the molecular groups of interest that will be analyzed through chemometrics and recognizing their absorption lines along the working wavelength range (see Figure 3.2–15).

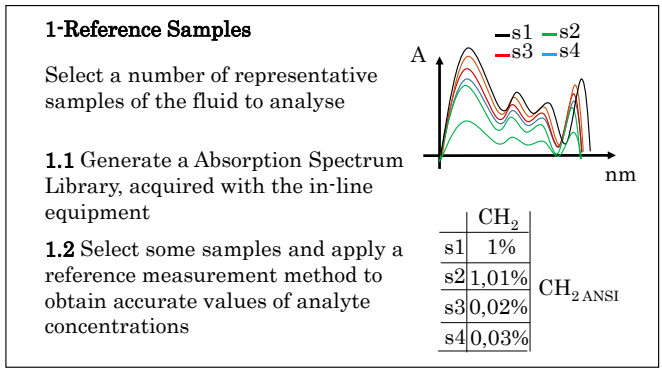

Figure 3.2–16: The second stage in any chemometric model development includes the spectrum library generation and the accomplishment of reference laboratory measurements.

After the hypothesis definition, the first stage in a chemometric method is the data pretreatment, which tries to mitigate the effects of amplitude differences from sample–to–sample. These systematic variations are originated mainly due to scattering effects at sample's non–homogeneities. The pretreatment is applied to the spectrum collection with the aim of normalizing the information for its further processing (see Figure 3.2–17). The literature covers several different pretreatment methods as Multiplicative Scatter Correction (MSC), Standard Normal Variate (SNV), Orthogonal Signal Correction (OSC), mean centering, first and second order derivatives, etc. [183].

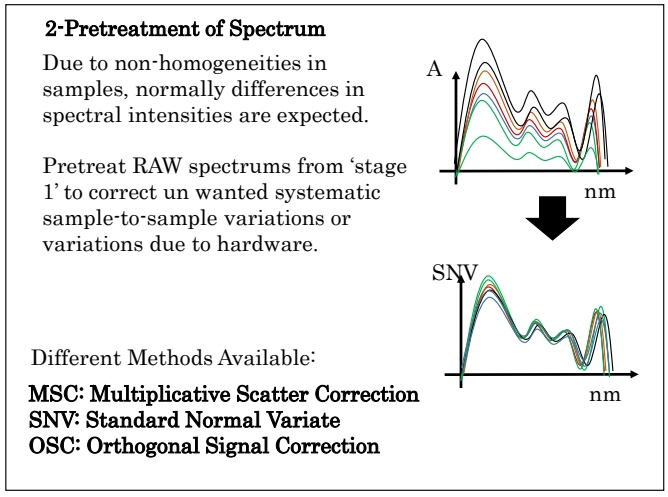

Figure 3.2–17: The pretreatment stage homogenizes the spectrum library for feeding these preprocessed data into the next stages.

The pretreatment stage is followed by different processing methods with the aim of reducing the large volume of information contained in the sample collection, filtering it to identify uncorrelated latent variables, known as Principal Components (PC). In qualitative

analysis, the Principal Component Analysis (PCA) is the most common method, while for quantitative methods, the Partial Least Square (PLS) regression is normally accomplished.

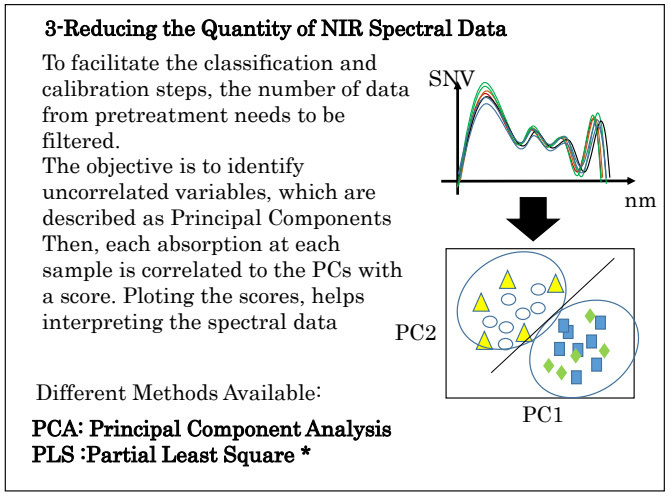

Figure 3.2–18: The large amount of data available for a chemometric model development is not practically processable, so significant information filtering is applied before model development.

While looking for the PCs, one should always take into account the theoretical analysis of the problem to solve. The PCs selected should be located in wavelength bands that have been previously identified as significant from a molecular point of view. Otherwise, the chemometrics may classify the samples according to an unwanted compound.

Once a sensible number of PCs have been identified, avoiding over–fitting or under–fitting the calibration, the spectrums can be graphically displayed according to their absorbance correspondence to the PCs, which is really helpful to understand the complexity of the calibration required.

The last stages are the multivariate calibration model development and its validation against the reference values (see Figure 3.2–19). The calibration is accomplished using appropriate models that describe relationships between the PCs and the absorbance values of different spectrums to provide prediction results about sample identification, qualification or quantification. Basically, the calibration looks for regression models that match the reference values with the analytical information pieces extracted in the previous stages. Indeed, this is a critical process and achieving reliable results that guarantee reliable predictions beyond the calibration library is not straightforward [184]. Normally, this reliability is related to the number of PCs used for the model regression, being 2 to 10 wavelengths a reasonable number for developing the model. Typical

regression models that may be used include Multiple Linear Regression (MLR), Partial Least Squares (PLS) regression, Principal Component Regression (PCR) and Artificial Neural Network (ANN) based regressions recommended when the relation between the spectral absorbance and the sample property to measure is non–linear [185].

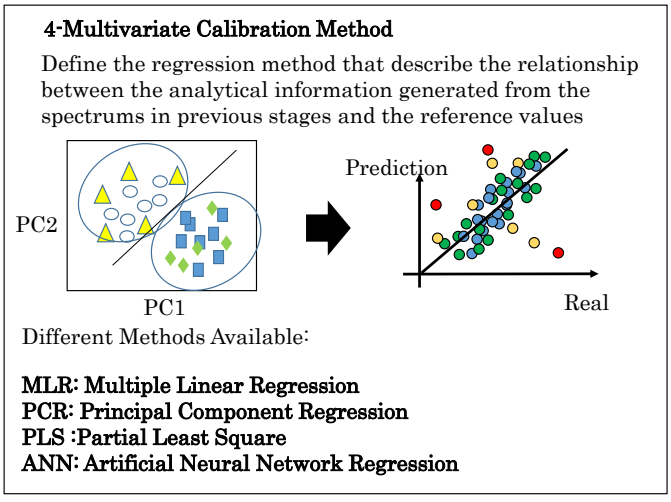

Figure 3.2–19: Calibration method development allows identifying, qualifying or quantifying new spectral information based on the insights gained in the thorough analysis of the spectrum library and reference values.

The model is assessed and verified with a validation set of samples (which have not taken part in the calibration of the model) to understand its predictive ability. The performance of the model is characterized by statistical parameters such as the root mean square error of calibration and prediction (RMSEC and RMSEP), which represent the deviation of the predicted values from the reference values.

It goes beyond the scope of this summary to cover every mathematical detail of the different pretreatment and calibration models and further insights into chemometrics can be obtained consulting examples in the vast literature about the topic, as [186].

3.2.2.3 Imaging and Machine Vision

Even if Imaging and Machine Vision techniques are a clear paradigm of a photonic system, they are often left apart from the pure analytical techniques as the afore mentioned ones. However, machine vision techniques are often really helpful at in–line applications where not only light radiation intensities and wavelengths are important but also when their spatial distribution amidst a volume or geometry, or when the morphology of the sample may contain significant

information. Machine vision or imaging techniques are able to automatize the extraction of these features.

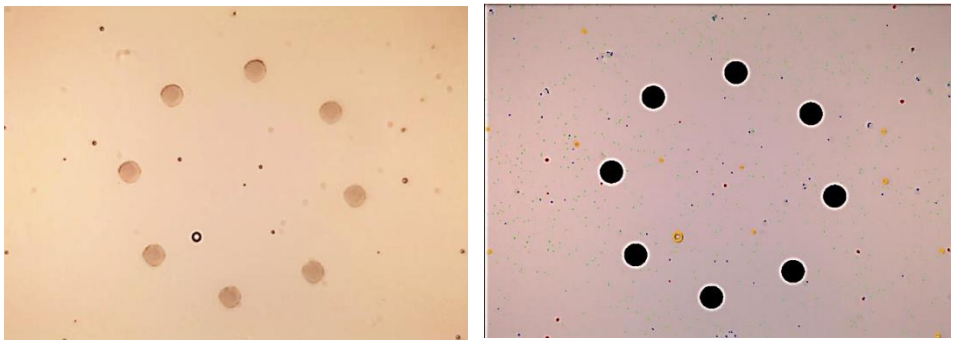

Figure 3.2–20: Results of machine vision algorithms for particle and bubble detection, as well as the self–calibration precision pattern that allows calibrating the size of the particles and bubbles at each image taken. Source: OilWear® sensor, Atten2 Technologies.

Sometimes machine vision or imaging techniques are used in combination with Fluorescence or Raman setups to analyze the presence of singular components that react to the excitation lights. Even if these approaches are not very common with industrial fluidics, these mixed techniques are being widespread in biological applications, such as cytometry or cell identification [187].

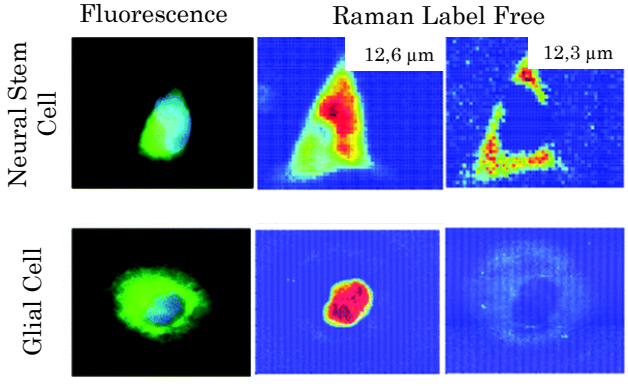

Figure 3.2–21: Fluorescent and Raman imaging used for demonstrating the differences between glial and neural stem cells. The Raman band at 788 cm−1 is associated with the nucleic acids of DNA and RNA, whilst the band at 813 cm−1 is associated with RNA only. Source [188].

The most accurate description for the Imaging or Machine Vision technologies is a combination of a set of algorithms of operations that a system is able to perform over an image or a sequence of images to extract significant information, based on geometrical forms, movements and other effects. For more information about machine vision techniques refer to literature references as [189].

The images used for imaging or machine vision processing are normally captured in the visible color region, at infrared region and

lately more and more examples can be seen in the near infrared hyperspectral domain [190][191].

The potentials of these technologies are evident and complementary to the previously mentioned signal analyzing techniques. This is the case, for instance, when machine vision helps identifying uncontrolled sample conditions that may jeopardize a chemometrics analysis (e.g. high concentration of air bubbles would not allow a correct fluid absorbance reading) or helping to localize regions of interest before accomplishing the full in–deep spectral analysis.

3.3 In Line Sensors

Integrating the aforementioned photonic setups and analysis methods is not an easy task, especially when requirements in terms of compactness and low cost becomes part of the equation. However, things get even more complex when these configurations need to deal with in–line operation, where the fluid sample is directly taken for the process under test and fed into the sensor element.

The advantages of acquiring in–situ and real-time information about the fluids directly from the process flow are evident: the fluid conditions remain unaltered; the reaction time is very fast and the sensors can be installed in locations relevant for process monitoring. The in–line monitoring helps guaranteeing and improving product quality and repeatability, enables increasing the efficiency and safety of the process, and also allows understanding the fundamentals of the process thanks to the acquired insights about process statistics.

Even if the cost of the in–line sensor is going down constantly, normally this is one of the factors hindering their deployment. However, this cost is rapidly paid off due to improved process efficiency, lower raw materials consumption and waste generation, and, most important, the ability to manufacture high quality products.

Nevertheless, dealing with an in–line operation imposes several challenging working conditions that need to be matched with the photonic and optoelectronic requirements. Different factors need to be addressed when designing and in–line sensor system:

i. Definition of the information and parameters necessary to monitor and control (chemical compounds, physical parameters, etc.).

ii. Accuracies, response times, reliabilities expected.

iii. Average values, normal fluctuations, dynamic ranges, extreme values of the parameters to monitorize

iv. Sampling frequencies with respect to the process timescale and expected dynamics of the changes.

v. Implications for installation, operation and calibration of the sensors, always assuring an easy deployment and automated operation

vi. Number and measurement locations

vii. Data output formats and compatibility with already deployed control systems

viii. Safety and certification considerations.

ix. Total cost of operation.

Next section will review the differences between the process monitoring approaches, from the off–line analysis to the proposed in–line systems, also covering the associated calibration issues entailed in the in–line operation solutions. Additionally, the requirements for the wettable parts of the sensors will be outlined, including the possible wear or fouling on these parts in contact with the fluid.

3.3.1 In–line, On–line, At–line and Off–line Sensors

Process Analysis at industrial deployments as production, processing, energy or manufacturing plants could be defined as the set of methods for providing sufficiently accurate and immediate information on variables that describe the state of the industrial activity. These process analyses can be accomplished in four options: Off–line or laboratory analysis, At–line measurements or On–Line and In–line systems (see Figure 3.3–1) [192]. However, there is no clear–cut line between the different classes, and these boundaries are even moving, with an increasing number of off–line techniques having been converted into on–line methods by automated, robot–assisted sample extraction from the processes or from bypasses that directly feed samples into in–line instruments [193].

For instance, the laboratory analysis of oil samples looking for wear evidences was first introduced in 1948 [194], and this traditional off–line fluid analysis is still an important asset for several maintenance programs, especially when high accuracy and low detection limits are needed. However, due to the potential benefits of real time operation, in situ sampling, reduced prices and size, and the decent accuracy and reliability (which increased day by day), the number of in–line sensor solutions is increasing unstoppably in the last decades [195][196].

Off–line analysis relies in high–end equipment operated by trained personal located in environmentally controlled laboratories. They offer the greatest versatility of analysis methods and achieve the

highest accuracies, reliabilities, etc. However, they require samples being physically extracted and sent to laboratory for their analysis, which, obviously implies long turnaround times and the delivery may change some sample properties that could be significant for the measurement.

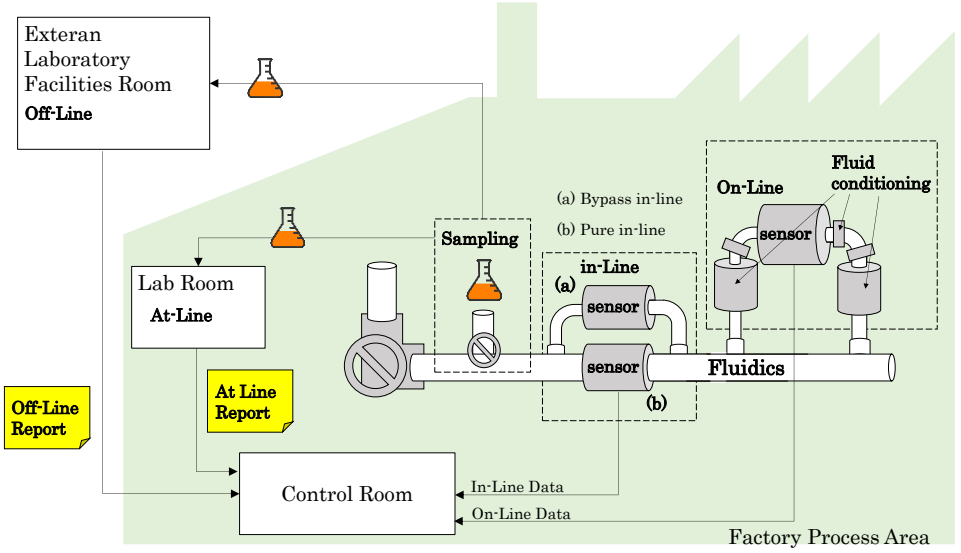

Figure 3.3–1: Diagram depicting the differences between the fluidic process analysis approaches.

At–Line systems are mini–laboratory solutions intended to be installed within the process area and used by a skilled operator. They still require extracted samples to perform measurements, but they are normally ready to deliver a high sample throughput (5–10 per hour) with high accuracies. Even if they can still be considered as laboratory equipment, they are designed to work under relatively dirt environments with no special environment conditioning.

In addition to the laboratory analysis performed either in–house (at–line) or in external facilities (off–line), there is another family of process measurement approach represented by the on–line and in–line sensor systems, terms which are sometimes used indistinctly.

On–line sensors are fully automated systems, located very close to the process under monitoring. Normally, an on–line system includes not only the sensor or transducer but also sample conditioning hydraulics as pumping, filters, electro–valves, heating, cooling, pressure reductions, and could also, sometimes, asides the hydraulic conditioning, include some sort of chemical preparation controlling external devices as dosing pump. Thanks to these pretreatments, on–line systems are able to include delicate transducers and offer very good sensor performances in terms of accuracy, reliabilities, etc. Additionally, on–line sensors deliver the measurement results directly

to the central point through a standardized communication protocol. However, the required external equipment makes on–line solutions normally expensive and bulky.

On the other hand, in–line system represents the most integrated version of process monitoring equipment since they need to be placed directly into the process stream. As it has already been detailed in chapter 1, these in–line devices have traditionally been used for measuring relatively simple parameters as pressure, PH, density, flows, etc. but with approaches as the one presented in this thesis, in–line sensors are evolving to offer readings of much more complex parameters.

One of the biggest difference between the on–line and in–line devices is that on–line sensors remove a lot of uncertainty sources thanks to the fluid conditioning applied before the measurement is done. For instance, on–line devices add bubble removing systems, may include particle filters, flow controllers that avoid turbulences and assure sample homogeneity, etc. [197][198][199], contributing to a much more stable sample conditions that lead to higher accuracies and repeatabilities in on–line sensor systems.

However, integrating more complicated transduction in harsh conditions as the ones imposed by the industrial fluidics requires a careful hydraulics, fluidics, optics, mechanics and electronics integration for offering reliable measurements. The next sections describe two important design considerations when dealing with photonics sensors in industrial fluidics applications: the calibration and the wettable parts.

Table 3.3–1: Comparison chart of process analysis approaches.

	Off–Line	**At–Line**	**On–Line**	**In–Line**
Installation Site	Laboratory	Plant	Process	Process
Sampling	manually	manually	Automatically	integrated
Sampling Points	Potentially many	Potentially many	few	few
Analysis Frequency	low	Low–mid	high	Real time
Sample Transport	To remote laboratory	To local analytical equipment	integrated	No transport
Analysis Procedure	Automated /manual	Automated/ quick check	Automated	Automated
Turnaround time	Hours / days	hours	minutes	Real time
Parameters Measured	many	1–10	1–2	1–2

Measurement Range	Flexible	Fixed	Fixed	Fixed
Accuracy	Very High	High	Medium	Medium
Sample Preparation	manually	manually	automatically	No preparation
Operation	Lab assistant	Plant Operator	Automatically	Automatically
Maintenance	Lab assistant	Plant Operator	Plant Operator	Plant Operator
Data communication	LIMS[31]	LIMS	Process Signal / LIMS*	Process Signal / LIMS*
Environmental compatibility	Room temp.	Room Temp.	Industrial range	Harsh environments
Environmental protection	IP23	IP54	IP67 / Hazardous area certified	IP67/ Hazardous area certified

*Smart sensors are supposed to be deliver LIMS

3.3.2 Calibrating in–Line sensors, White and Dark Level measurements

The different measurement techniques presented in the previous chapters are normally the integrated versions of well–stablished laboratory methods. Indeed, transmission, fluorescence, microscopy, etc. have been routine processes in laboratories since hundreds of years ago. However, the migrations of these methods to low cost compact settings does not only present integration problems, and meeting some of the method–fundamentals is almost no possible in systems as the ones presented in this thesis. We are talking about spectroscopy calibration (white and dark signals), detector calibration (as in colorimetry), or dimensional calibrations performed in microscopy.

Laboratory equipment normally include a calibration procedure, either for calibrating the instrument, or to be accomplished prior to the measurement acquisition as baseline signal. These reference values are used for normalizing measurements and for compensating the measured signal removing the effects of variations in emitters, detectors or optical settings.

For instance, in reflectance spectrometry, the standard procedure, require measuring the White and Dark signals. White signal represents the maximum value detectable, and thus requires using a mock sample that reflects ideally the 100% of the emitted light. Several reference samples are available for this purpose, but

[31] Laboratory Information Management System

basically are composed of a highly reflective material (see Figure 3.3–2). Dark signal represents the intensity value delivered by the detector whit the emitter lights switched off. The dark signal represents the noise level at the detector, which increases with integration times, gain, etc. In transmittance, even if some standard materials could be used, the White signal is acquired just measuring an empty cuvette. These reference spectrums are then mathematically applied to the sample's measured spectrum and its normalized and compensated reflectance is obtained, which is fed into subsequent processing stages (e.g. chemometrics).

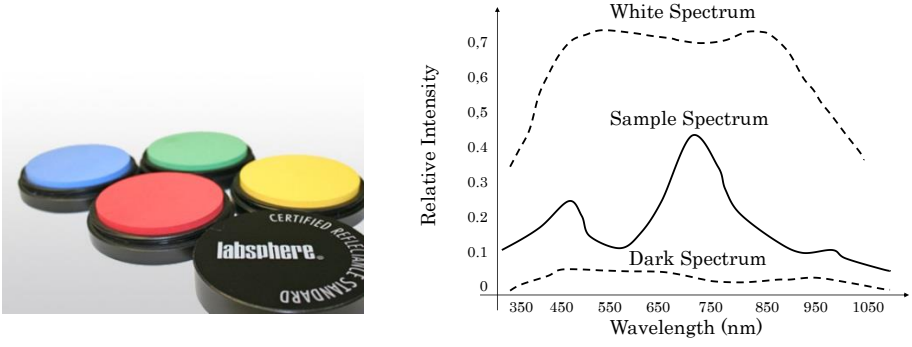

(a) (b)

Figure 3.3–2: (a) Reference samples for diffuse reflectance (Lapsphere, North Sutton, NH, USA). (b) Example representation of white, dark and real sample spectrums.

$$\text{Transmittance} = \frac{I_{SAMPLE} - I_{DARK}}{I_{WHITE} - I_{DARK}} \qquad \text{Eq. 3.3–1}$$

Something similar happens with microscopes, where either the equipment is calibrated on regular basis or reference patterns are used to determine the size of the measured targets. Colorimetric measurements are accomplished following the same approach, calibrated equipment or reference color.

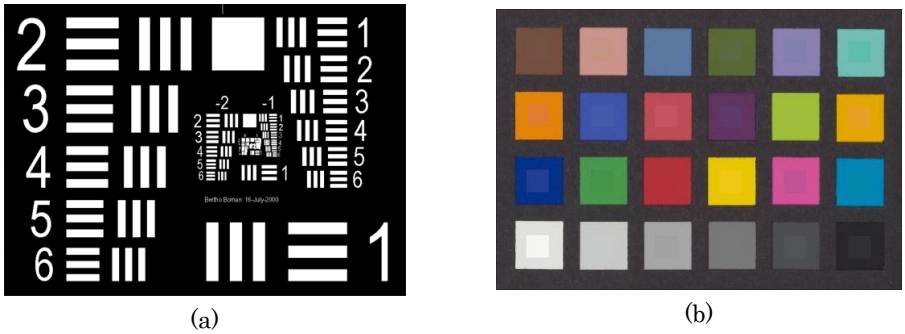

(a) (b)

Figure 3.3–3: (a) Microscope calibration and resolution resolving pattern (1951 USAF resolution test chart). (b) Color calibration patter (Leica, Wetzlar, Germany).

But, indeed, the migration of the aforementioned techniques is not straightforward, and in some occasions, is even practically impossible. Notice that the in–line sensors are permanently in contact with the sample fluid, with little or null possibilities of completely removing it for taking a reference reading.

In this situation, there are only two possible solutions left for the integrated in–line sensors: either they work without calibration, which could perfectly fit several applications where no absolute readings are required, or some sort of calibration system is included within the system.

Notice that we are not talking about detector or emitter compensation systems (already outlined in section 3.1.1.9 Calibration), but presenting the implications of enabling the in–line sensors to offer a calibrated measurement against a standard. And this requires somehow measuring the reference pattern along with the sample analysis [200].

For instance, the measurement of the white reference patterns is a traditional challenge that has been faced with several clever and even artistic engineering solutions, which at certain moments, between measurements, are able to introduce a physical component, named white tiles, for accomplishing a white signal reading. Even if sometimes, these engineering solutions use two parallel systems, one measuring the reference and the other the sample [201], the solutions normally require some sort of moving parts within the sensor system, either for displacing the physical white tile to the measurement point, blocking the sample, or, moving some optical component (e.g. mirror) that alternatively focuses the sample or the white tile [202] [203] [204] [205].

Regarding the calibration of in–line microscopy solutions, a good approximation is to include reference and accurate patterns within the FOV of the system [180]. This reduces the active area available for inspecting the sample, but removes all the dependencies with mechanical, optical and assembly tolerances.

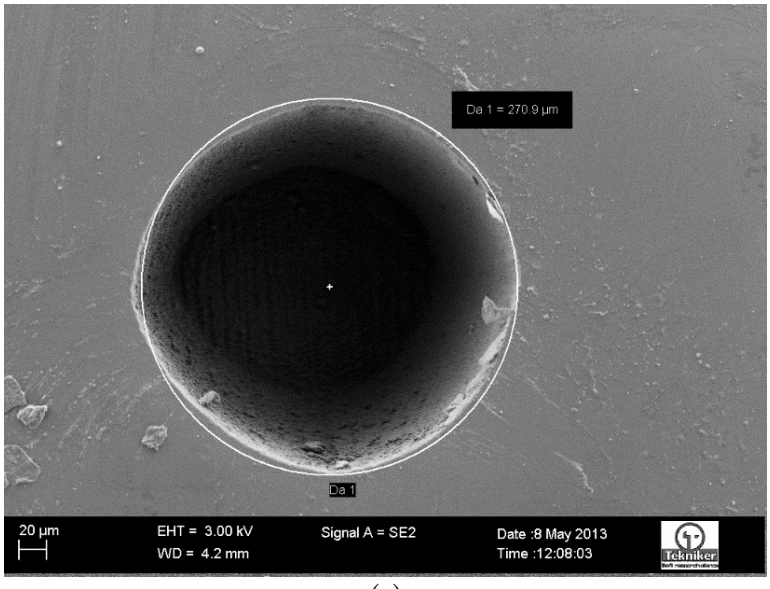

(a)

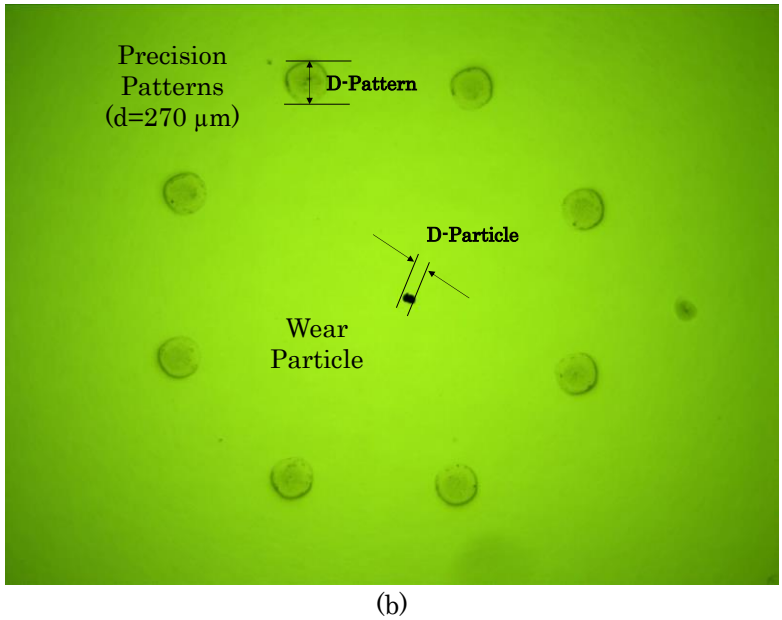

(b)

Figure 3.3–4: (a) Calibrated Pattern inspected in SEM microscope. (b) Rings of patterns included in the FOV of the in–line microscope. All the wear particle dimensions are calculated referenced to the precision pattern dimensions.

3.3.3 Wettable Parts

The wettable parts are one of the most critical parts within an in–line sensor for fluidics. Wettable parts are defined as all the components that will be in contact with the fluid, which individual properties and integration need to assure a reliable operation under the given working conditions (pressure, temperature, corrosion, wear…).

Regarding the compatibility of the sensor with the fluid, it needs to be assured in both directions, especially when dealing with bio samples that may be contaminated by the sensor itself. This is the case for the Food&Beverages and medical applications, where all the optics, seals and metals need to be accepted for the biological uses.

From the practical point of view, the design of the wettable parts normally relies in several laboratory analyses for compatibility studies, and simulations (see chapter 4) for assessing the reliability of the different parts under the working conditions.

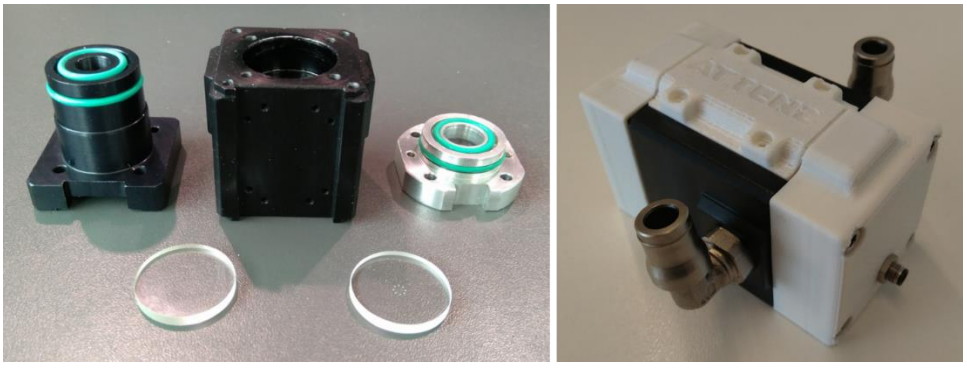

(a) (b)

Figure 3.3–5: Example of wettable parts included within a sensor prototype for wear particle detection. (a) Shows optics, mechanics, and sealings and (b) shows the hydraulic fittings.

Normally, these parts will include the following items:

3.3.3.1 Hydraulic fittings

These elements allow connecting the sensor with the hydraulic infrastructure to monitorize. Normally these parts are standard hydraulic components (BSP, GAS, etc. connectors) and are fully compatible with a large range of fluids and do not represent a major problem in sensor integration.

3.3.3.2 Sealings

The seals are required to assure a proper sealing between the different optic and metallic parts. These flexible elements are accommodated to absorb the effects of the mechanical imperfections and to seal the junctions avoiding leakages due to capillarity effects. The sealing material, normally elastomers, should be selected depending on the fluid to be monitorized, because not all the materials are suitable to all applications. For instance, when dealing with mineral or synthetic lubricant fluids fluorocarbon may be used for sealings, while Phosphate Ester based hydraulic fluids require the use of EPDM (Ethylene–Propylene) or Teflon.

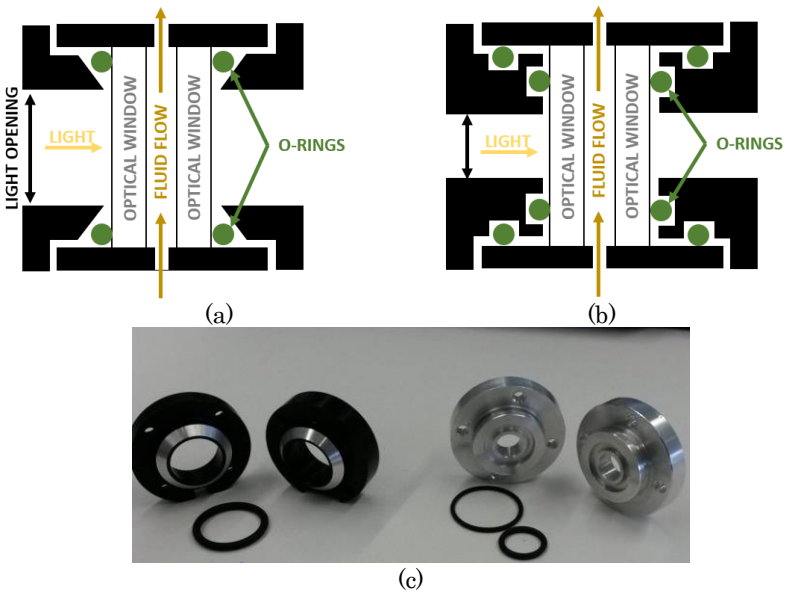

Figure 3.3–6: (a), (b) Different mechanical approaches for installing a single seal or double seal solution for photonic sensors. (c) Mechanical parts and seals according to the (a) and (b) designs.

3.3.3.3 Mechanical parts and sensor internal embodiment

Normally the channels by which the fluid moves within the sensor are made in metallic elements. Corrosion and chemical compatibility needs to be checked because not all the metals and metal surface treatments (e.g anodizing) are compatible with the different fluids.

3.3.3.4 Optics

This is perhaps the most challenging part in the structural design of the sensor. The optics in contact with the fluid may do not have any optical function but to let the light come in and out from the sample. However, as it needs to stand the fluidics pressure, temperature, etc. it has to be carefully selected not only for its transparency properties but also for its mechanical roughness. For instance, the following Eq. 3.3–2 describes the minimum thickness of glass disk before it breaks under a given pressure.

$$T(\text{inch}) = \sqrt{\frac{P\max(\text{psi}) \times A(\text{sq.inch}) \times F}{3.12 \times M}} \qquad \text{Eq. 3.3–2}$$

Whereas, T represents the minimum thickness in inches, A defines the unsupported area in sq/inches (see Figure 3.3–7 depicting different apertures), P is the maximum pressure in psi, F is a safety factor that normally is set to 7 and M defines the Modulus of Rupture of the glass (in psi). As reference a BK7 glass delivers a M~2,400 psi

and Gorilla® Glass from Corning (Corning, NY, USA) a M~100,000 psi, which allows a compatibility with higher working pressures.

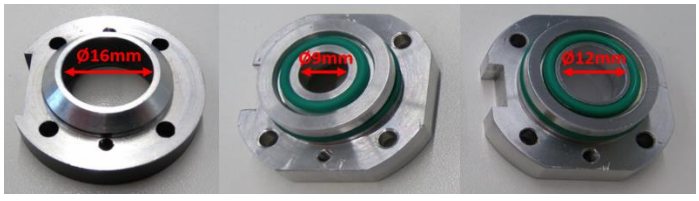

Figure 3.3–7: Different optical apertures. Increasing the diameter allow higher radiation flux availability, while reducing the compatible maximum pressure.

Besides, the ageing, fouling and scratches on the surfaces of the optical parts in contact with the fluid is also one of the major drawbacks of this kind of photonic sensors and hinders long life time of the sensors. The wear of the surface will produce a wrong measurement due to either increase or decrease the intensity of scattered light onto the sensor surface, changes in absorptivity, modified index of reflection, etc. Even if several coatings and surface nano–structuration, [206] [207] [208] [209], have been tried for protecting the optics against wear and fouling, they do not offer a definitive solution and only delay the effects of the surface degradation.

4.

Design Methodology for Cost Effective Photonic Sensor Product Development

Photonic component developers usually do not provide any specific support for bringing their systems into products, leaving an important technological gap to be faced by system integrators. Moreover, the intrinsic complexity of the fundamental processes involved in photonic measurement techniques, requires the availably of a multi-domain engineering team, including physicist, chemist, mechanics, optics, electronics and data processing experts. The integration of this bunch of heterogeneous domains is not evident, which, added to the uncertainties and risks typically entailed in complex and innovative products hinders the technological, economic and time-to-market success of the development. The situation aggravates if strict certification framework regulates the application, as it happens in the industrial, energy or manufacturing domains.

In this context, this chapter reviews different New Product Development processes targeting complex and innovative products. Since none of the state of the art models satisfy the abovementioned situation, a development methodology is presented and specified for guiding the design and development of cost effective photonic sensor products Development. The presented methodology merges contributions identified from different development models with customized approaches tailored to the use case of fluidics sensors. The definition of the methodology is continuously complemented with specific examples taken from real developments that illustrate different details at each stage of the design process.

4.1 Background and Main Objectives of the Design Methodology

The main challenges faced by a photonics–enabled smart sensor integrator derive from manifold reasons. First, the nature of the working principles (as described in Chapter 2) require a deep understanding of the physical and chemical processes behind the measurement principle, and normally, advanced knowledge in chemistry, fluid dynamics, thermodynamics, etc. is essential for specifying the problem–to–solve and formulating the solution hypothesis. Then, the interaction with the photonics starts, when the suitability of the properties of the light–matter interaction processes is assessed for enabling a solution to the identified problem. Therefore, it becomes evident that the insights and expertise of a photonic expert is required to evaluate the benefits and risks of applying a certain photonic principle to sort out a fluidics sensing problem.

At this stage, the engineering review starts, where the issues coming from the effective integration of the aforementioned techniques into a system need to be solved. Optical alignment of the photonic components, mechanical tolerances, fluid sample acquisition and conditioning, assuring the sensor performance under operational conditions (pressure, temperature, vibrations, etc.), enabling the easy calibration, installation and maintenance of the sensor, embedding all the data processing and communications, etc. are some of the task to be solved by the multidisciplinary engineering team (mechanics, hydraulics, electronics, control and automation and software engineers).

Besides the complexity inherited from the mentioned scientific, technological and operational challenges, photonics–enabled smart sensor integrators need to deal with severer regulatory requirements and the constantly increasing importance of reducing time–to–market and investment payback for successful device commercialization.

Fluid sensing problems looks solvable at laboratories, and the availability of continuously improving low cost, compact and feature–rich photonic emitters and detectors seems to enable the easy migration of multiple monitoring techniques from the lab to the market, requiring little effort and time. The real situation is completely opposite to this appreciation, because, asides the traditional difficulties found in bringing innovative products to the market, known as crossing the 'valley of the death' [210][211][212], in this case additional technological, integration, regulatory and market originated risks and strict requirements [213][214][215] [216][217][218] seriously jeopardize the successful evolution from photonic measurement principles into autonomous sensor systems.

The objective of the proposed methodology is to bridge the gap between the theoretical measurement principle formulation and the photonic smart sensor manufacturing, providing a device development model, which has been empirically formulated based on insights acquired during the sequence of different photonics–enabled product development.

One of the major concerns faced while shaping the model has been, indeed, the management of the aforementioned heterogeneity of technologies, but also how to deal with the uncertainty in terms of lack of specifications and lack of awareness about the risks involved in the project.

The reason behind this lack of information and knowledge about the product is because normally, the sort of sensors addressed by this methodology are novel devices. This novelty is generated either because the sensors target a new application scenario, which is quite common situation for the in–line sensors since they are supposed to replace or assist an off–line laboratory method but the conditions for the in–line operations are unclear. Alternatively, the novelty may be justified because, even if other sensor technologies might cover an application, the integration of photonic measurement principles for that specific case has not been tackled previously.

The proposed methodology is based on different approaches of New Product Development processes, specifically on those models focused on technological products and on incremental product developments, as the traditional Phase–Gate or Stage–Gate models [219], and the newer generation as the Triple A System (Adaptive, Agile, Accelerated) [220], because they accommodate better the uncertainty that normally surrounds the development of new sensor products.

The work presented here, describes the generic methodology but also highlights some specific steps which are considered critical for a successful development of a photonic–enabled smart sensor for in–line fluid monitoring. Notice that, even if the final goal of the methodology is to achieve a product, its business model formulation [221][222] is out of the scope of the topics covered here, so value propositions, distribution channels, revenue streams, etc. are not considered while formulating the product structure.

4.2 Product Innovation and Development Process Models

Bringing a new sensor product successfully from the laboratory to the real field is highly complex and depends heavily on the implementation of rigorous processes or methodologies. These

methodologies should allow or assist developers to optimally synchronize development, prototyping, verification, production, etc. successfully meeting manifold requirements of third parties, including end users, regulators and investors [223]. However, this traditional situation has evolved collaterally to the raise of Industry 4.0.

In the Industrial Internet of Things world, the boundaries between traditional industry and internet companies are becoming increasingly blurred, and connectivity is opening up new business opportunities for sensor manufacturers, which require very fast reaction times once the opportunity has been identified [224].

As described in section 4.2.1, dealing with this complex and innovative product development in successively shorter product life cycles is not straightforward, and different development strategies has been proposed in the last years. However, while various models may exist in the sensor industry, no comprehensive development process has been published so far.

The sections from 4.2.2 to 4.2.7 review different existing model representations, looking for the best approaches that might be applied to the formulation of a new development model that captures all aspects of photonic sensor system integration and commercialization from early–concept development to after–sales support.

4.2.1 Smart Photonic Sensors: Complex and Technological Product development

Known as novel, disruptive, vanguard, breakthrough, or exploratory projects, etc. what they all have in common is that, in this sort of project scenario neither the objectives, nor the capabilities, means and resources to achieve them, are clearly specified at the beginning of the development. This uncertain situation poses clear differences when compared to a routine project execution (see Table 4.2-1), and therefore, the management approaches for both project types could not share the same vision, tools and criteria [225] [226].

Table 4.2-1: Differences between routine and complex project execution [244].

	Routine Projects	Novel and Complex Projects
Objectives and Requirements	Fully specified with little probability of change	General view of the project known, but without detailed objectives and with emerging and evolving requirements
Tasks	Can be specified and could be derived from previous experience	Only the big picture of the project is envisaged

Means and Capabilities	Identified beforehand, with known sources or suppliers	Not necessarily existent, not necessarily specifiable
Uncertainty	Variation (plan deviations) and risks (stochastic estimable changes in known project variables)	Unexpected uncertainty: new variables, new effects, new actions, which could not be foreseen at the beginning
Risks	Normally known, and therefore, mitigation plans could be allocated early	Mostly unknown
Examples of Domains of Relevance	▪ Well Known markets and customer expectations ▪ Well Known performance drivers of the developed system ▪ Well Known environmental parameters	▪ New markets and unknown customer feedback and reaction ▪ New performance drivers of the developed system ▪ Unknown or new technology ▪ Complexity with unexpected interactions among parts ▪ New markets and application domains with unforeseeable regulatory constraints ▪ New stakeholders with unforeseeable requirements

Additionally, as mentioned earlier, in todays globalized and digitalized modern economy, it is often impossible to envisage how a digital product will evolve. The needs from the end users evolve, the economic and market conditions change rapidly and new competitive pressures arise suddenly from any part of the world. Therefore, apart from the uncertainty intrinsic to technologically complex projects, the volatility of the globalized economy does not contribute to having the full set of requirements defined at the outset of the projects [227].

If we narrow down to the photonics–enabled smart sensors, we found a set of challenges that the methodology is supposed to help developers dealing with.

Table 4.2-2: Description of the challenges present in the Smart Photonic Fluid Sensor product development.

Challenge	Description
Critical Requirements	▪ High sensibility ▪ Reliable and Autonomous operation ▪ harsh environments (corrosive ambient, high temperature range)

	▪ Almost zero maintenance ▪ Plug & Play installation and calibration free operation
Heterogeneous technology integration	▪ Physics and Chemistry, Optics, optoelectronics, micromechanics, hydraulics and microfluidics, hardware and software, algorithms, communications, industrial processes.
Multidisciplinary working teams	▪ Chemistry, Optics, Photonics, Mechanics, Design, Electronics, Software and data analytics.
Managing key providers	▪ Novel Photonic components
Uncertainty	▪ Novel applications ▪ Unspecified working conditions (environmental, sample conditions, contaminations…) ▪ Little accessibility to devices once deployed in the field (little feedback)
Little time to market	▪ From problem identification by the end–user, 0.5 years concept proto, ~1 years working prototype, ~1.5 years volume production
Regulatory, investment and market constraints	▪ Several Certifications may apply (e.g. CE, UL, FDA, IP, vibrations and Shock, ATEX…) ▪ Unit cost constraints, impacting on product margin ▪ Fierce competition

In addition to the challenges described in Table 4.2-1 and Table 4.2-2, the proposed methodology also needs to address the traditional objectives considered a must for any new product development technology [228]:

- Foster optimum Quality of Execution
- Sharp the focus for better project prioritization
- Focus the development of the competitive advantage of the product
- Keep a strong market and end–user orientation
- Sharp, early, and stable product definition
- Fast parallel and flexible processing by different disciplines
- Rely on a true cross–functional team approach

The next sections will review different development models, looking for the best contributions to the specific product we have in hands. Then from section 4.3 on, we will summarize these diverse contributions and visions in the Design Methodology for Cost Effective Photonic Sensor Product Development.

4.2.2 Design for Six Sigma

Design for Six Sigma (DFSS), which was introduced as an evolution from the traditional Six Sigma approach in the early 2000s [229], is a product development process that uses metrics, data, statistics, and project management tools with the final goal of having a robust and failure–free product in the market, and has been applied in the sensor product development industry [230]. The DFSS focuses all the development in the deep understanding of the customer needs, which are translated to requirements that drive design and development, which is then optimized and finally validated. In this situation, some interesting contributions from the DFSS philosophy [231] to the photonic sensor development have been identified:

i. Only if you focus on measuring the defects of a process, you will be able to figure out how to solve them,

ii. Use objective metrics or key performance indicators (KPI) to measure processes

iii. Track changes occurring at these KPIs for early problem identification

iv. Keep the customer in the loop for detecting problems and deviations occurring at customer's site

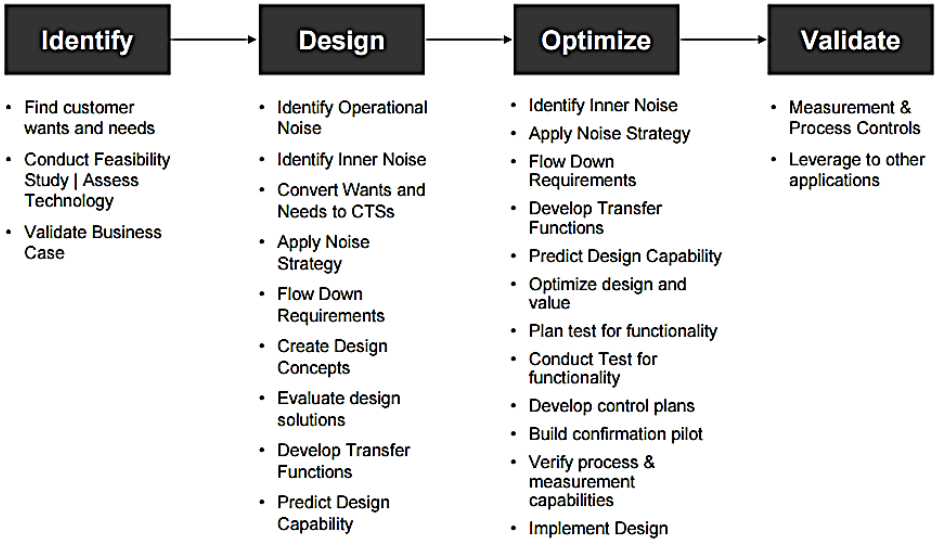

Figure 4.2-1: DFSS phases and internal actions [231].

4.2.3 Lean Product Development

Even if the Lean thinking was originated after the World War II in japan at the Toyota factories, it was reformulated during the nineties decade [232] for maximizing the value (meeting or exceeding customer requirements) while minimizing or removing the waste (cost reduction), by simplifying and continuously assessing and improving all processes and relationships in an environment of trust, respect and full employee involvement.

After being widely adopted, the Lean principles were shaped into the Lean Product Development (LPD) approach fifteen years later [233], with the aim of helping the design teams to be fast, flexible and highly effective to be able to answer the demands of today's globally competitive environment. Basically, the successful application of Lean models in product development involves improving the growth of knowledge about the product, customer and manufacturing [234], achieving a practical approach for accelerating the time–to–market focusing on efficient planning, resource management, design control, and interdisciplinary communication.

The LPD also highlights the importance of the deep knowledge and insight gathering about the product while it is being developed, and concludes that engineering decisions in product development must be based on proven knowledge and experience [235]. This asseveration should be directly translated to the Photonic sensor design flow, because due to their intrinsic complexity, design decisions that do not rely on proven scientific evidences may be prone to generate failures in later stages.

Besides interiorizing the importance of always relying on the knowledge for driving the design, the Photonic Sensor development could also benefit from LPD's proposals about team management and organizational procedures [233].

v. Develop a chief engineer system to integrate development from start to finish.

vi. Organize to balance functional expertise and cross–functional integration.

vii. Develop towering competence in all engineers.

viii. Fully integrate suppliers into the product development system.

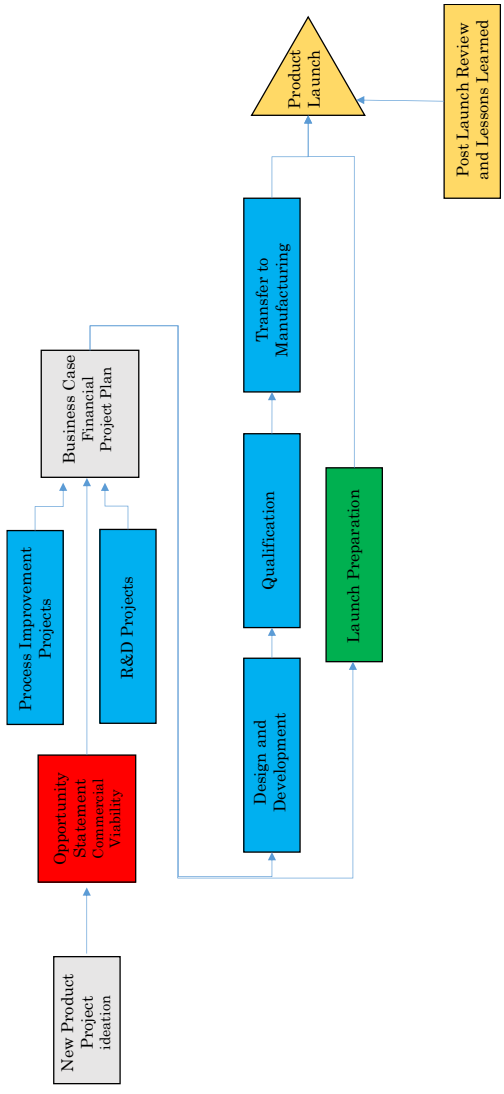

Figure 4.2-2: Lean Product Development process flow [233].

4.2.4 Lean Startup

The Lean for Startups is a particularization of the Lean process and provides a scientific approach to get the right product to the customer faster. Introduced around 2008 [236], the Lean Startup model suggests some interesting ideas based on eliminating the uncertainty, prototyping fast and validating with the customer the product concept as early as possible, rather than trying to perfecting it. Actually, the Lean Startup recommend including the potential customers in the loop from the very beginning of the product development, in order to incorporate their request in the design while it is being built. This approach should allow to reach the market with already stablished customers with the minimum investment possible.

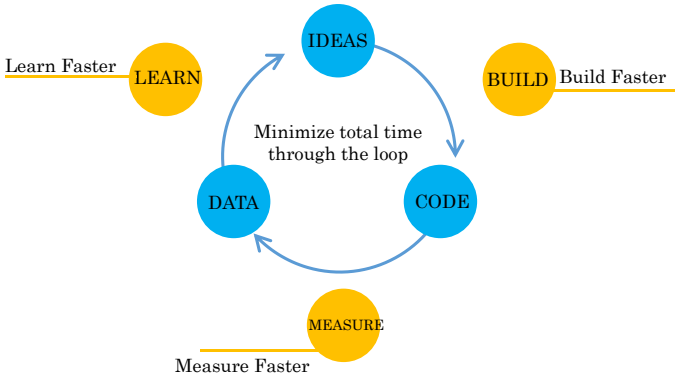

Figure 4.2-3 The Lean Startup process diagram [236].

The Lean Startup process is based on the Build–Measure–Learn feedback loop. *Build* is referred to focus the efforts on putting together the minimum pieces to have a working prototype, known as the Minimum Viable Product (see next section). The MVP is the version of the product that enables a full turn of the Build–Measure–Learn cycle with a minimum amount of effort in the minimum development time.

Measure defines the need to observe the performance of your prototypes, not only from your perspective, but also from the customers' point of view. This measurement requires a comprehensive and scientific assessment of the product and relies on the analysis of a predefined KPIs. The *Learn* word suggests the need to measure the effective progress achieved in the product development, which is the only way to progressively mitigate the uncertainty. This last part is also defined as *Validated Learning*, and suggests validating the learning by running scientific experiments that allow developers to test each element of our vision.

Even if Lean Startup method claims that is suitable for any kind of business, it addresses best the pure software and web products rather than a complex system like the Photonic Sensors. However, there are still some interesting points that could be applicable to our methodology proposal as:

ix. Shape the product specifications hand by hand with the customer.

x. Analyze thoroughly the progress of the development by scientific experiments and by the feedback of the customer.

4.2.5 Minimum Viable Product, Hardware products

As mentioned, the Lean Startup model does not consider with the appropriate importance the differences between the software and

the hardware developments, which dramatically impact on the Minimum Viable Product concept for non–software products. Regulatory compliances (e.g. CE or UL marks) are required to install or use almost any kind of hardware products. The tooling costs for being able to manufacture or even prototype the hardware MVP have a huge impact on the companies' finances. And, last but not least, even the most basic minimum viable hardware product will be bound to certain durability and reliability requirements that are not evident to meet for use cases as the industrial ones [237].

However, the MVP concept is not new to hardware designers, and it was a basic process applied by product design firms already twenty years ago or even earlier, as demonstrated by the popular Ideo's shopping cart example [238]. And even if the MVP concept has now gained attention due to its massive adoption by software and web engineers, hardware integrators need to understand the main differences between the two worlds and need to deal with them.

Getting hardware products to market is harder and costlier due to the need of building tools, managing manufacturing, acquisition of components and raw materials, shipping and distribution, stocking, etc. In this situation, it is evident that hardware products present a more probable risk of failure, because, asides the higher expenses, the expectations witch such products are normally also higher. Software is perceived and assumed to be ephemeral, and consumers are far more tolerant of imperfections, but this is not applicable to physical products, where the end users want their expectations to be met [239].

Moreover, the product type we have in hands, the Photonic Sensor, is not even a mere hardware product. The problem's complexity management, the smartness and the connectivity are to be solved by software means. Having a look at smart sensor products that combine an advanced hardware with several software applications, we realize that the development effort may fall around 60–70% in software and algorithm development [240].

Considering both, the budgetary requirements for launching the hardware series, and the importance of delivering advanced functionalities through customized software, the following statements could be assimilated for the Photonic Sensors development from the Minimum Viable Hardware Product philosophy.

xi. Plan scalable hardware and schedule different software releases for the same hardware.

xii. Plan modular hardware so that you can replace blocks with less effort.

xiii. Focus of minimum viable, but reliable, hardware products, shipping first versions with basic software functionalities.

4.2.6 Phase–Gate or Stage–Gate®

It is evident that efforts, time and budget for the development of photonic sensors, including not only hardware and software, but also optoelectronics, micromechanics, chemistry, etc. increases as the complexity of the system does. Therefore, providing means to control the progress of the development becomes crucial for the success of the product, or just for stopping the projects early to minimize the losses.

The sensor systems covered in this thesis could be considered as the result of research intensive activities, and normally address critical use cases, with important technical and regulatory specifications. In this challenging scenario, the probabilities of not meeting certain requirements are high. Consequently, the methodology suggested for assisting the integration of photonic sensors should cover the continuous technical, economical, regulatory and market assessment of the development, monitoring the progress and identifying risks.

This challenging scenario is well suited for the Phase–Gate, or Stage–Gate® methodologies, which suggest an operational roadmap for conceiving, developing and launching new products improving effectiveness and efficiency. Devised during the mid–1980s and implemented around 1995 [228], the core idea of these methods is a staging and gating process, where *Stages* represent the development of the project, executed by multidisciplinary teams, and the *Gates* symbolize intermediate assessment points. At each Gate the continuation of the project is decided based on the information generated within the previous Stages, including not only the technological progress but also the business case, risk analysis, and availability of necessary resources.

The structure of each stage is quite the similar, formed by the specific Activities to be carried out by the project leader and the team, a *Comprehensive Analysis* of the results and the preparation of the Deliverables which integrate the conclusions of the analysis and which are submitted to the Gate. There are 6 basic stages:

Table 4.2-3: Description of the Stages included in the traditional Stage–Gate development process.

Stage	Activities
0. Discovery	The phase covering the activities planned to discover opportunities and to generate new product ideas.

1. Scoping	During this step, the main goal is to launch an inexpensive assessment of the technical strengths, weaknesses, market prospects and status of the competence regarding the new product idea.
2. Build Business Case	This phase deals with the comprehensive analysis of the technical, marketing and business feasibility of the product and it is a difficult, complex and resource intensive task. There are four main components to be defined within this phase: product and project definition; project justification; project plan and feasibility review.
3. Development	Plans defined at early stages are translated into concrete deliverables. The actual design and development of the new product happens at this phase, as well as the scheduling of manufacturing and operations, and the test plans for the next stage are defined. The ultimate deliverable of this stage is the prototype, which will go through extensive testing and validation in the next stage of the process.
4. Testing and Validation	The objective of this stage is to validate the entire project, covering the product itself, the production and manufacturing process, customer acceptance, and the economics of the project. The tests include near testing, field testing and market testing
5. Launch	The product launch is the conclusion of the product having passed all previous gate. This phase covers the full commercialization of the product – the beginning of full production, selection of distributors and commercial launch.

As mentioned, prior to each Stage, we found a decision point, Gates, where the continuity of the project is decided based on the information generated so far. At each Gate, the next steps of the project are decided and resources are allocated based on three quality parameters: quality of execution, business rationale and quality of the action plan.

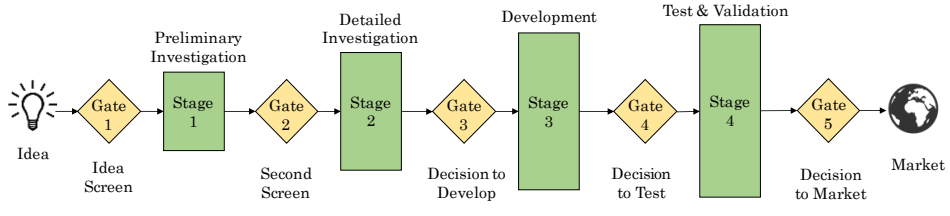

Figure 4.2-4: The generic Stage–Gate Process.

As it happens with the Stages, the Gates are structured in three components: *Deliverables*, which are the inputs to the Gate and collect all the information generated within the previous stages. The *Criteria* by which the project is validated, including normally technical, financial and qualitative parameters. And finally, the *Outputs* of each gate, which include a decision (go, kill, hold, recycle) and a path forward (approved project plan, date and deliverables for the next gate agreed upon).

The benefits from this paced process are evident and, since its launch, Stage–Gate has been present in more than 80% of the companies in the United States [241]. This method has also been reported as an ideal candidate for assisting the development of medical devices [242], covering from their embryonic research phases, clinical trials, clearance from regulatory bodies until the commercial launch. This is an interesting scenario, because medical devices is a really challenging development field, dealing with research intensive products, heterogeneous and multi–domain technologies, strict regulations and testing, and requiring huge investment that need to be carefully justified and allocated.

Additionally, as it can be seen in Figure 4.2-5, Stage–Gate has been merged with other traditional new product development processes as the DFSS.

There are also some references of application of Stage Gate modifications in the field of MEMS devices [243], which is also a challenging application field, intrinsically heterogeneous, highly dependable on functional prototypes for concept validations and with important investment requirements even at early stages.

As described in the next section, the traditional Stage Gate process is evolving to better accommodate iterative projects. However, some interesting contributions can be extracted even from its original principles, as:

xiv. Control the process development through a structured process, with clear check–points, helping to introduce discipline into an ordinarily chaotic process

xv. Create multi–domain working groups to cover both, the development and the assessment of the project

xvi. Focus on three different testing scenarios: near, field and market testing.

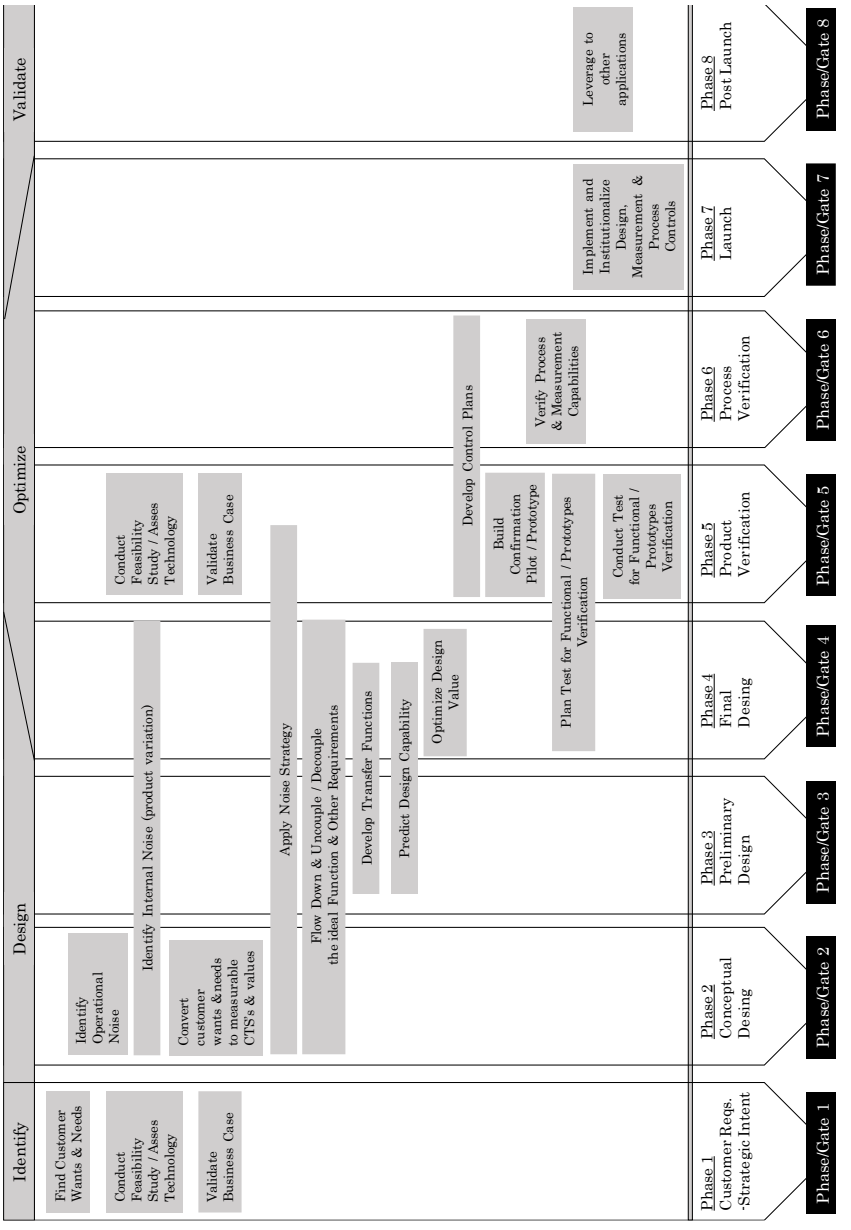

Figure 4.2-5: Design for Six Sigma phases mapped into a phase–gate development process [231].

4.2.7 New Development models: Hybrid Approaches

The traditional vision of the Stage–Gate process is clearly lineal or sequential, and may lack from the flexibility needed to accommodate to fast changing scenarios [244]. This weakness has led to the generation of different hybrid models lately, as the Agile Stage–Gate [245] [246] [247], Open Innovation and Stage–Gate [248], or the Triple A System (Adaptive, Agile, Accelerated) [220].

These evolutions are always looking for a better management of product development under evolving requirements, uncertain environments and unforeseeable risk management, which are the common denominator in ambitious novel projects [249] as the ones represented by the Smart Photonics Sensors, and described in Table 4.2-1. Basically, all the new features added to sequential processes like the Stage–Gate try to incorporate the iteration or looping approaches within the general project phases, as depicted in Figure 4.2-6, assuming that the information at the beginning of each phase is not solid.

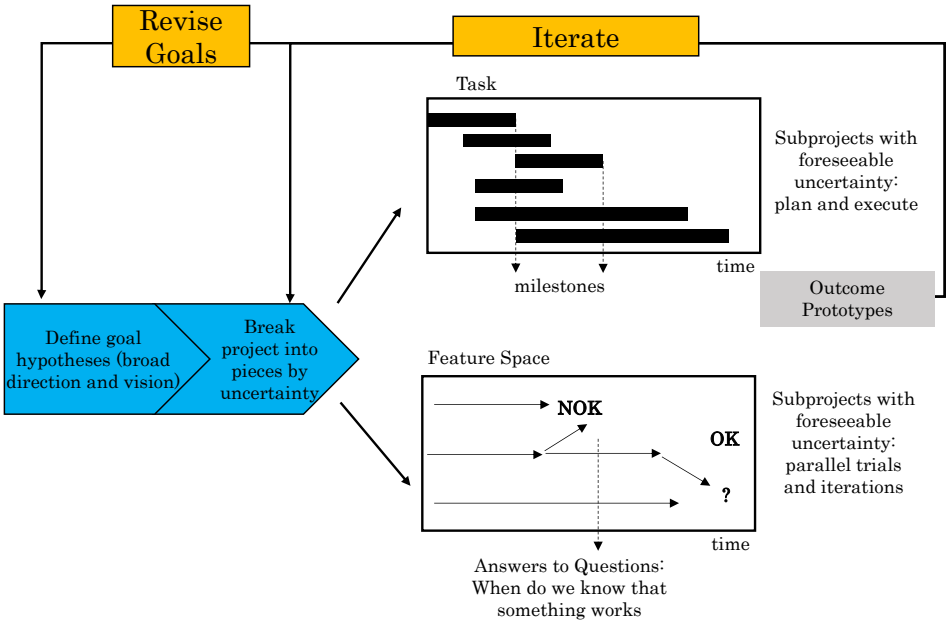

Figure 4.2-6: Template of flexible process to complement the Stage approach [244].

Agile development methods were elaborated by the software industry and described for the first time in the 2001 book, *Manifesto for Agile Software Development*. Basically, this approach splits the development into small incremental pieces, so–called 'sprints', requiring minimum planning, with clear goals, short delivery times (2–3 weeks) and focused on creating working version of the product, which will be used to demonstrate a certain functionality to stakeholders (management, customers, end users, investors, etc.). Therefore, this methodology suggests micro–planning management approach, with incremental and iterative design, where requirements and solutions evolve through cooperation between cross–functional and self–organizing teams.

While this approach has proved to be very suitable for software environments, as mentioned in section 4.2.5, physical products represent a much more complex challenge, and it may not be feasible

to manufacture a working version of the product in a few weeks. However, when applied to physical or hardware products, the goal of an Agile–based approach, the objective is similar: deliver something that is tangible and can be evaluated and tested with stakeholders.

xvii. Parallelize as much as possible the different proof–of–concepts required to validate technologies, mitigate risk, verify integrations, etc. considering each of work lines as an isolated sprint.

Understanding the differences between Agile and Stage–Gate models, displayed in Table 4.2-4 helps to assimilate the diverse approaches that have been proposed for their merge.

The first approach is to consider Agile as a useful micro–planning or project management method that can be used within Stage–Gate to accelerate some of its stages. The next evolution of the integration of Agile within Stage–Gate is the Spiral concept. This evolution was suggested to bridge the gap between the Agile principles and the requirements from physical product developers facing a dynamic and fluid market with changing product specifications. The spiral development devises a series of *build–test–feedback–revise* iterations with each iteration delivering an increasingly more complete version of the product.

When applying the Spiral approach to the development of physical products, unlike it happens with the software ones, each iteration does not deliver a working product, but a product version that the end user can respond to or give his feedback. These product versions can be virtual prototypes, crude models, working models, rapid prototypes, or early prototypes, i.e. usually something physical that the customer can respond to

Table 4.2-4: Key differences between Stage–Gate and Agile models, from [246]

Characteristic	Stage–Gate	Agile
Type of model	Macro–planning	Micro–planning, project management
Scope	Idea–to–Launch, end–to–end	Development & Testing stages only
Organizational breadth	Cross–functional: Development, Marketing, Sales, Operations	Technical (software code writers, engineers, IT people)
End point	A launched new product in the market	Developed and tested working software product

Decision model	Investment model: Go/Kill Involves a senior management group	Principally tactical: the actions needed for the next sprint

The next evolution of Stage–Gate under the influence of Agile is the Triple A System, which apart from the Agility, it empowers the Adaptive and Accelerated development. The Triple A system basically suggests to incorporate the *Agility* by the previously mentioned spiral's *build–test–feedback–revise* loop or iteration within each phase of the generic Stage–Gate approach. Additionally, the development needs to be *Adaptive*, to accommodate to new scenarios, because, especially for more innovative products, end users are not able to specify what they want or need until they see it.

However, continual adaptation without any forward progress accomplishes little to the project development [227]. Therefore, not only adaptability, but also means for fast progressing are required, and, we need to offer versions of the product very fast to enable the validations of the product concept by the end users early, cheaply and often. Consequently, an Accelerated development flow is expected.

The Triple A System also suggests to increase the development emphasis on the clarifying the key unknowns, risks and uncertainties of the project. The objective should be to identify them as early as possible and determine whether new technology or development might be required. Keeping the focus on specifying the uncertainty, many problems later in the project can be prevented and much time and money saved.

But the Triple A proposal it is clear on this specific point, for achieving a truly accelerated design, the resources should be properly accommodated and supported by a dedicated cross–functional team for maximum speed to market. According to the Tripe A System, to achieve this commitment, the integration of the Stage–Gate approach with the company's portfolio management and resource management is required. This technical and management integration should guarantee that the number of projects under development and the resources available are equilibrated so that project team members are not stretched too thin and a true Acceleration, Adaptation and Agility is achieved.

Even if several suggestions claimed by the Agile and Stage–Gate merged view are also present in the Lean Startup proposal, some interesting approaches have been also identified in these methods, as:

xviii. Integrate technical, economic and human resource management to enable a true accelerated project development.

xix. Prototype fast (generate something tangible) to enable the end user giving feedback about the project concept, contributing to its specification.

xx. Focus on the unknown, uncertain and risky parts of the project, to clarify them as early as possible with the aim of minimizing project development time and cost.

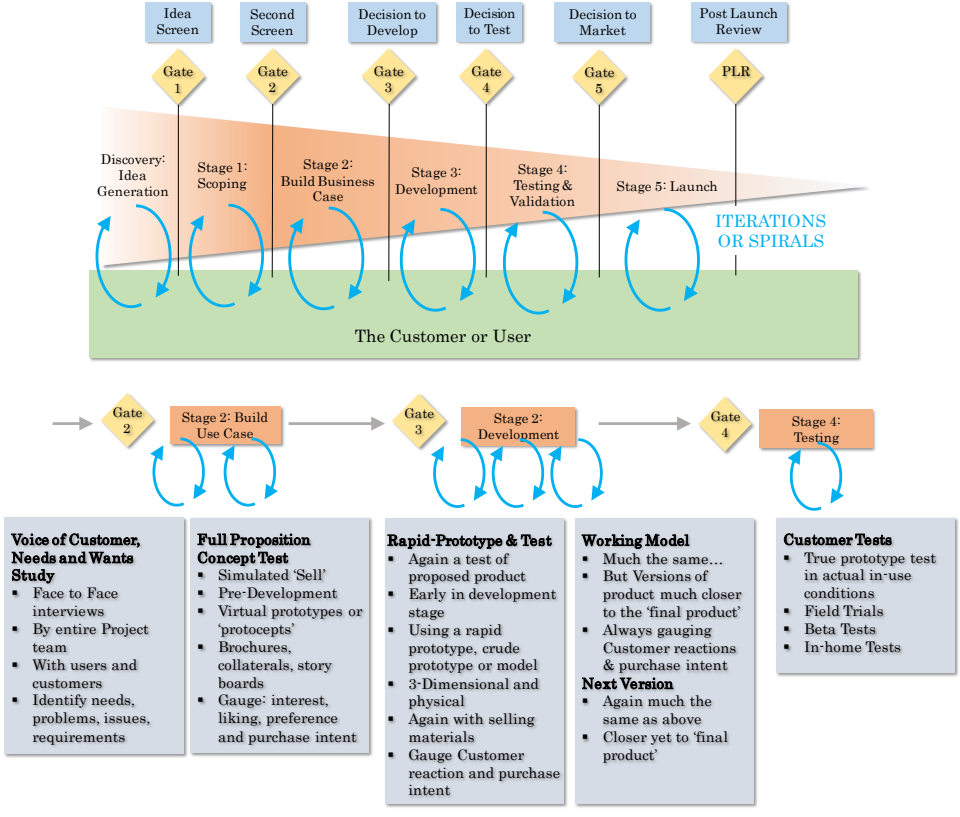

Figure 4.2-7: The Spiral development within the Stage–Gate process, from [220].

Continuing with the Stage–Gate evolutions, the Open Innovation Stage–Gate is found. Open Innovation is a concept pioneered around 2003 [250] with the aim of moving forward from the classic Closed Innovation scenario, where the companies rely solely on internal resources for envisaging new ideas, for developing them and for selling the final outcomes. The Open Innovation claims that projects may be generated inside or outside the boundaries of the companies, while their development and commercialization could, eventually, accommodate or be transferred to third parties. This new model is really suitable for helping companies to expand to new markets, to assimilate new technologies or to make profit from developments out of the companies' core businesses.

When merged with the Stage–Gate process, different activities are fitted into the Stages, and some new Criterions are considered at Gates. The philosophy change gets more evident at the first pre–Development stages (scoping and business model), including actions that involve potential partners or outsourced suppliers who may provide technical, marketing or manufacturing competences to develop and commercialize the product. Additionally, the Criteria at the Gates should deal with a completely new perspective like the lack of knowledge within the development team, or the unalignment with business of the company.

The new set of actions suggested by the Open Innovation Stage–Gate approach suits perfectly to the case of Photonics–enable Sensors. The multi–domain nature of these systems evidently could be benefited from the inclusion of external experts to support the development. This is clearly the case for the photonic component providers, whose insights are always an important asset for the sensor product design. Therefore, the Open Innovation version of the Stage–Gate could contribute to the specific case of this thesis with the following suggestions:

xxi. Identify the missing internal capabilities and seek potential partners or outsourced suppliers early in the projects.

xxii. Develop an IP strategy for the project to help handling the IP and legal issues with external firms.

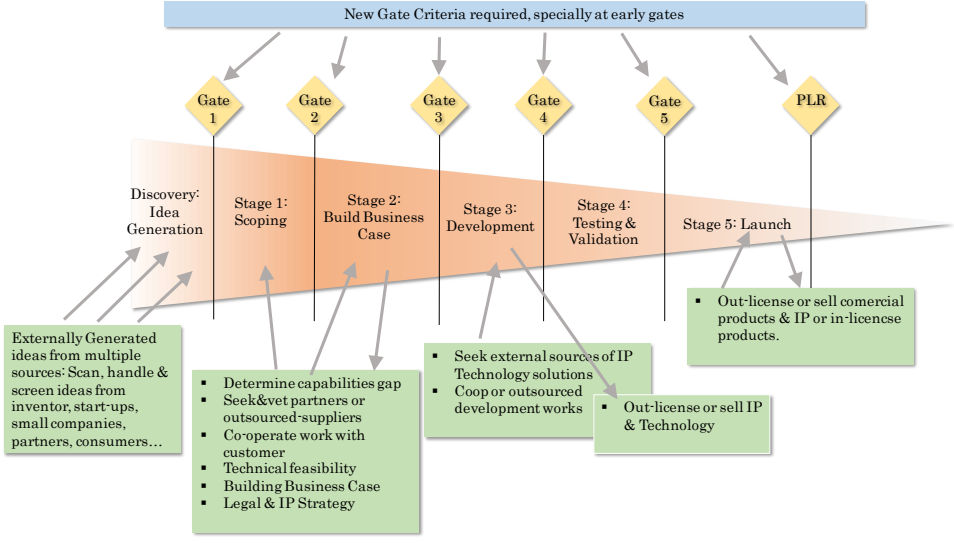

Figure 4.2-8: Open Innovation Stage–Gate, External interfaces (in–bound and out–bound) at multiple points in the process, from [250].

4.2.8 Summary of Key Contributions from Baseline Models

The review of the state of the art of the different models for the development of new products done in the sections so far, has served as starting point for our custom methodology elaboration. Different contributions have been identified while assessing the structure and approach of the baseline processes, which have been summarized in Table 4.2-5. These contributions have been fed into the different stages of the proposed methodology for photonics–enabled sensor engineering.

Table 4.2-5: Summary of identified contributions from the different new product development processes.

	Contribution	Baseline model
i.	Only if you focus on measuring the defects of a process, you will be able to figure out how to solve them,	DFSS
ii.	Use objective metrics or key performance indicators (KPI) to measure processes	
iii.	Track changes occurring at these KPIs for early problem identification	
iv.	Keep the customer in the loop for detecting problems and deviations occurring at customer's site	
v.	Develop a chief engineer system to integrate development from start to finish.	Lean Product Development
vi.	Organize to balance functional expertise and cross–functional integration.	
vii.	Develop towering competence in all engineers.	
viii.	Fully integrate suppliers into the product development system.	
ix.	Shape the product specifications hand by hand with the customer.	Lean Startup
x.	Analyze thoroughly the progress of the development by scientific experiments and by the feedback of the customer.	
xi.	Plan scalable hardware and schedule different software releases for the same hardware.	MVP Hardware
xii.	Plan modular hardware so that you can replace	

	blocks with less effort.	
xiii.	Focus of minimum viable, but reliable, hardware products, shipping first versions with basic software functionalities.	
xiv.	Control the process development through a structured process, with clear check–points, helping to introduce discipline into an ordinarily chaotic process	
xv.	Create multi–domain working groups to cover both, the development and the assessment of the project	Stage-Gate
xvi.	Focus on three different testing scenarios: near, field and market testing.	
xvii.	Parallelize as much as possible the different proof–of–concepts required to validate technologies, mitigate risk, verify integrations, etc. considering each of work lines as an isolated sprint.	Agile Stage Gate
xviii.	Integrate technical, economic and human resource management to enable a true accelerated project development.	
xix.	Prototype fast (generate something tangible) to enable the end user giving feedback about the project concept, contributing to its specification.	Tripe A Stage Gate
xx.	Focus on the unknown, uncertain and risky parts of the project, to clarify them as early as possible with the aim of minimizing project development time and cost.	
xxi.	Identify the missing internal capabilities and seek potential partners or outsourced suppliers early in the projects.	Open Innovation Stage Gate
xxii.	Develop an IP strategy for the project to help handling the IP and legal issues with external firms.	

4.3 Methodology proposal

This chapter introduces a comprehensive methodology for Photonics–enabled in–line fluid sensor engineering. The following sections give an overview of the method, and then dives deep down into the details of the individual methodology blocks. For each of the

Stages and Gates, a detailed description of their objectives, restrictions, inputs and outputs and criteria is given. The description of the different Stages is complemented with specific examples as well. Additionally a design flow chart that leads through the development of the project is provided.

4.3.1 Audience for the Methodology

This methodology is intended to answer the concerns and curiosities of Research and Development Teams, Design houses or Engineering teams that typically have to face the development and integration of products for end customers, being those either within the same company or outside. Therefore, even if innovative ideas may come up from the aforementioned teams, these are not normally the main promoters of the innovations neither they are the ones with the better insights on the final application.

However, these teams need to be imaginative, flexible and fast to adapt to the new development scenario and maximize the expertise and knowledge gained in previous experiences to generate a development team that answers and anticipates to the customers' needs.

The intention of the methodology is to help these design teams understanding the intrinsic complexity of the photonics-enabled sensors, providing a structured approach developed for uncertainty reduction, guiding on multi-domain and heterogeneous integration and to maximize the incremental outcomes towards the product development.

Indeed, customers promoting and requesting this kind of products would also benefit from this methodology because this approach should help them understanding the technological complexity of the product, allowing them to specify it better and plan de development in a more accurate way.

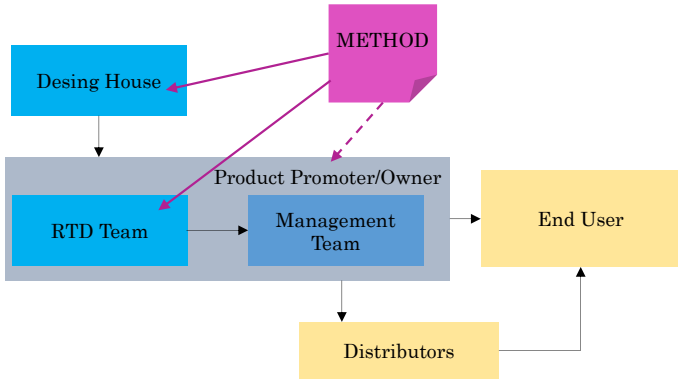

Figure 4.3-1: Schematic showing potential stake holders in a product structure and the main audience at which the methodology is aiming.

4.3.2 Overview

The assessment of the baseline methods reviewed in previous sections revealed that a combination of principles, suggestions and visions taken from the different models (see Table 4.2-5) represents a promising approach for New Product Development in the context of Photonics–enabled Smart Sensors for fluidics.

Additionally, we found that the backbone of the traditional **Stage–Gate process, enhanced with Agile and Open Innovation** concepts, could serve as an ideal framework for controlling the development process, from the management of the early stages to the materialization of the final product.

Sections 4.1 and 4.2.1 have already introduced the main objectives and challenges set out by the photonic sensor integration, and most of them deal with the **management of heterogeneous technologies** by a **multi-domain team** and with the **lack of awareness about specifications and risks** of the project. Therefore, these two conditions have been considered as the main drivers for the model elaboration, and all the focus and efforts of the different stages, iterations and gates are devoted to solve the heterogeneous integration in an efficient and reliable manner and to clarify the uncertainty (specifications and risks) as early as possible.

Another important asset in the suggested development model is the continuous **presence of the end–user or customer in the development loop**. Their insights and feedback is a key factor for the success of the idea generation, proof-of-concept validation, prototype testing, product shaping and product launch. This is because, the customers and end–users are the ones who really look after strengthening the competitive advantage and added value of the sensor under development.

The methodological approach proposed here is tailored for **projects that must integrate photonic component provided by third parties or outsourced into autonomous sensor products**. Therefore, the management of this supply chain, and the characterization and wise selection of these components is also addressed by the methodology.

The development **process has been divided into five different stages** with its corresponding gates where efforts and resource requirement increase with each subsequent stage. The stages are (i) Opportunity identification, (ii) Proof of concept validation, (iii) Prototypes and Test Bench design, (iv) Validation in real field, (v) Industrialization and commercialization (see Figure 4.3-2), and will be described in deep in the next sections. Notice that, from now on, the methodology will be called Photonic Sensor Development (PSD) process.

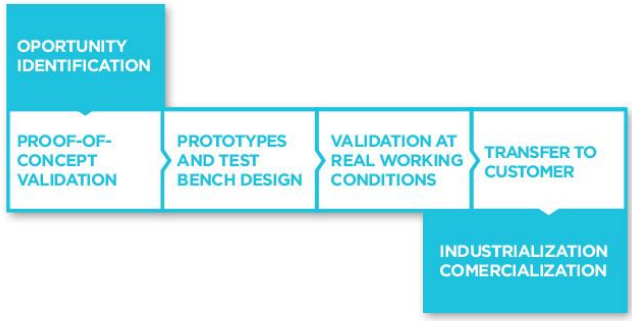

Figure 4.3-2: Basic structure of the Photonic Sensor Development (PSD) process.

4.4 Opportunity Identification

The first step towards a new product is to envisage an idea, vision, or concept that looks promising for a certain application or to identify a clear need to be covered. The first situation is known as technology push and the second is clearly a market pull scenario. Both innovation strategies are valid for generating the seed of a new product, because the first one looks for promoting or expanding a promising technology and the second one set outs a market need that may become an opportunity for technological developments. Even if both approaches may drive a new product conceptualization, the strategy to follow on each case should not be the same [251].

Some examples of market-pull product requests may be found in: (i) the enforcement of new regulations that require to measure or control a new parameter of the fluid (e.g. detection of allergens proteins in beverage production). (ii) The application of preventive maintenance programs, which requires to check the status of a certain fluid in real time to detect failures early and prevent them (e.g. monitoring wear debris on hydraulic fluids). (iii) The execution of cost cutting strategies that look for replacing certain fluid only when it is strictly needed to reduce the cost in consumables (fluid liters) and in human resources devoted to change the fluids (e.g. replacement of lubricant oils in automotive robots).

On the other hand, new developments driven by technological innovation are quite common in the photonics field. We should notice that photonic analysis techniques are very transversal to any application, and several use cases may benefit from the outcomes achieved in similar, but different, use cases. Imagine the possibilities of the spectroscopy analysis of a fluid; the capabilities of analyzing the presence of certain molecules by the measurement of the absorption bands happening in a fluid could be applied to recognize the

degradation of a lubricant (e.g. presence of oxidation molecules) or to quantify the fat proportion (e.g. presence of fatty acid molecules) on dairy products.

In this scenario, the purpose of the Opportunity Capturing Stage does not strictly deal with the process of new idea generation but with the evaluation of its feasibility. The Opportunity Identification is done almost exclusively by the customer company, however, for some preliminary investigations done within the stage, potential development partners might be included for consulting. Therefore, the focus of the proposed methodology with this regard is to perform a wise assessment of the opportunities identified.

The Opportunity Screening Gate is the place where the newly identified product ideas are assessed from technological and market views.

4.4.1 Opportunity Capturing Stage

Normally, we enter this stage with a rough formulation about the problem to solve made by the customer or end-user, with parameters of interest somehow defined and the process where to install the in-line monitoring system more or less identified. This situation represents an opportunity for the photonic sensor developer, who rapidly should identify the potential measurement principles that could address the problem or challenge outlined by the customer.

As mentioned earlier, the opportunities may come from different origins, but the first step is to identify if their nature is either technology push or a market pull. The reason behind this need for classification is because the origin of the idea will determine how the relationship with the end users and the specifications of requirements develop in later stages.

Additionally, the nature of the idea will modulate the efforts to be put on this early stage. Opportunities originated by market requests may require smaller efforts on the business model definition and the market assessment of the idea, but will entail a deeper technological review. On the other hand, technological ideas looking to be accommodated to an end user's need will have to focus on the economical feasibilities and implications of the new use case scenarios.

Once the basic idea has been defined, the objective of the Opportunity assessment stage is to briefly define technical, economical, intellectual property and business advantages that will help evaluating in more detail the suitability of the idea.

Usually, this Stage should not occupy more than one month, and the objective is to deliver the conclusions as soon as possible because a preliminary overview is requested rather than a deep

analysis. So far, the assessment work group should be composed of the headcount listed in the Table 4.4-1.

Table 4.4-1: Roles and equipment required and their expected activities for the Opportunity Identification Stage.

Headcount	
Role	**Activities expected**
Project Leader/ Senior Engineer	Deal with integration approach, IP and patent search, general feasibility, general plans, may require assistance from Legal and Financial depts.
Optoelectronic Engineer	Assessment of the proposed photonic method
Mechanical Engineer	Assessment of the proposed size, installation and environmental conditions
Chemical Engineer / Physicist	Assessment of the requested measurement performance, measurands
IP and Patent Advisor	Assessment of any potential IP or patent issue
Market and Financial Advisor	Assist the project leader on the economic plan
Equipment	
Item	**Use expected**
Bench-top Laboratory analyzers	Fast feasibility assessment

The specific deliverable outputs generated during this stage are described below, but it should be noticed that these documents will contain only basic and preliminary information that needs to be further elaborated in later stages. Notice that this is the only stage in the whole process where no physical deliverable is expected, since all these outputs deal with a generic feasibility assessment of the idea, each of them focusing on different aspects to be considered so far.

Table 4.4-2: Deliverables generated during the Opportunity Identification Stage and the involved team members.

id	Name	Participants
1.1	Technical Feasibility Report	Project Leader & Technical members
1.2	Capability Assessment Report	Project Leader
1.3	IP, Regulation and Legal Assessment Report	Project Leader & Technical members IP and Legal Advisor
1.4	Business and Economic Assessment Report	Project Leader Market and Financial Advisor

The first deliverable is the Technical Feasibility Report, which is coordinated by the Project Leader, but gathers the insights of the whole technical team. This document gives an overview about the measurement principle, the different implementation technologies and their interfaces, an estimation regarding the development plan, costs and times, an estimation about the expected unitary and volume prices of the product and the potential risks foreseen.

For the technical assessment of the measurement principle a bibliographic review and the internal technical expertise and resources are used. At this stage, the use of certain bench–top laboratory equipment (e.g. spectrometers, colorimeters, microscopes, rheometers) might be required. These laboratory analyzers could be useful for performing a rapid evaluation of the chemo–physical properties over some representative fluid samples provided by the end-user or for cross verifying some bibliographic findings.

At this stage already, the heterogeneous building blocks of the envisaged solutions should be, at least, identified. This enables not only a better estimation of resources and planning of the project, but also finding missing capabilities within the partners involved, which is critical for the next deliverables.

Another additional output of this stage is the Capability Assessment Report, which contains information concerning the foreseen capabilities and equipment required for project execution. Besides, the critical photonic components are listed and the associated key suppliers identified. Moreover, if any missing capability is found, a list of potential partners or outsourcers is provided. If required, this list is used in the following Gate by the stakeholders to decide which potential partners to approach for a joined engineering undertaking. An outline and example of this deliverable is given in Table 4.4-3.

.

Table 4.4-3: Example of information to be provided in the Deliverable 1.2 Capability Assessment Report

Equipment	
Item	**Activities expected**
Hydraulic Test Bench up to 15 bars	
UV/VIS/NIR Optic Test Bench	Preliminary feasibility test
Climatic Chamber	
Vibration and Shock generator	
Missing Equipment	
Item	**Potential Provider**
Hydraulic Test Bench up to 100 bars	Laboratory A
Fast prototyping of Plastic and Metallic pieces	Workshop A

Capabilities	
Role	**Activities expected**
Hardware Engineer	HW prototypes
Software Engineer	SW prototypes
Mechanical Engineer	Fluidics and Mechanics Simulations
Mechanical Designer	Micromechanical System design. Enclosure design
Optical Engineer	Optical design and simulations
UL and CE Advisor	Assessment of the envisaged regulatory requirements and their impact on design
Missing Capabilities	
Item	**Potential Provider**
Chemometrics Expert	University A, Company B
FDA Certification Expert	Company C
Core Photonic Component	
Item	**Potential Provider**
NIR micro–spectrometer 1600-2200nm	Company D, Company E

The next deliverable at this stage is the IP, Regulation and Legal Assessment Report, responsibility of the Project Leader and the IP and legal advisor and its content is outlined in Table 4.4-4. This document includes the declaration of the background knowledge for all the parties, and the list of the envisaged foreground technology generated during the project [252].

The background knowledge represents the pieces of technology that might be used during the project execution, but were developed previously and belong to the party's IP portfolio. The general conditions (e.g. license to use, deployment conditions, and royalties) for using these technological blocks should also be addressed here. On the contrary, the foreground knowledge is the innovation generated as the result of the project execution, and its ownership should be agreed among the partners, as well as its protection strategy (new patent submission, trade secret, etc.).

Of course, the information included in this very first version of the document is only an intention declaration, and should not be consider as legally binding. The specific term of each item will be later discussed and agreed among the partners, but having at least identified all the hot topics lubricates the forthcoming negotiations.

This deliverable should also include the conclusions of a preliminary patent review report, which has been accomplished with a twofold aim: early identifying any blocking or competing patent and

understanding the potential patentability of the foreground technology.

Last but not least, this report should gather the conclusions drawn by all the parties concerning the applicable regulations and potential compliance requirements, including the framework set up for monitoring the progress in terms of regulations along the next stages. Besides, this document needs to raise the awareness of the regulatory and compliance implications, especially concerning delivery time and cost of the development.

Table 4.4-4: Summary of the items and the expected information to collect in the 1.3 IP, Regulation and Legal Assessment Report deliverable.

Item
Background declaration
Foreground estimation
Patent review
Regulations and compliance requirements

The activities within this stage conclude with the Business and Economic Assessment Report. Notice that, as mentioned earlier in this chapter, the proposed methodology is not focusing on how to develop a comprehensive business and market review of the product; this is supposed to be the responsibility of the customer, and the information contained in this last deliverable must be generated with their close collaboration. The customer is supposed to have accomplished at least a preliminary scoping of the market existence, market size, potential sales, expected maximum investment, market opportunity window, competitors, and product placement. Based on this assessment, the information outlined below, and summarized in Table 4.4-5, should be included in this document.

The expected production volume and the approximated unit cost are significant information that may drive several technical decisions and may even jeopardize the whole feasibility of the project, either because the unit cost is not achievable, or because the project, or the non–recurring engineering (NRE) cost is not paid back by the margin profit of each unit at the expected commercialization volume.

Additionally, the market opportunity window will be used as baseline for the project planning and timeline, basically analyzing the feasibility and uncertainty of having the product ready by the time requested by the customer. The document is concluded with a very rough estimate of potential project cost, including personnel cost, consumable cost and equipment cost or amortization.

Table 4.4-5: Information contained in deliverable 1.4 Business and Economic Assessment Report.

Information	Responsibility of
Market existence, market size, potential sales, expected maximum investment, market opportunity window, competitors, and product placement	Customer
Production Volume and Target Unit Cost	Customer
Project Planning and Timeline	Project Leader
Project Cost (Personnel, Consumables, Equipment)	Project Leader & Economic Advisor

4.4.2 Opportunity Screen Gate

The main activity to accomplish at this first Gate is authorize or not the initialization of the project. This resolution is based on a thorough assessment performed by a decision group formed by customer representatives and the project leader. The particular decisions to be taken deal with the evaluation and acceptance of the individual deliverables generated during the Opportunity Capturing Stage (see Table 4.4-6). In addition to the continuation acceptance, a plan for the next stage is also provided, including the required resource allocation based on the estimations provided in the deliverable 1.4.

Table 4.4-6: Detailed inputs, decisions and outputs at 4.5.2 Opportunity Screen Gate.

Input	Decisions	Outputs
Technical Feasibility Report	Project risks and uncertainties acceptable	Approved initialization Proof-of-concept stage plan
Capability Assessment Report	Partner and provider list acceptable	Potential partners list
IP, Regulation and Legal Assessment Report	IP and regulatory perspective acceptable	Authorization to proceed
Business and Economic Assessment Report	Unit cost, project cost and project timeline acceptable	

4.5 Proof–of–Concept Validation

The objective of this second stage is to consolidate the estimations made on the previous one, confirming the measurement principle hypothesis, clarifying the integration needs, better understanding the project and technological risks and providing a more accurate vision on project's economics and schedule. Additionally, during this stage a first version of system requirements are expected.

During this stage, certain scientific or technological work is expected, but the level of detail and the intensity of these developments depend on the budget availability agreed at the Opportunity Screen Gate. The outcomes of this research will be decisive for the conclusions to be taken at the Prototype Development Decision Gate.

4.5.1 Proof–of–Concept Stage

The main objective during this Proof-of-Concept Stage is to confirm the feasibility of the envisaged sensor, and this is started primarily from the technical assessment of the devised measurement principles. In the previous stage, the customer's problem-to-solve has been somehow defined and the potential technical approaches have been identified based on internal expertise, literature review and some eventual laboratory measurements. At this point, these solution proposals will be further elaborated and verified against a first set of requirements already identified by the customer (see Table 4.5-3 for examples of requirement definition at this stage), with the aim of concluding if they are suitable for the use case, identifying their constraints and risk, and finally proposing a potential system architecture.

Normally, this stage should not cover more than one or two months, and the technical staff are the main active members. The roles, activities and required equipment and outsourcing for this stage is outlined in Table 4.5-1.

Table 4.5-1: Roles, equipment and outsourcing required and their expected activities for the Proof-of-Concept Stage.

Role	Headcount Activities expected
Project Leader/ Senior Engineer	Risk identification, identify the heterogeneous interfaces, provide the integrated view and assure the integrability of the proposed methods into an in-line sensor.

Optoelectronic Engineer	Define suitable optical and optoelectronic components. Define working settings.
Mechanical Engineer	Assess the feasibility mechanic, hydraulic, fluidic and environmental requirements. Validate the manufacturability of optoelectronic settings
Chemical Engineer / Physicist	Validate the chemo–physical measurement principles

Equipment	
Item	**Use expected**
Bench-top Laboratory analyzers (spectrometers, colorimeters, microscopes)	Validate the chemo–physical measurement principle
Sample optoelectronic equipment (emitter and detector evaluation systems)	Validate the integrability of the chemo–physical measurement principle into a sensor system
Climatic Chamber, Vibration test bed, etc.	Emulate different working conditions to validate the chemo–physical measurement principle under the required operation environment

Outsourcing	
Item	**Use expected**
Plastic/Metallic Fast Prototyping	Fabricate mechanical parts for the integration validation

The specific deliverables belonging to this stage (see Table 4.5-2) are generated during different sub–stage activities, which cover a theoretical approach to the problem, a laboratory validation of the theoretical hypothesis and a first assessment of the integrability of the method.

Table 4.5-2: Deliverables generated during the Proof-of-Concept Stage and the involved team members.

id	Name	Participants
2.1	Theoretical Description Report	Technical members
2.2	Laboratory Result Report	Technical members

2.3	Photonic Integration Report	Project Leader & Technical members
2.4	System Specification and Project Plan	Project Leader

4.5.1.1 Theoretical Approach

The vast majority of the applications of the fluid monitoring sensors are based on the measurement of a certain chemo-physical parameter. In the first stage, some photonic working mode have already been identified as potential candidates for extracting this relevant information from a fluid sample. In this sub-stage, the theoretical approach to the problem should be accomplished, which merges the theoretical principles with the very preliminary set of requirements already brought by the customer (see Table 4.5-3 for examples of this kind of requirements).

Table 4.5-3: examples of raw requirements brought by customer at this stage

Examples of Raw Requirements
Parameter to measure
Sensibility
Throughput
Size
Working conditions
Cost
Number of units required
Idea of potential regulations that may apply

This work is based on the application of the Photonic principles explained in the Chapter 2, to the specific use case under development. Thus, concepts like light transmission, reflection angles, absorption bands, focal points, etc. are particularized for the analysis of the parameters of interest of the target fluid. References to bibliographic sources as well as internal calculations are expected in this phase.

This theoretical study is fully dependent on the target application, and the experience of the chemo-physical and optoelectronics technicians is fundamental here for defining the right formulation of the problem. In the Table 4.5-4, we display some examples of possible outputs generated at this stage.

Table 4.5-4: Examples of parameters defined during the Proof-of-concept stage when analyzing a generic photonic system.

Example Parameters defined at Proof-of-Concept	Sub-stage
Absorption lines of compounds	Theoretical Approach
Working Spectral Range	
Sample Volume to analyze	
Expected Absorbance of typical sample	
Order of magnitude of the light source	
Order of magnitude of the detector sensibility	
Numerical Apertures of source and detector	
Optical Focal Lengths	
Optical Path Length	Lab. Validation
Optical Spot Size	
Field of View	
Deep of Field	
Integration time of detector	Integrated Validation
Intensity of emitters	

For instance, applications interested in either the identification of the material (qualitative analysis) or how much of a particular compound is present (quantitative analysis), require first to identify the functional groups of the target compound, map their absorption on the spectral region, and identify any other compound present in the sample that overlaps the absorption lines of interest (see Figure 4.5-1). This allows specifying the spectral working range for emitters and detectors.

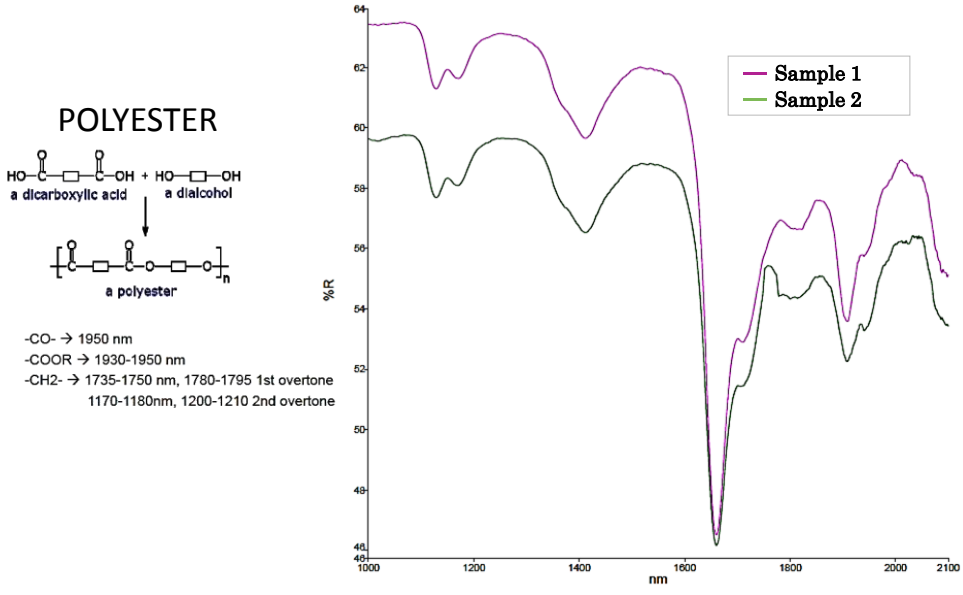

Figure 4.5-1: Functional groups of the Polyester compound, their absorption lines, and the correspondence of these lines with the reflectance spectra in the NIR region of two analyzed samples.

Then we should define the molar absorptivity of the compounds and apply theoretical models (e.g. Beer-Lambert, Kubelka–Munk or Kramers–Krönig) for estimating the light behavior and thus, the required emission light power and detector's sensibility. At this stage, the impact of other side effects should also be at least identified, such as the effect of the temperature changes in the absorption lines, or the variation of moisture concentration in the sample.

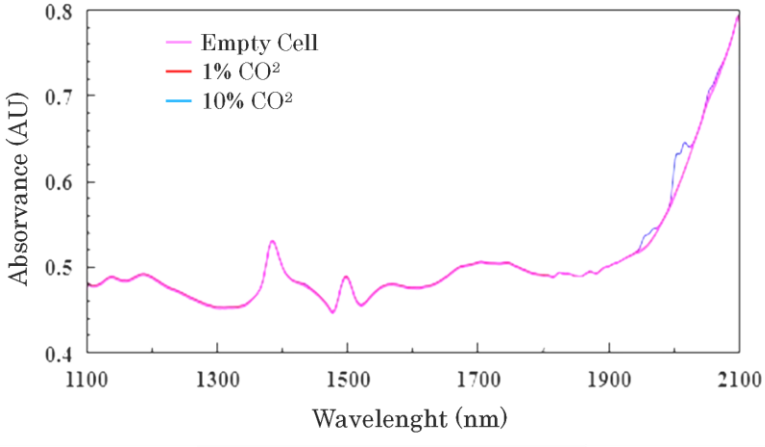

Figure 4.5-2: NIR spectra of empty cell, cell with 1% CO^2, and cell with 10% CO^2 sample. The differences between the empty cell and the 1% sample are insufficient to perform any measurement, and thus, this is the detection limit [253].

Some typical conclusions at this stage that could hinder the project execution could be that the analyte concentration is too little for a reliable measurement (see Figure 4.5-2), or that the overlapping noisy-compounds present stronger absorptions that hide the effect of the compound of interest, as depicted in the Figure 4.5-3.

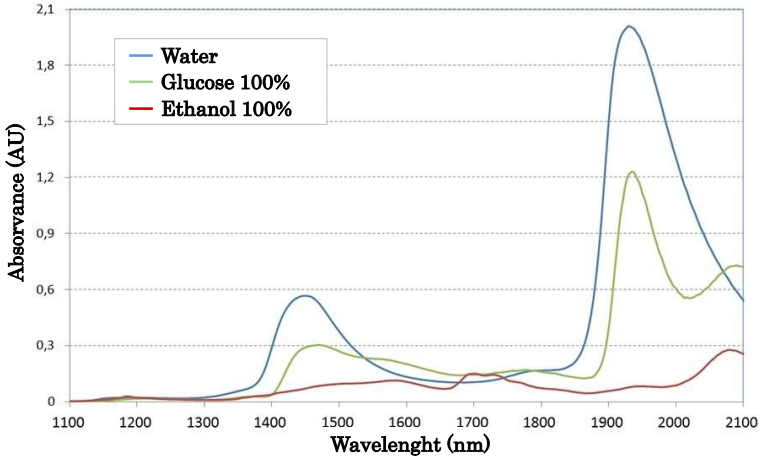

Figure 4.5-3: Absorption spectrum in the NIR range of Ethanol, Glucose and Water samples, showing the overlap of the absorption peaks. This situation complicates the quantitative analysis of mixed samples (e.g. fermentation of alcoholic beverages [254], or at bioreactor processes [255]) based on NIR spectroscopy.

Another example is the motorization of micro-particles. In this specific application, the problem to solve is the definition of the optical and focusing properties and the definition of the light intensity requirement at the detector to perform a valid detection through machine vision algorithms (see section 5.2).

Of course, this theoretical approach needs to be consolidated whit real experimentation, which is accomplished in the following sections.

Table 4.5-5: Summary of the items and the expected information to collect in the 2.1 Theoretical Description Report.

Item
Theoretical description of the measurement principle
Assessment of working conditions in the measurement principle
Identification of main Photonic Component
Formulae to calculate (orders of magnitude) emitters, detectors, …

4.5.1.2 Laboratory Verification

Basically, at this stage, the theoretical hypothesis and definitions are taken one step further and are validated against real measurements performed at bench-top laboratory equipment.

This is one of the first points where the cooperation of the end-user or customer is strictly required, since the availability of real and representative samples is mandatory. Depending on the photonic principle that is going to be used as measurement method, a different minimum number of samples will be required. For instance, a chemometrics-based method will require at least 50 or 70 representative samples.

These samples will be used as reference, so the validated values of the parameters of interest need to be provided as well, if not, we should also accomplish these measurements. Once the samples with their reference values have been identified, we proceed to apply the selected photonic measurement setup to extract the information.

Notice that applying a photonic inspection does not necessarily give a measurement result. Remember that the photonic techniques are mainly indirect methods for extracting relevant information from a sample, but always some sort of algorithm, method or processing mean is required to convert the photonic information into a valid sensor measurement.

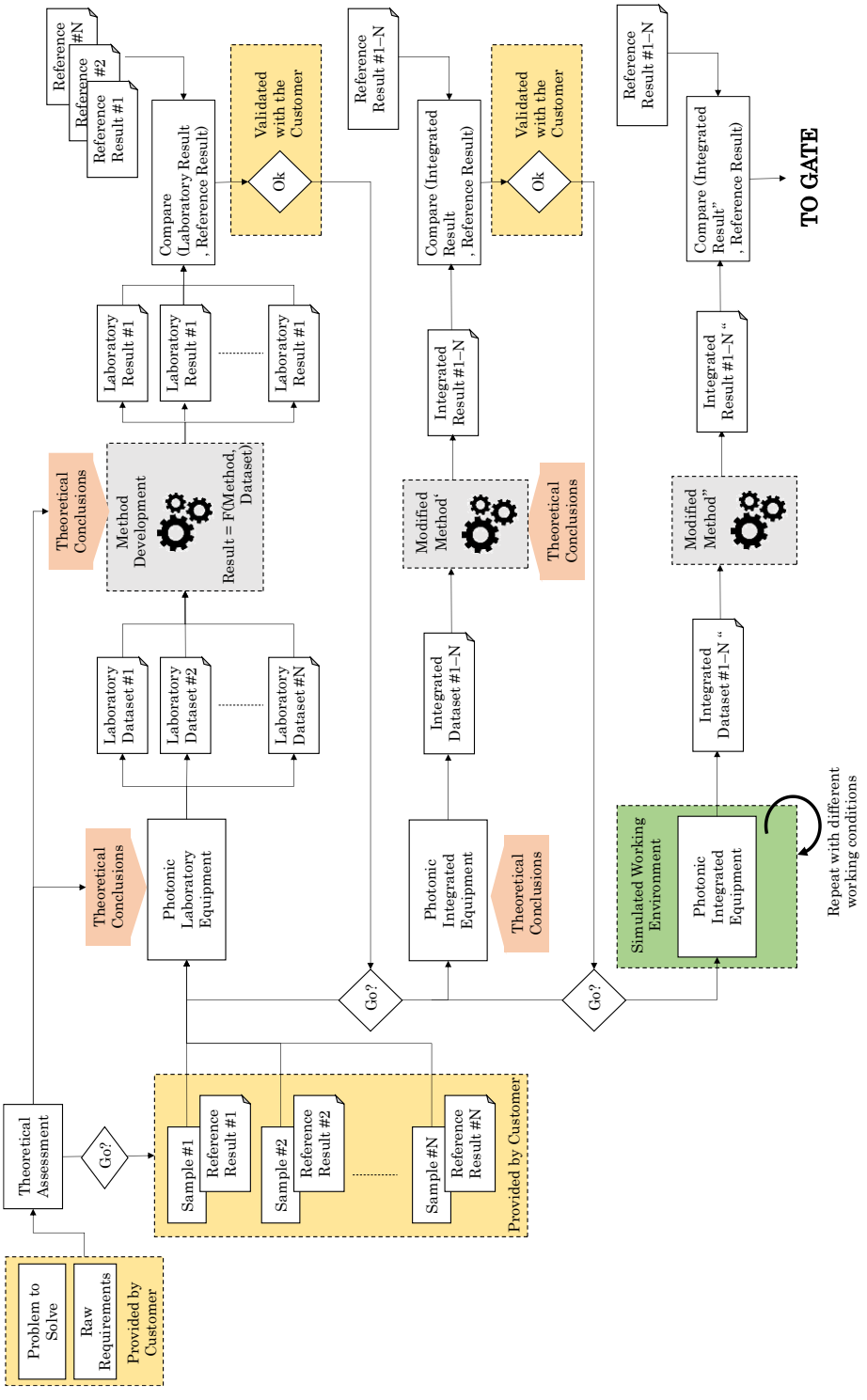

Figure 4.5-4: Workflow amidst the different sub-stages within the Proof-of-Concept phase.

Depending on the complexity of this method, including it within the Proof-of-Concept stage may be overambitious, because sometimes the method itself is the core of the photonic integration project. In these cases, the extent of the method development and the expected soundness of the laboratory results should be agreed with the customer. Same happens with the decisions about the feasibility of the idea, they may depend entirely on the capabilities of the method to be developed. In these cases, the experienced verdict given by the technicians after analyzing the laboratory data needs to be validated by the customer, assuming that with the current level of dedication no further guarantee is possible.

Concerning some specific information extracted during these laboratory studies, sample volume and inspection area are normally defined based on the settings of the laboratory equipment and the data obtained (see Table 4.5-4). For instance, for a transmission spectrometric system, the sample volume is defined by the path length (the section of the cuvette) and by the spot size, or the intersected area between the emitted light beam and the detectors viewing area. On the other hand, for an optical setup, the inspected volume equals the field of view by the deep of field. The specification of this kind of parameters and their tolerances is critical for the later hydraulic and mechanic system specification.

Notice that, apart from the abovementioned parameters and the photonic results, no relevant information may be taken from the photonic settings of the laboratory equipment, because normally, these include detectors, emitters and optical components which installation on the field is not feasible. This is the reason why we move forward to the next sub-stage.

4.5.1.3 Integrability assessment

The very first thing to take into account while planning to develop an integrated photonic sensor is that, likely, the performance and characteristics available in the integrated components will be worse than the ones available at laboratory equipment. And even if, as described in Chapter 1, the integrated photonic components are enhancing their features day by day, the reality is that the laboratory equipment is doing the same, so we will always have to consider this performance gap.

This is the reason why this third stage is required while validating the proof-of-concept, because the results achieved with the bench-top equipment may not be migrated into an embedded sensor system at the required cost, size, sensibility, etc.

Besides, it is almost impossible to replicate any industrial working condition with bench-top analyzers, basically because these have been designed to work under stabilized environments, rather

than dealing with broad temperature spans, humidity and vibrating conditions as expected for the in-line sensors. On the other hand, if required for the proof-of-concept, we could emulate different working conditions (e.g. using a climatic chamber, vibration bench, etc.) and have the integrated photonic components operating under these conditions for verifying the performance of the system.

Actually, the photonic components tested at this stage (emitters, detectors and optics) will become the first option to be integrated in the hypothetic forthcoming prototypes, and therefore, should be selected with the aim of meeting not only the technical specifications identified in the previous theoretical and laboratory studies, but also the requirements in terms of cost, size, and operation conditions specified by the customer.

However, even if the providers of the integrated photonic components offer a full range of evaluation systems to test their devices, at this stage we may require manufacturing mechanical mock parts for enabling the use of the devices more similar to their intended use once integrated in the sensor. These mechanical parts could be considered as the very first version of the sensor prototype (see Figure 4.5-5). Therefore, the implication of the mechanical and hydraulic engineers may be required for designing and accomplishing the fabrication and assembly of these parts with the optoelectronic components.

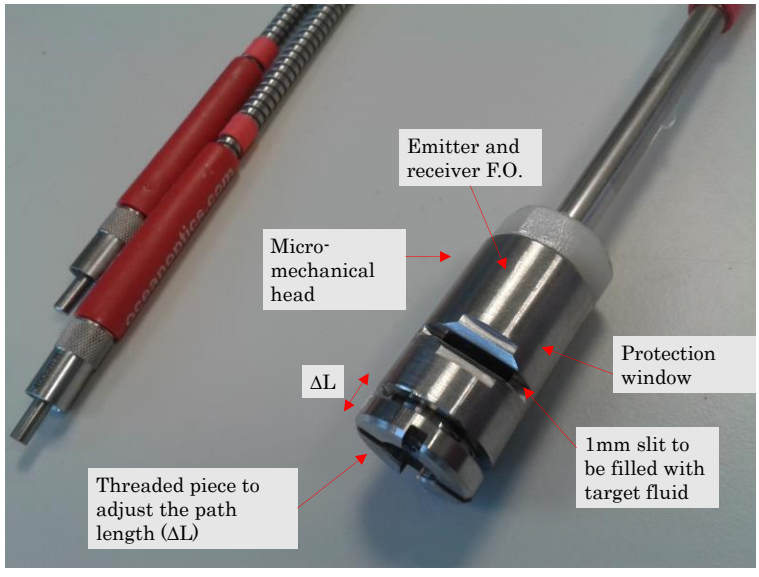

Figure 4.5-5: Example of customized mechanics system to enable the proof-of-concept of the integrated components. In this case, a micro mechanical head was developed to submerge a dual F.O. system into a running fluid to analyze it with visible spectrometry. Since the path length was not defined yet, the design includes a threaded piece that allows enlarging the path length. This specific prototype belongs to the proof-of-concept of the OilProbe® sensor.

In addition, in some occasions, dedicated electronic system is required for enabling certain working modes of the photonic components, and not all the features are available in the evaluation versions. In these situations, we may also require developing a custom hardware-software solution for the tests. In Figure 4.5-6, we display an example of this situation, with a CMOS detector required to drive and synchronize a stroboscopic lighting system; but with no evaluation board supporting this feature, a customized hardware was built. So, already at the proof-of-concept stage we realize about the multi-domain skill set required to accomplish the verification of the first integrated version of the measurement principle.

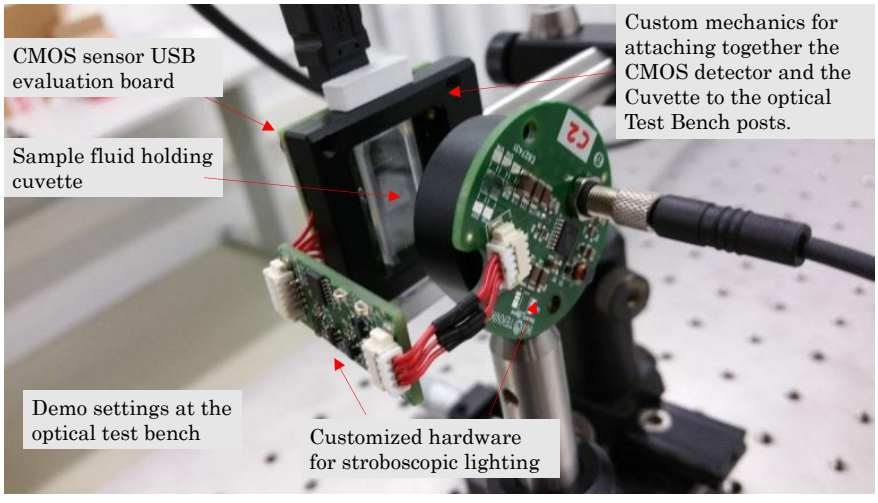

Figure 4.5-6: Example of customized hardware system to enable the proof-of-concept of the integrated components. In this case, the settings belong to the proof-of-concept of a micro-particle detector.

Even if we may require certain customized parts, our objective at this stage is using as much standard components as possible to keep the development cost down. The availably of an optical test bench is very useful at this point, because several optical and mechanic components are accessible at relatively low cost. Sometimes, as depicted in Figure 4.5-6, even if we develop our custom parts, we still fabricate them compatible with standard optical test benches to allow using them along with the rest of compatible optical components.

4.5.1.4 System Specification and Project Plan

This is the wrapping up sub-stage, where the developments and conclusions of the previous tasks are summed up to deliver a system architecture, with all the heterogeneous blocks clearly identified (see Figure 4.5-7), and including a first version of system

specification answering to the customers' requirements. If the project moves on to the next stage, these preliminary specifications will be the base for the prototype development.

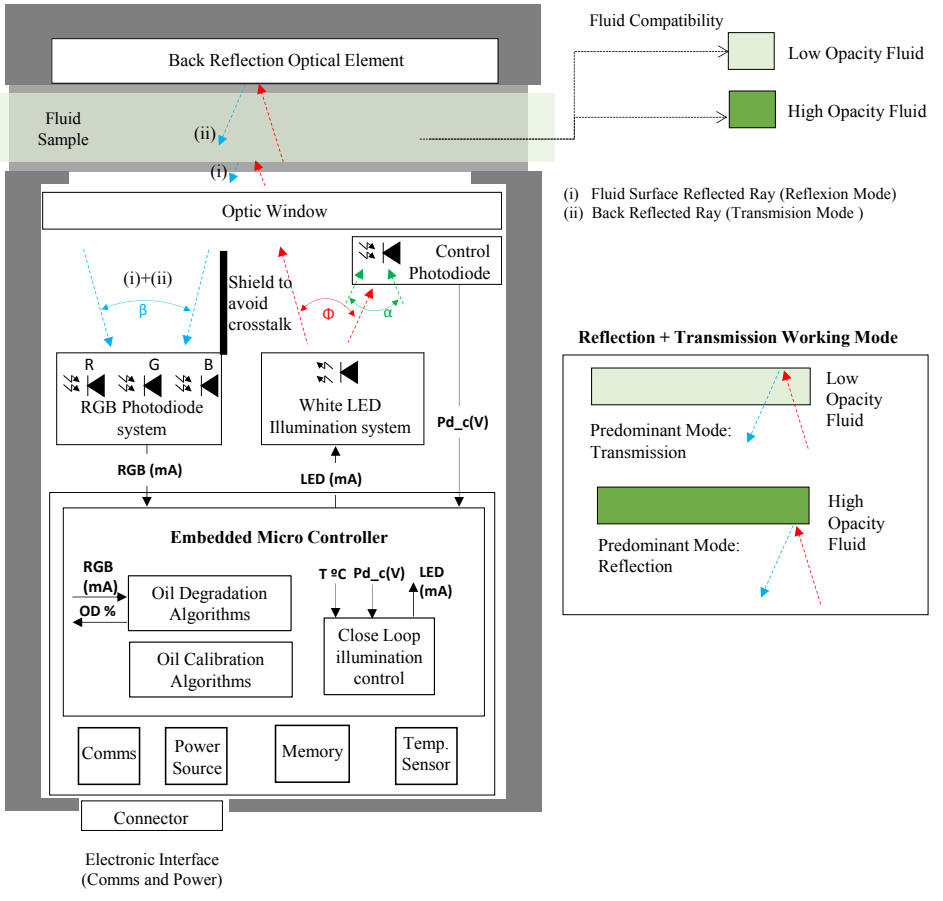

Figure 4.5-7: Typical block diagram of sensor system generated at this stage, where Different building blocks are depicted and working mode is outlined. In this case, the diagram belongs to the OilProbe® lubricant sensor.

Additionally, this is the place where the risks, uncertainties, and the potential heterogeneous integration problems are risen up. Besides, an updated and much more accurate view of the whole project cost and schedule is provided.

Table 4.5-6: Information contained in deliverable 2.4 System Specification and Project Plan.

Item
System Architecture
Heterogeneous blocks and interfaces
selection of photonic components and their settings

Identification of hydraulic components and their specifications
Identification of electronic component and their settings
Specification of working ranges
Revised expected unitary cost
Revised Project cost
Revised Project Plan
Revised Risk and Uncertainty assessment

4.5.2 Prototype Development Decision Gate

The main activity to accomplish at this second Gate is authorize or not the launch of the prototyping stage. Up to now only initial checks, feasibility tests and perhaps some minor prototypes have been performed. However, in the coming phase a real prototype of the product will be developed. Therefore, this Gate needs to be executed very thoroughly with higher management as well as customer involvement to reach sign-off on the product definition, and the development plan. Additionally, agreement on the commitment of the required resources (capital, personnel, etc.) needs to be achieved.

Notice that, even if this final Gate represents the final checkpoint, the stage's workflow (see Figure 4.5-4) already includes some internal decision points at which, in front of negative intermediate results or major risks, the customer may stop the development.

All the deliverables will be taken into consideration, but the continuation of the project normally depends on the following four questions. If all of them have a positive answer, very likely the project will proceed to the next stage.

1. Are we able to measure the parameters of interest with the envisaged photonic principles?
2. Are we able to integrate them into a sensor and maintain the performance over the industrial working condition span?
3. Does the unitary cost of the sensor and does the project cost meet the target?
4. Are the risks and uncertainties accepted by all the parties?

Table 4.5-7: Detailed inputs, decisions and outputs at 4.5.2 Prototype Development Decision Gate.

Input	Decisions	Outputs
Theoretical Description Report	Photonic Measurement principle proven	Prototypes stage plan and resources

Laboratory Result Report	Integrabiltity and reliability in operation conditions feasible	Potential partners list
Photonic Integration Report	Unit cost, project cost and project timeline meet target	Authorization to proceed
System Specification and Project Plan	Project risks and uncertainties acceptable	

4.6 Design of Prototypes and Test–Bench Verifications

The objective of this third stage is to iterate in the fabrication of the different versions of the sensor prototypes, until the whole set of client's requirements (the already known and the ones to be defined) are met and the system is ready for its validation in real environments in the next stage. The different technological developments will help us progressing in the system integration, will enable the optimization of the measurement principle, will allow reducing the uncertainties and mitigating risks, and will serve as the first pilot versions for the customer, enabling him to narrow down in the specification and to define unforeseen requirements or working modes.

Why we talk about Test-Benches along with Sensor Prototypes? This is because this stage is not only responsible for the prototype development, but also for its deep verification, and this task is usually underestimated when talking about photonic sensors. These prototypes need to be verified with many different fluid samples, at several operating environments, under different fluid conditions, etc. and this implies a huge effort and time spent in testing. Things get worse when not only a single device needs to be tested but a batch of them in order to provide the repeatability of the prototypes and the variance coefficient of the measurement. Consequently, any little support concerning the test would maximize our productivity, and this is the specific reason why we conceive the prototypes with their paired test-bench.

Test-benches are automatized and parameterizable hydraulic equipment, which may already exist at customer's or design house's premises, may be subcontracted or may be designed and developed within the project. These Test-benches usually enable to install more than one sensor simultaneously (in parallel and in series), allow modifying the hydraulic setup (e.g. pressure, flow, temperature of the sample) and normally permits an easy fluid sample interchangeability. Merging all these features, we are able to

dramatically speed up the prototype testing time and maximize our insights about the sensor performance.

This is a technological intensive stage, with all the technical members devoted to the definition and fabrication of the different working prototypes. In this case, the headcount and budget availability needs to be assured for enabling an accelerated work rhythm that allows iterating fast. In this occasion, only if the conclusions and results achieved at test benches and controlled environments are successful it will make sense to move forward to the next stage (Validation in real field), but this will be judged at the Real Field Deployment Decision Gate.

4.6.1 Prototype Development and Test Bench Setup Stage

This is the phase where the system briefly specified in the previous stage is crystalized in a physical system, with all the heterogeneous building blocks efficiently integrated to deliver an autonomous sensor system for in-line fluidics monitoring. Additionally, all the required efforts are put for having the system massively verified at laboratory scale, assuring its suitability for a real field validation. This verification implies the setup and use of dedicated Test-Benches that will allow achieving high productivity in testing activities.

Of course, all the project partner should assume an evolving design of the prototypes, which iteratively answer to the new specifications that arise as we, and the customer, learn about the problem and about the application, as new risks to mitigate are recognized, or as new use cases are identified.

The duration of this stage depends on the difficulty of the sensor system, but in the current fast Time-to-Market scenario, customers normally require having sound results in 6 - 9 months. Therefore, the resources should be dimensioned considering this tight schedule. The roles, hardware and software equipment and the outsourcing needs normally present in this stage are outlined in Table 4.6-1.

Table 4.6-1: Roles, equipment and outsourcing required and their expected activities for the Prototypes and Test-Bench Stage.

Headcount	
Role	**Activities expected**
Project Leader/ Senior Engineer	Risk identification, identify the heterogeneous interfaces, provide the integrated view and assure the integrability of the proposed methods into an in-line sensor.

Optoelectronic Engineer	Simulate the photonic subsystem
Mechanical Engineers	Simulate the hydraulics and mechanics Simulate the microfluidics Design and develop the different versions sensor body and enclosure Design/Modify the sensor Test-Bench
Hardware Engineers	Design and develop the sensor electronics
Software Engineers	Design and Develop the sensor control firmware Codify the measurement algorithms
Automation Engineers	Program the test bench and automate the tests
Verification Engineers	Define and implement the verification plans
Chemical Engineer / Physicist	Design the chemo–physical measurement method

Equipment/Software	
Item	**Use expected**
Hydraulic Test Benches	Emulate the different hydraulic operating conditions, enable fluid sample interchangeability, enable multi sensor measurements
CFD Simulation Software	Simulate the mechanical stresses, and the fluidics behavior across the micromechanical structures
Optics Simulation Software	Simulate the ray traces, absorptions, light intensities
Climatic Chamber, Vibration test bed, etc.	Emulate different working conditions to validate the prototypes under the required operation environment

Outsourcing	
Item	**Use expected**
Plastic/Metallic Fast Prototyping	Fabricate mechanical parts for the prototypes
Hardware Electronics manufacturing	Fabricate and assembly the prototype electronics
Photonic Components	Integrate as core part of the sensor system

Again, this stage is divided in different sub-stages that are supposed to generate specific deliverables for its later assessment at the stage's Gate. However, on this occasion, we found an iterative loop in the sensor prototyping and verification, because, until the customer's expectations are fulfilled (or the project is stopped), we should remain in this loop.

Table 4.6-2: Deliverables generated during the Proof-of-Concept Stage and the involved team members.

id	Name	Participants
3.1	Heterogeneous Integration Report	Project Leader & Technical members
3.2	Simulation Report	Technical members
3.3	Verification Plan	Project Leader & Technical members
3.4.i	Prototypes	Technical members
3.5.i	Verification Report	Project Leader & Technical members
3.6.i	Technical and Economic Progress Report	Project Leader
3.7	Final Version Prototype	Technical members
3.8	Validation and Industrialization Plan	Project Leader

i: 1…N, being N the number of iterations

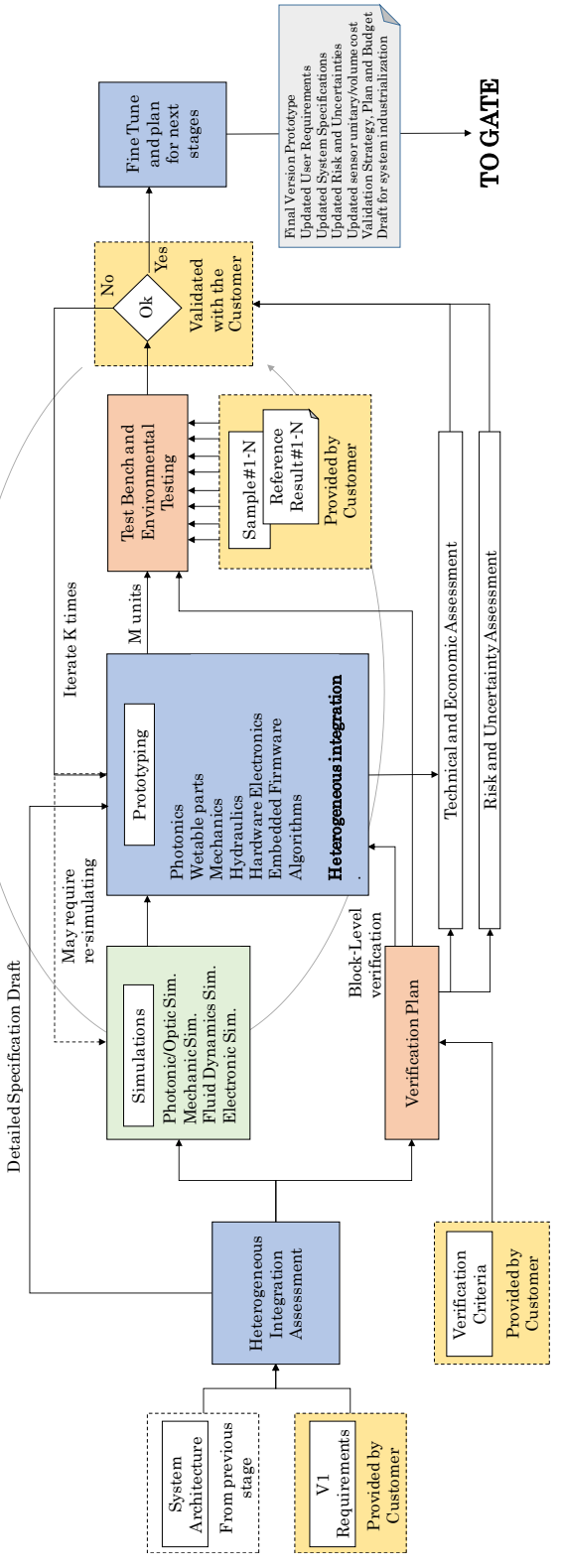

Figure 4.6-1: Workflow amidst the different sub-stages within the Prototyping phase.

4.6.1.1 Heterogeneous Integration Assessment

The heterogeneous integration does not only imply putting all the different building blocks together and having them running. It also implies performing a thorough study about the dependences between the blocks, identification of potential error propagation, definition of tolerances and recognition of weaknesses and risks. In this sub-stage, the system will be treated as a whole, and specifications for all the sub-systems will be generated.

The analysis of the dependences between the blocks is a crucial part before starting the integration. This is a task to accomplish among the whole technical work-team since it is a truly multi-domain activity. This study should reveal how the system works thanks to the internal connections between the blocks. Indeed, these connections and interfaces will pose a heterogeneous nature, and the blocks could be tied together through a physical, chemical, mechanical, electronic, photonic, etc. interface.

The analysis of the risks and uncertainties present in the system follows a similar multi-domain approach. However, due to this heterogeneity, it is not possible to define a single manner to proceed in this definition of dependences, but following the next steps may help:

1. To define a responsible person for each building block.
2. Make them define how their block works, and which are the limitations and risks within it
3. Make them define which are the inputs and outputs and their most important parameters (key performance indicators)
4. Make them define what can fail in their block
5. Make them define what concerns them about the boundary blocks and about the quality of their inputs
6. Merge all answers and define the sensor as a plant with several blocks connected (inputs and outputs), each of them with internal information (KPI) and different risks and weaknesses identified at each block level and at block interface level.

The outcome of this sound analysis reveals the dependences and the risks present in the sensor at this stage.

Additionally, and fully related with the analysis of the interfaces between the building blocks, we found the study of tolerances. Tolerance assessment and budgeting is the process of defining the required design specifications for each block within the context of the whole system to guarantee both the optimal performance and the manufacturability of the final sensor product. In a system that includes photonic elements, from source to detector,

with all the precision optics in between, the analysis of the tolerance of the optical design is critically important [256]; optical and mechanical engineers need to understand how tightly the size, surface figure, thickness, tilt, centering, and other parameters of the optics must be controlled. In addition, it is equally important to simultaneously analyze mechanical and assembly tolerances, to avoid overlooking at the optics and not to the entire system [257]. This task is extremely important because inadequate tolerance analysis during design frequently results in system shortfalls. Under-specifying tolerances may generate performance deficits or issues during final assembly, either of which will require expensive and time-consuming redesign. Similarly, over-specifying optical and mechanical tolerances normally implies incrementing unnecessarily cost, complexity, and lead time to a project.

Table 4.6-3: Information contained in deliverable 3.1 Heterogeneous Integration Report.

Item
Detailed System Architecture
Detailed identification of building blocks: Function, Input, Output and KPI
Detailed identification of interfaces between the building blocks
Detailed system and block specification
Detailed optical and mechanical tolerance definition
Risk and uncertainties at block and at system level

4.6.1.2 Simulation Support

Once all the building blocks have been clearly identified and the first version of the specifications has been defined, we now should take advantage of the benefits brought by the simulation tools to speed up the system design and to minimize uncertainties in a fast and flexible manner. The simulation tools enable to understand how different critical parts of the system will behave, and help us driving some design decision based on the simulation outputs.

The simulations rely on dedicated software tools, that must be configured properly and that normally require some engineering work to define the settings, to prepare the required input dataset and to interpret the output results. However, all the effort pays off, because all the conclusions are very valuable to specify the first version of the prototypes.

Normally, the simulation will be used in four different domains, each one with its own objectives, based on different software

tools, requiring different input information and generating different results.

i. **Optics and Optoelectronics:** The objective of these simulations is to clarify how the light behaves across the different elements of the system. It includes simulation models for emitters, receivers, optical components and mechanical parts, including their finishing materials, which is important for simulating the ray reflections and identifying potential stray rays. Normally, the photonic component manufacturers provide these simulation models for easing the integration work. However, if this data is not available, reference or standard models could be used instead, but the accuracy of the results will be less accurate. Besides the models of the individual components, a 3D model depicting their relative positions (e.g. a CAD model) is essential for the simulation, therefore, a collaborative work between the optic and mechanic engineers is required here.

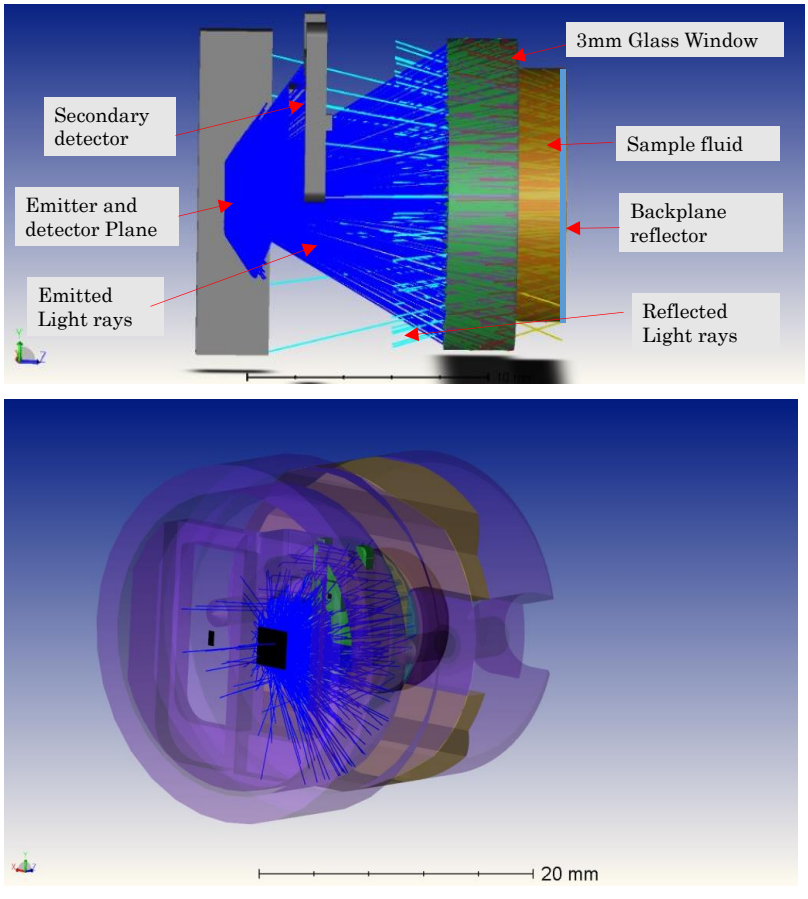

Figure 4.6-2: Simulation results of the optoelectronic, optic and mechanic components. This specific case belongs to the OilProbe® system already introduced in Figure 4.5-7

The results provided by these simulators illustrate the different trajectories followed by the light rays from the source to the detector (see Figure 4.6-2)., and help us defining for instance, positioning tolerances of the different components. Additionally, the intensities of these light beams are also provided (see Figure 4.6-3 and Figure 4.6-4), based on the light flux generated at the emitter and the different constructive or destructive interactions, reflections, absorptions, etc. This output is extremely useful for the light budget calculation and for validating the theoretical results from the previous stages.

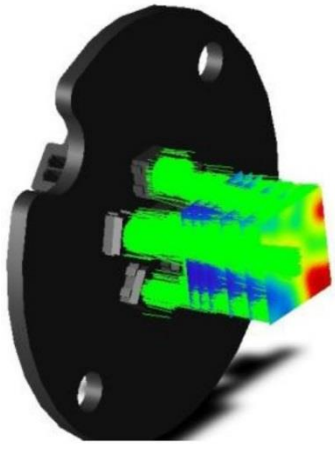

Figure 4.6-3: Simulation of the light irradiance generated by a custom multi-LED light source. This specific design belongs to the OilWear® product.

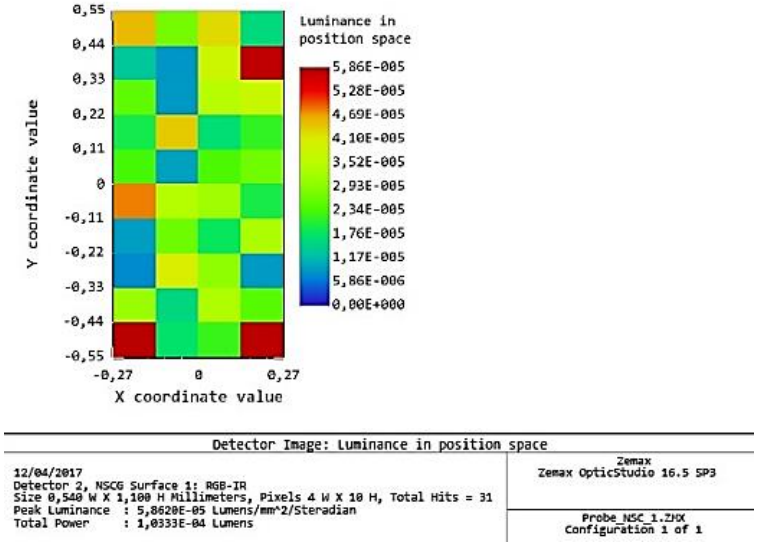

Figure 4.6-4: Example of results generated by simulation tool. This specific case represents the luminance getting to a 2D detector of the OilHealth® product.

Additionally, these tools are able to estimate the scattering, absorption and diffuse reflection that may occur at the sample fluids (see Figure 4.6-5). Setting up this feature in the simulation tools is not straightforward and normally requires very specific knowledge about the sample in order to generate a valid simulation model. These features are based on statistical and numerical approximations of Mie and Rayleigh scattering phenomena for calculating the estimated trajectory of the photons entering the sample. Using input parameterization about the particle distribution and absorption, the simulation tool usually performs a Monte-Carlo based statistical representation of the different light rays across the sample. This information is very useful for understanding where the light-matter interaction effectively happens, and eases the design and interpretation of quantitative measurement methods in spectrometry and fluorescence.

Some reference tools for optical design simulations include OpticsStudio from Zemax (Kirkland, WA, USA), TracePro from Lambda Research Corporation (Littleton, MA, USA) or ASAP by Breult Research (Tucson, Arizona, USA).

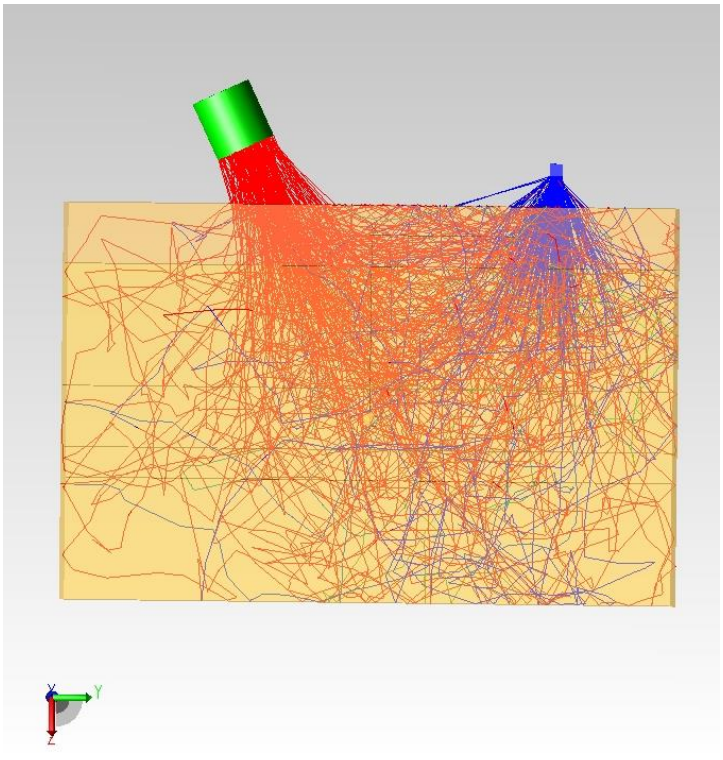

Figure 4.6-5: Ray trace simulation within a tissue, the emitter is on the left and the receiver on the right. Image courtesy of Lambda Research Corporation.

ii. **Structural Analysis of Wettable parts:** The objective of this simulation is to calculate how the glass; plastic or metallic parts behave under the extreme working conditions required for the sensor. The hydraulic conditions are often very challenging because the photonic sensors require a transparent interface between the optoelectronics and the fluid sample, which may be a high pressure, temperatures, etc. This wettable part is normally the weakest point of the system and solving it is not straightforward due to the high maximum pressures of the fluid and the necessity of keeping the compactness and the low cost of the components. Therefore, engineering and validating efforts are expected there for assuring the reliable design. The input parameters are normally mechanical properties of the materials (young modulus, shear limits, etc.), the 3D model or CAD file of the wettable part (see Figure 4.6-6-a), fluidic properties of the liquid (e.g. viscosity) and the hydraulic parameters to simulate with (e.g. temperature, pressure). Then a Finite Element Model of each part under test is developed (see Figure 4.6-6-b) and the finite element analysis is then executed by the tool.

The results generated by the simulation are normally the efforts and tensions suffered by the different mechanic parts at different points (see Figure 4.6-6-c), and thus, the engineer could verify if these values remain far from critical levels. Additionally, thanks to these simulators, we can directly calculate misalignments and tolerances in the parts may dramatically impact on the tension and effort values.

Some examples of tools performing this kind of simulations are: Mechanical from Ansys (Canonsburg, PA, USA), SolidWorks Simulation from Dassault Systemes (Vélizy-Villacoublay, France), or FEA tools from MSC Software (Newport Beach, CA, USA).

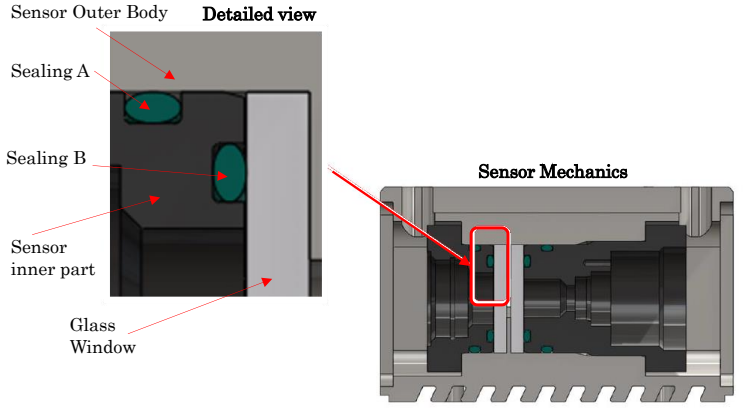

(a)

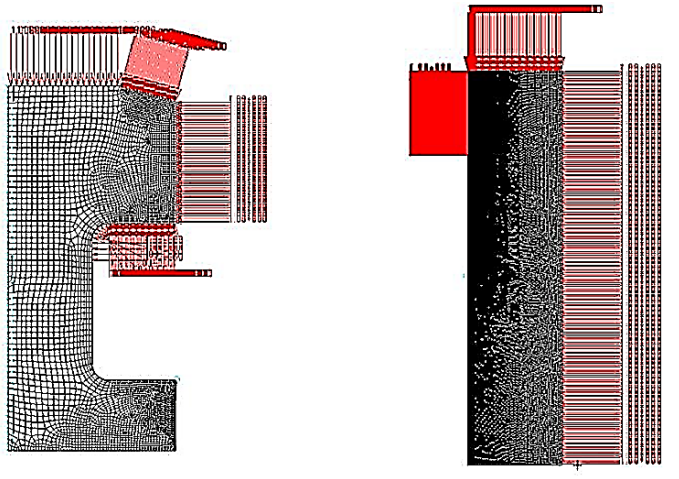

(b)

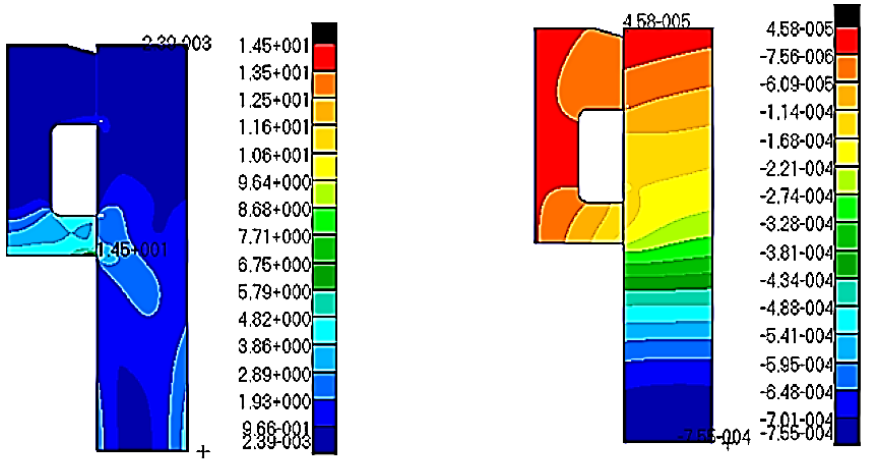

(c)

Figure 4.6-6: Example of Finite Element Model for simulation the different forces supported by the glass and metallic parts under 10bar fluidic pressure. This specific design belongs to the OilWear Piko® product.

iii. **Fluid Dynamics:** The aim of these simulations is to understand how the fluid behaves within the measurement cell, identifying potential turbulence vortexes, flow homogeneities, sample renovation, etc. The simulations are based on Computational Fluid Dynamics (CFD) calculations, which basically apply the Fluid Dynamics formulae to the specific problem configure into the simulation tool.

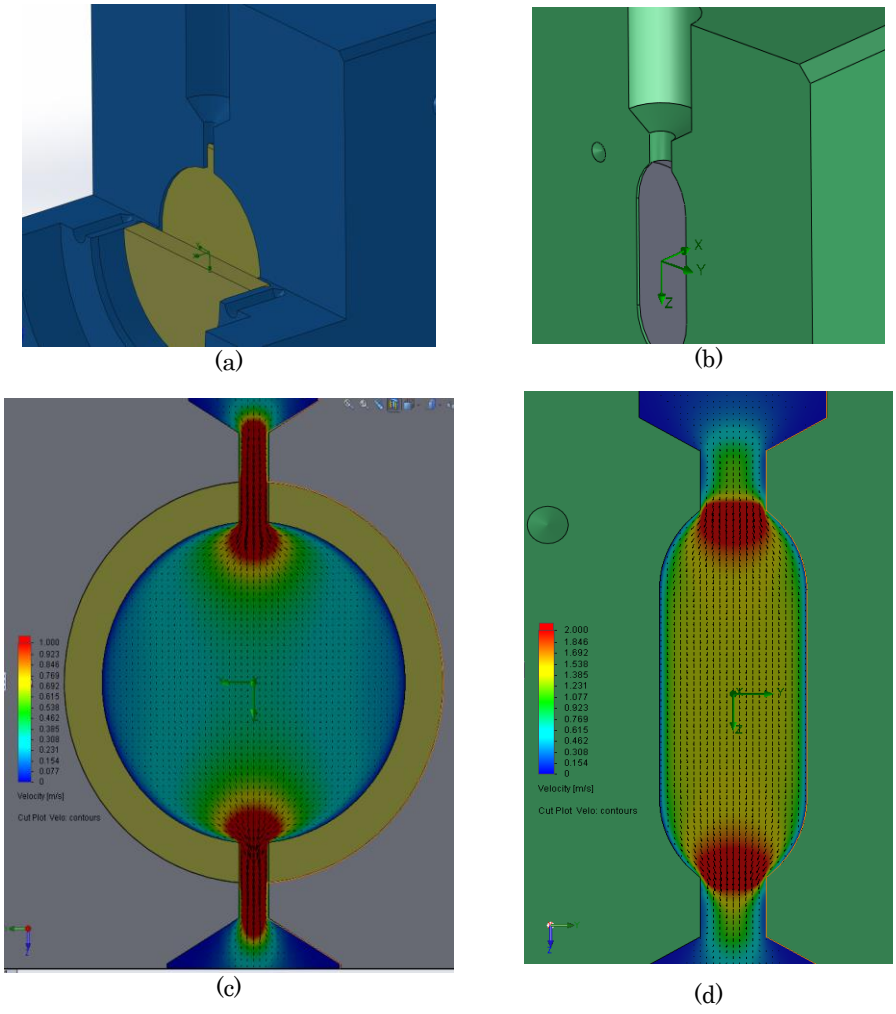

Figure 4.6-7: (a) and (b) represent Mechanical CAD model of different generations of OilWear® bypass sensors, where the geometry of the cavity was modified to homogenize the fluid flow. (c) and (d) Output results displaying how the fluid flows across the cavities and how the (d) version present a smaller flow speed gradient.

The input information is normally the 3D model of the mechanical cavities crossed by the fluid (see Figure 4.6-7-a and -b), hydraulic conditions (input and output pressures, temperature) and properties of the fluid (viscosity, density

and temperature). Then, the structure to be simulated is converted into a mesh (see Figure 4.6-8) and the tool calculates the 3D distribution of the flow speed across the mechanical structure (see Figure 4.6-7-c and -d). The typical system configurations for the fluidic sensors are in bypass, with a fluid inlet and a fluid outlet and the immersion systems, with the whole structure at the same pressure point (see Figure 4.6-9).

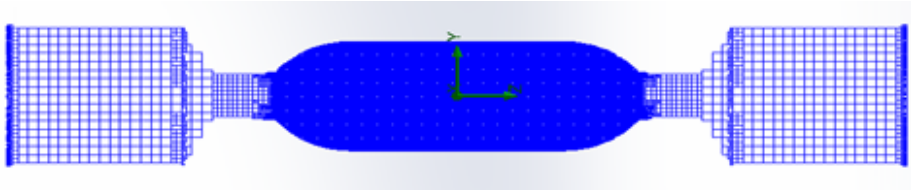

Figure 4.6-8: Mesh structure of the fluidic sensor cavity to setup the simulation.

These kinds of simulations are extremely useful for validating the geometry of the measurement cavity and assist the mechanical engineer in the selection of the best approach for solving the microfluidic structure.

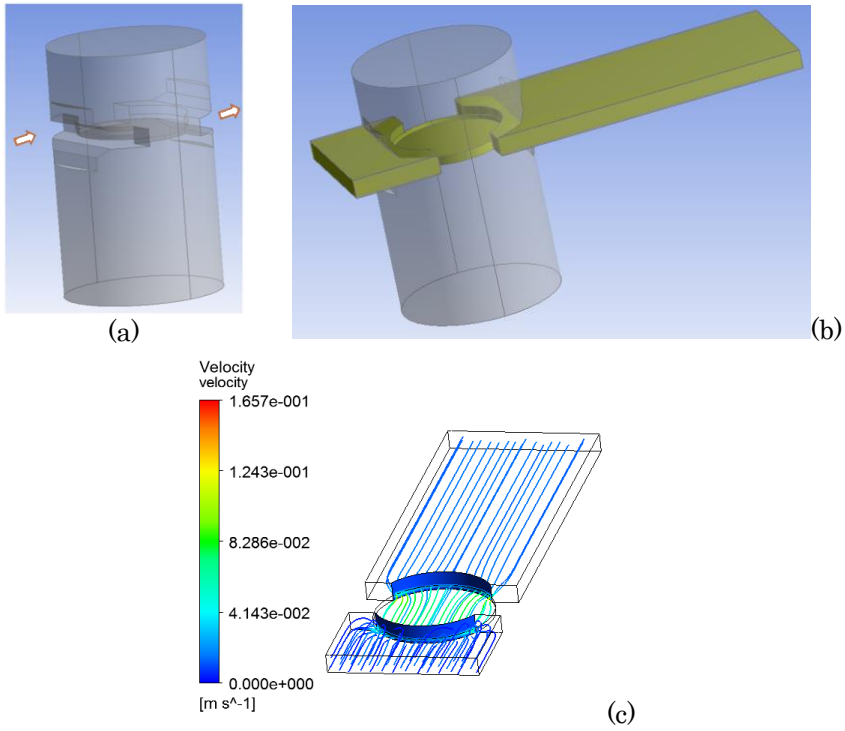

Figure 4.6-9: (a) Mechanical CAD model of the OilProbe® immersion sensor. (b) Geometry of the fluid section under simulation, considering not only the liquid contained in the measurement cavity, but also on its surroundings, simulating the immersion. (c) Output results displaying how the fluid flows across the cavity once the sensor is immersed.

Some example of simulation tools for CFD are Fluent from Ansys, scFLOW from MSC Software or Flow Simulations from SolidWorks.

iv. **Hardware Electronics:** The objective of these simulations is to assist in the design of the analog electronic subsystems, which are sometimes required either for driving and modulating the light sources, for reading out and conditioning of the signals coming from detectors or for synchronizing both. It is true that the integration of digitalized interfaces into current photonic components avoids the need of designing custom electronic solutions for controlling them, but not all the system includes these digital communication channels and in these occasions, some sort of analog electronic design should be delivered by the design team.

The analog circuit behavior simulators enable the designer to tailor the development avoiding any investment in hardware until the confidence in the design is much higher. Typical applications of these simulations include power sources and control system for light emitters (Figure 4.6-10-a), and signal conditioners for reading the information collected by the detector. Simulated results normally display the performance of Voltage, Intensity or Power signals in the time or frequency domains (see Figure 4.6-10-b).

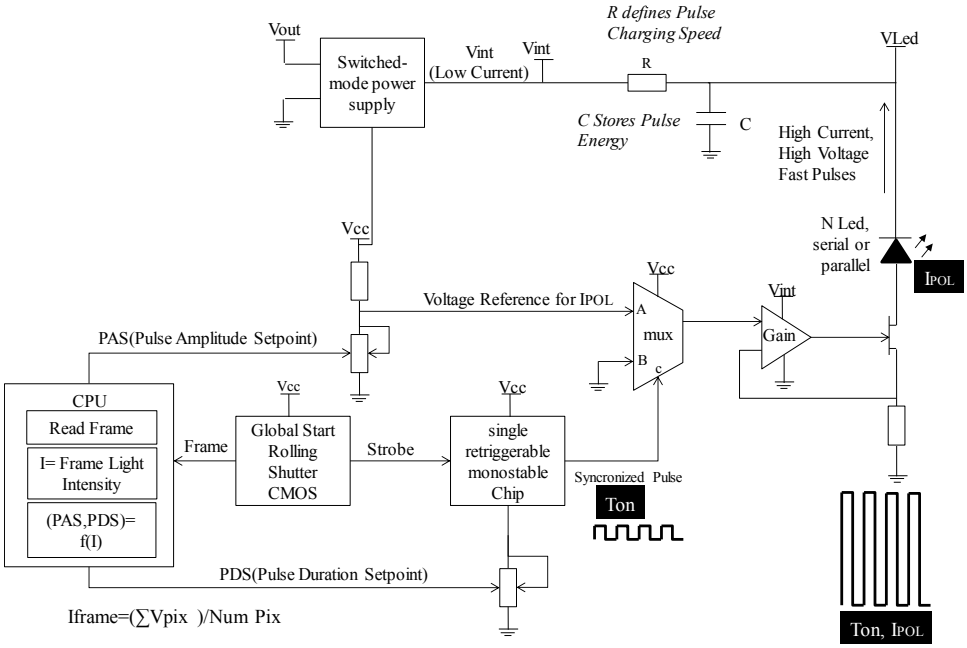

(a)

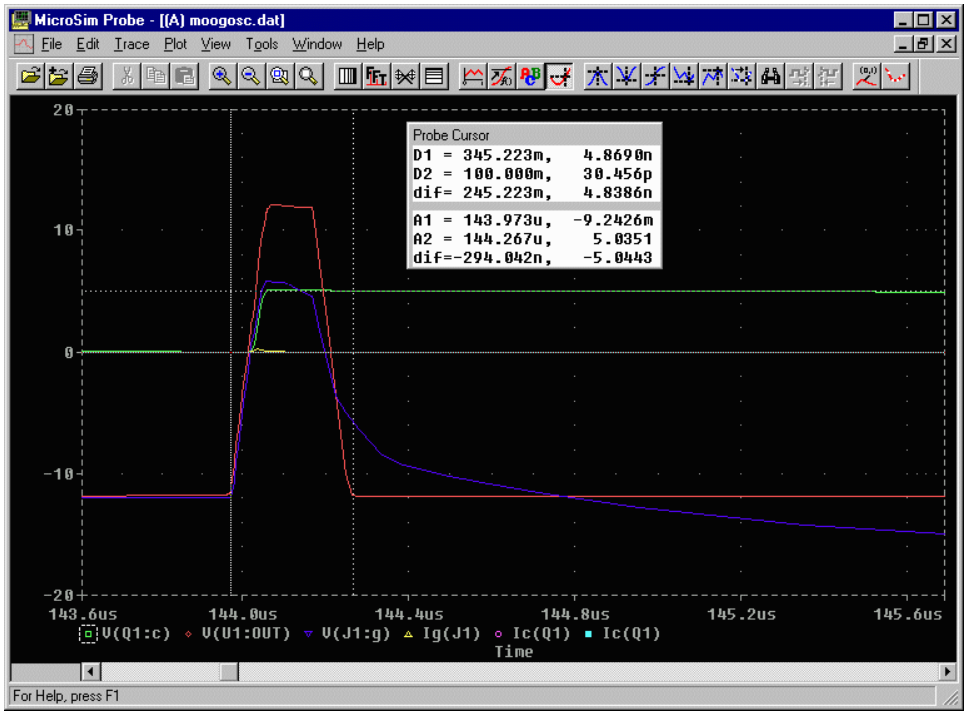

(b)

Figure 4.6-10: (a)Example of Analog Circuit for synchronizing and driving a stroboscopic illumination system for a Lens Free wear particle sensor system. (b) Simulation result of the stroboscopic light pulse generation circuit, where the x-axis shows the duration of the pulse in microseconds and the y-axis the amplitude in Amperes.

Typical simulation tools include Altium Simulator from Altium Designer (Sydney, Australia), LTSpice from Linear Technologies (Milpitas, CA, USA) or Orcad Pspice from Cadence (San José, CA, USA).

The results and conclusions from these simulations (included in the deliverable 3.2 Simulation Report) are directly fed into the design of the different building blocks of the prototypes. However, notice that simulated results need to be confirmed by real physical verifications. Additionally, the input data of these simulation environments may be updated as new information and new scenarios are being defined while progressing in the project development.

4.6.1.3 Verification Approach

This sub-stage is devoted to defining the verification plan to accomplish at the prototyping stage. The verification presents a manifold objective and should cover, among others the items outlined in Table 4.6-4.

Table 4.6-4: Examples of topics to be covered by the verification plan at the Prototyping Stage.

Topic to Verify
Performance of the measurement principle (e.g. algorithm result, stability and variance coefficient of the measurement) under different status conditions of the fluid.
Stability of the measurement under different hydraulic and operating conditions.
Stability of emitters and detectors under different operating conditions (e.g. Temperature, humidity).
Reliability of the sensor under hydraulic operating conditions (e.g. Pressure, flow, fluid temperature).
Reliability of the sensor under environmental conditions (e.g. temperature, humidity, vibrations, EMC).
Impact of fabrication/assembly tolerances.
Durability of wettable parts under the continuous contact with target fluid under different status of the fluid (e.g. degraded, contaminated) under different hydraulic and operating conditions.
Installation and operation easiness.

The analysis carried out at this sub-stage should be able to generate verification plans for the individual building blocks as well as for the entire, integrated, system. During this phase, the requirements for the test-benches and specific equipment (e.g. climatic chambers, vibration benches, anechoic chambers) are identified and the test to be performed there are also specified.

During the verification of the sensor, the availability of relevant samples is critical for performing a thorough assessment of the sensors operation, therefore, the verification team should agree with the customer the provision of these sample library. Additionally, the acceptance criteria for all the test is agreed with the customer and the required staff and resources are allocated for accomplishing the verification task, which include among others, the activities listed in the Table 4.6-5.

Table 4.6-5: Activities included in the Verification Approach sub-stage

Activity
Definition of Individual and Integrated Verification plans
Specification of tests
Agree with the customer the availability of representative samples
Agree the acceptance criteria with the customer
Specification of resources to accomplish the tests
Configure and operate the testing equipment
Configure, program and operate the test-benches
Execute the tests
Document the test and provide feedback about the successes

4.6.1.4 Prototype development

This is the sub-stage where the physical implementation of the different building blocks is accomplished. Based on the specifications and simulation results from previous tasks, here the efforts on technical developments ramp-up for having the different modules developed, individually verified and integrated into a working prototype. These prototypes are fed-into the test-benches and testing equipment's for their exhaustive verifications.

Due to the nature of the development already described in section 4.1, different iterations are expected for the prototype refinement until the customer's expectations are meet. Thanks to the agility applied to the development iterations (*build–test–feedback–revise*) these are delivered fast to the customer. These evolving prototypes serve as unique demonstrators for specifying the required sensing capabilities, identifying weaknesses, clarifying uncertainties,

and devising methods for mitigating the risks. The iterative development approach helps shaping the product much better and changes included at this relatively early phase impacts much less in project cost and times (see Figure 4.6-11) because late-stage design iterations (occurring at every product) are avoided [258].

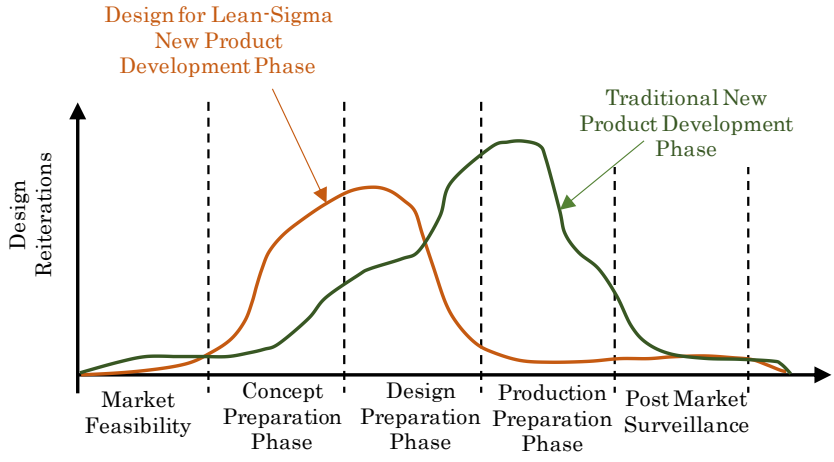

Figure 4.6-11: Example of how the design iterations move backwards on time using novel development technologies as LeanSigma [258].

These prototypes should encompass all the design variations, intermediate designs, etc. that may contribute in increasing the knowledge about the product and about the problem-to-solve. For instance, we may manufacture N different prototype versions where N different light sources are tested because neither the simulation results nor the theoretical studies clarified the most appropriate candidate, so this is solved by prototyping. Notice that prototype development comprises the following steps to be accomplished at each iteration:

- Development of individual building blocks,
- Fabrication and partial verification of individual blocks
- Integration and assembly
- Testing and customer feedback (see next section)

This is the sub-stage where the photonic components are integrated with the rest of blocks to form the photonic sensor. Therefore, a close collaboration with the component provider should be fostered, received their insights about reference designs, integration tips, verification details, etc.

Notice that this stage may represent an intense resource consumer. The technical efforts are high (e.g. 2-3 Full Time Person Efforts during 4-5 months) and the expenses to cover the fabrication of different prototypes are also considerable. Especially during these

early developments, the components, manufacturing and assembly costs are relatively high compared to the final prices and labor costs achieved in the later stages. Thus, the economic impact of each iteration needs to be validated by all the partners.

Additionally, expect an increasing budget allocation to cover the fabrication of an increased number of units at each iteration, even if sometimes components utilized in previous iterations are reused in the later ones. As the design is getting closer to the final specifications, a larger number of units is required for performing the different tests, as depicted in Table 4.6-6.

Table 4.6-6: Number of Units per prototype iteration for the OilWear-Piko® Product.

Iteration	Units	Prototype Example
1	2-3	Figure 4.6-12.a
2	5-10	Figure 4.6-12.b
3	10-20	-
4	10-20	Figure 4.6-12.c
5	40-50	Figure 4.6-12.d

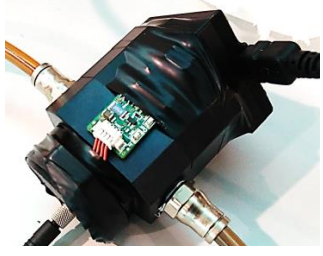

(a)

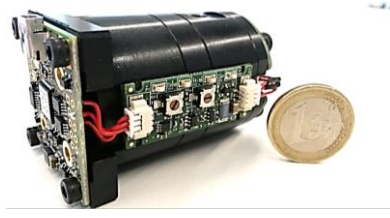

(b)

(c)

(d)

Figure 4.6-12: Examples of different prototypes accomplished during the OW-Piko® sensor design. (a) Concept prototype, (b) improved version, (c) first complete integration and (d) final prototype.

4.6.1.5 Test–Bench Verification

This stage is crucial for accomplishing a thorough verification of the sensor system performance under controlled conditions. These

conditions may be gradually modified towards being much closer to the real working conditions.

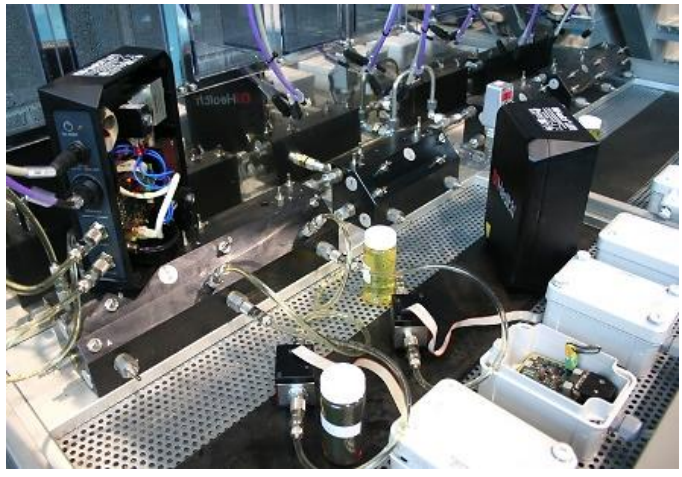

Figure 4.6-13: Example of test bench with different OilHealth® sensors installed simultaneously.

The availability of these kind of test-benches should serve a twofold purpose. First, they need to ease the testing of several units in a row to maximize the generation of results and to assess the sensor's performance, reliability and repeatability and stability of the measurements (see Figure 4.6-13). The second main outcome of the test-benches is to allow a fast test setup modification, either changing the sample under measure or by changing the sample or environmental conditions.

The test-benches are typically used for testing the whole integrated system, but sometimes they are a very useful tool for verifying system's sub–modules as for instance the Wettable parts (see Figure 4.6-14)

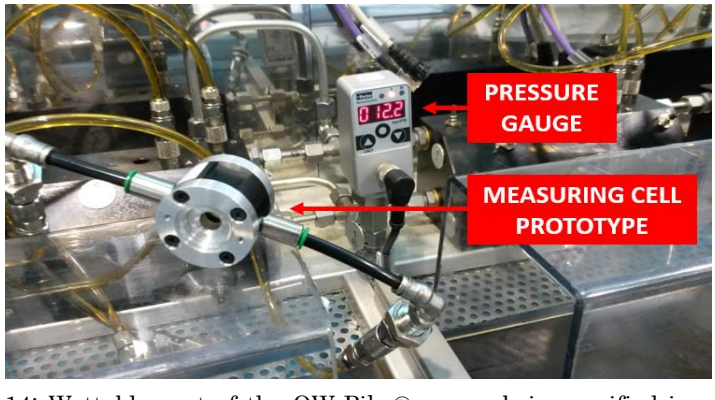

Figure 4.6-14: Wettable part of the OW-Piko® sensor being verified in a test-bench setup.

Notice that it is not required to combine all the test equipment within the same setup. Even if having the complete set of conditions and test parameters available in the same setting would be the ideal situation, this is not always feasible and different test-benches are normally designed or arranged for covering the different testing scenario. Thus, in fluidics sensor verification, it is quite typical to require the following types of test-equipment:

- Sample test bench, where different sensors can be installed in a row and the fluid samples are easily exchanged. These kinds of test-benches may include the option to modify some hydraulic conditions as flow or pressure.
- Hydraulic test bench, with controllable hydraulic conditions as pressure, flow, temperature and viscosity of the fluid.
- Climatic Chamber, with controllable temperature and relative humidity environment.
- Vibrations and shock test bench, with different vibration modes.
- EMC test equipment, to verify the electromagnetic compatibility of the device.

Some other test equipment as Saline mist and condensation chamber or UV irradiation chambers may be required if the sensor enclosure needs to be tested against harsh climatic conditions.

4.6.1.6 Technical and Economic Assessment

This parallel task basically tracks the technical and economic progress of the project at each prototype iteration, because new resource allocation may be required at the end of each iteration loop. The Project Leader is in charge of generating a periodic technical and economic report including the budgetary request for the next planed iteration. This information should be reviewed and accepted by the customer to proceed to the next iteration.

4.6.1.7 Fine–tuning and deployment plan for real scenarios

This is the last sub-stage within the Prototyping phase and includes the minor changes to apply to the prototypes preparing them for their deployment in the real use cases. During this task, the deployment of the prototypes in the real scenarios should be planned, identifying the responsibilities of each party (e.g. designer, customer, and end-user) and quoting the cost of the different activities, consumables, prototypes, etc. Additionally, this stage includes the final set of system specifications and risk identification for answering

the latest definition of the user requirement prepared by the customer. The different topics covered in the deliverables 3.7 Final Version Prototype and 3.8 Validation and Industrialization Plan, which belong to this phase are outlined in the Table 4.6-7.

Table 4.6-7: Topics covered in deliverables 3.7 Final Version Prototype and 3.8 Validation and Industrialization Plan

Item
Final Version Prototype, including all the photonic, mechanic, hydraulic, electronic and software elements integrated in a working prototype
Updated User Requirements
Updated System Specifications
Updated Risk and Uncertainty Assessment
Updated sensor unitary/volume cost estimation
Validation Strategy, Plan and Budget
Draft for system industrialization

4.6.2 Real Field Deployment Decision Gate

The conclusions from the test-bench verifications along with the economical assessment will determine the suitability of moving forward to the real scenarios for the sensor validation. Notice that once the sensor is installed in the field its accessibility will be very limited, and with little room for system modifications and improvements. Additionally, the impact of a sensor failure once at customer's premises may be critical for the system acceptance, and therefore, only sensors with a proven reliability at test-bench scale should move forward to the next stage.

4.7 Validation in real field

4.7.1 Validation and fine-tuning Stage

This stage represents the final validation of the sensor concept. At this point, all the insights gained about the sensor performance concerning measurement quality and system reliability are confronted with real working conditions, real sensor users and real samples.

Notice, that even the best test-bed could only give an approximate and not solid feedback about the sensor behavior. Additionally, normally, it is not even physically possible to simulate or emulate the different working conditions all together, so the coverage of the test performed at test station is, by definition, limited.

Therefore, expect unexpected conditions, unforeseen working modes and odd performances while executing the first set of tests at real deployment.

However, if the development so far has been accomplished in a sensible manner, the probabilities are high for overcoming from these initial disappointments.

The activities start with the sensor installation on end user's site. This might be carried out by the customer technicians, so, by now, the sensor installation may require to be easy enough for not requiring an expert supervisor. However, during the first field tests, it is recommended to accommodate resources for on-site assistance, since the first deployments are always complex and last-minute setting and tuning may be required. The suggestions for including tools enabling sensor remote monitoring, parameterization, performance assessment and even software update becomes a true requirement for sensor developers, and will ease all the validation activities.

Indeed, testing at customer's site, where all the definitive working conditions impact on the sensor together, may evidence some hidden weaknesses in sensor design and even some new and unforeseeable requirement may be included at this moment. Therefore, once sufficient feedback has been acquired, a fine-tuning stage starts, where the conclusions from the real validations are turned into specifications which may be integrated into the prototype system or perhaps leave the implementation for the latter industrialization stage.

4.7.2 Industrialization Decision Gate

This is one of the most important gate so far since it is the responsible for launching the final industrialization of the prototypes, which in terms of economy requirements may represent an amount of several times the already invested budget. Indeed, at this point, all the technical uncertainties and risk must be under control, and only minor concerns may remain in terms of the specific final product cost (e.g. ±5-10%). However, and specially in new products with no previous references in the market, doubts and uncertainties may remain until the final product hits the market, because even if feedback has been gathered from end users so far, their purchasing intentions may change once the final economic conditions are set.

Therefore, the people involved in this gate (technical and economic managers as well as the rest of stakeholders) gate should be responsible of taking the decision and for allocating the required resources based on estimations provided by the project manager.

4.8 Industrialization

This is the final stage, where the product finally crystalizes into an industrial reality. The objective of this stage is to accomplish all the modifications in the previous prototypes to assure the industrialization of the sensor, considering the outsourcing management, manufacturing, assembly and all the processes entailed in the volume production of the sensor system.

Additionally, this is the stage where the knowledge transference should be performed from the design house to the final customer. Actually, in some occasions, the relation may finish at this point because the customer may be able to manage the production by itself, provided that the knowledge transference has been managed in a proper way.

This stage also involves the regulatory and certification processes, and the definition of the product life-cycle management strategy, which in both cases, from this point on, becomes the responsibility of the product owner

Notice that the industrialization is a resource intensive stage, with high expenses not only due to development of the industrial version, but also because of subcontracting for certificate emissions and for the manufacturing of the first pre–series, which require investment in tooling and materials.

4.8.1 Industrialization of prototypes

The industrialization of the sensor system may be straightforward activity depending on the status of the final prototypes. Indeed, more mature prototypes could be reused in a larger extent and will be closer to industrial version. However, some short of redesigning is typically required, either in the electronic hardware, in mechanics or in software.

In addition to the sensor system itself, some extra technical side developments shall start at this stage, including design and fabrication of tools, molds and any other specific development for assisting the manufacturing and assembly of the mechanical parts. If custom optics are required, the associated tooling cost should also be covered during this stage.

Additionally, specific electronic hardware is normally required for series manufacturing of the sensors electronics, which include specific test and programming equipment. Aligned with this activity, additional software and firmware pieces are required by the Electronic Manufacturing Supplier for accomplishing the system factory verifications.

Production, assembly and calibration lines must be prepared and setup in time for the first production batches, which will serve for evaluating the final manufacturing costs because until now, the costs in terms of assembly and calibrations were based on estimations.

During this stage, the strategy for purchase and supplier management should be defined, as well as the production strategy (minimum stocking, delivery times, pre-orders, etc.)

Table 4.8-1: Items covered during the industrialization stage.

Item
Final Version of Hardware, Software, Mechanics and optics
Molds and Tools for series manufacturing of mechanics, optics and sensor embodiments
Test beds for series manufacturing of electronic hardware
Specific firmware and software for verification of electronic hardware
Specific firmware and software for sensor calibration
Production, Assembly and calibration plant
Purchases and supplier management plan
Production strategy: stock, delivery time, order management
Definitive unitary cost of the product

4.8.2 Certification and Regulatory affairs

Even if regulatory requirements have been considered from the early stages of the project, it is not until now when the project-product auditing starts by an authorized body. Indeed, different products may entail different certification and regulatory requirements, but even aside the critical markets as Medical, Automotive, Aeronautics or Military, industrial product certification may represent a difficult challenge to accomplish with.

With the aim of giving a brief overview of potential certifications that may apply to the sort of products covered by this thesis, three main categories may be found.

- Compatibility certifications as the EMC (Europe) or FCC (USA) directives, which defines the electronic compatibility tests and levels to be applied to the product.

- Operation Environment certifications, that normally defines the different tests and conditions at which the product performance must remain unaltered. These tests normally cover the International Protection Marking (IPXX), the temperature and humidity tests, vibrations and shocks, transportation, etc.
- Safety certifications as the UL for the USA market, which looks after electrical, fire, or risk of other nature that may impact of safety of the system users or installers. Additionally, if the sensor system is supposed to be installed and operative in explosive environments, ATEX certification is required, which takes its name from the French directive *Appareils destinés à être utilisés en Atmosphères Explosives*.
- Market Specific Regulations as the Food and Drug Administration (FDA) in the USA that regulates and provides clearance for the use of sensor system at food & beverage industries; or the Det Norske Veritas - Germanischer Lloyd (DNV-GL), formerly two different firms, which provides independent accredited certification services for the renewable energy industry.

Depending on the application, the documentation to be provided include, but are not limited to, user and installation manuals, risk assessments; historic design files describing the development methodology, design inputs and outputs, etc.; record of evidences, etc.

On the other hands, other certifications as the EMC, IP, Vibrations, Temperature, etc. require running real test at the certified body premises to verify that the system under test behaves as expected under the whole environmental condition span. For this purpose, normally specific test-assistance tools are required by the certification technicians.

Figure 4.8-1: The product is not able to reach the market without the corresponding certifications and regulatory clearance.

Be sure to allocate an important budget (several tens of thousands of euros) for accomplishing just the subcontracting of the certification agencies, without considering any possible modification of the product that might be required if any test is not successfully passed. Even if the product owner is the final, and legal, responsible for the regulatory issues, the design house is normally required for assisting the test and for compiling all the design documentation.

4.8.3 Life Cycle Management strategy

The kind of product presented in this thesis are complex product, which may require a continuous assessment of the performance especially when the first units are rolled out in the market. Even if the design house is typically required for giving support to the product owner, they are supposed to stablish a post-sales and life-cycle management strategy to support the product.

All, but specially this kind of advanced products, will require reviews, updates, amendments, etc. and the product owner must stablish an internal structure or a collaboration framework to assist the product launch, operation and maintenance of the sensor (installation, calibrations, etc.), substitution, evolution and disposal. Section 3.1.4 gives an outline of some of the most important points to consider in the life cycle management of sensor systems.

5.

Methodology Validation: Photonic Sensor Examples

While sections 1 to 3 have been focused on explaining the fundaments behind the photonic-sensors for cost effective in-line fluid monitoring, and section 4 describes the proposed methodology for accomplishing the development of such a product, this fifth chapter is all about the practice. Based on the real-world experience of the author in the photonic sensor development, three application scenario that have been benefited from the methodology are presented. First use case describes an in-line microscopy solution for detecting wear particles suspended on industrial fluids. The second use case is an evolution of the first, where holography, lens-free microscopy and stroboscopic photonic technologies are merged for delivering a real time flowing particle detector. The last use case deals with the application of NIR spectroscopy and chemometrics for analyzing alcoholic beverages with an in-line sensor.

5.1 In-Line Microscopy: Wear Debris Sensor

This use case deals with the development of a sensor product for the detection of micro particles suspended in hydraulic fluids. The detection of such wear particles is becoming an important asset for the predictive maintenance strategies since the presence of these microscopic particles is often the symptom of latent or incoming faults in the machines where the fluids are being used.

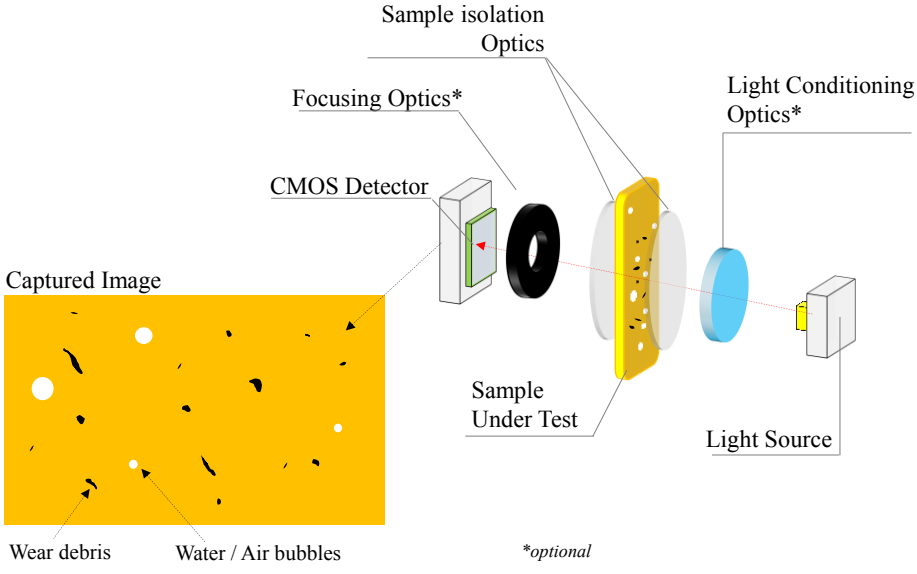

Figure 5.1-1: Working principle of the in-line microscopy. Block diagram depicting a direct imaging wear debris sensor analyzing a flowing lubricant

The working principle is based on a transmissive setup, with white light emitters, a diffuser, two transparent windows, and the light collection subsystem comprising a 2D CMOS imager and a macro lens optics. The optoelectronic system is illuminating a fluid volume, confined between the windows, and capturing a high-resolution image that enables the later detection and classification of solid particles above 4 µm. The key features of the system come not only from its ability to detect, count and classify by size and shape the particles, but also because it is a plug&play sensor, delivering standardized outputs (ISO normalized data over Modbus RTU or Modbus TCP) in a compact setting, and at very effective cost.

Indeed, the development of such a system, with no reference in the market was far from being a straightforward integration. The uncertainties where more than the specifications and the multi domain nature of the technology jeopardized any direct development. Therefore, a set of evolving prototypes were manufactured, each of them with incremental features answering to the newly discovered requirements. These prototypes were tested not only by the customer

(vendor of the technology) but also by end users who gave invaluable feedback that allowed having the right product at the right time.

Figure 5.1-2: OilWear S100 version (Atten2, Advanced Monitoring Technologies), the sensor module and the particularized embodiment for wind turbine applications.

Requirements in terms of reliability but without compromising the target cost effectiveness also hindered the time to market, due to the long verification periods. However, thanks to the use of specific test benches, the impact of these intensive testing sessions was kept under control.

The outcomes of this research and developments efforts where put together in an already accepted patent [259] and are now core part of a successful line of products of the Atten2 Advanced Monitoring Technologies in the field of in-line wear particle counting and classification (see Figure 5.1-2). Currently the devices are being used in wind turbines all over the world; it is also being installed on high load hydraulic and equipment in USA and Korea for serving automotive industry; the sensor is also being used for monitoring the status of gas turbines, compressors, presses, etc.

5.2 Lens Free and Stroboscopic Lighting: Next Generation of Wear Debris Sensor

This second use case, even if aligned with the wear detection applications, presents three completely different photonic technologies to accomplish several major changes to in-line microscopy approach followed by the Wear Debris Sensor of the section 5.1. While the operation of the previous development was based on light transmission and a macro focus system, the new developments integrated holography, lens-free imaging and stroboscopic lighting to remove the macro lens and allows working in continuous flow enabling the detection of particles below the 4 µm.

Achieving the aforementioned enhancements allows the OilWear product moving one step forward in terms of lowering the cost (avoid the macro lens) and size of the system, enabling a true hydraulic plug&play thanks to the compatibility with continuous flows, and reducing the minimum resolvable particle. However, the integration of holography and diffraction processes to setup a lens-free microscope presented several difficulties, because, even if it is well known technique, with several developments (specially from 2010 on), these have been always focusing to biological samples and low pressure; a scenario which has little in common with the highly absorptive and pressurized industrial fluidics.

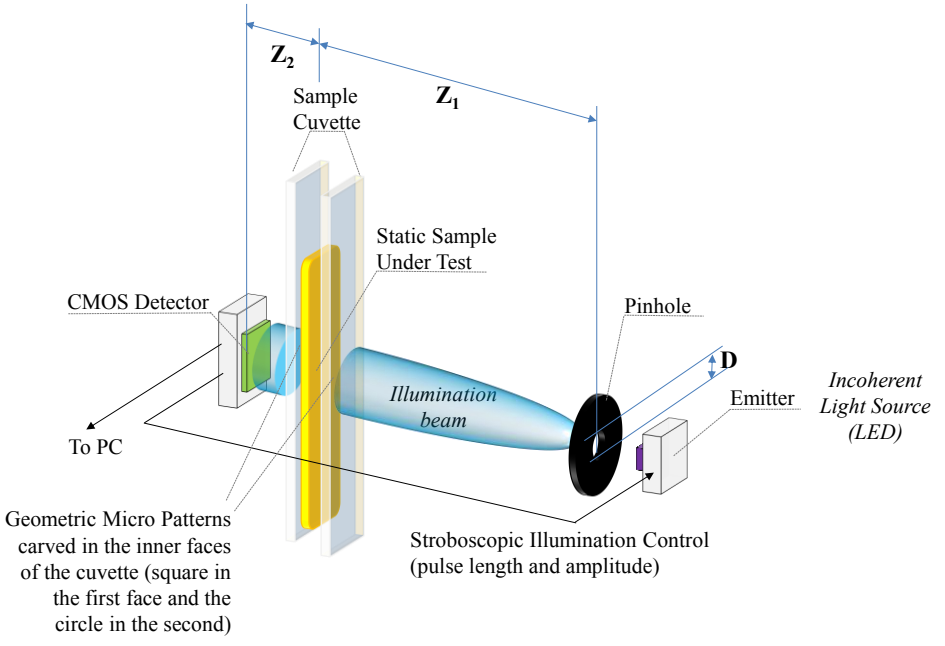

Figure 5.2-1: Schematic diagram of the Lens-Free sensor setup.

The situation was even worse because non-stationary samples had to be monitored to allow an effective particle detection on running fluids. Therefore, in addition to the spatial filtering of the light radiation required for generating the holographic pattern for the lens free operation, imaging moving objects requires to illuminate the sample during very short time slots (stroboscopic imaging). Thus, the available net light power was a real challenge in the prototype hypothesis.

Again, in order to assess the feasibility of the envisaged product idea, several simulations and prototyping sessions were accomplished iteratively, being some of them already used as examples during the methodology description in Chapter 4. A detailed description of the operation and working principles is described in [260] and [261].

During the prototype phases, two parallel development were followed, the first one dealt with the pure lens free operation setup, focusing on static hydraulic fluids (see [260] and Figure 5.2-1), while the second focused on the flowing particles part of the problem. When both investigations delivered relatively successful and potentially patentable results, (already submitted and pending approval [262][263]), the integrated approach was launched, as described in [261] (see Figure 5.2-2).

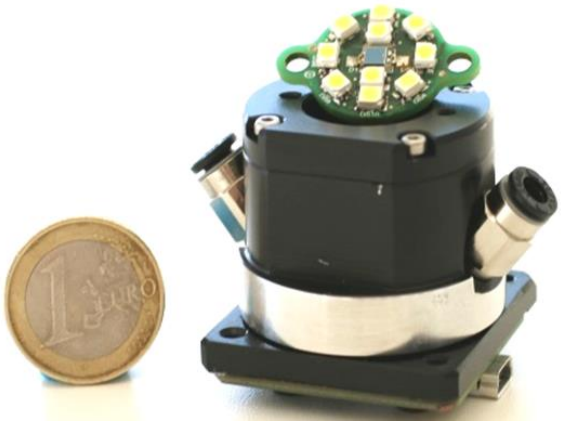

Figure 5.2-2: Prototype of Lens-Free sensor integrating the stroboscopic lighting system.

However, even if the scientific results demonstrated the feasibility of the Lens-Free sensor for flowing objects, the risks and uncertainties for having a reliable product jeopardized the whole product development. Therefore, at that GATE, the decision was to leave a part of the developments for the future, but to integrate the pieces of technology offering the highest confidence to the whole decision team.

Thus, lens-free operation was replaced by the lens based one but the system was enhanced with the stroboscopic lighting system and the integrated electronics, delivering a totally new product.

The figures summarizing this development are 2 patents issued and waiting for approval, and one new product (see Figure 5.2-3) which halves the price of the original version, in a much smaller form factor, offering a total new functionality enabling the monitoring of continuous flows. Additionally, even if the lens-free line was eventually stalled, it is now part of the new development lines with the aim of achieving sub-micron resolutions. It took around 16 months from the concept to the pre-series manufacturing, employing approximately 2.5-3 FTP effort.

Figure 5.2-3: Oilwear PIKO version (Atten2, Advanced Monitoring Technologies), renovated version of OilWear device including the outcomes from the developments of section 5.1 and section 5.2.

5.3 NIR Spectroscopy for Fluid Monitoring: Cider and Wine Use Cases

The last use case is focused on the integration of VIS-NIR spectroscopy in transmissive setup for the monitoring of the fermentation process of cider and wines. The objective of this kind of sensors is to monitorize the process of the alcoholic fermentation, which basically comprises the gradual conversion of glucoses and fructose molecules to Ethanol. Both molecular groups present absorption lines in the NIR (SWIR) range: CH3 and CH2 groups of Ethanol present at 1670-1780nm with the first overtone of the CH-stretch; 2200-2300 nm with the absorption of glucoses; at 380-780nm the phenolic compounds (anthocyanin); and at 1450 and 1950 nm the first overtone of the OH stretch is present, due to the water and ethanol molecules-

The solution integrates not only the sensor hardware but also the chemometric algorithms for delivering an estimation about the fermentation state rather than only providing RAW spectral information.

Due to technological availability of low cost spectrometers, the development started with a VIS-NIR spectrometer in the range of 400–1100 nm, but during the project development, larger wavelengths

become available at integrated spectrometer versions. The work accomplished for cider monitoring is referenced in [264].

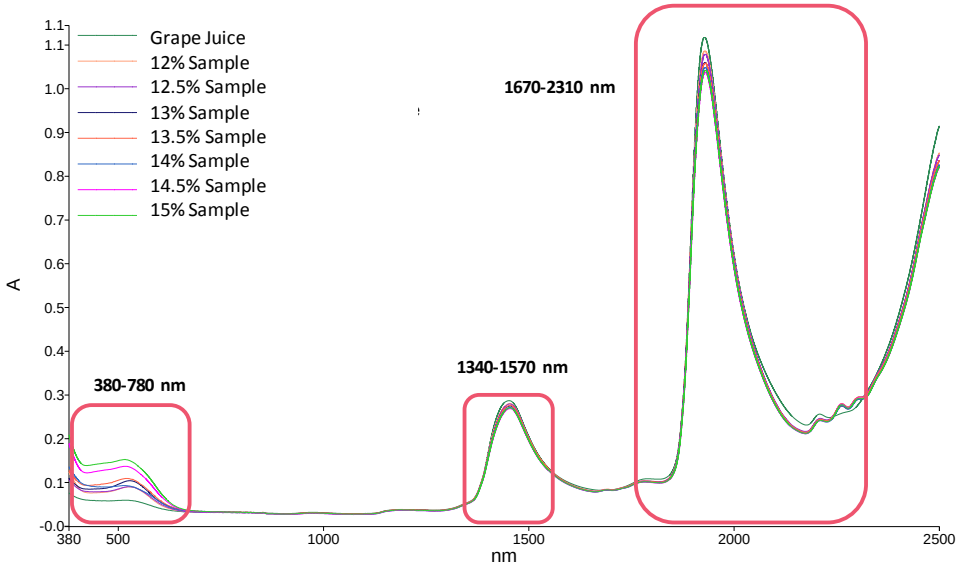

Figure 5.3-1: Absorbance spectra from different samples with incremental alcoholic concentration. As the alcohol concentration rises, the absorbance around 1670-1780nm increases.

Based on the feasibility study accomplished with the cider, the development of a compact and low version of the sensor was launched (see Figure 5.3-2), integrating a tungsten light source, sapphire windows, a collimating lens and a 1700 – 2200 nm spectrometer. The prototype was designed for operating on immersion mode, submerged in the wine/cider barrel using the cork hole (see Figure 5.3-3).

Figure 5.3-2: Detail of the NIR prototype, with the 1 mm slit designed to be filled by capillary forces of the fluid.

Figure 5.3-3: Wine-NIR prototype immersed in a barrel through the cork hole.

The work accomplished so far has led to a patent submission [265], but the cost of the prototypes is still too high, hindering the decision for the industrialization of the system. Newest spectrometers being launched during the 2017 are, however, opening new opportunities to move on the development of a second generation of devices based on the IPs and insights gathered with the early versions of the system. Actually, the knowledge in the field of the in-line chemometric analysis has also driven other families of products in the field of food sorting by reflectance measurements as the ones presented in the patent application [266].

6.
Conclusions

This chapter includes a discussion about the most significant results presented in this thesis together with the concluding remarks and the identified future research lines. The opportunity–challenge paradox, entailed in the outlook of photonics-based fluidics sensors, is highlighted as the main driver of the work accomplished during this thesis. In this context, a methodological hybrid and agile integration of photonic components within the rest of subsystems towards a sensor product development is presented as the main outcome of the thesis. The methodology has been validated in several industrial scenarios, being three of them included in this book, which covers from hydraulic fluid quality control and real-time monitoring of alcoholic beverage fermentation process.

Additionally, the future research lines are outlined, including some specific developments already requested by the industry, setting out new paradigms of the opportunity-challenge binomial in the landscape of photonics-enabled in-line fluidic sensors.

6.1 Low Cost Photonic Sensors, the opportunity-challenge paradox

It is evident that the paradigm of process monitoring has evolved in the last years, driven by a clear necessity for improving the production efficiency, quality and safety of products and processes. In this context, so-called Industry 4.0, sectors as manufacturing, energy, pharma, food and beverages, etc. are fostering the adoption of innovative methods for controlling their processes and products, in a non-destructive, in-place, reliable, fast, accurate and cost-efficient manner. Furthermore, the parameters of interest requested by the industry for the quality assessment are evolving from basic magnitudes as pressures, temperatures, humidity, etc. to complete chemical and physical fingerprints of these products and processes.

In this situation, the measurement techniques based on the UV/VIS/IR light-matter interaction appear to be optimum candidates to face the request of the industry. Moreover, at this moment, when we are witnessing a technological revolution in the field of optoelectronic components, which are required for setting up these light-based analyzers. A complete range of cost effective, compact and feature rich emitters, detectors, modules is being launched to the market paving the way for developing photonic sensor products.

Thus, the opportunity is, clear: the industry requests sensor systems, photonics arises as optimum candidate for answering their needs, and the fundamental pieces for delivering a complete solution are becoming a reality. However, being able to integrate these optoelectronic components with the rest of subsystems (electronics, optics, mechanics, hydraulics, data processing, etc.) is not straightforward.

The development of these multi-domain and heterogeneous sensor products, meeting not just technological but also market objectives, poses a considerable technical and organizational challenge for any company. The synchronizing of multidisciplinary working teams, the pressure to cut development times to launch new products into the market, and the complexity inherent in the technological bases of this kind of product, need to be managed efficiently throughout the design, development, validation and certification phases of the photonics-enabled sensors.

The review of the different development models concludes that even if these different processes propose interesting contributions, no one provides a comprehensive coverage for the kind of product we are presenting.

Therefore, a custom methodological solution is presented as the main outcome of the thesis, with the aim of answering the concerns

and curiosities of Research and Development Teams, Design houses or Engineering teams facing the design of Cost Effective Photonic Sensor Products for in-line fluid analysis.

6.2 Methodological Hybrid and Agile Integration for sensor product development

With the aim of fulfilling the requirements of the abovementioned situation, a custom methodology has been proposed to guide and help Engineering teams in the different steps from the proof-of-concept to the product launch in the area of photonic sensor systems. The thorough revision of the traditional and innovative methods for managing the development of complex technological projects involving a high hardware load, concluded that these methodologies were lacking important features for an effective management of the uncertainties, lack of specifications and risks in a multi domain environment.

The reason behind this lack of information and knowledge about the product is because, normally, the sort of sensors addressed by this methodology are novel devices. This novelty is generated either because the sensors target a new application scenario, which is quite common situation for the in–line sensors as they replace an off–line laboratory method but the conditions for the in–line operations are unclear. Alternatively, the novelty may be justified because, even if other sensor technologies might cover an application, the integration of photonic measurement principles for that specific case has not been tackled previously.

Therefore, assuming the Stage-Gate model as starting point, and taking contributions from Agile, Open Innovation, Lean and Six Sigma, a customized product development approach has been proposed. The methodology splits the development in five stages (Opportunity identification, Proof-of-Concept validation, Design of Prototypes and Test Benches, Validation in Real Field and Industrialization) but identifies specific activities, responsibilities and deliverables on each of them. Indeed, the focus is put on the integration of photonic components into complete smart sensor systems for delivering in-line and real-time measurement solutions in the field of industrial fluidics. The proposed methodology has been validated in several real industrial sensor domains and three of them have been included as use cases.

The main conclusions about the application of the methodology for the development of cost effective photonic sensors for in-line fluidics monitoring, is that it helps cutting the development times,

allows tailoring the product to the exact customer evolving demands without hindering the development cost, maximizes the exploitation of the generated IP cores, and assures the compliance with the identified regulations.

6.3 Future research lines

Three main reasons motivate the continuity in the structuration of a development process in the field of photonics sensors: (i) enabling the integration of new but complex core measurement techniques and increasing the autonomy of the deployed sensors; (ii) minimizing their maintenance and calibration needs and maximizing the lifetime; (iii) and providing the means for delivering hardware independent solutions.

Processes like Raman Spectroscopy presents important advantages in the field of fluid monitoring, especially due to its immunity against the interferences of water molecules. However, the required excitation powers, low detection limits and strict optical tolerances hinder the development of low cost and in-line solutions and push the limits of the proposed methodological approach.

On the other hand, the durability of optic sensors, in a continuous exposure to harsh fluid conditions is also a factor limiting the total and long-term autonomy of in-line photonic sensors. Solutions like protective coatings, the use of micro-actuated white tiles for self-calibration, etc. need to be incorporated to the photonic sensors and the methodology requires evolving to consider these new requirements.

Additionally, newer components, with better features, lower costs and higher compactness will continuously be hitting the market specially in the forthcoming years. Sensor product developers need tools for integrating new photonic components without being required to modify to legacy development (e.g. chemometrics or machine vision algorithms). Thus, the development methodology will also have to deal with this required hardware agnosticism to allow rapid migration to newer platforms.

7.

References

[1] Lee, J., Bagheri, B., Kao and H. A. (2015). A Cyber-Physical Systems architecture for Industry 4.0-based manufacturing systems. Manufacturing Letters, 3, pp. 18-23.

[2] Evans P.C. and Annunziata M., (2012). Industrial Internet: Pushing the Boundaries of Mind and Machines. White paper, General Electric.

[3] Drath R. and Horch, A. (2014). Industry 4.0 Hit or Hype? IEEE Industrial Electronics Magazine, 8(2), pp 56-58.

[4] Franklin, C. (2015). General Electric Announces Predix Cloud, The World's First Cloud Service Built for Industrial Data and Analytics. Press Release, General Electric, New York, NY, USA.

[5] Gantz, J. and Reinsel, D. (2012). The Digital Universe in 2020: Big Data, Bigger Digital Shadows, and Biggest Growth in the Far East. Report, International Data Corporation (IDC), retrieved from: https://www.emc.com/collateral/analyst-reports/idc-the-digital-universe-in-2020.pdf (accessed on 14/05/2017)

[6] Evans, D. (2011). The Internet of Things. How the Next Evolution of the Internet Is Changing Everything. White Paper, Cisco, retrieved from: http://www.cisco.com/web/innov/IoT_IBSG_0411FINAL.pdf (accessed on 16/04/2017)

[7] Simonds, D. (2016). Siemens and General Electric gear up for the internet of things. Press Article, The Economist, New York, USA, December 3, 2016. Retrieved from: http://www.economist.com/news/business/21711079-american-industrial-giant-sprinting-towards-its-goal-german-firm-taking-more (accessed on 16/05/2017)

[8] General Electric (2016). PREDIX, The industrial Internet Platform. White paper, General Electric Company.

[9] Möller, M. (2016). Industry 4.0 in action at Bosch Rexroth Homburg facility. White paper, Rexroth, Bosch Group.

[10] Hoenicke, C. (2016). Intelligent sensor systems for Industry 4.0. Press Release, Bosch Group, May 27, 2016.

[11] Thomä, M. (2016). Machine monitoring with smart sensors. Press Release, Bosch Group, July 26, 2016.

[12] Bertheau, T. (2016). ABB's new condition monitoring solution is a quantum leap for millions of motors. Press Release, January 21, 2016.

[13] Honeywell (2013). Analytical Sensors and Measurement Solutions. Brochure, Honeywell, retrieved from: https://www.honeywellprocess.com/library/marketing/brochures/HPS-SmartSensors-Analytical-Instruments-Brochure.pdf (accessed on 17/05/2017)

[14] Honeywell (2017). SmartLine Temperature Transmitters, Modular, Accurate and Reliable for the Lowest Cost of Ownership. Brochure, Honeywell, retrieved from: https://www.honeywellprocess.com/library/marketing/brochures/smartline-temperature-transmitter-brochure.pdf (accessed on 17/05/2017)

[15] Grönzin, H. (2017). Fit for Industry 4.0 with smart sensor business 4.0. White Paper, Leuze Electronics, retrieved from: http://www.leuze.it/media/assets/whitepaper/WP_I40_Smart_Sensor_Business_40_en.pdf (accessed on 20/04/2017).

[16] Lorenz, M., Rüssman, M., Strack, R. and Bolle, M. (2015). Man and Machine in Industry 4.0. White Paper, Boston Consulting, retrieved from:http://www.bcg.com.cn/en/files/publications/reports_pdf/BCG_Man_and_Machine_in_Industry_4_0_Sep_2015_ENG.pdf (accessed on 17/05/2017).

[17] Coronado, D. and Kupferschmidt, C. (2014). Assessment and Validation of Oil Sensor Systems for On-line Oil Condition Monitoring of Wind Turbine Gearboxes. Procedia Technology, 15, pp. 747-754.

[18] Amin, M., Majid, A. and Fudzin, F. (2017). Study on Robots Failures in Automotive Painting Line. ARPN Journal of Engineering and Applied Sciences, 12(1), pp. 62-67.

[19] Sumit, P., Legner, W., Krenkow, A. et al. (2010) Chemical Contamination Sensor for Phosphate Ester Hydraulic Fluids. International Journal of Aerospace Engineering, 2010, 156281.

[20] Kress-Rogers, E., Brimelow, C. (2001), Instrumentation and Sensors for the food Industry, CRC Press, Woodhead Publishing Limited, Cambridge, England, pp. 404-405.

[21] GEM Sensors (2017). Tackling Tough Fluid Sensing Challenges. White paper, GEM Sensors, retrieved from: http://www.gemssensors.com/
(accessed on 26/03/2017)

[22] (ed.) Bøving, K. G. (2014). NDE handbook: Non-destructive examination methods for condition monitoring. Butterworths, Silkerborg, Denmark, pp. 286-295.

[23] Qin, S. J. (2014). Process data analytics in the era of big data. AIChE Journal, 60(9), pp. 3092-3100.

[24] LIM, S. A. H., Jiju, A. and, Saja, A. (2014). Statistical Process Control (SPC) in the food industry–A systematic review and future research agenda. Trends in food science & technology, 37(2), pp 137-151.

[25] Bennet, S. (1993). A History of Control Engineering, 1930-1955. IEE Control Engineering series, 47, London, UK, pp. 28-34.

[26] Bennett, S. (1994). Automatic on-line fluid monitoring. Industrial Lubrication and Tribology, 46(4), pp.8-9.

[27] Yokogawa (2012). Flowmeter History. White Paper, LF 01E00A00-03EN, 2nd Edition, Yokogawa, retrieved from: https://web-material3.yokogawa.com/LF01E00A00-03EN.us.pdf
(accessed on 2017/04/28)

[28] Wemyss, C. (2017). Next Generation Flowmeters for Fluid Measurement and Control Solutions. White Paper, Litre Meter Ltd. Retrieved from: http://litremeter.info/tag/flowmeter-history/
(accessed on 2017/04/28)

[29] Pinto, J. (2010). Brief history of Industrial Instrumentation. InTech Magazine, ISA publications, January-February 2010.

[30] Dunn, W. C. (2006), Introduction to Instrumentation, Sensors, and Process Control. ARTECH HOUSE, INC, Boston,

[31] Yoder, J. (2003). Flow Meters and Their Application; an Overview. Sensors Magazine, 20 (10).

[32] Desmarais, R., and Breuer, J. (2001). How to Select the Right Temperature Sensor. Sensors Magazine, 18(1), January 2001.

[33] Wilson, J. S. (2003). Pressure Measurement Principles and Practice. Sensors Magazine, 20(1).

[34] ISO 7027-1 (2016). Water quality, Determination of turbidity, Part 1: Quantitative methods. International Organization for Standardization.

[35] Roveti, D. K. (2001). Choosing a Humidity Sensor. A Review of Three Technologies. Sensors Magazine, 18(7).

[36] Radiometer Analytical SAS, (2004). Conductivity Theory and Practice. White paper, Radiometer Analytical SAS, retrieved from: http://www.analytical-chemistry.uoc.gr/ (accessed on 2017/04/17).

[37] Hambrice, K., and Hooper, H. (2004). A Dozen Ways to Measure Fluid Level and How They Work. Sensors Magazine, 21(12).

[38] Gungor, V. C. and Hancke, G. P. (2009). Industrial Wireless Sensor Networks: Challenges, Design Principles, and Technical Approaches. IEEE Transactions On Industrial Electronics, 56(10), pp. 4258–4265.

[39] (ed.) Alioto, M. (2017). Enabling the Internet of Things: From Integrated Circuits to Integrated Systems, Springer International Publishing, Basel, Switzerland, pp. 35-36.

[40] (ed.) Wilson, J. (2005). Sensor Technology Handbook, Volume 1, Newnes, Elsevier, Burlington, MA, USA, pp. 591-597.

[41] Willner, A. E. et al. (2012). Optics and Photonics: Key Enabling Technologies. Proc. IEEE, Special Centennial Issue, 100, pp. 1604-1643.

[42] (ed.) Zheludev, N. I. (2009). The next photonic revolution. J. Opt. A: Pure Appl. Opt., 11, pp. 1-2.

[43] Forbes, H. (2016). The IIoT Edge: Why is Industrial Sensing Difficult and Expensive?.retrieved from: https://industrial-iot.com/2016/05/iiot-edge-industrial-sensing-difficult-expensive/ (accessed on 2017/03/28)

[44] Miller, S. E. (1969). Integrated optics: an introduction. Bell Syst. Tech. J., 48, pp. 2059– 2069.

[45] Smit, M., Tol, J. and Hill, M. (2012), Moore's law in photonics. Laser & Photon. Rev., 6, pp. 1–13.

[46] M. Smit et al. (2012). A generic foundry model for InP-based photonic ICs. OFC/NFOEC, Los Angeles, CA, pp. 1-3.

[47] Nomoto, T., Oike, Y. and Wakabayashi, H. (2016). Accelerating the Sensing world through imaging evolution. VLSI Circuits (VLSI-Circuits) 2016 IEEE Symposium on, pp. 1-4

[48] Sanderson, S. W. and Simons, K. L. (2012). Light Emitting Diodes and the Lighting Revolution: The Emergence of a Solid-State Lighting Industry. Rensselaer Polytechnic Institute, NY, USA.

[49] Wang, Y., Alonso, J. M. and Ruan, X. (2017). A Review of LED Drivers and Related Technologies. IEEE Transactions on Industrial Electronics, 99, pp. 1-1.

[50] Kim, J. K., Krames, M. R., Tu, L. W. and Strassburg, M. (2017). Proc. SPIE 10124 Light-Emitting Diodes: Materials, Devices, and Applications for Solid State Lighting XXI, 10124.

[51] Reichl, M. (2016). Osram presents the world's first broadband infrared LED. Osram, Regensburg, November 4, 2016, retrieved from: https://www.osram.com/os/press/press-releases/
(accessed on 2017/04/14)

[52] Cambou, P. and Jaffard, J. L. (2016). Status of the CMOS Image Sensor Industry 2016: New Market and Technology Dynamics. Yole Technologies, Market Report, Lyon, France.

[53] (ed.) Bannon, D. P. (2016). Hyperspectral Imaging Sensors: Innovative Applications and Sensor Standards 2016. Proc. SPIE, 9860.

[54] Warren, M. E. (2014). Micro-opto-electro-mechanical Systems (MOEMS). Access Science, McGraw-Hill Education, 2014.

[55] Fischer, A. C., Forsberg, F., Lapisa, M., Bleiker, S. J., Stemme, G., Roxhed, N. and Niklaus,F. (2015). Integrating MEMS and ICs. Nat. Microsyst. Nanoeng., 1, pp. 15005.

[56] Ford, J. (2005). Optical Mems: A Brief History and Future Trends. Mems Journal, 10 (8), pp.45-46.

[57] Antila, J., Tuohiniemi, M., Rissanen, A., Kantojärvi, U., Lahti, M., Viherkanto, K., Kaarre, M. and Malinen, J. (2014). MEMS- and MOEMS-Based Near-Infrared Spectrometers. Encyclopedia of Analytical Chemistry, John Wiley & Sons, Lt, pp. 1–36.

[58] Havermeyer, F., Ho, L. and Moser, C. (2012). Discrete Tunable Laser for 3D Imaging. International Conference on Optical MEMS and Nanophotonics, Banff, AB, 2012, pp. 11-12.

[59] Jayaraman, V., Jiang, J., Potsaid, B., Cole, G. and Fujimoto, J.C.A. (2012). Design and Performance of Broadly Tunable, Narrow Line-width, High Repetition Rate 1310nm VCSELs for Swept Source Optical Coherence Tomography. Proc. SPIE, 8276, 1–10.

[60] Sinning, S., Wullinger, I., Schmidt, J.-U., Friedrichs, M., Dauderstädt, U., Wolschke, S., Hughes, T., Pahner, D. and Wagner, M. (2012). One dimensional light modulator. Proc. SPIE 8252, MOEMS and Miniaturized Systems XI, 82520H.

[61] Johnson, R. C. (2010). Optical MEMS finally arriving. MEMS Journal, retrieved from:
http://www.memsjournal.com/2010/08/optical-mems-finally-arriving.html
(accessed on 2017/03/01)

[62] Kantojärvi et al. (2015). MEMS spectral sensors bring laboratory measurements to field use. Laser and Photonics, 10(1) pp. 66- 69.

[63] Parr, A. C. (2001). The Candela and Photometric and Radiometric Measurements. Journal of Research of the National Institute of Standards and Technology, 106(1), pp. 151–186.

[64] J. Flammer et al. (2013). Basic Sciences in Ophthalmology. Springer-Verlag Berlin, Germany, pp. 20-35.

[65] (ed.) Calmers, J.M. and Dent, G. (1976). Industrial Analysis with Vibrational Spectroscopy. The Royal Society of Chemistry, Cambridge, UK.

[66] Qingbo, F. (2012). Short-Wave Near- Infrared Spectrometer for Alcohol Determination and Temperature Correction Journal of Analytical Methods in Chemistry, 2012, Article ID 728128.

[67] Wulfert, F. and Smilde K. (1998). Influence of Temperature on Vibrational Spectra and Consequences for the Predictive Ability of Multivariate Models. Anal. Chem., 70, pp. 1761-1767.

[68] Scheeline, A. (2016). What must be specified to achieve a valid spectroscopic measurement? Hamamatsu Articles, retrieved from:
http://www.hamamatsu.com/us/en/community/optical_sensors/article/scheeline_spectroscopic_measurement/index.html
(accessed on 2017/17/04)

[69] (ed.) Polfer, N. C. and Dugourd, P. (2013). Laser Photodissociation and Spectroscopy of Mass-separated Biomolecular Ions. Lecture Notes in Chemistry 83, Springer International Publishing, Basel, Switzerland.

[70] Gong, Y. J. et al. (2016). A unique approach toward near-infrared fluorescent probes for bioimaging with remarkably enhanced contrast. Chem. Sci., 7, pp. 2275-2285.

[71] Abramowitz, M. and Davidson, M. W. (2015). Fluorescence: Overview of Excitation and Emission Fundamentals. The Florida State University, retrieved from: https://micro.magnet.fsu.edu/primer/lightandcolor/fluoroexcitation.ml (accessed on 2017/05/16).

[72] O'Sullivan, T. D., Heitz, R. T., Parashurama, N., Barkin, D. B., Wooley, B. A., Gambhir, S. S. and Levi, O. (2013). Real-time, continuous, fluorescence sensing in a freely-moving subject with an implanted hybrid VCSEL/CMOS biosensor. Biomedical Optics Express, 4(8), pp. 1332–1341.

[73] Banwell, C. N., (1972). Fundamentals of Molecular Spectroscopy. McGraw-Hill, Berkshire, UK, pp. 121-156.

[74] Struve, Walter S., (1989). Fundamentals of Molecular Spectroscopy, John Wiley & Sons, New York, NY, USA, pp. 307-330.

[75] Davis, B. J., Carney, P. S., and R. Bhargava, (2010). Theory of Mid-infrared Absorption Micro-spectroscopy: II. Heterogeneous Samples. Analytical Chemistry, 82(9), pp. 3487–3499.

[76] Davis, B. J., Carney, P. S., and R. Bhargava, (2010). Theory of Mid-infrared Absorption Micro-spectroscopy: I. Homogeneous Samples," Analytical Chemistry, 82(9), pp. 3474–3486

.

[77] Yamamoto, K. and Ishida, H. (1997). Kramers-Kronig analysis applied to reflection-absorption spectroscopy. Vibrational Spectroscopy, 15(1), pp. 27-36.

[78] Jacques, S.L. (2013). Optical properties of biological tissues: a review. Phys. Med. Bio., 58 (11), pp. R37-R61.

[79] Saccomandi, P. et al., (2014). Estimation of anisotropy coefficient and total attenuation of swine liver at 850 nm based on a goniometric technique: Influence of sample thickness. Proc. IEEE Eng. Med. Biol. Soc., pp. 5332-5335.

[80] Pu, Y., Chen, J. and Wang, W. (2014). Investigation of scattering coefficients and anisotropy factors of human cancerous and normal

prostate tissues using Mie theory. Proc. SPIE 8941, Optical Interactions with Tissue and Cells XXV; and Terahertz for Biomedical Applications, 894115.

[81] Mignon, C., Rodriguez, A., Palero, J., Varghese, B. and M. Jurna, (2016). Fractional laser photothermolysis using Bessel beams. Biomed. Opt. Express, 7, pp. 4974-4981.

[82] Armaroli1, T., Bécue, T. and Gautier, S. (2004). Diffuse Reflection Infrared Spectroscopy (DRIFTS): Application to the in situ Analysis of Catalysts. Oil & Gas Science and Technology – Rev. IFP, 59(2), pp. 215-237.

[83] Workman, J. (2016). The Concise Handbook of Analytical Spectroscopy: Theory, Applications, and Reference Materials. Volume 3. World Scientific Publishing, London, UK, pp. 52.

[84] Hamamatsu, Solid State Division (2017). Technical Information LEDs. Hamamatsu, retrieved from: http://www.hamamatsu.com/resources/pdf/ssd/led_kled9001e.pdf (accessed on 2017/02/01).

[85] Grum, F., Saunders, S. B. and Macadam, D. L. (1978). Concept of correlated color temperature. Color Res. Appl., 3, pp. 17–21.

.

[86] Osram (2001). Led Fundamentals, Thermal Characteristics of LEDs. Osram Opto Semiconductors, retrieved from: https://ledlight.osram-os.com/wp-content/uploads/2013/01/OSRAM-OS_LED-FUNDAMENTALS_Thermal-Characteristics-of-LEDs_v2_08-16-11_SCRIPT.pdf (accessed on 2017/02/13)

[87] Olafsen, L. J., Ice, L. D. and Ball, B. (2012). Nonlinear Temperature Dependence of Resonant Pump Wavelengths in Optical Pumping Injection Cavity Lasers. IEEE Journal of Selected Topics in Quantum Electronics, 17(5), pp. 1453-1459.

[88] Excelsys. Driving Halogen Lamps. Application Note 1604, Excelsys, retrieved from: http://www.excelsys.com/wp-content/uploads/2016/07/AN1604_Driving_Halogen_Lamps.pdf (accessed on 2017/03/14).

[89] Muramoto, Y., Kimura, M. and Nouda, S. (2014). Development and future of ultraviolet light-emitting diodes: UV-LED will replace the UV lamp. Semicond. Sci. Technol., 29, 084004.

[90] Liangfeng, S. et al. (2012). Bright infrared quantum-dot light-emitting diodes through inter-dot spacing control. Nature Nanotechnology, 7, pp. 369–373.

[91] Thorlabs (2009). Supercontinuum Generation in Photonics Crystal Fibers. Thorlabs Application Note, retrieved from: https://www.thorlabs.com/images/TabImages/SupercontinuumGeneralApplicationNoteThorlabs.pdf
(accessed on 2017/02/25).

[92] Michalzik, R. and Ebeling, K. J. (2003). Operating Principles of VCSELs. Chapter 3, in Vertical-Cavity Surface-Emitting Laser Devices, Springer Series in Photonics, 6, pp. 53-98.

[93] Overton, G. (2013). VCSEL Illumination: High-power VCSELs rule IR illumination. Laser Focus World, 49(08).

[94] O'Sullivan, T. D., Munro, E., Harris, J. S. and Levi, O. (2010). Fabrication of an integrated 670nm VCSEL-based sensor for miniaturized fluorescence sensing. Proc. SPIE, Vertical-Cavity Surface-Emitting Lasers XIV, 76150D.

[95] Van der Lee, A., Carpaij, M., Monch, H., Schemmann, M. and Pruijmboom, A. (2008). A miniaturized VCSEL based sensor platform for velocity measurement. Proc. IEEE Instrumentation and Measurement Tech. pp. 141-143.

[96] Maute, M. and Amann, M. C. (2004). Long-wavelength VCSELs. Proc. Indium Phosphide and Related Materials (IRPM), pp. 695-699.

[97] Koerperick, E. J. (2009). High power mid-wave and long-wave infrared light emitting diodes: device growth and applications. Thesis, University of Iowa.

[98] Weise, S., Steinbach, B. and Biermann, S. (2016). MEMS-based IR-sources. Proc. SPIE, 9752, 97521E 7.

[99] Chowdhury, M. F., Hopper, R., Ali, S. Z., Gardner, J. W. and Udrea, F. (2016). MEMS Infrared Emitter and Detector for Capnography Applications. Procedia Engineering, 168, pp. 1204 - 1207.

[100] Ali, S. Z. et al (2015). A Low-Power, Low-Cost Infra-Red Emitter in CMOS Technology. IEEE Sen Jour, 15(12), pp. 6775 – 6782.

[101] Calaza, C., Salleras, M., Sabaté, N., Santander, J., Cané, C. and Fonseca, L. (2012). A MEMS-based thermal infrared emitter for an integrated NDIR spectrometer. Microsystem Technologies, 18(7-8), pp. 1147-1154.

[102] Hossein, L. et al. (2013). Narrow-bandgap photovoltaic devices operating at room temperature and above with high open-circuit voltage. Applied Physics Letters, 102(21), 10.1063.

[103] Kosonocky, W. F. (1987). Infrared Image Sensors With Schottky-Barrier Detectors. Proc. SPIE, 869, pp.90 - 106.

[104] Watanabe, K. et al (2008). GaAs extrinsic photoconductors for the terahertz astronomy. Proc. SPIE 6840, Terahertz Photonics, 68401F.

[105] Giorgetta , F., Baumann , E., Graf, M. and Hofstetter , D. (2009). Quantum Cascade Detectors. IEEE Journal of Quantum Electronics, 45(8), pp. 1039 - 1052.

[106] Osi Optoelectronics. (2007). Photodiode Characteristics and Applications. Osi Optoelectronics, retrieved from: http://www.osioptoelectronics.com/application-notes/an-photodiode-parameters-characteristics.pdf (accessed on 2017/04/18)

[107] Pagano, R., Libertino, S., Corso, D., Valvo, G. and Sanfilippo, D. et al. (2014). Potentialities of silicon photomultiplier. Proc. SPIE 8990, Silicon Photonics IX, 899018.

[108] Haus, J. (2010). Optical Sensors: Basics and Applications, John Wiley & Sons, Weinheim, Germany.

[109] (ed.) Kubitscheck, U. (2017). Fluorescence Microscopy: From Principles to Biological Applications. John Wiley & Sons, NY, USA.

[110] Manzardo, O. (2002). Micro-Sized Fourier Spectrometers. Master Thesis, Universit´e de Neuchˆatel Institut de Microtechnique.

[111] Sabry, Y. M, Hassan, K., Anwar, M., Alharon, M. H., Medhat, M. et al. (2017). Ultra-compact MEMS FTIR spectrometer. Proc. SPIE 10210, Next-Generation Spectroscopic Technologies X, 102100H.

[112] Rissanen, A., Akujärvi, A., Antila, J., Blomberg, M. and Saari, H. (2012). MOEMS miniature spectrometers using tuneable Fabry-Perot interferometers. J. Micro/Nanolith. MEMS MOEMS. 11(2), 023003.

[113] Grüger, H., Knobbe, J., Pügner, T. and Schenk, H. (2013). Design and characterization of a hybrid-integrated MEMS scanning grating spectrometer. Proc. SPIE 8616, MOEMS and Miniaturized Systems XII, 86160L.

[114] Pügner, T., Knobbe, J., and Grüger, H. (2016). Near-Infrared Grating Spectrometer for Mobile Phone Applications. Applied Spectroscopy, 70(5), 734–745.

[115] Friedrich, D. M., Hulse, C. A., Gunten, M.V., Williamson, E. P., Pederson, C. G. and O'Brien, N. A. (2014). Miniature near-infrared

spectrometer for point-of-use chemical analysis. Proc. SPIE, 8992, Photonic Instrumentation Engineering, 899203.

[116] Huang, E. et al. (2017). Etalon Array Reconstructive Spectrometry. Scientific Reports, 7, 40693.

[117] Lapray, P. J., Wang, X., Thomas, J. B. and Gouton, P. (2014) Multispectral Filter Arrays: Recent Advances and Practical Implementation. Sensors 2014, 14, 21626-21659.

[118] Loewen, E. G. and Popov, E. (1997). Diffraction Gratings and Applications. CRC Press, NY, USA.

[119] Martin, A. E. (1980). Infrared interferometric spectrometers. Vibrational Spectra and Structure, 8, Elsevier, Amsterdam, The Netherlands.

[120] Middelhoek, S. and Audet, S. A. (1989). Silicon Sensors, Academic Press, London, UK.

[121] Hashemian, H. M and Knovel (Firm) (2005). Sensor performance and reliability. ISA - The Instrumentation, Systems, and Automation Society, Triangle Park, NC. pp. 23-40.

[122] Sassoli de Bianchi, M. (2013). The Observer Effect. Foundations of Science 18, pp. 213-243.

[123] Fraden, J. (2010). Handbook of Modern Sensors. Springer-Verlag New York. pp. 13-52.

[124] Kourosh, K. (2013). Sensors, An Introductory Course. Springer-Verlag New York. pp. 12-19.

[125] Meijer, G. (2008). Smart Sensor Systems. John Wiley & Sons, Sussex. pp. 23-50.

[126] Cree, (2016). Binning & Labeling, Cree® XLamp® XM Family LEDs. White Paper, Cree Inc., retrieved from: http://www.cree.com/led-components/media/documents/XLampXMBL.pdf (accessed on 2017/04/17).

[127] International Organization for Standardization (1997). ISO 11843-1. Capability of detection. Part 1: Terms and definitions. ISO, Genève.

[128] International Union of Pure and Applied Chemistry IUPAC (1995). Nomenclature in Evaluation of Analytical Methods including Detection and Quantification Capabilities, Pure & Appl. Chem., 67, pp. 1699-1723.

[129] El Gamal, A. (2001). High Dynamic Range Image Sensors. 392b Lectures and Class notes, Department of Electrical Engineering, Stanford University.

[130] Kavusi, S. and El Gamal, A. (2004). Quantitative study of high-dynamic-range image sensor architectures. Proc. SPIE 5301, Sensors and Camera Systems for Scientific, Industrial, and Digital Photography Applications V, 264.

[131] Arp, U., Shaw, P.S., Gupta, R. and Lykke, K. R. (2005). Damage to solid-state photodiodes by vacuum ultraviolet radiation, Journal of Electron Spectroscopy and Related Phenomena, 144–147, pp. 1039-1042

[132] Bostian, K. (2006). Long Term Stability and Reliability of Permanently Installed On-Line UV Sensors. Proc. Radtech Technical Conference.

[133] Liu, J.M. (2005). Photonic Devices. Cambridge University Press. Cambridge. pp. 941-942

[134] Rahimi, N., Patadia, A., Babic, D. and Grubisic, D. (2016). Characterization of the Linearity of InGaAs Photodetectors Using Series Resistance. GMA/ITG-Fachtagung Sensoren und Messsysteme 2016, pp. 519 - 523.

[135] L. P. Boivin, (1993). Automated absolute and relative spectral linearity measurements on photovoltaic detectors. Metrologia, 30(4), pp. 355-415.

[136] Martini, M., Guanche, R., Losada, I. J., and Vidal, C. (2017) Accessibility assessment for operation and maintenance of offshore wind farms in the North Sea. Wind Energy, 20, pp. 637–656.

[137] Whitby, D. (2012). Online condition monitoring of greases. Tribology and lubrication technology, STLE Publication, 68(5), pp. 72.

[138] Meyer, R. G., (2008). Inline photometer device and calibration method. Optek-Danulat Gmbh, US Patent, US2008100845 (A1).

[139] Lopez, P., Mabe, J., Iturbe, I. (2017). Sistema y Método de Monitorización del Estado de un Fluido (Spanish). IK4-Tekniker, Pending Patent, P201730848. See annexed documents.

[140] Rao, P. R. (2008). Signal and Systems. Tata McGraw Hill, New Delhi, pp. 415-420

[141] Hergert, E. (2015). WITS$- A Rough Guide to Selecting a Photodetector. Industrial Photonics, 2(3), pp.19 - 22.

[142] (ed.) Lasance, C. and Poppe, A. (2014). Thermal Management for LED Applications. Springer, New York, pp. 21 - 23.

[143] Du, Y. P., Liang, Y. Z., Kasemsuran, S., Maruo, K. and Ozaki, Y. (2004). Removal of Interference Signals Due to Water from in vivo Near-Infrared (NIR) Spectra of Blood Glucose by Region Orthogonal Signal Correction (ROSC). Analytical Sciences, 20(9), pp. 1339-1345.

[144] Newman, R. (1995). Visible light from a silicon p-n junction. Physics Review, 100(2), pp. 700 - 703.

[145] Mackowiak, V., Peupelmann, J. and Ma, Y. NEP – Noise Equivalent Power. Thorlabs White Paper, retrieved from: https://www.thorlabs.com/images/TabImages/Noise_Equivalent_Power_White_Paper.pdf
(accessed on 2017/04/29).

[146] Vishay Semiconductors (2002). Application of Optical Reflex Sensors. Application Note, 80107.

[147] Watson, C. and Vitic, M. (2011). Crosstalk mitigation in optical transceivers. Onechip Photonics Inc. , US Patent, US20110217045 A1.

[148] Osada, B. (2014). Handbook of Photodiodes. Hamamatsu, retrieved from: https://www.hamamatsu.com/resources/pdf/ssd/e02_handbook_si_photodiode.pdf
(accessed on 2017/03/17).

[149] (ed.) Dobkin, B. and Hamburger, J. (2015). Analog Circuit Design Volume Three: Design Note Collection. Elsevier, Oxford, UK.

[150] (ed.) Turchetta, R. (2016). Analog Electronics for Radiation Detection. CRC Press, Boca Ratón, FL, USA.

[151] Ping, W. and Qingjun, L., (2011). Biomedical Sensors and Measurement. Springer-Verlag, Hangzhou, China, pp. 25 - 27.

[152] Greanya, V. (2016). Bioinspired Photonics: Optical Structures and Systems Inspired by Nature. CRC press, London, UK, pp. 292 - 294.

[153] Gaigalas, A. K., Wang, L., Schwartz, A., Marti, G. E., and Vogt, R. F. (2005). Quantitating Fluorescence Intensity from Fluorophore: Assignment of MESF Values. Journal of Research of the National Institute of Standards and Technology, 110(2), pp. 101 - 114.

[154] Martelo-Vidal, M. J., Domínguez-Agis, F. and Vázquez, M. (2013), Ultraviolet/visible/near-infrared spectral analysis and chemometric tools for the discrimination of wines between subzones inside a

controlled designation of origin: a case study of Rías Baixas. Australian Journal of Grape and Wine Research, 19, pp. 62 - 67.

[155] Weeks, J. (2016). Why Hydraulic Oil Changes Color. Machine Lubrication, retrieved from http://machinerylubrication.com/Read/30495/hydraulic-oil-color
(accessed on 2017/04/17)

[156] Nørgaard, L., Haunstrup, I., Petersen, M., Weimann, J. and Sørensen, K. M., (2014). Chemometric terminology for qualitative and quantitative analysis. White Paper, P/N 1026715, Issue 1, Foss.

[157] Micklander, E. (2014). Quantitative, Qualitative and Exploratory Analysis of Food using Spectrometry and Quimiometry. The Royal Veterinary and Agricultural University Denmark.

[158] Denton, R. (2016). Sensor reliability impact on predictive maintenance program costs. Wilcoxon Research White paper, retrieved from:
https://wilcoxon.com/wp-content/uploads/2016/07/Sensor-reliability-impact-on-PdM-cost.pdf
(accessed on 2017/04/20).

[159] Ohba, R. (1992). Intelligent Sensor Technology. John Wiley & Sons, Ltd, Chichester, UK, pp. 5 -19.

[160] Brignell, J. E. and White, N. M. (1996). Intelligent Sensor Systems. Taylor & Francis, Oxford, UK, pp. 143 - 148.

[161] Kazior, T. E. (2014). Beyond CMOS: heterogeneous integration of III–V devices, RF MEMS and other dissimilar materials/devices with Si CMOS to create intelligent microsystems. Philosophical Transactions. Series A, Mathematical, Physical, and Engineering Sciences, 372.

[162] Geum, D.-M., Park, M.-S., Lim, J. Y., Yang, H.-D., Song, J. D., Kim, C. Z. and Choi, W. J. (2016). Ultra-high-throughput Production of III-V/Si Wafer for Electronic and Photonic Applications. Scientific Reports, 6, 20610.

[163] Roelkens, G. et al. (2015). III–V-on-silicon photonic integrated circuits for communication and sensing applications, 2015 IEEE Photonics Conference (IPC), pp. 593 - 594.

[164] IEEE Standard for a Smart Transducer Interface for Sensors and Actuators". IEEE Standards Association, IEEE STD.2007.4346346.

[165] International Electrotechnical Commission (2012). IEC 61076-2-101, Connectors for electronic equipment.

[166] Scheeline, A. (2016). What must be specified to achieve a valid spectroscopic measurement? Hamamatsu Articles, retrieved from: http://www.hamamatsu.com/us/en/community/optical_sensors/article/scheeline_spectroscopic_measurement/index.html (accessed on 2017/04/21).

[167] Scheeline, A. (2015). Is "good enough" good enough for portable visible and near-visible spectrometry? Proc. SPIE 9482, Next-Generation Spectroscopic Technologies VIII, 94820H.

[168] Workman, J. (2016). The Concise Handbook of Analytical Spectroscopy: Theory, Applications, and Reference Materials. World Scientific, London, UK, 3, pp. 21 - 23.

[169] (ed.) Coleman, P. C. (1994). Practical Sampling Techniques for Infrared Analysis. CRC Press, Boca Raton, FL, USA, pp. 151.

[170] (ed.) Lindon, J. C., Tranter, G. E. and Koppenaal, D. W. (2017). Encyclopedia of Spectroscopy and Spectrometry. Elsevier, Oxford, UK, pp. 752 - 755.

[171] Armaroli, T., Bécue, T. and Gautier, S. (2004). Diffuse Reflection Infrared Spectroscopy (DRIFTS): Application to the in situ Analysis of Catalysts. Oil & Gas Science and Technology - Rev. IFP, 59(2), pp. 215-237.

[172] Ocean Optics, (2015). Sampling Accessories for Reflection. Applications blog, retrieved from: https://oceanoptics.com/sampling-accessories-for-reflection/ (accessed on 2017/04/21).

[173] Padalkar, M. V. and Pleshko, N. (2015). Wavelength-Dependent Penetration Depth of Near Infrared Radiation into Cartilage. The Analyst, 140(7), pp. 2093 - 2100.

[174] Jianwei, Q. and Renfu, L. (2008). Measurement of the optical properties of fruits and vegetables using spatially resolved hyperspectral diffuse reflectance imaging technique. Postharvest Biology and Technology, 49(3), pp. 355 - 365.

[175] Huang, M., Kim, M.S., Chao, K., Qin, J., Mo, C., Esquerre, C., Delwiche, S. and Zhu, Q. (2016). Penetration Depth Measurement of Near-Infrared Hyperspectral Imaging Light for Milk Powder. Sensors. 16(4), pp. 441-449.

[176] Turner Designs (2014). Introduction to Fluorescence Measurements. Technical Note, retrieved from: https://www.turnerdesigns.com/t2/doc/appnotes/998-0050.pdf (accessed on 2017/04/26).

[177] Fischer, G., Ehlers, M., Andreas P., Zumbusch, A. and Daltrozzo, E. (2007). Near-Infrared Dyes and Fluorophores Based on Diketopyrrolopyrroles. Angewandte Chemie International Edition, 46, pp. 3750 - 3753.

[178] Gnyba, M., Smulko, J., Kwiatkowski, A. and Wierzba, P. (2011). Portable Raman spectrometer – design rules and applications. Bulleting of the Polish Academy of Sciences, 59(3).

[179] Bryan, A., Bonvallet, J., Rodriguez, J. and Olmstead, T. (2017). Miniature Raman spectroscopy utilizing stabilized diode lasers and 2D CMOS detector arrays. Proc. SPIE 10110, Photonic Instrumentation Engineering IV, 1011019.

[180] Gorritxategi, E. and Mabe, J. (2013). System and method for monitoring a fluid. Atten2 Monitoring Technologies, Patent EP2980557 A1.

[181] Salik, E. (2009). Optical phase measurement emphasized. Education and Training in Optics and Photonics, OSA Technical Digest Series (CD) (Optical Society of America), paper EMB3.

[182] Massart, D. L. (2003). Chemometrics: A Textbook. Elsevier Health Sciences, London, UK.

[183] Devos O., Downey G. and Duponchel L. (2014). Simultaneous data pre-processing and SVM classification model selection based on a parallel genetic algorithm applied to spectroscopic data of olive oils. Food Chem., 148, pp. 124 - 130.

[184] Sileoni V., van den Berg F., Marconi O., Perretti G. and Fantozzi P. (2011). Internal and external validation strategies for the evaluation of long-term effects in NIR calibration models. J. Agric. Food Chem. 59, pp. 1541–1547.

[185] Zhao, N., Wu, Z., Zhang, Q., Shi, X., Ma, Q., and Qiao, Y. (2015). Optimization of Parameter Selection for Partial Least Squares Model Development. Scientific Reports, 5, 11647.

[186] Brereton, R.G. (2003). Chemometrics: Data Analysis for the laboratory and Chemical Plant. Willey, Chichester, UK.

[187] (ed.) Johnson, R.W. (2016). Handbook of Fluid Dynamics. CRC Press, Boca Raton, FL, USA, pp. 502 - 506.

[188] Ghita, A., Pascut, F. C., Mather, M., Sottile, V. and Notingher, I. (2012). Cytoplasmic RNA in Undifferentiated Neural Stem Cells: A Potential Label-Free Raman Spectral Marker for Assessing the

Undifferentiated Status. Analytical Chemistry, 84 (7), pp. 3155 - 3162.

[189] Jain, R., Kasturi, R. and Schunk, B.G. (1995) Machine Vision. McGraw Hill, London, UK.

[190] Tack, N., Lambrechts, A., Soussan, P. and Haspeslagh, L. (2012). A compact, high-speed, and low-cost hyperspectral imager. Proc. SPIE 8266, Silicon Photonics VII, 82660Q.

[191] Lambrechts, A., Gonzalez, P., Geelen, B., Soussan, P., Tack, K. and Jayapala, M. (2014). A CMOS-compatible, integrated approach to hyper- and multispectral imaging. IEEE International Electron Devices Meeting, San Francisco, CA, USA, pp. 10.5.1-10.5.4.

[192] Hergeth, W.D. (2014). Process Analytical Chemistry. Wiley-VCH Verlag GmbH & Co. KGaA, Weinheim, Germany.

[193] Kress-Rogers, E. and Brimelow, C. J. B. (2000). Instrumentation and Sensors for the Food Industry. CRC Press, Boca Raton, FL, USA, pp. 404 - 410.

[194] Johnson, M. (2007). Past, Present and Future of Oil Analysis: An Expert Panel Discussion on the Future of Oil 705 Analysis. Tribology and Lubrication Transactions.

[195] Poley, J. (2011). Metallic wear Debris Sensors: promising Developments in Failure Prevention for Wind Turbine Gear sets and Similar Components. Wind turbine Condition Monitoring Workshop.

[196] Zhu, J., Yoon, J.M., He D. and Bechhoefer, E. (2014). Online particle-contaminated lubrication oil condition monitoring and remaining useful life prediction for wind turbines. Wind Energy, 18(6), pp. 1131-1149.

[197] O'Toole, M. and Diamond, D. (2008). Absorbance Based Light Emitting Diode Optical Sensors and Sensing Devices. Sensors (Basel, Switzerland), 8(4), pp. 2453 - 2479.

[198] (ed.) Gaonkar, A. G. (1995) Characterization of Food: Emerging Methods. Elsevier, New York, NY, USA, pp. 192 - 195.

[199] Siesler, H.W. and Eschenauer, U. (1998). NIR absorbance measuring instrument with ATR probe. Perstorp Analytical, Inc., US Patent, US5739537 A.

[200] Bereta, G. (1999). Spectrophotometer Calibration and Certification. HP Laboratories Palo Alto, HPL-1999-2.

[201] Gordon, D.A., Alguard, M. J. (1998). Dual spectrometer color sensor. Honeywell, Patent, US5793486 A.

[202] Color Sentinel Systems. In Line & Hand Held Self-Calibrating Modeling Spectrophotometers. White Paper, retrieved from: http://www.colorsentinelsystems.com/ (accessed on 2017/04/11).

[203] Ehbets, P., Frick, B., Wegmuller, M., Hunkemeier, J. and Niederer, G. (2014). Hand-Held Measurement Device for Capturing the Visual Impression of a Measurement Object. X-Rite Switzerland GmbH, Patent, US20140152990 A1.

[204] Frick, B. (2015). Color Measuring Apparatus. X-Rite Switzerland GmbH, Patent, US20160011052 A1.

[205] Frick, B., Feri, L. and Knechtle, S. (2012). Hand-held light measuring device. X-Rite Switzerland GmbH, Patent, US8279440 B2.

[206] Navarro-Villoslada, F., Orellana, G., Moreno-Bondi, M.C. Vick, T., Driver, M., Hildebrand, G. and Liefeith, K. (2001). Fiber-optic luminescent sensors with composite oxygen-sensitive layers and anti-biofouling coating. Anal. Chem., 73, pp. 5150 - 5156.

[207] Chae, K. H., Jang, Y. M., Kim, Y.H., Sohn, O. J. and Rhee, J. I. (2007). Anti-fouling epoxy coatings for optical biosensor application based on phosphorylcholine. Sensors and Actuators B: Chemical, 124(1), pp. 153 - 160.

[208] Omar, A. F. B. and MatJafri, M. Z. B. (2009). Turbidimeter Design and Analysis: A Review on Optical Fiber Sensors for the Measurement of Water Turbidity. Sensors (Basel, Switzerland), 9(10), 8311 - 8335.

[209] Mignani, A.G., Bizzarri, P. and Driver, M. (2002). Anti-biofouling coatings for optical fiber sensors. Proc. SPIE 4578, Sensor Technology and Applications, 0277-786X.

[210] Gulbrandsen, K. E. (2009). Bridging the valley of death: The rhetoric of technology transfer, PhD Thesis, Univ Iowa.

[211] Hargadon, A. (2011). Into the Valley of Death, University of California Davis Graduate School of Management.

[212] Cooper, R. G. and Scott J. E. (2012). Best Practices in the Idea-to-Launch Process and Its Governance. Research-Technology Management. 55 (2), pp. 43 - 54.

[213] Kuroda, R. and Sugawa, S. (2015). UV/VIS/NIR imaging technologies: challenges and opportunities. Proc. SPIE 9481, Image Sensing Technologies: Materials, Devices, Systems, and Applications II, 948108.

[214] Manuela Reitzig, M., Katzmann, J., Schuster, C. and Härtling, T. (2015). Optical nanosensor technology – from basic research to industrial applications. Proc. SENSOR 2015, AMA Science, pp. 25 – 29.

[215] European Commission. (2012). Towards 2020 - Photonics Driving Economic Growth in Europe. Photonics PPP Multi Annual Roadmap, pp.6-8, retrieved from: https://ec.europa.eu/research/industrial_ technologies/pdf/photonics-ppp-roadmap_en.pdf (accessed on 2017/04/ 21).

[216] El Hagrasy, A. S., Chang S.Y. and Kiang, S. (2006). Evaluation of Risk and Benefit in the Implementation of Near-Infrared Spectroscopy for Monitoring of Lubricant Mixing. Pharmaceutical Development and Technology, 11(3), pp. 303-315.

[217] Huang, H., Yu, H., Xu, H. and Ying, Y. (2008). Near infrared spectroscopy for on/in-line monitoring of quality in foods and beverages: A review. Food Engineering, 87(3), pp. 303-313.

[218] Tokhtuev, E., Owen, C. J., Skirda, A. and Christensen, W. M. (2015). Self-cleaning optical sensor. Ecolab Usa Inc., US Patent, US9001319 B2.

[219] Cooper, R. G. (2007). Managing Technology Development Projects, IEEE Engineering Management Review, 35 (1), pp. 67 - 76.

[220] Cooper, R. G. (2014). What's next? After Stage-Gate. Research Technology Management, 157(1), pp 20 - 31.

[221] Osterwalder, A. and Pigneur, Y. (2010). Business Model Generation: A Handbook for Visionaries, Game Changers, and Challengers. John Wiley and Sons, New York, NY, USA.

[222] Osterwalder, A. Pigneur, Y., Bernarda, G. and Smith, A. (2014). Value Proposition Design: How to Create Products and Services Customers Want. John Wiley and Sons, New York, NY, USA.

[223] Photonics 21, (2011). Our Vision for a Key Enabling Technology of Europe. White Paper, Photonics 21, pp. 8-12

[224] Resenhoeft, T. (2015). The fast track to success with agile product development, Bosch Press Release, June 16, 2015.

[225] McGrath, R. and McMillan, I. (2009). Discovery-Driven Growth. A Breakthrough Process to Reduce Risk and Seize Opportunity. Harvard Business School Press: Cambridge, MA, pp. 1 - 26.

[226] Loch, C., DeMeyer, A. and Pich, M. (2006). Managing the Unknown. A New Approach to Managing High Uncertainty and Risks in Projects. John Wiley & Sons, Hoboken, NJ, USA, pp. 1 - 5

[227] Pressman, R. (2009). Software Engineering: A Practitioner's Approach. McGraw-Hill, International Editions, 5th Ed...

[228] Cooper, R.G. (1998). Product Leadership – Creating and Launching Superior New Products. Perseus Books, New York, USA.

[229] Hasenkamp, T. and Olme, A. (2008). Introducing design for Six Sigma at SKF. International Journal of Six Sigma and Competitive Advantage, 4 (2), pp. 172 - 189.

[230] Korb, W. and Helmut, K. (2013). Innovation and robust sensor product development with Design for Six Sigma. Proc. SENSOR 2013, AMA Science, pp. 743 – 745.

[231] Eskandari, R. (2006). Role of Design for Six Sigma in Total Product Development. Six Sigma Academy International LCC, MIT LGO seminars May 2006.

[232] Womack, J. P., Jones, D. T. and Roos, D. (1990). The Machine that Changed the World: The Story of Lean Production. Harper Perennial, New York, NY, USA.

[233] Morgan, J. P. and Liker, J. K. (2006). The Toyota Product Development System: Integrating People, Process, and Technology. Productivity Press, New York, NY, USA.

[234] McMahon, T. (2010). Lean Product Development. CONNSTEP's 2010 Manufacturing and Business.

[235] Sorli, M., Maksimovic, M., Al-Ashaab, A., Sulowski, R., Shehab, E. and Sopelana, A. (2012). Development of KBE system to support LeanPPD application. 18th International ICE Conference on Engineering, Technology and Innovation, pp. 1 - 8.

[236] Ries, E. (2011). The Lean Startup: How Today's Entrepreneurs Use Continuous Innovation to Create Radically Successful Businesses. Crown Business, Crown Publishing Group, New York. NY, USA.

[237] Chen, E. (2015). Bringing a Hardware Product to Market: Navigating the Wild Ride from Concept to Mass Production. Concept Spring.com, pp. 9-31.

[238] Ideo (1999). Reimagining the shopping cart, Ideo, Palo Alto, CA, retrieved from:
https://www.ideo.com/post/reimagining-the-shopping-cart
(accessed on 2017/04/15).

[239] Ostrower, D. (2014). MVP for Hardware. Insight, page 8, retrieved from: http://www.altitudeinc.com (accessed on 2017/04/15).

[240] Hof, R. (2014). How Fitbit Survived as A Hardware Startup. Forbes, retrieved from: https://www.forbes.com/sites/roberthof/2014/02/04/how-fitbit-survived-as-a-hardware-startup/
(accessed on 2017/04/15).

[241] Sheehan, M. (2009). Ready, fire… aim: balancing speed and accuracy in new product development. PDMA Ontario, retrieved from: http://www.ontariopdma.ca/events/pastevents.htm
(accessed on 17/04/ 2017).

[242] Pietzsch, J.B., Shluzas, L.A., Paté-Cornell, M., Yock, P.G. and Linehan, J.H. (2009). Stage-Gate Process for the Development of Medical Devices. ASME. J. Med. Devices., 3(2), pp. 021004 - 021004-15.

[243] Ortloff, D. et al. (2014). MEMS Product Engineering: Handling the Diversity of an Emerging Technology. Best Practices for Cooperative Development. Springer-Verlag Wien, New York, USA, pp. 85 - 129.

[244] Lenfle, S. and Loch, C. (2010). Lost Roots: How Project Management Came to Emphasize Control Over Flexibility and Novelty. California Management Review, 53(1), pp. 32 - 55.

[245] Karlström, D. and Runeson, P. (2006). Integrating agile software development into stage-gate managed product development. Empirical Software Engineering, 11(2), pp. 203 - 225.

[246] Cooper, R. G. (2016). Agile–Stage-Gate Hybrids. Journal of Research-Technology Management, 59(1), pp. 21 - 29.

[247] Sommer, A. F., Hedegaard, C., Dukovska-Popovska, I., and Steger-Jensen, K. (2015). Improved product development performance through Agile/Stage-Gate hybrids: The next-generation Stage-Gate process? Research-Technology Management, 58(1), pp. 34 - 44.

[248] Grönlund, J., Rönnberg, D. and Frishammar, J. (2010). Open Innovation and the Stage-Gate Process: A Revised Model for New Product Development. California Management Review, 52(3), pp. 106-131.

[249] Unnger D. W., and Eppinger, S. D. (2009). Comparing product development processes and managing risk. Int. J. Product Development, 8(4), pp. 382 - 402.

[250] Chesbrough, H. W. (2003). Open Innovation: The new imperative for creating and profiting from technology. Boston: Harvard Business School Press, Boston, MA, USA.

[251] Mierzwa, T. J. (2016). Strategies for Managing Innovation. Lectures, University of Maryland's Master of Technology Entrepreneurship Program, Innovation Theory.

[252] European Commission, (2011). Guide to Intellectual Property Rules for FP7 projects. European Commission, Version 3, pp. 5 - 13.

[253] Metrohm AG. (2016). Using Online Near-Infrared Spectroscopy for Real-Time Analysis of Industrial Gases. Application Work, AW NIR-US-073-092015, Metrohm AG, retrieved from: https://www.metrohm.com/ (accessed on 2017/04/17)

[254] Di Egidio, V., Sinelli, N., Giovanelli, G. et al. (2010). NIR and MIR spectroscopy as rapid methods to monitor red wine fermentation. Eur Food Res Technol , 230(6), 947 - 955.

[255] Miller, R., Princz, S., Hessling, M. and Nurtdinow, I. (2012). Goal: online glucose sensor for bioreactors. Online Article. Ulm University of Applied Sciences, retrieved from: https://www.biooekonomie-bw.de/en/articles/news/goal-online-glucose-sensor-for-bioreactors/ (accessed on 2017/04/17).

[256] Filhaber, J. (2013). How Wedge and Decenter Affect Aspheric Optics. Photonics Spectra, Laurin Publishing, pp. 44 - 47.

[257] Hill, D. and McEuen, K. (2015). 4 Big Mistakes in Developing Photonics-Enabled Medical Devices. White Paper, Zygo Corporation.

[258] Mazurek, W. and Badve, A. (2017). Applying Design for LeanSigma® in the Medical Device Industry. White Paper, ConMed Corp. retrieved from: http://www.tbmcg.com.br/practitioner_assets/ Practitioner_Briefing_DLS.pdf (accessed on 2017/04/17)

[259] Mabe, J. and Gorritxategi, E. (2013). System and method for monitoring a fluid. Atten2 Advanced Monitoring Technologies, Patent, EP2980557A1, US20160069856, WO2014154915A1.

[260] Mabe, J., Zubia, J. and Gorritxategi, E. (2017). Lens-free imaging-based low-cost microsensor for in-line wear debris detection in lube

oils. Proc. SPIE 10110, Photonic Instrumentation Engineering IV, 101101D.

[261] Mabe, J., Zubia, J., Gorritxategi, E. (2017). Photonic Low Cost Micro-Sensor for in-Line Wear Particle Detection in Flowing Lube Oils. Sensors 2017, 17, 586.

[262] Mabe, J. (2016). Fluid Monitoring System, IK4-Tekniker, Pending Patent, EP16382179. See Annexed Documents.

[263] Mabe, J. (2017). Monitoring System and Method for Detecting Flowing Microscopic Objects. IK4-Tekniker, Pending Patent, EP17382007. See Annexed Documents.

[264] Villar, A., Vadillo, J., Santos, J.I., Gorritxategi, E., Mabe, J., Arnaiz, A. and Fernández, L. A. (2017) Cider fermentation process monitoring by Vis-NIR sensor system and chemometrics. Food Chemistry, 221(15), pp. 100-106.

[265] Gorritxategi, E., Mabe, J., Delgado, A. (2015). Fluid Monitoring System Based on Near-Infrared Spectroscopy. Atten2 Advanced Monitoring Technologies, Pending Patent, EP15382609.
See Annexed Documents.

[266] Villar, A., Mabe, J. et al. (2017). Equipo de Inspección para la Clasificación o Discriminación Automatizada de Almendras en Función de la Concentración de Amigdalina y Procedimiento de Inspección. (Spanish) Arboreto SL, Pending Patent, P201730562.